


United States Nuclear Regulatory Commission Official Hearing Exhibit		
In the Matter of: PSEG POWER, LLC AND PSEG NUCLEAR, LLC (Early Site Permit Application)		
	ASLBP #:	15-943-01-ESP-BD01
	Docket #:	05200043
	Exhibit #:	PSEG004B-MA-BD01
	Admitted:	03/24/2016
	Rejected:	
	Other:	
	Identified:	03/24/2016
	Withdrawn:	
	Stricken:	

PSEG004B

PSEG Site

ESP Application

Part 2

Site Safety Analysis Report

Revision 4

**PSEG Site
ESP Application
Part 2, Site Safety Analysis Report**

MASTER TABLE OF CONTENTS

<u>Section</u>	<u>Title</u>	<u>Page</u>
CHAPTER 1		
INTRODUCTION AND GENERAL DESCRIPTION		
1.1	INTRODUCTION	1.1-1
1.2	GENERAL PLANT DESCRIPTION	1.2-1
1.3	PLANT PARAMETER ENVELOPE	1.3-1
1.4	IDENTIFICATION OF AGENTS AND CONTRACTORS	1.4-1
1.5	REQUIREMENTS FOR FURTHER TECHNICAL INFORMATION.....	1.5-1
1.6	MATERIAL INCORPORATED BY REFERENCE	1.6-1
1.7	DRAWING AND OTHER DETAILED INFORMATION.....	1.7-1
1.8	INTERFACES WITH STANDARD DESIGNS	1.8-1
1.9	CONFORMANCE TO NRC REGULATIONS AND REGULATORY GUIDANCE	1.9-1
1.10	NUCLEAR POWER PLANTS TO BE OPERATED ON MULTI-UNIT SITES ..	1.10-1
CHAPTER 2		
SITE CHARACTERISTICS AND SITE PARAMETERS		
2.0	SITE CHARACTERISTICS	2.0-1
2.1	GEOGRAPHY AND DEMOGRAPHY	2.1-1
2.2	IDENTIFICATION OF POTENTIAL HAZARDS IN SITE VICINITY	2.2-1
2.3	METEOROLOGY	2.3-1
2.4	HYDROLOGIC ENGINEERING	2.4-1
2.5	GEOLOGY, SEISMOLOGY, AND GEOTECHNICAL INFORMATION	2.5-1
APPENDIX 2AA Boring Logs from ESPA Exploration		2AA-1
CHAPTER 3		
DESIGN OF STRUCTURES, COMPONENTS, EQUIPMENT, AND SYSTEMS		
3.5.1.6	Aircraft Hazards	3.5-1
CHAPTER 11		
RADIOACTIVE WASTE MANAGEMENT		
11.2.3	LIQUID RADIOACTIVE RELEASES	11.2-1
11.3.3	GASEOUS RADIOACTIVE RELEASES	11.3-1

**PSEG Site
ESP Application
Part 2, Site Safety Analysis Report**

MASTER TABLE OF CONTENTS (CONTINUED)

<u>Section</u>	<u>Title</u>	<u>Page</u>
CHAPTER 13 CONDUCT OF OPERATIONS		
13.3	EMERGENCY PLAN	13.3-1
13.6	INDUSTRIAL SECURITY	13.6-1
CHAPTER 15 TRANSIENT AND ACCIDENT ANALYSIS		
15.1	SELECTION OF ACCIDENTS	15.1-1
15.2	EVALUATION METHODOLOGY	15.2-1
15.3	SOURCE TERMS	15.3-1
15.4	RADIOLOGICAL CONSEQUENCES	15.4-1
CHAPTER 17 QUALITY ASSURANCE		
17.1	ESPA QUALITY ASSURANCE	17.1-1

**PSEG Site
ESP Application
Part 2, Site Safety Analysis Report**

**CHAPTER 1
INTRODUCTION AND GENERAL DESCRIPTION**

TABLE OF CONTENTS

<u>Section</u>	<u>Title</u>	<u>Page</u>
1.1	INTRODUCTION	1.1-1
1.2	GENERAL PLANT DESCRIPTION	1.2-1
1.2.1	SITE LOCATION.....	1.2-1
1.2.2	SITE DEVELOPMENT	1.2-1
1.3	PLANT PARAMETER ENVELOPE	1.3-1
1.3.1	PLANT PARAMETER ENVELOPE APPROACH.....	1.3-1
1.3.2	PPE DEVELOPMENT PROCESS.....	1.3-2
1.3.3	PSEG SITE PLANT PARAMETER ENVELOPE.....	1.3-3
1.4	IDENTIFICATION OF AGENTS AND CONTRACTORS	1.4-1
1.4.1	APPLICANT	1.4-1
1.4.1.1	PSEG Power, LLC and PSEG Nuclear, LLC.....	1.4-1
1.4.2	CONTRACTORS.....	1.4-1
1.4.2.1	Sargent & Lundy, LLC	1.4-1
1.4.2.2	MACTEC Engineering and Consulting, Inc.	1.4-1
1.4.3	OTHER CONSULTANTS	1.4-2
1.4.3.1	William Lettis & Associates, Inc.	1.4-2
1.5	REQUIREMENTS FOR FURTHER TECHNICAL INFORMATION	1.5-1
1.6	MATERIAL INCORPORATED BY REFERENCE.....	1.6-1
1.7	DRAWINGS AND OTHER DETAILED INFORMATION	1.7-1
1.8	INTERFACES WITH STANDARD DESIGNS.....	1.8-1
1.9	CONFORMANCE TO NRC REGULATIONS AND REGULATORY GUIDANCE.....	1.9-1
1.10	NUCLEAR POWER PLANTS TO BE OPERATED ON MULTI-UNIT SITES ...	1.10-1

**PSEG Site
ESP Application
Part 2, Site Safety Analysis Report**

LIST OF TABLES

<u>Number</u>	<u>Title</u>
1.1-1	Acronyms and Abbreviations Used in the SSAR
1.3-1	Plant Parameter Envelope
1.3-2	Blowdown Constituents and Concentrations
1.3-3	Single Unit Principal Radionuclides in Solid Radwaste
1.3-4	Emissions from Auxiliary Boilers
1.3-5	Emissions from Standby Diesel Generators
1.3-6	Standby Power System Gas Turbine Flue Gas Effluents
1.3-7	Single Unit Composite Average Annual Normal Gaseous Release
1.3-8	Single Unit Composite Average Annual Normal Liquid Release
1.3-9	Liquid-Containing Tank Failure Radionuclide Concentrations
1.9-1	Regulatory Conformance Matrix
1.9-2	Regulatory Conformance Matrix Clarifications

**PSEG Site
ESP Application
Part 2, Site Safety Analysis Report**

LIST OF FIGURES

<u>Number</u>	<u>Title</u>
1.2-1	PSEG Site Location – 6-Mile Radius
1.2-2	PSEG Site Location – 50-Mile Radius
1.2-3	Site Utilization Plan

**PSEG Site
ESP Application
Part 2, Site Safety Analysis Report**

CHAPTER 1

INTRODUCTION AND GENERAL DESCRIPTION

1.1 INTRODUCTION

This Site Safety Analysis Report (SSAR) supports PSEG Power's and PSEG Nuclear's (hereafter referred to as PSEG or Applicants) early site permit application (ESPA). The SSAR addresses site suitability issues and complies with applicable portions of Title 10, Part 52 of the Code of Federal Regulations (10 CFR 52), Subpart A, *Early Site Permits*.

The PSEG Site is located on the southern part of Artificial Island on the east bank of the Delaware River in Lower Alloways Creek Township, Salem County, New Jersey. The site is 15 miles south of the Delaware Memorial Bridge, 18 miles south of Wilmington, Delaware, 30 miles southwest of Philadelphia, Pennsylvania, and 7-1/2 miles southwest of Salem, New Jersey.

PSEG has not selected a particular reactor design to be constructed at the site. In order to provide sufficient design information to enable the NRC to determine that the site is suitable for a new plant, a surrogate design has been provided. The surrogate plant is a set of bounding parameters, the plant parameter envelope (PPE). The PPE approach has been accepted by the NRC in previous ESPAs. The combination of PPE values and site characteristics that form the permit basis for NRC's issuance of an early site permit (ESP) are identified in this SSAR and discussed further in Sections 1.3 and 2.0.

The SSAR also contains information about site characteristics, site safety, emergency preparedness, and quality assurance. The following paragraphs briefly describe the contents of the SSAR:

Chapter 1, *Introduction and General Description*, includes a general site description, an overview of reactor types, the PPE approach, and a summary of regulatory conformance.

Chapter 2, *Site Characteristics*, includes geography, demography, nearby industrial installations, transportation facilities, meteorology, hydrology, geology, and seismic characteristics of the site. It also includes descriptions of effluents, thermal discharges, and conformance with 10 CFR 100, *Reactor Site Criteria*, requirements.

Chapter 3, *Design of Structures, Components, Equipment, and Systems* contains information on aircraft hazards in the vicinity of the PSEG Site.

Chapter 11, *Radioactive Waste Management*, includes only information on liquid and gaseous radioactive releases.

Chapter 13, *Conduct of Operations*, includes only an overview of emergency planning for the site and surrounding area in case of plant accidents and of the physical security provided for the site and plant sensitive areas.

Chapter 15, *Transient and Accident Analyses*, includes a discussion of radiological consequence of bounding plant accidents and conformance with applicable 10 CFR 100, *Reactor Site Criteria* for the reactor technologies being considered.

Rev.4

**PSEG Site
ESP Application
Part 2, Site Safety Analysis Report**

Chapter 17, *Quality Assurance*, includes the Quality Assurance Program under which the ESPA was prepared.

Where possible, the SSAR section numbers correspond to the section numbers identified in NUREG-0800, *Standard Review Plan for the Review of Safety Analysis Reports for Nuclear Power Plants: LWR Edition*. Consistent with that guidance, there are some gaps in the numbering sequence. This is intentional. This approach is intended to facilitate subsequent integration of the information in this ESPA with a reactor design certification in a combined license (COL) application, in which the complete numbering sequence is used.

Table 1.1-1 provides a list of abbreviations and acronyms used in Part 2.

**PSEG Site
ESP Application
Part 2, Site Safety Analysis Report**

**Table 1.1-1 Sheet (1 of 15)
Acronyms and Abbreviations Used in the SSAR**

Acronym/Abbreviation	Definition
°C	degrees Celsius
°F	degrees Fahrenheit
σ_v'	Overburden pressure
μ	Poisson's Ratio
ϕ	Total stress internal friction angle
ϕ'	Effective stress internal friction angle
χ/Q	atmospheric dispersion factor
ABWR	Advanced Boiling-Water Reactor
ac.	acre
ac.-ft.	acre-feet
acfm	actual cubic feet per minute
ACI	American Concrete Institute
AFB	Air Force Base
AFCCC	Air Force Combat Climatology Center
ALOHA	Areal Locations of Hazardous Atmospheres
amax	foundation level acceleration due to the design earthquake and/or horizontal acceleration
AMC	antecedent moisture condition
ANSI/ANS	American National Standards Institute/American Nuclear Society
ANSS	Advanced National Seismic System
AP1000	Advanced Passive 1000
arc-min	arc minute
arc-sec	arc second

**PSEG Site
ESP Application
Part 2, Site Safety Analysis Report**

**Table 1.1-1 Sheet (2 of 15)
Acronyms and Abbreviations Used in the SSAR**

Acronym/Abbreviation	Definition
ASHRAE	American Society of Heating, Refrigerating and Air-Conditioning Engineers
AST	alternate source term
atm	atmosphere
bgs	below ground surface
BLEVE	Boiling Liquid Expanding Vapor Explosion
bpf	blows per foot
BTP	Branch Technical Position
Btu	British thermal units
BWR	boiling water reactor
c	total stress cohesion intercept
c'	effective stress cohesion intercept
CAV	Cumulative Absolute Velocity
Cc	coefficient of compression
CCW	component cooling water
C&D	Chesapeake & Delaware
CDF	confined disposal facility
CDF	core damage frequency
CEM	Coastal Engineering Manual
CEUS	central and eastern United States
CFR	Code of Federal Regulations
cfs	cubic feet per second
Ci	Curie

**PSEG Site
ESP Application
Part 2, Site Safety Analysis Report**

**Table 1.1-1 Sheet (3 of 15)
Acronyms and Abbreviations Used in the SSAR**

Acronym/Abbreviation	Definition
CL, CH	clay
cm/s	centimeters per second
COC	chain-of-custody
COL	Combined License
COLA	Combined License Application
CO-OPS	Center for Operational Oceanographic Products and Services
COOP	Cooperative Observing Program
CPT	cone penetration test
Cr	coefficient of recompression
CRM	Coastal Relief Model
CRR	cyclic resistance ratio
CRREL	Cold Regions Research and Engineering Laboratory
CSZ	Charlevoix seismic zone
CU	Consolidated-undrained
cu. ft.	cubic feet
cu. yd.	cubic yards
CVSZ	Central Virginia seismic zone
CWS	circulating water system
DANG	Delaware Air National Guard
DBF	design basis flood
dBA	A-weighted decibels
DBA	design basis accident
DBT	Design Basis Tornado

**PSEG Site
ESP Application
Part 2, Site Safety Analysis Report**

**Table 1.1-1 Sheet (4 of 15)
Acronyms and Abbreviations Used in the SSAR**

Acronym/Abbreviation	Definition
DBT	dry bulb temperature
DCD	Design Control Document
deg	degrees
Delaware DataMIL	Delaware Data Mapping and Integration Laboratory
delta-T	vertical temperature difference
DEM	digital elevation model
dia.	diameter
DMDS	demineralized water distribution system
DNAG	Decade of North America Geology
DOE	U.S. Department of Energy
D/Q	ground deposition factor
DRBC	Delaware River Basin Commission
dyn-cm	dyne-centimeters
EAB	Exclusion Area Boundary
EAL	Emergency Action Level
ECFS	East Coast fault system
ECFS-s	East Coast fault system - south
ECL	effluent concentration limit
EDG	emergency diesel generator
EIS	Environmental Impact Statement
Emb	estimated body wave magnitude
EPA	Environmental Protection Agency
EPRI	Electric Power Research Institute

**PSEG Site
ESP Application
Part 2, Site Safety Analysis Report**

**Table 1.1-1 Sheet (5 of 15)
Acronyms and Abbreviations Used in the SSAR**

Acronym/Abbreviation	Definition
EPRI-SOG	Electric Power Research Institute Seismic Owner's Group
Eq.	equation
ERO	emergency response organization
EPZ	Emergency Planning Zone
EWD	Engineering Weather Data
Es	Elastic Modulus (psf)
ESP	early site permit
ESPA	early site permit application
EST	Earth Science Team
ETE	Evacuation Time Estimate
FAA	Federal Aviation Administration
fc	corner frequency (units of Hertz)
FIRS	foundation input response spectra
fpm	feet per minute
fps	feet per second
FPS	fire protection system
FS	factor of safety
FSAR	Final Safety Analysis Report
ft.	feet
ft/day	feet per day
ft/ft	feet per foot
ft/mi.	feet per mile
ft/s	feet per second

**PSEG Site
ESP Application
Part 2, Site Safety Analysis Report**

**Table 1.1-1 Sheet (6 of 15)
Acronyms and Abbreviations Used in the SSAR**

Acronym/Abbreviation	Definition
ft/sec	feet per second
ft/yr	feet per year
g	gram
g	acceleration due to gravity
G	Shear Modulus (psf)
G/Gmax	shear modulus divided by the low strain shear modulus function of the cyclic shear strain described by the damping ratio and the modulus reduction ratio
Ga	billion years ago or Giga Annum
gal.	gallon
GHB	general head boundary
GI-LLI	gastrointestinal tract, lower-large intestine
GIS	Geographic Information System
GMRS	ground motion response spectra
gpd	gallons per day
gpm	gallons per minute
GTG	gas turbine generator
Gs	Specific Gravity
GWh	gigawatthour(s)
HCGS	Hope Creek Generating Station
HEC-HMS	Hydrologic Engineering Center -Hydrologic Modeling System
HEC-RAS	Hydrologic Engineering Center River Analysis System
HF	high-frequency
Hg	mercury

**PSEG Site
ESP Application
Part 2, Site Safety Analysis Report**

**Table 1.1-1 Sheet (7 of 15)
Acronyms and Abbreviations Used in the SSAR**

Acronym/Abbreviation	Definition
HMR	Hydrometeorological Reports
hr.	hour
HT	Hornerstown Formation
HUC	hydrologic unit code
Hz	hertz
I.D.	Inside Diameter
IDLH	Immediately Dangerous to Life and Health
in.	inch
ISFSI	independent spend fuel storage installation
ISMCS	International Surface Meteorological Climate Summary
ITAAC	Inspections, Test, Analysis, and Acceptance Criteria
J	joules
JFD	Joint Frequency Distribution
K	Kelvin
ka	thousand years ago
kg	kilogram
km	kilometer
km ³	cubic kilometers
Ko	coefficient of earth pressure at rest
ksf	kips per square foot and/or 1000 pounds per square foot
kt	knots
kW	kilowatts
KW	Kirkwood Formation

**PSEG Site
ESP Application
Part 2, Site Safety Analysis Report**

**Table 1.1-1 Sheet (8 of 15)
Acronyms and Abbreviations Used in the SSAR**

Acronym/Abbreviation	Definition
Lat	latitude
l or L	liter
L	Lower
lb.	pounds
LCD	local climatological data
LCSN	Lamont-Doherty Cooperative Seismographic Network
LEL	Lower Explosive Limit
LF	low-frequency
Lidar	resolution light detection and ranging
LMDCT	linear mechanical draft cooling tower
LOCA	loss of coolant accident
LL	Liquid Limit
Long	longitude
LPZ	low population zone
LWR	light water reactor
m	meter
Ma	million years ago
MAP	municipal airport
m_b	body wave magnitude
m_{bLg}	body wave magnitude
m_c	coda magnitude
MCWB	mean coincident wet bulb temperature
Md	duration magnitude

**PSEG Site
ESP Application
Part 2, Site Safety Analysis Report**

**Table 1.1-1 Sheet (9 of 15)
Acronyms and Abbreviations Used in the SSAR**

Acronym/Abbreviation	Definition
MEDRB	Maritime Exchange for the Delaware River and Bay
MEI	maximally exposed individual
mg/L	milligrams per liter
mGal	milli-Galileo
MGY	million gallons per year
mi.	miles
min	minute
MISLE	Marine Information for Safety and Law Enforcement
ML	local magnitude
ML, MH	silt
M _{Lg}	body-wave magnitude
Mmax	maximum magnitude
MMI	Modified Mercalli Intensity
MORB	mid-ocean ridge basalt
MOST	Method of Splitting Tsunami
MPa	megapascals
mph	miles per hour
MPSSZ	Middleton Place–Summerville seismic zone
mrad	millirad
mrem	millirem
MTBE	Methyl Tertiary-Butyl Ether
MTR	Military Training Route
MTU	metric ton uranium

**PSEG Site
ESP Application
Part 2, Site Safety Analysis Report**

**Table 1.1-1 Sheet (10 of 15)
Acronyms and Abbreviations Used in the SSAR**

Acronym/Abbreviation	Definition
msl	mean sea level
M _w	moment magnitude
MW	megawatt
MWD	megawatt days
MWe	megawatts electric
MWt	megawatts thermal
NAMAG	North American Magnetic Anomaly Group
NAVD	North American Vertical Datum 1988
NCDC	National Climatic Data Center
NDCT	natural draft cooling tower
NEC	not elsewhere classified
NEDB	National Earthquake Database
NEI	Nuclear Energy Institute
Neogene	Upper Tertiary Strata
NESN	New England Seismic Network
NID	National Inventory of Dams
NIOSH	National Institute of Occupational Safety and Health
NJDEP	New Jersey Department of Environmental Protection
NK	Navesink Formation
NM	nautical miles
NOAA	National Oceanic and Atmospheric Administration
NOS	National Ocean Service
NRC	U.S. Nuclear Regulatory Commission

**PSEG Site
ESP Application
Part 2, Site Safety Analysis Report**

**Table 1.1-1 Sheet (11 of 15)
Acronyms and Abbreviations Used in the SSAR**

Acronym/Abbreviation	Definition
NRCS	Natural Resources Conservation Service
nT	nanotesla
N-values	standard penetration resistance
OBE	operating basis earthquake
ODCM	Offsite Dose Calculation Manual
OX VT	Oxidized Portion of the Vincetown Formation
P	suspension compressional wave
PBL	Planetary Boundary Layer
pc	pre-consolidation stress
PHMSA	Pipeline and Hazardous Materials Safety Administration
PI	Plasticity Index
PL	Plastic Limit
PMF	probable maximum flood
PMH	probable maximum hurricane
PMP	probable maximum precipitation
PMS	probable maximum surge
PMT	probable maximum tsunami
PMWP	probable maximum winter precipitation
PM ₁₀	particulate matter smaller than 10 microns in diameter
PM _{2.5}	particulate matter smaller than 2.5 microns in diameter
Po	total overburden pressure
Po'	effective overburden pressure
PPE	plant parameter envelope

**PSEG Site
ESP Application
Part 2, Site Safety Analysis Report**

**Table 1.1-1 Sheet (12 of 15)
Acronyms and Abbreviations Used in the SSAR**

Acronym/Abbreviation	Definition
ppm	parts per million
ppt	parts per thousand
PRM	Potomac-Raritan-Magothy
PS	paleoshoreline
PSAR	Preliminary Safety Analysis Report
PSEG	PSEG Power, LLC and PSEG Nuclear, LLC
psf	pounds per square foot
psi	pounds per square inch
PSWS	potable and sanitary water system
PWR	pressurized water reactor
QAPD	Quality Assurance Program Description
RAI	request for additional information
RCC	roller-compacted concrete
RCRA	Resource Conservation and Recovery Act
RCTS	resonant column torsional shear
rd	stress reduction factor due to depth
Reg. Tons	Registered Tonnage
RERR	Radioactive Effluent Release Report
RG	Regulatory Guide
RM	river mile
RMB	estimate of mb used in rate and b-value calculations
RSZ	Ramapo seismic zone
s	second

**PSEG Site
ESP Application
Part 2, Site Safety Analysis Report**

**Table 1.1-1 Sheet (13 of 15)
Acronyms and Abbreviations Used in the SSAR**

Acronym/Abbreviation	Definition
S	shear wave
S/HC	Salem and Hope Creek
SAGE	SAIC Adaptive Grid Eulerian
SARA	Superfund Amendments and Reauthorization Act
SB	subbasin
scf	standard cubic feet
SCR	stable continental region
SC-SM	sand
SCS	Soil Conservation Service
sec.	second
SEIS	Supplemental Environmental Impact Statement
SER	Safety Evaluation Report
SGS	Salem Generating Station
SL	stream lineament
SM	silty sands
SMF	submarine mass failure
SOD	Summary of the Day
SOG	Seismicity Owners Group
SPT	Standard Penetration Test
sq.	square
sq. mi.	square miles
SRP	Standard Review Plan
SRV	safety/relief valve

**PSEG Site
ESP Application
Part 2, Site Safety Analysis Report**

**Table 1.1-1 Sheet (14 of 15)
Acronyms and Abbreviations Used in the SSAR**

Acronym/Abbreviation	Definition
SSAR	site safety analysis report
SSC	structures, systems and components
SSE	safe shutdown earthquake
SSI	Soil Structure Interaction
STEL	Short Term Exposure Limit
SWAN	Simulating Waves Nearshore
SWL	still water level
SWS	service water system
T ₁₀₀	100 percent consolidation
TC	Tonal contrast lineament
TDS	total dissolved solids
TEDE	Total Effective Dose Equivalent
TIN	Triangular Irregular Network
TL	Topographic lineament
TNT	Trinitrotoluene
TOC	top of casing
tsf	tons per square foot
TSS	total suspended solids
TWA	Time Weighted Average
UEL	Upper Explosive Limit
UFSAR	Updated Final Safety Analysis Report
UHS	Ultimate Heat Sink
USACE	U.S. Army Corps of Engineers

**PSEG Site
ESP Application
Part 2, Site Safety Analysis Report**

**Table 1.1-1 Sheet (15 of 15)
Acronyms and Abbreviations Used in the SSAR**

Acronym/Abbreviation	Definition
US-APWR	U.S. Advanced Passive Pressurized-Water Reactor
USCB	U.S. Census Bureau
USCG	U.S. Coast Guard
USCS	Unified Soil Classification System
USGS	U.S. Geological Survey
USEPA	U.S. Environmental Protection Agency
U.S. EPR	U.S. Evolutionary Power Reactor
UU	unconsolidated-undrained
VCE	Vapor Cloud Explosion
VL	vegetation lineament
VT	Vincentown Formation
W	watt
WBAN	Weather Bureau Army Navy
WBT	wet bulb temperature
WOH	Weight-of-hammer
WSEL	water surface elevation
wt.	weight
WWTP	Waste Water Treatment Plant
Ybt	Yellow Breaches thrust fault
yr	year

**PSEG Site
ESP Application
Part 2, Site Safety Analysis Report**

1.2 GENERAL PLANT DESCRIPTION

1.2.1 SITE LOCATION

The existing 734 acre PSEG property is located on the southern part of Artificial Island on the east bank of the Delaware River in Lower Alloways Creek Township, Salem County New Jersey. PSEG is developing an agreement in principle with the U.S. Army Corps of Engineers (USACE) to acquire an additional 85 acres immediately to the north of Hope Creek Generating Station (HCGS). Therefore, with the land acquisition, the PSEG Site will be 819 acres. The specific timing of land acquisition is not currently known and is subject to further PSEG and USACE actions. However the agreement in principle with the USACE will serve to establish the basis for eventual land acquisition and Exclusion Area Boundary (EAB) control, necessary to support the issuance of a future COL.

Subsequent to the agreement in principle with the USACE, PSEG will develop a lease agreement for the USACE Confined Disposal Facility (CDF) land to the north of the PSEG Site, depicted on the Site Utilization Plan (Figure 1.2-3) for the concrete batch plant and temporary construction/laydown use. At the completion of construction, the leased land will be returned to the USACE, subject to any required long-term EAB control conditions.

The site is 15 miles south of the Delaware Memorial Bridge, 18 miles south of Wilmington, Delaware, 30 miles southwest of Philadelphia, Pennsylvania, and 7-1/2 miles southwest of Salem, New Jersey. The site location is shown on Figures 1.2-1 and 1.2-2, and is discussed in more detail in Section 2.1.

1.2.2 SITE DEVELOPMENT

The PSEG Site currently has three operating nuclear reactors. Salem Units 1 and 2 are Westinghouse Pressurized Water Reactors (PWR), rated at 3459 MWt each. Hope Creek Unit 1 is located north of the Salem Units. Hope Creek is a General Electric Boiling Water Reactor, rated at 3840 MWt. Hope Creek Unit 2 was originally planned and partially constructed directly adjacent to Unit 1. Surrounding the Salem and Hope Creek units are many support facilities, including circulating and service water intake structures, switchyards, administration buildings, and an independent spent fuel storage installation (ISFSI).

The location selected for the new plant on the PSEG Site is north of the Salem and Hope Creek units, and is shown on the Site Utilization Plan, Figure 1.2-3. Site layouts for each of the four reactor technology configurations considered for the PSEG Site were established. The primary power generation areas (power block area, switchyard, cooling tower area, etc.) are located in the same general area on the PSEG Site for each layout considered. Once the layouts were established, the bounding footprint for each specific area (e.g., power block area) was developed. This approach provides a bounding depiction of overall land usage on the PSEG Site. In addition to the land acquired from the USACE, as noted above, PSEG will also obtain the right to temporarily use approximately 45 additional acres of USACE property north of the current PSEG property boundary for temporary construction use.

No specific plant design has been chosen for the PSEG Site. Instead, a set of bounding plant parameters is presented to envelop future PSEG Site development. This PPE is based on the addition of power generation from either a single or dual unit light water reactor (LWR) plant.

**PSEG Site
ESP Application
Part 2, Site Safety Analysis Report**

PSEG used design parameter information from the following reactor designs in development of the PPE.

- Single Unit U.S. Evolutionary Power Reactor (U.S. EPR)
- Single Unit Advanced Boiling Water Reactor (ABWR)
- Single Unit U.S. Advanced Pressurized-Water Reactor (US-APWR)
- Dual Unit Advanced Passive 1000 (AP1000)

The new plant on the PSEG Site may be any of the reactor designs identified or a different design that falls within the range of the information developed to characterize the new plant. The bounding new plant consists of a reactor design with a maximum thermal power that does not exceed 4614 MWt for a single unit or 6830 MWt for a dual unit. The new plant on the PSEG Site is capable of producing up to approximately 2200 MWe net of electrical power.

**PSEG Site
ESP Application
Part 2, Site Safety Analysis Report**

1.3 PLANT PARAMETER ENVELOPE

The required contents of an ESPA are specified in 10 CFR 52.17. As detailed in 10 CFR 52.17(a)(1), the SSAR portion of the application is required to specify, among other things:

- The number, type, and thermal power level of the facilities
- Boundaries of the site and proposed general location of each facility
- Type of cooling systems, intakes, and outflows
- Anticipated maximum levels of radiological and thermal effluents
- Site seismic, meteorological, hydrologic, and geologic characteristics
- Existing and projected future population profile of the area surrounding the site

The PSEG approach to providing this information is presented in the following subsections.

1.3.1 PLANT PARAMETER ENVELOPE APPROACH

A list of plant parameters necessary to define the plant-site interface was developed in the early 1990s based on work sponsored by the U.S. Department of Energy (DOE) and the nuclear industry, which included reactor vendors and utilities. The effort was intended to provide a comprehensive list of plant parameters to accurately characterize a plant at a site. The original list was reduced to identify information needed to support development of an ESPA, including the SSAR and the Environmental Report (ER).

The PPE is a set of postulated parameters that bound the parameters of a reactor or reactors that might be deployed at a site. This includes site parameters specified by the reactor vendor which must be met by the selected site.

- In terms of safety reviews, design characteristics of potential plant designs are no more demanding from a site suitability perspective than the bounding design parameters in the PPE.
- In terms of environmental reviews, impacts of the selected design are not significantly greater than impacts evaluated in the ESPA using the bounding design parameters in the PPE.

For the purposes of preparing ESPAs, the PPE serves as a surrogate for actual facility information. For example, values for maximum building height, acreage for plant facilities, ponds, etc., and cooling water requirements, are among the design parameters specified in the PPE.

PPE parameters, along with information established by features of the site itself (i.e., "site characteristics"), support the 10 CFR Part 52.17 analyses required to demonstrate site suitability. These analyses are provided in this SSAR and in the environmental impact assessments reported in the ER included with this application.

Prior to the submittal of the first three ESPAs, the PPE concept was discussed in several public meetings involving the NRC and nuclear industry representatives as part of the resolution of Generic Topic ESP-6 (*Use of Plant Parameters Envelope Approach for ESP*) and was the subject of associated correspondence between the NRC and the Nuclear Energy Institute (NEI).

**PSEG Site
ESP Application
Part 2, Site Safety Analysis Report**

Agreement on the PPE concept was attained and the SRP updated in 2007 to incorporate the concept.

In developing and refining the PPE concept, the industry and the NRC worked to establish a number of definitions for key terms to facilitate discussion and understanding of the PPE approach. These definitions are incorporated into the NRC regulations (10 CFR 52) and are provided below:

- **Site characteristics** are the actual physical, environmental and demographic features of a site. Site characteristics are specified in an early site permit or in a Final Safety Analysis Report for a combined license.
- **Site parameters** are the postulated physical, environmental and demographic features of an assumed site. Site parameters are specified in a standard design approval, standard design certification, or manufacturing license.
- **Design characteristics** are the actual features of a reactor or reactors. Design characteristics are specified in a standard design approval, a standard design certification, a combined license application, or a manufacturing license.
- **Design parameters** are the postulated features of a reactor or reactors that could be built at a proposed site. Design parameters are specified in an early site permit.

In a COL application, the site-specific engineering and design features of the selected reactor design are compared with the ESP basis to demonstrate they are bounded.

1.3.2 PPE DEVELOPMENT PROCESS

The PPE developed for the PSEG ESPA was prepared by reviewing the information developed by the industry prior to the submittal of the Grand Gulf, Clinton and North Anna ESPAs, reviewing the correspondence between the NRC and industry on the PPE subject, and reviewing safety evaluation reports (SER), environmental impact statements (EIS) and requests for additional information (RAIs) associated with the first three ESPA. Based upon these document reviews, the PSEG PPE includes only those parameters needed to support the issuance of an ESP.

The PPE tables are based on information supplied by the reactor vendors for the plant designs listed previously. Site-dependent PPE data was either based on a typical site as provided by the vendors (not a specific site and not the PSEG Site) or was modified to take into account site specific conditions, as appropriate. An example of adapting the vendor provided data to site specific conditions is in the design of the circulating water system, which is based on site-specific water supplies and meteorological conditions. The listed circulating water designs, which include mechanical, fan-assisted natural draft and natural draft towers, are based on a bounding plant design and location, and would be modified to meet the selected reactor design and site characteristics during preparation of a COL application.

The design parameter data included in the PPE was developed considering the values provided by various reactor vendors to characterize the surrogate facility. As applicable, the most limiting (maximum or minimum) bounding value is selected. The complete set of plant parameter values characterizes a new plant at the PSEG Site. This type of facility characterization is considered sufficient to assess the future use of the site for a nuclear electric generating facility from both a safety and environmental perspective.

Rev.4

**PSEG Site
ESP Application
Part 2, Site Safety Analysis Report**

1.3.3 PSEG SITE PLANT PARAMETER ENVELOPE

Tables 1.3-1 through 1.3-8 present the listing of the PPE values used in assessing the safety and environmental impact of constructing and operating the new plant on the PSEG Site. The numbering of the PPE listing is not meant to be sequential, and was compiled from and is consistent with the list developed by the industry and refined for the PSEG Site ESPA. Table 1.3-1 also provides a description or definition for the plant parameters used in evaluating the safety and/or environmental impact of locating the new plant at the PSEG Site.

**PSEG Site
ESP Application
Part 2, Site Safety Analysis Report**

**Table 1.3-1 (Sheet 1 of 14)
Plant Parameter Envelope**

PPE Item	Design Parameter	Definition
1	Structure	
1.1	Building Characteristics	
1.1.1	Height	234 ft. The height from finished grade to the top of the tallest power block structure, excluding cooling towers.
1.1.2	Foundation Embedment	39 ft. to 84.3 ft. The depth from finished grade to the bottom of the basemat for the most deeply embedded power block structure.
2	Normal Plant Heat Sink	
2.3	Condenser	
2.3.1	Max Inlet Temp Condenser	91° F Design assumption for the maximum acceptable circulating water temperature at the inlet to the condenser.
2.3.2	Condenser Heat Rejection	1.508E+10 Btu/hr Design value for the waste heat rejected to the circulating water system across the condensers.
2.3.3	Maximum Cooling Water Flow Rate Across Condenser	1,200,000 gpm Design value for the maximum flow rate of the circulating water system through the condenser tubes.
2.3.4	Maximum Cooling Water Temperature Rise Across Condenser	25.2° F Design value for the maximum temperature differential across the condenser.
2.4	Mechanical Draft Cooling Towers - Circulating Water System	
2.4.1	Acreage	50 ac. The land required for cooling towers, including support facilities.
2.4.2	Approach Temperature	14.4° F The difference between the cold water temperature and the ambient wet bulb temperature.
2.4.3	Blowdown Constituents and Concentrations	Table 1.3-2 The maximum expected concentrations for anticipated constituents in the circulating water system blowdown to the receiving water body.

**PSEG Site
ESP Application
Part 2, Site Safety Analysis Report**

**Table 1.3-1 (Sheet 2 of 14)
Plant Parameter Envelope**

PPE Item	Design Parameter	Definition
2.4.4	Blowdown Flow Rate (Normal)	50,516 gpm
		The normal flow rate of the blowdown stream from the circulating water system to the receiving water body for closed system designs during normal operations.
2.4.5	Blowdown Temperature (Normal)	91° F
		The maximum expected blowdown temperature at the point of discharge to the receiving water body during normal operations.
2.4.6	Cycles of Concentration	1.5
		The ratio of total dissolved solids in the circulating water system blowdown to the total dissolved solids in the make-up water.
2.4.7	Evaporation Rate (Normal)	25,264 gpm
		The expected 1 percent exceedance design rate at which water is lost by evaporation from the circulating water system during normal operations.
2.4.9	Makeup Flow Rate (Normal)	75,792 gpm
		The expected rate of removal of water from a natural source to replace water losses from a closed circulating water system during normal operations.
2.4.10	Noise	58 dBA at 1000 ft.
		The maximum expected sound level produced by operation of cooling towers, measured in feet from the noise source.
2.4.11	Cooling Tower Temperature Range (Normal)	25.2° F
		The temperature difference between the cooling water entering and leaving the towers during normal operations.
2.4.12	Cooling Water Flow Rate (Normal)	1,200,000 gpm
		The total cooling water flow rate through the condenser/heat exchangers during normal operations.
2.4.13	Heat Rejection Rate (Normal)	1.508E+10 Btu/hr
		The expected heat rejection rate to a receiving water body during normal operations.
2.4.17	Drift	12 gpm
		Rate of water lost from the tower as liquid droplets entrained in the vapor exhaust air stream.
2.4.18	Exhaust Stack exit velocity	1730 fpm
		The exit velocity of water vapor through the cooling tower exhaust stack.

**PSEG Site
ESP Application
Part 2, Site Safety Analysis Report**

**Table 1.3-1 (Sheet 3 of 14)
Plant Parameter Envelope**

PPE Item	Design Parameter	Definition
2.4.19 Exhaust Stack exit diameter	68 cells at 31.6 ft. each	The diameter of the cooling tower exhaust stack.
2.4.20 Exhaust Stack Height	46 ft.	The vertical height above finished grade of cooling towers associated with the circulating water system.
2.5 Natural Draft Cooling Towers - Circulating Water System		
2.5.1 Acreage	50 ac.	The land required for cooling towers, including support facilities.
2.5.2 Approach Temperature	14.4° F	The difference between the cold water temperature and the ambient wet bulb temperature.
2.5.3 Blowdown Constituents and Concentrations	Table 1.3-2	The maximum expected concentrations for anticipated constituents in the circulating water system blowdown to the receiving water body.
2.5.4 Blowdown Flow Rate (Normal)	50,516 gpm	The normal flow rate of the blowdown stream from the circulating water system to the receiving water body for closed system designs during normal operations.
2.5.5 Blowdown Temperature (Normal)	91° F	The maximum expected blowdown temperature at the point of discharge to the receiving water body during normal operations.
2.5.6 Cycles of Concentration	1.5	The ratio of total dissolved solids in the circulating water system blowdown to the total dissolved solids in the make-up water.
2.5.7 Evaporation Rate (Normal)	25,264 gpm	The expected 1 percent exceedance design rate at which water is lost by evaporation from the circulating water system during normal operations.
2.5.9 Makeup Flow Rate (Normal)	75,792 gpm	The expected rate of removal of water from a natural source to replace water losses from a closed circulating water system during normal operations.
2.5.10 Noise	50 dBA at 1000 ft.	The maximum expected sound level produced by operation of cooling towers, measured in feet from the noise source.

**PSEG Site
ESP Application
Part 2, Site Safety Analysis Report**

**Table 1.3-1 (Sheet 4 of 14)
Plant Parameter Envelope**

PPE Item	Design Parameter	Definition
2.5.11	Cooling Tower Temperature Range (Normal)	25.2° F The temperature difference between the cooling water entering and leaving the towers during normal operations.
2.5.12	Cooling Water Flow Rate (Normal)	1,200,000 gpm The total cooling water flow rate through the condenser/heat exchangers during normal operations.
2.5.13	Heat Rejection Rate (Normal)	1.508E+10 Btu/hr The expected heat rejection rate to a receiving water body during normal operations.
2.5.17	Drift	12 gpm Rate of water lost from the tower as liquid droplets entrained in the vapor exhaust air stream.
2.5.18	Exhaust Stack exit velocity	995 fpm The exit velocity of water vapor through the cooling tower exhaust stack.
2.5.19	Exhaust Stack exit diameter	242 ft. The diameter of the cooling tower exhaust stack.
2.5.20	Exhaust Stack Height	590 ft. The vertical height above finished grade of cooling towers associated with the circulating water system.
2.6	Fan Assisted Natural Draft Cooling Towers - Circulating Water System	
2.6.1	Acreage	50 ac. The land required for cooling towers, including support facilities.
2.6.2	Approach Temperature	14.4° F The difference between the cold water temperature and the ambient wet bulb temperature.
2.6.3	Blowdown Constituents and Concentrations	Table 1.3-2 The maximum expected concentrations for anticipated constituents in the circulating water system blowdown to the receiving water body.
2.6.4	Blowdown Flow Rate (Normal)	50,516 gpm The normal flow rate of the blowdown stream from the circulating water system to the receiving water body for closed system designs during normal operations.

**PSEG Site
ESP Application
Part 2, Site Safety Analysis Report**

**Table 1.3-1 (Sheet 5 of 14)
Plant Parameter Envelope**

PPE Item		Design Parameter	Definition
2.6.5	Blowdown Temperature (Normal)	91° F	The maximum expected blowdown temperature at the point of discharge to the receiving water body during normal operations.
2.6.6	Cycles of Concentration	1.5	The ratio of total dissolved solids in the circulating water system blowdown to the total dissolved solids in the make-up water.
2.6.7	Evaporation Rate (Normal)	25,264 gpm	The expected 1 percent exceedance design rate at which water is lost by evaporation from the circulating water system during normal operations.
2.6.9	Makeup Flow Rate (Normal)	75,792 gpm	The expected rate of removal of water from a natural source to replace water losses from a closed circulating water system during normal operations.
2.6.10	Noise	60 dBA at 1000 ft.	The maximum expected sound level produced by operation of cooling towers, measured in feet from the noise source.
2.6.11	Cooling Tower Temperature Range (Normal)	25.2° F	The temperature difference between the cooling water entering and leaving the towers during normal operations.
2.6.12	Cooling Water Flow Rate (Normal)	1,200,000 gpm	The total cooling water flow rate through the condenser/heat exchangers during normal operations.
2.6.13	Heat Rejection Rate (Normal)	1.508E+10 Btu/hr	The expected heat rejection rate to a receiving water body during normal operations.
2.6.17	Drift	12 gpm	Rate of water lost from the tower as liquid droplets entrained in the vapor exhaust air stream.
2.6.18	Exhaust Stack exit velocity	902 fpm	The exit velocity of water vapor through the cooling tower exhaust stack.
2.6.19	Exhaust Stack exit diameter	255 ft.	The diameter of the cooling tower exhaust stack.
2.6.20	Exhaust Stack Height	224 ft.	The vertical height above finished grade of cooling towers associated with the circulating water system.

**PSEG Site
ESP Application
Part 2, Site Safety Analysis Report**

**Table 1.3-1 (Sheet 6 of 14)
Plant Parameter Envelope**

PPE Item	Design Parameter	Definition
3	Ultimate Heat Sink (UHS)	
3.2	Heat Exchangers	
3.2.1	Maximum Inlet Temperature to CCW Heat Exchanger	95° F The maximum temperature of safety-related service water at the inlet of the UHS component cooling water heat exchanger.
3.2.2	CCW Heat Exchanger Duty	2.06E+8 Btu/hr (Normal) 4.72E+8 Btu/hr (Peak) The heat transferred to the safety-related service water system for rejection to the environment in UHS heat removal devices.
3.3	UHS Cooling Towers	
3.3.3	Blowdown Constituents and Concentrations	Table 1.3-2 The maximum expected concentrations for anticipated constituents in the UHS blowdown to the receiving water body.
3.3.4a	Blowdown Flow Rate (Normal)	1140 gpm The maximum flow rate of the blowdown stream from the UHS system to receiving water body for closed system designs during normal operations.
3.3.4b	Blowdown Flow Rate (Accident)	2280 gpm The maximum flow rate of the blowdown stream from the UHS system to receiving water body for closed system designs during accident conditions.
3.3.5a	Blowdown Temperature (Normal)	< 95° F The maximum expected UHS blowdown temperature at the point of discharge to the receiving water body during normal operations.
3.3.5b	Blowdown Temperature (Accident)	95° F The maximum expected UHS blowdown temperature at the point of discharge to the receiving water body during accident conditions.
3.3.6	Cycles of Concentration	2 The ratio of total dissolved solids in the UHS system blowdown streams to the total dissolved solids in the make-up water streams.
3.3.7a	Evaporation Rate (Normal)	1142 gpm The maximum rate at which water is lost by evaporation from the UHS system during normal operations.
3.3.7b	Evaporation Rate (Accident)	2284 gpm The maximum rate at which water is lost by evaporation from the UHS system during accident conditions.

**PSEG Site
ESP Application
Part 2, Site Safety Analysis Report**

**Table 1.3-1 (Sheet 7 of 14)
Plant Parameter Envelope**

PPE Item		Design Parameter	Definition
3.3.8a	Cooling Tower Deck Height	63 ft.	The height of the cooling tower deck above grade.
3.3.8b	Exhaust Stack Height	35 ft.	The height of the exhaust stacks above the deck.
3.3.9a	Makeup Flow Rate (Normal)	2404 gpm	The maximum rate of removal of water from a natural source to replace water losses from the UHS system during normal operations.
3.3.9b	Makeup Flow Rate (Accident)	4808 gpm	The maximum rate of removal of water from a natural source to replace water losses from the UHS system during accident conditions.
3.3.10	Noise	57 dBA at 200 ft.	The maximum expected sound level produced by operation of mechanical draft UHS cooling towers, measured in feet from the noise source.
3.3.12	Cooling Water Flow Rate	26,125 gpm (normal) 52,250 gpm (shutdown/accident)	The total cooling water flow rate through the UHS system.
3.3.13a	Heat Rejection Rate (Normal)	2.06E+8 Btu/hr	The maximum expected heat rejection rate to the atmosphere during normal operations.
3.3.13b	Heat Rejection Rate (Accident)	3.95E+8 Btu/hr	The maximum expected heat rejection rate to the atmosphere during accident conditions.
3.3.16	Stored Water Volume	30,600,000 gal.	The quantity of water stored in UHS impoundments.
3.3.17	Drift	2 gpm	Rate of water lost from the tower as liquid droplets entrained in the vapor exhaust air stream.

**PSEG Site
ESP Application
Part 2, Site Safety Analysis Report**

**Table 1.3-1 (Sheet 8 of 14)
Plant Parameter Envelope**

PPE Item	Design Parameter	Definition
5 Potable/Sanitary Water System		
5.1 Discharge to Site Water Bodies		
5.1.1	Flow Rate (Normal) 93 gpm	The expected effluent flow rate from the potable and sanitary water systems to the receiving water body.
5.1.2	Flow Rate (Maximum) 93 gpm	The maximum effluent flow rate from the potable and sanitary water systems to the receiving water body.
5.2 Raw Water Requirements		
5.2.1	Maximum Use 216 gpm	The maximum short-term rate of withdrawal from the water source for the potable and sanitary waste water systems.
5.2.2	Monthly Average Use 93 gpm	The average rate of withdrawal from the water source for the potable and sanitary waste water systems.
6 Demineralized Water System		
6.1 Discharge to Site Water Bodies		
6.1.1	Flow Rate 27 gpm	The expected (and maximum) effluent flow rate from the demineralized system to the receiving water body.
6.2 Raw Water Requirements		
6.2.1	Maximum Use 107 gpm	The maximum short-term rate of withdrawal from the water source for the demineralized water system.
6.2.2	Monthly Average Use 107 gpm	The average rate of withdrawal from the water source for the demineralized water system.

**PSEG Site
ESP Application
Part 2, Site Safety Analysis Report**

**Table 1.3-1 (Sheet 9 of 14)
Plant Parameter Envelope**

PPE Item	Design Parameter	Definition
7	Fire Protection System	
7.1	Raw Water Requirements	
7.1.1	Maximum Use	625 gpm The maximum short-term rate of withdrawal from the water source for the fire protection water system.
7.1.2	Monthly Average Use	5 gpm The average rate of withdrawal from the water source for the fire protection water system.
8	Miscellaneous Drain	
8.1	Discharge to Site Water Bodies	
8.1.1	Flow Rate (Expected)	39 gpm The expected effluent flow rate from miscellaneous drains to the receiving water body.
8.1.2	Flow Rate (Maximum)	55 gpm The maximum effluent flow rate from miscellaneous drains to the receiving water body.
8.2	Raw Water Requirements	
8.2.1	Maximum Use	5 gpm The maximum short-term rate of withdrawal from the water source for miscellaneous activities, such as floor washing.
8.2.2	Monthly Average Use	5 gpm The average rate of withdrawal from the water source for miscellaneous activities, such as floor washing.
9	Unit Vent/Airborne Effluent Release Point	
9.4	Release Point	
9.4.2	Elevation (Normal)	Ground Level The elevation above finished grade of the release point for routine operational releases.
9.4.3	Elevation (Post Accident)	Ground Level The elevation above finished grade of the release point for accident sequence releases.

**PSEG Site
ESP Application
Part 2, Site Safety Analysis Report**

**Table 1.3-1 (Sheet 10 of 14)
Plant Parameter Envelope**

PPE Item	Design Parameter	Definition
9.5 Source Term		
9.5.1 Gaseous (Normal)	Table 1.3-7	The expected annual activity, by isotope, contained in routine plant airborne effluent streams.
9.5.2 Gaseous (Post-Accident)	See Section 15.3	The activity, by isotope, contained in post-accident airborne effluents.
9.5.3 Tritium	Table 1.3-7	The expected annual activity of tritium contained in routine plant airborne effluent streams.
10 Liquid Radwaste System		
10.2 Release Point		
10.2.1 Flow Rate	11 gpm	The discharge flow rate of potentially radioactive liquid effluent streams from plant systems to the receiving waterbody.
10.2.2 Minimum Blowdown Rate	20,000 gpm	Minimum flow rate of the effluent stream discharging potentially radioactive liquid effluent to the receiving water body during normal operations.
10.3 Source Term		
10.3.1 Liquid	Table 1.3-8	The annual activity, by isotope, contained in routine plant liquid effluent streams.
10.3.2 Tritium	Table 1.3-8	The annual activity of tritium contained in routine plant liquid effluent streams.
11 Solid Radwaste System		
11.2 Solid Radwaste		
11.2.1 Activity	Table 1.3-3	The annual activity, by isotope, contained in solid radioactive wastes generated during routine plant operations.
11.2.2 Principal Radionuclides	Table 1.3-3	The principal radionuclides contained in solid radioactive wastes generated during routine plant operations.

**PSEG Site
ESP Application
Part 2, Site Safety Analysis Report**

**Table 1.3-1 (Sheet 11 of 14)
Plant Parameter Envelope**

PPE Item	Design Parameter	Definition
11.2.3 Volume	16,721.5 ft ³ /yr	The expected volume of solid radioactive wastes generated during routine plant operations.
13 Auxiliary Boiler System		
13.1 Exhaust Elevation	150 ft.	The height above finished plant grade at which the flue gas effluents are released to the environment.
13.2 Flue Gas Effluents	Table 1.3-4	The expected combustion products and anticipated quantities released to the environment due to operation of the auxiliary boilers.
13.3 Fuel Type	No. 2 Fuel Oil	The type of fuel required for proper operation of the auxiliary boilers.
13.4 Heat Input Rate (Btu/hr)	1.56E+8 Btu/hr	The average heat input rate (fuel consumption rate).
15 Onsite/Offsite Electrical Power System		
15.1 Acreage		
15.1.1 Switchyard	63 ac.	The land usage required for the high voltage switchyard used to connect the plant to the transmission grid.
16 Standby Power System		
16.1 Diesel		
16.1.1 Diesel Capacity (kW)	10,130 kW/unit (EDG) 5000 kW/unit (SBO)	The total generating capacity of the diesel generating system.
16.1.2 Diesel Exhaust Elevation	50 ft.	The elevation above finished grade of the release point for standby diesel exhaust releases.
16.1.3 Diesel Flue Gas Effluents	Table 1.3-5	The expected combustion products and anticipated quantities released to the environment due to operation of the emergency standby diesel generators.
16.1.4 Diesel Noise	55 dBA at 1000 ft.	The maximum expected sound level produced by operation of diesel generators, measured in feet from the noise source.

**PSEG Site
ESP Application
Part 2, Site Safety Analysis Report**

**Table 1.3-1 (Sheet 12 of 14)
Plant Parameter Envelope**

PPE Item	Design Parameter	Definition
16.1.5 Diesel Fuel Type	No. 2	The type of diesel fuel required for proper operation of the diesel generator.
16.1.6 Exhaust Stack Diameter	68 in.	The nominal diameter of the exhaust stack.
16.1.7 Flue Gas Flow Rate	68,960 acfm	The maximum flue gas flow rate exiting the exhaust stack.
16.1.8 Flue Gas Temperature	665 °F	The temperature of the flue gas exiting the exhaust stack.
16.1.10 Number of Units	EDG - 4 SBO - 2	The number of generator units.
16.1.11 Diesel Usage	150 hr/yr/unit (EDG) 100 hr/yr/unit (SBO)	The expected duration of usage for each diesel.
16.1.12 Heat Input Rate (Btu/hr)	77,384,160 Btu/hr	The average heat input rate (fuel consumption rate).
16.2 Gas-Turbine		
16.2.1 Gas-Turbine Capacity (kW)	26,000 kW	The total generating capacity of the gas turbine generating system.
16.2.2 Gas-Turbine Exhaust Elevation	50 ft.	The elevation above finished grade of the release point for standby gas-turbine exhaust releases.
16.2.3 Gas-Turbine Flue Gas Effluents	Table 1.3-6	The expected combustion products and anticipated quantities released to the environment due to operation of the standby gas-turbine generators
16.2.4 Gas-Turbine Noise	64.3 dBA at 1000 ft.	The maximum expected sound level produced by operation of gas-turbines, measured in feet from the noise source.
16.2.5 Gas-Turbine Fuel Type	Diesel Oil	The type of fuel required for proper operation of the gas-turbines.
16.2.6 Exhaust Stack Diameter	59.1 in.	The nominal diameter of the exhaust stack.
16.2.7 Flue Gas Flow Rate	128,899 acfm	The maximum flue gas flow rate exiting the exhaust stack.
16.2.8 Flue Gas Temperature	940 °F	The temperature of the flue gas exiting the exhaust stack.
16.2.10 Number of Units	4/2	The number of generator units (Class 1E / Non-Class 1E)

**PSEG Site
ESP Application
Part 2, Site Safety Analysis Report**

**Table 1.3-1 (Sheet 13 of 14)
Plant Parameter Envelope**

PPE Item	Design Parameter	Definition
16.2.11 Gas-Turbine Usage	48 hr/yr	The expected duration of usage for each gas-turbine.
16.2.12 Heat Input Rate (Btu/hr)	71,513,906 Btu/hr	The average heat input rate (fuel consumption rate).
17 Plant Characteristics		
17.2 Permanent Acreage		
17.2.2 Parking Lots	8 ac.	The land area required to provide space for parking lots.
17.2.3 Permanent Support Facilities	8 ac.	The land area required to provide space for permanent support facilities.
17.2.4 Power Block	70 ac.	The land area required to provide space for Power Block facilities. Power Block is defined as all structures, systems and components which perform a direct function in the production of, transport of, or storage of heat energy, electrical energy or radioactive wastes. Also included are structures, systems, and components that monitor, control, protect or otherwise support the above equipment.
17.2.6 Other Areas	26.4 ac.	The land area required to provide space for plant facilities not provided in Parameters 17.2.2 - 17.2.4.
17.3 Megawatts Thermal	4614 MWt (single unit) 6830 MWt (dual unit)	The thermal power generated by the nuclear steam supply system.
17.4 Plant Design Life	60 years	The operational life for which the plant is designed.
17.5 Plant Population		
17.5.1 Operation	600 people	The number of people required to operate the plant.
17.5.2 Refueling/Major Maintenance	1000 people	The additional number of temporary staff required to conduct refueling and major maintenance activities.
17.6 Station Capacity Factor	85 to 96.3 percent	The percentage of time that a plant is capable of providing power to the grid. Values within this range are conservatively applied as necessary in the ER analyses.

**PSEG Site
ESP Application
Part 2, Site Safety Analysis Report**

**Table 1.3-1 (Sheet 14 of 14)
Plant Parameter Envelope**

PPE Item	Design Parameter	Definition
17.7	Plant Operating Cycle	18 or 24 months The normal plant operating cycle length.
17.8	Megawatts Electric (net)	1350 to 1600 MWe (single unit) 2200 MWE (dual unit) The nominal electrical output from the plant to the electrical grid. This value does not include the plant's house loads.
18	Construction	
18.2	Acreage	
18.2.1	Laydown Area	128 ac. The land area required to provide space for construction support facilities.
18.2.2	Temporary Construction Facilities	77 ac.
18.3	Construction	
18.3.1	Noise	102 dBA at 50 ft. The maximum expected sound level due to construction activities, measured in feet from the noise source.
18.4	Plant Population	
18.4.1	Construction	3950 to 4100 people Number of workers on-site for construction of the new plant.
19	Miscellaneous Parameters	
19.7	Maximum Fuel Enrichment	5 percent wt. Concentration of U-235 in the fuel.
19.8	Maximum Average Assembly Burnup	54,200 MWD/MTU Maximum assembly average burnup at end of assembly life.
19.9	Peak Fuel Rod Burnup	62,000 MWD/MTU Peak fuel rod exposure at end of life.
19.11	Rated Thermal Power	4590 MWt (single unit) 6800 MWt (dual unit) Maximum core thermal power.
19.12	Liquid-Containing Tank Failure Radionuclide Concentrations	See Table 1.3-9 The concentrations of radionuclides and associated tank volumes for the analysis of liquid-containing tank failure.

**PSEG Site
ESP Application
Part 2, Site Safety Analysis Report**

**Table 1.3-2
Blowdown Constituents and Concentrations**

Constituents		CWS Blowdown	SWS/UHS Blowdown	SWS Water Treatment Discharge	Sanitary System Discharge	Other Plant Discharge^(a)	Combined Discharge^(b)
pH		7.6	7.5	7.1	8.1	8.1	7.6
Alkalinity	mg/l as CaCO ₃	70	64	47.1	283	293	71
Suspended Solids	mg/l	180	30	30	30	30	176
TDS	mg/l	9860	13,150	6280	624	545	9894
Total Hardness	mg/l as CaCO ₃	2020	2700	1330	134	120	2027
Calcium	mg/l	146	195	96	29	27	147
Magnesium	mg/l	403	537	264	15	12	404
Sodium	mg/l	3020	4030	1980	120	99	3030
Chloride	mg/l	5490	7330	3725	52	26	5508
Sulfate	mg/l	748	1020	507	33	16	751
Bicarbonate	mg/l	83	77	56.4	310	357	84
Ammonia	mg/l	0.5	0.6	0.313	25		0.5
ortho- Phosphate	mg/l	0.5	0.7	0.35	5		0.5
Silica	mg/l as SiO ₂	1.0	1.3	0.67	12	10	1.0
BOD ₅	mg/l				30		
Cycles of concentration		1.5	2				
H ₂ SO ₄ added	mg/l	0	14				
Max TDS		17,800	23,750				

a) Other plant discharges include demineralizer wastes and other plant drains.

b) Combined discharge is the mass-balanced combination of the five primary flow paths.

**PSEG Site
ESP Application
Part 2, Site Safety Analysis Report**

**Table 1.3-3 (Sheet 1 of 2)
Single Unit Principal Radionuclides in Solid Radwaste**

Radionuclide	ABWR Quantity (Ci/yr)	AP1000 Quantity (Ci/yr)	U.S. EPR Quantity (Ci/yr)	US-APWR Quantity (Ci/yr)	Bounding Value Quantity (Ci/yr)
H-3		1.61E+00	8.52E-02		1.61E+00
C-14		2.85E-01	2.70E-01		2.85E-01
Na-24				6.50E+01	6.50E+01
Cr-51	5.24E+03	2.92E-01	1.75E+00	2.73E+02	5.24E+03
Mn-54	7.51E+01	2.24E+01	3.60E+02	1.69E+03	1.69E+03
Fe-55	5.64E+02	3.11E+02	4.73E+02	2.60E+03	2.60E+03
Mn-56				3.64E+01	3.64E+01
Co-58	1.96E+02	6.23E+01	1.14E+02	1.14E+03	1.14E+03
Fe-59	2.87E+01		1.09E+00	5.20E+01	5.20E+01
Co-60	4.34E+02	2.87E+02	2.36E+02	1.04E+03	1.04E+03
Ni-63	1.09E+03	3.16E+02	4.46E+00		1.09E+03
Zn-65			9.34E+01	4.16E+02	4.16E+02
Br-82				3.38E+01	3.38E+01
Br-83				2.08E+01	2.08E+01
Br-84				2.47E+00	2.47E+00
Rb-86				2.21E+02	2.21E+02
Rb-88				8.19E+01	8.19E+01
Rb-89				1.56E+00	1.56E+00
Sr-89				2.60E+02	2.60E+02
Sr-90			2.63E+00	1.56E+02	1.56E+02
Y-90			2.55E+00	1.56E+02	1.56E+02
Sr-91				1.30E+00	1.30E+00
Y-91				4.81E+01	4.81E+01
Y-91m				8.19E-01	8.19E-01
Sr-92				2.08E-01	2.08E-01
Y-92				4.29E-01	4.29E-01
Y-93				2.73E-01	2.73E-01
Nb-95	7.73E+00	3.23E-01	7.59E+00	9.49E+01	9.49E+01
Zr-95	7.73E+00	7.16E-02	3.66E+00	6.24E+01	6.24E+01
Mo-99				3.25E+03	3.25E+03
Tc-99m				2.99E+03	2.99E+03
Mo-101				5.33E-01	5.33E-01
Rh-103m			1.12E+01		1.12E+01
Ru-103			1.25E+01	3.12E+01	3.12E+01
Ru-106			2.08E+01	7.80E+01	7.80E+01

Rev.4

**PSEG Site
ESP Application
Part 2, Site Safety Analysis Report**

**Table 1.3-3 (Sheet 2 of 2)
Single Unit Principal Radionuclides in Solid Radwaste**

Radionuclide	ABWR Quantity (Ci/yr)	AP1000 Quantity (Ci/yr)	U.S. EPR Quantity (Ci/yr)	US-APWR Quantity (Ci/yr)	Bounding Value Quantity (Ci/yr)
Ag-110m	1.06E+00	4.60E-02	1.11E+02	5.59E-01	1.11E+02
Te-125m				6.63E+01	6.63E+01
Te-127m				4.94E+02	4.94E+02
Te-129				9.49E-01	9.49E-01
Te-129m				5.20E+02	5.20E+02
I-130				8.06E+04	8.06E+04
I-131				3.38E+04	3.38E+04
Te-131				3.90E-01	3.90E-01
Te-131m				5.20E+01	5.20E+01
Cs-132				5.59E+02	5.59E+02
I-132				1.69E+03	1.69E+03
Te-132				1.43E+03	1.43E+03
I-133				6.37E+03	6.37E+03
Te-133m				1.69E+00	1.69E+00
Cs-134			1.83E+02	4.16E+05	4.16E+05
I-134				5.98E+01	5.98E+01
Te-134				2.21E+00	2.21E+00
Cs-135m				4.94E-01	4.94E-01
I-135				1.30E+03	1.30E+03
Cs-136				4.16E+03	4.16E+03
Ba-137m				2.99E+05	2.99E+05
Cs-137			3.48E+02	3.12E+05	3.12E+05
Cs-138				3.25E+01	3.25E+01
Ba-140	2.62E+02	8.73E-02	1.92E-01	7.80E+01	2.62E+02
La-140	2.62E+02	4.01E-02	1.92E-01	7.93E+01	2.62E+02
Ce-141				3.12E+01	3.12E+01
Ce-143				1.09E+00	1.09E+00
Ce-144			7.74E-01	1.69E+02	1.69E+02
Pr-144				1.69E+02	1.69E+02
Pm-147				3.12E+01	3.12E+01
Eu-154				3.51E+00	3.51E+00
Np-239	1.50E+03				1.50E+03
Pu-241		1.14E-01	3.39E-01		3.39E-01
Total w/o H-3	9.67E+03	1.00E+03	1.99E+03	1.17E+06	1.18E+06
Total w/ H-3	9.67E+03	1.00E+03	1.99E+03	1.17E+06	1.18E+06

**PSEG Site
ESP Application
Part 2, Site Safety Analysis Report**

**Table 1.3-4
Emissions from Auxiliary Boilers**

Pollutant Discharged	(lbs)^(a)
Particulates (PM ₁₀)	34,500
Sulfur Oxides	115,000
Carbon Monoxide	1749
Volatile Organic Compounds ^(b)	100,200
Nitrogen Oxides	19,022

a) Emissions based on 30 days continuous operation per boiler.

b) As total hydrocarbons

**PSEG Site
ESP Application
Part 2, Site Safety Analysis Report**

**Table 1.3-5
Emissions from Standby Diesel Generators**

Pollutant Discharged	Diesel Generators (lb/yr)^(a)
Particulates (PM ₁₀)	1620
Sulfur Oxides	5010
Carbon Monoxide	4600
Volatile Organic Compounds ^(b)	3070
Nitrogen Oxides	28,968

a) Emissions based on 4 hr/month operation
for all of the generators.

b) As total hydrocarbons

**PSEG Site
ESP Application
Part 2, Site Safety Analysis Report**

**Table 1.3-6
Standby Power System Gas Turbine Flue Gas Effluents**

Pollutant	Emission Factor^{(a)(b)} (lb/MMBtu)	Emission Rate (per GTG) ^(f) (Normal Operation)		
		(lb/hr)	(lb/24-hr)	(lb/2-yr)^(c)
NOx (Uncontrolled)	8.80E-01	66.25	1589.96	3179.93
NOx (Water- Steam Injection)	2.40E-01	18.07	433.63	867.25
CO (Uncontrolled)	3.30E-03	0.25	5.96	11.92
CO (Water-Steam Injection)	7.60E-02	5.72	137.32	274.63
SO ₂ ^(d)	5.05 E-02	3.8	91.24	182.48
Filterable Particulate Matter ^(e)	4.30E-03	0.32	7.77	15.54
Condensable Particulate Matter ^(e)	7.20E-03	0.54	13.01	26.02
Total Particulate Matter ^(e)	1.20E-02	0.9	21.68	43.36
Total Hydrocarbons ^(e)	4.00E-03	0.3	7.23	14.45

a) Emission factors obtained from AP 42, Fifth Edition, Volume I, Chapter 3: Stationary Internal Combustion Sources, Section 3.1: Stationary Gas Turbines; U.S. EPA.

b) Based on average distillate oil heating value of 139 MMBtu/103 gallons. To convert from (lb/MMBtu) to (lb/103 gallons), multiply by 139.

c) Value based on operation 1 hour per month and one additional 24-hour period every 24 months.

d) Emission Factor = 1.01S, where S=percent sulfur in fuel. Example if sulfur content in the fuel is 3.4 percent, then S=3.4. All sulfur in the fuel is assumed to be converted to SO₂.

e) Emission factor is based on combustion turbines using water-steam injection, which is not expected to have a large effect on particulate matter emissions. Particulate matter data for uncontrolled gas turbines were not available.

f) The bounding plant design has a total of six gas turbine generators.

**PSEG Site
ESP Application
Part 2, Site Safety Analysis Report**

**Table 1.3-7 (Sheet 1 of 3)
Single Unit Composite Average Annual Normal Gaseous Release**

Isotope	ABWR Release^(a) (Ci/yr)	AP1000 Release^(b) (Ci/yr)	U.S. EPR Release^(c) (Ci/yr)	US-APWR Release^(d) (Ci/yr)	Bounding Value Release (Ci/yr)
H-3	7.30E+01	3.50E+02	1.80E+02	1.80E+02	3.50E+02
C-14	9.19E+00	7.30E+00	1.89E+01 ^(e)	7.30E+00	1.89E+01
Na-24	4.05E-03				4.05E-03
P-32	9.19E-04				9.19E-04
Ar-41	6.76E+00	3.40E+01	3.40E+01	3.40E+01	3.40E+01
Cr-51	3.51E-02	6.10E-04	9.70E-05	6.10E-04	3.51E-02
Mn-54	5.41E-03	4.30E-04	5.70E-05	4.30E-04	5.41E-03
Fe-55	6.49E-03				6.49E-03
Mn-56	3.51E-03				3.51E-03
Co-57		8.20E-06	8.20E-06	8.20E-06	8.20E-06
Co-58	2.41E-03	2.30E-02	4.80E-04	2.30E-02	2.30E-02
Fe-59	8.11E-04	7.90E-05	2.80E-05	7.90E-05	8.11E-04
Co-60	1.30E-02	8.70E-03	1.10E-04	8.80E-03	1.30E-02
Ni-63	6.49E-06				6.49E-06
Cu-64	1.00E-02				1.00E-02
Zn-65	1.11E-02				1.11E-02
Kr-83m	8.38E-04				8.38E-04
Kr-85	5.68E+02	4.10E+03	2.80E+03 ^(e)	1.40E+03	4.10E+03
Kr-85m	2.11E+01	3.60E+01	1.50E+02	0.00E+00	1.50E+02
Kr-87	2.51E+01	1.50E+01	5.30E+01	0.00E+00	5.30E+01
Kr-88	3.78E+01	4.60E+01	1.80E+02	0.00E+00	1.80E+02
Kr-89	2.41E+02				2.41E+02
Rb-89	4.32E-05				4.32E-05
Sr-89	5.68E-03	3.00E-03	1.60E-04	3.00E-03	5.68E-03
Kr-90	3.24E-04				3.24E-04
Sr-90	7.03E-05	1.20E-03	6.30E-05	1.20E-03	1.20E-03
Y-90	4.59E-05				4.59E-05
Sr-91	1.00E-03				1.00E-03
Y-91	2.41E-04				2.41E-04
Sr-92	7.84E-04				7.84E-04
Y-92	6.22E-04				6.22E-04
Y-93	1.11E-03				1.11E-03
Nb-95	8.38E-03	2.50E-03	4.20E-05	2.50E-03	8.38E-03
Zr-95	1.59E-03	1.00E-03	1.00E-05	1.00E-03	1.59E-03
Mo-99	5.95E-02				5.95E-02
Tc-99m	2.97E-04				2.97E-04

**PSEG Site
ESP Application
Part 2, Site Safety Analysis Report**

**Table 1.3-7 (Sheet 2 of 3)
Single Unit Composite Average Annual Normal Gaseous Release**

Isotope	ABWR Release^(a) (Ci/yr)	AP1000 Release^(b) (Ci/yr)	U.S. EPR Release^(c) (Ci/yr)	US-APWR Release^(d) (Ci/yr)	Bounding Value Release (Ci/yr)
Ru-103	3.51E-03	8.00E-05	1.70E-05	8.00E-05	3.51E-03
Rh-103m	1.11E-04				1.11E-04
Rh-106	1.89E-05				1.89E-05
Ru-106	1.89E-05	7.80E-05	7.80E-07	7.80E-05	7.80E-05
Ag-110m	2.00E-06				2.00E-06
Sb-124	1.81E-04				1.81E-04
Sb-125		6.10E-05	6.10E-07	6.10E-05	6.10E-05
Te-129m	2.19E-04				2.19E-04
I-131	2.59E-01	1.20E-01	8.80E-03	4.20E-03	2.59E-01
Te-131m	7.57E-05				7.57E-05
Xe-131m	5.14E+01	1.80E+03	2.70E+03 ^(e)	2.60E+02	2.70E+03
I-132	2.19E+00	4.00E-01			2.19E+00
Te-132	1.89E-05				1.89E-05
I-133	1.70E+00		3.20E-02	6.40E-02	1.70E+00
Xe-133	2.41E+03	4.60E+03	7.20E+03 ^(e)	0.00E+00	7.20E+03
Xe-133m	8.65E-02	8.70E+01	1.70E+02 ^(e)	2.00E+00	1.70E+02
Cs-134	6.22E-03	2.30E-03	4.80E-05	2.30E-03	6.22E-03
I-134	3.78E+00				3.78E+00
I-135	2.41E+00				2.41E+00
Xe-135	4.59E+02	3.30E+02	1.20E+03	2.00E+00	1.20E+03
Xe-135m	4.05E+02	7.00E+00	1.40E+01	4.00E+00	4.05E+02
Cs-136	5.95E-04	8.50E-05	3.30E-05	8.50E-05	5.95E-04
Cs-137	9.46E-03	3.60E-03	9.00E-05	3.60E-03	9.46E-03
Xe-137	5.14E+02		0.00E+00	4.00E+00	5.14E+02
Ba-137m				3.60E-03	3.60E-03
Cs-138	1.70E-04				1.70E-04
Xe-138	4.32E+02	6.00E+00	1.20E+01	1.00E+00	4.32E+02
Xe-139	4.05E-04				4.05E-04
Ba-140	2.70E-02	4.20E-04	4.20E-06	4.20E-04	2.70E-02
La-140	1.81E-03				1.81E-03
Ce-141	9.19E-03	4.20E-05	1.30E-05	4.20E-05	9.19E-03
Ce-144	1.89E-05				1.89E-05
Pr-144	1.89E-05				1.89E-05
W-187	1.89E-04				1.89E-04
Np-239	1.19E-02				1.19E-02
Total w/o H-3	5.19E+03	1.11E+04	1.45E+04 ^(e)	1.71E+03	1.74E+04
Total w/ H-3	5.26E+03	1.14E+04	1.47E+04^(e)	1.89E+03	1.78E+04

Rev.4

**PSEG Site
ESP Application
Part 2, Site Safety Analysis Report**

**Table 1.3-7 (Sheet 3 of 3)
Single Unit Composite Average Annual Normal Gaseous Release**

Notes:

- a) The annual average normal gaseous release from the ABWR for each isotope was taken from ABWR DCD (Rev. 4) Table 12.2-20.
- b) The annual average normal gaseous release from the AP1000 for each isotope was taken from AP1000 DCD (Rev. 19) Table 11.3-3.
- c) The annual average normal gaseous release from the U.S. EPR for each isotope was taken from U.S. EPR DCD (Rev. 1) Table 11.3-3, except for specific isotopes identified by footnote e below.
- d) The annual average normal gaseous release from the US-APWR for each isotope was taken from US-APWR DCD (Rev. 3) Table 11.3-5.
- e) The annual average normal gaseous release for the U.S. EPR for this isotope was obtained from the Bell Bend Nuclear Power Plant (BBNPP) Final Safety Analysis Report (FSAR), Revision 2.

**PSEG Site
ESP Application
Part 2, Site Safety Analysis Report**

**Table 1.3-8 (Sheet 1 of 3)
Single Unit Composite Average Annual Normal Liquid Release**

Isotope	ABWR Release^(a) (Ci/yr)	AP1000 Release^(b) (Ci/yr)	U.S. EPR Release^(c) (Ci/yr)	US-APWR Release^(d) (Ci/yr)	Bounding Value Release (Ci/yr)
H-3	8.00E+00	1.01E+03	1.66E+03	1.60E+03	1.66E+03
C-14	0.00E+00				0.00E+00
Na-24	5.05E-03	1.63E-03	6.10E-03	4.70E-03	6.10E-03
P-32	5.68E-04			1.80E-04	5.68E-04
Cr-51	1.70E-02	1.85E-03	1.00E-03	6.00E-03	1.70E-02
Mn-54	3.97E-03	1.30E-03	5.40E-04	4.50E-03	4.50E-03
Fe-55	9.46E-03	1.00E-03	4.10E-04	7.70E-03	9.46E-03
Co-56	0.00E+00				0.00E+00
Mn-56	2.04E-03				2.04E-03
Co-57	0.00E+00				0.00E+00
Co-58	8.38E-03	3.36E-03	1.50E-03	9.80E-03	9.80E-03
Fe-59	2.23E-03	2.00E-04	1.00E-04	2.30E-03	2.30E-03
Co-60	1.54E-02	4.40E-04	1.80E-04	1.40E-02	1.54E-02
Ni-63	1.70E-03			1.70E-03	1.70E-03
Cu-64	1.26E-02				1.26E-02
Zn-65	4.41E-04	4.10E-04	1.70E-04	2.20E-04	4.41E-04
Br-84		2.00E-05			2.00E-05
Rb-88		2.70E-04		2.80E-02	2.80E-02
Rb-89	0.00E+00				0.00E+00
Sr-89	3.14E-04	1.00E-04	5.00E-05	1.50E-04	3.14E-04
Sr-90	2.68E-05	1.00E-05		1.80E-05	2.68E-05
Y-90	0.00E+00				0.00E+00
Sr-91	1.25E-03	2.00E-05	8.00E-05	6.80E-05	1.25E-03
Y-91	2.35E-04			9.00E-05	2.35E-04
Y-91m		1.00E-05	5.00E-05	4.40E-05	5.00E-05
Sr-92	4.43E-04				4.43E-04
Y-92	1.69E-03				1.69E-03
Y-93	1.36E-03	9.00E-05	3.60E-04	2.90E-04	1.36E-03
Nb-95	3.14E-04	2.10E-04	1.00E-04	2.00E-03	2.00E-03
Zr-95	1.11E-03	2.30E-04	1.30E-04	1.30E-03	1.30E-03
Mo-99	2.61E-03	5.70E-04	1.80E-03	1.70E-03	2.61E-03
Tc-99m	5.68E-03	5.50E-04	1.70E-03	1.70E-03	5.68E-03
Ru-103	3.27E-04	4.93E-03	2.50E-03	3.40E-03	4.93E-03
Rh-103m	0.00E+00	4.93E-03	2.50E-03	3.10E-03	4.93E-03
Rh-106	0.00E+00	7.35E-02	3.10E-02	3.90E-02	7.35E-02
Ru-106	8.89E-03	7.35E-02	3.10E-02	4.70E-02	7.35E-02
Ag-110		1.40E-04	6.00E-05	7.20E-05	1.40E-04

Rev.4

**PSEG Site
ESP Application
Part 2, Site Safety Analysis Report**

**Table 1.3-8 (Sheet 2 of 3)
Single Unit Composite Average Annual Normal Liquid Release**

Isotope	ABWR Release^(a) (Ci/yr)	AP1000 Release^(b) (Ci/yr)	U.S. EPR Release^(c) (Ci/yr)	US-APWR Release^(d) (Ci/yr)	Bounding Value Release (Ci/yr)
Ag-110m		1.05E-03	4.40E-04	1.80E-03	1.80E-03
Sb-124				4.30E-04	4.30E-04
Te-129		1.50E-04	4.00E-05	3.10E-04	3.10E-04
Te-129m	8.43E-05	1.20E-04	6.00E-05	7.80E-05	1.20E-04
I-131	9.05E-03	1.41E-02	3.40E-02	2.00E-03	3.40E-02
Te-131		3.00E-05	6.00E-05	7.60E-05	7.60E-05
Te-131m	8.38E-05	9.00E-05	3.10E-04	2.50E-04	3.10E-04
I-132	1.93E-03	1.64E-03	1.20E-03	3.10E-04	1.93E-03
Te-132	1.35E-05	2.40E-04	4.80E-04	4.70E-04	4.80E-04
I-133	3.73E-02	6.70E-03	3.50E-02	8.10E-04	3.73E-02
Cs-134	1.13E-02	9.93E-03	2.60E-03	1.20E-02	1.20E-02
I-134	1.14E-04	8.10E-04		8.90E-05	8.10E-04
I-135	1.09E-02	4.97E-03	1.50E-02	7.80E-04	1.50E-02
Cs-136	7.51E-04	6.30E-04	3.10E-04	2.20E-02	2.20E-02
Cs-137	1.78E-02	1.33E-02	3.50E-03	1.80E-02	1.80E-02
Ba-137m		1.25E-02	3.30E-03	4.60E-04	1.25E-02
Cs- 138	8.00E-07				8.00E-07
Ba-140	1.68E-03	5.52E-03	4.20E-03	5.80E-03	5.80E-03
La-140	0.00E+00	7.43E-03	7.60E-03	8.00E-03	8.00E-03
Ce-141	2.97E-04	9.00E-05	5.00E-05	2.90E-04	2.97E-04
Ce-143		1.90E-04	6.10E-04	5.00E-04	6.10E-04
Pr-143	8.11E-05	1.30E-04	5.00E-05	7.90E-05	1.30E-04
Ce-144	3.89E-03	3.16E-03	1.30E-03	5.60E-03	5.60E-03
Pr-144		3.16E-03	1.30E-03	1.70E-03	3.16E-03
Nd-147	2.00E-06				2.00E-06
W -187	2.23E-04	1.30E-04	4.60E-04	3.50E-04	4.60E-04
Np-239	9.49E-03	2.40E-04	5.80E-04	5.30E-04	9.49E-03
Other		2.00E-05	2.00E-05	1.20E-05	2.00E-05
Total w/o H-3	2.08E-01	2.56E-01	1.94E-01	2.62E-01	4.75E-01
Total w/ H-3	8.21E+00	1.01E+03	1.66E+03	1.60E+03	1.66E+03

**PSEG Site
ESP Application
Part 2, Site Safety Analysis Report**

**Table 1.3-8 (Sheet 3 of 3)
Single Unit Composite Average Annual Normal Liquid
Release**

Notes:

- a) The annual average normal liquid release from the ABWR for each isotope was taken from South Texas Project 3 & 4 FSAR (Rev.3) Table 12.2-22.
- b) The annual average normal liquid release from the AP1000 for each isotope was taken from AP1000 DCD (Rev. 19) Table 11.2-7.
- c) The annual average normal liquid release from the U.S. EPR for each isotope was taken from U.S. EPR DCD (Rev. 1) Table 11.2-4.
- d) The annual average normal liquid release from the US-APWR for each isotope was taken from US-APWR DCD (Rev. 3) Table 11.2-10.

**PSEG Site
ESP Application
Part 2, Site Safety Analysis Report**

**Table 1.3-9 (Sheet 1 of 3)
Liquid-Containing Tank Failure Radionuclide Concentrations**

Radionuclide	ABWR^(a)		AP-1000^(b)	US-APWR^(c)	U.S. EPR^(d)	Bounding Value
	(MBq)	($\mu\text{Ci/cc}^{(e)}$)	($\mu\text{Ci/cc}$)	($\mu\text{Ci/cc}$)	($\mu\text{Ci/cc}$)	($\mu\text{Ci/cc}$)
Br-82				3.50E-03		3.50E-03
Br-83				2.40E-02	3.20E-02	3.20E-02
Br-84				1.10E-02	1.70E-02	1.70E-02
Br-85					2.00E-03	2.00E-03
Rb-86m					3.00E-07	3.00E-07
Rb-86				1.10E-02	1.90E-03	1.10E-02
Rb-88			1.50E+00	1.40E+00	1.00E+00	1.50E+00
Rb-89	2.80E+02	8.41E-05	6.90E-02	2.50E-02	4.70E-02	6.90E-02
Sr-89	5.10E+03	1.53E-03	1.10E-04	8.30E-04	6.40E-04	1.53E-03
Sr-90	4.20E+02	1.26E-04		5.40E-05	3.30E-05	1.26E-04
Sr-91	7.00E+03	2.10E-03		4.70E-04	1.00E-03	2.10E-03
Sr-92	5.30E+03	1.59E-03		2.20E-04	1.70E-04	1.59E-03
Y-90	4.20E+02	1.26E-04		1.80E-04	7.70E-06	1.80E-04
Y-91m				2.70E-04	5.20E-04	5.20E-04
Y-91	2.00E+03	6.01E-04		1.30E-04	8.10E-05	6.01E-04
Y-92	4.10E+03	1.23E-03		2.10E-04	1.40E-04	1.23E-03
Y-93	6.80E+03	2.04E-03		9.00E-05	6.50E-05	2.04E-03
Zr-95	4.10E+02	1.23E-04		1.60E-04	9.30E-05	1.60E-04
Zr-97					6.70E-05	6.70E-05
Nb-95	3.70E+02	1.11E-04		1.80E-04	9.40E-05	1.80E-04
Mo-99	2.00E+04	6.01E-03	2.10E-01	1.80E-01	1.10E-01	2.10E-01
Mo-101				5.00E-03		5.00E-03
Tc-99m	2.00E+04	6.01E-03		1.10E-01	4.60E-02	1.10E-01
Ru-103	9.70E+02	2.91E-04		1.30E-04	7.80E-05	2.91E-04
Ru-105					9.50E-05	9.50E-05
Ru-106	1.80E+02	5.41E-05		4.70E-05	2.70E-05	5.41E-05
Rh-103m	9.70E+02	2.91E-04			6.80E-05	2.91E-04
Rh-105					4.40E-05	4.40E-05
Rh-106	1.80E+02	5.41E-05			2.70E-05	5.41E-05
Ag-110m	5.80E+01	1.74E-05		4.30E-07	2.00E-07	1.74E-05
Ag-110					1.10E-08	1.10E-08
Sb-125					8.00E-07	8.00E-07
Sb-127					5.00E-06	5.00E-06
Sb-129					6.80E-06	6.80E-06
Te-125m				1.90E-04		1.90E-04
Te-127m				7.50E-04	4.40E-04	7.50E-04
Te-127					2.20E-03	2.20E-03
Te-129m	1.80E+03	5.41E-04		2.50E-03	1.50E-03	2.50E-03
Te-129				2.00E-03	2.40E-03	2.40E-03
Te-131m	4.60E+02	1.38E-04		6.30E-03	3.70E-03	6.30E-03

**PSEG Site
ESP Application
Part 2, Site Safety Analysis Report**

**Table 1.3-9 (Sheet 2 of 3)
Liquid-Containing Tank Failure Radionuclide Concentrations**

Radionuclide	ABWR ^(a)		AP-1000 ^(b)	US-APWR ^(c)	U.S. EPR ^(d)	Bounding Value
	(MBq)	($\mu\text{Ci/cc}^{(e)}$)				
Te-131				2.20E-03	2.60E-03	2.60E-03
Te-132	1.10E+02	3.30E-05		7.00E-02	4.10E-02	7.00E-02
Te-133m				4.30E-03		4.30E-03
Te-134				7.60E-03	6.70E-03	7.60E-03
I-129					4.60E-08	4.60E-08
I-130				2.70E-02	5.00E-02	5.00E-02
I-131	1.20E+05	3.60E-02	7.10E-02	6.70E-01	7.40E-01	7.40E-01
I-132	1.70E+04	5.11E-03	9.30E-02	2.90E-01	3.70E-01	3.70E-01
I-133	1.10E+05	3.30E-02	1.30E-01	1.10E+00	1.30E+00	1.30E+00
I-134	1.10E+04	3.30E-03	2.20E-02	1.50E-01	2.40E-01	2.40E-01
I-135	5.20E+04	1.56E-02	7.80E-02	6.40E-01	7.90E-01	7.90E-01
Cs-132				2.20E-03		2.20E-03
Cs-134	1.60E+03	4.80E-04	6.90E-01	2.00E+00	1.70E-01	2.00E+00
Cs-135m				2.40E-03		2.40E-03
Cs-136	6.00E+02	1.80E-04	1.00E+00	2.50E-01	5.30E-02	1.00E+00
Cs-137	4.40E+03	1.32E-03	5.00E-01	1.20E+00	1.10E-01	1.20E+00
Cs-138	1.20E+03	3.60E-04	3.70E-01	2.60E-01	2.20E-01	3.70E-01
Ba-137m			5.00E-01	8.00E+00	1.00E-01	8.00E+00
Ba-139					2.20E-02	2.20E-02
Ba-140	1.30E+04	3.90E-03		9.80E-04	6.20E-04	3.90E-03
La-140	1.30E+04	3.90E-03		4.20E-04	1.60E-04	3.90E-03
La-141					5.30E-05	5.30E-05
La-142					3.10E-05	3.10E-05
Ce-141	1.40E+03	4.20E-04		1.50E-04	8.90E-05	4.20E-04
Ce-143				1.20E-04	7.60E-05	1.20E-04
Ce-144	1.70E+02	5.11E-05		1.20E-04	6.90E-05	1.20E-04
Pr-143	1.00E+02	3.00E-05			8.80E-05	8.80E-05
Pr-144				2.90E-03	6.90E-05	2.90E-03
Pm-147				1.30E-05		1.30E-05
Nd-147					3.40E-05	3.40E-05
Eu-154				1.20E-06		1.20E-06
Np-239	6.80E+04	2.04E-02			8.70E-04	2.04E-02
Pu-238					2.00E-07	2.00E-07
Pu-239					2.00E-08	2.00E-08
Pu-240					2.80E-08	2.80E-08
Pu-241					6.90E-06	6.90E-06
Am-241					7.80E-09	7.80E-09
Cm-242					1.90E-06	1.90E-06
Cm-244					1.00E-07	1.00E-07
Na-24	2.50E+04	7.51E-03		1.50E-02	3.70E-02	3.70E-02

**PSEG Site
ESP Application
Part 2, Site Safety Analysis Report**

**Table 1.3-9 (Sheet 3 of 3)
Liquid-Containing Tank Failure Radionuclide Concentrations**

Radionuclide	ABWR ^(a)		AP-1000 ^(b) (μCi/cc)	US-APWR ^(c) (μCi/cc)	U.S. EPR ^(d) (μCi/cc)	Bounding Value (μCi/cc)
	(MBq)	(μCi/cc ^(e))				
P-32	6.90E+03	2.07E-03				2.07E-03
Cr-51	2.70E+05	8.11E-02		1.60E-03	2.00E-03	8.11E-02
Mn-54	4.10E+03	1.23E-03		1.10E-03	1.00E-03	1.23E-03
Mn-56	2.50E+04	7.51E-03	1.70E-02	4.00E-02		4.00E-02
Fe-55	6.00E+04	1.80E-02		1.10E-03	7.60E-04	1.80E-02
Fe-59	1.50E+03	4.50E-04		1.90E-04	1.90E-04	4.50E-04
Co-58	1.10E+04	3.30E-03		2.60E-03	2.90E-03	3.30E-03
Co-60	2.40E+04	7.21E-03		3.90E-04	3.40E-04	7.21E-03
Ni-63	6.00E+01	1.80E-05				1.80E-05
Cu-64	6.40E+04	1.92E-02				1.92E-02
Zn-65	1.20E+04	3.60E-03		3.20E-04	3.20E-04	3.60E-03
W-187	1.10E+03	3.30E-04			1.80E-03	1.80E-03
H-3		1.00E-02	3.50E+00	1.00E+00	1.00E+00	3.50E+00

Notes:

- a) Data is based on ABWR DCD (Rev. 4) Table 12.2-13a and Section 11.1.2.3. The associated tank size is 90 m³ (23,778 gallons) per Table 12.2-13a of the ABWR DCD.
- b) Data is based on AP1000 DCD (Rev. 18) Table 12.2-9 and Section 11.1.1.3. The associated tank size is 28,000 gallons per Table 12.2-9 of the AP1000 DCD.
- c) Data is based on US-APWR DCD (Rev.3) Table 12.2-37 and Section 11.1.1.3. The associated tank size is 30,000 gallons per Table 11.2-3 of the US-APWR DCD.
- d) Data is based on U.S. EPR DCD (Rev. 1) Table 11.1-2. The associated tank size is 19,600 gallons per Table 11.2-2 of the U.S. EPR DCD.
- e) A conversion factor between MBq (in a 90 m³ tank) and μCi/cc is:

$$10^6 \text{ Bq} / 1 \text{ MBq} \times 1 \text{ μCi} / 3.7 \times 10^4 \text{ Bq} \times 1 \text{ m}^3 / 10^6 \text{ cc} \times 1 / 90 \text{ m}^3 = 3 \times 10^{-7} \text{ μCi/cc} \times \text{m}^3/\text{MBq}.$$

**PSEG Site
ESP Application
Part 2, Site Safety Analysis Report**

1.4 IDENTIFICATION OF AGENTS AND CONTRACTORS

1.4.1 APPLICANT

1.4.1.1 PSEG Power, LLC and PSEG Nuclear, LLC

PSEG Power, LLC submits this application for an Early Site Permit for itself and PSEG Nuclear, LLC.

PSEG Power, LLC is a Delaware limited liability company, which is wholly owned by Public Service Enterprise Group, Incorporated, a corporation formed under the laws of the State of New Jersey. PSEG Nuclear, LLC is a Delaware limited liability company formed to own and operate nuclear generating stations and is a wholly owned subsidiary of PSEG Power, LLC. PSEG Nuclear, LLC is the owner and licensed operator of the Hope Creek Generating Station and the partial owner and licensed operator of the Salem Nuclear Generating Station, Units 1 and 2. These existing nuclear generating stations are adjacent to the PSEG Site that is the subject of this Early Site Permit application. It is anticipated that PSEG Nuclear, LLC will be the licensed operator of the new plant at the PSEG site, which is the subject of this application.

1.4.2 CONTRACTORS

1.4.2.1 Sargent & Lundy, LLC

Sargent & Lundy, LLC is a full-service architect-engineering firm with considerable nuclear plant expertise. The firm has demonstrated and proven capabilities in the design and licensing of nuclear plants both domestically and overseas. Sargent & Lundy, LLC has engineered, designed, planned, evaluated, and managed large, complex nuclear projects including 30 new nuclear units.

Sargent & Lundy, LLC provided engineering, management, and consulting services to prepare the ESPA for PSEG. This included project management and engineering services, developing SSAR and ER sections, developing the emergency plan, and preparing the ESPA.

1.4.2.2 MACTEC Engineering and Consulting, Inc.

MACTEC Engineering and Consulting, Inc. is a leader in the engineering, environmental, and remedial construction industries and provides a full range of engineering consulting services to clients worldwide. These services include site development, planning and engineering design, construction phase services, environmental services, and facilities operations and maintenance services.

MACTEC Engineering and Consulting, Inc. performed hydrogeological, hydrological and geotechnical field investigations and laboratory testing in support of the ESPA for the PSEG Site. This includes performing standard penetration tests, obtaining core samples, and installing groundwater observation wells.

In June 2011, AMEC acquired MACTEC Engineering and Consulting, Inc. AMEC Environment and Infrastructure, Inc. is providing hydrogeological, hydrological and geotechnical engineering services in support of the ESPA for the PSEG Site.

**PSEG Site
ESP Application
Part 2, Site Safety Analysis Report**

1.4.3 OTHER CONSULTANTS

1.4.3.1 William Lettis & Associates, Inc.

William Lettis & Associates, Inc. performed geologic mapping and characterized seismic sources in support of SSAR Section 2.5, including literature review, geologic field reconnaissance, review and evaluation of existing seismic source characterization models, identification and characterization of any new or different sources, and preparation of the related SSAR sections.

In December 2007, William Lettis & Associates, Inc. was acquired by Fugro Consultants, Inc. William Lettis & Associates operated as a unit of Fugro Consultants until being integrated into Fugro Consultants. Fugro Consultants is supporting geoscience topics associated with SSAR Section 2.5.

**PSEG Site
ESP Application
Part 2, Site Safety Analysis Report**

1.5 REQUIREMENTS FOR FURTHER TECHNICAL INFORMATION

No technical development programs remain to be performed to support this application.

**PSEG Site
ESP Application
Part 2, Site Safety Analysis Report**

1.6 MATERIAL INCORPORATED BY REFERENCE

No material has been incorporated by reference in this application.

**PSEG Site
ESP Application
Part 2, Site Safety Analysis Report**

1.7 DRAWINGS AND OTHER DETAILED INFORMATION

No such information has been submitted separately as part of this application.

**PSEG Site
ESP Application
Part 2, Site Safety Analysis Report**

1.8 INTERFACES WITH STANDARD DESIGNS

This topic is not applicable to this ESPA and will be discussed at the COL Application stage.

**PSEG Site
ESP Application
Part 2, Site Safety Analysis Report**

1.9 CONFORMANCE TO NRC REGULATIONS AND REGULATORY GUIDANCE

This section discusses the conformance of the ESPA SSAR with applicable NRC regulations and guidance. NRC regulations are contained in Title 10 of the Code of Federal Regulations. NRC guidance is contained in NRC Regulatory Guides (RGs) and in NRC Standard Review Plan NUREG-0800, *Standard Review Plan for the Review of Safety Analysis Reports for Nuclear Power Plants: LWR Edition*.

The applicable NRC regulations, Regulatory Guides, and the Standard Review Plan are identified in Table 1.9-1 for each SAR section. Conformance with the regulation is determined using the acceptance criteria sections of NUREG-0800. The revision number and date are provided for applicable Regulatory Guides.

Clarifications are identified when guidance is met, but additional information is needed to provide complete understanding of the method of conformance. In certain instances, regulations and regulatory guides do not apply due to design features not being applicable or due to process timing (i.e., applies at COL application versus ESPA). Clarification explanations are provided in Table 1.9-2.

In some cases, the regulations or guidance documents in question contain requirements that apply only in part to an ESPA. This table indicates conformance with the portions of the regulations or guidance applicable to an ESPA.

PSEG Site
ESP Application
Part 2, Site Safety Analysis Report

Table 1.9-1 (Sheet 1 of 3)
Regulatory Conformance Matrix

Legend: X = Complies C = Clarification Required, See Table 1.9-2	Rev.	Date	Chapter 1	2.0	2.1.1	2.1.2	2.1.3	2.2.1-2.2.2	2.2.3	2.3.1	2.3.2	2.3.3	2.3.4	2.3.5	2.4.1	2.4.2	2.4.3	2.4.4	2.4.5	2.4.6	2.4.7	2.4.8	2.4.9	2.4.10	2.4.11	2.4.12	2.4.13	2.5.1	2.5.2	2.5.3	2.5.4	2.5.5	3.5.1.6	11.2.3	11.3.3	13.3	13.6	Chapter 15	Chapter 17		
Regulatory Requirements Document Title																																									
NRC Regulations																																									
10 CFR 20					X																																				
10 CFR 20, Appendix B, Table 2																																			X	X					
10 CFR 20.1301																																			X	X					
10 CFR 50.33			X																																		X				
10 CFR 50.34			X																																		X			X	
10 CFR 50.34(a)														X																											
10 CFR 50.34(a)(1)					X	X	X																																X		
10 CFR 50.47(b)												X																									X				
10 CFR 50, Appendix B												X																	X	X										X	
10 CFR 50, Appendix E												X																									X				
10 CFR 50, Appendix I												X		X																					X	X					
10 CFR 50, Appendix S																X													X	X											
10 CFR 52.16			X																																						
10 CFR 52.17			X	X			X																															X	X		
10 CFR 52.17(a)					X	X		X	X	X	X	X	X	X	X	X	X	X	X	X	X	X	X	X	X	X	X	X	X	X	X	X	X	X					X	X	
10 CFR 52.18																																						X			
10 CFR 73.55																																						X			
10 CFR 100				X			X																						X		X	X					X	X			
10 CFR 100.3					X	X																																X			
10 CFR 100.20							X																											X			X				
10 CFR 100.20(b)					X	X	X	X	X																																
10 CFR 100.20(c)										X	X	X				X		X	X	X	X	X	X	X	X	X	X														
10 CFR 100.21							X																											X							
10 CFR 100.21(c)												X																													
10 CFR 100.21(c)(2)													X	X																									X		
10 CFR 100.21(d)										X	X	X				X					X	X	X	X	X	X															
10 CFR 100.21(f)																																						X			
10 CFR 100.21(g)																																					X				
10 CFR 100.23																											X	X	X	X	X										
10 CFR 100.23(d)																	X	X	X	X		X	X	X	X	X															
40 CFR 190																																				X	X				

PSEG Site
ESP Application
Part 2, Site Safety Analysis Report

Table 1.9-1 (Sheet 2 of 3)
Regulatory Conformance Matrix

Legend: X = Complies C = Clarification Required, See Table 1.9-2	Rev.	Date	Chapter 1	2.0	2.1.1	2.1.2	2.1.3	2.2.1-2.2.2	2.2.3	2.3.1	2.3.2	2.3.3	2.3.4	2.3.5	2.4.1	2.4.2	2.4.3	2.4.4	2.4.5	2.4.6	2.4.7	2.4.8	2.4.9	2.4.10	2.4.11	2.4.12	2.4.13	2.5.1	2.5.2	2.5.3	2.5.4	2.5.5	3.5.1.6	11.2.3	11.3.3	13.3	13.6	Chapter 15	Chapter 17		
Regulatory Requirements Document Title																																									
NRC Guidance																																									
NRC RG 1.23	1	Mar-07								C	X	X	X	X																							X				
NRC RG 1.26	4	Mar-07																																						X	
NRC RG 1.27	2	Jan-76								X					X	X	X	X	X	X	X	X	X		X	X					X	X									
NRC RG 1.28	3	Aug-85																							X	X														C	
NRC RG 1.29	4	Mar-07													X		X	X	X	X	X	X	X	X	X															X	
NRC RG 1.59	2	Aug-77													X		X	X	X	X	X	X	X	X																	
NRC RG 1.60	1	Dec-73																										X													
NRC RG 1.70	3	Nov-78	C		X	X	X	X	X	X	X	X	X	X	X	X	X	X	X	X	X	X	X	X	X	X	X	X	X	X	X	X	X	X			X	X	X	X	
NRC RG 1.76	1	Mar-07								C																															
NRC RG 1.78	1	Dec-01							X				C	C																											
NRC RG 1.91	1	Feb-78							X																																
NRC RG 1.101	5	Jun-05																																				C			
NRC RG 1.102	1	Sep-76												X	X	X	X	X	X	X	X	X	X	X																	
NRC RG 1.109	1	Oct-77												X																						X	X				
NRC RG 1.111	1	Jul-77												X																							X				
NRC RG 1.112	1	Mar-07												C																					X	X					
NRC RG 1.113	1	Apr-77																								X									X						
NRC RG 1.125	2	Mar-09																	X	X		X																			
NRC RG 1.132	2	Oct-03																										X	X	X	X	X	X								
NRC RG 1.138	2	Dec-03																										X			X	X									
NRC RG 1.145	1	Feb-83											X																										X		
NRC RG 1.165	0	Mar-97																										X	X	X											
NRC RG 1.183	0	Jul-00																																					X		
NRC RG 1.198	0	Nov-03																										X		X	X	X	X								
NRC RG 1.206	0	Jun-07								X	X	X	X															X	X	X	X	X					C				
NRC RG 1.208	0	Mar-07																										X	X	X											
NRC RG 4.7	2	Apr-98					X																					X	X	X	X						X	X			
NUREG-0800																																									
NUREG-0800, Section 1.0	1	Nov-07	C																																						
NUREG-0800, Section 2.0	0	Mar-07		X																																					
NUREG-0800, Section 2.1.1	3	Mar-07			X																																				
NUREG-0800, Section 2.1.2	3	Mar-07				X																																			
NUREG-0800, Section 2.1.3	3	Mar-07					X																																		

PSEG Site
ESP Application
Part 2, Site Safety Analysis Report

Table 1.9-1 (Sheet 3 of 3)
Regulatory Conformance Matrix

Legend: X = Complies C = Clarification Required, See Table 1.9-2	Rev.	Date	Chapter 1	2.0	2.1.1	2.1.2	2.1.3	2.2.1-2.2.2	2.2.3	2.3.1	2.3.2	2.3.3	2.3.4	2.3.5	2.4.1	2.4.2	2.4.3	2.4.4	2.4.5	2.4.6	2.4.7	2.4.8	2.4.9	2.4.10	2.4.11	2.4.12	2.4.13	2.5.1	2.5.2	2.5.3	2.5.4	2.5.5	3.5.1.6	11.2.3	11.3.3	13.3	13.6	Chapter 15	Chapter 17	
Regulatory Requirements Document Title																																								
NUREG-0800, Section 2.2.1-2.2.2	3	Mar-07						X																																
NUREG-0800, Section 2.2.3	3	Mar-07							X																															
NUREG-0800, Section 2.3.1	3	Mar-07								X																														
NUREG-0800, Section 2.3.2	3	Mar-07									X																													
NUREG-0800, Section 2.3.3	3	Mar-07										X																												
NUREG-0800, Section 2.3.4	3	Mar-07											C																											
NUREG-0800, Section 2.3.5	3	Mar-07												X																										
NUREG-0800, Section 2.4.1	3	Mar-07													X																									
NUREG-0800, Section 2.4.2	4	Mar-07														X																								
NUREG-0800, Section 2.4.3	4	Mar-07															X																							
NUREG-0800, Section 2.4.4	3	Mar-07																X																						
NUREG-0800, Section 2.4.5	3	Mar-07																	X																					
NUREG-0800, Section 2.4.6	3	Mar-07																		X																				
NUREG-0800, Section 2.4.7	3	Mar-07																			X																			
NUREG-0800, Section 2.4.8	3	Mar-07																				X																		
NUREG-0800, Section 2.4.9	3	Mar-07																					X																	
NUREG-0800, Section 2.4.10	3	Mar-07																						X																
NUREG-0800, Section 2.4.11	3	Mar-07																							X															
NUREG-0800, Section 2.4.12	3	Mar-07																								X														
NUREG-0800, Section 2.4.13	3	Mar-07																									X													
NUREG-0800, Section 2.5.1	4	Mar-07																										X												
NUREG-0800, Section 2.5.2	4	Mar-07																											X											
NUREG-0800, Section 2.5.3	4	Mar-07																												X										
NUREG-0800, Section 2.5.4	3	Mar-07																													X									
NUREG-0800, Section 2.5.5	3	Mar-07																															X							
NUREG-0800, Section 3.5.1.6	3	Mar-07																																C						
NUREG-0800, Section 11.2	3	Mar-07																																	X					
NUREG-0800, Section 11.3	3	Mar-07																																		X				
NUREG-0800, Section 13.3	3	Mar-07																																			C			
NUREG-0800, Section 13.6	3	Mar-07																																				X		
NUREG-0800, Section 15.0.3	0	Mar-07																																					X	
NUREG-0800, Section 17.5	0	Mar-07																																						X

**PSEG Site
ESP Application
Part 2, Site Safety Analysis Report**

**Table 1.9-2 (Sheet 1 of 2)
Regulatory Conformance Matrix Clarifications**

SAR Section/Subsection	Document	Clarification
1.3	RG 1.70	The RG guidance for Section 1.3 is to provide a comparison with other facilities. Since the reactor technology is not selected at this stage, this section is used for presenting the PPE.
	NUREG-0800, Section 1.0	The SRP guidance for Section 1.3 is to provide a comparison with other facilities. Since the reactor technology is not selected at this stage, this section is used for presenting the PPE.
2.3.1	RG 1.23	ESPA data collected from the existing Salem and Hope Creek meteorological monitoring program prior to July 2008 conforms to RG 1.23, Revision 0. As of July 1, 2008 upgrades have been implemented to meet RG 1.23, Revision 1.
	RG 1.76	The AP1000 and ABWR Design Control Documents (DCDs) comply with RG 1.76, Revision 0. The U.S. EPR and US-APWR DCDs comply with RG 1.76, Revision 1.
2.3.4	RG 1.78	Control room habitability is addressed in the COL Application.
	NUREG-0800, Subsection 2.3.4	Control room habitability is addressed in the COL Application.
2.3.5	RG 1.78	Control room habitability is addressed in the COL Application.
	RG 1.112	Source terms for gaseous and liquid releases during normal plant operation are provided as part of the PPE and are listed in other sections involving dose assessment.
3.5.1.6	NUREG-0800, Subsection 3.5.1.6	U.S. Department of Energy methodology is used to evaluate the air hazard impact frequency (DOE-STD-3014-96).

**PSEG Site
ESP Application
Part 2, Site Safety Analysis Report**

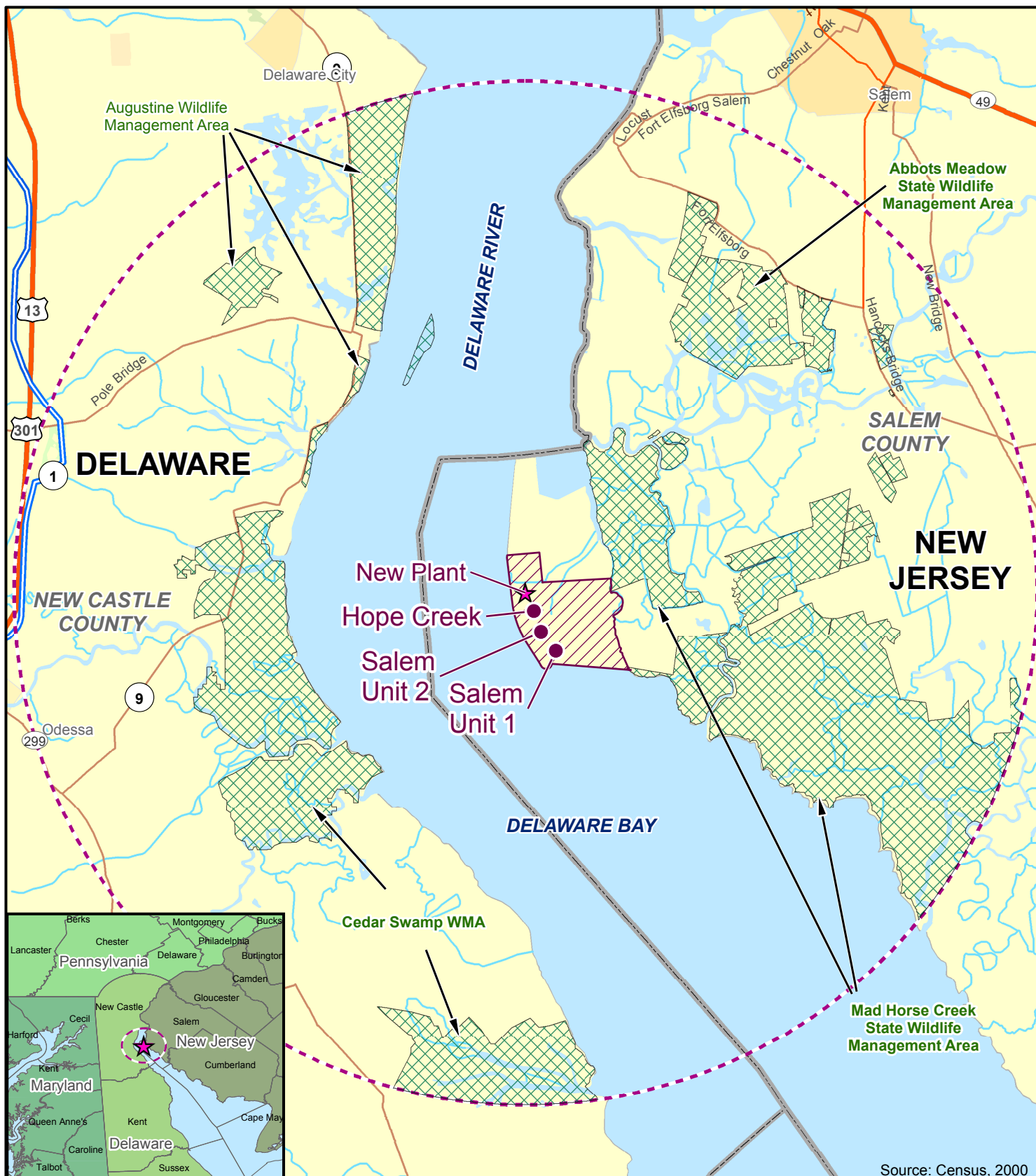
**Table 1.9-2 (Sheet 2 of 2)
Regulatory Conformance Matrix Clarifications**

SAR Section/Subsection	Document	Clarification
13.3	RG 1.101	NUREG-0654, Criterion II.B.5 defines a 30 and 60-minute augmentation time. The existing Salem/Hope Creek Nuclear Generating Station's Emergency Plan (E-Plan) describes an Emergency Response Organization (ERO) augmentation time of 90 minutes to augment the affected unit on-shift staff upon the declaration of an Alert or higher classification (E-Plan Section B.5). The existing on-shift staffing, as augmented by the capabilities for additions in 90 minutes, satisfies the staffing requirements of NUREG-0654, Table B-1. In the Safety Evaluation Report (SER) for the revision to the E-Plan that approved the on-shift ERO capabilities, as well as the 90 minute augmentation time capabilities, the NRC found that the ERO augmentation (response) time of 90 minutes meets the intent of the NRC-approved E-plan, and continues to meet the standards of 10 CFR 50.47(b) and the requirements of Appendix E to 10 CFR Part 50. The NRC Safety Evaluation Report is dated June 26, 2008 (ADAMS Ascension # ML081690552)
	RG 1.206 C.I.13.3	Certain aspects of the technology specific Emergency Action Levels (EAL) required by 10 CFR 50.47(b)(4) and 10 CFR 50 App. E Section IV.B cannot be completed until actual as-built information is available, and certain Technical Specifications are finalized. PSEG will adopt its EAL scheme prior to initial fuel load of the unit.
	NUREG-0800, Section 13.3	NUREG-0654, Criterion II.B.5 defines a 30 and 60-minute augmentation time. The existing Salem/Hope Creek Nuclear Generating Station's Emergency Plan (E-Plan) describes an Emergency Response Organization (ERO) augmentation time of 90 minutes to augment the affected unit on-shift staff upon the declaration of an Alert or higher classification (E-Plan Section B.5). The existing on-shift staffing, as augmented by the capabilities for additions in 90 minutes, satisfies the staffing requirements of NUREG-0654, Table B-1. In the Safety Evaluation Report (SER) for the revision to the E-Plan that approved the on-shift ERO capabilities, as well as the 90 minute augmentation time capabilities, the NRC found that the ERO augmentation (response) time of 90 minutes meets the intent of the NRC-approved E-plan, and continues to meet the standards of 10 CFR 50.47(b) and the requirements of Appendix E to 10 CFR Part 50. The NRC Safety Evaluation Report is dated June 26, 2008 (ADAMS Ascension # ML081690552)
17.5 QAPD Part IV	RG 1.28	Quality assurance requirements utilize the more recently NRC endorsed NQA-1 in lieu of the identified outdated standards.

**PSEG Site
ESP Application
Part 2, Site Safety Analysis Report**

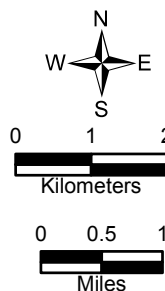
1.10 NUCLEAR POWER PLANTS TO BE OPERATED ON MULTI-UNIT SITES

This topic is not applicable to this ESPA and will be discussed at the COL Application stage.



LEGEND

- ★ New Plant
- Interstate Highway
- Highway
- Major Road
- County Boundary
- State Boundary
- PSEG Site Boundary
- 6-mile Radius
- State Owned Land
- Water



PSEG Power, LLC
PSEG Site ESPA
Part 2, Site Safety Analysis Report

PSEG Site Location -
6-Mile Radius
FIGURE 1.2-1

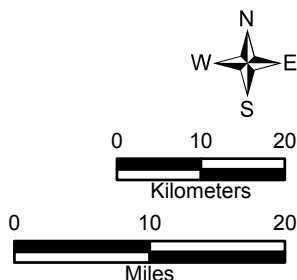
Rev 0



Source: Census, 2000

LEGEND

- ★ New Plant
- Interstate
- Highway
- Major Railroad Line
- County Boundary
- ▭ State Boundary
- ⬡ 50-Mile Radius
- ⬢ Water

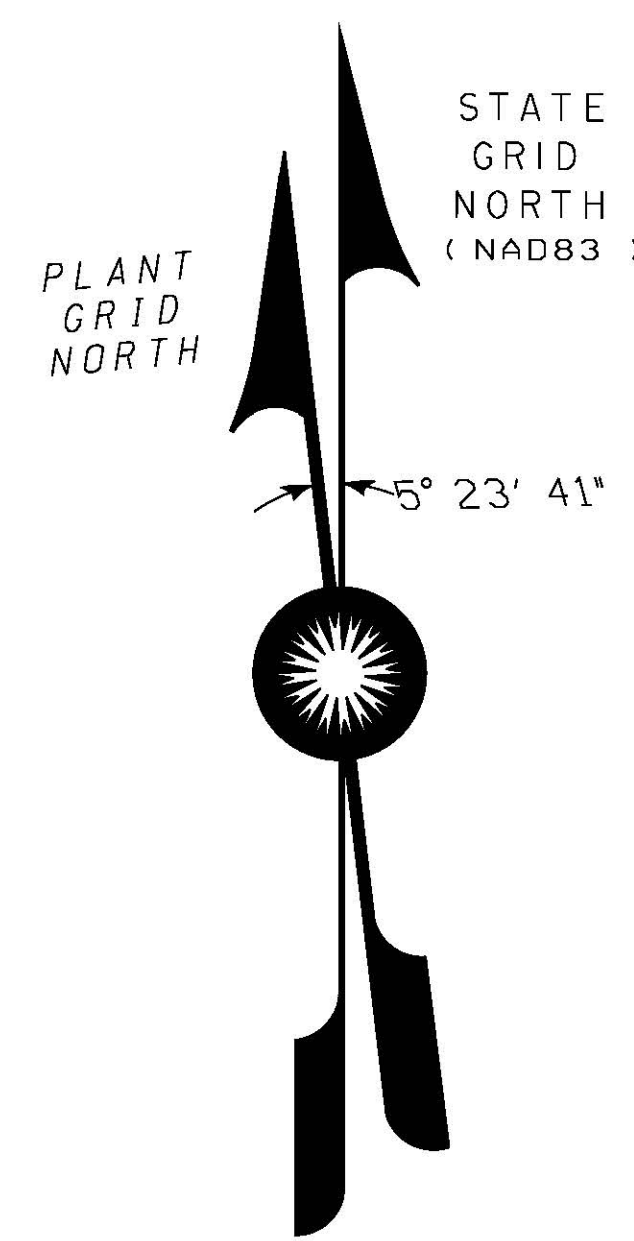


PSEG Power, LLC
PSEG Site ESPA
Part 2, Site Safety Analysis Report

PSEG Site Location -
50-Mile Radius

FIGURE 1.2-2

Rev 0



NOTES:

1. THE FOLLOWING ARE THE COORDINATES FOR NEW PLANT SITE CENTER:
NEW JERSEY STATE PLANE (NAD83)
NORTHING: 234,753,988.5 FT
EASTING: 196,529,293.8 FT
GEOGRAPHIC (NAD83)
LATITUDE: 39° 28' 23.7436"
LONGITUDE: 75° 32' 24.3316"
UNIVERSAL TRANSVERSE MERCATOR (NAD83 ZONE 18)
NORTHING: 14335392.324 FT
EASTING: 1488007.170 FT
U.S. NATIONAL GRID (NAD83)
USNG: 18SVJ5354569436
PLANT GRID COORDINATES
N632,536 FT
W980,666 FT
UNIVERSAL TRANSVERSE MERCATOR AND U.S. NATIONAL GRID DERIVED UTILIZING USACE CORPSCON V6.0.1.

2. TEMPORARY CONSTRUCTION IMPACT DUE TO INSTALLATION OF TRANSMISSION TOWERS IN THIS AREA (APPROXIMATELY 5 ACRES).
3. AREAS DESIGNATED AS "TEMPORARY CONSTRUCTION AREA" WILL INCLUDE CONSTRUCTION SUPPORT FACILITIES INCLUDING PARKING, CONSTRUCTION OFFICES, CONSTRUCTION FABRICATION AND SERVICES NECESSARY FOR CONSTRUCTION OF THE PROPOSED FACILITY.
4. PERMANENT IMPACT DUE TO INSTALLATION OF BARGE MOORING CAISSONS, LESS THAN 1 ACRE IMPACT.

LEGEND

- PERMANENT PLANT USE AREA
- TEMPORARY CONSTRUCTION USE AREA



PSEG Power, LLC
PSEG Site ESPA
Part 2, Safety Analysis Report

Site Utilization Plan

FIGURE 1.2-3

Rev.1

**PSEG Site
ESP Application
Part 2, Site Safety Analysis Report**

**CHAPTER 2
SITE CHARACTERISTICS AND SITE PARAMETERS**

TABLE OF CONTENTS

<u>Section</u>	<u>Title</u>	<u>Page</u>
2.0	SITE CHARACTERISTICS.....	2.0-1
2.1	GEOGRAPHY AND DEMOGRAPHY	2.1-1
2.1.1	SITE LOCATION AND DESCRIPTION.....	2.1-1
2.1.1.1	Specification of Location	2.1-1
2.1.1.2	Site Description and Site Map	2.1-1
2.1.1.3	Boundaries for Establishing Effluent Release Limits	2.1-2
2.1.2	EXCLUSION AREA AUTHORITY AND CONTROL	2.1-2
2.1.2.1	Authority	2.1-2
2.1.2.2	Control of Activities Unrelated to Plant Operation	2.1-3
2.1.2.3	Arrangements for Traffic Control	2.1-4
2.1.2.4	Abandonment or Relocation of Roads	2.1-4
2.1.2.5	Summary of Exclusion Area Authority and Control Issues	2.1-5
2.1.3	POPULATION DISTRIBUTION	2.1-5
2.1.3.1	Resident Population within 10 Miles	2.1-6
2.1.3.2	Resident Population between 10 and 50 Miles	2.1-7
2.1.3.3	Transient Population	2.1-7
2.1.3.3.1	Transient Population within 10 Miles	2.1-7
2.1.3.3.2	Transient Population between 10 and 50 Miles	2.1-8
2.1.3.4	Low Population Zone	2.1-8
2.1.3.5	Population Center	2.1-9
2.1.3.6	Population Density	2.1-10
2.1.4	REFERENCES	2.1-12
2.2	IDENTIFICATION OF POTENTIAL HAZARDS IN SITE VICINITY	2.2-1
2.2.1	LOCATIONS AND ROUTES.....	2.2-1
2.2.2	DESCRIPTIONS.....	2.2-3
2.2.2.1	Industrial Facilities.....	2.2-3
2.2.2.1.1	Hope Creek Generating Station	2.2-3
2.2.2.1.2	Salem Generating Station	2.2-3
2.2.2.1.3	Port Penn Sewage Treatment Plant.....	2.2-3
2.2.2.1.4	Lower Alloways Creek Township Buildings	2.2-3
2.2.2.2	Pipelines.....	2.2-4
2.2.2.3	Waterways.....	2.2-4
2.2.2.3.1	Alloway Creek	2.2-4
2.2.2.3.2	Delaware River.....	2.2-4
2.2.2.3.3	Chesapeake and Delaware Canal	2.2-5
2.2.2.3.4	Salem River.....	2.2-5
2.2.2.4	Mining Operations	2.2-5

**PSEG Site
ESP Application
Part 2, Site Safety Analysis Report**

TABLE OF CONTENTS (CONTINUED)

<u>Section</u>	<u>Title</u>	<u>Page</u>
2.2.2.5	Highways.....	2.2-5
2.2.2.6	Railroads	2.2-6
2.2.2.7	Airports, Airways, and Military Training Routes	2.2-6
2.2.2.7.1	Airports	2.2-6
2.2.2.7.2	Airways.....	2.2-6
2.2.2.8	Military	2.2-7
2.2.2.9	Projections of Industrial Growth	2.2-7
2.2.3	EVALUATIONS OF POTENTIAL ACCIDENTS.....	2.2-7
2.2.3.1	Determination of Design-Basis Events.....	2.2-8
2.2.3.2	Effects of Design-Basis Events	2.2-8
2.2.3.2.1	Probabilistic Analysis Methods.....	2.2-9
2.2.3.2.2	Explosions	2.2-12
2.2.3.2.3	Flammable Vapor Clouds	2.2-15
2.2.3.2.4	Toxic Chemicals	2.2-18
2.2.3.2.5	Fires	2.2-19
2.2.3.2.6	Conclusions.....	2.2-21
2.2.3.3	Collisions with Intake Structure	2.2-22
2.2.3.4	Liquid Spills	2.2-22
2.2.3.5	Radiological Hazards	2.2-23
2.2.4	REFERENCES	2.2-23
2.3	METEOROLOGY	2.3-1
2.3.1	REGIONAL CLIMATOLOGY.....	2.3-1
2.3.1.1	Landforms and Ground Surface Character of the Site Region.....	2.3-1
2.3.1.2	General Climate of the Site Region.....	2.3-1
2.3.1.3	Identification of Representative Regional Weather Monitoring Stations	2.3-5
2.3.1.4	Data Sources	2.3-8
2.3.1.5	Severe Weather	2.3-10
2.3.1.5.1	Extreme Wind.....	2.3-10
2.3.1.5.2	Tornadoes	2.3-10
2.3.1.5.3	Tropical Cyclones.....	2.3-11
2.3.1.5.4	Precipitation Extremes	2.3-11
2.3.1.5.5	Hail, Snowstorms, and Ice Storms	2.3-14
2.3.1.5.6	Thunderstorms	2.3-15
2.3.1.6	Meteorological Data for Evaluating the Ultimate Heat Sink.....	2.3-16
2.3.1.7	Design Basis Dry Bulb and Wet Bulb Temperatures	2.3-17
2.3.1.8	Restrictive Dispersion Conditions	2.3-20
2.3.1.9	Air Quality.....	2.3-20
2.3.1.10	Climate Changes.....	2.3-20
2.3.1.11	References.....	2.3-22
2.3.2	LOCAL METEOROLOGY	2.3-27
2.3.2.1	Data Sources	2.3-27

**PSEG Site
ESP Application
Part 2, Site Safety Analysis Report**

TABLE OF CONTENTS (CONTINUED)

<u>Section</u>	<u>Title</u>	<u>Page</u>
2.3.2.2	Normal, Mean, and Extreme Values of Meteorological Parameters...	2.3-29
2.3.2.2.1	Wind	2.3-30
2.3.2.2.1.1	Scales of Air Motion	2.3-30
2.3.2.2.1.2	On-Site Wind Roses during Three Year Period	2.3-30
2.3.2.2.1.3	On-Site Wind Roses during 32 Year Period	2.3-32
2.3.2.2.1.4	Comparison of Annual and Seasonal Three Year On-Site Wind Roses with Annual and Seasonal Regional Station Wind Roses	2.3-32
2.3.2.2.1.5	Wind Direction Persistence	2.3-33
2.3.2.2.2	Atmospheric Stability	2.3-33
2.3.2.2.3	Temperature	2.3-34
2.3.2.2.4	Water Vapor	2.3-34
2.3.2.2.5	Precipitation	2.3-35
2.3.2.2.6	Fog	2.3-35
2.3.2.3	Potential Influence of the Plant and Related Facilities on Local Meteorology	2.3-35
2.3.2.4	Current and Projected Site Air Quality	2.3-36
2.3.2.5	Topographic Description.....	2.3-37
2.3.2.6	References.....	2.3-37
2.3.3	ON-SITE METEOROLOGICAL MEASUREMENTS PROGRAM	2.3-38
2.3.3.1	On-Site Meteorological Measurements Program	2.3-38
2.3.3.2	General Program Description.....	2.3-38
2.3.3.3	Location, Elevation, and Exposure of Instruments	2.3-39
2.3.3.4	Instrument Maintenance.....	2.3-40
2.3.3.5	Data Collection and Analysis.....	2.3-40
2.3.4	SHORT-TERM (ACCIDENT) DIFFUSION ESTIMATES.....	2.3-41
2.3.4.1	Basis	2.3-41
2.3.4.2	PAVAN Modeling Results	2.3-44
2.3.5	LONG-TERM (ROUTINE) DIFFUSION ESTIMATES	2.3-44
2.3.5.1	Basis	2.3-44
2.3.5.2	XOQDOQ Modeling Results.....	2.3-46
2.3.5.3	References.....	2.3-47
2.4	HYDROLOGIC ENGINEERING	2.4-1
2.4.1	HYDROLOGIC DESCRIPTION.....	2.4-1
2.4.1.1	Site and Facilities	2.4-1
2.4.1.2	Hydrosphere.....	2.4-3
2.4.1.2.1	Hydrologic Characteristics	2.4-3
2.4.1.2.2	Local Drainage	2.4-5
2.4.1.2.3	Dams and Reservoirs.....	2.4-5
2.4.1.2.4	Proposed Water Management Changes	2.4-7
2.4.1.2.5	Surface-Water Users.....	2.4-7
2.4.1.2.6	Water Consumption.....	2.4-7
2.4.1.2.7	Potential Changes.....	2.4-8

**PSEG Site
ESP Application
Part 2, Site Safety Analysis Report**

TABLE OF CONTENTS (CONTINUED)

<u>Section</u>	<u>Title</u>	<u>Page</u>
2.4.1.3	References	2.4-8
2.4.2	FLOODS	2.4-23
2.4.2.1	Flood History	2.4-23
2.4.2.2	Flood Design Considerations	2.4-24
2.4.2.3	Effects of Local Intense Precipitation	2.4-26
2.4.2.4	References	2.4-27
2.4.3	PROBABLE MAXIMUM FLOOD ON STREAMS AND RIVERS	2.4-36
2.4.3.1	Design Bases for Flooding in Streams and Rivers	2.4-36
2.4.3.1.1	Identification and Analysis of the Probable Maximum Flood	2.4-38
2.4.3.1.1.1	Alternative Probable Maximum Precipitation Events	2.4-38
2.4.3.1.1.2	Basin Discharge	2.4-38
2.4.3.1.1.3	Delaware River Hydraulics	2.4-39
2.4.3.1.2	Coincident Wave Runup	2.4-40
2.4.3.1.3	Combined Events	2.4-40
2.4.3.1.3.1	Alternative I	2.4-41
2.4.3.1.3.2	Alternative II	2.4-41
2.4.3.2	Design Basis for Site Drainage	2.4-42
2.4.3.3	Effects of Sediment Erosion and Deposition	2.4-42
2.4.3.4	Conclusions	2.4-43
2.4.3.5	References	2.4-44
2.4.4	POTENTIAL DAM FAILURES	2.4-52
2.4.4.1	Selection of Dams and Their Combinations for Failure Scenarios	2.4-54
2.4.4.2	Analysis of Potential Dam Failures	2.4-55
2.4.4.3	Water Level at the New Plant Location	2.4-57
2.4.4.4	Effects of Sediment Deposition and Erosion	2.4-57
2.4.4.5	Dynamic Effects of Dam Failure-Induced Flood Waves on Structures, Systems and Components	2.4-59
2.4.4.6	Conclusions	2.4-59
2.4.4.7	References	2.4-60
2.4.5	PROBABLE MAXIMUM SURGE AND SEICHE FLOODING	2.4-67
2.4.5.1	Probable Maximum Winds (PMW) and Associated Meteorological Parameters	2.4-68
2.4.5.1.1	Probable Maximum Wind Storm (PMWS)	2.4-70
2.4.5.1.2	Appropriateness of PMH Determination	2.4-71
2.4.5.2	Surge and Seiche Water Levels	2.4-71
2.4.5.2.1	Historical Surges	2.4-72
2.4.5.2.2	Estimation of Probable Maximum Storm Surge	2.4-73
2.4.5.2.2.1	Estimation of 10 Percent Exceedance High Tide	2.4-74
2.4.5.2.2.2	Storm Surge at the Open Coast	2.4-75
2.4.5.2.2.3	Propagation of Surge through Delaware Bay	2.4-76
2.4.5.3	Coincident Wave Runup	2.4-77
2.4.5.3.1	Methodology	2.4-77
2.4.5.3.2	Wave Runup at the New Plant Location	2.4-79
2.4.5.4	Potential Sea Level Rise	2.4-79

**PSEG Site
ESP Application
Part 2, Site Safety Analysis Report**

TABLE OF CONTENTS (CONTINUED)

<u>Section</u>	<u>Title</u>	<u>Page</u>
2.4.5.5	Maximum Water Surface Elevation Associated with the PMH	2.4-80
2.4.5.6	PMH Design Basis Flood Level.....	2.4-80
2.4.5.6.1	Modeling System.....	2.4-81
2.4.5.6.1.1	Wind Model	2.4-81
2.4.5.6.1.2	ADCIRC+SWAN Model	2.4-81
2.4.5.6.1.3	Wave Runup Estimation	2.4-82
2.4.5.6.2	PMH Storm Simulations	2.4-83
2.4.5.6.3	PMH Design Basis Flood Level.....	2.4-84
2.4.5.7	Sediment Erosion and Deposition Associated with the PMH Surge.....	2.4-84
2.4.5.8	Seiche and Resonance	2.4-85
2.4.5.9	References	2.4-86
2.4.6	PROBABLE MAXIMUM TSUNAMI FLOODING	2.4-95
2.4.6.1	Historical Tsunami Record.....	2.4-95
2.4.6.1.1	Currituck Landslide	2.4-95
2.4.6.1.2	1755 Lisbon, Portugal Earthquake and Tsunami.....	2.4-96
2.4.6.1.3	Tsunami from 1918 Puerto Rico Earthquake	2.4-96
2.4.6.1.4	Tsunami Due to 1929 Earthquake at Grand Banks, Newfoundland, Canada.....	2.4-96
2.4.6.2	Probable Maximum Tsunami	2.4-97
2.4.6.3	Tsunami Source Characteristics.....	2.4-98
2.4.6.3.1	Currituck Landslide	2.4-98
2.4.6.3.2	La Palma Landslide in Canary Islands	2.4-99
2.4.6.3.3	Hispaniola Trench	2.4-99
2.4.6.4	Tsunami Analysis.....	2.4-99
2.4.6.4.1	Governing Equations.....	2.4-100
2.4.6.4.2	Model Simulations.....	2.4-100
2.4.6.4.3	Bathymetry and Topography Sources	2.4-101
2.4.6.4.4	Model Grids.....	2.4-101
2.4.6.4.5	Currituck Landslide Results.....	2.4-101
2.4.6.4.6	La Palma (Canary Islands) Landslide Results	2.4-103
2.4.6.4.7	Hispaniola Trench Earthquake Case.....	2.4-103
2.4.6.4.8	Summary of Tsunami Amplitudes at PSEG Site.....	2.4-104
2.4.6.5	Effects of Runup on Safety-Related Facilities	2.4-104
2.4.6.6	Consideration of Debris and Waterborne Projectiles	2.4-104
2.4.6.7	Effects of Sediment Erosion and Deposition	2.4-104
2.4.6.8	Consideration of Other Site-Related Evaluation Criteria	2.4-104
2.4.6.9	References	2.4-105
2.4.7	ICE EFFECTS	2.4-114
2.4.7.1	Historical Ice Accumulation	2.4-114
2.4.7.2	High and Low Water Levels	2.4-115
2.4.7.2.1	High Water Levels	2.4-116
2.4.7.2.1.1	Ice Jam Modeling	2.4-116
2.4.7.2.2	Low Water Levels.....	2.4-118
2.4.7.3	Ice Sheet Formation.....	2.4-118

**PSEG Site
ESP Application
Part 2, Site Safety Analysis Report**

TABLE OF CONTENTS (CONTINUED)

<u>Section</u>	<u>Title</u>	<u>Page</u>
2.4.7.4	Potential Ice-Induced Forces and Blockages	2.4-118
2.4.7.5	Conclusions	2.4-119
2.4.7.6	References	2.4-119
2.4.8	COOLING WATER CANALS AND RESERVOIRS	2.4-127
2.4.8.1	Cooling Water Intake Design	2.4-127
2.4.8.2	Conclusion	2.4-127
2.4.9	CHANNEL DIVERSIONS	2.4-128
2.4.9.1	Historical Channel Diversions	2.4-128
2.4.9.2	Regional Topographic Evidence	2.4-128
2.4.9.3	Ice Causes	2.4-129
2.4.9.4	Flooding of Site Due to Channel Diversion	2.4-129
2.4.9.5	Human-Induced Causes of Channel Diversion	2.4-129
2.4.9.6	Alternate Water Sources	2.4-130
2.4.9.7	Consideration of Other Site-Related Evaluation Criteria	2.4-130
2.4.9.8	References	2.4-130
2.4.10	FLOODING PROTECTION REQUIREMENTS	2.4-132
2.4.11	LOW WATER CONSIDERATIONS	2.4-133
2.4.11.1	Historical Low Water Conditions and the Effect of Tides	2.4-133
2.4.11.2	Low Water from Drought	2.4-134
2.4.11.2.1	HEC-RAS Simulation of Low Water Conditions	2.4-134
2.4.11.3	Low Water from Other Phenomena	2.4-135
2.4.11.3.1	Storm Surge Effects	2.4-136
2.4.11.3.2	Tsunami Effect	2.4-139
2.4.11.3.3	Winter Low Water Elevations with Ice Effects	2.4-139
2.4.11.4	Future Controls	2.4-140
2.4.11.5	Plant Requirements	2.4-140
2.4.11.6	Heat Sink Dependability Requirements	2.4-141
2.4.11.7	Conclusions	2.4-141
2.4.11.8	References	2.4-141
2.4.12	GROUNDWATER	2.4-146
2.4.12.1	Hydrogeology	2.4-146
2.4.12.1.1	Regional Hydrogeology	2.4-146
2.4.12.1.2	Local Hydrogeology	2.4-148
2.4.12.1.2.1	Fill Deposits	2.4-148
2.4.12.1.2.2	Alluvium	2.4-149
2.4.12.1.2.3	Kirkwood Formation	2.4-149
2.4.12.1.2.4	Cohansey Formation	2.4-150
2.4.12.1.2.5	Vincentown Formation	2.4-150
2.4.12.1.2.6	Hornerstown Formation	2.4-151
2.4.12.1.2.7	Navesink Formation	2.4-152
2.4.12.1.2.8	Mount Laurel Formation	2.4-152
2.4.12.1.2.9	Wenonah Formation	2.4-153
2.4.12.1.2.10	Marshalltown Formation	2.4-153
2.4.12.1.2.11	Englishtown Formation	2.4-154

**PSEG Site
ESP Application
Part 2, Site Safety Analysis Report**

TABLE OF CONTENTS (CONTINUED)

<u>Section</u>	<u>Title</u>	<u>Page</u>
2.4.12.1.2.12	Woodbury Formation	2.4-154
2.4.12.1.2.13	Merchantville Formation	2.4-155
2.4.12.1.2.14	Potomac-Raritan-Magothy Formation	2.4-155
2.4.12.1.3	Observation Well and Production Well Data	2.4-156
2.4.12.1.3.1	Hydrogeologic Properties	2.4-158
2.4.12.1.3.2	Hydraulic Gradients	2.4-158
2.4.12.1.3.3	Vertical Gradients	2.4-159
2.4.12.1.3.4	Hydraulic Conductivity	2.4-159
2.4.12.1.3.5	Groundwater Velocity	2.4-159
2.4.12.1.3.6	Tidal Influences	2.4-159
2.4.12.1.3.7	Hydraulic Communication Between Groundwater and Surface- Water Bodies	2.4-160
2.4.12.1.4	Conceptual Site Model	2.4-160
2.4.12.2	Groundwater Use	2.4-161
2.4.12.2.1	Regional Groundwater Use	2.4-161
2.4.12.2.2	Local Water Use	2.4-162
2.4.12.3	New Plant Water Use	2.4-164
2.4.12.3.1	Water Demands to Support Construction	2.4-164
2.4.12.3.2	Water Demands to Support Existing and New Plant Operations	2.4-164
2.4.12.3.3	Monitoring or Safeguard Requirements	2.4-166
2.4.12.4	Dewatering and Post-Construction Groundwater Simulations	2.4-167
2.4.12.4.1	Dewatering and Construction Activities	2.4-167
2.4.12.4.1.1	Groundwater Modeling in Support of Dewatering Activities	2.4-167
2.4.12.4.1.2	Model Calibration	2.4-169
2.4.12.4.1.3	Sensitivity Analysis	2.4-170
2.4.12.4.1.4	Conclusions	2.4-171
2.4.12.4.1.5	Dewatering Model Simulation Summary	2.4-173
2.4.12.4.2	Post-Construction Operations	2.4-173
2.4.12.5	Design Basis for Hydrostatic Loading	2.4-174
2.4.12.6	References	2.4-175
2.4.13	ACCIDENTAL RELEASE OF RADIOACTIVE LIQUID EFFLUENTS IN GROUNDWATER AND SURFACE WATERS	2.4-213
2.4.13.1	Groundwater	2.4-213
2.4.13.1.1	Assumptions and Methodology	2.4-213
2.4.13.1.2	Accident Scenario	2.4-214
2.4.13.1.3	Conceptual Model and Hydrogeologic Inputs	2.4-215
2.4.13.1.4	Radionuclide Transport Analysis	2.4-218
2.4.13.1.5	Radionuclides Determined to be a Potential Migration Threat	2.4-222
2.4.13.1.6	Transport with Advection and Radioactive Decay Only (Cases 1, 3 and 5)	2.4-222
2.4.13.1.7	Transport with Advection, Radioactive Decay and Dilution (Cases 2, 4 and 6)	2.4-223
2.4.13.1.8	Potential Effects from Increased Hydraulic Gradients (Mounding)	2.4-224
2.4.13.1.9	Comparison with 10 CFR Part 20	2.4-225

**PSEG Site
ESP Application
Part 2, Site Safety Analysis Report**

TABLE OF CONTENTS (CONTINUED)

<u>Section</u>	<u>Title</u>	<u>Page</u>
2.4.13.1.10	Conclusions.....	2.4-225
2.4.13.2	Surface-Water	2.4-226
2.4.13.3	References	2.4-226
2.5	GEOLOGY, SEISMOLOGY, AND GEOTECHNICAL INFORMATION	2.5-1
2.5.1	BASIC GEOLOGIC AND SEISMOLOGIC INFORMATION	2.5-2
2.5.1.1	Regional Geology.....	2.5-2
2.5.1.1.1	Regional Physiography and Geomorphology.....	2.5-2
2.5.1.1.1.1	Coastal Plain Physiographic Province.....	2.5-3
2.5.1.1.1.2	Continental Shelf, Slope, and Rise Physiographic Provinces	2.5-4
2.5.1.1.1.3	Piedmont Physiographic Province	2.5-5
2.5.1.1.1.4	Blue Ridge Physiographic Province	2.5-6
2.5.1.1.1.5	New England Physiographic Province	2.5-7
2.5.1.1.1.6	Valley and Ridge Physiographic Province.....	2.5-7
2.5.1.1.1.7	Appalachian Plateau Physiographic Province.....	2.5-7
2.5.1.1.2	Regional Geologic History.....	2.5-8
2.5.1.1.2.1	Grenville Orogeny and Subsequent Rifting	2.5-8
2.5.1.1.2.2	Penobscot/Potomac Orogeny	2.5-9
2.5.1.1.2.3	Taconic Orogeny	2.5-9
2.5.1.1.2.4	Acadian Orogeny	2.5-10
2.5.1.1.2.5	Alleghany Orogeny.....	2.5-10
2.5.1.1.2.6	Mesozoic Opening of the Atlantic Basin.....	2.5-10
2.5.1.1.2.7	Cenozoic Passive Margin Development	2.5-11
2.5.1.1.3	Regional Stratigraphy.....	2.5-12
2.5.1.1.3.1	Laurentian Continental Margin Stratigraphy.....	2.5-12
2.5.1.1.3.2	Gondwanan and Peri-Gondwanan Stratigraphy.....	2.5-15
2.5.1.1.3.3	Pangean Stratigraphy.....	2.5-16
2.5.1.1.3.4	North American Stratigraphy	2.5-17
2.5.1.1.3.4.1	Mesozoic Strata.....	2.5-17
2.5.1.1.3.4.2	Cenozoic Strata	2.5-18
2.5.1.1.3.4.3	Tertiary Strata	2.5-18
2.5.1.1.3.4.4	Quaternary Strata	2.5-20
2.5.1.1.4	Regional Tectonic Setting.....	2.5-20
2.5.1.1.4.1	Regional Stress	2.5-21
2.5.1.1.4.2	Principal Tectonic Structures	2.5-22
2.5.1.1.4.2.1	Late Proterozoic Tectonic Structures.....	2.5-23
2.5.1.1.4.2.2	Paleozoic Tectonic Structures	2.5-23
2.5.1.1.4.2.3	Mesozoic Tectonic Structures.....	2.5-24
2.5.1.1.4.2.4	Cenozoic Tectonic Structures.....	2.5-25
2.5.1.1.4.2.4.1	The Hypothesized Fault of Pazzaglia (1993)	2.5-26
2.5.1.1.4.2.4.2	Faults of Hansen (1978).....	2.5-26
2.5.1.1.4.2.4.3	River Bend Trend/Stafford Fault of Marple (2004).....	2.5-26
2.5.1.1.4.2.4.4	National Zoo Faults	2.5-27

**PSEG Site
ESP Application
Part 2, Site Safety Analysis Report**

TABLE OF CONTENTS (CONTINUED)

<u>Section</u>	<u>Title</u>	<u>Page</u>
2.5.1.1.4.2.4.5	Chesapeake Bay Impact Structure.....	2.5-27
2.5.1.1.4.2.4.6	Brandywine Fault System	2.5-27
2.5.1.1.4.2.5	Potential Quaternary Tectonic Features within the Site Region	2.5-28
2.5.1.1.4.2.5.1	Central Virginia Seismic Zone	2.5-28
2.5.1.1.4.2.5.2	Lancaster Seismic Zone and the Cacoosing Valley Earthquake.....	2.5-29
2.5.1.1.4.2.5.3	Fall Lines of Weems (1998)	2.5-30
2.5.1.1.4.2.5.4	Everona-Mountain Run Fault Zone	2.5-31
2.5.1.1.4.2.5.5	New Castle County Faults.....	2.5-32
2.5.1.1.4.2.5.6	The Stafford Fault System.....	2.5-33
2.5.1.1.4.2.5.7	Upper Marlboro Faults	2.5-34
2.5.1.1.4.2.5.8	Lebanon Church Fault.....	2.5-35
2.5.1.1.4.2.5.9	New York Bight Fault.....	2.5-35
2.5.1.1.4.2.5.10	East Border Fault	2.5-35
2.5.1.1.4.2.5.11	Ramapo Fault.....	2.5-35
2.5.1.1.4.2.5.12	Kingston Fault	2.5-40
2.5.1.1.4.2.5.13	Dobb's Ferry Fault Zone.....	2.5-40
2.5.1.1.4.2.5.14	Mosholu Fault.....	2.5-41
2.5.1.1.4.2.5.15	Offset Glacial Surfaces.....	2.5-41
2.5.1.1.4.2.5.16	Hopewell Fault	2.5-42
2.5.1.1.4.2.5.17	East Coast Fault System.....	2.5-42
2.5.1.1.5	Seismic Zones Defined By Regional Seismicity.....	2.5-42
2.5.1.1.5.1	Ramapo Seismic Zone	2.5-43
2.5.1.1.5.2	Proposed Peekskill-Stamford Seismic Boundary of Sykes et al.....	2.5-43
2.5.1.1.6	Site Regional Gravity and Magnetic Fields	2.5-44
2.5.1.1.6.1	Site Regional Gravity Field.....	2.5-44
2.5.1.1.6.2	Site Region Magnetic Field	2.5-48
2.5.1.1.6.3	Discussion and Synthesis of Regional Gravity and Magnetic Fields.....	2.5-52
2.5.1.2	Site Geology.....	2.5-54
2.5.1.2.1	Physiography and Geomorphology	2.5-54
2.5.1.2.1.1	Site Area.....	2.5-54
2.5.1.2.1.2	New Plant Location	2.5-54
2.5.1.2.2	Site Stratigraphy and Lithology	2.5-55
2.5.1.2.2.1	Site Area.....	2.5-55
2.5.1.2.2.1.1	Basement Complex.....	2.5-55
2.5.1.2.2.1.1.1	Carolina Superterrane	2.5-55
2.5.1.2.2.1.1.2	Philadelphia Terrane.....	2.5-56
2.5.1.2.2.1.2	Coastal Plain Stratigraphic Sequences	2.5-57
2.5.1.2.2.1.2.1	Lower Cretaceous Strata.....	2.5-57
2.5.1.2.2.1.2.2	Upper Cretaceous Strata.....	2.5-57
2.5.1.2.2.1.2.3	Lower Tertiary Strata (Paleocene).....	2.5-59
2.5.1.2.2.1.2.4	Upper Tertiary Strata (Neogene)	2.5-60
2.5.1.2.2.1.2.5	Quaternary Strata	2.5-60
2.5.1.2.2.2	Site Stratigraphy.....	2.5-61
2.5.1.2.2.2.1	Basement Complex.....	2.5-61

**PSEG Site
ESP Application
Part 2, Site Safety Analysis Report**

TABLE OF CONTENTS (CONTINUED)

<u>Section</u>	<u>Title</u>	<u>Page</u>
2.5.1.2.2.2.2	Coastal Plain Stratigraphic Sequences	2.5-62
2.5.1.2.2.2.2.1	Lower Cretaceous Strata	2.5-62
2.5.1.2.2.2.2.2	Upper Cretaceous Strata	2.5-62
2.5.1.2.2.2.2.3	Lower Tertiary Strata (Paleocene)	2.5-64
2.5.1.2.2.2.2.4	Upper Tertiary Strata (Neogene)	2.5-64
2.5.1.2.2.2.2.5	Quaternary Strata	2.5-64
2.5.1.2.3	Geologic History	2.5-65
2.5.1.2.3.1	Formation of Pangean Crust	2.5-65
2.5.1.2.3.2	Deposition of North American Sedimentary Sequences	2.5-66
2.5.1.2.4	Structural Geology	2.5-67
2.5.1.2.4.1	Site Vicinity	2.5-67
2.5.1.2.4.2	Site Area and Site	2.5-68
2.5.1.2.5	Site Engineering Geology Evaluation	2.5-69
2.5.1.2.5.1	Dynamic Behavior During Prior Earthquakes	2.5-69
2.5.1.2.5.2	Zones of Mineralization, Alteration, Weathering, Structural Weakness	2.5-69
2.5.1.2.5.3	Unrelieved Residual Stresses in Bedrock	2.5-70
2.5.1.2.5.4	Groundwater Conditions	2.5-70
2.5.1.2.5.5	Effects of Human Activity	2.5-70
2.5.1.3	References	2.5-70
2.5.2	VIBRATORY GROUND MOTION	2.5-99
2.5.2.1	Seismicity	2.5-100
2.5.2.1.1	Seismicity Catalog Used in CEUS-SSC Seismic Hazard Analysis	2.5-100
2.5.2.1.2	Updated Seismicity Catalogs	2.5-101
2.5.2.1.2.1	Updating the NUREG-2115 CEUS-SSC Seismicity Catalog	2.5-101
2.5.2.1.2.2	Mmax Distributions	2.5-102
2.5.2.1.2.3	PSEG Site Region Seismicity Catalog Update	2.5-102
2.5.2.1.2.4	Evaluation of AHEx-E Seismic Source Zone	2.5-103
2.5.2.1.3	Recent and Historical Seismicity	2.5-103
2.5.2.2	Geologic and Tectonic Characteristics of the Site and Region	2.5-107
2.5.2.2.1	Summary of CEUS-SSC Source Model	2.5-109
2.5.2.2.1.1	Mmax Sources	2.5-109
2.5.2.2.1.2	Seismotectonic Sources	2.5-109
2.5.2.2.1.3	RLME Sources	2.5-110
2.5.2.3	Correlation of Earthquake Activity with Seismic Sources	2.5-110
2.5.2.4	Probabilistic Seismic Hazard Analysis and Controlling Earthquake	2.5-110
2.5.2.4.1	CEUS-SSC Probabilistic Seismic Hazard Analysis	2.5-111
2.5.2.4.2	Revisions to CEUS-SSC Model Used for Probabilistic Seismic Hazard Analysis	2.5-111
2.5.2.4.2.1	Updated Seismicity Catalog	2.5-111
2.5.2.4.2.2	New Seismic Source Characterizations	2.5-112
2.5.2.4.2.2.1	Atlantic Highly Extended Crust – East (AHEx-E) Seismic Source Zone	2.5-112
2.5.2.4.2.2.2	Ramapo Seismic Zone	2.5-113

**PSEG Site
ESP Application
Part 2, Site Safety Analysis Report**

TABLE OF CONTENTS (CONTINUED)

<u>Section</u>	<u>Title</u>	<u>Page</u>
2.5.2.4.3	EPRI Ground Motion Models	2.5-113
2.5.2.4.4	Updated Probabilistic Seismic Hazard Analysis and Deaggregation	2.5-114
2.5.2.5	Seismic Wave Transmission Characteristics of the Site	2.5-116
2.5.2.5.1	Aleatory and Epistemic Uncertainty	2.5-117
2.5.2.5.2	Description of Site Response Analysis.....	2.5-117
2.5.2.5.2.1	Generation of Synthetic Profiles.....	2.5-117
2.5.2.5.2.2	Selection of Rock Input Motions.....	2.5-118
2.5.2.5.2.2.1	Site Response Calculations	2.5-118
2.5.2.6	Ground Motion and Site Response Analysis	2.5-119
2.5.2.6.1	Ground Motion Response Spectrum (GMRS).....	2.5-119
2.5.2.6.1.1	Horizontal GMRS Spectrum	2.5-120
2.5.2.6.1.2	Vertical GMRS Spectrum	2.5-121
2.5.2.7	References	2.5-122
2.5.3	SURFACE FAULTING	2.5-162
2.5.3.1	Geological, Seismological, and Geophysical Investigations	2.5-162
2.5.3.1.1	Published Geologic Mapping	2.5-163
2.5.3.1.2	Regional Geological Studies	2.5-163
2.5.3.1.3	Seismicity Data.....	2.5-164
2.5.3.1.4	Previous Site Investigations	2.5-164
2.5.3.1.5	Aerial Imagery Analysis	2.5-164
2.5.3.1.6	Current Aerial and Field Reconnaissance	2.5-165
2.5.3.1.7	Current Site Subsurface Investigations	2.5-166
2.5.3.2	Geological Evidence, or Absence of Evidence, for Tectonic Surface Deformation.....	2.5-166
2.5.3.2.1	Paleozoic Structures Exposed in the Piedmont	2.5-166
2.5.3.2.2	Faults Buried by Coastal Plain Sediments	2.5-167
2.5.3.2.3	Hypothesized Features	2.5-168
2.5.3.3	Correlation of Earthquakes with Capable Tectonic Sources	2.5-169
2.5.3.4	Ages of Most Recent Deformations	2.5-169
2.5.3.5	Relationship of Tectonic Structures in the Site Area to Regional Tectonic Structures	2.5-169
2.5.3.6	Characterization of Capable Tectonic Sources	2.5-169
2.5.3.7	Designation of Zones of Quaternary Deformation in the Site Region	2.5-169
2.5.3.8	Potential for Surface Tectonic Deformation or Non-Tectonic Deformation at the Site	2.5-170
2.5.3.9	References	2.5-170
2.5.4	STABILITY OF SUBSURFACE MATERIALS AND FOUNDATIONS	2.5-174
2.5.4.1	Geologic Features	2.5-174
2.5.4.1.1	PSEG Site Stratigraphy	2.5-174
2.5.4.1.1.1	PSEG Site Stratigraphic Units and Geologic Formations.....	2.5-175
2.5.4.1.2	Description of PSEG Site Stratigraphic Units and Geologic Formations	2.5-177
2.5.4.1.2.1	Lower Cretaceous Strata.....	2.5-177
2.5.4.1.2.1.1	Potomac Formation.....	2.5-177

**PSEG Site
ESP Application
Part 2, Site Safety Analysis Report**

TABLE OF CONTENTS (CONTINUED)

<u>Section</u>	<u>Title</u>	<u>Page</u>
2.5.4.1.2.2	Upper Cretaceous Strata	2.5-178
2.5.4.1.2.2.1	Magothy Formation	2.5-178
2.5.4.1.2.2.2	Merchantville Formation	2.5-178
2.5.4.1.2.2.3	Woodbury Formation	2.5-179
2.5.4.1.2.2.4	Englishtown Formation	2.5-179
2.5.4.1.2.2.5	Marshalltown Formation	2.5-179
2.5.4.1.2.2.6	Wenonah Formation	2.5-180
2.5.4.1.2.2.7	Mount Laurel Formation	2.5-180
2.5.4.1.2.2.8	Navesink Formation	2.5-181
2.5.4.1.2.3	Paleogene Strata (Lower Tertiary)	2.5-182
2.5.4.1.2.3.1	Hornerstown Formation	2.5-182
2.5.4.1.2.3.2	Vincentown Formation	2.5-182
2.5.4.1.2.4	Neogene Strata (Upper Tertiary)	2.5-183
2.5.4.1.2.4.1	Kirkwood Formation	2.5-183
2.5.4.1.2.5	Quaternary Strata	2.5-184
2.5.4.1.2.5.1	Alluvium	2.5-184
2.5.4.1.2.5.2	Artificial and Hydraulic Fill	2.5-185
2.5.4.1.3	Geologic Stability	2.5-185
2.5.4.1.4	References	2.5-187
2.5.4.2	Properties of Subsurface Materials	2.5-192
2.5.4.2.1	Laboratory Testing	2.5-193
2.5.4.2.1.1	Purpose and Scope	2.5-193
2.5.4.2.1.2	Sample Control	2.5-194
2.5.4.2.1.3	Testing Procedures	2.5-194
2.5.4.2.1.3.1	Consolidated-Undrained Triaxial Compression	2.5-194
2.5.4.2.1.3.2	Unconsolidated-Undrained Triaxial Compression	2.5-195
2.5.4.2.1.3.3	One-Dimensional Consolidation	2.5-195
2.5.4.2.1.3.4	Resonant Column and Torsional Shear	2.5-195
2.5.4.2.2	Material Engineering Properties	2.5-196
2.5.4.2.2.1	Static Material Properties	2.5-196
2.5.4.2.2.1.1	Artificial Fill (Mechanically Placed)	2.5-196
2.5.4.2.2.1.2	Hydraulic Fill	2.5-196
2.5.4.2.2.1.3	Alluvium	2.5-198
2.5.4.2.2.1.4	Kirkwood Formation	2.5-198
2.5.4.2.2.1.5	Vincentown and Hornerstown Formations	2.5-200
2.5.4.2.2.1.6	Navesink Formation	2.5-203
2.5.4.2.2.1.7	Mount Laurel Formation	2.5-204
2.5.4.2.2.1.8	Wenonah and Marshalltown Formations	2.5-205
2.5.4.2.2.1.9	Englishtown and Woodbury Formations	2.5-206
2.5.4.2.2.1.10	Merchantville Formation	2.5-207
2.5.4.2.2.1.11	Magothy Formation	2.5-208
2.5.4.2.2.1.12	Potomac Formation	2.5-208
2.5.4.2.2.2	Dynamic Material Properties	2.5-209
2.5.4.2.3	References	2.5-210

**PSEG Site
ESP Application
Part 2, Site Safety Analysis Report**

TABLE OF CONTENTS (CONTINUED)

<u>Section</u>	<u>Title</u>	<u>Page</u>
2.5.4.3	Foundation Interfaces	2.5-246
2.5.4.3.1	Site Exploration	2.5-246
2.5.4.3.1.1	Purpose and Scope	2.5-246
2.5.4.3.1.2	Exploratory Borehole Drilling and Sampling	2.5-246
2.5.4.3.1.3	In-Situ Geophysical Testing	2.5-249
2.5.4.3.1.4	Observation Well Installation and Testing	2.5-249
2.5.4.3.2	Foundation Interfaces	2.5-250
2.5.4.3.3	References	2.5-250
2.5.4.4	Geophysical Surveys	2.5-257
2.5.4.4.1	Downhole Geophysical Testing and Suspension Velocity Logging	2.5-257
2.5.4.4.2	Crosshole Seismic Velocity Testing	2.5-258
2.5.4.4.3	Downhole Seismic Velocity Testing	2.5-258
2.5.4.4.4	References	2.5-259
2.5.4.5	Excavation and Backfill	2.5-261
2.5.4.5.1	Plans and Sections	2.5-261
2.5.4.5.1.1	Lateral Limits of Excavation	2.5-261
2.5.4.5.1.2	Vertical Limits of Excavation	2.5-262
2.5.4.5.2	Construction Excavation and Dewatering	2.5-262
2.5.4.5.2.1	Excavation Support	2.5-263
2.5.4.5.2.2	Dewatering	2.5-263
2.5.4.5.2.3	Excavation Mapping and Photography	2.5-263
2.5.4.5.3	Backfill	2.5-263
2.5.4.5.3.1	Materials	2.5-264
2.5.4.5.3.2	Backfill Properties	2.5-264
2.5.4.5.3.3	Compaction Specifications	2.5-264
2.5.4.5.3.3.1	Lean Concrete and Roller-Compacted Concrete	2.5-264
2.5.4.5.3.3.2	Soil Backfill	2.5-265
2.5.4.5.3.4	Quality Control Testing	2.5-265
2.5.4.5.3.4.1	Lean Concrete or Roller-Compacted Concrete	2.5-265
2.5.4.5.3.4.2	Soil Backfill	2.5-266
2.5.4.5.4	Foundation Excavation Monitoring	2.5-266
2.5.4.5.4.1	Mat Foundation Evaluation	2.5-266
2.5.4.5.4.2	Geotechnical Instrumentation	2.5-267
2.5.4.5.5	References	2.5-267
2.5.4.6	Groundwater Conditions	2.5-269
2.5.4.6.1	Groundwater Occurrence	2.5-269
2.5.4.6.2	Field Hydraulic Conductivity Testing	2.5-271
2.5.4.6.3	Construction Dewatering	2.5-271
2.5.4.6.3.1	Dewatering Effects on Adjacent Structures	2.5-272
2.5.4.6.3.1.1	HCGS and SGS Nuclear Islands	2.5-273
2.5.4.6.3.1.2	HCGS Plant Area Buildings	2.5-273
2.5.4.6.3.1.3	Independent Spent Fuel Storage Installation	2.5-274
2.5.4.6.3.1.4	Buildings on Shallow Foundations	2.5-274
2.5.4.6.4	References	2.5-274

**PSEG Site
ESP Application
Part 2, Site Safety Analysis Report**

TABLE OF CONTENTS (CONTINUED)

<u>Section</u>	<u>Title</u>	<u>Page</u>
2.5.4.7	Response of Soil and Rock to Dynamic Loading	2.5-278
2.5.4.7.1	Soil Dynamic Property Data	2.5-278
2.5.4.7.2	Geologic Overview	2.5-278
2.5.4.7.3	Effects of Prior Earthquakes on Site	2.5-279
2.5.4.7.4	Calculation of Dynamic Soil Property Profiles	2.5-279
2.5.4.7.4.1	Shallow Soil Dynamic Profile.	2.5-279
2.5.4.7.4.2	Deep Soil Dynamic Profile.	2.5-281
2.5.4.7.5	Evaluation of Modulus Reduction and Damping Values	2.5-283
2.5.4.7.6	Development of Ground Motion Response Spectra	2.5-284
2.5.4.7.7	References	2.5-284
2.5.4.8	Liquefaction Potential	2.5-291
2.5.4.8.1	Site Conditions	2.5-291
2.5.4.8.2	Geologically Based Liquefaction Assessment	2.5-292
2.5.4.8.3	SPT-Based Liquefaction Assessment	2.5-293
2.5.4.8.4	Liquefaction Outside the Safety-Related Structure Area	2.5-294
2.5.4.8.5	Non-Seismic Liquefaction Potential	2.5-295
2.5.4.8.6	References	2.5-295
2.5.4.9	Earthquake Design Basis	2.5-298
2.5.4.9.1	References	2.5-298
2.5.4.10	Static Stability	2.5-299
2.5.4.10.1	General Foundation Information	2.5-299
2.5.4.10.2	Soil Bearing Capacity	2.5-300
2.5.4.10.3	Settlement	2.5-301
2.5.4.10.3.1	Deflection Monitoring	2.5-302
2.5.4.10.4	References	2.5-303
2.5.4.11	Design Criteria	2.5-305
2.5.4.12	Techniques to Improve Subsurface Conditions	2.5-306
2.5.4.12.1	Competent Layer Bearing Surface Preparation	2.5-306
2.5.5	STABILITY OF SLOPES	2.5-307
2.5.5.1	Slope Characteristics	2.5-307
2.5.5.2	Design Criteria and Analysis	2.5-308
2.5.5.3	Boring Logs	2.5-308
2.5.5.4	Compacted Fill	2.5-308
2.5.5.5	References	2.5-309
APPENDIX 2AA	Boring Logs from ESPA Exploration	2AA-1

**PSEG Site
ESP Application
Part 2, Site Safety Analysis Report**

LIST OF TABLES

<u>Number</u>	<u>Title</u>
2.0-1	PSEG Site Characteristics
2.1-1	Resident Population Distribution within 10 Miles of the PSEG Site
2.1-2	Resident Population Distribution between 10 and 50 Miles of the PSEG Site
2.1-3	Transient Population within 10 Miles of the PSEG Site by Source of Transients
2.1-4	Transient Population Distribution within 10 Miles of the PSEG Site
2.1-5	Employment in Major Economic Centers between 10 and 50 Miles of the PSEG Site
2.1-6	Major Public Recreation Areas between 10 and 50 Miles of the PSEG Site
2.1-7	Facilities and Institutions within the Low Population Zone
2.1-8	Population Centers (> 25,000 people) within 50 Miles of the PSEG Site
2.2-1	Industrial Facilities within 10 Miles of the PSEG Site
2.2-2a	Hope Creek Generating Station Chemical Storage
2.2-2b	Salem Generating Station Chemical Storage
2.2-3	SGS and HCGS Right-to-Know Chemical Storage
2.2-4	Port Penn Sewage Treatment Plant Chemical Storage
2.2-5	Lower Alloways Creek Township Chemical Storage
2.2-6	Chemical Commodities Transported on the Delaware River from 2003 through 2007
2.2-7	Number of Vessels Traveling to Oil/ Petroleum/Chemical Berths on the Delaware River in Each State from 1995 through 2008
2.2-8	Largest Net Tonnage of Hazardous Cargo Traveling on the Delaware River from 2003 through May 2009
2.2-9	Chemical Commodities Transported on the Chesapeake and Delaware Canal from 2003 through 2007
2.2-10	State and Federal Highways within 10 Miles of the PSEG Site

**PSEG Site
ESP Application
Part 2, Site Safety Analysis Report**

LIST OF TABLES (CONTINUED)

<u>Number</u>	<u>Title</u>
2.2-11	Airport Operations within the PSEG Site Region
2.2-12	Breakdown of the Probabilities of Chemical Spill Sizes
2.2-13	Results for Calculation of Frequency of a Hazard per Trip of Propane Past the PSEG Site
2.2-14	Number of Allowable Trips of Chemical Hazards Past the PSEG Site Each Year Based on a Probabilistic Analysis for a Flammable Vapor Cloud and Solid Explosive Hazards
2.2-15	Estimated Number of Trips of Chemical Hazards Past the PSEG Site Each Year and the Frequency of each Explosive Hazard
2.2-16	Hazardous Commodities Transported by Vessel and the Chemical Analyzed for Each Commodity
2.2-17	Chemicals Stored at Nearby Facilities (Including the Salem and Hope Creek Generating Stations) that are Analyzed
2.2-18	Explosion Event Analysis
2.2-19	Flammable Vapor Cloud Event Analysis
2.2-20	Toxicity Event Analysis
2.2-21	Chemical Fire Event Analysis
2.2-22	Number of Non-Self Propelled Vessels that Passed the PSEG Site from 2003 through 2007
2.3-1	NOAA Climate Summary for Wilmington, Delaware
2.3-2	NOAA Climate Summary for Atlantic City, New Jersey
2.3-3	NOAA Climate Summary for Philadelphia, Pennsylvania
2.3-4	Available NOAA Regional Meteorological Monitoring Stations
2.3-5	Tornado Site Characteristics
2.3-6	Tornado Missile Site Characteristics
2.3-7	Regional Tornadoes and Water Spouts

**PSEG Site
ESP Application
Part 2, Site Safety Analysis Report**

LIST OF TABLES (CONTINUED)

<u>Number</u>	<u>Title</u>
2.3-8	Regional Tropical Cyclones by Storm Category
2.3-9	Regional Tropical Cyclones by Month
2.3-10	NOAA Regional Stations for Precipitation Data
2.3-11	Precipitation Extremes at the Salem/Hope Creek Site and at NOAA Regional Meteorological Monitoring Stations
2.3-12	Location and Date of Hail Events
2.3-13	Estimated 100 Year Annual Maximum and Minimum Return DBT, Historic Maximum WBT and Estimated 100 Year Annual Maximum Return WBT
2.3-14	Design Wet and Dry Bulb Temperatures
2.3-15	Dry Bulb Temperature Extremes at the Salem/Hope Creek Site and at NOAA Regional Meteorological Monitoring Stations
2.3-16	Variation of Mean Precipitation and Mean Temperature Climate Parameters between Normal Periods and Variation of Extreme Precipitation, Extreme Temperature, and Tornado Occurrence Climate Parameters between Historic Periods
2.3-17	Number of Tropical Cyclones per Decade Period within 115 Statute Miles of the PSEG Site
2.3-18	Mean Monthly and Annual Rainfall at the Salem/Hope Creek Site and at NOAA Regional COOP Meteorological Monitoring Stations
2.3-19	Mean Monthly and Annual Snowfall at the NOAA Regional COOP Meteorological Monitoring Stations
2.3-20	Mean Monthly and Annual Dry Bulb Temperatures at the Salem/Hope Creek Site and at NOAA Regional COOP Meteorological Monitoring Stations
2.3-21	Wind Direction Persistence/Wind Speed Distributions at the Salem/Hope Creek Primary Meteorological Tower 33 ft. Level 2006-2008 Period Wind Speed Greater than or Equal to 2.24 m/sec
2.3-22	Wind Direction Persistence/Wind Speed Distributions at the Salem/Hope Creek Primary Meteorological Tower 33 ft. Level 2006-2008 Period Wind Speed Greater than or Equal to 4.47 m/sec

**PSEG Site
ESP Application
Part 2, Site Safety Analysis Report**

LIST OF TABLES (CONTINUED)

<u>Number</u>	<u>Title</u>
2.3-23	Wind Direction Persistence/Wind Speed Distributions at the Salem/Hope Creek Primary Meteorological Tower 33 ft. Level 2006-2008 Period Wind Speed Greater than or Equal to 6.71 m/sec
2.3-24	Wind Direction Persistence/Wind Speed Distributions at the Salem/Hope Creek Primary Meteorological Tower 33 ft. Level 2006-2008 Period Wind Speed Greater than or Equal to 8.94 m/sec
2.3-25	Wind Direction Persistence/Wind Speed Distributions at the Salem/Hope Creek Primary Meteorological Tower 33 ft. Level 2006-2008 Period Wind Speed Greater than or Equal to 11.18 m/sec
2.3-26	Mean Annual Pasquill Stability Class Distributions at the Salem/Hope Creek Primary Meteorological Tower 33 ft. Level Wind and 150-33 ft. Delta-T 2006-2008 and 1977-2008 Periods Frequency
2.3-27	Joint Frequency Distribution of Wind Speed and Wind Direction versus Atmospheric Stability Class Based at the Salem/Hope Creek Primary Meteorological Tower 33 ft. Level Wind 150-33 ft. Delta-T and 2006-2008 Period (Pasquill Stability Class A - G)
2.3-28	Meteorological Instrumentation Descriptions and Accuracies for the On-Site Meteorological Monitoring System
2.3-29	Annual Data Recovery Statistics for the On-Site Meteorological Monitoring System
2.3-30	Summary of PAVAN χ/Q Results (0.5%) January 1, 2006- December 31, 2008 Meteorological Data
2.3-31	PAVAN 0-2 Hour 0.5% Exclusion Area Boundary χ/Q Values
2.3-32	PAVAN 0-30 Day Low Population Zone χ/Q Values
2.3-33	Shortest Distances Between the New Plant Site Center and Receptors of Interest for Routine Releases
2.3-34	XOQDOQ Predicted Maximum χ/Q and D/Q Values at Receptors of Interest for Routine Releases
2.3-35	XOQDOQ Predicted Annual Average χ/Q Values at the Standard Radial Distances and Distance-Segment Boundaries for Routine Releases

**PSEG Site
ESP Application
Part 2, Site Safety Analysis Report**

LIST OF TABLES (CONTINUED)

<u>Number</u>	<u>Title</u>
2.3-36	XOQDOQ Predicted Annual Average D/Q Values at the Standard Radial Distances and Distance-Segment Boundaries for Routine Releases
2.3-37	XOQDOQ Predicted Annual Average χ /Q and D/Q Values at the Site Boundary for Routine Releases
2.3-38	Hurricane Missile Site Characteristics for PSEG Site
2.4.1-1	Hydrologic Features in the Vicinity of the PSEG Site
2.4.1-2	Delaware River Subbasins and Drainage Areas Above and Below the PSEG Site
2.4.1-3	NOAA Tidal Gage Data for the Delaware Bay and Delaware River
2.4.1-4	Tidal Values at NOAA Reedy Point, DE Tidal Gage (Gage Number 8551910)
2.4.1-5	USGS Gage Data for the Delaware River and Tributaries
2.4.1-6	Daily Mean Flow Data for the Delaware River at Trenton, NJ (USGS Gage 01463500)
2.4.1-7	Inventory of Reservoirs in the Delaware River Basin
2.4.1-8	Surface-Water Users on the Tidal Delaware River
2.4.1-9	Plant Water Use
2.4.2-1	Events Resulting in Storm Surges in the Delaware River near the PSEG Site
2.4.2-2	Peak Discharge for USGS Gage 01463500 on the Delaware River at Trenton, NJ
2.4.2-3	Reedy Point MSL Elevation Monthly Variation, 1987 – 2008
2.4.2-4	PMF Determination in Accordance with ANSI/ANS-2.8-1992 “Determining Design Basis Flooding at Power Reactor Sites”
2.4.2-5	PMP Values for Point Rainfall at the PSEG Site
2.4.2-6	HEC-HMS Input Parameters for PMP
2.4.2-7	HEC-HMS Results for PMP
2.4.3-1	Criteria for PMP Events

**PSEG Site
ESP Application
Part 2, Site Safety Analysis Report**

LIST OF TABLES (CONTINUED)

<u>Number</u>	<u>Title</u>
2.4.3-2	HEC-RAS Simulation Results of PMP Events
2.4.3-3	Worst Historical Storm Surge
2.4.3-4	Resulting PMF at the PSEG Site (RM 52) From Alternative I of ANSI/ANS-2.8-1992 Section 9.2.2.2
2.4.3-5	Resulting PMF at the PSEG Site (RM 52) From Alternative II of ANSI/ANS-2.8-1992, Section 9.2.2.2
2.4.4-1	Delaware River Basin Selected Water Control Structures
2.4.4-2	Summary of Tributary Dam Failure Input Parameters
2.4.4-3	Summary of Tributary Dam Failure Output Data Excluding Tidal Effects
2.4.4-4	Summary of Reservoir Sedimentation Rates
2.4.4-5	Resulting Maximum Water Surface Elevation at the PSEG Site (RM 52) From Dam Failure (Combined Events Alternative II of ANS)
2.4.5-1	Resulting Water Elevations at the PSEG Site (RM 52)
2.4.5-2	Maximum Sustained Wind Speed (kt) for Multiple PMH Scenarios
2.4.5-3	Maximum Surge (ft. NAVD) for Multiple PMH Scenarios from Screening Simulations
2.4.5-4	PMH Storm Parameters and Maximum Total Water Surface Elevation
2.4.5-5	Wave Runup Parameters and Results
2.4.6-1	Historical Record of Tsunamis Affecting the U.S. East Coast
2.4.6-2	Parameters for Seven Individual Okada Sources Which Make Up the Composite Hispaniola Trench Source
2.4.6-3	Grids A, B, and C for Currituck Landslide Case
2.4.6-4	Grids A, B and C for La Palma, Canary Island Landslide Case
2.4.6-5	Grids A, B, and C for the Hispaniola Trench Earthquake Case
2.4.6-6	Summary of Maximum Runup and Drawdown Values at PSEG Salem Site for Each Case

**PSEG Site
ESP Application
Part 2, Site Safety Analysis Report**

LIST OF TABLES (CONTINUED)

<u>Number</u>	<u>Title</u>
2.4.7-1	Historic Ice Jam Events on the Delaware River and Tributaries
2.4.7-2	Historical Ice Events on the Delaware Bay at the PSEG Site Winter 1998/1999 – Winter 2004/2005
2.4.7-3	Resulting Water Surface Elevations at the PSEG Site from the 1904 Ice Jam at Trenton, NJ
2.4.11-1	Negative Surge Associated with Bypassing Hurricanes
2.4.11-2	Resulting Water Surface Elevations at the New Plant
2.4.12-1	Summary of Hydraulic Properties for Local and Regional Aquifers and Aquitards
2.4.12-2	Summary of Public Water Supply Wells Within a 25-Mile Radius of the PSEG Site
2.4.12-3	Summary of Groundwater Users Within the 25-Mile Radius
2.4.12-4	Observation Well Installation Details
2.4.12-5	Groundwater Elevations (ft. NAVD), January 2009 to December 2009
2.4.12-6	Groundwater Elevation Data Range (in Feet NAVD 88) for HCGS and SGS Groundwater Wells, 2000 – 2009
2.4.12-7	Summary of Horizontal Hydraulic Gradients
2.4.12-8	Summary of Vertical Hydraulic Gradients
2.4.12-9	Summary of Average Hydraulic Conductivities
2.4.12-10	Summary of Tidal Study Results
2.4.12-11	Summary of Surface Water and Shallow Groundwater Elevations at Piezometers
2.4.12-12	Summary Dewatering Simulation and Sensitivity Results Drawdowns and Heads at Selected Locations
2.4.12-13	Summary Dewatering Simulation and Sensitivity Results Dewatering Rates at Times into Simulation
2.4.13-1	Initial Concentrations of Radionuclides

**PSEG Site
ESP Application
Part 2, Site Safety Analysis Report**

LIST OF TABLES (CONTINUED)

<u>Number</u>	<u>Title</u>
2.4.13-2	Radionuclides Concentrations – Advection and Decay Only Average Groundwater Flow Rate Conditions
2.4.13-3	Radionuclides Concentrations – Advection, Decay and Dilution Average Groundwater Flow Rate Conditions
2.4.13-4	Radionuclides Concentrations – Advection and Decay Only; Maximum Groundwater Flow Rate Conditions – West Flow Path
2.4.13-5	Radionuclides Concentrations – Advection, Decay, and Dilution Maximum Groundwater Flow Rate Conditions – West Flow Path
2.4.13-6	Radionuclides Concentrations – Advection and Decay Only; Maximum Groundwater Flow Rate Conditions – Northeast Flow Path
2.4.13-7	Radionuclides Concentrations – Advection, Decay, and Dilution Maximum Groundwater Flow Rate Conditions – Northeast Flow Path
2.5.1-1	Potential Cenozoic Features in the PSEG Site Region
2.5.1-2	Definition of Classes Used to Compile Quaternary Faults, Liquefaction Features and Deformations in the Eastern United States
2.5.2-1	Not Used
2.5.2-2	Not Used
2.5.2-3	Not Used
2.5.2-4	Not Used
2.5.2-5	Not Used
2.5.2-6	Not Used
2.5.2-7	Not Used
2.5.2-8	Not Used
2.5.2-9	Not Used
2.5.2-10	Not Used
2.5.2-11	Not Used

**PSEG Site
ESP Application
Part 2, Site Safety Analysis Report**

LIST OF TABLES (CONTINUED)

<u>Number</u>	<u>Title</u>
2.5.2-12	Not Used
2.5.2-13	Not Used
2.5.2-14	Not Used
2.5.2-15	Not Used
2.5.2-16	Not Used
2.5.2-17	Base-Case Soil Profile Mean Shear Wave Velocity
2.5.2-18	Parameters for Layer-Depth Randomization
2.5.2-19	Calculation of Durations and Effective Strain Ratios for Input Rock Motions
2.5.2-20	Amplification Factors for High-Frequency (HF) Motions
2.5.2-21	Amplification Factors for Low-Frequency (LF) Motions
2.5.2-22	Mean and Fractile Soil Seismic Hazard Curves at GMRS Elevation
2.5.2-23	Mean and Median UHRS Values for Soil Seismic Hazard (SA in g)
2.5.2-24	Calculation of Horizontal and Vertical GMRS
2.5.2-25	Mmax Comparisons Based on the CEUS-SSC Seismicity Catalog Update
2.5.2-26	Regional Updated Seismicity Catalog for the PSEG Site ($M \geq 2.9$)
2.5.2-27	CEUS-SSC Mmax Zones (Modified from Table H-3-1 of NUREG-2115)
2.5.2-28	CEUS-SSC Seismotectonic Zones (Modified from Table H-4-1 of NUREG-2115)
2.5.2-29	CEUS-SSC RLME Sources (Modified from Table 4.2.2-1 of NUREG-2115)
2.5.2-30	CEUS-SSC Seismic Sources Used in the PSEG Site PSHA Calculations
2.5.2-31	Mean and Fractile Rock Seismic Hazard Curves
2.5.2-32	Mean and Median UHRS Values for Rock Seismic Hazard at the PSEG Site (Spectral Acceleration in g)
2.5.2-33	Percent Contribution to Hazard by Magnitude and Distance

**PSEG Site
ESP Application
Part 2, Site Safety Analysis Report**

LIST OF TABLES (CONTINUED)

<u>Number</u>	<u>Title</u>
2.5.2-34	Mean Magnitudes (M) and Distances (R) from the 10-4, 10-5, and 10-6 Deaggregations at Low and High Frequencies
2.5.4.1-1	Summary of ESPA Investigation Stratigraphic Data Elevation at the Top of Formations
2.5.4.1-2	Comparison of PSEG ESPA and HCGS Stratigraphic Data
2.5.4.1-3	Key to Soil Descriptions at the PSEG Site
2.5.4.2-1	Summary of the Type and Number of Laboratory Tests Performed for the PSEG ESP Application
2.5.4.2-2	Summary of Static Indices Laboratory Analysis
2.5.4.2-3a	Summary of Unconsolidated-Undrained (UU) Triaxial Test Results Data from ESPA Investigation
2.5.4.2-3b	Summary of Unconfined Compression (UC) and Unconsolidated-Undrained (UU) Test Results Data from the Hope Creek Generating Station UFSAR
2.5.4.2-4	Summary of Consolidated Undrained Triaxial Test Results Data from ESPA Investigation
2.5.4.2-5a	Summary of One-Dimensional Consolidation Tests Results Data from the ESPA Investigation
2.5.4.2-5b	Summary of One-Dimensional Consolidation Tests Results Data from the Hope Creek Generating Station UFSAR
2.5.4.2-6	Summary of Unit Weight for Intact Samples Data from ESPA Investigation
2.5.4.2-7	Summary of Unit Weight of Soil Data from Hope Creek Foundation Investigation
2.5.4.2-8	Design Values for Static Engineering Properties of Subsurface Materials
2.5.4.2-9	Summary of RCTS Test Results Data from ESPA Investigation
2.5.4.3-1	Summary of Exploratory Borehole Drilling, Sampling and Testing Locations
2.5.4.3-2	Observation Well Location and Construction Summary
2.5.4.3-3	Summary of SPT Energy Measurements

**PSEG Site
ESP Application
Part 2, Site Safety Analysis Report**

LIST OF TABLES (CONTINUED)

<u>Number</u>	<u>Title</u>
2.5.4.4-1	Summary of Exploratory Borehole Drilling, Sampling and Testing Locations
2.5.4.5-1	Summary of Nuclear Plant Technologies
2.5.4.6-1	Summary of Groundwater Elevations, January 2009 to December 2009 – New Plant Area
2.5.4.6-2	Summary of In-Situ Hydraulic Conductivity (Slug Test) Results
2.5.4.6-3	Summary of Drawdowns at Existing Structures
2.5.4.7-1	Summary of Geologic Strata Elevations
2.5.4.7-2	Summary of Stratigraphic Layer Thicknesses, New Plant Area
2.5.4.7-3	Summary of Shear Wave Velocities and Layers
2.5.4.7-4	Shear Wave Velocity Parameters for Dynamic Profile Layers
2.5.4.7-5	Summary of Modulus Reduction and Damping Layer Information
2.5.4.8-1	Screening for Potential Liquefaction
2.5.4.8-2	Summary of Liquefaction Safety Factors (FS) for each Geologic Formation
2.5.4.10-1	Summary of Properties for Settlement Analysis Properties for Average Shear Wave Velocity Values

**PSEG Site
ESP Application
Part 2, Site Safety Analysis Report**

LIST OF FIGURES

<u>Number</u>	<u>Title</u>
2.1-1	PSEG Site 10 Mile Region with Direction Sectors Identified
2.1-2	PSEG Site 50 Mile Region with Direction Sectors Identified
2.1-3	PSEG Site 10 Mile Resident Population Distribution – 2000
2.1-4	PSEG Site 10 Mile Resident and Transient Population Distribution – 2010
2.1-5	PSEG Site 10 Mile Resident and Transient Population Distribution – 2021
2.1-6	PSEG Site 10 Mile Resident and Transient Population Distribution – 2031
2.1-7	PSEG Site 10 Mile Resident and Transient Population Distribution – 2041
2.1-8	PSEG Site 10 Mile Resident and Transient Population Distribution – 2051
2.1-9	PSEG Site 10 Mile Resident and Transient Population Distribution – 2061
2.1-10	PSEG Site 10 Mile Resident and Transient Population Distribution – 2071
2.1-11	PSEG Site 10 Mile Resident and Transient Population Distribution – 2081
2.1-12	PSEG Site 10 to 50-Mile 2000 Resident Population Distribution
2.1-13	PSEG Site 10 to 50-Mile 2010 Resident Population Distribution
2.1-14	PSEG Site 10 to 50-Mile 2021 Resident Population Distribution
2.1-15	PSEG Site 10 to 50-Mile 2031 Resident Population Distribution
2.1-16	PSEG Site 10 to 50-Mile 2041 Resident Population Distribution
2.1-17	PSEG Site 10 to 50-Mile 2051 Resident Population Distribution
2.1-18	PSEG Site 10 to 50-Mile 2061 Resident Population Distribution
2.1-19	PSEG Site 10 to 50-Mile 2071 Resident Population Distribution
2.1-20	PSEG Site 10 to 50-Mile 2081 Resident Population Distribution
2.1-21	PSEG Site 2010 Resident Population Within the Low Population Zone
2.1-22	PSEG Site Cumulative Population within 30 Miles Compared to NRC Siting Criteria

**PSEG Site
ESP Application
Part 2, Site Safety Analysis Report**

LIST OF FIGURES (CONTINUED)

<u>Number</u>	<u>Title</u>
2.1-23	Exclusion Area Boundary
2.2-1	Industrial and Transportation Facilities within 10 Miles of the PSEG Site
2.2-2	Airports and Airways within 10 Miles of the PSEG Site
2.2-3	Vessel Route near the PSEG Site Showing the Distance and Wind Direction
2.3-1	New Jersey Landform Areas
2.3-2	Local Topographic Map
2.3-3	Regional Topographic Map
2.3-4	New Jersey Climate Zones
2.3-5	Pattern of New Jersey Average January Dry Bulb Temperature
2.3-6	Pattern of New Jersey Average July Dry Bulb Temperature
2.3-7	Pattern of New Jersey Average Annual Water Equivalent Precipitation
2.3-8	Pattern of New Jersey Average January Relative Humidity
2.3-9	Pattern of New Jersey Average July Relative Humidity
2.3-10	Typical Tracks of Low-Pressure Storm Systems Across the Northeastern United States
2.3-11	Locations and Categories of Regional Weather Monitoring Stations
2.3-12	Annual Mean Wind Rose at S/HC Primary Meteorological Tower 33 ft. Level During Three Year Period 2006-2008
2.3-13	January Mean Wind Rose at S/HC Primary Meteorological Tower 33 ft. Level During Three Year Period 2006-2008
2.3-14	February Mean Wind Rose at S/HC Primary Meteorological Tower 33 ft. Level During Three Year Period 2006-2008
2.3-15	March Mean Wind Rose at S/HC Primary Meteorological Tower 33 ft. Level During Three Year Period 2006-2008
2.3-16	April Mean Wind Rose at S/HC Primary Meteorological Tower 33 ft. Level During Three Year Period 2006-2008

**PSEG Site
ESP Application
Part 2, Site Safety Analysis Report**

LIST OF FIGURES (CONTINUED)

<u>Number</u>	<u>Title</u>
2.3-17	May Mean Wind Rose at S/HC Primary Meteorological Tower 33 ft. Level During Three Year Period 2006-2008
2.3-18	June Mean Wind Rose at S/HC Primary Meteorological Tower 33 ft. Level During Three Year Period 2006-2008
2.3-19	July Mean Wind Rose at S/HC Primary Meteorological Tower 33 ft. Level During Three Year Period 2006-2008
2.3-20	August Mean Wind Rose at S/HC Primary Meteorological Tower 33 ft. Level During Three Year Period 2006-2008
2.3-21	September Mean Wind Rose at S/HC Primary Meteorological Tower 33 ft. Level During Three Year Period 2006-2008
2.3-22	October Mean Wind Rose at S/HC Primary Meteorological Tower 33 ft. Level during Three Year Period 2006-2008
2.3-23	November Mean Wind Rose at S/HC Primary Meteorological Tower 33 ft. Level During Three Year Period 2006-2008
2.3-24	December Mean Wind Rose at S/HC Primary Meteorological Tower 33 ft. Level During Three Year Period 2006-2008
2.3-25	Winter Mean Wind Rose at S/HC Primary Meteorological Tower 33 ft. Level During Three Year Period 2006-2008
2.3-26	Spring Mean Wind Rose at S/HC Primary Meteorological Tower 33 ft. Level During Three Year Period 2006-2008
2.3-27	Summer Mean Wind Rose at S/HC Primary Meteorological Tower 33 ft. Level During Three Year Period 2006-2008
2.3-28	Autumn Mean Wind Rose at S/HC Primary Meteorological Tower 33 ft. Level During Three Year Period 2006-2008
2.3-29	Annual Mean Wind Rose at S/HC Primary Meteorological Tower 33 ft. Level During 32 Year Period 1977-2008
2.3-30	Seasonal Wind Roses at S/HC Primary Meteorological Tower 33 ft. Level During 32 Year Period 1977-2008
2.3-31	Winter Wind Roses by Hour of Day at S/HC Primary Meteorological Tower 33 ft. Level During 32 Year Period 1977-2008

**PSEG Site
ESP Application
Part 2, Site Safety Analysis Report**

LIST OF FIGURES (CONTINUED)

<u>Number</u>	<u>Title</u>
2.3-32	Spring Wind Roses by Hour of Day at S/HC Primary Meteorological Tower 33 ft. Level During 32 Year Period 1977-2008
2.3-33	Summer Wind Roses by Hour of Day at S/HC Primary Meteorological Tower 33 ft. Level During 32 Year Period 1977-2008
2.3-34	Autumn Wind Roses by Hour of Day at S/HC Primary Meteorological Tower 33 ft. Level During 32 Year Period 1977-2008
2.3-35	Precipitation Hours Only by Season at S/HC Primary Meteorological Tower 33 ft. Level during 32 Year Period 1977-2008
2.3-36	Annual Mean Wind Roses at SHC Primary Meteorological Tower 33 ft. Level During Three Year Period 2006-2008 and Long-Term at Wilmington, Millville, and Dover
2.3-37	Winter Mean Wind Roses at SHC Primary Meteorological Tower 33 ft. Level During Three Year Period 2006-2008 and Long-Term at Wilmington, Millville, and Dover
2.3-38	Spring Mean Wind Roses at SHC Primary Meteorological Tower 33 ft. Level During Three Year Period 2006-2008 and Long-Term at Wilmington, Millville, and Dover
2.3-39	Summer Mean Wind Roses at SHC Primary Meteorological Tower 33 ft. Level During Three Year Period 2006-2008 and Long-Term at Wilmington, Millville, and Dover
2.3-40	Autumn Mean Wind Roses at SHC Primary Meteorological Tower 33 ft. Level During Three Year Period 2006-2008 and Long-Term at Wilmington, Millville, and Dover
2.3-41	PSEG Site Directional Elevation Profiles within 50 Miles of PSEG Site
2.3-42	Elevation Profiles to a 50 Mile Radius for N and NNE Direction Sectors
2.3-43	Elevation Profiles to a 50 Mile Radius for NE and ENE Direction Sectors
2.3-44	Elevation Profiles to a 50 Mile Radius for E and ESE Direction Sectors
2.3-45	Elevation Profiles to a 50 Mile Radius for SE and SSE Direction Sectors
2.3-46	Elevation Profiles to a 50 Mile Radius for S and SSW Direction Sectors
2.3-47	Elevation Profiles to a 50 Mile Radius for SW and WSW Direction Sectors

**PSEG Site
ESP Application
Part 2, Site Safety Analysis Report**

LIST OF FIGURES (CONTINUED)

<u>Number</u>	<u>Title</u>
2.3-48	Elevation Profiles to a 50 Mile Radius for W and WNW Direction Sectors
2.3-49	Elevation Profiles to a 50 Mile Radius for NW and NNW Direction Sectors
2.4.1-1	Local Area Drainage
2.4.1-2	Delaware River Watersheds and Stations
2.4.1-3	Reservoirs of the Delaware River Basin
2.4.1-4	PSEG Site Drainage
2.4.2-1	Peak Annual Discharge from the Delaware River at Trenton, NJ (01463500)
2.4.2-2	Comparison of Discharge at Trenton with River Stage at Reedy Point for June 2006 Event
2.4.2-3	Drainage Basin Sizes for PMP Determination
2.4.2-4	Probable Maximum Precipitation Values as a Function of Duration of Point Rainfall at the PSEG Site
2.4.2-5	Local Precipitation Model Drainage Pathways
2.4.2-6	HEC-HMS Link-Node Network
2.4.2-7	Datum and Water Level Relationship
2.4.3-1	Delaware River Basin Watershed
2.4.3-2	PMP Isohyetals Centered over Delaware River Basin near Doylestown, PA
2.4.3-3	PMP Isohyetals Centered over Delaware River Basin near Philadelphia, PA
2.4.3-4	Estimation of the 96-hr. PMP Depths of Isohyetal A Centered over the Delaware River Basin near Philadelphia, PA
2.4.3-5	96-hr. PMP Hyetograph for Isohyetal A Centered over the Delaware River Basin near Doylestown, PA
2.4.3-6	96-hr. PMP Hyetograph for Isohyetal A Centered over the Delaware River Basin near Philadelphia, PA
2.4.3-7	Cross-Section of Delaware River at RM 52 (PSEG Site)

**PSEG Site
ESP Application
Part 2, Site Safety Analysis Report**

LIST OF FIGURES (CONTINUED)

<u>Number</u>	<u>Title</u>
2.4.3-8	PMF Plot for the PSEG Site per Approximate Method from RG 1.59
2.4.3-9	Individual Components of the Combined Event Alternative I of ANSI/ANS-2.8-1992, Section 9.2.2.2 Stage Hydrograph at the PSEG Site
2.4.3-10	Individual Components of the Combined Event Alternative II of ANSI/ANS-2.8-1992, Section 9.2.2.2 Stage Hydrograph at the PSEG Site
2.4.4-1	Delaware River Basin Dams
2.4.4-2	Minimum Settled Particle Diameter at PSEG Intake Structure
2.4.4-3	Water Surface Elevations at the New Plant Location Following Failure of the Cannonsville and Pepacton Dams
2.4.4-4	Flow Rates at the New Plant Location Following Failure of the Pepacton and Cannonsville Dams
2.4.5-1	PMH Track
2.4.5-2	Hurricanes Producing Significant Storm Surges in Delaware Bay
2.4.5-3	Comparison of Bodine Method and Observed WSEL in Delaware Bay for the Chesapeake-Potomac Hurricane
2.4.5-4	Comparison of Calculated and Observed Surge at Reedy Point, DE
2.4.5-5	Determination of 10% Exceedance High Tide at Lewes and Reedy Point, DE
2.4.5-6	Probable Maximum Hurricane Surge Still Water Level at the New Plant Location
2.4.5-7	Probable Maximum Hurricane Surge Plus Additional Effects of Wave Runup and Potential Sea Level Rise
2.4.5-8	FEMA Region III ADCIRC Mesh
2.4.5-9	ADCIRC Mesh Refinement at PSEG Site
2.4.5-10	Comparison of Refined PSEG Site Mesh versus Unmodified FEMA Region III Mesh
2.4.5-11	Wave Runup Computation Locations around the Power Block
2.4.6-1	Slope at the Site Using Grid C

**PSEG Site
ESP Application
Part 2, Site Safety Analysis Report**

LIST OF FIGURES (CONTINUED)

<u>Number</u>	<u>Title</u>
2.4.6-2	Comparison of Water Surface Elevation Generated by the Currituck Slide With and Without Friction
2.4.6-3	Current Speeds Generated by the Currituck Slide
2.4.6-4	Nested Model Grids for Currituck Landslide Case
2.4.6-5	Nested Model Grids for the La Palma, Canary Islands Landslide Case
2.4.6-6	Nested Model Grids for the Hispaniola Trench Earthquake Case
2.4.6-7	40-Hour Simulation for Seiche Effects Currituck Landslide Case
2.4.6-8	Representative Model Stations 1 (Mouth of Delaware Bay) to 6 (PSEG Site)
2.4.6-9	Time Series Water Surface Elevations Currituck Slide Case
2.4.6-10	Initial Water Surface Elevations at Source Currituck Slide Case
2.4.6-11	2-D Image for Currituck Slide at 02 hours
2.4.6-12	2-D Image for Currituck Slide at 03 hours
2.4.6-13	2-D Image for Currituck Slide at 04 hours
2.4.6-14	2-D Image for Currituck Slide at 05 hours
2.4.6-15	Time Series Water Surface Elevations La Palma Slide Case
2.4.6-16	Initial Water Surface Elevations at Source La Palma Slide Case
2.4.6-17	2-D Image for La Palma Slide at 08 hours
2.4.6-18	2-D Image for La Palma Slide at 09 hours
2.4.6-19	2-D Image for La Palma Slide at 10 hours
2.4.6-20	2-D Image for La Palma Slide at 11 hours
2.4.6-21	Time Series Water Surface Elevations Hispaniola Trench Earthquake Case
2.4.6-22	Initial Water Surface Elevations at Source Hispaniola Trench Earthquake Case
2.4.6-23	2-D Image for Hispaniola Trench Earthquake at 04 hours

**PSEG Site
ESP Application
Part 2, Site Safety Analysis Report**

LIST OF FIGURES (CONTINUED)

<u>Number</u>	<u>Title</u>
2.4.6-24	2-D Image for Hispaniola Trench Earthquake at 05 hours
2.4.6-25	2-D Image for Hispaniola Trench Earthquake at 06 hours
2.4.6-26	2-D Image for Hispaniola Trench Earthquake at 07 hours
2.4.7-1	Cross-Section of Delaware River at RM 52 (PSEG Site)
2.4.9-1	Topography Near the PSEG Site
2.4.11-1	New Plant Location
2.4.11-2	River Mile 52 Cross-Section
2.4.11-3	Historical Hurricane Tracks
2.4.11-4	Negative Surge Caused by Hurricane Gloria
2.4.11-5	Negative Surge Caused by Hurricane Floyd
2.4.11-6	Track of PMH Producing Maximum Negative Surge
2.4.11-7	Basis for Determining Negative Surge from Hurricanes
2.4.12-1	Hydrostratigraphic Classification for the PSEG Site
2.4.12-2	Regional Hydrogeology, Extent of Major Aquifers or Aquifer Systems in New Jersey
2.4.12-3	NJ & DE Well Head Protection Areas and NJ Public Supply Wells Within 25 Miles of the PSEG Site
2.4.12-4	Cross Section Orientation
2.4.12-5	Cross Section A-A'
2.4.12-6	Cross Section B-B'
2.4.12-7	Average and Monthly Precipitation Data for 2009
2.4.12-8	Surface and Groundwater Sampling Locations
2.4.12-9	Not Used
2.4.12-10	Groundwater Elevations: Upper Wells in New Plant Location

**PSEG Site
ESP Application
Part 2, Site Safety Analysis Report**

LIST OF FIGURES (CONTINUED)

<u>Number</u>	<u>Title</u>
2.4.12-11	Potentiometric Contour Map – New Plant Location – Alluvium – February 2009
2.4.12-12	Potentiometric Contour Map – New Plant Location – Alluvium – April, 2009
2.4.12-13	Potentiometric Contour Map – New Plant Location – Alluvium – July 2009
2.4.12-14	Summary of Potentiometric Contours for Alluvium, PSEG Site – September, 2009
2.4.12-15	Groundwater Elevations: Lower Wells in New Plant Location
2.4.12-16	Potentiometric Contour Map – New Plant Location – Vincentown Formation – February 2009
2.4.12-17	Potentiometric Contour Map – New Plant Location – Vincentown Formation – April 2009
2.4.12-18	Potentiometric Contour Map – New Plant Location – Vincentown Formation – July 2009
2.4.12-19	Potentiometric Contour Map – New Plant Location – Vincentown Formation – September 2009
2.4.12-20	Tidal Effects – Summary of Water Level Elevation vs. Time
2.4.12-21	Tidal Effects – Barge Slip Location and Observation Well NOW-1U
2.4.12-22	Tidal Effects – Barge Slip Location and Observation Well NOW-1L
2.4.12-23	Tidal Effects – Barge Slip Location and Observation Well NOW-3U
2.4.12-24	Tidal Effects – Barge Slip Location and Observation Well NOW-3L
2.4.12-25	Drawdown Contours in Hydraulic Fill During Dewatering Activities
2.4.12-26	Drawdown Contours in Alluvium During Dewatering Activities
2.4.12-27	Drawdown Contours in Vincentown Formation During Dewatering Activities
2.4.12-28	Potentiometric Surface Contours in Alluvium Post-Construction
2.4.12-29	Potentiometric Surface Contours in Vincentown Formation Post-Construction
2.4.12-30	Comparison of Observed and Computed Water Level Contours

**PSEG Site
ESP Application
Part 2, Site Safety Analysis Report**

LIST OF FIGURES (CONTINUED)

<u>Number</u>	<u>Title</u>
2.4.13-1	Location of Hypothetical Accidental Release
2.5.1-1	Site Region Physiographic Provinces
2.5.1-2a	Site Region Geologic Map
2.5.1-2b	Site Region Geologic Map Explanation
2.5.1-3a	Site Regional Geologic Map of the Coastal Plain
2.5.1-3b	Site Regional Geologic Map of the Coastal Plain Explanation
2.5.1-4	Site Region Physiographic Features
2.5.1-5	Site Regional Physiographic Subprovinces of the Coastal Plain
2.5.1-6	Site Vicinity Physiographic Subprovinces of the Coastal Plain
2.5.1-7	Fall Lines of Weems
2.5.1-8a	Site Region Lithostratigraphic Map
2.5.1-8b	Site Region Lithostratigraphic Map Explanation
2.5.1-9	Mesozoic Basins by Benson
2.5.1-10	Site Region Structures
2.5.1-11	Generalized Stratigraphic Table for New Jersey
2.5.1-12a	Site Vicinity Geologic Map
2.5.1-12b	Site Vicinity Geologic Map Explanation
2.5.1-13	Regional Stratigraphic Correlations for Fluvial and Marine Neogene Strata
2.5.1-14	Regional Cross-Section
2.5.1-15	Alternative Basin Compilations
2.5.1-16	Cenozoic Features
2.5.1-17	Potential Quaternary Features
2.5.1-18	Site Region Seismicity

**PSEG Site
ESP Application
Part 2, Site Safety Analysis Report**

LIST OF FIGURES (CONTINUED)

<u>Number</u>	<u>Title</u>
2.5.1-19	New Castle County Faults
2.5.1-20a	Site Region Gravity Field
2.5.1-20b	Site Region Gravity Field Features
2.5.1-20c	Site Region Gravity Field with Mesozoic Basins
2.5.1-21	Gravity and Magnetic Profiles
2.5.1-22a	Site Region Magnetic Field
2.5.1-22b	Site Region Magnetic Field Features
2.5.1-22c	Site Region Magnetic Field with Mesozoic Basins
2.5.1-23	Site Vicinity Gravity Map
2.5.1-24a	Site Vicinity Magnetic Anomaly Map
2.5.1-24b	Site Vicinity Magnetic Anomaly Map Explanation
2.5.1-25	Site Region Crustal Zones
2.5.1-26	Site Vicinity Magnetic Anomaly Map Features
2.5.1-27	Site Area Topography and Physiography
2.5.1-28	Site Area Geologic Map
2.5.1-29	New Plant Location Geology
2.5.1-30	New Plant Location Aerial Photography
2.5.1-31	Site Location and Historical Aerial Photography
2.5.1-32	Site Topography
2.5.1-33	Site Area Stratigraphy
2.5.1-34	Site Location Stratigraphy
2.5.1-35	Depth to Basement
2.5.1-36	Site Vicinity Cross-Section

**PSEG Site
ESP Application
Part 2, Site Safety Analysis Report**

LIST OF FIGURES (CONTINUED)

<u>Number</u>	<u>Title</u>
2.5.1-37	Geotechnical Boring Location
2.5.1-38	Cross-Section A-A'
2.5.1-39	Cross-Section B-B'
2.5.1-40	Structure Contour Map – Top of Vincentown Formation
2.5.2-1	ANSS-Defined Regions of Authority and the Catalog Search Region
2.5.2-2	Seismicity Catalogs
2.5.2-3	Regional Seismicity
2.5.2-4	Seismicity within 200 Miles and 50 Miles of the Site
2.5.2-5	Bechtel Seismic Source Zones
2.5.2-6	Dames & Moore Seismic Source Zones
2.5.2-7	Law Seismic Source Zones
2.5.2-8	Rondout Seismic Source Zones
2.5.2-9	Weston Seismic Source Zones
2.5.2-10	Woodward Clyde Consultants Seismic Source Zones
2.5.2-11	Comparison of Seismicity Rates
2.5.2-12	EPRI-SOG EST's Charleston Map
2.5.2-13	UCSS Map
2.5.2-14	Regional Charleston Tectonic Features
2.5.2-15	Local Charleston Tectonic Features
2.5.2-16	Updated Charleston Seismic Source (UCSS) Logic Tree
2.5.2-17	Ramapo Seismic Zone
2.5.2-18	Mean and Fractile Rock Seismic Hazard Curves for PGA

**PSEG Site
ESP Application
Part 2, Site Safety Analysis Report**

LIST OF FIGURES (CONTINUED)

<u>Number</u>	<u>Title</u>
2.5.2-19	Mean and Fractile Rock Seismic Hazard Curves for 25 HZ Spectral Acceleration
2.5.2-20	Mean and Fractile Rock Seismic Hazard Curves for 10 HZ Spectral Acceleration
2.5.2-21	Mean and Fractile Rock Seismic Hazard Curves for 5 HZ Spectral Acceleration
2.5.2-22	Mean and Fractile Rock Seismic Hazard Curves for 2.5 HZ Spectral Acceleration
2.5.2-23	Mean and Fractile Rock Seismic Hazard Curves for 1 HZ Spectral Acceleration
2.5.2-24	Mean and Fractile Rock Seismic Hazard Curves for 0.5 HZ Spectral Acceleration
2.5.2-25	Rock Deaggregation for 1 and 2.5 Hz at Amplitudes Corresponding to 10^{-4} Annual Frequency of Exceedance
2.5.2-26	Rock Deaggregation for 5 and 10 Hz at Amplitudes Corresponding to 10^{-4} Annual Frequency of Exceedance
2.5.2-27	Rock Deaggregation for 1 and 2.5 Hz at Amplitudes Corresponding to 10^{-5} Annual Frequency of Exceedance
2.5.2-28	Rock Deaggregation for 5 and 10 Hz at Amplitudes Corresponding to 10^{-5} Annual Frequency of Exceedance
2.5.2-29	Rock Deaggregation for 1 and 2.5 Hz at Amplitudes Corresponding to 10^{-6} Annual Frequency of Exceedance
2.5.2-30	Rock Deaggregation for 5 and 10 Hz at Amplitudes Corresponding to 10^{-6} Annual Frequency of Exceedance
2.5.2-31	High- and Low-frequency Rock Spectra for 10^{-4} , with 10^{-4} UHRS Amplitudes
2.5.2-32	High- and Low-frequency Rock Spectra for 10^{-5} , with 10^{-5} UHRS Amplitudes
2.5.2-33	High- and Low-frequency Rock Spectra for 10^{-6} , with 10^{-6} UHRS Amplitudes
2.5.2-34	Synthetic Profiles
2.5.2-35	Synthetic Profiles (Shallow Portion)
2.5.2-36	Comparison of Input and Modeled Velocity Profiles

**PSEG Site
ESP Application
Part 2, Site Safety Analysis Report**

LIST OF FIGURES (CONTINUED)

<u>Number</u>	<u>Title</u>
2.5.2-37	Comparison of Input and Modeled Velocity Profiles (Shallow Portion)
2.5.2-38	Not Used
2.5.2-39	Not Used
2.5.2-40	Amplification Factors Calculated with the 60 Synthetic Profiles, for the 10 ⁻⁵ High-Frequency Rock Input
2.5.2-41	Amplification Factors Calculated with the 60 Synthetic Profiles, for the 10 ⁻⁵ Low-Frequency Rock Input
2.5.2-42	Logarithmic Mean Amplification Factors for High-Frequency (HF) Rock Inputs and Associated Logarithmic Standard Deviations
2.5.2-43	Logarithmic Mean Amplification Factors for Low-Frequency (LF) Rock Inputs and Associated Logarithmic Standard Deviations
2.5.2-44	Strain as a Function of Depth for the 10 ⁻⁵ High-Frequency Rock Input (Shallow Portion of Profile)
2.5.2-45	Strain as a Function of Depth for the 10 ⁻⁵ Low-Frequency Rock Input (Shallow Portion of Profile)
2.5.2-46	Mean and Fractile Soil Seismic Hazard Curves at the GMRS Elevation for 100 Hz (PGA) Spectral Acceleration
2.5.2-47	Mean and Fractile Soil Seismic Hazard Curves at the GMRS Elevation for 25 HZ Spectral Acceleration
2.5.2-48	Mean and Fractile Soil Seismic Hazard Curves at the GMRS Elevation for 10 HZ Spectral Acceleration
2.5.2-49	Mean and Fractile Soil Seismic Hazard Curves at the GMRS Elevation for 5 HZ Spectral Acceleration
2.5.2-50	Mean and Fractile Soil Seismic Hazard Curves at the GMRS Elevation for 2.5 HZ Spectral Acceleration
2.5.2-51	Mean and Fractile Soil Seismic Hazard Curves at the GMRS Elevation for 1 HZ Spectral Acceleration
2.5.2-52	Mean and Fractile Soil Seismic Hazard Curves at the GMRS Elevation for 0.5 HZ Spectral Acceleration

**PSEG Site
ESP Application
Part 2, Site Safety Analysis Report**

LIST OF FIGURES (CONTINUED)

<u>Number</u>	<u>Title</u>
2.5.2-53	Horizontal Soil UHRS
2.5.2-54	Horizontal and Vertical Soil GMRS
2.5.2-55	Recommended V/H Ratios
2.5.2-56	CEUS-SSC (NUREG-2115) Seismicity Catalog
2.5.2-57	Large Updated Seismicity Catalog for CEUS SSC Study Region
2.5.2-58	ANSS Authoritative Regions
2.5.2-59	Updated Seismicity Catalog for CEUS SSC Study Region
2.5.2-60	Updated Seismicity Catalog – CEUS SSC Mmax Source Zones (Wide Configuration)
2.5.2-61	Updated Seismicity Catalog – CEUS SSC Mmax Source Zones (Narrow Configuration)
2.5.2-62	Updated Seismicity Catalog – CEUS SSC Seismotectonic Source Zones (MIDC-A Configuration)
2.5.2-63	Updated Seismicity Catalog – CEUS SSC Seismotectonic Source Zones (MIDC-B Configuration)
2.5.2-64	Updated Seismicity Catalog – CEUS SSC Seismotectonic Source Zones (MIDC-C Configuration)
2.5.2-65	Updated Seismicity Catalog – CEUS SSC Seismotectonic Source Zones (MIDC-D Configuration)
2.5.2-66	Regional Catalog
2.5.2-67	Master Logic Tree for CEUS SSC Model
2.5.2-68	Mmax Branch of Logic Tree for CEUS SSC Model
2.5.2-69a	Seismotectonic Branch of Logic Tree for CEUS SSC Model
2.5.2-69b	Seismotectonic Branch of Logic Tree for CEUS SSC Model (cont.)
2.5.2-70	Comparison of Earthquake Counts
2.5.2-71	AHEX-E Seismic Source Zone Logic Tree Branch

**PSEG Site
ESP Application
Part 2, Site Safety Analysis Report**

LIST OF FIGURES (CONTINUED)

<u>Number</u>	<u>Title</u>
2.5.2-72	Total Mean and Median Rock UHRS
2.5.2-73	Contribution of AHEx-E to Total Mean Background and Site Hazard at 1 Hz
2.5.2-74	Contribution of AHEx-E to Total Mean Background and Site Hazard at 10 Hz
2.5.2-75	Contribution of AHEx-E to Total Mean Background and Site Hazard at 100 Hz (PGA)
2.5.2-76	Smooth Mean Rock 10-4, 10-5, and 10-6 Annual Frequency of Exceedance UHRS
2.5.2-77	G/Gmax and Material Damping Curves for Soil Layer 1
2.5.2-78	G/Gmax and Material Damping Curves for Soil Layers 2 through 5
2.5.2-79	G/Gmax and Material Damping Curves for Soil Layers 6 through 8
2.5.2-80	G/Gmax and Material Damping Curves for Soil Layers 9A and 9B
2.5.2-81	10-4 and 10-5 Horizontal Unsmoothed Soil Mean UHRS and Smoothed GMRS
2.5.3-1	Site Vicinity Geology and Seismicity
2.5.3-2	Lineament Investigation
2.5.4.1-1	PSEG Site Location Map
2.5.4.1-2	ESP Geotechnical Boring Location Map
2.5.4.1-3	Site Stratigraphic Column
2.5.4.1-4	Geologic Cross-Section A-A'
2.5.4.1-5	Geologic Cross-Section B-B'
2.5.4.1-6	Structure Contour Map-Top of Vincentown Formation
2.5.4.1-7	SPT Histogram-Mount Laurel Formation
2.5.4.1-8	SPT Histogram-Navesink Formation
2.5.4.1-9	SPT Histogram-Hornerstown Formation
2.5.4.1-10	SPT Histogram-Vincentown Formation

**PSEG Site
ESP Application
Part 2, Site Safety Analysis Report**

LIST OF FIGURES (CONTINUED)

<u>Number</u>	<u>Title</u>
2.5.4.1-11A	Boring Profile – NB-1 (Page 1)
2.5.4.1-11B	Boring Profile – NB-1 (Page 2)
2.5.4.1-11C	Boring Profile – NB-1 (Page 3)
2.5.4.1-12A	Boring Profile – NB-8 (Page 1)
2.5.4.1-12B	Boring Profile – NB-8 (Page 2)
2.5.4.1-13A	Boring Profile – EB-3 (Page 1)
2.5.4.1-13B	Boring Profile – EB-3 (Page 2)
2.5.4.1-13C	Boring Profile – EB-3 (Page 3)
2.5.4.1-14A	Boring Profile – EB-8/EB-8G (Page 1)
2.5.4.1-14B	Boring Profile – EB-8/EB-8G (Page 2)
2.5.4.2-1	Grain Size Distribution Envelope for the Samples Tested from Vincentown and Hornerstown Formations
2.5.4.2-2	Grain Size Distribution Envelope for the Samples Tested from Navesink Formations
2.5.4.2-3	Grain Size Distribution Envelope for the Samples Tested from Mount Laurel Formations
2.5.4.2-4	Shear Modulus Reduction Curves and RCTS Data at In-Situ Confining Stress
2.5.4.2-5	Damping Ratio Curves and RCTS Data at In-Situ Confining Stress
2.5.4.2-6	Shear Modulus Reduction Curves and RCTS Data at Four Times In-Situ Confining Stress
2.5.4.2-7	Damping Ratio Curves and RCTS Data at Four Times In-Situ Confining Stress
2.5.4.3-1	ESP Site Exploration
2.5.4.3-2	Cross-Section and Geotechnical Boring Location Plan
2.5.4.3-3	Reactor Building Vertical Extent Bounds on Geologic Section A-A'
2.5.4.3-4	Reactor Building Vertical Extent Bounds on Geologic Section B-B'

**PSEG Site
ESP Application
Part 2, Site Safety Analysis Report**

LIST OF FIGURES (CONTINUED)

<u>Number</u>	<u>Title</u>
2.5.4.4-1	ESPA Site Exploration
2.5.4.4-2A	Boring Profile – NB-1 (Page 1)
2.5.4.4-2B	Boring Profile – NB-1 (Page 2)
2.5.4.4-2C	Boring Profile – NB-1 (Page 3)
2.5.4.4-3A	Boring Profile – NB-8 (Page 1)
2.5.4.4-3B	Boring Profile – NB-8 (Page 2)
2.5.4.4-4A	Boring Profile – EB-3 (Page 1)
2.5.4.4-4B	Boring Profile – EB-3 (Page 2)
2.5.4.4-4C	Boring Profile – EB-3 (Page 3)
2.5.4.4-5A	Boring Profile – EB-8/EB-8G (Page 1)
2.5.4.4-5B	Boring Profile – EB-8/EB-8G (Page 2)
2.5.4.4-6	Crosshole Vs and P-S Vs Comparison, NB-1
2.5.4.4-7	P- and S- Wave Comparison for Crosshole and P-S Suspension Techniques, NB-8
2.5.4.4-8	Velocity Comparison P-S and Downhole, NB-1
2.5.4.5-1	Conceptual Lateral Limits of Excavation
2.5.4.5-2	Conceptual Excavation Section A-A'
2.5.4.6-1	ESP Site Observation Well Locations
2.5.4.6-2	Conceptual Dewatering Plan Well Locations
2.5.4.6-3	Drawdowns in Fill After One Year of Dewatering
2.5.4.6-4	Drawdowns in Vincentown Formation After One Year
2.5.4.6-5	Drawdowns in Fill After One Year and Structure Locations
2.5.4.6-6	Drawdowns in Vincentown Formation After One Year and Structure Locations

**PSEG Site
ESP Application
Part 2, Site Safety Analysis Report**

LIST OF FIGURES (CONTINUED)

<u>Number</u>	<u>Title</u>
2.5.4.7-1A	Boring Profile – NB-1 (Page 1)
2.5.4.7-1B	Boring Profile – NB-1 (Page 2)
2.5.4.7-1C	Boring Profile – NB-1 (Page 3)
2.5.4.7-2A	Boring Profile – NB-8 (Page 1)
2.5.4.7-2B	Boring Profile – NB-8 (Page 2)
2.5.4.7-3A	Boring Profile – EB-3 (Page 1)
2.5.4.7-3B	Boring Profile – EB-3 (Page 2)
2.5.4.7-3C	Boring Profile – EB-3 (Page 3)
2.5.4.7-4A	Boring Profile – EB-8/EB-8G (Page 1)
2.5.4.7-4B	Boring Profile – EB-8/EB-8G (Page 2)
2.5.4.7-5A	Slope Plot for Depth vs Travel Time (Page 1)
2.5.4.7-5B	Slope Plot for Depth vs Travel Time (Page 2)
2.5.4.7-5C	Slope Plot for Depth vs Travel Time (Page 3)
2.5.4.7-5D	Slope Plot for Depth vs Travel Time (Page 4)
2.5.4.7-6A	Velocity Layer Comparison to Data
2.5.4.7-6B	Velocity Layer Comparison to Data
2.5.4.7-6C	Velocity Layer Comparison to Data
2.5.4.7-6D	Velocity Layer Comparison to Data
2.5.4.7-7	Shear Wave Velocities Aligned to Navesink Formation
2.5.4.7-8a	Dynamic Profile – Shear Wave Velocity
2.5.4.7-8b	Dynamic Profile – Comprehensive Wave Velocity
2.5.4.7-9	Basement Contours
2.5.4.7-10	Summit Site Location Map

**PSEG Site
ESP Application
Part 2, Site Safety Analysis Report**

LIST OF FIGURES (CONTINUED)

<u>Number</u>	<u>Title</u>
2.5.4.7-11	Correlation Cross-Section
2.5.4.7-12	Delmarva Velocity Profile 1
2.5.4.7-13	Delmarva Velocity Profile 2
2.5.4.7-14	Correlation of Summit Site Velocity Layering to Regional Stratigraphy
2.5.4.7-15	Summit Site Velocity Layers
2.5.4.7-16	Oyo Suspension Logger Shear Wave Measurements at Savannah River Site
2.5.1.7-17	Shear Modulus Reduction Curves and RCTS Data at In-Situ Confining Stress
2.5.4.7-18	Damping Ratio Curves and RCTS Data at In-Situ Confining Stress
2.5.4.7-19	Shear Modulus Reduction Curves and RCTS Data at Four Times In-Situ Confining Stress
2.5.4.7-20	Damping Ratio Curves and RCTS Data at Four Times In-Situ Confining Stress
2.5.4.7-21	Computed Modulus Reduction Curve Layer A
2.5.4.7-22	Computed Damping Variation Curve Layer A
2.5.4.7-23	Computed Modulus Reduction Curve Layer B
2.5.4.7-24	Computed Damping Variation Curve Layer B
2.5.4.7-25	Computed Modulus Reduction Curve Layer C
2.5.4.7-26	Computed Damping Variation Curve Layer C
2.5.4.7-27	Computed Modulus Reduction Curve Layer D
2.5.4.7-28	Computed Damping Variation Curve Layer D
2.5.4.8-1	Potential Impact of Liquefaction Outside Excavation Support
2.5.5-1	Approximate Site Fill Boundaries
2.5.5-2	General Section A-A' Slope Configuration

**PSEG Site
ESP Application
Part 2, Site Safety Analysis Report**

CHAPTER 2

SITE CHARACTERISTICS AND SITE PARAMETERS

2.0 SITE CHARACTERISTICS

Chapter 2 describes the characteristics of the PSEG Site. The site location, characteristics, and site-related design parameters, as described in the following sections, are provided in sufficient detail to support a safety assessment of the proposed site:

- Geography and Demography (Section 2.1)
- Identification of Potential Hazards in Site Vicinity (Section 2.2)
- Meteorology (Section 2.3)
- Hydrology (Section 2.4)
- Geology, Seismology, and Geotechnical Engineering (Section 2.5)

Table 2.0-1 presents a representative list of characteristics that describe the PSEG Site. The listing presented in Table 2.0-1 does not include all of the characteristics developed in Chapter 2.

**PSEG Site
ESP Application
Part 2, Site Safety Analysis Report**

**Table 2.0-1 (Sheet 1 of 9)
PSEG Site Characteristics**

Site Characteristic		PSEG Site Value	SSAR Section	Definition
Geography and Demography				
Exclusion Area Boundary		The EAB is a circle at least 600 meters (1968 feet) from the edge of the power block area in all directions.	2.1.1.2	The area surrounding the reactor(s), in which the reactor licensee has the authority to determine all activities, including exclusion or removal of personnel and property from the area.
Low Population Zone		The area falling within a 5-mile radius circle from the PSEG Site New Plant Site Center.	2.1.3.4	The area immediately surrounding the exclusion area that contains residents.
Population Center Distance		14.8 mi. (Wilmington, DE)	2.1.3.5	The distance from the reactor to the nearest boundary of a densely populated center containing more than about 25,000 residents.
Identification of Potential Hazards in Site Vicinity				
External Hazards on Plant SSCs		Refer to Subsection 2.2.3	2.2.3	Identification and evaluation of potential accident situations in the vicinity of the plant.
Meteorology				
Ambient Air Temperature and Humidity				
Maximum Dry-Bulb Temperature	2% annual exceedance	88°F (DBT) 73°F (MCWB)	Table 2.3-14	The ambient dry-bulb temperature (and mean coincident wet-bulb temperature) that will be exceeded 2% of the time annually.
	1% annual exceedance	90°F (DBT) 75°F (MCWB)	Table 2.3-14	The ambient dry-bulb temperature (and mean coincident wet-bulb temperature) that will be exceeded 1% of the time annually.
	0.4% annual exceedance	93°F (DBT) 76°F (MCWB)	Table 2.3-14	The ambient dry-bulb temperature (and mean coincident wet-bulb temperature) that will be exceeded 0.4% of the time annually.

**PSEG Site
ESP Application
Part 2, Site Safety Analysis Report**

**Table 2.0-1 (Sheet 2 of 9)
PSEG Site Characteristics**

Site Characteristic		PSEG Site Value	SSAR Section	Definition
	0% annual exceedance (record)	108°F (DBT) 79°F (MCWB)	2.3.1.7	The highest recorded ambient dry-bulb temperature and mean coincident wet-bulb temperature
	100-year return period	105.9°F (DBT) 82.4°F (MCWB)	Table 2.3-13 2.3.1.7	The ambient dry-bulb temperature (and mean coincident wet-bulb temperature) that has a 1% annual probability of being exceeded (100-year mean recurrence interval).
Minimum Dry-Bulb Temperature	99% annual exceedance	14°F	Table 2.3-14	The ambient dry-bulb temperature below which dry-bulb temperatures will fall 1% of the time annually.
	99.6% annual exceedance	10°F	Table 2.3-14	The ambient dry-bulb temperature below which dry-bulb temperatures will fall 0.4% of the time annually.
	100% annual exceedance (record)	-15°F	2.3.1.7	Lowest recorded dry-bulb temperature.
	100-year return period	-18.7°F	Table 2.3-13	The ambient dry-bulb temperature for which a 1% annual probability of a lower dry-bulb temperature exists (100-year mean recurrence interval).
Maximum Wet-Bulb Temperature	1.0% annual exceedance	77°F	Table 2.3-14	The ambient wet-bulb that will be exceeded 1.0% of the time annually.
	0.4% annual exceedance	79°F	Table 2.3-14	The ambient wet-bulb that will be exceeded 0.4% of the time annually.

**PSEG Site
ESP Application
Part 2, Site Safety Analysis Report**

**Table 2.0-1 (Sheet 3 of 9)
PSEG Site Characteristics**

Site Characteristic		PSEG Site Value	SSAR Section	Definition
	0% annual exceedance (record)	86.2°F	Table 2.3-13	Highest recorded wet-bulb temperature.
	100-year return period	87.4°F	Table 2.3-13	The ambient wet-bulb temperature that has a 1% annual probability of being exceeded (100-year mean recurrence interval).
UHS Ambient Air Temperature and Humidity				
Meteorological Conditions Resulting in the Minimum Water Cooling During any 1 Day		82.69°F WBT 87.12°F DBT	2.3.1.6	Historic worst 1-day daily average wet-bulb temperature and coincident dry-bulb temperature.
Meteorological Conditions Resulting in the Minimum Water Cooling During any Consecutive 5 Days		78.02°F WBT 83.47°F DBT	2.3.1.6	Historic worst 5-day daily average wet-bulb temperature and coincident dry-bulb temperature.
Meteorological Conditions Resulting in the Maximum Evaporation and Drift Loss During any Consecutive 30 Days		75.87°F WBT 82.65°F DBT	2.3.1.6	Historic worst 30-day daily average wet-bulb temperature and coincident dry-bulb temperature.
Basic Wind Speed				
3-Second Gust		117.7 mph	2.3.1.5.1	The nominal 3-second gust wind speeds in miles per hour (mph) at 33 ft. above ground associated with a 100-year return period.
Importance Factors		1.15	2.3.1.5.1	Multiplication factor applied to basic wind speed used to assess wind impacts on structures.

**PSEG Site
ESP Application
Part 2, Site Safety Analysis Report**

**Table 2.0-1 (Sheet 4 of 9)
PSEG Site Characteristics**

Site Characteristic	PSEG Site Value	SSAR Section	Definition
Hurricane			
Hurricane Wind Speed	159 mph	2.3.1.5.3	Maximum nominal 3-second gust wind speed at 33 ft. above ground over open terrain having a probability of exceedance of 10^{-7} per year.
Tornado			
Maximum Wind Speed	200 mph	Table 2.3-5	Maximum wind speed resulting from passage of a tornado having a probability of occurrence of 10^{-7} per year.
Maximum Translational Speed	40 mph	Table 2.3-5	Translation component of the maximum tornado wind speed.
Maximum Rotational Speed	160 mph	Table 2.3-5	Rotation component of the maximum tornado wind speed.
Radius of Maximum Rotational Speed	150 ft.	Table 2.3-5	Distance from the center of the tornado at which the maximum rotational wind speed occurs.
Maximum Pressure Drop	0.9 psi	Table 2.3-5	Decrease in ambient pressure from normal atmospheric pressure resulting from passage of the tornado.
Rate of Pressure Drop	0.4 psi/sec	Table 2.3-5	Rate of pressure drop resulting from the passage of the tornado.
Winter Precipitation			
100-year Snowpack	24 lb/ft ²	2.3.1.5.4	The weight of the 100-year return period snowpack (to be used in determining normal precipitation loads for roofs).
48-hour Probable Maximum Winter Precipitation	21 inches of water	2.3.1.5.4	PMP during the winter months (to be used in conjunction with the 100-year snowpack in determining extreme winter precipitation loads for roofs).

**PSEG Site
ESP Application
Part 2, Site Safety Analysis Report**

**Table 2.0-1 (Sheet 5 of 9)
PSEG Site Characteristics**

Site Characteristic	PSEG Site Value	SSAR Section	Definition
Normal winter precipitation event	24 lb/ft ²	2.3.1.5.4	The highest ground-level weight (in lb/ft ²) among: (1) the 100-year return period snowpack; (2) the historical maximum snowpack; (3) the 100-year return period two-day snowfall event; or (4) the historical maximum two-day snowfall event in the site region. (to be used in determining the precipitation load for roofs)
Extreme frozen winter precipitation event	20.51 lb/ft ²	2.3.1.5.4	The highest of (1) the 100-year return period two-day snowfall event; and (2) the historical maximum snowfall event in the site region. (to be used in determining the precipitation load for roofs)
Short-Term (Accident Release) Atmospheric Dispersion			
0-2 hr χ/Q (EAB)	4.71×10^{-4} s/m ³	Table 2.3-30	The 0-2 hour atmospheric dispersion factor to be used to estimate dose consequences of accidental airborne releases at the EAB.
0-8 hr χ/Q (LPZ)	8.47×10^{-6} s/m ³	Table 2.3-30	The 0-8 hour atmospheric dispersion factor to be used to estimate dose consequences of accidental airborne releases at the LPZ.
8-24 hr χ/Q (LPZ)	5.50×10^{-6} s/m ³	Table 2.3-30	The 8-24 hour atmospheric dispersion factor to be used to estimate dose consequences of accidental airborne releases at the LPZ.
1-4 day χ/Q (LPZ)	2.15×10^{-6} s/m ³	Table 2.3-30	The 1-4 day atmospheric dispersion factor to be used to estimate dose consequences of accidental airborne releases at the LPZ.
4-30 day χ/Q (LPZ)	5.60×10^{-7} s/m ³	Table 2.3-30	The 4-30 day atmospheric dispersion factor to be used to estimate dose consequences of accidental airborne releases at the LPZ.
Long-Term (Normal Release) Atmospheric Dispersion			
Annual Average Undepleted/No Decay χ/Q Value @ Site Boundary, east-northeast, 0.24 mile	1.00×10^{-5} s/m ³	Table 2.3-34	The maximum annual average site boundary undepleted/no decay atmospheric dispersion factor (χ/Q) value for use in determining gaseous pathway doses to the maximally exposed individual.

**PSEG Site
ESP Application
Part 2, Site Safety Analysis Report**

**Table 2.0-1 (Sheet 6 of 9)
PSEG Site Characteristics**

Site Characteristic	PSEG Site Value	SSAR Section	Definition
Annual Average Undepleted/2.26-day Decay χ/Q Value @ Site Boundary, east-northeast, 0.24 mile	$1.00 \times 10^{-5} \text{ s/m}^3$	Table 2.3-34	The maximum annual average site boundary undepleted/2.26-day decay χ/Q value for use in determining gaseous pathway doses to the maximally exposed individual.
Annual Average Depleted/8.00-day Decay χ/Q Value @ Site Boundary, east-northeast, 0.24 mile	$9.50 \times 10^{-6} \text{ s/m}^3$	Table 2.3-34	The maximum annual average site boundary depleted/8.00-day decay χ/Q value for use in determining gaseous pathway doses to the maximally exposed individual.
Annual Average D/Q Value @ Site Boundary, east-northeast, 0.24 mile	$4.10 \times 10^{-8} \text{ 1/m}^2$	Table 2.3-34	The maximum annual average site boundary relative deposition factor (D/Q) value for use in determining gaseous pathway doses to the maximally exposed individual.
Annual Average Undepleted/No Decay χ/Q Value @ Nearest Resident, northwest, 2.8 mile	$2.40 \times 10^{-7} \text{ s/m}^3$	Table 2.3-34	The maximum annual average resident undepleted/no decay atmospheric dispersion factor (χ/Q) value for use in determining gaseous pathway doses to the maximally exposed individual.
Annual Average Undepleted/2.26-day Decay χ/Q Value @ Nearest Resident, northwest, 2.8 mile	$2.40 \times 10^{-7} \text{ s/m}^3$	Table 2.3-34	The maximum annual average resident undepleted/2.26-day decay χ/Q value for use in determining gaseous pathway doses to the maximally exposed individual.
Annual Average Depleted/8.00-day Decay χ/Q Value @ Nearest Resident, northwest, 2.8 mile	$1.90 \times 10^{-7} \text{ s/m}^3$	Table 2.3-34	The maximum annual average resident depleted/8.00-day decay χ/Q value for use in determining gaseous pathway doses to the maximally exposed individual.
Annual Average D/Q Value @ Nearest Resident, northwest, 2.8 mile	$9.60 \times 10^{-10} \text{ 1/m}^2$	Table 2.3-34	The maximum annual average resident relative deposition factor (D/Q) value for use in determining gaseous pathway doses to the maximally exposed individual.

**PSEG Site
ESP Application
Part 2, Site Safety Analysis Report**

**Table 2.0-1 (Sheet 7 of 9)
PSEG Site Characteristics**

Site Characteristic	PSEG Site Value	SSAR Section	Definition
Annual Average Undepleted/No Decay χ/Q Value @ Nearest Farm, northwest, 4.9 mile	$1.10 \times 10^{-7} \text{ s/m}^3$	Table 2.3-34	The maximum annual average farm undepleted/no decay atmospheric dispersion factor (χ/Q) value for use in determining gaseous pathway doses to the maximally exposed individual.
Annual Average Undepleted/2.26-day Decay χ/Q Value @ Nearest Farm, northwest, 4.9 mile	$1.10 \times 10^{-7} \text{ s/m}^3$	Table 2.3-34	The maximum annual average farm undepleted/2.26-day decay χ/Q value for use in determining gaseous pathway doses to the maximally exposed individual.
Annual Average Depleted/8.00-day Decay χ/Q Value @ Nearest Farm, northwest, 4.9 mile	$8.20 \times 10^{-8} \text{ s/m}^3$	Table 2.3-34	The maximum annual average farm depleted/8.00-day decay χ/Q value for use in determining gaseous pathway doses to the maximally exposed individual.
Annual Average D/Q Value @ Nearest Farm, northwest, 4.9 mile	$3.50 \times 10^{-10} \text{ 1/m}^2$	Table 2.3-34	The maximum annual average farm relative deposition factor (D/Q) value for use in determining gaseous pathway doses to the maximally exposed individual.
Hydrology			
Proposed Facility Boundaries	Figure 1.2-3 presents the proposed facility boundary.	2.1	PSEG Site boundary map.
Maximum Ground Water	10 ft. NAVD	2.4.12.5	The maximum elevation of groundwater at the PSEG Site.
Maximum Stillwater Flood Elevation (including 10 percent exceedance high tide)	24.7 ft. NAVD	Table 2.4.5-4	The stillwater elevation, without accounting for wind induced waves that the water surface reaches during a flood event.
Wave Runup	7.4 ft.	Table 2.4.5-4	The height of water reached by wind-induced waves running up on the site.
Combined Effects Maximum Flood Elevation	32.1 ft. NAVD	Table 2.4.5-4	The water surface elevation at the point in time where the combination of the still water level and wave runup is at its maximum.

**PSEG Site
ESP Application
Part 2, Site Safety Analysis Report**

**Table 2.0-1 (Sheet 8 of 9)
PSEG Site Characteristics**

Site Characteristic	PSEG Site Value	SSAR Section	Definition
Local Intense Precipitation	18.4 in/hr	Table 2.4.2-5	The depth of PMP for duration of one hour on a one square-mile drainage area. The surface water drainage system should be designed for a flood produced by the local intense precipitation.
Frazil, Surface or Anchor Ice	The PSEG Site has the potential for Frazil and Surface Ice.	2.4.7.1	Potential for accumulated ice formation in a turbulent flow condition.
Minimum River Water Surface Elevation	- 15.9 ft. NAVD for less than 6 hours	2.4.11.7	The river surface water elevation and duration for which the low water level conditions exist at the PSEG Site.
Site Grade	36.9 ft. NAVD	2.4.10	Finished plant grade for the power block area on the PSEG Site.
Maximum Ice Thickness	17.8 in.	2.4.11.3.3	Maximum potential ice thickness on the Delaware River at the PSEG Site.
Hydraulic Conductivity	Table 2.4.12-9	2.4.12	Groundwater flow rate per unit hydraulic gradient.
Hydraulic Gradient	Table 2.4.12-7 and 8	2.4.12	Slope of groundwater surface under unconfined conditions or slope of hydraulic pressure head under confined conditions.
Geology, Seismology, and Geotechnical Engineering			
Basic Geological and Seismic Information			
Capable Tectonic Structures	No capable tectonic structures within the site region.	2.5.1	The presence of a fault or structure capable of producing both tectonic surface deformation and earthquakes.
Vibratory Ground Motion			
Ground Motion Response Spectra (Site Safe Shutdown Earthquake)	Figure 2.5.2-54	2.5.2	Site specific response spectra.

**PSEG Site
ESP Application
Part 2, Site Safety Analysis Report**

**Table 2.0-1 (Sheet 9 of 9)
PSEG Site Characteristics**

Site Characteristic	PSEG Site Value	SSAR Section	Definition
Stability of Subsurface Materials and Foundations			
Liquefaction	Soils below the competent layer are not susceptible to liquefaction.	2.5.4.8	Liquefaction potential for the subsurface soils at a site.
Minimum Ultimate Bearing Capacity	420,000 psf	2.5.4.10	Load bearing capacity of the competent soil layer supporting the loads exerted by plant structures without soil failure.
Minimum Shear Wave Velocity	1613 ft/sec	Table 2.5.4.7-3	The minimum propagation velocity of shear waves through the foundation materials.

**PSEG Site
ESP Application
Part 2, Site Safety Analysis Report**

2.1 GEOGRAPHY AND DEMOGRAPHY

2.1.1 SITE LOCATION AND DESCRIPTION

2.1.1.1 Specification of Location

The new plant location is on the PSEG Site in Lower Alloways Creek Township, Salem County, New Jersey (NJ). The PSEG Site consists of 734 acres (ac.) of property located on the southern part of Artificial Island on the east bank of the Delaware River. PSEG Power, LLC and PSEG Nuclear, LLC (PSEG) are developing an agreement in principle with the U.S. Army Corps of Engineers (USACE) to acquire an additional 85 ac. immediately to the north of the existing site property as shown on Figure 1.2-3. Therefore, with the land acquisition, the PSEG Site will be 819 ac. The specific timing of land acquisition is not currently known and is subject to further PSEG and USACE actions. However, the agreement in principle with the USACE will serve to establish the basis for eventual land acquisition and Exclusion Area Boundary (EAB) control, necessary to support the issuance of a future combined license.

Artificial Island is connected to the mainland of NJ by a strip of tideland formed by hydraulic fill from dredging operations conducted by the USACE. The river area adjacent to the PSEG Site is in the Delaware River's Estuary Transition Zone. The site is situated within the Atlantic Coastal Plain Physiographic Province.

The PSEG Site is located 30 miles (mi.) southwest of Philadelphia, Pennsylvania, 15 mi. south of the Delaware Memorial Bridge, and 7-1/2 mi. southwest of Salem, New Jersey. The site location is shown on Figures 1.2-1 and 1.2-2, which identify major towns, roads, and other prominent features within 6 mi. and 50 mi., respectively, of the PSEG Site.

The nearest railroad to the PSEG Site, the Southern Railroad Company of New Jersey, is located 8.2 mi. to the northeast at its nearest point. The nearest highway, Delaware Route 9, is 3.1 mi. to the west, across the Delaware River from the PSEG Site. The nearest accessible highway, New Jersey Route 49, is 7.5 mi. to the northeast of the site. Land access to the site is limited to a road that PSEG constructed to connect its property with an existing secondary road 3.6 mi. to the east of the site. A new site access causeway is proposed to support construction and operation of the new plant.

2.1.1.2 Site Description and Site Map

The location selected for the new plant on the PSEG Site is north of the existing Hope Creek Generating Station (HCGS), as shown in Figure 1.2-3. The power block area, shown in Figure 1.2-3 bounds the area within which power block structures are located for each of the new reactor designs.

Figure 1.2-3 also shows the new plant center point, which is established by defining the locations of the reactor containment centerlines (or the mid-point between the containment centerlines of a dual unit plant) for the reactor technologies under consideration. The center point of the new plant is located at the centroid of these points. The coordinates of this center point are as follows:

**PSEG Site
ESP Application
Part 2, Site Safety Analysis Report**

Latitude and Longitude (NAD83)

39° 28' 23.744" North
75° 32' 24.332" West

Universal Transverse Mercator Coordinates (NAD83, Zone 18)

N14335392.324 ft.
E1488007.170 ft.

Figure 1.2-3 shows the new plant's proposed EAB, which is a circle at least 600 meters (1968 feet) from the edge of the power block area in all directions. A specific reactor design has not been selected, therefore Figure 1.2-3 does not show the location and orientation of principal plant structures for the new plant. It shows the boundaries of the power block area and theoretical plant center point within the power block area. The distance from these features to the site boundary and the proposed EAB can be scaled from Figure 1.2-3.

As shown in Figure 2.1-23 the proposed EAB extends beyond the PSEG Site property line to the west (into the Delaware River) and to the north and northeast. The total area encompassed by the EAB is 743 ac., of which 224 ac. is in the Delaware River and 288 ac. is in land currently owned by PSEG. An additional 85 ac. of land will be owned when PSEG completes property acquisition from the USACE as discussed in Subsection 2.1.1.1. The land within the EAB that will not be owned by PSEG consists of 146 ac. owned by the federal government. No public roads, railroads, or structures other than existing PSEG power plant facilities are located within any part of the EAB.

2.1.1.3 Boundaries for Establishing Effluent Release Limits

The land boundary, on which technical specification limits for release of gaseous radioactive effluents are based, is the PSEG Site property line shown in Figure 1.2-3. However, the χ/Q and D/Q values (Table 2.3-37) at the site boundary, adjacent to the Delaware River (sectors SE to NW in clockwise direction), are not considered in the associated analyses for radiological exposure due to routine gaseous effluents. This is acceptable because of the negligible time any individual is expected to spend in this area during any one-year period. The χ/Q and D/Q values that are considered in the associated analyses for radiological exposure due to the routine gaseous effluents are those in sectors NNW to ESE (clockwise direction). The distance from the new plant center point to the property line in any direction can be scaled from Figure 1.2-3. The minimum distance from the center point to the property line is 872 feet in the west direction.

2.1.2 EXCLUSION AREA AUTHORITY AND CONTROL

2.1.2.1 Authority

As discussed in Subsection 2.1.1.2, PSEG owns 288 ac. of the land within the proposed EAB for the new plant. PSEG has fee simple ownership, including mineral rights, of this land. In addition, PSEG is working with the USACE to develop an agreement in principle to acquire 85 ac. of land, including mineral rights, that will be within the proposed EAB. Therefore, when

**PSEG Site
ESP Application
Part 2, Site Safety Analysis Report**

property acquisition is complete PSEG will have ownership of 373 ac. of land within the proposed EAB as shown in Figure 2.1-23.

The only land area within the proposed EAB that will not be owned by PSEG is 146 ac. located to the north and northeast of the PSEG property line. This land is owned by the federal government and controlled by the USACE. PSEG will obtain legal authority from the USACE prior to the issuance of the COL that will either allow PSEG and its surrogates to determine all activities including exclusion or removal of personnel and property from the area or to insist that the USACE exercise that control in a specified manner. The agreement will specify that no residences are allowed within the Exclusion Area. Some public uses of the land may be allowed, but PSEG will acquire the ability to remove and exclude people.

Under the existing PSEG Site Radiological Emergency Response Plan, the U.S. Coast Guard (USCG) is responsible for warning people in boats, assisting in traffic control of boats, and notifying persons participating in swimming, fishing, and boating on the Delaware River in the site vicinity in the event of a radiological emergency. This agreement will be extended to address all open water areas within the proposed EAB for the new plant.

The USACE and USCG are the two primary agencies who interface with PSEG in establishing the control of the EAB. The USCG establishes control over the Delaware River portion of the EAB, while PSEG or the USACE controls the land area associated with the EAB that is not on PSEG's property. Other agencies, such as state and local police, fire departments, state and county emergency management agencies, etc., are active in the event of an Emergency Response situation and can be called upon to support the situation. Details of the Emergency Plan, including roles and responsibilities, are included in Part 5 of the ESPA. Emergency Response Support and Resources are presented in Section 4 of the Emergency Plan. Certification Letters and Memoranda of Understanding with offsite support agencies are presented in Attachments 2 and 3, respectively, of the Emergency Plan.

2.1.2.2 Control of Activities Unrelated to Plant Operation

The part of the proposed EAB that includes the Delaware River is sometimes used for boating, swimming, and/or fishing. The existing PSEG Site Security Plan provides for a maritime exclusion zone or "security zone" as described in 33 CFR Part 165, Subpart F, Section 165.553 around the existing power plant facilities. As part of developing the Site Security Plan, PSEG and the USCG will establish the specific boundaries and enforcement provisions of the extended maritime exclusion zone, and promulgate revisions to associated regulations regarding an extension to the "security zone" currently specified at 33 CFR Part 165, Subpart F, Section 165.553. A portion of the proposed EAB will be within this extended exclusion zone. Beyond the exclusion zone, no additional limitations are proposed for legal public use activities, maximum number of people, or maximum frequency of use in the open water portions of the EAB.

The land area of the proposed EAB includes a confined disposal facility (CDF) used by the USACE for the disposal of dredged material. The CDF currently stretches into the 85 acre parcel of land that PSEG intends to acquire from the USACE. After the land is acquired, this 85 acre parcel of land will be PSEG property and no longer used as a CDF, because structures associated with the power block and cooling towers will occupy this land. The northern portion of the CDF (labeled as Laydown and Batch Plant on Figure 1.2-3) will be returned to the

**PSEG Site
ESP Application
Part 2, Site Safety Analysis Report**

USACE after construction and potentially could continue to be used by the USACE as a CDF for dredge spoils. PSEG will develop notification provisions related to USACE use of the CDF that is within the EAB.

Access to the CDF by land is via the PSEG property from the existing site access road or the proposed causeway as shown on Figure 1.2-3. PSEG will allow USACE personnel vehicular access to the CDF north of the proposed site. During past usage of the CDF, access by water was generally made at the northern tip of the CDF, at a location outside of the EAB.

The USACE does not have a defined schedule for disposal of spoils in the CDF, nor do they delineate the number or kinds of persons who are engaged in the activity, the location of those persons, or the length of time the activity occurs. However, based on typical dredge spoils disposal activities conducted by the USACE at other sites, approximately five or less people would be present within the CDF during the dredging operation. A USACE representative inspects the CDF annually by traveling through the PSEG Site. Activities associated with the USACE CDF occur infrequently, and PSEG would maintain awareness of the CDF activities ongoing in the vicinity of the site.

The land area of the proposed EAB includes 146 acres of land that is owned by the federal government and controlled by the USACE. The USACE does not officially permit recreational use of this land; however, there are no physical barriers to prevent access. In the context of the EAB, PSEG considers the land to be accessible by the public for recreational use such as hunting and fishing during the respective seasons. There are no pre-established features (e.g., trails or launches) to enable access to this undeveloped land. Unauthorized recreational access to this land is by water via the Delaware River or, in a limited capacity, coastal salt marshes. The physical limitations on both access and the use result in infrequent use. PSEG will establish provisions for evacuation of this land in the agreements with the USACE, USCG, or other agencies.

Salem and Hope Creek have provisions to notify people in the EAB of the need to evacuate in an emergency. This includes sirens, plant page, and an agreement with the U.S. Coast Guard. Provisions will be established for the new plant similar to that of Salem and Hope Creek Generating Stations. These provisions provide reasonable assurance that the Exclusion Area can be evacuated in a manner that prevents radiation exposure in excess of guideline values.

2.1.2.3 Arrangements for Traffic Control

As discussed in Subsection 2.1.2.1, a small part of the Delaware River is within the proposed Exclusion Area, and the USCG is responsible for controlling traffic on the Delaware River in the event of an emergency. No other arrangements for traffic control are required, because no public roads, railways, or other waterways traverse the proposed Exclusion Area.

2.1.2.4 Abandonment or Relocation of Roads

There are no public roads to be abandoned or relocated in the proposed Exclusion Area.

**PSEG Site
ESP Application
Part 2, Site Safety Analysis Report**

2.1.2.5 Summary of Exclusion Area Authority and Control Issues

As discussed above, PSEG already owns 288 ac. of land within the proposed EAB for the new plant. PSEG will enter into the appropriate agreements to ensure the necessary authority and control over the remainder of the Exclusion Area. First, PSEG will complete the acquisition of 85 ac. of land, including mineral rights, from the USACE that is currently part of the confined disposal facility north of the site. Second, PSEG will modify the existing PSEG Site Radiological Emergency Response Plan and the existing PSEG Site Security Plan, and reach agreements with the USCG, to extend the protections for the Delaware River portion of the existing Salem and Hope Creek Exclusion Area to cover the Delaware River portion of the Exclusion Area related to the ESP. Third, PSEG will reach agreement with the USACE for any land within the EAB that will not be owned by PSEG to obtain legal authority from the USACE to either allow PSEG and its surrogates to determine all activities including exclusion or removal of personnel and property from the area or insist that the USACE exercise that control in a specified manner.

Consistent with the NRC regulations in 10 CFR Part 100, which applies the Exclusion Area requirements to "licensees," and Section 2.1.2 of the Standard Review Plan (NUREG-0800, Rev. 3), PSEG may enter into the agreements following issuance of an Early Site Permit. Consistent with the Standard Review Plan, PSEG proposes the following Permit Condition to require PSEG to notify the Nuclear Regulatory Commission staff when PSEG has acquired the required authority and control over the Exclusion Area and the basis for that conclusion.

PSEG will notify the Nuclear Regulatory Commission staff when PSEG has acquired the required authority and control over the Exclusion Area (no later than issuance of any combined license that references this ESP) and the basis for that conclusion, including the following agreements:

1. PSEG will complete the acquisition of 85 ac. of land, including mineral rights, from the USACE that is currently part of the confined disposal facility north of the site.
2. PSEG will modify the existing PSEG Site Radiological Emergency Response Plan and the existing PSEG Site Security Plan, and reach agreements with the USCG, to extend the protections for the Delaware River portion of the existing Salem and Hope Creek Exclusion Area to cover the Delaware River portion of the Exclusion Area related to the ESP.
3. PSEG will reach agreement with the USACE for any land within the EAB that will not be owned by PSEG to obtain legal authority from the USACE to either allow PSEG and its surrogates to determine all activities including exclusion or removal of personnel and property from the area or insist that the USACE exercise that control in a specified manner.

2.1.3 POPULATION DISTRIBUTION

This subsection describes the population distribution within 50 mi. of the PSEG Site. The characterization includes a description of the resident and transient populations from 0 to 10 mi. and from 10 to 50 mi. around the site. Population estimates are obtained from various sources including the U.S. Census Bureau (USCB). These estimates are used to develop population projections for the current year (2010), the expected first year of operation for the new plant

**PSEG Site
ESP Application
Part 2, Site Safety Analysis Report**

(2021), and 10-year increments over the potential operating life of the new plant (through 2081). The characterization also includes a description of the Low Population Zone (LPZ), the nearest population centers, and the population density within 30 mi. of the PSEG Site.

Using USCB 2000 census block data (Reference 2.1-9), population estimates are provided within the concentric bands from 0 to 1 mi., 1 to 2 mi., 2 to 3 mi., 3 to 4 mi., 4 to 5 mi., 5 to 10 mi., 10 to 20 mi., 20 to 30 mi., 30 to 40 mi., and 40 to 50 mi. for each of the sixteen directional sectors, with each directional sector consisting of 22.5 degrees. These distance bands and directional sectors for the 0 to 10 mi. and 10 to 50 mi. areas are shown in Figures 2.1-1 and 2.1-2, respectively. For each segment formed by a distance band and directional sector, the percentage of each census block's land area that fell, either completely or partially, within that segment is calculated using geographic information system (GIS) software ArcMap9.2 (Reference 2.1-15). The equivalent proportion of each census block's population is then assigned to each segment. If portions of two or more census blocks fell within the same segment, the proportional population estimates for each census block are summed to obtain the population estimate for that segment.

The GIS baseline, which includes the population estimates distributed by segment, is used to develop projections of future populations. The 2010 populations are projected by using USCB growth rates for the 2000 through 2008 period (Reference 2.1-16). From 2010 onward, population growth rates are derived from county population projections developed by the states of Delaware, Maryland, New Jersey, and Pennsylvania. New Jersey (Reference 2.1-6) has published population projections out to 2025, while Delaware (Reference 2.1-1), Maryland (Reference 2.1-4), and Pennsylvania (Reference 2.1-7) have published population projections out to 2030. The county population growth rates derived from these projections are used to extrapolate the baseline 2010 projections out to 2021 and 2031 for appropriate counties within each of the four states. No official published data were found that could be applied beyond the 2031 projections. Population projections beyond 2031 are based on the county-specific annual growth rate calculated for each county between 2021 and 2031. The county-specific growth rates for this 10-year period are used to obtain the population projections for each successive 10-year period (2041, 2051, 2061, 2071 and 2081).

2.1.3.1 Resident Population within 10 Miles

Resident population data are calculated for each directional sector for the 0 to 1 mi., 1 to 2 mi., 2 to 3 mi., 3 to 4 mi., 4 to 5 mi., and 5 to 10 mi. distances from the PSEG Site. The resultant population distributions are summarized in Table 2.1-1 by distance and by year. Based on 2000 census data, 33,871 people are estimated to reside within 10 mi. of the site. No population exists within 2 mi. of the site, and an estimated 75 individuals reside within 2 to 3 mi.

Using the population projection methodology described above to determine future populations, the population within 10 mi. of the PSEG Site is expected to increase to 42,743 in 2010, 45,527 in 2021 (first year of plant operation), and 60,892 in 2081 (end of plant operating life).

Figure 2.1-3 shows only the resident population in each distance band and directional sector within 10 mi. of the PSEG Site based on year 2000 census data. Reliable transient population data for the year 2000 is not available. Figures 2.1-4 through 2.1-11 show the projected resident population plus transient population (Subsection 2.1.3.3) in each distance band and directional sector within 10 mi. of the PSEG Site for the years 2010 through 2081.

**PSEG Site
ESP Application
Part 2, Site Safety Analysis Report**

2.1.3.2 Resident Population between 10 and 50 Miles

Resident population data are calculated for each of the sixteen directional sectors for the 10 to 20 mi., 20 to 30 mi., 30 to 40 mi., and 40 to 50 mi. distances from the PSEG Site. The resultant population distributions are summarized in Table 2.1-2 by distance and by year. Based on 2000 census data, an estimated 5,230,454 residents are located within 50 mi. of the PSEG Site, of which an estimated 5,196,583 people reside between 10 and 50 mi. from the site. Less than 1 percent of the regional population (the population within 50 mi.) resides within 10 mi. of the site.

Using the population projection methodology described above to determine future populations, the population between 10 and 50 mi. from the PSEG Site is projected to increase to 5,418,212 in 2010, 5,760,985 in 2021, and 8,077,743 in 2081.

Figures 2.1-12 through 2.1-20 show the resident population in each distance band and directional sector between 10 and 50 mi. from the PSEG Site for the years 2000 through 2081.

2.1.3.3 Transient Population

2.1.3.3.1 Transient Population within 10 Miles

In addition to the permanent residents within 10 mi. of the PSEG Site, there are people that enter this area on a regular basis for employment, education (schools and daycare), recreation (parks, wildlife areas, resorts, beaches, and associated lodging and restaurants), and medical care (hospitals and assisted living). These transient populations are based primarily on 2009 surveys conducted by KLD Engineering (Reference 2.1-2). The surveys conducted by KLD Engineering are part of the ongoing emergency evacuation planning for the new plant. Based on these surveys, Table 2.1-3 provides the sources of transient populations within 10 miles of the PSEG Site and provides estimated populations for 2008. Transient populations are assumed to grow at the same rate as resident populations. Projected transient populations in each distance band for 2010 through 2081 are provided in Table 2.1-4. The total transient population within 10 mi. is projected to be 12,549 in 2010, increasing to 13,378 in 2021 and 18,063 in 2081.

Although Tables 2.1-3 and 2.1-4 do not identify any transient populations within 3 mi. of the PSEG Site, the area within 3 mi. is used infrequently for recreational purposes such as hunting, fishing, and boating. Much of this recreational use is concentrated in Mad Horse Creek Wildlife Management Area (in New Jersey) and in Cedar Swamp and Augustine Wildlife Management Areas (in Delaware). Portions of these Wildlife Management Areas fall within the 3 mi. radius, but the main access points are beyond 3 mi. The Wildlife Management Areas provide very limited land access to areas beyond the main access points. The daily usage data collected at these points reflect where most of the recreational transient population is located. Therefore, transient populations in the Cedar Swamp and Augustine Wildlife Management Areas are shown in the 3 to 4 mi. and 4 to 5 mi. bands in Tables 2.1-3 and 2.1-4. Transient populations for the Mad Horse Creek Wildlife Management Area are shown in the 5 to 10 mi. band.

**PSEG Site
ESP Application
Part 2, Site Safety Analysis Report**

2.1.3.3.2 Transient Population between 10 and 50 Miles

The major employment centers located between 10 and 50 mi. from the PSEG Site are shown in Table 2.1-5. These major employment centers include Philadelphia, which is the core of the Philadelphia Standard Metropolitan Statistical Area, as well as subregional centers such as Camden, Vineland, Millville, and Bridgeton, New Jersey; and Wilmington, Newark, and Dover, Delaware. The estimated total 2008 employment for the metropolitan areas that include these centers is 1,676,400, as shown in Table 2.1-5.

Philadelphia generates the largest student population in the area due to a concentration of major colleges and universities. Students at colleges and universities are counted in the USCB census as year-round residents in their place of residence in February and March. Therefore, virtually all students are considered permanent, not transient, persons.

Major public recreation areas located between 10 and 50 mi. from the PSEG Site are shown in Table 2.1-6. Independence National Historical Park in Philadelphia generates the largest number of annual visitors, followed by Valley Forge National Historical Park in Pennsylvania. The total annual visitors for these recreation areas are 5,814,971 as shown in Table 2.1-6.

Other potentially significant sources of transient population between 10 and 50 mi. from the PSEG Site include Christiana Mall, a shopping mall located in Newark, Delaware, that reports approximately 17,000,000 annual visitors; and Delaware Park, a casino and racetrack located in Wilmington, Delaware, that reports approximately 2,900,000 annual visitors.

2.1.3.4 Low Population Zone

The proposed LPZ consists of a 5 mi. radius around the center point of the new plant as shown in Figure 2.1-21. This area is dominated by the open waters of Delaware Bay and low coastal wetlands to the east and west of the bay. Much of these coastal wetlands are under state ownership and managed as wildlife areas that are protected from future development. Additionally, most of the land on the New Jersey side within 2 mi. of the new plant center point is owned by PSEG, the USACE, or the New Jersey Department of Environmental Protection. Most of the privately owned land within the LPZ is managed for agricultural production and/or private access hunting/fishing.

Figure 2.1-21 shows the projected 2010 resident population in each distance band and directional sector within the LPZ. The projected 2010 resident population within the LPZ is 2047 people. Figure 2.1-21 also shows the locations of the facilities and institutions listed in Table 2.1-7, as well as the locations of existing public roads within the LPZ. All of these roads potentially could be used for evacuation purposes.

Table 2.1-7 lists facilities and institutions identified within the LPZ. The directional sector, distance from the new plant center point, and associated 2008 peak transient populations are also shown in Table 2.1-7. It can be seen that the total 2008 peak transient population within the LPZ is estimated to be 260 people, almost all of whom are associated with recreation areas. One small day care facility, located 4.8 mi. from the plant center point, contributes seven students and two employees to the transient population. As discussed in Subsection 2.1.3.3.1, portions of Mad Horse Creek Wildlife Management Area are within the LPZ, but transient population use is concentrated beyond the LPZ.

**PSEG Site
ESP Application
Part 2, Site Safety Analysis Report**

Combining the projected 2010 resident and transient populations within the LPZ (from Tables 2.1-1 and 2.1-4, respectively) provides the totals shown below.

Projected 2010 Population in the Low Population Zone						
Type of Population	Distance in Miles					Total
	0 to 1	1 to 2	2 to 3	3 to 4	4 to 5	0 to 5
Resident	0	0	82	600	1365	2047
Transient	0	0	0	166	98	264
Total	0	0	82	766	1463	2311

2.1.3.5 Population Center

A list of the population centers (defined in 10 CFR 100.3 as densely populated communities containing more than about 25,000 residents) located within 50 mi. of the PSEG Site is presented in Table 2.1-8. The distance band, directional sector, 2000 census population, and 2007 estimated population are also shown in Table 2.1-8. While there are no population centers within 10 mi. of the site, seventeen population centers exist within 10 to 50 mi. The nearest population center is the city of Wilmington, DE, with the nearest boundary 14.8 mi. north of the new plant center point. For this purpose, the population center boundary is based on the corporate boundary of the city of Wilmington as identified in USCB GIS population data.

As shown in Table 2.1-8, Wilmington had an estimated population of 72,868 people in 2007. The next closest population centers are Newark, DE, with an estimated 2007 population of 29,992, and Dover, DE, with an estimated 2007 population of 35,811. The nearest boundary of Newark is 15.9 mi. northwest, and the nearest boundary of Dover is 18.1 mi. south of the new plant center point. The town of Bridgeton, NJ, has an estimated 2007 population of 24,575, and therefore may be considered a population center per the 10 CFR 100.3 definition of "about 25,000 residents". The nearest boundary of Bridgeton is 15.5 mi. east of the new plant center point. All of the population center distances discussed in this paragraph are based on the corporate boundaries as identified in USCB GIS population data.

Nuclear facility siting criteria (10 CFR 100.21) require that the boundary of the nearest population center must be at least one and one-third times the distance from the center of the reactor to the LPZ boundary. For the PSEG Site, one and one-third times the distance from the new plant center point to the proposed LPZ boundary is 6.7 mi. Given that the boundary of the nearest population center (Wilmington, DE) is 14.8 mi. from the new plant center point, the PSEG Site complies with the 10 CFR 100.21 siting requirement.

NUREG-0800, *Standard Review Plan for the Review of Safety Analysis Reports for Nuclear Power Plants: LWR Edition*, states that communities that are closer than the design population center should be evaluated to determine the likelihood that their population will grow to greater than 25,000 people within the lifetime of the proposed plant. An examination of Figure 2.1-11 shows that none of the segments within 10 miles have a projected resident and transient population in 2081 that exceeds the 25,000 people criteria. The only segment that approaches the 25,000 criterion is the segment west of the PSEG Site from 5 to 10 miles. This segment includes the town of Middletown, DE, which also extends somewhat into the west-southwest sector between 5 and 10 miles and into both the west and west-southwest sectors beyond 10 miles. Middletown appears to be the only community within 10 miles of the site that has the

**PSEG Site
ESP Application
Part 2, Site Safety Analysis Report**

potential to reach “about 25,000 residents” within the lifetime of the new plant. Therefore, the potential future population and population boundaries of the Middletown area were examined in greater detail.

The Middletown Comprehensive Plan (Reference 2.1-17) reports a 2005 population estimate of “10,000 or more” and describes rapid population growth in recent years. Based on analysis of local residential permit activity and assumptions about the average household size, the Middletown Comprehensive Plan includes the projection that the population will range between 23,000 and 33,000 residents by the year 2020. Therefore, it appears likely that Middletown will reach a population of “about 25,000 residents” within the lifetime of the new plant. Middletown will then become the nearest population center to the PSEG Site.

Based on the corporate boundaries delineated in USCB GIS map data, the nearest boundary of Middletown is approximately 7.0 miles west of the new plant center point. This nearest boundary location is on the west side of State Route 1, a controlled-access divided highway that separates Middletown from areas farther east and nearer to the PSEG Site. The Middletown Comprehensive Plan indicates that there are no plans for the town to annex land or otherwise expand to the east of State Route 1. Population growth east of State Route 1 will be controlled by the New Castle County Unified Development Code (Reference 2.1-18) and associated zoning districts. An analysis of the zoning districts indicates that allowable housing densities in the areas of New Castle County east of State Route 1 are significantly lower than the density in the town of Middletown. Therefore, population densities east of State Route 1 are expected to remain significantly below the density in the town of Middletown for the foreseeable future. This information indicates that the Middletown corporate boundary location on the west side of State Route 1 is the appropriate location to use in measuring the distance to the nearest future population center boundary. As stated above, this location is approximately 7.0 miles west of the new plant center point, which complies with the 10 CFR 100.21 siting requirement.

2.1.3.6 Population Density

Future population projections and ArcMap9.2 are used to determine population density characteristics around the PSEG Site. Figure 2.1-22 provides a graphical representation of the cumulative population within 30 mi. of the site, based on the 2010, 2021 (first year of operation), 2061 (end of normal license period), and 2081 (end of plant life) population projections. These population projections are compared to hypothetical cumulative populations based on population densities of 500 and 1000 people per sq. mi.

USNRC Regulatory Guide (RG) 1.70 states that the residential population density within 30 mi. of a proposed plant site should be compared to a density of 500 people per sq. mi. for the initial year of plant operation and 1000 people per sq. mi. for the last year of plant operation. As shown in Figure 2.1-22, the projected population density in 2021 is comparable to 500 people per sq. mi. for the entire distance out to 30 mi. from the PSEG Site. At 20 mi. the projected 2021 residential population density is 497 people per sq. mi., and at 30 mi. the projected 2021 residential population density is 508 people per sq. mi. Figure 2.1-22 also shows that the projected population density in 2061 and 2081 is well below 1000 people per sq. mi. for the entire area out to 30 mi. from the PSEG Site. At 30 mi. the projected 2081 population density is 782 people per sq. mi.

**PSEG Site
ESP Application
Part 2, Site Safety Analysis Report**

RG 4.7 and NUREG-0800 recommend that the population density including weighted transient populations, at all radial distances within 20 mi. of a proposed plant site not exceed 500 people per sq. mi. at the time of initial site approval and 5 years thereafter. For the PSEG Site, the expected year of initial site approval is expected to be 2013, and the year 5 years after the initial site approval is expected to be 2018. Consistent with RG 4.7, transient populations identified within 20 mi. of the PSEG Site are weighted according to the percentage of each day the populations could reasonably be expected to be present in the area, and these weighted populations are added to the residential populations projected for 2013 and 2018. The resulting population density at 20 mi. from the PSEG Site is 477 people per sq. mi. in 2013 and 494 people per sq. mi. in 2018. As illustrated in Figure 2.1-22, the population density is lower at all distances closer to the site than at 20 mi.; therefore, it is clear that all radial distances within 20 mi. comply with the RG 4.7/NUREG-0800 guideline for the years 2013 and 2018.

Although the 2013 and 2018 population densities, including weighted transient populations, are below 500 people per sq. mi. at all radial distances out to 20 mi., the 2018 density at 20 mi. approaches the criteria provided in RG 4.7 and NUREG-0800. Given that the population density is close to the criteria, PSEG did consider population density in the Alternative Site Evaluation performed in support of the siting determination for the Early Site Permit effort. As reported in Part 3 of the PSEG ESP application, Environmental Report, Section 9.3, the PSEG Site was selected as the Proposed Site on the basis of a comprehensive site selection study as summarized below.

The PSEG Site was one of five Candidate Sites evaluated in detail through both numerical scoring and qualitative evaluations. The numerical scoring covered 40 site characteristics related to nuclear licensing issues, environmental issues, and engineering and economic issues. These numerical scores were summed both in an unweighted form and with weighting factors based on judgments about the relative importance of the site characteristics. The PSEG Site had the highest total scores with both weighted and unweighted scoring. In addition, the PSEG Site had the highest scores on environmental issues, and the second-highest scores for both nuclear licensing issues and engineering/cost issues. No other Candidate Site ranked among the top two sites in all three categories.

In addition to the numerical scoring, PSEG considered several qualitative factors related to the site location. On the basis of this evaluation, the PSEG Site was found to have important advantages compared with the other Candidate Sites, including the following:

- The lowest existing population density in the probable Low Population Zone area, and limited risk of substantial future population growth in the Low Population Zone due to surrounding land use and land cover conditions.
- Abundant existing site data and regulatory knowledge, including detailed geology and seismic data.
- Favorable security considerations, including opportunities for an integrated security strategy and protected area in common with the existing Salem and Hope Creek reactors.
- Existing emergency management infrastructure and support agreements with the states of New Jersey and Delaware, and with Salem and Cumberland counties in New Jersey and

**PSEG Site
ESP Application
Part 2, Site Safety Analysis Report**

New Castle County in Delaware. Existing emergency plans can be used as necessary, and a consistent Emergency Planning Zone can be maintained.

- Significant community and key stakeholder support in Lower Alloways Creek Township and Salem County, New Jersey.
- Minimal community and regional disruptions associated with new transmission lines, pipelines, and road and rail systems as compared with the other Candidate Sites.

In summary, the PSEG Site was selected as the Proposed Site because it was the highest-ranked site using objective numerical criteria and it has significant additional benefits related to the specific site location.

2.1.4 REFERENCES

- 2.1-1 The Delaware Population Consortium (DPC), Annual Population Projections Data Tables, Version 2008.0 (Excel), http://stateplanning.delaware.gov/information/dpc_projections.shtml, October 31, 2008, accessed May 18, 2009.
- 2.1-2 KLD Engineering, P.C., Salem and Hope Creek Nuclear Generating Stations, Development of Evacuation Time Estimates, Commack, New York, 2009.
- 2.1-3 Manta, profile based on data provided by Dun and Bradstreet accessed on June 11, 2009:
Air Liquide America LP <http://www.manta.com/company/mm77bp3>,
Autotype Holdings (USA), Inc. <http://www.manta.com/company/mm2s0m1>,
Delstar Technologies, Inc. <http://www.manta.com/company/mm29ctk>
Letica Corporation <http://www.manta.com/company/mmj9wv0>
Memorial Hospital of Salem County, Inc. http://www.manta.com/coms2/dnbcompany_dy11qv
- 2.1-4 Maryland State Data Center, 2009 Population Projections, Projections by Type for All Counties - Historic Census 1970 to 2000, Projected 2005 to 2030, Population Projections: XLS, http://www.mdp.state.md.us/msdc/dw_Popproj.htm, accessed May 18, 2009
- 2.1-5 National Park Service. Division of Economics U.S. Fish and Wildlife Service, "Banking on Nature 2004," September 2005. Division of Economics U.S. Fish and Wildlife Service, "Banking on Nature 2006," September 2007 Website, <http://www.nature.nps.gov/stats/>, accessed August 17, 2009.
- 2.1-6 New Jersey Department of Labor, Population & Labor Force Projections, Projections of Total Population by County: New Jersey, 2004 to 2025, <http://www.wnjp.inet/OneStopCareerCenter/LaborMarketInformation/Imi03/index.html>, accessed May 18, 2009.

**PSEG Site
ESP Application
Part 2, Site Safety Analysis Report**

- 2.1-7 Pennsylvania County Population Projections, 2000-2030, http://pasdc.hbg.psu.edu/pasdc/PA_Stats/estimates_and_projections/estimates.html, accessed May 18, 2009.
- 2.1-8 U.S. Census Bureau, 2008 TIGER/Line® Shapefiles, <http://www.census.gov/geo/www/tiger/tgrshp2008/tgrshp2008.html>, accessed May 05, 2009.
- 2.1-9 U.S. Census Bureau, Census 2000 Summary File 1 ASCII text data files, <http://www.census.gov/support/SF1ASCII.html>, accessed May 05, 2009.
- 2.1-10 U.S. Census Bureau, American Fact Finder, Lower Alloways Creek township, New Jersey – Population Finder, Website, <http://factfinder.census.gov/servlet/SAFFPopulation>, accessed June 8, 2009.
- 2.1-11 U.S. Census Bureau, Population Estimates, County Datasets, http://www.census.gov/popest/CO-EST2008-popchg2000_2008.html. Accessed County datasets for New Jersey, Delaware, Maryland and Pennsylvania accessed on May 15, 2009.
- 2.1-12 U.S. Census Bureau, 2008, Table 4: Annual Estimates of the Population for Incorporated Places in Delaware, Listed Alphabetically: April 1, 2000 to July 1, 2007 (SUB-EST2007-04-10). <http://census.gov/popest/cities/SUB-EST2007-04-10>, accessed on May 15, 2009.
U.S. Census Bureau, 2008, Table 4: Annual Estimates of the Population for Incorporated Places in New Jersey, Listed Alphabetically: April 1, 2000 to July 1, 2007 (SUB-EST2007-04-10). <http://census.gov/popest/cities/SUB-EST2007-04-34>, accessed on May 15, 2009.
U.S. Census Bureau, 2008, Table 4: Annual Estimates of the Population for Incorporated Places in Pennsylvania, Listed Alphabetically: April 1, 2000 to July 1, 2007 (SUB-EST2007-04-10). <http://census.gov/popest/cities/SUB-EST2007-04-42>, accessed on May 15, 2009.
- 2.1-13 U.S. Census Bureau, American Fact Finder, Bel Air North CDP, Maryland, Fact Sheet, 2005-2007 American Community Survey 3-Year Estimates, http://factfinder.census.gov/servlet/ACSSAFFFacts?_event=Search&geo_id=&_geoContext=&_street=&_county=Bel+Air+North+CDP&_cityTown=Bel+Air+North+CDP&_state=04000US24&_zip=&_lang=en&_sse=on&_pctxt=fph&_pgsl=010, accessed on May 15, 2009.
http://factfinder.census.gov/servlet/ACSSAFFFacts?_event=Search&geo_id=16000US2405950&_geoContext=01000US%7C04000US24%7C16000US2405950&_street=&_county=Essex&_cityTown=Essex&_state=04000US24&_zip=&_lang=en&_sse=on&_ActiveGeoDiv=geoSelect&_useEV=&_pctxt=fph&_pgsl=160&_submenuId=factsheet_1&ds_name=ACS_2007_3YR_SAFF&ci_nbr=null&qtr_name=null&req=null%3Anul&_keyword=&_industry=, accessed on May 15, 2009.
U.S. Census Bureau, American Fact Finder, Perry Hall CDP, Maryland, Fact Sheet, 2005-2007 American Community Survey 3-Year Estimates. http://factfinder.census.gov/servlet/ACSSAFFFacts?_event=Search&geo_id=16000US2426600&_geoContext=01000US%7C04000US24%7C16000US2426600&_street=

**PSEG Site
ESP Application
Part 2, Site Safety Analysis Report**

[=& county=Perry+Hall& cityTown=Perry+Hall& state=04000US24& zip=& lang=en
& sse=on&ActiveGeoDiv=geoSelect& useEV=&pctxt=fph&pgsl=160& submenuld=f
actsheet 1&ds name=ACS 2007 3YR SAFF& ci nbr=null&qtr name=null®=nul
l%3Anull& keyword=& industry=](#). Accessed on May 15, 2009.

U.S. Census Bureau, American Fact Finder, Drexel Hill CDP, Pennsylvania, Fact Sheet, 2005-2007 American Community Survey 3-Year Estimates.

[http://factfinder.census.gov/servlet/ACSSAFFFacts? event=&geo id=16000US4219
920& geoContext=01000US%7C04000US42%7C16000US4219920& street=& cou
nty=Drexel+Hill+Township& cityTown=Drexel+Hill+Township& state=04000US42&
zip=& lang=en& sse=on&ActiveGeoDiv=geoSelect& useEV=&pctxt=fph&pgsl=160
& submenuld=factsheet 1&ds name=null& ci nbr=null&qtr name=null®=null%3
Anull& keyword=& industry=](#). Accessed on May 15, 2009.

- 2.1-14 Bureau of Labor Statistics, Website, <http://www.bls.gov/sae/eetables/annav108.pdf>, accessed August 7, 2009.
- 2.1-15 Environmental Science Research Institute, ArcMap9.2 software, 2006.
- 2.1-16 U.S. Census Bureau, Geographical Comparison Tables, Population Estimates 2000 to 2008, by State and County, Website:
http://factfinder.census.gov/servlet/GCTGeoSearchByListServlet?ds_name=PEP_2008_EST& lang=en& ts=281556534886, accessed on June 8, 2009.
- 2.1-17 Institute for Public Administration, Town of Middletown Comprehensive Plan, adopted and certified November 2005
- 2.1-18 New Castle County Department of Land Use, Unified Development Code, <http://www.nccde.org/czo/acc/>, accessed on September 19, 2011

**PSEG Site
ESP Application
Part 2, Site Safety Analysis Report**

**Table 2.1-1
Resident Population Distribution within 10 Miles of the PSEG Site**

Year	Distance in Miles						
	0-1	1-2	2-3	3-4	4-5	5-10	Total 0-10
2000	0	0	75	562	1292	31,942	33,871
2010	0	0	82	600	1365	40,696	42,743
2021	0	0	85	642	1451	43,349	45,527
2031	0	0	91	670	1525	45,486	47,772
2041	0	0	96	701	1601	47,731	50,129
2051	0	0	99	731	1681	50,099	52,610
2061	0	0	105	764	1767	52,593	55,229
2071	0	0	110	797	1856	55,219	57,982
2081	0	0	117	835	1951	57,989	60,892

References 2.1-1, 2.1-4, 2.1-6, 2.1-7, 2.1-8, 2.1-9, and 2.1-11

**PSEG Site
ESP Application
Part 2, Site Safety Analysis Report**

**Table 2.1-2
Resident Population Distribution between 10 and 50 Miles of the PSEG Site**

Year	Distance in Miles					
	10-20	20-30	30-40	40-50	Total 10-50	Total 0-50
2000	495,708	663,385	1,839,777	2,197,713	5,196,583	5,230,454
2010	535,164	737,825	1,907,693	2,237,530	5,418,212	5,460,955
2021	579,362	811,029	2,024,369	2,346,225	5,760,985	5,806,512
2031	612,502	875,214	2,134,825	2,434,175	6,056,716	6,104,488
2041	648,433	946,388	2,257,452	2,530,748	6,383,021	6,433,150
2051	687,502	1,025,479	2,393,789	2,636,891	6,743,661	6,796,271
2061	730,126	1,113,552	2,545,595	2,753,673	7,142,946	7,198,175
2071	776,789	1,211,819	2,714,864	2,882,300	7,585,772	7,643,754
2081	828,052	1,321,698	2,903,867	3,024,126	8,077,743	8,138,635

References 2.1-1, 2.1-4, 2.1-6, 2.1-7, 2.1-8, 2.1-9, and 2.1-11

**PSEG Site
ESP Application
Part 2, Site Safety Analysis Report**

**Table 2.1-3
Transient Population within 10 Miles of the PSEG Site by Source of Transients**

Distance in Miles	2008 Population Estimate by Source					
	Employers	Lodging	Recreation (Parks, Resorts, Wildlife Areas, etc.)	Schools and Daycare	Medical Care (Hospitals and Assisted Living)	Totals
0-1	0	0	0	0	0	0
1-2	0	0	0	0	0	0
2-3	0	0	0	0	0	0
3-4	0	0	163	0	0	163
4-5	2	0	88	7	0	97
5-10	4144	121	2843	4114	603	11,825
0-10	4146	121	3094	4121	603	12,085
Delaware	2244	80	1899	3432	336	7991
New Jersey	1902	41	1195	689	267	4094

References 2.1-2 and 2.1-3

**PSEG Site
ESP Application
Part 2, Site Safety Analysis Report**

**Table 2.1-4
Transient Population Distribution within 10 Miles of the PSEG Site**

Year	Distance in Miles						
	0-1	1-2	2-3	3-4	4-5	5-10	Total 0-10
2010	0	0	0	166	98	12,285	12,549
2021	0	0	0	176	105	13,097	13,378
2031	0	0	0	183	109	13,765	14,057
2041	0	0	0	191	116	14,470	14,777
2051	0	0	0	199	122	15,212	15,533
2061	0	0	0	206	129	15,997	16,332
2071	0	0	0	215	136	16,824	17,175
2081	0	0	0	224	143	17,696	18,063

References 2.1-1 and 2.1-2

**PSEG Site
ESP Application
Part 2, Site Safety Analysis Report**

**Table 2.1-5
Employment in Major Economic Centers between 10 and 50 Miles of the PSEG Site**

Economic Center^(d)	State	Directional Sector	Distance Band (miles)	2008 Employment
Camden	NJ	NE	30 to 40	536,000
Dover-Kent County ^(b)	DE	S	20 to 30	65,400
Philadelphia	PA	NNE	30 to 40	662,500
Vineland-Millville-Bridgeton ^(c)	NJ	E	10 to 30	61,800
Wilmington-Newark ^(a)	DE	NNW	10 to 20	350,700
Total	-	-	-	1,676,400

a) Newark and Wilmington are not reported separately.

b) Dover is not reported separately from Kent County.

c) Vineland is not reported separately.

d) Values are reported from the Bureau of Labor Statistics and represent geographic areas larger than the jurisdictions listed.

Reference 2.1-14

**PSEG Site
ESP Application
Part 2, Site Safety Analysis Report**

**Table 2.1-6
Major Public Recreation Areas between 10 and 50 Miles of the PSEG Site**

Recreation Area	State	Directional Sector	Distance Band (miles)	Annual Visitors^(a)
Independence National Historical Park	PA	NNE	30 to 40	4,076,638
Valley Forge National Historical Park	PA	N	40 to 50	1,275,871
Bombay Hook National Wildlife Refuge	DE	SSE	10 to 20	119,500
Prime Hook National Wildlife Refuge	DE	SSE	40 to 50	106,525
John Heinz National Wildlife Refuge	PA	NNE	30 to 40	106,491
Eastern Neck National Wildlife Refuge	MD	SW	40 to 50	103,946
Cape May National Wildlife Refuge	NJ	ESE	40 to 50	26,000
Wharton State Forest	NJ	ENE	40 to 50	NA(b)
Belleplain State Forest	NJ	ESE	40 to 50	NA(b)
Total	--	--	--	5,814,971

a) Visitor numbers are for the most recent year for which statistics are available.
Visitor number for Bombay Hook National Wildlife Refuge represents the average annual number of visitors from 2008 through 2010.

b) "NA" indicates that statistics are not available.

Reference 2.1-5

**PSEG Site
ESP Application
Part 2, Site Safety Analysis Report**

**Table 2.1-7
Facilities and Institutions within the Low Population Zone**

Facility	State	Directional Sector	Distance (miles)	2008 Peak Daily Transient Population
Augustine Beach Boat Ramp	DE	NW	3.1	88
Augustine Wildlife Management Area	DE	NNW	3.6	50
Port Penn Interpretive Center	DE	NW	3.7	25
Cedar Swamp: Wildlife Management Area	DE	SW	4.1	58
Abbott's Meadow Wildlife Management Area	NJ	NE	4.4	10
Sugar & Spice Pre-School Day Care Center	NJ	ENE	4.8	7
Hancock House	NJ	ENE	4.9	20
Total	--	--	--	260

Reference 2.1-2

**PSEG Site
ESP Application
Part 2, Site Safety Analysis Report**

**Table 2.1-8
Population Centers (> 25,000 people) within 50 Miles of the PSEG Site**

Population Center	2000 Population Census	2007 Population Estimate	Distance Sector^(a)	Direction Sector
Bel Air North, MD	25,798	28,179	40 - 50	W
Bel Air South, MD	39,711	45,345	40 - 50	W
Bridgeton, NJ	22,771	24,575	10 - 20	E
Camden, NJ	79,904	78,675	30 - 40	NE
Chester, PA	36,854	36,695	20 - 30	NNE
Dover, DE	32,135	35,811	10 - 20	S
Drexel Hill, PA	29,364	30,036	30 - 40	NNE
Essex, MD	39,078	39,643	40 - 50	WSW
Millville, NJ	26,847	28,459	20 - 30	ESE
Newark, DE	28,547	29,992	10 - 20	NW
Norristown, PA	31,282	31,108	40 - 50	NNE
Pennsauken, NJ	35,737	35,116	40 - 50	NE
Perry Hall, MD	28,705	28,997	40 - 50	W
Philadelphia, PA	1,517,550	1,449,634	30 - 40	NNE
Radnor Township, PA	30,878	31,163	30 - 40	NNE
Vineland, NJ	56,271	58,505	20 - 30	E
Wilmington, DE	72,664	72,868	10 - 20	N

a) Distance Sector is to closest boundary of population centers

References 2.1-10, 2.1-12, and 2.1-13

**PSEG Site
ESP Application
Part 2, Site Safety Analysis Report**

2.2 IDENTIFICATION OF POTENTIAL HAZARDS IN SITE VICINITY

2.2.1 LOCATIONS AND ROUTES

The purpose of this section is to identify present and potential industrial, transportation, and military installations and operations within the vicinity of the PSEG Site. In accordance with Regulatory Guide (RG) 1.206, *Combined License Applications for Nuclear Power Plants (LWR Edition)*, Revision 0, 2007, all facilities and activities within 5 miles (mi.) are considered. Industrial, transportation, and military installations and operations beyond 5 mi. are included as appropriate to their significance.

The identified facilities and transportation routes within 5 mi. of the PSEG Site are:

- a. Industrial Facilities
 - Hope Creek Generating Station (HCGS)
 - Salem Generating Station (SGS) Units 1 & 2
 - Port Penn Sewage Treatment Plant
 - Lower Alloways Creek Township Buildings
- b. Transportation Routes
 - Alloway Creek Neck Road
 - Delaware Route 9
 - Quinton Hancocks Bridge Road
- c. Waterways
 - Delaware River
 - Alloway Creek
- d. Airports and Airways
 - Airway V123-312
 - Airway V29
 - Jet Route J42-150
 - Salem/Hope Creek Generating Station Helipad

The identified facilities and transportation routes between 5 and 10 mi. from the PSEG Site are:

- a. Industrial Facilities
 - Air Liquide
 - Anchor Glass Container Corporation
 - Cooper Interconnect
 - Delaware City Wastewater Treatment Plant
 - Formosa Plastics Corporation
 - Johnson Controls Inc. Battery Division

**PSEG Site
ESP Application
Part 2, Site Safety Analysis Report**

- Mannington Mills
- Quaker City Motor Parts/ NAPA Distribution Center
- Valero Delaware City Refinery

b. Pipelines

- Hazardous Liquid Pipeline
- Natural Gas Pipeline

c. Transportation Routes

- Delaware Route 1
- Delaware Route 299
- Delaware Route 72
- Delaware Route 7
- Delaware Route 71
- Delaware Route 896
- New Jersey Route 49
- New Jersey Route 45
- U.S. Route 13
- U.S. Route 301
- The Southern Railroad Company of NJ
- Norfolk Southern Railroad

d. Waterways

- Chesapeake and Delaware Canal
- Salem River

e. Airports and Airways

- Airway V157
- Airway V213
- Airway V214
- Hidden Acres Airport
- Jet Route J191
- Jet Route J51
- Okolona Plantation Airport
- Paruszewski Farm Strip Airport
- PSEG Training Center Heliport
- Salem Airport
- Scotty's Airport
- Stoe Creek Farm Airport
- Townsend Airport

**PSEG Site
ESP Application
Part 2, Site Safety Analysis Report**

Figure 2.2-1 is a site vicinity map that shows the location of the identified industrial and transportation facilities, with the exception of airports and airways, within 10 mi. of the PSEG Site. Figure 2.2-2 shows the airports and airways within 10 mi. of the PSEG Site.

2.2.2 DESCRIPTIONS

The following subsections describe the industrial, transportation, and military facilities identified within 5 mi. and beyond 5 mi. as appropriate to their significance.

2.2.2.1 Industrial Facilities

The industrial facilities identified are facilities that use, produce, or potentially transport chemicals within 5 mi. of the PSEG Site. Four facilities are identified within 5 mi. of the PSEG Site: HCGS, SGS, Port Penn Sewage Treatment Plant, and Lower Alloways Creek Township Buildings. Nine additional facilities are identified for review within 5 to 10 mi. Table 2.2-1 provides a concise description of these facilities, including the primary functions and chemicals that are used or produced, as well as the number of persons employed. The facilities identified within 5 mi. are described in the following subsections.

2.2.2.1.1 Hope Creek Generating Station

The centerline of the HCGS reactor building is located 1730 feet (ft.) south of the nearest point where power block structures are located for the new plant (the nearest edge of the power block area as shown in Figure 1.2-3). Surrounding the HCGS reactor building are operational support facilities, including chemical storage facilities. The HCGS chemicals identified for analysis and their locations are presented in Table 2.2-2a and Table 2.2-3.

2.2.2.1.2 Salem Generating Station

The centerline of the SGS Unit 1 reactor building is located 3249 ft. south of the nearest edge of the power block area for the new plant. The centerline of the SGS Unit 2 reactor building is located 2929 ft. south of the new plant power block area. Surrounding the reactor buildings are operational support facilities, including chemical storage facilities. The SGS chemicals identified for analysis and their locations are presented in Table 2.2-2b and Table 2.2-3.

2.2.2.1.3 Port Penn Sewage Treatment Plant

The Port Penn Sewage Treatment Plant is located in Delaware, 3.4 mi. northwest of the new plant power block area. The sewage treatment plant is a small facility that does not require continuous site supervision. The facility receives chemicals by truck, with the closest possible approach being on Delaware Route 9, which is 3.1 mi. west of the new plant power block area. The chemicals identified for possible analysis and their locations associated with Port Penn Sewage Treatment Plant are presented in Table 2.2-4.

2.2.2.1.4 Lower Alloways Creek Township Buildings

Lower Alloways Creek Township has several buildings that perform functions such as government administration, vehicle maintenance, and storage for the township. The chemicals

**PSEG Site
ESP Application
Part 2, Site Safety Analysis Report**

identified for possible analysis and their locations are presented in Table 2.2-5. There are no township buildings within 3 mi. of the new plant power block area.

2.2.2.2 Pipelines

No natural gas or hazardous liquid pipelines are located within 5 mi. of the PSEG Site. The nearest pipeline is a gas transmission line that runs along the U.S. Route 13 corridor in Delaware, 5.9 mi. west of the new plant power block area.

2.2.2.3 Waterways

The Delaware River, Alloway Creek, the Chesapeake and Delaware Canal, and the Salem River are the only navigable waterways within 10 mi. of the PSEG Site.

2.2.2.3.1 Alloway Creek

Alloway Creek is located 1.9 mi. northeast to the PSEG Site. Alloway Creek has 10 mi. of navigable waters with no commercial freight traffic.

2.2.2.3.2 Delaware River

The Delaware River is located adjacent to the PSEG Site and is used for commercial freight traffic to and from ports in New Jersey, Delaware, and Pennsylvania. The waterway has a channel depth maintained at 39.3 ft. at low tide. The shipping channel is 0.9 miles from the PSEG Site at the closest approach.

There are two anchorages within five miles of the PSEG Site: General Anchorage 2 and General Anchorage 3. Anchorage 2 lies between roughly 0.7 and 3.1 mi. to the North/Northwest of the PSEG Site. Anchorage 3 lies between roughly 3.8 and 5.8 mi. to the North/Northwest of the PSEG Site.

Table 2.2-6 details the total quantities of materials identified as chemical commodities transported on freight traffic, inbound and outbound, on the Delaware River. There are no reported bulk shipments of chlorine on the Delaware River.

Table 2.2-7 identifies the number of oil and chemical shipments on the Delaware River.

Table 2.2-8 identifies the largest maximum net tonnage of chemical commodities transported on the Delaware River.

Several small marinas and docks exist along the Delaware River within 10 mi. of the PSEG Site. These marinas are located in: Woodland Beach, Delaware; Delaware City, Delaware; Fort Mott, New Jersey; and Salem City, New Jersey. Most facilities are limited to recreational boating; however, the Fort Mott and Delaware City facilities are also home to ferry services. There are no planned expansions or new facilities within 10 mi. of the PSEG Site. The closest planned new facility is a mixed use marina, with recreational boat dockage and waterfront stores, in Pennsville, New Jersey, located 11.5 mi. away.

**PSEG Site
ESP Application
Part 2, Site Safety Analysis Report**

2.2.2.3.3 Chesapeake and Delaware Canal

The Chesapeake and Delaware Canal carries commercial freight traffic between the Delaware River and the Chesapeake Bay. The canal's nearest approach to the new plant power block area is 5.9 mi to the north-northwest. The canal has a mean low water depth of 35 ft.

Table 2.2-9 details the total quantities of materials identified as chemical commodities transported on freight traffic, inbound and outbound, on the Chesapeake and Delaware Canal.

2.2.2.3.4 Salem River

The mouth of the Salem River is 6.6 mi. northeast of the new plant power block area. The river has one industrial port, the Salem River Terminal in Salem, New Jersey, located 7.5 mi. northeast of the new plant power block area. The Salem River is a shallow water channel, with a depth of 16 ft. or less. The largest two quantities of commodities shipped on the river are soil or fill dirt and food products (Reference 2.2-10).

2.2.2.4 Mining Operations

There are no mining activities within 5 miles of the PSEG Site. The nearest identified mine is a sand and gravel mine, located just east of Middletown, Delaware, 7.0 miles west of the new plant power block area.

2.2.2.5 Highways

Alloways Creek Neck Road is a secondary road that provides access to the PSEG Site, Mad Horse Creek Wildlife Management Area, and several farms. Starting at the PSEG Site access road, Alloway Creek Neck Road runs east to the town of Hancocks Bridge, where it connects to Quinton-Hancocks Bridge Road. New Jersey Route 49 is the closest highway east of the site; its closest approach is 7.5 mi. northeast of the new plant power block area.

A new second road is proposed to be constructed for dedicated vehicular access to the site. The proposed causeway is conceptually designed as a 48 foot wide elevated structure that extends from the PSEG site towards the northeast along, or adjacent to, the existing Red Lion 500 kV transmission right-of-way ending at the intersection of Money Island Road and Mason Point Road in Elsinboro Township. The proposed causeway's land approach to the PSEG site is depicted in SSAR Figure 1.2-3.

Delaware Route 9 is the only highway within 5 miles of the PSEG Site. The closest approach is 3.1 miles west of the new plant power block area. Route 9 runs along the Delaware River coast including the region near the PSEG Site from Taylors Bridge through the town of Port Penn. The road is designated as a scenic route. A maximum weight of 80,000 pounds (lb.) is used to conservatively estimate chemical transportation. Table 2.2-10 provides a description of Delaware Route 9 and the other highways within 10 mi., including the closest approach to the PSEG Site.

Information is not available about the materials transported on the roads within 5 mi. of the PSEG Site; therefore, Superfund Amendments and Reauthorization Act (SARA) Title III, Tier II reports for facilities within 10 mi. and the results of a survey completed to obtain data for the

**PSEG Site
ESP Application
Part 2, Site Safety Analysis Report**

early site permit application (ESPA) were reviewed to determine chemicals that may be transported on roads within 5 mi. It is assumed that any of the chemicals listed for the industrial facilities in Table 2.2-1 could be transported on Delaware Route 9 or New Jersey Route 49. However, when considering the locations of the facilities that receive chemical shipments, it is apparent that normal delivery routes are away from the PSEG Site.

2.2.2.6 Railroads

There are no railroads within 5 mi. of the PSEG Site. The closest railroad line is the Southern Railroad Company of New Jersey, which connects Salem to Alloway, and has its closest approach at 8.2 mi. to the northeast. The company transports primarily freight and does not have any current plans for track expansion.

2.2.2.7 Airports, Airways, and Military Training Routes

2.2.2.7.1 Airports

The helipad for SGS and HCGS is the only heliport or airport within 5 mi. of the PSEG Site. Additionally, there are seven airports and one heliport located within 5 to 10 mi.

The helipad is owned by PSEG and is located on the PSEG Site, 3848 feet southeast of the new plant power block area. Helipad operations are sporadic and are limited primarily to medical emergencies and corporate management use. Permission from PSEG is required to land at the helipad.

Table 2.2-11 shows the number of operations at several private airports, helipads, and heliports within the vicinity of the PSEG Site. All facilities within 10 mi. are included, and public airports with operations greater than 25,000 per year are included within 35 mi. The nearest public airport is the Summit Airport, which is located 10.4 mi. from the new plant power block area. The airport has a 4488 ft. north-south oriented asphalt runway, and a 3601 ft. turf runway. Operations involve primarily single-engine light aircraft (Reference 2.2-26).

There are no airports within 10 mi. of the PSEG Site that have active plans for expansion. The Summit Airport, which is 10.4 mi. away, plans to add a 39,000 square foot hangar and 80,000 square feet of warehouse space.

An evaluation of hazards associated with identified airports is presented in Subsection 3.5.1.6.

2.2.2.7.2 Airways

There are four federal airways within 10 mi. of the PSEG Site: V123-312, V29, V157, and V213 (Reference 2.2-12). There are also two high altitude routes J42-150 and J191 (Reference 2.2-14). The closest military routes are six slow speed low-altitude military training routes as indicated on Figure 2.2-2 (SR800, SR805, SR844, SR845, SR846 and SR847). The nearest edges of the military training routes are located within five statute miles of the PSEG Site.

The centerline of Airway V123-312 is located 0.5 mi. northwest of the site. Additionally, Airway V29 is 1.1 mi. west of the site, Airway V157 is 7.1 mi. east of the site, and Airway V213 is 9.4 mi. southeast of the site. The centerline of jet way J42-150 is 0.8 mi. east of the site, with an

**PSEG Site
ESP Application
Part 2, Site Safety Analysis Report**

additional jet way J191, located 9.7 mi. east of the site. The width of a federal airway is typically 8 nautical mi., 4 nautical mi. on each side of the centerline. When airway width is considered, airways passing closer than 2 statute mi. to the nearest edge of the PSEG site are evaluated along with air traffic hazards in Subsection 3.5.1.6.

2.2.2.8 Military

There are no military facilities within 10 mi. of the PSEG Site. New Castle County Airport is the closest facility with military operations (Air National Guard), and it is located 14.5 mi. northeast of the site. The closest dedicated military facility is Dover Air Force Base, which is located 23.8 mi. south of the site. The operations at Dover Air Force Base are 100 percent military, and the numbers are identified in Table 2.2-11 (Reference 2.2-11).

2.2.2.9 Projections of Industrial Growth

No industrial growth projections are available for Salem County. However, the Salem County Utilities Authority identified areas of the county which are expected to undergo economic development. Projects include a possible recycling center in the city of Salem and a business/industrial park addition in Oldmans Township and Carneys Point, New Jersey. The projects identified in Salem County are more than 5 mi. away from the PSEG Site.

New Castle County, Delaware, has a comprehensive plan prepared in 2008 indicates most of the land in the county is expected to remain agricultural or open space (Reference 2.2-23). The closest zoned industrial plot is the Delaware City Industrial Complex, located on the northwest side of Delaware City, 8.9 mi. from the PSEG Site. A new wastewater treatment plant is planned at 5.9 mi. west of the site, situated along U.S. Route 13. The planned wastewater treatment plant chemical delivery is not expected to approach any closer than the existing facilities in New Castle County.

A review of available Salem and New Castle County planning documents does not indicate any significant expansion of military or transportation facilities located within the 5 mi. of the PSEG Site.

2.2.3 EVALUATIONS OF POTENTIAL ACCIDENTS

On the basis of the information provided in Subsections 2.2.1 and 2.2.2, the potential design-basis events that affect the new plant are identified and evaluated in this subsection. These events include those that could cause design parameters (e.g., structural overpressure) to be exceeded or cause physical phenomena (e.g., concentration of flammable or toxic chemical vapor clouds at building structures) that are hazardous to the new plant. The events are identified and evaluated in accordance with:

- Title 10 Code of Federal Regulations (CFR) 20
- 10 CFR 52.79(a)(1)(vi)
- 10 CFR 50.34
- 10 CFR 100.20
- 10 CFR 100.21
- RG 1.70
- RG 1.78

**PSEG Site
ESP Application
Part 2, Site Safety Analysis Report**

- RG 1.91
- RG 1.206
- RG 4.7

The selection of design-basis events is discussed in the subsection below.

2.2.3.1 Determination of Design-Basis Events

Design-basis events are defined as those hazards that could cause design parameters to be exceeded or cause physical phenomena that affect operation of the plant. A hazard is an incident with a consequence serious enough to affect the safety of the plant to the extent that the dose guidelines in 10 CFR Part 100 could be exceeded. NUREG-0800 Section 2.2.3, states that a hazard occurring with a probability of 1.0×10^{-7} per year, or greater, is a design-basis event when accurate data is used. If data are not available to make an accurate estimate, a hazard is a design-basis event if the probability of occurrence is greater than 1.0×10^{-6} per year, provided qualitative arguments can be made to show the realistic probability is lower (Subsection 2.2.3.2.6 for a discussion of conservatisms used herein). The following hazard categories are considered to determine which hazards are design-basis events:

- Chemical releases that could result in an explosion, flammable vapor cloud (delayed ignition), toxicity hazard, or fires
- Collisions with cooling water intake structure
- Liquid spills that could be drawn into the cooling water intake structure
- Radiological hazards

These hazard categories are discussed in the following subsections.

2.2.3.2 Effects of Design-Basis Events

The chemical hazards are analyzed at the following locations (for this section, chemicals refer to all materials that could result in explosive, flammable, or toxic hazards to the PSEG Site, including, but not limited to, ammonia, gasoline, propane, and other fuel storage):

- Nearby transportation routes such as local roads in both New Jersey and Delaware
- River vessel traffic on the Delaware River
- Nearby chemical and fuel storage facilities (in Lower Alloways Creek (LAC) Township Buildings or Port Penn Sewage Treatment Plant)
- Chemical storage at Salem and Hope Creek (S/HC)

On-site chemical storage for the new plant is not included in the ESPA and is analyzed for the combined license application (COLA) when the new plant reactor technology is selected.

The subsections that follow detail the major potential hazards due to chemical releases. The primary source of hazards to the new plant is chemical shipments on the Delaware River. Many of these chemicals are analyzed using a probabilistic analysis in order to show that the frequency of the hazard is sufficiently low so as not to pose a threat to the new plant. The methods and results of the analysis for chemical shipments on the Delaware River are

**PSEG Site
ESP Application
Part 2, Site Safety Analysis Report**

presented first, followed by the methods and results for other chemical sources (i.e., nearby facilities, local transportation, and S/HC chemicals).

2.2.3.2.1 Probabilistic Analysis Methods

A probabilistic analysis is used to determine the frequency of hazards due to chemicals that are transported on the Delaware River. This method is used to determine the threat due to solid explosions, vapor cloud ignition explosions and toxic vapor clouds. This method is consistent with RG 1.70, RG 1.78, *Evaluating the Habitability of a Nuclear Power Plant Control Room During a Postulated Hazardous Chemical Release*, December 2001, RG 1.91, *Evaluations of Explosions Postulated to Occur on Transportation Routes Near Nuclear Power Plants*, February 1978, and NUREG-0800 Section 2.2.3. These references state that a chemical is hazardous to the new plant if the probability of a hazardous event is greater than 10^{-7} hazards per year or 10^{-6} hazards per year if arguments are made to show that the analysis is conservative. Per the Standard Review Plan, NUREG-0800 Section 2.2.3, if the total aggregated frequency of a hazardous condition is greater than 10^{-6} hazards per year, then it must be shown that the probability of a radiological release to the public is less than 10^{-7} releases per year or 10^{-6} releases per year if arguments are made to show the analysis is conservative.

The probability analysis is based on Equation 2 in RG 1.91, but is modified to more accurately represent the analyzed situation. Equation 2 in RG 1.91 is (note that for the following discussion, “shipment” refers to known vessels on the Delaware River such as shipment size, and “trip” refers to a hypothetical vessel containing the chemical being analyzed):

$$r = n \cdot f \cdot s \quad \text{(Equation 2.2-1)}$$

Where:

- r = exposure rate in hazards per year (i.e., rate of a hazardous event)
- n = explosion rate for the substance and transportation mode in question in explosions per mile (mi.)
- f = frequency of trips for the substance in question in trips per year
- s = exposure distance in mi. (i.e., mi. of transportation route within the standoff distance)

For the purposes of this analysis, the previous equation is modified to account for additional features. The equation used to determine the frequency of vessel hazards is:

$$R_{\text{haz}} = P_{\text{spill}} \cdot R_{\text{accident}} \cdot P_{\text{weather}} \cdot D_{\text{trip}} \quad \text{(Equation 2.2-2)}$$

Where:

- R_{haz} = Rate of hazards per vessel trip near the PSEG Site (hazardous conditions at the site/trip)
- P_{spill} = Probability of a spill, dependent on amount released (spills/accident)
- R_{accident} = Rate of vessel accidents (accidents/vessel mi.)
- P_{weather} = Adverse wind direction probability (hazardous conditions at the site/spill)
- D_{trip} = Hazardous trip length, the total number of mi. that a vessel travels past the PSEG Site each trip where an accident would result in a hazardous condition (vessel mi/trip)

The total number of allowable trips is calculated using Equation 2.2-3:

**PSEG Site
ESP Application
Part 2, Site Safety Analysis Report**

$$T_{\text{allowable}} = 10^{-6} / \sum R_{\text{haz}} \quad (\text{Equation 2.2-3})$$

Where: $T_{\text{allowable}}$ = Allowable number of trips (trips/year)
 10^{-6} = Total allowable number of hazards per year as specified in RG 1.91

The hazard rate is split into several different cases. Each case is a combination of weather conditions (i.e., Pasquill Stability Class and wind speed) and spill size. For each combination of Pasquill Stability Class and spill size, Equation 2.2-2 is used to determine the rate of a hazard for that combination. The total rate of a hazard for a single vessel trip of a chemical is the sum of each of the hazard rates for each case.

To determine the total probability of a radiological release to the public, the sum of all the individual explosive hazard frequencies is multiplied by the conditional core damage probability given an explosion and by the conditional radiological release probability given core damage, as shown in Equation 2.2-3a.

$$\sum_{\text{hazards}} H_f \times \text{CCDP} \times \text{CRRP} < 10^{-6} \text{ per year} \quad (\text{Equation 2.2-3a})$$

Where: H_f = chemical hazard frequency (events per year)
CCDP = conditional core damage probability given an event
CRRP = conditional radiological release probability given core damage

Hazardous Trip Length (D_{trip})

The total number of miles that the vessel travels near the new plant where a spill would result in a hazardous condition (the hazardous trip length) is calculated deterministically using the methods presented in RG 1.78 for toxicity or flammable vapor cloud analyses, or using the methods presented in RG 1.91 for explosion analyses. The trip length is dependent on the standoff distance for each case. The standoff distance is the smallest distance the release can be from the PSEG Site without the site experiencing a hazardous condition. The standoff distance is dependent on the chemical, the stability class, the wind speed and the amount of chemical released. The relationship between the standoff distance, the trip length, and the wind direction is shown in Figure 2.2-3. For example, within a 2 mi. standoff distance, there is 4.3 mi. of navigable channel between south and north-northwest of the PSEG Site.

Adverse Wind Direction Probability (P_{weather})

The adverse wind direction term is the probability that the wind blows from the direction of the spill toward the PSEG Site. The adverse wind direction is different for each case because each case uses a specific stability class and wind speed. The wind direction, stability class and wind speeds are correlated with each other (Section 2.3 for the correlation between wind direction, stability class and wind speed). Only winds blowing from the spill toward the new plant can lead to a hazardous condition at the PSEG Site. The relationship between the standoff distance, the trip length, and the wind direction is shown in Figure 2.2-3.

**PSEG Site
ESP Application
Part 2, Site Safety Analysis Report**

Probability of a Spill (P_{spill}) and Rate of Accidents Terms (R_{accident})

Several tools including the Marine Information for Safety and Law Enforcement (MISLE) (Reference 2.2-20) Database and the Pipeline and Hazardous Materials Safety Administration (PHMSA) Incident Reports database (Reference 2.2-24) are used to calculate the largest chemical releases that can be expected to occur near the PSEG Site. The largest chemical spill reported in the PHMSA Database between 2001 and 2008 is roughly 1000 gallons (gal.) of chemical. The largest chemical spill reported in the MISLE database, which includes spills from vessels that were outside of United States waters, is 3,629,526 gal. of ethyl alcohol from the vessel Bow Mariner in February 2004. There are 9913 vessels with reported spill volumes in the MISLE database (out of 10,287 vessel incidents in the database between July 2001 and February 2007 per Reference 2.2-20). Table 2.2-12 shows the breakdown of the size of spills reported in the MISLE database.

Several of the more explosive chemicals identified as being transported by vessel near the PSEG Site are examined to determine which is the most hazardous in terms of a vapor cloud explosion. Propane is the most explosive. It is released as a single instantaneous puff (as opposed to gasoline which is stored at atmospheric conditions and evaporates over time following a release) and it has a lower explosive limit (LEL) than most other petroleum gases (2.1 percent for propane, 3.0 percent for ethane, 4.4 percent for methane [Reference 2.2-27]).

Probability Analysis for Propane Vapor Cloud Explosions

The analysis shown below is the probability analysis for propane vapor cloud explosions. Many other chemicals are analyzed for explosive and toxic analyses using the same method. The cases run for propane are shown in Table 2.2-13. The deterministic results for each case are also shown in Table 2.2-13 and are detailed below.

For any release less than 2000 gal. (~99 percent of all releases), an explosion has a standoff distance less than the distance between the vessel channel and the nearest safety-related building (less than 0.9 mi.). The standoff distance is less than the distance from the release to the PSEG Site, therefore the hazardous trip length is 0 mi.

Following a release of 10,000 gal., the standoff distance for a propane explosion with Pasquill Stability Class G is 1.8 mi. Pasquill Stability Class G (extremely stable atmosphere) is the most conservative stability class and, therefore, provides an upper bound for standoff distance. The hazardous trip length within the 1.8 mi. standoff distance of the PSEG Site is 4 mi. The standoff distance for Pasquill Stability Class F is 1.1 mi. The hazardous trip length within the 1.1 mi. standoff distance is 1.2 mi. The standoff distance is less than 0.9 mi. for all Pasquill Stability Class E weather. Only wind that blows the puff toward the plant would lead to adverse conditions. The worst case (most frequent) wind direction for each stability class is used. Additional spill sizes are then modeled at each stability class. Results from each set of conditions are summed to determine a total hazard rate. The results of this analysis are shown in Table 2.2-13.

The number of allowable trips of propane is calculated by dividing 10^{-6} by the frequency of hazards per trip. The result is 397 allowable trips per year. Using this same analysis method, the total number of allowable trips of each chemical is shown in Table 2.2-14.

**PSEG Site
ESP Application
Part 2, Site Safety Analysis Report**

The U.S. Army Corps of Engineers (USACE) (Reference 2.2-28), the U.S. Coast Guard (USCG) (Reference 2.2-20) and the Maritime Exchange for the Delaware River and Bay (MEDRB) (References 2.2-21 and 2.2-22) were each contacted to determine the actual number of trips of each chemical past the new plant each year. None of these sources is able to provide the number of trips; however, each is able to provide information that is used to develop a conservative estimate for the number of trips. Table 2.2-16 provides chemicals that are analyzed to bound the transported commodities.

The USACE provided data including the total tonnage of chemicals shipped past the PSEG Site (Reference 2.2-28). This tonnage is listed by a 4-digit commodity code. The 4-digit commodity code provides sufficient information such that an analysis can be performed. The USACE also provided the Registered Tonnage (Reg. Tons) of vessels that contain that chemical. The Reg. Tons is used to estimate the mass of chemical in a shipment.

The MEDRB provided information about specific shipments on the Delaware River; however, the commodity type does not provide sufficient detail to be used independently in an analysis (Reference 2.2-22). In addition, the total tonnage of chemicals reported to the MEDRB is much less than the tonnage from the USACE. The MEDRB data is used to provide a second estimate for the average mass of chemical in each shipment.

The MISLE database from the USCG is also used (Reference 2.2-20). The largest spill reported in the MISLE database is compared with the average tonnage estimated from the USACE and the MEDRB to ensure all three are consistent with each other.

Using all three sets of data, a conservatively low average shipment size is selected. Smaller shipment sizes maximize the estimated number of trips, thereby maximizing the total probability of a hazard. The total tonnage, the average and minimum mass per shipment from the USACE and MEDRB, the mass per shipment selected for the analysis, and the estimated number of trips are shown in Table 2.2-15.

The smallest margin between the number of allowable trips and the estimated number of trips is for propane. From Table 2.2-14, for propane, the number of allowable trips is 397, and from Table 2.2-15, the estimated number of trips is 129.

2.2.3.2.2 Explosions

Explosive hazards are considered for facilities and activities in the vicinity of the plant. These hazards include the detonation of high explosives, munitions, chemicals, or liquid and gaseous fuels that are processed, stored, used, or transported near the PSEG site. The effects of explosions are a concern in analyzing structural response to blast pressures. The effects of blast pressure from explosions from nearby chemical sources (e.g., navigable waterways, external facilities, etc.) to critical plant structures are evaluated to determine if the explosion has an adverse effect on plant operation or would prevent a safe shutdown.

The allowable and actual distances of hazardous chemicals transported or stored are determined in accordance with RG 1.91 which cites 1 pound per square inch (psi) as a conservative value of peak positive incident overpressure, below which no significant damage would be expected. RG 1.91 defines this safe distance by the relationship $R \geq kW^{1/3}$ where R is the distance in feet from an exploding charge of W pounds (lb.) of trinitrotoluene (TNT); and the

**PSEG Site
ESP Application
Part 2, Site Safety Analysis Report**

value k is a constant. For hydrocarbons, the TNT mass equivalent, W , is determined following guidance in RG 1.91, where W is taken as being 240 percent of the explosive mass of the chemical. For non-hydrocarbons (ammonia and hydrogen), an equation from the Fire Protection Engineering Handbook (Reference 2.2-27) comparing the heats of combustion to TNT is also used to determine the TNT mass equivalent. For solids, the TNT mass equivalent is the explosive mass of the chemical per RG 1.91.

Conservative assumptions are used to determine a safe distance, or minimum separation distance, required for an explosion to have less than 1 psi peak incident pressure. When the heat of combustion method is used, an explosion yield factor of 10 percent is applied. The yield factor is an estimation of the available combustion energy released during the explosion as well as a measure of the explosion confinement. Use of a 10 percent yield is conservative because it is the highest in the range of expected yields based on past large explosions (Reference 2.2-27).

For some atmospheric liquids (e.g., diesel, gasoline) the storage vessel is assumed to contain the fuel vapors at the upper explosive limit (UEL). This is conservative because this scenario produces the maximum flammable mass given that it is the fuel vapor, not the liquid fuel that explodes. The density of chemical vapor is higher when temperatures are lower, therefore, the design low temperature is used to determine the amount of chemical vapor that exists at the UEL. To be consistent with Chapter 15 of NUREG-1805, *Fire Dynamics Tools (FDTs) Quantitative Fire Hazard Analysis Methods for the US Nuclear Regulatory Commission Fire Protection Inspection Program*, it is assumed that for compressed or liquefied gases (e.g., propane, hydrogen), the entire contents of the storage vessel is between the UEL and the LEL, therefore, the entire contents of the storage vessel is considered as the flammable mass.

Salem and Hope Creek site chemicals, nearby facilities chemicals, chemicals transported by vessel, and chemicals assumed to be driven on roadways near the PSEG Site are evaluated to ascertain the chemicals that have the potential to explode, thereby requiring further analysis. Hazardous materials potentially on the Delaware River are identified in Table 2.2-16. Hazardous materials transported on nearby roads or at nearby facilities, and Salem and Hope Creek Generating Stations, are identified in Table 2.2-17. The effects of limiting explosion events are summarized in Table 2.2-18 and in the following subsections.

Hazard distances are generally determined as the distance from the hazard to the edge of the power block. For hazards analyzed that exceed the acceptance criteria at the power block boundary, the distances to technology specific safety-related structures are used. The distances used are based on preliminary site drawings. A review of the supporting calculations for this section, including a review of the distances from chemicals to safety-related buildings, will be analyzed at the COLA stage when a reactor technology is selected.

Salem and Hope Creek Site

Four bounding chemicals at the S/HC site are identified as requiring further explosion analysis: a 6000 gal. tank of gasoline, the 8000 gal. truck that refills the tank of gasoline, a 1,000,000 gal. capacity tank of diesel fuel, and a bank of hydrogen cylinders.

An analysis of the identified chemicals is conducted using the TNT equivalency methods described in Subsection 2.2.3.2.2. The results indicate that the minimum allowable separation

**PSEG Site
ESP Application
Part 2, Site Safety Analysis Report**

distances (safe distances) for all tanks are less than the actual distance from the tanks to the nearest postulated safety-related building at the new plant. The safe distance for the diesel tank is 0.13 mi. and the actual distance to any proposed safety-related building is 0.14 mi. The safe distance for the hydrogen tanks is 0.11 mi. and the actual distance to the power block boundary is 0.35 mi. The road used to deliver to the gasoline tank is 0.07 mi. from a proposed safety-related building. The safe distance for the gasoline truck is 0.02 mi. The gasoline tank is bounded by the gasoline truck both in terms of distance from a potential safety-related building and in terms of volume of the tank.

Nearby Facilities

The only off-site chemicals identified for further analysis for a stationary explosion are a tank of gasoline and a tank of propane at the LAC Township Buildings, over 3 mi. away. For both tanks, the safe distances are much less than the actual distance. The safe distance for the 6000 gal. gasoline tank is 0.02 mi., and the safe distance for the propane tank is 0.14 mi.

Vessels on the Delaware River

Two types of explosions are analyzed for vessels on the Delaware River. The first is liquid/vapor explosions. The MISLE database and the PHMSA database are examined to identify the largest chemical explosions that have occurred. The largest chemical explosion in either database is the explosion and sinking of the Bow Mariner in 2004 (Reference 2.2-17). The ship contained 22 recently emptied tanks that had been carrying the fuel additive methyl tertiary-butyl ether (MTBE). The vapors in those tanks were ignited by a spark and exploded in quick succession. The total mass of MTBE vapor is estimated to be 116 tons. The standoff distance for 116 tons of MTBE is 0.50 miles. If the total mass of explosive chemical is multiplied by a factor of six, the safe distance is 0.90 mi., which is the actual distance from the vessel channel to the power block. The next largest chemical explosion in either database is 550 gal., which is on the order of 2.5 tons (assuming 9 lb. per gal). The largest explosion in either database is too small by a factor of 6 to lead to a hazardous overpressure at the PSEG Site, therefore liquid/vapor explosions of chemicals on vessels are not hazards to the PSEG Site.

The second analysis is solid explosives. The standoff distance equation in RG 1.91 is used. The smallest mass that can have a 1 psid explosive overpressure at a distance of 0.9 mi. is 589 tons. Historically large vessel explosions are examined to determine an upper bound for explosive mass. The two largest vessel explosions are the Halifax Explosion in 1917 and the Texas City Disaster in 1947. Both cases involved external factors that are not present within 5 mi. of the PSEG Site on the Delaware River. The Halifax Explosion involved vessel contact in a crowded harbor, and the Texas City Disaster occurred during unloading. The Delaware River is very wide near the new plant and there are no large docks within 5 mi. Both of these explosions are estimated to be on the order of 2500 tons of solid explosive.

A probability analysis is used to determine the number of allowable trips of solid explosive. The probability of an explosive hazard is the probability of an explosion per vessel mile multiplied by the distance that the vessel travels within the standoff distance multiplied by the number of vessels that carry solid explosives near the PSEG Site. Data from MISLE and PHMSA is used in evaluating the probability of an explosion, similar to the method for determining spill probabilities described in Subsection 2.2.3.2.1. The standoff distance for a 2500 ton explosion of TNT, the surrogate solid explosive recommended by Regulatory Guide 1.91, Rev. 1, is 1.46

**PSEG Site
ESP Application
Part 2, Site Safety Analysis Report**

miles. For each trip on the Delaware River, a vessel will travel 2.5 miles within 1.46 miles of the PSEG Site. The total frequency of explosions within 1.46 miles of the PSEG Site is calculated to be 1.125×10^{-9} explosions per trip. Solid explosive shipments less than 589 tons are determined to pose no threat to the PSEG Site. Using the methods in Regulatory Guide 1.91, Rev. 1, the maximum number of allowable solid explosive trips of 589 tons or greater is therefore 888 trips. From the USACE data (Reference 2.2-28), the largest total annual amount of “explosives” or “ordnance” that is transported on the Delaware River in any year between 2003 and 2007 is 610 tons per year, and the largest total amount of “ammonium nitrate” or other fertilizers is 165,412 tons per year. The total sum of solid explosives and ammonium nitrate fertilizer is 166,022 tons/year. This is the equivalent of 282 trips of solid explosive ($=166,022 / 589$). Since the annual number of trips containing 589 tons of solid explosive is less than 888 trips per year, the hazard risk associated with solid explosions near the PSEG Site is acceptable.

In addition to the above analysis, the frequency of a solid explosion affecting the site is included in the aggregate explosion frequency used to assess the rate of radiological releases to the public. This assessment is presented in Subsection 2.2.3.2.6.

A probabilistic analysis was performed for vessels in the two anchorages on the Delaware River within five miles of the PSEG Site. The analysis utilized anchorage usage data from the USCG as well as failure rates for anchored vessels. The probability of plant damage due to stationary explosions on vessels in these anchorages is negligible compared to the results of the probability analysis for the vessels that travel past the site.

Roadways

The only chemical transported by roadway identified for use in this analysis is the gasoline delivery truck to the S/HC site. This analysis is detailed above.

2.2.3.2.3 Flammable Vapor Clouds

Flammable gases in the liquid or gaseous state can form an unconfined vapor cloud that could drift toward the plant before ignition occurs. When a flammable chemical is released into the atmosphere and forms a vapor cloud it disperses as it travels downwind. The parts of the cloud where the concentration is within the flammable range, between the lower and upper flammability limits, can burn if the cloud encounters an ignition source. The speed at which the flame front moves through the cloud determines whether it is a deflagration or a detonation. If the cloud burns fast enough to create a detonation an explosive force is generated.

Potentially hazardous materials on the Delaware River are identified in Table 2.2-16. Hazardous materials transported on nearby roads or at nearby facilities, and SGS and HCGS, are identified in Table 2.2-17. These chemicals are evaluated to ascertain which hazardous materials have the potential to form a flammable vapor cloud or vapor cloud explosion. For those chemicals with an identified flammability range, an air dispersion model based on the methods and equations in RG 1.78 and NUREG-0570, *Toxic Vapor Concentration in the Control Room Following a Postulated Accidental Release*, is used to determine the distance that the vapor cloud can travel before the concentration is less than the LEL. This distance (called the LEL distance) is used in three ways. First, if the LEL distance is greater than the distance to a safety-related building, then the cloud is flammable at the PSEG Site and is hazardous. Second, if it can be shown that there are no ignition sources within the LEL distance, then that vapor cloud

**PSEG Site
ESP Application
Part 2, Site Safety Analysis Report**

does not explode. Third, if there are potential ignition sources (i.e., buildings or other man made objects), the LEL distance is used as the center of an explosion of the chemical vapor. All of the mass of chemical between the release point and the LEL distance is modeled in an explosion centered at the LEL distance. This maximizes the explosive energy and minimizes the distance between the center of the explosion and safety-related buildings.

Conservative assumptions are used in the analyses with regard to meteorological inputs and identified scenarios. The following meteorological conditions are used as inputs to the model: Pasquill Stability Class G (very stable), with a wind speed of 2.84 miles per hour (mph); ambient temperature of 80.8 degrees Fahrenheit (°F); and an atmospheric pressure of 1 atmosphere (atm). Each of these meteorological conditions represents the 5 percent worst case at the PSEG Site. Pasquill Stability Class G represents the most limiting 5 percent of meteorological conditions observed at the PSEG Site. Wind speeds less than 2.84 mph occur only 5 percent of the time. Temperatures greater than 80.8°F only occur 5 percent of the time. An atmospheric pressure of 1 atm is used because the PSEG Site is very close to sea level. For each of the identified chemicals, it is conservatively assumed that the entire contents of the vessel leaked forming a puddle or that the entire contents are released instantaneously as a gas. For liquid releases, a large puddle provides a significant surface area to maximize evaporation and the formation of a vapor cloud. For gaseous releases, the instantaneous release maximizes the peak gas concentration.

Additional mitigating factors (plume rise, plume meander, etc.) are considered in the analysis. The Safety Evaluation Report related to the construction of Hartsville Nuclear Power Plants, NUREG-0014, *Safety Evaluation Report Related to Construction of Hartsville Nuclear Plants*, concluded that “the state of knowledge concerning the chemical reactions of natural gas mixed with air is sufficiently well established to form a basis for the judgment that the detonation of unconfined natural gas dispersal in air is not a credible event.” If it can be shown that the vapor cloud rises to an elevation such that the concentration is below the lower flammable limit at the highest point of the plant structures, the cloud is completely unconfined, and a vapor cloud detonation does not occur. Also, at that elevation there would be no credible ignition source. To determine if the vapor cloud is above the plant structures, a plume buoyancy model is used. In addition, for a plume release, RG 1.145, *Atmospheric Dispersion Models for Potential Accident Consequence Assessments at Nuclear Power Plants*, February 1983, indicates that meander can be considered in calculating the concentration at a point.

The analyzed effects of flammable vapor clouds and vapor cloud explosions from internal and external sources are summarized in Table 2.2-19 and are described in the following subsections relative to the release source.

Salem and Hope Creek Site

Three bounding chemicals at the S/HC site are identified as requiring further explosion analysis; a 6000 gal. tank of gasoline, the 8000 gal. truck that refills the tank of gasoline, and a hydrogen tube farm.

The results indicate that the minimum allowable separation distances (safe distance) for the gasoline is greater than the actual distance from the tanks to the nearest postulated safety-related building at the new plant. The safe distance for the 8000 gal. gasoline truck is 0.27 mi. and the actual distance to any proposed safety-related building is 0.07 mi. The safe distance for

**PSEG Site
ESP Application
Part 2, Site Safety Analysis Report**

the 6000 gal. gasoline tank is 0.24 mi. The Hope Creek gasoline tank will be relocated for construction of the new plant, and the delivery truck route to the new tank will be analyzed for its effects on the new plant.

The safe distance for the hydrogen tanks is 0.24 mi. and the actual distance to the power block boundary is 0.35 mi.

Nearby Facilities

The only off-site chemicals identified for further analysis for a stationary explosion are a tank of gasoline and a tank of propane at the LAC Township Buildings, over 3 mi. away. For both tanks, the safe distances are much less than the actual distance. The safe distance for the 6000 gal. gasoline tank is 0.239 mi., and the safe distance for the propane tank is 0.814 mi.

Vessels on the Delaware River

Based on reports from the MEDRB (Reference 2.2-22) and from the USACE (Reference 2.2-28), several chemicals are identified as the bounding chemicals that are transported along the Delaware River. These chemicals are propane, gasoline, benzene, alcohols (methanol, ethanol), carboxylic acids, ammonia, naphtha & solvents, methane, acetone and vinyl chloride. The closest point that vessel traffic approaches the new plant is 0.9 mi.

A vapor cloud of alcohols has a standoff distance of less than 0.9 mi., and is therefore not a hazard to the PSEG Site. The hazardous carboxylic acids (acetic acid, formic acid, and benzoic acid) have vapor pressures lower than their lower flammable limits. Therefore, carboxylic acids do not support a flammable vapor cloud. The rest of the chemicals identified as being transported on the Delaware River are analyzed using the probabilistic analysis presented in Subsection 2.2.3.2.1.

The vessels of gasoline, benzene, ammonia, naphtha, methane, acetone and vinyl chloride are analyzed in the same method as the propane analysis that is presented in Subsection 2.2.3.2.1. The table of total allowable trips is shown in Table 2.2-14 and the table of estimated number of trips is shown in Table 2.2-15. For each chemical, the total number of allowable trips is greater than the estimated number of trips; therefore, none of these chemicals pose a threat greater than 10^{-6} hazards per year.

The frequency of each individual chemical vapor cloud explosion affecting the site is included in the aggregated explosion frequency used to assess the rate of radiological releases to the public. This assessment is presented in Subsection 2.2.3.2.6.

A probabilistic analysis was performed for vessels in the two anchorages on the Delaware River within five miles of the PSEG Site. The analysis utilized anchorage usage data from the USCG as well as failure rates for anchored vessels. The probability of plant damage due to a flammable vapor cloud from an accident on a vessel in these anchorages is negligible compared to the results of the probability analysis for the vessels that travel past the site.

**PSEG Site
ESP Application
Part 2, Site Safety Analysis Report**

Roadways

The only chemical transported by roadway identified for use in this analysis is the gasoline delivery truck to the S/HC site. This analysis is detailed above.

2.2.3.2.4 Toxic Chemicals

Toxic chemical hazards are considered for facilities and activities in the vicinity of the PSEG Site. These hazards include chemicals that are processed, stored, used, or transported near the PSEG site. NRC RG 1.78, Revision 1, *Evaluating the Habitability of a Nuclear Power Plant Control Room During a Postulated Hazardous Chemical Release*, requires evaluation of control room habitability after a postulated external release of hazardous chemicals from mobile or stationary sources, off-site or on-site. PSEG has not selected a reactor technology. Control room characteristics (i.e., the control room volume and outside air infiltration and circulation rates) are unknown. Therefore, chemicals that lead to concentrations above the Immediately Dangerous to Life and Health (IDLH) at the power block boundary will be evaluated during the development of the COLA.

Hazardous materials potentially on the Delaware River are identified in Table 2.2-16. Hazardous materials transported on nearby roads or at nearby facilities, and SGS and HCGS, are identified in Table 2.2-17. Only those chemicals at nearby facilities were evaluated to determine if the chemical posed a threat to the new plant. All other chemicals will be evaluated during the generation of the COLA when the new plant technology has been selected.

The dispersion model based on RG 1.78 and NUREG-0570 is used to determine the maximum distance various postulated vapor clouds travel before they dispersed enough to fall below the associated National Institute of Occupational Safety and Health (NIOSH) defined Immediately Dangerous to Life and Health (IDLH) limit.

The IDLH is defined by the NIOSH as a situation that poses a threat of exposure to airborne contaminants when that exposure is likely to cause death or immediate or delayed permanent adverse health effects or prevent escape from such an environment. The IDLH limits determined by NIOSH are established such that workers are able to escape such an environment without suffering permanent health damage.

Some chemicals, for example gasoline, do not have an IDLH limit. For these chemicals, other toxicity limits are used. The short term exposure limit (STEL) is defined as the limit that a person can tolerate without any side effects for 15 minutes. The time weighted average (TWA) is defined as the average concentration that a person can be exposed to for 8 hours a day, 5 days a week, without adverse effects. For chemicals with no defined IDLH, both of these exposure limits must be met.

The meteorological parameters that are used to determine chemical concentrations are: Pasquill Stability Class G (stable), a wind speed of 2.84 mph; an ambient temperature of 80.8°F; and an atmospheric pressure of 1 atm. As previously stated, each of these meteorological conditions represents the 5 percent worst case at the new plant. An atmospheric pressure of 1 atm is used because the PSEG Site is very close to sea level.

**PSEG Site
ESP Application
Part 2, Site Safety Analysis Report**

The effects of toxic chemical releases from nearby facilities are summarized in Table 2.2-20 and are described as follows:

Nearby Facilities

The only off-site chemicals identified for further analysis for toxicity are a tank of gasoline and a tank of propane at the LAC Township Buildings, over 3 mi. away. For both chemicals, the peak concentration at the power block boundary is less than the toxicity limits. The peak concentration at the power block boundary for gasoline is 206 parts per million (ppm), which is less than the STEL for gasoline, 500 ppm, and the TWA for gasoline, 300 ppm. The peak concentration at the power block boundary for propane is 710 ppm, which is less than the IDLH for propane, 2100 ppm. Both of these chemical releases are not a threat to the new plant.

2.2.3.2.5 Fires

Hazards leading to high heat fluxes, smoke, non-flammable gases or chemical bearing clouds from the release of materials, as the consequence of fires in the vicinity of the plant are considered. Fires in adjacent industrial plants and storage facilities, oil and gas pipelines, brush and forest fires, and fires from transportation accidents were evaluated as events that could lead to high heat fluxes or to the formation of chemical bearing clouds.

For chemical fires, the goal is to show that the heat flux from the fire does not raise the surface temperature of the walls of safety-related buildings above acceptable values. American Concrete Institute (ACI) Standard 349-01, *Code Requirements for Nuclear Safety-Related Concrete Structures*, states that the maximum long term temperature of a concrete wall must be less than 150°F, and that the maximum short term temperature must be less than 350°F (Reference 2.2-1). Therefore, a chemical fire must not increase the surface of a concrete wall by more than 200°F. To calculate the temperature increase, an equation from, *Introduction to Heat Transfer*, by Incropera (Reference 2.2-16) is used. The equation simplifies to:

$$T(0,t) - T_i = \frac{2q_0''(\alpha t/\pi)^{\frac{1}{2}}}{k} \quad (\text{Equation 2.2-4})$$

Where:

- $T(0,t)$ = Wall surface temperature at time t (degrees Celsius °C)
- T_i = Initial temperature of the wall before the fire (°C)
- q_0'' = Steady state heat flux (watts (W)/ meter (m)²)
- t = Time (seconds, sec.)
- α = Thermal diffusivity of the material = $k/\rho \cdot c_p$ (m²/sec)
- k = Thermal conductivity (W/m· Kelvin (K))
- ρ = Density (kilogram (kg)/m³)
- c_p = Specific heat (joules (J)/kg·K)

The chemical releases that are analyzed for potentially leading to high heat fluxes at safety-related buildings are: a hydrogen tank jet fire from the tank farm on the Hope Creek site, a gasoline pool fire due to a spill of the Hope Creek delivery truck, a diesel pool fire due to a spill of the Hope Creek tank, a boiling liquid expanding vapor explosion (BLEVE) fireball of the propane tank at the LAC Township Buildings, a pool fire from the spill of gasoline from a vessel

**PSEG Site
ESP Application
Part 2, Site Safety Analysis Report**

on the Delaware River, and a BLEVE fireball of a propane vessel on the Delaware River. The results are shown in Table 2.2-21.

These releases are modeled in the computer program Areal Locations of Hazardous Atmospheres (ALOHA). ALOHA provides the heat flux at a location as a function of time for jet and pool fires, and provides the peak heat flux and the duration of BLEVE fireballs. Most atmospheric conditions do not affect the heat flux results: only relative humidity can change the results. A low relative humidity leads to less energy absorption by the air. A relative humidity of 5 percent is used in this analysis.

The results from ALOHA show that none of the fires are hazardous to the new plant. The propane at LAC Township Buildings is so far away that the heat flux is negligible (0.011 kilowatts (kW) per m², whereas solar radiation alone is close to 1 kW per m²). The gasoline vessel spill pool fire is far enough away that the heat flux is negligible (0.008 kW per m²). The heat flux from the hydrogen jet fire is negligible (0.05 kW per m²). The heat flux from a pool fire of the 1,000,000 gal. diesel tank is negligible (0.0497 kW per m²), which leads to a temperature increase of 3.6°F.

The gasoline truck pool fire (using the current route, see Subsection 2.2.3.2.3 for discussion of changing the gasoline tank location and gasoline truck route) results in a heat load of 0.39 kW per m² at a standoff distance of 0.07 mi. The fire lasts a total of 5 minutes. The surface of a concrete wall of a building heats up by 8.2°F as a result of this fire. This is less than the 200°F allowable temperature rise and therefore, the fire is not a hazard to the new plant. The BLEVE fireball of propane from a vessel on the Delaware River is modeled as being a complete fireball of 5000 tons of propane based on the largest explosion data detailed in Subsection 2.2.3.2.2. The fireball would last for 42 sec. and causes a peak heat load of 22.3 kW/m². The surface of a concrete wall of a building heats up by 174°F as a result of this fireball. This is less than the 200°F allowable, however, it is a very high temperature increase and very high heat load. Therefore, further evaluation of the likelihood of a propane vessel BLEVE is provided.

The full 5000 ton fireball analyzed above has a standoff distance of 1.9 mi. for a 5 kW/m² heat load. There is 4.2 mi. of vessel route within 1.9 mi. of the PSEG Site. In the MISLE database, there is only one reported instance of a release of more than 322,000 gal. of chemical. A fireball of 322,000 gal. of liquid propane would last 25 sec. and result in a heat load of 6.36 kW/m² on the power block. This fireball would increase the wall temperature only 37°F. The probability of a spill of any kind greater than 322,000 gal. is 1.82×10^{-10} spills per vessel mile (Table 2.2-12). The total frequency of a heat load greater than 6.36 kW/m is 7.644×10^{-10} hazards per trip. This is less than the hazard rate for a propane vapor cloud explosion; therefore the vapor cloud hazard is bounding over the BLEVE fireball.

Based on the frequency of BLEVEs in general a propane BLEVE is unlikely to occur. The largest spill in the MISLE database is the Bow Mariner. As detailed above, the mass of chemical that exploded in the Bow Mariner incident is estimated to be 116 tons. From the MISLE database, there have been no other explosions or fires within an order of magnitude of 5000 tons. Therefore, the frequency of a fireball on the order of 5000 tons of chemical is very low.

**PSEG Site
ESP Application
Part 2, Site Safety Analysis Report**

2.2.3.2.6 Conclusions

Based on the analyses presented in Subsections 2.2.3.2.1 through 2.2.3.2.5, there are no chemical hazards that are design-basis events, provided:

- A review of the supporting calculations for these sections will be performed following technology selection.
- The HCGS 6000 gal. tank of gasoline and the delivery truck route to that tank, will be relocated.
- Chemicals identified for toxicity and control room habitability analysis will be performed for the COLA.

This conclusion is reached using the acceptance criterion for a probabilistic analysis. This analysis determines that the frequency is less than 10^{-6} hazards per year for each chemical. The total aggregated frequency of an explosion, both due to solid explosives and vapor cloud explosions, that adversely affects the PSEG Site is 2.31×10^{-6} hazards per year which is greater than 10^{-6} . From Equation 2.2-3a, the probability of a release to the public includes the conditional core damage probability (CCDP) given an explosion at the site. The conditional probability is unknown at this time and will be evaluated at COL when a reactor technology is selected. However, based on existing data, an order of magnitude estimate can be established. The CCDP was previously evaluated for small aircraft hazards. The four reactor technology vendors were contacted for the CCDP for the small aircraft analysis. The highest reported CCDP is 0.318%. The frequency of core damage due to chemical explosions with a CCDP of 0.318% is 7.35×10^{-9} , which is over two orders of magnitude less than the 10^{-6} acceptance criteria in NUREG-0800. Several conservatisms are used in the probability analyses; the more significant conservatisms are listed here.

- The spill size for each case is the maximum in the range of spill sizes. For instance, a spill of 51,000 gal. is modeled as a spill of 322,000 gal. of chemical since the applicable range is 50,000 gal. to 322,000 gal. (Table 2.2-12).
- The estimated number of trips of each chemical is high since the estimated ship cargo sizes are biased low.
- Storage conditions for chemicals are selected in order to maximize the release rate, which would maximize the concentration at the PSEG Site. Many chemicals that would typically be stored or transported as liquids are modeled as gases (e.g., propane, methane).
- For vessels, bounding chemicals are selected for each commodity category (e.g., propane is modeled for "Unknown NEC" where NEC is the shipping acronym for Not Elsewhere Classified). While there may have been a commodity as hazardous as propane that is classified as "Unknown NEC", it is very unlikely that all trips classified as "Unknown NEC" are as hazardous as propane.
- It is very likely that a chemical vapor cloud explosion would occur near the vessel following a massive release given that a vessel provides many ignition sources. This on or near-vessel explosion would consume the flammable vapor before the vapor reaches the PSEG Site. Therefore, a vapor cloud explosion at the site is much less likely than modeled here.

**PSEG Site
ESP Application
Part 2, Site Safety Analysis Report**

2.2.3.3 Collisions with Intake Structure

The cooling water intake structure for the new plant is located on the Delaware River, which is a navigable waterway. One of the four reactor technologies being considered by PSEG requires a safety-related intake structure on the Delaware River. Therefore, an evaluation is performed which considered the probability of an accident involving a run-away barge carrying flammable material that could cause a significant release resulting in fire or explosion upon striking the intake. This evaluation is described below.

Five factors are determined to yield the probability of the event of concern (a runaway barge striking the safety-related section of the intake structure and causing a fire or explosion). The factors and the basis for their determination are described below:

- Number of non-self propelled vessels that pass the site per year identified in Table 2.2-22. Conservatively, this is determined to be 2825 vessels based on the study of USACE statistics for years 2003 through 2007 (Reference 2.2-28).
- Proportion of traffic on the Delaware River having potentially flammable material listed in Table 2.2-6. This is determined to be 0.071 based on the summary of chemical shipment data USACE for the years 2003 through 2007 (Reference 2.2-28).
- Accident rate for non-self propelled vessels. This is determined to be 1.8×10^{-6} per year, as provided in NUREG/CR-6624.
- Proportion of accidents causing significant release of contents. This is determined to be 0.025, as provided in NUREG/CR-6624.
- Conditional probability that a runaway vessel strikes the intake of length L. This is calculated assuming that once a vessel becomes runaway, the angle at which it travels is uniformly distributed over all possible angles.

The probability is calculated using the values listed above, and the length of the safety-related section of the intake structure of 68 ft. The probability of a significant release is found to be 0.59×10^{-7} per year. Since this probability is much smaller than the 1.0×10^{-7} per year threshold for a design basis event (Subsection 2.2.3.1), no further consideration of this hazard is necessary. There is an additional conservatism related to the fact that not every significant release causes a fire or explosion. The current calculation does not take credit for this fact and conservatively assumes the conditional probability of fire and explosion for a given release to be unity.

The above evaluation does not address damage to the intake structure due to the physical impact of any run-away barge. If the reactor technology selected requires a safety-related intake structure on the Delaware River this type of hazard will be addressed at the COLA stage, when information on the detailed design of the intake structure is available.

2.2.3.4 Liquid Spills

As discussed in Subsection 2.2.3.3, one of the four reactor technologies being considered by PSEG requires a safety-related intake structure on the Delaware River. According to the intake structure conceptual design, the circulating water system makeup pumps and service water

**PSEG Site
ESP Application
Part 2, Site Safety Analysis Report**

system makeup pumps draw water through the intake structure forebay on the bank of the river. Present at the forebay of the intake structure is a baffle wall that assists in preventing floating pollutants, such as petroleum products, from reaching the intake pump suction.

Materials that are transported on the Delaware River and could potentially be spilled into the waterway are listed in Table 2.2-6. Other than coal, tar-like oil, and asphalt, each of the transported materials has a specific gravity of less than one, meaning it would float on the surface of the water if spilled. Therefore, these liquids would not only be diluted by the large quantity of Delaware River water, but would float on the surface and consequently would not likely be drawn into the intake system. Cryogenics do not appear in the list of hazardous materials in Table 2.2-6.

In the unlikely event of a spill of coal, tar-like oil, or asphalt into the Delaware River, any substance that reached the intake structure would be removed by the bar rack or traveling screen in the intake structure system.

In summary, the intake structure is well protected. It is likely that any chemical spills would be sufficiently diluted before reaching the intake structure or would be swept away from the intake structure by the Delaware River current. Any floating liquids that reached the intake structure would likely be prevented from reaching the intake pump suction by the baffle wall in the forebay. Any spills that solidified in the water and reached the intake structure would be removed by the traveling screens. In each case, there would be no significant damage to the intake structure. As a result, the unlikely event of a liquid spill would not impact the safe shutdown of the new plant.

2.2.3.5 Radiological Hazards

Potential hazards due to the release of radioactive material from Hope Creek Generating Station (HCGS) or Salem Generating Station (SGS), as a result of normal operations or an unanticipated event, would not threaten the safety of the new plant. The information in Section 6.4 in the Design Control Document (DCD) or Final Safety Analysis Report (FSAR) associated with the reactor technologies under consideration by PSEG indicates that the control room outside air intakes are monitored for radiation. Upon detection of high radiation in the outside air intakes, each control room design automatically reconfigures the control room ventilation system to provide a habitable environment for the operators as described in the respective DCD or FSAR.

Radiation detectors and smoke detectors in the outside control room air intakes provide the required initiating signal to reconfigure the control room ventilation system into the protective mode of operation. The control room shielding design and habitability systems for the new plant are capable of maintaining the main control room environment suitable for prolonged occupancy throughout the duration of the postulated accidents that require protection from external airborne radioactivity. Therefore, the release of radioactive material from either HCGS or SGS would not threaten the safety of the new plant.

2.2.4 REFERENCES

- 2.2-1 ACI Standard 349-01, "Code Requirements for Nuclear Safety-Related Concrete Structures," American Concrete Institute, 2001.

**PSEG Site
ESP Application
Part 2, Site Safety Analysis Report**

- 2.2-2 Anchor Glass Container Corporation Tier Two Emergency and Hazardous Chemical Inventory, Website, https://www11.state.nj.us/DEP_RSP/Orchestrate.do?initiate=true&orchestrationId=NJD-EP-RTKPPP-RTKSurvey&service_category_id=4&service_class_id=6, login required, (find DEP Apps, then choose Right to Know and Pollution Prevention Program, then choose Community Right to Know survey, finally locate the facility in the facilities search bar), accessed April 13, 2009.
- 2.2-3 Cooper Interconnect Tier Two Emergency and Hazardous Chemical Inventory, Website, https://www11.state.nj.us/DEP_RSP/Orchestrate.do?initiate=true&orchestrationId=NJD-EP-RTKPPP-RTKSurvey&service_category_id=4&service_class_id=6, login required, (find DEP Apps, then choose Right to Know and Pollution Prevention Program, then choose Community Right to Know survey, finally locate the facility in the facilities search bar), accessed April 13, 2009.
- 2.2-4 Delaware Division of Air & Waste Management, (DNREC), "Air Liquide Tier Two Emergency and Hazardous Chemical Inventory January 1-December 31, 2008. April 2009.
- 2.2-5 Delaware Division of Air & Waste Management, (DNREC), "Delaware City Wastewater Treatment Plant Tier Two Emergency and Hazardous Chemical Inventory January 1-December 31, 2008", April 2009.
- 2.2-6 Delaware Division of Air & Waste Management, (DNREC), "Formosa Plastics Tier Two Emergency and Hazardous Chemical Inventory January 1-December 31, 2008. April 2009.
- 2.2-7 Delaware Division of Air & Waste Management, (DNREC), "Johnson Controls Tier Two Emergency and Hazardous Chemical Inventory January 1-December 31, 2008. May 2009.
- 2.2-8 Delaware Division of Air & Waste Management, (DNREC), "Port Penn Sewage Treatment Plant Tier Two Emergency and Hazardous Chemical Inventory January 1-December 31, 2008. April 2009.
- 2.2-9 Delaware Division of Air & Waste Management, (DNREC), "Valero Refinery Tier Two Emergency and Hazardous Chemical Inventory January 1-December 31, 2008. April 2009.
- 2.2-10 Department of the Army Corps of Engineers Institute for Water Resources, Website, "Waterborne Commerce of the United States Calendar Year 2003-2007 Part 1- Waterways and Harbors, Atlantic Coast," Available at <http://www.iwr.usace.army.mil/ndc/wcsc/wcsc.htm>, accessed February 27, 2009.
- 2.2-11 Dover Air Force Base, Website, <http://www.airnav.com/airport/KDOV/>, accessed October 5, 2009.

**PSEG Site
ESP Application
Part 2, Site Safety Analysis Report**

- 2.2-12 Federal Aviation Administration "Federal Aviation Administration Sectional Raster Aeronautical Charts, East, Vol." 77 Edition, published June 29, 2009.
- 2.2-13 Federal Aviation Administration APO Terminal Area Forecast Detail Report, <http://aspm.faa.gov/main/taf.asp>, accessed July 29, 2009.
- 2.2-14 Federal Aviation Administration Enroute U.S High 9/10 Chart, Website, <http://www.naco.faa.gov/ecom/ProductsDetails.aspx?ProductID=DEHUS9>, accessed July 29, 2009.
- 2.2-15 Hope Creek and Salem Electric Generating Station Tier Two Emergency and Hazardous Chemical Inventory, Website, https://www11.state.nj.us/DEP_RSP/Orchestrate.do?initiate=true&orchestrationId=NJD-EP-RTKPPP-RTKSurvey&service_category_id=4&service_class_id=6, login required, (find DEP Apps, then choose Right to Know and Pollution Prevention Program, then choose Community Right to Know survey, finally locate the facility in the facilities search bar), accessed April 13, 2009.
- 2.2-16 Introduction to Heat Transfer, Fourth Edition, Incropera and DeWitt, John Wiley & Sons, 2002.
- 2.2-17 "Investigation into the Explosion and Sinking of the Chemical Tanker Bow Mariner," United States Coast Guard and U.S. Department of Homeland Security, December 14, 2005.
- 2.2-18 Lower Alloways Creek Municipal Township Building "Tier Two Emergency and Hazardous Chemical Inventory," January 1-December 31, 2008. April 2009.
- 2.2-19 Mannington Mills Tier Two Emergency and Hazardous Chemical Inventory, Website, Hope Creek and Salem Electric Generating Station Tier Two Emergency and Hazardous Chemical Inventory, Website, https://www11.state.nj.us/DEP_RSP/Orchestrate.do?initiate=true&orchestrationId=NJD-EP-RTKPPP-RTKSurvey&service_category_id=4&service_class_id=6, login required, (find DEP Apps, then choose Right to Know and Pollution Prevention Program, then choose Community Right to Know survey, finally locate the facility in the facilities search bar), accessed April 13, 2009.
- 2.2-20 "Marine Casualty and Pollution Data for Researchers," Subset of the MISLE Database, <http://homeport.uscg.mil/mycg/portal/ep/home.do> (click on Investigations, then Marine Casualty/Pollution Investigations, then Marine Casualty and Pollution Data for Researchers). Accessed October 13, 2009.
- 2.2-21 Maritime Exchange, "Annual Summary of Cargo and Piers, for the Delaware River 1995-2008," Maritime Exchange. Philadelphia, PA. January, 2009.
- 2.2-22 Maritime Exchange, "CDC Net Tonnage 2003-2007, Delaware River," Maritime Exchange. Philadelphia, PA. September 24, 2009.

**PSEG Site
ESP Application
Part 2, Site Safety Analysis Report**

- 2.2-23 New Castle County Comprehensive Plan, Website, <http://www2.nccde.org/landuse/Planning/ComprehensivePlan/default.aspx>, accessed May 14, 2009.
- 2.2-24 "Office of Hazardous Materials Safety Incident Reports Database Search," <https://hazmatonline.phmsa.dot.gov/IncidentReportsSearch/>, U.S. Department of Transportation Pipeline and Hazardous Materials Safety Administration. Accessed October 22, 2009.
- 2.2-25 PSEG, "Requirements for Compliance with Discharge Prevention, Containment, and Countermeasure (DPCC) Regulations." Prepared in 2001.
- 2.2-26 Summit Airport, Website, www.airnav.com/airport/KEVY/, accessed October 5, 2009.
- 2.2-27 The SFPE Handbook of Fire Protection Engineering, 2nd Edition, Society of Fire Protection Engineers, 1995.
- 2.2-28 "Waterborne Commerce of the United States Pass the Point for the Delaware River, RM 52," Department of the Army Corps of Engineers Waterborne Commerce Statistics Center. September, 11, 2009.

**PSEG Site
ESP Application
Part 2, Site Safety Analysis Report**

**Table 2.2-1 (Sheet 1 of 2)
Industrial Facilities within 10 miles of the PSEG Site**

Facility	Concise Description	Number of Employees	Distance from PSEG Power Block Area	Chemicals Used or Produced
Hope Creek Generating Station	Nuclear power plant licensed by the Nuclear Regulatory Commission.	1554 Total Employees for Salem and Hope Creek Generating Stations	1730 ft.	Itemized in Table 2.2-2a and Table 2.2-3
Salem Generating Station	Nuclear power plant licensed by the Nuclear Regulatory Commission.	1554 Total Employees for Salem and Hope Creek Generating Stations	3249 ft., 2929 ft.	Itemized in Table 2.2-2b and Table 2.2-3
Port Penn Sewage Treatment Plant	Public sewage treatment plant	No Full Time Employees	3.4 mi.	Itemized in Table 2.2-4
Lower Alloways Creek Township Buildings	Local administration, township storage, etc.	30 Total Employees	More than 3.0 mi.	Itemized in Table 2.2-5
Delaware City Wastewater Treatment Plant	Public sewage treatment plant.	No Full Time Employees	7.5 mi.	Sodium Hypo-Chlorite
Cooper Interconnect	Manufacturer of electrical products.	114 (maximum per shift)	7.6 mi.	Sulfuric Acid, Vinyl Chloride
Anchor Glass Container Corporation	Manufacturer of glass containers.	130 (maximum per shift)	8.0 mi.	Propane, Heating Oil
Mannington Mills	Manufacturer of residential and commercial flooring.	550 (maximum per shift)	8.7 mi.	Propane, Gasoline, Nitrogen (compressed or liquefied)
Valero Delaware City Refinery ^(a)	Crude oil refinery with power generation facility.	600 (maximum per shift)	8.9 mi.	Hydrogen gas, Ethylene Glycol, Petroleum

**PSEG Site
ESP Application
Part 2, Site Safety Analysis Report**

**Table 2.2-1 (Sheet 2 of 2)
Industrial Facilities within 10 miles of the PSEG Site**

Facility	Concise Description	Number of Employees	Distance from PSEG Power Block Area	Chemicals Used or Produced
Air Liquide	Producer of chemical and industrial gases.	27 (estimated)	9.2 mi.	Fuel Oil, Anhydrous Ammonia
Formosa Plastics Corporation	Producer of Polyvinyl Chloride (PVC) resins.	56 (maximum per shift)	9.6 mi.	Propane, Gasoline, Nitrogen (compressed or liquefied)
Johnson Controls Inc. Battery Division	Supplier of lead acid batteries.	113 (maximum per shift)	9.7 mi.	Lead, Sulfuric Acid, Kerosene
Quaker City Motor Parts/ NAPA Distribution Center	Distribution center for auto parts and accessories.	86 (maximum per shift)	9.7 mi.	No information available

a) Valero Delaware City Refinery ceased operations in 2009.

References 2.2-2 through 2.2-9, 2.2-15, 2.2-18, and 2.2-19

**PSEG Site
ESP Application
Part 2, Site Safety Analysis Report**

**Table 2.2-2a
Hope Creek Generating Station Chemical Storage**

Chemical	Container Type	Location	Tank Capacity Gallons
50% Sodium Hydroxide Solution	Lined Carbon Steel	West-Southwest of Cooling Tower	21,154
50% Sodium Hydroxide Solution	Steel	Turbine Building	2 @ 16,000
Sodium Hydroxide	Steel	Auxiliary Building	1 @ 27,500 1 @ 12,000
Sodium Hydroxide	Steel	Auxiliary Building Rad-Waste Area	1 @ 4500 1 @ 12,000 1 @ 27,500
15% Sodium Hypochlorite Solution	Durakane 411 Lined Carbon Steel	West-Southwest of Cooling Tower	2 @ 30,000
15% Sodium Hypochlorite Solution	Durakane 411 Lined Carbon Steel	East of Service Water Intake Structure	2 @ 15,254
Sulfuric Acid	Steel	Turbine Building	2 @ 16,000
Hydrazine	Stainless Steel	West-Southwest Boiler Building	25
Hydrazine	Steel	Auxiliary Boiler Building	2 @ 35
No. 2 Fuel Oil	Steel	North of Hope Creek Barge Slip	1,000,000
No. 2 Fuel Oil	Steel	Outside of Fire Pump House	300
No. 2 Fuel Oil	Steel	Northwest of Auxiliary Boiler Building	18,000
No. 2 Fuel Oil	Steel	Auxiliary Building	8 @ 26,500
No. 2 Fuel Oil	Steel	Auxiliary Building Diesel Room	4 @ 550
Gasoline	Steel	North of Barge Slip	6000
Diesel Fuel	Steel	North of Barge Slip	6000
70% Ammonium Bisulfate Solution	Coated FRP	West-Southwest of Cooling Tower	5000
Petroleum Oil	Steel	Turbine Building	12,275 2 @ 22,000 3 @ 425
Petroleum Oil	Steel	Emergency Diesel Generator Building	2 @ 275
Triphenyl Phosphate	Steel	Turbine Building	450
Ammonium Hydroxide	Stainless Steel	Auxiliary Boiler Building	50

Reference 2.2-25

**PSEG Site
ESP Application
Part 2, Site Safety Analysis Report**

**Table 2.2-2b
Salem Generating Station Chemical Storage**

Chemical	Container Type	Location	Tank Capacity Gallons
<28% Ammonium Hydroxide Solution	Steel	Unit 1 Turbine Building	2 @ 250
<28% Ammonium Hydroxide Solution	Steel	Unit 1 Turbine Building	3500
15% Sodium Hypochlorite Solution	Lined Steel	Yard, Southwest of Unit 1 Reactor	2 @ 88,000
50% Sodium Hydroxide Solution	Epoxy Enamel Coated Steel	Unit 1 Turbine Building	2 @ 4000
50% Sodium Hydroxide Solution	FRP – Durakane 411	Chemical Treatment Building	5000
50% Sodium Hydroxide Solution	Lined Steel	Unit 2 Turbine Building	2 @ 2250
Sodium Hydroxide	Steel	Unit 1 Auxiliary Building	4000
Sodium Hydroxide	Steel	Unit 2 Auxiliary Building	4000
5-35% Hydrazine Solution	Steel	Unit 1 Turbine Building	2 @ 250
5-35% Hydrazine Solution	Poly	Unit 1 Turbine Building	300
98% Sulfuric Acid	Baked Phenolic Resin Coated Steel	Unit 1 Turbine Building	4000
98% Sulfuric Acid	Lined Steel	Unit 2 Turbine Building	2250
Hydrazine	Steel	House Heating Boiler Building	50
Propylene Glycol	Steel	East of House Heating Boiler	5200
Potassium Chromate	Steel	Unit 1 Auxiliary Building	2000
Potassium Chromate	Steel	Unit 2 Auxiliary Building	2000
Potassium Dichromate	Steel	Unit 1 Auxiliary Building	2000
Potassium Dichromate	Steel	Unit 2 Auxiliary Building	2000
Fuel Oil	Steel	Auxiliary Boiler Building	3 @ 300
Fuel Oil	Steel	Inside Fire Pump House	2 @ 350
No. 2 Fuel Oil	Steel	Unit 2 Auxiliary Building	3 @ 550 2 @ 30,000
No. 2 Fuel Oil	Steel	Unit 1 Auxiliary Building	3 @ 550 2 @ 30,000
No. 2 Fuel Oil	Steel	East of Cooling Water Intake	840,000
Petroleum Lube Oil	Steel	Unit 1 Turbine Building	1 @18,000 2 @14,000 1 @ 550 1 @ 6000
Petroleum Lube Oil	Steel	Unit 2 Turbine Building	1 @ 1100 1 @18,000 2 @14,000 1 @ 500

Reference 2.2-25

**PSEG Site
ESP Application
Part 2, Site Safety Analysis Report**

**Table 2.2-3
SGS and HCGS Right-to-Know Chemical Storage**

Chemical	Container Type	Location	Max Daily Inventory Pounds
Ammonium Hydroxide	Stainless Steel	Facility Wide	9999
Tetrafluoroethane	Cylinder	Facility Wide	99,999
Acetone	Bottles/ Jugs (glass)	Facility Wide	499
Carbon Dioxide	Cylinder	Salem Gas Bottle Storage	999
Dichlorodifluoromethane	Cylinder	Material Center	9999
Difluoroethane	Cylinder	Material Center	24,999
Ethylbenzene	Other	Material Center	99
Hydrazine	Stainless Steel	Facility Wide	9999
Hydrogen	Cylinder	South of the Hope Creek Turbine/Admin. Building ^(a)	120,000 cu. ft. ^(a)
Methoxypropylamine	Tote Bin	Facility	24,999
Monochloropentafluoroethane	Cylinder	Salem Gas Bottle Storage	99,999
Nitrogen	Cylinder	Facility Wide	24,999
Toluene	Can	Material Center	99
N-Butyl Acetate	Other	Material Center	499
Trichlorofluoromethane	Steel Drum	Material Center	999
Xylene	Can	Material Center	9999

Reference 2.2-15

- a) The location and storage conditions of the hydrogen were identified using site drawings and a walkdown conducted by on-site PSEG employees separate from Reference 2.2-15.

**PSEG Site
ESP Application
Part 2, Site Safety Analysis Report**

**Table 2.2-4
Port Penn Sewage Treatment Plant Chemical Storage**

Chemical	Container Type	Location	Tank Capacity Gallons
Sodium Hypochlorite	55 Gallon Drums	On-site	220
Various Oil	Plastic Container	On-site	12.5

Reference 2.2-8

**PSEG Site
ESP Application
Part 2, Site Safety Analysis Report**

**Table 2.2-5
Lower Alloways Creek Township Chemical Storage**

Chemical	Container Type	Location	Tank Capacity Gallons
Waste Oil	Above Ground Tank	End of Lower Alloways Creek Road Garage	500
Diesel	Above Ground Tank	Fuel Area Road Garage	6000
Gasoline	Above Ground Tank	Fuel Area Road Garage	6000
Propane	Above Ground Tank	Behind Waste Oil Tank	1000
Fuel Oil	Above Ground Tank	Rear of Ambulance Building	500
Fuel Oil	Above Ground Tank	Rear of Garage Wash Bay	3000
Fuel Oil	Above Ground Tank	Carpenter Shop	500
Fuel Oil	Above Ground Tank	North End of Bus Garage	2000

Reference 2.2-18

**PSEG Site
ESP Application
Part 2, Site Safety Analysis Report**

**Table 2.2-6
Chemical Commodities Transported on the Delaware River from 2003 through 2007 (in short tons)**

Commodity	2007	2006	2005	2004	2003
Acyclic Hydrocarbons	41,996	3076	3949	5111	3103
Alcohols	1,164,742	1,250,092	138,530	145,797	162,620
Ammonia	572	11,493	288	611	668
Asphalt, Tar & Pitch	922,674	1,148,749	1,193,995	1,301,665	1,346,674
Benzene & Toluene	313,448	284,947	331,515	328,656	358,551
Carboxylic Acids	123,225	66,736	68,481	51,464	53,206
Chemical Products NEC ^(a)	98,013	55,031	53,505	112,678	134,498
Chemical Additives	7546	149,793	634,609	455,020	1,043,777
Crude Petroleum	65,725,325	65,878,419	67,224,045	63,008,462	63,784,587
Distillate Fuel Oil	6,049,563	6,355,416	5,268,342	4,550,148	3,071,968
Explosives	163	117	71	191	56
Fertilizers & Mixes NEC ^(a)	8067	3118	5508	11,644	10,989
Gasoline	3,350,946	3,875,778	4,044,285	3,251,643	2,861,138
Hydrocarbon & Petrol Gases, Liquefied and Gaseous	309,113	398,585	99,671	246,260	162,861
Inorganic Chem. NEC ^(a)	3908	43,936	14,389	8809	5110
Kerosene	115,671	53,893	174,099	150,168	128,648
Lube Oil & Greases	200,362	123,978	163,153	589,717	159,205
Naphtha & Solvents	360,720	731,221	448,858	286,849	362,017
Nitrogen Function Compound	9297	13,255	12,929	8037	5470
Nitrogenous Fertilizer	99,947	54,095	58,870	66,636	143,843
Ordnance & Access	447	440	323	162	266
Organic Comp. NEC ^(a)	20,736	258,869	736,476	1,102,373	752,678
Organo - Inorg. Comp.	11,761	12,120	13,209	11,697	4791
Other Hydrocarbons	101,532	103,617	83,180	182,955	171,914
Pesticides	1365	1392	1528	1405	1794
Petroleum Jelly & Waxes	50,748	35,574	59,058	55,682	79,332
Petroleum Products NEC ^(a)	81,554	70,568	13,063	Not Reported	23,287
Residual Fuel Oil	6,965,965	6,368,542	5,862,399	5,395,237	6,431,300
Sodium Hydroxide	14,639	89,095	159,013	206,272	176,723
Sulfuric Acid	80	77	119	201	2396
Unknown or NEC ^(a)	279,535	319,087	312,986	498,031	221,554

a) NEC represents Not Elsewhere Classified.

Reference 2.2-28

**PSEG Site
ESP Application
Part 2, Site Safety Analysis Report**

**Table 2.2-7
Number of Vessels Traveling to Oil/Petroleum/Chemical Berths on the Delaware River in
Each State from 1995 through 2008**

Year	Pennsylvania	New Jersey	Delaware
1995	530	278	91
1996	428	301	115
1997	457	310	125
1998	620	392	165
1999	632	397	151
2000	678	426	150
2001	648	458	151
2002	622	434	142
2003	575	432	126
2004	585	452	158
2005	611	457	187
2006	587	528	241
2007	622	516	223
2008	592	508	197
Total	8187	5889	2222

Reference 2.2-21

**PSEG Site
ESP Application
Part 2, Site Safety Analysis Report**

**Table 2.2-8
Largest Net Tonnage of Hazardous Cargo Traveling on the Delaware River from 2003
through May 2009**

Cargo	Largest Net Tonnage (tons)
Acetone	15,121
Benzene	13,959
Butane	18,807
Chemicals	30,092
Diesel	14,356
Ethanol	13,154
Fuel Oil	48,785
Gasoline	32,163
Jet Fuel	15,276
Liquid Gas	17,024
Methyl Tertiary Butyl Ether	107,829
Oil	110,526
Propane	17,305
Urea	14,177

Reference 2.2-22

**PSEG Site
ESP Application
Part 2, Site Safety Analysis Report**

**Table 2.2-9
Chemical Commodities Transported on the Chesapeake and Delaware Canal from 2003
through 2007 (in thousand short tons)**

Chemical Commodity Description	2007	2006	2005	2004	2003
Crude petroleum	Not Reported	88	69	Not Reported	8
Gasoline	1948	2089	1698	1061	1759
Kerosene	6	5	22	18	56
Distillate Fuel Oil	1002	1442	772	819	510
Residual Fuel Oil	1350	1378	1272	1259	1280
Lube Oil & Greases	48	156	9	52	9
Petroleum Jelly & Waxes	3	15	48	30	48
Naphtha & Solvents	75	182	163	125	106
Asphalt, Tar & Pitch	1027	1066	1191	1139	1199
Petroleum Coke	73	190	Not Reported	20	12
Hydrocarbon & Petroleum Gases, Liquefied and Gaseous	Not Reported	26	21	53	42
Petroleum Products NEC ^(a)	26	41	17	Not Reported	Not Reported
Nitrogenous Fertilizer	18	12	6	46	11
Benzene & Toluene	Not Reported	17	59	26	27
Other Hydrocarbons	7	4	10	21	291
Alcohols	709	954	265	270	293
Organic Compound NEC ^(a)	37	9	1	19	6
Sodium Hydroxide	146	75	46	76	120
Inorganic Elements, Oxides & Halogen Salts	Not Reported	3	Not Reported	4	Not Reported
Metallic Salts	87	74	81	91	87
Chemical Additives	Not Reported	32	96	110	170
Chemical Products NEC ^(a)	69	137	215	90	98

a) NEC represents Not Elsewhere Classified.

Reference 2.2-10

**PSEG Site
ESP Application
Part 2, Site Safety Analysis Report**

**Table 2.2-10
State and Federal Highways within 10 Miles of the PSEG Site**

Highway	Closest Approach to the New Plant Power Block Area	Chemical Products
Delaware Route 9	3.1 mi. west	Chemical delivery not specified
Delaware Route 1	5.8 mi. west	Chemical delivery not specified
U.S. Route 13	5.9 mi. west	Chemical delivery not specified
Delaware Route 299	6.0 mi. west	Chemical delivery not specified
Delaware Route 896	6.1 mi. west	Chemical delivery not specified
New Jersey Route 49	7.5 mi. northeast	Chemical delivery not specified
New Jersey Route 45	7.8 mi. northeast	Chemical delivery not specified
Delaware Route 72	9.3 mi. northwest	Chemical delivery not specified
Delaware Route 7	9.7 mi. west	Chemical delivery not specified
Delaware Route 71	9.7 mi. west	Chemical delivery not specified
U.S. Route 301	9.7 mi. west	Chemical delivery not specified

**PSEG Site
ESP Application
Part 2, Site Safety Analysis Report**

**Table 2.2-11
Airport Operations within the PSEG Site Region**

Airport	Annual Number of Operations	Distance from new power block area
Salem/Hope Creek Helipad	Sporadic	3848 ft.
Paruszewski Farm Strip Airport	Sporadic	5.2 mi.
PSEG Training Center Heliport	Sporadic	6.9 mi.
Stoe Creek Farm Airport	Sporadic	7.0 mi.
Townsend Airport	Sporadic	7.6 mi.
Hidden Acres Airport	Sporadic	7.8 mi.
Salem Airport	Sporadic	7.9 mi.
Scotty's Place Airport	Sporadic	8.2 mi.
Okolona Plantation Airport	Sporadic	8.5 mi.
Summit Airport	60,612 (2007) 77,819 (2025)	10.4 mi.
New Castle County Airport	127,902 (2007) 108,881 (2025)	14.5 mi.
Delaware Airpark	28,661 (2007) 53,697 (2025)	17.2 mi.
Dover Air Force Base	123,735 (2007) ^(a)	23.8 mi
Millville Airport	42,610 (2007) 42,610 (2025)	25.4 mi.
Philadelphia International Airport	504,528 (2007) 696,175 (2025)	32.2 mi.

a) Number of annual operations based on 339 operations per day which are 100 percent military.

References 2.2-11 and 2.2-13

**PSEG Site
ESP Application
Part 2, Site Safety Analysis Report**

**Table 2.2-12
Breakdown of the Probabilities of Chemical Spill Sizes**

Spill Size	Occurrences ^(b)	Probability ^(b)	Spills per Vessel Mile ^(a)
0-100 Gallons	9260	0.9341	1.68×10^{-6}
100-1000 Gallons	494	0.0498	8.97×10^{-8}
1000-2000 Gallons	58	0.0059	1.05×10^{-8}
2000-10,000 Gallons	61	0.0062	1.11×10^{-8}
10,000-50,000 Gallons	27	0.0027	4.90×10^{-9}
50,000-322,000 Gallons	12	0.0012	2.18×10^{-9}
>322,000 Gallons	1	0.0001	1.82×10^{-10}
Total	9913	1	1.80×10^{-6}

- a) NUREG/CR-6624 states that barge incidents occur at a rate of 1.8×10^{-6} incidents per mile. The probability for each spill size is used to determine the rate of spills per mile. For example, the rate of spills per mile for 0 to 100 gallons is 1.68×10^{-6} spills per mile ($=1.8 \times 10^{-6} \times 0.9341$).
- b) The number of occurrences is based on data from the Coast Guard MISLE database (Reference 2.2-20). The probability is the number of occurrences of that spill size divided by the total number of occurrences, 9913.

**PSEG Site
ESP Application
Part 2, Site Safety Analysis Report**

**Table 2.2-13
Results for Calculation of Frequency of a Hazard per Trip of Propane Past the PSEG Site**

Spill Volume (gallons)	Weather (Stability)	Standoff Distance (miles)	Hazardous Trip Length D_{trip} (miles)	Directions from Vessel to Site	Worst Wind Direction	Adverse Wind Probability P_{weather}	Spill Rate (spills/mile) P_{spill}·R- accident	Total Hazard R_{haz}
2000	G	<0.9	0			0	1.05×10^{-8}	0
10,000	G	1.8	4	S-NNW	S	0.51%	1.11×10^{-8}	2.26×10^{-10}
10,000	F	1.1	1.2	WSW- WNW	WSW	0.69%	1.11×10^{-8}	9.19×10^{-10}
10,000	E	<0.9	0			0	1.11×10^{-8}	0
50,000	G	3.4	7.7	SSE-N	N	0.69%	4.90×10^{-9}	2.60×10^{-10}
50,000	F	2.0	4.3	S-NNW	NNW	1.17%	4.90×10^{-9}	2.47×10^{-10}
50,000	E	1.2	1.7	SW-NW	NW	4.14%	4.90×10^{-9}	3.45×10^{-10}
322,000	G	5.0	11	SSE-N	N	0.69%	2.18×10^{-9}	1.65×10^{-10}
322,000	F	4.3	9.7	SSE-N	N	1.19%	2.18×10^{-9}	2.52×10^{-10}
322,000	E	2.5	5.5	S-NNW	NW	4.14%	2.18×10^{-9}	4.96×10^{-10}
322,000	D	1.7	3.8	SSW- NNW	NW	2.63%	2.18×10^{-9}	2.18×10^{-10}
322,000	C	<0.9	0			0	2.18×10^{-9}	0
>322,000	All	5.0	11	SSE-N	NW	10.79%	1.82×10^{-10}	2.16×10^{-10}
Total								2.52×10^{-9}
Allowable Trips								397

**PSEG Site
ESP Application
Part 2, Site Safety Analysis Report**

**Table 2.2-14
Number of Allowable Trips of Chemical Hazards Past the PSEG Site Each Year Based on
a Probabilistic Analysis for a Flammable Vapor Cloud and Solid Explosive Hazards**

Chemical	Allowable Number of Trips
Propane	397
Gasoline	3753
Benzene	9131
Ammonia	4629
Naphtha	3753
Methane	708
Acetone	3753
Vinyl Chloride	520
Solid Explosive	888
Ammonium Nitrate	888

**PSEG Site
ESP Application
Part 2, Site Safety Analysis Report**

**Table 2.2-15
Estimated Number of Trips of Chemical Hazards Past the PSEG Site Each Year
and the Frequency of each Explosive Hazard^(a)**

Chemical	Maximum Total Tons per Year (2003-2007 USACE)	USACE Average Shipment Tons (2003-07)	USACE Minimum Shipment Tons (2003-07)	Maritime Exchange Average Shipment Tons (2003-07)	Maritime Exchange Minimum Shipment Tons (2003-07)	Tons per Vessel Used in this Analysis	Estimated Number of Trips ^(b)	Allowable Number of Trips	Probability of Explosive Hazard per year^{(d)(e)}
Propane	514,839	7238	2307	7592	1269	4000	129	397	3.25E-7
Gasoline	4,044,285	5062	614	14,922	10,400	4000	1012	3,753	2.70E-7
Benzene	358,551	10,424	823	5234	2351	800	449	9,131	4.92E-8
Ammonia	140,636	9035	4272	8109	829	800	176	4,629	3.80E-8
Naphtha	731,221	5375	1347	11,280	4527	1000	732	3,753	1.95E-7
Methane	398,585	1999	1999	N.A.	N.A.	1000	399	708	5.64E-7
Acetone	1,102,373	15,276	8815	7512	829	800	1378	3,753	3.67E-7
Vinyl Chloride	182,955	11,411	1922	N.A.	N.A.	1900	97	520	1.87E-7
Solid Explosives ^(c)	610	N.A.	N.A.	N.A.	N.A.	589	2	888	2.25E-9
Ammonium Nitrate ^(c)	165,412	N.A.	N.A.	N.A.	N.A.	589	282	888	3.18E-7

- a) N.A. - Not Available
- b) The estimated number of trips is rounded up for conservatism.
- c) See Subsection 2.2.3.2.2 for a discussion of the shipment sizes of solid explosives.
- d) Based on the estimated number of trips for each chemical.
- e) Total Aggregated Frequency of an Explosion adversely affecting the PSEG Site is 2.31E-6/year

**PSEG Site
ESP Application
Part 2, Site Safety Analysis Report**

**Table 2.2-16
Hazardous Commodities Transported by Vessel and the Chemical
Analyzed for Each Commodity**

USACE 4 Digit Commodity ^(b)	Chemical Analyzed for each Types of Hazard ^(a)
Acyclic Hydrocarbons	Propane for both VCE and toxicity
Alcohols	Both methanol and ethanol for both VCE and toxicity
Ammonia	Ammonia for both VCE and toxicity
Benzene & Toluene	Benzene for both VCE and toxicity
Carboxylic Acids	Acetic acid for VCE, formic acid for toxicity
Chem. Products NEC ^(c)	Ammonia for both VCE and toxicity
Chemical Additives	No hazard – Low vapor pressure
Explosives	TNT for a stationary explosion
Fert. & Mixes NEC ^(c)	Ammonium nitrate for a stationary explosion
Gasoline	Gasoline for both VCE and toxicity
Hydrocarbon & Petrol Gases, Liquefied and Gaseous	Methane for both VCE and toxicity
Inorganic Chem. NEC ^(c)	Ammonium nitrate for a stationary explosion, hydrogen peroxide for toxicity
Naphtha & Solvents	Naphtha for both VCE and toxicity
Nitrogen Func. Comp.	Ammonium nitrate for a stationary explosion, ammonia for both VCE and toxicity
Nitrogenous Fert.	Ammonium nitrate for a stationary explosion
Ordnance & Access.	TNT for a stationary explosion
Organic Comp. NEC ^(c)	Acetone for both VCE and toxicity
Organo - Inorg. Comp.	Propane for a VCE, ammonia for toxicity
Other Hydrocarbons	Vinyl chloride for a VCE, ethylene dichloride for toxicity
Pesticides	Herbicide and insecticide for toxicity
Petro. Products NEC ^(c)	Propane for both VCE and toxicity
Unknown or NEC ^(c)	Propane for a VCE, ammonia for toxicity

- a) Toxicity analyses will be developed for the COLA after a reactor technology has been selected.
- b) The USACE delineates commodities based on commodity codes. The four digit codes are associated with the commodity families listed in this table.
- c) NEC represents Not Elsewhere Classified.

**PSEG Site
ESP Application
Part 2, Site Safety Analysis Report**

**Table 2.2-17
Chemicals Stored at Nearby Facilities (Including the Salem
and Hope Creek Generating Stations) that are Analyzed**

Chemical	Amount	Location	Distance to the Power Block Boundary (miles)	Distance to Safety- Related Buildings (miles)	Hazardous Conditions
Gasoline	6000 (gal.)	Lower Alloways Creek Township Buildings	3	3	Explosion, Flammable Vapor Cloud, Toxicity
Propane	1000 (gal.)	Lower Alloways Creek Township Buildings	3	3	Explosion, Flammable Vapor Cloud, Toxicity
Gasoline	6000 (gal.)	Hope Creek	0.12	0.19	Explosion, Flammable Vapor Cloud, Toxicity
Gasoline	8000 (gal.)	Delivery to Salem/ Hope Creek Site	0.01	0.07	Explosion, Flammable Vapor Cloud, Toxicity
Diesel	1,000,000 (gal.)	Hope Creek	0.05	0.14	Explosion
Hydrogen	120,000 (standard cubic feet, scf)	S/HC Site	0.35	0.44	Explosion, Flammable Vapor Cloud, Toxicity

**PSEG Site
ESP Application
Part 2, Site Safety Analysis Report**

**Table 2.2-18
Explosion Event Analysis**

Chemical	Location	Distance to the Power Block Boundary (miles)	Distance to Safety-Related Buildings (miles)	Safe Distance for an Explosion (miles)
Gasoline	Lower Alloways Creek Township Buildings	3	3	0.02
Propane	Lower Alloways Creek Township Buildings	3	3	0.14
Gasoline	Hope Creek	0.12	0.19	0.02
Gasoline	Delivery to Salem/ Hope Creek Site	0.01	0.07	0.02
Diesel	Hope Creek	0.05	0.14	0.13
Hydrogen	S/HC Site	0.35	0.44	0.11
Explosive Chemical Vapors	Vessel on the Delaware River	0.9	0.9	0.5

**PSEG Site
ESP Application
Part 2, Site Safety Analysis Report**

**Table 2.2-19
Flammable Vapor Cloud Event Analysis ^(a)**

Chemical	Location	Distance to the Power Block Boundary (miles)	Distance to Safety-Related Buildings (miles)	Safe Distance for a Flammable Vapor Cloud (miles)
Gasoline	Lower Alloways Creek Township Buildings	3	3	0.239
Propane	Lower Alloways Creek Township Buildings	3	3	0.814
Gasoline	Hope Creek	0.12	0.19	0.239 ^(b)
Gasoline	Delivery to Salem/ Hope Creek site	0.01	0.07	0.274 ^(b)
Hydrogen	S/HC Site	0.35	0.44	0.24
Alcohols (Methanol/ Ethanol)	Vessel on the Delaware River	0.90	0.90	<0.90
Acetic Acid	Vessel on the Delaware River	0.90	0.90	<0.90

- a) This table does not include those chemicals for which a probabilistic analysis was performed. The chemicals for which a probabilistic analysis was performed are shown in Table 2.2-14.
- b) The Hope Creek Generating Station gasoline tank and the delivery route to that tank do not meet the safe standoff distance acceptance criteria. The tank location and the route for the delivery truck will be relocated and the new location analyzed after a reactor technology is selected.

**PSEG Site
ESP Application
Part 2, Site Safety Analysis Report**

**Table 2.2-20
Toxicity Event Analysis ^(a)**

Chemical	Location	Distance to the Power Block Boundary (miles)	Distance to Safety- Related Buildings (miles)	Peak Power Block Concentration (ppm)	Toxicity Limit (ppm)
Gasoline	Lower Alloways Creek Twsp. Municip. Bldg.	3	3	206	500
Propane	Lower Alloways Creek Twsp. Municip. Bldg.	3	3	710	2100

- a) The technology has not been selected, therefore only the concentration at the new plant location can be determined. For all adjacent site chemicals and chemicals that are transported on the Delaware River, a full toxicity analysis will be performed during creation of the COLA.

**PSEG Site
ESP Application
Part 2, Site Safety Analysis Report**

**Table 2.2-21
Chemical Fire Event Analysis**

Chemical	Location	Distance to the Power Block Boundary (miles)	Distance to Safety- Related Buildings (miles)	Peak Heat Load (kW/m²)	Wall Temperature Increase (°F)
Propane	Lower Alloways Creek Twsp. Municip. Bldg.	3	3	0.011	Negligible
Gasoline	Delivery to Salem/ Hope Creek site	0.01	0.07	0.39	8.2
Diesel	Hope Creek	0.05	0.14	0.0497	3.6
Hydrogen	Adjacent Site	0.35	0.44	0.05	Negligible
Propane	Vessel on the Delaware River	0.90	0.90	22.3 ^(a)	174 ^(a)
Gasoline	Vessel on the Delaware River	0.90	0.90	0.008	Negligible

a) The worst case propane fireball results in a large heat load and a large increase in wall temperature; however, the acceptance criteria for a concrete wall, based on ACI Standard 349-01 (Reference 2.2-27), are met. An additional examination the frequency of a fireball of that size was performed. The results show that complete ruptures of 5000 tons of propane occur very infrequently (Table 2.2-12) and that the probability that a fireball has a heat load greater than 6.36 kW/m² is less than the probability of a flammable vapor cloud at the site (Table 2.2-13). A full sized explosion is therefore bounded by the flammable vapor cloud. The temperature increase for the smaller fireball is 37°F.

**PSEG Site
ESP Application
Part 2, Site Safety Analysis Report**

**Table 2.2-22
Number of Non-Self Propelled Vessels that Passed the PSEG Site
from 2003 through 2007**

Year	Number of Vessels
2003	2464
2004	2722
2005	2825
2006	2772
2007	2499

**PSEG Site
ESP Application
Part 2, Site Safety Analysis Report**

2.3 METEOROLOGY

2.3.1 REGIONAL CLIMATOLOGY

2.3.1.1 Landforms and Ground Surface Character of the Site Region

The climate of the PSEG Site region is the combined result of several geographic factors, including passage of large-scale (synoptic) weather systems, the character of approaching air masses, and the character of the regional ground surface. This and following subsections include background information on these factors.

The PSEG Site is located on the east shoreline of the Delaware River at the southwest corner of New Jersey, on the Outer Coastal Plain (Reference 2.3.1-1).

The region surrounding the PSEG Site at the southern end of New Jersey includes three major landform areas, as shown in Figure 2.3-1. Those areas are the Delaware River to the west, and to the east the Inner Coastal Plain and the Outer Coastal Plain. The difference between the ground surfaces of those two plains is primarily in the age and constituents of the ground surface sediments. The boundary between those two plains is a low, eroded ridge that runs generally northeast to southwest, parallel to the Atlantic Ocean coastline. The width of the Delaware River adjacent to the PSEG Site is 2.5 miles (mi.). The width in the east-west direction of the combined inner and outer coastal plains widens from 25 mi. at Raritan Bay to the north, to 60 mi. between the lower Delaware River and the Atlantic Ocean at the south end of the state. Highest ground surface elevation on the combined inner and outer coastal plains is 400 feet (ft.). One-half of the ground surface of the combined inner and outer coastal plains is below 100 ft.

Land use character of the region surrounding the PSEG Site includes the following ground surface types. In New Jersey on the eastern shore of the Delaware River, and within a distance of 5 mi. from the site, the surface is primarily marsh (References 2.3.1-1, 2.3.1-2, 2.3.1-3, and 2.3.1-4) Figure 2.3-2 presents a local topographic map. At distances greater than 5 mi., the surface is a mixture of cleared area, coastal dune vegetation, forest including oak, beach, and pine, and urban centers. Figure 2.3-3 presents a regional topographic map.

As described in Subsection 2.3.2.5, elevation profiles for a radial distance range of 50 mi. show that the terrain in the PSEG Site area out to a distance of 20 mi. is flat to gently rolling. The nearest significant topography is at distances ranging from 20 through 50 mi., and ranges in elevation from 200 to 800 ft. mean sea level (msl). The highest elevation at a radial distance of 25 mi. is 400 ft. msl. The overall highest elevation within a radius of 50 mi. is 975 ft. msl at a distance of 48 mi.

2.3.1.2 General Climate of the Site Region

Climate is a statistical description of the weather conditions that occur during a long period of time, usually several decades. Weather is short-term variations (minutes to months) of the atmosphere.

Sources of weather data input to analysis of climate at a site include weather maps (depictions of areal weather phenomena at one instant of time), atlas maps summarizing long-term climate,

**PSEG Site
ESP Application
Part 2, Site Safety Analysis Report**

records of weather at specific monitoring stations at single instants of time, and long-term climatic statistics at specific monitoring stations.

The purpose of analysis of regional climate is to understand the local climate at the PSEG Site in the context of the climate of the surrounding area. Phenomena are then analyzed at progressively smaller scales and within progressively smaller areas. As the area being analyzed shrinks, some stations that are considered initially in the broad analysis are excluded because they are found to be unrepresentative of the site climate. The end result is a documented, systematic approach that defines local climate within a context that includes a broad surrounding region.

According to the Koppen classification system (as modified and simplified by Trewartha, Reference 2.3.1-5), the PSEG Site is near (just south of) a boundary region between two climates. To the north and west is a “Daf” or Boreal climate, defined as humid continental with hot summers and cold winters. To the south and east is a “Caf” climate, defined as humid subtropical with hot summers (Reference 2.3.1-6).

Overall, New Jersey has a continental climate, with variations of that continental climate type on a regional basis (Reference 2.3.1-1). Those regional variations are caused by differences in elevation and variation of intensity of continentality due to the moderating influences of the Atlantic Ocean and the Delaware Bay. As described above, elevation variations at the southern end of the state including the PSEG Site region are minor. Therefore, the primary remaining factors that control local variation of the continental climate in the PSEG Site region are the moderating influences of the Delaware Bay and Atlantic Ocean.

A more detailed breakdown of New Jersey climate zones is presented on the map in Figure 2.3-4 (Reference 2.3.1-7). The Northern Zone has elevated highlands and valleys, and has colder temperatures than the other regions. The Central Zone has considerable urbanization and related pollution emissions. Heavily developed parts of the zone have urban heat island effects. The Pine Barrens Zone is in the interior south part of the state, and has scrub pine and oak forests. The soils are sandy and porous and quickly become dry after precipitation. Solar radiation is absorbed by the ground more quickly during the day and radiated into space more quickly during the night because of the low heat capacity of the dry soils. This results in large daily temperature ranges and significantly lower minimum temperatures. Extreme temperatures at the Coastal Zone, adjacent to the Atlantic Ocean, are moderated by the water because of its high heat capacity. Sea breezes often penetrate 5 to 10 mi. inland, and occasionally penetrate 25 to 40 mi. inland. Those breezes are most frequent during spring and summer. Coastal storms called Nor’easters are most frequent during the period October through April. They move over the coastal plain or up to several hundred miles offshore. Their effects include strong winds and heavy rains. Most winters include one such storm, and some winters include more than ten. Tropical storms also affect the coast, and frequently cause significant precipitation.

The Southwest Zone includes the PSEG Site region. Its elevation ranges between sea level and 100 ft. msl. The Delaware Bay has a maritime influence. The Southwest Zone is the warmest and driest part of the state. Winds from the south bring high humidity and moderate temperatures. The Delaware Bay moderates temperature extremes and produces the state’s longest growing season.

**PSEG Site
ESP Application
Part 2, Site Safety Analysis Report**

The PSEG Site lies within the very broad mid-latitude prevailing westerly wind belt. Across southern New Jersey from the Atlantic Ocean shoreline at the southeast corner of the state, to the Delaware River Valley at the southwest corner of the state, there is some variation of those prevailing, generally westerly winds.

The regional map presented in Figure 2.3-11 shows geographic locations relative to the PSEG Site of several available regional weather monitoring stations, including those at Atlantic City, Wilmington, and Philadelphia.

Atlantic City airport is at the Atlantic Ocean shoreline, and is located 50 mi. east of the PSEG Site. Per the statistics in Table 2.3-2 from Reference 2.3.1-9, the prevailing wind at Atlantic City is from the northwest during autumn, winter, and spring months, and from the south-southwest during summer months. The wind climate at Atlantic City is not representative of the PSEG Site vicinity, because of its Atlantic Ocean shoreline location.

Wilmington airport (New Castle County airport) is located 14.5 mi. northwest of the PSEG Site, near the Delaware River. Per the statistics in Table 2.3-1 from Reference 2.3.1-8, the prevailing wind at Wilmington is from the northwest during autumn, winter, and spring months, and generally from the south during summer months. The wind climate at Wilmington is representative of a portion of the PSEG Site vicinity, as discussed below.

Philadelphia International Airport (designation KPHL) is at a slightly more northerly location on the Delaware River, 30 mi. north-northeast of the PSEG Site. Per the statistics in Table 2.3-3 from Reference 2.3.1-10, the prevailing wind at Philadelphia is from the northwest during winter and early spring months and from the southwest during late spring, summer, and autumn months. The wind climate at Philadelphia is representative of a portion of the PSEG Site vicinity, as discussed below.

Overall, the Wilmington and Philadelphia wind patterns show fewer summer winds from south or near-south directions than Atlantic City. Those patterns reflect more frequent advances of air masses from within the continent at locations farther to the west and north than the Atlantic Ocean shoreline, such as Atlantic City.

Summarizing, the broad climate of the PSEG Site region at the southern end of New Jersey is, in general, dominated by winds with offshore components (eastward components, with respect to the Atlantic Ocean shoreline) except in the immediate vicinity of the shoreline. Therefore, the regional climate, in general, has a lee shore character which allows features of a continental climate to be present over inland areas. The wind climates of Wilmington and Philadelphia represent those conditions over inland areas such as at the PSEG Site. In contrast, the wind climate of Atlantic City does not represent those conditions because of its Atlantic Ocean shoreline location, and is not considered further as a source of wind data for the PSEG Site vicinity.

In the PSEG Site region, summer temperatures, humidity, and precipitation are influenced by several factors (Reference 2.3.1-1). Nearby water bodies, including the Delaware River, the Delaware Bay, and the Atlantic Ocean, are locations at which approaching air masses are modified. As described above, winds during summer are primarily from the south, which bring maritime tropical air masses that originate over the tropical ocean and are quite moist. Summer air masses over the state generally include plentiful moisture and support considerable

**PSEG Site
ESP Application
Part 2, Site Safety Analysis Report**

precipitation, frequently including local thunderstorms. Near-shore temperatures are moderated by the water surfaces, which absorb heat from the air more effectively than do the land surfaces. Therefore, extreme high summer temperatures are less likely over near-shore regions than they are at locations farther inland to the west.

PSEG Site region winter temperatures are influenced and moderated by the Appalachian Mountains to the west. Those mountains somewhat disrupt the advance of eastward-moving polar air masses. Additionally, descent of eastward-moving cold air masses from the mountains to the coastal plains causes some adiabatic warming. That warming moderates extreme low air temperatures, versus at locations farther inland to the west. Also, the typical presence of colder air aloft results in colder ground temperatures on the mountains to the west than on the coastal plain.

In spite of the summer and winter moderation effects described above, the lee shore and continental aspects of the climate of New Jersey result in summer maximum dry bulb temperatures over 100 degrees Fahrenheit (°F) and winter minimum dry bulb temperatures below 0°F in every county in the state.

As shown by the sketch in Figure 2.3-10 (Reference 2.3.1-1), one of the major tracks followed over the northeastern United States by synoptic-scale low pressure storm systems extends along the Atlantic coastline from Georgia to New England. That track is associated with the warm temperatures of the Gulf Stream, which lies just offshore and moves warm water northward along the coast. Higher ocean temperatures in that current induce a trough of lower atmospheric pressure that helps channel storms along the coast. The storm track fluctuates somewhat, and is closest to the coast during winter. Winter storms that follow the track frequently tap large amounts of maritime moisture and produce heavy snowfalls over New Jersey.

Figures 2.3-5, 2.3-6, 2.3-7 (Reference 2.3.1-1), 2.3-8, and 2.3-9 (Reference 2.3.1-11) present sketches of patterns across New Jersey of the following parameters: average January dry bulb temperature, average July dry bulb temperature, average annual water equivalent precipitation, average January relative humidity, and average July relative humidity.

As shown by the temperature patterns presented in Figures 2.3-5 and 2.3-6, temperature differences between the northwest and southeast portions of New Jersey are greatest during winter (approximately 8°F), and least during summer (approximately 4°F). In the PSEG Site region in southern New Jersey, the temperature patterns in Figure 2.3-5 reflect the warming influence of the Delaware Bay and Atlantic Ocean during winter. The southern New Jersey temperature patterns in Figure 2.3-6 reflect the cooling influence of maritime air masses drawn inland from the Atlantic Ocean by storm centers moving north along the coastal storm track during summer.

As shown in Figure 2.3-7, New Jersey annual precipitation totals are largest at the northern highlands and along the shoreline of the Atlantic Ocean, the primary source of moisture. Although most winter precipitation falls as rain, winter snowfall is highly variable and ranges from one inch (in.) to 50 in. (Reference 2.3.1-7).

**PSEG Site
ESP Application
Part 2, Site Safety Analysis Report**

As shown in Figures 2.3-8 and 2.3-9 (Reference 2.3.1-11), humidity in southern New Jersey is high year round, but are slightly higher during summer along the Delaware Bay shoreline (10 percent higher than during winter).

During late summer and autumn seasons, hurricanes occasionally cause heavy rainfall over the PSEG Site region. However, winds seldom reach hurricane force in that area (Reference 2.3.1-8). New Jersey receives 25 to 30 thunderstorms per year, with fewer such storms near the Atlantic Ocean coastline (Reference 2.3.1-7). Approximately five tornadoes occur each year in the state. In general, they tend to be weak.

Considered together, the information presented above indicates that the climate of southern New Jersey in the PSEG Site region is continental in character, includes extremes, has a marine influence, and is quite changeable.

2.3.1.3 Identification of Representative Regional Weather Monitoring Stations

As stated above in the introduction to Subsection 2.3.1.2, the objective of analysis of regional climate is to verify understanding of the local climate at the PSEG Site in the context of the climate of the surrounding area. Phenomena are analyzed at progressively smaller scales and within progressively smaller areas. As the area being analyzed shrinks, some stations that are considered initially in the broad analysis are excluded because they are found to be unrepresentative of the site climate. The end result is a documented, systematic approach that defines local climate within a context that includes a broad surrounding region. In this subsection, a subset of all regional weather monitoring stations is identified. That smaller group of stations is representative of the PSEG Site climate. Data from that smaller group of stations and from the area in which they are located are used to further analyze the PSEG Site climate.

Selected National Oceanic and Atmospheric Administration (NOAA) weather monitoring stations in the site region are identified, for which raw observations and summaries of climatological statistics are available. Those include the following:

- a. Automated Surface Observing System (ASOS) stations for which Integrated Surface Hourly Global (DS 3505) digital datasets are available. DS 3505 datasets are official U.S. Government NOAA NCDC quality-controlled archives for those hourly observations. They also have standardized and well-known digital formats, such that commercial software tools are available for processing and summarization of them. Therefore, ASOS stations are a logical choice as part of the input to the regional climate analysis.
- b. First-order surface observing stations (stations with 24 hour per day, year round observing schedules with trained, certified observers) for which Local Climatological Data (LCD) summaries and International Station Meteorological Climate Summary (ISMCS) temperature joint frequency distributions (JFDs) are available from the NCDC. The LCD and ISMCS summaries are widely-used, quality-controlled, official U.S. Government documents. They are a source of statistical summaries including means, extremes, and frequency distributions of meteorological parameters such as temperature, humidity, and wind. Periods summarized include both the record at observing stations and official NOAA 30-year "normals" periods. Therefore, first-order stations are a logical choice as part of the input to the regional climate analysis.

**PSEG Site
ESP Application
Part 2, Site Safety Analysis Report**

- c. Cooperative Network Observing Program (COOP) surface observing stations for which Climatology of the United States No. 20 (Clim-20) summaries or Daily Surface Data (DS 3200) digital datasets are available. Clim-20 reports include statistical summaries of the means and extremes of meteorological parameters. Included are such parameters as daily rainfall and snowfall totals, and daily maximum, minimum and mean dry bulb temperature. DS 3200 datasets are sequential files with the actual daily values for the multi-year periods of record at COOP stations. Although available parameters are generally limited to daily precipitation and temperature, the COOP network is the most numerous available and therefore has a higher spatial resolution than, for example, LCD stations. Therefore, COOP stations are a logical choice as part of the input to the regional climate analysis.
- d. Hourly surface observing stations for which American Society of Heating, Refrigerating and Air-Conditioning Engineers (ASHRAE) climatic design information tables are available. ASHRAE tables are a standardized source of already-summarized weather information. They contain values of statistical extremes for selected NOAA first-order and ASOS stations at which hourly surface observations are recorded. The table includes such statistics as percentile temperatures with coincident values. Therefore, ASHRAE stations are a logical choice as part of the input to the regional climate analysis.

Table 2.3-4 presents a list of information on NOAA regional meteorological monitoring stations across a broad area in New Jersey, Delaware, Maryland, and Pennsylvania that are available for use in this section. Included in that table are station names, station type categories, state and county locations, approximate distances and directions from the new plant site, approximate elevations, COOP and Weather Bureau Army Navy (WBAN) identification numbers, and COOP station periods of record analyzed. Figure 2.3-11 presents a map of locations and categories of the regional weather monitoring stations listed in Table 2.3-4. References 2.3.1-12 through 2.3.1-36 contain the information that is used to identify those stations.

A subset of the region shown on the map in Figure 2.3-11 is selected as representative of the climate of the PSEG Site and surrounding area. That subset area has approximate rather than precisely defined boundaries. The basis for that selected subset area included the following five factors.

- Limit the selected area to the inner and outer coastal plains.

This factor is used because the PSEG Site is located on the outer coastal plain, and near (five miles south of) the boundary between those two plains, as shown on the map in Figure 2.3-1.

- Exclude from the selected area all points within a distance of 10 mi. from the Atlantic Ocean shoreline.

Purpose of this factor is to minimize influence of ocean breeze circulations on weather datasets. Those circulations do not typically penetrate as far west from the ocean shoreline as the PSEG Site, as discussed above in Subsection 2.3.1.2. Additionally,

**PSEG Site
ESP Application
Part 2, Site Safety Analysis Report**

wind speed effects of hurricanes are greater near the ocean coastline than in the new plant site region.

- Exclude from the selected area any points on the hills and mountains to the northwest in Delaware, Maryland, and Pennsylvania.

Purpose of this factor is to minimize effects on climate of that higher, more complex terrain. That terrain is unlike the relatively flat terrain at the PSEG Site, as shown on the map in Figure 2.3-11.

- Exclude from the selected area shorelines and vicinities of major water bodies other than the Delaware Bay.

The effects of those water bodies on local climate may be identical to those of the Delaware Bay. The vicinity of the Delaware Bay is preferred because the PSEG Site is adjacent to it. Excluded major water bodies are the Atlantic Ocean and Chesapeake Bay.

- Exclude points farther than 40 mi. from the PSEG Site.

On the basis of factors 1 through 4 above, the selected area is already bounded by: The Chesapeake Bay (and its vicinity) to the west and southwest, the hills and mountains to the north and northwest, and the Atlantic Ocean (and its primary ocean breeze zone) to the southeast and east. Therefore, this factor is primarily used to define how far the selected area would extend to the northeast on the inner and outer coastal plains of New Jersey, and to the south near the border between Maryland and Delaware. Towards the northeast, the 40 mi. distance includes the Southwest New Jersey climate zone as defined on the map in Figure 2.3-4, plus a sample of the adjacent Pine Barrens New Jersey climate zone.

The selected subset geographic area based on the five factors listed and explained above is used to eliminate stations that are located within a broader surrounding area that is first examined in Sec. 2.3.1.2 above, but are not located within the subset area. Those eliminated stations include the following: Aberdeen Phillips Field, Atlantic City IAP, Baltimore-Wash. IAP, Belleplain STN Forest, Cape May 2NW, Centreville, Chadds Ford 2 NE, Chestertown, Conowingo Dam, Denton 2 E, Newark Univ. Farm, Sussex, and West Chester 2NW.

Based on the selected subset area described above, the following remaining subset of regional weather stations (listed in Table 2.3-4 and plotted on the map in Figure 2.3-11) are considered to be sufficiently representative of the climate of the site and the surrounding area:

- Dover (Dover AFB), DE
- Millington 1 SE, MD
- Wilmington, DE
- Marcus Hook, PA
- Philadelphia IAP, PA
- Hammonton 1 NE, NJ
- Glassboro 2 NE, NJ
- Woodstown Pittsgrove 4 E, NJ

**PSEG Site
ESP Application
Part 2, Site Safety Analysis Report**

- Seabrook Farms, NJ
- Millville MAP, NJ

2.3.1.4 Data Sources

Several sources of data are used to characterize regional climatological conditions. A list of those sources, and explanations why they are appropriate for this regional climate analysis, follows.

- Published Clim-20 (References 2.3.1-21 through 2.3.1-33) and Clim-81 (References 2.3.1-13 through 2.3.1-16) statistical summaries, and DS 3200 raw daily digital data files from the National Climatic Data Center for COOP daily weather monitoring stations located within in the representative area defined above in Subsection 2.3.1.3.

Clim-20 publications are station summaries of particular interest to agriculture, industry, and engineering applications. They are typically available for COOP network stations. They include a variety of climate statistics of interest for this climate analysis. Parameters include: temperature, precipitation, snow, and degree days. Statistical parameters include: means, median precipitation and snow, extremes, mean number of days exceeding threshold values, and probabilities for monthly precipitation and freeze.

- LCD, ISMCS, ASHRAE, and Air Force Combat Climatology Center (AFCCC) statistical summaries for hourly weather monitoring stations located within the representative area defined above in Subsection 2.3.1.3.

LCD annual summaries are typically available for major airport weather stations. They include climatic normals, averages, and extremes of interest for this climate analysis. Normals cover 30-year averages for the standardized period (1971-2000). Thirty-year monthly histories are provided for the following parameters: mean temperature, total precipitation, total snowfall, and heating and cooling degree days. A narrative climate description is also provided.

ISMCS summaries are available for many airports and military installations. They include tabulations of statistics for several parameters of interest for this climate analysis. Those include: wind, clouds, temperature, humidity, precipitation, and weather phenomena. Station climatic narratives are also included. Particularly useful and unique statistics are tabulations of joint frequency distributions of dry bulb versus wet bulb temperature depression, and independent frequency distributions of dry bulb, wet bulb, and dew point temperature.

ASHRAE climatic design information is available for 5564 worldwide locations including many U.S. airports with hourly surface observation stations. The information is commonly used for design, sizing, distribution, installation, and marketing of heating, ventilating, air-conditioning, and dehumidification equipment. It is also used for other energy-related processes in residential, agricultural, commercial, and industrial applications. Statistical summaries include values of: dry bulb, wet bulb, and dew point temperature, wind speed and direction frequencies, monthly degree days, and radiation calculation methods. Also included are: statistical design values of dry bulb with mean coincident wet bulb temperature, design wet bulb with mean coincident dry bulb

Rev. 4

**PSEG Site
ESP Application
Part 2, Site Safety Analysis Report**

temperature, and design dew point with mean coincident dry bulb temperature. These data allow designers to consider various extreme operating conditions.

The AFCCC statistical summaries include the following data and information: design criteria values for dry and wet bulb temperatures and humidity ratios, average annual climate summaries, psychrometric summaries, binned temperature data, annual temperature and humidity summaries, heating and cooling degree data summaries for building envelope loads, ventilation and infiltration loads, solar radiation data, and seasonal wind direction and speed summaries.

- American Society of Civil Engineers (ASCE) structure design standards for the PSEG Site area.

The ASCE standards provide minimum load requirements for the design of buildings and other structures that are subject to building code requirements. Particularly useful and unique statistics of interest for this climate analysis are values of basic wind speed on a map of the U.S. The basic speed is required by the standard for the determination of design wind loads. Also included are various adjustments and supplementary information dependent on site and structure characteristics.

- Tornado, waterspout, hurricane, and other weather event statistics for counties at and in the area of the new plant site, from the National Climatic Data Center (NCDC) online Storm Events Database (Reference 2.3.1-40).

This online database is maintained by the U.S. official repository for climatological data, the NCDC. It contains a chronological listing, by state, of climate statistics of interest for this climate analysis. Those statistics include: hurricanes, tornadoes, thunderstorms, hail, floods, drought conditions, lightning, high winds, snow, temperature extremes, and other weather phenomena. Also included are statistics on personal injuries and damage estimates.

- Tracks of tropical cyclones from an NOAA Coastal Services Center (CSC) historical database, for an area within a radius of 115 nautical miles (NM) from the PSEG Site.

The CSC, part of the U. S. Government NOAA, works with private and public sector partners to address coastal issues, and supports environmental, social, and economic well being of the coast. One of its missions is to analyze hazardous tropical weather. The CSC provides an online Historical Hurricane Tracks tool of interest for this climate analysis. It is an interactive mapping application that allows search and display of Atlantic Basin and Eastern North Pacific Basin tropical cyclone data. Input options include latitude and longitude coordinates. Selected tracks are viewed on a map. Details are listed in tabular form including storm name and date of occurrence.

- Maps of relative humidity in the PSEG Site region from the Climate Atlas of the United States (Reference 2.3.1-11).

The atlas is published by the NCDC, the U.S. official repository for climatological data. It features climate maps of interest for this climate analysis. The atlas includes all 50 states, and provides color maps of climatic elements such as: temperature, precipitation,

Rev. 4

**PSEG Site
ESP Application
Part 2, Site Safety Analysis Report**

snow, wind, and pressure. The period of record for most maps is 1961-1990. The user chooses: a parameter (e.g. temperature), a statistical measure (e.g. mean), and a state.

2.3.1.5 Severe Weather

2.3.1.5.1 Extreme Wind

A statistic known as the “basic” wind speed is used for design and operating bases. Basic wind speeds are the “nominal design 3-second gust wind speeds in miles per hour (mph) at 33 ft. above ground for Exposure C category”, as defined in Figures 6-1 and 6-1C of Reference 2.3.1-38.

PSEG considered several sources to determine the wind speed for the PSEG Site. The basic wind speed for the PSEG Site is 90 mph, based on the plot of basic wind speeds in Figure 6-1C of Reference 2.3.1-38. Basic wind speeds reported in Reference 2.3.1-39 for hourly weather monitoring stations in the site area are as follows: 100 mph for Dover AFB DE, 110 mph for Philadelphia, Pennsylvania, and 100 mph for Wilmington, Delaware. Therefore, the highest of the four basic wind speed values is selected, the 110 mph wind speed for Philadelphia. These values apply to a recurrence interval of 50 years. Section C6.5.5 of Reference 2.3.1-38 provides a method to calculate wind speeds for other recurrence intervals. Based on that method, a 100 year return period value is calculated by multiplying the 50 year return period value by a factor of 1.07. That approach produces a 100 year return period three second gust wind speed for the new plant site area of 117.7 mph.

Reference 2.3.1-38 provides an importance factor for wind loads, “I”, which is used to assess wind impacts on structures. For the PSEG Site, it has a value of 1.15 per Table 6-1 of Reference 2.3.1-38. That value is based on further classification of the site as within a hurricane prone region with basic wind speed greater than 100 mph, as described above, and using the design provisions for Category IV of Reference 2.3.1-38.

2.3.1.5.2 Tornadoes

The new plant conforms to regulatory guidance as follows. The AP1000 and ABWR designs conform to Regulatory Guide (RG) 1.76, *Design Basis Tornado and Tornado Missiles for Nuclear Power Plants*, Revision 0. The AREVA and US-APWR designs conform to RG 1.76, Revision 1.

Tornado site characteristics (Table 2.3-5) are from RG 1.76, Revision 1, March 2007. Per the U. S. map in Figure 1 of RG 1.76, the PSEG Site is located within tornado intensity Region II. Tornado missile site characteristics correspond to those for Region II, including the characteristics in Table 2.3-6.

The NCDC Storm Events Database (Reference 2.3.1-40) provides information on historic storm events on a county basis. To use that database, eight regional counties centered on the PSEG Site are selected. Those eight counties approximate the representative climate region defined above in Subsection 2.3.1.3, and have a combined area of 4023 square miles (sq. mi.). The eight counties include: New Castle and Kent in Delaware, Cumberland, Salem, and Gloucester in New Jersey, and Queen Anne’s, Kent, and Cecil in Maryland.

**PSEG Site
ESP Application
Part 2, Site Safety Analysis Report**

The NCDC Storm Events Database (Reference 2.3.1-40) is accessed to extract statistics on regional tornadoes and waterspouts. Information is extracted for the eight regional counties (Reference 2.3.1-41). Those statistics, for the 59.4 year period of record January 1, 1950 through May 31, 2009, are included in Table 2.3-7.

As shown in Table 2.3-7, total tornadoes and waterspouts recorded in the eight-county area during the 59.4 year period of record are 82 and 1, respectively.

The strongest tornadoes found in the database for Salem County, New Jersey were both rated F2. The first Salem County F2 tornado occurred on July 14, 1960. That storm damaged and destroyed several rural and residential structures, and had a path length of eight miles and width of 450 yards. The second Salem County F2 tornado occurred on August 17, 1988. That storm had a path length of two miles and width of 400 yards. It uprooted large diameter trees, some of which fell on automobiles and a house.

The strongest tornado found in the database for New Castle County, Delaware is rated F3 and occurred on April 28, 1961. That storm damaged a warehouse, and had a path length of one-quarter mi. and width of 30 yards.

2.3.1.5.3 Tropical Cyclones

A National Hurricane Center online historical database of tracks of tropical cyclones, including the years 1851 through 2008 (Reference 2.3.1-42), is accessed for an area within a radius of 115 mi. around the new plant site. The total number of storms identified is 109. Frequencies of tropical storms of various intensities during the 158 year period of record are listed in Table 2.3-8.

Tropical cyclones occur within this area as early in the year as May and as late as November. The highest frequency of 41 storms is during September. Monthly frequencies are identified in Table 2.3-9.

The hurricane site characteristic wind speed is extracted from RG 1.221 *Design-Basis Hurricane Missiles for Nuclear Power Plants*, October 2011. Per RG 1.221, the site characteristic wind speed is the highest nominal 3-second gust wind speed at the 33 ft. level above ground over open terrain with a probability of exceedance of 10^{-7} per year. Per the U.S. East Coast map in Figure 3 of RG 1.221, the interpolated hurricane site characteristic wind speed at the PSEG Site is 159 mph. Corresponding site characteristic hurricane horizontal missile speeds from RG 1.221 Table 2 are provided in Table 2.3-38.

2.3.1.5.4 Precipitation Extremes

This subsection examines and compares precipitation extremes within the site climate region and at the PSEG Site itself. Water equivalent precipitation is measured at both the PSEG Site and at regional government monitoring stations. Snowfall measurements are not made at the PSEG Site, so historic snowfall measurements are only presented for the regional government monitoring stations.

This subsection also presents a probable maximum precipitation (PMP) value and the extreme frozen winter precipitation event for the PSEG Site.

**PSEG Site
ESP Application
Part 2, Site Safety Analysis Report**

Historic precipitation measurements for regional government monitoring stations are obtained from two sources: Clim-20 summaries (References 2.3.1-24, 2.3.1-25, 2.3.1-26, 2.3.1-27, 2.3.1-28, 2.3.1-30, 2.3.1-31, 2.3.1-32, and 2.3.1-33) and TD 3200 daily digital data files (Reference 2.3.1-43). Regional data are obtained for government stations that are identified per the discussion in Subsection 2.3.1.3 above as being within an area considered representative of the PSEG Site and its surroundings. Those stations are identified in Table 2.3-10.

Historic precipitation measurements at the Salem and Hope Creek (S/HC) sites are based on site measurements during the 32 year period 1977 through 2008. Available site measurements do not include dates of occurrence.

Table 2.3-11 presents and compares measurements for the S/HC site and the regional government stations listed in Tables 2.3-10. As shown in Table 2.3-11, overall historic maximum recorded 24-hour water-equivalent precipitation from records for either the S/HC site or the regional stations is 11.68 in. at Marcus Hook, Pennsylvania on September 16, 1999. That daily rainfall total is associated with Tropical Storm Floyd. Note that the maximum 10.03 in. total at the PSEG Site is also due to Floyd.

As also shown in Table 2.3-11, overall maximum monthly water-equivalent precipitation from records for the S/HC site or the regional stations is 16.13 in. at Marcus Hook, Pennsylvania during September 1999. That monthly precipitation total is primarily due to Tropical Storm Floyd.

Maximum recorded 24 hour snowfall from records for the regional government stations is 30.7 in. at Marcus Hook, Pennsylvania on January 8, 1996.

Maximum monthly snowfall from records for the regional government stations is 40.0 in. at Hammonton, NJ during February 1899.

As shown by comparison of the statistics in Table 2.3-11, there is considerable variability of extreme rainfall and snowfall events across the site climate region and across the period of record. That is consistent with the explanation of regional climate character as discussed in Subsection 2.3.1.2. That is, distance and direction of a specific monitoring station from the Delaware Bay and from the Atlantic Ocean shoreline significantly affect temperatures and moisture levels during snowstorms. Also, distance and direction of a specific monitoring station from a storm system and its rain cells, including a tropical storm, significantly affect total rainfall amounts. However, some of the precipitation extreme events at different stations are the result of the same individual tropical or winter storms. Overall, the order of magnitude of rainfall and snowfall extremes are similar across the climate region and at the PSEG Site, supporting conclusions regarding climate region representativeness.

The weight of the 100 year return period ground level snowpack for the PSEG Site is 24 lb/ft². This value is determined as follows. First, a 50 year return value of 20 lb/ft² is obtained from Figure 7 of the ASCE Standard 7-05, *Minimum Design Loads for Buildings and Other Structures* (Reference 2.3.1-38). Second, per directions in "Section C7.3.3 Importance Factor, I" of that standard, the 100 year value is obtained by multiplying the 50 year value by a conversion factor of 1.2.

**PSEG Site
ESP Application
Part 2, Site Safety Analysis Report**

A highest winter season (December through February) 48 hour PMP value is determined by linear interpolation between 24 hour and 72 hour PMP values for December (based on Figures 35 and 45 of NOAA, *Hydrometeorological Report No. 53* [Reference 2.3.1-44]). The result is a value of 21 in. One inch of liquid water is equivalent to 5.2 lb/ft². Therefore, the weight of the 48 hour probable maximum winter precipitation (PMWP) is 109 lb/ft².

The Interim Staff Guidance (ISG) DC/COL-ISG-07, "Interim Staff Guidance on Assessment of Normal and Extreme Winter Precipitation Loads on the Roofs of Seismic Category I Structures" (Reference 2.3.1-53) defines the extreme frozen winter precipitation event as the higher ground level weight (in lb/ft²) between: (1) the 100-year return period two-day snowfall event; and (2) the historical maximum two-day snowfall event in the area. The 100-year return period two-day snowfall event and the historical maximum two-day snowfall event are available from *United States Snow Climatology* (Reference 2.3.1-54) and TD3200 daily digital data files (Reference 2.3.1-43). The representative climate area is defined in Subsection 2.3.1.3.

The maximum 100-year two-day snowfall event in the area was 26.3 in. at Milford 4 SE, Delaware (Reference 2.3.1-54). The historical maximum two-day snowfall in the area was 30.7 in. recorded at Marcus Hook, Pennsylvania and Philadelphia, Pennsylvania on January 7-8, 1996 (Reference 2.3.1-54 and Reference 2.3.1-43).

ISG DC/COL-ISG-07 states that the maximum 100-year two-day snowfall event and the historical maximum two-day snowfall are converted to snow load (in lb/ft²). According to the ISG, the corresponding observed (liquid) precipitation, when available, should be used to determine the snow load for historical maximum snowfall events. Liquid precipitation is converted to a snow load (in lb/ft²) by multiplying the observed (liquid) precipitation (in inches) by 5.2 lb/ft². When the corresponding observed (liquid) precipitation is not available for a corresponding snowfall, the ISG provides the following algorithm for converting a 100-year snowfall event to a snow load (in lb/ft²):

$$L = 0.15 \times S \times 5.2$$

where S is the 100-year snow event (in inches)
5.2 is the weight of one inch of water (in lb/ft²)
 L is the resulting snow load (in lb/ft²)

The maximum 100-year two-day snowfall event (26.3 in.) is a statistically-derived parameter. Therefore, a corresponding observed liquid precipitation measurement is not available. Following this algorithm, the 26.3 in. snowfall is converted to an equivalent weight for the 100-year return period two-day snowfall event of 20.51 lb/ft².

The historical maximum two-day snowfall in the area (30.7 in.) was recorded at Marcus Hook, Pennsylvania and Philadelphia, Pennsylvania on January 7-8, 1996. The observed liquid water equivalent precipitation is not available from Marcus Hook, Pennsylvania for the January 7-8, 1996 snowfall. However, the observed liquid equivalent precipitation is available from Philadelphia, Pennsylvania (1.55 in.). Multiplying the observed liquid precipitation measured at Philadelphia (1.55 in.) by 5.2 lb/ft² produces an equivalent snow weight of 8.06 lb/ft². Since the extreme frozen winter precipitation event is defined as the higher ground-level weight (in lb/ft²) between: (1) the 100-year return period two-day snowfall event; and (2) the historical maximum

**PSEG Site
ESP Application
Part 2, Site Safety Analysis Report**

two-day snowfall event, the extreme frozen winter precipitation event is the higher of 8.06 lb/ft², and 20.51 lb/ft², or 20.51 lb/ft².

ISG DC/COL-ISG-07 defines the normal winter precipitation event as the highest ground-level weight (in lb/ft²) among: (1) the 100-year return period snowpack, (2) the historical maximum snowpack, (3) the 100-year return period two-day snowfall event, or (4) the historical maximum snowfall event in the site region.

The 100-year return period snowpack (24 lb/ft²) is computed from Reference 2.3.1-38 as described in Subsection 2.3.1.5.4.

The historical maximum snowpack for the area is 25 inches, which was observed at Wilmington, Delaware and Dover, Delaware. The historical maximum snowpack at Wilmington, had an observed 1.93 in. liquid equivalent and the historical maximum snowpack at Dover had an observed 1.13 in. liquid equivalent (Reference 2.3.1-43). Multiplying the observed liquid precipitation measured at Wilmington (1.93 in.) by 5.2 lb/ft² produces an equivalent weight of 10.04 lb/ft². Multiplying the observed liquid precipitation measured at Dover (1.13 in.) by 5.2 lb/ft² produces an equivalent weight of 5.88 lb/ft². The historical maximum snowpack (in lb/ft²) is the higher of 10.04 lb/ft², and 5.88 lb/ft², or 10.04 lb/ft².

ISG DC/COL-ISG-07 defines the normal winter precipitation load as the highest ground-level weight (in lb/ft²) among: (1) the 100-year return period snowpack [24 lb/ft²], (2) the historical maximum snowpack [10.04 lb/ft²], (3) the 100-year return period two-day snowfall event [20.51 lb/ft²], or (4) the historical maximum snowfall event in the site region [8.06 lb/ft²]. Therefore, the normal winter precipitation load is 24 lb/ft².

Application of design basis loads to roof design of plant structures will be described in the COL application.

2.3.1.5.5 Hail, Snowstorms, and Ice Storms

Climatic Atlas of the United States (Reference 2.3.1-11) and the NCDC, *Storm Events Database* (Reference 2.3.1-40) are used to review historic hail, snow, and ice storms in the site climate region. As explained above in Subsection 2.3.1.4, the atlas and the database are published by the NCDC, the U.S. official repository for climatological data. These two references feature climate maps and statistics of interest for this climate analysis.

Climatic Atlas of the United States (Reference 2.3.1-11) indicates that Salem County, New Jersey, in which the PSEG Site is located, and New Castle County, Delaware, to the west of the site, experience on the average less than 0.5 days per year with hail greater than approximately one inch in diameter.

The NCDC, *Storm Events Database* (Reference 2.3.1-40) indicates that the largest hailstones that Salem County, New Jersey, and New Castle County, Delaware, have experienced are of diameter 1.75 in. (golf ball size). Those hailstones occurred on three occasions in Salem County and on three occasions in New Castle County during the 60 year period covered by that reference. The locations and dates of these six hail events are identified in Table 2.3-12.

**PSEG Site
ESP Application
Part 2, Site Safety Analysis Report**

Climatic Atlas of the United States (Reference 2.3.1-11) indicates that, on average, snow fall occurs at the PSEG Site and within the surrounding area during only 2.5 to 5.4 days per year, and freezing precipitation occurs in that area during only 5.5 to 10.4 days per year.

As described above in Subsection 2.3.1.2, annual snowfall is highly variable and ranges from one inch to 50 in. The largest recorded daily snowfall for the site climate region, as described above in Subsection 2.3.1.3.4 and in Table 2.3-11, is 30.7 in. at Marcus Hook Pennsylvania on January 8, 1996. The highest monthly total of 40.0 in. occurred at Hammonton 1 NE, New Jersey during February 1899.

Information in the NCDC, *Storm Events Database* (Reference 2.3.1-40) on freezing precipitation events in Salem County, New Jersey and New Castle County, Delaware is reviewed for the period of record 1950 through 2009. Those results indicate that freezing precipitation events tend to occur each year. However, maximum thicknesses of ice accumulation are usually 0.1 or 0.2 in. The maximum observed ice thickness in the two counties is 0.5 in.

2.3.1.5.6 Thunderstorms

Analysis of thunderstorms considers detailed records of thunderstorm occurrence on an hourly basis. Only first order surface weather monitoring stations make such observations. Those detailed hourly thunderstorm records are then made available by NCDC in their LCD publications. As indicated in Table 2.3-4, only four first-order stations exist within the broad area initially examined as part of this climate analysis: Atlantic City IAP, Baltimore-Wash. IAP, Philadelphia IAP, and Wilmington (New Castle County). As discussed above in Subsection 2.3.1.3, two of those four first order stations, Atlantic City IAP and Baltimore-Wash. IAP, are eliminated from the PSEG Site climate analysis because they are outside of a selected subset area that is representative of the climate of the PSEG Site its surrounding area. Remaining are the Philadelphia IAP and Wilmington (New Castle County) first-order stations. LCD publications for Philadelphia and Wilmington are used to describe thunderstorm frequencies.

LCD tables for Wilmington and Philadelphia are presented as Tables 2.3-1 and 2.3-3. The data in Tables 2.3-1 and 2.3-3 indicate that thunderstorms occur at the PSEG Site and in its surrounding climate area at any time of year. On the average, the month with greatest occurrence is July, with 5.9 days at Wilmington and 5.5 days at Philadelphia. The majority of thunderstorm days occur during the months May through August. During the remaining months of September through April, the number of thunderstorm days averages 0.9 days per month at Wilmington and 1.0 day per month at Philadelphia.

The storm statistics are clearly very similar at Wilmington and Philadelphia, verifying some consistency across the site climate region.

The mean frequency of lightning strikes to earth is calculated via a method from the Electric Power Research Institute (EPRI), per the U. S. Department of Agriculture Rural Utilities Service, in Reference 2.3.1-45. The method assumes a relationship between the average number of thunderstorm days per year (T), and the number of lightning strikes to earth per square mile per year (N). The mathematical relationship is as follows.

$$N = [0.31][T] \quad \text{(Equation 2.3-1)}$$

**PSEG Site
ESP Application
Part 2, Site Safety Analysis Report**

Based on the average number of thunderstorm days per year at Wilmington during a 61 year period of record (27.7, per Table 2.3-1, which is slightly higher than the value of 27.3 days for Philadelphia and is therefore used here), the frequency of lightning strikes to earth per square mile per year is 8.6 for the PSEG Site and surrounding area. For comparison, based on a five year period of record, Reference 2.3.1-46 indicates 1 to 2 flashes per square kilometer per year value for the site, which corresponds to 2.6 to 5.2 flashes per square mile per year. The EPRI value therefore is shown to be a reasonable indicator.

The power block area of the new plant is an area of 70 acres or 0.11 (sq. mi.). Given the annual average lightning strike to earth frequency of 8.6 per square mile per year, the frequency of lightning strikes in the power block area is calculated using the following mathematical relationship.

$$[8.6 \text{ strikes/sq. mi./year}] [0.11 \text{ sq. mi.}] = 0.95 \text{ strikes/year}$$

The result is about once per year in the power block area.

2.3.1.6 Meteorological Data for Evaluating the Ultimate Heat Sink

The evaluation for determining the meteorological conditions resulting in the maximum evaporation and drift loss of water from and the minimum cooling by the ultimate heat sink (UHS) is in accordance with the guidance of RG 1.27, *Ultimate Heat Sink for Nuclear Power Plants*, Revision 2, January 1976. The evaluation uses data from Dover, Millville, and Wilmington (Reference 2.3.1-52). The controlling parameters for the type of UHS selected for the early site permit application (ESPA) (i.e., mechanical draft cooling tower over a buried water storage basin or other passive water storage facility, as required by the reactor design) are the wet-bulb temperature and coincident dry-bulb temperature.

Sequential hourly surface meteorological data sets are analyzed with a Fortran computer program named Rolavgwb that is used to move a rolling time window. A rolling 30-day period is identified that has the highest average wet bulb temperature, which represents maximum evaporation and drift loss. Similarly, that computer program is used to move a rolling time window through the digital data set to identify rolling five-day and one-day periods with maximum average wet bulb temperatures, which represent minimum water cooling. Inputs to the computer program are formatted TD-3280 digital files with lengths of multiple decades, obtained from the National Climatic Data Center (NCDC). Such files are available for the following National Oceanic and Atmospheric Administration (NOAA) monitoring stations within the site climate region: Wilmington, Dover, Millville, and Philadelphia.

Recognizing that a TD-3280 file is not available at the PSEG Site itself, and also complying with guidance to use most representative data available, the best approach is to identify several monitoring stations, for which TD-3280 data sets are available, that geographically bracket the PSEG Site. Wilmington, Dover, and Millville are selected to meet those criteria. Wilmington is located 14.5 mi. northwest of the PSEG Site, Dover is located 22 mi. south of the PSEG Site, and Millville is located 30 mi. southeast of the PSEG Site. As shown by the map presented in SSAR Figure 2.3-11, Wilmington, Dover, and Millville form a triangular bracket around the PSEG Site. Wilmington best represents the north quadrant, Dover best represents the west and south quadrants, and Millville best represents the east quadrant. The Philadelphia monitoring station, which is located 30 mi. north-northeast of the PSEG Site, is within the PSEG Site

**PSEG Site
ESP Application
Part 2, Site Safety Analysis Report**

climate region and is therefore available and valid for input to analyses. However, Philadelphia is not as representative as Wilmington because it is twice as distant. It also duplicates coverage of the north quadrant provided by Wilmington.

The meteorological conditions resulting in the maximum evaporation and drift loss of water from the UHS are the worst 30-day average combination of the controlling atmospheric parameters. Calculating “running, 30-day,” daily averages and selecting the 30-day period with the highest daily average wet-bulb temperature, determined the worst 30-day period. The worst 30-day daily averages of wet-bulb temperatures and coincident dry-bulb temperatures are 75.87°F and 82.65°F, respectively. Those values are based on analysis of the referenced data, which include 61 years of record from Dover, 35 years of record from Millville, and 39 years of record from Wilmington.

The meteorological conditions resulting in minimum water cooling are the worst combination of controlling atmospheric parameters, including diurnal variations where appropriate, for the critical time periods unique to the UHS design. The worst 1-day and the worst 5-day daily average of wet-bulb temperatures and coincident dry-bulb temperatures are considered to conservatively represent these conditions.

The worst 1-day is the day having the highest daily average wet-bulb temperature. Calculating “running, 5-day,” daily averages and selecting the 5-day period with the highest daily average wet-bulb temperature determined the worst 5-day period. Both the worst 1-day and the worst 5-day temperatures are determined using the same reference data over the same period of record as the worst 30-day temperatures.

The worst 1-day wet-bulb temperature and coincident dry-bulb temperature is 82.69°F and 87.12°F, respectively. The worst 5-day daily average of the wet-bulb temperatures and coincident dry-bulb temperatures is 78.02°F and 83.47°F, respectively.

2.3.1.7 Design Basis Dry Bulb and Wet Bulb Temperatures

Site design basis dry bulb temperature (DBT) and WBTs are defined for the new plant site and its climate area. Those include the following statistics:

- a. Maximum DBT with annual exceedance probability of 0.4 percent
- b. Mean coincident WBT (MCWB) at the 0.4 percent DBT
- c. Maximum DBT with annual exceedance probability of 2.0 percent
- d. MCWB at the 2.0 percent DBT
- e. Minimum DBT with annual exceedance probability of 0.4 percent
- f. Minimum DBT with annual exceedance probability of 1.0 percent
- g. Maximum WBT with annual exceedance probability of 0.4 percent
- h. 100 year return maximum annual DBT
- i. 100 year return maximum annual WBT
- j. 100 year return minimum annual DBT
- k. Maximum DBT with annual exceedance probability of 5 percent
- l. Minimum DBT with annual exceedance probability of 5 percent
- m. Maximum DBT with annual exceedance probability of 1.0 percent
- n. MCWB at the 1.0 percent DBT
- o. Maximum WBT with annual exceedance probability of 1.0 percent

**PSEG Site
ESP Application
Part 2, Site Safety Analysis Report**

One hundred-year return-interval parameters, including: maximum annual dry bulb temperature, maximum annual wet bulb temperature, and minimum annual dry bulb temperature, are developed via an overall approach that is similar to that used for the UHS analysis. A computer program is used to analyze TD-3280 digital data files from the most representative regional monitoring stations. Those stations, Wilmington, Dover, and Millville, are the same group of three stations as are selected for the UHS TD-3280 analysis, and they are selected for the same reasons. That is, the required TD-3280 files are available for them, and they are the most representative stations available and cover the four compass quadrants around the PSEG Site.

Percentile dry bulb and wet bulb temperatures are extracted from a convenient, rapid source of already-published values, the Air Force Combat Climatology Center (AFCCC) Engineering Weather Data (EWD) CD (Reference 2.3.1-39). However, although the EWD CD includes the Wilmington and Dover stations that are used for the UHS and 100-year return temperature analyses, it does not include statistics for Millville. Therefore, to compensate somewhat for the lack of statistics for Millville, statistics from Philadelphia are conservatively included in the percentile temperatures. Even though those Philadelphia statistics somewhat duplicate coverage of the north quadrant from the PSEG Site, it is the next most representative, and only remaining EWD CD station available within the site climate region.

Worst case values are selected from the three EWD CD regional stations that are located within the site climate region: Wilmington, Philadelphia, and Dover. To maintain consistency between dry bulb temperatures and coincident wet bulb temperatures, DBT/MCWB pairs are always retained from a single station.

Results for the statistics are presented in Table 2.3-13 and Table 2.3-14.

A technique provided as Equation (1) on page 14.6 of Chapter 14 of ASHRAE Reference 2.3.1-34 allows estimation of 100-year return interval maximum annual DBTs and WBTs.

The ASHRAE technique uses the following equation.

$$T_n = M + Ifs \quad \text{(Equation 2.3-2)}$$

where:

T_n = n-year return period value of the extreme temperature computed, in years

M = mean annual extreme maximum or minimum temperature

I = 1 if the maximum temperature is computed; -1 if the minimum temperature is computed

s = standard deviation of the annual extreme maximum or minimum temperatures

n = number of years in a return period

$$f = -\frac{\sqrt{6}}{\pi} \left(0.5772 + \ln \left(\ln \left(\frac{n}{n-1} \right) \right) \right)$$

A function that is developed to convert the return period variable (in years) of an extreme temperature parameter (such as the mean

**PSEG Site
ESP Application
Part 2, Site Safety Analysis Report**

annual extreme temperature in °F) to a new “reduced” variable that has a linear relationship to the extreme temperature parameter.

Use of that technique involves analysis of hourly surface TD3280 digital datasets from NCDC. As discussed above in Subsection 2.3.1.6, TD 3280 digital data files with hourly WBTs are available from NCDC only for the following stations within the PSEG Site climate region: Dover, Millville, Philadelphia, and Wilmington. To be consistent with work for Subsection 2.3.1.6, we select the same subset of three stations for this 100-year return analysis. That station subset is: Dover, Millville, and Wilmington. Philadelphia is excluded for the same reasons as discussed above in Subsection 2.3.1.6.

The highest and lowest DBT and highest WBT are identified for each year through the available period of record for each regional station (61 years for Dover, 35 years for Millville, 39 years for Wilmington). Those values are input to the ASHRAE technique. Estimated 100-year return period DBTs, and estimated 100-year return period WBTs determined via the ASHRAE technique are listed in Table 2.3-13.

An additional review of regional extreme DBT data is done using NCDC TD 3200 SOD (summary of the day) digital datasets for the same 10 regional COOP monitoring stations for which daily precipitation data are reviewed above in Subsection 2.3.1.3.4. Those stations are: Dover, Millington 1 SE, Wilmington, Marcus Hook, Philadelphia IAP, Hammonton 1 NE, Glassboro 2 NE, Woodstown Pittsgrove 4 E, Seabrook Farms, and Millville MAP.

Those ten stations do not measure WBT, and do not record hourly DBT. They only record maximum and minimum daily DBTs and daily precipitation totals. Therefore, it is not possible to identify WBTs that are coincident with extreme DBTs identified in the TD 3200 datasets. Table 2.3-15 presents results of review of TD 3200 datasets for the 10 regional stations. That table also includes results of review of 32 years of S/HC hourly on-site data. As shown in Table 2.3-15, overall maximum and minimum recorded DBTs at the site and in its surrounding climate area are 108 and -15 °F.

As discussed above, WBTs coincident with extreme DBTs identified in the TD 3200 datasets are not directly available in existing publications for two reasons. First, the COOP monitoring stations that record the extreme DBTs do not record WBTs. Second, a frequency distribution of DBT versus WBT depression available for Wilmington on the International Station Meteorological Climate Summary CD (ISMCS, Reference 2.3.1-20) has a DBT upper limit of 102 °F. Therefore, the coincident WBT is estimated, rather than directly identified in an hourly database.

A graphical extrapolation is used to estimate the WBT that would occur during the peak overall DBT of 108 °F. A simple graphical approach is most appropriate for several reasons.

- A simple graphical approach is appropriate because at the extreme high end of the DBT range there are only a small number of observations. Use of an objective numerical technique to project larger DBT values using such a small population as input is unjustified because it is effectively no less subjective than the graphical approach.

**PSEG Site
ESP Application
Part 2, Site Safety Analysis Report**

- The requirement is for only a mean coincident WBT value. A mean WBT value is simply identified for any DBT value on the graph, therefore a set of such means is easily plotted, and form the basis for an extrapolation line.
- A DBT/WBT JFD table from Reference 2.3.1-20 for Wilmington is already published and is suitable for use in sketching the graphical relationship between regional DBT and WBT during conditions of the peak DBT.

Graphical extrapolation of the DBT/WBT depression relationship to a DBT of 108 °F results in estimation of a WBT depression of 29 °F, and a MCWB of 79 °F. Application of a similar graphical extrapolation technique to the 100-year DBT (105.9 °F) results in a MCWB of 82.4 °F.

2.3.1.8 Restrictive Dispersion Conditions

Major air pollution episodes are typically a result of persistent surface high pressure weather systems that cause light and variable surface winds and stagnant meteorological conditions for four or more consecutive days. Estimates of stagnation frequency are provided in *Air Stagnation Climatology for the United States* (Reference 2.3.1-47, Figures 1 and 2). Those estimates indicate that, on the average, the PSEG Site experiences 11 days per year with stagnation conditions, or 2 cases per year with the mean duration of each case lasting 5 days.

2.3.1.9 Air Quality

Salem County, New Jersey, in which the PSEG Site is located, is non-attainment for ozone (8 hour standard). New Castle County in Delaware is non-attainment for ozone (8 hour standard) and PM_{2.5} standard (Reference 2.3.1-48).

2.3.1.10 Climate Changes

Trends in global climatic conditions are currently the subject of considerable discussion in the scientific community and in the media. There are differences of opinion regarding the nature and causes of such trends. There is also controversy regarding the reliability of projections. Generally, projections of climatic changes have been done at global scales. Attempts to predict changes at regional scales, for example for the northeastern U.S., have been problematic. And, certainly, predictions of changes at a single station location or at a relatively small area such as the site climate region are not reliable.

It is not appropriate to attempt to predict climate changes in the site climate region because of the above uncertainties. It is also not appropriate to try to use such predictions to enhance or replace the standard approach of identifying historical extreme climatic conditions in the site climate region. Plant design is most reliably based on a standard approach of projecting via scientifically defensible statistical methods, using the historic statistics as input.

It is nevertheless valid to examine historic records for indications of long-term trends for informational purposes. Trends of interest are those of climate elements such as temperature, pressure, or winds that are sustained over periods of several decades or longer (Reference 2.3.1-49).

**PSEG Site
ESP Application
Part 2, Site Safety Analysis Report**

Trends of the following parameters are examined, for the climate region within which the PSEG Site is located:

- a. 30-year division normal period values of mean annual dry bulb temperature and mean annual precipitation.
- b. During five separate periods of record, extremes of hourly dry bulb temperature, one-day precipitation, strong tornadoes, and decadal frequency of tropical cyclones.

Division normals are climate normals for 30-year periods within climate divisions. Climate divisions are segments of individual states that the NOAA has identified as being climatologically homogeneous. Division normals for the PSEG Site that are reviewed included the northern section of Delaware labeled DE-01, and the southern half of New Jersey labeled NJ-02 (References 2.3.1-50 and 2.3.1-51).

Variation of mean annual dry bulb temperature and mean annual precipitation from division normal data and other data sources are identified in the top half of Table 2.3-16. By definition, the division normal periods: (1) are 30 years long, (2) overlap, and (3) are updated every 10 years. The statistics show the following.

- a. Largest mean annual precipitation totals occurred for both states during the latest normals period 1971 to 2000. That period is largest by one inch. However, there is no trend across all five normals periods. Second-largest total occurred during the period 1931 to 1960 in both states.
- b. Highest mean annual dry bulb temperatures occurred for both states during the latest normals period 1971 to 2000. That period is highest by one-half °F. However, there is no trend across all five normals periods. Second-highest mean occurred during the period 1931 to 1960 in Delaware and during 1931 to 1960 and 1961 to 1990 in New Jersey.

Variations of several historic meteorological parameters are also identified in the bottom half of Table 2.3-16. The time periods are selected to the normals periods in the top half of Table 2.3-16, but without overlaps. Those parameters are: regional extreme high daily precipitation, regional extreme high daily snowfall, regional extreme high DBT, regional extreme low DBT, New Castle County Delaware strongest tornado, and Salem County New Jersey strongest tornadoes. Those statistics show the following.

- a. Maximum daily precipitation 11.68 inches and maximum daily snowfall 30.7 inches are both during the latest decade 1991 to 2000.
- b. The extreme high DBT 108 °F is during the earliest period 1931 to 1960. The extreme low DBT -15 °F is during the fourth period 1981 to 2000.
- c. The strongest tornado F3 in New Castle County Delaware is during the second period 1961 to 1970. The strongest tornadoes F2 in Salem County New Jersey occur during both the earliest period 1931 to 1960 and during the period 1981 to 1990.
- d. The extremes are spread across the periods examined, and do not exhibit any trend towards more extremes during later years.

**PSEG Site
ESP Application
Part 2, Site Safety Analysis Report**

Additional information is reviewed on a decadal basis for tropical cyclone frequency, from data that is presented previously in the above subsections. Those tropical cyclone statistics are identified in Table 2.3-17. Those statistics show that the total number of tropical cyclones per year has fluctuated across virtually the set of decadal periods. The decade with most numerous storms, 14, is the 1880s. The smallest total, 2, is during the 1970s. Second highest total, 11 storms, is during both the 1900s and 1940s. No obvious trend is observed, and certainly no trend that peaks during any of the most recent three decades.

2.3.1.11 References

- 2.3.1-1 Stansfield, C. A., "A Geography of New Jersey", Rutgers University Press, Piscataway, New Jersey, 1998.
- 2.3.1-2 U. S. Geological Survey (USGS), "Taylors Bridge Quadrangle, Delaware-New Jersey 7.5 Minute Series (Topographic) Map", published by USGS, Denver, Colorado, 1999.
- 2.3.1-3 U. S. Geological Survey (USGS), "Wilmington, Eastern United States 1:250,000 Series (Topographic) Map", published by USGS, Denver, Colorado, 1972.
- 2.3.1-4 U. S. Geological Survey (USGS), "Topographic Map Symbols", published by USGS, Denver, Colorado, 2009.
- 2.3.1-5 Trewartha, G. T., "The Earth's Problem Climates", The University of Wisconsin Press, Madison, Wisconsin, 1961.
- 2.3.1-6 Strahler, A. N., "Physical Geography", third edition, John Wiley and Sons, Inc., New York, New York, 1969.
- 2.3.1-7 Office of the New Jersey State Climatologist (ONJSC), "The Climate of New Jersey", report available at ONJSC website, <http://climate.rutgers.edu/stateclim/?section=uscp&target=NJCoverview>, accessed August 2009.
- 2.3.1-8 National Climatic Data Center (NCDC), "2008 Local Climatological Data, Annual Summary with Comparative Data, Wilmington, Delaware (KILG)", published by NCDC, Asheville, North Carolina, 2009(a).
- 2.3.1-9 National Climatic Data Center (NCDC), "2008 Local Climatological Data, Annual Summary with Comparative Data, Atlantic City, N.A.F.E.C. (KACY)", published by NCDC, Asheville, North Carolina, 2009(b).
- 2.3.1-10 National Climatic Data Center (NCDC), "2008 Local Climatological Data, Annual Summary with Comparative Data, Philadelphia, Pennsylvania (KPHL)", published by NCDC, Asheville, North Carolina, 2009l.
- 2.3.1-11 National Climatic Data Center (NCDC), "The Climate Atlas of the United States", Version 2.0 CD, published by NCDC, Asheville North Carolina, September 2002.

**PSEG Site
ESP Application
Part 2, Site Safety Analysis Report**

- 2.3.1-12 National Climatic Data Center (NCDC), "NOAA surface weather monitoring station identification and descriptive information, obtained from the MMS: Multi-Network Metadata System", NCDC, Asheville North Carolina, available at NCDC website, <http://mi3.ncdc.noaa.gov/mi3qry/search.cfm?PleaseWait=OK>, accessed August-September 2009(d).
- 2.3.1-13 National Climatic Data Center (NCDC), "Climatography of the United States No. 81, Monthly Station Normals of Temperature, Precipitation, and Heating and Cooling Degree Days 1971-2000, 07 Delaware", published by NCDC, Asheville North Carolina, available at NCDC website, <http://www.ncdc.noaa.gov/oa/mpp/>, 2002.
- 2.3.1-14 National Climatic Data Center (NCDC), "Climatography of the United States No. 81, Monthly Station Normals of Temperature, Precipitation, and Heating and Cooling Degree Days 1971-2000, 18 Maryland", published by NCDC, Asheville North Carolina, available at NCDC website, <http://www.ncdc.noaa.gov/oa/mpp/>, 2002.
- 2.3.1-15 National Climatic Data Center (NCDC), "Climatography of the United States No. 81, Monthly Station Normals of Temperature, Precipitation, and Heating and Cooling Degree Days 1971-2000, 28 New Jersey", published by NCDC, Asheville North Carolina, available at NCDC website, <http://www.ncdc.noaa.gov/oa/mpp/>, 2002.
- 2.3.1-16 National Climatic Data Center (NCDC), "Climatography of the United States No. 81, Monthly Station Normals of Temperature, Precipitation, and Heating and Cooling Degree Days 1971-2000, 36 Pennsylvania", published by NCDC, Asheville North Carolina, available at NCDC website, <http://www.ncdc.noaa.gov/oa/mpp/>, 2002.
- 2.3.1-17 National Climatic Data Center (NCDC), "Climatological Data Annual Summary, New Jersey, 2008", Volume 113 Number 3, published by NCDC, Asheville North Carolina, 2009(e).
- 2.3.1-18 National Climatic Data Center (NCDC), "Climatological Data Annual Summary, Maryland and Delaware, 2008", Volume 132 Number 13, published by NCDC, Asheville North Carolina, 2009(f).
- 2.3.1-19 National Climatic Data Center (NCDC), "Climatological Data Annual Summary, Pennsylvania, 2008", Volume 113 Number 13, published by NCDC, Asheville North Carolina, 2009(g).
- 2.3.1-20 Fleet Numerical Meteorology and Oceanography Detachment, National Climatic Data Center (NCDC), and USAFETAC OL-A, "International Station Meteorological Climate Summary", Ver 4.0 CD, published by NCDC, Asheville North Carolina, September 1996.
- 2.3.1-21 National Climatic Data Center (NCDC), "Climatography of the United States No. 20, 1971-2000, Aberdeen Phillips Field, MD", published by NCDC, Asheville North Carolina, available at NCDC website, <http://www.ncdc.noaa.gov/oa/mpp/>, 2001(a).

**PSEG Site
ESP Application
Part 2, Site Safety Analysis Report**

- 2.3.1-22 National Climatic Data Center (NCDC), "Climatology of the United States No. 20, 1971-2000, Chestertown, MD", published by NCDC, Asheville North Carolina, available at NCDC website, <http://www.ncdc.noaa.gov/oa/mpp/>, 2001(b).
- 2.3.1-23 National Climatic Data Center (NCDC), "Climatology of the United States No. 20, 1971-2000, Conowingo Dam, MD", published by NCDC, Asheville North Carolina, available at NCDC website, <http://www.ncdc.noaa.gov/oa/mpp/>, 2001(l).
- 2.3.1-24 National Climatic Data Center (NCDC), "Climatology of the United States No. 20, 1971-2000, Dover, DE", published by NCDC, Asheville North Carolina, available at NCDC website, <http://www.ncdc.noaa.gov/oa/mpp/>, 2001(d).
- 2.3.1-25 National Climatic Data Center (NCDC), "Climatology of the United States No. 20, 1971-2000, Glassboro 2 NE, NJ", published by NCDC, Asheville North Carolina, available at NCDC website, <http://www.ncdc.noaa.gov/oa/mpp/>, 2001(e).
- 2.3.1-26 National Climatic Data Center (NCDC), "Climatology of the United States No. 20, 1971-2000, Marcus Hook, PA", published by NCDC, Asheville North Carolina, available at NCDC website, <http://www.ncdc.noaa.gov/oa/mpp/>, 2001(f).
- 2.3.1-27 National Climatic Data Center (NCDC), "Climatology of the United States No. 20, 1971-2000, Millington 1 SE, MD", published by NCDC, Asheville North Carolina, available at NCDC website, <http://www.ncdc.noaa.gov/oa/mpp/>, 2001(g).
- 2.3.1-28 National Climatic Data Center (NCDC), "Climatology of the United States No. 20, 1971-2000, Millville Municipal AP, NJ", published by NCDC, Asheville North Carolina, available at NCDC website, <http://www.ncdc.noaa.gov/oa/mpp/>, 2001(h).
- 2.3.1-29 National Climatic Data Center (NCDC), "Climatology of the United States No. 20, 1971-2000, Newark University Farm, DE", published by NCDC, Asheville North Carolina, available at NCDC website, <http://www.ncdc.noaa.gov/oa/mpp/>, 2001(i).
- 2.3.1-30 National Climatic Data Center (NCDC), "Climatology of the United States No. 20, 1971-2000, Philadelphia INTEL AP, PA", published by NCDC, Asheville North Carolina, available at NCDC website, <http://www.ncdc.noaa.gov/oa/mpp/>, 2001(j).
- 2.3.1-31 National Climatic Data Center (NCDC), "Climatology of the United States No. 20, 1971-2000, Seabrook Farms, NJ", published by NCDC, Asheville North Carolina, available at NCDC website, <http://www.ncdc.noaa.gov/oa/mpp/>, 2001(k).
- 2.3.1-32 National Climatic Data Center (NCDC), "Climatology of the United States No. 20, 1971-2000, Wilmington New Castle AP, DE", published by NCDC, Asheville North Carolina, available at NCDC website, <http://www.ncdc.noaa.gov/oa/mpp/>, 2001(l).
- 2.3.1-33 National Climatic Data Center (NCDC), "Climatology of the United States No. 20, 1971-2000, Woodstown Pittsgrove 4 E, NJ", published by NCDC, Asheville North Carolina, available at NCDC website, <http://www.ncdc.noaa.gov/oa/mpp/>, 2001(m).

**PSEG Site
ESP Application
Part 2, Site Safety Analysis Report**

- 2.3.1-34 American Society of Heating, Refrigerating and Air-Conditioning Engineers, Inc. (ASHRAE), "The Handbook CD 2009 Fundamentals", CDR, published by ASHRAE, Atlanta Georgia, 2009.
- 2.3.1-35 National Climatic Data Center (NCDC), "ASOS Station List", available in digital database form at NCDC website, <http://lwf.ncdc.noaa.gov/oa/climate/surfaceinventories.html#inventories>, accessed August-September 2009(h).
- 2.3.1-36 National Climatic Data Center (NCDC), "List of NOAA stations for which LCD reports may be purchased and downloaded", available at NCDC website, <http://www7.ncdc.noaa.gov/IPSLcd/lcd.html>, accessed August-September 2009(i).
- 2.3.1-37 Not used.
- 2.3.1-38 American Society of Civil Engineers (ASCE), "Minimum Design Loads for Buildings and Other Structures", ASCE Standard ASCE/SEI 7-05 Including Supplement No. 1, published by ASCE, Reston, Virginia, 2006.
- 2.3.1-39 Air Force Combat Climatology Center (AFCCC), National Climatic Data Center (NCDC), "Engineering Weather Data, 2000 Interactive Edition", developed by the AFCCC and published by the NCDC, Asheville North Carolina, 1999.
- 2.3.1-40 National Climatic Data Center (NCDC), "NCDC Storm Event Database", available at NCDC website, <http://www4.ncdc.noaa.gov/cgi-win/wwwcgi.dll?wwEvent~Storms>, accessed September-October 2009(j).
- 2.3.1-41 U. S. Census Bureau, "County and City Data Book: 2007", accessed at Census Bureau Internet site, http://www.census.gov/statab/ccdb/cc07_tabB1.pdf, accessed October 2009(k).
- 2.3.1-42 National Oceanic and Atmospheric Administration (NOAA), "Historical Hurricane Tracks Storm Query", NOAA Coastal services Center, available at Internet site: <http://csc-s-maps-q.csc.noaa.gov/hurricanes/viewer.html>, accessed October 2009(l).
- 2.3.1-43 National Climatic Data Center (NCDC), "Data set 3200 (DSI-3200) Surface Land Daily Cooperative Summary of the Day files for periods of record for the following COOP stations: Dover DE, Glassboro2 NE NJ, Marcus Hook PA, Millington 1 SE MD, Millville MAP NJ, Philadelphia IAP PA, Seabrook Farms NJ, Wilmington Newcastle AP DE, Woodstown Pittsgrove 4 E NJ", NCDC Asheville North Carolina, purchased and downloaded, 2009(m).
- 2.3.1-44 National Oceanic and Atmospheric Administration (NOAA), "Hydrometeorological Report No. 53, "Seasonal Variation of 10-Square-Mile Probable Maximum Precipitation Estimates, United States East of the 105th Meridian", NUREG/CR-1486, Washington, D.C., 1980.
- 2.3.1-45 U. S. Department of Agriculture (USDA), "Rural Utilities Service Summary of Items of Engineering Interest", published August 1998.

**PSEG Site
ESP Application
Part 2, Site Safety Analysis Report**

- 2.3.1-46 National Lightning Safety Institute (NLSI), "Vaisala 5-Year Flash Density Map – U.S. (1996-2000)", available at NLSI Internet site at: <http://www.lightningsafety.com/>, accessed August 2009.
- 2.3.1-47 Wang, J. X. L., J. K. Angell, "Air Stagnation Climatology for the United States (1948-1998)", NOAA/Air Resources Laboratory Atlas No. 1, published by Air Resources Laboratory, Environmental Research Laboratories, Office of Oceanic and Atmospheric Research, Silver Spring, Maryland, April 1999.
- 2.3.1-48 U. S. Environmental Protection Agency (US EPA), attainment status information for U.S. counties, available online at Internet site: <http://www.epa.gov/oaqps001/greenbk/index.html>, accessed October 2009.
- 2.3.1-49 American Meteorological Society (AMS), "Glossary of Meteorology", available online at AMS Internet site at URL: <http://amsqglossary.allenpress.com/glossary/>, accessed October 2009.
- 2.3.1-50 National Climatic Data Center (NCDC), "Divisional Normals and Standard Deviations of Temperature, Precipitation, and Heating and Cooling Degree Days, 1971-2000 (and previous normals periods), Section 1: Temperature", Climatology of the United States No. 85, published by NCDC Asheville North Carolina, June 2002.
- 2.3.1-51 National Climatic Data Center (NCDC), "Divisional Normals and Standard Deviations of Temperature, Precipitation, and Heating and Cooling Degree Days, 1971-2000 (and previous normals periods), Section 2: Precipitation", Climatology of the United States No. 85, published by NCDC Asheville North Carolina, June 2002.
- 2.3.1-52 National Climatic Data Center (NCDC), "TD 3280 - Airways Surface Observations", Surface weather observations in TD 3280 digital format for: Dover Delaware from 1943-2008, for Millville New Jersey from 1973-2008, and for Wilmington Delaware from 1943-2008, data purchased from NCDC, Published by NCDC, Asheville, NC, 2009.
- 2.3.1-53 U.S. Nuclear Regulatory Commission Interim Staff Guidance, DC/COL-ISG-07, "Assessment of Normal and Extreme Winter Precipitation Loads on Roofs of Seismic Category I Structures." June 23, 2009. Accession Number ML091490565.
- 2.3.1-54 U.S. Department of Commerce "United States Snow Climatology." National Climatic Data Center, NOAA, available at Internet site: <http://www.ncdc.noaa.gov/ussc/index.jsp>, accessed April-May, 2011.

**PSEG Site
ESP Application
Part 2, Site Safety Analysis Report**

2.3.2 LOCAL METEOROLOGY

This subsection summarizes the local meteorological data, compares local data to regional data, and describes the potential influence of the new plant on local meteorological conditions.

2.3.2.1 Data Sources

We consider the following primary sources of data use in characterization of meteorology and climatology at the PSEG Site and its surroundings:

- a. Thirty-two years of data collected during the period of record 1977 through 2008 by the existing S/HC primary on-site meteorological monitoring system.
- b. Regional Automated Surface Observing Systems (ASOS) stations for which Integrated Surface Hourly Global (DS 3505) digital datasets are available.
- c. Regional first-order surface observing stations for which Local Climatological Data (LCD) summaries and International Station Meteorological Climate Summary (ISMCS) temperature JFDs are available.
- d. Regional COOP surface observing stations for which *Climatology of the United States No. 20* (Clim-20) summaries, *Daily Surface Data* (DS 3200) digital datasets, or *Climatology of the United States No. 81* (Clim-81) summaries are available.
- e. Regional hourly surface observing stations for which ASHRAE climatic design information tables are available.

A detailed description of the government-run regional stations above is presented in Subsection 2.3.1.3 above. That detailed description defines the station types, and describes the value for this analysis of various dataset and summary products that are created by NCDC for each station type.

Twenty-three regional monitoring stations of the types listed above are available and considered for use in the characterization. Table 2.3-4 lists those stations, including their approximate distances and directions from the PSEG Site. The regional map in Figure 2.3-11 provides the locations of the 23 available stations. Of those stations, 10 are selected for use and are listed in Subsection 2.3.1.3. They are selected because they are representative of the PSEG Site and its climatic surroundings. Several of the regional stations include, at a single location, two or more of the monitoring station types listed above.

The on-site primary meteorological tower is located 5470 ft. southeast of the new plant power block area, as shown in Figure 1.2-3. As discussed in Subsection 2.3.3.3, this location is sufficiently far from S/HC stations and other structures such that they do not affect the results of monitoring at the tower.

Available statistical summaries of data recorded at regional COOP stations are used to characterize climatological normals and period-of-record means and extremes of temperature, rainfall, and snowfall in the vicinity of the PSEG Site. Government statistical summaries are also available for regional first order stations which monitor other weather elements including winds,

**PSEG Site
ESP Application
Part 2, Site Safety Analysis Report**

relative humidity, dew point temperature, wet bulb temperature, and observed weather phenomena such as fog and thunderstorms.

Government information sources include the following.

- a. *Climatology of the United States No. 20*, 1971-2000 (Clim-20) summaries for nine of the regional COOP stations: Dover, Glassboro 2 NE, Marcus Hook, Millington 1 SE, Millville MAP, Philadelphia IAP, Seabrook Farms, Wilmington New Castle Regional Airport, and Woodstown Pittsgrove 4 E (References: 2.3.1-24, 2.3.1-25, 2.3.1-26, 2.3.1-27, 2.3.1-28, 2.3.1-30, 2.3.1-31, 2.3.1-32, and 2.3.1-33).

Clim-20 publications are station summaries of particular interest to agriculture, industry, and engineering applications. They are typically available for COOP network stations. They include a variety of climate statistics of interest for this analysis. Parameters include: temperature, precipitation, snow, and degree days. Statistical parameters include: means, median precipitation and snow, extremes, mean number of days exceeding threshold values, and probabilities for monthly precipitation and freeze.

- b. Digital dataset 3200 (DSI-3200) Surface Land Daily Cooperative Summary of the Day for nine of the regional COOP stations: Dover, Glassboro 2 NE, Marcus Hook, Millington 1 SE, Millville MAP, Philadelphia IAP, Seabrook Farms, Wilmington New Castle AP, and Woodstown Pittsgrove 4 E (Reference 2.3.1-43).

DS-3200 summary of the day datasets are sequential files with the actual daily values for the multi-year periods of record at COOP stations. They include a variety of meteorological parameters of interest for this analysis. Those once-per-day parameters include: maximum/minimum temperatures, precipitation, and snowfall/snow depth. Some stations have additional data such as evaporation, soil temperature, peak wind gust, etc.

- c. *Climatology of the United States No. 81*, Monthly Station Normals of Temperature, Precipitation, and Heating and Cooling Degree Days 1971-2000 (Clim-81) for four regional states: Delaware, Maryland, New Jersey, and Pennsylvania (References 2.3.1-13 through 2.3.1-16).

Clim-81 summaries include several meteorological parameters of interest for this analysis, including the following: normals (for the standard normals period 1971 to 2000) of average monthly and annual maximum, minimum, and mean temperature, monthly and annual total precipitation, and heating and cooling degree days. Those data are available for normals stations, which include both COOP and first-order surface weather monitoring locations in the U.S.

- d. Local Climatological Data 2008 Annual Summaries with Comparative Data for two of the regional stations: Wilmington New Castle County AP and Philadelphia IAP (References 2.3.1-8 and 2.3.1-10).

LCD annual summaries are typically available for major airport weather stations. They include climatic normals, averages, and extremes of interest for this climate analysis. Normals cover 30-year averages for the standardized normals period (1971 to 2000). Thirty-year monthly histories are provided for the following parameters: mean

**PSEG Site
ESP Application
Part 2, Site Safety Analysis Report**

temperature, total precipitation, total snowfall, and heating and cooling degree days. A narrative climate description is also provided.

Wind speed, wind direction, and atmospheric stability statistical summaries are based on data collected by the existing S/HC on-site meteorological monitoring system. Two separate periods are summarized. The 32-year period 1977 through 2008 is summarized to define medium length climatic averages and extremes at the site. The three year period 2006 through 2008 is summarized to define averages and extremes in the same data set that is also used as input to estimates of χ/Q and radiological dose assessments.

2.3.2.2 Normal, Mean, and Extreme Values of Meteorological Parameters

For the S/HC site and the 10 selected regional COOP stations, historical extremes of rainfall and snowfall are presented in Table 2.3-11. That table does not include S/HC snowfall measurements because no snowfall measurements are made at the site. For those same stations, historical extremes of dry bulb temperature are presented in Table 2.3-15. For the two selected regional COOP stations that are also first order stations, normals tabulations are presented in Tables 2.3-1 and 2.3-3. Table 2.3-18 presents a comparison of monthly and annual mean rainfall at the S/HC site and at the 10 selected regional COOP stations for which those statistics have been published in Clim-20 or Clim-81 summaries. Table 2.3-19 presents a comparison of monthly and annual mean snowfall at the nine selected regional COOP stations for which it is available in published Clim-20 summaries. Table 2.3-20 presents a comparison of monthly and annual mean dry bulb temperatures at the S/HC site and the 10 selected regional COOP stations for which those statistics have been published in Clim-20 or Clim-81 summaries.

As discussed in Subsection 2.3.1.2, on a statewide basis, New Jersey annual precipitation totals are largest at the northern highlands and along the Atlantic Ocean shoreline. This pattern is caused by topographic controls on local mesoscale weather systems which produce precipitation and by distance from the primary moisture source, the ocean. As shown in Table 2.3-18, the PSEG Site has the lowest precipitation on a monthly basis, by 0.5 inch, compared to the other regional stations in the site climate region. This pattern appears to be a result of combination of the following factors.

First, the PSEG Site is immediately adjacent to the Delaware Bay shoreline. As discussed in Subsection 2.3.2.2.1.2, considerable mesoscale air movement occurs over the Delaware Bay. It includes both upstream and downstream breezes. It appears that these breezes bring relatively colder air into the bay adjacent to the PSEG Site during cold months and colder air into the bay during warm months, versus temperatures at inland surroundings where the other regional climate stations are located. That year-round colder surface air has a stabilizing effect on local airflow, acting to suppress some precipitation over the bay and its immediate surroundings.

Second, it is well known that tipping bucket rain gauges such as used at the PSEG Site do not record all precipitation during heavy, rapid rainfall events. In contrast, the standard NOAA manual rain gauge does not have that limitation.

As shown in Table 2.3-20, the PSEG Site has the lowest DBT on a monthly basis, by 2 °F to 5 °F, compared to the other regional stations in the site climate region. This pattern appears to also be a result of the cooling effect of Delaware Bay breezes discussed above.

**PSEG Site
ESP Application
Part 2, Site Safety Analysis Report**

Note that overall, consistent monthly average differences of 0.5 inch precipitation and 5 °F dry bulb temperature would not by themselves indicate a different climate at the location of a particular station. Also, some variation is observed between the ten regional stations and is to be expected. That is, these consistent differences do not change any conclusions made here regarding the site region climate zone.

2.3.2.2.1 Wind

2.3.2.2.1.1 Scales of Air Motion

Wind direction and speed distributions are important factors in characterization of site dispersion climatology. Those distributions are results of air motions at several spatial and temporal scales, including those referred to as macroscale, mesoscale, and microscales.

The macroscale includes synoptic weather events with scales of thousands of kilometers. Those events are influenced by general circulation patterns of the atmosphere and by large topographic features such as mountain ranges and ocean coastlines. Macroscale phenomena are addressed in Subsection 2.3.1.2.

Mesoscale airflow patterns have horizontal scales from a few to several hundred kilometers. Those patterns are influenced by mesoscale weather systems such as thunderstorms, squall lines, fronts, cyclone precipitation bands, and sea breezes. They are also influenced by regional scale topographic features.

Microscale airflow patterns have horizontal scales less than two kilometers. These patterns are measured by on-site monitoring systems such as the existing system at the PSEG Site. Microscale measurements reflect the larger macroscale and mesoscale patterns, but are primarily influenced by local topographic and geographic features.

2.3.2.2.1.2 On-Site Wind Roses during Three Year Period

Subsection 2.3.3 describes the existing on-site primary meteorological monitoring system at the PSEG Site. As described in that section, system wind direction and speed measurements that are presently used for χ/Q and radiological dose assessments are collected at the 33 ft. level of the primary tower. For consistency, the following descriptions of on-site winds present data from the same 33 ft. elevation.

Presented in Figures 2.3-12 through 2.3-40 are annual, monthly and seasonal windroses for the 33 ft. level of the on-site primary tower. The period of record on which those plots are based is the three years January 1, 2006 through December 31, 2008. That period is also used for the χ/Q and radiological dose assessments in this report. Figures 2.3-29 through 2.3-34 include data from 1977 to 2008.

The annual on-site three year wind rose (Figure 2.3-12) shows dominant frequencies from the northwest (11 percent of the time) and from the southeast (9 percent of the time). The remaining directions include a large group (SSE, S, SSW, SW, WSW, W, WNW, NNW, N, NNE, and NE) with frequencies of occurrence that range from 6 to 8 percent of the time, and a small group (ENE, E, and ESE) with frequencies of occurrence that range from 3 to 4 percent of the time.

**PSEG Site
ESP Application
Part 2, Site Safety Analysis Report**

The on-site annual dominant wind direction from the northwest reflects flow over the site region of air masses that originate within large surface high pressure systems over the continental interior. The on-site annual frequent wind direction from the southeast reflects Delaware Bay breezes that flow from the southeast along the length of that bay (Reference 2.3.2-1).

On-site winds from directions other than the two dominant directions northwest and southeast, appear to be due to a complex mix of several minor phenomena including: flows around transient storm systems, local shoreline breezes, and flow around the southwest perimeter of the Atlantic Ocean high pressure system.

The winter wind rose (Figure 2.3-25) shows more frequent flow from the northwest than any other season. It verifies that during winter, modified continental polar air masses streaming over the Appalachian Mountains towards the Atlantic Ocean shoreline dominate the site regional airflow.

The spring season wind rose (Figure 2.3-26) shows a high frequency of continental polar air mass intrusion from the northwest, like the winter wind rose. It also indicates an even higher frequency of flow from the southeast. That bimodal distribution is an indicator of two phenomena. First, it indicates that the spring season is transitional between winter and summer synoptic regimes in the region, and that modified continental polar air masses continue to occasionally penetrate to New Jersey during the year. Second, it indicates the high frequency of Delaware Bay breezes during spring.

The summer season wind rose (Figure 2.3-27), in addition to characteristic prevalent flows from the northwest (of modified continental polar air masses) and southeast (Delaware Bay breeze), also indicates somewhat larger frequencies of flows from the minor directions.

The autumn season wind rose (Figure 2.3-28), reflects the characteristic prevalent northwest (modified continental polar air mass) and southeast (Delaware Bay breeze) flows.

No calms are detected during the three years of on-site monitoring because of the sensitivity of the on-site sonic wind sensor and the open exposure of the flat terrain and Delaware Bay at the site.

As stated above, the annual on-site wind rose reflects a complex mix of several minor airflow phenomena. The mix is complex, but not the airflows themselves. There are frequent annual site winds from the southeast, which include airflow from over the smooth surface of the Delaware Bay. The bay acts as a relatively low-friction path for airflow from the southeast directional sector.

While the PSEG Site is located on the shore of the Delaware River, the river “valley” is extremely flat and open in this area. The types of channeled airflows that are typically associated with deep “v-shaped” river valleys do not occur, because the marshy land areas bordering the water are only slightly higher than the river level in the region.

The PSEG Site is not located on the coastline of a large body of water, such as the Atlantic Ocean or the Great Lakes, and is not considered a coastal location. Therefore, the PSEG Site is not subject to the frequent sea-breeze mesoscale circulations that arise from the differential heating of the land and water surfaces and are commonly observed at coastal locations. Such

**PSEG Site
ESP Application
Part 2, Site Safety Analysis Report**

closed sea-breeze mesoscale circulations do not occur at the PSEG Site, and recirculation of airflow during periods of prolonged atmospheric stagnation seldom occurs.

Summarizing, the on-site meteorological tower provides representative measurements of PSEG Site airflows and atmospheric stability, and of the meteorological conditions under which effluents are released. The site is not an ocean coastal location. No spatial or temporal circulations of airflow are expected due to land-water boundary sea-breeze effects.

2.3.2.2.1.3 On-Site Wind Roses during 32 Year Period

Figures 2.3-29 through 2.3-34 present annual and seasonal wind roses for the 33 ft. level of the on-site primary tower for the 32 year period of record 1977 through 2008.

Comparison of three year (Figure 2.3-12, 2006-2008) and 32 year (Figure 2.3-29, 1977-2008) annual mean wind roses shows very similar distributions, verifying that the three years of data used for χ/Q and dose calculations are representative of longer term climatological conditions at the PSEG Site.

Comparison of three year (Figures 2.3-25 through 2.3-28, 2006-2008) and 32 year (Figure 2.3-30, 1977-2008) seasonal mean wind roses also shows very similar distributions. Those similarities also support the conclusion that the three years of data used for χ/Q and radiological dose calculations are representative of longer term climatological conditions at the new plant site.

Figures 2.3-31 through 2.3-34 present seasonal wind roses by hour of day. They indicate development during mid-day and late afternoon hours of strong Delaware Bay breezes (from the southeast) during spring, summer, and autumn seasons.

Figure 2.3-35 presents seasonal mean wind roses during only hours with precipitation. They consistently show wind components from the northeast and southeast. Airflows from those directions are expected during precipitation events, as moist maritime air masses are drawn into low pressure systems to the southwest and west, to feed precipitation areas east and northeast of synoptic-scale low-pressure areas.

2.3.2.2.1.4 Comparison of Annual and Seasonal Three Year On-Site Wind Roses with Annual and Seasonal Regional Station Wind Roses

Software used to create wind roses uses TD 3505 hourly surface digital dataset files as input. Those files are available from NCDC only for the following stations within the PSEG Site climate region: Dover, Millville, Philadelphia, and Wilmington. To be consistent with work for Subsections 2.3.1.6 and 2.3.1.7, we select the same subset of three stations for wind rose creation. That station subset is: Dover, Millville, and Wilmington. Philadelphia is excluded for the same reasons as discussed above in Subsection 2.3.1.6. Those three regional stations are identified in Subsection 2.3.1.3 as representative of the regional climate zone.

Figures 2.3-36 through 2.3-40 present comparisons of three-year annual and seasonal wind roses for the on-site system with seasonal wind roses for the three regional stations Wilmington, Millville, and Dover. Annual and seasonal wind roses are constructed. Periods of record input to the annual and seasonal wind roses include: 66 years for Wilmington, 36 years for Millville, and

**PSEG Site
ESP Application
Part 2, Site Safety Analysis Report**

65 years for Dover. Annual and seasonal wind roses for the S/HC site are based on the three year period 2006 through 2008.

The annual and seasonal wind roses at Wilmington, Millville, and Dover show overall similar patterns to the seasonal wind roses from the PSEG Site. At the PSEG Site, Delaware Bay breeze circulations are evident as a distinctively higher frequency of winds from the southeast versus from the south at the Wilmington and Dover regional stations, which are not Delaware Bay shoreline sites. Millville is found to have very few winds from the south, apparently because it is located farthest inland.

Summarizing, the patterns of wind observed at the PSEG Site and at the three nearest regional hourly observing stations, Dover, Millville, and Wilmington, are consistent and explainable in terms of the effects of regional geography. That consistency verifies the representativeness of on-site measurements for purposes of dispersion modeling.

2.3.2.2.1.5 Wind Direction Persistence

The duration of atmospheric transport for a given wind direction sector, combined with wind speed, provides an indicator of which upwind sectors have relatively more or less potential for dilution of air pollutants.

Tables 2.3-21 through 2.3-25 present wind direction/persistence/wind speed distributions for the on-site primary meteorological tower 33 ft. level, for the three year period 2006 through 2008. Included are distributions for selected durations from one through 48 hours for the standard 16 wind directions ranging from north through north-northwest. Each of those wind directions spans a 22.5 degree upwind sector.

2.3.2.2.2 Atmospheric Stability

Table 2.3-26 presents a comparison of annual mean Pasquill stability class frequency distributions based on three year (2006 to 2008) and 32 year (1977 to 2008) on-site meteorological data. Stability data are based on primary tower 150-33 ft. delta-T.

Comparison indicates that the three and 32-year distributions are very similar. That result provides additional support for the conclusion that the three years of data used for χ/Q and radiological dose calculations are representative of longer term climatological conditions at the PSEG Site.

For the reactor technologies used to develop the Plant Parameter Envelope, Unit Vent/Airborne Release Point Elevation is considered Ground Level as shown in PPE items 9.4.2 and 9.4.3 of Table 1.3-1 of the SSAR. Therefore, short term and long term diffusion estimates treat those emissions as ground level releases.

The on-site meteorological tower includes delta-T measurements between 300 ft – 33 ft, and between 150 ft – 33 ft. Comprehensive data are available from the 150 ft – 33 ft instrumentation for the three year period January 1, 2006 through December 31, 2008.

The delta-T values used to determine stability classes for use in diffusion estimates of χ/Q values are determined using a 150 ft – 33 ft delta-T. The use of these values is appropriate for

Rev. 4

**PSEG Site
ESP Application
Part 2, Site Safety Analysis Report**

this application for the following reasons: the instrument more closely represents the atmospheric layer closest to the ground, therefore the instrument elevation is consistent with the plant parameter envelope ground level release point; and the instrument vertical height difference of 117 ft (35 m) is close to the 50 m vertical height difference specified in Regulatory Guide 1.23, Revision 1.

In summary, the 150 ft – 33 ft instrumentation measurements best represent the layer into which the ground level releases will be emitted, comply with regulatory requirements, and provide the most appropriate input for diffusion estimates.

Table 2.3-27 presents annual mean JFDs of wind direction and wind speed versus Pasquill atmospheric stability class for the three year period 2006 to 2008. Stability class is based on the S/HC on-site primary meteorological tower 150-33 ft. delta-T, and winds are based on 33 ft. level measurements.

Statistics in Tables 2.3-26 and 2.3-27 show that E (slightly stable) stability class is most frequent at the site, occurring 34 percent of the time. Class D (neutral) is next most frequent, at 26 percent of the time. Class G (extremely stable), which is associated with the highest estimated χ/Q for the new plant ground level release, occurs 7 percent of the time.

2.3.2.2.3 Temperature

Extreme temperatures at the PSEG Site and in its climatic vicinity are described in Subsection 2.3.1.5, based on statistics from the 10 representative regional COOP monitoring stations: Dover, Millington 1 SE, Wilmington, Marcus Hook, Philadelphia IAP, Hammonton 1 NE, Glassboro 2 NE, Woodstown Pittsgrove 4 E, Seabrook Farms, and Millville MAP. Those statistics indicate that extreme temperatures in the region that includes the site and its surrounding climate area range from 108°F (at Marcus Hook, Pennsylvania) to -15°F (at Millington 1 SE, New Jersey). Mean temperatures are described in Subsection 2.3.2.2. Those statistics indicate that mean conditions are relatively homogeneous across the region that includes the site and the climate area that surrounds it. The mean annual temperature ranges from 56.8°F at Dover, Delaware to 53.9°F at Hammonton 1 NE, New Jersey.

2.3.2.2.4 Water Vapor

NOAA publishes LCD summaries for standard first-order weather monitoring stations. Those summaries provide water vapor statistics, including wet bulb temperature, dew point temperature, and relative humidity. Water vapor statistics from the LCD summary for a single representative regional station first-order station is sufficient to define mean water vapor conditions for the PSEG Site climate region. Wilmington is the closest such station. The only other such station within the PSEG Site climate region is Philadelphia, which is more distant than Wilmington, and is eliminated from consideration for mean water vapor data for that reason.

As shown in Table 2.3-1, the mean annual wet bulb temperature at Wilmington, Delaware is 48.9°F. Maximum monthly mean wet bulb temperature at Wilmington is 69.0°F in July, and lowest mean monthly is 29.0°F in January.

**PSEG Site
ESP Application
Part 2, Site Safety Analysis Report**

Mean annual dew point temperature at Wilmington is 44.6°F. Highest and lowest mean monthly dew point temperatures at Wilmington are 66.1°F in July and 24.1°F in January. Based on 32 years of on S/HC site data: the mean annual dew point is 41.1°F and highest and lowest monthly mean dew points are 61.5°F in July and 21.0°F in January.

Mean annual relative humidity at Wilmington and S/HC (based on 32 years of on-site data at S/HC) are 68 and 65.6 percent, respectively. Based on Wilmington statistics, relative humidity typically reaches a diurnal maximum during early morning (at 0700 local time) and a diurnal minimum typically during early afternoon (at 1300 local time). Mean Wilmington early morning relative humidity (at 0100 local time) exceeds 80 percent during the months of June through October.

2.3.2.2.5 Precipitation

As described in Subsection 2.3.2.2, mean annual total rainfall for the S/HC site and its climate surroundings ranges from 36.04 in. at the site, to 46.28 in. at Dover Delaware. Mean annual total snowfall at those same stations ranges from 7.5 in. at Glassboro 2 NE New Jersey, to 19.3 in. at Philadelphia IAP Pennsylvania.

2.3.2.2.6 Fog

For the same reasons as described above in Subsection 2.3.2.2.4, water vapor statistics from the LCD summary for a single representative regional station first-order station, Wilmington, is sufficient to define mean fog conditions for the PSEG Site climate region. As described in Table 2.3-1, at Wilmington, Delaware the mean annual number of days with heavy fog and visibility less than or equal to ¼ mi. is 26.1. The frequency of fog at the PSEG Site is similar to the frequency at Wilmington because of similar geographic features (Delaware River shoreline) at both locations.

2.3.2.3 Potential Influence of the Plant and Related Facilities on Local Meteorology

The existing S/HC plants and the new plant design include cooling systems, structures, and modified ground surfaces. Those systems, structures and surfaces are not expected to cause discernible long term changes in local meteorological conditions.

If natural draft cooling towers (NDCTs) are used, they produce elevated plumes that somewhat alter overall local frequencies of overhead clouds. However, no increases of ground level fog are expected from the cooling systems because of the high release elevation. Additionally, no lasting changes in ground level temperature or moisture are expected due to high elevations of those plumes, which are typically several hundred feet above the tops of the towers.

If linear mechanical draft cooling towers (LMDCTs) are used, like NDCTs they also produce elevated plumes that somewhat alter overall local frequencies of overhead clouds. LMDCTs are also expected to produce small increases of ground level fog. An additional 50 hours, or less, of fog are expected per year. A majority of that fog occurs within a distance of 984 ft. from the LMDCTs, and most occur on-site, not affecting roadway conditions in the PSEG Site vicinity or commercial traffic on the Delaware River. No icing events are expected due to the LMDCTs. Additionally, no lasting changes in ground level temperature or moisture are expected due to the very limited number of hours of increased fog.

**PSEG Site
ESP Application
Part 2, Site Safety Analysis Report**

As described in Subsection 2.3.3.3, the tallest power block structure and cooling towers are 234 and 590 ft. high, respectively. Airflow is altered to a distance of approximately ten building heights downwind of those large site structures. Those alterations depend on structure layout/wind direction geometry, and are therefore brief as wind directions fluctuate.

Excavation, landscaping, leveling, and clearing during construction of the new plant results in site terrain profiles that do not differ significantly from the flat to gently rolling character of the topography already present at, and in the vicinity of, the site. Therefore, the overall local meteorology of the site is not affected.

Air temperatures immediately above structure roofs and modified site ground surfaces may at times increase above ambient. Air temperature changes are also very limited in vertical and horizontal extent because of the relatively small horizontal dimensions of those roofs and ground surfaces. Therefore, they are not expected to cause long term changes in local temperatures.

2.3.2.4 Current and Projected Site Air Quality

As described in Subsection 2.3.1.7, Salem County, New Jersey, in which the PSEG Site is located, is in attainment for all U. S. Environmental Protection Agency (USEPA) criteria pollutants except ozone. Salem County is non-attainment for ozone (8 hour). New Castle County, Delaware, which is located to the north and west of the PSEG Site, is also in attainment for all criteria pollutants except ozone (8 hour) and PM_{2.5}, for which it is in non-attainment.

The only Federal Class I area in New Jersey, Delaware, Pennsylvania, and Maryland is the Brigantine Wilderness at the Edwin B. Forsythe National Wildlife Refuge, an area of 6603 acres on the Atlantic Ocean shoreline located 70 mi. from the PSEG Site and 10 mi. northeast of Atlantic City, New Jersey (Reference 2.3.2-2).

The new plant itself is not a source of criteria or toxic pollutants. Supporting equipment such as cooling towers, auxiliary boilers, and emergency diesel generators and/or combustion turbines emit some criteria pollutants. Cooling tower emissions are discussed below. The other supporting equipment is operated on an intermittent basis and is not expected to significantly impact ambient air quality in the vicinity of the PSEG Site. The distance between the PSEG Site and the Brigantine Wilderness is large, therefore visibility at that Class I Federal Area is not expected to be significantly impacted by project construction or operation.

Evaporative cooling tower drift emissions are as follows.

Input:

Water circulating flow rate =	1,200,000 gal/min (based on 2 towers operating at 600,000 gal/min of circulating water)
Drift rate =	0.001 % of circulating water flow
Liters per gallon =	3.785
Maximum water salt = concentration	12,900 mg/liter

Rev. 4

**PSEG Site
ESP Application
Part 2, Site Safety Analysis Report**

Drift emission rate estimation:

$$\begin{aligned}(1,200,000 \text{ gal/min}) (.001) (1/100) &= 12.000 \text{ gal/min} \\ (12 \text{ gal/min}) (3.785 \text{ liter/gal}) (12,900 \text{ mg/liter}) (1/1000) &= 585.9 \text{ g of dry salt/min} \\ (585.9 \text{ g/min}) / (453.6 \text{ g/lb}) &= 1.292 \text{ lb/min} \\ (1.292 \text{ lb/min}) (60 \text{ min/hr}) &= 77.5 \text{ lb/hr} \\ (77.5 \text{ lb/hr}) (8,760 \text{ hr/year}) &= 678,900 \text{ lb/year} \\ (678,900 \text{ lb/year}) / (2,000 \text{ lb/ton}) &= 339.45 \text{ ton/year}\end{aligned}$$

Initial analyses suggest that the emissions from the cooling towers and auxiliary boilers at the new plant result in a slight exceedance of the National Ambient Air Quality Standards. When a reactor technology is selected and detail design is completed for the cooling towers and combustion sources (including auxiliary boiler equipment), PSEG will consult with New Jersey Department of Environmental Protection and perform more detailed multi-source modeling. Applicable emissions rates in effect at the time will be used in detail design and specification of equipment, along with identification of the appropriate engineering and operational controls. The final modeling will demonstrate that the new plant will comply with the applicable air quality regulations.

2.3.2.5 Topographic Description

Figures 2.3-41 through 2.3-49 present elevation profiles, for a radial distance range of 50 mi. from the PSEG Site, for each of the 16 directional sectors. The profiles show that the terrain in the PSEG Site area out to a distance of 20 mi. is flat to gently rolling. The nearest significant topography is at distances ranging from 20 through 50 mi., and in sectors NW clockwise through NNE. That topography ranges in elevation from 200 to 800 ft. msl. The highest elevation at a radial distance of 25 mi. is 400 ft. msl, in sectors NW, NNW, and N. The overall highest elevation, through all direction sectors and within a radius of 50 mi., is 975 ft. msl at a distance of 48 mi. in the NNW direction.

2.3.2.6 References

- 2.3.2-1 Bowers, L., R. Dunk, J. Kohut, H. Roarty, S. Glenn, A. Cope, "Sea Breeze Forecasting and Applications along the New Jersey Coast", Rutgers University Coastal Ocean Observation Lab, Office of the New Jersey State Climatologist, Rutgers University, New Brunswick, New Jersey, presented at the American Meteorological Society (AMS) Fifth Conference on Coastal Atmospheric and Oceanic Prediction and Processes - August 2003, <http://ams.confex.com/ams/pdfpapers/63768.pdf>, accessed October 2009.
- 2.3.2-2 U. S. Environmental Protection Agency (USEPA), 40 CFR Part 81, Subpart D, "Identification of Mandatory Class I Federal Areas where Visibility is an Important Value", http://ecfr.gpoaccess.gov/cgi/t/text/text-idx?c=ecfr&tpl=ecfrbrowse/Title40/40cfr81_main_02.tpl, accessed October 2009.

**PSEG Site
ESP Application
Part 2, Site Safety Analysis Report**

2.3.3 ON-SITE METEOROLOGICAL MEASUREMENTS PROGRAM

2.3.3.1 On-Site Meteorological Measurements Program

PSEG plans to use measurements from the existing on-site meteorological monitoring program to support licensing, and ongoing and future operation of the new plant. The existing program is described in the following subsections.

2.3.3.2 General Program Description

The current on-site S/HC meteorological monitoring program conforms to the requirements of RG 1.23, *Onsite Meteorological Programs*, Revision 0, 1972. PSEG maintains an existing on-site primary meteorological tower. It is a 300 ft. structure and is supported by guy wires. Its geographic coordinates are: 39° 27' 48.9" north latitude, 75° 31' 11.76" west longitude. The primary tower location is 5470 ft. southeast of the new plant power block area. The base of the primary tower is at 11.9 ft. NAVD. The new plant site grade elevation is established at 36.9 ft. NAVD. That raised ground elevation will not affect the applicability of the meteorological tower measurements or affect the suitability of future tower measurements for use during operation of the new plant.

The site region topographic relief is minimal. The major local feature is the Delaware River, which is 2.5 miles wide and is oriented north-south adjacent to and west of the PSEG Site. Regional ground surface character is mixed marsh, cropland, and woodland. The maximum terrain elevation within 5 mi. of the PSEG Site is less than 60 ft. above grade, in the west direction. The nearest topographic elevations greater than 500 ft. above grade are at a distance of 15 mi. in the northwest direction. Local topography is not a factor in meteorological instrumentation siting or exposure because it does not have significant effects on local airflow.

PSEG maintains a backup meteorological tower, consisting of a 10 m (33 ft.) utility pole. It is located 386 ft. south of the primary tower. The primary tower serves as the main source of site meteorological data. The backup tower is used as a backup for periods of equipment unavailability on the primary tower. Measurements at the backup tower include wind speed, wind direction, and sigma-theta determinations at the 10 m (33 ft.) elevation only.

The existing primary and backup on-site meteorological systems include instrumentation as described in Table 2.3-28.

The primary tower is of lattice construction, which minimizes its effects on airflow. Primary tower instrumentation is mounted on booms oriented into the prevailing wind, which is from the northwest. The sensors are mounted on the booms at distances equal to more than twice the tower maximum horizontal width. The primary tower has been in operation for more than 30 years and has been a reliable source of data on site meteorological conditions during that period to support plant operations and reporting for the existing Salem and Hope Creek (S/HC) power plants.

Enhancements made to instrumentation on the primary meteorological tower occurred during June 2008. Relative humidity sensor additions are at the 300 ft. and 33 ft. levels. A dry bulb temperature sensor is added at the 300 ft. level. Wind direction, wind speed, sigma theta, and 197-33 ft. delta-temperature sensor additions are at the 197 ft. level. Vertical temperature

**PSEG Site
ESP Application
Part 2, Site Safety Analysis Report**

difference resolution is upgraded to 0.01° C. Those enhancements improved on a system that is already providing high quality data. As of July 1, 2008, those upgrades are implemented to meet RG 1.23, *Meteorological Monitoring Programs for Nuclear Power Plants*, Revision 1, 2007.

2.3.3.3 Location, Elevation, and Exposure of Instruments

As described above, the location of the primary tower is 5470 ft. southeast of the new plant power block area. The backup tower, as described above, is located 386 ft. south of the primary tower.

Whenever possible, wind measurements should be made at a distance of at least 10 times the height of any nearby obstruction that exceeds one-half the height of the wind measurement. The tallest site structures are the existing S/HC reactors and cooling towers, and the new plant reactors and cooling towers. The existing S/HC reactors are located at least 4500 ft. west of the meteorological towers and the tallest (HCGS) is 203 ft. high. This distance and height yield a distance/height ratio of 22.2:1, which meets the 10:1 distance/height ratio criterion. The existing HCGS cooling tower is located 4700 ft. northwest of the meteorological towers and is 512 ft. high. This distance and height yield a distance/height ratio of 9.2:1, which does not precisely meet the 10:1 distance/height ratio criterion. However, the 10:1 distance/height ratio criterion is based on rectangular structures. A tall and aerodynamically smooth structure such as the existing HCGS cooling tower produces a downwind wake influence smaller than predicted by the 10:1 ratio. Therefore, the HCGS cooling tower does not have an adverse aerodynamic effect on tower wind measurements.

The reactors for the new plant are located 5470 ft. northwest of the meteorological towers (measuring from the nearest point at the southeast corner of the new plant power block area). The new plant cooling towers are located 6800 ft. northwest of the meteorological towers (measuring from the nearest point at the southeast corner of the new plant cooling tower area). As shown in Table 1.3-1, the bounding plant parameter envelope values for the new plant reactor heights and cooling tower heights are 234 ft. and 590 ft., respectively. These values yield distance/height ratios of 23.3:1 for the reactors and 11.5:1 for the cooling towers. Both of these ratios meet the 10:1 distance/height ratio criterion in RG 1.23.

Generally, as described above, the local topography is quite flat. There are no significant groups of trees in the vicinity. Therefore, topographic features and trees will not affect meteorological tower wind measurements.

The maximum height of influence of a structure wake generally does not exceed 2.5 times the structure height for a squat building (width greater than height) such as the meteorological building at the base of the primary meteorological tower. The meteorological building is 12 ft. high. Based on that height, the upper limit of the meteorological building aerodynamic wake will not exceed a height of 30 ft., which is below the height of the lowest 33 ft. wind measurements on the primary tower. Therefore, the meteorological building aerodynamic wake does not affect meteorological tower wind measurements. Additionally, the 10:1 distance/height ratio criterion does not apply to the meteorological building because its height (12 ft.) does not exceed one-half the height of the lowest wind measurement (33 ft.).

Overall, the topography (including raising the grade for a portion of the site) and existing and new plant structures in the vicinity of the on-site meteorological towers are not expected to

**PSEG Site
ESP Application
Part 2, Site Safety Analysis Report**

adversely affect meteorological measurements. Similarly, vegetation and minor structures in the vicinity of the meteorological towers, such as the meteorological building, will not adversely affect meteorological measurements.

In addition to the on-site meteorological data for the January 1, 2006, through December 31, 2008, period of record, National Oceanic and Atmospheric Administration (NOAA) regional meteorological datasets are used to supplement evaluations of atmospheric dispersion. The following datasets are used: Wilmington, Delaware, hourly surface observations; and Sterling, Virginia, upper-air soundings and twice-daily mixing heights. The representativeness of Wilmington surface data is described in Subsection 2.3.1.5.6. Upper-air and mixing height data from Sterling Virginia Dulles Airport are appropriate because that station is the closest representative upper-air station.

2.3.3.4 Instrument Maintenance

Meteorological instrumentation is inspected and serviced regularly. Sensor and system repairs are made as needed. Data are reviewed daily by a meteorologist. Meteorological technicians make weekly surveillance checks. Meteorological technicians make monthly indicator checks including zero/spans. On a quarterly basis, full calibrations are done, from sensor to data acquisition system. On an annual basis, during every fourth calibration, the wind sensors are swapped out and returned to Met One for a wind tunnel calibration. Guyed towers are inspected annually and anchors are inspected every three years.

2.3.3.5 Data Collection and Analysis

The on-site meteorological monitoring system includes display, processing, and communication components. A meteorological building at the base of the primary meteorological tower houses the equipment for processing, display, and transmission of data measured at the primary and backup towers.

Measurements are digitally sampled once per second. Meteorological data averages in the real time system are calculated and stored in separate 15 minute and hourly average files. Those values are running averages. The hourly data that are archived and used in χ/Q and dose assessment calculations are from the hourly running average files, sampled at the ends of the hour.

Real time system measurements are available for real-time display at the tower base meteorological building. Real time displays of 15 minute averages are available at the S/HC Control Rooms and Technical Support Centers via fiber optic cable or modem. Precipitation values are hourly totals. Daily, meteorological data are downloaded and reviewed via software and manual checks for reasonableness. Data are reviewed and validated for archive.

Archived on-site meteorological data collected by the monitoring system during the three-year period from January 1, 2006, through December 31, 2008, are used to describe local meteorology and to evaluate atmospheric dispersion. Table 2.3-29 presents year-by-year values of percent data recovery for the measured meteorological parameters during those three years. Composite recovery values for JFDs (of 33 ft. wind direction and 33 ft. wind speed versus Pasquill stability class based on 150-33 ft. ΔT) of 95 percent or greater are achieved during each of the three years. The only parameter with annual data recovery values less than the 90

**PSEG Site
ESP Application
Part 2, Site Safety Analysis Report**

percent target is 33 ft. dew point temperature during 2006 and 2008. The 33-ft. dew point temperature sensor failed during several periods. Together those periods caused annual data recovery to be 83.9 percent during 2006 and 79.2 percent during 2008, and therefore less than the 90 percent target.

The 33-ft. dew point temperature sensor failed on October 19, 2008, which caused a 90 percent data recovery goal to not be met for the dew point parameter during the year 2008. However, that dew point sensor failure occurred after the June 2008 equipment upgrade which included installation of a 33-ft. relative humidity sensor. The new redundant instruments enabled PSEG to meet the 90 percent data recovery goal. The 33-ft. dew point sensor was subsequently replaced in 2009.

On-site dew point temperature measurements recorded during the three-year period 2006-2008 are not used for any purpose that is affected by the missing observations.

2.3.4 SHORT-TERM (ACCIDENT) DIFFUSION ESTIMATES

2.3.4.1 Basis

The consequence of a design basis accident in terms of personnel exposure is a function of the atmospheric dispersion conditions at the site of the potential release. Atmospheric dispersion consists of two components: 1) atmospheric transport due to organized or mean airflow within the atmosphere and 2) atmospheric diffusion due to disorganized or random air motions. Atmospheric diffusion conditions are represented by atmospheric dispersion factor (χ/Q) values.

The magnitude of the atmospheric diffusion is a function of the wind speed, wind direction and atmospheric stability class. The more unstable the atmospheric characteristics, the more rapid the atmospheric dispersion. The lower the alphabetic atmospheric class designation (Class A) in RG 1.145 *Atmospheric Dispersion Models for Potential Accident Consequence Assessments at Nuclear Power Plants*, Revision 1, 1982, (Re-issued February 1983), the more unstable the atmosphere, the more rapid the atmospheric dispersion. Thus, the atmospheric class designations in RG 1.145 run from most rapid atmospheric dispersion (Class A) to least rapid atmospheric dispersion (Class G).

For accident analysis, the χ/Q calculations are based on the theory that material released to the atmosphere is normally distributed (Gaussian) about the plume centerline. A straight-line trajectory is assumed between the point of release and all distances for which χ/Q values are calculated. A straight-line trajectory approach is appropriate for the meteorological conditions at the PSEG Site as described in Subsection 2.3.2.2.1.2.

To evaluate potential health effects for the new plant on the PSEG Site, a design basis accident is postulated to predict upper-limit concentrations and doses that might occur in the event of a containment release to the atmosphere.

RG 4.7, *General Site Suitability Criteria for Nuclear Power Stations*, Revision 2, 1998, states that for site approval, each applicant should collect at least one year's worth of meteorological information that is representative of the site conditions for calculating radiation doses resulting from the release of fission products as a consequence of a postulated accident.

**PSEG Site
ESP Application
Part 2, Site Safety Analysis Report**

This on-site meteorological information is used to calculate the short term diffusion, also known as the accident χ/Q values, which are used to calculate the radiological consequences of a postulated accident.

As stated in RG 4.7, the applicant is required to establish an Exclusion Area Boundary (EAB) and a low population zone (LPZ) such that the following accident criteria are met:

“A reactor licensee is required by 10 CFR 100.21(a) to designate an exclusion area and to have authority to determine all activities within that area, including removal of personnel and property. In selecting a site for a nuclear power station, it is necessary to provide for an exclusion area in which the applicant has such authority. Transportation corridors such as highways, railroads, and waterways are permitted to traverse the exclusion area provided (1) these are not so close to the facility as to interfere with normal operation of the facility and (2) appropriate and effective arrangements are made to control traffic on the highway, railroad, or waterway in case of emergency to protect the public health and safety.

In 10 CFR 50.34(a)(1)(ii)(D)(1), the exclusion area is required to be of such a size that an individual assumed to be located at any point on its boundary would not receive a radiation dose in excess of 25 rem total effective dose equivalent (TEDE) over any 2-hour period following a postulated fission product release into the containment. The required exclusion area size involves consideration of the atmospheric characteristics of the site as well as plant design.

A reactor licensee is also required by 10 CFR 100.21(a) to designate an area immediately beyond the exclusion area as a low population zone (LPZ). The size of the LPZ must be such that the distance to the boundary of the nearest densely populated center containing more than about 25,000 residents must be at least one and one-third times the distance from the reactor to the outer boundary of the LPZ. The boundary of the population center should be determined upon consideration of population distribution, not political boundaries.

In 10 CFR 50.34(a)(1)(ii)(D)(2), the LPZ is required to be of such a size that an individual located on its outer radius for the course of the postulated accident (assumed to be 30 days) would not receive a radiation dose in excess of 25 rem TEDE. The size of the LPZ depends upon atmospheric dispersion characteristics and population characteristics of the site as well as aspects of plant design.”

Site-specific meteorological data covering the three-year period of record from January 1, 2006 through December 31, 2008 are used to quantitatively evaluate a design basis accident at the PSEG Site. On-site data provide representative measurements of local dispersion conditions appropriate to the PSEG Site and a three-year period is considered to be reasonably representative of long-term conditions.

Meteorological data are used to determine various postulated accident conditions as specified in RG 1.145. Compared to an elevated release, a ground-level release usually results in higher ground-level concentrations at downwind receptors. Since the ground-level release scenario provides a bounding case, elevated releases are not considered in this ESPA.

**PSEG Site
ESP Application
Part 2, Site Safety Analysis Report**

The NRC-sponsored PAVAN computer code (NUREG/CR-2858, PAVAN: *An Atmospheric Dispersion Program for Evaluating Design Basis Accidental Releases of Radioactive Materials from Nuclear Power Stations*, PNL-4413, November 1982) is used to estimate ground-level χ/Q s at the EAB and the outer boundary of the LPZ for potential accidental releases of radioactive material to the atmosphere. Such an assessment is required by 10 CFR Part 100.

The computer program PAVAN implements the guidance provided in RG 1.145. Mainly the code computes the χ/Q values at the EAB and the outer boundary of the LPZ for each joint combination of wind direction distributed into 16 sectors (i.e., north, north-northeast, northeast, etc.), and atmospheric stability distributed into seven classes. The χ/Q values for each sector are then ordered from greatest to smallest and an associated cumulative frequency distribution is derived based on the frequency distribution of wind speed and stabilities for that sector. The smallest χ/Q value in the distribution has a corresponding cumulative frequency equal to the wind-direction frequency for that sector. The program then determines for each sector an upper envelope curve based on these data (plotted as χ/Q versus probability of being exceeded) such that no plotted point is above the curve. From this upper envelope, the χ/Q value which is equaled or exceeded 0.5 percent of the total time is obtained. The maximum 0.5 percent χ/Q value from the 16 sectors becomes the maximum sector χ/Q value. This is done for both the EAB and LPZ.

PAVAN also combines all χ/Q values independent of wind direction into a cumulative frequency distribution for the site. An upper envelope curve is then determined, and PAVAN selects the χ/Q value which is equaled or exceeded 5 percent of the total time.

The larger of the two values (i.e., the maximum sector-dependent 0.5 percent χ/Q or the overall site 5 percent χ/Q value) is used to represent the χ/Q value for a 0- to 2-hour time period. To determine χ/Q s for longer time periods, the program calculates an annual average χ/Q value using the procedure described in RG 1.111, *Methods for Estimating Atmospheric Transport and Dispersion of Gaseous Effluents in Routine Releases from Light-Water-Cooled Reactors*, Revision 1, 1977. The program then uses logarithmic interpolation between the 0- to 2-hour χ/Q values for each sector and the corresponding annual average χ/Q values to calculate the values for intermediate time periods (i.e., 8 hours, 16 hours, 72 hours, and 624 hours).

The PAVAN model uses building cross-sectional area and containment height to estimate wake related χ/Q values. Conservatively, the EAB χ/Q for the new plant is determined without accounting for the reduction due to building wake effect, i.e. building cross-sectional area set to zero, and at a ground level release height of 10 meters (m) (33 ft.). The outer boundary of the LPZ is located beyond the building wake effect zone. The new plant location within the PSEG Site is not yet determined. Conservatively, the EAB is measured from the new plant power block envelope boundary in all directions. The outer boundary of the LPZ is measured from the new plant power block envelope boundary. This permits the analysis of any number of locations of the new plant on the PSEG Site without relocating the EAB and LPZ boundaries for each analysis. The EAB value of 600 m (1968 ft.) is based on the PAVAN analysis using the site-specific three year meteorology data and the not-to exceed plant parameter envelope (PPE) χ/Q value of $5.0E-04 \text{ sec/m}^3$. The outer boundary value of 5 mi. for the LPZ, 8045 m at 1609 m per mile, for the new plant is taken from the Salem Units 1 and 2 UFSAR, and the corresponding χ/Q values are determined using PAVAN and the three year site-specific meteorology data. The

Rev. 4

**PSEG Site
ESP Application
Part 2, Site Safety Analysis Report**

EAB minimum distance of 600 m (1968 ft.) as measured from the power block envelope and the location of the new plant site center is shown in the Site Utilization Plan, Figure 1.2-3.

The PAVAN model input data are presented below:

- Meteorological data: 3-year (January 1, 2006 through December 31, 2008) composite wind speed, wind direction, and atmospheric stability
- Type of release: Ground-level
- Wind sensor height: 10 m, (33 ft.)
- Vertical temperature difference: 150 ft.-33 ft.
- Number of wind speed categories: 11
- Release height: 10 m, (33 ft.) (Default height)
- Distances from release point to EAB: 600 m (1968.5 ft.), for all down wind sectors
- Distances from release point to outer boundary of the LPZ: 5 miles (8045 m), for all down wind sectors

2.3.4.2 PAVAN Modeling Results

As presented in Table 2.3-31, the maximum 0- to 2-hour, 0.5 percent, direction-dependent χ/Q value of $4.71\text{E-}04 \text{ sec/m}^3$ is greater than the corresponding 5 percent overall site χ/Q value of $3.74\text{E-}04 \text{ sec/m}^3$ at the EAB. Therefore, the 0.5 percent direction dependent χ/Q is used as the proper χ/Q at the EAB. Similarly, Table 2.3-32 shows that the maximum 0- to 2-hour, 0.5 percent, direction-dependent χ/Q value of $2.08\text{E-}05 \text{ sec/m}^3$ is greater than the corresponding 5 percent overall site χ/Q value of $1.95\text{E-}05 \text{ sec/m}^3$ at the outer boundary of the LPZ. Therefore, the 0.5 percent direction dependent χ/Q is used as the proper χ/Q at the outer boundary of the LPZ for the 0-2 hour time period. The χ/Q values at the outer boundary of the LPZ for longer time periods out to 30 days are also provided in Table 2.3-32. Note that sectors that cover substantial bodies of water are included in the comparison of χ/Q values.

The maximum χ/Q values presented in Tables 2.3-31 and 2.3-32 for the EAB and the outer boundary of the LPZ, respectively are summarized in Table 2.3-30, both evaluated by the PAVAN model. Examination of the results for the outer boundary of the LPZ shows a shift in the maximum direction dependent χ/Q for the 0 to 2-hour time period from the SW sector to the NW sector for the 0 to 8-hour time period and for the remaining time period out to 30 days.

2.3.5 LONG-TERM (ROUTINE) DIFFUSION ESTIMATES

2.3.5.1 Basis

For routine releases, receptor locations for the new plant are evaluated by determining χ/Q and/or D/Q at points of potential maximum concentration outside the site boundary. Points of maximum individual exposure are determined using a radial grid of sixteen $22\frac{1}{2}$ degree sectors (centered on true north, north-northeast, northeast, etc.) extending to a distance of 80 kilometers (km) (50 mi.) from the station. A set of data points is located within each sector:

- From the site boundary at increments of 0.4 km (0.25 mi.) to a distance of 1.6 km (1 mi.) from the plant

**PSEG Site
ESP Application
Part 2, Site Safety Analysis Report**

- From a distance of 1.6 km (1 mi.) at increments of 0.8 km (0.5 mi.) from a distance of 1.6 km (1 mi.) to 8 km (5 mi.)
- From a distance of 8 km (5 mi.) at increments of 4 km (2.5 mi.) to 16 km (10 mi.)
- From 16 km (10 mi.) at increments of 8 km (5 mi.) to a distance of 80 km (50 mi.)

Estimates of χ/Q (undecayed and undepleted; depleted for radioiodines) and D/Q radioiodines and particulates are provided at each of these grid points.

The NRC-sponsored XOQDOQ computer program (NUREG/CR-2919, *XOQDOQ: Computer Program for the Meteorological Evaluation of Routine Effluent Releases at Nuclear Power Stations*, PNL-4380, September 1982) is used to estimate χ/Q and D/Q values due to routine releases of gaseous effluents to the atmosphere. The XOQDOQ computer code calculates the χ/Q values and D/Q values at receptors of interest (e.g., site boundary, the nearest milk cow, residence, garden, meat animal). χ/Q and D/Q values due to intermittent releases, which occur during routine operation, may also be evaluated using the XOQDOQ model.

The XOQDOQ dispersion model implements the assumptions outlined in RG 1.111. The program assumes that the material released to the atmosphere follows a Gaussian distribution around the plume centerline. Atmospheric diffusion parameters are the standard Pasquill-Gifford diffusion parameters. In estimating concentrations for longer time periods, the Gaussian distribution is assumed to be evenly distributed within a given directional sector. A straight-line trajectory is assumed between the release point and all receptors. A straight-line trajectory approach is appropriate for the meteorological conditions at the PSEG Site as described in Subsection 2.3.2.2.1.2.

Conservatively, the χ/Q values for the new plant are determined without accounting for the reduction due to building wake effect, i.e. building cross-sectional area set to zero, and a ground level release height of 10 meters (m) (33 ft.). The new plant location within the PSEG Site is not yet determined. The downwind distances from 0.25 to 50 mi. are measured from the center of the power block, known as the new plant site center, in all directions. Additionally, distances, to the site boundary, the nearest residence and the nearest farm containing the milk/meat animals and vegetable garden greater than 50 m² are also measured from the new plant site center at this time.

Four reactor technologies are considered at the PSEG Site: ABWR, AP1000, U.S. EPR, and US-APWR. The primary gaseous effluent release pathways for the ABWR, U.S. EPR, and US-APWR are via the associated vent stacks that are adjacent to the corresponding reactor buildings. The vent stacks for these three technologies are located approximately at the center of the power block. The distances between the vent stacks and the site boundary vary slightly for these reactor technologies but they are within 10% of the distance between the center of the power block and the site boundary currently used in the SSAR. Therefore, the approach in the SSAR to use the center of the power block as a release point to determine the χ/Q and D/Q values at the PSEG Site is a reasonable approximation.

The new plant using two AP1000 units has multiple gaseous effluent release points around the center of the power block. The release points associated with one of the reactors are farther away from the site boundary than the modeled center of the power block, while the release points associated with the other reactor are closer to the site boundary than the modeled center

**PSEG Site
ESP Application
Part 2, Site Safety Analysis Report**

of the power block. The release point used to determine the χ/Q and D/Q values at the PSEG Site is therefore a representative location for all the release points of the two AP1000 units.

As stated in SSAR Subsection 2.3.5.1, the building wake effects are conservatively not credited in the χ/Q and D/Q calculation. This methodology provides a reasonable justification for the use of the center of the power block as the representative release point for all the reactor technologies being considered for the PSEG Site.

The following input data and assumptions are used in the XOQDOQ modeling analysis:

- Meteorological data: Three way JFD based on three years of on-site meteorological data for the period January 1, 2006 through December 31, 2008
- Type of release: Ground-level
- No vertical plume rise
- Conservatively, terrain is flat
- Wind sensor height: 10 m, (33 ft.)
- Vertical temperature difference: 150 ft.-33 ft.
- Number of wind speed categories: 11
- Release height: 10 m, (33 ft.), (default height)
- Distances from the postulated release point at the new plant site center to the nearest residence, nearest site boundary, vegetable garden, and meat animal

These values are used in the XOQDOQ model to predict the required annual average χ/Q and D/Q values. The location of the nearest meat animal and vegetable garden is assumed to be the dairy farm located 4.9 mi. WSW of the new plant site center. This assumption is acceptable because the specified location is the nearest identified farm, and hence the nearest point where a meat animal or a garden (greater than 50 m²) could be maintained. Moreover, the S/HC Offsite Dose Control Document requires a land census to identify a garden location for the site dose calculation. The dairy farm located 4.9 mi. west of the existing S/HC site is used for this analysis in the *2008 Annual Radioactive Effluent Release Report for the Salem and Hope Creek Generating Stations* (Reference 2.3.5-1). Therefore, it is reasonable to use this farm to analyze the radiological impact of normal effluents from the new plant. The nearest residence that could be conservatively determined is 2.8 mi. WNW. The nearest distances for the residence, farm and site boundary are presented in Table 2.3-33.

2.3.5.2 XOQDOQ Modeling Results

The values are summarized in Table 2.3-34. A complete set of the χ/Q and D/Q values at the site boundary is provided in Table 2.3-37. The largest χ/Q value for the site boundary is 1.6E-05 sec/m³ in the South direction. Note however that the limiting values for sectors SE to NW (clockwise direction) is disregarded due to the fact that the site boundary for these sectors is bordered by the Delaware River (greater than a mile radially out from new plant site center). Therefore, the only sectors that are used to obtain the limiting χ/Q value for the site boundary are between the NNW and ESE directions (clockwise direction).

Table 2.3-33 shows the shortest distance between the new plant site center and the receptor points of interest. Table 2.3-34 summarizes the maximum χ/Q and D/Q values predicted by the XOQDOQ model for identified sensitive receptors in the vicinity of the new plant site center due

**PSEG Site
ESP Application
Part 2, Site Safety Analysis Report**

to routine releases of gaseous effluents. As stated above, results for Delaware River sectors for the site boundary are not presented. The listed maximum χ/Q values reflect several plume depletion scenarios that account for radioactive decay (i.e., no decay, and the default half-life decay periods of 2.26 and 8 days).

The overall maximum annual average χ/Q value (with no decay) is $1.00\text{E-}05 \text{ sec/m}^3$ and occurs at the site boundary at a distance of 0.24 mi. to the ENE of the new plant site center. The maximum annual average χ/Q values (along with the direction and distance of the receptor locations relative to the new plant site center) for the other sensitive receptor types are: $2.40\text{E-}07 \text{ sec/m}^3$ for the nearest residence occurring in the northwest sector at a conservative distance of 2.8 mi. and $1.10\text{E-}07 \text{ sec/m}^3$ at the farm 4.9 mi. to the northwest. Table 2.3-35 summarizes the annual average χ/Q values at the XOQDOQ model's 22 standard radial distances between 0.25 and 50 mi. and for the model's 10 distance segment boundaries between 0.5 and 50 mi. downwind along each of the 16 standard direction radials (i.e., separated by 22.5 degrees). Table 2.3-36 summarizes the annual average D/Q values (for no decay).

2.3.5.3 References

- 2.3.5-1 *2008 Annual Radioactive Effluent Release Report for the Salem and Hope Creek Generating Stations*

**PSEG Site
ESP Application
Part 2, Site Safety Analysis Report**

**Table 2.3-1 (Sheet 1 of 3)
NOAA Climate Summary for Wilmington, Delaware^(a)**

	Element	POR	JAN	FEB	MAR	APR	MAY	JUN	JUL	AUG	SEP	OCT	NOV	DEC	YEAR
Temperature °F	Normal Daily Maximum	30	39.3	42.5	51.9	62.6	72.5	81.1	86	84.1	77.2	65.9	55	44.4	63.5
	Mean Daily Maximum	61	40	42.7	51.6	63.1	72.7	81.4	85.9	84.1	77.5	66.6	55.3	44.2	63.8
	Highest Daily Maximum	61	75	78	86	94	96	100	102	101	100	91	85	75	102
	Year of Occurrence		1950	1985	1998	1985	1996	1994	1966	1955	1983	1951	1950	1998	Jul 1966
	Mean of Extreme Max	61	60.3	62.3	73.2	82.4	88	93.1	95.4	93.3	89.8	81.8	72.7	63.6	79.7
	Normal Daily Minimum	30	23.7	25.8	33.4	42.1	52.4	61.8	67.3	65.8	58.1	45.6	36.9	28.4	45.1
	Mean Daily Minimum	61	24.1	25.6	32.9	42.2	52	61.5	66.9	65.4	57.9	46	36.7	27.9	44.9
	Lowest Daily Minimum	61	-14	-6	2	18	30	41	48	43	36	24	14	-7	-14
	Year of Occurrence		1985	1979	1984	1982	1978	1972	1988	1982	1974	1976	1955	1983	Jan 1985
	Mean of Extreme Min	61	7.6	9.6	18	29.1	38.6	49.1	56	53.5	42.9	31.9	22.3	12.7	30.9
	Normal Dry Bulb	30	31.5	34.2	42.7	52.4	62.5	71.5	76.6	75	67.7	55.8	45.9	36.4	54.4
	Mean Dry Bulb	61	32.1	34.2	42.3	52.6	62.4	71.6	76.4	74.9	67.7	56.3	46	36.1	54.4
	Mean Wet Bulb	25	29	30.2	36.6	45	55.6	64.7	69	67.9	61.8	51	41.7	32.9	48.9
	Mean Dew Point	25	24.1	24.6	30.9	40.7	51.7	61.1	66.1	65.3	58.9	47.3	37	27.8	44.6
	Normal Number of Days:														
	Maximum >=90	30	0	0	0	0.2	1	3.5	9	5.4	1.5	0	0	0	20.6
	Maximum <=32	30	7.7	5	0.7	0	0	0	0	0	0	0	0.1	3.5	17
	Minimum <=32	30	24.9	21	13.7	2.8	*	0	0	0	0	1.3	9.8	21.2	94.7
	Minimum <=0	30	0.5	0.3	0	0	0	0	0	0	0	0	0	0.1	0.9
H/C	Normal Heating Deg. Days	30	1029	864	687	376	132	15	1	2	49	297	564	872	4888
	Normal Cooling Deg. Days	30	0	0	2	9	62	315	368	317	135	16	1	0	1125
RH	Normal (Percent)	30	68	65	63	63	68	69	70	72	73	72	69	69	68
	Hour 01 LST	30	73	71	70	71	79	81	81	83	84	82	76	74	77
	Hour 07 LST	30	76	74	73	72	76	77	79	83	85	85	80	76	78
	Hour 13 LST	30	60	55	51	50	54	55	55	57	57	55	56	59	55
	Hour 19 LST	30	67	62	59	57	63	64	64	68	71	69	67	67	65

**PSEG Site
ESP Application
Part 2, Site Safety Analysis Report**

**Table 2.3-1 (Sheet 2 of 3)
NOAA Climate Summary for Wilmington, Delaware^(a)**

	Element	POR	JAN	FEB	MAR	APR	MAY	JUN	JUL	AUG	SEP	OCT	NOV	DEC	YEAR
S	Percent Possible Sunshine														
W/O	Mean Number Days with:														
	Heavy Fog (VSBY <= 1/4 mi.)	45	3.4	2.6	2.4	1.7	1.7	1.3	1.1	1.2	1.6	3.1	3	3	26.1
	Thunderstorms	61	0.2	0.3	1	2.1	3.8	5.4	5.9	5.1	2.3	0.8	0.6	0.2	27.7
Cloudiness^(b)	Mean:														
	Sunrise-Sunset (OKTAS)														
	Midnight-Midnight (OKTAS)														
	Mean No. Days with:														
	Clear	1	2	2	6		8	9	3	7	5	9		5	
	Partly Cloudy	1	1	1	6		4	5	1	4	3	2		2	
	Cloudy	1	4	5	11		6	8		2	7	3		8	
Pressure	Mean Station Pressure (in.)	25	30.01	29.99	29.96	29.9	29.9	29.89	29.9	29.94	29.98	30.01	30.01	30.02	29.96
	Mean Sea-Level Pressure (in.)	25	30.1	30.08	30.05	29.98	29.99	29.98	29.99	30.03	30.07	30.1	30.1	30.11	30.05
Winds	Mean Speed (mph)	25	9.3	9.7	10.4	9.9	8.6	7.9	7.6	7.1	7.6	7.6	8.6	8.9	8.6
	Prevailing Direction (Tens of Deg.)	33	31	31	31	31	31	17	31	19	32	32	31	31	31
	Max 2-Min. Speed (mph)	14	51	43	47	46	48	41	45	40	43	38	47	45	51
	Direction (Tens of Deg.)		15	31	24	33	24	27	32	14	13	28	29	31	15
	Year of Occurrence		1999	2006	2008	1995	1999	1998	1995	1997	2003	2008	2003	2008	Jan 1999
	Max 3-Sec. Speed (mph)	14	61	54	56	60	61	52	56	53	53	51	61	59	61
	Direction (Tens of Deg.)		23	29	24	29	23	27	26	15	12	29	29	32	29
	Year of Occurrence		1999	1996	2008	2007	1999	1998	2006	1997	2003	2008	2005	2008	Nov 2005

**PSEG Site
ESP Application
Part 2, Site Safety Analysis Report**

**Table 2.3-1 (Sheet 3 of 3)
NOAA Climate Summary for Wilmington, Delaware^(a)**

	Element	POR	JAN	FEB	MAR	APR	MAY	JUN	JUL	AUG	SEP	OCT	NOV	DEC	YEAR
Precipitation	Normal (in.)	30	3.43	2.81	3.97	3.39	4.15	3.59	4.28	3.51	4.01	3.08	3.19	3.4	42.81
	Maximum Monthly (in.)	61	8.41	7.02	9.17	8.55	7.38	9.9	12.63	12.09	12.68	8.01	7.84	7.96	12.68
	Year of Occurrence		1978	1979	2000	2007	1983	2003	1989	1955	1999	1995	1972	1996	Sep 1999
	Minimum Monthly (in.)	61	0.52	0.43	0.29	0.35	0.22	0.21	0.16	0.25	0.44	0.08	0.49	0.19	0.08
	Year of Occurrence		1981	2002	2006	1985	1964	1988	1955	1972	2005	2000	1976	1955	Oct 2000
	Maximum in 24 Hours (in.)	61	2.53	2.35	4.87	4.39	2.72	4.35	6.83	4.11	8.43	3.88	3.83	2.38	8.43
	Year of Occurrence		1998	2003	2000	2007	1990	1972	1989	1971	1999	1966	1956	2008	Sep 1999
	Normal no. Days with:														
	Precipitation >=0.01	30	10.9	9.5	10.5	10.7	11.5	10.4	9.3	8.5	9	8	9.2	10.3	117.8
	Precipitation >=1.0	30	1	0.6	1.1	0.8	0.9	0.8	1.2	1.1	1.2	0.8	0.8	1	11.3
Snowfall	Normal (in.)	30	7.5	6.3	2.2	0.3	0	0	0	0	0	0.1	0.6	1.9	18.9
	Maximum Monthly (in.)	57	26.2	31.6	20.3	2.6	T	T	T	0	0	2.5	11.9	21.5	31.6
	Year of Occurrence		1996	2003	1958	1982	1991	1992	2007			1979	1953	1966	Feb 2003
	Minimum Monthly (in.)	57	22	17	15.6	2.4	T	T	T	0	0	2.5	11.9	12.4	22
	Year of Occurrence		1996	2003	1958	1987	1991	1992	1990			1979	1953	1966	Jan 1996
	Maximum in 24 Hours (in.)	52	13	25	8	2	0	0	0	0	0	T	9	12	25
	Year of Occurrence		1987	2003	1956	1987						1962	1953	1966	Feb 2003
	Normal no. Days with:														
	Snowfall >=1.0	30	2.2	1.4	0.5	0.2	0	0	0	0	0	0	0.2	0.7	5.2

a) Blank entries denote missing or unreported data.

b) When at least one of the elements used to determine cloudiness (ceilometer or satellite) is missing, the daily cloudiness is not computed and the table entry is blank.

**PSEG Site
ESP Application
Part 2, Site Safety Analysis Report**

**Table 2.3-2 (Sheet 1 of 3)
NOAA Climate Summary for Atlantic City, New Jersey^(a)**

	Element	POR	JAN	FEB	MAR	APR	MAY	JUN	JUL	AUG	SEP	OCT	NOV	DEC	YEAR
Temperature °F	Normal Daily Maximum	30	41.4	43.9	51.9	61.3	71.1	80	85.1	83.3	76.6	66.3	56	46.4	63.6
	Mean Daily Maximum	50	41.3	43.3	51.4	61.6	71.3	80.1	84.9	83.5	77	66.4	56.2	45.7	63.6
	Highest Daily Maximum	65	78	75	87	94	99	106	104	103	99	90	84	77	106
	Year of Occurrence		1967	1985	1998	2002	1969	1969	1966	2001	1983	2007	1950	1998	Jun 1969
	Mean of Extreme Max	50	62	63	72.9	82.3	88.3	93.4	95.5	93.9	89.3	81.6	72.5	63.4	79.8
	Normal Daily Minimum	30	22.8	24.5	31.7	39.8	49.8	59.3	65.4	63.7	56	43.9	35.7	27.1	43.3
	Mean Daily Minimum	50	23	24.2	31.5	40.3	49.8	59.2	65.5	64.1	56.4	44.6	36.2	26.9	43.5
	Lowest Daily Minimum	65	-10	-11	4	12	25	37	42	40	32	20	10	-7	-11
	Year of Occurrence		1977	1979	2007	1969	1966	1980	1988	1976	1969	1988	1989	1950	Feb 1979
	Mean of Extreme Min	50	4.2	7	15.4	25.6	35	45.3	53.3	50.9	40.4	29.4	19.9	9.9	28
	Normal Dry Bulb	30	32.1	34.2	41.8	50.6	60.5	69.7	75.3	73.5	66.3	55.1	45.9	36.8	53.5
	Mean Dry Bulb	50	32.2	33.8	41.5	50.9	60.6	69.9	75.2	73.8	66.7	55.5	46.2	36.3	53.6
	Mean Wet Bulb	25	30	30.7	36.4	45.1	54.3	63.9	68.9	67.9	61.8	51.2	42.3	33.7	48.9
	Mean Dew Point	25	25.5	25.8	31.4	40.4	50.7	60.9	66.5	65.9	59.4	48.1	38.2	29.2	45.2
	Normal Number of Days:														
	Maximum >=90	30	0	0	0	0.1	1	3.3	7.8	4.4	1.1	0	0	0	17.7
	Maximum <=32	30	6.4	4.7	0.6	0	0	0	0	0	0	0	0.1	3.2	15
	Minimum <=32	30	25.1	21.7	16.6	6.3	0.4	0	0	0	0	3.2	12.5	22.2	108
	Minimum <=0	30	0.6	0.4	0	0	0	0	0	0	0	0	0	0.2	1.2
H/C	Normal Heating Deg. Days	30	1019	873	725	437	187	32	1	6	69	323	573	868	5113
	Normal Cooling Deg. Days	30	0	0	1	5	44	168	322	269	110	15	1	0	935
RH	Normal (Percent)	30	72	70	67	68	72	73	74	77	78	76	73	72	73
	Hour 01 LST	30	76	76	76	78	84	87	88	89	89	87	81	77	82
	Hour 07 LST	30	79	79	77	77	79	81	83	87	88	88	84	79	82
	Hour 13 LST	30	59	56	53	52	56	57	57	59	59	56	57	58	57
	Hour 19 LST	30	71	69	65	65	69	70	71	76	80	79	74	72	72

**PSEG Site
ESP Application
Part 2, Site Safety Analysis Report**

**Table 2.3-2 (Sheet 2 of 3)
NOAA Climate Summary for Atlantic City, New Jersey^(a)**

	Element	POR	JAN	FEB	MAR	APR	MAY	JUN	JUL	AUG	SEP	OCT	NOV	DEC	YEAR
S	Percent Possible Sunshine	36	50	53	55	56	56	60	61	65	61	59	51	47	56
W/O	Mean Number Days with:														
	Heavy Fog (VSBY <= 1/4 mi.)	45	2.8	2.6	2.8	3.2	3.8	3.4	3.4	3	3.1	3.8	3.1	2	37
	Thunderstorms	50	0.1	0.3	0.8	1.8	2.8	3.8	5.4	4.4	1.5	0.7	0.4	0.2	22.2
Cloudiness^(b)	Mean:														
	Sunrise-Sunset (OKTAS)														
	Midnight-Midnight (OKTAS)														
	Mean No. Days with:														
	Clear														
	Partly Cloudy														
	Cloudy														
Pressure	Mean Station Pressure (in.)	25	30	29.99	29.96	29.9	29.91	29.9	29.91	29.95	29.99	30.01	30.01	30.01	29.96
	Mean Sea-Level Pressure (in.)	25	30.08	30.06	30.03	29.97	29.98	29.97	29.98	30.02	30.06	30.08	30.09	30.09	30.03
Winds	Mean Speed (mph)	25	9.6	10.1	10.8	10.5	9.1	8.1	7.5	7.1	7.4	7.8	8.9	9.3	8.9
	Prevailing Direction (Tens of Deg.)	29	30	31	31	19	19	20	19	19	20	30	31	30	30
	Max 2-Min. Speed (mph)	13	47	41	49	41	43	36	41	31	39	38	43	41	49
	Direction (Tens of Deg.)		30	28	5	13	4	30	26	28	7	28	27	10	5
	Year of Occurrence		2000	2006	2007	2005	2008	1998	2006	2007	2003	2003	2003	2003	Mar 2007
	Max 3-Sec. Speed (mph)	13	56	53	60	54	59	46	59	41	50	54	54	58	60
	Direction (Tens of Deg.)		30	5	5	23	4	31	25	28	9	28	28	9	5
	Year of Occurrence		2000	2003	2007	1996	2008	1998	2006	2007	2006	2003	2003	2003	Mar 2007

**PSEG Site
ESP Application
Part 2, Site Safety Analysis Report**

**Table 2.3-2 (Sheet 3 of 3)
NOAA Climate Summary for Atlantic City, New Jersey^(a)**

	Element	POR	JAN	FEB	MAR	APR	MAY	JUN	JUL	AUG	SEP	OCT	NOV	DEC	YEAR
Precipitation	Normal (in.)	30	3.6	2.85	4.06	3.45	3.38	2.66	3.86	4.32	3.14	2.86	3.26	3.15	40.59
	Maximum Monthly (in.)	65	7.71	5.98	9.25	7.95	11.51	6.99	13.09	16.06	6.32	9.04	9.65	7.33	16.06
	Year of Occurrence		1948	1958	1994	1952	1948	2003	1959	1997	2006	2005	1972	1969	Aug 1997
	Minimum Monthly (in.)	65	0.26	0.74	0.37	0.84	0.4	0.1	0.51	0.34	0.41	0.06	0.68	0.62	0.06
	Year of Occurrence		1955	2002	2006	1976	1957	1954	1983	1943	1970	2000	1976	1955	Oct 2000
	Maximum in 24 Hours (in.)	65	2.86	2.59	3	3.37	4.15	3.69	6.46	6.4	3.98	2.95	3.93	4.36	6.46
	Year of Occurrence		1944	1966	2000	1952	1959	2007	1959	1997	1954	1958	1953	2008	Jul 1959
	Normal no. Days with:														
	Precipitation >=0.01	30	10.5	9.2	10.4	10.7	10.8	8.7	8.8	8.7	8.2	7.6	9.4	10.3	113.3
	Precipitation >=1.0	30	0.8	0.6	1.2	0.8	0.7	0.7	1	1.3	0.8	0.8	0.8	0.8	10.3
Snowfall	Normal (in.)	30	4.6	5.5	1.3	0.3	0	0	0	0	0	0	0.3	1.5	13.5
	Maximum Monthly (in.)	60	20.3	35.2	17.6	3.9	T	T	T	0	0	T	7.8	9.3	35.2
	Year of Occurrence		1987	1967	1969	1990	1989	1994	1991			2008	1967	1989	Feb 1967
	Minimum Monthly (in.)	60	16.3	17.1	11.5	3.9	T	T	T	0	0	T	7.8	7.5	17.1
	Year of Occurrence		1987	1979	1969	1990	1989	1994	1991			1990	1967	1960	Feb 1979
	Maximum in 24 Hours (in.)	40	19	23	11	3	0	0	0	0	0	0	6	7	23
	Year of Occurrence		1987	1979	1969	1990							1989	1982	Feb 1979
	Normal no. Days with:														
	Snowfall >=1.0	30	1.6	1.3	0.5	0.1	0	0	0	0	0	0	0	0.5	4

a) Blank entries denote missing or unreported data.

b) When at least one of the elements used to determine cloudiness (ceilometer or satellite) is missing, the daily cloudiness is not computed and the table entry is blank.

**PSEG Site
ESP Application
Part 2, Site Safety Analysis Report**

**Table 2.3-3 (Sheet 1 of 3)
NOAA Climate Summary for Philadelphia, Pennsylvania^(a)**

	Element	POR	JAN	FEB	MAR	APR	MAY	JUN	JUL	AUG	SEP	OCT	NOV	DEC	YEAR
Temperature °F	Normal Daily Maximum	30	39	42.1	51.3	62	72.1	80.6	85.5	84	76.7	65.7	54.8	44.2	63.2
	Mean Daily Maximum	61	39.7	42.5	51.5	63.4	73.3	82	86.6	84.8	77.7	66.7	55.3	44	64
	Highest Daily Maximum	67	74	74	87	95	97	100	104	101	100	96	81	73	104
	Year of Occurrence		1950	1997	1945	2002	1991	1994	1966	2001	1953	1941	1993	1998	Jul 1966
	Mean of Extreme Max	61	60.2	61.7	73.1	83.1	88.5	93.7	95.9	94.1	90.3	81.8	72.6	63.1	79.8
	Normal Daily Minimum	30	25.5	27.5	35.1	44.2	54.8	64	59.7	68.5	60.9	48.7	39.5	30.6	47.4
	Mean Daily Minimum	61	24.9	36.4	33.6	43.1	53.1	62.3	68	66.8	59.3	47.6	38.1	29.1	46
	Lowest Daily Minimum	67	-7	-4	7	19	28	44	51	44	35	25	15	1	-7
	Year of Occurrence		1984	1961	1984	1982	1966	1984	1966	1986	1963	1969	1976	1983	Jan 1984
	Mean of Extreme Min	61	9	10.8	19	30.3	40.8	50.6	58.1	55.8	45	33.8	24.1	14.3	32.6
	Normal Dry Bulb	30	32.3	34.8	43.2	53.1	63.5	72.3	77.6	76.3	68.8	57.2	47.1	37.4	55.3
	Mean Dry Bulb	61	32.3	34.5	42.5	53.3	63.2	72.4	77.3	75.8	68.5	57.1	46.7	36.6	55
	Mean Wet Bulb	25	29.3	30.4	36.7	46	55.5	64.6	69.1	67.9	61.9	51.5	42.1	33.2	49
	Mean Dew Point	25	24.1	24.6	31	40.5	51.1	60.9	65.8	65	58.6	47.7	37.3	27.6	44.5
	Normal Number of Days:														
	Maximum >=90	30	0	0	0	0.4	1.3	4.6	10.5	7.3	1.6	0	0	0	25.7
	Maximum <=32	30	8	5.3	0.7	0	0	0	0	0	0	0	0.1	3.6	17.7
	Minimum <=32	30	24.8	20.8	12.6	2	0	0	0	0	0	0.7	7.3	19.2	87.4
	Minimum <=0	30	0.4	0.1	0	0	0	0	0	0	0	0	0	0	0.5
H/C	Normal Heating Deg. Days	30	1020	858	681	362	113	12	1	2	39	269	545	857	4759
	Normal Cooling Deg. Days	30	0	0	2	10	70	234	395	351	152	19	2	0	1235
RH	Normal (Percent)	30	67	64	62	61	66	68	69	70	72	71	68	68	67
	Hour 01 LST	30	71	69	70	70	77	80	80	82	82	82	75	72	76
	Hour 07 LST	30	74	73	73	71	75	77	78	81	83	83	48	75	77
	Hour 13 LST	30	60	55	52	50	53	54	54	55	56	55	56	58	55
	Hour 19 LST	30	65	61	58	55	59	61	62	65	68	69	66	66	63

**PSEG Site
ESP Application
Part 2, Site Safety Analysis Report**

**Table 2.3-3 (Sheet 2 of 3)
NOAA Climate Summary for Philadelphia, Pennsylvania^(a)**

	Element	POR	JAN	FEB	MAR	APR	MAY	JUN	JUL	AUG	SEP	OCT	NOV	DEC	YEAR
S	Percent Possible Sunshine	59	49	53	55	55	56	62	61	62	59	59	52	49	56
W/O	Mean Number Days with:														
	Heavy Fog (VSBY <= 1/4 mi.)	45	2	1.5	1	0.8	0.7	0.6	0.7	0.4	0.8	2	1.5	1.6	13.6
	Thunderstorms	61	0.3	0.3	1	2.2	4	5.2	5.5	4.9	2.4	0.8	0.5	0.2	27.3
Cloudiness^(b)	Mean:														
	Sunrise-Sunset (OKTAS)														
	Midnight-Midnight (OKTAS)														
	Mean No. Days with:														
	Clear	1	3	2	8		8	11							
	Partly Cloudy			1	4		5	3							
	Cloudy	1	3	6	8		7	9							
Pressure	Mean Station Pressure (in.)	25	30.06	30.05	30.02	29.95	29.95	29.94	29.95	29.99	30.03	30.06	30.03	30.08	30.01
	Mean Sea-Level Pressure (in.)	25	30.09	30.08	30.05	29.98	29.98	29.97	29.98	30.02	30.07	30.09	30.1	30.1	30.04
Winds	Mean Speed (mph)	25	10	10.4	11	10.3	9.2	8.8	8.5	8.1	8.4	7.8	9.4	9.9	9.4
	Prevailing Direction (Tens of Deg.)	45	30	31	30	24	24	24	24	24	24	24	24	30	24
	Max 2-Min. Speed (mph)	13	44	45	49	37	52	51	41	41	39	45	46	45	52
	Direction (Tens of Deg.)		27	27	24	33	28	30	33	25	32	24	27	27	28
	Year of Occurrence		2008	2008	2008	2002	2005	1998	1999	1997	1998	2003	2003	2000	May 2005
	Max 3-Sec. Speed (mph)	13	57	52	56	51	69	71	48	52	49	55	58	53	71
	Direction (Tens of Deg.)		18	31	24	28	27	30	28	24	13	20	28	28	30
	Year of Occurrence		1996	1996	2008	2000	2005	1998	2006	1997	2003	2003	2003	2000	Jun 1998

**PSEG Site
ESP Application
Part 2, Site Safety Analysis Report**

**Table 2.3-3 (Sheet 3 of 3)
NOAA Climate Summary for Philadelphia, Pennsylvania^(a)**

	Element	POR	JAN	FEB	MAR	APR	MAY	JUN	JUL	AUG	SEP	OCT	NOV	DEC	YEAR
Precipitation	Normal (in.)	30	3.52	2.74	3.81	3.49	3.89	3.29	4.39	3.82	3.88	2.75	3.16	3.31	42.05
	Maximum Monthly (in.)	66	8.86	6.44	7.01	9.05	7.41	8.08	10.42	9.7	13.07	8.68	9.06	8.47	13.07
	Year of Occurrence		1978	1979	1980	2007	1948	2003	1994	1955	1999	2005	1972	1996	Sep 1999
	Minimum Monthly (in.)	66	0.45	0.55	0.68	0.52	0.47	0.11	0.64	0.49	0.21	0.09	0.32	0.25	0.09
	Year of Occurrence		1955	2002	1966	1985	1964	1949	1957	1964	2005	1963	1976	1955	Oct-1963
	Maximum in 24 Hours (in.)	66	2.7	3.52	3.08	4.36	3.18	4.62	4.68	5.68	6.77	5.94	3.99	3.18	6.77
	Year of Occurrence		1979	2008	2000	2007	1984	1973	2004	1971	1999	2005	1977	2008	Sep 1999
	Normal no. Days with:														
	Precipitation >=0.01	30	10.9	9.7	10.5	10.9	11.7	10	9.4	8.4	9.1	8	9.4	10.6	118.6
	Precipitation >=1.0	30	0.9	0.6	1	0.8	0.8	0.8	1.3	1.2	1.1	0.7	0.6	0.8	10.6
Snowfall	Normal (in.)	30	6.4	6.6	3.2	0.6	0	0	0	0	0	0.1	0.4	2	19.3
	Maximum Monthly (in.)	65	23.4	29.6	13.4	4.3	T	T	T	0	0	2.1	8.8	18.8	29.6
	Year of Occurrence		1978	2003	1958	1971	1963	1993	2008			1979	1953	1966	Feb 2003
	Minimum Monthly (in.)	65	33.8	21.3	12	4.3	T	T	T	0	0	2.1	8.7	14.6	33.8
	Year of Occurrence		1996	1983	1993	1971	1963	1993	2006			1979	1953	1960	Jan-1996
	Maximum in 24 Hours (in.)	60	12	23	12	3	0	0	0	0	0	0	8	12	23
	Year of Occurrence		1961	2003	1993	1997							1953	1966	Feb 2003
	Normal no. Days with:														
	Snowfall >=1.0	30	1.9	1.5	0.8	0.2	0	0	0	0	0	0	0.2	0.5	5.1

a) Blank entries denote missing or unreported data.

b) When at least one of the elements used to determine cloudiness (ceilometer or satellite) is missing, the daily cloudiness is not computed and the table entry is blank.

**PSEG Site
ESP Application
Part 2, Site Safety Analysis Report**

**Table 2.3-4 (Sheet 1 of 2)
Available NOAA Regional Meteorological Monitoring Stations^(a)**

Station Name	Station Type(s)	State	County	Approx Distance from New Plant Site (mi.)	Approx Direction from New Plant Site	Approx Elevation (ft. msl)	COOP ID no.	WBAN ID no.	COOP Station Period of Record Analyzed
Aberdeen Phillips Field	COOP	MD	Harford	34	W	57	180015	13701	1919 to 2009
Atlantic City IAP	COOP, ASOS, LCD, ASHRAE	NJ	Atlantic	53	E	60	280311	13724	Not analyzed
Baltimore-Wash. IAP	COOP, ASOS, LCD, ASHRAE	MD	Baltimore	63	WSW	156	180465	93721	Not analyzed
Belleplain STN Forest	COOP	NJ	Cape May	38	SE	30	280690	n/a	Not analyzed
Cape May 2NW	COOP, ASHRAE	NJ	Cape May	60	SSE	20	281351	n/a	Not analyzed
Centreville	COOP	MD	Queen Anne's	33	WSW	59	181627	n/a	1953 to 1985
Chadds Ford 2 NE	COOP	PA	Delaware	27	N	229	361342	n/a	Not analyzed
Chestertown	COOP	MD	Kent	32	SW	40	181750	n/a	1893 to 2009
Conowingo Dam	COOP	MD	Harford	34	WNW	40	182060	n/a	Not analyzed
Denton 2 E	COOP	MD	Caroline	47	SSW	49	182523	n/a	Not analyzed
Dover	COOP, ASOS	DE	Kent	23	S	30	072730	13707	1893 to 2009
Glassboro 2 NE	COOP	NJ	Gloucester	26	NE	100	283291	n/a	1948 to 2004
Hammonton 1 NE	COOP	NJ	Atlantic	43	ENE	90	283662	n/a	1893 to 2009
Marcus Hook	COOP	PA	Delaware	26	NNE	10	365390	n/a	1919 to 2009
Millington 1 SE	COOP	MD	Kent	23	SW	30	185985	n/a	1898 to 2001
Millville MAP	COOP, ASOS, ASHRAE	NJ	Cumberland	23	ESE	70	285581	13709	1947 to 2009
Newark Univ. Farm	COOP	DE	New Castle	19	NW	90	076410	n/a	1894 to 2006
Philadelphia IAP	COOP, ASOS, LCD, ASHRAE	PA	Philadelphia	30	NNE	10	366889	13739	1948 to 2009

**PSEG Site
ESP Application
Part 2, Site Safety Analysis Report**

**Table 2.3-4 (Sheet 2 of 2)
Available NOAA Regional Meteorological Monitoring Stations**

Station Name	Station Type(s)	State	County	Approx Distance from New Plant Site (mi.)	Approx Direction from New Plant Site	Approx Elevation (ft. msl)	COOP ID no.	WBAN ID no.	Available Period of Record (COOP DS 3200 Database)
Seabrook Farms	COOP	NJ	Cumberland	17	E	90	287936	n/a	1949 to 2009
Sussex	COOP, ASOS, ASHRAE	DE	Sussex	55	SSE	52	n/a	n/a	Not analyzed
West Chester 2NW	COOP	PA	Chester	33	N	375	369464	n/a	Not analyzed
Wilmington New Castle R	COOP, ASOS, LCD, ASHRAE	DE	New Castle	13	N	74	079595	13781	1948 to 2009
Woodstown Pittsgrove 4E	COOP	NJ	Salem	20	ENE	98	289910	n/a	1901 to 2003

a) n/a – not available

References 2.3.1-12 through 2.3.1-36

**PSEG Site
ESP Application
Part 2, Site Safety Analysis Report**

**Table 2.3-5
Tornado Site Characteristics^(a)**

DBT Characteristic	Value
Maximum total wind speed	200 mph
Translational wind speed	40 mph
Maximum rotational wind speed	160 mph
Radius of maximum rotational wind speed	150 ft.
Pressure drop	0.9 psi
Rate of pressure drop	0.4 psi/sec

a) Definitions:

- “Maximum total wind speed” is the sum of the tornado translational wind speed and the tornado maximum rotational wind speed.
- “Translational wind speed” is the horizontal velocity of the tornado.
- “Maximum rotational speed” is the maximum rotation speed around the circular vortex of the tornado.
- “Radius of maximum rotational wind speed” is the radial distance from the center of the tornado vortex at which the maximum rotational speed occurs.
- “Pressure drop” is the pressure difference between the center and the outer rim of the tornado vortex.
- “Rate of pressure drop” is the rate at which the atmospheric pressure changes at one point on the ground surface as the tornado vortex passes overhead.
- These tornado site characteristics correspond to those for U.S. geographic Region II as defined in RG 1.76 Revision 1.

**PSEG Site
ESP Application
Part 2, Site Safety Analysis Report**

**Table 2.3-6
Tornado Missile Site Characteristics^(a)**

Missile Type	Dimensions	Mass	$C_D A/m$	V_{Mh}^{max}
Schedule 40 Pipe	6.625 in. dia x 15 ft. long	287 lb.	0.0212 ft ² /lb	112 ft./sec
Automobile	16.4 ft. x 6.6 ft. x 4.3 ft.	4000 lb.	0.0343 ft ² /lb	112 ft./sec
Solid Steel Sphere	1 in. dia	0.147 lb	0.0166ft ² /lb	23 ft./sec

a) Definitions:

- “ $C_D A/m$ ” is a parameter that is the product of an aerodynamic drag coefficient “ C_D ” and a tornado missile cross sectional area “ A ” divided by the missile mass “ m ”. This product is used as one of the terms in the equation for calculation of drag force on a tornado missile.
- “ V_{Mh}^{max} ” is the maximum horizontal speed of a tornado missile.
- These tornado missile site characteristics correspond to those for U.S. geographic Region II as defined in RG 1.76 Revision 1.

**PSEG Site
ESP Application
Part 2, Site Safety Analysis Report**

**Table 2.3-7
Regional Tornadoes and Water Spouts^(a)**

State	County	Area (sq. mi.)	Number of Tornadoes	Number of Waterspouts
DE	New Castle	494	21	1
DE	Kent	800	18	0
MD	Queen Anne's	510	7	0
MD	Kent	414	4	0
MD	Cecil	418	14	0
NJ	Cumberland	677	8	0
NJ	Salem	373	4	0
NJ	Gloucester	337	6	0
		Total	82	1

a) Period of record covered is 1950 through 2009.

**PSEG Site
ESP Application
Part 2, Site Safety Analysis Report**

**Table 2.3-8
Regional Tropical Cyclones by Storm Category^(a)**

Tropical Cyclone Classification	Frequency
Hurricanes Category 2	3
Hurricanes Category 1	6
Tropical Storms	60
Tropical Depressions	9
Extra Tropical Depressions	31

a) Period of record covered is 1851 through 2008.

**PSEG Site
ESP Application
Part 2, Site Safety Analysis Report**

**Table 2.3-9
Regional Tropical Cyclones by Month^(a)**

Month	Tropical Cyclone Frequency
May	2
June	6
July	6
August	31
September	41
October	21
November	2

a) Period of record covered is 1851 through 2008.

**PSEG Site
ESP Application
Part 2, Site Safety Analysis Report**

**Table 2.3-10
NOAA Regional Stations for Precipitation Data**

Station	State	1971-2000 Clim-20 Publication Reviewed	TD 3200 Data File Reviewed	TD 3200 Period of Record
Dover	DE	yes	yes	1893-2009
Glassboro 2NE	NJ	yes	yes	1948-2004
Hammonton 1NE	NJ	not available	yes	1893-2009
Marcus Hook	PA	yes	yes	1919-2009
Millington 1SE	MD	yes	yes	1898-2001
Millville MAP	NJ	yes	yes	1947-2009
Philadelphia IAP	PA	yes	yes	1948-2009
Seabrook Farms	NJ	yes	yes	1949-2009
Wilmington AP	DE	yes	yes	1948-2009
Woodstown Pittsgrove 4E	NJ	yes	yes	1901-2003

**PSEG Site
ESP Application
Part 2, Site Safety Analysis Report**

**Table 2.3-11
Precipitation Extremes at the Salem/Hope Creek Site and at NOAA Regional
Meteorological Monitoring Stations^(a)**

Station Name	State	County	Maximum Recorded 24-Hour Rainfall (inches)	Maximum Recorded Monthly Rainfall (inches)	Maximum Recorded 24-Hour Snowfall (inches)	Maximum Recorded Monthly Snowfall (inches)
S/HC Site	NJ	Salem	10.03	13.51	not measured	not measured
Dover	DE	Kent	8.50	16.08	25.0	36.5
Glassboro 2 NE	NJ	Gloucester	6.67	15.37	14.0	27.0
Hammonton 1 NE	NJ	Atlantic	7.55	14.01	26.0	40.0
Marcus Hook	PA	Delaware	11.68	16.13	30.7	30.7
Millington 1 SE	MD	Kent	10.77	15.58	20.0	25.6
Millville MAP	NJ	Cumberland	9.06	12.90	14.8	26.2
Philadelphia IAP	PA	Philadelphia	6.63	13.07	27.6	33.8
Seabrook Farms	NJ	Cumberland	6.57	12.99	11.0	23.6
Wilmington New Castle R	DE	New Castle	8.29	12.68	22.0	31.6
Woodstown Pittsgrove 4E	NJ	Salem	7.24	12.53	19.0	38.3
Overall Maximum			11.68	16.13	30.7	40.0

a) Periods of record reviewed:

- S/HC site 1977-2008
- Dover 1893-2009
- Glassboro 1948-2004
- Hammonton 1893-2009
- Marcus Hook 1919-2009
- Millington 1898-2001
- Millville 1947-2009
- Philadelphia IAP 1948-2009
- Seabrook Farms 1949-2009
- Wilmington 1948-2009
- Woodstown Pittsgrove 1901-2003

**PSEG Site
ESP Application
Part 2, Site Safety Analysis Report**

**Table 2.3-12
Location and Date of Hail Events^{(a) (b)}**

Location of Hail Event	Date of Hail Event
Near Pedricktown, NJ	May 12, 1987
Near Pennsville, NJ	June 2, 1989
Near Deepwater, NJ	August 10, 2008
Near Talleyville, DE	May 31, 1980
Near Smyrna, DE	April 1, 1993
Near Newark, DE	May 24, 1999

a) Period of record addressed is 1950 through 2009.

b) Only hailstorms with hailstones of size 1.75 inch diameter and larger are included.

**PSEG Site
ESP Application
Part 2, Site Safety Analysis Report**

**Table 2.3-13
Estimated 100 Year Annual Maximum and Minimum Return DBT, Historic Maximum WBT,
and Estimated 100 Year Annual Maximum Return WBT**

Station	Estimated 100 Year Annual Maximum Return DBT (°F)	Historic Maximum Recorded WBT (°F)	Estimated 100 Year Annual Maximum Return WBT (°F)	Estimated 100 Year Annual Minimum Return DBT (°F)
Wilmington	104.7	85.5	85.2	-18.7
Millville	104.7	85.0	86.9	-16.4
Dover	105.9	86.2	87.4	-8.2
Bounding Value	105.9	86.2	87.4	-18.7

**PSEG Site
ESP Application
Part 2, Site Safety Analysis Report**

**Table 2.3-14
Design Wet and Dry Bulb Temperatures**

Statistic	Value (°F)
Maximum DBT with annual exceedance probability of 0.4 percent.	93 (Philadelphia)
Mean coincident WBT (MCWB) at the 0.4 percent DBT.	76 (Philadelphia)
Maximum DBT with annual exceedance probability of 2.0 percent.	88 (Philadelphia)
MCWB at the 2.0 percent DBT.	73 (Philadelphia)
Minimum DBT with annual exceedance probability of 99.6 percent.	10 (Wilmington)
Minimum DBT with annual exceedance probability of 99 percent.	14 (Wilmington)
Maximum WBT with annual exceedance probability of 0.4 percent.	79 (Dover and Philadelphia)
Maximum DBT with annual exceedance probability of 5 percent	83 (Wilmington and Philadelphia)
Minimum DBT with annual exceedance probability of 95 percent	25 (Wilmington and Philadelphia)
Maximum DBT with annual exceedance probability of 1.0 percent.	90 (Philadelphia)
MCWB at the 1.0 percent DBT.	75 (Philadelphia)
Maximum WBT with annual exceedance probability of 1.0 percent	77 (Dover, Philadelphia, and Wilmington)

**PSEG Site
ESP Application
Part 2, Site Safety Analysis Report**

**Table 2.3-15
Dry Bulb Temperature Extremes at the Salem/Hope Creek Site and at NOAA Regional
Meteorological Monitoring Stations^(a)**

Station Name	State	County	Maximum Dry Bulb Temperature (° F)	Minimum Dry Bulb Temperature (° F)
S/HC Site	NJ	Salem	97.4	-5.8
Dover	DE	Kent	104	-11
Glassboro 2 NE	NJ	Gloucester	104	-8
Hammonton 1 NE	NJ	Atlantic	105	-13
Marcus Hook	PA	Delaware	108	-12
Millington 1 SE	MD	Kent	105	-15
Millville MAP	NJ	Cumberland	102	-10
Philadelphia IAP	PA	Philadelphia	104	-7
Seabrook Farms	NJ	Cumberland	101	-13
Wilmington New Castle R	DE	New Castle	102	-14
Woodstown Pittsgrove 4E	NJ	Salem	103	-13
Overall Extreme			108	-15

a) Periods of record reviewed:

- S/HC site 2007-2008
- Dover 1893-2009
- Glassboro 1948-2004
- Hammonton 1893-2009
- Marcus Hook 1919-2009
- Millington 1898-2001
- Millville 1947-2009
- Newark Univ. Farm 1894-2006
- Philadelphia IAP 1948-2009
- Seabrook Farms 1949-2009
- Wilmington 1948-2009
- Woodstown Pittsgrove 1901-2003

**PSEG Site
ESP Application
Part 2, Site Safety Analysis Report**

**Table 2.3-16
Variation of Mean Precipitation and Mean Temperature Climate Parameters between Normal Periods and Variation of
Extreme Precipitation, Extreme Temperature, and Tornado Occurrence Climate Parameters between Historic Periods**

	Normal Period				
	1931-1960	1941-1970	1951-1980	1961-1990	1971-2000
Delaware Precipitation (in)	44.48	40.95	42.22	42.45	45.5
New Jersey Precipitation (in)	44.95	43.1	44.58	44.31	45.98
Delaware Temperature (°F)	54	53.7	53.7	53.7	54.3
New Jersey Temperature(°F)	53.2	53.1	53.1	53.2	53.6

	Historic Period				
	1931-1960	1961-1970	1971-1980	1981-1990	1991-2000
Regional Extreme High Daily Pcp (in)					11.68
Regional Extreme high Daily Snow (in)					30.7
Regional Extreme High Temperature (°F)	108				
Regional Extreme Low Temperature (°F)				-15	
New Castle County DE Strongest Tornado		F3			
Salem County NJ Strongest Tornadoes	F2			F2	

**PSEG Site
ESP Application
Part 2, Site Safety Analysis Report**

**Table 2.3-17
Number of Tropical Cyclones per Decade Period
within 115 Statute Miles of the PSEG Site**

Decade Period	Number of Tropical Cyclones within 100 NM^(a) of PSEG Site
1850s	5
1860s	6
1870s	9
1880s	14
1890s	9
1900s	11
1910s	4
1920s	5
1930s	7
1940s	11
1950s	9
1960s	4
1970s	2
1980s	3
1990s	3
2000-2008	7

a) Reference 2.3.1-42 provides the data in nautical miles (NM)

**PSEG Site
ESP Application
Part 2, Site Safety Analysis Report**

**Table 2.3-18
Mean Monthly and Annual Rainfall (in.) at the Salem/Hope Creek Site and at NOAA
Regional COOP Meteorological Monitoring Stations^(a)**

Station Name	Jan	Feb	Mar	Apr	May	Jun	Jul	Aug	Sep	Oct	Nov	Dec	Annual
S/HC Site	2.81	2.02	3.49	3.10	3.25	3.49	3.50	3.40	3.34	2.52	2.55	2.57	36.04
Dover	3.94	3.04	4.40	3.47	4.29	3.77	4.16	4.73	4.56	3.26	3.16	3.50	46.28
Glassboro 2 NE	3.88	2.83	4.27	3.83	4.17	3.64	4.16	4.42	3.80	3.40	3.44	3.70	45.54
Hammon-ton 1 NE	3.93	2.90	3.91	3.93	3.96	4.01	3.93	4.05	3.90	3.23	3.59	3.77	45.11
Marcus Hook	2.92	2.75	3.63	3.27	4.16	3.20	4.01	3.32	4.23	2.84	3.21	3.12	40.66
Millington 1 SE	3.50	2.95	4.22	3.36	4.32	3.88	4.05	4.05	4.27	3.39	3.22	3.57	44.78
Millville MAP	3.62	3.19	4.38	3.53	3.94	3.27	3.59	4.35	3.47	3.04	3.25	3.57	43.20
Philadel-phia IAP	3.52	2.74	3.81	3.49	3.89	3.29	4.39	3.82	3.88	2.75	3.16	3.31	42.05
Sea-brook Farms	3.96	2.94	4.33	3.58	4.07	3.37	4.30	4.18	3.83	3.36	3.19	3.76	44.87
Wilmington New Castle AP	3.43	2.81	3.97	3.39	4.15	3.59	4.28	3.51	4.01	3.08	3.19	3.40	42.81
Woods-town Pitts-grove 4E	3.80	2.89	4.21	3.75	3.97	3.89	4.41	4.27	4.01	3.40	3.46	3.70	45.76

a) Periods of record reviewed:

- S/HC site 1977-2008
- All other stations 1971-2000

References 2.3.1-15, 2.3.1-24 through 2.3.1-33

**PSEG Site
ESP Application
Part 2, Site Safety Analysis Report**

**Table 2.3-19
Mean Monthly and Annual Snowfall (in.) at the NOAA Regional COOP Meteorological
Monitoring Stations^(a)**

Station Name	Jan	Feb	Mar	Apr	May	Jun	Jul	Aug	Sep	Oct	Nov	Dec	Annual
Dover	4.5	6.9	0.9	0.0	0.0	0.0	0.0	0.0	0.0	0.0	0.1	1.5	13.9
Glassboro 2 NE	3.7	1.9	0.1	0.1	0.0	0.0	0.0	0.0	0.0	trace	0.0	1.7	7.5
Marcus Hook	5.4	4.8	1.4	0.0	0.0	0.0	0.0	0.0	0.0	trace	0.2	1.3	13.1
Millington 1 SE	5.5	6.0	1.1	0.0	0.0	0.0	0.0	0.0	0.0	trace	0.3	1.4	14.3
Millville MAP	4.8	5.0	1.4	0.3	0.0	0.0	0.0	0.0	0.0	trace	0.2	1.4	13.1
Philadelphia IAP	6.4	6.6	3.2	0.6	0.0	0.0	0.0	0.0	0.0	0.1	0.4	2.0	19.3
Seabrook Farms	5.0	6.0	0.8	0.6	0.0	0.0	0.0	0.0	0.0	0.0	0.3	1.1	13.8
Wilmington New Castle AP	7.5	6.3	2.3	0.3	0.0	0.0	0.0	0.0	0.0	0.1	0.6	1.9	19.0
Woodstown Pittsgrove 4E	5.9	4.8	1.6	0.5	trace	0.0	0.0	0.0	0.0	0.1	0.3	2.1	15.3

a) Period of record reviewed:

- 1971-2000

References 2.3.1-24 through 2.3.1-33

**PSEG Site
ESP Application
Part 2, Site Safety Analysis Report**

**Table 2.3-20
Mean Monthly and Annual Dry Bulb Temperatures (°F) at the Salem/Hope Creek Site and
at NOAA Regional COOP Meteorological Monitoring Stations^(a)**

Station Name	Jan	Feb	Mar	Apr	May	Jun	Jul	Aug	Sep	Oct	Nov	Dec	Annual
S/HC Site	30.2	31.9	39.1	48.5	57.4	65.7	70.2	68.9	62.7	52.6	43.8	35.0	50.5
Dover	35.3	37.7	45.4	54.6	64.3	72.9	77.8	76.2	69.9	58.8	49.2	39.9	56.8
Glassboro 2 NE	31.8	34.1	42.4	52.0	62.0	71.1	76.1	74.5	67.5	55.6	46.2	36.7	54.2
Hammon-ton 1 NE	31.7	34.1	42.1	51.9	61.9	70.6	76.0	74.1	66.4	54.9	46.0	36.6	53.9
Marcus Hook	33.7	36.4	44.2	54.4	64.7	73.8	78.7	76.9	69.2	57.7	47.8	38.4	56.3
Milling-ton 1 SE	32.8	35.5	44.0	53.3	62.8	71.3	75.9	74.4	67.8	56.5	46.8	37.5	54.9
Millville MAP	32.7	34.7	42.7	52.0	61.9	70.9	76.3	74.7	67.6	56.0	46.4	37.3	54.4
Philadel-phia IAP	32.3	34.8	43.2	53.1	63.5	72.3	77.6	76.3	68.8	57.2	47.1	37.4	55.3
Sea-brook Farms	32.3	34.1	42.7	52.1	62.2	71.3	76.3	74.8	67.6	56.1	46.5	37.2	54.4
Wilmington New Castle AP	31.5	34.2	42.7	52.4	62.5	71.5	76.6	75.0	67.7	55.8	45.9	36.4	54.4
Woods-town Pitts-grove 4E	32.9	35.3	43.6	53.4	63.4	72.3	76.9	75.1	68.2	56.7	46.8	37.4	55.2

a) Periods of record reviewed:

- S/HC site 1977-2008
- All other stations 1971-2000

References 2.3.1-15; 2.3.1-24 through 2.3.1-33

**PSEG Site
ESP Application
Part 2, Site Safety Analysis Report**

**Table 2.3-21
Wind Direction Persistence/Wind Speed Distributions at the Salem/Hope Creek Primary Meteorological Tower 33 ft. Level
2006-2008 Period Wind Speed Greater than or Equal to 2.24 m/sec**

Hours	N	NNE	NE	ENE	E	ESE	SE	SSE	S	SSW	SW	WSW	W	WNW	NW	NNW
1	323	261	210	118	99	152	253	399	341	295	331	323	350	360	327	324
2	106	104	99	42	22	43	119	143	102	121	124	141	145	125	139	156
4	22	37	25	9	5	16	37	44	31	32	29	38	40	45	51	46
8	5	2	2	0	1	3	23	4	4	4	7	2	5	9	18	4
12	1	3	2	0	0	0	6	0	0	0	2	0	2	4	9	2
18	0	0	0	0	0	0	0	0	0	0	0	0	0	0	3	0
24	0	0	0	0	0	0	0	0	0	0	0	0	0	0	1	0
30	0	0	0	0	0	0	0	0	0	0	0	0	0	0	0	0
36	0	0	0	0	0	0	0	0	0	0	0	0	0	0	0	0
48	0	0	0	0	0	0	0	0	0	0	0	0	0	0	0	0

**PSEG Site
ESP Application
Part 2, Site Safety Analysis Report**

**Table 2.3-22
Wind Direction Persistence/Wind Speed Distributions at the Salem/Hope Creek Primary Meteorological Tower 33 ft. Level
2006-2008 Period Wind Speed Greater than or Equal to 4.47 m/sec**

Hours	N	NNE	NE	ENE	E	ESE	SE	SSE	S	SSW	SW	WSW	W	WNW	NW	NNW
1	66	42	37	16	8	19	120	188	124	90	87	76	144	146	142	111
2	29	26	20	7	3	12	65	57	38	50	28	27	50	54	63	59
4	4	5	9	1	1	4	33	26	14	14	13	3	19	31	26	14
8	0	0	0	0	0	2	13	0	2	1	0	1	4	4	16	1
12	0	1	2	0	0	0	1	0	1	0	1	0	2	4	5	1
18	0	0	0	1	0	0	0	0	0	0	0	0	0	0	1	0
24	0	0	0	0	0	0	0	0	0	0	0	0	0	0	0	0
30	0	0	0	0	0	0	0	0	0	0	0	0	0	0	1	0
36	0	0	0	0	0	0	0	0	0	0	0	0	0	0	0	0
48	0	0	0	0	0	0	0	0	0	0	0	0	0	0	0	0

**PSEG Site
ESP Application
Part 2, Site Safety Analysis Report**

**Table 2.3-23
Wind Direction Persistence/Wind Speed Distributions at the Salem/Hope Creek Primary Meteorological Tower 33 ft. Level
2006-2008 Period Wind Speed Greater than or Equal to 6.71 m/sec**

Hours	N	NNE	NE	ENE	E	ESE	SE	SSE	S	SSW	SW	WSW	W	WNW	NW	NNW
1	5	6	8	2	1	7	36	53	32	23	17	19	38	44	71	36
2	4	8	1	1	0	1	19	12	7	11	4	4	14	18	16	12
4	0	2	0	0	0	1	11	7	1	5	3	2	5	13	4	3
8	0	0	0	0	0	0	4	0	1	1	0	0	2	1	4	0
12	0	1	1	0	0	0	0	0	0	0	0	0	1	4	2	0
18	0	0	0	0	0	0	0	0	0	0	0	0	0	0	2	0
24	0	0	0	0	0	0	0	0	0	0	0	0	0	0	0	0
30	0	0	0	0	0	0	0	0	0	0	0	0	0	0	0	0
36	0	0	0	0	0	0	0	0	0	0	0	0	0	0	0	0
48	0	0	0	0	0	0	0	0	0	0	0	0	0	0	0	0

**PSEG Site
ESP Application
Part 2, Site Safety Analysis Report**

**Table 2.3-24
Wind Direction Persistence/Wind Speed Distributions at the Salem/Hope Creek Primary Meteorological Tower 33 ft. Level
2006-2008 Period Wind Speed Greater than or Equal to 8.94 m/sec**

Hours	N	NNE	NE	ENE	E	ESE	SE	SSE	S	SSW	SW	WSW	W	WNW	NW	NNW
1	0	1	0	0	0	1	8	9	5	8	2	3	15	16	15	2
2	0	2	0	0	0	0	7	2	1	0	1	1	2	7	3	4
4	0	0	0	1	0	0	0	0	1	1	1	0	1	2	4	0
8	0	0	0	0	0	0	1	0	0	0	0	0	0	0	0	0
12	0	0	0	0	0	0	0	0	0	0	0	0	0	1	1	0
18	0	0	0	0	0	0	0	0	0	0	0	0	0	0	0	0
24	0	0	0	0	0	0	0	0	0	0	0	0	0	0	0	0
30	0	0	0	0	0	0	0	0	0	0	0	0	0	0	0	0
36	0	0	0	0	0	0	0	0	0	0	0	0	0	0	0	0
48	0	0	0	0	0	0	0	0	0	0	0	0	0	0	0	0

**PSEG Site
ESP Application
Part 2, Site Safety Analysis Report**

**Table 2.3-25
Wind Direction Persistence/Wind Speed Distributions at the Salem/Hope Creek Primary Meteorological Tower 33 ft. Level
2006-2008 Period Wind Speed Greater than or Equal to 11.18 m/sec**

Hours	N	NNE	NE	ENE	E	ESE	SE	SSE	S	SSW	SW	WSW	W	WNW	NW	NNW
1	0	0	0	0	0	0	1	0	0	1	0	1	3	5	1	0
2	0	0	0	0	0	0	1	0	1	1	0	0	0	2	2	0
4	0	0	0	0	0	0	0	0	0	0	0	0	0	0	0	0
8	0	0	0	0	0	0	0	0	0	0	0	0	0	1	0	0
12	0	0	0	0	0	0	0	0	0	0	0	0	0	0	0	0
18	0	0	0	0	0	0	0	0	0	0	0	0	0	0	0	0
24	0	0	0	0	0	0	0	0	0	0	0	0	0	0	0	0
30	0	0	0	0	0	0	0	0	0	0	0	0	0	0	0	0
36	0	0	0	0	0	0	0	0	0	0	0	0	0	0	0	0
48	0	0	0	0	0	0	0	0	0	0	0	0	0	0	0	0

**PSEG Site
ESP Application
Part 2, Site Safety Analysis Report**

**Table 2.3-26
Mean Annual Pasquill Stability Class Distributions at the Salem/Hope Creek Primary
Meteorological Tower 33 ft. Level Wind and 150-33 ft. Delta-T 2006-2008 and 1977-2008
Periods Frequency (Percent)**

Period	A	B	C	D	E	F	G
2006-2008	11.8	5.6	3.6	26.0	34.2	11.8	7.2
1977-2008	12.8	3.7	3.6	27.2	33.2	12.9	6.7

**PSEG Site
ESP Application
Part 2, Site Safety Analysis Report**

**Table 2.3-27 (Sheet 1 of 7)
Joint Frequency Distribution of Wind Speed and Wind Direction versus Atmospheric
Stability Class Based at the Salem/Hope Creek Primary Meteorological Tower 33 ft. Level
Wind 150-33 ft. Delta-T and 2006-2008 Period (Pasquill Stability Class A)**

Speed (M/S)	N	NNE	NE	ENE	E	ESE	SE	SSE	S	SSW	SW	WSW	W	WNW	NW	NNW	Total
Calm																	0
0.00<WS< 0.50	0	0	0	0	0	0	0	0	0	0	0	0	0	0	0	0	0
0.51<WS< 1.05	1	0	0	0	1	0	1	0	0	0	0	0	1	0	0	0	4
1.05<WS< 1.55	2	1	0	0	0	1	0	0	0	0	1	0	2	1	1	0	9
1.55<WS< 2.05	8	1	3	1	2	0	5	9	3	7	4	4	2	4	1	3	57
2.05<WS< 3.05	33	16	17	17	8	8	14	65	41	29	41	27	20	14	19	45	414
3.05<WS< 4.05	53	27	26	22	12	6	56	70	27	29	35	73	41	33	34	89	633
4.05<WS< 5.05	54	27	36	10	11	14	66	57	22	17	39	53	65	50	76	82	679
5.05<WS< 6.05	18	17	17	5	5	7	79	44	11	7	14	20	45	51	67	53	460
6.05<WS< 8.05	4	6	5	6	2	7	110	70	11	4	8	17	46	70	153	53	572
8.05<WS< 10.00	0	1	0	0	0	0	47	20	5	1	0	1	17	35	48	5	180
WS>10.00	0	0	0	0	0	0	1	0	0	0	0	0	1	3	10	1	16
Totals	173	96	104	61	41	43	379	335	120	94	142	195	240	261	409	331	3024
Speed (M/S)																	
Calm																	0
0.00<WS< 0.50	0	0	0	0	0	0	0	0	0	0	0	0	0	0	0	0	0
0.50<WS< 1.05	0	0	0	0	0	0	0	0	0	0	0	0	0	0	0	0	0.02
1.05<WS< 1.55	0.01	0	0	0	0	0	0	0	0	0	0	0	0.01	0	0	0	0.03
1.55<WS< 2.05	0.03	0	0.01	0	0.01	0	0.02	0.03	0.01	0.03	0.02	0.02	0.01	0.02	0	0.01	0.22
2.05<WS< 3.05	0.13	0.06	0.07	0.07	0.03	0.03	0.05	0.25	0.16	0.11	0.16	0.1	0.08	0.05	0.07	0.17	1.61
3.05<WS< 4.05	0.21	0.1	0.1	0.09	0.05	0.02	0.22	0.27	0.1	0.11	0.14	0.28	0.16	0.13	0.13	0.35	2.46
4.05<WS< 5.05	0.21	0.1	0.14	0.04	0.04	0.05	0.26	0.22	0.09	0.07	0.15	0.21	0.25	0.19	0.3	0.32	2.64
5.05<WS< 6.05	0.07	0.07	0.07	0.02	0.02	0.03	0.31	0.17	0.04	0.03	0.05	0.08	0.17	0.2	0.26	0.21	1.79
6.05<WS< 8.05	0.02	0.02	0.02	0.02	0.01	0.03	0.43	0.27	0.04	0.02	0.03	0.07	0.18	0.27	0.59	0.21	2.22
8.05<WS< 10.00	0	0	0	0	0	0	0.18	0.08	0.02	0	0	0	0.07	0.14	0.19	0.02	0.7
WS>10.00	0	0	0	0	0	0	0	0	0	0	0	0	0	0.01	0.04	0	0.06
Totals	0.67	0.37	0.4	0.24	0.16	0.17	1.47	1.3	0.47	0.37	0.55	0.76	0.93	1.01	1.59	1.29	11.76

**PSEG Site
ESP Application
Part 2, Site Safety Analysis Report**

**Table 2.3-27 (Sheet 2 of 7)
Joint Frequency Distribution of Wind Speed and Wind Direction versus Atmospheric
Stability Class Based at the Salem/Hope Creek Primary Meteorological Tower
33 ft. Level Wind 150-33 ft. Delta-T and 2006-2008 Period (Pasquill Stability Class B)**

Speed (M/S)	N	NNE	NE	ENE	E	ESE	SE	SSE	S	SSW	SW	WSW	W	WNW	NW	NNW	Total
Calm																	0
0.00<WS< 0.50	0	0	0	0	0	0	0	0	0	0	0	0	0	0	0	0	0
0.51<WS< 1.05	0	1	0	0	0	1	0	0	0	1	0	1	0	0	0	0	4
1.05<WS< 1.55	3	1	1	1	0	0	2	1	5	0	1	1	1	0	3	1	21
1.55<WS< 2.05	12	6	5	2	3	1	2	22	16	11	10	4	4	4	7	8	117
2.05<WS< 3.05	32	14	25	13	13	6	16	40	37	40	51	29	24	19	26	34	419
3.05<WS< 4.05	23	23	36	11	7	5	22	19	8	3	9	30	24	18	32	41	311
4.05<WS< 5.05	12	9	22	9	1	3	17	7	1	3	10	14	22	15	40	25	210
5.05<WS< 6.05	5	3	8	1	0	2	26	7	1	0	3	4	12	20	19	21	132
6.05<WS< 8.05	1	3	6	1	2	2	25	23	4	4	2	5	16	23	50	8	174
8.05<WS< 10.00	0	0	0	0	0	0	7	3	1	0	0	1	3	10	7	1	33
WS>10.00	0	0	0	0	0	0	4	0	0	0	0	0	1	3	2	1	11
Totals	88	60	103	38	26	20	121	121	73	62	86	89	107	112	186	140	1432
Speed (M/S)																	
Calm																	0
0.00<WS< 0.50	0	0	0	0	0	0	0	0	0	0	0	0	0	0	0	0	0
0.50<WS< 1.05	0	0	0	0	0	0	0	0	0	0	0	0	0	0	0	0	0.02
1.05<WS< 1.55	0.01	0	0	0	0	0	0.01	0	0.02	0	0	0	0	0	0.01	0	0.08
1.55<WS< 2.05	0.05	0.02	0.02	0.01	0.01	0	0.01	0.09	0.06	0.04	0.04	0.02	0.02	0.02	0.03	0.03	0.45
2.05<WS< 3.05	0.12	0.05	0.1	0.05	0.05	0.02	0.06	0.16	0.14	0.16	0.2	0.11	0.09	0.07	0.1	0.13	1.63
3.05<WS< 4.05	0.09	0.09	0.14	0.04	0.03	0.02	0.09	0.07	0.03	0.01	0.03	0.12	0.09	0.07	0.12	0.16	1.21
4.05<WS< 5.05	0.05	0.03	0.09	0.03	0	0.01	0.07	0.03	0	0.01	0.04	0.05	0.09	0.06	0.16	0.1	0.82
5.05<WS< 6.05	0.02	0.01	0.03	0	0	0.01	0.1	0.03	0	0	0.01	0.02	0.05	0.08	0.07	0.08	0.51
6.05<WS< 8.05	0	0.01	0.02	0	0.01	0.01	0.1	0.09	0.02	0.02	0.01	0.02	0.06	0.09	0.19	0.03	0.68
8.05<WS< 10.00	0	0	0	0	0	0	0.03	0.01	0	0	0	0	0.01	0.04	0.03	0	0.13
WS>10.00	0	0	0	0	0	0	0.02	0	0	0	0	0	0	0.01	0.01	0	0.04
Totals	0.34	0.23	0.4	0.15	0.1	0.08	0.47	0.47	0.28	0.24	0.33	0.35	0.42	0.44	0.72	0.54	5.57

**PSEG Site
ESP Application
Part 2, Site Safety Analysis Report**

**Table 2.3-27 (Sheet 3 of 7)
Joint Frequency Distribution of Wind Speed and Wind Direction versus Atmospheric
Stability Class Based at the Salem/Hope Creek Primary Meteorological Tower
33 ft. Level Wind 150-33 ft. Delta-T and 2006-2008 Period (Pasquill Stability Class C)**

Speed (M/S)	N	NNE	NE	ENE	E	ESE	SE	SSE	S	SSW	SW	WSW	W	WNW	NW	NNW	Total
Calm																	0
0.00<WS< 0.50	0	0	0	0	0	0	0	0	0	0	0	0	0	0	0	0	0
0.51<WS< 1.05	0	1	0	1	0	0	0	0	0	1	0	0	0	0	0	0	3
1.05<WS< 1.55	1	2	5	0	1	0	2	2	5	2	2	0	1	1	2	1	27
1.55<WS< 2.05	10	2	1	4	5	3	5	8	10	9	9	8	6	8	6	7	101
2.05<WS< 3.05	20	18	14	18	11	6	10	23	14	14	17	24	15	14	18	31	267
3.05<WS< 4.05	21	19	16	3	4	3	12	6	6	5	8	16	18	16	9	20	182
4.05<WS< 5.05	9	13	14	2	1	2	7	10	5	5	5	9	13	13	23	18	149
5.05<WS< 6.05	1	3	6	1	0	0	13	4	6	1	2	1	7	5	18	5	73
6.05<WS< 8.05	0	1	1	0	0	3	19	9	5	2	0	1	7	17	14	3	82
8.05<WS< 10.00	0	0	0	2	0	0	4	0	1	0	0	3	5	8	6	0	29
WS>10.00	0	0	0	0	0	0	0	0	0	0	0	0	0	2	2	0	4
Totals	62	59	57	31	22	17	72	62	52	39	43	62	72	84	98	85	917
Speed (M/S)																	
Calm																	0
0.00<WS< 0.50	0	0	0	0	0	0	0	0	0	0	0	0	0	0	0	0	0
0.50<WS< 1.05	0	0	0	0	0	0	0	0	0	0	0	0	0	0	0	0	0.01
1.05<WS< 1.55	0	0.01	0.02	0	0	0	0.01	0.01	0.02	0.01	0.01	0	0	0	0.01	0	0.1
1.55<WS< 2.05	0.04	0.01	0	0.02	0.02	0.01	0.02	0.03	0.04	0.03	0.03	0.03	0.02	0.03	0.02	0.03	0.39
2.05<WS< 3.05	0.08	0.07	0.05	0.07	0.04	0.02	0.04	0.09	0.05	0.05	0.07	0.09	0.06	0.05	0.07	0.12	1.04
3.05<WS< 4.05	0.08	0.07	0.06	0.01	0.02	0.01	0.05	0.02	0.02	0.02	0.03	0.06	0.07	0.06	0.03	0.08	0.71
4.05<WS< 5.05	0.03	0.05	0.05	0.01	0	0.01	0.03	0.04	0.02	0.02	0.02	0.03	0.05	0.05	0.09	0.07	0.58
5.05<WS< 6.05	0	0.01	0.02	0	0	0	0.05	0.02	0.02	0	0.01	0	0.03	0.02	0.07	0.02	0.28
6.05<WS< 8.05	0	0	0	0	0	0.01	0.07	0.03	0.02	0.01	0	0	0.03	0.07	0.05	0.01	0.32
8.05<WS< 10.00	0	0	0	0.01	0	0	0.02	0	0	0	0	0.01	0.02	0.03	0.02	0	0.11
WS>10.00	0	0	0	0	0	0	0	0	0	0	0	0	0	0.01	0.01	0	0.02
Totals	0.24	0.23	0.22	0.12	0.09	0.07	0.28	0.24	0.2	0.15	0.17	0.24	0.28	0.33	0.38	0.33	3.57

**PSEG Site
ESP Application
Part 2, Site Safety Analysis Report**

**Table 2.3-27 (Sheet 4 of 7)
Joint Frequency Distribution of Wind Speed and Wind Direction versus Atmospheric
Stability Class Based at the Salem/Hope Creek Primary Meteorological Tower
33 ft. Level Wind 150-33 ft. Delta-T and 2006-2008 Period (Pasquill Stability Class D)**

Speed (M/S)	N	NNE	NE	ENE	E	ESE	SE	SSE	S	SSW	SW	WSW	W	WNW	NW	NNW	Total
Calm																	0
0.00<WS< 0.50	0	0	0	0	1	0	0	0	0	0	0	0	0	0	0	0	1
0.51<WS< 1.05	7	10	7	12	6	3	3	4	8	5	2	5	4	5	6	8	95
1.05<WS< 1.55	19	20	22	31	30	17	9	13	34	29	28	14	14	7	15	24	326
1.55<WS< 2.05	29	49	35	47	39	12	21	26	45	30	33	26	30	21	29	34	506
2.05<WS< 3.05	74	91	109	101	69	35	65	83	101	81	81	74	54	71	75	79	1243
3.05<WS< 4.05	85	95	105	63	36	29	66	86	102	83	83	120	82	80	77	80	1272
4.05<WS< 5.05	51	69	83	33	15	20	103	97	125	61	75	65	69	74	118	77	1135
5.05<WS< 6.05	21	46	41	16	4	15	85	114	120	36	24	18	68	93	106	55	862
6.05<WS< 8.05	15	60	33	8	1	8	120	113	61	22	19	22	96	124	166	71	939
8.05<WS< 10.00	0	4	5	1	0	3	36	15	2	2	4	2	24	55	63	14	230
WS>10.00	0	1	5	4	0	0	4	0	0	0	0	0	11	21	22	0	68
Totals	301	445	445	316	201	142	512	551	598	349	349	346	452	551	677	442	6677
Speed (M/S)																	
Calm																	0
0.00<WS< 0.50	0	0	0	0	0	0	0	0	0	0	0	0	0	0	0	0	0
0.50<WS< 1.05	0.03	0.04	0.03	0.05	0.02	0.01	0.01	0.02	0.03	0.02	0.01	0.02	0.02	0.02	0.02	0.03	0.37
1.05<WS< 1.55	0.07	0.08	0.09	0.12	0.12	0.07	0.03	0.05	0.13	0.11	0.11	0.05	0.05	0.03	0.06	0.09	1.27
1.55<WS< 2.05	0.11	0.19	0.14	0.18	0.15	0.05	0.08	0.1	0.17	0.12	0.13	0.1	0.12	0.08	0.11	0.13	1.97
2.05<WS< 3.05	0.29	0.35	0.42	0.39	0.27	0.14	0.25	0.32	0.39	0.31	0.31	0.29	0.21	0.28	0.29	0.31	4.83
3.05<WS< 4.05	0.33	0.37	0.41	0.24	0.14	0.11	0.26	0.33	0.4	0.32	0.32	0.47	0.32	0.31	0.3	0.31	4.95
4.05<WS< 5.05	0.2	0.27	0.32	0.13	0.06	0.08	0.4	0.38	0.49	0.24	0.29	0.25	0.27	0.29	0.46	0.3	4.41
5.05<WS< 6.05	0.08	0.18	0.16	0.06	0.02	0.06	0.33	0.44	0.47	0.14	0.09	0.07	0.26	0.36	0.41	0.21	3.35
6.05<WS< 8.05	0.06	0.23	0.13	0.03	0	0.03	0.47	0.44	0.24	0.09	0.07	0.09	0.37	0.48	0.65	0.28	3.65
8.05<WS< 10.00	0	0.02	0.02	0	0	0.01	0.14	0.06	0.01	0.01	0.02	0.01	0.09	0.21	0.24	0.05	0.89
WS>10.00	0	0	0.02	0.02	0	0	0.02	0	0	0	0	0	0.04	0.08	0.09	0	0.26
Totals	1.17	1.73	1.73	1.23	0.78	0.55	1.99	2.14	2.32	1.36	1.36	1.35	1.76	2.14	2.63	1.72	25.96

**PSEG Site
ESP Application
Part 2, Site Safety Analysis Report**

**Table 2.3-27 (Sheet 5 of 7)
Joint Frequency Distribution of Wind Speed and Wind Direction versus Atmospheric
Stability Class Based at the Salem/Hope Creek Primary Meteorological Tower
33 ft. Level Wind 150-33 ft. Delta-T and 2006-2008 Period (Pasquill Stability Class E)**

Speed (M/S)	N	NNE	NE	ENE	E	ESE	SE	SSE	S	SSW	SW	WSW	W	WNW	NW	NNW	Total
Calm																	0
0.00<WS< 0.50	0	0	0	0	1	2	2	1	0	1	0	1	2	1	2	0	13
0.51<WS< 1.05	11	16	17	27	35	13	6	14	16	15	9	14	21	21	25	24	284
1.05<WS< 1.55	33	29	47	48	53	25	21	16	20	26	43	40	43	44	38	33	559
1.55<WS< 2.05	49	42	38	72	53	41	26	28	29	61	51	64	82	78	51	47	812
2.05<WS< 3.05	107	154	123	56	80	116	119	118	103	163	235	255	153	163	161	115	2221
3.05<WS< 4.05	95	88	90	25	18	63	155	96	88	155	176	272	175	201	244	132	2073
4.05<WS< 5.05	46	43	53	8	2	28	153	74	78	107	110	72	138	144	242	130	1428
5.05<WS< 6.05	28	21	15	3	0	4	84	40	36	42	62	17	94	87	148	61	742
6.05<WS< 8.05	24	27	13	4	0	1	63	22	15	19	19	16	36	82	123	69	533
8.05<WS< 10.00	0	8	1	1	0	0	17	5	0	6	4	6	10	9	27	8	102
WS>10.00	0	0	1	4	0	0	7	0	0	0	0	1	3	9	3	1	29
Totals	393	428	398	248	242	293	653	414	385	595	709	758	757	839	1064	620	8796
Speed (M/S)																	
Calm																	0
0.00<WS< 0.50	0	0	0	0	0	0.01	0.01	0	0	0	0	0	0.01	0	0.01	0	0.05
0.50<WS< 1.05	0.04	0.06	0.07	0.1	0.14	0.05	0.02	0.05	0.06	0.06	0.03	0.05	0.08	0.08	0.1	0.09	1.1
1.05<WS< 1.55	0.13	0.11	0.18	0.19	0.21	0.1	0.08	0.06	0.08	0.1	0.17	0.16	0.17	0.17	0.15	0.13	2.17
1.55<WS< 2.05	0.19	0.16	0.15	0.28	0.21	0.16	0.1	0.11	0.11	0.24	0.2	0.25	0.32	0.3	0.2	0.18	3.16
2.05<WS< 3.05	0.42	0.6	0.48	0.22	0.31	0.45	0.46	0.46	0.4	0.63	0.91	0.99	0.59	0.63	0.63	0.45	8.63
3.05<WS< 4.05	0.37	0.34	0.35	0.1	0.07	0.24	0.6	0.37	0.34	0.6	0.68	1.06	0.68	0.78	0.95	0.51	8.06
4.05<WS< 5.05	0.18	0.17	0.21	0.03	0.01	0.11	0.59	0.29	0.3	0.42	0.43	0.28	0.54	0.56	0.94	0.51	5.55
5.05<WS< 6.05	0.11	0.08	0.06	0.01	0	0.02	0.33	0.16	0.14	0.16	0.24	0.07	0.37	0.34	0.58	0.24	2.88
6.05<WS< 8.05	0.09	0.1	0.05	0.02	0	0	0.24	0.09	0.06	0.07	0.07	0.06	0.14	0.32	0.48	0.27	2.07
8.05<WS< 10.00	0	0.03	0	0	0	0	0.07	0.02	0	0.02	0.02	0.02	0.04	0.03	0.1	0.03	0.4
WS>10.00	0	0	0	0.02	0	0	0.03	0	0	0	0	0	0.01	0.03	0.01	0	0.11
Totals	1.53	1.66	1.55	0.96	0.94	1.14	2.54	1.61	1.5	2.31	2.76	2.95	2.94	3.26	4.14	2.41	34.2

**PSEG Site
ESP Application
Part 2, Site Safety Analysis Report**

**Table 2.3-27 (Sheet 6 of 7)
Joint Frequency Distribution of Wind Speed and Wind Direction versus Atmospheric
Stability Class Based at the Salem/Hope Creek Primary Meteorological Tower
33 ft. Level Wind 150-33 ft. Delta-T and 2006-2008 Period (Pasquill Stability Class F)**

Speed (M/S)	N	NNE	NE	ENE	E	ESE	SE	SSE	S	SSW	SW	WSW	W	WNW	NW	NNW	Total
Calm																	0
0.00<WS< 0.50	2	1	1	1	0	0	0	0	0	0	1	0	0	1	0	0	7
0.51<WS< 1.05	14	12	15	20	15	3	11	1	7	7	14	7	11	8	13	7	165
1.05<WS< 1.55	16	18	25	28	33	18	15	14	10	9	10	14	16	17	26	19	288
1.55<WS< 2.05	38	42	26	25	21	31	23	21	13	20	26	29	22	24	31	24	416
2.05<WS< 3.05	134	152	73	35	22	66	81	51	22	31	61	68	44	33	141	159	1173
3.05<WS< 4.05	93	67	23	7	6	28	56	25	21	31	25	43	22	14	73	80	614
4.05<WS< 5.05	7	14	3	0	0	2	46	11	7	11	27	9	3	4	6	10	160
5.05<WS< 6.05	1	0	0	0	0	0	19	10	8	13	12	4	0	1	1	1	70
6.05<WS< 8.05	0	0	0	0	0	0	21	2	15	30	11	2	1	0	0	0	82
8.05<WS< 10.00	0	0	0	0	0	0	14	0	6	18	9	1	0	0	0	0	48
WS>10.00	0	0	0	0	0	0	1	0	3	5	0	0	0	0	0	0	9
Totals	305	306	166	116	97	148	287	135	112	175	196	177	119	102	291	300	3032
Speed (M/S)																	
Calm																	0
0.00<WS< 0.50	0.01	0	0	0	0	0	0	0	0	0	0	0	0	0	0	0	0.03
0.50<WS< 1.05	0.05	0.05	0.06	0.08	0.06	0.01	0.04	0	0.03	0.03	0.05	0.03	0.04	0.03	0.05	0.03	0.64
1.05<WS< 1.55	0.06	0.07	0.1	0.11	0.13	0.07	0.06	0.05	0.04	0.03	0.04	0.05	0.06	0.07	0.1	0.07	1.12
1.55<WS< 2.05	0.15	0.16	0.1	0.1	0.08	0.12	0.09	0.08	0.05	0.08	0.1	0.11	0.09	0.09	0.12	0.09	1.62
2.05<WS< 3.05	0.52	0.59	0.28	0.14	0.09	0.26	0.31	0.2	0.09	0.12	0.24	0.26	0.17	0.13	0.55	0.62	4.56
3.05<WS< 4.05	0.36	0.26	0.09	0.03	0.02	0.11	0.22	0.1	0.08	0.12	0.1	0.17	0.09	0.05	0.28	0.31	2.39
4.05<WS< 5.05	0.03	0.05	0.01	0	0	0.01	0.18	0.04	0.03	0.04	0.1	0.03	0.01	0.02	0.02	0.04	0.62
5.05<WS< 6.05	0	0	0	0	0	0	0.07	0.04	0.03	0.05	0.05	0.02	0	0	0	0	0.27
6.05<WS< 8.05	0	0	0	0	0	0	0.08	0.01	0.06	0.12	0.04	0.01	0	0	0	0	0.32
8.05<WS< 10.00	0	0	0	0	0	0	0.05	0	0.02	0.07	0.03	0	0	0	0	0	0.19
WS>10.00	0	0	0	0	0	0	0	0	0.01	0.02	0	0	0	0	0	0	0.03
Totals	0.19	1.19	0.65	0.45	0.38	0.58	1.12	0.52	0.44	0.68	0.76	0.69	0.46	0.4	1.13	1.17	11.79

**PSEG Site
ESP Application
Part 2, Site Safety Analysis Report**

**Table 2.3-27 (Sheet 7 of 7)
Joint Frequency Distribution of Wind Speed and Wind Direction versus Atmospheric
Stability Class Based at the Salem/Hope Creek Primary Meteorological Tower
33 ft. Level Wind 150-33 ft. Delta-T and 2006-2008 Period (Pasquill Stability Class G)**

Speed (M/S)	N	NNE	NE	ENE	E	ESE	SE	SSE	S	SSW	SW	WSW	W	WNW	NW	NNW	Total
Calm																	0
0.00<WS< 0.50	0	1	2	0	0	0	0	0	0	0	0	0	0	0	1	0	4
0.51<WS< 1.05	4	7	3	8	19	4	5	4	5	0	2	2	1	0	3	5	72
1.05<WS< 1.55	8	16	23	33	22	15	18	9	18	9	3	2	1	2	6	6	191
1.55<WS< 2.05	17	29	32	36	20	31	23	25	16	11	12	4	3	3	10	8	280
2.05<WS< 3.05	79	72	74	27	11	46	86	41	18	9	26	14	5	3	19	44	574
3.05<WS< 4.05	69	51	9	6	0	13	81	22	8	8	15	9	2	0	12	35	340
4.05<WS< 5.05	0	1	0	0	0	0	58	20	16	13	15	2	0	0	0	1	126
5.05<WS< 6.05	0	0	0	0	0	0	42	14	21	25	9	1	0	0	0	0	112
6.05<WS< 8.05	0	0	0	0	0	0	39	7	20	43	7	0	0	0	0	0	116
8.05<WS< 10.00	0	0	0	0	0	0	5	3	7	5	3	0	0	0	0	0	23
WS>10.00	0	0	0	0	0	0	3	0	1	1	0	0	0	0	0	0	8
Totals	177	177	143	110	72	109	360	145	130	124	92	34	12	8	51	99	1843
Speed (M/S)																	
Calm																	0
0.00<WS< 0.50	0	0	0.01	0	0	0	0	0	0	0	0	0	0	0	0	0	0.02
0.50<WS< 1.05	0.02	0.03	0.01	0.03	0.07	0.02	0.02	0.02	0.02	0	0.01	0.01	0	0	0.01	0.02	0.28
1.05<WS< 1.55	0.03	0.06	0.09	0.13	0.09	0.06	0.07	0.03	0.07	0.03	0.01	0.01	0	0.01	0.02	0.02	0.74
1.55<WS< 2.05	0.07	0.11	0.12	0.14	0.08	0.12	0.09	0.1	0.06	0.04	0.05	0.02	0.01	0.01	0.04	0.03	1.09
2.05<WS< 3.05	0.31	0.28	0.29	0.1	0.04	0.18	0.33	0.16	0.07	0.03	0.1	0.05	0.02	0.01	0.07	0.17	2.23
3.05<WS< 4.05	0.27	0.2	0.03	0.02	0	0.05	0.31	0.09	0.03	0.03	0.06	0.03	0.01	0	0.05	0.14	1.32
4.05<WS< 5.05	0	0	0	0	0	0	0.23	0.08	0.06	0.05	0.06	0.01	0	0	0	0	0.49
5.05<WS< 6.05	0	0	0	0	0	0	0.16	0.05	0.08	0.1	0.03	0	0	0	0	0	0.44
6.05<WS< 8.05	0	0	0	0	0	0	0.15	0.03	0.08	0.17	0.03	0	0	0	0	0	0.45
8.05<WS< 10.00	0	0	0	0	0	0	0.02	0.01	0.03	0.02	0.01	0	0	0	0	0	0.09
WS>10.00	0	0	0	0	0	0	0.01	0	0	0	0	0	0	0	0	0	0.02
Totals	0.69	0.69	0.56	0.43	0.28	0.42	1.4	0.56	0.51	0.48	0.36	0.13	0.05	0.03	0.2	0.38	7.17

**PSEG Site
ESP Application
Part 2, Site Safety Analysis Report**

**Table 2.3-28 (Sheet 1 of 3)
Meteorological Instrumentation Descriptions and Accuracies for the On-Site Meteorological Monitoring System ^{(a) (b)}**

Measured Parameter	Primary Tower 300 ft. Wind Direction	Primary Tower 300 ft. Wind Speed	Primary Tower 300 ft. Sigma Theta	Primary Tower 300-33 ft. Delta-T	Primary Tower 150 ft. Wind Direction	Primary Tower 150 ft. Wind Speed	Primary Tower 150 ft. Sigma Theta	Primary Tower 150-33 ft. Delta-T
Manufacturer	Met One	Met One	Met One	Met One	Met One	Met One	Met One	Met One
Model	Model 50.5H Sonic Wind Sensor	Model 50.5H Sonic Wind Sensor	Model 50.5H Sonic Wind Sensor	Model 062MP (matched pair)	Model 50.5H Sonic Wind Sensor	Model 50.5H Sonic Wind Sensor	Model 50.5H Sonic Wind Sensor	Model 062MP (matched pair)
Units	degrees azimuth	mph	degrees	°C per 267 ft.	degrees azimuth	mph	degrees	°C per 117 ft.
Precision	to nearest degree	to 0.1 mph	to nearest degree (to 0.1 degree)	to 0.1° C (to 0.01° C)	to nearest degree	to 0.1 mph	to nearest degree	to 0.1° C (to 0.01° C)
Range	0 to 360	0.0 to 111.8 mph		-5.0 to 10.0 °C	0 to 360	0.0 to 111.8 mph		-5.0 to 10.0 °C
System Accuracy	+/- 3 degrees	+/- 0.15 m/sec for < 5 m/sec; +/- 2.0% for > 5 m/sec; 2.24 mph at 112 mph max speed		+/- 0.02 ° C for matched sets; Up to +/- 0.1 °C for 15 °C max delta-T	+/- 3 degrees	+/- 0.15 m/sec for < 5 m/sec; +/- 2.0% for > 5 m/sec; 2.24 mph at 112 mph max speed		+/- 0.02 ° C for matched sets; Up to +/- 0.1 °C for 15 °C max delta-T
Starting Threshold	0.1 m/sec.	0.1 m/sec.			0.1 m/sec.	0.1 m/sec.		

**PSEG Site
ESP Application
Part 2, Site Safety Analysis Report**

**Table 2.3-28 (Sheet 2 of 3)
Meteorological Instrumentation Descriptions and Accuracies for the On-Site Meteorological Monitoring System ^{(a) (b)}**

Measured Parameter	Primary Tower 33 ft. Wind Direction	Primary Tower 33 ft. Wind Speed	Primary Tower 33 ft. Sigma Theta	Primary Tower 33 ft. Temperature	Primary Tower 33 ft. Dew Point	Primary Tower Ground Barometric Pressure	Primary Tower Ground Precipitation	Primary Tower Ground Solar Radiation
Manufacturer	Met One	Met One	Met One	Met One	Edge Tech	Met One	Met One	Met One
Model	Model 50.5 Sonic Wind Sensor	Model 50.5 Sonic Wind Sensor	Model 50.5 Sonic Wind Sensor	Model 060A-2	200M Chilled Mirror Sensor	Model 090D	Model 375 Tipping Rain/Snow Gauge	Model 95
Units	degrees azimuth	mph	degrees	°C	°F or °C	inches Hg	inches	Langleys per min.
Precision	to nearest degree	to 0.1 mph	to nearest degree	to 0.1° C	to 0.1 °C	to 0.01 inch	to 0.01 inch	to 0.01 Langley
Range	0 to 360	0.0 to 111.8 mph		-50.0 to 50.0° C	-75.0 to 60.0° C	26 to 32 inches Hg	0.00 to 1.00 inch/hour	0.00 to 2.00 Langleys
System Accuracy	+/- 3 degrees	+/- 0.15 m/sec for < 5 m/sec; +/- 2.0% for > 5 m/sec; 2.24 mph at 112 mph max speed		+/- 0.1 °C	+/- 0.25 °C		+/- 1 % at 1 to 3 inches/hour	
Starting Threshold	0.1 m/sec.	0.1 m/sec.						

**PSEG Site
ESP Application
Part 2, Site Safety Analysis Report**

**Table 2.3-28 (Sheet 3 of 3)
Meteorological Instrumentation Descriptions and Accuracies for the On-Site Meteorological Monitoring System ^{(a) (b)}**

Measured Parameter	Backup Tower 33 ft. Wind Direction	Backup Tower 33 ft. Wind Speed	Backup Tower 33 ft. Sigma Theta	Time (recorded by data logger and work stations)
Manufacturer	Met One	Met One	Met One	Met One
Model	Model 50.5H Sonic Wind Sensor	Model 50.5H Sonic Wind Sensor	Model 50.5H Sonic Wind Sensor	Model 0455A
Units	degrees azimuth	mph	degrees	
Precision	to nearest degree	to 0.1 mph	to nearest degree	1 sec.
Range	0 to 360	0.0 to 111.8 mph		
System Accuracy	+/- 3 degrees	+/- 0.15 m/sec for < 5 m/sec; +/- 2.0% for > 5 m/sec; 2.24 mph at 112 mph max speed		+/- 2 min.
Starting Threshold	0.1 m/sec.	0.1 m/sec.		

a) Upgrades implemented as of July 1, 2008 to meet RG 1.23, Revision 1 include the following.

Relative humidity sensors (0.1% precision) added at the 300 ft. and 33 ft. levels.

Dry bulb temperature sensor added at the 300 ft. level.

Wind direction, wind speed, sigma theta, and 197-33 ft. delta-temperature (0.01° C precision) sensors added at the 197 ft. level.

All vertical temperature difference resolutions upgraded to 0.01° C.

b) Precisions and accuracies in parentheses are values for upgraded equipment, if different.

**PSEG Site
ESP Application
Part 2, Site Safety Analysis Report**

**Table 2.3-29
Annual Data Recovery Statistics for the On-Site Meteorological Monitoring System**

Tower	Parameter	Year		
		2006	2007	2008
Primary	300 ft. Wind Direction	99.1	97.8	94.11
Primary	300 ft. Wind Speed	99.1	97.8	94.11
Primary	300-33 ft. Delta-T	99.9	98.7	99.23
Primary	150 ft. Wind Direction	97.8	99.9	98.44
Primary	150 ft. Wind Speed	97.8	99.9	98.44
Primary	150-33 ft. Delta-T	99.9	97.8	99.11
Primary	33 ft. Wind Direction	99.5	98.1	98.7
Primary	33 ft. Wind Speed	99.5	98.1	98.7
Primary	33 ft. Temperature	99.9	99.6	99.74
Primary	33 ft. Dew Point Temperature	83.9	99.6	79.19
Primary	Ground Barometric Pressure	100.0	99.98	99.86
Primary	Ground Precipitation	91.7	97.4	99.35
Primary	Ground Solar Radiation	100.0	99.98	99.84
Backup	33 ft. Wind Direction	97.3	98.0	98.5
Backup	33 ft. Wind Speed	97.3	98.0	98.5
Not applicable	JFD (150-33 ft. frequency using delta-T based stability class, and 33 ft. wind direction and speed on primary tower)	99.44	95.98	97.93

**PSEG Site
ESP Application
Part 2, Site Safety Analysis Report**

**Table 2.3-30
Summary of PAVAN χ/Q Results (0.5 %) January 1, 2006-December 31, 2008 Meteorological Data**

Source Location	Receptor Location	0-2 hr (NW, 600 m) sec/m³	0-8 hr (NA) sec/m³	8-24 hr (NA) sec/m³	1-4 days (NA) sec/m³	4-30 days (NA) sec/m³	Annual average sec/m³
New Plant Power Block Envelope	EAB	4.71E-04	N/A	N/A	N/A	N/A	N/A
		0-2 hr (SW,8045 m) sec/m³	0-8 hr (NW,8045 m) sec/m³	0-24 hr (NW,8045 m) sec/m³	1-4 days (NW,8045 m) sec/m³	4-30 days (NW,8045 m) sec/m³	(NW,8045 m)
New Plant Power Block Envelope	LPZ (Outer Boundary)	2.08E-05	8.47E-06	5.50E-06	2.15E-06	5.60E-07	1.08 E-07

**PSEG Site
ESP Application
Part 2, Site Safety Analysis Report**

**Table 2.3-31
PAVAN 0-2 Hour 0.5% Exclusion Area Boundary χ/Q Values ^(a)**

Downwind Sector	Distance (feet)	Distance (meters)	χ/Q (sec/m³)
S	1968.5	600	3.76E-04
SSW	1968.5	600	3.70E-04
SW	1968.5	600	3.42E-04
WSW	1968.5	600	2.88E-04
W	1968.5	600	2.47E-04
WNW	1968.5	600	2.81E-04
NW	1968.5	600	4.71E-04
NNW	1968.5	600	3.36E-04
N	1968.5	600	3.13E-04
NNE	1968.5	600	3.19E-04
NE	1968.5	600	2.90E-04
ENE	1968.5	600	2.33E-04
E	1968.5	600	2.03E-04
ESE	1968.5	600	1.92E-04
SE	1968.5	600	2.73E-04
SSE	1968.5	600	3.14E-04
Max Sector (0.5%)	1968.5	600	4.71E-04
Site Overall (5%)	1968.5	600	3.74E-04
PPE χ/Q (sec/m ³)	N/A	N/A	5.00E-04

a) Distance measured from the boundary of the new plant power block envelope

**PSEG Site
ESP Application
Part 2, Site Safety Analysis Report**

**Table 2.3-32
PAVAN 0-30 Day Low Population Zone χ/Q Values ^{(a) (b) (c)}**

Downwind Sector ^(b)	Distance (mi.)	Distance (meters)	0 to 2 Hours	0 to 8 Hours	8 to 24 Hours	1 to 4 Days	4 to 30 Days
S	5	8045	1.92E-05	7.93E-06	5.10E-06	1.95E-06	4.93E-07
SSW	5	8045	2.00E-05	8.34E-06	5.39E-06	2.09E-06	5.36E-07
SW	5	8045	2.08E-05	8.42E-06	5.37E-06	2.02E-06	4.95E-07
WSW	5	8045	1.88E-05	7.57E-06	4.80E-06	1.79E-06	4.34E-07
W	5	8045	1.36E-05	5.67E-06	3.66E-06	1.41E-06	3.60E-07
WNW	5	8045	1.57E-05	6.26E-06	3.96E-06	1.46E-06	3.51E-07
NW	5	8045	2.01E-05	8.47E-06	5.50E-06	2.15E-06	5.60E-07
NNW	5	8045	1.47E-05	6.05E-06	3.89E-06	1.49E-06	3.75E-07
N	5	8045	1.17E-05	4.97E-06	3.24E-06	1.28E-06	3.37E-07
NNE	5	8045	1.09E-05	4.70E-06	3.09E-06	1.24E-06	3.37E-07
NE	5	8045	1.19E-05	5.20E-06	3.44E-06	1.40E-06	3.83E-07
ENE	5	8045	9.88E-06	4.41E-06	2.94E-06	1.22E-06	3.48E-07
E	5	8045	8.63E-06	3.86E-06	2.59E-06	1.08E-06	3.09E-07
ESE	5	8045	8.05E-06	3.65E-06	2.46E-06	1.05E-06	3.05E-07
SE	5	8045	1.30E-05	5.85E-06	3.92E-06	1.65E-06	4.73E-07
SSE	5	8045	1.48E-05	6.35E-06	4.16E-06	1.66E-06	4.44E-07
Site Limit ^(c)			1.95E-05	8.28E-06	5.39E-06	2.12E-06	5.56E-07

a) Distances measured from the boundary of the new plant power block envelope

b) Sector results are 0.5 percent χ/Q values

c) Site limit results are 5 percent χ/Q values

**PSEG Site
ESP Application
Part 2, Site Safety Analysis Report**

**Table 2.3-33
Shortest Distances between the New Plant Site Center and Receptors of Interest for Routine Releases**

		Distance [mi.]
Residence	NW	2.8
Farm	NW	4.9
Site Boundary	ENE	0.24

**PSEG Site
ESP Application
Part 2, Site Safety Analysis Report**

**Table 2.3-34
XOQDOQ Predicted Maximum χ/Q and D/Q Values at Receptors of Interest for Routine Releases^(a)**

Receptor Type	Sector	Distance	χ/Q			D/Q
			No Decay/ Undepleted	2.26-Day Half- life/ Undepleted	8-Day Half- life/ Depleted	
		[mi.]	[sec/m ³]	[sec/m ³]	[sec/m ³]	[1/m ²]
Residence	NW	2.8	2.40E-07	2.40E-07	1.90E-07	9.60E-10
Farm	NW	4.9	1.10E-07	1.10E-07	8.20E-08	3.50E-10
Site Boundary	ENE	0.24	1.00E-05	1.00E-05	9.50E-06	4.10E-08

a) Distances measured from the new plant site center

**PSEG Site
ESP Application
Part 2, Site Safety Analysis Report**

**Table 2.3-35 (Sheet 1 of 9)
XOQDOQ Predicted Annual Average χ/Q Values
at the Standard Radial Distances and Distance-Segment Boundaries for Routine Releases^(a)**

No Decay/Undepleted											
Distance (mi.)	0.25	0.5	0.75	1	1.5	2	2.5	3	3.5	4	4.5
Sector											
S	1.02E-05	3.22E-06	1.61E-06	1.00E-06	5.28E-07	3.42E-07	2.46E-07	1.88E-07	1.51E-07	1.25E-07	1.06E-07
SSW	1.12E-05	3.56E-06	1.78E-06	1.11E-06	5.86E-07	3.79E-07	2.72E-07	2.09E-07	1.67E-07	1.38E-07	1.17E-07
SW	9.92E-06	3.14E-06	1.57E-06	9.77E-07	5.16E-07	3.33E-07	2.39E-07	1.83E-07	1.47E-07	1.21E-07	1.02E-07
WSW	8.51E-06	2.70E-06	1.35E-06	8.42E-07	4.45E-07	2.88E-07	2.06E-07	1.58E-07	1.27E-07	1.05E-07	8.84E-08
W	7.49E-06	2.38E-06	1.19E-06	7.43E-07	3.92E-07	2.54E-07	1.82E-07	1.39E-07	1.12E-07	9.22E-08	7.80E-08
WNW	6.61E-06	2.12E-06	1.06E-06	6.62E-07	3.51E-07	2.27E-07	1.64E-07	1.26E-07	1.01E-07	8.32E-08	7.05E-08
NW^(b)	1.17E-05	3.73E-06	1.86E-06	1.16E-06	6.16E-07	4.00E-07	2.88E-07	2.21E-07	1.77E-07	1.47E-07	1.24E-07
NNW	8.09E-06	2.51E-06	1.25E-06	7.75E-07	4.08E-07	2.63E-07	1.88E-07	1.44E-07	1.15E-07	9.47E-08	8.00E-08
N	7.82E-06	2.43E-06	1.21E-06	7.52E-07	3.95E-07	2.53E-07	1.81E-07	1.38E-07	1.10E-07	9.06E-08	7.64E-08
NNE	8.06E-06	2.51E-06	1.25E-06	7.77E-07	4.07E-07	2.62E-07	1.87E-07	1.43E-07	1.14E-07	9.36E-08	7.89E-08
NE	9.29E-06	2.89E-06	1.44E-06	8.95E-07	4.69E-07	3.02E-07	2.16E-07	1.65E-07	1.31E-07	1.08E-07	9.12E-08
ENE	9.05E-06	2.79E-06	1.39E-06	8.61E-07	4.51E-07	2.89E-07	2.06E-07	1.57E-07	1.25E-07	1.03E-07	8.66E-08
E	8.30E-06	2.55E-06	1.27E-06	7.83E-07	4.09E-07	2.61E-07	1.86E-07	1.42E-07	1.13E-07	9.25E-08	7.78E-08
ESE	8.48E-06	2.60E-06	1.29E-06	7.99E-07	4.16E-07	2.66E-07	1.89E-07	1.44E-07	1.14E-07	9.39E-08	7.90E-08
SE^(b)	1.23E-05	3.81E-06	1.90E-06	1.18E-06	6.16E-07	3.96E-07	2.83E-07	2.16E-07	1.72E-07	1.41E-07	1.19E-07
SSE	1.04E-05	3.23E-06	1.61E-06	9.96E-07	5.24E-07	3.37E-07	2.41E-07	1.84E-07	1.47E-07	1.21E-07	1.03E-07

**PSEG Site
ESP Application
Part 2, Site Safety Analysis Report**

**Table 2.3-35 (Sheet 2 of 9)
XOQDOQ Predicted Annual Average χ/Q Values
at the Standard Radial Distances and Distance-Segment Boundaries for Routine Releases^(a)**

No Decay/Undepleted											
Distance (mi.)	5	7.5	10	15	20	25	30	35	40	45	50
Sector											
S	9.11E-08	5.20E-08	3.52E-08	2.05E-08	1.40E-08	1.05E-08	8.28E-09	6.79E-09	5.72E-09	4.92E-09	4.30E-09
SSW	1.01E-07	5.75E-08	3.88E-08	2.25E-08	1.54E-08	1.15E-08	9.08E-09	7.44E-09	6.27E-09	5.39E-09	4.71E-09
SW	8.82E-08	5.02E-08	3.39E-08	1.97E-08	1.34E-08	1.00E-08	7.91E-09	6.48E-09	5.46E-09	4.69E-09	4.10E-09
WSW	7.62E-08	4.34E-08	2.93E-08	1.70E-08	1.16E-08	8.64E-09	6.81E-09	5.58E-09	4.69E-09	4.03E-09	3.52E-09
W	6.72E-08	3.83E-08	2.58E-08	1.50E-08	1.02E-08	7.61E-09	5.99E-09	4.91E-09	4.13E-09	3.55E-09	3.10E-09
WNW	6.09E-08	3.48E-08	2.36E-08	1.37E-08	9.39E-09	7.02E-09	5.54E-09	4.54E-09	3.83E-09	3.29E-09	2.88E-09
NW^(b)	1.07E-07	6.15E-08	4.17E-08	2.44E-08	1.67E-08	1.25E-08	9.91E-09	8.14E-09	6.87E-09	5.92E-09	5.18E-09
NNW	6.89E-08	3.91E-08	2.64E-08	1.52E-08	1.04E-08	7.75E-09	6.10E-09	5.00E-09	4.20E-09	3.61E-09	3.15E-09
N	6.57E-08	3.70E-08	2.48E-08	1.42E-08	9.66E-09	7.17E-09	5.63E-09	4.60E-09	3.86E-09	3.31E-09	2.88E-09
NNE	6.79E-08	3.82E-08	2.56E-08	1.47E-08	9.95E-09	7.37E-09	5.78E-09	4.71E-09	3.95E-09	3.38E-09	2.95E-09
NE	7.84E-08	4.42E-08	2.97E-08	1.70E-08	1.15E-08	8.56E-09	6.71E-09	5.47E-09	4.59E-09	3.93E-09	3.42E-09
ENE	7.44E-08	4.18E-08	2.79E-08	1.59E-08	1.07E-08	7.94E-09	6.21E-09	5.05E-09	4.23E-09	3.62E-09	3.14E-09
E	6.68E-08	3.73E-08	2.49E-08	1.41E-08	9.51E-09	7.01E-09	5.47E-09	4.44E-09	3.71E-09	3.17E-09	2.75E-09
ESE	6.77E-08	3.78E-08	2.51E-08	1.43E-08	9.58E-09	7.05E-09	5.50E-09	4.46E-09	3.72E-09	3.18E-09	2.76E-09
SE	1.03E-07	5.78E-08	3.87E-08	2.22E-08	1.50E-08	1.11E-08	8.71E-09	7.10E-09	5.95E-09	5.09E-09	4.43E-09
SSE	8.82E-08	5.00E-08	3.36E-08	1.94E-08	1.32E-08	9.81E-09	7.72E-09	6.30E-09	5.30E-09	4.54E-09	3.96E-09

**PSEG Site
ESP Application
Part 2, Site Safety Analysis Report**

**Table 2.3-35 (Sheet 3 of 9)
XOQDOQ Predicted Annual Average χ/Q Values
at the Standard Radial Distances and Distance-Segment Boundaries for Routine Releases^(a)**

2.26-Day Half-life Decay/Undepleted											
Distance (mi.)	0.25	0.5	0.75	1	1.5	2	2.5	3	3.5	4	4.5
Sector											
S	1.02E-05	3.21E-06	1.60E-06	9.96E-07	5.26E-07	3.40E-07	2.44E-07	1.87E-07	1.49E-07	1.23E-07	1.04E-07
SSW	1.12E-05	3.55E-06	1.77E-06	1.10E-06	5.83E-07	3.76E-07	2.70E-07	2.06E-07	1.65E-07	1.36E-07	1.15E-07
SW	9.91E-06	3.14E-06	1.56E-06	9.73E-07	5.13E-07	3.30E-07	2.37E-07	1.81E-07	1.44E-07	1.19E-07	1.00E-07
WSW	8.50E-06	2.70E-06	1.35E-06	8.38E-07	4.42E-07	2.85E-07	2.04E-07	1.56E-07	1.25E-07	1.03E-07	8.67E-08
W	7.48E-06	2.38E-06	1.19E-06	7.39E-07	3.90E-07	2.51E-07	1.80E-07	1.37E-07	1.10E-07	9.04E-08	7.63E-08
WNW	6.61E-06	2.11E-06	1.06E-06	6.59E-07	3.49E-07	2.26E-07	1.62E-07	1.24E-07	9.94E-08	8.21E-08	6.94E-08
NW^(b)	1.17E-05	3.73E-06	1.86E-06	1.16E-06	6.14E-07	3.98E-07	2.86E-07	2.19E-07	1.76E-07	1.45E-07	1.23E-07
NNW	8.08E-06	2.51E-06	1.25E-06	7.73E-07	4.06E-07	2.61E-07	1.87E-07	1.43E-07	1.14E-07	9.37E-08	7.90E-08
N	7.81E-06	2.43E-06	1.21E-06	7.50E-07	3.93E-07	2.52E-07	1.80E-07	1.37E-07	1.09E-07	8.95E-08	7.53E-08
NNE	8.05E-06	2.51E-06	1.25E-06	7.75E-07	4.06E-07	2.60E-07	1.86E-07	1.41E-07	1.13E-07	9.25E-08	7.79E-08
NE	9.29E-06	2.89E-06	1.44E-06	8.92E-07	4.67E-07	3.00E-07	2.14E-07	1.63E-07	1.30E-07	1.07E-07	9.00E-08
ENE	9.04E-06	2.79E-06	1.39E-06	8.59E-07	4.49E-07	2.87E-07	2.05E-07	1.56E-07	1.24E-07	1.02E-07	8.54E-08
E	8.30E-06	2.54E-06	1.27E-06	7.81E-07	4.07E-07	2.60E-07	1.85E-07	1.40E-07	1.11E-07	9.13E-08	7.67E-08
ESE	8.47E-06	2.59E-06	1.29E-06	7.96E-07	4.14E-07	2.64E-07	1.88E-07	1.43E-07	1.13E-07	9.27E-08	7.78E-08
SE^(b)	1.23E-05	3.81E-06	1.90E-06	1.17E-06	6.13E-07	3.93E-07	2.80E-07	2.13E-07	1.70E-07	1.40E-07	1.18E-07
SSE	1.04E-05	3.22E-06	1.60E-06	9.93E-07	5.21E-07	3.35E-07	2.40E-07	1.83E-07	1.46E-07	1.20E-07	1.01E-07

**PSEG Site
ESP Application
Part 2, Site Safety Analysis Report**

**Table 2.3-35 (Sheet 4 of 9)
XOQDOQ Predicted Annual Average χ/Q Values
at the Standard Radial Distances and Distance-Segment Boundaries for Routine Releases^(a)**

2.26-Day Half-life Decay/Undepleted											
Distance (mi.)	5	7.5	10	15	20	25	30	35	40	45	50
Sector											
S	8.96E-08	5.08E-08	3.41E-08	1.95E-08	1.31E-08	9.67E-09	7.52E-09	6.07E-09	5.04E-09	4.27E-09	3.68E-09
SSW	9.90E-08	5.60E-08	3.75E-08	2.14E-08	1.44E-08	1.06E-08	8.19E-09	6.60E-09	5.47E-09	4.62E-09	3.98E-09
SW	8.64E-08	4.87E-08	3.25E-08	1.85E-08	1.24E-08	9.06E-09	7.01E-09	5.63E-09	4.65E-09	3.92E-09	3.36E-09
WSW	7.46E-08	4.20E-08	2.80E-08	1.59E-08	1.06E-08	7.76E-09	5.99E-09	4.80E-09	3.96E-09	3.33E-09	2.85E-09
W	6.56E-08	3.69E-08	2.46E-08	1.39E-08	9.26E-09	6.74E-09	5.19E-09	4.15E-09	3.41E-09	2.86E-09	2.44E-09
WNW	5.98E-08	3.39E-08	2.27E-08	1.30E-08	8.76E-09	6.43E-09	5.00E-09	4.03E-09	3.34E-09	2.82E-09	2.43E-09
NW^(b)	1.06E-07	6.03E-08	4.07E-08	2.34E-08	1.59E-08	1.17E-08	9.17E-09	7.44E-09	6.20E-09	5.28E-09	4.56E-09
NNW	6.79E-08	3.83E-08	2.56E-08	1.46E-08	9.82E-09	7.22E-09	5.61E-09	4.53E-09	3.76E-09	3.19E-09	2.75E-09
N	6.47E-08	3.62E-08	2.41E-08	1.36E-08	9.09E-09	6.64E-09	5.14E-09	4.13E-09	3.42E-09	2.88E-09	2.48E-09
NNE	6.69E-08	3.74E-08	2.49E-08	1.41E-08	9.40E-09	6.87E-09	5.32E-09	4.28E-09	3.54E-09	2.99E-09	2.57E-09
NE	7.72E-08	4.33E-08	2.88E-08	1.63E-08	1.09E-08	7.94E-09	6.14E-09	4.93E-09	4.08E-09	3.44E-09	2.96E-09
ENE	7.33E-08	4.08E-08	2.71E-08	1.52E-08	1.01E-08	7.39E-09	5.70E-09	4.57E-09	3.77E-09	3.18E-09	2.72E-09
E	6.57E-08	3.64E-08	2.41E-08	1.34E-08	8.91E-09	6.46E-09	4.97E-09	3.97E-09	3.27E-09	2.75E-09	2.35E-09
ESE	6.67E-08	3.69E-08	2.43E-08	1.36E-08	8.98E-09	6.51E-09	5.00E-09	3.99E-09	3.28E-09	2.76E-09	2.36E-09
SE	1.01E-07	5.64E-08	3.74E-08	2.11E-08	1.41E-08	1.03E-08	7.92E-09	6.35E-09	5.24E-09	4.42E-09	3.79E-09
SSE	8.70E-08	4.89E-08	3.27E-08	1.86E-08	1.25E-08	9.13E-09	7.08E-09	5.71E-09	4.73E-09	4.00E-09	3.44E-09

**PSEG Site
ESP Application
Part 2, Site Safety Analysis Report**

**Table 2.3-35 (Sheet 5 of 9)
XOQDOQ Predicted Annual Average χ /Q Values
at the Standard Radial Distances and Distance-Segment Boundaries for Routine Releases^(a)**

8-Day Half-life Decay/Depleted											
Distance (mi.)	0.25	0.5	0.75	1	1.5	2	2.5	3	3.5	4	4.5
Sector											
S	9.62E-06	2.94E-06	1.43E-06	8.74E-07	4.48E-07	2.83E-07	1.99E-07	1.49E-07	1.17E-07	9.54E-08	7.95E-08
SSW	1.06E-05	3.25E-06	1.58E-06	9.69E-07	4.97E-07	3.13E-07	2.20E-07	1.65E-07	1.30E-07	1.06E-07	8.80E-08
SW	9.38E-06	2.87E-06	1.40E-06	8.54E-07	4.37E-07	2.75E-07	1.93E-07	1.45E-07	1.14E-07	9.24E-08	7.70E-08
WSW	8.05E-06	2.47E-06	1.20E-06	7.36E-07	3.77E-07	2.38E-07	1.67E-07	1.25E-07	9.83E-08	7.98E-08	6.65E-08
W	7.09E-06	2.17E-06	1.06E-06	6.49E-07	3.33E-07	2.09E-07	1.47E-07	1.10E-07	8.67E-08	7.04E-08	5.86E-08
WNW	6.26E-06	1.93E-06	9.45E-07	5.79E-07	2.97E-07	1.88E-07	1.32E-07	9.94E-08	7.82E-08	6.36E-08	5.31E-08
NW^(b)	1.11E-05	3.41E-06	1.66E-06	1.02E-06	5.23E-07	3.30E-07	2.33E-07	1.75E-07	1.38E-07	1.12E-07	9.37E-08
NNW	7.65E-06	2.29E-06	1.11E-06	6.78E-07	3.46E-07	2.17E-07	1.52E-07	1.14E-07	8.94E-08	7.25E-08	6.03E-08
N	7.39E-06	2.22E-06	1.08E-06	6.58E-07	3.35E-07	2.09E-07	1.46E-07	1.09E-07	8.56E-08	6.93E-08	5.75E-08
NNE	7.63E-06	2.29E-06	1.12E-06	6.79E-07	3.46E-07	2.16E-07	1.51E-07	1.13E-07	8.85E-08	7.16E-08	5.95E-08
NE	8.79E-06	2.64E-06	1.29E-06	7.82E-07	3.98E-07	2.49E-07	1.74E-07	1.30E-07	1.02E-07	8.27E-08	6.87E-08
ENE	8.56E-06	2.55E-06	1.24E-06	7.53E-07	3.82E-07	2.39E-07	1.67E-07	1.24E-07	9.72E-08	7.86E-08	6.52E-08
E	7.86E-06	2.32E-06	1.13E-06	6.85E-07	3.47E-07	2.16E-07	1.50E-07	1.12E-07	8.76E-08	7.07E-08	5.86E-08
ESE	8.02E-06	2.37E-06	1.15E-06	6.98E-07	3.53E-07	2.20E-07	1.53E-07	1.14E-07	8.90E-08	7.18E-08	5.95E-08
SE^(b)	1.17E-05	3.48E-06	1.69E-06	1.03E-06	5.23E-07	3.27E-07	2.28E-07	1.71E-07	1.34E-07	1.08E-07	8.98E-08
SSE	9.82E-06	2.95E-06	1.43E-06	8.71E-07	4.44E-07	2.79E-07	1.95E-07	1.46E-07	1.15E-07	9.29E-08	7.72E-08

**PSEG Site
ESP Application
Part 2, Site Safety Analysis Report**

**Table 2.3-35 (Sheet 6 of 9)
XOQDOQ Predicted Annual Average χ/Q Values
at the Standard Radial Distances and Distance-Segment Boundaries for Routine Releases^(a)**

8-Day Half-life Decay/Depleted											
Distance (mi.)	5	7.5	10	15	20	25	30	35	40	45	50
Sector											
S	6.76E-08	3.64E-08	2.34E-08	1.26E-08	8.04E-09	5.67E-09	4.25E-09	3.32E-09	2.67E-09	2.20E-09	1.85E-09
SSW	7.47E-08	4.02E-08	2.58E-08	1.38E-08	8.82E-09	6.21E-09	4.65E-09	3.63E-09	2.92E-09	2.40E-09	2.02E-09
SW	6.54E-08	3.51E-08	2.25E-08	1.20E-08	7.66E-09	5.39E-09	4.03E-09	3.14E-09	2.52E-09	2.08E-09	1.74E-09
WSW	5.65E-08	3.03E-08	1.94E-08	1.04E-08	6.60E-09	4.64E-09	3.46E-09	2.70E-09	2.17E-09	1.78E-09	1.49E-09
W	4.98E-08	2.67E-08	1.71E-08	9.10E-09	5.80E-09	4.07E-09	3.03E-09	2.36E-09	1.89E-09	1.56E-09	1.30E-09
WNW	4.51E-08	2.44E-08	1.57E-08	8.40E-09	5.38E-09	3.79E-09	2.84E-09	2.22E-09	1.78E-09	1.47E-09	1.24E-09
NW^(b)	7.97E-08	4.31E-08	2.78E-08	1.50E-08	9.63E-09	6.81E-09	5.11E-09	4.00E-09	3.23E-09	2.67E-09	2.25E-09
NNW	5.12E-08	2.74E-08	1.76E-08	9.36E-09	5.97E-09	4.20E-09	3.14E-09	2.45E-09	1.97E-09	1.63E-09	1.37E-09
N	4.87E-08	2.59E-08	1.65E-08	8.74E-09	5.55E-09	3.88E-09	2.89E-09	2.25E-09	1.81E-09	1.49E-09	1.24E-09
NNE	5.04E-08	2.68E-08	1.71E-08	9.02E-09	5.72E-09	4.00E-09	2.98E-09	2.31E-09	1.86E-09	1.52E-09	1.28E-09
NE	5.82E-08	3.10E-08	1.98E-08	1.05E-08	6.62E-09	4.63E-09	3.45E-09	2.68E-09	2.15E-09	1.77E-09	1.48E-09
ENE	5.52E-08	2.93E-08	1.86E-08	9.77E-09	6.17E-09	4.30E-09	3.20E-09	2.48E-09	1.98E-09	1.63E-09	1.36E-09
E	4.95E-08	2.61E-08	1.65E-08	8.66E-09	5.45E-09	3.79E-09	2.81E-09	2.17E-09	1.73E-09	1.42E-09	1.18E-09
ESE	5.03E-08	2.65E-08	1.67E-08	8.74E-09	5.49E-09	3.81E-09	2.82E-09	2.18E-09	1.74E-09	1.42E-09	1.19E-09
SE	7.61E-08	4.04E-08	2.57E-08	1.36E-08	8.60E-09	6.01E-09	4.47E-09	3.47E-09	2.78E-09	2.28E-09	1.91E-09
SSE	6.55E-08	3.50E-08	2.24E-08	1.19E-08	7.58E-09	5.32E-09	3.97E-09	3.09E-09	2.49E-09	2.05E-09	1.72E-09

**PSEG Site
ESP Application
Part 2, Site Safety Analysis Report**

**Table 2.3-35 (Sheet 7 of 9)
XOQDOQ Predicted Annual Average χ/Q Values
at the Standard Radial Distances and Distance-Segment Boundaries for Routine Releases^(a)**

No Decay/Undepleted										
Sector Segment (mi.)	0.5-1	1-2	2-3	3-4	4-5	5-10	10-20	20-30	30-40	40-50
Sector										
S	1.70E-06	5.50E-07	2.48E-07	1.52E-07	1.06E-07	5.32E-08	2.09E-08	1.05E-08	6.80E-09	4.93E-09
SSW	1.88E-06	6.10E-07	2.75E-07	1.68E-07	1.17E-07	5.88E-08	2.30E-08	1.16E-08	7.46E-09	5.40E-09
SW	1.66E-06	5.37E-07	2.42E-07	1.47E-07	1.03E-07	5.14E-08	2.01E-08	1.01E-08	6.50E-09	4.70E-09
WSW	1.43E-06	4.63E-07	2.09E-07	1.27E-07	8.87E-08	4.44E-08	1.73E-08	8.69E-09	5.59E-09	4.04E-09
W	1.26E-06	4.09E-07	1.84E-07	1.12E-07	7.82E-08	3.92E-08	1.53E-08	7.65E-09	4.92E-09	3.55E-09
WNW	1.12E-06	3.65E-07	1.65E-07	1.01E-07	7.07E-08	3.56E-08	1.40E-08	7.06E-09	4.56E-09	3.30E-09
NW^(b)	1.97E-06	6.41E-07	2.91E-07	1.78E-07	1.25E-07	6.29E-08	2.48E-08	1.26E-08	8.16E-09	5.92E-09
NNW	1.32E-06	4.25E-07	1.90E-07	1.15E-07	8.03E-08	4.01E-08	1.56E-08	7.80E-09	5.01E-09	3.62E-09
N	1.28E-06	4.11E-07	1.83E-07	1.11E-07	7.66E-08	3.80E-08	1.46E-08	7.22E-09	4.61E-09	3.31E-09
NNE	1.32E-06	4.25E-07	1.89E-07	1.14E-07	7.92E-08	3.92E-08	1.50E-08	7.42E-09	4.73E-09	3.39E-09
NE	1.52E-06	4.89E-07	2.18E-07	1.32E-07	9.15E-08	4.54E-08	1.74E-08	8.61E-09	5.49E-09	3.94E-09
ENE	1.47E-06	4.70E-07	2.08E-07	1.26E-07	8.69E-08	4.28E-08	1.63E-08	8.00E-09	5.07E-09	3.62E-09
E	1.34E-06	4.27E-07	1.88E-07	1.13E-07	7.81E-08	3.83E-08	1.45E-08	7.06E-09	4.46E-09	3.18E-09
ESE	1.36E-06	4.35E-07	1.92E-07	1.15E-07	7.92E-08	3.88E-08	1.46E-08	7.10E-09	4.48E-09	3.18E-09
SE^(b)	2.00E-06	6.43E-07	2.86E-07	1.73E-07	1.20E-07	5.92E-08	2.27E-08	1.12E-08	7.12E-09	5.10E-09
SSE	1.70E-06	5.46E-07	2.44E-07	1.48E-07	1.03E-07	5.12E-08	1.98E-08	9.87E-09	6.32E-09	4.55E-09

**PSEG Site
ESP Application
Part 2, Site Safety Analysis Report**

**Table 2.3-35 (Sheet 8 of 9)
XOQDOQ Predicted Annual Average χ/Q Values
at the Standard Radial Distances and Distance-Segment Boundaries for Routine Releases^(a)**

2.26-Day Decay/Undepleted										
Sector Segment (mi.)	0.5-1	1-2	2-3	3-4	4-5	5-10	10-20	20-30	30-40	40-50
Sector										
S	1.69E-06	5.48E-07	2.46E-07	1.50E-07	1.04E-07	5.20E-08	1.99E-08	9.74E-09	6.09E-09	4.28E-09
SSW	1.87E-06	6.07E-07	2.73E-07	1.66E-07	1.15E-07	5.73E-08	2.19E-08	1.06E-08	6.62E-09	4.63E-09
SW	1.65E-06	5.34E-07	2.39E-07	1.45E-07	1.01E-07	4.99E-08	1.89E-08	9.12E-09	5.65E-09	3.93E-09
WSW	1.42E-06	4.60E-07	2.07E-07	1.25E-07	8.70E-08	4.30E-08	1.63E-08	7.82E-09	4.82E-09	3.34E-09
W	1.25E-06	4.06E-07	1.82E-07	1.10E-07	7.65E-08	3.78E-08	1.42E-08	6.79E-09	4.16E-09	2.87E-09
WNW	1.12E-06	3.63E-07	1.64E-07	9.99E-08	6.96E-08	3.47E-08	1.33E-08	6.48E-09	4.04E-09	2.83E-09
NW^(b)	1.96E-06	6.39E-07	2.89E-07	1.76E-07	1.23E-07	6.17E-08	2.39E-08	1.18E-08	7.46E-09	5.29E-09
NNW	1.32E-06	4.23E-07	1.89E-07	1.14E-07	7.92E-08	3.92E-08	1.49E-08	7.27E-09	4.54E-09	3.19E-09
N	1.28E-06	4.10E-07	1.82E-07	1.09E-07	7.56E-08	3.71E-08	1.39E-08	6.69E-09	4.15E-09	2.89E-09
NNE	1.32E-06	4.23E-07	1.88E-07	1.13E-07	7.82E-08	3.84E-08	1.44E-08	6.93E-09	4.29E-09	3.00E-09
NE	1.52E-06	4.87E-07	2.17E-07	1.31E-07	9.02E-08	4.44E-08	1.67E-08	8.00E-09	4.95E-09	3.45E-09
ENE	1.46E-06	4.68E-07	2.07E-07	1.24E-07	8.57E-08	4.19E-08	1.56E-08	7.44E-09	4.59E-09	3.19E-09
E	1.33E-06	4.25E-07	1.87E-07	1.12E-07	7.69E-08	3.74E-08	1.38E-08	6.52E-09	3.99E-09	2.75E-09
ESE	1.36E-06	4.33E-07	1.90E-07	1.14E-07	7.81E-08	3.79E-08	1.39E-08	6.56E-09	4.01E-09	2.77E-09
SE^(b)	2.00E-06	6.40E-07	2.84E-07	1.71E-07	1.18E-07	5.78E-08	2.16E-08	1.03E-08	6.38E-09	4.43E-09
SSE	1.69E-06	5.43E-07	2.42E-07	1.47E-07	1.02E-07	5.01E-08	1.90E-08	9.20E-09	5.73E-09	4.01E-09

**PSEG Site
ESP Application
Part 2, Site Safety Analysis Report**

**Table 2.3-35 (Sheet 9 of 9)
XOQDOQ Predicted Annual Average χ/Q Values
at the Standard Radial Distances and Distance-Segment Boundaries for Routine Releases^(a)**

8-Day Decay/Depleted										
Sector Segment (mi.)	0.5-1	1-2	2-3	3-4	4-5	5-10	10-20	20-30	30-40	40-50
Sector										
S	1.52E-06	4.69E-07	2.01E-07	1.18E-07	7.98E-08	3.76E-08	1.30E-08	5.73E-09	3.34E-09	2.21E-09
SSW	1.68E-06	5.20E-07	2.23E-07	1.31E-07	8.83E-08	4.15E-08	1.43E-08	6.28E-09	3.65E-09	2.41E-09
SW	1.48E-06	4.58E-07	1.96E-07	1.15E-07	7.73E-08	3.62E-08	1.24E-08	5.45E-09	3.16E-09	2.08E-09
WSW	1.28E-06	3.95E-07	1.69E-07	9.89E-08	6.67E-08	3.13E-08	1.07E-08	4.69E-09	2.71E-09	1.79E-09
W	1.13E-06	3.48E-07	1.49E-07	8.72E-08	5.88E-08	2.76E-08	9.41E-09	4.11E-09	2.37E-09	1.56E-09
WNW	1.00E-06	3.11E-07	1.34E-07	7.87E-08	5.33E-08	2.51E-08	8.67E-09	3.83E-09	2.23E-09	1.48E-09
NW^(b)	1.76E-06	5.47E-07	2.36E-07	1.39E-07	9.40E-08	4.45E-08	1.55E-08	6.88E-09	4.03E-09	2.68E-09
NNW	1.18E-06	3.63E-07	1.54E-07	9.00E-08	6.05E-08	2.83E-08	9.68E-09	4.25E-09	2.47E-09	1.63E-09
N	1.15E-06	3.51E-07	1.48E-07	8.62E-08	5.78E-08	2.68E-08	9.05E-09	3.93E-09	2.27E-09	1.49E-09
NNE	1.18E-06	3.62E-07	1.53E-07	8.90E-08	5.97E-08	2.77E-08	9.34E-09	4.05E-09	2.33E-09	1.53E-09
NE	1.36E-06	4.17E-07	1.77E-07	1.03E-07	6.90E-08	3.20E-08	1.08E-08	4.69E-09	2.70E-09	1.77E-09
ENE	1.31E-06	4.01E-07	1.69E-07	9.79E-08	6.55E-08	3.03E-08	1.01E-08	4.36E-09	2.50E-09	1.63E-09
E	1.20E-06	3.64E-07	1.53E-07	8.82E-08	5.88E-08	2.71E-08	8.98E-09	3.84E-09	2.19E-09	1.43E-09
ESE	1.22E-06	3.71E-07	1.55E-07	8.96E-08	5.97E-08	2.74E-08	9.07E-09	3.86E-09	2.20E-09	1.43E-09
SE^(b)	1.79E-06	5.48E-07	2.32E-07	1.35E-07	9.02E-08	4.18E-08	1.41E-08	6.08E-09	3.49E-09	2.29E-09
SSE	1.52E-06	4.65E-07	1.98E-07	1.15E-07	7.75E-08	3.62E-08	1.23E-08	5.38E-09	3.11E-09	2.05E-09

a) Distances measured from the new plant site center.

b) Values in bold font identify bounding values for all sectors.

**PSEG Site
ESP Application
Part 2, Site Safety Analysis Report**

**Table 2.3-36 (Sheet 1 of 3)
XOQDOQ Predicted Annual Average D/Q Values
at the Standard Radial Distances and Distance-Segment Boundaries for Routine Releases ^(a)**

Sector Segment (mi.)	0.5-1	1-2	2-3	3-4	4-5	5-10	10-20	20-30	30-40	40-50
Sector										
S	6.09E-09	1.88E-09	7.48E-10	4.09E-10	2.60E-10	1.12E-10	3.46E-11	1.37E-11	7.33E-12	4.54E-12
SSW	6.38E-09	1.97E-09	7.84E-10	4.29E-10	2.72E-10	1.17E-10	3.63E-11	1.44E-11	7.68E-12	4.75E-12
SW	5.75E-09	1.78E-09	7.07E-10	3.86E-10	2.46E-10	1.06E-10	3.27E-11	1.30E-11	6.92E-12	4.29E-12
WSW	3.74E-09	1.15E-09	4.59E-10	2.51E-10	1.60E-10	6.85E-11	2.13E-11	8.42E-12	4.50E-12	2.78E-12
W	2.85E-09	8.80E-10	3.50E-10	1.91E-10	1.22E-10	5.22E-11	1.62E-11	6.42E-12	3.43E-12	2.12E-12
WNW	3.14E-09	9.69E-10	3.85E-10	2.11E-10	1.34E-10	5.75E-11	1.78E-11	7.07E-12	3.77E-12	2.34E-12
NW	9.68E-09	2.99E-09	1.19E-09	6.50E-10	4.13E-10	1.78E-10	5.51E-11	2.18E-11	1.17E-11	7.21E-12
NNW	7.16E-09	2.21E-09	8.80E-10	4.81E-10	3.06E-10	1.31E-10	4.07E-11	1.61E-11	8.62E-12	5.33E-12
N	5.97E-09	1.84E-09	7.34E-10	4.01E-10	2.55E-10	1.10E-10	3.40E-11	1.35E-11	7.19E-12	4.45E-12
NNE	5.84E-09	1.80E-09	7.18E-10	3.92E-10	2.49E-10	1.07E-10	3.32E-11	1.32E-11	7.03E-12	4.35E-12
NE	6.57E-09	2.03E-09	8.07E-10	4.41E-10	2.80E-10	1.20E-10	3.74E-11	1.48E-11	7.91E-12	4.89E-12
ENE	6.75E-09	2.08E-09	8.29E-10	4.53E-10	2.88E-10	1.24E-10	3.84E-11	1.52E-11	8.12E-12	5.03E-12
E	7.14E-09	2.21E-09	8.78E-10	4.80E-10	3.05E-10	1.31E-10	4.06E-11	1.61E-11	8.60E-12	5.32E-12
ESE	7.95E-09	2.46E-09	9.77E-10	5.34E-10	3.39E-10	1.46E-10	4.52E-11	1.79E-11	9.57E-12	5.92E-12
SE^(b)	1.13E-08	3.48E-09	1.39E-09	7.57E-10	4.81E-10	2.07E-10	6.41E-11	2.54E-11	1.36E-11	8.40E-12
SSE	8.19E-09	2.53E-09	1.01E-09	5.50E-10	3.50E-10	1.50E-10	4.66E-11	1.85E-11	9.86E-12	6.10E-12

**PSEG Site
ESP Application
Part 2, Site Safety Analysis Report**

**Table 2.3-36 (Sheet 2 of 3)
XOQDOQ Predicted Annual Average D/Q Values
at the Standard Radial Distances and Distance-Segment Boundaries for Routine Releases ^(a)**

Distance (mi.)	0.25	0.5	0.75	1	1.5	2	2.5	3	3.5	4	4.5
Sector											
S	3.37E-08	1.14E-08	5.86E-09	3.60E-09	1.79E-09	1.09E-09	7.36E-10	5.33E-10	4.05E-10	3.19E-10	2.59E-10
SSW	3.54E-08	1.20E-08	6.14E-09	3.77E-09	1.88E-09	1.14E-09	7.71E-10	5.59E-10	4.25E-10	3.35E-10	2.71E-10
SW	3.19E-08	1.08E-08	5.53E-09	3.40E-09	1.69E-09	1.03E-09	6.95E-10	5.03E-10	3.83E-10	3.02E-10	2.44E-10
WSW	2.07E-08	7.00E-09	3.60E-09	2.21E-09	1.10E-09	6.68E-10	4.51E-10	3.27E-10	2.49E-10	1.96E-10	1.59E-10
W	1.58E-08	5.34E-09	2.74E-09	1.68E-09	8.39E-10	5.09E-10	3.44E-10	2.49E-10	1.90E-10	1.49E-10	1.21E-10
WNW	1.74E-08	5.88E-09	3.02E-09	1.85E-09	9.24E-10	5.60E-10	3.79E-10	2.75E-10	2.09E-10	1.64E-10	1.33E-10
NW	5.37E-08	1.82E-08	9.32E-09	5.72E-09	2.85E-09	1.73E-09	1.17E-09	8.48E-10	6.45E-10	5.08E-10	4.11E-10
NNW	3.97E-08	1.34E-08	6.89E-09	4.23E-09	2.11E-09	1.28E-09	8.65E-10	6.27E-10	4.77E-10	3.76E-10	3.04E-10
N	3.31E-08	1.12E-08	5.75E-09	3.53E-09	1.76E-09	1.07E-09	7.21E-10	5.23E-10	3.97E-10	3.13E-10	2.54E-10
NNE	3.24E-08	1.10E-08	5.62E-09	3.45E-09	1.72E-09	1.04E-09	7.06E-10	5.11E-10	3.89E-10	3.06E-10	2.48E-10
NE	3.64E-08	1.23E-08	6.32E-09	3.88E-09	1.94E-09	1.17E-09	7.93E-10	5.75E-10	4.37E-10	3.44E-10	2.79E-10
ENE	3.74E-08	1.26E-08	6.49E-09	3.99E-09	1.99E-09	1.21E-09	8.15E-10	5.91E-10	4.49E-10	3.54E-10	2.86E-10
E	3.96E-08	1.34E-08	6.88E-09	4.22E-09	2.11E-09	1.28E-09	8.63E-10	6.25E-10	4.76E-10	3.75E-10	3.03E-10
ESE	4.41E-08	1.49E-08	7.65E-09	4.70E-09	2.34E-09	1.42E-09	9.60E-10	6.96E-10	5.29E-10	4.17E-10	3.37E-10
SE^(b)	6.25E-08	2.11E-08	1.09E-08	6.66E-09	3.32E-09	2.01E-09	1.36E-09	9.87E-10	7.51E-10	5.91E-10	4.79E-10
SSE	4.54E-08	1.54E-08	7.88E-09	4.84E-09	2.41E-09	1.46E-09	9.90E-10	7.17E-10	5.45E-10	4.30E-10	3.48E-10

**PSEG Site
ESP Application
Part 2, Site Safety Analysis Report**

**Table 2.3-36 (Sheet 3 of 3)
XOQDOQ Predicted Annual Average D/Q Values
at the Standard Radial Distances and Distance-Segment Boundaries for Routine Releases ^(a)**

Distance (mi.)	5	7.5	10	15	20	25	30	35	40	45	50
Sector											
S	2.14E-10	1.05E-10	6.57E-11	3.32E-11	2.01E-11	1.35E-11	9.66E-12	7.26E-12	5.64E-12	4.51E-12	3.68E-12
SSW	2.24E-10	1.10E-10	6.89E-11	3.48E-11	2.11E-11	1.41E-11	1.01E-11	7.60E-12	5.91E-12	4.72E-12	3.86E-12
SW	2.02E-10	9.90E-11	6.21E-11	3.14E-11	1.90E-11	1.27E-11	9.13E-12	6.85E-12	5.33E-12	4.26E-12	3.47E-12
WSW	1.31E-10	6.43E-11	4.04E-11	2.04E-11	1.23E-11	8.28E-12	5.93E-12	4.45E-12	3.46E-12	2.77E-12	2.26E-12
W	1.00E-10	4.90E-11	3.07E-11	1.55E-11	9.41E-12	6.31E-12	4.52E-12	3.39E-12	2.64E-12	2.11E-12	1.72E-12
WNW	1.10E-10	5.40E-11	3.39E-11	1.71E-11	1.04E-11	6.94E-12	4.98E-12	3.74E-12	2.91E-12	2.32E-12	1.89E-12
NW	3.40E-10	1.67E-10	1.05E-10	5.29E-11	3.20E-11	2.14E-11	1.54E-11	1.15E-11	8.97E-12	7.17E-12	5.85E-12
NNW	2.52E-10	1.23E-10	7.73E-11	3.91E-11	2.37E-11	1.59E-11	1.14E-11	8.53E-12	6.63E-12	5.30E-12	4.33E-12
N	2.10E-10	1.03E-10	6.45E-11	3.26E-11	1.97E-11	1.32E-11	9.48E-12	7.12E-12	5.53E-12	4.42E-12	3.61E-12
NNE	2.05E-10	1.01E-10	6.31E-11	3.19E-11	1.93E-11	1.29E-11	9.27E-12	6.96E-12	5.41E-12	4.32E-12	3.53E-12
NE	2.31E-10	1.13E-10	7.09E-11	3.58E-11	2.17E-11	1.46E-11	1.04E-11	7.83E-12	6.09E-12	4.86E-12	3.97E-12
ENE	2.37E-10	1.16E-10	7.28E-11	3.68E-11	2.23E-11	1.49E-11	1.07E-11	8.04E-12	6.25E-12	4.99E-12	4.08E-12
E	2.51E-10	1.23E-10	7.71E-11	3.90E-11	2.36E-11	1.58E-11	1.13E-11	8.51E-12	6.62E-12	5.29E-12	4.32E-12
ESE	2.79E-10	1.37E-10	8.58E-11	4.34E-11	2.63E-11	1.76E-11	1.26E-11	9.47E-12	7.37E-12	5.88E-12	4.80E-12
SE^(b)	3.96E-10	1.94E-10	1.22E-10	6.15E-11	3.72E-11	2.50E-11	1.79E-11	1.34E-11	1.05E-11	8.35E-12	6.81E-12
SSE	2.88E-10	1.41E-10	8.85E-11	4.47E-11	2.71E-11	1.81E-11	1.30E-11	9.76E-12	7.59E-12	6.06E-12	4.95E-12

a) Distances measured from the new plant site center.

b) Values in bold font identify bounding values for all sectors.

**PSEG Site
ESP Application
Part 2, Site Safety Analysis Report**

**Table 2.3-37
XOQDOQ Predicted Annual Average X/Q and D/Q Values at the Site Boundary for Routine Releases^(a)**

Sector	Distance [miles]	χ/Q			D/Q [1/m ²]
		No Decay/ Undepleted [s/m ³]	2.26 Day Half-life/ Undepleted [s/m ³]	8 Day Half-life/ Depleted [s/m ³]	
S	0.41	4.5E-06	4.5E-06	4.2E-06	1.6E-08
SSW	0.25	1.1E-05	1.1E-05	1.1E-05	3.6E-08
SW	0.18	1.6E-05	1.6E-05	1.5E-05	5.0E-08
WSW	0.17	1.6E-05	1.6E-05	1.6E-05	3.8E-08
W	0.17	1.4E-05	1.4E-05	1.4E-05	2.9E-08
WNW	0.17	1.2E-05	1.2E-05	1.1E-05	3.0E-08
NW	0.22	1.5E-05	1.5E-05	1.4E-05	6.7E-08
NNW	0.36	4.5E-06	4.5E-06	4.2E-06	2.3E-08
N	0.46	2.8E-06	2.8E-06	2.6E-06	1.3E-08
NNE	0.34	4.9E-06	4.9E-06	4.6E-06	2.1E-08
NE	0.24	9.8E-06	9.8E-06	9.3E-06	3.8E-08
ENE	0.24	1.0E-05	1.0E-05	9.5E-06	4.1E-08
E	0.78	1.2E-06	1.2E-06	1.1E-06	6.4E-09
ESE	1.07	7.2E-07	7.1E-07	6.2E-07	4.2E-09
SE	1.03	1.1E-06	1.1E-06	9.8E-07	6.4E-09
SSE	0.83	1.3E-06	1.3E-06	1.2E-06	6.6E-09

Notes:
a) The χ/Q and D/Q values that are considered in the associated analyses for radiological exposure due to the routine gaseous effluents are those in sectors NNW to ESE (clockwise direction). Sectors SE to NW (clockwise direction) are adjacent to the Delaware River and are not used.

**PSEG Site
ESP Application
Part 2, Site Safety Analysis Report**

**Table 2.3-38
Hurricane Missile Site Characteristics for PSEG Site^(a)**

Missile Type	Dimensions	Mass	$C_D A/m$	$V_{Mh\ hn}^{max}$
Schedule 40 Pipe	6.625 in. dia x 15 ft. long	287 lb.	0.0212 ft ² /lb	99 ft/sec
Automobile	16.4 ft. x 6.6 ft. x 4.3 ft.	4000 lb.	0.0343 ft ² /lb	130 ft/sec
Solid Steel Sphere	1 in. dia.	0.147 lb.	0.0166 ft ² /lb	86 ft/sec

(a) Definitions

- $C_D A/m$ is a parameter that is the product of an aerodynamic drag coefficient " C_D " and a hurricane missile cross section area " A " divided by the missile mass " m ". This product is used in one of the terms in the equation for calculation of drag force on a hurricane missile.
- $V_{Mh\ hn}^{max}$ is the maximum horizontal speed of a hurricane missile from RG 1.221 Table 2, linearly interpolated to the corresponding hurricane site characteristic wind speed of 159 mph.

**PSEG Site
ESP Application
Part 2, Site Safety Analysis Report**

2.4 HYDROLOGIC ENGINEERING

Section 2.4 describes the hydrological characteristics of the PSEG Site. This section is divided into 13 subsections:

- 2.4.1 Hydrologic Description
- 2.4.2 Floods
- 2.4.3 Probable Maximum Flood on Streams and Rivers
- 2.4.4 Potential Dam Failures
- 2.4.5 Probable Maximum Surge and Seiche Flooding
- 2.4.6 Probable Maximum Tsunami Flooding
- 2.4.7 Ice Effects
- 2.4.8 Cooling Water Canals and Reservoirs
- 2.4.9 Channel Diversions
- 2.4.10 Flooding Protection Requirements
- 2.4.11 Low Water Considerations
- 2.4.12 Groundwater
- 2.4.13 Accidental Release of Radioactive Liquid Effluent in Groundwater and Surface Waters

2.4.1 HYDROLOGIC DESCRIPTION

The site location is described in detail to support the safety analysis. This subsection addresses hydrologic characteristics and phenomena having the potential to affect the design basis for the new plant.

2.4.1.1 Site and Facilities

The existing 734 acre PSEG property is located on the southern part of Artificial Island on the east bank of the Delaware River in Lower Alloways Creek Township, Salem County New Jersey (NJ) as shown on Figure 2.4.1-1. The site is located 52 river miles (RM) upstream of the mouth of Delaware Bay. Important hydrologic features close to the site are the Delaware River, the head of the Delaware Bay (RM 48), and the Chesapeake and Delaware (C&D) Canal channel entrance (RM 59). The PSEG Site is 17 RM downstream of the Delaware Memorial Bridge (RM 69) and 40 RM southwest of Philadelphia, Pennsylvania (PA) (RM 92) (Reference 2.4.1-2).

The City of Salem, NJ (7-1/2 miles [mi.] to the northeast of the site) and Pennsville, NJ (9 mi. north of the site) are the nearest sizable municipalities in NJ (populations in 2007 of approximately 6000 and 13,000, respectively). Middletown, Delaware (DE) (7 mi. due west of the site) and New Castle, DE (13 mi. north-northwest of the site) are the nearest sizable municipalities in DE (populations in 2007 of approximately 11,000 and 5000, respectively). (Reference 2.4.1-22)

The land mass on which the PSEG Site is located, known as Artificial Island, was created beginning early in the twentieth century by disposal of hydraulic dredge spoils within a progressively enlarged diked area around a natural sandbar that projected into the Delaware River. Now a peninsula, the elevation of the terrain across the PSEG Site generally ranges from 5 to 15 ft. NAVD. Developed areas are nominally 10 to 12 ft. NAVD (Reference 2.4.1-5).

**PSEG Site
ESP Application
Part 2, Site Safety Analysis Report**

Salem Generating Station (SGS) and Hope Creek Generating Station (HCGS) are located in the western portion of the PSEG Site. SGS has two Westinghouse pressurized water reactors (PWRs) with once-through condenser cooling systems. Units 1 and 2 entered commercial service in June 1977 and October 1981, respectively. Each unit is licensed for 3459 megawatts thermal (MWt). The nuclear steam supply system for each unit includes a PWR, reactor coolant system, and associated auxiliary fluid systems. SGS is located in an area of engineered backfill at a grade elevation of 9.7 ft. NAVD (Reference 2.4.1-14).

HCGS is a single-unit plant utilizing a General Electric boiling water reactor (BWR) with a natural draft cooling tower; the unit is currently licensed for 3840 MWt. HCGS entered commercial service in December 1986. The nuclear steam supply system includes a BWR, reactor coolant system, and associated auxiliary fluid systems. The Hope Creek plant is located in an area of engineered backfill at an elevation of 11.7 ft. NAVD. The Turbine and Auxiliary Building ground floor levels are at a grade elevation of 12.2 ft. NAVD. (Reference 2.4.1-13)

The new plant location is to the north of the HCGS. Most of the area for the new plant lies within the current property boundary. However, PSEG is developing an agreement in principle with the U.S. Army Corps of Engineers (USACE) to acquire an additional 85 acres immediately to the north of the HCGS. A specific reactor technology has not been selected for construction at the PSEG Site. Designs under consideration are:

- Single Unit U.S. Evolutionary Power Reactor (U.S. EPR)
- Single Unit Advanced Boiling Water Reactor (ABWR)
- Single Unit U.S. Advanced Pressurized-Water Reactor (US-APWR)
- Dual Unit Advanced Passive 1000 (AP1000)

The circulating water system (CWS) for the new plant includes cooling tower(s). The Delaware River is used for makeup water for the CWS and the turbine plant cooling systems. In addition to the circulating water cooling tower, service water cooling tower(s) are included in the new plant design.

The design basis flood (DBF) is 32.1 ft. NAVD as calculated in Subsection 2.4.5. Floor elevations for safety-related structures, systems and components (SSC) for the new plant, other than the intake structure, will be established to maintain at least one foot of clearance above the DBF, as required by Tier 1 of the design control document (DCD) for the technology selected. The area surrounding the safety-related SSC will be graded such that the runoff from probable maximum precipitation (PMP) on the site drains away from the SSC into a system of swales and pipes that carry runoff to the Delaware River.

The design basis low water level at the ultimate heat sink (UHS) makeup water intake is -15.9 ft. NAVD as discussed in Subsection 2.4.11 and shown on Figure 2.4.2-7.

Elevations reported in Section 2.4 are in NAVD. Some components of hydrologic events, such as storm surge and wave height, are customarily expressed in feet, which are not tied to a datum.

**PSEG Site
ESP Application
Part 2, Site Safety Analysis Report**

2.4.1.2 Hydrosphere

The Delaware River and the Delaware Bay are the main hydrologic features that may affect or be affected by new plant construction at the PSEG Site. Other hydrologic features considered include Alloway Creek, Hope Creek and the C&D Canal. Table 2.4.1-1 lists these and other hydrological features and their distances from the PSEG Site. The Delaware River and the Delaware Bay are the overwhelming hydrologic drivers at the PSEG Site, therefore other hydrologic features have minimal or no impact on the site and therefore are not discussed.

The Delaware River Basin covers 13,600 square miles (sq. mi.) and includes portions of DE, Maryland (MD), NJ, New York (NY), and PA (Reference 2.4.1-3). The basin crosses through five physiographic provinces. These are the Coastal Plain, Piedmont, New England, Valley and Ridge, and the Appalachian Plateaus. Topography varies from the relatively flat Coastal Plain, consisting of unconsolidated sediments, to the rolling lowlands and a series of broad uplands in the Piedmont. The New England and Valley and Ridge provinces consist of rock layers that have been deformed into a series of steep ridges and parallel folds. The Appalachian Plateaus occupy the upper one-third of the basin. Intricately dissected plateaus, broad ridges and rugged hills characterize this province. (Reference 2.4.1-26) The Delaware Estuary extends from the fall line in Trenton, NJ, and Morrisville, PA, south to Cape May, NJ, and Cape Henlopen, DE, including all of Delaware Bay and the tidal reaches of the Delaware River.

The Delaware River Basin and its subbasins, delineated as 8-digit hydrologic unit code (HUC) subbasins (SB) by the U.S. Geological Survey (USGS), are shown in Figure 2.4.1-2. The drainage area of each basin upstream and downstream of the PSEG Site is given in Table 2.4.1-2. The total drainage area upstream of the PSEG Site is 11,500 sq. mi.

Average annual precipitation in the Delaware River Basin ranges from 42 inches (in.) for southern NJ in the lower basin, to 50 in. for the Catskill Mountains of southern NY in the upper basin. Annual snowfall ranges from 13 in. for southern NJ to 80 in. for the Catskill Mountains. In general, precipitation is evenly distributed in the basin throughout the year. (Reference 2.4.1-26)

A detailed description of local aquifers is presented in Subsection 2.4.12.

2.4.1.2.1 Hydrologic Characteristics

The Delaware Estuary is comprised of the Delaware Bay and the tidally influenced portion of the Delaware River. The transition between the head of the bay and the mouth of the river occurs at RM 48, 4 mi. downstream from the PSEG Site. The PSEG Site is located in a transition zone between the bay and the river (References 2.4.1-6 and 2.4.1-23). The Delaware River is subject to tidal influence from the mouth of the Delaware River to the upstream limit of the estuary, which is defined by the head of tide where the deepest part of the Delaware River rises high enough to be outside of the influence of astronomical tides. The limit of tidal influence on the Delaware River is located at RM 134 in Trenton, NJ (Reference 2.4.1-18). At the PSEG Site, under normal flow conditions, tidal flow dominates over freshwater discharges. Tidal flow at the PSEG Site ranges from 400,000 cubic feet per second (cfs) to 472,000 cfs (References 2.4.1-16 and 2.4.1-23). Freshwater flow at the PSEG Site is approximately 15,000 cfs (Reference 2.4.1-16). Most of the freshwater flow that enters the Delaware Bay near the PSEG Site comes from the non-tidal Delaware River and the Schuylkill River (Reference 2.4.1-23).

**PSEG Site
ESP Application
Part 2, Site Safety Analysis Report**

The Delaware Bay is periodically affected by storm surges generated in the Atlantic Ocean. The largest surges result from hurricanes. Storm surge associated with hurricanes is discussed in Subsection 2.4.5. Less likely to affect the PSEG Site is a tsunami. There have been few recorded incidents of wave runup resulting from tsunamis affecting the Atlantic coast. These are discussed in Subsection 2.4.6.

The Delaware River, Delaware Estuary, and Delaware Bay system is a continuum of environments: freshwater, tidal freshwater, tidal brackish water, and marine. Currents in the upper estuary near Trenton, NJ are dominated by freshwater river flow. Current speed and direction in the Delaware Bay and lower portions of the estuary are primarily determined by tides. However, circulation patterns in the Delaware Estuary are influenced by river discharge. In general, the ratio of freshwater to saltwater creates a variation of the vertical salinity in the estuary. During the summer, the vertical stratification is weak. Increased freshwater discharge from the river in the spring creates vertical stratification with salinity variations of 5 – 15 parts per thousand (ppt). (Reference 2.4.1-15)

Tides enter Delaware Bay from the Atlantic Ocean and propagate upstream. The tide of the Delaware Estuary is semidiurnal in character. There are two high waters and two low waters in a tidal day, with comparatively little diurnal inequality. The Reedy Point station is the tidal gage station nearest the PSEG Site, as shown on Figure 2.4.1-2. The mean tide range at this location is 5.34 ft. (Reference 2.4.1-10), indicating a significant influence of tide on flows. National Oceanic and Atmospheric Administration (NOAA) tidal gage stations are used to calibrate hydraulic models for the tidally influenced sections of the Delaware River and Delaware Bay. Table 2.4.1-3 identifies location, and tidal range for NOAA gage stations used in this analysis. Tidal gages used for the modeling in Section 2.4 are tied to a constant datum so that comparisons and calibrations can be made. Table 2.4.1-4 summarizes tidal ranges at the Reedy Point gage. These ranges are similar to those at the PSEG Site because the Reedy Point gage is the closest tidal gage to the PSEG Site, located 7 mi. upriver.

Upstream of the head of tide, average daily and annual peak flow series data are tabulated by the USGS for nine stream gages maintained along the Delaware River between Trenton, NJ (RM 134) and Callicoon, NY (RM 303) (Reference 2.4.1-2 and Figure 2.4.1-2). USGS gage stations are used to calibrate hydraulic models for the non-tidal sections of the Delaware River system. USGS gages are selected based on their long-term available flow data and relevance of that data to modeling efforts. Gages used to model non-tidal sections of the Delaware River and its tributaries are listed in Table 2.4.1-5.

At the Trenton USGS gage station, average daily flow is 11,900 cfs, calculated as the mean of the average daily flows for each day of the 96-year (1912 – 2008) record (Table 2.4.1-6). The daily mean flow varies from a minimum of 5040 cfs in September, to a maximum of 28,900 cfs in April. Maximum flow recorded at the Trenton USGS gage is 329,000 cfs, which occurred during a flood event in 1955. (Reference 2.4.1-43) River flooding affecting the PSEG Site is discussed in detail in Subsection 2.4.3. The minimum target stream flow at Trenton is 3000 cfs. This flow is intended to maintain the salt line at RM 98, safely downstream of intakes for public water supply. (Reference 2.4.1-3) Water releases from dams designated for flow augmentation ensure minimum flows are achieved.

According to the Delaware River Basin Commission (DRBC), there are 24 reservoirs in the Delaware River Basin (Figure 2.4.1-3). Of these, nine reservoirs are dedicated for water supply,

**PSEG Site
ESP Application
Part 2, Site Safety Analysis Report**

two generate hydropower, three are dedicated for flood loss reduction, and one is solely for flow augmentation. The remaining nine reservoirs are multipurpose, providing water for a combination of water supply, flow augmentation, and flood loss reduction. Dedicated water supply reservoirs fill during the winter and spring months to ensure water supply during dry months. Multipurpose reservoirs and those dedicated to flood reduction maintain year-round flood storage voids to mitigate flooding. (Reference 2.4.1-3) Flow management of the Delaware River is accomplished through coordinated releases from major reservoirs on its tributaries. Coordinated management of reservoir flows ensures the maintenance of minimum flows under normal conditions at Montague (1750 cfs) (Reference 2.4.1-33) and Trenton (3000 cfs) (Reference 2.4.1-3). Flow diversions, reservoir releases, and flow objectives, which are based on water quantity stored and the season, are listed in the DRBC Flexible Flow Management Program (Reference 2.4.1-1).

2.4.1.2.2 Local Drainage

Local drainage, developed from the Taylor's Bridge, Canton, Salem, and Delaware City USGS quadrangle sheets, is shown in Figure 2.4.1-1. The transition between Delaware Bay and the Delaware River (RM 48) downstream of the PSEG Site is the most significant hydrologic feature to note. Tidal flows have a much larger impact on the PSEG Site than freshwater flows. Records indicate that under normal flow conditions tidal flows are approximately 30 times larger than freshwater flows at the PSEG Site (Reference 2.4.1-16). The C&D Canal (RM 59), shown on Figure 2.4.1-1, hydraulically connects Chesapeake Bay at the Elk River with the Delaware River. Average net flow moves from Chesapeake Bay to the Delaware Estuary (Reference 2.4.1-23). High water at the Delaware River end generally occurs two hours later than in the Elk River. The C&D Canal averages 35 ft. deep and 450 ft. wide and runs between the Delaware River to deep water in Chesapeake Bay (Reference 2.4.1-21). Smaller tributary creeks and rivers are listed in Table 2.4.1-1.

The PSEG Site is generally flat with drainage flowing toward marshes and the Delaware River. The area drainage system consists of ditches that collect and convey runoff to piping that discharges into the Delaware River (Reference 2.4.1-13). Existing PSEG Site drainage characteristics are shown in Figure 2.4.1-4, which shows the new plant footprint in conjunction with the existing topography and drainage patterns.

The new plant primarily affects drainage on the northwest side of the PSEG Site and requires the installation of additional stormwater conveyance structures to route stormwater from the top of fill through swales and pipes into the Delaware River. A more detailed discussion of local drainage for the new plant and existing PSEG Site is provided in Subsection 2.4.2.

2.4.1.2.3 Dams and Reservoirs

The Delaware River is the longest undammed river east of the Mississippi River (Reference 2.4.1-3). Tributaries of the Delaware River are dammed to create reservoirs used for water supply, to provide flood protection, to generate hydropower, augment river flow during droughts, and facilitate recreation. Table 2.4.1-7 provides a summary of location, purpose and size of the 24 reservoirs in the Delaware River Basin. Figure 2.4.1-3 is a DRBC-based map showing the location and use of the reservoirs in the Delaware River Basin.

**PSEG Site
ESP Application
Part 2, Site Safety Analysis Report**

The largest reservoirs in terms of water volume are located in the upper Delaware River Basin. Reservoir storage volumes tend to decrease in the Piedmont and Coastal Plain physiographic regions. Subsection 2.4.4 describes coincident dam breaks based on geographic groupings and reservoir size. The four largest reservoirs in the Delaware River Basin are:

Pepacton Reservoir
Cannonsville Reservoir
Neversink Reservoir
Lake Wallenpaupack

Pepacton Reservoir (460,000 acre-feet [ac.-ft.]), Cannonsville Reservoir (303,000 ac.-ft.), and Neversink Reservoir (142,000 ac.-ft.) all serve dual purposes. They serve as water supply and are used for flow augmentation in the event of a drought; to maintain the mandated flow level of 1750 cfs at Montague, NJ (References 2.4.1-3 and 2.4.1-33). Pepacton Reservoir is located on the East Branch Delaware River in NY, and it has been in service since 1954. Cannonsville Reservoir is located on the West Branch Delaware River in NY, and has been in service since 1963. Neversink Reservoir is located on the Neversink River in NY, and has been in service since 1953. (Reference 2.4.1-20) Approximately half of the water stored in the reservoirs in the Delaware River Basin is held in these three reservoirs in the upper watershed (Reference 2.4.1-3). Lake Wallenpaupack (209,000 ac.-ft.) is used to generate hydroelectric power. It is located on the Wallenpaupack Creek in northeastern PA and has been in service since 1925. (Reference 2.4.1-20)

Reservoirs used for flood control maintain storage capacity to capture and slowly release flood waters to mitigate downstream flooding. The three reservoirs dedicated for flood control are located in the upper and central portions of the Delaware River Basin. Listed below, these three reservoirs are operated by the USACE, Philadelphia District.

- General Edgar Jadwin Reservoir
- Prompton Reservoir
- F.E. Walter Reservoir

Jadwin Reservoir is located on Dyberry Creek in northeast PA, and has been in operation since 1960. Prompton Reservoir is located on the Lackawaxen River in PA, and has been in operation since 1961. F.E. Walter Reservoir is located on the Lehigh River in PA, and it has been in operation since 1961. (Reference 2.4.1-20) These reservoirs were constructed following a devastating flood on the Delaware River in 1955. The 1955 flood is the worst flood recorded since USGS started measuring floods through their gage system network in the Delaware River Basin.

Merrill Creek Reservoir, located on Merrill Creek in the central portion of the basin, is dedicated to flow augmentation. This reservoir has been in operation since 1988. PSEG is a co-owner of this reservoir. Operation of the reservoir ensures minimum flows downstream during a drought so that the Merrill Creek co-owners can continue to withdraw water from the Delaware River to maintain power generation operations.

The reservoirs nearest the PSEG Site are small in terms of storage volume and are used for water supply. These reservoirs are:

**PSEG Site
ESP Application
Part 2, Site Safety Analysis Report**

- Springton Reservoir (Geist Dam) (10,700 ac.-ft.)
- Hoopes Reservoir (11,000 ac.-ft.)
- Newark Reservoir (920 ac.-ft.)

These reservoirs have small storage volumes and therefore have little impact on flows at the PSEG Site. Springton Reservoir is located on Crum Creek in southeastern PA and it has been in operation since 1931. Hoopes Reservoir is located on Red Clay Creek and it has been in operation since 1931. (Reference 2.4.1-20) Newark Reservoir is located adjacent to White Clay Creek and it has been in operation since 2006. These two small water supply reservoirs are located in northern DE.

2.4.1.2.4 Proposed Water Management Changes

The USACE is authorized by Congress (Water Resources Development Act of 1992, modified in 1996) to deepen the existing Delaware River Federal Navigation Channel from 40 ft. to 45 ft. from Philadelphia, PA, and Camden, NJ, to the mouth of the Delaware Bay, with appropriate bend widening. This project also includes partial deepening of the Marcus Hook anchorage and relocation and addition of aids to navigation (Reference 2.4.1-18). An Environmental Assessment was published in April 2009 to consolidate into one document the results of the 1992 Environmental Impact Statement (EIS), 1997 Supplemental Environmental Impact Statement (SEIS), 1998 Record of Decision, and results of post-SEIS monitoring and data collection efforts (Reference 2.4.1-19). Since fiscal year 1999, Congress has appropriated funds for the project. The project partnership agreement with USACE headquarters and the Philadelphia Regional Port Authority was executed on June 23, 2008. Construction of the project is planned to start in 2010, subject to resolution of permitting and other regulatory or legal issues (Reference 2.4.1-17).

2.4.1.2.5 Surface-Water Users

The Delaware River is a major transportation corridor to Philadelphia, PA, a major port. The Delaware River is also a primary source of water for industry and municipalities, a receiving body for effluent, a resource for power generation, and a location for recreational activities.

Surface-water withdrawals are authorized from the Delaware River for industrial and public water supply purposes in DE, PA, and NJ. The majority of surface-water users are located upstream of the PSEG Site. The primary surface-water users of the Delaware River, as listed in Table 2.4.1-8, are industrial, power, commercial, and water supply (Reference 2.4.1-4). In-stream use of the Delaware River includes port traffic, barge traffic, fishing, boating, and other recreational activities.

Subsection 2.4.12 presents information about groundwater users.

2.4.1.2.6 Water Consumption

The detailed design of the water supply systems and the cooling water systems for the new plant are not finalized. Plant water use is defined in the plant parameter envelope (PPE) in Section 1.3. The PPE outlines the water consumption requirements for the bounding plant and is based on representative plant designs that result in the highest water consumption values. Water is required to support the needs of a new facility during construction and operation,

Rev. 4

**PSEG Site
ESP Application
Part 2, Site Safety Analysis Report**

including the requirements of the CWS, cooling water systems for plant auxiliary components (e.g., the service water system [SWS]), and makeup for the UHS cooling system (if required). The majority of the water is withdrawn from the Delaware River via an intake structure. The freshwater aquifer supplies water for general site purposes including the potable and sanitary water system (PSWS), demineralized water distribution system (DMDS), fire protection system (FPS), and other miscellaneous systems.

Average and maximum water consumption and discharge by the various cooling and water systems are given in Table 2.4.1-9. Water not consumed is returned to the Delaware River. Liquid radwaste, sewage, and other wastewater is treated before being released back to the river.

2.4.1.2.7 Potential Changes

Mean sea level (msl) trends are evaluated by NOAA at Reedy Point, DE, 7 mi. upstream of the PSEG Site. Based on sea level trend data, the sea level rise is conservatively estimated to be 1.35 feet/century using the upper 95 percent confidence limit (Reference 2.4.1-11). An increase in sea level moves the head of tide further upstream, affecting the salinity of the water in the Delaware River.

2.4.1.3 References

- 2.4.1-1 Delaware River Basin Commission, "Flexible Flow Management Program," Website, <http://www.state.nj.us/drbc/FFMP/index.htm>, accessed August 14, 2009.
- 2.4.1-2 Delaware River Basin Commission, 2007, "Stream River Mileage July 2007," Website, <http://www.state.nj.us/drbc/StreamMileageJuly2007.pdf>, p. 10, 11, 24 – 27, accessed February 16, 2009.
- 2.4.1-3 Delaware River Basin Commission, 2008, "State of the Delaware River Basin Report 2008," Website, <http://www.nj.gov/drbc/SOTB/entire-singles.pdf>, p. 6; 8 – 27; 73, accessed February 19, 2009.
- 2.4.1-4 Delaware River Basin Commission 2005, "Year 2005 Water Withdrawal and Consumptive Use by Large Water Users on the Tidal Delaware River," Website: http://www.state.nj.us/drbc/wateruse/largeusers_05.htm, p. 1 – 3; accessed July 30, 2009.
- 2.4.1-5 MASER Consulting, PA ALTA/ACSM Land Title Survey for PSEG Nuclear LLC of Block 26, Lots 4, 4.01, 5 and 5.01, Job Number 05001694D, Index Number HASU023453 dated June 13, 2008.
- 2.4.1-6 National Oceanic and Atmospheric Administration, "Delaware Estuary Watershed Database and Mapping Project," Website, <http://mapping2.orr.noaa.gov/website/portal/Delaware/>, accessed August 14, 2009.

**PSEG Site
ESP Application
Part 2, Site Safety Analysis Report**

- 2.4.1-7 National Oceanic and Atmospheric Administration, “Lewes, DE Tidal Data,” Website,
http://tidesandcurrents.noaa.gov/station_info.shtml?stn=8557380%20Lewes,%20DE, accessed August 3, 2009.
- 2.4.1-8 National Oceanic and Atmospheric Administration, “Newbold, PA Tidal Data,” Website,
http://tidesandcurrents.noaa.gov/station_info.shtml?stn=8548989%20Newbold,%20PA, accessed August 3, 2009.
- 2.4.1-9 National Oceanic and Atmospheric Administration, “Philadelphia, PA Tidal Data,” Website,
http://tidesandcurrents.noaa.gov/station_info.shtml?stn=8545530%20Philadelphia,%20PA, accessed August 3, 2009.
- 2.4.1-10 National Oceanic and Atmospheric Administration, 1996 – 2008, “Reedy Point Tidal Data,” Website,
http://tidesandcurrents.noaa.gov/station_info.shtml?stn=8551910%20Reedy%20Point,%20DE, accessed February 2, 2009.
- 2.4.1-11 National Oceanic and Atmospheric Administration, “Sea Level Trends Online, 8551910 Reedy Point, Delaware,” Website,
http://tidesandcurrents.noaa.gov/sltrends/sltrends_station.shtml?stnid=8551910, accessed April 27, 2009.
- 2.4.1-12 Pennsylvania Department of Conservation and Natural Resources, Crum Creek Watershed Conservation Plan, Website,
<http://www.dcnr.state.pa.us/brc/rivers/riversconservation/registry/CrumCreek/VI.WATER%20RESOURCES.final.pdf>, p. 28, accessed June 4, 2009.
- 2.4.1-13 Public Service Enterprise Group (PSEG), “Hope Creek Generating Station Updated Final Safety Analysis Report,” Revision 16, Subsection 2.4.1, May 15, 2008.
- 2.4.1-14 Public Service Enterprise Group (PSEG), “Salem Generating Station Updated Final Safety Analysis Report,” Revision 23, Subsection 2.4.1, October 17, 2007.
- 2.4.1-15 Sharp, J.H., L.A. Cifuentes, R.B Coffin, J.R. Pennock, and K.C. Wong, “The Influence of River Variability on the Circulation, Chemistry, and Microbiology of the Delaware Estuary,” *Estuaries*, Volume 9 No. 4A, p. 263 – 264, December 1986.
- 2.4.1-16 U.S. Army Corps of Engineers, “Delaware River Comprehensive Navigation Study Main Channel Deepening Final Interim Feasibility Report,” Philadelphia District, Philadelphia, Pennsylvania, p. 18, 1992.
- 2.4.1-17 U.S. Army Corps of Engineers, *Delaware River Main Channel Deepening PA, NJ, & DE Project Factsheet*, April 2009.

**PSEG Site
ESP Application
Part 2, Site Safety Analysis Report**

- 2.4.1-18 U.S. Army Corps of Engineers, Delaware River Main Channel Deepening Project Design Memorandum, Philadelphia District, Philadelphia, Pennsylvania, p. 1; 55 – 59, 1996.
- 2.4.1-19 U.S. Army Corps of Engineers, Delaware River Main Stem and Channel Deepening Project Environmental Assessment, April 2009.
- 2.4.1-20 U.S. Army Corps of Engineers, National Inventory of Dams, Website, <https://nid.usace.army.mil/>, accessed July 16, 2009.
- 2.4.1-21 U.S. Army Corps of Engineers, Rules and Regulations to Govern the Use, Administration, and Navigation of the Inland Waterway from Delaware River to Chesapeake Bay, June 1972.
- 2.4.1-22 U.S. Census Bureau, 2008, American FactFinder, 2007 Population Estimates, DE. http://factfinder.census.gov/servlet/SAFFPopulation?_submenuId=population_0&_sse=on, accessed on May 8, 2009.
- 2.4.1-23 U.S. Environmental Protection Agency, “Case Study Analysis for the Proposed Section 316(b) Phase II Existing Facilities Rule,” Part B, EPA-821-R-02-002, p. B1-1, B1-6, February 2002.
- 2.4.1-24 U.S. Geological Survey, “01459350 Nockamixon Reservoir Near Ottsville, PA, 1999a,” Website, <http://pa.water.usgs.gov/ar/wy99/pdfs/01459350.pdf>, p. 1, accessed February 22, 2009.
- 2.4.1-25 U.S. Geological Survey, “1:250,000 – scale Hydrologic Units of the United States, 1994,” Website, <http://water.usgs.gov/GIS/metadata/usgswrd/XML/huc250k.xml#stdorder>, accessed February 2, 2009.
- 2.4.1-26 U.S. Geological Survey, “Delaware River Study Unit Description,” National Water-Quality Assessment Program, Website, <http://nj.usgs.gov/nawqa/delr/su.descrpt.html>, accessed June 16, 2009
- 2.4.1-27 U.S. Geological Survey, “Lakes & Reservoirs in Christina River Basin, 2005,” Website, <http://pa.water.usgs.gov/ar/wy05/new-pdfs/christina-lakes.pdf>, p. 1, accessed February 22, 2009.
- 2.4.1-28 U.S. Geological Survey, “Lakes & Reservoirs in Delaware River Basin, 2004,” Website, <http://ny.water.usgs.gov/pubs/wdr/wdrny041/rept.delaware2004.pdf>, p. 1 – 2, accessed February 22, 2009.
- 2.4.1-29 U.S. Geological Survey, “Lakes & Reservoirs in Lackawaxen River Basin, 1999b,” Website, <http://pa.water.usgs.gov/ar/wy99/pdfs/lackawaxen-lakes.pdf>, p. 1, accessed February 22, 2009.

**PSEG Site
ESP Application
Part 2, Site Safety Analysis Report**

- 2.4.1-30 U.S. Geological Survey, "Lakes & Reservoirs in Lehigh River Basin, 2001a," Website, <http://pa.water.usgs.gov/ar/wy01/pdfs/lehigh-lakes.pdf>, p. 1, accessed February 22, 2009.
- 2.4.1-31 U.S. Geological Survey, "Lakes & Reservoirs in Schuylkill River Basin, 2001b," Website, <http://pa.water.usgs.gov/ar/wy01/pdfs/schuylkill-lakes.pdf>, p. 1, accessed February 22, 2009.
- 2.4.1-32 U.S. Geological Survey (USGS), "National Elevation Dataset," Website, <http://seamless.usgs.gov/website/seamless/viewer.htm>, accessed February 2, 2009.
- 2.4.1-33 U.S. Geological Survey, "Office of the Delaware River Master," Website, <http://water.usgs.gov/osw/odrm/intro.html>, accessed July 3, 2009.
- 2.4.1-34 U.S. Geological Survey, "Reservoirs in Delaware River Basin," Website, <http://pubs.usgs.gov/wdr/2005/wdr-nj-05-1/pdf/Delaware05.pdf>, accessed July 31, 2009.
- 2.4.1-35 U.S. Geological Survey, "USGS Stream Gage 01427510 Delaware River at Callicoon, NY. 2009," Website, http://waterdata.usgs.gov/ny/nwis/nwisman/?site_no=01427510&agency_cd=USGS, accessed June 4, 2009.
- 2.4.1-36 U.S. Geological Survey, "USGS Stream Gage 01428500 Delaware River above Lackawaxen River near Barryville, NY," Website, http://waterdata.usgs.gov/ny/nwis/nwisman/?site_no=01428500&agency_cd=USGS, accessed June 4, 2009.
- 2.4.1-37 U.S. Geological Survey, "USGS Stream Gage 01434000 Delaware River at Port Jervis, NY," Website, http://waterdata.usgs.gov/ny/nwis/nwisman/?site_no=01434000&agency_cd=USGS, accessed June 4, 2009.
- 2.4.1-38 U.S. Geological Survey, "USGS Stream Gage 01438500 Delaware River at Montague, NJ," Website, http://waterdata.usgs.gov/nwis/nwisman/?site_no=01438500&agency_cd=USGS, accessed June 4, 2009.
- 2.4.1-39 U.S. Geological Survey, "USGS Stream Gage 01440200 Delaware River near Delaware River Gap, PA," Website, http://waterdata.usgs.gov/pa/nwis/nwisman/?site_no=01440200&agency_cd=USGS, accessed June 4, 2009.
- 2.4.1-40 U.S. Geological Survey, "USGS Stream Gage 01446500 Delaware River at Belvidere, NJ.," Website, http://waterdata.usgs.gov/nj/nwis/nwisman/?site_no=01446500&agency_cd=USGS, accessed June 4, 2009.

**PSEG Site
ESP Application
Part 2, Site Safety Analysis Report**

- 2.4.1-41 U.S. Geological Survey, "USGS Stream Gage 01457500 Delaware River at Riegelsville, NJ," Website, http://waterdata.usgs.gov/nj/nwis/nwisman/?site_no=01457500&agency_cd=USGS, June 4, 2009.
- 2.4.1-42 U.S. Geological Survey, "USGS Stream Gage 01462000 Delaware River at Lambertville, NJ," Website, http://waterdata.usgs.gov/nj/nwis/nwisman/?site_no=01462000&agency_cd=USGS, accessed June 4, 2009.
- 2.4.1-43 U.S. Geological Survey, "USGS Stream Gage 01463500 Delaware River at Trenton, NJ," Website, http://waterdata.usgs.gov/nj/nwis/nwisman/?site_no=01463500&agency_cd=USGS, accessed June 4, 2009.
- 2.4.1-44 U.S. Geological Survey, "USGS Stream Gage 01474500 Schuylkill River at Philadelphia, PA," Website, http://waterdata.usgs.gov/nwis/nwisman/?site_no=01474500&agency_cd=USGS, accessed August 3, 2009.
- 2.4.1-45 U.S. Geological Survey, "USGS Stream Gage 01481500 Brandywine Creek at Wilmington, DE," Website, http://waterdata.usgs.gov/nwis/nwisman/?site_no=01481500&agency_cd=USGS, accessed August 3, 2009.
- 2.4.1-46 U.S. Geological Survey, "Digital Raster Graphics," Website, <http://seamless.usgs.gov/index.php>, accessed February 2, 2009.

**PSEG Site
ESP Application
Part 2, Site Safety Analysis Report**

**Table 2.4.1-1
Hydrologic Features in the Vicinity of the PSEG Site**

Hydrologic Feature Name	Delaware RM	Distance (RM) from PSEG Site
Delaware River	--	--
Lower Deep Creek	44	8
Smyrna River	45	7
Mad Horse Creek	45	7
Fishing Creek	47	5
Hope Creek	48	4
Head of Delaware Bay	48	4
Blackbird Creek	50	2
Appoquinimink River	51	1
Silver Run	53	1
Augustine Creek	53	1
Alloway Creek	54	2
St. Georges Creek	56	4
Salem River	58	6
Chesapeake and Delaware Canal	59	7
Mill Creek	60	8

Reference 2.4.1-2

**PSEG Site
ESP Application
Part 2, Site Safety Analysis Report**

**Table 2.4.1-2
Delaware River Subbasins and Drainage Areas Above and Below the PSEG Site**

ID	USGS 8-digit HUC	U.S. Geological Survey Subbasin Name	Drainage Area, sq. mi.		Total ^(a)
			Upstream of Site ^(a)	Downstream of Site ^(a)	
1	02040101	Upper Delaware	1191	0.0	1191
2	02040102	East Branch Delaware	836	0.0	836
3	02040104	Middle Delaware-Mongaup- Brodhead	1532	0.0	1532
4	02040103	Lackawaxen	593	0.0	593
5	02040105	Middle Delaware-Musconetcong	1345	0.0	1345
6	02040106	Lehigh	1367	0.0	1367
7	02040203	Schuylkill	1924	0.0	1924
8	02040201	Crosswicks-Neshaminy	543	0.0	543
9	02040202	Lower Delaware	1092	0.0	1092
10	02040205	Brandywine-Christina	731	34.4	765
11	02040204	Delaware Bay	70.3	676	746
12	02040206	Cohansey-Maurice	250	794	1044
13	02040207	Broadkill-Smyrna	0.0	638	638
Delaware River drainage area			11,474	2142	13,616

a) As estimated from HUC-8 shape files

Reference 2.4.1-25

**PSEG Site
ESP Application
Part 2, Site Safety Analysis Report**

**Table 2.4.1-3
NOAA Tidal Gage Data for the Delaware Bay and Delaware River**

NOAA Gage ID	Location	RM^(a)	Coordinates		Established^(b)	Mean Range (ft.)	Diurnal Range (ft.)
8557380	Lewes, DE	0	38° 46.9' N	75° 7.2' W	1/14/1919	4.08	4.65
8551910	Reedy Point, DE	59	39° 33.5' N	75° 34.4' W	7/30/1956	5.34	5.84
8545530	Philadelphia, PA	100	39° 57.2' N	75° 8.3' W	7/1/1900	6.24	6.82
8548989	Newbold, PA	126	40° 8.2' N	74° 45.1' W	10/27/2001	7.86	8.44

a) River miles measured from the mouth of the Delaware River as reported by DRBC.

b) The established column lists the date the gage was originally installed. The period of record for different data sets available at each gage can be found at the corresponding references listed below.

References 2.4.1-7, 2.4.1-8, 2.4.1-9, and 2.4.1-10

**PSEG Site
ESP Application
Part 2, Site Safety Analysis Report**

**Table 2.4.1-4
Tidal Values at NOAA Reedy Point, DE Tidal Gage (Gage Number 8551910)
(ft. NAVD)**

Identifier	Level	Description
MHHW	2.9	Mean Higher-High Water
MHW	2.6	Mean High Water
DTL	-0.05	Mean Diurnal Tide Level
MTL	-0.1	Mean Tide Level
msl	-0.05	Mean Sea Level
MLW	-2.8	Mean Low Water
MLLW	-3.0	Mean Lower-Low Water
GT	5.8 ^(b)	Great Diurnal Range
MN	5.3 ^(b)	Mean Range of Tide
10% EHT ^(a)	4.6	10% Exceedance High Tide
90% ELT ^(a)	-5.2	90% Exceedance Low Tide
Maximum	5.91	Highest Water Level
Minimum	-6.98	Lowest Water Level

a) Values calculated from monthly MHHW and MLLW values from 1987-2008

b) N/A. Reported results are the difference between two elevations: therefore, not referred to a datum.

Reference 2.4.1-10

**PSEG Site
ESP Application
Part 2, Site Safety Analysis Report**

**Table 2.4.1-5
USGS Gage Data for the Delaware River and Tributaries**

USGS Gage ID	Location	RM ^(a)	Coordinates	Elevation, ft. ^(b)	Area drained, sq. mi.	Average daily flow series			Annual peak flow series			
						Start	End	No. of records	Start	End	No. of records	
01427510	Delaware River at Callicoon, NY	302.70	41° 45' 24" N	75° 03' 28" W	734.33	1820	06/27/1975	09/30/2008	12,150	01/27/1976	03/09/2008	33
01428500	Delaware River above Lackawaxen River near Barryville, NY	279.16	41°30' 32" N	74° 59' 10" W	599.69	2020	10/01/1940	09/30/2008	24,837	12/30/1940	03/09/2008	68
01434000	Delaware River at Port Jervis, NY	254.80	41° 22' 14" N	74° 41' 52" W	414.78	3070	10/01/1904	09/30/2008	37,986	10/10/1903	03/09/2008	105
01438500	Delaware River at Montague, NJ	246.44	41° 18' 33" N	74° 47' 43" W	369.33	3480	10/01/1939	11/30/2008	25,264	10/10/1903	04/16/2007	73
01440200	Delaware River near Delaware Water Gap, PA	215.90	41° 00' 48" N	75° 05' 10" W	293.07	3850	06/02/1964	01/31/1996	11,566	08/19/1955	04/17/2007	39
01446500	Delaware River at Belvidere, NJ	197.67	40° 49' 35" N	75° 04' 57" W	225.75	4535	10/01/1922	12/31/2008	31,504	10/10/1903	04/17/2007	86
01457500	Delaware River at Riegelsville, NJ	174.87	40° 35' 41" N	75° 11' 23" W	124.32	6328	07/01/1906	09/30/1971	23,833	01/08/1841	04/17/2007	103
01462000	Delaware River at Lambertville, NJ	148.64	40° 21' 53" N	74° 56' 56" W	48.11	6680	10/01/1897	09/30/1906	3286	10/06/1786	04/17/2007	48
01463500	Delaware River at Trenton, NJ	134.32	40° 13' 18" N	74° 46' 41" W	-1.05	6780	10/01/1912	01/31/2009	35,187	12/16/1897	04/17/2007	110
01474500	Schuylkill River at Philadelphia, PA	~92	39° 58' 04" N	75° 11' 20" W	4.64	1893	10/01/1931	09/30/2008	28,125	10/04/1869	02/13/2008	79
01481500	Brandywine Creek at Wilmington, DE	~71	39° 46' 09.9" N	75° 34' 23.8" W	67.17	314	10/01/1946	09/30/2008	22,646	04/30/1947	02/14/2008	62

a) River miles measured from the mouth of the Delaware River as reported by USGS

b) NAVD

There are other USGS gage stations on the Delaware River that are not used in the analysis because they either lack flow data, have old flow data, or too short a record.

References 2.4.1-35, 2.4.1-36, 2.4.1-37, 2.4.1-38, 2.4.1-39, 2.4.1-40, 2.4.1-41, 2.4.1-42, 2.4.1-43, 2.4.1-44, and 2.4.1-45

**PSEG Site
ESP Application
Part 2, Site Safety Analysis Report**

**Table 2.4.1-6
Daily Mean Flow Data for the Delaware River at Trenton, NJ (USGS Gage 01463500)**

Day of Month	Mean of Daily Mean Values for this Day for 96 Years of Record ^(a) (in cfs)											
	January	February	March	April	May	June	July	August	September	October	November	December
1	13,200	11,800	15,300	26,700	16,000	12,000	9520	6260	5340	7580	8970	13,600
2	12,600	12,000	15,000	26,700	15,400	12,100	8790	6230	5650	7620	8490	13,900
3	12,900	12,500	14,800	27,400	14,900	11,700	7980	6140	5720	6960	8570	14,000
4	13,100	12,700	15,000	28,100	14,700	11,100	7430	6180	5820	6400	8930	13,500
5	12,600	12,300	16100	27,600	14,600	10,700	6850	6260	5940	6080	9310	13,900
6	12,500	11,700	17,200	28,600	14,400	10,200	6660	5990	5550	6010	8860	14,100
7	12,700	11,800	18,300	28,900	14,400	10,100	6820	5740	5300	6230	8720	14,000
8	13,200	12,200	18,100	27,300	14,000	10,700	6360	5610	5180	6790	9030	13,900
9	14,000	11,200	18,700	25,000	13,600	10,100	6610	5750	5290	6940	9860	14,200
10	13,800	10,700	18,900	24,200	13,400	9430	7850	5740	5150	6600	11,000	13,500
11	12,800	10,600	19,000	23,100	13,600	8930	7930	5610	5040	6670	11,000	13,500
12	12,100	11,800	19,200	22,200	14,400	8910	7060	5830	5050	6270	10,600	14,100
13	12,200	12,400	20,400	22,000	14,800	9110	6910	6270	5460	6150	10,400	13,900
14	11,600	11,800	20,000	21,500	15,200	8950	6810	6510	5840	6320	10,500	14,100
15	11,900	11,700	21,300	21,600	14,700	8780	6860	6080	5650	6420	10,700	14,000
16	11,700	12,400	21,800	22,900	14,200	8760	7020	5680	6210	6690	10,600	13,500
17	11,300	12,500	21,500	23,500	14,100	8920	6670	5730	6910	6930	11,500	12,900
18	11,100	12,600	22,400	22,500	13,900	8520	6600	5970	6830	6840	12,000	12,500
19	11,700	12,600	23,000	21,100	13,600	8670	6410	7190	7860	7350	11,600	12,200
20	12,400	12,700	22,000	19,800	13,600	8620	6610	8190	7570	8540	11,400	11,800
21	13,000	12,900	21,900	18,700	13,300	8450	6660	6030	7110	8640	11,500	12,600
22	12,400	13,900	23,000	18,700	13,300	8370	6790	5670	7100	8400	11,800	13,200
23	12,100	14,400	24,000	18,200	14,000	8880	7450	5700	7100	8040	11,800	12,200
24	12,800	14,900	22,800	17,900	14,200	8780	7490	6130	6580	7920	11,200	11,800
25	14,700	15,400	22,000	17,800	13,400	8250	7260	6540	6300	8230	11,100	12,300
26	15,500	17,100	22,300	17,900	13,700	7740	6710	6080	6120	8210	11,400	12,300
27	15,500	16,800	23,000	17,800	13,300	7990	6460	5520	6310	8340	11,900	11,800
28	15,400	16,200	24,900	17,500	12,600	8910	6760	5690	7120	8640	12,200	11,800
29	14,400	14,400	26,400	17,100	12,200	9790	7120	5330	7750	8810	13,500	11,800
30	13,100	--	25,900	16,400	13,200	10,500	7200	5200	7010	8810	14,500	12,000
31	12,200	--	25,300	--	12,600	--	6480	5170	--	8800	--	12,900
Average:	12,919	12,966	20,629	22,290	13,977	9465	7101	6001	6195	7362	10,765	13,090
Overall Average Daily Discharge:							11,888					

a) Available period of record may be less than value shown for certain days of the year.

Adapted from USGS 2009 (Reference 2.4.1-43)

**PSEG Site
ESP Application
Part 2, Site Safety Analysis Report**

**Table 2.4.1-7 (Sheet 1 of 2)
Inventory of Reservoirs in the Delaware River Basin**

Name of Dam or Reservoir	Owner or Operator	Primary Purpose	Source	Drainage Area Above Dam (sq. mi.)	Total Storage, (100's of ac.-ft.)	Spillway Elevation, ft. NAVD 1988	Date Completed
Pepacton Reservoir	NY City Department of Environmental Protection	Water supply and flow augmentation	East Branch Delaware River	372	4600	1279	1954
Cannonsville Reservoir	NY City Department of Environmental Protection	Water supply and flow augmentation	West Branch Delaware River	454	3030	1150	1963
Neversink Reservoir	NY City Department of Environmental Protection	Water supply and flow augmentation	Neversink River	92.5	1420	1439	1953
Jadwin Reservoir	USACE	Flood control	Dyberry Creek	65	473	1052	1960
Prompton Reservoir	USACE	Flood control	West Branch Lackawaxen River	60	728	1204	1961
Lake Wallenpaupack	Pennsylvania Power & Light	Hydroelectric	Wallenpaupack Creek	228	2090	1189	1925
Mongaup System	Mirant NY – Gen, LLC	Hydroelectric	Mongaup River	varies	varies	varies	varies
F.E. Walter Reservoir	USACE	Flood control and recreation	Lehigh River	289	1110	1449	1961
Wild Creek Reservoir	Bethlehem Authority	Water supply	Wild Creek	22	125	819	1941
Penn Forest Reservoir	Bethlehem Authority	Water supply	Wild Creek	17	185	1000	1958
Beltzville Reservoir	USACE	Multipurpose	Pohopoco Creek	96	1040	650	1969
Still Creek Reservoir	Tamaqua Area Water Authority	Water supply	Still Creek	7	83	1181	1933
Lake Hopatcong	NJ Division of Parks and Forestry	Water supply	Musconetcong River	25	482	923	1887
Merrill Creek Reservoir	Merrill Creek Owner's Group	Flow augmentation	Merrill Creek	3	460	928	1988
Blue Marsh Reservoir	USACE	Flood control and water supply	Schuylkill River	175	500	306	1979
Nockamixon Reservoir	Delaware Commission of Natural Resources	Recreation	Tohickon Creek	73	665	394	1973

Rev. 4

**PSEG Site
ESP Application
Part 2, Site Safety Analysis Report**

**Table 2.4.1-7 (Sheet 2 of 2)
Inventory of Reservoirs in the Delaware River Basin**

Name of Dam or Reservoir	Owner or Operator	Primary Purpose	Source	Drainage Area Above Dam (sq. mi.)	Total Storage, (100's of ac.-ft.)	Spillway Elevation, ft. NAVD 1988	Date Completed
Ontelaunee Reservoir	Reading Area Water Authority	Water supply	Maiden Creek	192	228	--	1935
Lake Galena	Bucks County Commissioners	Water supply	Neshaminy Creek	16	171	--	1973
Green Lane Reservoir	Aqua Pennsylvania, Inc.	Water supply	Perkiomen Creek	71	134	285	1957
Chambers Lake	Chester County Water Resources Authority	Multipurpose	Birch Run	5	20	587	1997
Marsh Creek Reservoir	Delaware Commission of Natural Resources	Water supply, flood control, and recreation	Brandywine Creek	20	222	359	1973
Springton Dam (Geist Reservoir)	Aqua Pennsylvania, Inc.	Water supply	Crum Creek	21.5	107	266 ^(a)	1931
Hoopes Reservoir	City of Wilmington, DE	Water supply	Red Clay Creek	N/A	110	339 ^(a)	1931
Newark Reservoir	City of Newark, DE	Water supply	White Clay Creek	0	9.2	188	2006

a) Estimated by digital mapping

References 2.4.1-12, 2.4.1-24, 2.4.1-27, 2.4.1-28, 2.4.1-29, 2.4.1-30, 2.4.1-31, 2.4.1-32, and 2.4.1-34

**PSEG Site
ESP Application
Part 2, Site Safety Analysis Report**

**Table 2.4.1-8
Surface-Water Users on the Tidal Delaware River**

Owner Name	Facility Type	Withdrawal (MGY)^(a)	Data Year
Exelon – Delaware	Power	1,544	2005
Exelon - Eddystone - Units 1-4	Power	320,057	2005
FPL Energy MH 50, Marcus Hook	Power	30	2005
FPL Energy MH 750, Marcus Hook	Power	1427	2005
Fairless Energy, LLC (Dominion)	Power	736	2005
Kimberly-Clark Corporation	Industry	2404	2005
Philadelphia Gas Works – Richmond	Industry	2938	2005
Rohm & Haas – Bristol	Industry	1752	2005
Rohm & Haas – Philadelphia	Industry	598	2005
Sun Refining Co. - Marcus Hook	Industry	3526	2005
Tosco/BP Oil/Bayway Refining	Industry	33,718	2005
USX-US Steel Div. - Fairless Works	Industry	12,555	2005
Wheelabrator – Falls	Industry	275	2005
Lower Bucks County Joint Municipal Authority	Public Water Supply	2870	2005
Aqua Pennsylvania - Bristol Division	Public Water Supply	2027	2005
Philadelphia Water Dept. – Torresdale	Public Water Supply	57,785	2005
Conectiv - Edgemoor Units 1-4	Power	68,543	2005
Conectiv - Edgemoor Unit 5	Power	67,201	2005
Conectiv - Hay Road	Power	470	2005
CitiSteel	Industry	45	2005
E.I. DuPont – Edgemoor	Industry	2650	2005
Premcor	Industry	134,238	2005
SPI Polyols	Industry	699	2005
Connectiv - Deepwater Station	Power	32,842	2005
Logan Generating Company	Power	843	2005
PSEG - Hope Creek Station	Power	19,561	2005
PSEG - Mercer Station	Power	233,679	2005
PSEG - Salem Station	Power	1,067,892	2005
Sunoco Eagle Point	Industry	2394	2005
E.I. DuPont – Chambers Plant	Industry	14,388	2005
E.I. DuPont - Repauno Plant	Industry	1407	2005
MAFCO Worldwide Corporation	Industry	53	2005
National Gypsum Company	Industry	91	2005
Valero Refining Corp.	Industry	2775	2005
Wheelabrator - Gloucester Co.	Industry	5138	2005
Burlington City	Public Water Supply	538	2005
New Jersey American Water Company	Public Water Supply	7930	2005

a) MGY=million gallons per year

Reference 2.4.1-4

**PSEG Site
ESP Application
Part 2, Site Safety Analysis Report**

**Table 2.4.1-9
Plant Water Use**

System	Average Flow (gpm)	Maximum Flow^(a) (gpm)	PPE Item (SSAR Table 1.3-1)
River Water Streams			
Circulating Water System (CWS) ^(d)			
Evaporation	25,264	25,264	2.4.7, 2.5.7, 2.6.7
Drift ^(b)	12	12	2.4.17, 2.5.17, 2.6.17
Makeup	75,792	75,792	2.4.9, 2.5.9, 2.6.9
Blowdown	50,516	50,516	2.4.4, 2.4.5, 2.4.6
Service Water System			
Evaporation	1142	2284	3.3.7a and 3.3.7b
Drift ^(c)	2	4	3.3.17
Makeup (before filter)	2404	4808	3.3.9a and 3.3.9b
Makeup (after filter)	2284	4568	N/A
Blowdown	1140	2280	3.3.4a and 3.3.4b
Makeup Filter Backwash	120	240	N/A
UHS Makeup (emergency only)	4568	4568	N/A
Fresh Water Aquifer Streams^(f)			
Plant Makeup			
PSWS Makeup	93	216	5.2.2 and 5.2.1
DWDS Makeup	107	107	6.2.2 and 6.2.1
FPS Makeup	5	625	7.1.2 and 7.1.1
Floor Wash Drain Makeup	5	5	8.2.2 and 8.2.1
Discharge Streams			
Plant Blowdown			
PSWS Blowdown	93	93	5.1.1 and 5.1.2
DWDS Blowdown	27	27	6.1.1
Misc. Drains Blowdown	39	55	8.1.1 and 8.1.2
Liquid Radwaste Blowdown	11	11	10.2.1
Combined Plant Blowdown ^(e)	51,946	53,222	N/A

a) These flows are not necessarily concurrent.

b) The cooling tower drifts are 0.001% of circulating water system flow.

c) The cooling tower drifts are <0.005% of the service water system flow.

d) The average and maximum flow rates for the CWS are evaluated at a single design point (1% exceedance meteorological conditions)

e) Includes CWS Blowdown, SWS Blowdown SWS Makeup Filter Backwash, and Plant Blowdown

f) Fresh Water Aquifer Streams total average makeup flow is 210 gpm from groundwater aquifers

**PSEG Site
ESP Application
Part 2, Site Safety Analysis Report**

2.4.2 FLOODS

In this subsection, historical flooding is described, flood-producing phenomena are identified, and the potential effects of local intense precipitation are discussed for the PSEG Site. Floods described in this subsection are presented to provide input in determining the design elevation of the new plant.

Potential causes of flooding at the PSEG Site include local runoff events due to intense point-rainfall near the site (discussed in this subsection), Delaware River flooding from precipitation in the watershed (Subsection 2.4.3), dam failures (Subsection 2.4.4), storm surge and seiche effects (Subsection 2.4.5), tsunamis (Subsection 2.4.6), and ice effects (Subsection 2.4.7).

2.4.2.1 Flood History

Historical records show that the highest flood events recorded near the mouth of the Delaware River and within Delaware Bay are caused by storm surge. The PSEG Site is located along the Delaware River at RM 52. Table 2.4.2-1 summarizes storm events resulting in significant surge near the site, including those recorded at NOAA tidal stations at Reedy Point, DE, at RM 59 (7 mi. upstream), and Philadelphia, PA at RM 92 (40 mi. upstream) (Reference 2.4.2-4). Anecdotal reporting of the hurricane of 1878 suggests that at Fort Delaware, DE, on Pea Patch Island at RM 60 (8 mi. upstream of the PSEG Site), water rose to 5 – 8 ft. above mean high water (Reference 2.4.2-2). The Chesapeake-Potomac hurricane of 1933 produced the highest identified recorded storm surge for Reedy Point at 7.7 ft. (Table 2.4.2-1) (Reference 2.4.2-14). Hurricane Hazel, in 1954, produced the maximum identified recorded storm surge of 9.4 ft. at Philadelphia (Reference 2.4.2-19). Hurricane events and storm surge are further discussed in Subsection 2.4.5.

There are NOAA tidal gage stations along the Delaware River from the mouth of the river up to Trenton, NJ. Above Trenton, the river is no longer tidally influenced. Gaging stations upstream from Trenton are operated by the USGS. Flows from the Trenton USGS gage station (gage 01463500) are used as an initial base flows for major flooding events in the watershed basin. Significant non-tidal floods on the Delaware River are based on recorded annual peak flows at Trenton. These peak flows are listed in Table 2.4.2-2. The period of record for the Trenton gage at RM 134 is from 1900 to 2007, as recorded by the USGS (References 2.4.2-4 and 2.4.2-18).

Annual peak flood data at Trenton include estimated flow and water surface elevation (WSEL) values from major floods recorded in 1904, 1936, 1955, 2005, and 2006 (Figure 2.4.2-1). Each of these five events produced peak discharges greater than 225,000 cfs and peak river stages greater than 23 ft. NAVD at Trenton. The maximum peak flow at Trenton for the period of record is 329,000 cfs which occurred August 20, 1955 (Reference 2.4.2-18). The Chesapeake-Potomac hurricane of 1933 and Hurricane Hazel in 1954 did not produce peak discharge or stage elevations at Trenton as high as these five events. Flood elevations downstream of Trenton are tidally influenced, therefore Trenton is the last gage at which discharge values for the Delaware River are determined based solely on freshwater discharge. Locations further downstream on the Delaware River (and its tributaries) are heavily influenced by tidal conditions, and many of the tributaries do not have non-tidal discharge gages. Therefore, the gage at Trenton represents the closest true discharge gage (independent of tide) on the Delaware River.

**PSEG Site
ESP Application
Part 2, Site Safety Analysis Report**

Flooding due to the probable maximum flood (PMF) is discussed in Subsection 2.4.3. Tidal gages near the PSEG Site show cyclic tidal variation with little effect from major flood events (Figure 2.4.2-2). Therefore, the model is calibrated to the June 2006 flood event (peak discharge of 237,000 cfs) to determine flood elevations at the PSEG Site, as discussed in Subsection 2.4.3. The June 2006 event is selected for model calibration for several reasons. More detailed and reliable rainfall data are available for the 2006 storm than for the 1955 flooding event. Substantial reservoir capacity was added within the basin after the 1955 flood (Table 2.4.1-7), including all reservoirs whose primary purposes are flood control. The June 2006 storm event is relatively recent and consequently represents the present day hydrology of the Delaware River Basin. The 2006 storm is more appropriate for model calibration than the 2005 storm because rainfall totals in the 2006 storm were more uniform over the basin, allowing calibration of all major sub-basins. Translating the June 2006 flood recorded in Trenton downriver to Delaware Bay, hydraulic model results indicate that the maximum river water surface level at the PSEG Site is 4.0 ft. NAVD; predominately as a result of the tidal high water level (further discussed in Subsection 2.4.3), rather than as a result of runoff from the Delaware River Basin.

One of the most severe tracks for a hurricane to cause storm surge in Delaware Bay is a storm moving from the southeast to the northwest. Although storms moving in this direction are rare, the bathymetry and shape of the bay can produce storm surge in response to hurricanes that more commonly make landfall to the west of the bay while traveling in a northward direction. Hurricanes producing severe storm surge at Philadelphia include the Chesapeake-Potomac hurricane of August 1933, Hazel (1954), Connie (1955), Floyd (1999), and Isabel (2003) (References 2.4.2-5, 2.4.2-6, 2.4.2-14, and 2.4.2-19). Hazel made landfall as a Category 4 hurricane near the border of North Carolina (NC) and South Carolina. It then moved north-northeast. Hazel produced a storm surge at Philadelphia of 9.4 ft. Storm surge and seiche events and models are discussed in Subsection 2.4.5.

Historical records of tsunamis reveal a tsunami amplitude of 2.2 ft. at Atlantic City, NJ, resulting from a 1929 earthquake occurring near Grand Banks, Canada (Reference 2.4.2-7). Historic tsunami events and models are discussed in Subsection 2.4.6.

Ice sheets have been reported to form on the Delaware River. However, review of the USACE Cold Regions Research and Engineering Laboratory (CRREL) Ice Jam Database, indicates no record of downstream ice jams causing flooding at the PSEG Site (Reference 2.4.2-15). The most notable ice jam on record causing flooding on the Delaware River occurred March 8, 1904, over 80 miles upstream of the PSEG Site. During that event, the Trenton USGS gage station recorded a peak stage of 29.6 ft. NAVD (Reference 2.4.2-18).

The Delaware River is the longest undammed river east of the Mississippi, extending from the confluence of the East Branch Delaware River and West Branch Delaware River, near Hancock, NY, to the mouth of the Delaware Bay where it meets the Atlantic Ocean (Reference 2.4.2-3). The potential consequences of any significant dam failure of surface-water impoundments on tributaries to the Delaware River are described in Subsection 2.4.4.

2.4.2.2 Flood Design Considerations

Tidal effects within the Delaware River extend upstream to Trenton, 134 RM from the mouth of Delaware Bay. Tidal flows at the PSEG Site range between 400,000 and 472,000 cfs

**PSEG Site
ESP Application
Part 2, Site Safety Analysis Report**

(References 2.4.2-13 and 2.4.2-17). This is approximately 30 times greater than the mean freshwater discharge of the Delaware River near the site. Tides within the Delaware Estuary are semidiurnal (Reference 2.4.2-10). The nearest tidal gage station to the PSEG Site is NOAA's Reedy Point, DE, tidal station, located upstream at RM 59. Mean tidal range at the Reedy Point tidal station is 5.34 ft. (Reference 2.4.2-11). Seasonal variations in the tidal cycle at Reedy Point (Reference 2.4.2-11) show higher msl elevations from April through October, as compared to November through March (Table 2.4.2-3).

Mean sea level trends at Reedy Point are evaluated by NOAA. The upper 95 percent confidence interval for sea level rise, based on monthly msl data, is estimated to be 1.35 feet/century (Reference 2.4.2-12). Flood elevations at the PSEG Site are affected by the regional tidal influences. Tidal variations are addressed in applicable modeling scenarios for determination of the design basis flood (DBF).

The DBF for the PSEG Site is determined by selecting the maximum flood elevation on the Delaware River adjacent to the site. This determination is obtained by considering possible flooding scenarios, singular and in combination, as applicable to the site. Flooding scenarios investigated for the site include:

- Flooding due to PMP on the site (Subsection 2.4.2)
- PMF on rivers and streams (Subsection 2.4.3)
- Potential dam failures (Subsection 2.4.4)
- Maximum surge and seiche flooding (Subsection 2.4.5)
- Probable maximum tsunami (PMT) (Subsection 2.4.6)
- Ice effect flooding (Subsection 2.4.7)
- Channel diversions (Subsection 2.4.9)

Flooding due to underwater landslides is evaluated with the PMT and detailed in Subsection 2.4.6. Each of these flooding scenarios is evaluated in conjunction with other flooding and meteorological events, such as wind-generated waves and/or 10 percent exceedance high tide, in accordance with guidelines provided in Regulatory Guide (RG) 1.59, *Design Basis Floods for Nuclear Power Plants*, 1977 and American National Standards Institute/American Nuclear Society (ANSI/ANS)-2.8-1992, *Determining Design Basis Flooding at Power Reactor Sites* (Reference 2.4.2-1), as detailed in Subsections 2.4.2 through 2.4.7.

Evaluation of the above-referenced flooding scenarios indicates that the DBF for the new plant is the probable maximum surge and seiche associated with the probable maximum hurricane (PMH). As described in Subsection 2.4.5, the DBF includes still water level, 10 percent exceedance high tide, wind setup, and wave runup. The DBF flood level derived from storm surge associated with the PMH, including sea level rise, is elevation 32.1 ft. NAVD. A summary of the types of floods considered and their associated flood levels is presented in Table 2.4.2-4. Results of select flooding events and other relevant elevations are shown on Figure 2.4.2-7. Sea level rise is only added to the worst case flooding scenario to develop a conservative design basis flood.

Floor elevations for safety-related SSC for the new plant will be established to maintain clearance above the DBF, as required by Tier 1 of the DCD for the technology selected. The area surrounding the safety-related SSCs will be graded such that the runoff from the PMP on the site drains away from the structures.

**PSEG Site
ESP Application
Part 2, Site Safety Analysis Report**

2.4.2.3 Effects of Local Intense Precipitation

The design basis for local intense precipitation at the site is the PMP (Reference 2.4.2-1), which is defined as “the theoretically greatest depth of precipitation for a given duration that is physically possible over a particular drainage area at a certain time of year.” The PMP rainfall distribution is determined using procedures outlined in the NOAA Hydrometeorological Reports (HMR) listed in Section 12.1 of ANSI/ANS-2.8-1992 (Reference 2.4.2-1). NOAA publishes maps of PMP rainfall depths for durations ranging from 6 to 72 hours (hr.), and watershed areas ranging from 10 to 20,000 square miles (sq. mi.) (References 2.4.2-8 and 2.4.2-9). Runoff volumes generated by the PMP are determined using the USACE *Hydrologic Engineering Center-Hydrologic Modeling System* (HEC-HMS), version 3.3 (Reference 2.4.2-20).

HEC-HMS is designed to simulate the precipitation-runoff processes in watershed systems. It is applicable to a wide range of geographic areas for modeling a broad range of events. Model input includes subbasin characteristics, conveyance feature characteristics, time of concentration and lag times, U.S. Department of Agriculture Natural Resources Conservation Service runoff curve numbers (Reference 2.4.2-16), existing site topography, and precipitation characteristics (Table 2.4.2-6). The HEC-HMS model is prepared based on current and proposed site information, including existing survey information. The PSEG Site is divided into 12 subbasins (SB). The new plant is located in the SB designated as SB Proposed North and SB Proposed South. Figure 2.4.2-5 shows the SB locations with drainage features, and Figure 2.4.2-6 shows the conceptual layout of the link-node network in the HEC-HMS model. For modeling purposes, it is assumed that most of the new plant slopes north and west, mainly away from the existing facilities (Figure 2.4.2-5). The new plant location is conservatively modeled as impervious; resulting in virtually all of the rainfall (99 percent) converted into runoff.

The PSEG Site is approximately 1-sq. mi., therefore a 1-sq. mi. PMP (also called the ‘point’ PMP) is determined. Figure 2.4.2-3 illustrates the relative size of the 1-sq. mi. and 10-sq. mi. drainage basins for PMP determination at the PSEG Site. PMP depths are used to develop a relationship between rainfall intensity and duration for the PMP. To obtain PMP depths, the 10-sq. mi., 6-hr., all season average PMP depth for the new plant location is determined using data published by NOAA (Reference 2.4.2-8). Next, a range of durations (5 minutes, 15 minutes, 30 minutes, and 60 minutes) for the 1-sq. mi. PMP is calculated using multipliers from the 10-sq. mi., 6-hr. PMP (Reference 2.4.2-9). The multiplier values used for developing the relationship are listed in Table 2.4.2-5, and the trend line is plotted in Figure 2.4.2-4. This linear relationship is then used to determine the 1-sq. mi. 2-hr., and 3-hr. PMP depths.

The resulting 5-minute, 15-minute, 1-hr., 2-hr., 3-hr., and 6-hr. duration PMP depths listed in Table 2.4.2-5 are input into the HEC-HMS model frequency storm option to develop the 6-hr. storm distribution. The 6-hr. storm is selected for this model because this storm provides the highest peak discharge value. A longer storm provides more overall runoff volume but a lower peak discharge. The model assumes the ground is saturated and storage in subbasins is full so that runoff is maximized. The rainfall distribution follows a bell curve where peak rainfall intensity occurs at the center of the curve. The time increment of the peak intensity period with respect to the total storm duration is an input parameter to the model. A time increment of 5 minutes is used for the meteorological data, to coincide with the time step used in the model. Table 2.4.2-7 shows results of the peak discharge from the HEC-HMS model. The resulting peak flows are used to determine the maximum WSEL resulting from the PMP event. This analysis can be refined once a technology is selected and the site grading and drainage systems are designed.

**PSEG Site
ESP Application
Part 2, Site Safety Analysis Report**

A detailed local PMP analysis to establish the maximum WSEL near new plant safety-related SSC is not performed. This analysis cannot be performed until the relevant technology is determined and the grading plan developed. The new plant area will be graded to ensure that PMP runoff drains away from safety-related SSC via overland flow to outfalls that discharge to the Delaware River. The local PMP event will not affect the new plant safety-related facilities.

The location and design of stormwater management systems for the new plant have not been determined for this early site permit application. This will be done as part of detailed engineering design and will be described in the combined license application. In general, the stormwater management system developed for new plant facilities is integrated with the existing facilities. The storm drain system will be designed in accordance with good engineering practice, following all applicable federal, state, and local stormwater management regulations. In addition, site grading will be sufficiently sloped to convey runoff overland from the PMP event, away from all buildings and safety-related equipment, without flooding, even if all culverts, pipe drains, catch basins and roof drains are assumed to be blocked.

2.4.2.4 References

- 2.4.2-1 American National Standards Institute/American Nuclear Society-2.8-1992, "Determining Design Basis Flooding at Power Reactor Sites," American National Standards Institute/American Nuclear Society, 1992.
- 2.4.2-2 Delaware Geological Survey, "The Hurricane of October 21 – 24, 1878," Special Publication No. 22, p. 5, 2002.
- 2.4.2-3 Delaware River Basin Commission, "The Delaware River Basin," Website, <http://www.state.nj.us/drbc/thedrb.htm>, accessed June 17, 2009.
- 2.4.2-4 Delaware River Basin Commission 2007, "Stream River Mileage July 2007," Website, <http://www.state.nj.us/drbc/StreamMileageJuly2007.pdf>, p. 10, 11, 24 – 27, accessed February 16, 2009.
- 2.4.2-5 National Oceanic and Atmospheric Administration, "Effects of Hurricane Floyd on Water Levels Data Report," NOAA Technical Report NOS CO-OPS 027, p. 14, 21, 2000.
- 2.4.2-6 National Oceanic and Atmospheric Administration, "Effects of Hurricane Isabel on Water Levels Data Report," NOAA Technical Report NOS CO-OPS 040, p. 22, 27, 2004.
- 2.4.2-7 National Oceanic and Atmospheric Administration, "Historical Tsunami Database at National Geophysical Data Center," Website, http://www.ngdc.noaa.gov/tsu_db.shtml, accessed June 8, 2009.
- 2.4.2-8 National Oceanic and Atmospheric Administration, HMR 51 1978, "Hydrometeorological Report No. 51, Probable Maximum Precipitation Estimates, United States East of the 105th Meridian," U.S. Department of Commerce, p. 2, 48, 1978.

**PSEG Site
ESP Application
Part 2, Site Safety Analysis Report**

- 2.4.2-9 National Oceanic and Atmospheric Administration, HMR 52 1982, "Hydrometeorological Report No. 52, Application of Probable Maximum Precipitation Estimates, United States East of the 105th Meridian," U.S. Department of Commerce, p. 78, 94 – 96, 1982.
- 2.4.2-10 National Oceanic and Atmospheric Administration, "Reedy Point (8551910) Historic Tide Data," Website, http://tidesandcurrents.noaa.gov/data_menu.shtml?stn=8551910%20Reedy%20Point,%20DE&type=Historic+Tide+Data, accessed June 17, 2009.
- 2.4.2-11 National Oceanic and Atmospheric Administration, 1996 – 2008, "Reedy Point Tidal Data," Website, http://tidesandcurrents.noaa.gov/station_info.shtml?stn=8551910%20Reedy%20Point,%20DE, accessed February 2, 2009.
- 2.4.2-12 National Oceanic and Atmospheric Administration, "Sea Level Trends Online, 8551910 Reedy Point, Delaware," Website, http://tidesandcurrents.noaa.gov/sltrends/sltrends_station.shtml?stnid=8551910, accessed April 27, 2009.
- 2.4.2-13 U.S. Army Corp of Engineers, "Delaware River Main Channel Deepening Project Design Memorandum," Philadelphia District, Philadelphia, Pennsylvania, p. 55 – 60, 1996.
- 2.4.2-14 U.S. Army Corp of Engineers, "Hurricane Surge Predictions for Delaware Bay and River, Miscellaneous Paper No. 4-59," Beach Erosion Board, p. 8 – 9, 1959.
- 2.4.2-15 U.S. Army Corp of Engineers, "Ice Jam Database," Website, <https://rsgis.crrel.usace.army.mil/icejam/>, accessed June 9, 2009.
- 2.4.2-16 U.S. Department of Agriculture, Soil Conservation Service, Urban Hydrology for Small Watersheds (Technical Release 55), June 1986.
- 2.4.2-17 U.S. Environmental Protection Agency, "Case Study Analysis for the Proposed Section 316(b) Phase II Existing Facilities Rule," Part B, EPA-821-R-02-002, p. B1-1, B1-6, February 2002.
- 2.4.2-18 U.S. Geological Survey, "USGS Stream Gage 01463500 Delaware River at Trenton, NJ," Website, http://waterdata.usgs.gov/nj/nwis/uv/?site_no=01463500&PARAMeter_cd=00065,00060, accessed April 24, 2009.
- 2.4.2-19 U.S. Navy (2008), "Hurricane Havens Handbook," last modified November 2008, Website, <http://www.nrlmry.navy.mil/~cannon/tr8203nc/0start.htm>, accessed June 10, 2009
- 2.4.2-20 U.S. Army Corps of Engineers, HEC-HMS 3.3 Software, Website, <http://www.hec.usace.army.mil/software/hec-hms/download.html>, accessed February 23, 2009.

**PSEG Site
ESP Application
Part 2, Site Safety Analysis Report**

**Table 2.4.2-1
Events Resulting in Storm Surges in the Delaware River near the PSEG Site**

Storm Event	Year	Estimated Storm Surge, ft. ^(a)		Reference
		Reedy Point	Philadelphia	
Hurricane of 1878	1878	5 to 8	5 to 8	2.4.2-2
Chesapeake-Potomac Hurricane	1933	7.7	7.1	2.4.2-14
Hurricane Hazel	1954	n.a. ^(b)	9.4	2.4.2-19
Hurricane Connie	1955	n.a. ^(b)	5.0	2.4.2-19
Hurricane Floyd	1999	2.9	4.0	2.4.2-5
Hurricane Isabel	2003	5.0	5.4	2.4.2-6

a) surge above predicted tide

b) n.a. = not available

References 2.4.2-2, 2.4.2-5, 2.4.2-6, 2.4.2-14, and 2.4.2-19

**PSEG Site
ESP Application
Part 2, Site Safety Analysis Report**

**Table 2.4.2-2
Peak Discharge for USGS Gage 01463500 on the Delaware River at Trenton, NJ**

Water Year	Date	Flow (cfs)	Gage Height NAVD (ft.)	Water Year	Date	Flow (cfs)	Gage Height NAVD (ft.)
1900	March 2, 1900	104,000	--	1954	December 8, 1953	46,300	12.74
1901	March 22, 1901	77,600	--	1955	August 20, 1955	329,000	27.55
1902	March 2, 1902	214,000	22.6	1956	October 17, 1955	133,000	18.65
1903	March 1, 1903	134,000	--	1957	April 7, 1957	77,500	15.13
1904	October 11, 1903	295,000	27.5 ^{a)}	1958	December 22, 1957	108,000	17.19
1905	March 28, 1905	88,500	-	1959	January 23, 1959	84,800	15.65
1906	April 16, 1906	112,000	--	1960	April 5, 1960	124,000	18.13
1907	January 26, 1907	--	15.8	1961	February 27, 1961	96,600	16.44
1908	December 12, 1907	--	17.4	1962	April 2, 1962	67,100	14.38
1909	February 21, 1909	--	16.7	1963	March 28, 1963	87,300	15.82
1910	April 23, 1910	--	17.4	1964	March 11, 1964	80,900	15.37
1911	January 5, 1911	--	14.6	1965	February 8, 1965	48,700	12.94
1912	March 16, 1912	--	17.7	1966	March 7, 1966	33,100	11.53
1913	March 28, 1913	160,000	20.1	1967	March 7, 1967	47,500	12.83
1914	March 29, 1914	143,000	19.2	1968	May 31, 1968	68,300	14.47
1915	February 26, 1915	85,000	--	1969	July 29, 1969	83,100	15.53
1916	April 3, 1916	93,800	16.3	1970	April 3, 1970	100,000	16.66
1917	March 29, 1917	90,600	16.0	1971	August 28, 1971	66,400	14.33
1918	October 31, 1917	89,100	15.9	1972	June 23, 1972	103,000	16.81
1919	July 22, 1919	69,200	14.6	1973	June 30, 1973	135,000	18.73
1920	March 14, 1920	121,000	18.0	1974	December 22, 1973	119,000	17.85
1921	March 11, 1921	108,000	17.2	1975	February 26, 1975	94,600	16.30
1922	November 30, 1921	105,000	17.0	1976	January 28, 1976	113,000	17.47
1923	March 24, 1923	74,800	15.0	1977	March 15, 1977	117,000	17.70
1924	April 8, 1924	132,000	18.6	1978	January 10, 1978	89,500	16.21
1925	February 13, 1925	154,000	19.8	1979	January 25, 1979	117,000	17.65
1926	April 10, 1926	48,100	12.92	1980	March 21, 1980	104,000	16.78
1927	November 18, 1926	123,000	18.02	1981	February 13, 1981	79,900	15.12
1928	October 20, 1927	116,000	17.63	1982	April 5, 1982	54,900	13.34
1929	March 16, 1929	84,800	15.65	1983	April 17, 1983	138,000	18.84
1930	March 10, 1930	47,400	12.80	1984	May 30, 1984	152,000	19.59
1931	March 30, 1931	53,200	13.32	1985	September 28, 1985	87,200	15.63
1932	April 2, 1932	66,100	14.35	1986	March 16, 1986	140,000	19.17
1933	August 25, 1933	147,000	19.38	1987	April 6, 1987	90,700	16.38
1934	March 6, 1934	80,000	15.37	1988	March 28, 1988	40,600	12.32
1935	July 10, 1935	129,000	18.46	1989	May 7, 1989	83,300	15.90
1936	March 19, 1936	227,000	23.38	1990	October 21, 1989	76,700	15.40
1937	February 23, 1937	74,200	14.88	1991	November 12, 1990	64,900	14.45
1938	September 23, 1938	125,000	18.17	1992	June 6, 1992	46,800	12.93
1939	December 7, 1938	99,500	16.58	1993	April 2, 1993	109,000	17.58
1940	April 1, 1940	151,600	19.57	1994	April 15, 1994	75,600	15.31
1941	April 7, 1941	56,800	13.47	1995	March 10, 1995	49,300	13.15
1942	May 24, 1942	161,200	20.07	1996	January 20, 1996	179,000	21.15
1943	January 1, 1943	118,900	17.72	1997	December 3, 1996	101,000	16.82
1944	November 10, 1943	78,000	15.19	1998	May 12, 1998	69,500	14.62
1945	July 21, 1945	82,200	15.47	1999	September 16, 1999	112,000	17.48
1946	May 29, 1946	82,300	15.46	2000	February 29, 2000	62,400	14.07
1947	April 7, 1947	98,500	16.32	2001	December 19, 2000	80,100	15.40
1948	March 23, 1948	125,600	18.01	2002	May 15, 2002	43,400	12.47
1949	January 1, 1949	139,100	18.78	2003	March 22, 2003	83,100	15.61
1950	April 6, 1950	79,800	15.32	2004	September 19, 2004	201,000	22.36
1951	April 1, 1951	133,200	18.67	2005	April 4, 2005	242,000	24.28
1952	July 11, 1952	95,400	16.36	2006	June 29, 2006	237,000	24.04
1953	December 12, 1952	139,000	19.02	2007	April 17, 2007	116,000	17.77

a) The maximum gage height at Trenton, NJ in water year 1904 was not the result of peak streamflow (which was 27.5 ft. NAVD and occurred on October 11, 1903). The maximum gage height during water year 1904 at Trenton, NJ of 29.6 ft. NAVD occurred as a result of an ice jam on March 8, 1904. A hydrologic water year runs from October through September and is designated by the calendar year in which it ends.

Reference 2.4.2-18; Data gaps reflect gaps in USGS record and significant figures reflect USGS reporting.

**PSEG Site
ESP Application
Part 2, Site Safety Analysis Report**

**Table 2.4.2-3
Reedy Point MSL^(a) Elevation Monthly Variation, 1987 – 2008**

Month	msl (ft.)
January	-0.40
February	-0.39
March	-0.20
April	0.07
May	0.19
June	0.17
July	0.16
August	0.24
September	0.32
October	0.14
November	-0.12
December	-0.33

a) msl = mean sea level ft., NAVD

Reference 2.4.2-10

**PSEG Site
ESP Application
Part 2, Site Safety Analysis Report**

**Table 2.4.2-4
PMF Determination in Accordance with ANSI/ANS-2.8-1992
“Determining Design Basis Flooding at Power Reactor Sites”**

Type of Flooding	SSAR Subsection	Max. WSEL (ft. NAVD)
Local PMP	2.4.2	(a)
PMF on Streams and Rivers	2.4.3	21.0
Potential Dam Failures	2.4.4	9.4
PMS and Seiche Flooding	2.4.5	32.1
Probable Maximum Tsunami	2.4.6	5.7
Ice Effects	2.4.7	8.1
Channel Diversions	2.4.9	n.a. ^(b)

a) WSEL depends on the stormwater drainage system design for the new plant and cannot be evaluated until the reactor technology is selected and the site grading plan, which is dependent of the selected technology, is developed.

b) n.a. = not applicable

**PSEG Site
ESP Application
Part 2, Site Safety Analysis Report**

**Table 2.4.2-5
PMP Values for Point Rainfall at the PSEG Site**

Duration	Watershed Area, sq. mi.	Multiplier	Applied to	Source	PMP Depth (in.)
6 hours ^(a)	10	n.a. ^(b)	n.a. ^(b)	HMR-51, Fig 18 (2.4.2-8)	27.4
3 hours ^(a)	1	n.a. ^(b)	n.a. ^(b)	Fig 2.4.2-2	23.6
2 hours ^(a)	1	n.a. ^(b)	n.a. ^(b)	Fig 2.4.2-2	21.5
1 hour ^(a)	1	0.67	6-hr. 10 sq. mi. value	HMR-52, Fig 23 (2.4.2-9)	18.4
30 minutes	1	0.753	1-hr. 10 sq. mi. value	HMR-52, Fig 38 (2.4.2-9)	13.9
15 minutes ^(a)	1	0.525	1-hr. 10 sq. mi. value	HMR-52, Fig 37 (2.4.2-9)	9.7
5 minutes ^(a)	1	0.334	1-hr. 10 sq. mi. value	HMR-52, Fig 36 (2.4.2-9)	6.1

a) Required input for the HEC-HMS frequency storm meteorologic model.

b) n.a. = not applicable

References 2.4.2-8 and 2.4.2-9

**PSEG Site
ESP Application
Part 2, Site Safety Analysis Report**

**Table 2.4.2-6
HEC-HMS Input Parameters for PMP^(a)**

Subbasin	Subbasin Area (sq. mi.)	Lag Time (minutes)
SB 1	0.016	6.14
SB 2	0.091	18.6
SB 3	0.070	14.7
SB 4	0.039	11.7
SB 5	0.032	7.72
SB 6	0.036	11.2
SB 7	0.110	10.2
SB 8	0.042	11.5
SB 9	0.225	29.9
SB 10	0.392	28.6
SB Proposed North	0.069	9.20
SB Proposed South	0.025	7.42

a) The SCS runoff curve number for all subbasins is 98

**PSEG Site
ESP Application
Part 2, Site Safety Analysis Report**

**Table 2.4.2-7
HEC-HMS Results for PMP**

Subbasin	Peak Discharge (cfs)
SB 1	423
SB 2	1560
SB 3	1320
SB 4	820
SB 5	827
SB 6	780
SB 7	2390
SB 8	889
SB 9	2970
SB 10	5320
SB Proposed North	1600
SB Proposed South	646

**PSEG Site
ESP Application
Part 2, Site Safety Analysis Report**

2.4.3 PROBABLE MAXIMUM FLOOD ON STREAMS AND RIVERS

In this subsection, the hydrometeorological design basis is developed to determine the extent of flood protection required for those safety-related SSC necessary to ensure the capability to shut down the reactor and maintain it in a safe shutdown condition. The PMF on streams and rivers is investigated to determine peak WSEL in the Delaware River near the new plant location. The PMF on streams and rivers is the hypothetical flood “that is considered to be the most severe reasonably possible, based on comprehensive hydrometeorological application of PMP and other hydrologic factors favorable for maximum flood runoff such as sequential storms and snowmelt” (Reference 2.4.3-1).

This subsection presents the calculated maximum WSEL at the PSEG Site based on the PMF. The methods used to determine the PMF follow ANSI/ANS-2.8-1992 (Reference 2.4.3-1); and NRC RG 1.59.

The Delaware River Basin drains to the Atlantic Ocean and is located in portions of five states: Pennsylvania (PA), New York (NY), New Jersey (NJ), Maryland (MD), and Delaware (DE). The basin is 13,600 square miles (sq. mi.) (Reference 2.4.3-4). The river is tidally influenced up to the U.S. Geological Survey (USGS) Gage Station 01463500, at Trenton, NJ, located at river mile (RM) 134 (Reference 2.4.3-16).

The new plant location is at RM 52, north of the existing HCGS, on the PSEG Site. The new plant is located on the shoreline of the Delaware River, where tidal fluctuations have a dominant effect on water levels under normal meteorological conditions, but severe precipitation in the basin and hurricanes can also affect water levels. The overall Delaware River Basin watershed is depicted in Figure 2.4.3-1. Floor elevations for safety-related SSC for the new plant will be established to maintain clearance above the design basis flood, as required by Tier 1 of the design control document for the technology selected. The area surrounding the safety-related SSC will be graded such that the runoff from the PMP on the site drains away from the structures.

2.4.3.1 Design Bases for Flooding in Streams and Rivers

This subsection presents the simulation details and results of the PMF analysis. Three different methods are used to determine the PMF. Two of the methods simulate river flood levels resulting from two different PMP events. The third method determines the PMF flood level using the Approximate Method from NRC RG 1.59. The resulting PMF water levels are then combined with other flood-producing events which may occur simultaneously. The highest water level at the plant location resulting from these three methods is considered the PMF.

Two potential PMP events are developed using NOAA HMR Number (No.) 51 and No. 52 (References 2.4.3-8 and 2.4.3-9). The first of the two potential PMP events evaluated is designed to yield maximum rainfall throughout the Delaware River Basin. The second potential PMP event is designed to yield more intense rainfall in the portion of the basin near and upstream of the new plant location.

- Flooding is simulated for PMP of a 15,000 sq. mi. storm centered over Doylestown, PA, oriented to produce maximum total rainfall within the Delaware River Basin (Reference 2.4.3-1).

**PSEG Site
ESP Application
Part 2, Site Safety Analysis Report**

- Flooding is simulated for PMP of a 2150 sq. mi. storm centered over Philadelphia, PA, oriented to produce more intense rainfall in the portion of the lower Delaware River Basin upstream of the new plant location (Reference 2.4.3-1).

Of these two PMP events, the one resulting in the highest water levels at the new plant location is selected to simulate a PMF. Alternatively, a PMF is determined using discharge from the Approximate Method from NRC RG 1.59, Appendix B. Of these two simulations, the one producing the highest water levels at the new plant, without tidal influence, is identified as the PMF.

Once the PMF is defined, additional calculations are performed to address a reasonable combination of flooding events to arrive at DBF conditions comparable in frequency of occurrence with a PMF in accordance with RG 1.59. The PMF can affect water levels at the new plant location, but tide and storm surge have been observed to have a greater effect than precipitation events. ANSI/ANS-2.8-1992 (Reference 2.4.3-1) is used to determine a conservative combination of events to establish the flood level associated with the PMF event. Section 9.2.2 of ANSI/ANS-2.8-1992 describes three alternatives that include PMF events, Alternatives I, II, and IV. Alternative IV is not evaluated because the drainage area is greater than 300 sq. mi. The combined events simulated for the new plant location include:

Alternative I

- One-half PMF or 500-year flood, whichever is less
- Surge and seiche from the worst regional hurricane or windstorm with wind-wave activity
- 10 percent exceedance high tide

Analysis of Alternative I is described in Subsection 2.4.3.1.3.1.

Alternative II

- PMF
- 25-year surge and seiche with wind-wave activity
- 10 percent exceedance high tide

Analysis of Alternative II is described in Subsection 2.4.3.1.3.2.

Simulation of the PMF is performed using the USACE HEC-HMS (Reference 2.4.3-18) and the USACE *Hydrologic Engineering Center River Analysis System* (HEC-RAS) (Reference 2.4.3-19) modeling software. HEC-HMS is used to calculate PMF discharge to the Delaware River from the watershed. Results of the HEC-HMS models are then applied as inputs to the HEC-RAS model, which simulates hydraulic processes within the Delaware River, routing subbasin runoff downstream for determination of maximum WSEL at the new plant location. To develop the combined events simulations, inputs into the HEC-RAS model include the 10 percent exceedance high tide and surge and seiche. Wind-wave activity is calculated in accordance with the USACE *Coastal Engineering Manual* (Reference 2.4.3-14).

**PSEG Site
ESP Application
Part 2, Site Safety Analysis Report**

2.4.3.1.1 Identification and Analysis of the Probable Maximum Flood

2.4.3.1.1.1 Alternative Probable Maximum Precipitation Events

As part of the analysis carried out for stream and river flooding at the new plant location, PMF discharge for the Delaware River at this location are determined using the PMP events described in Subsection 2.4.3.1. To determine the resultant flooding for these PMP events, a local PMP depth is obtained, the PMP event is centered over two different locations, models are developed for each PMP centered storm and the average precipitation depth is extrapolated from the 72 hour event to a 96-hr event.

Estimates of local PMP depths are obtained from PMP isohyets published in NOAA HMR No. 51 (Reference 2.4.3-8). Maps of PMP rainfall depths are published for durations ranging from 6 to 72 hr. and for storm areas ranging from 10 to 20,000 sq. mi. (Reference 2.4.3-8).

Two PMP events are modeled for the PSEG Site. The first PMP event is centered over the Delaware River Basin (Figure 2.4.3-2) near Doylestown, PA, while the second is centered in the upper estuary portion of the Delaware River at Philadelphia, PA (Figure 2.4.3-3). All storm spatial distributions are performed based on procedures in NOAA HMR No. 52 (Reference 2.4.3-9). The size and orientation of the storm for each PMP event are adjusted to maximize the average depth of rainfall within the basin.

The PMP analysis for the isohyets centered over Doylestown indicates that the greatest storm volume is produced by a 15,000 sq. mi. storm with an orientation of 222 degrees (deg) relative to north azimuth. This results in an average precipitation depth of 12.1 in. over a 72-hr. period. This storm produces an average depth of 4.3 in. during the first 6 hrs. (Table 2.4.3-1).

The selection of the storm size for the upper estuary portion of the Delaware River Basin is determined based on the average depth of rain in the subbasins contributing to the upper estuary portion of the Delaware River. Limiting the storm to the upper estuary simulates a more intense, localized event. The PMP analysis for the isohyets centered over Philadelphia indicates that the greatest storm depth is produced by a 2150 sq. mi. storm with an orientation of 263 degrees; resulting in an average depth of 22.2 in. over the portion of the basin within isohyet K, as shown on Figure 2.4.3-3, over a 72-hr. period; with an average depth of 11.3 in. occurring within isohyet K in the first 6 hrs. (Table 2.4.3-1).

A 96-hr. storm precipitation depth for each simulation is determined by extrapolating the rainfall data obtained from NOAA HMR No. 52 (Reference 2.4.3-9 and Figure 2.4.3-4). Center-weighted hourly PMP hyetographs are developed for both events based on a typical rainfall event distribution (Figures 2.4.3-5 and 2.4.3-6). The precipitation depth is input into HEC-HMS and spatially weighted for each subbasin.

2.4.3.1.1.2 Basin Discharge

HEC-HMS is used to determine a runoff hydrograph for the Delaware River Basin as a result of each PMP event (Reference 2.4.3-18). HEC-HMS modeling is performed using the Natural Resources Conservation Service (NRCS) (formerly known as the Soil Conservation Service) method for calculating runoff for the PMP events. The resulting discharge hydrographs are used as input to the HEC-RAS model.

**PSEG Site
ESP Application
Part 2, Site Safety Analysis Report**

The parameters used in the hydrologic model, including subbasin delineation and drainage patterns, precipitation losses, runoff response and attenuation, antecedent moisture conditions (AMC), and base flows are summarized further in this subsection.

Runoff is generated by precipitation falling onto subbasins (watersheds). Subbasin maps obtained from the DRBC Geographic Information System (GIS) at the 11-digit hydrologic unit code (HUC 11) level of resolution are used to define subbasin areas and boundaries. For modeling purposes, the Delaware River Basin is split into the non-tidal upper Delaware River Basin (upstream from Trenton), and the tidally-influenced lower Delaware River Basin (downstream from Trenton). Subbasins range in size from 1 sq. mi. to 676 sq. mi. Inflow is set equal to outflow for all reservoirs and in all subbasins during the PMP events to conservatively eliminate storage and peak discharge attenuation.

The NRCS method is used in HEC-HMS to determine subbasin precipitation losses and time of concentrations for the subbasins. Precipitation losses are determined using the runoff curve numbers developed from the land use codes provided by the USGS, and the soil survey information available from the NRCS. The runoff curve numbers control the portion of the precipitation amount that runs off to streams and rivers. In order to represent sequential storms, AMC III curve numbers are used. AMC III curve numbers represent ground that is nearly saturated, consistent with more than 2 in. of antecedent rainfall within 5 days of the PMP events. This AMC produces greater runoff volume, discharge, and higher Delaware River water levels for the PMP event.

Reach routing within the Delaware River Basin is modeled for the Delaware River and upland watershed tributaries. Routing through upland tributaries affects the timing of discharges to the Delaware River due to the PMP event. The lag method is used for reach routing, which translates floodwave hydrographs without any representation of attenuation or diffusion processes and is, therefore, conservative (Reference 2.4.3-18).

Prior to the PMP event, upland tributaries are assumed to flow at an average rate. Monthly base flow values are calculated by averaging available USGS stream flow gage data for available stations to determine an average monthly stream flow. Average monthly stream flow values are multiplied by the base flow index established by the USGS (Reference 2.4.3-20) to determine monthly average base flow values. These values are then used as initial discharge values for HEC-HMS flood simulations.

2.4.3.1.1.3 Delaware River Hydraulics

The HEC-RAS model is used to route the runoff through the Delaware River (Reference 2.4.3-19). This model is developed using channel geometry and floodplain elevations for the Delaware River. Bathymetry and floodplain topographic information for portions of the Delaware River from the Trenton, NJ, USGS gage station (RM 134) to the Lewes, DE, NOAA tidal gage station (RM 0) (Reference 2.4.3-5), are extrapolated from the Triangular Irregular Network (TIN) terrain model. The TIN terrain model is developed from the USGS National Elevation Dataset (Reference 2.4.3-22) digital elevation model (DEM), the NOAA Estuarine Bathymetry DEM (Reference 2.4.3-11), USGS quad sheets (Reference 2.4.3-21), and the USACE Bathymetry Data (Reference 2.4.3-17). Figure 2.4.3-7 shows a cross-section of the Delaware River at RM 52 (the PSEG Site). The Manning's n coefficients in the HEC-RAS model for the lower Delaware River are calibrated using astronomical tide data and stage-discharge data for Trenton. These n

**PSEG Site
ESP Application
Part 2, Site Safety Analysis Report**

values range from 0.013 to 0.027. Discharge hydrographs from the individual drainage areas (developed in HEC-HMS for the PMP events) define the discharge inputs to the HEC-RAS model, and the resultant flooding at the new plant location for each PMP event is simulated without tidal influence, for each PMP input.

In addition to the two HEC-HMS simulated PMP flood events, a third flood event alternative estimate of discharge for the PMF is determined by the Approximate Method. The Approximate Method, as outlined in NRC RG 1.59, Appendix B, applies to nontidal streams and consists of interpolating the PMF isoline discharge map for regions of the United States east of the 105th meridian as a function of drainage area. Figure 2.4.3-8 depicts this linear interpolation at the PSEG Site, which results in a discharge of 1,130,000 cfs. The discharges determined by the Approximate Method are input to the HEC-RAS hydraulic model to determine the effect of those discharges on water levels at the new plant location.

Table 2.4.3-2 shows the Delaware River discharge and resultant water levels for the three alternative methods of determining the PMF, without tidal influence, at the Trenton USGS gage station (RM 134), the new plant (RM 52), and Lewes NOAA tidal gage station (RM 0) (Reference 2.4.3-5). Comparative analysis of the results of the three alternative methods for estimating the PMF, without tidal influence, indicates that the highest WSEL at the new plant location results from the PMP centered over the upper estuary (Philadelphia, PA).

2.4.3.1.2 Coincident Wave Runup

Coincident wave runup in association with the 25-year surge and seiche is determined using procedures described by USACE *Coastal Engineering Manual* (Reference 2.4.3-14). Winds coincident with the maximum surge of the 1933 hurricane are determined at the new plant location using information provided by Bretschneider (Reference 2.4.3-2) and procedures described by NOAA (Reference 2.4.3-10). These winds are determined to be 43 miles per hour (mph) from the east-southeast at the new plant location, coincident with the maximum surge from the simulated storm. Water depth is determined from the TIN terrain model using coincident calculated water levels. The wave field is fetch- and duration-limited, as defined by USACE (Reference 2.4.3-14). Wind vectors are averaged over the time required for the wave heights to reach steady-state as specified by USACE (Reference 2.4.3-14). The smaller of the maximum wave height or the maximum breaker height is used to determine runup, as described in Sections 7.4.3 and 7.4.4.5 of ANSI/ANS-2.8-1992 (Reference 2.4.3-1). The new plant facilities are assumed to be constructed on engineered fill at a 3 (horizontal):1 (vertical) slope, or flatter, with the slope protected by riprap.

2.4.3.1.3 Combined Events

Following determination of the PMF, simulations of the combined events Alternatives I and II, from Section 9.2.2.2 of ANSI/ANS-2.8-1992, are performed (Reference 2.4.3-1). Although these events exceed ANSI/ANS 2.8 requirements for this analysis, they are simulated to provide conservative maximum WSEL associated with the PMF, which is not the DBF.

**PSEG Site
ESP Application
Part 2, Site Safety Analysis Report**

2.4.3.1.3.1 Alternative I

Alternative I is simulated to determine the maximum WSEL resulting from the one-half PMF or 500-year flood, whichever is less, combined with the 10 percent exceedance high tide and surge and seiche from the worst regional hurricane or windstorm with wind-wave activity.

To calculate the discharge hydrograph for one-half of the PMF, the discharge hydrographs for the HEC-HMS simulation of the PMP centered over the upper estuary are multiplied by 0.5 (one-half), and set up as lateral inflow hydrographs for the HEC-RAS simulation. The 500-year flood results in a lower water surface elevation at the new plant than one-half the PMF (Subsection 2.4.4.2). The one-half PMF is used in this simulation to provide a conservative estimate of water surfaces resulting from the PMF. Even using conservative assumptions, this scenario does not provide the DBF. The 10 percent exceedance high tide is incorporated into HEC-RAS as a downstream boundary condition. Maximum monthly high tide values from 1987 through 2008 are analyzed to determine the 10 percent exceedance high tide (Reference 2.4.3-7) in accordance with ANSI/ANS-2.8-1992 (Reference 2.4.3-1). The 10 percent exceedance high tide is 4.2 ft. NAVD at Lewes NOAA tide gage 8557380 (RM 0), and 4.6 ft. NAVD for NOAA tide gage 8551910 (RM 59) located at Reedy Point. From these values, the resulting 10 percent exceedance high tide at the new plant location (RM 52) is determined by linear interpolation to be 4.5 ft. NAVD. The maximum WSEL resulting from the one-half PMF and the 10 percent exceedance high tide, determined using the HEC-RAS model, is 6.6 ft.

Maximum historical surge and seiche activity is determined by reviewing the four worst regional historical storm events. These storm events are associated with hurricanes, which exceed surge and seiche values associated with other wind storms, and therefore are the more conservative analysis approach. Three of the events have water elevation data at Philadelphia and Reedy Point gage stations. There is data at the Philadelphia gage station for the worst hurricane event, Hurricane Hazel, but none at Reedy Point or downstream (Table 2.4.3-3). To determine the surge at Reedy Point for Hurricane Hazel, the surge at Philadelphia is multiplied by a 95 percent confidence limit adjustment factor of 20 percent (Table 2.4.3-3). This results in the maximum historical surge at Reedy Point totaling 11.3 ft. Coincident wave runup, calculated as described in Subsection 2.4.3.1.2, is 3.1 ft.

This combination of events, defined by Alternative I, produces a maximum WSEL at the PSEG Site of 21.0 ft. NAVD (Table 2.4.3-4). The components of this total include one-half the PMF with 10 percent exceedance high tide, 6.6 ft. NAVD, surge and seiche from the worst regional hurricane, 11.3 ft., and coincident wave runup, 3.1 ft. The stage hydrograph at the PSEG Site for the combined events of the Alternative I simulation with each component illustrated is presented in Figure 2.4.3-9.

2.4.3.1.3.2 Alternative II

Combined events Alternative II is simulated to determine the maximum WSEL resulting from the PMF, combined with 10 percent exceedance high tide, and the 25-year surge and seiche with wind-wave activity.

The 10 percent exceedance high tide downstream boundary condition is simulated in HEC-RAS to produce a maximum WSEL of 4.5 ft. NAVD at the new plant. The PMF discharge hydrographs for the HEC-HMS simulation of the PMP centered over the upper estuary are

**PSEG Site
ESP Application
Part 2, Site Safety Analysis Report**

entered into the HEC-RAS simulation as lateral inflow hydrographs. The combination of the downstream boundary condition of 10 percent exceedance high tide (4.5 ft. NAVD) and the PMF lateral inflows produce a maximum WSEL at the new plant of 7.3 ft. NAVD. Combining the inflow and downstream boundary condition in HEC-RAS changes the magnitude of the PMF at the site.

The 25-year surge and seiche is determined using the Chesapeake-Potomac hurricane of 1933. The 1933 hurricane is described in detail by Bretschneider (Reference 2.4.3-2). Its maximum water surface elevation, 8.3 ft. NAVD (Figure 2.4.5-4) surge exceeds the estimated 25-year recurrence interval surge and seiche of 5.7 ft. NAVD, at Reedy Point, DE, near the new plant location (Reference 2.4.3-15). For a conservative approach, the 1933 hurricane surge plus 10 percent exceedance high tide is used as the downstream boundary condition in the HEC-RAS model. This 1933 hurricane is described in greater detail in Subsection 2.4.5.2.1. The HEC-RAS simulation of the PMF and 10 percent exceedance high tide plus the 25-year surge and seiche produces a maximum WSEL at the new plant of 13 ft. NAVD. Coincident wave runoff on a 3 (horizontal):1 (vertical) slope or flatter with riprap, in association with the 25-year surge and seiche, is determined to be 3.1 ft. Coincident wave runoff is calculated using the methodology described in Subsection 2.4.3.1.2.

This combination of events, defined by Alternative II, produces a maximum WSEL at the PSEG Site of 16.1 ft. NAVD (Table 2.4.3-5). The simulated components of this total are 4.5 ft. from the 10 percent exceedance high tide, plus an additional 2.8 ft. from the simulated PMF, plus 5.7 ft. from the simulation of the surge and wind setup from the 25-year hurricane. The coincident wave runoff, 3.1 ft., is added to the HEC-RAS modeled output. The stage hydrograph at the new plant for the combined events of the Alternative II simulation with each component illustrated is presented in Figure 2.4.3-10.

2.4.3.2 Design Basis for Site Drainage

The existing topography in the vicinity of the new plant location is low and flat, with an elevation ranging from 5 to 15 ft. NAVD (Reference 2.4.3-6). The maximum WSEL determined in this subsection is 21.0 ft. NAVD (Table 2.4.3-4). The grade elevation for the new plant will be set at a level that provides for clearance above the DBF, as required by Tier 1 of the DCD for the selected technology. The new plant location will be graded to ensure that runoff drains away from safety-related SSC via overland flow to outfalls that discharge to the Delaware River. At the new plant elevation, debris and waterborne projectiles are not expected to come into contact with safety-related SSC other than the intake structure. The intake structure will be designed to protect it from debris resulting from the PMF.

2.4.3.3 Effects of Sediment Erosion and Deposition

Water velocities determined by the HEC-RAS model simulation of the PMF may exceed 7 feet per second (ft/sec) in Delaware Bay. Normal tidal velocities approach 3 ft/sec. Suspended sediment concentrations in Delaware Bay were observed by Cook (Reference 2.4.3-3). These values routinely range from 450 to 525 milligrams per liter (mg/L) near the bottom of the water column during flood and ebb periods in the tidal cycle. The value of the critical velocity (resuspension velocity) for the bay was estimated to be 30 centimeters per second (cm/s) +/- 8 cm/s (0.98 ft/sec +/- 0.23 ft/sec). Therefore, at typical water velocities in the bay, resuspension

**PSEG Site
ESP Application
Part 2, Site Safety Analysis Report**

does occur. Safety-related SSC will be protected against erosion and deposition that could affect the integrity of those facilities.

Having determined that sediment resuspension occurs during the hypothetical PMF, the next step is to determine to what extent resuspension occurs during a major flood. Several studies indicate that total suspended solids (TSS) concentrations increase by an order of magnitude (factor of 10) during severe storm events (Reference 2.4.3-3). Applying this factor to typical TSS levels in the Delaware Bay (450 to 525 mg/L) gives a conservative estimate of 5000 mg/L of TSS during a PMF.

The next step is to determine the deposition rate and flow patterns resulting in the most deposition in the vicinity of the PSEG Site intake structures. During the flood, while water velocities are still greatly elevated, deposition does not occur because water velocities keep sediment in suspension. Deposition occurs when the storm and tide weaken, water velocities slow, and the larger particles begin to drop out.

A conservative assumption is that all of the excess TSS drop out of the water and are uniformly distributed across the area near the intake structure. There is no temporal aspect to this analysis because over time water tends to deposit sediment uniformly, so any water entering this area at a later time has already deposited some of its sediment load, just as any water leaving the system at a later time still has some sediment load left to deposit.

The volume of water analyzed conservatively represents 10.3 pounds of sediment deposited per square foot due to the PMF, with the settled material having a bulk density of 112 pounds per cubic foot, representing 0.09 cubic feet of deposition per square foot. This translates to 1.1 in. of deposition per square foot near the intake structure. This is not a significant accumulation or a threat to the operation of any safety-related SSC.

Based on extended operating experience at the Hope Creek service water intake structure, which is of similar design to the intake structure at the new plant, short-term sedimentation events have not impacted the operation of the intake. Similarly, long-term sedimentation has required very limited periodic maintenance dredging. The approach to the Hope Creek service water intake structure is dredged approximately once every ten years. Desilting of the intake structure in the intake bays is performed routinely. It is anticipated that the new plant's intake structure will require similar maintenance programs to mitigate any effects of sedimentation.

2.4.3.4 Conclusions

Two PMP events are simulated to determine the PMF. Based on the results of these simulations, a PMP event centered over the upper estuary (Philadelphia, PA) produces the PMF maximum WSEL at the new plant location. The combined effects of coincident stream flooding due to precipitation, high tides, and a hurricane storm surge are evaluated in this subsection, using two alternative combinations of extreme flood-producing events, as defined by ANSI/ANS-2.8-1992 (Reference 2.4.3-1). Of these two alternatives, the coincident effects of one-half of the PMF, coincident with the 10 percent exceedance high tide, and the additional effects of the storm surge from the worst regional hurricane, and coincident wave runup, results in a flood elevation of up to 21.0 ft. NAVD at the PSEG Site.

**PSEG Site
ESP Application
Part 2, Site Safety Analysis Report**

The flood elevations determined in this subsection are less than the maximum WSEL from the storm surge associated with the PMH evaluated in Subsection 2.4.5. The grade elevation for the new plant will be set at a level that provides for clearance above the DBF, as required by Tier 1 of the DCD for the technology selected. In addition, sedimentation and erosion associated with the PMF do not represent a significant threat to operation of any safety-related SSC.

Subsection 2.4.10 addresses flooding protection requirements for the new plant location and considers the most severe flooding condition identified in this and other subsections of this report.

2.4.3.5 References

- 2.4.3-1 American National Standards Institute/American Nuclear Society, "Determining Design Basis Flooding at Power Reactor Sites," ANSI/ANS-2.8-1992, (historical), p. 1, 32, 1992.
- 2.4.3-2 Bretschneider, C.L. Hurricane Surge Predictions for Delaware Bay and River, Department of the Army Corps of Engineers Beach Erosion Board, Miscellaneous Paper No. 4-59, 1959.
- 2.4.3-3 Cook, T.L, "Observations of Sediment Transport in the Delaware Estuary During Spring Runoff Conditions," University of Delaware, Master of Science in Marine Studies Thesis, 2004, http://www.geo.umass.edu/grads/cook/tcook_thesis.pdf, accessed July 21, 2009.
- 2.4.3-4 Delaware River Basin Commission, "State of the Basin Report," Cover and Introduction, Website <http://www.state.nj.us/drbc/SOTB/index.htm>, p. 6, accessed June 16, 2009.
- 2.4.3-5 Delaware River Basin Commission 2007b, "Stream River Mileage July 2007," Website, <http://www.state.nj.us/drbc/StreamMileageJuly2007.pdf>, p. 11, accessed February 16, 2009.
- 2.4.3-6 MASER Consulting, PA ALTA/ACSM Land Title Survey for PSEG Nuclear LLC of Block 26, Lots 4, 4.01, 5 and 5.01, Job Number 05001694D, Index Number HASU023453 dated June 13, 2008.
- 2.4.3-7 National Oceanic and Atmospheric Administration, "Historic Tide Data," Website http://tidesandcurrents.noaa.gov/station_retrieve.shtml?type=Historic%20Tide%20Data&state=Delaware&id1=855, accessed April 7, 2009.
- 2.4.3-8 National Oceanic and Atmospheric Administration, HMR-51 1978, "Hydrometeorological Report No. 51, Probable Maximum Precipitation Estimates, United States East of the 105th Meridian," U.S. Department of Commerce, p. 2; 48, 1978.
- 2.4.3-9 National Oceanic and Atmospheric Administration, HMR-52 1982, "Hydrometeorological Report No. 52, Application of Probable Maximum

**PSEG Site
ESP Application
Part 2, Site Safety Analysis Report**

Precipitation Estimates – United States East of the 105th Meridian,” U.S. Department of Commerce, p. 78, 94 – 96, 1982.

- 2.4.3-10 National Oceanic and Atmospheric Administration, “Meteorological Criteria for Standard Project Hurricane and Probable Maximum Hurricane Windfields, Gulf and East Coasts of the United States,” NOAA Technical Report NWS 23, 1979.
- 2.4.3-11 National Oceanic and Atmospheric Administration, “NOS Estuarine Bathymetry: Delaware Bay DE/NJ (M090),” Website, <http://egisws01.nos.noaa.gov/servlet/BuildPage?template=bathy.txt&parm1=M090&B1=Submit>, accessed January, 28, 2009.
- 2.4.3-12 National Oceanic and Atmospheric Administration, “Effects of Hurricane Floyd on Water Levels Data Report,” NOAA Technical Report NOS CO-OPS 027, 2000.
- 2.4.3-13 National Oceanic and Atmospheric Administration, “Effects of Hurricane Isabel on Water Levels Data Report,” NOAA Technical Report NOS CO-OPS 040, 2004.
- 2.4.3-14 U.S. Army Corps of Engineers, “Coastal Engineering Manual,” Engineer Manual 1110-2-1100, U.S. Army Corps of Engineers, Washington, D.C. (in 6 volumes), 2002.
- 2.4.3-15 U.S. Army Corp of Engineers, “Coast of Delaware, Hurricane Stage-Frequency Analysis,” Philadelphia District, Philadelphia, Pennsylvania, p. A1, 1997.
- 2.4.3-16 U.S. Army Corp of Engineers, “Delaware River Main Stem and Channel Deepening Project Environmental Assessment,” p.51, April, 2009.
- 2.4.3-17 U.S. Army Corp of Engineers, “Delaware River Philadelphia to the Sea Examination,” Bathymetric Survey Data, Philadelphia, Pennsylvania, 2007 – 2009.
- 2.4.3-18 U.S. Army Corp of Engineers, “HEC-HMS 3.3 Software,” Website, <http://www.hec.usace.army.mil/software/hec-hms/download.html>, accessed February 23, 2009.
- 2.4.3-19 U.S. Army Corp of Engineers, “HEC-RAS 4.0 Software,” Website, <http://www.hec.usace.army.mil/software/hec-ras/hecras-download.html>, accessed February 23, 2009.
- 2.4.3-20 U.S. Geological Survey, “Base-Flow Index Grid for the Conterminous United States,” Website, <http://water.usgs.gov/GIS/metadata/usgswrd/XML/bfi48grd.xml>, accessed March 17, 2009.
- 2.4.3-21 U.S. Geological Survey, “7.5 Minute Quadrangle Topographic Maps,” Website, <http://datagateway.nrcs.usda.gov/>, accessed April 21, 2009.

**PSEG Site
ESP Application
Part 2, Site Safety Analysis Report**

- 2.4.3-22 U.S. Geological Survey, "National Elevation Dataset," Website, <http://seamless.usgs.gov/index.php>, accessed February 2, 2009.
- 2.4.3-23 U.S. Navy. "Hurricane Havens Handbook for the North Atlantic Ocean," Websites, <http://www.nrlmry.navy.mil/~cannon/tr8203nc/0start.htm> and <http://www.nrlmry.navy.mil/~cannon/tr8203nc/philadel/text/frame.htm>, accessed April 9, 2009.
- 2.4.3-24 Delaware River Basin Commission, "Delaware River Basin Boundary" Website <http://www.state.nj.us/drbc/gis.htm>, accessed 2/20/2009.

**PSEG Site
ESP Application
Part 2, Site Safety Analysis Report**

**Table 2.4.3-1
Criteria for PMP Events**

Center of Storm	Storm Size (sq. mi.)	Orientation of Storm (degrees relative to north azimuth)	Peak Intensity (in/hr)	Average Rainfall Depth - 6 Hours (in.)	Average Rainfall Depth – 72 Hours (in.)	Cumulative Volume for Storm Event (in-sq. mi.)
Doylestown, PA	15,000	222	3.3	4.3	12.1	180,000
Philadelphia, PA	2150	263	9.5	11.3	22.2	84,000

**PSEG Site
ESP Application
Part 2, Site Safety Analysis Report**

**Table 2.4.3-2
HEC-RAS Simulation Results of PMP Events**

Event	Parameter	RM 134 Station	RM 52 Station	RM 0 Station
PMP Over Entire Basin	Maximum Water Surface Elevation (ft. NAVD)	54.6	2.3	0.0
PMP Over Upper Estuary		23.8	2.6	0.0
RG 1.59		52.3	1.4	0.0
PMP Over Entire Basin	Flow Rate Concurrent to Maximum Water Surface Elevation (cfs)	1,190,000	1,450,000	n.a. ^(a)
PMP Over Upper Estuary		181,000	1,478,000	n.a. ^(a)
RG 1.59		1,040,000	1,100,000	n.a. ^(a)

a) n.a. = not available; Model output at RM 0 is not meaningful because RM 0 is a stage boundary. Tidal influence is not included in the model.

**PSEG Site
ESP Application
Part 2, Site Safety Analysis Report**

**Table 2.4.3-3
Worst Historical Storm Surge**

Storm Event	Year	Estimated Storm Surge, ft.^(a)		Percent Change
		Reedy Point	Philadelphia	
Chesapeake-Potomac Hurricane	1933	7.7	7.1	8
Hurricane Hazel	1954	11.3	9.4	20
Hurricane Floyd	1999	2.9	4.0	-28
Hurricane Isabel	2003	5.0	5.4	-7

- a) There are three storm events to compare the percent change from Philadelphia to Reedy Point. The surge at Reedy point is calculated by multiplying the surge at Philadelphia by the upper 95 percent confidence limit of the differences in the three known storm events (1.20).

References: 2.4.3-2, 2.4.3-12, 2.4.3-13, and 2.4.3-23

**PSEG Site
ESP Application
Part 2, Site Safety Analysis Report**

**Table 2.4.3-4
Resulting PMF at the PSEG Site (RM 52)
From Alternative I of ANSI/ANS-2.8-1992, Section 9.2.2.2**

Simulated One-Half PMF Water Surface Elevation (ft. NAVD)^(a)	Surge and Seiche from the Worst Regional Hurricane (ft.)	Coincident Wave Runup^(b) (ft.)	PMF Maximum Water Surface Elevation (ft. NAVD)
6.6	11.3	3.1	21.0

a) Results from simulation include coincident 10 percent exceedance high tide.

b) Coincident wave runup is described in detail in Subsection 2.4.3.1.2.

**PSEG Site
ESP Application
Part 2, Site Safety Analysis Report**

**Table 2.4.3-5
Resulting PMF at the PSEG Site (RM 52)
From Alternative II of ANSI/ANS-2.8-1992, Section 9.2.2.2**

Simulated PMF Water Surface Elevation^(a) (ft. NAVD)	Simulated 25-year Storm Surge (ft.)	Coincident Wave Runup^(b) (ft.)	PMF Maximum Water Surface Elevation (ft. NAVD)
7.3	5.7	3.1	16.1

a) Results include coincident 10 percent exceedance high tide.

b) Coincident wave runup is described in detail in Subsection 2.4.3.1.2.

**PSEG Site
ESP Application
Part 2, Site Safety Analysis Report**

2.4.4 POTENTIAL DAM FAILURES

In this subsection, the hydrological design basis for the new plant is developed to ensure any potential hazard to the safety-related SSC at the new plant due to failure of water control structures are considered in its design. Water control structures for the purpose of these analyses are reservoirs with dams retaining large volumes of water within the Delaware River watershed. There are no dams on the Delaware River. No safety-related water control or storage structures (e.g., reservoirs) will be constructed on the PSEG Site. The new plant's UHS or SWS may include mechanical draft cooling towers with basins designed to hold water volumes as required by RG 1.27, *Ultimate Heat Sink for Nuclear Power Plants*, Revision 2, 1976, and the appropriate design control document. These basins will be designed to not adversely impact operation of any safety-related SSC following a design basis event. Therefore, only upstream dam failures on tributaries to the Delaware River are considered in this analysis. The areas of review include consideration of flood waves from severe breaching of upstream dams, simultaneous dam failures, and effects of sediment deposition and erosion.

Maximum WSEL at the new plant location is calculated based on the dam breach analysis. The approach used to determine the maximum WSEL from the dam breach analysis follows ANSI/ANS-2.8-1992 (Reference 2.4.4-1) and RG 1.59.

Per ANSI/ANS-2.8-1992, Section 9.2.4, there is no specific guidance or specific event combinations provided due to uncertainty in postulating a realistic dam failure from nonhydrologic and nonseismic causes. Therefore, ANSI/ANS-2.8, Section 9.2.1.2, is conservatively used as guidance for the combined events criteria associated with the dam failure models presented in this subsection.

Seismic failure of a dam is modeled as the immediate breaching of the dam and release of water within the reservoir, as opposed to an extreme rain event which is modeled as the breach of a dam structure over a longer specified time period. A seismic dam failure is considered the worst case scenario releasing an immediate flood wave into the downstream tributary.

Two alternative combined events described in ANSI/ANS-2.8-1992, Section 9.2.1.2 are the basis for determining the maximum WSEL and flows at the new plant location.

Alternative I

- 25-year flood
- Dam failure caused by the safe shutdown earthquake (SSE) coincident with the peak flood
- 2-year wind speed applied in the critical direction

Alternative II

- One-half PMF or 500-year flood, whichever is less
- Dam failure caused by the operating basis earthquake (OBE) coincident with the peak flood
- 2-year wind speed applied in the critical direction

**PSEG Site
ESP Application
Part 2, Site Safety Analysis Report**

The Delaware River is tidally influenced at the PSEG Site, therefore the 10 percent exceedance high tide is included in the results. This is consistent with other flood analyses performed at the new plant location, and makes initial conditions consistent for comparison of calculated flood WSEL. It is also a conservative assumption.

There are hundreds of reservoirs within the Delaware River watershed with storage capacity ranging from 15 ac.-ft. to 460,000 ac.-ft. Subsection 2.4.4.1 describes the method of dam selection for those dams included in the dam breach modeling and the method used to determine the combination of dams used in simultaneous failures.

The approach and sequence of steps taken to calculate the maximum WSEL, peak flows and velocities caused by dam failure are as follows:

- USACE HEC-HMS, version 3.3 (Reference 2.4.4-8) is used to calculate the flows from the dam breach analysis.
- USACE HEC-RAS, version 4.0 (Reference 2.4.4-9) is used to calculate WSEL and flow velocities from the dam breaches to Delaware Bay using flow input from HEC-HMS and bathymetry and topography of the Delaware River, its tributaries, and their floodplains.
- The high water level at the site is used as the basis for calculating the wave height and wave runup from the 2-year wind speed in the critical direction.

The dam breach modeling is presented in Subsection 2.4.4.2.

The velocities from the output of the HEC-RAS model are used in the calculation of the sediment deposition at RM 52. Subsection 2.4.4.4 addresses sediment erosion and deposition associated with the dam failure analysis and its potential effects on the safety-related intake structure at the new plant.

The DRBC recognizes 24 reservoirs used for water supply, flood control, flow augmentation, and hydropower on tributaries to the Delaware River upstream from the PSEG Site as being within the Delaware River Basin. The largest reservoirs in terms of water volume are located in the upper Delaware River Basin. Notably, 68 percent of all the water stored in the 24 reservoirs is contained in three water supply reservoirs located in New York (NY). (Reference 2.4.4-3)

Reservoirs selected for inclusion in the dam breach analysis are chosen based on volume of water stored and distance from the new plant. Reservoirs with storage greater than 60,000 ac.-ft. are included in the analysis. Reservoirs within a 70 mi. radius of the site with more than 6000 ac.-ft. of storage are also included. Reservoir storage volumes tend to decrease in the Piedmont and Coastal Plain physiographic regions (Reference 2.4.4-3). Table 2.4.4-1 lists the locations and sizes of the seven largest reservoirs in the Delaware River Basin and the four largest reservoirs within 70 mi. of the site. These are all freshwater dams and are selected for analysis of dam failure permutations as discussed in subsequent subsections. Locations of the dams are shown on Figure 2.4.4-1.

The dams along the Christina River watershed are nearest to the PSEG Site, therefore their failures represent the highest potential for sediment deposition at the new plant intake structure. Based on evaluation of the settling velocity, water velocity and depth of the Christina and Delaware rivers, in addition to the distance between the dam breach location and the new plant,

**PSEG Site
ESP Application
Part 2, Site Safety Analysis Report**

erosion and sediment deposition at the intake structure due to dam breach, as described in Subsection 2.4.4.4, is not significant.

There are no dams located downstream of the new plant location on the Delaware River. Therefore, a loss of water supply due to downstream dam failure is not considered in this analysis. Subsection 2.4.11 addresses low water considerations for the new plant.

2.4.4.1 Selection of Dams and Their Combinations for Failure Scenarios

According to the USACE National Inventory of Dams (NID) (Reference 2.4.4-11), the Delaware River Basin contains four dams with reservoir storage volumes greater than 6000 ac.-ft. within a 70 mi. radius of the new plant location. Due to their physiographic locations, coincident seismic failure of these four dams is modeled to determine effects at the new plant location. There are seven large (greater than 60,000 ac.-ft. of total storage) reservoirs in the basin, which are modeled to determine effects at the site (Figure 2.4.4-1). Combinations of seismic dam failures are discussed in RG 1.59 and ANSI/ANS-2.8-1992, Section 9.2.1.2 (Reference 2.4.4-1). None of the dams identified above are located in series relative to each other. Therefore, flood waves from failure of any of the dams (listed in Table 2.4.4-1) do not route through downstream dams. Consequently, a domino-type dam failure analysis is not considered in this model. Coincident dam failures, as a result of seismic activity, are used to calculate peak flows. Evaluation of failures representing the worst case scenario is presented in the following subsections.

The exact timing of the dam breaches in each scenario are conservatively set to occur at discrete times resulting in a single combined breach flood wave arriving at the PSEG Site.

Four scenarios are considered for the dam break analysis to determine the maximum WSEL at the new plant location. These scenarios are based on the geographic locations of dams within the basin. These scenarios consist of two combinations of two large reservoirs, one combination of three reservoirs and one combination of the four largest reservoirs within 70 mi. of the plant failing during a single event. Though failure of multiple reservoirs may be possible within a geographic region, the failure of two large reservoirs or four smaller reservoirs due to a single seismic event is highly improbable because the reservoirs are not located within close proximity to each other. However, this approach is selected for conservatism. See Figure 2.4.4-1 for the location of the dams chosen for this analysis.

The first scenario is failure of the Pepacton and Cannonsville dams such that their resultant flood waves reach the PSEG Site simultaneously. The flood waves due to failure of these dams are combined in the analysis because both dams are located in the Catskill Mountains in New York. The NID indicates these are the two largest reservoirs in the Delaware River Basin. The Pepacton and Cannonsville dams are earthfill, rock-faced dams, storing 460,000 ac.-ft. and 303,000 ac.-ft. of water, respectively. The Pepacton Dam is located on the East Branch Delaware River. The Cannonsville Dam is located on the West Branch Delaware River (Reference 2.4.4-25).

The second scenario includes failure of the Lake Wallenpaupack and Neversink dams such that their resultant flood waves reach the PSEG Site simultaneously. These two dams are combined in the dam breach analysis because they are both located in the transition between the Catskills and the Valley and Ridge physiographic provinces. The Lake Wallenpaupack and Neversink dams are both earthfill dams with concrete spillways, storing 209,000 ac.-ft. and 142,000 ac.-ft.

**PSEG Site
ESP Application
Part 2, Site Safety Analysis Report**

of water, respectively. Lake Wallenpaupack Reservoir is located on Wallenpaupack Creek . Neversink Reservoir is located on the Neversink River. (References 2.4.4-20 and 2.4.4-11)

The third scenario consists of failure of the F.E. Walter, Beltzville and Nockamixon dams such that their resultant flood waves reach the PSEG Site simultaneously. These dams are combined in the dam breach analysis because they straddle the Valley and Ridge physiography in the central part of the Delaware River Basin. These dams are constructed of earthfill with concrete spillways, storing 111,000 ac.-ft., 104,000 ac.-ft., and 66,500 ac.-ft. of water, respectively. The F.E. Walter Dam is located on the Lehigh River. The Beltzville Reservoir is located on Pohopoco Creek; a tributary to the Lehigh River. The Nockamixon Dam is located on Tohickon Creek. (References 2.4.4-21, 2.4.4-11, and 2.4.4-17)

The fourth scenario involves failure of the Blue Marsh, Marsh Creek, Geist, and Edgar Hoopes dams; all located within 70 mi. of the new plant location (Figure 2.4.4-1). The Marsh Creek Reservoir stores 22,200 ac.-ft. of water. It is constructed of earthfill with a concrete spillway and is located on Marsh Creek (Reference 2.4.4-19). The Springton Reservoir (Geist Dam) stores 10,700 ac.-ft. of water and is located on Crum Creek (Reference 2.4.4-6). The Edgar Hoopes Reservoir stores 11,000 ac.-ft. of water and is located on Old Mill Stream-Red Clay Creek (Reference 2.4.4-11). The Blue Marsh Reservoir stores 50,000 ac.-ft. of water and is located on Tulpehocken Creek (Reference 2.4.4-22).

Combining the dam failures based on geographic regions is considered a worst case scenario for flooding at the new plant location. Discharge hydrographs from the dam breach analysis are used as input conditions into the hydraulic model. These hydrographs are used in combination with flooding, 10 percent exceedance high tide, and wave runup to calculate the maximum WSEL at the new plant location.

2.4.4.2 Analysis of Potential Dam Failures

Modeling conducted to establish the maximum WSEL for the combined events dam failure analyses includes developing individual dam breach hydrographs, establishing the river model, 500-year flood modeling and adding wave effects.

Individual Dam Breach Hydrographs

Dam failure hydrographs are developed using the USACE HEC-HMS model to produce the dam breach hydrograph for each reservoir (Reference 2.4.4-8). All reservoirs are considered to be full prior to failure, and breach dimensions are conservatively assumed to be equal to the extent of the dam. Information obtained from the USACE NID includes dam height, dam length, spillway width, and maximum volume of storage (Reference 2.4.4-11). Bottom elevations of the dams are obtained from the USGS National Elevation Dataset (Reference 2.4.4-23). Dam break hydrographs are developed assuming complete dam failure within 0.2 hr., which is the equivalent of an instantaneous dam failure in the model (Reference 2.4.4-12). Table 2.4.4-2 provides a summary of tributary dam failure HEC-HMS input parameters.

The River Model

To route dam failure discharge through the respective stream reaches and the Delaware River to the new plant location, a TIN terrain model is prepared using the USGS National Elevation

**PSEG Site
ESP Application
Part 2, Site Safety Analysis Report**

Dataset (Reference 2.4.4-23) DEM. The DEM uses the geometry of the tributary floodplain to route the flood waves. Geometry of the tributary floodplains is incorporated into the USACE HEC-RAS model (Reference 2.4.4-9).

Bathymetry from the NOAA tidal gage at Lewes, DE, up to RM 71 (Reference 2.4.4-4) is from the NOAA Estuarine Bathymetry DEM (Reference 2.4.4-5). This data is developed using the TIN terrain model and input into the HEC-RAS model. Bathymetry from RM 71 to the USGS gage station at Trenton, NJ (RM 134) is determined manually from the USGS 7.5 minute quadrangle sheets (Reference 2.4.4-16). The Delaware River and the tributaries that are modeled for dam breach routing are illustrated in Figure 2.4.4-1. A Manning's n roughness coefficient of 0.05 is used for the floodplains of all tributaries, and a Manning's n of 0.025 is used for the channels of all tributaries in the model. These values correspond to the n value for the floodplain and channel of a natural stream, respectively. (Reference 2.4.4-10)

The 500-year Flood

The combined events alternatives for dam breach analysis are as defined in Section 9.2.1.2 of ANSI/ANS-2.8-1992 (Reference 2.4.4-1). Alternative I requires modeling the 25-year flood, whereas Alternative II requires modeling the one-half PMF or 500-year flood, whichever is less. Alternative II is selected because it is more conservative than Alternative I. The 500-year flood results in a lower surface-water elevation at the new plant, 6.56 ft. NAVD, than one-half the PMF, 6.59 ft. NAVD. The 500-year flood event is used in the analysis because it is less than one-half the PMF. It includes a flow of 372,000 cfs at Trenton according to the flood frequency analysis performed by the USGS for the Delaware River Basin (Reference 2.4.4-18). This flooding event is added into the HEC-RAS model as a stage boundary condition.

Per each scenario discussed in Subsection 2.4.4.1, the dam failure hydrographs are added together and used as lateral inflows into the model. Flood hydrographs are routed through selected tributaries using the HEC-RAS model. Table 2.4.4-3 summarizes tributary dam failure output data and the 500-year frequency flood. To clarify the effect of the dam failure on water levels from the various scenarios, these results are extracted from the simulation without the effect of the tide.

To simulate the worst case scenario, dam breach is set to occur at a time resulting in the flood wave arriving at the site coincident with the 10 percent exceedance high tide. This is done by adjusting the time the dam breach hydrographs are simulated to break. The 10 percent exceedance high tide is 4.2 ft. NAVD at the Lewes NOAA tide gage 8557380 (RM 0); and 4.6 ft. NAVD at the Reedy Point NOAA tide gage 8551910 (RM 59). From these values, the resulting 10 percent exceedance high tide at the new plant location (RM 52) is determined by linear interpolation to be 4.5 ft. NAVD. The 10 percent exceedance high tide is added to the HEC-RAS model as a downstream boundary condition. The 500-year frequency flood with the 10 percent exceedance high tide results in a WSEL of 6.5 ft. NAVD at the new plant, corresponding to a flow of 480,000 cfs in the Delaware River.

Wave Effects

In addition to flood discharge in the Delaware River from the 500-year flood, wave runup with the 2-year wind speed in the critical direction at the new plant location is applied to flood elevations resulting from the various dam break scenarios to conservatively determine

**PSEG Site
ESP Application
Part 2, Site Safety Analysis Report**

maximum flood elevations, as presented in ANSI/ANS-2.8-1992, Section 9.2.1.2. Wave runup is determined using 2-year annual extreme wind speed of 50 mph, as shown in Section 9.1.4 of ANSI/ANS-2.8-1992 (Reference 2.4.4-1). Wind speeds are adjusted for duration in accordance with the Coastal Engineering Manual (Reference 2.4.4-7). Fetch directions are evaluated in 22.5 degree increments and the fetch direction that yields the highest wave runup is presented. Wave conditions are limited by fetch for the critical direction, which is wind blowing from the west across a flooded fetch of 4 miles. The flooded fetch is calculated at elevation 6.8 ft. NAVD, as discussed in Subsection 2.4.4.3, for a total length of 4 miles. The smaller of the maximum wave height or the maximum breaker height is used to determine runup, as described in Sections 7.4.3 and 7.4.4.5 of ANSI/ANS-2.8-1992 (Reference 2.4.4-1). The maximum wave height of 5.6 ft. is controlling. Subsection 2.4.3.1.2 provides a detailed discussion of the methods used to determine wave runup and wind setup.

The plant facilities are assumed to be constructed on fill at a 3 (horizontal):1 (vertical) or flatter slope with the slope protected by riprap.

Water Level at the New Plant Location

The inflow hydrographs from the 500-year flood calculations are incorporated into the HEC-RAS model along with discharge hydrographs from the selected tributaries for the four dam break scenarios. The maximum WSEL at the new plant location due to dam failure under any of the modeled scenarios is 9.4 ft. NAVD.

2.4.4.3 Water Level at the New Plant Location

HEC-HMS and HEC-RAS modeling show that maximum WSELs at the new plant location result from the simultaneous failure of the Pepacton and Cannonsville dams, excluding the influence of tides (Table 2.4.4-3). Conservative parameters used in this analysis include the combination of multiple dam failures timed to reach the new plant location simultaneously, the reservoirs being full at the time they are breached and the dam failures occurring instantaneously due to seismic activity. The maximum WSEL at the new plant location resulting from this scenario, including the influence of tides, is 6.8 ft. NAVD (Figure 2.4.4-3). Figure 2.4.4-4 illustrates the maximum flow rates for this scenario.

In accordance with ANSI/ANS-2.8-1992 standards (Reference 2.4.4-1), maximum wave height and wave runup are simulated coincident with dam failure flood levels through the Delaware River. The combined effect of dam failure with 10 percent exceedance high tide, the 500-year frequency flood, and the 2-year wind-wave runup, produces a maximum WSEL at the new plant location of 9.4 ft. NAVD (Figure 2.4.4-3 and Table 2.4.4-5).

2.4.4.4 Effects of Sediment Deposition and Erosion

The settling of particles carried downstream from the Marsh Creek and Hoopes Reservoir dam breaks are calculated to address the potential for suspended sediments from dam failures that may adversely affect the operation of the intake structure at the new plant. These two reservoirs are chosen because they are the closest reservoirs to the PSEG Site and represent the highest potential for sediment deposition at the PSEG Site due to dam failure. Both are located on the Christina River, a tributary entering the Delaware River at RM 71. The Hoopes Reservoir is located 37 RM upstream from the PSEG Site and Marsh Creek Reservoir is located 53 RM

**PSEG Site
ESP Application
Part 2, Site Safety Analysis Report**

upstream from the site. Other reservoirs are located on tributaries further upstream (Figure 2.4.4-1) and have additional time for sediment to settle prior to reaching the PSEG Site.

To determine the potential particle sizes that might be carried to the PSEG Site, soil characteristics for the Hoopes Reservoir watershed are determined using soil profiles from New Castle County, DE, where the reservoir is located. A majority of soils in New Castle County are listed as silty loam, sandy loam, and silt (Reference 2.4.4-13). Silt typically has an average particle diameter of 2 to 50 microns (Reference 2.4.4-14), while silty loam and sandy loam are larger in diameter. Using the smaller particle size (2 to 50 microns) as the critical particle diameter is a conservative assumption because smaller particles settle more slowly than larger particles. Thus, they are more likely to remain in suspension until they reach the new plant's intake structure. Other assumptions include:

- At channel depths of 20 ft. or more and water velocities below 4 ft/sec, resuspension is unlikely to occur, regardless of particle size (Reference 2.4.4-15). Conversely, to be conservative it is assumed that no settling of fine particles occurs in tributaries where water velocities exceed 4 ft/sec, due to resuspension.
- The Delaware River water velocity is assumed to be 5.7 ft/sec. This is the 90th percentile from the combined event modeling analysis, and represents a conservative assumption, as it decreases travel time and minimizes the time available for settling upstream.
- Suspended sediment particle geometry is spherical.

Using these assumptions, the particle settling velocity is determined using Stokes' Law (Reference 2.4.4-2). This law relates particle settling rates to particle diameter, and predicts that larger particles settle faster than smaller particles. If particles are settling in the Delaware River as they approach the PSEG Site, the cleanest water is near the surface, where most particles (small and large) have had a chance to settle out. (Figure 2.4.4-2). Therefore, solving Stokes' law, particles 20 microns (or larger) in diameter completely settle out of a 20 ft. deep water column prior to reaching the intake structure, 18 miles away. Particles smaller than 10 microns in diameter readily form colloids (Reference 2.4.4-2). Thus, particles of this size likely stay suspended in the water column indefinitely. Particles between 10 and 20 microns can potentially settle out near the intake structure, but the overall quantity of particles in this size range is small.

It is possible that some particles reach the PSEG Site during a dam break, therefore a conservative scenario is used to quantify the total volume of sediment deposition at the PSEG Site. A combination of the Marsh Creek and the Hoopes Reservoir failures is modeled, along with the assumption that sediment does not settle out until it reaches the Delaware River.

A review of regional reservoirs with capacities within an order of magnitude of the Hoopes Reservoir (1000 to 100,000 ac.-ft.) shows that they accumulate sediments at the rate of 0.2 percent of their storage volume per year (Table 2.4.4-4). This analysis conservatively assumes both reservoirs' storage capacity is 25 percent sediment which equates to 13.4 million cubic yards of sediment. This represents 125 years of sediment buildup. The Hoopes Reservoir is 78 years old and the Marsh Creek Reservoir is 36 years old.

Conservatively, sediment does not begin to deposit until it reaches the mouth of the Christina River (RM 70). This results in an average of 5 in. of sediment buildup from the mouth of the Christina River to the PSEG Site (RM 52). The majority of the deposition is close to the

**PSEG Site
ESP Application
Part 2, Site Safety Analysis Report**

confluence of the Christina and Delaware rivers, with less deposition occurring at the intake structure. Therefore, dam breaks of the Marsh Creek and Hoopes reservoirs do not represent a significant buildup of sedimentation at the intake structure.

2.4.4.5 Dynamic Effects of Dam Failure-Induced Flood Waves on Structures, Systems and Components

The maximum WSEL caused by dam-failure induced flood waves is 9.4 ft. NAVD. This is lower than the DBF elevation caused by probable maximum storm surge, described in Subsection 2.4.5. Floor elevations for safety-related structures, systems and components (SSC) for the new plant, other than the intake structure, will be established to maintain at least one foot of clearance above the DBF, as required by Tier 1 of the DCD for the technology selected. With the exception of the intake structure, no safety-related SSC will be subject to dynamic forces associated with the flood wave caused by dam failures in the Delaware River Basin. The intake structure of the new plant will be designed to protect it from dynamic effects associated with dam-failure induced flood waves.

2.4.4.6 Conclusions

There are no dams in series to model a domino-type failure. Combinations of failure of large dams on tributaries to the Delaware River are modeled to determine worst case flooding elevations due to dam failures at the new plant location. Based on the settling velocity of soils and distance to the site, deposition of sediment due to dam breach is not significant at the intake structure. Low water as a result of dam breach is not considered because there are no dams on-site or downstream that affect the availability of safety-related water supply to the new plant.

Flood elevations determined by these dam failure analyses are developed using conservative assumptions through modeling procedures that include:

- Addition of the downstream stage boundary condition of 10 percent exceedance of the high tide
- Multiple dam failures peak flows reaching the site at high tide
- Dams are considered full at the time of the breach
- Failures occur instantaneously due to seismic activity

Of the four seismic dam breach scenarios modeled, the scenario producing the maximum WSEL at the new plant location is the combined failure of the Pepacton and Cannonsville dams. This breach scenario results in a flood elevation of 9.4 ft. NAVD at the PSEG Site (Table 2.4.4-5) and includes the following components: the 10 percent exceedance high tide at 4.5 ft. NAVD, coincident with the 500-year frequency storm event of 2.0 ft., the combined Pepacton and Cannonsville dam breaches of 0.3 ft., and the 2-year wind speed applied in the critical direction of 2.6 ft. However, the maximum WSEL resulting from potential dam failures is exceeded by the maximum storm surge associated with the PMH, as described in Subsection 2.4.5.

**PSEG Site
ESP Application
Part 2, Site Safety Analysis Report**

2.4.4.7 References

- 2.4.4-1 American National Standards Institute/American Nuclear Society, "Determining Design Basis Flooding at Power Reactor Sites," ANSI/ANS-2.8-1992, (historical), p. 24, 30, 32, 1992.
- 2.4.4-2 Chapra, Steven, "Surface Water-Quality Modeling, McGraw-Hill, p. 299 – 300, 1997.
- 2.4.4-3 Delaware River Basin Commission, "Delaware River State of the Basin Report 2008," Website <http://www.state.nj.us/drbc/SOTB/index.htm>, p. 11, 73, accessed July 2, 2009.
- 2.4.4-4 Delaware River Basin Commission 2007b, "Stream Mileage July 2007," Website, <http://www.state.nj.us/drbc/StreamMileageJuly2007.pdf>, p. 11, accessed February 16, 2009.
- 2.4.4-5 National Oceanic and Atmospheric Administration (NOAA), "NOS Estuarine Bathymetry: Delaware Bay DE/NJ (M090)," Website <http://egisws01.nos.noaa.gov/servlet/BuildPage?template=bathy.txt&parm1=M090&B1=Submit>, accessed February 2, 2009.
- 2.4.4-6 Pennsylvania Department of Conservation and Natural Resources, Crum Creek Watershed Conservation Plan, Website, <http://www.dcnr.state.pa.us/brc/rivers/riversconservation/registry/CrumCreek/Vl.WATER%20RESOURCES.final.pdf>, p. 28, accessed June 4, 2009.
- 2.4.4-7 U.S. Army Corps of Engineers, "Coastal Engineering Manual. Engineer Manual 1110-2-1100," U.S. Army Corps of Engineers, Washington, D.C. (in 6 volumes), 2006.
- 2.4.4-8 U.S. Army Corps of Engineers, "HEC-HMS 3.3 Software," Website, <http://www.hec.usace.army.mil/software/hec-hms/download.html>, accessed February 23, 2009.
- 2.4.4-9 U.S. Army Corps of Engineers, "HEC-RAS 4.0 Software," Website, <http://www.hec.usace.army.mil/software/hec-ras/hecras-download.html>, accessed February 23, 2009.
- 2.4.4-10 U.S. Army Corps of Engineers, "Hydraulic Reference Manual Version 3.1, November 2002," Website, <http://www.hec.usace.army.mil/software/hec-ras/documents/hydref/>, accessed April 4, 2009.
- 2.4.4-11 U.S. Army Corps of Engineers, "National Inventory of Dams," Website, <https://nid.usace.army.mil/>, accessed July 16, 2009.
- 2.4.4-12 U.S. Bureau of Reclamation, "Predicting Embankment Dam Breach Parameters – A Needs Assessment," XXVIIth IAHR Congress, San Francisco California, August 10 – 15, 1997.

**PSEG Site
ESP Application
Part 2, Site Safety Analysis Report**

- 2.4.4-13 U.S. Department of Agriculture, NRCS, Soil Survey, Website, <http://websoilsurvey.nrcs.usda.gov/app/WebSoilSurvey.aspx>, accessed July 16, 2009.
- 2.4.4-14 U.S. Department of Agriculture, NRCS, Soil Survey Manual, Website, <http://soils.usda.gov/technical/manual/contents/chapter3e.html>, accessed July 16, 2009.
- 2.4.4-15 U.S. Department of Transportation, "Hydraulics Engineering," Website, <http://www.fhwa.dot.gov/engineering/hydraulics/pubs/07026/03.cfm>, accessed July 16, 2009.
- 2.4.4-16 U.S. Geological Survey, "7.5 Minute Quadrangle Topographic Maps," Website <http://datagateway.nrcs.usda.gov/>, accessed April 21, 2009.
- 2.4.4-17 U.S. Geological Survey, "01459350 Nockamixon Reservoir near Ottsville, PA, 1999a," Website, <http://pa.water.usgs.gov/ar/wy99/pdfs/01459350.pdf>, p. 1, accessed February 22, 2009.
- 2.4.4-18 U.S. Geological Survey, "Flood Magnitude and Frequency of the Delaware River in New Jersey, New York, and Pennsylvania," Open-File Report 2008-1203, 2008, Website, <http://pubs.usgs.gov/of/2008/1203/pdf/ofr2008-1203.pdf>.
- 2.4.4-19 U.S. Geological Survey, "Lakes and Reservoirs in Christina River Basin, 2005," Website, <http://pa.water.usgs.gov/ar/wy05/new-pdfs/christina-lakes.pdf>, p. 1, accessed February 22, 2009.
- 2.4.4-20 U.S. Geological Survey, "Lakes and Reservoirs in Lackawaxen River Basin, 1999b," Website, <http://pa.water.usgs.gov/ar/wy99/pdfs/lackawaxen-lakes.pdf>, p. 1, accessed February 22, 2009.
- 2.4.4-21 U.S. Geological Survey, "Lakes and Reservoirs in Lehigh River Basin, 2001a," Website, <http://pa.water.usgs.gov/ar/wy01/pdfs/lehigh-lakes.pdf>, p. 1, accessed February 22, 2009.
- 2.4.4-22 U.S. Geological Survey, "Lakes and Reservoirs in Schuylkill River Basin, 2001b," Website, <http://pa.water.usgs.gov/ar/wy01/pdfs/schuylkill-lakes.pdf>, p. 1, accessed February 22, 2009.
- 2.4.4-23 U.S. Geological Survey, "National Elevation Dataset," Website, <http://seamless.usgs.gov/website/seamless/viewer.htm>, accessed February 2, 2009.
- 2.4.4-24 U.S. Geological Survey, Reservoir Sedimentation Database, Website, <http://ida.water.usgs.gov/ressed/>, accessed July 16, 2009.
- 2.4.4-25 U.S. Geological Survey, "Reservoirs in Delaware River Basin, 2004," Website, <http://ny.water.usgs.gov/pubs/wdr/wdrny041/rept.delaware2004.pdf>, p. 1 – 2, accessed February 22, 2009.

**PSEG Site
ESP Application
Part 2, Site Safety Analysis Report**

**Table 2.4.4-1
Delaware River Basin Selected Water Control Structures ^(e)**

Name of Dam or Reservoir	Owner or Operator	Tributary	Drainage Area Above Dam (sq. mi.)	Total Storage, in 100's of ac.-ft.	Spillway Elevation, ft. NAVD 1988	Date Completed	Delaware RM ^(a)
Pepacton Reservoir	New York City Department of Environmental Protection	East Branch Delaware River	372	4600 ^(c)	1279	1954	331
Cannonsville Reservoir	New York City Department of Environmental Protection	West Branch Delaware River	454	3030 ^(c)	1150	1963	331
Lake Wallenpaupack	Pennsylvania Power & Light	Wallenpaupack Creek	228	2090	1189	1925	278
Neversink Reservoir	City of New York – Department of Environmental Protection	Neversink River	92.5	1420	1439	1953	254
F.E. Walter Reservoir	USACE North Atlantic Division, Philadelphia District	Lehigh River	289	1110	1449	1961	184
Beltzville Reservoir	USACE North Atlantic Division, Philadelphia District	Pohopoco Creek	96	1040	650	1969	184
Blue Marsh Reservoir	USACE North Atlantic Division, Philadelphia District	Tulpehocken Creek	175	500	306	1979	92
Nockamixon Reservoir	Pennsylvania Department of Conservation and Natural Resources	Tohickon Creek	73	665	394	1973	157
Marsh Creek Reservoir	Pennsylvania Department of Conservation and Natural Resources	Marsh Creek	20	222	359	1973	71
Springton Reservoir (Geist Dam)	Aqua Pennsylvania, Inc.	Crum Creek	21.5	107	266 ^(b)	1931	85
Edgar Hoopes Reservoir	City of Wilmington	Old Mill Stream - Red Clay Creek	n.a. ^(d)	110	339 ^(b)	1931	71

a) Delaware RM of confluence of tributary with the Delaware River

b) Determined by digital mapping (Reference 2.4.4-23)

c) Conversion from gallons to ac.-ft.: 1 ac.-ft. = 325,872 gallons

d) n.a. = not available - Minimal drainage area determined from aerial mapping and Reference 2.4.4-11

e) Table shows the seven largest reservoirs within the Delaware River Basin and the four largest reservoirs within 70 mi. of the PSEG Site

References 2.4.4-6, 2.4.4-11, 2.4.4-17, 2.4.4-19, 2.4.4-20, 2.4.4-21, 2.4.4-22, 2.4.4-23, and 2.4.4-25

**PSEG Site
ESP Application
Part 2, Site Safety Analysis Report**

**Table 2.4.4-2
Summary of Tributary Dam Failure Input Parameters**

Name of Dam or Reservoir	Top Elevation of Dam Breach (ft. NAVD)	Bottom Elevation of Dam Breach (ft. NAVD)	Bottom Width of Dam Breach (ft.)	Time of Failure (mm/dd/yyyy hh:mm)^(b)
Pepacton Reservoir	1279	1100	1450	6/28/2006 3:00
Cannonsville Reservoir	1150	990	1160	6/28/2006 3:00
Lake Wallenpaupack	1189	1120	230	6/28/2006 4:00
Neversink Reservoir	1439	1275	1550	6/28/2006 4:00
F.E. Walter Reservoir	1449	1265	170	6/28/2006 17:00
Beltzville Reservoir	650	510	400	6/28/2006 18:00
Nockamixon	394	385	1230	6/29/2006 0:00
Blue Marsh Reservoir	306	235	380	6/28/2006 18:00
Marsh Creek Reservoir	359	300	460	6/29/2006 5:00
Springton Reservoir (Geist Dam)	266 ^(a)	195	50	6/29/2006 5:00
Edgar Hoopes Reservoir	339 ^(a)	240	50	6/29/2006 5:00

a) Determined by digital mapping (Reference 2.4.4-23)

b) The simulation dates for the HEC-RAS model started at time 00:00 on 06/20/2006 and ended at 00:00 on 07/03/2006

**PSEG Site
ESP Application
Part 2, Site Safety Analysis Report**

**Table 2.4.4-3
Summary of Tributary Dam Failure Output Data Excluding Tidal Effects**

Name of Dam or Reservoir	Failure Scenario	Maximum Discharge at Breach (cfs)^[c]	Discharge at New Plant Location at Peak Water Surface Elevation at Maximum Water Surface Elevation (cfs)^(a)	Maximum Water Surface Elevation at PSEG Site (ft. NAVD)	Time of Peak Discharge (mm/dd/yyyy hh:mm)^(b)
Pepacton Reservoir	1	7,590,000	839,000	0.8	6/29/2006 22:00
Cannonsville Reservoir		6,530,000			
Lake Wallenpaupack	2	1,080,000	721,000	0.6	6/29/2006 21:00
Neversink Reservoir		1,790,000			
F.E. Walter Reservoir	3	2,210,000	686,000	0.6	6/29/2006 22:00
Beltzville Reservoir		1,120,000			
Nockamixon Reservoir		455,000			
Blue Marsh Reservoir	4	1,070,000	634,000	0.5	6/29/2006 18:00
Marsh Creek Reservoir		214,000			
Springton Reservoir (Geist Dam)		113,000			
Edgar Hoopes Reservoir		51,600			

a) Includes 500-year flood discharge of 639,000 cfs at Trenton, NJ (RM 134)

Maximum Discharge (cfs) and maximum water surface elevation (ft. NAVD) do not always occur at the same time.

b) The simulation dates for the HEC-RAS model started at time 00:00 on 06/20/2006 and ended at 00:00 on 07/03/2006

c) cfs = cubic feet per second

**PSEG Site
ESP Application
Part 2, Site Safety Analysis Report**

**Table 2.4.4-4
Summary of Reservoir Sedimentation Rates**

Reservoir/Impoundment Name	Location (County, State)	Initial Storage (ac.-ft.)	Final Storage (ac.-ft.)	Timespan (years)	Annual Storage Loss (ac.-ft.)	Annual Rate of Storage Loss
Gilboa Dam	Schoharie, NY	63,821	62,702	24	46.6	0.1%
Batavia Kill Site 4a	Greene, NY	1563	1562	7	0.2	0.0%
Carnegie Lake	Hunterdon-Mercer, NJ	1256	822	52	8.3	0.7%
Loch Raven Reservoir	Baltimore, MD	70,169	64,072	47	129.7	0.2%
Prettyboy	Baltimore, MD	60,979	59,864	28	39.8	0.1%
Lake Williams	York, PA	2686	2232	27	16.8	0.6%
Coatesville Reservoir	Chester, PA	1019	970	35	1.4	0.1%
Elmhurst	Lackawanna, PA	3746	3686	51	1.2	0.0%
Williams Bridge	Lackawanna, PA	1051	1046	48	0.1	0.0%
Griffin	Lackawanna, PA	1991	1953	53	0.7	0.0%
					Mean	0.2%

Reference 2.4.4-24

**PSEG Site
ESP Application
Part 2, Site Safety Analysis Report**

**Table 2.4.4-5
Resulting Maximum Water Surface Elevation at the PSEG Site (RM 52) From Dam Failure
(Combined Events Alternative II of ANS)**

10% Exceedance High Tide (ft. NAVD)	500-Year Flood (ft.)	Failure of Cannonsville and Pepacton Reservoirs (ft.)	Wave Runup from 2- Year Wind Speed in the Critical Direction (ft.)^(a)	Maximum Water Surface Elevation (ft. NAVD)
4.5	2.0	0.3	2.6	9.4

a) Coincident wave runup is described in detail in Subsection 2.4.3.1.2

**PSEG Site
ESP Application
Part 2, Site Safety Analysis Report**

2.4.5 PROBABLE MAXIMUM SURGE AND SEICHE FLOODING

In this subsection, the hydrometeorological design basis is developed to ensure that potential hazards to the safety-related structures, systems and components (SSC) at the new plant location, due to the effects of probable maximum hurricane (PMH) surge and seiche, are considered in the design of the new plant. The new plant is located on the eastern shore of the Delaware River estuary. The existing topography at the new plant location ranges from 5 to 15 feet (ft.) NAVD (Reference 2.4.5-11). Consequently, the new plant may be affected by hurricane storm surge.

The approach used to determine the PMH surge, seiche flooding, and wave runup are presented. The methodologies used to determine storm surge from the PMH are in accordance with American National Standards Institute/American Nuclear Society (ANSI/ANS)-2.8-1992 (Reference 2.4.5-1) and RG 1.59.

Methods used to determine maximum surge and seiche flooding include:

- Bodine storm surge model (Reference 2.4.5-2), coupled with the HEC-RAS model (Reference 2.4.5-28) and the wind setup model of Kamphuis (Reference 2.4.5-10)
- NOAA, *Sea, Lake, and Overland Surges from Hurricanes* (SLOSH) model (References 2.4.5-22 and 2.4.5-23)
- RG 1.59
- ADCIRC+SWAN Model (Reference 2.4.5-41)

The design basis flood level established in this subsection is conservatively based on the ADCIRC+SWAN model's simulation of the storm surge due to the PMH. Initially, the Bodine storm surge model, is used to screen storm surge water levels based on varying PMH parameters in combination with HEC-RAS and the Kamphuis wind setup model. The Bodine model calculates storm surge at the open coast. HEC-RAS determines the PMH surge water level as the surge propagates through Delaware Bay to the new plant location. The Kamphuis method calculates additional effects on water levels at the new plant caused by wind blowing over the Delaware Bay.

The alternative methods listed above (SLOSH and RG 1.59) are investigated, and results are discussed in this subsection, but the alternative methods are determined to have limitations for determining the PMH surge at the site. Those limitations are discussed in Subsection 2.4.5.2.

The overall approach and sequence of steps are as follows. Subsection 2.4.5.1 documents that the PMH, as defined by NOAA's *Meteorological Criteria for Standard Project Hurricane and Probable Maximum Hurricane Windfields* National Weather Service Technical Report NWS 23 (NWS 23) (Reference 2.4.5-18), represents the Probable Maximum Wind Storm (PMWS) at the new plant location. As defined by NOAA, the PMH may exhibit a range of meteorological characteristics, so preliminary screening level calculations are performed that identify the PMH characteristics that produce the PMH surge at the new plant location. The PMH with these specific characteristics is used to specify the PMWS.

Determination of the maximum still water level (SWL) of the PMH surge based on the Bodine, HEC-RAS and Kamphuis method is presented in Subsection 2.4.5.2. The analysis commences with the effects of the hurricane over the continental shelf, producing a surge at the mouth of

**PSEG Site
ESP Application
Part 2, Site Safety Analysis Report**

Delaware Bay, which is determined using the Bodine model. The surge is superimposed on a coincident 10% exceedance high tide. Outputs of the Bodine model are used as input to HEC-RAS, defining the surge at the mouth of the bay as a stage boundary condition. The upstream boundary of HEC-RAS is the head of tide at Trenton, NJ, where the discharge hydrograph reflects the effects of hurricane-associated precipitation. The additional effects of wind blowing over Delaware Bay, not simulated by HEC-RAS, are calculated using a formula for wind setup in semi-enclosed bodies of water as presented by Kamphuis (Reference 2.4.5-10).

Wave heights and wave runup coincident with the maximum SWL are determined in Subsection 2.4.5.3, using the hurricane wind field specified by NWS 23. Wave runup is calculated in accordance with USACE's *Coastal Engineering Manual* (CEM) (Reference 2.4.5-27). Wave runup is added to the maximum SWL of the PMH surge.

In Subsection 2.4.5.4, the potential future effects of sea level rise are evaluated and added to the maximum WSEL from the PMH surge, which includes coincident wind wave activity, to determine the future maximum WSEL through the projected life of the new plant in Subsection 2.4.5.5.

Subsections 2.4.5.6 presents the final design basis flood WSEL due to the PMH surge using a conservative, current practice approach predicted by a two-dimensional storm surge model. The ADCIRC+SWAN model is used in conjunction with the CEM wave runup equations to determine the design basis flood level for the PSEG Site.

Subsection 2.4.5.7 addresses sediment erosion and deposition associated with the PMH and their potential effects on the safety-related intake structure. Subsection 2.4.5.8 demonstrates that Delaware Bay does not resonate with meteorological or seismic forcing, providing further confirmation that the PMH surge as calculated in this section represents the most severe flooding that could occur at the new plant.

2.4.5.1 Probable Maximum Winds (PMW) and Associated Meteorological Parameters

This subsection identifies the meteorological characteristics of the PMH that causes the PMH surge and demonstrates that the PMH wind field represents the PMWS at the new plant location. The basic meteorological parameters that define the PMH are varied within limits given by NOAA (Reference 2.4.5-18) to determine the most severe combination that results. The detailed analysis of surge (in Subsection 2.4.5.2) is based on the most severe combination of these parameters.

The meteorological parameters associated with the PMH at the mouth of Delaware Bay are based on NWS 23. The mouth of Delaware Bay is defined as a point bisecting the line from Cape May, New Jersey (NJ) to Cape Henlopen, Delaware (DE), at latitude 38°51'30"N, longitude 75°01'30"W. At this location, NOAA provides the following meteorological parameters for the PMH:

- Central pressure, p_0 = 26.65 inches of mercury [in. of Mercury (Hg)].
- Pressure drop, Δp = 3.5 in. of Hg.
- Radius of maximum winds, R = from 11 to 28 nautical miles (NM).
- Forward speed, T = from 26 to 42 knots (kt).

**PSEG Site
ESP Application
Part 2, Site Safety Analysis Report**

- Coefficient related to density of air, $K = 68$ (when parameters are in units of in. of Hg and kt)
- Track direction, from 138 degrees (moving northwest).

The northwest track direction is perpendicular to bathymetric contours of the continental shelf offshore of the mouth of Delaware Bay (Reference 2.4.5-20). The track of this storm is illustrated in Figure 2.4.5-1. This track direction is within the range of directions that NOAA specifies for the PMH at the mouth of Delaware Bay. The inflow angle, which varies with distance from the storm center, is as specified by NOAA (Reference 2.4.5-18). From these parameters, the maximum winds range from 128 to 135 kt, as shown in Table 2.4.5-2. Thus, the PMH is a relatively strong Category 4 hurricane by the Saffir-Simpson hurricane scale. Category 4 hurricanes have maximum sustained winds ranging from 114 to 135 kt.

NOAA specifies that the PMH may occur within a range of radius of maximum winds (R) and forward speed (T) (Reference 2.4.5-18). The method described in Subsection 2.4.5.2.2.2 is used to calculate the maximum storm surge at the open coast for nine possible combinations of R (11, 20, and 28 NM) with T (26, 34, and 42 kt) spanning the ranges of these parameters specified by NOAA. This analysis follows methodology described in ANSI/ANS-2.8-1992 Section 7.2.1.4. In these preliminary simulations, designed to identify the PMH producing the maximum storm surge, a static high tide condition is specified. This tide condition differs from the dynamic tidal input used in Subsection 2.4.5.2.2. These preliminary screening level analyses (presented in Table 2.4.5-3) show that the surge at the mouth of Delaware Bay increases with R and T, with a maximum surge at the mouth of the bay when both R and T are high, specifically for the PMH with $R = 28$ NM, and $T = 42$ kt. This result is consistent with modeling performed in support of RG 1.59, which determined that the maximum surge at the coast consistently resulted from the PMH with high R and T.

The hurricane producing the maximum surge at the open coast may not produce maximum WSEL in bays and estuaries. A storm that progresses at approximately the same speed as the tide propagates is expected to produce maximum surges within Delaware Bay (Reference 2.4.5-3). The speed of propagation of the tide in Delaware Bay is approximately 14 kt (References 2.4.5-3 and 2.4.5-8). Therefore, it may be expected that a PMH with a high forward speed (42 kt) may not produce the highest storm surge at the new plant location, even though it produces the highest surge at the mouth of Delaware Bay. A fast-moving storm moves ahead of the storm surge wave, while a slower moving storm tends to reinforce the surge. Since the surge at the mouth of Delaware Bay is strongly dependent on the radius of maximum winds, R, but weakly dependent on the forward speed, (T), the three storms with $R = 28$ are further investigated using HEC-RAS and the Kamphuis wind setup method to determine the potential effects of these storms on SWLs at the new plant location. This analysis (presented in Table 2.4.5-3) shows that the PMH with $R = 28$ NM, and $T = 26$ kt produces the maximum surge at the new plant location consistent with Bretschneider's evaluation.

A PMH with $R = 28$ NM, and $T = 26$ kt produces the PMH surge at the new plant location. The PMH with $R = 28$ NM and $T = 26$ kt, is simulated in more detail in Subsections 2.4.5.2 and 2.4.5.3. Specifically, the storm is simulated with a fluctuating tide at the mouth of Delaware Bay, which produces the 10 percent exceedance high tide at the new plant location. The phase of the tide is established in relation to the development of the storm surge such that the 10 percent exceedance high tide coincides with the peak storm surge at the new plant location.

**PSEG Site
ESP Application
Part 2, Site Safety Analysis Report**

The pressure distribution and wind field associated with this storm are determined as specified by NOAA (Reference 2.4.5-18) for a PMH. Wind speed and direction at any point depend on Δp , T and R; the distance and angular orientation of the specified point relative to the center of the storm and the direction of storm movement. Wind speed varies with time at a point as the storm moves along its track relative to that point. Latitude and the density of air also affect the wind speed calculations. The maximum sustained winds over the ocean are calculated to be 128 kt; while the maximum winds over Delaware Bay are 126 kt, and maximum winds at the new plant location are 116 kt.

The HEC-RAS hydraulic simulation does not account for wind stress acting on water within Delaware Bay, therefore, the effect of wind stress within the bay is determined using the steady state wind setup method described by Kamphuis (Reference 2.4.5-10). Wind setup refers to the response of water surface elevations in enclosed or semi-enclosed bodies of water to winds blowing across the water surface. The method presented by Kamphuis assumes wind setup in Delaware Bay to be a steady state response to steady, uniform wind over the bay. This simplification is appropriate because Delaware Bay is less extensive in area than the continental shelf, and winds are more uniform. The assumption that the bay exhibits a steady state response to winds that change with time is a conservative assumption (Reference 2.4.5-4) because the bay would not reach a steady state condition instantaneously.

ANSI/ANS-2.8-1992 (Reference 2.4.5-1), recommends use of the parameterization of the wind stress, k , as discussed in Bodine (Reference 2.4.5-2), unless other values can be justified using better observational data. Recent research shows that the Bodine parameterization overestimates the wind stress coefficient at hurricane force winds. Recent observations of the wind stress coefficient at hurricane force winds have been made possible by the development of observational devices not available in 1971 when the Bodine technical memorandum was published (References 2.4.5-26 and 2.4.5-7). Observations, utilizing advanced devices, have determined k values at hurricane force winds ranging from 1.4×10^{-6} to 3.0×10^{-6} (References 2.4.5-4, 2.4.5-26, and 2.4.5-7). Above the threshold of hurricane force winds, k does not increase with wind speed (Reference 2.4.5-7). Therefore, the Bodine relationship for the wind stress coefficient is modified at high wind speeds so that the wind stress coefficient does not exceed 3.0×10^{-6} , the highest observed value reported at hurricane force winds (References 2.4.5-4, 2.4.5-26, and 2.4.5-7). Use of a maximum value of k of 3.0×10^{-6} is conservative based on measured values at hurricane force winds.

2.4.5.1.1 Probable Maximum Wind Storm (PMWS)

The PMH represents the PMWS that could cause flooding at the new plant location. A 31-year record (1978 through 2008) of wind speed and direction data from Dover, DE (11 miles west of the center of Delaware Bay) was analyzed. The Dover weather station is the closest to the center of Delaware Bay, and thus the most appropriate location for evaluating winds over the bay that could cause wind setup or seiche activity. Setup of Delaware Bay has been observed when strong winds parallel to its long axis (i.e., northwest-southeast) persist for durations of 2 to 12 hours (Subsection 2.4.11). Winds at Dover were averaged over 4 hours, a sufficient duration to cause wind setup of Delaware Bay, based on the observations summarized in Subsection 2.4.11. The analysis shows that 4 hour average winds parallel to the long axis of Delaware Bay did not exceed 35 mph (30 kt) at Dover. Overwater winds are expected to be 50 kt when overland winds are 30kt (Reference 2.4.5-18). Therefore winds of sufficient duration to cause wind setup or seiche did not exceed 50 kt over Delaware Bay during the period 1978 through

Rev. 4

**PSEG Site
ESP Application
Part 2, Site Safety Analysis Report**

2008. By comparison, the wind speeds associated with the PMH exceed 125 kt over Delaware Bay. Therefore, the PMH represents the PMWS for the new plant location.

2.4.5.1.2 Appropriateness of PMH Determination

The probable maximum storm surge water level estimation described in Subsection 2.4.5.5 uses the PMH parameters defined by NWS 23 for coastal locations on the United States (U.S.) Gulf and East coasts. NWS 23 is recognized as a reliable source of information to characterize the PMH (Reference 2.4.5-1). The PMH parameters in NWS 23 are based on historical data for hurricanes making landfall on the U.S. coasts between 1851 and 1975. Comparisons of hurricane climatology during the period evaluated in NWS 23 with hurricanes making landfall after 1975 indicate that the NWS 23 parameters for the PMH are still applicable.

NOAA (Reference 2.4.5-15) has summarized variations in the frequency of major hurricanes that relate to variations in climatologic conditions. The Atlantic Multi-decadal Oscillation, which refers to cyclic fluctuations in oceanic surface temperature over periods that last as long as several decades, appears to affect the frequency of hurricanes; resulting in periods of 20 years or more with a high frequency of major hurricanes, which may be followed by a similar period with lower hurricane frequency. Atlantic Ocean hurricanes were significantly more active from 1995 to 2005 than in the previous two decades (1970 to 1985). Prior to that, the period 1945 through 1970 was relatively active, as active as the 1995 to 2005 period. NOAA published a technical memorandum (Reference 2.4.5-24) analyzing the number and strength of hurricane strikes by decade and location in the U.S. According to this publication, on average, a Category 4 or stronger hurricane hits the U.S. once every 7 years. However, in the 35 years from 1970 to 2005, only three Category 4 or larger hurricanes have reached the U.S., which is less than the expected number of 5 in 35 years. Based on this information, it is reasonable to conclude that the number and strength of hurricanes since NWS 23 was published are not greater than hurricanes prior to 1975. The NWS 23 climatological data set includes the relatively active period of 1945 through 1970. Therefore, meteorological criteria for hurricanes affecting the gulf and east coasts of the U.S., described in NWS 23, are conservative even considering potential future climatic variability.

2.4.5.2 Surge and Seiche Water Levels

Assessment of the PMH meteorological parameters that produce the maximum SWL surge at the PSEG Site is presented in this subsection. The most severe hurricane storm surges historically reported for the site and surrounding area are characterized in Subsection 2.4.5.2.1. The PMH surge SWL calculations are presented in Subsection 2.4.5.2.2. Analysis of the PMH surge begins with the effects of the hurricane as it moves over the continental shelf, producing a surge at the mouth of Delaware Bay, determined using the Bodine model. The surge is superimposed on a coincident 10% exceedance high tide. Outputs of the Bodine model are used as input to HEC-RAS, defining the surge at the mouth of the bay as a stage boundary condition. The upstream boundary of HEC-RAS is the head of tide at Trenton, NJ, where the discharge reflects a historical rainfall event that conservatively represents the effects of hurricane-associated precipitation. The additional effects of wind blowing over the Delaware Bay are calculated using a formula for wind setup in semi-enclosed bodies of water as presented by Kamphuis (Reference 2.4.5-10).

**PSEG Site
ESP Application
Part 2, Site Safety Analysis Report**

Results are compared with results from alternative methods. The methodology used to determine the PMH surge SWL are validated by reproducing the storm surge observed in Delaware Bay from one of the historical hurricanes summarized in Subsection 2.4.5.2.1.

2.4.5.2.1 Historical Surges

Delaware, New Jersey, and Pennsylvania did not experience a direct hit from a major hurricane during the period 1851-2006 (Reference 2.4.5-24). Although storms that create substantial surges in Delaware Bay are rare, the bathymetry and shape of Delaware Bay can produce storm surge in response to hurricanes that make landfall to the west of the bay while traveling in a northward direction. Hurricanes producing severe storm surge at Philadelphia, PA (on the Delaware River estuary 30 miles northeast of the PSEG Site) include the Chesapeake-Potomac hurricane (1933), Hazel (1954), Connie (1955), Floyd (1999), and Isabel (2003). Tracks of these storms are shown in Figure 2.4.5-2, based on data accessed from NOAA's Coastal Services Center (Reference 2.4.5-12). This list of storms is assembled from published descriptions of hurricanes producing significant surges in Delaware Bay and from review of hurricane tracks passing within 100 NM of the new plant location, while making landfall to the west of the mouth of Delaware Bay.

The Chesapeake-Potomac hurricane made landfall as a Category 1 hurricane near Currituck, North Carolina (NC). Traveling northwest, its track paralleled the western shore of Chesapeake Bay. It then turned northeasterly, bringing the storm center within 80 NM of the new plant location (Reference 2.4.5-12). It produced a maximum storm surge of 3.8 ft. near the mouth of Delaware Bay; 7.7 ft. at Reedy Point, DE (nearest tidal gage to the new plant location), and 7.1 ft. at Philadelphia (Reference 2.4.5-3).

Hazel made landfall as a Category 4 hurricane near the border of NC and South Carolina (SC). It moved north, with Category 1 status at its nearest approach to the new plant location, when the storm center was 98 NM west of the new plant location (Reference 2.4.5-12). Hazel produced a maximum storm surge at Philadelphia of 9.4 ft. (Reference 2.4.5-31).

Connie made landfall near Cape Charles, Virginia, as a tropical storm, and its inland track generally followed the eastern shore of Chesapeake Bay. At its nearest point, the storm center was within 43 NM of the new plant location (Reference 2.4.5-12). It produced a maximum surge at Philadelphia of 5.0 ft. (Reference 2.4.5-31).

The storm center of Floyd bypassed Delaware Bay to the south and east, 70 NM from the new plant location, moving northeast as a Category 1 hurricane (Reference 2.4.5-12). It produced a storm surge (after correcting for astronomical tide) of 3.0 ft. at Cape May, NJ (mouth of Delaware Bay); 2.9 ft. at Reedy Point; and 4.0 ft. at Philadelphia (Reference 2.4.5-13).

Traveling northwest, Isabel made landfall as a Category 1 hurricane near Beaufort, NC. The storm center was closest to the new plant location at 163 NM to the southwest. At this point, it was a tropical storm (Reference 2.4.5-12). Isabel produced a storm surge of 3.1 ft. at Lewes, DE; 5.0 ft. at Reedy Point; and 5.4 ft. at Philadelphia (Reference 2.4.5-14).

Hurricane Hazel and the Chesapeake-Potomac hurricane produced the maximum historical storm surges recorded in Delaware Bay. Of these, the Chesapeake-Potomac hurricane storm center passed closer to the new plant location, exhibiting a northwesterly track most similar to

**PSEG Site
ESP Application
Part 2, Site Safety Analysis Report**

the hypothetical storm track of the PMH (References 2.4.5-18 and 2.4.5-17). Based on the storm track and adequate available data related to this storm, the Chesapeake-Potomac hurricane of August 1933 is selected to validate the storm surge model used to determine the PMH surge.

2.4.5.2.2 Estimation of Probable Maximum Storm Surge

In order to satisfy the combined events criteria specified in Section 9.2.2 of ANSI/ANS-2.8-1992, (Reference 2.4.5-1) storm surge at the new plant is evaluated combining probable maximum surge and seiche with wind wave activity concurrent with the 10 percent exceedance high tide, and effects of hurricane-associated precipitation. This subsection outlines the sequence of steps taken to calculate the maximum surge SWL due to PMH. Subsequent subsections describe wave runup and sea level rise estimates.

Surge at the open coast results from meteorological and oceanographic processes occurring offshore over a scale of 500 NM. Between the mouth of the bay and the new plant location, a distance of 50 NM, the propagation of the surge is controlled by the geometry and hydraulics of the estuary. Water levels further increase due to wind blowing directly over the bay. Wave runup addresses processes occurring upwind of the new plant location on spatial scales (fetch lines) of less than 10 NM which are discussed in Subsection 2.4.5.3. The analysis proceeds from the large, offshore spatial scales to smaller spatial scales proximal to the new plant location near the head of Delaware Bay. Details of the storm surge analysis are presented in the remainder of this subsection.

The PMH surge SWL is determined by combining the effects of surge at the open Atlantic coast coincident with the 10 percent exceedance high tide. That surge plus tide is propagated through Delaware Bay to the new plant location; and the effects of wind setup resulting from wind stress over Delaware Bay are superimposed, by addition, on the propagated surge. The overall approach uses:

- Bodine method to determine storm surge at the open coast
- HEC-RAS analysis to propagate that surge through Delaware Bay to the site
- Kamphuis method to determine wind setup at the site caused by winds blowing over the Delaware Bay

The storm surge water levels determined by the Bodine method are used as a stage boundary condition at the mouth of Delaware Bay for the HEC-RAS simulation within the Delaware River estuary. The upstream boundary conditions input into the HEC-RAS model, consisting of discharge of the Delaware River at Trenton, and discharge of tributaries downstream of Trenton, are based on a 2006 event to account for hurricane-related precipitation. The water levels determined by HEC-RAS, and winds defined by NOAA (Reference 2.4.5-18) for the PMH, are used to determine wind setup at the new plant location. The combination of HEC-RAS surge, which includes the 10 percent exceedance high tide, and Kamphuis wind setup determines the PMH surge SWL at the new plant location.

The Bodine model was used by the NRC to develop default storm surge estimates at the open coast in support of RG 1.59 and is cited as an acceptable methodology for such analyses by ANSI/ANS-2.8-1992 (Reference 2.4.5-1).

**PSEG Site
ESP Application
Part 2, Site Safety Analysis Report**

HEC-RAS is a widely accepted model for dynamic flood routing in rivers developed by the U.S. Army Corps of Engineers. It incorporates the ability to simulate hydraulics of estuaries by using a stage hydrograph as a downstream (tailwater) boundary condition. According to ANSI/ANS 2.8-1992, Section 7.3.2.1, a transient one-dimensional model can be used to compute resonance effects for a narrow body of water with a bay entrance. HEC-RAS is one-dimensional, and does not account for flow perpendicular to the primary longitudinal axis of the Delaware Bay and estuary. This model simplification does not have a significant effect on HEC-RAS ability to simulate either the tide or storm surge at the new plant.

Flow in Delaware Bay and near the new plant is predominantly longitudinal (References 2.4.5-36 and 2.4.5-37). Bretschneider determined that cross-wind effects on storm surge are virtually negligible (less than 3 percent) upstream of the head of Delaware Bay (upstream of RM 48), and reduces surge on the east side of the estuary at the new plant location (Reference 2.4.5-3), therefore neglecting cross-wind effects is conservative at the new plant location. The wind setup algorithm of Kamphuis is a steady-state analytical solution of the fundamental equations governing hydrodynamics, which can be found in reference texts (References 2.4.5-27 and 2.4.5-4). Its primary assumption, that water levels exhibit a steady state response to varying winds, is conservative because the bay does not respond to the winds instantaneously. The combination of these methods is demonstrated to be valid by reproducing the storm surge of an actual historical hurricane as described in the remaining paragraphs of this subsection.

These methods are validated by reproducing the surge observed during the Chesapeake-Potomac hurricane of 1933. The pressure distribution and winds associated with this storm are specified as described by Bretschneider (Reference 2.4.5-3) and NOAA (Reference 2.4.5-18). Bretschneider reports a pressure drop of 0.85 in. of Hg. This value is used with NOAA (Reference 2.4.5-18) formulas for the Standard Project Hurricane to determine the pressure distribution and wind field throughout the storm. Bretschneider reports maximum sustained winds over the ocean of 58 mph (50 kt), and maximum sustained winds over Delaware Bay of 50 mph (43 kt). The simulated storm exhibits maximum winds of 64 mph (56 kt) over the ocean, and 47 mph (41 kt) over Delaware Bay, similar to the wind speeds reported for the Chesapeake-Potomac hurricane.

Coincident astronomical tides are specified at the mouth of Delaware Bay. Comparison of model results with the actual response to the Chesapeake-Potomac hurricane is expressed as storm surge, the difference between actual water levels and the predicted astronomical tide level. The storm surge calculated at the mouth of Delaware Bay, using the Bodine method, reproduces the observed surge as described by Bretschneider (Reference 2.4.5-3). Comparison of observed and simulated surge at the mouth of the bay is illustrated in Figure 2.4.5-3. The peak storm surge at Reedy Point, DE, is calculated to be 7.9 ft., while the observed surge at Reedy Point was 7.7 ft. Water surface elevations (surge plus tide) at Reedy Point are illustrated in Figure 2.4.5-4. The Delaware Bay storm surge model described here is demonstrated to be conservative. The margin of error is consistent with comparable models, such as NOAA's SLOSH model which has a stated margin of error of +/- 20 percent (Reference 2.4.5-23).

2.4.5.2.2.1 Estimation of 10 Percent Exceedance High Tide

Maximum monthly high tide values from 1987 through 2008 are analyzed at NOAA tidal gage stations upstream and downstream from the new plant location to determine the 10 percent exceedance high tide at the site (Reference 2.4.5-16). This analysis calculates a 10 percent

**PSEG Site
ESP Application
Part 2, Site Safety Analysis Report**

exceedance high tide of 4.2 ft. NAVD at the Lewes, DE, NOAA tidal gage (8557380) at river mile (RM) 0, and 4.6 ft. NAVD for the Reedy Point, DE, NOAA tidal gage (8551910) at RM 59 as illustrated in Figure 2.4.5-5. Based on these values, the 10 percent exceedance high tide at the new plant location at RM 52 is determined by linear interpolation to be 4.5 ft. NAVD.

This approach for estimating 10 percent exceedance high tide, based on recorded tides, intrinsically includes the effects of sea level anomaly (also known as initial rise). ANSI/ANS-2.8-1992, Section 7.3.1.1.2, concludes sea level anomaly need not be included when 10-percent exceedance high tide is based on recorded tides. Sea level anomaly is not included in this analysis because recorded tide data is used to calculate the 10-percent exceedance high tide.

2.4.5.2.2.2 Storm Surge at the Open Coast

Calculations presented by Bodine are verified by reproducing a sample problem provided by Bodine (Reference 2.4.5-2). The model reproduced Bodine's results for maximum surge to four significant figures.

Inputting the PMH identified in Subsection 2.4.5.1 into the Bodine calculations, a maximum surge elevation of 20.9 ft. NAVD is calculated at the mouth of Delaware Bay. This value includes a fluctuating tide at the mouth of the bay that generates the 10 percent exceedance high tide at the new plant coincident with the peak storm surge (Figure 2.4.5-6).

As a point of comparison, other methodologies available from NOAA and NRC to determine storm surge at the open coast are NOAA's SLOSH program and RG 1.59 Appendix C. SLOSH results are accessed using the SLOSH Display Program v. 1.61g (Reference 2.4.5-22) and adjusted to account for the 10 percent exceedance high tide and NAVD datum. NOAA uses SLOSH to determine hurricane surge levels for a large number of potential hurricanes and provides access to the results via the SLOSH Display Program. The storms presented in the Display Program include a Category 4 storm on the Saffir-Simpson scale, but the Delaware Basin v3 SLOSH dataset does not include a storm with the same parameters as the PMH determined for the PSEG Site. Using the SLOSH Display Program, the highest surge elevation at the mouth of Delaware Bay is 17.6 ft. NAVD. Accounting for the 10 percent exceedance high tide indicates a Category 4 storm elevation of 19.8 ft. NAVD.

RG 1.59 is applicable to determine PMH surge levels on open coast sites on the Atlantic Ocean and Gulf of Mexico. Therefore, it is appropriate to use this methodology for estimating storm surge up to the mouth of Delaware Bay, but it is not appropriate to use it beyond the area where a hurricane makes initial landfall. As such, it is not an acceptable method for estimating surge at the new plant. RG 1.59, Appendix C, results for the mouth of Delaware Bay are based on interpolating results from Atlantic City, NJ, and Ocean City, MD, and then adjusting to NAVD. Including the 10 percent exceedance high tide, RG 1.59 estimates a maximum storm surge of 21.7 ft., NAVD at the mouth of the Delaware Bay.

While the three methods do not compare the exact same hurricane parameters, the three models produce similar storm surge estimates at the mouth of Delaware Bay for Category 4 hurricanes. The Delaware Basin v3 SLOSH dataset does not include a storm with the same parameters as the PMH determined for the PSEG Site. Therefore, SLOSH is not used to determine the peak surge at the mouth of the Bay. RG 1.59 cannot be used to determine surge at the new plant location, and cannot be used as a substitute for the Bodine method because it

**PSEG Site
ESP Application
Part 2, Site Safety Analysis Report**

does not provide a stage hydrograph for the simulated hurricane to input into HEC-RAS. Further, RG 1.59 does not simulate the PMH as defined by NWS 23 (References 2.4.5-32 and 2.4.5-18). The Bodine method produces a more conservative result than SLOSH, and can specifically simulate the response to the PMH. Therefore, the Bodine model is selected as the basis for determining the PMH surge. The stage hydrograph, including the peak surge at the mouth of the bay calculated using the Bodine method, is input to the HEC-RAS model which propagates the storm surge through Delaware Bay.

2.4.5.2.2.3 Propagation of Surge through Delaware Bay

The propagation of surge through Delaware Bay is calculated using the HEC-RAS computer program. The HEC-RAS model is developed using channel geometry and floodplain elevations for the Delaware River between Trenton, NJ, and the head of Delaware Bay determined from the Triangular Irregular Network (TIN) terrain model developed from the U.S. Geological Survey (USGS) National Elevation Dataset (NED) (Reference 2.4.5-30) digital elevation model (DEM), and the NOAA Estuarine Bathymetry DEM (Reference 2.4.5-19). The HEC-RAS model is calibrated using observed tidal data. The calibrated model is then used to simulate the propagation of the surge from the mouth of Delaware Bay to the new plant.

In order to simulate the propagation of the PMH surge, the surge hydrograph generated by the Bodine calculations for the PMH is used as the stage boundary condition at RM 0. Discharge hydrographs generated by the Hydrologic Engineering Center-Hydrologic Modeling System (HEC-HMS) for the Delaware River at Trenton and its major tributaries downstream of Trenton are used to simulate flow conditions in the Delaware River resulting from a historical rainfall event that conservatively represents the effects of hurricane-associated precipitation. Specifically, the HEC-RAS model uses a historical rainfall event that occurred in June 2006 that produced a basin average rainfall of 6 inches in the Delaware River Basin.

A discharge boundary condition at Trenton, defined by the HEC-HMS model response to the June 2006 rainfall event is input into the HEC-RAS model (Reference 2.4.5-29). Discharges from tributaries downstream of Trenton are also based on the HEC-HMS hydrographs for the June 2006 event, representing hurricane-associated precipitation. The output from the Bodine method describing the surge at the open coast is specified as the stage boundary condition at RM 0.

The effect of winds blowing over Delaware Bay, referred to as wind setup, is calculated using a standard method presented by Kamphuis (Reference 2.4.5-10), and is added to the HEC-RAS simulated water levels. Wind setup depends on wind speed and direction over the center of Delaware Bay; a coefficient accounting for wind and bottom stress; and water depth. The winds over the center of Delaware Bay at model time step 20.5 hours are 120 kt from the south-southeast, determined in accordance with NWS 23 (Reference 2.4.5-18). The stress coefficient is 3.3×10^{-6} (Reference 2.4.5-3). The cross-section average depth of water varies with RM and time, and is determined from the HEC-RAS water levels and channel geometry. The calculated wind setup at time 20.5 hours is 14.0 ft. at the new plant location. The wind setup is added to the HEC-RAS water level to determine the SWL, 26.86 ft. at $t = 20.5$ hours (Table 2.4.5-1).

Using the methods described in this subsection, the PMH surge SWL at the new plant location is 26.9 ft. NAVD (Table 2.4.5-1 and Figure 2.4.5-6). This maximum still water surface elevation combines the coincident effects of the 10 percent exceedance high tide, the propagation of the

**PSEG Site
ESP Application
Part 2, Site Safety Analysis Report**

open coast surge through Delaware Bay, hurricane-associated precipitation, and the effect of winds over Delaware Bay.

The maximum SWL may be compared with maximum surge levels calculated by the NOAA SLOSH model, accessed using the SLOSH Display Program v. 1.61g (Reference 2.4.5-22). However, the Delaware Basin v3 SLOSH dataset does not include a storm with the same parameters as the PMH determined for the PSEG Site, nor do results include the 10 percent exceedance high tide, or effects of river flow. The maximum surge level reported by the SLOSH Display Program at the new plant location is 22.8 ft. NAVD. Adjusting to include the 10 percent exceedance high tide indicates a Category 4 storm elevation of 25.3 ft. NAVD using the SLOSH Display Program.

Based on the analyses described in Subsection 2.4.5.2, the PMH surge SWL at the new plant location is 26.9 ft. NAVD. The maximum WSEL, including wave runup, occurs one-half hour later, when the still water level is 26.7 ft. NAVD (Subsection 2.4.5.5 and Table 2.4.5-1).

2.4.5.3 Coincident Wave Runup

Subsection 2.4.5.3.1 presents the methodology used to determine wave runup coincident with the PMH surge. Results of the analysis are provided in Subsection 2.4.5.3.2. The resultant wave runup is added to the maximum SWL.

2.4.5.3.1 Methodology

Coincident wave runup, in association with the PMH surge, is determined using the approach described by USACE (Reference 2.4.5-27). Winds are estimated at the new plant location in accordance with NOAA (Reference 2.4.5-18). Water depth is determined from the TIN terrain model, using coincident water levels determined by the Delaware Bay storm surge model, as defined in Subsection 2.4.5.2. The wave field is fetch- and duration-limited, as defined by USACE. Wind vectors are averaged over time consistent with the fetch and duration limitations, as specified by USACE. The significant wave height and period are calculated using the straight line fetch and the friction velocity. A check is made to validate the use of deep water equations, comparing the calculated significant wave period with the limiting spectral peak period. If the calculated period is less than the limiting spectral peak period, then the deep water equations are valid. Otherwise, the wave heights are limited by breaking. The maximum breaker height is determined using the Miche criterion (Reference 2.4.5-27).

The SWL and wave data (significant wave height, period, and direction) over the course of the PMH storm surge event are shown in Table 2.4.5-5. The wave runup calculations described below are performed at each half hour interval.

Wave runup calculations for the new plant are based upon the latest design guidance found in the USACE CEM, Chapter VI-5 (Reference 2.4.5-27). The new plant's powerblock will be constructed on engineering fill with riprap protection, with facing slopes of 3:1 (horizontal:vertical), as shown on Figure 2.5.4.5-2.

Although the CEM prescribes the use of significant wave height to calculate wave runup, one alteration from the methodology presented in the CEM is the use of the lesser of (a) the maximum wave height, or (b) the "breaker height" (0.78 times depth of water) for computation of

**PSEG Site
ESP Application
Part 2, Site Safety Analysis Report**

wave runup as required by Reference 2.4.5-1. Per Reference 2.4.5-1, the maximum wave height, H_{max} , is defined as the 1 percent wave, $H_{1\%}$, and for deep water waves, $H_{max} = 1.67$ times the significant wave height, H_s . CEM Equation II-1-132 also defines $H_{1\%}$ as 1.67 times H_s (Reference 2.4.5-27). Consequently, H_s is replaced by H_{max} (H_s times 1.67) in the CEM equations for both the surf similarity parameter and the wave runup for the PSEG Site. This alteration essentially yields the highest runup of any single wave running up the embankment.

CEM Equation VI-5-3 provides a general form for the wave runup equation for structures as (Reference 2.4.5-27):

$$R_{ui\%} / H_s = (A \xi + C) \gamma_r \gamma_b \gamma_h \gamma_\beta \quad (\text{Equation 2.4.5-1})$$

where:

- $R_{ui\%}$ runup level exceeded by i percent of the incident waves
- H_s significant wave height of incident waves at the toe of the structure, in this case, the maximum wave height ($H_{max} = 1.67H_s$)
- ξ surf similarity parameter, ξ_{om} or ξ_{op} (defined below)
- A, C coefficients dependent on ξ and i but related to the reference case of a smooth, straight impermeable slope, long-crested head-on waves and Rayleigh-distributed wave heights
- γ_r reduction factor for influence of surface roughness
- γ_b reduction factor for influence of a berm ($\gamma_b = 1$ for non-bermed profiles)
- γ_h reduction factor for influence of shallow-water conditions where the wave height distribution deviates from the Rayleigh distribution ($\gamma_r = 1$ for Rayleigh distributed waves)
- γ_β factor for influence of angle of incidence β of the waves ($\gamma_\beta = 1$ for head-on long-crested waves, i.e., $\beta = 0^\circ$). The influence of directional spreading in short-crested waves is included in γ_β as well.

The surf similarity parameter for random waves is defined as:

$$\xi_{om} = \frac{\tan \alpha}{\sqrt{S_{om}}} \quad \text{or} \quad \xi_{op} = \frac{\tan \alpha}{\sqrt{S_{op}}} \quad (\text{Equation 2.4.5-2})$$

where:

$$S_{om} = \frac{2\pi}{g} \frac{H_s}{T_m^2}$$

$$S_{op} = \frac{2\pi}{g} \frac{H_s}{T_p^2}$$

$\tan \alpha$ is the structure slope

**PSEG Site
ESP Application
Part 2, Site Safety Analysis Report**

T_m is the mean wave period

T_p is the spectral peak wave period

For the new plant an i value of 2 percent is adopted. This establishes values for A and C in Equation 2.4.5-1 depending on the surf similarity parameter as provided by CEM Equation VI-5-6:

$$A=1.5 \xi_{op} ; C = 0 \text{ for } 0.5 < \xi_{op} \leq 2$$

$$A=0.0 ; C = 3.0 \text{ for } 2 < \xi_{op} \leq 3-4$$

In establishing the y parameters to be used in the calculations of wave runup at the new plant, the berm factor γ_b is set equal to 1.0 because there is no berm in the design cross-section. The shallow water reduction factor is conservatively set to 1.0 as there will be storm surge conditions where the waves impinging on the new plant's slope will be non-breaking (i.e., Rayleigh distributed). The roughness factor γ_r as provided by Table VI-5-3 of the CEM is between 0.5 and 0.6, dependent upon the number of layers of rock to be placed on the slope. As this design detail has yet to be determined, the least restrictive value of 0.6 is selected for conservatism. Finally, it is assumed that the waves are head-on; i.e., normally-incident to the slope, so that γ_β is set equal to 1.0.

2.4.5.3.2 Wave Runup at the New Plant Location

Wave runup is determined at a time coinciding with the maximum PMH surge SWL at the new plant location, as well as half-hour intervals immediately before and after that time. Calculations during the extended time are performed to ensure that the maximum PMH flood level, consisting of the SWL plus wave runup, is identified. Coincident wave runup in association with the PMH is determined using the methodology described in Subsection 2.4.5.3.1. Winds coincident with the maximum surge are determined at the new plant location using the methodology described by NOAA (Reference 2.4.5-18).

At the time when SWL plus wave runup peaks, the wind speed is 104 kt from the east-southeast. Due to the flood levels associated with the PMH surge, the inundated fetch line upwind to the east-southeast is 8.3 mi. The wave field reaches steady state along this fetch line if winds blow steadily along the fetch line for 1.5 hours (hr.). Therefore, wind speed is averaged over the prior 1.5 hr. to determine an appropriate wind speed and direction.

The significant deep water wave height is 14.7 ft., and its period is 5.6 seconds. The maximum wave height is 24.5 ft.; however, the average depth along the fetch line is 22.0 ft. Thus, the deepwater equations are not valid: waves of this height would break. The maximum breaker height is 14.5 ft. Wave runup is estimated from the maximum wave height or the maximum breaker height, whichever is less; in this case the maximum breaker height. The wave runup is calculated to be 14.3 ft., using the procedure described in Subsection 2.4.5.3.1. Table 2.4.5-5 presents the wave runup results at each time step calculated.

2.4.5.4 Potential Sea Level Rise

NOAA has evaluated the trend of sea level at the NOAA Reedy Point tidal gage station. Measurements at any given tide station include both global sea level rise and vertical land motion, such as subsidence, glacial rebound, or large-scale tectonic motion. The monthly sea

Rev. 4

**PSEG Site
ESP Application
Part 2, Site Safety Analysis Report**

level trend based on monthly mean sea level data from 1956 through 2006 is 1.14 ft./century, with an upper 95 percent confidence limit of 1.35 ft./century (Reference 2.4.5-21). The maximum flood level determined at the new plant location includes 1.35 ft. to conservatively account for sea level rise over the projected 60 year life of the new plant.

2.4.5.5 Maximum Water Surface Elevation Associated with the PMH

The PMH, defined in Subsection 2.4.5.1, is determined to produce the PMH surge, as defined in NRC RG 1.59. Specifically, the storm used to determine maximum WSEL is the PMH that causes the PMH surge as it approaches the site along a critical path at an optimum rate of movement. At the time when water levels including wave runup peak, the SWL at the new plant location is calculated to be 26.7 ft. NAVD using the Bodine, HEC-RAS and Kamphuis method. The addition of wave runup, 14.3 ft., creates a water surface elevation of 41.0 ft. NAVD. Future sea level rise of 1.35 ft. per century is added to the effects of storm surge and wave runup for a maximum water surface elevation that could occur during the projected life of the new plant of 42.4 ft. NAVD at the new plant location. This result is illustrated in Figure 2.4.5-7, and water elevations from the combined events are presented in Table 2.4.5-1, which discusses rounding the result to tenths of ft.

Maximum wave runup does not occur simultaneously with maximum still water level (Table 2.4.5-1). When the SWL reaches its maximum at 26.9 ft. NAVD, wave runup is 12.8 ft, which combines to an elevation of 39.7 ft. NAVD. One half-hour later, still water level drops to 26.7 ft. NAVD and wave runup increases to 14.3 ft., which combines to 41.0 ft. NAVD (Figure 2.4.5-7), 0.3 ft. higher than the previous time step.

2.4.5.6 PMH Design Basis Flood Level

The maximum SWL results reported in Subsection 2.4.5.5 are based on a simplified modeling approach available at the time of the initial ESPA preparation. Subsequently, high-resolution storm surge modeling systems, and the computational resources required to run them, have become the standard for more accurate determination of flood levels due to hurricane storm surge. NUREG/CR-7046, *Design-Basis Flood Estimation for Site Characterization at Nuclear Power Plants in the United States of America*, supports use of these high-resolution models as they allow more detailed and accurate simulations of storm surges because they are based on more recent understanding of the physics of the hurricane-storm surge processes; resolve the spatial heterogeneity in bathymetry, topography, and hydrologic characteristics; and can explicitly account for coastal structures that may impede or enhance the movement of storm surge inland. NUREG/CR-7046 also introduces the hierarchical hazard assessment (HHA) process. The HHA is a progressively refined, stepwise estimation of site-specific hazards that evaluates the safety of SSCs with the most conservative plausible assumptions consistent with available data. Consistent with this process, this subsection presents a more site-specific storm surge hazard assessment using the high-resolution storm surge modeling system described below.

The design basis flood level for the PSEG Site is established by using the PMH meteorological parameters determined in Subsection 2.4.5.2 and simulating the surge response in a current day two-dimensional storm surge modeling system. This subsection presents information on

**PSEG Site
ESP Application
Part 2, Site Safety Analysis Report**

the development of the modeling system, the PMH cases run in the model and the design basis flood level determined at the PSEG Site.

2.4.5.6.1 Modeling System

The modeling system used for the analysis of the PMH surge at the PSEG Site uses a suite of state-of-the-art numerical wind, wave, and surge models and methods to compute surge still and total WSELs at the points of interest. The model suite consists of the Oceanweather Planetary Boundary Layer (PBL) wind model for tropical storms, the wave-field model Simulating Waves Nearshore (SWAN), and the storm surge and tidal model ADCIRC. This wind, wave, and surge modeling approach is very similar to the recent FEMA-sponsored Region III floodplain-mapping project (Reference 2.4.5-44). In addition to the numerical models, estimation of wave runup at the points of interest to establish a maximum total WSEL is determined using the approach described by USACE (Reference 2.4.5-27). The input to the modeling system is a series of parameters that represent the synthetic storm (i.e., storm track, which consists of time, position, central pressure, Holland B parameter [which controls the shape of the pressure and wind fields], radius to maximum winds, and peripheral pressure). The output from the modeling system is the maximum SWL and total WSEL for the PSEG Site associated with each individual storm modeled.

2.4.5.6.1.1 Wind Model

The Oceanweather PBL model is used to develop wind and pressure fields for the synthetic storms (Reference 2.4.5-40). For each storm, defined by a track and time varying wind field parameters, the Oceanweather PBL model is applied to construct wind and atmospheric pressure fields every 15 minutes for driving surge and wave models. Oceanweather generates wind and pressure fields with a highly refined meso-scale moving vortex formulation developed originally by Chow (Reference 2.4.5-39) and modified by Cardone et al. (Reference 2.4.5-38). The model is based on the equation of horizontal motion, vertically averaged through the depth of the planetary boundary layer.

2.4.5.6.1.2 ADCIRC+SWAN Model

Storm surge simulations are performed using the tightly coupled ADCIRC+SWAN state of-the-art coastal circulation and wave model. ADCIRC is based on the two-dimensional, vertically integrated shallow water equations that are solved in Generalized Wave Continuity Equation form (Reference 2.4.5-41). The equations are solved over complicated bathymetry encompassed by irregular seashore boundaries using an unstructured finite-element method. This algorithm allows for flexible spatial discretizations over the entire computational domain. The advantage of this flexibility in developing a computational mesh is that larger elements can be used in open-ocean regions where coarser resolution is needed, whereas smaller elements can be applied in the nearshore and estuary areas where finer resolution is required to resolve hydrodynamic details and more accurately simulate storm surge propagation onto a complex coastal landscape. (Reference 2.4.5-45)

The recent FEMA Region III storm surge study developed a high-resolution ADCIRC mesh that covers the entire Delaware Bay and PSEG Site region (see Figure 2.4.5-8). The ADCIRC mesh is comprised of a high-resolution grid covering FEMA Region III that was appended to a

**PSEG Site
ESP Application
Part 2, Site Safety Analysis Report**

previously developed grid of the western North Atlantic, the Gulf of Mexico and the Caribbean Sea. Specifically, the grid covers the area from the 60 degrees west meridian to the US mainland. Within FEMA Region III, the grid extends inland to the 49.2 ft. NAVD (15 m) contour to allow for inland storm surge flooding. In this region, the grid was designed to resolve major bathymetric and topographic features such as: inlets; dunes; and river courses, as identifiable on the detailed FEMA digital elevation model (DEM), satellite images, and National Oceanic and Atmospheric Administration (NOAA) charts. (References 2.4.5-42 and 2.4.5-43)

After confirming the FEMA developed ADCIRC mesh was operating correctly on the project computing platform, the mesh is refined in the vicinity of the PSEG Site to more accurately represent the topographic features of the site. To properly describe the topographic features important to the hydrodynamic and wave characteristics at the PSEG Site, high resolution, site-specific topographic data including the controlling vertical features important to surge conveyance and wave propagation were incorporated into the finite element mesh. The refined mesh for the PSEG Site area is shown on Figure 2.4.5-9. The refined PSEG Site mesh is inserted into the overall FEMA Region III mesh and the model is re-validated using the same Hurricane Isabel and Nor'easter Ida test storm input files as the FEMA Model validation report prepared by USACE (Reference 2.4.5-44). A graphical comparison of water levels from the Hurricane Isabel storm simulation on the refined PSEG Site mesh and unmodified FEMA Region III at locations around the PSEG Site is shown in Figure 2.4.5-10. This process confirms that the refined mesh produces results that are essentially the same as the unmodified FEMA Region III mesh in the vicinity of the PSEG Site.

2.4.5.6.1.3 Wave Runup Estimation

The ADCIRC+SWAN simulations of each storm produce SWL and wave data (significant wave height, period, and direction) over the course of each storm surge event. Wave field data on each of the four sides of the site (see Figure 2.4.5-11) are provided at 15-minute intervals. The data is analyzed and captured for the subsequent wave runup calculations. The wave runup calculations described below are performed at each time step and at each of the four locations around the site. After the calculations are performed, the maximum total WSEL value, defined as the SWL plus wave runup, at any of the four points is captured as the maximum value for that storm event.

Wave runup calculations for the new plant are based upon the latest design guidance found in the USACE CEM, Chapter VI-5 (Reference 2.4.5-29). The new plant's powerblock will be constructed on engineered fill with riprap protection, with facing slopes of 3:1 (horizontal:vertical), as shown on Figure 2.5.4.5-2. The wave runup equations described in Subsection 2.4.5.3.1 are used for the analysis. Additionally, the angle of incidence factor is considered variable in this analysis because more detailed wave direction information is available from the ADCIRC+SWAN model.

Based upon Equation VI-5-11 from the CEM and the expectation that waves impinging on the slope will be short-crested, the angle reduction factor is given by:

**PSEG Site
ESP Application
Part 2, Site Safety Analysis Report**

$$Y_{\beta} = 1 - 0.0022 \beta \quad \text{(Equation 2.4.5-3)}$$

where:

β (in degrees) is computed based upon the mean wave direction produced by SWAN and the orientation of the new plant's embankment.

The angle, β , is oriented such that it is zero when the incident wave direction is normal to a particular side of the new plant's embankment and is valid up to $\pm 90^\circ$ from due perpendicular. For example, at the Western point of interest (see Figure 2.4.5-11) a wave would need to have an easterly direction component to be impinging on the site. If the wave is traveling due East, then the angle β is zero and no reduction factor for wave direction is included in the wave runup calculation. If the wave is traveling in an easterly direction with some north/south component to it, then the wave runup is reduced according to the factor determined using Equation 2.4.5-3. This reduction factor is conservatively set to be very small and is only 20 percent when the wave is parallel to the shore (i.e., ± 90 degrees).

2.4.5.6.2 PMH Storm Simulations

Using the modeling system described in Subsection 2.4.5.6.1, three PMH storm simulations are run with differing antecedent water level conditions to compare the sensitivity of the resultant WSEL at the PSEG Site to the effects of potential sea level rise and 10 percent exceedance high tides. The PMH parameters described in Subsection 2.4.5.2 are used as an input to the modeling system. Table 2.4.5-4 provides the input parameters for each PMH model simulation.

One additional parameter not identified by NOAA (Reference 2.4.5-18), but required by the Oceanweather PBL wind field model is the Holland B parameter. A Holland B parameter of 1.1 is selected for these simulations, as this represents the mean value for the region.

As described in Subsection 2.4.5.2.2, the combined events criteria specified in Section 9.2.2 of ANSI/ANS-2.8-1992, (Reference 2.4.5-1) for determining the storm surge at the new plant is evaluated by combining probable maximum surge and seiche with wind wave activity concurrent with the 10 percent exceedance high tide, and effects of hurricane-associated precipitation. The modeling system developed for the PMH analysis accounts for the surge with wind wave activity concurrent with the 10 percent exceedance high tide through the use of antecedent water levels. The effects of hurricane-associated precipitation are not included in the analysis.

Analysis of the effects of precipitation based flooding in the Delaware River Basin is discussed in Subsections 2.4.3 and 2.4.4. These subsections estimate the resultant WSEL at the PSEG Site from the 500 year flood and various probable maximum precipitation events. While the ANSI/ANS-2.8-1992 combined events criteria only requires assessment of hurricane-associated precipitation, even these extreme precipitation events do not significantly increase the WSEL at the PSEG Site due to the size of the Delaware River at this location. Based on the limited response in WSEL at the PSEG Site to extreme precipitation events and the significantly higher WSEL when the PMH storm is modeled in the ADCIRC+SWAN modeling system, effects of hurricane-associated precipitation are not expected to affect the peak WSEL identified in the analysis.

**PSEG Site
ESP Application
Part 2, Site Safety Analysis Report**

2.4.5.6.3 PMH Design Basis Flood Level

Table 2.4.5-4 presents the resulting maximum WSEL's at the PSEG Site for each PMH event modeled. The only difference between each of the ADCIRC+SWAN simulations of the PMH is the antecedent water levels. Varying the antecedent water levels of the model simulations from 0 ft. NAVD to 5.85 ft. NAVD to conservatively account for potential sea level rise and the 10 percent exceedance high tide results in an approximate 1 ft. difference in maximum WSEL at the PSEG Site. The PMH simulations in the ADCIRC+SWAN modeling system produce maximum WSELs approximately 10 ft. below the equivalent maximum WSEL of the Bodine, Kamphuis, and HEC-RAS modeling approach.

The design basis flood level due to a PMH storm surge event at the PSEG Site is established using the results of Run No. 2 (Table 2.4.5-4). This simulation conservatively sets the antecedent water level of the entire model domain to the estimated sea level rise value at the end of the life of the new plant (see Subsection 2.4.5.4). Run No. 3 includes an antecedent water level that includes sea level rise and 10 percent exceedance high tide applied to the entire model domain. Raising the domain water level to reflect an increase in sea level rise is appropriate, due to the global effects of this phenomenon. Tidal variations are localized effects, and, therefore, it is more accurate to account for tides as a localized increase in the results of the model, rather than an antecedent water level increase. Therefore, Run No. 3 is considered unrealistic and not considered as the design basis level. The PMH maximum WSEL of 32.1 ft. NAVD using the high-resolution modeling system described in Subsection 2.4.5.6.1 represents the design basis flood for the new plant location.

2.4.5.7 Sediment Erosion and Deposition Associated with the PMH Surge

Tidal current velocities normally range from 2 to 3 ft/sec. Velocities determined by the HEC-RAS model's simulation of the PMH surge show that velocities throughout Delaware Bay exceed 4.9 ft/sec; while velocities in the river channel near the new plant exceed 8 ft/sec. These calculated current velocities are sufficient to cause resuspension of natural sediments and cause erosion (Reference 2.4.5-5). Safety-related SSC will be protected against erosion that could affect the integrity of those facilities.

Gross deposition is determined by conservatively assuming that all total suspended solids in the water column are deposited within a few days after passage of the hurricane. Observations of total suspended solids concentrations (TSS) in other bays and estuaries shortly after passage of hurricanes indicate that TSS increase approximately tenfold more than normal pre-storm levels (References 2.4.5-9, 2.4.5-34, and 2.4.5-35). TSS levels near the bottom of the Delaware Bay normally range between 450 and 525 mg/L during the flood and ebb periods in the tidal cycle (Reference 2.4.5-5). Therefore, TSS levels immediately after the storm could reach 5000 mg/L, ten times greater than the normal level of approximately 500 mg/L. Since current velocities are higher in the river channel near the new plant than would generally occur throughout Delaware Bay, net erosion is more likely to occur than net deposition. Since the intake structure would be protected from erosion, net deposition could occur immediately around the intake structure. Calculations based on the assumption that 5000 mg/L of total suspended solids deposit shortly after the passage of the hurricane indicate that deposition is not expected to exceed 2 in. of sediment.

**PSEG Site
ESP Application
Part 2, Site Safety Analysis Report**

The effect of the PMH surge on sediment deposition and erosion is not expected to adversely affect operation of safety-related SSC.

2.4.5.8 Seiche and Resonance

Seiche is an extreme sloshing of an enclosed or partially enclosed body of water excited by meteorological causes (e.g., barometric fluctuations, storm surges, and variable winds), interaction of wave trains with geometry and bathymetry of the water body (e.g., from tsunamis), and seismic causes (e.g., a local seismic displacement resulting in sloshing of the water body).

Seiche motion can be complex in water bodies with variable width and depth. The simplest seiche motion in an estuary like Delaware Bay causes the largest water level fluctuations at the head of tide (near Trenton, NJ) while water levels are relatively constant at the mouth of the bay. This type of seiche is called the fundamental mode (Reference 2.4.5-27). The free oscillation period of the fundamental mode seiche propagating along the length of the Delaware Estuary from its mouth at RM 0 to the head of tide at Trenton (RM 134) is 31 hrs.

Shorter length seiche waves (with shorter oscillation periods) are possible. The effect of winds blowing along the axis of Delaware Bay (northwest-southeast) may excite a seiche within Delaware Bay, but with little effect on the upper estuary, due to the change in orientation of the river in the upper estuary (more nearly northeast-southwest) and less surface area for the wind to act on. Therefore, winds from the northwest tend to excite a shorter length wave with greater effect in Delaware Bay and less effect in the upper estuary. Fluctuations in the strength of northwest winds could generate seiche waves of the second mode, which have a period of 10 hrs. (Reference 2.4.5-27).

Researchers have observed water level fluctuations in Delaware Bay that have lower frequency than tides, which are semidiurnal (indicating 12-hour periods). Water level fluctuations that have lower frequency than tides are referred to as subtidal. The magnitude of such subtidal oscillations observed by these researchers at the new plant location was less than 2 ft. Researchers further determined that these water level fluctuations are associated with wind forces of two types. The first type is direct wind stress on the surface of Delaware Bay, while the second is an indirect forcing associated with wind stress fluctuations over the Atlantic Ocean. The fluctuations in wind stress are associated with fluctuations in water levels in the Delaware Bay at periods of more than 3 days. Together, these direct and indirect wind stress fluctuations are associated with nearly all subtidal fluctuations of water surface elevations observed at Reedy Point, DE, 7 mi. from the new plant location. (References 2.4.5-36 and 2.4.5-37)

From the observations reported, it can be seen that the atmospheric forcing, associated with seiche motion in Delaware Bay, occurs with longer periods (more than 3 days) than the natural period of oscillation of the Delaware Estuary (30 hrs. or less). Therefore, Delaware Bay does not resonate with the meteorologically-induced wave periods. This lack of resonance contributes to the relatively small magnitude of seiche motion in Delaware Bay.

The Delaware Bay also would not resonate with seismic activity. Seismic waves have a period of 1 hr. or less (Reference 2.4.5-25). Subsection 2.4.6 documents the effect of tsunami-induced seiche motion in Delaware Bay, showing that the magnitudes of water level fluctuations are too small to affect safety-related SSC.

**PSEG Site
ESP Application
Part 2, Site Safety Analysis Report**

Due to the lack of resonance with identified forcing functions, as well as observational evidence of the relatively small magnitude of seiche motions, potential seiche waves produce much smaller flood levels than the PMH surge.

2.4.5.9 References

- 2.4.5-1 American National Standards Institute/American Nuclear Society, "Determining Design Basis Flooding at Power Reactor Sites," ANSI/ANS-2.8-1992, p. 1, 20, 32, 1992.
- 2.4.5-2 Bodine, B.R. 1971, "Storm Surge on the Open Coast Fundamental and Simplified Prediction," U.S. Army Corps of Engineers, Coastal Engineering Research Center Technical Memorandum No. 35, 1971.
- 2.4.5-3 Bretschneider, C.L, "Hurricane Surge Predictions for Delaware Bay and River," Department of the Army Corps of Engineers, Beach Erosion Board, Miscellaneous Paper No. 4-59, 1959.
- 2.4.5-4 Bretschneider, C.L, "Engineering Aspects of Hurricane Surge," Estuary and Coastline Dynamics, A.T. Ippen, ed., McGraw-Hill, New York, p. 231 – 256, 1966.
- 2.4.5-5 Cook, T.L., C.K. Sommerfield and K. Wong, "Observations of Tidal and Springtime Sediment Transport in the Upper Delaware Estuary," Estuarine Coastal and Shelf Science, 72: p. 235 – 246, 2007.
- 2.4.5-6 d'Angremond, K. and F.C. van Roode, "Breakwaters and Closure Dams," Taylor and Francis, London, p. 148, 2004.
- 2.4.5-7 Donelan, M.A., B.K. Haus, N. Reul, W.J. Plant, M. Stiassnie, H.C. Graber, O.B. Brown and E.S. Saltzman, "On the Limiting Aerodynamic Roughness of the Ocean in Very Strong Winds," Geophysical Research Letters, 31:L18306(5 pp.), 2004.
- 2.4.5-8 Harleman, D.R.F, "Tidal Dynamics in Estuaries, Part II: Real Estuaries," Estuary and Coastline Hydrodynamics, A.T. Ippen, ed., McGraw-Hill, New York, 1966.
- 2.4.5-9 Jones, S.H., et al., "Transport and Fate of Microbial Contaminants and Suspended Sediments in the Great Bay: Effects on Water Quality and Management Implications," Technical Completion Report #59 (USGS Grant), 1992.
- 2.4.5-10 Kamphuis, J.W., "Introduction to Coastal Engineering and Management," World Scientific Publishing Co., River Edge, New Jersey, 2000.
- 2.4.5-11 MASER Consulting, PA ALTA/ACSM Land Title Survey for PSEG Nuclear LLC of Block 26, Lots 4, 4.01, 5 and 5.01, Job Number 05001694D, Index Number HASU023453, dated June 13, 2008.

**PSEG Site
ESP Application
Part 2, Site Safety Analysis Report**

- 2.4.5-12 National Oceanic and Atmospheric Administration, Coastal Services Center, "Historical Storm Tracks," Website, <http://csc-s-maps-q.csc.noaa.gov/hurricanes/download.jsp>, accessed April 1 – April 9, 2009.
- 2.4.5-13 National Oceanic and Atmospheric Administration, "Effects of Hurricane Floyd on Water Levels Data Report," NOAA Technical Report NOS CO-OPS 027, 2000.
- 2.4.5-14 National Oceanic and Atmospheric Administration, "Effects of Hurricane Isabel on Water Levels Data Report," NOAA Technical Report NOS CO-OPS 040, 2004.
- 2.4.5-15 National Oceanic and Atmospheric Administration, "FAQ / State of the Science: Atlantic Hurricanes and Climate," 2 pp., 2006.
- 2.4.5-16 National Oceanic and Atmospheric Administration, "Historic Tide Data," Website, http://tidesandcurrents.noaa.gov/station_retrieve.shtml?type=Historic%20Tide%20Data&state=Delaware&id1=855, accessed April 7, 2009.
- 2.4.5-17 National Oceanic and Atmospheric Administration, "Hurricane Climatology for the Atlantic and Gulf Coasts of the United States," NOAA Technical Report NWS 38, 1987.
- 2.4.5-18 National Oceanic and Atmospheric Administration, "Meteorological Criteria for Standard Project Hurricane and Probable Maximum Hurricane Windfields, Gulf and East Coasts of the United States," NOAA Technical Report NWS 23, 1979.
- 2.4.5-19 National Oceanic and Atmospheric Administration, "NOS Estuarine Bathymetry: Delaware Bay DE/NJ (M090)," Website <http://egisws01.nos.noaa.gov/servlet/BuildPage?template=bathy.txt&parm1=M090&B1=Submit>, accessed January, 28, 2009.
- 2.4.5-20 National Oceanic and Atmospheric Administration, "Outer Continental Shelf Resource Management Map – Bathymetric Map, Salisbury," NOS NJ 18-5 (OCS), 1975.
- 2.4.5-21 National Oceanic and Atmospheric Administration, "Sea Level Trends Online, 8551910 Reedy Point, Delaware," Website, http://tidesandcurrents.noaa.gov/sltrends/sltrends_station.shtml?stnid=8551910, accessed April 27, 2009.
- 2.4.5-22 National Oceanic and Atmospheric Administration, "SLOSH Display Program v. 1.61g," October 20, 2009.
- 2.4.5-23 National Oceanic and Atmospheric Administration, "SLOSH: Sea, Lake, and Overland Surges from Hurricanes," NOAA Technical Report NWS 48, 1992.
- 2.4.5-24 National Oceanic and Atmospheric Administration, "The Deadliest, Costliest, and Most Intense United States Tropical Cyclones from 1851 to 2006 (and Other Frequently Requested Hurricane Facts)," NOAA Technical Memorandum NWS TPC-5, 2007.

**PSEG Site
ESP Application
Part 2, Site Safety Analysis Report**

- 2.4.5-25 Oliver, J., "A Summary of Observed Seismic Surface Wave Dispersion," Bulletin of the Seismological Society of America, 52: p. 81 – 86, 1962.
- 2.4.5-26 Powell, M.D., P.J. Vicker and T.A. Reinhold, "Reduced Drag Coefficient for High Wind Speeds in Tropical Cyclones," Nature 422: p. 279 – 283, 2003.
- 2.4.5-27 U.S. Army Corps of Engineers, "Coastal Engineering Manual," Engineer Manual 1110-2-1100, United States Army Corps of Engineers, Washington, D.C. (in 6 volumes), 2002.
- 2.4.5-28 U.S. Army Corps of Engineers, "HEC-RAS 4.0 Software," Website, <http://www.hec.usace.army.mil/software/hecras/hecras-download.html>, accessed February 23, 2009.
- 2.4.5-29 U.S. Geological Survey, "Flood Magnitude and Frequency of the Delaware River in New Jersey, New York, and Pennsylvania," USGS Open File Report 2008-1203, 2008.
- 2.4.5-30 U.S. Geological Survey, "National Elevation Dataset", Website, <http://seamless.usgs.gov/index.php>, accessed February 2, 2009.
- 2.4.5-31 U.S. Navy, "Hurricane Havens Handbook for the North Atlantic Ocean," Websites, <http://www.nrlmry.navy.mil/~cannon/tr8203nc/0start.htm> and , accessed April 9, 2009.
- 2.4.5-32 Not Used
- 2.4.5-33 Not Used
- 2.4.5-34 Walker, Nan, "Tropical Storm and Hurricane Wind Effects on Water Level, Salinity, and Sediment Transport in the River-Influenced Atchafalaya-Vermilion Bay System, Louisiana, USA," Estuaries 24(4): p. 498 – 506, 2001.
- 2.4.5-35 Wilber, D.H., et al, "Suspended Sediment Concentrations Associated with a Beach Nourishment Project on the Northern Coast of New Jersey," Journal of Coastal Research 22(5): p. 1035 – 1042, 2006.
- 2.4.5-36 Wong, K. and J.E. Moses-Hall, "On the Relative Importance of the Remote and Local Wind Effects to the Subtidal Variability in a Coastal Plain Estuary," Journal of Geophysical Research, 103: p. 18,393 – 404, 1998.
- 2.4.5-37 Wong, K. and R.W. Garvine, "Observations of Wind-Induced, Subtidal Variability in the Delaware Estuary," Journal of Geophysical Research 89: p. 10,589 – 597, 1984.
- 2.4.5-38 Cardone, V.J., C.V. Greenwood, and J.A. Greenwood, 1992. Unified program for the specification of hurricane boundary layer winds over surfaces of specified

**PSEG Site
ESP Application
Part 2, Site Safety Analysis Report**

roughness. Final Report. Contract Report CERC-92- 1. Dept. of the Army, Waterways Experiment Station, Vicksburg, MS.

- 2.4.5-39 Chow, S. H., 1971. A study of the wind field in the planetary boundary layer of a moving tropical cyclone. Master of Science Thesis in Meteorology, School of Engineering and Science, New York University, New York, N.Y.
- 2.4.5-40 Thompson, E. F. and V. J. Cardone, 1996. "Practical modeling of hurricane surface wind fields," ASCE Journal of Waterway, Port, Coastal and Ocean Engineering. 122, 4, 195-205.
- 2.4.5-41 University of North Carolina, "Introduction – ADCIRC," Website, <http://adcirc.org/home/documentation/users-manual-v50/introduction/>, accessed October 14, 2013.
- 2.4.5-42 U.S. Army Corps of Engineers, "FEMA Region III Storm Surge Study, Coastal Storm Surge Analysis System Digital Elevation Model," ERDC/CHL TR-11-1, Report 1, 2011.
- 2.4.5-43 U.S. Army Corps of Engineers, "FEMA Region III Storm Surge Study, Coastal Storm Surge Analysis: Computational System," ERDC/CHL TR-11-1, Report 2, 2011.
- 2.4.5-44 U.S. Army Corps of Engineers, "FEMA Region III Storm Surge Study, Coastal Storm Surge Analysis: Modeling System Validation," ERDC/CHL TR-11-1, Report 4, 2013.
- 2.4.5-45 U.S. Nuclear Regulatory Commission, "The Estimation of Very-Low Probability Hurricane Storm Surges for Design and Licensing of Nuclear Power Plants in Coastal Areas," NUREG/CR-7134, October 2012.

**PSEG Site
ESP Application
Part 2, Site Safety Analysis Report**

**Table 2.4.5-1
Resulting Water Elevations at the PSEG Site (RM 52)^{(a)(b)(c)(d)}**

Model Time Step (hr.)	Hurricane Surge Stillwater Level (ft. NAVD)	Wave Runup (ft.)	Hurricane Surge with Wave Runup (ft. NAVD)	Sea Level Rise (ft.)	PMH Surge Maximum Water Surface Elevation (ft. NAVD)
20.5	26.9	12.8	39.7	1.35	41.1
21.0	26.7	14.3	41.0	1.35	42.4

- a) PMH surge results include coincident 10 percent exceedance high tide.
- b) PMH surge SWL occurs one-half hour earlier than the PMH surge maximum water surface elevation, and is equal to 26.9 ft. NAVD.
- c) Calculations are performed using more significant figures than shown in the Table, and the result is rounded to tenths of a ft. If intermediate results were rounded prior to addition the result would not be correct.
- d) These results are based on the Bodine, HEC-RAS, and Kamphuis model described in Subsection 2.4.5.2.

**PSEG Site
ESP Application
Part 2, Site Safety Analysis Report**

**Table 2.4.5-2
Maximum Sustained Wind Speed (kt) for Multiple PMH Scenarios^(a)**

		Radius of Maximum Winds, R (NM)		
		11	20	28
Forward Speed, T (kt)	42	135	133	132
	34	133	131	130
	26	131	129	128

a) Each PMH evaluated in the above table exhibited a central pressure, $p_0 = 26.65$ inches of mercury; pressure drop, $\Delta p = 3.5$ inches of mercury; and track direction from 138 degrees (moving northwest). These parameters, and the ranges considered, represent the PMH that can affect the project site according to NOAA (Reference 2.4.5-18).

**PSEG Site
ESP Application
Part 2, Site Safety Analysis Report**

**Table 2.4.5-3
Maximum Surge (ft. NAVD) for Multiple PMH Scenarios from Screening Simulations^(a)**

		Radius of Maximum Winds, R (NM)			
		11	20	28	28
		At Mouth of Delaware Bay (RM 0)		At the Site (RM 52)	
Forward Speed, T (kt)	42	18.5	21.7	22.7	23.4
	34	18.4	21.2	22.1	25.3
	26	18.1	21.2	22.1	27.8

a) Each PMH evaluated in the above table exhibited a central pressure, p_0 = 26.65 inches of mercury; pressure drop, Δp = 3.5 inches of mercury; and track direction from 138 degrees (moving northwest). The tide is specified as static at the 10% exceedance high tide at the mouth of the Delaware Bay. Consequently these results cannot be compared with results presented in table 2.4.5-1 where a dynamic tide input is specified.

|

**PSEG Site
ESP Application
Part 2, Site Safety Analysis Report**

**Table 2.4.5-4
PMH Storm Parameters and Maximum Total Water Surface Elevation**

Storm Description	PMH Storm	ADCIRC Run #1	ADCIRC Run #2	ADCIRC Run #3
Modeling System	Bodine and HEC-RAS	ADCIRC	ADCIRC	ADCIRC
Central Pressure (mb)	902	902	902	902
Peripheral Pressure (mb)	1021	1021	1021	1021
Radius to Maximum Winds (NM)	28	28	28	28
Forward Speed (kt)	26	26	26	26
Storm Track Heading (deg. West of North)	42	42	42	42
Holland B Parameter	N/A ^a	1.1	1.1	1.1
Antecedent Water Level^b (ft. NAVD)	Dynamic 10% Exceedance High Tide	0	1.35	5.85
Maximum SWL (ft. NAVD)	26.7	18.6	20.2	25.3
Wave Runup (ft.)	14.3	7.5	7.4	7.7
10% Exceedance High Tide (ft.)	N/A ^d	4.5	4.5	N/A ^d
Sea Level Rise (ft.)	1.35	1.35	N/A ^d	N/A ^d
Maximum Total Water Surface Elevation^c (ft. NAVD)	42.4	32.0	32.1	33.0

- a) The NOAA wind field model (Reference 2.4.5-18) does not use the Holland B parameter.
- b) HEC-RAS is used to dynamically model the 10 percent exceedance high tide coincident with the PMH surge; whereas, the ADCIRC+SWAN model uses a static initial water surface elevation set to the elevations indicated in the table.
- c) These values include the 10 percent exceedance high tide, wave runup and potential sea level rise.
- d) This component of the maximum total WSEL is included in the antecedent water level for the corresponding simulation.

**PSEG Site
ESP Application
Part 2, Site Safety Analysis Report**

**Table 2.4.5-5
Wave Runup Parameters and Results**

Model Time Step (hr.)	Fetch Direction	Still WSEL (ft. NAVD)	Hs (ft.)	Wave Period (sec)	Hmax (ft.)	Surf Similarity Parameter	Wave Runup (ft.)
19.0	NE	9.3	7.2	4.0	4.6	1.40	5.8
19.5	ENE	15.4	9.5	4.7	7.9	1.25	8.8
20.0	ENE	23.3	11.7	5.1	11.8	1.11	11.7
20.5	E	26.9	13.1	5.3	12.8	1.11	12.8
21.0	ESE	26.7	14.7	5.6	14.4	1.10	14.3
21.5	ESE	25.7	14.0	5.5	14.1	1.10	13.9
22.0	ESE	24.4	13.3	5.4	13.1	1.12	13.2
22.5	ESE	22.9	11.5	5.1	12.1	1.11	12.1
23.0	ESE	21.5	9.9	4.9	11.2	1.10	11.1
23.5	ESE	19.5	8.6	4.7	9.8	1.12	9.9
24.0	S	17.0	9.0	4.5	12.8	0.95	11.0

**PSEG Site
ESP Application
Part 2, Site Safety Analysis Report**

2.4.6 PROBABLE MAXIMUM TSUNAMI FLOODING

This subsection develops the geohydrological design basis to ensure that potential hazards to the safety-related SSC important to safety due to the effects of a PMT are considered in the new plant design. NUREG/CR-6966, *Tsunami Hazard Assessment at Nuclear Power Plant Sites in the United States of America*, is used to support the conclusions described below.

Determination of PMT is based on evaluation of multiple source locations of the worst possible submarine landslide, volcanic cone flank failure, and submarine fault displacement that could affect the PSEG Site. The volume of material displaced causing the tsunami is based on recent research contained in “*Evaluation of Tsunami Sources with the Potential to Impact the U.S. Atlantic and Gulf Coasts*,” USGS Administrative Report to the NRC (Reference 2.4.6-21). The Method of Splitting Tsunami (MOST) model, originally developed at the University of Southern California and currently maintained by NOAA’s Pacific Marine Environmental Laboratory is used to propagate the tsunami from its source to the PSEG Site.

2.4.6.1 Historical Tsunami Record

Table 2.4.6-1 provides a list of recorded tsunamis affecting the eastern United States (U.S.) and Canada from 1755 to 2009 (Reference 2.4.6-15). Four potential tsunamigenic sources are identified that could affect the new plant location and include the following:

- A submarine landslide on the continental shelf along the U.S. East Coast.
- Seismic or volcanic tsunamigenic sources along the Atlantic Ocean’s eastern boundary, including those near the Portuguese coast and Canary Islands.
- Co-seismic activity associated with subduction zones in several Caribbean trenches.
- Earthquake zones in the northern Atlantic Ocean, primarily near Newfoundland, Canada.

Of these, historical records and published studies indicate that the greatest severity of tsunami waves in the Mid-Atlantic region of the U.S. East Coast, including Delaware Bay, would most likely stem from the first three sources (Reference 2.4.6-15). The historical record does not contain detailed earthquake source parameters. Estimates of such parameters as displacement volume, focal depth, and fault dimension and orientation are based on anecdotal accounts and resulting impacts on shorelines and coastal populations.

As discussed in Subsection 2.5.1.2.3.2, there is geologic evidence for a tsunami event occurring at the end of the Cretaceous Period (paleotsunami). The geologic record discussed in Section 2.5.4.1.3 indicates that review of samples from the 16 soil borings performed in the area of the PSEG ESPA Site indicated strata or features that are consistent with the depositional environments described in the literature, and the site deposits are not interpreted to represent a paleotsunami occurrence.

2.4.6.1.1 Currituck Landslide

Mapping and geological analysis of the sea floor indicates that a large submarine mass failure (SMF) event took place off the coast of NC in the late Pleistocene era. This slide is known as the Currituck slide. The slide is surmised to have happened in either one or two stages, with a total slide volume of around 2.16E11 cubic yards (cu. yd.) (165 cubic kilometers). Simulations of a number of scenarios based on the one- or two-stage partitioning of the event and on a range

Rev. 4

**PSEG Site
ESP Application
Part 2, Site Safety Analysis Report**

of slide velocities for each state indicate that coastlines immediately facing the slide location could experience tsunami amplitudes on the order of 20 ft. (6 meters [m]). Impact on regions upcoast or downcoast is mainly through refracted portions of the main generated waves or to edge waves propagating out of the immediately impacted areas, and effects are determined to be on the order of 6.6 feet. (Reference 2.4.6-21)

The Currituck slide is one of several apparent Paleolithic slide events occurring on the outer slope of the U.S. East Coast continental shelf. Landslide-generated tsunamis typically cause the greatest levels of inundation on shorelines immediately landward of the slide event. Therefore, it is most relevant to consider additional historical or potential slides in the Mid-Atlantic Bight region, spanning from the Hudson Canyon to Cape Hatteras. Review of morphological studies of slide deposits in this region (Reference 2.4.6-30) concludes that the most prominent slides are fluvial in origin, being linked to river delta deposits formed during the late Quaternary low stand of sea level, when major rivers of the regions reached across the present shelf. In particular, the Currituck slide is associated with the delta of the Susquehanna River. Additional deltas of the Delaware and Hudson Rivers also have associated slide deposits. Information in Reference 2.4.6-31 on the distribution of slide volumes shows that the Currituck slide is the largest slide occurring in the region, making it the most logical candidate for study.

2.4.6.1.2 1755 Lisbon, Portugal Earthquake and Tsunami

One significant Atlantic Ocean tsunami that affected the U.S. East Coast was generated off the coast of Portugal in 1755. The tsunami was generated at the Gorringe Bank, approximately 125 mi. (200 kilometers [km]) from the Portuguese coast, due to a displacement in the submarine fault. The highest runup from this tsunami was approximately 100 ft. (30.0 m), near Lagos, Portugal. At Lisbon, Portugal, runup reached a height of approximately 40 ft. (12.2 m). (Reference 2.4.6-15) Numerical simulations indicate that maximum tsunami amplitudes along the U.S. East Coast could have reached 9.8 ft. (3 m) (Reference 2.4.6-9).

2.4.6.1.3 Tsunami from 1918 Puerto Rico Earthquake

Puerto Rico experienced an earthquake and subsequent landslide event in 1918 with a moment magnitude (M_w) of 7.3. The M_w is a logarithmic scale of 1 to 10 (a widely used successor to the Richter scale) that enables seismologists to compare the energy released by different earthquakes on the basis of the area of the geological fault that ruptured in the quake. The epicenter of the Puerto Rico earthquake was located 9.4 mi. off the northwest coast of the island, within the Mona Passage. The resulting landslide and tsunami created runup ranging from 13 ft. to 20 ft. (4 m – 6 m) along the Puerto Rican coast. The tsunami had transatlantic reach, with effects of the tsunami recorded as a surge of 0.2 ft. at a tide gage in Atlantic City, NJ, located 40 mi. northeast of the mouth of Delaware Bay (Reference 2.4.6-15).

2.4.6.1.4 Tsunami Due to 1929 Earthquake at Grand Banks, Newfoundland, Canada

The 1929 earthquake which generated the Grand Banks landslide had an M_w of 7.2; producing the largest recorded tsunami in the northern part of the North American east coast. The recorded damage attributed to this tsunami was mostly confined to the Newfoundland coast. The epicenter of the earthquake was located near the mouth of the Laurentian Channel, south of the Burin Peninsula and on the south coast of Newfoundland. The earthquake triggered an

**PSEG Site
ESP Application
Part 2, Site Safety Analysis Report**

underwater landslide that generated a tsunami with a runup height of 89 ft. (27 m) at the Burin Peninsula. Water level records at Atlantic City show that the maximum tsunami amplitude at this location from the tsunami was 2.2 ft. (0.68 m) (Reference 2.4.6-15).

2.4.6.2 Probable Maximum Tsunami

Tsunami events that could affect the Delaware Bay environs and the PSEG Site could be generated by a range of local or distant geoseismic activities. Local sources include SMF events associated with slope failures on the continental shelf margin, or large sediment movements in the form of turbidity currents. These occur on the shelf margin or in submarine canyons that incise the shelf at locations along the eastern coast of the United States. Delaware Bay is a low-lying coastal plain estuary bounded by nearly flat terrain on both shores (Reference 2.4.6-24). Therefore, the occurrence of locally-generated waves due to subaerial or submarine landslide events is unlikely. Figure 2.4.6-1 shows the naturally occurring angular topography slopes on a grid in the vicinity of the PSEG Site, and shows a maximum slope value of 0.3° occurring inland of the site. Stability analysis will be conducted during the COLA phase of the project, and will include consideration of failure surfaces that extend into the Delaware River adjacent to the site as discussed in SSAR Section 2.5.5.1.

Distant sources include co-seismic activity in subduction zones, such as the Hispaniola and Puerto Rico trenches, or faulting zones such as the region west and south of Portugal. In addition, large scale SMF events have been identified along the Mid-Atlantic Ridge and British Isles. Possible catastrophic failure of volcanic cones and the subsequent generation of tsunamis due to subaerial landslide entry into the ocean has been suggested (Reference 2.4.6-21), with the cone on the island of La Palma in the Canary Islands hypothesized to be a site of major concern (Reference 2.4.6-25).

The range of possible Atlantic Ocean tsunami-generating events has been surveyed to provide guidance on potential Atlantic Ocean sources (Reference 2.4.6-21). Based on these studies and historical tsunami events recorded along the United States East Coast, three potential tsunamigenic sources have been chosen for study that could lead to the arrival of significant tsunami waves at the entrance to Delaware Bay.

Submarine landslide off the coast of NC or Virginia (VA)

Analysis of geology along the Mid-Atlantic continental margin shows the presence of historical landslide deposits at the base of the continental slope (Reference 2.4.6-21). Larger events are often associated with low sea level such as occurred at the beginning of or during the last ice age event. Of these larger events, the Currituck landslide has drawn interest as an indicator of potential risk to the Mid-Atlantic coastline. Submarine landslides in this area along the VA and NC continental shelf could produce tsunami amplitudes of 6.6 – 13 ft. (2 – 4 m) along beaches from NC to New York (NY) (References 2.4.6-4 and 2.4.6-26).

Large Atlantic tsunami generated by volcanic cone flank failure: La Palma, Canary Islands

The possible generation of a large Atlantic Ocean tsunami by a volcanic cone flank failure, as occurred in the Mount Saint Helens event in the United States, is predicted to lead to large tsunami waves along the western Atlantic Ocean boundary, including the Mid-Atlantic region

**PSEG Site
ESP Application
Part 2, Site Safety Analysis Report**

(Reference 2.4.6-25). Subsequent studies have led to reduced wave height predictions, but still reaching up to 10 ft. (3 m) at various East Coast locations (References 2.4.6-8 and 2.4.6-18).

Tsunami due to submarine fault displacement: Hispaniola Trench

The Caribbean Island chain is bounded on the north by a sequence of submarine trenches formed by subduction zone activity. The Puerto Rico Trench is often indicated as a possible source of tsunamigenic activity. However, the Hispaniola Trench to the west has slip characteristics which are more conducive to vertical motion (Reference 2.4.6-21) and, therefore, has a greater tsunamigenic potential (Reference 2.4.6-3). The eastern portion of the Hispaniola Trench has been seismically active, with a series of events with M_w of 6.8 to 7.6 occurring between 1946 and 1953. In the present study, a set of sources along the Hispaniola Trench that combine to produce an event with a total M_w of 9.0, approaching the scale of the catastrophic Indian Ocean tsunami of 2004, is used. This event magnitude is consistent with a failure of the entire length of the fault with a slip of 33 ft. (10 m) (Reference 2.4.6-21).

The PMT maximum positive amplitude and negative drawdown at the PSEG Site are computed for each of the three potential tsunami sources, using the MOST model described in Subsection 2.4.6.4. Numerical values are taken from model grid points located close to the north-south portion of the PSEG Site's western shoreline using the maximum and minimum tsunami-induced WSEL. Results for each case are reported in Subsections 2.4.6.4.5 through 2.4.6.4.7. None of the cases studied produced tsunami-induced water elevations that result in the design basis flood at the site.

2.4.6.3 Tsunami Source Characteristics

Simulations of tsunami events (Subsection 2.4.6.4) require a specification of properties of the tsunamigenic sources, including physical size, location and magnitude of ground movement. Values used in this study have been taken from available literature sources. Information about the source description for each of the three events considered is contained in Subsections 2.4.6.3.1 through 2.4.6.3.3.

2.4.6.3.1 Currituck Landslide

For the Currituck landslide, a total slide volume of 2.16×10^{11} cu. yd. (165 cubic kilometers [km^3]), and a vertical slide displacement of 5740 ft. (1750 m) are used (Reference 2.4.6-21). The source has a maximum along-shelf width of 72,768 ft. (22,180 m) and a cross-shelf length of 109,152 ft. (33,270 m), with maximum excavation depth of 2461 ft. (750 m). The source for the tsunami motion is given in the form of a static instantaneous surface displacement, specified using the equations and procedure outlined in two sources (References 2.4.6-27 and 2.4.6-28). The tsunami source location is taken as being near the location of the actual Currituck landslide, with the initial source center located at 36.4°N and 74.5°W . The slide moves along a straight line track oriented at an angle of 100° relative to North. Three additional sites to the north were tested in order to determine sensitivity to slide location at the study site.

The source for the Currituck slide simulations were developed using the TOPICS program (References 2.4.6-27 and 2.4.6-28) using the source geometry as given in Reference 2.4.6-21. TOPICS itself is based on a set of parameterized curve fits to calculated sea surface displacements based on numerical solutions of a fully nonlinear potential flow model, which in

**PSEG Site
ESP Application
Part 2, Site Safety Analysis Report**

turn has been validated against extensive laboratory data obtained using rigid models for translating slide masses (Reference 2.4.6-32). TOPICS has recently been validated against field measurements for the Papua New Guinea landside event of 1998 (Reference 2.4.6-33). TOPICS has thus been shown to be an appropriate means for prescribing initial conditions for landside tsunamis.

2.4.6.3.2 La Palma Landslide in Canary Islands

The source for this event is a possible volcanic cone collapse on the flank of the Cumbre Vieja volcano on the island of La Palma, in the Canary Islands. This hypothetical event has been extensively studied with a variety of techniques. The main input to the choice of a source is based on scientific literature. The Science Applications International Corporation (SAIC) SAIC Adaptive Grid Eulerian (SAGE) program multimaterial model has previously been applied to simulate the propagation of the landslide (Reference 2.4.6-5). SAGE is a geodynamic model used to model a moving landslide (Reference 2.4.6-5). Recently, a Boussinesq model was used to simulate near-field tsunami wave propagation across the Atlantic Ocean (Reference 2.4.6-7). The results indicate that the maximum predicted WSEL in the Canary Islands range from 33 ft. to 590 ft. (10 m to 188 m) for landslide depths between 895 ft. and 5363 ft. (273 m and 1695 m) (Reference 2.4.6-7). The recent Boussinesq model predicts smaller WSEL than Ward and Day previously predicted (Reference 2.4.6-25), but larger than the predicted results of Mader (Reference 2.4.6-8). Although these results represent qualitatively improved dynamics, as they included the full 3-dimensional representation of the wave generation, a more conservative larger surface displacement is used. The N-wave source, based on initial displacement estimated from Ward and Day (Reference 2.4.6-25), represents the largest estimate of the tsunamigenic event appearing in the literature to date and is thus conservative in that it produces a tsunami which is presently thought to be excessively large by most investigators. The N-wave source is implemented as a static, instantaneous displacement of the water surface with a leading maximum positive elevation of 1640 ft. (500 m) and a following depression of 2133 ft. (650 m). The N-wave source is centered at 18.2°W and 28.5°N, and is oriented with its principal propagation direction lying along an axis rotated 225 degrees from North. The distance between the maximum elevation and depression in the N-wave is set as 75,590 ft. (23 km), consistent with estimates of the initial tsunami wavelength computed in Reference 2.4.6-5. The width of the wave crest is chosen to be 86,449 ft. (26.35 km), consistent with source widths described in References 2.4.6-5 and 2.4.6-7.

2.4.6.3.3 Hispaniola Trench

The source for this event is a subduction zone slip event occurring on the full-length of the Hispaniola Trench. This event is modeled by dividing the trench into seven segments. Vertical displacement is then determined for each of the segments using the half-plane solution (Reference 2.4.6-17) to obtain an M_w equaling 9.0. Parameters and locations for the individual sources are shown in Table 2.4.6-2. The model is initialized with a static surface displacement corresponding to the superposed displacements resulting from the seven sources taken together.

2.4.6.4 Tsunami Analysis

Tsunami simulations are performed within the Delaware Bay and for portions of the Atlantic Ocean using the MOST model system (Reference 2.4.6-22). The MOST model has been

**PSEG Site
ESP Application
Part 2, Site Safety Analysis Report**

extensively verified against test data (References 2.4.6-10 and 2.4.6-19). The model operation is verified by comparing numerical results to results from the operational version of the code at the University of Southern California. Computations are based on MOST model code in effect between July and November 2009.

The MOST model provides a hierarchical environment describing tsunami generation, propagation in open water, and inundation at coastal sites. The computational scheme is comprised of a nesting of three model grids that move the computation for a lower resolution large scale grid A, through an intermediate resolution grid B, to a high resolution grid C encompassing the study site. The grids for the present tests and construction of the grids are discussed in the following subsections.

2.4.6.4.1 Governing Equations

The propagation and inundation phases of the modeling in MOST use the nonlinear shallow water equations in spherical coordinate form, based on a latitude (lat) -longitude (long) grid with horizontal coordinates in degrees-minutes-seconds (Reference 2.4.6-22). The model also incorporates bottom friction effects through a formulation using Manning's n as a free parameter. The three simulated tsunami cases described below are run using values of Manning's n equal to 0.01. The selected Manning's roughness coefficient value represents smooth bed conditions to conservatively model the worst case WSEL resulting from a tsunami propagating up Delaware Bay (Reference 2.4.6-6). The model is also run based on the Currituck landslide with no bottom friction to illustrate the magnitude of frictional effects on the simulations. Figure 2.4.6-2 shows a comparison of tsunami WSEL resulting from the Currituck landslide at the PSEG Site modeled with and without bottom friction. The difference in WSEL is 0.2 ft. (0.06 m).

2.4.6.4.2 Model Simulations

The MOST model is employed to simulate tsunami water levels at the PSEG Site. The simulations are performed within Delaware Bay and in relevant portions of the Atlantic Ocean for three possible cases to determine the PMT. The potential tsunamigenic sources for PMT at the PSEG Site are discussed in Subsection 2.4.6.1 and the source characteristics are described in Subsection 2.4.6.3.

The following simulations all employ the chosen source information to generate the tsunami wave at its source location. The resulting tsunami waves are then propagated across the ocean and into the confined area of Delaware Bay. Two sets of simulations are performed for each of the three scenarios: a set of simulations at a water level corresponding to 10 percent exceedance high tide at the study site, from which maximum runups are obtained; and a set of simulations at a water level corresponding to 90 percent exceedance low tide at the study site, from which maximum drawdowns are obtained. Simulated runup values are reported as runups above a water level in Delaware Bay corresponding to 10 percent exceedance high tide at the PSEG Site (interpolated between NOAA tide gage values at Reedy Point, DE and Lewes, DE) that represents a static water elevation at 4.5 ft. NAVD (4.45 ft. msl) (Reference 2.4.6-13). msl is the datum for NOAA National Geophysical Data Center (NGDC) Coastal Relief Model (CRM) and NOAA National Ocean Service (NOS) Arc Global Relief Model (ETOPO 1) bathymetry data sets. ETOPO 1 is a 1 arc-minute global relief model of the earth's surface that integrates land topography and ocean bathymetry. Mean sea level (msl) is -0.049 ft. NAVD (-0.015 m) at Reedy

**PSEG Site
ESP Application
Part 2, Site Safety Analysis Report**

Point (Reference 2.4.6-13). Resulting runup and drawdown levels are reported relative to NAVD in Subsection 2.4.6.4.8.

2.4.6.4.3 Bathymetry and Topography Sources

Topography and bathymetry data for the model domains are obtained from NOAA NOS ETOPO 1, NOAA NGDC CRM, and NJ and DE Digital Elevation Grids.

Atlantic domain grids (Grid A for the Canary Island case and Grid A for the Hispaniola earthquake case) are generated based on ETOPO 1 (Reference 2.4.6-1). ETOPO 1 uses msl as a vertical datum origin. The Currituck Grid A includes the continental shelf and offshore areas in the Atlantic Ocean. Each case employs a different Grid A.

Grids for regional scale domains (Grid B) are based on CRM with 3 arc-second resolution (Reference 2.4.6-2). Data is available from NOAA (Reference 2.4.6-11). CRM also uses msl as the vertical datum origin. The Canary Island case and Hispaniola earthquake case use the same Grid B. The Currituck case uses a different Grid B.

All three cases studied here use the same local Grid C, developed from the CRM for bathymetry and NJ and DE digital elevation grids, and for subaerial topography (References 2.4.6-16 and 2.4.6-23). NJ and DE digital elevation data are extracted from the USGS 30 m DEM data (7.5-minute DEM, horizontal North American datum NAD83, UTM-18N, and vertical datum NAVD 88 [NAVD]).

Conversions are needed to merge the bathymetry data and the topography data in generating the local Grid C, because NOS CRM data uses mean sea level. VDatum, NOAA's vertical datum transformation tool (Reference 2.4.6-14), is used to convert the topography data to mean sea level. In simulations, depth is based on 10 percent exceedance high tide obtained from historical data at NOAA's Center for Operational Oceanographic Products and Services (CO-OPS) Station 8557380 at Lewes, DE, located at the mouth of the Delaware Bay (Reference 2.4.6-12).

2.4.6.4.4 Model Grids

Areas of grid coverage and spatial resolution for the three cases studied are given in Tables 2.4.6-3, 2.4.6-4, and 2.4.6-5 and shown in Figures 2.4.6-4, 2.4.6-5, and 2.4.6-6. Numerical simulations are performed for each of the cases using a Manning's n value of 0.01, and calculations are repeated with no bottom friction for the Currituck landslide case (Reference 2.4.6-6). Results for water levels are discussed for each case. Model calculations were carried out for varying simulated elapsed times depending on the source location. The Currituck slide tsunami model ran calculations for elapsed times up to 40 hours after the initial tsunami generation event. No evidence was found of significant seiche effects within Delaware Bay after the initial arrival of the tsunami front at the PSEG Site. Results from this simulation are shown in Figure 2.4.6-7.

2.4.6.4.5 Currituck Landslide Results

Parameters used for the Currituck landslide case include a slide volume of 2.16×10^{11} cu. yd. (165 km^3), a depth of middle slide of 5740 ft. (1750 m), and a slope along the failure plane of 2.5

**PSEG Site
ESP Application
Part 2, Site Safety Analysis Report**

degrees (Reference 2.4.6-21). The slide has a maximum along-shelf width of 72,768 ft. (22,180 m) and a cross-shelf length of 109,152 ft. (33,270 m), with maximum excavation depth of 2461 ft. (750 m). Initial water surface displacements based on these parameters are generated using formulae and methodology for SMF (References 2.4.6-27 and 2.4.6-28). The resulting instantaneous surface displacement used for input to MOST has a maximum elevation of 47.44 ft. (14.46 m) and a maximum surface depression of 79.82 ft. (24.33 m).

For the original Currituck event, the landslide center is located at 36.4°N, 74.5°W, and oriented in the direction of slide motion at 100 degrees clockwise from north. Three additional events, each with a source moved progressively further north, have been considered, in order to investigate the sensitivity of simulated runup results to exact location of the slide event. The additional source centers are located at 36.6°N, 74.49°W; 36.9°N, 74.48°W; and 37.2°N, 74.47°W. Numerical experiments with the four landslide locations do not indicate that wave height predictions in Delaware Bay are sensitive to the choice of landslide location, because offshore shelf bathymetry, rather than source location, controls wave height distribution and focusing patterns. Therefore, remaining simulations for this site are performed using the historic landslide location. Further numerical examples also indicate that Delaware Bay wave conditions are not sensitive to the chosen width of the landslide, given a constant total landslide volume.

The tests carried out here were done primarily to address questions on how the shelf geometry controls hydrodynamic behavior of tsunamis associated with slides in the region of the PSEG Site. Although there has been some recent literature suggesting that the region covered by the additional slide locations may be vulnerable to failure (Reference 2.4.6-4), more recent literature (Reference 2.4.6-21) suggests that slides would be less likely at the additional source locations since these locations move out of the vicinity of old river delta deposits.

Model outputs compare time series of surface elevation at Cape May, NJ, and the PSEG Site for the cases with and without bottom friction. Model results indicate that Delaware Bay effectively filters high frequency components of the tsunami signal, leaving only a low frequency response at the PSEG Site. These results occur for each of the cases studied. Low frequency waves propagate up the bay like flood waves in a river, experiencing less damping. Additional model runs using finer spatial grid resolution show a greater penetration of high frequency energy into the upper reaches of the Bay, but do not change the conclusions on the dominance or magnitude of the lower frequency components. Model results using the chosen grid resolution have thus been shown to be appropriate.

Model output indicates that there is a region of high waves in the Delaware Bay entrance extending from Cape May towards the shipping channel in the mid-bay area. This region is in an area of large sandbanks which extends 3.1 mi. in each direction. The high wave energy seen over this area is persistent for all the cases studied, and the high wave energy does not continue into the bay itself. Figures 2.4.6-8, 2.4.6-9, 2.4.6-10, 2.4.6-11, 2.4.6-12, 2.4.6-13, and 2.4.6-14 illustrate model results for the Currituck Landslide through time.

The simulated WSEL relative to 10 percent exceedance high tide at the PSEG Site for the simulations with and without bottom friction indicates that the inclusion of bottom friction in the simulation reduces both the magnitude of runup and drawdown for both low and high frequency components. The effect on drawdown, computed using the 90 percent exceedance low tide water level, is more accentuated. Runup values with friction are reduced by 0.15 ft. Maximum runup at the site (computed with 10 percent exceedance high tide water level and no friction) is

**PSEG Site
ESP Application
Part 2, Site Safety Analysis Report**

+5.65 ft. NAVD. Maximum drawdown (computed with 90 percent exceedance low tide water level and no friction) is -6.16 ft. NAVD.

2.4.6.4.6 La Palma (Canary Islands) Landslide Results

A simulation of the La Palma event is conducted using an N-wave source. An N-wave represents the geometry of a wave crest in tsunami models (Reference 2.4.6-20). This source is introduced in the model as a static initial condition, with a leading maximum positive elevation wave of height 1640 ft. (500m) and a following depression wave with trough depth of 2133 ft. (650 m). The N-wave source is centered at 18.2° W and 28.5° N, and is oriented with its principal propagation direction lying along an axis rotated 225 degrees from North. The distance between the maximum elevation and depression in the N-wave is set as 75,590 ft. (23 km), consistent with estimates of the initial tsunami wavelength computed in Reference 2.4.6-5. The width of the wave crest is chosen to be 86,449 ft. (26.35 km), consistent with source widths described in References 2.4.6-5 and 2.4.6-7. The incident wave at Cape May, NJ, is more organized than the wave in the Currituck example. This incident wave represents a wave train that has dispersed from an initial pulse over oceanic distances. The incident wave has a dominant wave period of approximately 25 minutes. This wave is filtered by the lower Delaware Bay, as in the Currituck example. There is a residual low frequency motion at the PSEG Site producing a runup elevation of 0.26 ft., with a leading wave of elevation, or positive surge at the site. The wave heights experienced from this event do not exceed 6.6 ft. in amplitude in the area covered by Grid B. Maximum runup at the site is +4.76 ft. NAVD. Maximum drawdown is -5.30 ft. NAVD. Figures 2.4.6-15, 2.4.6-16, 2.4.6-17, 2.4.6-18, 2.4.6-19, and 2.4.6-20 illustrate model results for the La Palma Landslide through time.

2.4.6.4.7 Hispaniola Trench Earthquake Case

The last case considered is the Hispaniola Trench, which represents a conventional subduction zone co-seismic event.

The tsunami source chosen for this case is based on a composite source utilizing seven individual Okada (1985) elastic sources with a total M_w equaling 9.0. The trench segment is located between longitudes 68°W and 62°W, and stretches for a distance of 419 mi. (675 km) (Reference 2.4.6-17). Properties of the individual Okada sources are given in Table 2.4.6-2.

Time series of WSEL for the Hispaniola Trench case for Cape May, NJ, and the PSEG Site indicate that maximum runup elevations within the boundaries of the A and B grids are up to 11.5 ft. (3.5 m). This is higher than values obtained for the La Palma case. As in all cases studied here, refraction directs waves away from the Delaware Bay entrance, reducing wave heights entering the bay to the 3 ft. – 5 ft. (1 m – 1.5 m) range, except for a concentration of energy over the shoal area south of Cape May. As in previous cases, results indicate that the bay effectively filters the high frequency components of the tsunami signal, leaving only a low frequency signal at the PSEG Site. Maximum runup at the site is +5.22 ft. NAVD. Maximum drawdown is -5.56 ft. NAVD. Figures 2.4.6-21, 2.4.6-22, 2.4.6-23, 2.4.6-24, 2.4.6-25 and 2.4.6-26 illustrate model results for the Hispaniola Trench earthquake through time.

**PSEG Site
ESP Application
Part 2, Site Safety Analysis Report**

2.4.6.4.8 Summary of Tsunami Amplitudes at PSEG Site

Runup values calculated during simulations are relative to 10 percent exceedance high tide, which serves as the static initial water level in the simulations. Maximum runup values are reported in Table 2.4.6-6 relative to the 10 percent exceedance high tide elevation. Drawdown values are reported in Table 2.4.6-6 relative to the 90 percent exceedance low tide elevation. The 10 percent exceedance high tide is 4.5 ft. NAVD and 90 percent exceedance low tide is -5.08 ft. NAVD based on values from the NOAA tidal gage at Reedy Point (Reference 2.4.6-13). This provides an approximation for extreme water levels reached for wave runup events arriving coincident with high astronomical tide, or for drawdown events arriving coincident with low astronomical tide. The PMT at the PSEG Site is caused by the Currituck Landslide. In the most conservative model without bottom friction, maximum runup at the PSEG Site is 5.65 ft. NAVD and maximum drawdown is -6.16 ft. NAVD.

These results indicate that a landslide tsunami on the U.S. East Coast continental shelf margin represents the PMT case.

2.4.6.5 Effects of Runup on Safety-Related Facilities

The new plant grade will be established at an elevation of 36.9 ft. NAVD. As indicated in Table 2.4.6-6, none of the maximum predicted runup elevations obtained in this study overtop this elevation. Therefore, PMT events do not constitute a limiting design basis for the new plant nor do hydrodynamic and hydrostatic forces impact any safety-related structures. The DBF caused by storm surge and associated wave runup caused by the PMH, described in Subsection 2.4.5, governs the design to protect safety-related structures from wave runup.

2.4.6.6 Consideration of Debris and Waterborne Projectiles

The grade elevation for the new plant will be established at a level providing for clearance above the DBF, as required by Tier 1 of the DCD for the selected technology. Therefore, debris and waterborne projectiles do not come into contact with safety-related structures. The intake structure at the new plant will be designed to protect it from impacts of waves and waterborne projectiles.

2.4.6.7 Effects of Sediment Erosion and Deposition

Strong water currents associated with tsunami wave activity can cause erosion and deposition, rapidly changing the morphology of an impacted area. In order to examine whether this mechanism is likely to have an impact at the new plant location, the speed of current at the site for the Currituck cases, both with and without friction, is considered. Figure 2.4.6-3 shows that water current speeds for the case without friction are significantly higher than for the case with friction, but each value falls within the range of normal tidal current activity in the bay (Reference 2.4.6-29). A rapid morphological response to tsunami activity at the site is not expected.

2.4.6.8 Consideration of Other Site-Related Evaluation Criteria

Three tsunami sources are selected to analyze the PMT at the new plant location. Two tsunami sources (Currituck and Canary Islands) are assumed to generate the tsunami due to submarine landslides, which are not necessarily tied to strong seismic activity. The Currituck landslide is

**PSEG Site
ESP Application
Part 2, Site Safety Analysis Report**

assumed to be triggered by gas hydrate decomposition. The Canary Islands flank landslide is assumed to be generated by volcanism. A potential tsunami in the Hispaniola Trench would be generated by the fault displacement due to an earthquake. Due to the distance of the earthquake from the new plant location, 1550 mi., the earthquake magnitude will be significantly attenuated during the propagation toward the PSEG Site. A tsunami associated with an earthquake would originate a significant distance from the new plant location. Therefore, combining a tsunami event and seismic event at the new plant location will not be considered in designing safety-related SSC for the new plant. Subsection 2.5.3 discusses the design basis earthquake.

2.4.6.9 References

- 2.4.6-1 Amante, C. and B.W. Eakins, "ETOPO1 1 Arc-Minute Global Relief Model: Procedures, Data Sources and Analysis," National Geophysical Data Center, NESDIS, NOAA, U.S. Department of Commerce, Boulder, CO, August, 2008, Website, <http://www.ngdc.noaa.gov/mgg/global/global.html>, accessed June 9, 2009.
- 2.4.6-2 Divins, D.L. and D. Metzger, "NGDC Coastal Relief Model", Volume 2, Website, <http://www.ngdc.noaa.gov/mgg/coastal/coastal.html>, accessed June 8, 2009.
- 2.4.6-3 Dolan, J.F. and D.J. Wald, "The 1943-1953 North-Central Caribbean Earthquakes: Active Tectonic Setting, Seismic Hazards, and Implications for Caribbean-North America Plate Motions," Geological Society of America Special Publications, 326, p. 143 – 170, 1998.
- 2.4.6-4 Driscoll, N.W., J.K. Weissel and J.A. Goff, "Potential for Large-Scale Submarine Slope Failure and Tsunami Generation Along the U.S. Mid-Atlantic Coast," Geology, 28(5), p. 407 – 410, 2000.
- 2.4.6- 5 Gisler, G., R. Weaver and M. Gittings, "SAGE Calculations of the Tsunami Threat from La Palma," Science of Tsunami Hazards, 24, p. 288 – 301, 2006.
- 2.4.6-6 Harig, S., C. Chaeroni, W. Pranowo and J. Behrens, "Tsunami Simulations on Several Scales," Ocean Dynamics, 58, p. 429 – 440, 2008.
- 2.4.6-7 Lovholt, F., G. Pedersen and G. Gisler, "Oceanic Propagation of a Potential Tsunami from the La Palma Island," Journal of Geophysical Research, 113, C09026, doi:10.1029/2007JC004603, 2008.
- 2.4.6-8 Mader, C.L., "Modeling the La Palma Landslide Tsunami," Science of Tsunami Hazards, 19, p. 150 –170, 2001a.
- 2.4.6-9 Mader, C.L., "Modeling the 1755 Lisbon Tsunami," Science of Tsunami Hazards, 19, p. 93 – 98, 2001b.
- 2.4.6-10 MOST Model Introduction, Website, <http://nctr.pmel.noaa.gov/model.html>, accessed: July 15, 2009.

**PSEG Site
ESP Application
Part 2, Site Safety Analysis Report**

- 2.4.6-11 National Oceanic and Atmospheric Administration Satellite and Information Service, Website, www.ngdc.noaa.gov/mgg/coastal/grddas02/grddas02.htm, accessed: July 15, 2009.
- 2.4.6-12 National Oceanic and Atmospheric Administration, "Tides and Currents, Lewes, Delaware, Station 8557380," Website, <http://tidesandcurrents.noaa.gov/>, accessed: July 15, 2009.
- 2.4.6-13 National Oceanic and Atmospheric Administration, "Tides and Currents, Reedy Point, Delaware, Station 8551910," Website, <http://tidesandcurrents.noaa.gov/>, accessed: July 15, 2009.
- 2.4.6-14 National Oceanic and Atmospheric Administration Vertical Datum Transformation, Website, <http://vdatum.noaa.gov/>, accessed June 9, 2009.
- 2.4.6-15 National Oceanic and Atmospheric Administration/World Data Center Historical tsunami database, Website, http://www.ngdc.noaa.gov/hazard/tsu_db.shtml, accessed June 8, 2009.
- 2.4.6-16 New Jersey Geological Survey, Website, <http://www.njgeology.org/geodata/dgs99-1.htm>, accessed July 15, 2009.
- 2.4.6-17 Okada, Y., "Surfaced Deformation Due to Shear and Tensile Faults in a Half-Space," Bulletin of the Seismological Society of America, 75: p. 1135 – 1154, 1985.
- 2.4.6-18 Pararas-Carayannis, G., "Evaluation of the Threat of Mega Tsunami Generation from Postulated Massive Slope Failures of Island Stratovolcanoes on La Palma, Canary Islands, and on the Island of Hawaii," Science of Tsunami Hazards, 20: p. 251 – 277, 2002.
- 2.4.6-19 Synolakis, C.E., E.N. Bernard, V.V. Titov, U. Kanoglu and F.I. Gonzalez, "Standards, Criteria and Procedures for NOAA Evaluation of Tsunami Numerical Models," NOAA Technical Memorandum OAR PMEL-135, Pacific Marine Environmental Laboratory, Seattle, WA, 2007.
- 2.4.6-20 Tadeipalli, S. and C.E. Synolakis, "Model for the Leading Waves of Tsunamis," Physical Review Letters, 77, p. 2141 – 2144, 1996.
- 2.4.6-21 ten Brink, U., D. Twichell, E. Geist, J. Chaytor, J. Locat, H. Lee, B. Buczkowski, R. Barkan, A. Solow, B. Andrews, T. Parsons, P. Lynett, J. Lin and M. Sansoucy, "Evaluation of Tsunami Sources with the Potential to Impact the U.S. Atlantic and Gulf Coasts," USGS Administrative report to the U.S. Nuclear Regulatory Commission, 300 pp., August 22, 2008.
- 2.4.6-22 Titov, V.V. and F.I. Gonzalez, "Implementation and Testing of the Method of Splitting Tsunami (MOST) Model," NOAA Technical Memorandum ERL PMEL-112, 1997.

**PSEG Site
ESP Application
Part 2, Site Safety Analysis Report**

- 2.4.6-23 University of Delaware Spatial Analysis Lab, Website, <http://www.udel.edu/FREC/spatlab/dems/>, accessed July 15, 2009.
- 2.4.6-24 U.S. Geological Survey, "Delaware River Study Unit Description," National Water-Quality Assessment Program, Website, <http://nj.usgs.gov/nawqa/delr/su.descript.html>, accessed June 16, 2009.
- 2.4.6-25 Ward, S.N. and S. Day, "Cumbre Vieja Volcano – Potential Collapse and Tsunami at La Palma, Canary Island," Geophysical Research Letters, 28(17), p. 3397 – 3400, 2001.
- 2.4.6-26 Ward, S.N., "Landslide Tsunami," Journal of Geophysical Research, 106: p. 11,201 – 11,215, 2001.
- 2.4.6-27 Watts, P., S.T. Grilli, D.R. Tappin, G.J. Fryer, "Tsunami Generation by Submarine Mass Failure. II: Predictive Equations and Case Studies," Journal of Waterway, Port, Coastal and Ocean Engineering, 131(6), p. 298 – 310, 2005.
- 2.4.6-28 Watts, P., S.T. Grilli, J.T. Kirby, G.J. Fryer, D.R. Tappin, "Landslide Tsunami Case Studies Using a Boussinesq Model and a Fully Nonlinear Tsunami Generation Mode I," Natural Hazards and Earth System Science, 3(5), 391 – 402, 2003.
- 2.4.6-29 Whitney, M.M. and R.W. Garvine, "Estimating Tidal Current Amplitudes Outside Estuaries and Characterizing the Zone of Estuarine Tidal Influence", Continental Shelf Research, 28: p. 380 – 390, 2008.
- 2.4.6-30 Twichell, D. C., J. D. Chaytor, U. S. ten Brink and B. Buczkowski, B., "Morphology of late Quaternary submarine landslides along the U. S. Atlantic continental margin", Marine Geology, 264, 4-15, 2009.
- 2.4.6-31 Chaytor, J. D., U. S. ten Brink, A. R. Solow, and B. D. Andrews, "Size distribution of submarine landslides along the U. S. Atlantic margin", Marine Geology, 264, 16-27.
- 2.4.6-32 Enet, F. and Grilli, S. T., 2007, "Experimental study of tsunami generation by three-dimensional rigid underwater landslides", J. Waterway, Port, Coastal and Ocean Engineering, 133, 442-454.
- 2.4.6-33 Tappin, D. R., Watts, P. and Grilli, S. T., 2008, "The Papua New Guinea tsunami of 17 July 1998: anatomy of a catastrophic event", Natural Hazards and Earth Systems Science, 8, 243-266.

**PSEG Site
ESP Application
Part 2, Site Safety Analysis Report**

**Table 2.4.6-1
Historical Record of Tsunamis Affecting the U.S. East Coast**

Date	Tsunami Source Location				Earthquake Magnitude ^(a)	Tsunami Cause	Maximum Tsunami Water Height
	Country	City	Lat	Long			
11/01/1755	Portugal	Lisbon	36.000	-11.000	n.a. ^(e)	Earthquake	98.4 ft. (30 m) (Lagos) ^(b) 9.8 ft. (3 m) (East Coast) ^(d)
06/27/1864	Canada	Avalon Peninsula, Newfoundland	46.500	-53.700	n.a. ^(e)	Earthquake	n.a. ^(e)
09/01/1886	U.S.	Charleston, SC	32.900	-80.000	M _w 7.7	Earthquake	n.a. ^(e)
09/01/1895	U.S.	High Bridge, NJ	40.667	-74.883	M _f a 4.3	Earthquake	n.a. ^(e)
10/11/1918	U.S.	Mona Passage, Puerto Rico	18.500	-67.500	M _w 7.3	Earthquake	20 ft. (6.10 m) (Punta Agujereada) ^(b) 0.2 ft. (0.06 m) (Atlantic City) ^(c)
11/18/1929	Canada	Grand Banks, Newfoundland	44.690	-56.000	M _w 7.2	Earthquake and Submarine Landslide	23 ft. (7.00 m) (Taylor's Bay) ^(b) 2.2 ft. (0.68 m) (Atlantic City) ^(c)
08/04/1946	Dominican Republic	Northeastern Coast	19.300	-68.940	Unk 8.1	Earthquake	16.4 ft. (5.0 m) (Rio Boba) ^(b)
08/08/1946	Dominican Republic	Northeastern Coast	19.710	-69.510	Unk 7.9	Earthquake	2 ft. (0.60 m) (San Juan) ^(c)
08/08/1964	U.S.	Long Island, NY	n.a. ^(e)	n.a. ^(e)	n.a. ^(e)	Submarine Landslide	0.92 ft. (0.28 m) (Plum Island) ^(c)
12/26/2004	Indonesia	Off West Coast of Sumatra	3.295	95.982	M _w 9.0	Earthquake	167 ft. (50.9 m) (Labuhan) ^(b) 0.75 ft. (0.23 m) (Atlantic City) ^(c)

a) M_w is moment magnitude scale, M_fa is logarithmic magnitude scale, and Unk is unknown scale.

b) Tide gage record.

c) Deep ocean gage record.

d) Determined from numerical simulation.

e) n.a. - Not available. Information not provided in NOAA Historical Tsunami database

Reference 2.4.6-15

The data presented on this table is modified from the NOAA website; 4 events related to the New Madrid earthquakes are reported on the NOAA website. New Madrid is located near the Mississippi River in Missouri. According to the tsunami records, New Madrid earthquakes generated several waves in the rivers. As this tsunami source is not located along the East Coast of the United States or in the Atlantic Ocean, this kind of tsunami would not affect the water level at the site. Thus, tsunami sources in New Madrid are excluded from the table to be consistent with its title "Historical Tsunamis arriving at the Shores of the Eastern United States and Canada."

**PSEG Site
ESP Application
Part 2, Site Safety Analysis Report**

**Table 2.4.6-2
Parameters for Seven Individual Okada Sources Which Make Up the
Composite Hispaniola Trench Source**

Location (deg)	Length (km)	Width (km)	Dip (deg)	Rake (deg)	Strike (deg)	Slip (m)	Depth (km)
293.00E 18.75N	100.0	100.0	20	90	84	10	10
293.00E 18.75N	100.0	100.0	20	90	84	10	10
294.00E 18.85N	100.0	100.0	20	90	84	10	10
294.00E 18.95N	100.0	100.0	20	90	84	10	10
294.00E 19.00N	100.0	100.0	20	90	84	10	10
295.00E 19.00N	100.0	100.0	20	90	84	10	10
296.10E 19.00N	100.0	100.0	20	90	84	10	10

**PSEG Site
ESP Application
Part 2, Site Safety Analysis Report**

**Table 2.4.6-3
Grids A, B, and C for Currituck Landslide Case**

Grid	Coverage	Resolution	Dimension	Simulation Time
Grid A	35° 30' N-40° 00' N 75° 45' W-73° 00' W	30 arc-second (arc-sec)	166x271	15 hours
Grid B	38° 36' N-39° 40' N 75° 40' W-74° 47' W	6 arc-sec	641x531	15 hours
Grid C	39° 15' N-39° 39' N 75° 37' W-75° 10' W	3 arc-sec	541x481	15 hours

**PSEG Site
ESP Application
Part 2, Site Safety Analysis Report**

**Table 2.4.6-4
Grids A, B and C for La Palma, Canary Island Landslide Case**

Grid	Coverage	Resolution	Dimension	Simulation Time
Grid A	20° 00' N-45° 00' N 80° 00' W-13° 00' W	2 arc-minute (arc-min)	2011x750	18 hours
Grid B	37° 50' N-40° 00' N 75° 40' W-73° 00' W	15 arc-sec	641x521	18 hours
Grid C	39° 15' N-39° 39' N 75° 37' W-75° 10' W	3 arc-sec	541x481	18 hours

**PSEG Site
ESP Application
Part 2, Site Safety Analysis Report**

**Table 2.4.6-5
Grids A, B, and C for the Hispaniola Trench Earthquake Case**

Grid	Coverage	Resolution	Dimension	Simulation Time
Grid A	13° 00' N-42° 30' N 82° 00' W-52° 00' W	2 arc-min	901x886	18 hours
Grid B	37° 50' N-40° 00' N 75° 40' W-73° 00' W	15 arc-sec	641x521	18 hours
Grid C	39° 15' N-39° 39' N 75° 37' W-75° 10' W	3 arc-sec	541x481	18 hours

**PSEG Site
ESP Application
Part 2, Site Safety Analysis Report**

**Table 2.4.6-6
Summary of Maximum Runup and Drawdown Values at PSEG Salem Site for Each Case**

Case	Maximum Runup	Maximum Drawdown	Wave Period
Currituck submarine landslide	+1.0 ft. (+0.31m) 10%E +5.5 ft. (+1.68m) NAVD	-0.62 ft. (-0.19 m) 90%E -5.62 ft. (-1.71 m) NAVD	250 min
Currituck submarine landslide without bottom friction	+1.15 ft. (+0.35m) 10%E +5.65 ft. (+1.72m) NAVD	-1.16 ft. (-0.34 m) 90%E -6.16 ft. (-1.86 m) NAVD	223 min
La Palma, Canary Island submarine landslide	+0.26 ft. (+0.08m) 10%E +4.76 ft. (+1.45m) NAVD	-0.30 ft. (-0.09 m) 90%E -5.30 ft. (-1.61 m) NAVD	260 min
Hispaniola Trench earthquake	+0.72 ft. (+0.22m) 10%E +5.22 ft. (+1.59m) NAVD	-0.56 ft. (-0.17 m) 90%E -5.56 ft. (-1.69 m) NAVD	266 min

Maximum runups are shown relative to a datum based on the 10% exceedance elevation (10%E) for tidal motions and converted to NAVD elevations. Maximum drawdown is relative to a datum based on the 90% exceedance elevation (90%E) for tidal motions, also converted to NAVD.

**PSEG Site
ESP Application
Part 2, Site Safety Analysis Report**

2.4.7 ICE EFFECTS

The hydrometeorological design basis is developed in this subsection to ensure that water supply and safety-related SSC are not affected by ice induced hazards.

Adverse ice effects can include ice cover or ice jams in streams and canals causing backwater; frazil and anchor ice affecting intake screens, racks, pumps, casings, valves and control works; ice-produced forces on intake structures, racks, gates, dams, and control works; ice ridges on lakes, and windrowed ice piles (Reference 2.4.7-1). Ice effects are analyzed to determine any adverse effects at the new plant location.

Potential ice effects at the new plant location are evaluated, including the review of ice formations or ice jams; modeling combined events to ensure protection of the safety-related facilities from ice-affected floods, and mitigation to protect safety-related structures from ice. Analysis of ice effects at the new plant includes review of historic winter conditions and the simulation of flooding due to an upstream ice jam break.

Flooding caused by upstream ice jam failures is simulated using recorded historic WSEL and discharges resulting from the failure of a historic upstream ice jam. Water surface elevations from the ice jam failure in combination with 10 percent exceedance high tide, average spring base flows, and coincident wave runup resulting from the maximum 2-year wind, are modeled to obtain a peak WSEL at the new plant location.

2.4.7.1 Historical Ice Accumulation

The PSEG Site is located on the east (E) bank of the Delaware River, in the southwest portion of Salem County, NJ. The new plant location is in the northwest corner of the PSEG Site, at RM 52. Meteorological data from Wilmington, DE, 18 mi. north of the new plant, shows normal low temperatures in January range between 23°Fahrenheit (F) and 25°F, for the period of record from 1971 to 2000. A record low temperature of -15°F in Wilmington was recorded on February 9, 1934, for the period of record of 1894 to 2009. (Reference 2.4.7-9) These temperatures are lower than temperatures observed at the PSEG Site, where 32 years of site meteorological data show the average minimum temperature in January is 27°F, with a record low of -6°F (see Subsection 2.3.3). The lower temperatures in Wilmington are used in this analysis to provide more conservative temperatures.

Ice is typically present in the northern areas of the upper Delaware River, Delaware Bay, and Chesapeake and Delaware Canal in January, and is generally thawed by the end of February (Reference 2.4.7-22). Water temperature gradients from Trenton, NJ to the mouth of the bay at the Atlantic Ocean can be as large as 9°F. The shallow waters and tidal flow produce horizontal gradients in water temperature that vary 4°F or more on daily cycles. (Reference 2.4.7-12)

The normal range of ocean salinity is 32 to 37 ppt of salt. Salinity at the PSEG Site ranges from 5 to 18 ppt, with a daily variation due to tidal influence (Reference 2.4.7-23). Sea water has a freezing point of 29°F (Reference 2.4.7-13), the freezing point of the Delaware Estuary at the PSEG Site ranges from 30°F to 31°F.

Research of the USACE CRREL Ice Jam Database records show no recorded ice jams on the Delaware River downstream of Trenton. Records in the database start as far back as 1780 and

**PSEG Site
ESP Application
Part 2, Site Safety Analysis Report**

continue through 2009. The closest ice jam to the PSEG Site on record in the CRREL Ice Jam Database was located on Brandywine Creek, in Wilmington, DE, on February 14, 1948 (Reference 2.4.7-15). Brandywine Creek discharges into the Christina River, which discharges into the Delaware River at RM 71 (Reference 2.4.7-2). This ice jam caused backwater elevations to reach 75.9 ft. NAVD at USGS gage 01481500 (Brandywine Creek) (Reference 2.4.7-15), in comparison to a bankfull stage of 82.4 ft. NAVD (Reference 2.4.7-28).

Numerous ice jams occurred in the Delaware River Basin due to record-breaking snowfall in January, 1996. Major ice jams caused flooding on the Schuylkill River and the Delaware River. These ice jams caused the Delaware River to rise 12 ft. in 10 hr., producing flooding in Trenton, NJ (Reference 2.4.7-15). The effect at Reedy Point was not significant, as the maximum WSEL at the Reedy Point NOAA gage station (8551910) during January 1996 was 3.2 ft. NAVD, which is 0.6 ft. above the mean high water at Reedy Point.

The highest recorded flooding as a result of an ice jam on the Delaware River closest to the PSEG Site occurred at Trenton (RM 134), 82 mi. upstream from the new plant. This ice jam occurred on March 8, 1904 as reported in the CRREL Ice Jam Database. (Reference 2.4.7-15) Severe flooding in Trenton resulted from a combination of heavy rains, ice melt upstream, and an ice jam at Terriwig Bar in South Trenton, which caused the Delaware River to rise rapidly. This ice jam produced a maximum gage height of 22.8 ft. (29.6 ft. NAVD) at Trenton, NJ USGS gage 01463500 (Reference 2.4.7-26).

Table 2.4.7-1 summarizes the most significant historical ice jams on record within the Delaware River Basin. Ice jams of these magnitudes have the potential to cause flooding or low water at the site (Reference 2.4.7-15) and, therefore, are analyzed. This table includes the closest ice jams upstream of the new plant location, the ice jams producing the highest gage height, and the ice jams producing the highest discharge in the Delaware River or its tributaries within 15 mi. of the Delaware River. There have been no ice jams recorded downstream of the PSEG Site (Reference 2.4.7-15).

Surface ice has historically been observed at the PSEG Site. The National Ice Center's archive data, from the winter of 1998/1999 to the winter of 2004/2005, shows surface ice typically occurring in January and February on the Delaware River near the PSEG Site (Reference 2.4.7-4) (Table 2.4.7-2).

The potential for frazil ice exists at the PSEG Site, as frazil ice forms when the water is supercooled below its freezing temperature. Conditions that lead to supercooling include air temperatures of 21°F (-6 degrees Celsius [C]) and below, along with open water and clear nights (Reference 2.4.7-14). There are numerous instances in the historical meteorological data indicating that air temperatures have dropped below 21°F in the vicinity of the PSEG Site; therefore, frazil ice can potentially occur.

2.4.7.2 High and Low Water Levels

The topography at the new plant location ranges from 5 to 15 ft. NAVD (Reference 2.4.7-3). The surrounding land is of a similar low and flat nature. As the proposed safety-related structures will be elevated above the surrounding land, the potential for flooding of the safety-related structures caused by snow or ice slides from adjacent areas is unlikely, due to the topographic

**PSEG Site
ESP Application
Part 2, Site Safety Analysis Report**

relief at the new plant location and along the banks of the Delaware River (References 2.4.7-10 and 2.4.7-17).

2.4.7.2.1 High Water Levels

As described in Subsection 2.4.7.1, the January 21, 1996 ice jam located on the Delaware River near Trenton occurred upstream of the PSEG Site. The result of this ice jam, in combination with rapid snow melt, caused a peak stage at Trenton USGS gage 01463500, of 21.2 ft. NAVD, and a peak discharge of 179,000 cfs (Reference 2.4.7-30). Review of gage data between January 10 and February 10, 1996 shows a maximum WSEL of 3.2 ft. NAVD at the Reedy Point NOAA tidal gage 8551910 on January 21, 1996 (Reference 2.4.7-7). This data indicates the flood levels from this ice jam dissipated by the time floodwaters reached the PSEG Site.

The highest recorded elevation produced from the March 8, 1904, ice jam flood event at Trenton USGS gage 01463500 produced a WSEL of 29.6 ft. NAVD (Reference 2.4.7-26). No discharge value at the Trenton USGS gage station is on record for the March 8, 1904 flood event.

2.4.7.2.1.1 Ice Jam Modeling

The USACE HEC-RAS model (Reference 2.4.7-20) is used to simulate the March 8, 1904 ice jam event at Trenton and determine the resulting effect on the new plant location, in combination with a 10 percent exceedance high tide, average spring flows, and a 2-year wind speed applied in the critical direction. There is no specific source for combined events for ice effects. Using a wind event similar to the other types of flooding in addition to the worst recorded ice jam on the Delaware River is considered to be a conservative approach.

The HEC-RAS model is used to route the runoff through the Delaware River. This model is developed using channel geometry and floodplain elevations for the Delaware River. Bathymetry and floodplain topography for portions of the Delaware River from the USGS gage station at Trenton (RM 134) to the NOAA tidal gage station at Lewes (RM 0) (Reference 2.4.7-2), are developed using the TIN terrain model based on the USGS National Elevation Dataset (Reference 2.4.7-29) DEM, the NOAA Estuarine Bathymetry DEM (Reference 2.4.7-5), USGS quad sheets (Reference 2.4.7-24), and the USACE Bathymetry Data (Reference 2.4.7-18). Figure 2.4.7-1 shows a typical cross-section of the Delaware River at RM 52 (the PSEG Site). The Manning's n roughness coefficients in the HEC-RAS model for the lower Delaware River are calibrated using astronomical tide data, and stage-discharge data for Trenton.

Discharge hydrographs from the individual drainage areas developed in the USACE HEC-HMS (Reference 2.4.7-19) define the discharge inputs to the HEC-RAS model. Cross-sections between Lambertville, NJ (RM 149) and Trenton (RM134) (Reference 2.4.7-2) are added to the tidal calibrated hydraulic model in order to incorporate the storage upstream of the ice jam. The Manning's n values from Lambertville to Trenton are determined from the HEC-RAS Hydraulic Reference Manual Table 3.1. The non-tidal portion of the HEC-RAS model uses 0.025 as the Manning's n value for a clean, straight, full channel and 0.05 as the Manning's n value for the flood plain (Reference 2.4.7-21). The hydraulic model for the ice jam is checked by simulating the average April base flow conditions in conjunction with the 10 percent exceedance high tide value, and evaluating the results as compared to a simulation performed using the tidal calibrated hydraulic model developed for the PMF in Subsection 2.4.3.

**PSEG Site
ESP Application
Part 2, Site Safety Analysis Report**

The 10 percent exceedance high tide is 4.2 ft. NAVD at Lewes NOAA tide gage 8557380 (RM 0); and 4.6 ft. NAVD for NOAA tide gage 8551910 (RM 59) located at Reedy Point. From these values, the resulting 10 percent exceedance high tide at the new plant location (RM 52) is determined by linear interpolation to be 4.5 ft. NAVD. The average spring base flows are then applied to this 10 percent exceedance high tide. In order to simulate average springtime base flow in the lower Delaware River, a simulation using the HEC-HMS base flow model is performed for a day in April where no rainfall occurred in the lower Delaware River Basin. The average monthly base flow values for April are selected following a review of the USGS water data report for gage 01463500 at Trenton, which shows that the highest monthly mean discharge between the period of record of 1913 to 2008 occurs in April (Reference 2.4.7-27). The streamflow gage at Trenton is the most direct measurement of the streamflow for the Delaware River Basin. Therefore this is used as the selection criterion for the highest average monthly base flow. Application of the HEC-RAS model with spring base flow discharge at Trenton and 10 percent exceedance high tide at the mouth of the bay results in a maximum water surface elevation of 5.2 ft. NAVD (Table 2.4.7.-3), which is 0.7 ft higher than the 10 percent exceedance high tide at the new plant location, implying that the spring base flow discharge causes a 0.7 ft increase in water level at the new plant.

The stage hydrograph at RM 0 is set to simulate the 10 percent exceedance high tide at the lower limit of the HEC-RAS model. An initial flow of 48,800 cfs is incorporated into the HEC-RAS model at the upstream limit of the model, reflecting the measured discharge on March 8, 1904, at USGS gage 01462000 in Lambertville, NJ (Reference 2.4.7-25). An ice dam at Trenton is input into the model to produce an upstream WSEL similar to the stage produced by the ice jam of 1904. The modeled WSEL is 29.8 ft. NAVD, which is 0.2 ft. higher than the 1904 stage, and produces a more conservative estimate of flooding. The ice jam is then instantaneously breached in the model, simulating the ice jam failure and subsequent release of accumulated water down the Delaware River. A 2-year wind speed is then applied on the resulting water level in the critical direction, and a coincident wave runup is determined. The wave field is fetch- and duration-limited, as defined by USACE (Reference 2.4.7-13).

Wave runup is determined using 2-year annual extreme-mile wind speed of 50 mph, in accordance with Section 9.1.4 of ANSI/ANS-2.8-1992 (Reference 2.4.7-1). Wind speeds are adjusted for duration in accordance with the Coastal Engineering Manual (Reference 2.4.7-13). Fetch directions are evaluated in 22.5 degree increments and the fetch direction that yields the highest wave runup is reported. Wave conditions are limited by fetch for the critical direction, which is wind blowing from the west-northwest across a flooded fetch of 4 mi. The smaller of the maximum wave height or the maximum breaker height is used to determine runup, as described in Section 7.4.3 and Subsection 7.4.4.5 of ANSI/ANS-2.8-1992 (Reference 2.4.7-1). The maximum wave height of 5.6 ft. is controlling.

It is assumed the waves break on the existing ground slope because the maximum WSEL resulting from an upstream ice jam is less than the average grade of the new plant location. The modified Hunt formula as described in the USACE Coastal Engineering Manual determines wave runup as a function of shoreline slope, incident wave height, and wave steepness. This formula is valid for beach slopes from 1:10 to vertical. The actual ground slope is less than 1:10. Wave runup increases with slope, so assuming a 1:10 slope produces a conservative estimate of wave runup. This assumption is reasonable because waves will break before reaching the fill placed to elevate the new reactor above the DBF.

**PSEG Site
ESP Application
Part 2, Site Safety Analysis Report**

The resulting WSEL at the PSEG Site, due to the 10 percent exceedance high tide (4.5 ft. NAVD), plus the spring base flows (0.7 ft.), plus the rise in the Delaware River resulting from the upstream ice jam breach at Trenton (0.1 ft.), plus the coincident wave runup from a 2-year wind speed applied in the critical direction (2.8 ft.) is 8.1 ft. NAVD. Table 2.4.7-3 presents the water surface levels determined from the model.

2.4.7.2.2 Low Water Levels

There are no ice jams recorded in the CRREL database for the Delaware River downstream of the PSEG Site. In addition, the Delaware River width and cross-section increase significantly immediately to the south of the new plant. Therefore, backwater flooding from downstream ice jams has not been considered (Reference 2.4.7-15). However, numerous ice jams located on the Delaware River upstream of the PSEG Site have been recorded, as discussed in Subsection 2.4.7.1. Therefore, the potential for low water elevations in the Delaware River due to upstream river blockage from an ice jam is evaluated. A detailed analysis of winter low water elevations at the new plant due to winter low flows and ice jams is presented in Subsection 2.4.11.

The mean lower low water elevation at the Reedy Point NOAA tidal gage station (gage 8551910) is -3.0 ft. NAVD. Based on historic information of the Reedy Point gage, the minimum water level recorded since inception of the gage (in 1956) is -7.0 ft. NAVD. This occurred on April 7, 1982 (Reference 2.4.7-6). A USGS paper identifies a low water event which occurred on December 31, 1962 due to north-northwestern winds blowing downstream. The paper identified a low water reading at Reedy Point of -8.6 ft. msl (-9.5 ft. NAVD) (Reference 2.4.7-11). Tidal flow at the PSEG Site, which ranges from 400,000 cubic feet per second (cfs) to 472,000 cfs (References 2.4.1-16 and 2.4.1-23), dominates the freshwater flow of the Delaware River. The tidal flow is much greater than the flow required by the intake structure, making the effects of an ice jam upstream and the resulting reduced Delaware River freshwater flow not a critical factor in the design of the new plant intake.

The invert elevations of the new plant intake structure will be set at an elevation to maintain operations during low water conditions. Intakes will be designed to assure that adequate water is available in the event of low water conditions. Design features to address floating and frazil ice will be included. Low water effects are further discussed in Subsection 2.4.11.

2.4.7.3 Ice Sheet Formation

No safety-related water reservoirs are located on the PSEG Site. Therefore there is no potential for surface ice to reduce the volume of liquid water available in a reservoir for safety-related cooling. Depending on the technology chosen, any basins for the new plant will be designed to withstand internal and external ice effects, and the intake structure on the Delaware River will have protective measures to mitigate potential effects from surface ice.

2.4.7.4 Potential Ice-Induced Forces and Blockages

Frazil ice, fine needle-like structures or thin, flat circular plates of ice, can form on intake structures, thereby causing blockages of the intakes and reducing access to available water (Reference 2.4.7-16). Frazil ice begins to form when the water becomes supercooled (below its

**PSEG Site
ESP Application
Part 2, Site Safety Analysis Report**

freezing temperature). Conditions that lead to supercooling include air temperatures of 21°F (-6 C) and below, open water, and clear nights (Reference 2.4.7-14).

As discussed in Subsection 2.4.7.1, surface ice has been observed on the Delaware River at the PSEG Site, primarily during the months of January and February (Reference 2.4.7-4). This is consistent with the U.S. Coast Guard (USCG) Ice Guide (Reference 2.4.7-22). Table 2.4.7-2 summarizes the thickness and concentration of ice reported near the PSEG Site during the period of record from the 1998/1999 winter to the 2004/2005 winter. The concentration of ice is defined as the fraction of an area that is covered by sea ice. The National Ice Center reports this concentration data in tenths (Reference 2.4.7-8). A review of the National Ice Center data shows the thickest ice in the vicinity of the new plant was reported as code 741 on January 31, 2000. Using the World Meteorology Organization's ice chart symbology, this translates to a thickness of 12 to 28 in. for the most mature portions of ice on the Delaware River, 4 to 6 in. for newer portions of formed ice, and 0 to 4 in. for the most recently formed ice. The highest concentration of ice reported during this period of record is 9-tenths to 10-tenths in the mid- to upper-Delaware Bay, occurring during the week of January 26, 2004 (Reference 2.4.7-4). This means that the ice formed in the mid and upper portions of Delaware Bay was concentrated enough to allow formation of a solid sheet of ice, but was not concentrated enough to be considered fast ice (ice anchored to the shoreline). The new plant is located at the transition from the Delaware Bay to the Delaware River. Table 2.4.7-2 summarizes the thickness and concentration of ice reported near the PSEG Site during this period of record.

In accordance with ANS 2.8, Section 8.3, the intake structure at the new plant location will be designed with protective measures to mitigate potential effects from frazil ice, surface ice, and other dynamic forces associated with ice effects.

2.4.7.5 Conclusions

The new plant design will ensure that all above-grade safety-related SSC are situated at least one foot higher than the DBF elevation, as required by Tier 1 of the DCD for the technology selected. Based on review of historical ice jam information and model simulation of a major historic ice jam event, the flooding potential resulting from historic ice jam discharge is elevation 8.1 ft. NAVD. This is significantly lower than the DBF elevation of 32.1 ft. NAVD. The DBF is further discussed in Subsection 2.4.5. Surface ice has been observed at the site. Based on historic meteorological data, the potential for frazil ice exists at the PSEG Site (as discussed in Subsection 2.4.7.1). The new plant intake structure will be designed to address ice effects, including surface ice, frazil ice, and other dynamic forces and blockages associated with ice effects. The icing events presented in this subsection represent the worst case icing scenarios adjacent to and at the PSEG Site.

2.4.7.6 References

- 2.4.7-1 American National Standards Institute/American Nuclear Society, "Determining Design Basis Flooding at Power Reactor Sites," ANSI/ANS-2.8-1992, (historical), p. 1; 32, 1992.
- 2.4.7-2 Delaware River Basin Commission 2007b, "Stream River Mileage July 2007," Website, <http://www.state.nj.us/drbc/StreamMileageJuly2007.pdf>, p. 11, accessed February 16, 2009.

**PSEG Site
ESP Application
Part 2, Site Safety Analysis Report**

- 2.4.7-3 MASER Consulting, PA ALTA/ACSM Land Title Survey for PSEG Nuclear LLC of Block 26, Lots 4, 4.01, 5 and 5.01, Job Number 05001694D, Index Number HASU023453, dated June 13, 2008.
- 2.4.7-4 National Oceanic and Atmospheric Administration, National Ice Center, Website, <http://www.natice.noaa.gov/>, accessed July 13, 2009.
- 2.4.7-5 National Oceanic and Atmospheric Administration, "NOS Estuarine Bathymetry: Delaware Bay DE/NJ (M090)," Website, <http://egisws01.nos.noaa.gov/servlet/BuildPage?template=bathy.txt&parm1=M090&B1=Submit>, accessed February 2, 2009.
- 2.4.7-6 National Oceanic and Atmospheric Administration, "Tides and Currents, Reedy Point, DE (Gage 8551910) Datums," Website, http://tidesandcurrents.noaa.gov/data_menu.shtml?stn=8551910%20Reedy%20Point,%20DE&type=Datums, accessed July 10, 2009.
- 2.4.7-7 National Oceanic and Atmospheric Administration, "Tides and Currents, Reedy Point, DE (Gage 8551910), Historic Tide Data," Website, http://tidesandcurrents.noaa.gov/data_menu.shtml?bdate=19960101&edate=19960331&wl_sensor_hist=W3&relative=&datum=6&unit=1&shift=g&stn=8551910+Reedy+Point%2C+DE&type=Historic+Tide+Data&format=View+Plot, accessed July 11, 2009.
- 2.4.7-8 National Oceanic and Atmospheric Administration, National Ice Center, Ice Chart Symbolology, Website, http://www.natice.noaa.gov/products/egg_code.html, accessed July 14, 2009.
- 2.4.7-9 National Weather Service, "Forecast Office, Records & Normals for Wilmington, DE," Website, http://www.erh.noaa.gov/phi/climate/recsAndNormals/xml/KILG_recAndNorms.xml, accessed July 13, 2009.
- 2.4.7-10 Public Service Enterprise Group (PSEG), "Applicant's Environmental Report- Operating License Renewal Stage Salem Generating Station Unit 1 and 2," Docket No. 50-272 and 50-311, Revision 2a, p. 2-3, 3-3 – 3-5, 3-7, 3-8, 2008a.
- 2.4.7-11 U. S. Department of the Interior, Report # 1586-E, "Record Low Tide of December 31, 1962 on the Delaware River" 1966, prepared by A.C. Lendo.
- 2.4.7-12 Public Service Enterprise Group, "Salem Generating Station NJPDES Permit Renewal Application," p. 52 – 53, 1999.
- 2.4.7-13 U.S. Army Corps of Engineers, "Coastal Engineering Manual," Engineer Manual 1110-2-1100, U.S. Army Corps of Engineers, Washington, D.C. (in 6 volumes), 2002.

**PSEG Site
ESP Application
Part 2, Site Safety Analysis Report**

- 2.4.7-14 U.S. Army Corps of Engineers, Cold Regions Research and Engineering Laboratory, Cold Regions Technical Digest No 91-1, "Frazil Ice Blockage of Intake Trash Racks," Stephen F. Daly, p. 2, March 1991.
- 2.4.7-15 U.S. Army Corps of Engineers, Cold Regions Research and Engineering Laboratory, "Ice Jam Database," Website, <http://www.crrel.usace.army.mil/icejams/>, accessed June 24, 2009.
- 2.4.7-16 U.S. Army Corps of Engineers, Cold Regions Research and Engineering Laboratory, "River Ice Guide and Glossary," Website, http://www.crrel.usace.army.mil/ierd/ice_guide/iceguide.htm, accessed July 13, 2009.
- 2.4.7-17 U.S. Army Corps of Engineers, Corpscon 6.0 Computer Program, downloaded February 2009.
- 2.4.7-18 U.S. Army Corp of Engineers, "Delaware River Philadelphia to the Sea Examination," Bathymetric Survey Data, Philadelphia, Pennsylvania, 2007 – 2009.
- 2.4.7-19 U.S. Army Corp of Engineers, "HEC-HMS 3.3 Software," Website, <http://www.hec.usace.army.mil/software/hec-hms/download.html>, accessed February 23, 2009.
- 2.4.7-20 U.S. Army Corp of Engineers, "HEC-RAS 4.0 software," Website, <http://www.hec.usace.army.mil/software/hec-ras/hecras-download.html>, accessed February 23, 2009.
- 2.4.7-21 U.S. Army Corp of Engineers, "Hydraulic Reference Manual Version 3.1, November 2002," Website, <http://www.hec.usace.army.mil/software/hec-ras/documents/hydref/>, accessed August 5, 2009.
- 2.4.7-22 U.S. Coast Guard, Sector Delaware Bay, "2008 – 2009 Ice Guide," Website, <http://www.uscg.mil/d5/sectDelawareBay/Sector/IceReport/IceReporting.asp>, accessed July 13, 2009.
- 2.4.7-23 U.S. Environmental Protection Agency, "Condition of the Mid Atlantic Estuaries," Office of Research and Development, p. 7, November 1998.
- 2.4.7-24 U.S. Geological Survey, "7.5 Minute Quadrangle Topographic Maps," Website, <http://datagateway.nrcs.usda.gov/>, accessed April 21, 009.
- 2.4.7-25 U.S. Geological Survey, Gage 01462000 Delaware River at Lambertville NJ, Website, http://waterdata.usgs.gov/nwis/dvstat?referred_module=sw&site_no=01462000&por_01462000_1=147714,00060,1,1897-10-01,1906-09-30&start_dt=1904-03-01&end_dt=1904-03-15&format=html_table&stat_cds=max_va&date_format=YYYY-MM-DD&rdb_compression=file&submitted_form=parameter_selection_list, accessed July 15, 2009.

**PSEG Site
ESP Application
Part 2, Site Safety Analysis Report**

- 2.4.7-26 U.S. Geological Survey, Gage 01463500 Delaware River at Trenton NJ, Website, http://waterdata.usgs.gov/usa/nwis/uv?site_no=01463500, accessed July 13, 2009.
- 2.4.7-27 U.S. Geological Survey, "Water Data Report USGS Gage 01463500 Delaware River at Trenton, NJ," Website, <http://wdr.water.usgs.gov/wy2008/pdfs/01463500.2008.pdf>, accessed July 16, 2009.
- 2.4.7-28 U.S. Geological Survey, Gage 01481500 Brandywine Creek at Wilmington, DE, Streamflow Statistics, Website, <http://md.water.usgs.gov/surfacewater/streamflow/brandywine.html>, accessed July 13, 2009.
- 2.4.7-29 U.S. Geological Survey, "National Elevation Dataset," Website, <http://seamless.usgs.gov/index.php>, accessed February 2, 2009.
- 2.4.7-30 U.S. Geological Survey, Statewide Floods in Pennsylvania, January 1996, Website, http://water.usgs.gov/wid/FS_103-96/FS_103-96.html, accessed July 23, 2009.

**PSEG Site
ESP Application
Part 2, Site Safety Analysis Report**

**Table 2.4.7-1 (Sheet 1 of 2)
Historic Ice Jam Events on the Delaware River and Tributaries^(a)**

City	State	River	Jam Date	Gage Station ID	Description
Barryville	NY	Delaware River	2/11/1981	01428500	A gage height of 20.9 ft. occurred on Delaware River above Lackawaxen River near Barryville, NY, on February 11, 1981 as a result of an ice jam with an associated discharge of 15,000 cfs. This was the maximum gage height for the year. The next day, February 12, the maximum annual discharge of 52,800 cfs occurred as the ice jam released.
Barryville	NY	Delaware River	2/15/1971	01428500	The USGS reported an ice jam on February 15, 1971 at Barryville, NY, on the Delaware River. The estimated water discharge was 12,000 cfs. Maximum gage height was 15.62 ft.
Barryville	NY	Delaware River	2/24/1961	01428500	Maximum annual gage height of 18.19 ft., affected by backwater from ice, reported at USGS gage Delaware River (above Lackawaxen River) near Barryville, on February 24, 1961.
Callicoon	NY	Delaware River	2/12/1981	01427510	A gage height of 13.19 ft. and a discharge of 75,300 cfs occurred on Delaware River at Callicoon NY, on February 12, 1981, as a result of an ice jam release. This was the maximum gage height and discharge for the year as well as for the period of record 1975 – 1981.
Hale Eddy	NY	West Branch Delaware River	3/5/1934	01426500	Maximum annual gage height of 11.43 ft., affected by backwater from ice, reported at USGS gage West Branch Delaware River at Hale Eddy, on March 5, 1934. Discharge 13,000 cfs.
Harvard	NY	East Branch Delaware River	2/20/1948	01417500	Gage height of 12.12 ft., affected by backwater from ice, reported at USGS gage East Branch Delaware River at Harvard, on February 20, 1948. Discharge 11,900 cfs.
Harvard	NY	East Branch Delaware River	2/27/1945	01417500	Maximum annual gage height of 12.74 ft., affected by backwater from ice, reported at USGS gage East Branch Delaware River at Harvard, on February 27, 1945. Discharge 14,800 cfs.
Langhorne	PA	Neshaminy Creek	1/2/1959	01465500	Maximum annual gage height of 6.79 ft., affected by backwater from ice, reported at USGS gage Neshaminy Creek near Langhorne, on January 2, 1959. Bankfull stage 7 ft.
Langhorne	PA	Neshaminy Creek	12/27/1943	01465500	Gage height of 7.24 ft., affected by backwater from ice, reported at USGS gage Neshaminy Creek near Langhorne, on December 27, 1943. Bankfull stage 7 ft.
Langhorne	PA	Neshaminy Creek	1/15/1940	01465500	Gage height of 8.05 ft., affected by backwater from ice, reported at USGS gage Neshaminy Creek near Langhorne, on January 15, 1940. Additional ice-affected gage height of 11.12 ft., reported on February 20, 1940. Bankfull stage 7 ft.
Langhorne	PA	Neshaminy Creek	2/27/1936	01465500	Gage height of 7.59 ft., affected by backwater from ice, reported at USGS gage Neshaminy Creek near Langhorne, on February 27, 1936. Bankfull stage 7 ft.
Langhorne	PA	Neshaminy Creek	2/15/1935	01465500	Maximum annual gage height of 11.80 ft., affected by backwater from ice, reported at USGS gage Neshaminy Creek near Langhorne, on February 15, 1935. Bankfull stage 7 ft.
Montague	NJ	Delaware River	2/21/1948	01438500	Gage height of 17.88 ft., affected by backwater from ice, reported at USGS gage Delaware River at Montague, on February 21, 1948.

**PSEG Site
ESP Application
Part 2, Site Safety Analysis Report**

**Table 2.4.7-1 (Sheet 2 of 2)
Historic Ice Jam Events on the Delaware River and Tributaries^(a)**

City	State	River	Jam Date	Gage Station ID	Description
Montague	NJ	Delaware River	3/4/1945	01438500	Maximum annual gage height of 17.54 ft., affected by backwater from ice, reported at USGS gage Delaware River at Montague, on March 4, 1945. Additional ice-affected gage height of 15.42 ft., reported on February 28, 1945.
Philadelphia	PA	Schuylkill River	1/21/1996	01474500	Ice jams were reported on the Susquehanna, Delaware, and Schuylkill Rivers on January 21, 1996. These jams caused severe flooding in Trenton, NJ. The Delaware had risen 12 ft. in 10 hours. This began with a winter storm dumping incredible amounts of snow across PA. Of the 40 inches that was on the ground, 28 of it melted. There were also high winds reaching 58 mph. The Fort Washington interchange of the PA turnpike was closed. In Chester County Routes 30 and 100 were closed as well.
Port Jervis	NY	Delaware River	12/18/2000	01434000	As a result of an ice jam release on Delaware River at Port Jervis, NY a maximum annual gage height of 11.76 ft. and maximum annual discharge of 57,700 cfs occurred on December 18, 2000.
Port Jervis	NY	Delaware River	2/5/1982	01434000	The maximum annual gage height of 15.82 ft. occurred on Delaware River at Port Jervis, NY on 5 February 1982, as a result of an ice jam. The average daily discharge recorded was 13,000 cfs.
Port Jervis	NY	Delaware River	2/12/1981	01434000	On February 12, 1981 a gage height of 26.6 ft. occurred on the Delaware River at Port Jervis, NY, due to an ice jam. This was the maximum for the year as well as for the period of record of record 1904-1981. The discharge was not determined. (see also entry for February 7, 1981) This gage height remained the maximum as of Sep 2001.
Port Jervis	NY	Delaware River	2/7/1981	01434000	Midwinter jam at Port Jervis followed by the spring break-up appear to cause this flood. Solutions suggested were a permanent hydraulic structure, ice booms, high-level diversion channels, and levee protection.
Port Jervis	NY	Delaware River	1/1/1904	01434000	An ice jam caused flooding for the town of Port Jervis in 1904. It was reported that the river stage was 25.5 ft. above the river gage while the flood stage is 18 ft. over the river gage. Other New York jams took place in February and March 1904.
Trenton	NJ	Delaware River	3/8/1904	01463500	Maximum annual gage height of 22.8 ft., affected by backwater from ice, reported at USGS gage Delaware River at Trenton, on March 8, 1904. Note: The ice jam flood of February 8, 1857, may have had a stage at Trenton equal to or higher than the ice jam flood of March 8, 1904 (highest known stage at Trenton).
Water Gap	PA	Delaware River	2/4/1970	01440200	The USGS reported an ice jam on February 4, 1970 at Water Gap, PA on the Delaware River. The estimated water discharge was 15,000 cfs. Maximum gage height was 18.85 ft.
Wilmington	DE	Brandywine Creek	2/14/1948	01481500	Maximum annual gage height of 8.72 ft., affected by backwater from ice, reported at USGS gage Brandywine Creek at Wilmington, on February 14, 1948.

a) The period of data collected ranges from 1780 to 2009.
Reference 2.4.7-15

**PSEG Site
ESP Application
Part 2, Site Safety Analysis Report**

**Table 2.4.7-2
Historical Ice Events on the Delaware Bay at the PSEG Site^(b)
Winter 1998/1999 – Winter 2004/2005**

Analysis Date / Week	Stage of Development^(c)	Ice Thickness (inches)	Total Concentration^(a)
January 31, 2000	741	0 – 28	8/10 – 10/10
February 4, 2000	541	0 – 12	8/10 – 10/10
February 9, 2000	54	2 – 12	6/10 – 8/10
February 11, 2000	54	2 – 12	6/10 – 8/10
February 14, 2000	54	2 – 12	2/10 – 4/10
Week of January 26, 2004	541	0 – 12	9/10 – 10/10
Week of February 9, 2004	541	0 – 12	6/10 – 8/10

- a) Total concentration is the fraction of an area covered by sea ice, reported in tenths (Egg Code Ct, Reference 2.4.7-8).
- b) The PSEG Site data was interpreted from maps produced for the Delaware Bay.
- c) Stage of development represents the ice age and associated thickness (Egg Code Sx, Reference 2.4.7-8).

Reference 2.4.7-4

**PSEG Site
ESP Application
Part 2, Site Safety Analysis Report**

**Table 2.4.7-3
Resulting Water Surface Elevations at the PSEG Site from the 1904 Ice Jam
at Trenton, NJ**

10 Percent Exceedance High Tide and Spring Base Flow Base Water Surface Elevation (ft. NAVD)	Trenton Ice Jam Breach (ft.)	Coincident Wave Runup (ft.)	Ice Jam Breach Maximum Water Surface Elevation (ft. NAVD)
5.2	0.1	2.8	8.1

**PSEG Site
ESP Application
Part 2, Site Safety Analysis Report**

2.4.8 COOLING WATER CANALS AND RESERVOIRS

This subsection addresses the design requirements for canals and reservoirs used to transport and store water for safety-related SSC.

2.4.8.1 Cooling Water Intake Design

The new plant location is in the northwest corner of the PSEG Site. The new plant design does not include any safety-related canals or reservoirs used to transport or impound plant cooling water. Makeup to the safety-related UHS system and the non-safety-related CWS for the new plant is provided by an intake structure located on the east bank of the Delaware River, north of the existing Hope Creek service water intake structure. As the reactor technology for the new plant has not been chosen, the specific design of the intake structure is not finalized. The intake structure will be set at an elevation low enough that it can provide an uninterrupted supply of water to the new plant, even under extreme low water conditions, as discussed in Subsection 2.4.11.

In order to maintain capacity and unobstructed flow into the intake structure, limited maintenance dredging may be required. Interior intake bay desilting is periodically performed. The maximum WSEL in the intake structure is controlled by the PMH, as discussed in Subsection 2.4.5. The intake structure and forebay area will be designed to provide protection from the maximum WSEL and associated hydrodynamic forces.

2.4.8.2 Conclusion

Appropriate erosion control technology, such as riprap and vertical earth retaining structures, would be implemented where applicable to protect the intake structure from wind-induced waves, runup and associated erosion caused by hydrodynamic forces. The forebay protects the intake structure from sedimentation, and the forebay area can be periodically dredged to remove accumulated sediment to maintain the required invert elevation for new plant water supply.

As there are no safety-related reservoirs or canals proposed with the new plant design, the requirements outlined in the NRC Standard Review Plan for the Review of Safety Analysis Reports for Nuclear Power Plants (NUREG-0800), Subsection 2.4.8, *Cooling Water Canals and Reservoirs*, pertaining to the hydraulic design bases for the protection of safety-related canals and reservoirs, are not applicable.

**PSEG Site
ESP Application
Part 2, Site Safety Analysis Report**

2.4.9 CHANNEL DIVERSIONS

The potential for stream channel diversions and their potential effects on the safety-related SSC at the new plant location are discussed in this subsection. Stream channel diversions could direct water away from the site (leading to loss of water supply for safety-related purposes) or towards the site (leading to flooding). A historic review along with potential causes and effects on the new plant SSC and water supplies is included in this subsection.

The new plant is located on the east bank of the Delaware River in the lower estuary. This section of the Delaware River is influenced by both tides and river flow from the Delaware River watershed. Depending on the type of reactor technology chosen, the new plant uses water from the Delaware River as a source of makeup water to the safety-related UHS.

Given the seismic, topographical, geologic, and thermal evidence in the region, there is very limited potential for upstream diversion or rerouting of the Delaware River (due to channel migration, river cutoffs, ice jams, or subsidence) and adverse impacts to safety-related SSCs.

2.4.9.1 Historical Channel Diversions

The Delaware River has been flowing in its current channel at least since the last ice age, approximately 10,000 years ago (Reference 2.4.9-2). There is no historical evidence of channel diversions of significance in the Delaware River Basin. There are no levees on the Delaware River, only on tributaries to the river. The collapse or breaching of a levee or dam on upstream tributaries would not cause a catastrophic flood at the new plant, as discussed in Subsection 2.4.4.

2.4.9.2 Regional Topographic Evidence

The PSEG Site is located in the Atlantic Coastal Plain. The Atlantic Coastal Plain consists of a wedge of unconsolidated sediment. Large amounts of water are stored in these deposits, which transmit water much more readily than the consolidated rocks underlying the piedmont and mountain provinces (Reference 2.4.9-3). The topography of this area is flat and low. Elevations rise very gently from the Delaware River, and throughout most of the Atlantic Coastal Plain. Although there is significant variation, natural elevations in the vicinity of the PSEG Site are less than 10 ft. NAVD for 1 – 4 mi. to the west and east of the site (Figure 2.4.9-1). The highest elevations in the vicinity of the PSEG Site are manmade embankments less than 20 ft. high which intermittently line the banks of the river (Reference 2.4.9-7). The river banks at the PSEG Site are lined with heavy riprap, sheet piling and/or wood piling to protect the banks from erosion. Other sections of river bank upstream of the site are similarly protected. Some areas further upriver are also protected by concrete structures to prevent erosion and lateral migration of the river.

The river channel is 2.5 mi. wide at the PSEG Site (Reference 2.4.9-6). Five mi. downstream of the PSEG Site, channel width increases to over 4 mi. as the Delaware River enters Delaware Bay (Figure 2.4.9-1 and Reference 2.4.9-7). Due to this width and the geologic and topographic conditions found in the Atlantic Coastal Plain, a blockage occurring downstream of the PSEG Site cannot completely block the flow, causing water to back up and create flooding. There are no bluffs or topographic features which could cause significant blockage downstream of the

**PSEG Site
ESP Application
Part 2, Site Safety Analysis Report**

PSEG Site. Therefore, channel diversions do not pose a significant threat to the function of safety-related SSC.

2.4.9.3 Ice Causes

Complete blockage of the river upstream and downstream of the site concurrently, due to ice effects, has not historically occurred. As the river is influenced by tides and freshwater at the new plant, tidal waters supply sufficient cooling water for the new plant if the Delaware River is blocked upstream. Therefore, potential river blockage due to ice effects does not pose a threat to the function of safety-related SSCs. This is discussed further in Subsection 2.4.7.

2.4.9.4 Flooding of Site Due to Channel Diversion

Site flooding as a result of channel diversion does not affect the PSEG Site. However, the DBF elevation for the PSEG Site is determined by considering a number of different flooding possibilities. The possibilities applicable and investigated for the site include the PMF on streams and rivers, potential dam failures, probable maximum surge and seiche flooding, PMT and ice effect flooding. Each of these flooding scenarios is investigated in conjunction with other flooding and meteorological events, such as wind-generated waves, as required in accordance with guidelines presented in RG 1.59 and ANSI/ANS-2.8-1992 (Reference 2.4.9-1). Detailed discussions on each of these flooding events and how they are determined are found in Subsection 2.4.2 through Subsection 2.4.7. Adequate drainage capacity will be provided to prevent flooding of safety-related SSCs.

The PSEG Site has drainage ditches near the site that could overflow and cause local flooding as a result of ditch channel diversions. Assuming the drainage ditches on-site are partially blocked due to ice formation, the blockage is bypassed by the flowing water as the water rises. Grading in the vicinity of the safety-related structures will be sloped away from the individual structures such that PMP ground and roof runoff flows away from each of these structures towards the collection ditches.

The potential for channel diversions caused by landslide, mudslide, or other temporary blockage of flow either directly upstream or downstream of the new plant and the intake structures is highly unlikely due to the shallow nature of the lower Delaware River and the flat topography near the PSEG Site. This, in combination with the tidal influence of the Delaware River at the PSEG Site, does not cause a loss in plant intake water availability.

2.4.9.5 Human-Induced Causes of Channel Diversion

The USACE actively maintains the Delaware River as a shipping channel (Reference 2.4.9-5). Channel maintenance includes dredging. This maintenance along with shoreline protection reduces river morphological activity to the existing Delaware River channel. The Delaware River is the main drainage mechanism for the watershed of over 11,000 sq. mi. Based on these considerations, human-induced causes of channel diversion do not pose a significant threat to the new plant.

**PSEG Site
ESP Application
Part 2, Site Safety Analysis Report**

2.4.9.6 Alternate Water Sources

The safety-related water supply to the new plant is the tidally-influenced portion of the Delaware River. Therefore sources of cooling water include both freshwater discharge and tidal waters. Freshwater upstream of the site is supplied primarily by stormwater runoff and, to a limited extent, by ice and snow melt during the spring. In the unlikely event that the river flow or the tidal flow is interrupted due to a channel diversion (and there is no historic evidence to indicate that this has occurred in the recorded past), the second, uninterrupted tidal flow source continues to supply water to the new plant. Average annual discharge of the Delaware River at Trenton, NJ is 11,780 cfs (Reference 2.4.9-8). As shown in Table 2.4.1-9, the new plant intake from the Delaware River is 175 cfs (75,792 gpm for circulating water system plus 2404 gpm service water system makeup water). This is 1.5 percent of the average annual freshwater discharge of the non-tidal Delaware River. During a drought emergency, the flow objective for the Delaware River is 3000 cfs at Trenton (Reference 2.4.9-8). This flow is supplemented by reservoir releases and inputs from the Schuylkill River, Christina River, and other tributaries before it reaches the PSEG Site. River flows are discussed further in Subsections 2.4.2 and 2.4.11. Tidal flow at the PSEG Site ranges from 400,000 cfs to 472,000 cfs (References 2.4.9-6 and 2.4.9-4). New plant intake flow is less than 1 percent of the tidal flow at the PSEG Site. If the channel of the Delaware River upstream of the site becomes diverted, the tidal water level is sufficient to supply the required water to the plant.

2.4.9.7 Consideration of Other Site-Related Evaluation Criteria

The potential for channel diversion from seismic or other severe weather events is not considered to result in a loss of cooling water supply. Other severe weather-related threats are discussed in Subsections 2.4.2 through 2.4.7. The shoreline near the PSEG Site is flat and low and neither a seismic nor severe weather event result in a major shoreline collapse. Any silt deposition due to events caused by seismic activity is discussed in Subsections 2.4.4 and 2.4.6. The forebay extends into the Delaware River, and is dredged to an adequate bottom elevation lower than the required low water elevation in the Delaware River, as discussed in Subsection 2.4.11. Accumulated silt and sedimentation can be removed via periodic maintenance dredging in order to maintain the required invert elevation in the forebay.

2.4.9.8 References

- 2.4.9-1 American National Standards Institute/American Nuclear Society, "Determining Design Basis Flooding at Power Reactor Sites," ANSI/ANS-2.8-1992, (historical), p. 1, 32, 1992.
- 2.4.9-2 Delaware Department of Transportation, Archaeology/Historic Preservation, Website, http://www.deldot.gov/archaeology/3_bridges/pdf/env_set.pdf, accessed August 5, 2009.
- 2.4.9-3 Delaware River Basin Commission, "Delaware River State of the Basin Report 2008," Website, <http://www.state.nj.us/drbc/SOTB/index.htm>, p. 73, accessed July 2, 2009.
- 2.4.9-4 U.S. Army Corp of Engineers, "Delaware River Main Channel Deepening Project Design Memorandum," Philadelphia District, Philadelphia, Pennsylvania, p. 55 – 60, 1996.

**PSEG Site
ESP Application
Part 2, Site Safety Analysis Report**

- 2.4.9-5 U.S. Army Corp of Engineers, "Delaware River Main Stem & Channel Deepening Project", Philadelphia District, Website, <http://www.nap.usace.army.mil/cenap-pl/drmcdp/overview.html>, accessed September 12, 2009.
- 2.4.9-6 U.S. Environmental Protection Agency, "Case Study Analysis for the Proposed Section 316(b) Phase II Existing Facilities Rule," EPA-821-R-02-002, p. 19, February 2002.
- 2.4.9-7 U.S. Geological Survey, "7.5 Minute Quadrangle Topographic Maps," Website, <http://datagateway.nrcs.usda.gov/>, accessed Delaware maps for Bennetts Pier, Bombay Hook Island, Cape Henlopen, Dover, Frederica, Lewes, Little Creek, Milford, Milton, Mispillion River, Smyrna, Wyoming, Ben Davis Point, Canton, Cape May, Cedarville, Dividing Creek, Fortescue, Heislerville, Port Norris, Rio Grande, Shiloh and Taylors Bridge, accessed April 21, 2009.
- 2.4.9-8 U.S. Geological Survey, "USGS Stream Gage 1463500 Delaware River at Trenton, NJ Daily Stream Flow Statistics," Website, http://waterdata.usgs.gov/nwis/annual/?referred_module=sw&site_no=01463500&por_01463500_5=147753,00060,5,1913,2009&year_type=W&format=html_table&date_format=YYYY-MM-DD&rdb_compression=file&submitted_form=parameter_selection_list, accessed September 22, 2009.
- 2.4.9-9 Delaware River Basin Commission, "Delaware River Basin Boundary" Website <http://www.state.nj.us/drbc/gis.htm>, accessed 2/20/2009.

**PSEG Site
ESP Application
Part 2, Site Safety Analysis Report**

2.4.10 FLOODING PROTECTION REQUIREMENTS

Maximum WSEL, including wave runup, is evaluated for different flood-producing events in Subsections 2.4.3 through 2.4.7. The results are summarized in Subsection 2.4.2 (specifically Table 2.4.2-4). The combined events evaluation for probable maximum surge and seiche flooding, presented in Subsection 2.4.5, represents the maximum flood level and, therefore, becomes the DBF at the new plant. That alternative includes the effects of the probable maximum hurricane surge associated with the PMH.

Floor elevations for safety-related SSC for the new plant, with the exception of the intake structure, will be established to maintain clearance above the DBF, as required by Tier 1 of the DCD for the selected technology. The area surrounding the safety-related SSC will be graded such that runoff from the PMP on the site drains away from new and existing structures to the Delaware River. To create the worst case scenario, the model assumes that all drainage structures (e.g. culverts, storm drains, and bridges) are blocked during the PMP event. Drainage systems for the new plant location will be designed so that the peak discharge from the local PMP does not produce WSEL that cause flooding of any safety-related SSC at the site.

The storm surge associated with the PMH is discussed in Subsection 2.4.5. This surge is calculated coincident with the 10 percent exceedance high tide. Wave runup is added to the storm surge to give the maximum WSEL at the site. The maximum WSEL combined with the potential sea level rise produces a water level of 32.1 ft. NAVD (see Subsection 2.4.5.6). All safety-related SSC (with the exception of the intake structure) for the new plant will be constructed at least one foot higher than the DBF. The new plant site grade is established at 36.9 ft. NAVD. This meets the requirements of a dry site as defined in NRC RG 1.102. Riprap protection will be provided on the slopes of the site to provide protection from wave runup.

The maximum WSEL in the intake forebay is controlled by the PMH, as discussed in Subsection 2.4.5. Appropriate erosion control technology will be implemented, where applicable, to protect the intake structure from wind-induced waves, runup and associated erosion. Flood protection for the intake structure will be designed as part of the detailed design of the new plant. The intake structure will be designed to be protected from the effects of flooding and to withstand the applicable hydrodynamic forces, including wave forces, in accordance with RG 1.27, 1.59, and 1.102.

Procedures to address flooding protection requirements will be developed based on the detailed site design.

**PSEG Site
ESP Application
Part 2, Site Safety Analysis Report**

2.4.11 LOW WATER CONSIDERATIONS

This subsection investigates natural events that reduce or limit the available safety-related cooling water supply to ensure that an adequate water supply exists to shut down the plant under conditions requiring safety-related cooling. Specifically, the potential for low water conditions to occur in the Delaware Estuary is investigated.

The new plant is located on the northwest corner of the PSEG Site, on the east bank of the Delaware River, in the southwest portion of Salem County, NJ. The site is located 52 RM upstream of the mouth of Delaware Bay. A cross-section of the Delaware River at RM 52 is shown on Figure 2.4.3-7. The intake structure located on the east bank of the Delaware River provides a nonsafety-related and, depending on the type of reactor technology selected, safety-related source of water for the new plant. The effect of low water conditions on the new plant requirements are further discussed in Subsection 2.4.11.5.

Under normal flow and weather conditions, water levels at the new plant location are primarily determined by tides. The Delaware River is subject to tidal influence from the mouth of the Delaware River to the head of tide at RM 134 in Trenton (Reference 2.4.11-13). Therefore, the influence of the tide must be addressed for all other potential natural events that result in low water conditions.

Water levels in the Delaware River at the new plant location are influenced by tides; flooding conditions within the Delaware River Basin, and storms, including hurricanes, that affect Delaware Bay. Historical low water conditions and the effect of tides are summarized in Subsection 2.4.11.1. The combined effects of low tides and drought conditions in the Delaware River Basin are addressed in Subsection 2.4.11.2. The effect of negative storm surge, seiches, tsunamis, and ice effects are addressed in Subsection 2.4.11.3.

2.4.11.1 Historical Low Water Conditions and the Effect of Tides

The tide of the Delaware Estuary is semidiurnal in character. There are two high waters and two low waters in a tidal day, with comparatively little diurnal inequality. The Reedy Point, DE station at RM 59 is the tidal gage station nearest the PSEG Site, as shown on Figure 2.4.11-1.

A 22-year record (1987 to 2008) of water levels at the Reedy Point gage shows an extreme low water elevation of -6.8 ft. NAVD, which occurred during November 1989. The extreme low water in the 22-year record is attributed to a negative surge associated with strong northwest winds that occurred on November 21, 1989. Winds at Dover, DE, near Delaware Bay, were consistently from the northwest, ranging from 21 to 37 mph and averaging 28 mph for approximately 18 hours on that day (Reference 2.4.11-6). The wind event was associated with passage of a cold front (Reference 2.4.11-20). A USGS paper identifies a low water event which occurred on December 31, 1962 due to north-northwesterly winds blowing downstream. The paper identified a low water reading at Reedy Point of -8.6 ft. msl (-9.5 ft. NAVD) (Reference 2.4.11-11).

Mean low water at Reedy Point is -2.8 ft. NAVD (Reference 2.4.11-23), and the 90 percent exceedance low tide is -5.15 ft. NAVD (Reference 2.4.11-21). The 90 percent exceedance low tide at the new plant is determined to be -5.1 ft. NAVD by interpolation between the 90 percent

**PSEG Site
ESP Application
Part 2, Site Safety Analysis Report**

exceedance low tides at Reedy Point and Lewes, DE at RM 0 (-4.6 ft. NAVD, Reference 2.4.11-22).

2.4.11.2 Low Water from Drought

Minimum flows in the Delaware River have been regulated since 1931, with additional regulations established in 1954 (Reference 2.4.11-3). Flow management of the Delaware River is accomplished through coordinated releases from reservoirs on its tributaries dictated by the Delaware River Basin Commission (DRBC) Flexible Flow Management Program (Reference 2.4.11-2). Within the Delaware River Basin, nine reservoirs are multipurpose, providing water for water supply, flow augmentation, and flood loss reduction. The Merrill Creek Reservoir, located on Merrill Creek in the central portion of the basin, is dedicated to flow augmentation. This reservoir has been in operation since 1988. PSEG is a co-owner of this reservoir, which ensures sufficient flows downstream during a drought so PSEG may continue to withdraw water from the Delaware River to maintain power generation operations. Under normal conditions, coordinated management of reservoir flows ensures the maintenance of minimum flows of 1750 cfs at Montague, NJ and 3000 cfs at Trenton, NJ (Reference 2.4.11-3).

The USGS evaluated discharge at Trenton (RM 134) from 1913 through 2001. The minimum daily flow in this 89-year record is 1240 cfs. This low flow, which is less than the DRBC objective of 3000 cfs, occurred after implementation of the current low flow augmentation policies. By statistical analysis, USGS estimated the 20-year recurrence interval daily low flow to be 1530 cfs, based on discharge data collected from 1956 through 2001, after the current low flow regulatory policies were established. Considering only the winter season, the 20-year daily low flow determined by USGS from the same period of record is 1840 cfs.

2.4.11.2.1 HEC-RAS Simulation of Low Water Conditions

The USACE HEC-RAS model is used to simulate low flow conditions in order to analyze the surface-water levels at the new plant in conjunction with drought effects (Reference 2.4.11-15). The HEC-RAS application to the Delaware River, estuary, and bay has been calibrated to reproduce normal tidal fluctuations, and validated by reproducing water levels at the new plant location under varying river flow rates.

The HEC-RAS model (Reference 2.4.11-15) is used to route the flows through the Delaware River. This model is developed using channel geometry and floodplain elevations for the Delaware River. Bathymetry and floodplain topography for portions of the Delaware River from the USGS gage station at Trenton to the NOAA tidal gage station, at Lewes (Reference 2.4.11-4), are determined from the TIN terrain model developed from the USGS National Elevation Dataset (Reference 2.4.11-18) DEM, the NOAA Estuarine Bathymetry DEM (Reference 2.4.11-9), USGS quad sheets (Reference 2.4.11-17), and the USACE Bathymetry Data (Reference 2.4.11-14). Figure 2.4.11-2 shows a typical cross-section of the Delaware River at RM 52 (the PSEG Site). The Manning's n coefficients in the HEC-RAS model are calibrated using astronomical tide data, and stage-discharge data for Trenton. The downstream boundary condition in the HEC-RAS model is set to represent the 90 percent exceedance low tide. To generate a tide cycle at RM 0 that is representative of the 90 percent exceedance low tide, a stage hydrograph is generated for RM 0 that is equal to the 90 percent exceedance value at RM 0.

**PSEG Site
ESP Application
Part 2, Site Safety Analysis Report**

Two low flow simulations are performed for the low water analysis at the new plant. The first simulation is representative of the 20-year daily low flow in Trenton, as determined by USGS, and is in conjunction with the 90 percent exceedance low tide. For this simulation, an inflow at Trenton of 1530 cfs is used in the model. This flow is routed through the Delaware River and the resulting WSEL at the new plant site is evaluated. The second simulation performed is representative of a no flow condition at Trenton in conjunction with the 90 percent exceedance low tide. An inflow at Trenton of 1 cfs is used in the model, representing a no flow condition. This flow is routed through the Delaware River and the resulting WSEL at the new plant site is evaluated.

The minimum water level at the PSEG Site resulting from the no flow model simulation, in conjunction with the 90 percent exceedance low tide, is -5.1 ft. NAVD. The minimum water level at the PSEG Site resulting from the 20-year drought low flow model simulation, in conjunction with the 90 percent exceedance low tide, is -5.0 ft. NAVD. This result demonstrates that the WSEL at the new plant are dependent on tidal influences rather than upstream flow conditions. Thus, the Delaware River at the new plant provides a sufficient water supply source, even in low flow conditions. Likewise, due to the sensitivity of the model it can be deduced that all low flows below the 20-year drought low flow produce the same WSEL results at the new plant site. Therefore, the 20-year drought low flow simulation can be used to simulate a minimum WSEL at the new plant site.

2.4.11.3 Low Water from Other Phenomena

The potential for low WSEL caused by various hydrometeorological events and potential blockage of intakes by sediment, debris, littoral drift, and ice is evaluated in this subsection. Specific hydrometeorological events evaluated are negative surge caused by cyclonic storms, seiche, and tsunami events.

Storm surge from hurricanes is found to have the potential to cause the most severe flooding at the site (Subsections 2.4.2 and 2.4.5). Hurricanes that bypassed the bay, traveling towards the northeast and staying offshore, have resulted in negative surge (water levels lower than the predicted astronomical tide) at the NOAA tide gage stations at both Reedy Point (the NOAA tide gage closest to the plant location, at RM 59), and Lewes (at the mouth of Delaware Bay, at RM 0). Setdown, or negative surge resulting from hurricanes that pass east of Delaware Bay, traveling north-northeast, represent the hydrometeorological events with the greatest potential to lower water levels in the vicinity of the safety-related intake structure.

A meteorological event causing strong sustained winds from the northwest over the Delaware Bay could cause negative surge at the new plant location. As discussed in Subsection 2.4.5.1.1, however, winds from a hypothetical PMH are much stronger than winds from other meteorological phenomena that have been observed in the region of the new plant. During the 31-year period from 1978 through 2008 winds of sufficient duration to cause negative surge did not exceed 50 knots (kt) (58 mph) over Delaware Bay. Conversely, as shown in Subsection 2.4.11.3.1, PMH winds from the northwest of sufficient duration to cause negative surge could reach 93 mph, and exceed 50 kt for over 4 hours. Therefore, the negative surge from PMH winds would be more severe than the surge from any other expected wind storm.

**PSEG Site
ESP Application
Part 2, Site Safety Analysis Report**

2.4.11.3.1 Storm Surge Effects

Hurricanes that passed within 100 nautical miles (NM) of the mouth of Delaware Bay during the 30-year period from 1979 through 2008 include Charley (1986), Gloria (1985), and Floyd (1999) (Reference 2.4.11-7). Water levels at Lewes (near the mouth of the bay) and Reedy Point (near the new plant at RM 59), and winds at Dover, DE, associated with these storm events were obtained and reviewed (References 2.4.11-10 and 2.4.11-6). The Dover, DE, weather station is near the center of the longitudinal axis of Delaware Bay. Figure 2.4.11-3 shows the tracks of these storms, and Table 2.4.11-1 summarizes the effects of these storms on Delaware Bay. Each passed Delaware Bay to the east, traveling northeast. At its closest approach to Delaware Bay (68 mi.), Charley was a tropical storm with maximum sustained winds of 60 mph. Charley created an insignificant negative surge of -0.12 ft. at Lewes. Floyd was also a tropical storm at its closest approach, but passed so near the mouth of the bay (17 mi.) that it caused a substantial negative surge of -1.59 ft. at Lewes and -2.68 ft. at Reedy Point. This indicates that the negative surge is more severe at Reedy Point than at the mouth of the bay.

Positive storm surges are also more extreme at Reedy Point than at Lewes (Subsection 2.4.5). The observed relationship of greater negative surge at Reedy Point than at Lewes is expected from storm surge theory (Reference 2.4.11-1), which finds that water levels are lowest at the upwind end of semi-enclosed bodies of water. Winds associated with storms causing negative surge at the new plant location are from the northwest, so Reedy Point is on the upwind end and is expected to experience greater negative surge than Lewes. Of these three storms, Gloria produced the largest negative surge at Lewes (-2.45 ft.). Gloria was a Category 1 hurricane with sustained winds of 85 mph at its closest approach to Delaware Bay (43 mi.). These data show that both the strength of the storm and its proximity to Delaware Bay affect the magnitude of the negative surge that occurs when tropical cyclones pass to the east of the bay.

Figures 2.4.11-4 and 2.4.11-5 show wind stress over the center of Delaware Bay, water levels in Delaware Bay, and properties of Gloria and Floyd as they made their closest approaches to Delaware Bay. The wind stress over the center of Delaware Bay is determined using observed winds at Dover, DE (the nearest weather station to the center of Delaware Bay), with observations available for both storms. Water levels at Reedy Point are not available for Hurricane Gloria. Note that the negative (northwesterly) wind stress is strongest for a short time as the storms pass near the mouth of the bay, while the maximum negative surge occurs 2 to 10 hours after the storm passes. Negative surges associated with these bypassing tropical cyclones were of short duration, lasting less than 6 hrs.

Conclusions drawn from this review of data for historical tropical cyclones passing east of Delaware Bay are:

- Negative surge in Delaware Bay has been caused by wind stress from tropical cyclones passing near and to the east of Delaware Bay.
- The negative surge is larger if the storm passes close to the mouth of the bay while remaining offshore.
- The negative surge increases with the maximum sustained winds at the point of closest approach.
- The negative surge at Reedy Point is greater than the negative surge at Lewes.
- Maximum negative surge occurs 2 to 10 hrs. after the closest approach, and negative surge events last less than 6 hrs.

Rev. 4

**PSEG Site
ESP Application
Part 2, Site Safety Analysis Report**

Hurricanes have a predictable relationship between wind speed, direction, and distance from the storm center (Reference 2.4.11-8). This relationship is determined from the pressure drop, forward speed, and location relative to the storm center and the storm's track direction. As a result, the maximum wind stress along the longitudinal axis of Delaware Bay, associated with storms having a similar track (north or northeast and passing east of the bay), are proportional to the square of the maximum sustained wind speed of the storm and inversely proportional to its distance from the bay. As a result, the negative surge is predictable by the following relationship:

$$\text{Negative surge (ft.)} = A \times (\text{maximum sustained winds})^2 \quad (\text{Equation 2.4.11-1})$$

Where

A is a constant dependent on distance of the storm center from the bay at the storm's closest approach, and maximum sustained winds are given in kt.
(References 2.4.11-5 and 2.4.11-1)

The negative surge observed during these three hurricanes, in particular Floyd and Gloria, supports the determination of the value of A as a function of the closest approach of the storm center to the mouth of Delaware Bay. The functional relationship between A and the closest approach is illustrated in Figure 2.4.11-7. To apply this relationship, the characteristics of the PMH with the potential to cause the most severe negative surge need to be determined.

Reference 2.4.11-8 is used to define the range of meteorological parameters associated with the PMH at the mouth of Delaware Bay. The mouth of Delaware Bay is defined as a point bisecting the line from Cape May to Cape Henlopen at 38°51'30"N, 75°01'30"W. At this location, NOAA (Reference 2.4.11-8) indicates the following meteorological parameters for the PMH:

- Central pressure, p_0 = 26.65 in mercury (Hg)
- Pressure drop, Δp = 3.5 in Hg
- Radius of maximum winds, R = from 11 to 28 NM
- Forward speed, T = from 26 to 42 kt
- Track Direction (storm coming from) = from 70 to 185 degrees
- Coefficient related to density of air, K = 68 (when parameters are in units of kt and in Hg)

For a hurricane to produce maximum negative surge in Delaware Bay it must parallel the coast and stay offshore to the east of the mouth of the bay. Storms coming from the southeast (specifically with a track direction of 135 degrees) make landfall and weaken. This weakening reduces the negative surge. A storm coming from 185 degrees (moving toward the north) stays over the ocean longer, maintaining stronger northwesterly winds over the bay. Thus, the optimal track direction is from 185 degrees (5 degrees west of south).

A hurricane with a large forward speed produces higher wind speeds to the right of the storm center than a hurricane with slower forward speed. However, a fast forward speed reduces the wind speeds to the left (west) of the storm center (Reference 2.4.11-8). Maximum wind speeds over Delaware Bay, associated with a storm that passes to the east of the bay, result from a slow moving PMH. In addition, the slower progress of the storm results in a longer duration of high wind speeds over Delaware Bay. Therefore, the PMH producing the maximum negative surge has a forward speed, T , of 26 kt.

Rev. 4

**PSEG Site
ESP Application
Part 2, Site Safety Analysis Report**

A larger storm, as indicated by the radius of maximum winds, produces higher wind speeds at the same distance from the storm center, which is necessary to produce maximum northwesterly winds over Delaware Bay. Therefore, the optimal radius of maximum winds, R , to produce maximum negative surge in Delaware Bay is the largest indicated R for the PMH of 28 NM.

The remaining variable that can affect the negative surge is the distance of the storm track from the mouth of Delaware Bay. As shown in Figure 2.4.11-7, negative surge is greater for storms that closely approach, but bypass the bay. Given the track direction of the PMH, however, the hypothetical PMH makes landfall on the NJ coastline and weakens after landfall. Therefore, there is an optimal distance of closest approach to the bay given the PMH track direction and the orientation of the NJ shoreline. A storm passing close to the mouth makes landfall and weakens prior to generating a significant negative surge, while a storm passing farther away has less wind over the bay due to distance from the storm center. The optimal track direction is identified by determining the winds over the center of the bay for a series of storms tracking north, but differing in the distance of closest approach. Winds are determined near the center of the bay using procedures defined by NOAA (Reference 2.4.11-8). These calculations show that the maximum northwesterly winds over Delaware Bay occur for a PMH with $R = 28$ NM, $T = 26$ kt, track direction from 185 degrees, and distance of closest approach to the mouth of Delaware Bay of 20 NM (23 mi).

Thus, the PMH that produces the maximum negative surge has the following characteristics:

- Central pressure, $p_0 = 26.65$ in Hg.
- Pressure drop, $\Delta p = 3.5$ in Hg.
- Radius of maximum winds, $R = 28$ NM.
- Forward speed, $T = 26$ kt.
- Track direction (storm coming from) = 185 degrees.
- Distance at closest approach = 20 NM (23 mi.) east of the mouth of Delaware Bay.
- Coefficient related to density of air, $K = 68$.

The maximum sustained winds for this PMH are 128 kt, and its maximum northwesterly winds over the center of Delaware Bay are 81 kt (Reference 2.4.11-8). Its track is shown on Figure 2.4.11-6.

Negative surges associated with hurricanes Floyd, Gloria, and Charley observed at Lewes are used to determine the relationship between negative surge, maximum sustained winds of each hurricane, and the distance of each storm from Delaware Bay at its point of closest approach. The calculated value of A (from Equation 2.4.11-1) for each of the three storms at Lewes, and the value at Reedy Point for Floyd are plotted on Figure 2.4.11-7. The factor A exhibits the expected dependence on distance at its closest approach at Lewes. As expected from storm surge theory, it is greater at Reedy Point than at Lewes for Floyd. It is assumed that the surge at Reedy Point for Gloria and Charley was proportional to the surge at Lewes by the same ratio as observed during Floyd. Finally, it is assumed that the surge at the new plant location can be linearly interpolated, by RM, from the results at Reedy Point and Lewes. These relationships are illustrated in Figure 2.4.11-7, which shows that A at the new plant location is 0.000664 for the PMH that produces maximum negative surge. Therefore, the maximum negative surge at the new plant location is determined to be:

**PSEG Site
ESP Application
Part 2, Site Safety Analysis Report**

$$\begin{aligned}\text{Negative surge (ft.)} &= A \times (\text{maximum sustained winds})^2 \\ \text{Negative surge (ft.)} &= 0.000664 \times (128)^2 \\ \text{Negative surge (ft.)} &= 10.9 \text{ ft.}\end{aligned}$$

It is possible that the maximum negative surge could coincide with the 20-year low flow in the Delaware River at Trenton and the 90 percent exceedance low tide. Together, the 20-year low flow and 90 percent exceedance low tide produces a low flow level of -5.0 ft. NAVD, as discussed in Subsection 2.4.11.2.1. Combining this with the negative surge of 10.9 ft. results in a low water level of -15.9 ft. NAVD, as shown in Table 2.4.11-2. Figure 2.4.2-7 presents this low water level relative to other significant water levels at the new plant.

2.4.11.3.2 Tsunami Effect

Various tsunami sources in the Atlantic Ocean are analyzed for the PSEG Site, as discussed in Subsection 2.4.6, in order to determine the resulting PMT height at the new plant. Low water levels associated with these tsunami events occurring simultaneously with the 90 percent exceedance low tide are also evaluated in Subsection 2.4.6.

The following tsunami sources are considered in the tsunami evaluation in Subsection 2.4.6:

- Currituck submarine landslide
- Currituck submarine landslide without bottom friction
- La Palma, Canary Island submarine landslide
- Hispaniola Trench earthquake

The maximum drawdown at the site resulting from the above analysis is due to the Currituck submarine landslide without bottom friction. The resulting low water elevation from this simulation is -6.2 ft. NAVD. Details of the tsunami effects are presented in Subsection 2.4.6.

2.4.11.3.3 Winter Low Water Elevations with Ice Effects

The effects from ice at the new plant occurring in conjunction with 90 percent exceedance low tide and winter low flow conditions are evaluated to produce a minimum winter low WSEL at the PSEG Site. Ice thickness is then determined using the modified Stefan equation (Reference 2.4.11-12). This thickness is then subtracted from the winter low WSEL to determine the water elevation in the Delaware River at the new plant once surface ice has formed.

The historic winter low flow at Trenton for the period of record from 1913 to 2001 is 1840 cfs. This historic winter low flow of 1840 cfs is input into the HEC-RAS model as an inflow at Trenton, in conjunction with the 90 percent exceedance low tide, to simulate the surface-water elevations at the PSEG Site (Reference 2.4.11-19).

The modified Stefan equation is used to determine the maximum historic ice thickness (Reference 2.4.11-12). The modified Stefan equation uses a coefficient representative of the subject body of water, along with accumulated freezing degree days to predict ice thickness on the body of water. Based on this evaluation, the maximum historic ice thickness determined at the PSEG Site is 17.8 in. This represents a conservative approach, as the water in the

**PSEG Site
ESP Application
Part 2, Site Safety Analysis Report**

Delaware River at the new plant location is brackish, and, therefore, does not have a freezing point of 32°F, as is assumed in the modified Stefan equation.

The surface-water elevation from the winter low flow model is -5.0 ft. NAVD. Therefore, assuming ice thickness is consistent with the calculated ice thickness based on historic data, and assuming it occurs in conjunction with the winter low flow condition, the bottom elevation of the ice is -6.5 ft. NAVD. Based on this analysis, the intake structure will be designed such that surface ice effects occurring during low flow conditions would not prohibit or block the operations of the intake structures.

2.4.11.4 Future Controls

The Delaware River is the longest undammed river east of the Mississippi River (Reference 2.4.11-3). Tributaries of the Delaware River contain surface-water impoundments used to manage water supply, provide flood protection, and facilitate recreation. No impoundments are located on the main stem of the Delaware River.

The water elevations at the new plant are primarily dependent on tidal fluctuations as opposed to flow conditions within the Delaware River. Therefore, there are no known proposed future controls on the Delaware River that could affect the availability of water or result in extreme low water elevations at the new plant location.

2.4.11.5 Plant Requirements

Design of the new plant has not been finalized and a specific reactor technology has not been chosen. Plant water requirements are defined using the information in the PPE from Section 1.3 of this Site Safety Analysis Report. The PPE outlines the water consumption requirements for the bounding plant and is based on representative plant designs that result in the highest water consumption values. Raw water is required to support the needs of a new facility during construction and operation, including the requirements of the CWS, cooling water systems for plant auxiliary components (e.g., the SWS), and makeup for the UHS cooling system.

Average and maximum water consumption and discharge by the various cooling and water systems is provided in Table 2.4.1-9. Tidal flow at the PSEG Site ranges from 400,000 cfs to 472,000 cfs (References 2.4.11-13 and 2.4.11-16). Therefore, the new plant site is located in an area where the tidal flow is much greater than the flow required by the intake structure for the selected reactor technology, thus making the WSEL the critical factor in plant design, as opposed to the available flow in the Delaware River.

During extreme low water conditions, the Delaware River at the new plant location reaches a minimum elevation of -15.9 ft. NAVD, as discussed in Subsection 2.4.11.3.1. The mean lower low water elevation at the Reedy Point NOAA tidal gage station (gage 8551910) is -3.0 ft. NAVD (Reference 2.4.11-10). The intake structure provides a non-safety-related and, depending on the type of reactor technology selected, potentially a safety-related source of water for the new plant. Therefore, the safety-related intake structure for the selected reactor technology will be designed for operation considering the low water conditions identified in this subsection.

**PSEG Site
ESP Application
Part 2, Site Safety Analysis Report**

2.4.11.6 Heat Sink Dependability Requirements

The intake structure located on the east bank of the Delaware River provides a nonsafety-related and, depending on type of reactor technology selected, potentially a safety-related source of water for the new plant. Both the CWS and the UHS makeup bays are housed in this intake structure. The extreme low water conditions produced at the new plant are a direct result of the negative surge from the PMH in conjunction with the 20-year low flow and the 90 percent exceedance low tide. The PMH that produces the extreme low water elevations at the new plant is only expected to affect the new plant location for a short duration of time, consistent with the effects observed during historical tropical cyclones (Subsection 2.4.11.3.1, Figures 2.4.11-4 and 2.4.11-5). Therefore, the low water levels produced at the new plant as a result of this storm last for duration of less than 6 hrs. Based on this analysis, the UHS portion of the intake structure will be designed to withstand extreme meteorological events, such as the PMT, the PMH, extreme low water conditions, winter ice effects, and flooding from streams and rivers. The invert of the UHS makeup pumps will be set at an elevation so as to maintain plant operations during extreme low water conditions, and to maintain sufficient net positive suction head with margin. The need to construct a deep intake invert for low water considerations is dependent upon the specific reactor technology chosen.

2.4.11.7 Conclusions

Based on the low water conditions simulations and analysis, the new plant will be operational during low flow and low water conditions. The most extreme low water event is associated with a bypassing hurricane. Negative surge from the hurricane reduces water elevations in the vicinity of the PSEG Site by 10.9 ft. If this hurricane is coincident with a 20-year low flow in the Delaware River at Trenton and 90 percent exceedance low tide, the water elevation could be as low as -15.9 ft. NAVD, however this extreme low water level would not persist. The negative surge, or deviation from the astronomical tide, would not persist for more than six (6) hours, and the low tide level is also of short duration. Even during the six hour period of significant negative surge, the tidal level would increase by more than 3 ft. from the extreme low tide, increasing water levels. Figure 2.4.2-7 shows this low water level relative to other significant water levels at the new plant location (as discussed in Section 2.4). Water levels associated with other low flow conditions evaluated, which could be more persistent, such as low flow in the Delaware River, would not produce water levels lower than -6.5 ft. NAVD (Table 2.4.11-2). The safety-related intake structure for the selected reactor technology will be designed to operate during the low water conditions presented in this subsection.

2.4.11.8 References

- 2.4.11-1 Bretschneider, C.L., "Engineering Aspects of Hurricane Surge," Estuary and Coastline Dynamics, A.T. Ippen, ed., McGraw-Hill: New York. p. 231 – 256, 1966.
- 2.4.11-2 Delaware River Basin Commission, 2008, "Flexible Flow Management Program," Website, <http://www.state.nj.us/drbc/FFMP/index.htm>, accessed August 14, 2009.

**PSEG Site
ESP Application
Part 2, Site Safety Analysis Report**

- 2.4.11-3 Delaware River Basin Commission, "State of the Delaware River Basin Report 2008," Website, <http://www.nj.gov/drbc/SOTB/hydrology.pdf>, p. 8 – 27, 73, accessed February 19, 2009.
- 2.4.11-4 Delaware River Basin Commission, 2007b, "Stream River Mileage July 2007," Website, <http://www.state.nj.us/drbc/StreamMileageJuly2007.pdf>, p. 11, accessed February 16, 2009.
- 2.4.11-5 Einarsson, E. and A. B. Lowe, "Seiches and Set-Up on Lake Winnipeg," American Society of Limnology and Oceanography, Limnology and Oceanography Vol. 13 No. 2, p. 257 – 271, April 1968.
- 2.4.11-6 National Climatic Data Center, "TD3505 Format Digitized Hourly Surface Weather Observations for Wilmington Delaware (1942-2009), Dover Delaware (1942-2009), and Millville New Jersey (NJ) (1972-2009)," purchased from NCDC, Asheville North Carolina, downloaded from NCDC file transfer protocol website, <ftp://ftp.ncdc.noaa.gov/pub/data/>, accessed February 19, 2009
- 2.4.11-7 National Oceanic and Atmospheric Administration, Coastal Services Center, Historical Storm Tracks, Website, <http://csc-s-maps-q.csc.noaa.gov/hurricanes/download.jsp>, accessed August 12, 2009.
- 2.4.11-8 National Oceanic and Atmospheric Administration, "Meteorological Criteria for Standard Project Hurricane and Probable Maximum Hurricane Windfields, Gulf and East Coasts of the United States," NOAA Technical Report NWS 23, 1979.
- 2.4.11-9 National Oceanic and Atmospheric Administration, "NOS Estuarine Bathymetry: Delaware Bay DE/NJ (M090)," Website, <http://egisws01.nos.noaa.gov/servlet/BuildPage?template=bathy.txt&parm1=M090&B1=Submit>, accessed February 2, 2009.
- 2.4.11-10 National Oceanic and Atmospheric Administration, Tides and Currents, Website, http://tidesandcurrents.noaa.gov/station_retrieve.shtml?type=Historic%20Tide%20Data&state=Delaware&id1=855, accessed July 10, 2009.
- 2.4.11-11 U. S. Department of the Interior, Report # 1586-E, "Record Low Tide of December 31, 1962 on the Delaware River" 1966, prepared by A.C. Lendo.
- 2.4.11-12 U.S. Army Corp of Engineers, Cold Regions Research and Engineering Laboratory, Technical Note 04-3, "Method to Estimate River Ice Thickness Based on Meteorological Data," June 2004.
- 2.4.11-13 U.S. Army Corp of Engineers, "Delaware River Main Channel Deepening Project Design Memorandum," Philadelphia District, Philadelphia, Pennsylvania, p. 1, 55 – 59, 1996.
- 2.4.11-14 U.S. Army Corp of Engineers, "Delaware River Philadelphia to the Sea Examination," Bathymetric Survey Data, Philadelphia, Pennsylvania, 2007 – 2009.

**PSEG Site
ESP Application
Part 2, Site Safety Analysis Report**

- 2.4.11-15 U.S. Army Corps of Engineers, "HEC-RAS 4.0 Software," website, <http://www.hec.usace.army.mil/software/hec-ras/hecras-download.html>, accessed February 23, 2009.
- 2.4.11-16 U.S. Environmental Protection Agency, "Case Study Analysis for the Proposed Section 316(b) Phase II Existing Facilities Rule," [EPA-821-R-02-002](#), p. 19, February 2002.
- 2.4.11-17 U.S. Geological Survey, "7.5 Minute Quadrangle Topographic Maps," website <http://datagateway.nrcs.usda.gov/>, accessed April 21, 2009.
- 2.4.11-18 U.S. Geological Survey, "National Elevation Dataset," Website, <http://seamless.usgs.gov/index.php>, accessed February 2, 2009.
- 2.4.11-19 U.S. Geological Survey, "Streamflow Characteristics and Trends in NJ, Water Years 1897-2003," Scientific Investigations Report 2005-5150, 2005.
- 2.4.11-20 Yurkonic, K., "Electrical Storm Charges across Valley, Poconos," The Morning Call, Inc., Allentown, Pennsylvania, November 21, 1989.
- 2.4.11-21 National Oceanic and Atmospheric Administration, 1996 – 2008, "Reedy Point Tidal Data," Website, http://tidesandcurrents.noaa.gov/station_info.shtml?stn=8551910%20Reedy%20Point,%20DE, accessed February 2, 2009.
- 2.4.11-22 National Oceanic and Atmospheric Administration, "Lewes, DE Tidal Data," Website, http://tidesandcurrents.noaa.gov/station_info.shtml?stn=8557380%20Lewes,%20DE, accessed August 3, 2009.
- 2.4.11-23 National Oceanic and Atmospheric Administration, "Reedy Point, DE - Datums," Website, http://tidesandcurrents.noaa.gov/data_menu.shtml?stn=8551910%20Reedy%20Point,%20DE&type=Datums, accessed September 4, 2009.

**PSEG Site
ESP Application
Part 2, Site Safety Analysis Report**

**Table 2.4.11-1
Negative Surge Associated with Bypassing Hurricanes**

Storm (Year)	Closest Approach to Delaware Bay (mi.)	Maximum Sustained Winds at Closest Approach (kt)	Maximum Negative Surge at Lewes, DE (ft.)	Maximum Negative Surge at Reedy Pt., DE (ft.)
Charley (1986)	68	60	-0.12	n.a. ^(a)
Floyd (1999)	17	55	-1.59	-2.68
Gloria (1985)	43	85	-2.45	n.a. ^(a)

a) n.a. = not available; hourly water levels at Reedy Point, DE, are not available prior to 1996

Reference 2.4.11-8

**PSEG Site
ESP Application
Part 2, Site Safety Analysis Report**

**Table 2.4.11-2
Resulting Water Surface Elevations at the New Plant**

Simulation	Minimum Water Surface Elevation (ft. NAVD)
20-Year Low Flow Conditions with 90 Percent Exceedance Low Tide	-5.0
Tsunami Effects with 90 Percent Exceedance Low Tide	-6.2
Ice Effects with 90 Percent Exceedance Low Tide and Winter Low Flow Conditions	-6.5
Negative Surge from PMH with 90 Percent Exceedance Low Tide and 20 Year Low Flow Conditions ^(a)	-15.9

a) This includes a surge associated with the PMH of -10.9 ft.

References 2.4.11-12 and 2.4.11-15

**PSEG Site
ESP Application
Part 2, Site Safety Analysis Report**

2.4.12 GROUNDWATER

This subsection describes the hydrogeological characteristics of the PSEG Site and vicinity and assesses the potential effects of groundwater on plant foundations and the reliability of safety-related water supply and dewatering systems at the new plant location.

The new plant is located along the east bank of the Delaware River at river mile (RM) 52. The new plant location occupies the southern portion of the 1500-acre (ac.) Artificial Island, located in southwestern New Jersey (NJ) (Figure 2.4.1-1), in Lower Alloways Creek Township, Salem County. Artificial Island is a man-made land form created through the deposition of dredge spoils behind a naturally occurring sandbar and bulkhead. The developed portions of the site occupy 373 ac. of the parcel owned by PSEG. The remaining portion of the property is comprised of a variety of wetland types, desilting basins, and stormwater management facilities.

In constructing the new plant, the power block area will be excavated to approximately -67 ft. NAVD to remove the soils overlying the Vincentown Formation. The excavation will then be backfilled as described in Subsection 2.5.4.5. Foundations for the new plant will be constructed on the new backfill material and the fill material will be placed around the structures to a final grade of 36.9 ft. NAVD.

2.4.12.1 Hydrogeology

The PSEG Site is located within the NJ Coastal Plain aquifer system 18 miles (mi.) south of the fall line. The fall line is a low, east-facing feature, with the exposed scarp generally trending parallel to the Atlantic coastline and extending from NJ to the Carolinas. The fall line separates the hard Paleozoic metamorphic rocks of the Appalachian Piedmont to the west from the softer Mesozoic and tertiary sedimentary rocks of the Coastal Plain.

The hydrogeologic units within the NJ Coastal Plain can be summarized as southeast dipping permeable fine-grained to coarse-grained materials separated by less permeable fine-grained materials, resulting in a multiple aquifer system. The shallow aquifers in the vicinity of the site are saline and tidally-influenced. Regional and local hydrogeology are described in this subsection.

New Jersey designated two Critical Water-Supply Management Areas in the NJ Coastal Plain in response to long-term declines in groundwater levels where groundwater is a primary water supply. The PSEG Site is southwest of the management areas and is not subject to groundwater withdrawal restrictions except as defined in applicable permits. The U.S. Environmental Protection Agency (EPA) has determined that the NJ Coastal Plain Aquifer System is a sole or principal source of drinking water (References 2.4.12-28 and 2.4.12-31).

2.4.12.1.1 Regional Hydrogeology

The regional hydrogeology of southwestern NJ includes overburden sequences that thicken as the underlying bedrock surface dips from the fall line toward the southeast and the Atlantic Ocean. The overlying unconsolidated units reflect this topography and show a corresponding southeasterly dip of approximately 30 feet per mile (ft/mi). Aquifers are generally thicker near the ocean and thin progressively towards the northwest. In some instances, aquifers may thin

**PSEG Site
ESP Application
Part 2, Site Safety Analysis Report**

out entirely. Generally, the ages of the underlying units include Cretaceous, Tertiary, and Quaternary, as shown in the hydrostratigraphic summary on Figure 2.4.12-1. Note that the formations shown on Figure 2.4.12-1 only include the major or more geographically continuous formations. The complete list of aquifers/aquitard units is described below.

Groundwater in the shallow aquifers is generally encountered within 20 ft. of the ground surface and flow is generally toward the Delaware River. The deeper aquifers (greater than 700 ft. below ground surface [bgs]) generally flow southeast, toward the Atlantic Ocean.

Regionally, the aquifer/aquitard sequence generally consists of the following units (Reference 2.4.12-19):

- Alluvium
- Kirkwood-Cohansey Formations
- Vincentown Formation
- Navesink-Hornerstown Formation
- Mount Laurel-Wenonah Formations
- Marshalltown Formation
- Englishtown Formation
- Woodbury Formation
- Merchantville Formation
- Potomac-Raritan-Magothy (PRM) Formations

The Delaware River is the primary surface-water body that interacts with shallow site groundwater. The river is tidal adjacent to the PSEG Site with a bottom elevation of approximately -40 ft. NAVD near mid-channel. Three other smaller surface waters, which may locally interact with groundwater, include Alloway Creek, Hope Creek, and the Salem River (see Figure 2.4.1-1). These flow into the Delaware River and are located 2 mi. northeast, 2.5 mi. east, and 7 mi. north of the site, respectively. Several surface-water bodies occupy parts of the undeveloped portion of the property. Subsection 2.3.1.1 describes these water bodies.

At the PSEG Site, groundwater is encountered within the shallow hydraulic fill and Alluvium. Regionally, where man-made deposits are not present, shallow groundwater is first encountered in alluvial deposits or in the Kirkwood-Cohansey units east of the site.

Near-surface aquifers are recharged at areas where they outcrop the surface near the PSEG Site. Recharge of these aquifers is provided from adjacent aquifers through leaky aquitards, and/or through surface-water interactions with groundwater. In some areas, these near-surface aquifers may receive induced recharge from the Delaware River. The deeper aquifers are recharged through leaky aquitards and in areas where they outcrop further northwest of the site. Figure 2.4.12-2 shows the extent of these recharge areas in New Jersey. Table 2.4.12-1 summarizes the aquifer and aquitard characteristics of the regional aquifer system.

Groundwater wells (NJ) and wellhead protection areas (DE) within a 25-mi. radius of the site are shown on Figure 2.4.12-3. These are the two states with the most potential impact from site operations, and therefore wells from Maryland and Pennsylvania are not listed. Table 2.4.12-2 summarizes the public supply wells from NJ and DE in the area. Table 2.4.12-3 summarizes the

**PSEG Site
ESP Application
Part 2, Site Safety Analysis Report**

significant groundwater users, or those sites that use more than 100,000 gpd, in the same region.

The PRM aquifer system is a significant regional potable groundwater resource. The nearest off-site supply wells of any significance that withdraw from the PRM system are located 8.5 mi. across the Delaware River in Delaware (DE), and 15 mi. to the northeast in Salem County, NJ. There are no off-site public water supply wells or private wells within 1 mi. of the PSEG Site. The nearest off-site potable water supply well is located more than 3.5 mi. west of the PSEG Site, across the Delaware River, in DE (Reference 2.4.12-29).

2.4.12.1.2 Local Hydrogeology

The shallow soils of the PSEG Site consist of fill materials or spoils (hydraulic fill) historically dredged from the adjacent Delaware River. Beneath the hydraulic fill are alluvial deposits (riverbed sands, gravels, and clays). These alluvial deposits represent the original ground surface (which was submerged as the river bed in this area at the time the dredge spoils were initially placed) (Reference 2.4.12-29). The hydraulic fill and the alluvial sands and gravels also constitute the shallow groundwater flow system that overlies either the alluvial clay or the top of the Upper Kirkwood Formation (a clay-rich, semi-confining unit at approximately -39 ft. NAVD). The shallow aquifer is recharged directly by infiltration of precipitation where not impeded by buildings, pavement, or other stormwater diversion structures from the existing plants. The groundwater surface is typically encountered at depths ranging from 5 to 10 ft. bgs. However, the hydraulic fill acts as an aquitard. The shallow artificial ponds in the PSEG desilt basin, and U.S. Army Corps of Engineers (USACE) confined disposal facility (CDF) are likely perched, creating moist to saturated soils extending from ground surface through the hydraulic fill.

Sixteen observation well pairs and 16 geotechnical borings were completed at the PSEG Site in support of the early site permit application (ESPA). Geotechnical boring logs from this effort, in conjunction with existing data from the PSEG Site, are used to characterize the local hydrogeologic units. Geologic cross-sections are developed to depict the local geology and represent the associated hydrogeological units. The orientations of these cross-sections are shown on Figure 2.4.12-4, with the cross-sections presented on Figures 2.4.12-5 and 2.4.12-6.

Each of the units encountered at the PSEG Site is described below. The results of hydraulic conductivity tests, as well as interpreted gradients and velocities, are presented in Subsections 2.4.12.1.3.2 through 2.4.12.1.3.5.

2.4.12.1.2.1 Fill Deposits

Artificial fill comprises the surface material at the PSEG Site. It consists of typically grayish-brown to brown, silt, clay, and sand with variable silt and clay content, and clayey and silty gravels. The thickness of the artificial fill ranges from 2 to 10 ft., and averages 4 ft. across the northern and eastern portions of the site. These materials were placed at the site during previous construction activities and grade downward into hydraulic fill. Groundwater identified in these borings is likely perched and is not indicative of a continuous hydrogeologic unit.

Hydraulic fill was deposited at the site as the result of channel dredging of the Delaware River. It consists typically of dark gray to dark greenish-gray, highly plastic clay and silt with trace to some organic material, and locally interbedded discontinuous layers of clayey and silty, fine-

**PSEG Site
ESP Application
Part 2, Site Safety Analysis Report**

grained to medium-grained sand up to 5 ft. thick. The thickness of the hydraulic fill ranges from 24 to 44 ft., with an average thickness of 33 ft. across the northern and eastern portions of the site. The combined artificial and hydraulic fill stratigraphic sequence overlies Alluvium at an average elevation of -21 ft. NAVD in the eastern portion of the site. Average elevation of the bottom of the fill materials (top of the Alluvium) in the northern portion of the site is -29 ft. NAVD. Due to the clay and silt content of these units, the fill deposits represent an aquitard creating semi-confining conditions for the underlying Alluvium. The hydraulic conductivity of the hydraulic fill is reportedly 1,000 to 10,000 times less than that of the underlying Alluvium (Reference 2.4.12-1). This is further supported by the piezometric data discussed in Subsection 2.4.12.1.3.7. The average hydraulic conductivity measured from slug tests for one well (NOW-5U), located at the new plant location and screened in hydraulic fill, was 0.2 ft/day (See Table 2.4.12-9).

2.4.12.1.2.2 Alluvium

The Alluvium underlies the fill deposits and consists of Quaternary age sediments that formerly comprised the bed of the Delaware River. Alluvial soils consist typically of gray to grayish-brown, fine-grained to coarse-grained sand with trace to little, rounded to angular, fine to coarse gravel, and trace to little silt and clay content. In borings completed in the northern and eastern portions of the PSEG Site, 2 to 5 ft. thick discontinuous layers of fine-grained soils consisting of sandy silts and clays, and highly organic soils consisting of peat, were encountered. In the eastern portion of the PSEG Site, a 4 to 15 ft. thick discontinuous layer of non-organic silt and clay was locally encountered below the alluvial sand and gravel.

The Alluvium stratigraphic layer was typically encountered at elevations ranging from -22 to -35 ft. NAVD in the northern portion of the PSEG Site, and at elevations ranging from -16 to -25 ft. NAVD in the eastern portion of the site. The slightly undulating upper surface of the unit generally slopes gently westward towards the Delaware River. The thickness of the Alluvium ranges from 5 to 24 ft. across the PSEG Site. Average thickness in the northern portion of the site is 13 ft., and average thickness in the eastern portion of the site is 18 feet.

The Alluvium represents the shallowest saturated unit having appreciable hydraulic conductivity and transmissivity. Horizontal hydraulic conductivity for this unit, reported from prior studies at Salem and Hope Creek Station, ranges from 0.03 to 2.27 ft/day (see Table 2.4.12-1). Horizontal hydraulic conductivity measurements from aquifer tests conducted in observation wells located at the proposed new plant site range from 0.4 to 8.0 ft/day (see Table 2.4.12-9).

2.4.12.1.2.3 Kirkwood Formation

The Kirkwood Formation unconformably underlies the Alluvium and consists of Miocene age marine sediments deposited in a near-shore environment associated with a marine regression. The sediments of the Kirkwood Formation consist of two distinct units. The upper unit of the formation typically consists of dark gray, green, and brown to olive-gray, highly plastic clay and silt with trace fine sand and rounded gravel, trace shell fragments, and trace to little organic content. Locally, interbeds of silty and clayey, fine-grained to medium-grained sand occur within this upper unit. In the eastern portion of the PSEG Site, a thick section of light greenish-gray, silty, fine-grained to medium-grained sand was locally encountered above the finer grained sediments. The upper unit is considered an aquitard separating the Alluvium from the lower Kirkwood and Vincentown water-bearing zones.

**PSEG Site
ESP Application
Part 2, Site Safety Analysis Report**

There are no site-specific hydraulic conductivity testing data available for the Kirkwood aquitard. Regionally, estimates of the vertical hydraulic conductivity for the Alloway Clay member, the finer grained member of the Kirkwood unit, range from 0.00002 to 0.000052 ft/day (Reference 2.4.12-37).

The lower basal unit of the Kirkwood Formation typically consists of a 2-ft. to 14-ft. thick layer composed of dark greenish-gray, olive-gray, and dark gray to brown, silty and clayey, fine-grained to medium-grained sand and fine to coarse gravel. The sand and gravel in this lower unit is typically rounded to subangular. The lower Kirkwood is directly above the Vincentown Formation and is in hydraulic communication with the Vincentown where the sands and gravels are present.

The Kirkwood Formation rests on the erosional unconformity formed on top of the underlying Vincentown Formation and its upper surface forms an erosional unconformity with the overlying Alluvium. This makes the elevation of its upper surface as well as the thickness of the unit somewhat variable. In the northern portion of the PSEG Site, the top of the Kirkwood Formation ranges from elevations -34 to -43 ft. NAVD. In the eastern portion of the site, the top of the formation ranges from elevations -31 to -49 ft. NAVD. The thickness of the Kirkwood Formation ranges from 12 to 29 ft. and averages 17 ft. in the northern area of the site. The thickness of the Kirkwood Formation in the eastern portion of the PSEG Site ranges from 14 to 54 ft. and averages 37 ft. The large variation in thickness observed in the Kirkwood Formation is directly related to the undulating contact with the underlying Vincentown Formation, which displays up to 37 ft. of relief in the northern portion of the site, and up to 51 ft. of relief in the eastern portion of the site. Conversely, where the top of the Vincentown Formation is topographically low, the Kirkwood Formation is generally thick. Where the top of the Vincentown Formation is topographically high, the Kirkwood Formation is generally thin.

A few of the borings completed during the ESPA investigation did not encounter the lower unit of the Kirkwood Formation, indicating that the lower unit has some discontinuity across the site or, more likely, that the layer was thinner than the distance between sampling intervals. At boring NB-2, completed in the northern portion of the site, the upper unit of the Kirkwood Formation was not encountered, probably due to fluvial scour during deposition of the overlying Alluvium at this location. At boring NB-7, which was completed in the northern portion of the site, sediments of the Kirkwood Formation are completely absent, with alluvial sand and gravel unconformably overlying strongly oxidized Vincentown Formation sediments. This is most likely due to fluvial scour during deposition of the Alluvium at this location.

2.4.12.1.2.4 Cohansey Formation

The Cohansey Formation is often associated with the Kirkwood Formation and the two form an aquitard. However, the Cohansey was not identified in the vicinity of the PSEG Site.

2.4.12.1.2.5 Vincentown Formation

The Vincentown Formation serves as the water-bearing zone for much of the shallow groundwater transport in areas where alluvial deposits do not exist. It is the formation on which the foundations of the existing nuclear units (Hope Creek Generating Station [HCGS] and Salem Generating Station [SGS]) were constructed. This foundation will serve as the competent

**PSEG Site
ESP Application
Part 2, Site Safety Analysis Report**

layer for structures at the PSEG Site. The formation unconformably underlies the Kirkwood Formation and consists of Paleocene age marine sediments deposited in a neritic (shallow) marine environment during a marine regression. The Vincentown Formation shows significant erosional relief on its upper surface. This makes both the elevation of its upper contact and thickness somewhat variable..

In the northern portion of the PSEG Site, the elevation of the top of the formation ranges from -33 to -70 ft. NAVD. In the eastern portion of the site, the elevation ranges from -45 to -91 ft. NAVD. The thickness of the Vincentown Formation ranges from 35 to 79 ft. and averages 52 ft. in the northern portion of the site. Thickness ranges from 37 to 93 ft. and averages 55 ft. in the eastern portion of the site. Due to the erosional nature of the upper surface of the Vincentown Formation, the sediments of the uppermost portion of the unit typically show signs of weathering characterized by oxidation of iron-bearing minerals such as glauconite. The weathering and oxidation of the formation is subject to several post-depositional processes, such as subaerial exposure and fluvial erosion prior to deposition of the overlying sediments, as well as groundwater movement through the formation. This results in distinct but highly erratic contacts with the underlying unoxidized sediments that are not the result of depositional or stratigraphic control. Oxidized sediments are typically yellowish-brown to reddish-brown and unoxidized sediments are typically light greenish-gray to dark greenish-gray. The oxidized and unoxidized Vincentown Formation sediments are typically composed of glauconitic, calcareous, silty and clayey, fine-grained to medium-grained sand with variable silt content. Glauconite is typically present in trace amounts with locally higher concentrations observed during field sampling. The formation contains many discontinuous, friable to indurated, carbonate cemented sandstone layers. These indurated zones are typically 0.1 to 1 ft. thick, as observed from split-spoon sampling and drilling operations. The oxidized and unoxidized sediments display a weak to strong reaction with 10 percent hydrochloric acid.

The Vincentown Unit is described both locally and regionally as a significant water-bearing unit and is comprised of sediments of the Vincetown Formation and the lower portion of the overlying Kirkwood Formation. The hydrogeologic parameter data for the Vincentown Unit have been compiled from a number of pumping and aquifer tests at Salem and Hope Creek Stations. Previously reported site-specific horizontal hydraulic conductivity values range from 0.95 to 14 ft/day (Reference 2.4.12-11 and 2.4.12-12). Horizontal hydraulic conductivity measurements from aquifer tests conducted in observation wells installed for this proposed new plant site range from 0.3 to 10.7 ft/day (See Table 2.4.12-9).

In general, groundwater in the Vincentown Formation beneath the PSEG Site has relatively high concentrations of chloride and is not adequate for use as a water supply.

2.4.12.1.2.6 Hornerstown Formation

The Hornerstown Formation underlies the Vincentown Formation and is considered an aquitard. However, in several areas, the sand content suggests that it is in hydraulic communication with the overlying Vincentown Formation. Sediments of the Hornerstown Formation are typically composed of greenish-gray to very dark greenish-gray, silty and clayey, fine-grained to medium-grained sand, with trace to few shell fragments, trace to few friable to indurated layers, and trace to some glauconite. Glauconite content typically increases with depth and is estimated from field sample observations to comprise greater than 30 percent of the sand fraction near the base of the formation. The formation contains numerous discontinuous, friable to indurated,

**PSEG Site
ESP Application
Part 2, Site Safety Analysis Report**

carbonate cemented sandstone layers. These properties classify it as an aquitard. These cemented zones are typically 0.1 to 1 ft. thick, as observed from the split-spoon sampling and drilling operations. In general, the Hornerstown Formation is differentiated from the overlying Vincentown Formation on the basis of increasing silt/clay content and increasing glauconite content.

The Hornerstown Formation consists of upper Cretaceous to Paleocene age marine sediments deposited in a neritic environment during a marine transgression. Borings in the northern portion of the site encountered the top of the Hornerstown Formation at elevations ranging from -105 to -114 ft. NAVD, and in the eastern portion of the site at elevations ranging from -127 to 137 ft. NAVD. The formation averages 20 ft. thick across the PSEG Site.

The Hornerstown Formation, together with the underlying Navesink Formation comprise an aquitard between the Vincentown and Mount Laurel Formations. There are no site-specific hydraulic conductivity testing data available for the Hornerstown unit. Regionally, estimates of the vertical hydraulic conductivity for the Hornerstown and Navesink Formations range from 0.0005 to 9 ft/day (Reference 2.4.12-33 and 2.4.12-37). The relatively higher range of values (e.g., 9 ft/day) are reportedly measures of minor sand layers that are not representative of this unit's overall vertical hydraulic conductivity (Reference 2.4.12-37). Horizontal hydraulic conductivity measurements for the Navesink Formation and Hornerstown Sand in Gloucester County range from 30 to 65 gpd/ft² (4 to 8.7 ft/day) (Reference 2.4.12-33).

2.4.12.1.2.7 Navesink Formation

The Navesink Formation underlies the Hornerstown Formation and as described in the previous subsection, these two units together comprise an aquitard between the Vincentown and Mount Laurel formations. Sediments of the Navesink Formation are typically composed of very dark greenish-gray to very dark grayish-green and greenish-black, silty and clayey, fine-grained to medium-grained glauconite and quartz sand with trace to little shell fragments.

The Navesink Formation consists of Upper Cretaceous age marine sediments deposited in a neritic environment during a marine transgression. The borings in the northern portion of the PSEG Site encountered the top of the Navesink Formation at elevations ranging from -121 to -133 ft. NAVD, and in the eastern portion of the site at elevations ranging from -147 to -157 ft. NAVD. The thickness of the unit averages 24 ft. in the northern portion of the site and thins slightly to the southeast, with an average thickness of 20 ft. in the eastern portion of the site.

2.4.12.1.2.8 Mount Laurel Formation

The Mount Laurel Formation and underlying Wenonah Formation create the next major water-bearing zones. Two standby production wells at SGS, PW-2 and PW-3, are screened in this aquifer. Sediments of the Mount Laurel Formation typically consist of dark olive-gray, dark grayish-brown, and greenish-gray, clayey and silty, fine-grained to medium-grained sand, grading with depth into fine-grained to medium-grained sand with variable silt and clay content; all with trace to little glauconite and shell fragments. The amount of glauconite and shell fragments decreases to trace amounts with increasing depth. The upper 15 to 20 ft. of the formation typically contains trace to little, subrounded, coarse-grained sand and fine gravel, and is locally composed of sandy clay.

**PSEG Site
ESP Application
Part 2, Site Safety Analysis Report**

The Mount Laurel Formation consists of Upper Cretaceous age marine sediments deposited in a near-shore environment during a marine regression. All geotechnical borings advanced during the ESPA investigation penetrated the top of the formation. Borings in the northern portion of the PSEG Site encountered the top of this formation at elevations ranging from -145 to -157 ft. NAVD, and at elevations ranging from -168 to -177 ft. NAVD in the eastern portion of the site. This corresponds to an apparent southeasterly dip of approximately 30 ft/mi. The unit has an average thickness of 103 ft. in the northern portion of the site and thickens slightly to the southeast, with an average thickness of 111 ft. in the eastern portion of the site.

Together with the top of the underlying Wenonah Formation, the Mount Laurel-Wenonah Aquifer ranges from approximately 100 to 125 feet in thickness. The horizontal hydraulic conductivity calculated from a pumping test at the PSEG Site ranges from 0.67 to 18.7 ft/day (Reference 2.4.12-12).

2.4.12.1.2.9 Wenonah Formation

The upper Wenonah Formation underlies the Mount Laurel Formation. The Mount Laurel and Wenonah formations are used as a drinking water source for several communities. The Wenonah Formation typically consists of very dark gray to greenish-black, sandy clay with trace shell fragments and trace to little glauconite, and locally consists of clayey and silty, fine-grained to medium-grained sand with trace to little glauconite. The lower Wenonah Formation has an increase in clays and silts and is considered, with the underlying Marshalltown Formation, to be an aquitard.

The Wenonah Formation is of Upper Cretaceous age and consists of marine sediments deposited in a neritic environment during a marine regression. Six of the borings completed during the ESPA investigation penetrated the top of the formation. In the northern portion of the site, the top of the Wenonah Formation was encountered at elevations ranging from -250 to -259 ft. NAVD, and in the eastern portion of the site at elevations ranging from -279 to -289 ft. NAVD. The Wenonah Formation has an average thickness of 15 ft. across the site.

The Lower Wenonah Formation, together with the upper portion of the underlying Marshalltown Formation comprise the Marshalltown-Wenonah aquitard. There are no site-specific hydraulic conductivity testing data available for this aquitard. Regionally, estimates of the vertical hydraulic conductivity for the Marshalltown-Wenonah Unit range from 0.0000057 to 0.13 ft/day (Reference 2.4.12-37).

2.4.12.1.2.10 Marshalltown Formation

The Marshalltown Formation consists of Upper Cretaceous age marine sediments deposited in a neritic environment during a marine transgression and, with the lower Wenonah, acts as an aquitard. Sediments of this unit typically consist of greenish-gray to very dark gray and black, clayey and silty, fine-grained to medium-grained sand, and fine sandy clay of variable plasticity, all with trace to little glauconite content. Trace amounts of shell fragments, pyrite nodules, friable layers, and subrounded fine gravel were locally encountered within the Marshalltown Formation. A natural gamma peak was observed in the geophysical logs at the top of the Marshalltown Formation/base of the overlying Wenonah Formation. This may represent a thin (less than 3 ft. thick) phosphatic hard-ground or lag deposit that formed during the transition from deposition of the Marshalltown Formation to deposition of the Wenonah Formation, and

**PSEG Site
ESP Application
Part 2, Site Safety Analysis Report**

was used to differentiate the two formations at the PSEG Site. The Marshalltown Formation, in general, shows an elevated natural gamma response in comparison to the overlying Wenonah Formation, but is similar to the underlying Englishtown Formation.

Five of the borings completed during the ESPA investigation penetrated the top of the Marshalltown Formation at elevations ranging from -265 to -277 ft. NAVD in the northern portion of the PSEG Site and at elevation -293 ft. NAVD in the eastern portion of the site. This corresponds to an apparent southeasterly dip of approximately 30 ft/mi. The Marshalltown Formation is typically 25 ft. thick across the PSEG Site.

2.4.12.1.2.11 Englishtown Formation

The Englishtown Formation consists of Upper Cretaceous age marine sediments deposited in a near-shore environment associated with a marine regression. Sediments in the upper portion of the Englishtown Formation consist of micaceous, very dark greenish-gray to very dark gray and black, sandy silt and clay to clayey sand, with trace shell fragments and trace to little glauconite; grading downward into micaceous, black, highly plastic silt and clay with trace to few fine sand and trace shell fragments. The upper portion of this formation is considered a water-bearing zone with good water quality.

There are no site-specific hydraulic conductivity testing data available for the Englishtown Aquifer as this aquifer has not been evaluated locally as a source of water. Regionally, estimates of the horizontal hydraulic conductivity for this unit range from 12 to 67 ft/day based on aquifer and laboratory tests for the unit as represented in Monmouth County, New Jersey (Reference 2.4.12-37).

Four of the borings advanced during the ESPA investigation penetrated the top of the unit at elevation -291 ft. NAVD in the northern portion of the site and at elevation -319 ft. NAVD in the eastern portion of the site. The thickness of the Englishtown Formation ranges from 44 to 49 ft. across the PSEG Site.

2.4.12.1.2.12 Woodbury Formation

The Woodbury Formation consists of Upper Cretaceous age marine sediments deposited in an inner shelf environment associated with a marine regression. Together with the underlying Merchantville Formation, these units are an aquitard between the overlying Englishtown Formation and the underlying PRM. Sediments of the Woodbury Formation consist of very dark gray and black to greenish-black, highly plastic clay with trace glauconite, fine sand, mica, and shell fragments and, locally, with trace indurated layers. Sediments of the Woodbury Formation are very similar to those of the upper portion of the overlying Englishtown Formation and the two formations appear to have a gradational contact.

Two deep borings completed during the ESPA investigation penetrated the top of this unit at elevation -336 ft. NAVD in the northern portion of the site and at elevation -368 ft. NAVD in the eastern portion of the site. The thickness of the Woodbury Formation ranges from 30 to 36 ft. across the PSEG Site.

**PSEG Site
ESP Application
Part 2, Site Safety Analysis Report**

2.4.12.1.2.13 Merchantville Formation

The Merchantville Formation and overlying Woodbury Formation comprise an aquitard between the overlying Englishtown water-bearing zone and the underlying PRM. Sediments of the Merchantville Formation consist of greenish-black to black, glauconitic, silt and clay with trace to some fine sand, trace mica, locally with trace friable to moderately indurated layers.

There are no site-specific hydraulic conductivity testing data available for the Merchantville-Woodbury Confining Unit. This unit acts as a confining unit over the PRM aquifer and regionally, estimates of the vertical hydraulic conductivity range from 0.000004 to 0.0004 ft/day (Reference 2.4.12-37).

The Merchantville Formation consists of Upper Cretaceous age marine sediments deposited in a neritic environment during a marine transgression. The two deep borings advanced during the ESPA investigation penetrated the top of the Merchantville Formation at an elevation of -372 ft. NAVD in the northern portion of the PSEG Site and at an elevation of -398 ft. NAVD in the eastern portion of the site. The unit is approximately 30 ft. thick.

2.4.12.1.2.14 Potomac-Raritan-Magothy Formation

Hydrogeologically, the Potomac, Raritan and Magothy (PRM) formations are identified as a continuous water-bearing zone used as a significant potable water source at the PSEG Site as well as regionally. There are confining units between water-bearing zones, but for the purpose of this ESPA, the PRM is discussed as one unit.

The Magothy Formation disconformably overlies the Potomac Formation and consists of Upper Cretaceous age non-marine sediments deposited in deltaic to nearshore environments. Sediments of the Magothy Formation typically consist of gray to very dark gray, carbonaceous/lignitic clay and silt at the top of the formation, interbedded with sands with variable silt and clay content at the bottom of the formation. The two deep borings advanced during the ESPA investigation penetrated the top of the Magothy Formation at elevation -402 ft. NAVD in the northern portion of the PSEG Site, and in the eastern portion of the site at elevation -429 ft. NAVD. The unit ranges from 52 to 55 ft. thick.

The Raritan Formation, although recognized as a distinct formation, is considered to be part of the Potomac Formation at the PSEG Site. Hydrogeologically, the Upper Raritan aquifer provides good quality groundwater and is tapped by three production wells used by the HCGS (HC-1 and HC-2) and SGS (PW-5) which each produce, on average, 364 gallons per minute (gpm). The remaining deep production well at the site, PW-6, is in the next deeper aquifer, the Middle PRM, but it supplies only a small portion of the SGS's groundwater supply needs (6.4 gpm, on average from 2002 to 2007).

The Middle Raritan Clay, 260 to 290 ft. thick, separates the Upper PRM from the Middle PRM. The Middle PRM is thinner (45 to 55 ft. thick) and generally has a lower transmissivity than the Upper PRM. However, transmissivity in the Upper PRM appears to vary more widely than in the Middle PRM. The Middle PRM supplies only a relatively low percentage of the groundwater used at SGS due to higher chloride levels. (Reference 2.4.12-12) A relatively lower specific capacity and transmissivity is reported for the Middle PRM as compared to the Upper PRM (Table 2.4.12-1).

**PSEG Site
ESP Application
Part 2, Site Safety Analysis Report**

The Potomac Formation is the deepest stratigraphic unit encountered by the ESPA borings at the site. The Potomac Formation consists of Lower Cretaceous age non-marine, continentally-derived sediments deposited in fluvial to deltaic environments (Reference 2.4.12-309). Two borings completed during the ESPA investigation penetrated the top of the Potomac Formation. The top of the formation is at elevation -454 ft. NAVD in the northern portion of the site, and at elevation -484 ft. NAVD in the eastern portion of the site. These two borings are along a southeasterly line, approximately in the regional dip direction. The vertical elevation difference corresponds to an apparent southeasterly dip of approximately 34 feet per mile. This apparent dip is consistent with published range of dip for the NJ Coastal Plain. The top of the Potomac Formation was identified mainly from the geophysical testing conducted in the two deepest borings completed as part of the ESPA.

2.4.12.1.3 Observation Well and Production Well Data

Sixteen observation well pairs were installed at the PSEG Site to support the ESPA development (Figure 2.4.12-8). Hydraulic conductivity tests were conducted on the observation wells installed at the new plant location to calculate the estimated hydraulic conductivity of the Alluvium or upper water-bearing zone, and the Vincentown Formation or lower water-bearing zone. In addition to these activities, a limited tidal study was completed for two well pairs at the new plant location to better characterize the hydraulic communication between the Delaware River and the adjacent upper and lower water-bearing zones.

Groundwater level data was used, in conjunction with existing data from the PSEG Site, to prepare groundwater potentiometric surface maps. New wells were installed on both the new plant location, and on the eastern location, which is used for construction support and/or laydown areas during construction. Well pairs installed at the new plant location are designated as NOW-1U (upper) and L (lower) through NOW-8U and L. Well pairs installed in the eastern location were completed to support potential environmental impacts and, therefore, are not discussed here. For all well identifications, the “U” designation in the well identification indicates that the well was screened in the shallow or “upper” water bearing units. Similarly, the “L” designation indicates that the well was screened in the “lower” water bearing units.

As the northern portion of the site is the new plant location, the remaining discussion pertains to those wells only. At each well pair, the lower or deeper well was installed within the Vincentown or lower Kirkwood aquifer. With the exception of NOW-5U and NOW-7U, the upper or shallow wells were installed within the Alluvium. Observation well NOW-5U was installed in the hydraulic fill to assess the properties of the shallow hydraulic fill aquitard. NOW-7U was installed in the Vincentown Formation just below the Alluvium, as it was identified as the first adequate water-bearing zone encountered. Table 2.4.12-4 summarizes observation well construction details.

Monthly water levels were measured at each observation well to collect sufficient data to characterize groundwater conditions at the site, including seasonal fluctuations (Table 2.4.12-5). These data were then supplemented during the September 2009 sampling event with data from selected existing wells at the PSEG Site. The purpose of the monthly water-level measurements is to characterize groundwater flow directions, calculate hydraulic gradients, and ascertain seasonal variations in groundwater levels and flow directions in the two shallow water-bearing units. Table 2.4.12-5 presents a 12-month data set representing January 2009 through December 2009. In addition to the 12 months of data, historic, longer-term data are available for

**PSEG Site
ESP Application
Part 2, Site Safety Analysis Report**

some of the existing production wells installed in Mount Laurel-Wenonah and the PRM. Data from these wells show fluctuations in water elevations due to the influence of groundwater withdrawals (pumping) to support SGS and HCGS. Data from 2000 to 2009 is presented in Table 2.4.12-6.

As groundwater levels may be impacted by rainfall, the average and measured regional precipitation data for 2009, obtained from the Delaware Environmental Observing System Network at the Wilmington Delaware Location are presented in Figure 2.4.12-7. Groundwater responses are typically measured with respect to regional precipitation.

Alluvium

Six wells were screened in the Alluvium that underlie the hydraulic fill. These materials represent the uppermost interval where groundwater transport is likely. As presented on Figure 2.4.12-10 the 2009 water-level measurements collected for the wells installed on the new plant location show slight seasonal variations with higher water levels in the summer months. These data are not adjusted for slight tidal impacts. This is evidenced by the fluctuation in water levels over the measurement period (January 2009 through December 2009). It is apparent that the observation well installed within the hydraulic fill, NOW-5U, represents perched conditions and is not as responsive to seasonal variation as the wells installed within the Alluvium. NOW-7U was installed within the Vincentown Formation, as this was identified as the first encountered transmissive zone and appears to be in hydraulic communication with the overlying Alluvium.

Groundwater potentiometric contours were interpreted for each measuring event. Groundwater quality samples were collected on a quarterly basis during this period as well. The estimated potentiometric surface contours of the shallow water-bearing zone (Alluvium) are shown for each of the quarterly sampling events in 2009. Potentiometric contours, or groundwater flow directions, for February, April, July and September sampling events are presented in Figures 2.4.12-11 through 2.4.12-14. To further investigate the groundwater below the new plant location, the September 2009 data was supplemented with selected water-level measurements from HCGS and SGS as well as the eastern location wells. The gradients are not corrected for tidal influences, but groundwater flow is generally toward the Delaware River, with a slightly more northerly component during the summer months.

Vincentown Formation

Nine wells were screened within the Vincentown or Vincentown-Kirkwood formations. As depicted on Figure 2.4.12-15, groundwater levels for these wells show more variation over time. (As noted above, data from NOW-7U was used to contour the upper water-bearing zone.) This is most likely due to tidal influences. As noted in both previous studies (References 2.4.12-1 and 2.4.12-12) and Subsection 2.4.12.1.3, the overlying Kirkwood Formation is an aquitard creating semi-confining conditions. Additionally, the Vincentown Formation is in direct hydraulic communication with the Delaware River. Therefore, the tidal influences are seen with greater amplitude and farther eastward than as noted in the shallow water-bearing zone.

Groundwater contours were estimated for each round of sampling. During quarterly events, groundwater quality samples were also collected. The estimated potentiometric surface contours for the deeper water-bearing zone (Lower Kirkwood and Vincentown formations) are shown for each of the quarterly events in 2009. Potentiometric surface contours, or groundwater

**PSEG Site
ESP Application
Part 2, Site Safety Analysis Report**

flow directions, for February, April, July and September 2009 sampling events are presented in Figures 2.4.12-16 through 2.4.12-19.

Groundwater elevation data used to estimate the potentiometric surface for the lower water-bearing zone were not corrected for tidal effects. However, the data show that groundwater within the Vincentown aquifer flows west, toward the Delaware River.

2.4.12.1.3.1 Hydrogeologic Properties

Sixteen observation wells were installed at the PSEG Site in the vicinity of the new plant location to support the ESPA development. Additionally, hydraulic conductivity tests were conducted to calculate the estimated hydraulic conductivity of the Alluvium or upper water-bearing zone, and the Vincentown aquifer or lower water-bearing zone. In addition to these activities, a limited tidal study was completed for two well pairs to better characterize the hydraulic communication between the Delaware River and the adjacent upper and lower water-bearing zones.

In addition to the site specific data, regional data on the hydrogeological properties of the formations at the new plant site are presented in Table 2.4.12-1. These include hydraulic conductivity, transmissivities, porosity, storage coefficients, specific capacity and leakance.

The following sections present the findings from the data collected for this ESPA.

2.4.12.1.3.2 Hydraulic Gradients

The potentiometric surface of the groundwater in both the upper and lower water-bearing zones follows the regional and local topography and is relatively flat. Groundwater at the new plant location flows generally westward toward the Delaware River.

Groundwater elevations were determined from wells installed for this ESPA and the data were used to characterize groundwater flow. During the September 2009 sampling event, additional selected wells from SGS and HCGS were measured to obtain a broader spatial distribution of data points between the new plant and eastern locations.

Groundwater flow directions and hydraulic gradients are determined for each month by contouring the isopleths from the piezometric head elevations. These contours are established for each data set and are based on distance between the contours that represented the steepest gradients. Table 2.4.12-7 presents calculated groundwater gradients. The average measured gradient for the Alluvium is calculated to be 0.00042 feet per foot (ft/ft) for the new plant location. The maximum gradient is calculated to be 0.00235 ft/ft for the new plant location. The average measured groundwater gradient in the Vincentown aquifer is calculated at 0.00048 ft/ft with the maximum gradient calculated to be 0.0020 ft/ft.

As the maximum hydraulic gradient is the steepest gradient from the 12 months of groundwater readings, and because it is tidally affected, the maximum is a transient and short-term condition. Due to the shallow horizontal gradients in both water-bearing zones, it is expected that overall groundwater velocity, calculated from these gradients, is slower than the conservative estimate provided above. Groundwater velocities are discussed further in Subsection 2.4.12.1.3.5.

**PSEG Site
ESP Application
Part 2, Site Safety Analysis Report**

2.4.12.1.3.3 Vertical Gradients

Vertical gradients are calculated for each well pair. The average vertical gradients water levels are shown in Table 2.4.12-8. In general, there is a slight downward gradient between the upper and lower water-bearing zones. However, because the lower unit is more strongly influenced by tidal fluctuations, this downward gradient will not significantly impact groundwater flow. Note that the Kirkwood Formation, where present, acts as an aquitard between the two zones, further limiting the hydraulic communication between the two formations.

2.4.12.1.3.4 Hydraulic Conductivity

Hydraulic conductivity tests (slug tests) were completed in all wells installed at the new plant location for the ESPA. The data were evaluated using the Bouwer and Rice, Cooper et al., and Hvorslev methods to calculate hydraulic conductivity estimates (References 2.4.12-3; 2.4.12-4; and 2.4.12-19). Table 2.4.12-9 summarizes these slug test results.

Based on the results of the slug tests, the upper wells in the Alluvium exhibited an average hydraulic conductivity of 3.75 feet per day (ft/day), while the lower wells, screened in the Vincentown Formation (excluding NOW 7U), exhibited an average hydraulic conductivity of 3.85 ft/day. Observation well NOW-5U was completed in the hydraulic fill and has a calculated average hydraulic conductivity of 0.145 ft/day. These values are within the ranges presented in Table 2.4.12-1.

2.4.12.1.3.5 Groundwater Velocity

Groundwater velocities are dependent on the hydraulic gradients and the hydraulic conductivity of the water-bearing zone. Average horizontal travel times, or velocities, in the upper alluvial aquifer are calculated at 0.0078 ft/day (2.9 feet per year [ft/yr]) with a maximum velocity calculated at 0.094 ft/day (34 ft/yr). Average horizontal travel times, or velocities, in the lower Vincentown aquifer are calculated at 0.0091 ft/day (3.3 ft/yr) with a maximum velocity calculated at 0.107 ft/day (39 ft/yr). As the maximum velocities are calculated using maximum local gradients (i.e. from the steepest contours from shorter distances and not from distances that extend over the entire site) the maximum velocities represent limiting conservative conditions.

Due to the tidal fluctuations and minimal vertical gradients and the location of the Kirkwood aquitard between the Alluvium and Vincentown Formation, the horizontal velocity of groundwater is much greater than the vertical velocity. Therefore, any vertical migration of groundwater is negligible with respect to contaminant transport.

2.4.12.1.3.6 Tidal Influences

A 72-hour tidal study was completed on observation wells NOW-1L and NOW-1U, and NOW-3L and NOW-3U. Similar to the studies completed by ARCADIS at SGS and HCGS, a slight tidal influence was observed in the wells installed in the Alluvium, or upper water-bearing zone. A stronger tidal influence is observed in the lower wells installed in the Vincentown Formation. (Reference 2.4.12-2)

Observation wells NOW-3U and NOW-3L exhibit average tidal shifts of 0.56 ft. and 2.26 ft., respectively, over the course of the tidal study. The NOW-3 well pair is located 205 ft. from the

**PSEG Site
ESP Application
Part 2, Site Safety Analysis Report**

Delaware River. The NOW-1 pair is located 765 ft. inland to the east. Observation well NOW-1L exhibited an average tidal shift of 0.49 ft. over the course of the tidal study. These data indicate that the semi-confined condition of the Vincentown Formation results in an amplified response to tidal change. Both the upper and lower aquifers are in hydraulic communication with the Delaware River, but there is greater response in the wells screened in the lower aquifer. For both units, tidal influences dampen or decrease with distance from the river. Figures 2.4.12-20 through 2.4.12-24 present the responses of the four wells, as compared to the stilling well installed at the barge slip. Table 2.4.12-10 summarizes the tidal study results.

2.4.12.1.3.7 Hydraulic Communication Between Groundwater and Surface-Water Bodies

Ten shallow piezometers were installed at depths ranging from 2 to 5 ft. below the bottoms of surface-water bodies at sampling locations AS-1 through AS-6, and AS-8 through AS-11. Each piezometer was constructed with a 1.5-ft. screen interval. These piezometers were used to collect data to characterize the hydraulic communication between the surface-water and underlying groundwater. Figure 2.4.12-8 shows these piezometer locations.

Monthly water-level measurements were collected from the six piezometers installed at the PSEG Site. Measurements from the four piezometers installed off-site (AS-1 through AS-3 and AS-11) were collected quarterly. Water-level measurements and construction details are provided in Table 2.4.12-11.

Based on the data from each piezometer location, and when compared to the potentiometric surface of the water table, the surface-water bodies on-site and within the tidal marsh appear to be perched. There is no conclusive data that indicates that they are receiving bodies or that they recharge the underlying groundwater. It is interpreted that these surface-water bodies on-site and within the tidal marsh are perched on the silty hydraulic fill materials. The streams are strongly influenced by the tides whereas the ponds are relatively stagnant and are recharged by precipitation and stormwater runoff.

These data also indicate that the surface-water bodies do not strongly influence the groundwater flow within the Alluvium of the upper aquifer. Both the measurements from within the piezometers (representative of shallow groundwater) and outside the piezometers (representative of surface-water) are similar for the standing waters and do not correlate to the groundwater measurements collected from the observation wells screened in the upper alluvial deposits. In some of the tidal marshes (i.e. locations AS-4, 5, and 11) the difference between the surface water and groundwater are more pronounced due to the tidal impacts, however the data demonstrate that the shallow groundwater is perched and not in hydraulic communication with the groundwater present in the Alluvium. These differences were also seen in the other piezometers installed in the tidal marshes (Locations AS-1, 2 and 3) although the differences are not as pronounced.

2.4.12.1.4 Conceptual Site Model

The PSEG Site is located in the NJ Coastal Plain. The regional geology and hydrogeology consists of southeasterly dipping sands, silts and clays. The shallow aquifers beneath the site (Alluvium and Vincentown aquifer), are in direct contact with the Delaware River, are tidally-influenced, and saline (and therefore, are not considered to be an adequate source for potable water).

**PSEG Site
ESP Application
Part 2, Site Safety Analysis Report**

Observation wells were installed at the PSEG Site to better characterize the upper Alluvium aquifer deposits as well as the underlying lower (Vincentown) aquifer. Potentiometric contour maps generated from the site data indicate that groundwater flow in these units is generally westward towards the Delaware Estuary, with localized influences from tides and the surrounding marsh. The tidal study indicated there is a stronger response to the tidal cycle in the lower (Vincentown) aquifer when compared to the response in the shallow Alluvium groundwater.

Average horizontal travel times, or velocities in the upper Alluvium aquifer are calculated at 0.0078 ft/day (2.9 ft/yr) with a maximum velocity calculated at 0.094 ft/day (34 ft/yr). Average horizontal travel times, or velocities in the lower Vincentown Aquifer are calculated at 0.0091 ft/day (3.3 ft/yr) with a maximum velocity calculated at 0.1070 ft/day (39 ft/yr). The maximum velocities are partially attributable to tidal influences on the gradients and have been measured from the steepest portion, causing the values to be conservative (fast). These are temporary conditions, therefore these maximum rates are not applicable to extended periods of time.

The deeper aquifers, such as the Mount Laurel-Wenonah and PRM, are water supply aquifers. The Mount Laurel-Wenonah has been previously used for water supply at PSEG, but the required pumping rate introduced the potential for induced chloride migration (saline water transmission through leaky aquitards) from the overlying Vincentown aquifer and pumping was limited to retard migration (Reference 2.4.12-12). These water-bearing zones are also designated by EPA as sole source aquifers (Reference 2.4.12-32). HCGS and SGS currently withdraw water from the PRM. The new plant withdraws groundwater for potable water and sanitary water systems as well as fire protection systems from the PRM. The site water balance calculation gives estimates of projected groundwater increased demand as discussed further in Subsection 2.4.12.2.

This conceptual model provides the basis in Subsection 2.4.13 for the evaluation of subsurface pathways and more specifically the conservative analysis of critical groundwater pathways for a hypothetical liquid effluent release at the site.

2.4.12.2 Groundwater Use

The anticipated water source to meet the water demand requirements for the new plant during operations is groundwater from the PRM aquifer. Table 2.4.1-9 shows the new plant will use up to 210 gpm or 110 million gallons per year (Mgy). When a reactor technology is selected and a final site water balance is developed, PSEG will re-evaluate total site (SGS, HCGS, and new plant) water use against the site water allocation permit limits. The current permits and authorizations will be modified as necessary to include the new plant, or new permit(s) for water withdrawal will be obtained. Groundwater will be used for sanitary/potable water, demineralized makeup water, and fire suppression. Subsection 2.4.12.3.2 discusses the anticipated water demands for plant construction and operations.

2.4.12.2.1 Regional Groundwater Use

In 1986, NJ designated two Critical Water-Supply Management Areas in the NJ Coastal Plain in response to long-term declines in groundwater levels where groundwater is the primary water supply. Critical Water-Supply Management Area 1 includes portions of Middlesex, Monmouth, and Ocean counties along the Atlantic Ocean shore. Critical Water-Supply Management Area 2,

**PSEG Site
ESP Application
Part 2, Site Safety Analysis Report**

which is closer to and northeast of the site, includes portions of Ocean, Burlington, Camden, Atlantic, Gloucester, and Cumberland counties, and a small portion of eastern Salem County. In Critical Water-Supply Management Area 2, groundwater withdrawals were reduced and new allocations limited from the PRM Aquifer. The PSEG Site is southwest of the management area, along the Delaware River. The site is not in a Critical Water-Supply Management Area, and is not subject to the groundwater withdrawal restrictions associated with these areas (Reference 2.4.12-28). As described in Subsection 2.4.12.1, regional aquifers within the NJ Coastal Plain have been designated sole source aquifers by the EPA (Reference 2.4.12-32).

Salem County contains five aquifers that supply groundwater for domestic and industrial users. The PRM aquifer and the Cohansey Sands aquifers provide water in excess of 500 gpm. The PRM outcrops in the northwestern portion of the county. The Cohansey Sands outcrops over most of the eastern portion of the county and were not encountered at the PSEG Site.

Figure 2.4.12-3 shows well head protection areas in both NJ and DE and public supply wells in NJ that are within a 25-mi. radius of the site. Table 2.4.12-2 identifies withdrawal rates and well depths for public supply wells, excluding well head protection areas, within 25 mi. of the PSEG Site in NJ and DE. Table 2.4.12-3 shows the primary groundwater users within the same radius in NJ and DE that use more than 100,000 gallons per day.

The regional groundwater demand placed on the PRM resulted in a decrease in the elevation of the piezometric surface that was historically observed in the counties of Camden, Middlesex, and Monmouth (Reference 2.4.12-36). The development of these piezometric surface reductions was observed in wells completed in the middle and lower aquifers between 1973 and 1978. The declines may have been a result of an increase in the amount of extraction from the lower aquifer which began in 1973. Coincident cones of depression in the upper and middle/lower PRM suggest that significant communication occurs between these aquifers. Furthermore, PRM aquifer withdrawals in Camden County have been previously shown to influence water levels at significant lateral distances resulting in water level reductions in Salem and Gloucester counties (Reference 2.4.12-36).

Groundwater withdrawals in central and southern NJ increased from 1904 to a peak in the mid/late 1970s. They then dropped off in the mid-1980s (References 2.4.12-36 and 2.4.12-39). A slower rate of declining withdrawals continued until 1995 (Reference 2.4.12-39). Water levels in lower PRM observation wells located in NJ and DE generally increased during the period from the mid-1980s to the late-1990s, as documented by the USGS (Reference 2.4.12-409). Decreased consumptive use and greater controls on groundwater withdrawals by NJ, in favor of surface water withdrawals, allowed groundwater levels in the PRM to recover in central NJ from the over-pumping of the 1970s (Reference 2.4.12-39).

2.4.12.2.2 Local Water Use

PSEG has authorization from the New Jersey Department of Environmental Protection (NJDEP) (Reference 2.4.12-22) and Delaware River Basin Commission (DRBC) (Reference 2.4.12-15) for consumptive use of up to 43.2 million gallons of groundwater per month at HCGS and SGS combined. The discussion of groundwater in this subsection includes use at both HCGS and SGS for the following reasons.

- NJDEP issued a single permit for the combined sites. Although each site uses its own wells and there are individual pumping limits for each site's wells, the permit limits are for

**PSEG Site
ESP Application
Part 2, Site Safety Analysis Report**

the combined sites. The current permit allows a combined maximum diversion rate for HCGS and SGS of 2900 gpm and limits of actual water diverted to 43.2 million gallons per month (Mgm), and 300 MGY.

- The groundwater distribution systems for HCGS and SGS are interconnected in order to transfer water between the stations, if needed.

Groundwater is the only source of freshwater at HCGS and SGS. Both sites use freshwater for potable, industrial process makeup, fire protection, and sanitary purposes. There are no off-site public water supply wells or private wells within 1 mi. of the PSEG Site. The nearest potable supply well is located west of the site, across the Delaware River, in Delaware (Reference 2.4.12-2).

HCGS draws groundwater from two production wells (HC-1 and HC-2) installed to depths of 816 ft. in the Upper Raritan Formation of the PRM aquifer (Reference 2.4.12-22). The wells supply two 350,000-gallon storage tanks. Of the total storage volume, 656,000 gallons of water are reserved for fire protection; the remainder is for potable, sanitary, and industrial purposes, including demineralized makeup water. The demineralized water makeup system uses ion exchange resin to provide the required ultrapure water.

Groundwater at SGS is withdrawn primarily from two production wells, PW-5 and PW-6, which are installed to depths of 840 ft. and 1135 ft., respectively, in the upper and middle Raritan Formation of the PRM aquifer. SGS also has the capability of using two shallower wells, PW-2 and PW-3, currently classified as standby wells by NJDEP (Reference 2.4.12-22). These wells are installed to depths of 281 ft. and 293 ft., respectively, in the Mount Laurel-Wenonah aquifer. The wells supply two 350,000-gallon storage tanks. Of the total storage volume, 600,000 gallons of water are reserved for fire protection; the remainder is for potable, sanitary, and industrial purposes, including demineralized makeup water. The demineralized water makeup system uses reverse osmosis to provide the required ultrapure water (Reference 2.4.12-29).

SGS and HCGS pumping wells completed in the PRM exhibited relatively stable to slightly decreasing water levels during the period 2000 to 2009. A study by the U.S. Geological Survey (USGS) (Reference 2.4.12-40) indicates that the pumping centers north of the Chesapeake and Delaware Canal influence water levels in the lower PRM in the vicinity of the PSEG Site. The interconnected nature of the lower and middle units of the PRM in conjunction with this study (Reference 2.4.12-40) indicate that water levels in the middle PRM are influenced by/related to water levels in the lower PRM. A more recent USGS study (Reference 2.4.12-40) indicates that Delaware withdrawals from the middle and lower PRM had increased as of 2003. This appears to have resulted in reduced regional water levels in this area of the lower PRM. These effects continue to influence water levels at the PSEG Site in both the lower and middle units of the PRM. Water-level monitoring at the station is consistent with the regional water-level changes resulting from the increased withdrawals in Delaware (Reference 2.4.12-34).

This indicates that the observed decrease in water levels in observation wells located at Artificial Island are part of a larger regional trend rather than a result of station-related withdrawals. This conclusion is supported by data documenting increased water withdrawals (both location and quantity) in lower New Castle County, DE and water-level maps prepared by the USGS as part of a long-term groundwater monitoring program. Artificial Island is not included in either the Southeastern Pennsylvania Ground Water Protected Area, or a New Jersey critical area, and the DRBC monitors these regional groundwater sources (Reference 2.4.12-16). PSEG currently

**PSEG Site
ESP Application
Part 2, Site Safety Analysis Report**

withdraws less than the allocation authorized by DRBC and NJDEP. The calculated zone of influence for the new plant water demand does not overlap or impact any off-site water users. Therefore the additional groundwater demands required by the new plant do not impact regional groundwater supply (Reference 2.4.12-28).

2.4.12.3 New Plant Water Use

Groundwater withdrawal is required to support the new plant. The projected volumes are estimated, the pumps and storage requirements will be determined after a reactor technology is determined and plant layout is finalized. The following subsections present the additional groundwater needs to support both plant construction and the existing and new plant operations.

2.4.12.3.1 Water Demands to Support Construction

Water use requirements for construction of a nuclear plant are similar to those for other large industrial construction projects. Water is required for typical construction uses such as dust suppression and concrete mixing.

The amount of water needed to support new plant construction is estimated using the historical water use data from construction of the existing plants. The new plant will use 119 gpm of groundwater to support concrete batch plant operations, dust suppression, and potable use. The existing water supply system currently provides 378 gpm to support HCGS and SGS operations. The existing water allocation permit allows for additional withdrawal beyond the current SGS and HCGS uses. There is sufficient capacity to provide the groundwater needed to support the new plant construction within the current NJDEP and DRBC allocations. The current permits and authorizations will be modified as necessary to include the new plant, or new permit(s) for water withdrawal will be obtained. The existing capacity and permitted withdrawal levels are discussed further in Subsection 2.4.12.3.2. This additional volume will not alter groundwater flow directions in the lower PRM aquifer.

2.4.12.3.2 Water Demands to Support Existing and New Plant Operations

Groundwater in the region is used for both potable and plant needs, with the closest non-PSEG well located 3.5 mi. away. Groundwater withdrawal during normal plant operation supports makeup to the demineralizer system, fire protection system, sanitary and potable systems, and other miscellaneous uses.

The groundwater withdrawal for the new plant is 210 gpm, which equals 110.4 Mgy (see Table 2.4.1-9). The withdrawal for normal operation, including SGS and HCGS average historic withdrawals (see Table 2.4.12-6) and the new plant, is 309 Mgy. This value is approximately 3% percent above the current SGS and HCGS site permitted annual water withdrawal. The highest SGS and HCGS historic groundwater withdrawal is 232.5 Mgy (1995). PSEG will continue to manage water use to further reduce the potential impact of the new plant on groundwater resources.

When a reactor technology is selected and a final site water balance developed, PSEG will re-evaluate total site (SGS, HCGS, and new plant) water use against the site water allocation

**PSEG Site
ESP Application
Part 2, Site Safety Analysis Report**

permit limits. The current permits and authorizations will be modified as necessary to include the new plant, or new permit(s) for water withdrawal will be obtained.

As described In Subsection 2.4.12.2.2, there are currently four pumping wells and two backup wells providing groundwater to HCGS and SGS. Pumping wells PW-5 (maximum limit 800 gpm), HC-1 (maximum limit 750 gpm), HC-2 (maximum limit 750 gpm), and PW-6 (maximum limit 600 gpm) extract groundwater from the PRM aquifer. Backup wells PW-2 (maximum limit 300 gpm) and PW-3 (maximum limit 600 gpm) extract groundwater from the Mount Laurel-Wenonah aquifer.

To support the initial HCGS/SGS groundwater use permit, groundwater modeling was conducted to evaluate aquifer properties. This modeling was conducted by Dames and Moore in 1988. Dames and Moore used the Princeton Transport Code model to run simulations at different rates to evaluate potential aquifer responses to changes in withdrawal rates, as well as to understand the potential impacts of saline intrusion on the Mount Laurel-Wenonah and PRM aquifers (Reference 2.4.12-12). The model is calibrated using field observations from 1973 forward, when some of the supply came from the Mount Laurel-Wenonah aquifer. Since the model focused on the potential effects of pumping in the deeper aquifers, shallower aquitards and aquifers above the Mount Laurel-Wenonah aquifer are not included in the model. The seven layers in the model (shallowest to deepest), with approximate thicknesses in parentheses, represented: 1) the Mount Laurel-Wenonah aquifer (100-125 feet); 2) the Matawan Aquitard, including the Merchantville, Woodbury, Englishtown, and Marshalltown Formations (140-150 feet); 3) the Magothy Sand (20-45 feet); 4) Upper Raritan Clay (250-320 feet); 5) Upper Raritan Sand (70-100 feet); 6) Middle Raritan Clay (260-270 feet); and 7) Middle Raritan Sand (45-55 feet). The Dames and Moore model covers an area of approximately 6.25 by 8 miles, with rectangular element sizes varying from 4500 by 5000 feet at the model perimeter to 500 by 500 feet covering the site, centered in the model grid.

Dames and Moore simulated continued water withdrawals (at the 1987 rates of 736 gpm average) for the period of 1987 to 2007. Additional simulations included eliminating withdrawals from the Mount Laurel-Wenonah wells and from PW-6 in the Middle PRM, with a new hypothetical well, "PW-7" in the Magothy sand, added in conjunction with increases at HC-1 and HC-2. This results in a modeled increase in flow rate to 875 gpm. A final simulation held the same withdrawal rate with a different well configuration. The final simulation configuration (PW-5 at 200 gpm, HC-1 and HC-2 at 268 gpm each, and hypothetical PW-7 at 139 gpm) provided adequate supply with appropriately limited drawdown and without any significant increases in chloride levels at the production wells. Note that the total withdrawal simulated in the increased demand scenario (875 gpm) is considerably more than the current total of 371 gpm (average demand over 2002 to 2007), with differing distribution of flow rates among wells. Pumping rates in this simulation were also greater than those projected for future post-expansion construction normal use. The model was run for 20 years, ending in 2007. Monitoring required by NJDEP has determined that salinity concentrations remain acceptable. Therefore, the Dames and Moore model results are applicable to the evaluation of future use and capabilities of the groundwater supplies.

The results of the Dames and Moore analysis indicate that there are no significant impacts on the region and that the PRM can support volumes of withdrawal up to levels almost twice the current usage. These model runs also demonstrate that additional withdrawals will not cause a significant increase in chloride concentrations in the Upper PRM, even at simulated flow rates of nearly twice those of current operation (Reference 2.4.12-12).

**PSEG Site
ESP Application
Part 2, Site Safety Analysis Report**

The results of the Dames and Moore modeling remain conservative and applicable. The grid size is consistent with, and smaller across the facility than, USGS modeling studies of the New Jersey coastal plain aquifer system (References 2.4.12-35 and 2.4.12-38). In addition, the simulations performed by Dames and Moore in evaluating future potential groundwater use included a 20-year simulation wherein present water supply well rates for HC-1, HC-2 and PW-5 are increased to a total annual demand of 736 gpm, or 387 million gallons per year (Reference 2.4.12-12). This is approximately 25% in excess of the projected demand on the Upper PRM as projected for the expanded site and above the current permit limit. The Dames and Moore modeling indicates no significant increase in expected chloride concentrations relative to the supply criterion of 250 milligrams per liter (mg/L). Since the Dames and Moore model was constructed, no significant degradation of the water supply from the Upper PRM has been observed. The results of the Dames and Moore modeling remain conservative and applicable to projected groundwater use.

Three existing groundwater supply wells (HC-1, HC-2, and PW-5) will remain as the primary supply wells for the site. A new well in the PRM may be installed within the property boundary north of HC-1 and HC-2. Due to the isolating effects of the several intervening aquitards (Kirkwood, Navesink, Marshalltown, and Merchantville), no new transport pathways are anticipated due to the projected increase in the groundwater supply pumping from the Upper PRM. In addition, the dispersion of the projected water demand over a wider area within the Upper PRM with a new well will serve to limit changes to vertical and horizontal hydraulic gradients and overall groundwater flow regime to less than those that might arise solely from increases at the existing well locations.

The Dames and Moore study was conducted independently of the regional trends; additional groundwater withdrawals to support the new plant do not impact regional groundwater supply.

2.4.12.3.3 Monitoring or Safeguard Requirements

Once the final technology is selected and the footprint of the new plant determined, the existing PSEG groundwater monitoring programs will be evaluated with respect to placement of the new plant to determine if any additional monitoring of existing or construction of new observation wells will be required to adequately monitor groundwater levels. This evaluation will include a review of the observation wells installed for the ESPA to determine if they may be used as part of a longer-term groundwater monitoring program. The results will be presented in the combined license (COL) application (Reference 2.4.12-1).

Best management practices and safeguards will be used to minimize the potential for adverse impacts to the groundwater. These practices will be implemented in conjunction with NJDEP and EPA requirements such as the use of lined containment structures and secondary containment and hazardous materials storage areas as required under the EPA Resource Conservation and Recovery Act (RCRA).

**PSEG Site
ESP Application
Part 2, Site Safety Analysis Report**

2.4.12.4 Dewatering and Post-Construction Groundwater Simulations

2.4.12.4.1 Dewatering and Construction Activities

Prior to facility construction, the main power block area will be excavated and dewatered to facilitate construction. By means of a dewatering system, the upper aquifer will be dewatered in the immediate vicinity of the excavation. The groundwater in the Vincentown aquifer, the second aquifer encountered below the land surface at the site, was modeled to simulate a draw down to approximately elevation -70 ft. NAVD. Upon completion of construction and backfilling in this area, dewatering will be discontinued. Following decommissioning of the dewatering system, the groundwater will return to a natural condition, which will be slightly higher than preconstruction water levels. The soil retention barrier walls will be left in place, therefore groundwater levels inside the barrier are predicted to be at or slightly above the elevation of the top of the barrier. The plant grade will be established at 36.9 ft NAVD, and therefore, groundwater levels will be lower than the maximum levels indicated in the PPE. Permanent dewatering is not required and the reliability of safety-related dewatering systems is not addressed.

2.4.12.4.1.1 Groundwater Modeling in Support of Dewatering Activities

To assess the potential impacts to existing safety-related structures, a numerical groundwater flow model is developed to provide estimates of groundwater flow during proposed dewatering activities at the new plant. By modeling the dewatering scenarios, the data is used to estimate the drawdowns in aquifers across the site and specifically to identify where dewatering could impact the existing safety-related structures, systems, and components (SSC). The dewatering model outputs are also used to estimate post-construction groundwater flow conditions and to estimate potential hydrostatic loadings on proposed and existing safety-related SSCs.

The dewatering model for the ESPA is performed in support of calculations to provide estimates of temporary construction dewatering rates and potential effects on safety-related structures in the vicinity of the proposed PSEG plant. The dewatering model is focused on the potential effects of construction dewatering for the new plant on the shallow aquifers. Thus, the dewatering model includes strata only from ground surface down through the Mount Laurel-Wenonah aquifer, the underlying Marshelltown aquitard being considered suitably thick and of sufficiently low permeability to be considered impermeable for purposes of this modeling. The dewatering model is distinct from the Dames and Moore model (see Subsection 2.4.12.3.2) in purpose and focus, and the only formation the models share in common is the Mount Laurel-Wehnonah. Thus, the dewatering model for the ESPA temporary construction dewatering does not incorporate the layers, grid or other model parameters from the Dames and Moore model.

The groundwater dewatering model is constructed to cover the PSEG Site and extends 7520 feet in a north-south direction and 7000 feet in an east-west direction. The model is bounded to the west and south by the Delaware River and employs a uniform grid spacing of 20 feet, resulting in a model with 376 rows and 350 columns. The Delaware River provides a natural hydrogeologic boundary to the west and south of the model, while no-flow boundaries are assumed to the north and east where wetlands provide natural discharge locations for the shallow aquifer and are distant from the location as represented in the model domain. The modeled area covers approximately 1200 acres to simulate the effect on groundwater elevation of the dewatering within the power block area of the new plant location. The model includes the shallow aquifer system, with seven layers, each representing the identified shallow

**PSEG Site
ESP Application
Part 2, Site Safety Analysis Report**

hydrogeologic units (i.e., the fill materials, the Alluvium aquifer, the Kirkwood aquitard, the Vincentown Formation, the Hornerstown Formation, the Navesink aquitard, and the Mount Laurel-Wenonah aquifer). The top of the next lower formation, the Marshalltown aquitard, is considered impermeable and serves as the base of the model domain.

Following successful calibration of the dewatering model to observed water levels in the alluvial aquifer, the model is used with modifications to the layering to depict the dewatering scheme and to provide estimates of dewatering rates for a dewatering scenario. A reactor technology has not been selected; therefore, the construction dewatering model is based on an excavation size that bounds the anticipated excavation dimensions and location for the technologies being considered. The dewatering scenario includes the dewatering of the plant area (bounding dimensions of 1950 ft. by 1700 ft.) (Figure 2.4.12-27) down to the Kirkwood aquitard. A smaller, deeper excavation is advanced in the central area beneath the safety-related structures to access the competent layer, as discussed in Subsection 2.5.4.5. This deeper excavation extends through the Kirkwood Formation and into the founding layer in the Vincentown Formation. The majority of the dewatering is accomplished using dewatering wells installed at the perimeter of the shallow and deeper excavation limits. Both the shallow and deep excavations also include the installation of soil retention barriers having low permeability characteristics that affect groundwater flow.

The modeling of the dewatering approach considered for construction provides an estimate of approximately 5600 gpm to dewater the larger (plan view), shallower excavation to the top of the Kirkwood Formation. The transition into dewatering the smaller (plan view), deeper excavation, into the Vincentown Formation, is estimated to require dewatering rates of about 5230 gpm. These are initial rates for each phase of the excavation, and taper off with time, eventually requiring a total long-term rate of about 3600 gpm for the entire excavation. Analyses of dewatering rates performed on sensitive input parameters suggested a range of long-term flow rates from 3400 to 5400 gpm. This range of rates does not include influx of water from storm events, which must be dealt with separately.

The proximity of the power block excavation area to the Delaware River and the model perimeter boundary conditions are also considered. The use of river and general head boundary (GHB) type boundary conditions rather than constant head boundaries is chosen to alleviate a potential concern for constant heads providing an unlimited sink or source of water in the model. Further, in evaluating the results of the base dewatering simulation, relative contributions to wells along the perimeters of the proposed excavations nearer these boundaries are compared with those farther away. These comparisons indicate that the combined pumping for the northern wells (both inner and outer rings of wells) at the end of the simulated period as compared to the southern wells are in the ratio of 53 to 47 percent. Similarly, comparing the western wells nearer the river to the eastern wells further away resulted in a ratio of 55 to 45 percent. This is realistic considering the setting. The resultant head and drawdown contours projected by the model, while compressed near the boundaries (i.e., steeper), are considered realistic for areas interior to the model and in the vicinities of the safety-related structures.

The dewatering scenario and dewatering estimates provided in the ESP are preliminary and are based on the bounding excavation dimensions. Groundwater modeling will be refined after the reactor vendor is selected, and the final excavation geometry is determined. Preparation of the combined license application (COLA) requires additional data, which is obtained from pumping

**PSEG Site
ESP Application
Part 2, Site Safety Analysis Report**

tests or other methods, to further refine hydrogeologic parameters and model estimates of dewatering rates and drawdowns beneath existing site structures.

Note that dewatering the shallow hydraulic fill and alluvium may be difficult to accomplish with dewatering wells located far from the center of the power block. It may be necessary to include other measures, such as sand drains, to dewater the fill and alluvium in a timely manner. However, the design of the dewatering system is further evaluated in the COL application after the technology and plant layout is selected.

The dewatering scenario estimated pumping rates do not specifically include simulation of short-term storm events which could introduce significant amounts of precipitation into an open excavation. These are common events during large-scale excavation projects. Suitable storm pumps will be made available during the excavation period to rapidly remove the storm water.

The excavation area, as well as the results of the modeled steady-state dewatering (shown as contours of the potentiometric surface for formations of interest), are shown on Figures 2.4.12-25 through 2.4.12-27.

2.4.12.4.1.2 Model Calibration

Calibration of the steady-state numerical groundwater dewatering model to existing conditions consists of adjusting hydrogeologic parameters, including boundary conditions, to approximate observed piezometric heads over the site within the alluvial and Vincentown aquifers, and to be consistent with observed hydraulic gradients and interpreted groundwater flow directions. Monthly groundwater level data were collected from January 2009 through December 2009 from observation wells installed in the Alluvium and the Vincentown Formation. Other hydrogeologic parameters were adjusted during calibration. The values used in the model are consistent with either site-specific tests or observations, or literature reported ranges of the parameters (e.g., hydraulic conductivity or transmissivity).

Dewatering model calibration is performed by varying key parameter inputs to approach the calibration criteria (i.e., minimizing residuals [the difference between observed and model computed piezometric head values] analysis statistics) while matching observed and interpreted groundwater heads, gradients and flow directions within reasonable ranges of site-specific or literature-reported aquifer parameter values for each of the aquifer units. These key parameters included horizontal and vertical hydraulic conductivity for aquifers, vertical hydraulic conductivity for aquitards, reference heads for river and other specified boundary conditions, and areal distribution of recharge. These adjustments in model parameters are first conducted manually and then through the use of the parameter estimating program PEST (Reference 2.4.12-43). Final calibrated model parameter values are presented in Table 2.4.12-14. Each of these values is within ranges provided by site-specific or literature reported values. Vertical and horizontal hydraulic conductivity values are specified as one single value per layer except where hydraulic fills have been replaced with structural fill. The statistical analysis of residuals is summarized on Table 2.4.12-15. The match of computed groundwater heads and groundwater flow directions and gradients with observed values is depicted on Figure 2.4.12-30.

The calibration process is augmented by a sensitivity analysis which varied dewatering model input parameter values individually to see the effects of uncertainty in model input values. The calibration is guided by using the averages of site-specific water level measurement events

**PSEG Site
ESP Application
Part 2, Site Safety Analysis Report**

taken monthly over 2009 in 30 newly installed Alluvium and Vincentown wells. This data was augmented by the use of September 2009 water level measurements in 12 previously existing Alluvium monitoring wells distributed across the facility. The September 2009 water levels in the 12 older Alluvium wells are very similar to levels measured in these same wells in 2006 (Reference 2.4.12-2).

A statistical approach is used to assess the average data set for water levels. This approach is not intended to directly analyze the individual tidal responses or responses to specific precipitation events. The objective of the approach is to infer from the data which wells are affected by these influences. It is also intended to determine to what degree that effect might have on the mean of the water level data for each well. The year's data allows the use of the average as a target calibration water level data set for the dewatering model. The elimination of probable outliers (possible measurement errors) from the data set is followed by the successive trimming of maximum and minimum values at each well through three stages of trimming. This process indicated that tidal and precipitation effects have little effect on the stability of the mean of the year's data except for two wells (NOW-2L and NOW-2U). The effect at these wells appears to be only on the order of 0.2 to 0.3 feet. These results also suggest that there are no abnormal tidal or precipitation events that might significantly skew the data set. The averages of the target locations are sufficient for model calibration at steady-state conditions.

Hydraulic conductivities are varied by factors of from 0.25 to 4, and reference heads from minus to plus two feet over calibrated values. The more sensitive model input parameters relative to the calibration (residuals analysis) are determined to be recharge, vertical conductance of the Kirkwood aquitard, specified conductances and reference heads for Vincentown and Mount-Laurel-Wenonah aquifer boundary conditions, reference head for the Delaware River, and horizontal hydraulic conductivity of the Alluvium and Mount Laurel-Wenonah aquifer units.

For the dewatering simulations, the applied stresses overcome generally occurring hydrogeologic conditions, and the results of the dewatering simulations are subject to a somewhat differing set of sensitive parameter values. In developing an estimate of anticipated pumping rates to attain target drawdowns during dewatering, the calibrated model is first used to develop what is considered to be the best estimate. Then a sensitivity analysis is conducted to identify the sensitive parameters for the dewatering scenarios and then vary these over reasonable ranges (e.g., horizontal hydraulic conductivities by factors ranging from 0.5 to 2 times the calibration value). The sensitivity analysis is summarized and the resultant ranges of estimated dewatering pumping rates summarized as indicated in Subsection 2.4.12.4.1.3.

2.4.12.4.1.3 Sensitivity Analysis

A sensitivity analysis is performed on the calibrated dewatering model, indicating the most sensitive parameters in the model include the net recharge rate, the horizontal hydraulic conductivity of the alluvium, the vertical hydraulic conductivity of the Kirkwood and Navesink aquitards, and hydraulic conductivity of the Mount Laurel-Wenonah formation and boundary reference heads in the Alluvium, Vincentown and Hornerstown aquifers. Table 2.4.12-12 summarizes the model input parameters included in this sensitivity analysis and the effects on the summary fit point-wise statistics.

A second sensitivity analysis is performed for the dewatering simulations, varying key model parameters to determine a reasonable range of expected dewatering rates that could be

**PSEG Site
ESP Application
Part 2, Site Safety Analysis Report**

encountered. This sensitivity analysis is summarized in Table 2.4.12-13, and discussed further in the following section.

2.4.12.4.1.4 Conclusions

The conclusions from the dewatering model can be grouped into several categories as listed below:

Dewatering Rates and Long-Term Rate Sensitivity

The modeling of the dewatering approach considered for the new plant construction indicates an estimate of 5600 gpm to dewater the larger (plan view), shallower excavation to the top of the Kirkwood Formation. The transition into dewatering the smaller (plan view), deeper excavation, into the Vincentown Formation, is estimated to require dewatering rates of 5230 gpm. These are initial rates for each phase of the excavation, and taper off with time, resulting in a total long-term rate of approximately 3600 gpm. Sensitivity analyses indicate a range of long-term flow rates from 3400 to 5400 gpm. These rates do not include influx of water from storm events.

Drawdown of Aquifer at Existing Structures

Dewatering results in considerable drawdowns of the groundwater level in order to maintain these levels below the target excavation depths. Dewatering may also affect existing site structures. Figures 2.4.12-25 through 2.4.12-27 show the zones of influence for the three primary water-bearing units (the hydraulic fill, the riverbed deposits, and the Vincentown aquifer). Based on the zone of influence, the below existing structures are within the projected zone of dewatering influence. The effect of dewatering on these structures is discussed in Subsection 2.5.4.6.3.1.

- Hope Creek Cooling Tower
- Independent Spent Fuel Storage Installation
- Wastewater Treatment Plant
- Hope Creek Switchyard
- Learning and Development Center
- Hope Creek Nuclear Island
- Fuel Oil Tank
- Material Center
- Low Level Radioactive Waste Building

Anticipated Changes in Shallow Groundwater Flow Patterns

Modeling of post-construction conditions indicates that groundwater flow patterns and water levels return to the preconstruction conditions over most of the model domain. Only slight increases of 0.5 ft. are noted in some portions of the model. Changes to the site following construction also include:

**PSEG Site
ESP Application
Part 2, Site Safety Analysis Report**

- The presence of the abandoned in place soil retention barriers
- A localized portion of the Kirkwood aquitard that is replaced with structural fill
- Placement of fill to establish a plant grade to 36.9 NAVD
- Removal of shallow perched ponds within the excavation footprint
- Replacement of existing vegetation with developed hard surface

These physical changes cause some variation in flow patterns. However, the projected piezometric heads in the fill and alluvial deposits are not expected to be much greater than the current static conditions.

Simulations of post-development groundwater conditions are based on a soil retention barrier top elevation of 5 ft. NAVD. Modeling indicates an average hydrostatic loading of 3 to 4 ft. at the center of the proposed development area, and a maximum elevation of 5.2 ft. NAVD within the power block area. Based on these results, a design loading of 6 ft. is recommended, and is consistent with that proposed for HCGS. The elevations of the bottom of the new structures may be deeper than the groundwater table. Preconstruction and post-construction water levels in shallow units appear to be similar. Post-construction shallow water levels are only 0.5 ft. higher in some areas of existing structures (e.g., HCGS cooling tower) requiring no permanent long-term dewatering.

The characteristics of the soil retention barriers left in place, may also locally affect the hydrostatic loading. The new plant grade will be raised to 36.9 ft. NAVD, therefore, groundwater levels within the area will be at or near the top of the groundwater barrier walls (6 ft. NAVD). Thus, the anticipated hydrostatic loading on the future structures is less than the conservative hydrostatic water-level on which the DCDs are based.

Therefore, the proposed development only slightly alters groundwater flow patterns from current conditions in the areas of present facilities, and there is no need for a permanent dewatering system.

Sensitive Parameters in Model Calibration

Based on calibration of the dewatering model to observed conditions in the alluvial and Vincentown aquifers, the most sensitive input parameters include recharge applied over the model area (including seepage losses from existing artificial ponds in the new plant location), horizontal hydraulic conductivity of the aquifer units, vertical hydraulic conductivity of the Kirkwood and Navesink aquitards, and general head boundary reference heads in the Alluvium, Vincentown, and Hornerstown formations.

**PSEG Site
ESP Application
Part 2, Site Safety Analysis Report**

Sensitive Parameters in the Dewatering Simulation

Based on the dewatering simulations, the most sensitive parameters controlling anticipated dewatering pumping rates include the hydraulic conductivity of the Vincentown and Hornerstown formations, and the vertical hydraulic conductivity of the Navesink leaky aquitard. In these simulations, the majority of the groundwater pumped during dewatering came from the Vincentown and Hornerstown formations. A much lesser contribution came from the alluvium and hydraulic fill. Some upwelling from the Mount Laurel-Wenonah aquifer occurred as the drawdown created by the dewatering in the Vincentown caused an upward gradient across the leaky Navesink aquitard.

Sensitivity analyses were performed on the dewatering model run, varying key parameters of the hydraulic conductivity of the Vincentown Formation, the vertical hydraulic conductivity of the leaky Navesink aquitard, and the vertical hydraulic conductivity of the Kirkwood aquitard. Averaging short-term initial rates, the model provided best estimates from 5200 to 5600 gpm over a year's simulation. The sensitivity analysis indicated the expected range might vary from 3000 to 7600 gpm (averaging short-term initial rates). Estimated dewatering rates are generally consistent with those documented during the construction of HCGS. The dewatering rates do not include stormwater which may fall within the excavation limits.

2.4.12.4.1.5 Dewatering Model Simulation Summary

The dewatering model provides the expected groundwater response to dewatering and post-construction scenarios. However, the dewatering scenario and dewatering estimates are based on the assumed excavation boundaries. Groundwater modeling will be refined after a reactor technology is selected, and the final excavation geometry is determined.

Data gathered in support of the ESPA, combined with the location and size of the proposed plant excavation area, indicates that additional data is needed to refine estimates of dewatering rates and the potential for excessive drawdown at existing structures during the dewatering period. Once PSEG determines the technology and site layout, pumping tests will be performed at the site to further refine the groundwater model. The pumping tests are used to determine:

- aquifer characteristics of the Vincentown Formation in the proposed area of construction
- determine the effectiveness of the Kirkwood aquitard to limit drawdown in the alluvial aquifer and fill (as it is absent in some locations)
- assess potentials for upwelling from the underlying Mount Laurel-Wenonah formations during dewatering
- assess the potential for encountering recharge boundaries in the Vincentown Formation in the northern portion of the proposed power block area

2.4.12.4.2 Post-Construction Operations

Post-construction, the natural groundwater recharge regime to the shallow aquifer will be modified as compared to the natural preconstruction conditions. The final ground surface will be raised to 36.9 ft. NAVD. Pavement and structures reduce or prevent groundwater recharge beneath their footprints. Unpaved areas covered by permeable gravel or fill receive additional recharge compared to preconstruction conditions. Groundwater modeling indicates that the

**PSEG Site
ESP Application
Part 2, Site Safety Analysis Report**

effect of the power block intrusion into the shallow aquifer could be a slight increase of 0.6 ft. in the up gradient direction above current average water-level conditions in the area.

The model constructed to evaluate the impact of dewatering is also used to evaluate groundwater contours following plant construction. Figures 2.4.12-28 and 2.4.12-29 show the estimated potentiometric contours for groundwater in the Alluvium, and Vincentown aquifer.

2.4.12.5 Design Basis for Hydrostatic Loading

The design elevation of the new plant is 36.9 ft. NAVD. The ground surface will be elevated by approximately 27 ft. Following decommissioning of the dewatering system, the groundwater will return to a natural condition, which will be slightly higher than preconstruction water levels. The soil retention barrier walls will be left in place, therefore groundwater levels inside the barrier are predicted to be at or slightly above the elevation of the top of the barrier.

Based on the plant elevation and groundwater conditions, permanent dewatering is not required and the reliability of safety-related dewatering systems is not addressed.

Prior to construction and dewatering of the site, as demonstrated by the current conditions (Subsection 2.4.12.1), the water table is several feet below the land surface and within the hydraulic fill. Though the water table within the hydraulic fill is perched, the water elevations measured from wells screened within the underlying Alluvium have been measured to be -0.5 ft. to 2.2 ft. NAVD or 8 to 11 ft. below ground surface.

With the replacement of large areas of hydraulic fill with structural fill, the water levels observed in the Alluvium are representative of water levels in this area. Water levels in the upper aquifer (Alluvium) at the proposed new plant location have been observed to range from -0.5 ft. to +2.2 ft. (January 2009 to December 2009 data), with a hydraulic gradient of 0.1 percent across the new plant location toward the Delaware River.

Groundwater levels in the deeper aquifer (Vincentown aquifer) were observed to range from -1.0 ft. to +2.8 ft. NAVD (January 2009 to December 2009 data). Generally, vertical gradients are downward from the alluvial aquifer to the Vincentown aquifer across the confining Kirkwood aquitard unit, but greater tidal influence in the Vincentown aquifer may reverse this intermittently.

The hydrogeologic setting, under normal conditions, is one of slight recharge through the land surface and vertically downward through the low permeable hydraulic fill to the alluvial aquifer. Groundwater migrating westward through the alluvial aquifer toward the Delaware River may discharge upward through river sediments into the water column. Some exchange between the Alluvium and Vincentown aquifers may occur, especially where the Kirkwood is thin or absent, but generally, the low permeable Kirkwood forms a barrier between the two confined aquifers.

The Vincentown aquifer may receive some seepage from above, but is generally recharged some distance to the north as the Vincentown Formation slopes upward toward the fall line and daylights. Structural fill placed around and beneath the various safety-related structures of the proposed plant is expected to form a permeable hydraulic conduit connecting the shallow aquifer with the Vincentown aquifer. Therefore, when the excavation is completely backfilled and the dewatering system is decommissioned, water levels outside the barrier wall in the two

**PSEG Site
ESP Application
Part 2, Site Safety Analysis Report**

aquifers are predicted to return to near preconstruction levels. The new normal level is expected to be the same for both aquifers under the site.

It is unlikely that the tidal influence observed in the confined Vincentown aquifer will be manifested in the more shallow soils following construction. This is consistent with the post-construction groundwater regime at SGS (Reference 2.4.12-1).

For purposes of foundation analysis, the maximum groundwater elevation within the new power block area is expected to range from 6 to 10 ft. NAVD. This range is dependent on the final design height of the top of the soil retention barrier as well as factors such as recharge of precipitation over the area, the thickness and permeability of the barrier, and the degree of connection between the fill areas and the Vincentown aquifer.

2.4.12.6 References

- 2.4.12-1 ARCADIS, Remedial Investigation Report. PSEG Nuclear, LLC, Salem Generating Station, Hancock's Bridge, New Jersey, March 2004.
- 2.4.12-2 ARCADIS G&M, Inc., Site Investigation Report, Salem Generating Station. PSEG Nuclear, LLC, Salem Generating Station, Hancock's Bridge, New Jersey, July 15, 2006.
- 2.4.12-3 Bouwer, H., and R.C. Rice, "A Slug Test for Determining Hydraulic Conductivity of Unconfined Aquifers with Completely or Partially Penetrating Wells," Water Resources Research, v. 12, no. 3, pp. 423 – 428, 1976.
- 2.4.12-4 Cooper, H.H., J.D. Bredehoeft, and I.S. Papadopoulos, "Response of a Finite-Diameter Well to an Instantaneous Charge of Water," Water Resources Research, v. 3, no. 1, pp. 263 – 269, 1967.
- 2.4.12-5 Dames & Moore, "Groundwater Supply Investigation, Proposed Nuclear Power Plant Near Salem NJ," 1968.
- 2.4.12-6 Dames & Moore, "Investigation of Saline Production Well No. 4," 1970.
- 2.4.12-7 Dames & Moore, "Groundwater Supply Well #5," 1974.
- 2.4.12-8 Dames & Moore, "Groundwater Supply Investigation, Hope Creek," 1974.
- 2.4.12-9 Dames & Moore, "Report of Foundation Studies, Proposed Salem Nuclear Generating Station, Salem, New Jersey, Public Service Electric & Gas Company," August 28, 1968
- 2.4.12-10 Dames & Moore, "Report of Foundation Studies, Proposed Hope Creek Generating Station, Lower Alloways Creek Township, New Jersey Public Service Electric and Gas Company," May 23, 1974.

**PSEG Site
ESP Application
Part 2, Site Safety Analysis Report**

- 2.4.12-11 Dames & Moore, Report, "Stages 3 to 10, Excavation/Dewatering, Hope Creek Generating Station, Lower Alloways Creek Township, New Jersey" PSE&G Company, October 1977.
- 2.4.12-12 Dames & Moore, "Final Report Study of Groundwater Conditions and Future Water-Supply Alternatives Salem/Hope Creek Generating Station, Artificial Island, Salem County, New Jersey," PSE&G. July 15, 1988.
- 2.4.12-13 Delaware Department of Natural Resources and Environmental Control, Well Database, Division of Water Resources, Water Supply Section, Well Permits Branch, August 25, 2009
- 2.4.12-14 Delaware River Basin Commission, "Delaware River, State of the Delaware River Basin Report 2008," Website, <http://www.nj.gov/drbc/SOTB/index.htm>, 2008, accessed June 26, 2009.
- 2.4.12-15 Delaware River Basin Commission, Groundwater Withdrawal, Docket No. D-90-71 Renewal, West Trenton, New Jersey, November 1, 2000.
- 2.4.12-16 Delaware River Basin Commission, Information about the Delaware River, <http://www.state.nj.us/drbc/thedrb.htm> , Trenton, New Jersey, 2008.
- 2.4.12-17 Delaware Environmental Observing System, Website http://www.deos.udel.edu/monthly_retrieval.html, accessed December 23, 2009.
- 2.4.12-18 Dugan, B. et al, "Hydrogeologic Framework of Southern New Castle County, Open File Report No. 49, Delaware Geological Survey, Newark, Delaware, 2008.
- 2.4.12-19 Hvorslev, M. J., "Time Lag and Soil Permeability in Ground Water Observations," U.S. Army Corps of Engineers, Waterways Experiment Station, Bulletin Number 36, 50 pp., 1951.
- 2.4.12-20 New Jersey Department of Conservation and Economic Development, Division of Water Policy and Supply, Special Report 33 – Geology and Groundwater Resources of Salem County New Jersey, 1969.
- 2.4.12-21 New Jersey Department of Environmental Protection, Open Public Records, Website, http://datamine2.state.nj.us/DEP_OPRA/OpraMain/get_long_report?, accessed April 30, 2009.
- 2.4.12-22 New Jersey Department of Environmental Protection, Water Allocation Permit WAP040001, Trenton, New Jersey, December 30, 2004,
- 2.4.12-23 New Jersey Department of Environmental Protection, Public Community Water-Supply Wells of New Jersey, Website <http://www.state.nj.us/dep/njgs/geodata/dgs97-1.htm>, accessed March 5, 2009.

**PSEG Site
ESP Application
Part 2, Site Safety Analysis Report**

- 2.4.12-24 New Jersey Department of Environmental Protection, Digital Geodata Series, DGS98-5 Aquifers of New Jersey, Website
<http://www.state.nj.us/dep/njgs/geodata/dgs98-5.htm>, Accessed July 23, 2009.
- 2.4.12-25 PSEG, Letter to Ms. Diane E. Zalaskus, NJDEP, PSEG Nuclear LLC Water Allocation Permit, Program Interest ID 2216P, Activity Number WAP040001, First Quarter Report – 2009 dated April 17, 2009.
- 2.4.12-26 PSEG, Letter to Ms. Diane E. Zalaskus, NJDEP, PSEG Nuclear LLC Water Allocation Permit, Program Interest ID 2216P, Activity Number WAP040001, Second Quarter Report – 2009 dated July 21, 2009.
- 2.4.12-27 PSEG, Letter to Ms. Diane E. Zalaskus, NJDEP, PSEG Nuclear LLC Water Allocation Permit, Program Interest ID 2216P, Activity Number WAP040001, Third Quarter Report – 2009 dated October 29, 2009.
- 2.4.12-28 PSEG, Letter to Ms. Diane E. Zalaskus, NJDEP, PSEG Nuclear LLC Water Allocation Permit, Program Interest ID 2216P, Activity Number WAP040001, Fourth Quarter Report – 2009 dated January 14, 2010.
- 2.4.12-29 PSEG, Applicant's Environmental Report – Operating License Renewal Stage Salem Operating Generating Station, Unit 1 Docket No. 50-272, Unit 2 Docket No. 50-311,
- 2.4.12-30 Sugarman, P. et al., "Hydrostratigraphy of the New Jersey Coastal Plain: Sequences and Facies Predict Continuity of Aquifers and Confining Units," Stratigraphy, Vol. 2, no.3, pp. 259 – 275, 2005.
- 2.4.12-31 Salem County Government, Farmland Preservation, Website:
http://www.salemcountynj.gov/cmssite/downloads/Farmland_Preservation/Ch1_2.pdf, accessed September 2, 2009
- 2.4.12-32 U.S. Environmental Protection Agency, 2009, Federal Register Notice, Volume 53, No. 122, Page 23791, "Sole Source Aquifer Determination for the NJ Coastal Plain Aquifer System," Website,
http://www.epa.gov/r02earth/water/eauifer/coast/fr_coast.htm, June 24, 1988, accessed September 8, 2009.
- 2.4.12-33 U.S. Geological Survey/State of New Jersey, "Geology and Ground-Water Resources of Salem County, New Jersey," State of New Jersey Department of Conservation and Economic Development, Division of Water Policy and Supply, Special Report No. 33. J. Rosenau, J, Lang, S, Hilton, G, and Rooney, J, 1969.
- 2.4.12-34 U.S. Geological Survey, "Delaware River Study Unit Description," National Water-Quality Assessment Program, Website,
<http://NJ.usgs.gov/nawqa/delr/su.descrpt.html>, accessed July 28, 2009.

**PSEG Site
ESP Application
Part 2, Site Safety Analysis Report**

- 2.4.12-35 U.S. Geological Survey, "Documentation of Revisions to the Regional Aquifer System Analysis Model of the New Jersey Coastal Plain," Lois M. Veronin, Water-Resources Investigations Report 03-4268, 2003.
- 2.4.12-36 U.S. Geological Survey 1983. Walker, R. L., "Evaluation of Water Levels in Major Aquifers of the New Jersey Coastal Plain, 1978," U. S. Department of the Interior, U.S. Geological Survey, Water- Resources Investigations Report 82-4077.
- 2.4.12-37 U.S. Geological Survey, "Ground-Water Flow in the New Jersey Coastal Plain," Martin, Mary, Professional Paper 1404-H, 1998.
- 2.4.12-38 U.S. Geological Survey, "Simulation of Ground-Water Flow and Movement of the Freshwater-Saltwater Interface in the New Jersey Coastal Plain," Pope, D. and A. Gordon. Water-Resources Investigations Report 98-4216, 1999.
- 2.4.12-39 U.S. Geological Survey 2001, Lacombe, P.J., and R. Rosman, "Water Levels in, Extent of Freshwater in, And Water Withdrawals from Ten Confined Aquifers, New Jersey and Delaware Coastal Plain, 1998," Reston, Virginia, U. S. Department of the Interior, U.S. Geological Survey, Water- Resources Investigations 00-4143.
- 2.4.12-40 U.S. Geological Survey 2001. Schreffler, C.L. "Simulation of Ground-Water Flow in the Potomac-Raritan- Magothy Aquifer System Near the Defense Supply Center Philadelphia, and the Point Breeze Refinery, Southern Philadelphia County, Pennsylvania," 48 p., New Cumberland, Pennsylvania, U. S. Department of the Interior, U.S. Geological Survey, Water-Resources Investigations 01-4218.
- 2.4.12-41 U.S. Geological Survey 2009. V. T. DePaul, R. Rosman, and P. J. Lacombe, "Water-Level Conditions in Selected Confined Aquifers of the New Jersey and Delaware Coastal Plain, 2003," 135p., Reston, Virginia, U. S. Department of the Interior, U.S. Geological Survey, Scientific Investigations Report 2008-5145.
- 2.4.12-42 Page, Leo, No. 6 Test and Production Well, 1981.
- 2.4.12-43 Doherty, J., 2004, PEST Model-Independent Parameter Estimation, Watermark Numerical Computing, Australia.

**PSEG Site
ESP Application
Part 2, Site Safety Analysis Report**

**Table 2.4.12-1 (Sheet 1 of 2)
Summary of Hydraulic Properties for Local and Regional Aquifers and Aquitards**

Formation	Transmissivity	Hydraulic Conductivity	Total Porosity	Storage Coefficient	Specific Capacity	Leakance	Reference
Structural Fill		0.09 to 4.3 ft/d; 6.5 ft/d					2.4.12-2 ^(a)
Alluvium Aquifer	13.2 to 440 gpd/ft	0.9 to 13.1 gpd/ft ²					2.4.12-12 ^(a)
		0.12 to 1.75 ft/d					2.4.12-12 ^(a)
		0.03 to 2.27 ft/d					2.4.12-2 ^(a)
Kirkwood Aquitard		Kv = 0.00002 to 0.00005 ft/d					2.4.12-37
						1E-05/d	2.4.12-38
Basal Kirkwood-Vincentown Aquifer					0.5 to 8.3 gpm/ft		2.4.12-33
	5000 to 11,000 gpd/ft	0.95 to 2.5 ft/d			0.3 to 1.9 gpm/ft		2.4.12-12 ^(a)
	530 ft ² /d						2.4.12-37
	2000 to 2500 ft ² /d						2.4.12-38
		14 ft/d					2.4.12-11 ^(a)
		2.95 ft/d					2.4.12-2 ^(a)
Hornerstown - Navesink Aquitard							2.4.12-35
		30 to 65 gpd/ft ²	0.522 to 0.543				2.4.12-33
		Kv = 0.42 gpd/ft ²					2.4.12-33
		Kv = 0.0005 to 9 ft/d					2.4.12-37
						5E-05/d	2.4.12-38
Mount Laurel - Wenonah Aquifer						3.35E-05 to 6.87E-05/d	2.4.12-35
	7000 gpd/ft	18.7 ft/d					2.4.12-5 ^(a)
		10 ft/d	0.444		0.7 to 9 gpm/ft		2.4.12-33
	7500 to 14,000 gpd/ft						2.4.12-6 ^(a)
	4900 to 8700 gpd/ft	0.67 to 4.5 ft/d			0.2 to 3.8 gpm/ft		2.4.12-12 ^(a)
	360 to 1430 ft ² /d	13 to 19 ft/d					2.4.12-37
	1000 ft ² /d						2.4.12-38
	815 ft ² /d						2.4.12-18
Marshalltown-Wenonah Aquitard							2.4.12-35
		0.001 to 0.01 gpd/ft ²					2.4.12-33
		Kv = 0.0000057 to 0.13 ft/d					2.4.12-37
						6E-06/d	2.4.12-38
						5.91E-06 to 7.13E-06/d	2.4.12-35

**PSEG Site
ESP Application
Part 2, Site Safety Analysis Report**

**Table 2.4.12-1 (Sheet 2 of 2)
Summary of Hydraulic Properties for Local and Regional Aquifers and Aquitards**

Formation	Transmissivity	Hydraulic Conductivity	Total Porosity	Storage Coefficient	Specific Capacity	Leakance	Reference
Englishtown Aquifer					up to 10 gpm/ft		2.4.12-33
	1,100 to 2,100 ft ² /d	12 to 67 ft/d					2.4.12-37
	500 ft ² /d						2.4.12-38
	415 to 552 ft ² /d						2.4.12-35
Merchantville-Woodbury Confining Unit		Kv = 0.00000087 to 0.03 ft/d					2.4.12-37
						3E-06/d	2.4.12-38
						2.15E-06 to 3.85E-06/d	2.4.12-35
Upper PRM Aquifer	10,000 to 25,000 gpd/ft						2.4.12-7 ^(a)
	15,000 to 25,000 gpd/ft						2.4.12-8 ^(a)
	9,000 to 27,000 gpd/ft				10.6 to 26.7 gpm/ft		2.4.12-12 ^(a)
	870 to 24,210 gpd/ft	240 ft/d					2.4.12-37
	2,000 ft ² /d						2.4.12-38
	1,086 to 2,419 ft ² /d						2.4.12-35
Confining Unit, Upper to Middle PRM		Kv = 0.084 ft/d					2.4.12-37
						2E-06/d	2.4.12-38
						1.797E-07 to 2.69E-07/d	2.4.12-35
Middle PRM Aquifer	4,700 to 11,500 gpd/ft						2.4.12-7 ^(a)
	8,590 gpd/ft	129.5 ft/d		0.0025			2.4.12-41
	670 to 4,000 gpd/ft						2.4.12-12 ^(a)
	4,000 ft ² /d						2.4.12-38
	3,024 to 3,813 ft ² /d						2.4.12-35
Confining Unit, Middle to Lower PRM						5E-06/d	2.4.12-38
						7.19E-07 to 1.67E-05/d	2.4.12-35
Lower PRM Aquifer	2,300 to 16,600 ft ² /d						2.4.12-37
	4,000 to 5,000 ft ² /d						2.4.12-38
	4,844 to 5,299 ft ² /d						2.4.12-35

a) Hydraulic properties based on local (site) studies.

**PSEG Site
ESP Application
Part 2, Site Safety Analysis Report**

**Table 2.4.12-2 (Sheet 1 of 12)
Summary of Public Water Supply Wells Within a 25-Mile Radius of the PSEG Site^(c)**

Well Identification^(b)	Owner	County (NJ) / Watershed (DE)	Total Depth (ft.)^(a)	Pump Rate (gpm)	State
NJGS0000000260	J & J Community Park	Cumberland	0	14.6	NJ
NJGS0000000261	J & J Community Park	Cumberland	0	14.6	NJ
NJGS0000000365	Handy's Mobile Park	Salem	0	9	NJ
NJGS0000000366	Handy's Mobile Park	Salem	0	20	NJ
NJGS0000000368	Country Club Estates Mobile Home	Salem	0	0	NJ
WSWL0000066937	South Jersey Water Supply Co.	Gloucester	270	250	NJ
WSWL0000066939	Penns Grove Water Supply Co.	Gloucester	0	270	NJ
WSWL0000066944	Penns Grove Water Supply Co.	Salem	371	400	NJ
WSWL0000067026	Woodstown Water Dept.	Salem	0	600	NJ
WSWL0000067035	Penns Grove Water Supply Co.	Salem	79	450	NJ
WSWL0000067056	NJ American Water Co.	Gloucester	219	700	NJ
WSWL0000067059	Pennsville Township Water Dept.	Salem	119	700	NJ
WSWL0000067065	Penns Grove Water Supply Co.	Salem	62	250	NJ
WSWL0000067068	Penns Grove Water Supply Co.	Gloucester	104	270	NJ
WSWL0000067075	Penns Grove Water Supply Co.	Salem	96	300	NJ
WSWL0000067102	Pennsville Township Water Dept.	Salem	106	700	NJ
WSWL0000067105	NJ American Water Co.	Gloucester	166	0	NJ
WSWL0000067119	Harrisonville Mobile Home Park	Gloucester	151	48	NJ
WSWL0000067142	Penns Grove Water Supply Co.	Salem	87	250	NJ
WSWL0000067145	Swedesboro Water Dept.	Gloucester	322	500	NJ
WSWL0000067147	South Jersey Water Supply Co.	Gloucester	398	500	NJ
WSWL0000067153	NJ American Water Co.	Gloucester	106	0	NJ
WSWL0000067154	Woodstown Water Dept.	Salem	151	400	NJ

Rev. 4

**PSEG Site
ESP Application
Part 2, Site Safety Analysis Report**

**Table 2.4.12-2 (Sheet 2 of 12)
Summary of Public Water Supply Wells Within a 25-Mile Radius of the PSEG Site^(c)**

Well Identification^(b)	Owner	County (NJ) / Watershed (DE)	Total Depth (ft.)^(a)	Pump Rate (gpm)	State
WSWL0000067168	Auburn Village Water Supply	Salem	0	0	NJ
WSWL0000067201	Woodstown Water Dept.	Salem	1143.8	550	NJ
WSWL0000067202	Consumers NJ Water Co.	Gloucester	240	0	NJ
WSWL0000067203	Consumers NJ Water Co.	Gloucester	235	0	NJ
WSWL0000067213	South Jersey Water Supply Co.	Gloucester	256	1200	NJ
WSWL0000067214	Salem Water Dept.	Salem	171	250	NJ
WSWL0000067340	Elmer Borough Water Dept.	Salem	573	400	NJ
WSWL0000067516	Picnic Grove Mobile Homes	Salem	0	47	NJ
WSWL0000067529	Harding Woods Mobile Home Park	Salem	0	180	NJ
WSWL0000067530	Harding Woods Mobile Home Park	Salem	0	175	NJ
WSWL0000067634	Elmer Borough Water Dept.	Salem	520	400	NJ
WSWL0000081691	Christy Enterprises	Gloucester	310	12	NJ
WSWL0000065052	Fairton Trailer Park	Cumberland	60	45	NJ
WSWL0000066928	Pennsville Township Water Dept.	Salem	242	400	NJ
WSWL0000066988	Penns Grove Water Supply Co.	Salem	84	500	NJ
WSWL0000067001	Auburn Village Water Supply	Salem	270	100	NJ
WSWL0000067007	Swedesboro Water Dept.	Gloucester	343	600	NJ
WSWL0000067021	NJ American Water Co.	Gloucester	0	120	NJ
WSWL0000067022	NJ American Water Co.	Gloucester	229	700	NJ
WSWL0000067545	Harrisonville Mobile Home Park	Gloucester	247	70	NJ
WSWL0000067579	Picnic Grove Mobile Homes	Salem	0	47	NJ
WSWL0000068642	Fairton Trailer Park	Cumberland	59	20	NJ
WSWL0000068645	Bridgeton Water Dept.	Cumberland	107	200	NJ

Rev. 4

**PSEG Site
ESP Application
Part 2, Site Safety Analysis Report**

**Table 2.4.12-2 (Sheet 3 of 12)
Summary of Public Water Supply Wells Within a 25-Mile Radius of the PSEG Site^(c)**

Well Identification^(b)	Owner	County (NJ) / Watershed (DE)	Total Depth (ft.)^(a)	Pump Rate (gpm)	State
WSWL0000068652	Bridgeton Water Dept.	Cumberland	126	500	NJ
WSWL0000068666	Bridgeton Water Dept.	Cumberland	136	500	NJ
WSWL0000068673	Bridgeton Water Dept.	Cumberland	120	500	NJ
WSWL0000068684	Bridgeton Water Dept.	Cumberland	152	800	NJ
WSWL0000068685	Bridgeton Water Dept.	Cumberland	114	350	NJ
WSWL0000068686	Bridgeton Water Dept.	Cumberland	193	350	NJ
WSWL0000068699	Leisure Arms Complex	Salem	0	25	NJ
WSWL0000068700	Leisure Arms Complex	Salem	0	25	NJ
WSWL0000068717	Tips Trailer Park & Sales	Cumberland	70	60	NJ
WSWL0000068767	Tips Trailer Park & Sales	Cumberland	0	40	NJ
WSWL0000068795	Upper Deerfield Township Water Dept.	Cumberland	186	0	NJ
WSWL0000068800	Bridgeton Water Dept.	Cumberland	110	0	NJ
WSWL0000068807	Bridgeton Water Dept.	Cumberland	126	0	NJ
WSWL0000068809	Upper Deerfield Township Water Dept.	Cumberland	196	0	NJ
WSWL0000068837	Seabrook Water Co.	Cumberland	185	800	NJ
WSWL0000068881	Fairton Trailer Park	Cumberland	52	45	NJ
WSWL0000069155	U.S. Dept of Justice/Federal Bureau of Prisons	Cumberland	130	250	NJ
WSWL0000069166	U.S. Dept of Justice/Federal Bureau of Prisons	Cumberland	120	250	NJ
WSWL0000069176	Millville Water Dept.	Cumberland	153	700	NJ
WSWL0000069083	Holly Tree Acres	Salem	0	30	NJ
WSWL0000069105	Holly Tree Acres	Salem	137	30	NJ

**PSEG Site
ESP Application
Part 2, Site Safety Analysis Report**

**Table 2.4.12-2 (Sheet 4 of 12)
Summary of Public Water Supply Wells Within a 25-Mile Radius of the PSEG Site^(c)**

Well Identification^(b)	Owner	County (NJ) / Watershed (DE)	Total Depth (ft.)^(a)	Pump Rate (gpm)	State
WSWL0000069106	Holly Tree Acres	Salem	137	30	NJ
WSWL0000070413	Swedesboro Water Dept.	Gloucester	0	400	NJ
WSWL0000070414	Woodstown Water Dept.	Salem	0	425	NJ
WSWL0000070417	Pennsville Township Water Dept.	Salem	248	250	NJ
WSWL0000070418	Salem Water Dept.	Salem	157	500	NJ
WSWL0000070420	South Jersey Water Supply Co.	Gloucester	285	120	NJ
WSWL0000070435	Penns Grove Water Supply Co.	Salem	392	275	NJ
WSWL0000070444	Laux Lakeview Mobile Home Park Inc.	Gloucester	0	100	NJ
WSWL0000070445	Laux Lakeview Mobile Home Park Inc.	Gloucester	0	100	NJ
WSWL0000070446	Laux Lakeview Mobile Home Park Inc.	Gloucester	0	65	NJ
WSWL0000070447	Laux Lakeview Mobile Home Park Inc.	Gloucester	0	100	NJ
WSWL0000070835	Bridgeton Water Dept.	Cumberland	93	525	NJ
WSWL0000070838	Seabrook Water Co.	Cumberland	0	600	NJ
WSWL0000070839	Seabrook Water Co.	Cumberland	0	600	NJ
WSWL0000070888	Tips Trailer Park & Sales	Cumberland	0	0	NJ
WSWL0000070889	Tips Trailer Park & Sales	Cumberland	0	40	NJ
WSWL0000078126	Consumers NJ Water Co.	Gloucester	0	350	NJ
WSWL0000078127	Consumers NJ Water Co.	Gloucester	0	350	NJ
WSWL0000091158	South Jersey Water Supply Co.	Gloucester	270	1200	NJ
WSWL0000138942	Bridgeton Water Dept.	Cumberland	94	0	NJ
WSWL0000138947	Bridgeton Water Dept.	Cumberland	400	500	NJ
WSWL0000138948	Bridgeton Water Dept.	Cumberland	0	500	NJ

**PSEG Site
ESP Application
Part 2, Site Safety Analysis Report**

**Table 2.4.12-2 (Sheet 5 of 12)
Summary of Public Water Supply Wells Within a 25-Mile Radius of the PSEG Site^(c)**

Well Identification^(b)	Owner	County (NJ) / Watershed (DE)	Total Depth (ft.)^(a)	Pump Rate (gpm)	State
WSWL0000138949	Salem Water Dept.	Salem	165	324	NJ
WSWL0000138950	Bridgeton Water Dept.	Cumberland	405	500	NJ
WSWL0000139268	Bridgeton Water Dept.	Cumberland	108	0	NJ
WSWL0000139269	Bridgeton Water Dept.	Cumberland	92	0	NJ
WSWL0000176817	Pennsville Township Water Dept.	Salem	153	0	NJ
WSWL0000176818	Pennsville Township Water Dept.	Salem	269	0	NJ
WSWL0000190792	NJ American Water Co.	Gloucester	105	700	NJ
WSWL0000191667	Hopewell Place Senior Apartments	Cumberland	82	75	NJ
WSWL0000191528	Holly Tree Acres	Salem	0	20	NJ
WSWL0000191530	Fairton Trailer Park	Cumberland	60	0	NJ
WSWL0000191565	Picnic Grove Mobile Homes	Salem	0	24	NJ
WSWL0000191567	Country Club Estates Mobile Home	Salem	0	50	NJ
WSWL0000191568	Harrison Mobile Park	Salem	93	25	NJ
WSWL0000191573	Harrison Mobile Park	Salem	0	25	NJ
WSWL0000191681	Handy's Mobile Park	Salem	187	30	NJ
WSWL0000191682	Harding Woods Mobile Home Park	Salem	105	200	NJ
WSWL0000215097	Seabrook Water Co.	Cumberland	335	30	NJ
WSWL0000215958	Pennsville Township Water Dept.	Salem	0	500	NJ
WSWL0000293710	Country Club Estates Mobile Home	Salem	0	15	NJ
WSWL0000454591	Rainbow Convalescent Center	Salem	88	30	NJ
WSWL0000475741	Rainbow Convalescent Center	Salem	90	30	NJ
WSWL0000708077	J & J Community Park	Cumberland	563	20	NJ

**PSEG Site
ESP Application
Part 2, Site Safety Analysis Report**

**Table 2.4.12-2 (Sheet 6 of 12)
Summary of Public Water Supply Wells Within a 25-Mile Radius of the PSEG Site^(c)**

Well Identification^(b)	Owner	County (NJ) / Watershed (DE)	Total Depth (ft.)^(a)	Pump Rate (gpm)	State
WSWL0000824635	Pennsville Township Water Dept.	Salem	0	500	NJ
WSWL0000831109	Woodstown Water Dept.	Salem	155	200	NJ
WSWL0000842061	Penns Grove Water Supply Co.	Salem	0	275	NJ
84445	St. Georges	C & D Canal East	142	10	DE
168612	DeIDOT	Dragon Run Creek	59	10	DE
69050	Hollingsworth, Diamond State	Dragon Run Creek	250	10	DE
69051	Petroleum, Eastern	Dragon Run Creek	160	10	DE
69052	Stapleford, Charles Sr.	Dragon Run Creek	302	10	DE
90632	Parkway Gravel Inc.	C & D Canal East	160	30	DE
171554	Edwards, Richard	Red Lion Creek	85	10	DE
177079	71 Holding Company	C & D Canal East	275	15	DE
65280	Madic Inc., Michael	C & D Canal East	76	20	DE
63015	Thirty Three, Forty Limited	C & D Canal East	37	10	DE
80752	Motiva Enterprises LLC	Red Lion Creek	45	10	DE
77305	St Georges Association	Dragon Run Creek	275	20	DE
94029	DeIDOT	Dragon Run Creek	64	20	DE
79910	Blaschko, John W.	Red Lion Creek	50	10	DE
90632	Parkway Gravel Inc.	C & D Canal East	160	30	DE
91916	Parkway Gravel	C & D Canal East	200	30	DE
96341	Blaschko, John W.	Red Lion Creek	35	10	DE
102661	Buttcoula, Louis	Appoquinimink River	152	10	DE
192969	Whiteman, Marty	Appoquinimink River	125	10	DE

**PSEG Site
ESP Application
Part 2, Site Safety Analysis Report**

**Table 2.4.12-2 (Sheet 7 of 12)
Summary of Public Water Supply Wells Within a 25-Mile Radius of the PSEG Site^(c)**

Well Identification^(b)	Owner	County (NJ) / Watershed (DE)	Total Depth (ft.)^(a)	Pump Rate (gpm)	State
102872	Genes Body Shop	Appoquinimink River	39	10	DE
103777	New Castle County	Appoquinimink River	190	60	DE
105016	Hearne, William A.	Appoquinimink River	200	0	DE
107232	Whiteman, Mike	Appoquinimink River	100	50	DE
105151	Zoar Methodist Church	Appoquinimink River	201	20	DE
154043	Glorious Church of God	Blackbird Creek	140	20	DE
158489	Frog Hollow LLC	Appoquinimink River	162	30	DE
161541	Artesian Water Company Inc.	Appoquinimink River	118	20	DE
167920	McKeown, Robert	Appoquinimink River	157	10	DE
185045	Stanley Builders	Appoquinimink River	184	10	DE
190088	Delaware Solid WASTE Authority	Blackbird Creek	132	20	DE
204315	Averill, Ron	Blackbird Creek	70	10	DE
202974	New Castle County	Appoquinimink River	121	20	DE
36214	Wyoming Block Co.	Blackbird Creek	157	60	DE
50682	Tappahanna	Blackbird Creek	30	5	DE
62905	Mummford & Miller, Concrete	Appoquinimink River	200	20	DE
72425	Salvage, Fred D.	Blackbird Creek	150	20	DE
74671	Calotex, Delaware Inc.	Blackbird Creek	120	10	DE
77049	Middletown Seventh-Day Adventist	Appoquinimink River	95	20	DE
77648	Mumford & Mille	Appoquinimink River	90	10	DE
83331	Harvey & Harvey	Blackbird Creek	130	20	DE
91490	DEL DOT Div of Highways	Appoquinimink River	118	10	DE

**PSEG Site
ESP Application
Part 2, Site Safety Analysis Report**

**Table 2.4.12-2 (Sheet 8 of 12)
Summary of Public Water Supply Wells Within a 25-Mile Radius of the PSEG Site^(c)**

Well Identification^(b)	Owner	County (NJ) / Watershed (DE)	Total Depth (ft.)^(a)	Pump Rate (gpm)	State
43962	Kirkwood Soccer Club	Army Creek	215	900	DE
43963	Artesian Water Company Inc.	Army Creek	225	300	DE
101760	Artesian Water Company Inc.	Army Creek	170	700	DE
103480	Crab Rib	C & D Canal East	105	10	DE
106649	United Water Delaware	Dragon Run Creek	295	25	DE
194042	Parkway Gravel	Red Lion Creek	152	25	DE
194043	Parkway Gravel	Red Lion Creek	187	25	DE
194044	Parkway Gravel	Red Lion Creek	402	25	DE
36504	City of Delaware City	Dragon Run Creek	720	300	DE
62314	Chesapeake, Canal Partners	C & D Canal East	280	10	DE
83253	Colonial School	Dragon Run Creek	350	30	DE
88603	Mullins, William F.	C & D Canal East	80	20	DE
80405	Shopping Center (undesignated)	Dragon Run Creek	120	20	DE
78555	Carroll, Chester	Dragon Run Creek	250	20	DE
80167	Colonial School,	Dragon Run Creek	700	0	DE
10429	State of DE DAS/DFM	C & D Canal East	190	100	DE
90048	Crab Rib	C & D Canal East	120	20	DE
99719	U.S. Postal Service	Army Creek	208	10	DE
1 ^(b)	Gunning Bedford	Dragon Run Creek	341	0	DE
169693	Diamond State Realty Co.	C & D Canal East	125	20	DE
89283	Farm Land Holdings LLC	C & D Canal East	125	30	DE
89284	Farm Land Holdings LLC	C & D Canal East	135	30	DE

Rev. 4

**PSEG Site
ESP Application
Part 2, Site Safety Analysis Report**

**Table 2.4.12-2 (Sheet 9 of 12)
Summary of Public Water Supply Wells Within a 25-Mile Radius of the PSEG Site^(c)**

Well Identification^(b)	Owner	County (NJ) / Watershed (DE)	Total Depth (ft.)^(a)	Pump Rate (gpm)	State
89285	Farm Land Holdings LLC	C & D Canal East	130	30	DE
101153	Stanley Builders	C & D Canal East	505	300	DE
102151	Artesian Water Company Inc	C & D Canal East	400	400	DE
102224	Hickey, John & Amy	C & D Canal East	135	10	DE
104063	U.S. Army Corps of Engineers	C & D Canal East	268	20	DE
105156	Artesian Water Company Inc.	C & D Canal East	495	100	DE
105157	Davis, Leola B.	C & D Canal East	792	0	DE
156288	Artesian Water Company Inc.	C & D Canal East	625	50	DE
162618	Artesian Water Company Inc.	C & D Canal East	152	0	DE
199537	Tidewater Utilities	C & D Canal East	170	0	DE
41871	Lester, Earl	C & D Canal East	80	30	DE
39786	Mazik, Ken	Dragon Run Creek	289	20	DE
53347	Buckson, Newlin	C & D Canal East	37	10	DE
43368	Reybold Homes	Dragon Run Creek	240	80	DE
68944	Tidewater Utilities, Inc.	C & D Canal East	80	0	DE
68945	Norfolk Southern Railroad	C & D Canal East	230	75	DE
59152	Walker, Guy	C & D Canal East	165	20	DE
54126	Mt. Pleasant Trailer Park	C & D Canal East	45	25	DE
75180	Common Wealth	C & D Canal East	115	10	DE
78973	Tidewater Utilities, Inc.	C & D Canal East	160	160	DE
99469	Artesian Water Company Inc.	C & D Canal East	534	580	DE
82242	Tidewater Utilities, Inc.	C & D Canal East	80	160	DE

Rev. 4

**PSEG Site
ESP Application
Part 2, Site Safety Analysis Report**

**Table 2.4.12-2 (Sheet 10 of 12)
Summary of Public Water Supply Wells Within a 25-Mile Radius of the PSEG Site^(c)**

Well Identification^(b)	Owner	County (NJ) / Watershed (DE)	Total Depth (ft.)^(a)	Pump Rate (gpm)	State
82244	Tidewater Utilities, Inc.	C & D Canal East	95	160	DE
74785	Gentlemens Farmers Rest Inc.	C & D Canal East	103	150	DE
84135	Tidewater Utilities, Inc.	C & D Canal East	120	0	DE
10757	Commodore Macdo	Dragon Run Creek	35	0	DE
1202	DNREC-Fish & Wildlife	C & D Canal East	105	0	DE
98112	Artesian Water Company	C & D Canal East	300	0	DE
93214	New Group Investments	Appoquinimink River	160	30	DE
99806	Artesian Water Company Inc.	Appoquinimink River	740	800	DE
102217	Gilchrist, Robert A.	Appoquinimink River	200	80	DE
109874	Artesian Water Company Inc.	Appoquinimink River	435	0	DE
110612	Artesian Water Company Inc.	Appoquinimink River	330	200	DE
108202	Artesian Water Company Inc.	Appoquinimink River	450	300	DE
111065	Artesian Water Company Inc.	Appoquinimink River	740	300	DE
111968	Artesian Water Company Inc.	Appoquinimink River	238	0	DE
168004	Conoco, Inc.	Appoquinimink River	220	15	DE
178412	St Andrews School of DE, Inc.	Appoquinimink River	389	15	DE
188292	Artesian Water Company Inc.	Appoquinimink River	983	550	DE
179292	Tidewater Utilities, Inc.	Appoquinimink River	180	90	DE
185186	Artesian Water Company Inc.	Appoquinimink River	300	250	DE
185232	Tidewater Utilities, Inc.	Appoquinimink River	230	75	DE
196919	Artesian Water Company Inc.	Blackbird Creek	300	250	DE
39676	Town of Middletown	Appoquinimink River	846	250	DE

Rev. 4

**PSEG Site
ESP Application
Part 2, Site Safety Analysis Report**

**Table 2.4.12-2 (Sheet 11 of 12)
Summary of Public Water Supply Wells Within a 25-Mile Radius of the PSEG Site^(c)**

Well Identification^(b)	Owner	County (NJ) / Watershed (DE)	Total Depth (ft.)^(a)	Pump Rate (gpm)	State
37195	New Castle County	Appoquinimink River	70	25	DE
58805	Pre Holding Hampstead LLC	Appoquinimink River	201	35	DE
53259	Bailey, James	Blackbird Creek	310	20	DE
72100	Justice of the Peace	Appoquinimink River	118	10	DE
89852	Reed, Charolet	Appoquinimink River	170	40	DE
70172	Howard Cohen, Middletown	Appoquinimink River	165	25	DE
82787	Diamond	Appoquinimink River	201	20	DE
10454	Wicks, Christopher	Appoquinimink River	375	250	DE
10745	Cantwell Water	Appoquinimink River	228	0	DE
10746	Cantwell Water	Appoquinimink River	168	0	DE
10765	Children Castle	Appoquinimink River	150	0	DE
10766	St Andrews School of DE, Inc	Appoquinimink River	650	0	DE
10767	St Andrews School of DE, Inc	Appoquinimink River	181	0	DE
10772	Delaware State	Appoquinimink River	206	0	DE
71254	Tidewater Utilities, Inc.	Appoquinimink River	163	250	DE
96299	Tidewater Utilities, Inc.	C & D Canal East	160	150	DE
96300	Tidewater Utilities, Inc.	C & D Canal East	170	150	DE
98363	Fas Mart	Blackbird Creek	160	10	DE
30021	Camp Ground Inco, Delmarva	Blackbird Creek	165	0	DE
30022	Williams Assoc.	Blackbird Creek	178	0	DE
97960	Tidewater Utilities, Inc.	Appoquinimink River	220	80	DE
33392	Hampson, Leonora	Appoquinimink River	200	50	DE

Rev. 4

**PSEG Site
ESP Application
Part 2, Site Safety Analysis Report**

**Table 2.4.12-2 (Sheet 12 of 12)
Summary of Public Water Supply Wells Within a 25-Mile Radius of the PSEG Site^(c)**

Well Identification^(b)	Owner	County (NJ) / Watershed (DE)	Total Depth (ft.)^(a)	Pump Rate (gpm)	State
84852	Reed, Charolet	Appoquinimink River	160	40	DE
585	South Market	Appoquinimink River	200	0	DE
30148	Townsend	Blackbird Creek	206	150	DE
10099	City of Delaware City	Dragon Run Creek	235	100	DE
58900	Odessa Motel, Larry Cox	Appoquinimink River	201	20	DE

a) Depths provided in feet below ground surface.

b) Permit number is as presented in the DE DNR database. The well identifier number is likely an error.

c) Public water supply wells within DE and NJ not inclusive of wells that are mapped in wellhead protection areas. Wellhead protection areas in DE and NJ are shown on Figure 2.4.12-3.

Reference 2.4.12-13; Reference 2.4.12-21

**PSEG Site
ESP Application
Part 2, Site Safety Analysis Report**

**Table 2.4.12-3 (Sheet 1 of 6)
Summary of Groundwater Users Within the 25-Mile Radius^{(a)(b)}**

Program Interest ID	Program Interest Name	Activity Number^(a)	Activity Type Description	Effective Start Date	Expiration Date
Gloucester County, NJ					
2029P	Air Products & Chemicals Inc.	WAP980001	Water Allocation Permit - Renewal	6/23/1999	12/31/2010
5383	Aqua New Jersey Inc. (Woolwich)	WAP050002	Water Allocation Permit - Minor Modification	1/1/2006	12/31/2010
2272P	Beckett Golf Club Inc.	WAP990001	Water Allocation Permit - Renewal	10/30/2002	12/31/2010
2401P	BP Terminal No. 4555	WAP070001	Water Allocation Permit - Renewal	12/1/2008	11/30/2018
2530P	Bridgeport Disposal LLC	WAP050001	Water Allocation Permit - Minor Modification	6/1/2005	4/30/2014
2495E	Chemical Leaman Tanklines	EQP080001	Water Allocation Permit Equivalency - Renewal	10/1/2008	9/30/2018
5244	Clayton Borough Water Dept.	WAP040001	Water Allocation Permit - Modification	4/1/2005	3/31/2015
2014P	Colonial Estates	WAP080001	Water Allocation Permit - Renewal	11/1/2008	10/31/2018
5336	Deptford Township Municipal Utilities Authority	WAP070001	Water Allocation Permit - Administrative Modification	5/1/2007	12/31/2010
5142	East Greenwich Township	WAP060001	Water Allocation Permit - Renewal	1/1/2007	12/31/2016
2251P	E.I. Dupont Denemours & Company Inc. Repauno Plant	WAP040002	Water Allocation Permit - Renewal	9/1/2005	8/31/2015
2099P	Ferro Corp	WAP070001	Water Allocation Permit - Minor Modification	5/9/2007	7/31/2014
5135	Glassboro Borough Water Dept.	WAP080001	Water Allocation Permit - Renewal	11/1/2008	10/31/2018
2280P	Gloucester County Pitman Golf Course	WAP030001	Water Allocation Permit - Renewal	10/1/2004	12/31/2013
2423P	Grasso Foods Inc.	WAP990001	Water Allocation Permit - Renewal	6/30/2000	12/31/2010
5253	Greenwich Township Water Dept.	WAP000001	Water Allocation Permit - Renewal	10/19/2001	12/31/2010

**PSEG Site
ESP Application
Part 2, Site Safety Analysis Report**

**Table 2.4.12-3 (Sheet 2 of 6)
Summary of Groundwater Users Within the 25-Mile Radius^{(a)(b)}**

Program Interest ID	Program Interest Name	Activity Number^(a)	Activity Type Description	Effective Start Date	Expiration Date
Gloucester County, NJ (continued)					
2469E	Helen Kramer Landfill Superfund Site	EQP080001	Water Allocation Permit Equivalency - Renewal	10/1/2008	9/30/2018
2227P	Hercules Groundwater Treatment	WAP070002	Water Allocation Permit - Minor Modification	1/1/2008	4/30/2012
2391P	Inversand Co.	WAP960001	Water Allocation Permit - Renewal	1/20/1998	12/31/2010
4059PS	Logan Generating Company LP	WAP050001	Water Allocation Permit - Renewal	11/1/2006	10/31/2016
5314	Mantua Township Municipal Utilities Authority	WAP080001	Water Allocation Permit - Minor Modification	9/1/2008	6/30/2012
2291P	Maple Ridge Golf Course	WAP010001	Water Allocation Permit - Renewal	10/24/2002	12/31/2011
5161	Monroe Township Municipal Utilities Authority	WAP050001	Water Allocation Permit - Modification	6/1/2007	5/31/2017
5153	National Park Borough Water Dept.	WAP070001	Water Allocation Permit - Renewal	4/1/2008	3/31/2018
5147	Newfield Borough Water Dept.	WAP030001	Water Allocation Permit - Renewal	8/1/2004	6/30/2014
5375	NJ American Water - Bridgeport	WAP070001	Water Allocation Permit - Modification	8/1/2008	7/31/2018
5183	NJ American Water - Harrison	WAP070002	Water Allocation Permit - Hearing Appeal Modification	4/1/2008	7/31/2017
5003	NJ American Water Logan System	WAP030001	Water Allocation Permit - Renewal	3/1/2004	12/31/2013
2425P	Nustar Asphalt Refining LLC	WAP040001	Water Allocation Permit - Minor Modification	9/1/2005	10/31/2012
5130	Paulsboro Water Dept.	WAP070001	Water Allocation Permit - Renewal	10/1/2007	9/30/2017
5137	Pitman Borough Water Dept.	WAP000001	Water Allocation Permit - Renewal	10/30/2002	2/28/2011
2215P	Preferred Real Estate Investments	WAP060001	Water Allocation Permit - Renewal	4/1/2007	3/31/2012
2336P	RE Pierson Materials Corp.	WAP020001	Water Allocation Permit - Renewal	9/1/2003	2/28/2013

**PSEG Site
ESP Application
Part 2, Site Safety Analysis Report**

**Table 2.4.12-3 (Sheet 3 of 6)
Summary of Groundwater Users Within the 25-Mile Radius^{(a)(b)}**

Program Interest ID	Program Interest Name	Activity Number^(a)	Activity Type Description	Effective Start Date	Expiration Date
Gloucester County, NJ (continued)					
4073PS	River Winds at West Deptford	WAP990001	Water Allocation Permit - New	4/17/2003	11/30/2012
2543P	Sahara Sand ff Franklin Inc.	WAP020001	Water Allocation Permit - New	3/26/2003	11/30/2012
2234P	Solvay Solaxis Inc.	WAP080001	Water Allocation Permit - Modification	4/1/2009	3/31/2019
2205P	Sunoco Inc. (R&M) Eagle Point Facility	WAP060001	Water Allocation Permit - Administrative Modification	10/1/2006	6/30/2015
5105	Swedesboro Water Dept.	WAP010001	Water Allocation Permit - Renewal	11/26/2001	10/31/2011
2424E	USEPA Lipari Landfill Superfund Site	EQP910001	Water Allocation Permit Equivalency - New	12/2/1991	--
2204P	Valero Refining Co. - NJ	WAP070002	Water Allocation Permit - Renewal	7/1/2008	6/30/2018
1281D	Valero Refining Co. NJ	DWP080001	Temporary Dewatering Permit - New	6/1/2009	7/31/2012
2177P	Violet Packing LLC	WAP980001	Water Allocation Permit - Renewal	12/30/1999	12/31/2010
5194	Washington Township Municipal Utilities Association	WAP060001	Water Allocation Permit - Modification	2/1/2008	1/31/2018
5192	Wenonah Borough Water Dept.	WAP010001	Water Allocation Permit - Renewal	9/11/2002	1/31/2011
5304	West Deptford Township - Public Works	WAP050001	Water Allocation Permit - Renewal	11/1/2006	10/31/2016
5319	Westville Borough Water Dept.	WAP000001	Water Allocation Permit - Renewal	1/31/2003	12/31/2010
2257P	Westwood Golf Club	WAP060001	Water Allocation Permit - Renewal	5/1/2007	4/30/2017
2365P	Wheelabrator Gloucester Co. LP	WAP980001	Water Allocation Permit - Renewal	12/30/1999	12/31/2010
5347X	Woodbury City Water Dept	WAP030001	Water Allocation Permit - Renewal	9/1/2004	8/31/2012
5347X	Woodbury City Water Dept	WAP990001	Water Allocation Permit - Modification	9/1/2004	8/31/2012
5159	Woodbury Heights Borough Water Utility	WAP060001	Water Allocation Permit - Renewal	4/1/2007	3/31/2017
Salem County, NJ					
2413P	B & B Poultry Co. Inc.	WAP060001	Water Allocation Permit - Renewal	12/1/2007	11/30/2017
2104P	Deepwater Generating Station	WAP980001	Water Allocation Permit - Renewal	3/20/2001	12/31/2010

Rev. 4

**PSEG Site
ESP Application
Part 2, Site Safety Analysis Report**

**Table 2.4.12-3 (Sheet 4 of 6)
Summary of Groundwater Users Within the 25-Mile Radius^{(a)(b)}**

Program Interest ID	Program Interest Name	Activity Number^(a)	Activity Type Description	Effective Start Date	Program Interest ID
Salem County, NJ (continued)					
2122P	Dupont Chambers Works	WAP070002	Water Allocation Permit - Minor Modification	11/1/2007	5/31/2012
5215	Elmer Borough Water Dept.	WAP990001	Water Allocation Permit - Renewal	12/1/2003	11/30/2013
5170	Harding Woods Mobile Home Park	WAP040001	Water Allocation Permit - Administrative Modification	7/29/1999	2/28/2009
5328	NJ American Water - Pennsgrove	WAP070002	Water Allocation Permit - Minor Modification	6/1/2007	7/31/2016
2421P	Pedricktown Cogeneration Company	WAP070001	Water Allocation Permit - Renewal	7/1/2008	6/30/2018
5047	Pennsville Township Water Dept.	WAP020001	Water Allocation Permit - Modification	10/1/2005	9/30/2015
2166P	Polyone Corp.	WAP080001	Water Allocation Permit - Minor Modification	12/1/2008	12/30/2014
2216P	Salem and Hope Creek Generating Station	WAP040001	Water Allocation Permit - Minor Modification	1/1/2005	1/31/2010
5290	Salem City Water Dept.	WAP020001	Water Allocation Permit - Modification	5/1/2005	3/31/2015
2528P	Town & Country Golf Links	WAP010001	Water Allocation Permit - New	1/1/2006	12/31/2015
2497P	Wild Oaks Country Club	WAP050001	Water Allocation Permit - Renewal	5/1/2007	4/30/2012
5167	Woodstown Borough Water Dept.	WAP070001	Water Allocation Permit - Modification	6/1/2009	5/31/2019
Cumberland County, NJ					
2095P	Alcan Packaging Inc.	WAP070001	Water Allocation Permit - Minor Modification	8/1/2008	6/30/2012
2010P	Atlantic Coast Freezers	WAP080001	Water Allocation Permit - Renewal	10/1/2008	9/30/2018
5398	Berrymans Branch Mobile Home Park	WAP070001	Water Allocation Permit - New	7/1/2008	6/30/2018
5032	Bridgeton City Water Dept.	WAP980001	Water Allocation Permit - Modification	8/1/2003	1/31/2013

**PSEG Site
ESP Application
Part 2, Site Safety Analysis Report**

**Table 2.4.12-3 (Sheet 5 of 6)
Summary of Groundwater Users Within the 25-Mile Radius^{(a)(b)}**

Program Interest ID	Program Interest Name	Activity Number^(a)	Activity Type Description	Effective Start Date	Program Interest ID
Cumberland County, NJ (continued)					
2448P	Cape May Foods LLC doing business as Lamonica Fine Foods	WAP020001	Water Allocation Permit - Renewal	11/1/2003	9/30/2012
2220P	Clement Pappas Co. Inc.	WAP010001	Water Allocation Permit - Renewal	9/27/2002	1/31/2011
5364	Fairton Federal Correctional Institute	WAP970001	Water Allocation Permit - Renewal	12/23/1997	12/31/2010
5399	Fairview Manor Mobile Home Park	WAP070001	Water Allocation Permit - New	5/1/2008	4/30/2018
2552P	Gerresheimer Glass Inc.	WAP030001	Water Allocation Permit - Minor Modification	8/12/2004	7/31/2014
2254P	Hanson Aggregates	WAP990001	Water Allocation Permit - Modification	3/26/2003	12/31/2012
2098P	Kimble Glass Inc.	WAP980001	Water Allocation Permit - Renewal	6/14/2002	12/31/2010
2436P	Mays Landing Sand & Gravel Co. Dorchester Plant	WAP070001	Water Allocation Permit - Renewal	3/1/2008	2/28/2018
5316	Millville City Water Dept.	WAP980001	Water Allocation Permit - Renewal	9/10/2002	6/30/2011
2467E	Nascolite (Potentially Responsible Parties) Group	EQP950001	Water Allocation Permit Equivalency - New	3/24/1995	
5367	NJ State Prison Bayside	WAP980001	Water Allocation Permit - Modification	2/21/2002	3/31/2010
2443P	Purex Industries	WAP010001	Water Allocation Permit - Renewal	10/30/2002	10/31/2011
2030P	Ricci Brothers Sand Co.	WAP070001	Water Allocation Permit - Minor Modification	5/1/2007	5/31/2016
2221P	Seabrook Farms	WAP050001	Water Allocation Permit - Renewal	4/1/2006	3/31/2016
2237P	Shieldalloy Metallurgical Corp.	WAP060001	Water Allocation Permit - Renewal	8/1/2007	7/31/2017
2440P	South State Inc.	WAP980001	Water Allocation Permit - Renewal	12/29/1998	12/31/2010
2219P	Unimin Corp	WAP050002	Water Allocation Permit - Renewal	7/1/2006	6/30/2016
5376	Upper Deerfield Township	WAP070001	Water Allocation Permit - Modification	4/1/2008	3/31/2018

**PSEG Site
ESP Application
Part 2, Site Safety Analysis Report**

**Table 2.4.12-3 (Sheet 6 of 6)
Summary of Groundwater Users Within the 25-Mile Radius^{(a)(b)}**

Program Interest ID	Program Interest Name	Activity Number^(a)	Activity Type Description	Effective Start Date	Program Interest ID
Cumberland County, NJ (continued)					
2485E	USEPA Region II Vineland Chemical Co. Superfund	EQP070002	Water Allocation Permit Equivalency - Modification	8/1/2008	7/31/2018
2003P	US Silica Co	WAP040001	Water Allocation Permit - Modification	4/1/2005	3/31/2015
2282P	US Silica Co. Port Elizabeth Plant	WAP080001	Water Allocation Permit - Renewal	7/1/2008	6/30/2018
5148	Vineland City Water Utility	WAP060001	Water Allocation Permit - Modification	8/1/2007	7/31/2017
2405P	Vineland Kosher Poultry Co.	WAP040001	Water Allocation Permit - Minor Modification	5/1/2004	12/31/2010
2026P	Whibco Inc.	WAP970001	Water Allocation Permit - Renewal	6/30/1997	5/31/2008
Delaware					
53066	Star Enterprises	NA	Dragon Run Creek	2/1/1983	10/24/1983
53066	Star Enterprises	NA	Dragon Run Creek	2/1/1983	10/24/1983
216229	Highland View LLC	NA	Dragon Run Creek	10/3/2006	3/2/2007
216229	Highland View LLC	NA	Dragon Run Creek	10/3/2006	3/2/2007
10059	Motiva Enterprises LLC	NA	Dragon Run Creek	1/1/1956	1/1/1956
10059	Motiva Enterprises LLC	NA	Dragon Run Creek	1/1/1956	1/1/1956
43962	Kirkwood Soccer Club	NA	Army Creek	7/23/1979	9/17/1979
163874	Motiva Enterprises LLC	NA	Dragon Run Creek	2/19/1999	9/16/1999
163874	Motiva Enterprises LLC	NA	Dragon Run Creek	2/19/1999	9/16/1999

a) NA – “Activity numbers” are not a Delaware Department of Natural Resources database field

b) Summary includes permitted groundwater use of greater than 100,000 gallons per day.

References 2.4.12-13 and 2.4.12-21

**PSEG Site
ESP Application
Part 2, Site Safety Analysis Report**

**Table 2.4.12-4
Observation Well Installation Details**

Well ID	Northing (U.S. Feet, NAD83)	Easting (U.S. Feet, NAD83)	Screen Interval (ft. bgs)^(a)	Reference Point Elevation (ft NAVD)	Formation
New Plant Location					
NOW-1U	234542.7	198443.4	46 to 56	15.20	Alluvium
NOW-1L	234564.0	198449.8	80 to 90	15.19	Vincetown
NOW-2U	235207.4	197754.9	52 to 62	10.80	Alluvium
NOW-2L	235227.7	197752.8	103 to 113	11.18	Vincetown
NOW-3U	234552.8	197885.2	40 to 50	7.71	Alluvium
NOW-3L	234565.5	197897.9	90 to 100	7.66	Vincetown
NOW-4UB ^(b)	233963.0	198147.1	42 to 52	13.56	Alluvium
NOW-4L	233972.7	198147.9	73 to 83	14.08	Vincetown
NOW-5U	234907.5	198444.5	20 to 30	10.23	Hydraulic Fill
NOW-5L	234927.5	198438.4	90 to 100	10.54	Vincetown
NOW-6U	235269.4	198313.5	35 to 45	8.59	Alluvium
NOW-6L	235287.9	198312.8	80 to 90	7.95	Vincetown
NOW-7U	234975.8	199694.3	48 to 58	8.25	Vincetown
NOW-7L	234973.4	199675.9	85 to 95	8.70	Vincetown
NOW-8U	234141.6	199755.9	37 to 47	11.68	Alluvium
NOW-8L	234139.1	199736.2	100 to 110	11.61	Vincetown
Eastern Location					
EOW-1U	232321.6	202758.0	38 to 48	18.01	Alluvium
EOW-1L	232297.6	202758.1	95 to 105	17.91	Vincetown
EOW-2U	233274.6	202157.9	39 to 49	16.51	Alluvium
EOW-2L	233271.5	202177.7	99 to 109	16.73	Vincetown
EOW-4U	231791.9	202012.1	22 to 32	22.73	Hydraulic Fill
EOW-4L	231772.9	202021.2	110.2 to 120.2	22.31	Vincetown
EOW-5U	233056.8	203007.3	35 to 45	15.85	Alluvium
EOW-5L	233039.7	203021.5	110 to 120	16.17	Vincetown
EOW-6U	232587.1	203281.4	47 to 57	15.99	Alluvium
EOW-6L	232588.1	203300.7	90 to 100	15.23	Vincetown
EOW-8U	231144.2	203520.4	30 to 40	18.38	Alluvium
EOW-8L	231163.5	203516.0	67 to 77	17.89	Vincetown
EOW-9U	230917.2	202826.0	50 to 60	20.67	Alluvium
EOW-9L	230925.6	202844.6	117.5 to 127.5	18.21	Vincetown
EOW-10U	231687.2	203521.3	17 to 27	14.79	Alluvium
EOW-10L	231706.7	203521.9	85 to 95	14.27	Vincetown

a) ft. bgs = feet below ground surface per well installation records

b) B = Designates a replacement of the original NOW-4U due to well installation difficulties. NOW-4UB was installed prior to start of data collection.

**PSEG Site
ESP Application
Part 2, Site Safety Analysis Report**

**Table 2.4.12-5
Groundwater Elevations (ft. NAVD), January 2009 to December 2009^(b)**

	Jan	Feb	Mar	Apr	May	Jun	Jul	Aug	Sept	Oct	Nov	Dec	Avg	Std dev	Range
New Plant Area – Hydraulic Fill															
NOW-5U	2.54	2.04	2.12	2.07	1.20	2.74	2.59	2.12	2.55	2.87	2.53	3.20	2.38	0.51	2.0
New Plant Area – Alluvium															
NOW-1U		0.36	0.61	0.59	0.66	1.32	1.14	0.94	1.13	1.22	1.18	-0.48	0.79	0.53	1.80
NOW-2U	-0.10	-0.42	-0.48	-0.17	-0.08	2.04	-0.41	1.72	2.08	2.19	-0.20	0.88	0.59	1.11	2.67
NOW-3U	-0.21	-0.36	0.15	-0.19	0.18	1.20	0.56	0.66	1.13	1.18	0.60	1.23	0.51	0.59	1.59
NOW-4UB		0.03	0.46	0.36	0.40	1.18	1.00	0.75	0.95	1.09	0.95	1.34	0.77	0.41	1.31
NOW-6U	0.50	0.35	0.76	0.62	0.65	1.35	1.12	0.98	1.31	1.31	1.15	1.44	0.96	0.37	1.09
NOW-7U	0.40	0.18	0.74	0.77	0.79	1.40	1.14	1.07	1.41	1.46	1.01	1.64	1.00	0.44	1.46
NOW-8U	0.72	0.41	0.84	0.74	0.86	1.57	1.24	1.21	1.38	1.39	1.15	1.57	1.09	0.37	1.16
New Plant Area – Vincentown															
NOW-1L		0.25	0.56	0.50	0.65	1.58	1.07	1.14	1.54	1.66	1.02	1.67	1.06	0.51	1.42
NOW-2L	-0.05	-0.31	-0.32	-0.20	0.74	2.16	-0.17	1.86	2.82	2.15	-0.01	1.10	0.81	1.16	3.14
NOW-3L	-0.14	-0.25	-0.40	0.10	-0.99	1.63	0.10	1.69	1.90	1.38	0.61	1.25	0.57	0.97	2.89
NOW-4L	-0.71	-0.30	-0.01	-0.16	0.37	1.70	0.43	1.20	1.80	1.56	0.43	1.45	0.65	0.86	2.51
NOW-5L	0.54	-0.19	0.31	0.35	0.52	1.54	0.93	0.73	1.54	1.59	0.65	1.57	0.84	0.60	1.78
NOW-6L	-0.11	-0.08	0.26	0.17	-0.58	1.56	0.88	0.80	1.54	1.63	1.04	0.21	0.61	0.74	2.21
NOW-7L	0.39	-0.81	0.59	0.70	0.71	1.11	0.87	0.94	1.34	1.39	0.75	1.51	0.79	0.61	2.32
NOW-8L	0.50	0.36	0.70	0.79	0.90	1.54	1.15	1.14	1.44	1.43	1.08	1.51	1.05	0.40	1.18
Eastern Location – Hydraulic Fill															
EOW-4U	13.66	13.20	12.90	13.91	13.88	13.50	12.33	12.26	13.99	13.35	14.03	15.33	13.36	0.63	1.77
Eastern Location – Alluvium															
EOW-1U	0.95	0.90	1.20	1.08	1.18	1.74	1.51	(a)	2.54	1.59	1.52	1.79	1.45	0.47	1.64
EOW-2U	2.92	2.80	2.83	2.49	2.70	3.02	2.96	(a)	2.74	3.09	2.87	3.40	2.89	0.24	0.91
EOW-5U	1.03	0.83	1.16	1.10	1.19	1.70	1.45	1.43	1.61	1.59	0.51	1.78	1.28	0.38	1.27
EOW-6U	1.00	0.79	1.20	1.12	1.16	1.71	1.45	1.43	1.59	1.60	1.49	1.78	1.36	0.30	0.99
EOW-8U	0.72	1.02	1.47	0.95	1.27	-0.21	1.73	1.65	1.46	1.70	1.46	2.27	1.29	0.63	2.48
EOW-9U	-0.06	0.08	0.50	0.55	0.35	1.20	0.78	0.75	1.21	1.13	0.86	2.69	0.84	0.71	2.75
EOW-10U	0.52	1.43	1.37	1.32	1.39	2.07	1.58	1.52	1.71	1.85	1.86	2.30	1.58	0.45	1.78
Eastern Location – Vincentown															
EOW-1L	0.79	0.62	0.92	0.98	0.95	1.59	1.29	(a)	1.59	1.59	1.27	1.59	1.20	0.36	0.97
EOW-2L	1.06	0.74	1.25	1.18	1.12	1.74	1.42	1.39	1.76	1.67	1.43	1.72	1.37	0.32	1.02
EOW-4L	0.62	0.51	1.09	0.90	1.00	1.75	1.33	1.19	1.85	1.91	*	1.59	1.25	0.48	1.40
EOW-5L	1.09	0.92	1.30	1.25	0.86	1.79	1.51	2.39	1.78	1.74	1.49	1.77	1.49	0.44	1.53
EOW-6L	0.98	0.70	1.30	1.14	1.06	-0.12	1.45	0.47	1.80	0.74	1.45	1.74	1.06	0.55	1.92
EOW-8L	0.12	0.13	0.60	0.55	0.68	1.48	0.94	0.85	1.59	1.61	1.05	1.27	0.91	0.52	1.49
EOW-9L	0.45	0.41	0.68	0.77	0.97	1.68	1.28	1.05	1.86	1.86	1.18	1.49	1.14	0.51	1.45
EOW-10L	0.60	0.66	1.12	0.94	0.35	1.66	1.36	1.24	1.71	1.76	1.34	1.61	1.20	0.47	1.41

a) Data evaluated as inconsistent with data set and therefore not used for ESPA evaluation.

b) Blank cell indicates no reading.

**PSEG Site
ESP Application
Part 2, Site Safety Analysis Report**

**Table 2.4.12-6
Groundwater Elevation Data Range (in Feet NAVD 88) for HCGS and SGS Groundwater Wells, 2000 – 2009**

	2000	2001	2002	2003	2004	2005	2006	2007	2008	2009
Mount Laurel/Wenonah^(a)	3.08 to -3.12	3.68 to -1.12	4.08 to 0.16	3.28 to 0.86	3.48 to -7.82	13.78 to 0.68	3.58 to 1.08	3.56 to 0.96	3.88 to 1.58	3.78 to 1.36
Salem Well (PW-2)	2.36 to -1.64	2.26 To -0.14	2.96 to 0.16	2.66 to 0.86	2.96 to -0.14	10.06 to 1.36	2.66 to .56	3.56 to 0.96	2.76 to 1.66	3.26 to 1.36
Salem Well (PW-3)	3.08 to -3.12	3.68 to -1.12	3.48 to 0.28	3.28 to 0.88	3.48 to -7.82	13.78 to 0.68	3.58 to 1.08	2.98 to 0.98	3.88 to 1.58	3.78 to 1.48
Middle Raritan^(a)	-35.85 to -64.75	-42.45 to -54.15	-42.45 to -45.15	-40.45 to -45.65	-41.55 to -52.65	-35.75 to -45.45	-44.75 to -46.25	-45.35 to -48.35	-45.35 to -51.35	-43.65 to -48.75
Salem Well (PW-6)	-35.85 to -64.75	-42.45 to -54.15	-42.45 to -45.15	-40.45 to -45.65	-41.55 to -52.65	-35.75 to -45.45	-44.75 to -46.25	-45.85 To -48.35	-45.35 to -51.35	-43.65 to -48.75
Upper Raritan^(a)	-28.93 to -68.35	-41.53 to -72.13	-54.33 to -74.94	-55.73 to -74.35	-57.94 to -84.35	-60.94 to -86.35	-53.94 to -81.35	-55.94 to -83.35	-53.93 to -88.35	-57.73 to -83.94
Salem Well (PW-5)	-28.93 to -67.73	-41.53 to -72.13	-54.33 to -66.23	-55.73 to -70.73	-58.23 to -78.13	-64.33 to -80.73	-59.33 to -75.33	-63.03 to -79.63	-54.63 to -74.33	-57.73 to -71.03
Hope Creek Well (HC-1)	-59.94 to -67.94	-58.94 to -65.94	-57.94 to -74.94	-60.94 to -71.94	-57.94 to -83.94	-60.94 to -74.94	-53.94 to -73.94	-55.94 to -65.94	-53.94 to -71.94	-60.94 to -83.94
Hope Creek Well (HC-2)	-61.35 to -68.35	-60.35 to -70.35	-58.35 to -74.35	-61.35 to -74.35	-69.35 to -84.35	-73.35 to -86.35	-69.35 to -81.35	-70.35 to -83.35	-63.35 to -88.35	-60.35 to -75.45

- a) The aquifer range includes data from all production wells monitored in that aquifer. Individual well ranges are provided directly below the summary line (shown in bold).
b) The water levels presented in this Table may be the result of groundwater pumping and may be monitored from within the wells. The water levels presented are not considered natural groundwater variations.

Reference 2.4.12-31

**PSEG Site
ESP Application
Part 2, Site Safety Analysis Report**

**Table 2.4.12-7
Summary of Horizontal Hydraulic Gradients**

	Maximum Hydraulic Gradient (ft/ft)	Average Gradients(ft/ft)	Gradients From Average Potentiometric Surface^(b) (ft/ft)
New Plant Location – Alluvium			
Measured	0.00235	0.00042	0.00050
Fixed Locations ^(a)	0.00139	0.00066	0.00050
New Plant Location – Vincentown			
Measured	0.00200	0.00048	0.00062
Fixed Locations ^(a)	0.00293	0.00069	0.00088
Eastern Location – Alluvium			
Measured	0.00407	0.00188	0.00092
Fixed Locations ^(a)	0.00099	0.00045	0.00045
Eastern Location – Vincentown			
Measured	0.00167	0.00024	0.00019
Fixed Locations ^(a)	0.00025	0.00004	0.00004

- a) Gradients calculated from the fixed locations: gradients are calculated from the head differenced between NOW-1U/L and NOW-3U/L for the new plant location and between EOW 1U/L and EOW 9L/U for the eastern location.
- b) Gradients from Average Potentiometric Surface are calculated from the contours generated from the average groundwater elevations considering data collected from January 2009 through December 2009.

**PSEG Site
ESP Application
Part 2, Site Safety Analysis Report**

**Table 2.4.12-8
Summary of Vertical Hydraulic Gradients**

Well ID	Screen Interval^(a) (ft. bgs)	Reference Point Elevation (ft. NAVD)	Observed Aquifer/Aquitard	Average Groundwater Elevation (ft. NAVD)	Center Point of Well Screen (ft. bgs)	Vertical Distance (ft .)	Average Vertical Gradient ^(b) (ft.)
New Plant Location							
NOW-1U	46 to 56	15.20	Alluvium	0.92	51		
NOW-1L	80 to 90	15.19	Vincentown	1.06	85	34	-0.00412
NOW-2U	52 to 2	10.80	Alluvium	0.59	57		
NOW-2L	103 to 113	11.18	Vincentown	0.81	108	51	-0.00431
NOW-3U	40 to 50	7.71	Alluvium	0.51	45		
NOW-3L	90 to 100	7.66	Vincentown	0.57	95	50	-0.00120
NOW-4UB	42 to 52	13.56	Alluvium	0.77	47		
NOW-4L	73 to 3	14.08	Vincentown	0.65	78	31	0.00387
NOW-5U	20 to 30	10.23	Hydraulic Fill	2.6	25		
NOW-5L	90 to 100	10.54	Vincentown	0.84	95	70	0.02514
NOW-6U	35 to 45	8.59	Alluvium	0.96	40		
NOW-6L	80 to 90	7.95	Vincentown	0.61	85	45	0.00778
NOW-7U	48 to 58	8.25	Vincentown / Alluvium	1.0	53		
NOW-7L	85 to 95	8.70	Vincentown	0.94	90	37	0.00162
NOW-8U	37 to 47	11.68	Alluvium	1.09	42		
NOW-8L	100 to 110	11.61	Vincentown	1.05	105	63	0.00063
Eastern Wells							
EOW-1U	38 to 48	18.01	Alluvium	1.45	43		
EOW-1L	95 to 105	17.91	Vincentown	1.2	100	57	0.00439
EOW-2U	39 to 49	16.51	Alluvium	2.89	44		
EOW-2L	99 to 109	16.73	Vincentown	1.37	104	60	0.02533
EOW-4U	22 to 32	22.73	Hydraulic Fill	14.56	27		
EOW-4L	110 to 120	22.31	Vincentown	1.25	115	88	0.15125
EOW-5U	35 to 45	15.85	Alluvium	1.28	40		
EOW-5L	110 to 120	16.17	Vincentown	1.49	105	65	-0.00323
EOW-6U	47 to 57	15.99	Alluvium	1.36	52		
EOW-6L	90 to 100	15.23	Vincentown	1.17	95	43	0.00442
EOW-8U	30 to 40	18.38	Alluvium	1.43	35		
EOW-8L	67 to 77	17.89	Vincentown	0.91	72	37	0.01405
EOW-9U	50 to 60	20.67	Alluvium	0.67	55		
EOW-9L	117.5 to 127.5	18.21	Vincentown	1.14	122.5	67.5	-0.00696
EOW-10U	17 to 27	14.79	Alluvium	1.67	22		
EOW-10L	85 to 95	14.27	Vincentown	1.2	90	68	0.00691

a) ft bgs = feet below ground surface, determined from well installation records

b) Negative values indicate an upward vertical hydraulic gradient

**PSEG Site
ESP Application
Part 2, Site Safety Analysis Report**

**Table 2.4.12-9
Summary of Average Hydraulic Conductivities**

Well	Formation	Average Result (feet/day)
Shallow		
NOW-1U	Alluvium	8.0
NOW-2U	Alluvium	8.0
NOW-3U	Alluvium	0.3
NOW-4UB	Alluvium	0.9
NOW-5U	Hydraulic fill	0.2
NOW-6U	Alluvium	3.5
NOW-7U	Vincentown	1.4
NOW-8U	Alluvium	0.4
Deep		
NOW-1L	Vincentown	4.5
NOW-2L	Vincentown	3.6
NOW-3L	Vincentown	1.4
NOW-4L	Vincentown	10.7
NOW-5L	Vincentown	1.7
NOW-6L	Vincentown	6.2
NOW-7L	Vincentown	2.4
NOW-8L	Vincentown	0.3

**PSEG Site
ESP Application
Part 2, Site Safety Analysis Report**

**Table 2.4.12-10
Summary of Tidal Study Results**

Measurement Location	Unit	Barge Slip	NOW-1L	NOW-1U	NOW-3L	NOW-3U
Max High Tide	Elevation (ft.)	3.57	1.38	<i>Tidal influence not observed in this observation well</i>	2.03	0.95
Min High Tide	Elevation (ft.)	2.36	1.12		1.5	0.58
Max Low Tide	Elevation (ft.)	-3.52	0.65		-0.75	0.41
Min Low Tide	Elevation (ft.)	-2.27	0.86		-0.18	0.09
Average Tidal Shift	Feet	5.85	0.49		2.26	0.56
Average Periodicity	Hours	6.9	6.5		7	7.3
Average Phase Lag to Barge Slip	Minutes	N/A	-66		-19	-62

All elevations reported in ft. NAVD 88

**PSEG Site
ESP Application
Part 2, Site Safety Analysis Report**

**Table 2.4.12-11
Summary of Surface Water and Shallow Groundwater Elevations at Piezometers^{(a)(b)(c)}**

Location ID	1/30/2009	2/27/2009	3/29/2009	4/24/2009	5/22/2009	6/19/2009	7/23/2009	8/16/2009	9/17/2009	10/16/2009	11/11/2009	12/10/2009
AS-01 - inside	N/A	NM	N/A	N/A	0.64	N/A	NM	N/A	NM	N/A	N/A	1.12 ^(d)
AS-01 - outside	N/A	NM	N/A	N/A	Dry	N/A	NM	N/A	NM	N/A	N/A	-0.43 ^(d)
AS-02 - inside	N/A	NM	N/A	N/A	-0.04	N/A	0.20	N/A	0.14	N/A	N/A	N/A
AS-02 - outside	N/A	NM	N/A	N/A	2.52	N/A	1.75	N/A	1.59	N/A	N/A	N/A
AS-03 - inside	N/A	NM	N/A	N/A	-1.99	N/A	-1.94	N/A	-2.02	N/A	N/A	N/A
AS-03 - outside	N/A	NM	N/A	N/A	-0.23	N/A	-0.15	N/A	-2.02	N/A	N/A	N/A
AS-04 - inside	Frozen	4.19	4.04	4.49	4.34	4.09	3.55	3.02	3.73	3.55	3.88	4.32
AS-04 - outside	4.32	4.18	4.16	4.38	4.30	4.16	3.63	3.12	3.67	3.52	3.82	4.37
AS-05 - inside	-0.41	0.54	0.17	0.58	-0.23	1.40	1.15	-3.63	1.63	1.21	1.27	1.46
AS-05 - outside	0.58	-0.09	-0.21	-0.13	-0.29	1.23	0.10	0.25	3.31	2.98	0.48	0.97
AS-06 - inside	0.80	0.93	1.14	0.83	0.86	1.74	Dry	0.73	3.09	3.23	1.95	1.87
AS-06 - outside	1.20	Dry	Dry	Dry	Dry	2.51	1.09	dry	dry	dry	dry	dry
AS-08-pre-outside ^(e)	0.70	0.82	0.68	0.70	0.73	2.71	0.81	1.47	3.50	1.46	1.42	0.80
AS-08-pre-inside ^(e)	0.51	0.76	0.89	1.43	1.00	1.54	1.37	1.11	1.86	3.42	-2.17	2.27
AS-08-post-outside ^(e)	1.70	NM	2.25	1.87	1.26	Dry	0.76	1.48	3.25	NM	Dry	0.77
AS-08-post-inside ^(e)	0.46	NM	1.43	1.21	1.04	Dry	1.34	2.80	1.90	NM	Dry	2.00
AS-09 - inside	Frozen	5.76	5.45	6.00	5.84	5.94	3.98	5.82	5.85	3.00	5.82	5.97
AS-09 - outside	6.24	5.87	5.89	5.97	5.81	5.93	5.37	5.83	5.83	5.75	5.80	6.17
AS-10 - inside	1.84	3.12	2.99	3.45	3.15	3.32	2.62	3.02	3.47	-0.06	3.42	3.70
AS-10 - outside	3.52	3.14	3.12	3.24	3.09	3.11	2.95	3.02	3.25	3.08	3.17	3.68
AS-11 - inside	N/A	NM	N/A	N/A	0.09	N/A	1.08	N/A	1.06	N/A	N/A	N/A
AS-11 - outside	N/A	NM	N/A	N/A	0.70	N/A	2.11	N/A	2.04	N/A	N/A	N/A

a) Elevation data reported in ft. NAVD88

b) N/A = not applicable

c) NM = could not be sampled / not measured.

d) * = Data measured on 1/07/10

e) ** = the first and last reading of each event is conducted at PZ-8 so that a tidal change encompassing all water measurements could be evaluated

**PSEG Site
ESP Application
Part 2, Site Safety Analysis Report**

**Table 2.4.12-12 (Sheet 1 of 2)
Summary Dewatering Simulation and Sensitivity Results
Drawdowns and Heads at Selected Locations^(a, b, c, d, e, f, g)**

Base simulation			
Drawdown, ft at 365 days	HC Cooling Tower	HC Unit 1	Salem 1&2
Alluvium	9.3	3.3	0.9
Vincentown Formation	33	17.7	6.4
Head, ft at 365 days at nuclear island			
Vincentown Formation	-68.3		
Halve VT/HT Kh to 5.35 ft/d			
Drawdown, ft at 365 days	HC Cooling Tower	HC Unit 1	Salem 1&2
Alluvium	7.4	2.5	0.6
Vincentown Formation	27.3	14.9	5.4
Head, ft at 365 days at nuclear island			
Vincentown Formation	-53.9		
Double VT/HT Kh to 21.4 ft/d			
Drawdown, ft at 365 days	HC Cooling Tower	HC Unit 1	Salem 1&2
Alluvium	9.6	3.4	1
Vincentown Formation	34.2	18.4	6.7
Head, ft at 365 days at nuclear island			
Vincentown Formation	-70		
Decrease Kv of Navesink to 0.0272 ft/d			
Drawdown, ft at 365 days	HC Cooling Tower	HC Unit 1	Salem 1&2
Alluvium	9.2	3.1	0.8
Vincentown Formation	32.8	17.1	6
Head, ft at 365 days at nuclear island			
Vincentown Formation	-70.3		
Increase Kv of Navesink to 0.109 ft/d			
Drawdown, ft at 365 days	HC Cooling Tower	HC Unit 1	Salem 1&2
Alluvium	9.3	3.4	0.9
Vincentown Formation	33.3	18	6.5
Head, ft at 365 days at nuclear island			
Vincentown Formation	-66.7		
Increase Kh of MLW to 15 ft/d			
Drawdown, ft at 365 days	HC Cooling Tower	HC Unit 1	Salem 1&2
Alluvium	8.7	3	0.8
Vincentown Formation	31.4	16.8	6.2
Head, ft at 365 days at nuclear island			
Vincentown Formation	-68.3		

**PSEG Site
ESP Application
Part 2, Site Safety Analysis Report**

**Table 2.4.12-12 (Sheet 2 of 2)
Summary Dewatering Simulation and Sensitivity Results
Drawdowns and Heads at Selected Locations**

Increase Kv of VT/HT to 1.0 ft/d			
Drawdown, ft at 365 days	HC Cooling Tower	HC Unit 1	Salem 1&2
Alluvium	8.7	3	0.8
Vincentown Formation	31.4	16.8	6.2
Head, ft at 365 days at nuclear island			
Vincentown Formation	-66.7		
Increase Kv of Kirkwood to 0.01 ft/d			
Drawdown, ft at 365 days	HC Cooling Tower	HC Unit 1	Salem 1&2
Alluvium	20.7	10.2	2.7
Vincentown Formation	31.2	16.2	5.3
Head, ft at 365 days at nuclear island			
Vincentown Formation	-67.6		
Decrease Kz of Kirkwood to 0.001 ft/d			
Drawdown, ft at 365 days	HC Cooling Tower	HC Unit 1	Salem 1&2
Alluvium	2.6	0.4	0.1
Vincentown	34.7	19	7.2
Head, ft at 365 days at nuclear island			
Vincentown	-69.2		

- a) VT/HT = Vincentown and Hornerstown Formations.
- b) MLW = Mount Laurel-Wenonah aquifer
- c) Kh = horizontal hydraulic conductivity.
- d) Kv = vertical hydraulic conductivity
- e) The drawdowns are taken at the approximate centers of the listed structures
- f) The head is taken in the upper Vincentown (model layer 5) mid-point in the deeper excavation
- g) The nuclear island refers to that of the new unit.

**PSEG Site
ESP Application
Part 2, Site Safety Analysis Report**

**Table 2.4.12-13
Summary Dewatering Simulation and Sensitivity Results
Dewatering Rates at Times into Simulation**

	Flow rates (gpm) after start of dewatering simulation					
	0.48 days	1.06 days	90 days	90.6 days	91.3 days	365 days
Base simulation	6541	4613	3434	5477	4989	3566
Sensitivity change to input parameter						
Halve VT/HT Kh to 5.35 ft/d	4449	2149	1955	3062	2421	2223
Double VT/HT Kh to 21.4 ft/d	8524	6686	5170	7257	6906	5345
Halve Navesink Kv to 0.0272 ft/d	6455	4532	3300	5267	4797	3375
Double Navesink Kv to 0.109 ft/d	6617	4685	3549	5631	5135	3727
Decrease Kirwood Kv to 0.001 ft/d	6507	4569	3329	5315	4845	3495
Increase Kirkwood Kv to 0.01 ft/d	6615	4717	3633	5710	5211	3635
Increase MLW Kh to 15 ft/d	6592	4473	3587	5692	5072	3796
Increase VT/HT Kv to 1.0 ft/d	7022	5076	3744	6129	5633	3883

Abbreviations:

VT/HT - Vincentown and Hornerstown Formations
MLW - Mount Laurel-Wenonah aquifer
Kh - horizontal hydraulic conductivity
Kv - vertical hydraulic conductivity

**PSEG Site
ESP Application
Part 2, Site Safety Analysis Report**

**Table 2.4.12-14
Calibrated Model – Input Parameter Values** (a, b, c)

Hydraulic conductivities, ft/d	Horizontal	Vertical	
Hydraulic fill	0.1	0.03	
Structural fill	6.5	0.65	
Alluvium	3.89	0.48	
Kirkwood aquitard	0.02	0.003	
Vincentown	10.7	0.2	
Hornerstown	10.7	0.2	
Navesink	0.4	0.0545	
Mount Laurel-Wenonah	10	10	
Recharge	Ft/d	in/yr	
Zone 1 Wetlands north	0.00003521	0.15	
Zone 2 Buildings, pavement	0	0	
Zone 3 Developed facility	0.0002907	1.27	
Zone 4 Wetlands east	0.0001385	0.61	
Zone 5 Semi-impermeable	0.0004176	1.83	
Zone 6 Near Salem units 1 & 2	0.001826	8	
Storage coefficient	Confined	Specific yield	Total Porosity
Aquifers	0.0001	0.2	0.35
Aquitards	0.0001	0.1	0.4
River package	Ref Elev	Conductance	
Delaware River	-0.1	56.6	
Ponds	4 to 5.4	0.0282 to 0.0566	
Streams	0	5.66 to 11.3	
General Head Boundaries	Ref Elev	Conductance	
Alluvium	-0.5	25.1	
Vincentown	0.5 to 2.0	408 to 640	
Hornerstown	0.5 to 2.0	148	
Mount Laurel-Wenonah	-1 to 0.8	3590 to 3940	

a) Reference elevations are in feet NAVD88

b) Units of conductance are square feet per day

c) GHB conductances are a function of thickness and generally vary along their lengths.

**PSEG Site
ESP Application
Part 2, Site Safety Analysis Report**

**Table 2.4.12-15
Residuals Statistical Analysis
Final Calibrated Model (Sheet 1 of 2)**

Name	Easting	Northing	Layer	Observed	Computed	Residual
NOW-1U	198443	234543	2	0.93	1.04	-0.11
NOW-1L	198450	234564	4	1.08	0.79	0.29
NOW-2U	197755	235207	2	0.53	0.50	0.03
NOW-2L	197753	235228	4	0.73	0.60	0.13
NOW-3U	197885	234553	2	0.53	0.39	0.14
NOW-3L	197898	234565	4	0.60	0.64	-0.04
NOW-4UB	198147	233963	2	0.79	0.90	-0.11
NOW-4L	198148	233973	4	0.67	0.70	-0.03
NOW-5L	198438	234927	4	0.87	0.81	0.06
NOW-6U	198314	235269	2	0.98	1.13	-0.15
NOW-6L	198313	235288	4	0.63	0.80	-0.17
NOW-7U	199694	234976	2	1.02	1.11	-0.09
NOW-7L	199676	234973	4	0.93	1.01	-0.08
NOW-8U	199756	234142	2	1.11	1.99	-0.88
NOW-8L	199736	234139	4	1.06	0.97	0.09
EOW-1U	202758	232322	2	1.40	2.04	-0.64
EOW-1L	202758	232298	4	1.22	0.89	0.33
EOW-2U	202158	233275	2	2.88	2.14	0.74
EOW-2L	202178	233271	4	1.40	0.98	0.42
EOW-4L	202021	231733	4	1.26	0.83	0.43
EOW-5U	203007	233057	2	1.31	1.75	-0.44
EOW-5L	203021	233040	4	1.46	0.96	0.50
EOW-6U	203281	232587	2	1.38	1.76	-0.38
EOW-6L	203301	232588	4	1.17	0.93	0.24
EOW-8U	203520	231144	2	1.41	1.51	-0.10
EOW-8L	203516	231163	4	0.91	0.80	0.11
EOW-9U	202826	230917	2	0.69	1.54	-0.85
EOW-9L	202845	230926	4	1.14	0.76	0.38
EOW-10U	203521	231687	2	1.64	1.55	0.09
EOW-10L	203522	231707	4	1.22	0.85	0.37
Well BA	199984	230320	2	1.97	1.80	0.17
Well BF	199322	231301	2	1.88	1.96	-0.08
Well BG	199212	231829	2	2.30	2.36	-0.06
Well BH	198752	231891	2	1.77	1.54	0.23
Well BL	198390	232627	2	1.69	1.38	0.31
Well BM	198936	232658	2	2.26	2.66	-0.40
Well BP	198010	233572	2	1.09	0.85	0.24
Well BQ	198966	233401	2	2.95	2.72	0.23
Well BR	198711	234004	2	1.72	1.91	-0.19
Well BS	200475	234137	2	2.71	1.77	0.94
Well BT	199958	232909	2	3.13	3.08	0.05
Well BU	200236	231883	2	2.95	3.00	-0.05

**PSEG Site
ESP Application
Part 2, Site Safety Analysis Report**

**Table 2.4.12-15
Residuals Statistical Analysis
Final Calibrated Model (Sheet 2 of 2)**

Name	Easting	Northing	Layer	Observed	Computed	Residual
			Residual Mean			0.04
			Res. Std. Dev.			0.36
			Sum of Squares			5.48
			Abs. Res. Mean			0.27
			Min. Residual			-0.88
			Max. Residual			0.94
			Range in Target Values			2.60
			Std. Dev./Range			0.138

- a) Target water level data were selected as the average of the acceptable data (see Table 3) with the high and low value also deleted.

**PSEG Site
ESP Application
Part 2, Site Safety Analysis Report**

**2.4.13 ACCIDENTAL RELEASE OF RADIOACTIVE LIQUID EFFLUENTS IN
GROUNDWATER AND SURFACE WATERS**

2.4.13.1 Groundwater

This subsection provides an analysis of an accidental liquid release of effluents or radioactive wastes to the groundwater at the PSEG Site. The postulated accident scenarios are combined with the conceptual site model to evaluate potential impacts to receptors should a catastrophic tank rupture occur during plant operations and instantaneously release radionuclides to the groundwater environment. The resulting calculated concentrations that would reach the potential receptors are then compared to the effluent concentration limits (ECLs) published in 10 CFR Part 20, Appendix B.

The calculated concentrations are then assessed using the unity rule: the sum of the ratios of the calculated concentrations to the corresponding ECLs for all radionuclides in the effluent may not exceed "1", or unity, without requiring further dose assessment.

2.4.13.1.1 Assumptions and Methodology

The assumptions and basis for the evaluations provide a conservative determination of the potential exposure point concentrations and are consistent with guidance in NUREG-0800. Exposure point concentrations are compared to ECLs in 10 CFR Part 20 to determine regulatory compliance.

The groundwater conceptual site model used to evaluate the hypothetical releases is described in Subsection 2.4.12. Due to potential for migration in different directions following construction, two accidental release locations are hypothesized. One hypothetical release location is on the western edge of the power block and assumes migration west toward the Delaware River. The second hypothetical release location is at the northeast corner of the power block, and assumes migration northeast toward a Delaware River tributary named Fishing Creek. Hydrogeologic parameters, measured and calculated from data at the proposed new plant location are used to calculate the time of travel from each hypothetical release location to the primary point of exposure, and to determine decreases in concentrations of radionuclides due to decay. Hydraulic gradients, hydraulic conductivities and estimated average and maximum groundwater velocities determined in the field investigation of actual site conditions are presented in Subsection 2.4.12.1.3. The evaluation of hypothetical northeastern migration pathway utilizes the hydraulic conductivities from Subsection 2.4.12.1.3 and a gradient based on the observed groundwater elevations and the postulated flow distance. Thus, the flow velocity for the hypothetical northeastern flow path is calculated and does not correspond with the maximum groundwater velocities presented in Subsection 2.4.12.1.3.

The Delaware River lies immediately to the west of the proposed new plant location. Marshlands and Fishing Creek lie to the east and northeast of the new plant location, while the Hope Creek Generating Station (HCGS) is immediately to the south. Groundwater level data for the new plant location collected in monitoring wells in the Alluvium and in the Vincentown Formation indicate predominately westerly groundwater flow toward the Delaware River. While northeast and eastern components of groundwater flow are apparent in some instances due to

**PSEG Site
ESP Application
Part 2, Site Safety Analysis Report**

diurnal tidal effects, the average and sustained flow direction to the nearest potential exposure point is to the west, i.e., the Delaware River.

However, due to uncertainty and a possibility that an easterly flow component will develop in the Alluvium due to groundwater mounding after construction, a groundwater pathway toward the nearest water body toward the east, Fishing Creek, is assessed. Other potential receptors, such as public water supply wells, are further east and in deeper strata (See Subsection 2.4.12.2). This creek, which flows northward, is located along the former eastern river bank of the Delaware River. The trace of the former riverbank, at its nearest point approximately 4200 feet from the power block, is an area where the depth to the top of the Alluvium would be expected to be less than that in areas further away from the former shoreline and closer to the power block. Therefore, this area represents the nearest plausible discharge point for the groundwater discharge from the Alluvium.

The smaller surface water channels in the marshland area between the power block and Fishing Creek, are shallow channels with little to no flow at low tide. Surface water in the marsh area is underlain by low permeability hydraulic fill above the Alluvium and therefore there is little hydraulic communication between the surface water and the Alluvium. Water levels measured in shallow piezometers east of the power block demonstrate poor hydraulic communication between surface water and the shallow portion of the hydraulic fill (See Subsection 2.4.12.1.3.7). The presence of hydraulic fill also precludes upward vertical migration from the deeper Alluvium. Therefore, flow through the more permeable Alluvium to the point of discharge is taken as more conservative based on distance and time of travel.

The first step in the evaluation includes a screening approach considering only advection and decay to limit the number of radionuclides carried forward into the more complex evaluations. Next, dilution upon discharge of the radionuclide plume to surface-water is considered by estimating a dilution ratio of groundwater plume rates to receiving water flows. The most conservative values are used (i.e., fastest velocities, highest hydraulic conductivities); therefore, alternative conceptual site models would only show lower resulting concentrations, and are not evaluated. Subsection 2.4.13.1.3 discusses the groundwater flow and migration potentials to determine the most conservative release scenario.

2.4.13.1.2 Accident Scenario

The hypothetical accident scenario involves instantaneous release (NUREG-0800, 15.7.3, III.1.a, 1981 for the ABWR and AP1000, and Branch Technical Position [BTP] 11-6 for the U.S. EPR and US-APWR) of 80 percent of the contents of a liquid radioactive waste tank into nearby groundwater. This scenario represents the most conservative results of a release to groundwater and potentially affected groundwater receptors.

The final technology and plant layout have not yet been determined. Therefore, two independent points of release of the hypothetical tank failure are conservatively assumed to occur. The first is at the western edge of the proposed power block and the second is at the northeast edge of the power block. The distance from the point of release, along the postulated flow path to the Delaware River (the nearest probable receptor of the contaminated groundwater for a westerly migration pathway) is 285 feet (ft.) (Figure 2.4.13-1). This is a conservative value because it represents the horizontal distance from the western edge of the power block to the

**PSEG Site
ESP Application
Part 2, Site Safety Analysis Report**

shoreline. As discussed below, the aquifer's discharge point to the river is likely beyond the shoreline due to the depths of the aquifers relative to the bottom of the river at the shoreline.

The distance from the point of release, along the postulated flow path to Fishing Creek (the nearest probable receptor of the contaminated groundwater for an easterly or northeasterly migration pathway) is 4200 ft. (Figure 2.4.13-2). Hydraulic gradient data from the 12-months of groundwater readings indicate a release along the eastern side of the power block would most likely migrate west toward the river. However, an alternative migration pathway toward the northeast is conservatively postulated to allow for the potential that gradients may be altered as a result of construction. While a significantly longer pathway to the river to the northeast or conversely to the east and then south to the Delaware River would be a more plausible alternative pathway, a shorter migration pathway to the northeast toward Fishing Creek is conservatively assumed. At this distance, the postulated flow path would meet the location of the trace of the former river bank where the depth to the top of the Alluvium would likely be less than that in the filled marsh area.

The proposed tank size is 30,000 gallons, so a release of 24,000 gallons of liquid radioactive effluent is postulated. Concentrations of radionuclides contained in this hypothetical release are specified as the bounding concentrations for the four DCDs (ABWR, AP1000, US-APWR and U.S. EPR), as is the 30,000 gallons specified for the tank volume. Table 2.4.13-1 contains the initial list of radionuclides considered and their bounding concentrations. The initial list of radionuclides considered, the associated bounding concentrations, and the bounding tank volume is obtained from SSAR Table 1.3-9.

2.4.13.1.3 Conceptual Model and Hydrogeologic Inputs

The PSEG Site facility is isolated. There are no public water supply wells within 3.5 miles of the facility (the nearest being across the river in Delaware). In addition, the two immediately underlying aquifers, the Alluvium and the Vincentown, which are the evaluated release paths, are brackish and unsuitable as potable water sources.

The hydrogeologic setting consists of low permeable fill (mainly hydraulic fill materials historically dredged from the Delaware River) placed over more permeable Alluvium. It is expected that natural recharge within the fill materials results in vertical migration into the Alluvium which overlies the Kirkwood Formation confining layer. The top of the Alluvium aquifer has an elevation ranging from -22 to -35 ft. North America Vertical Datum 1988 (NAVD) through the northern portion of the PSEG Site, and an average thickness of 13 ft. The river immediately adjacent to the site is not dredged and is relatively shallow (7 to 11 ft. deep). This corresponds to an elevation of -7 to -11 ft. NAVD. The discharge of effluent through the Alluvium to the river more likely occurs at some distance from the shoreline where the river deepens and the overlying material thins. To support new plant construction, the river bottom will be dredged to an elevation of approximately -15 to -18 ft. NAVD. Following dredging, the discharge from the groundwater to the river could be nearer the shoreline than under existing conditions. Therefore, as a conservative estimate, the westerly migration pathway is assumed to be the distance from the postulated release point to the river shoreline.

With respect to the easterly migration pathway, the elevation of the bottom of Fishing Creek is not published on coastal survey maps. However, the depth is estimated to be slightly less than the mean low water elevation (approximately -2 to -4 ft. NAVD) based on the observation that

**PSEG Site
ESP Application
Part 2, Site Safety Analysis Report**

little flow occurs in this channel at low tide. Therefore, discharge is conservatively assumed to occur upward into Fishing Creek from the Alluvium without impedance by lower permeability hydraulic fill or marsh sediments that are present.

Dredging of the river in the vicinity of the proposed expansion locations may improve the connection of the river to the Alluvium for the westerly flow path and tidal effects in the Alluvium may be increased as a result. Although the flow into the river may be slowed by remaining sediments above the Alluvium, no resistance is assumed in the calculations for the migration pathway toward the west. The added resistance of high organic material sediments would allow for greater retardation, travel times, and radioactive decay. Tidal responses in the Alluvium are relatively small, especially at distances more than a few hundred feet east of the river. While a greater tidal response might occur due to an improved connection with the river after dredging, the tidal effects are manifest more as a change in hydrostatic pressure in the confined Alluvium rather than actual intrusion of water from the river for any significant distance in towards the site. Any intrusion that might occur would help set up a narrow mixing zone just prior to discharge of groundwater to the river that would result in lowered concentrations at the river. The net tidal effects in the Alluvium due to dredging will be minimal as the river is the sink for groundwater flow in this unit and total discharge of groundwater over a tidal cycle would remain the same despite any diurnal tidal cycle effects.

Assuming there is hydraulic communication between the Alluvium and the surface water at Fishing Creek, a similar tidal mixing zone is hypothesized for discharge of groundwater to the northeast. This mixing zone would also result in lowered concentrations prior to discharge into the creek.

Local horizontal hydraulic gradients in the Alluvium for the westerly flow path are reflected by piezometric heads or groundwater levels presented in Subsection 2.4.12. The data may indicate inward flow toward the site during high tide in some instances, but these would be counter-balanced by higher outward local gradients at low tide. Thus the average horizontal hydraulic gradient, taking into account seasonality and tidal effects, results in a net flow direction from the new plant location west towards the Delaware River.

A flow path toward the northeast is not directly supported by water level data, but rather an assumption for this flow direction is made to account for changes in hydraulic gradients that may occur after construction. The discharge location is chosen as the closest point easterly to the former eastern bank of the Delaware River and at the current location of Fishing Creek where the depth to the top of the Alluvium is expected to be less than that in other locations of the marsh. Other flow directions further north or southeast from the power block would result in longer flow paths to the Delaware River, and thus would be less conservative. To calculate the hydraulic gradient for the northeast migration pathway to the Fishing Creek, the maximum groundwater water level along the east side of the power block and a groundwater elevation equivalent to mean sea level at the point of discharge (south end of Fishing Creek) are assumed.

While structural fill with potentially higher hydraulic conductivity may be placed as foundation support material, the migration pathway between the power block and the two discharge points will remain within the lower permeability Alluvium. This evaluation assumes that the releases occur at the western or northeastern edges of the proposed power block, at distances of 285 ft. and 4200 ft. respectively, to the receptors. The edge of the power block is chosen because a

**PSEG Site
ESP Application
Part 2, Site Safety Analysis Report**

reactor technology has not been selected, nor has the specific building layout been determined (Figures 2.4.13-1 and 2.4.13-2). Also, the release is conservatively assumed to occur directly into the Alluvium, and no time for decay is provided by the vertical migration through the hydraulic fills or the structural fill to the aquifer. A release further from the river or the creek, interior to the power block area, into the structural fill, would allow additional travel time for radioactive decay to occur and provide additional attenuation by dispersion, dilution, and sorption effects.

Water-level data have been collected monthly from the observation wells installed for this ESPA at the new plant location (Subsection 2.4.12.1.3) over the period from January 2009 to December 2009. Calculated horizontal hydraulic gradients, based on these water-level measurements and the interpreted probable migration pathway, indicate an average gradient along the projected westerly migration pathway of 0.00042 feet per foot (ft/ft), with a maximum gradient of 0.00235 ft/ft. As the data indicate, the precipitation that actually percolates down through the hydraulic and structural fills reaches the Alluvium and creates a mounded piezometric surface. This directs groundwater movement in the Alluvium toward natural sinks for groundwater, namely the Delaware River to the west and south for site groundwater in the western portion of the site, and to the east and south for groundwater in the eastern portion of the facility. The mounding is a function of the hydrogeologic properties of the Alluvium, the distribution of recharge across the site, and distances and directions to groundwater sinks, i.e., places where groundwater would discharge to surface water. Groundwater flow at the site is generally radially outward (see Figure 2.4.12-30).

While an easterly groundwater flow component is not postulated from any part of the power block, a migration direction to the marshy areas to the east, if it were to occur, is also hypothesized to occur in the Alluvium. Migration upward through a thicker sequence (approximately 30 to 40 ft.) of low permeability hydraulic fill or natural marsh sediments before discharging to the surface water (see Figures 2.4.12-5 and 2.4.12-6) results in a longer travel time as the hydraulic conductivity of the Alluvium is reported to be 1,000 to 10,000 times more than that of the overlying hydraulic fill (Reference 2.4.12-1). To assess the easterly migration pathway, hydraulic parameter values determined by testing performed in the proposed power block area are used.

Slug test analyses of monitoring wells installed in the Alluvium at the new plant location suggest an average hydraulic conductivity of 3.8 feet per day (ft/day), and a maximum of 8 ft/day.

Considering an effective porosity of 0.20, the estimated average groundwater velocity along the postulated migration pathway of the release to the Delaware River from the west side of the power block is 0.00788 ft/day (2.9 feet per year [ft/yr]). Maximum groundwater velocity is estimated as 0.094 ft/day (34 ft/yr).

For the migration pathway to the east or northeast, only the maximum hydraulic parameters (hydraulic conductivity and estimated maximum gradient) are considered. To calculate the maximum horizontal hydraulic gradient for the northeast migration pathway to the Fishing Creek, the maximum water level along the east side of the power block and a groundwater elevation equivalent to mean sea level at the point of discharge are used. The maximum water level from the 2009 data set (12 months) for the two wells located along the eastern side of the power block (NOW-7U and NOW-8U) is selected. Since the well NOW-7U is actually screened in the upper Vincentown, the maximum level is chosen from NOW-8U at 1.57 ft. NAVD (See

**PSEG Site
ESP Application
Part 2, Site Safety Analysis Report**

Table 2.4.12-5). Since the travel time is expected to be significantly longer to the east, the gradient assumes local mean sea level (a value equivalent to -0.05 ft. NAVD as taken from the NOAA station at Reedy Point, Delaware, Reference 2.4.13-6) to estimate groundwater elevation at the discharge point (Fishing Creek). From the water elevation data (1.57 ft. and -0.05 ft. NAVD) and the distance (4200 ft.) a maximum horizontal hydraulic gradient of 0.00039 ft/ft is calculated for a northeasterly migration pathway. Assuming the same effective porosity (0.20) and maximum hydraulic conductivity (8 ft/d) used for the western migration pathway and the maximum hydraulic gradient to the northeast, a maximum groundwater velocity of 0.0154 ft/d is calculated for the northeast flow path toward Fishing Creek.

If a release were to migrate downward through the Kirkwood aquitard to the Vincentown or through areas where the Kirkwood aquitard may be absent, there are two possible flow paths through the Vincentown that could be considered. The first is westward toward the Delaware and upward through overlying materials which may include the Kirkwood aquitard, the Alluvium, and river bottom sediments at a location near the river bank. This, however, would result in a longer flow path and travel time than through the Alluvium alone. The second is through the Vincentown to a location approximately 1 to 2 miles to the northwest of the site where the Vincentown outcrops to the Delaware River (Reference 2.4.12-39). The thickness of the Vincentown is much greater than that of the Alluvium, so that there is a greater potential for vertical spread in the Vincentown, which both dilutes the flow and allows for greater dispersion of the plume. Although groundwater velocity through the Vincentown is similar to that in the Alluvium (see Subsection 2.4.12.1.4), this is a much longer potential pathway and therefore much less conservative when compared to a release through the Alluvium alone.

While deeper aquifers exist below the Vincentown, vertical gradients are relatively small, and intervening thick and low-permeability aquitards protect them against deeper migration of an accidental release. The longer flow paths of such migration pathways would require longer travel times with greater decay, dispersion, dilution, and retardation, which would be less conservative than migration through the Alluvium. It is this conservative pathway, through the Alluvium, that is selected for the following evaluation.

2.4.13.1.4 Radionuclide Transport Analysis

The analysis of an accidental release to groundwater is based on a conceptual model of a catastrophic release of a volume of radionuclide-contaminated water from a containment vessel or tank (assuming a release of 80 percent of the total vessel volume). This release instantaneously displaces an equal volume of groundwater in the underlying Alluvium aquifer. The release then proceeds to migrate at the estimated groundwater flow velocity to a location taken conservatively as 285 ft. from the point of release (along the western edge of the power block) to the Delaware River. The second independent release location considered is from the northeast edge of the power block to Fishing Creek, approximately 4200 ft. to the northeast.

This accidental release screening analysis is conducted in three stages, with the results compared to 10 CFR Part 20 ECLs. First, the list of potentially released radionuclides (Table 2.4.13-1) contains a number with very short half-lives, which are excluded (thus limiting the number of radionuclides for further consideration); constituents with initial concentrations equal to or less than their respective ECLs are also deleted. Given the setting and the hypothetical release location, this screening step decreases the number of radionuclides that need to be considered further (see Table 2.4.13-1). Second, a conservative assumption of decrease in

**PSEG Site
ESP Application
Part 2, Site Safety Analysis Report**

activity/concentration due to radioactive decay and advective transport only is applied. Finally, if contaminated groundwater discharges to surface-water, dilution of radionuclides in groundwater takes place in the surface-water discharge in proportion to their relative flow rates. For large surface-water flows, such as flows in the Delaware River, this dilution is large. For the case of dilution in Fishing Creek, a minimum amount of flow needed to reduce concentrations below ECLs is calculated, since by advection and decay only, the unity rule is nearly achieved.

Using these remaining radionuclides and the average and maximum estimated groundwater velocities for the west flow path, concentrations at the river edge and examples of concentrations within the river are computed. The remaining radionuclides and maximum estimated groundwater velocities are also used for the northeast flow path to calculate concentrations at the edge of Fishing Creek and to provide an example showing the minimum amount of dilution needed for the discharge to be below ECLs. These are identified as the following cases for later reference:

- Case 1 (west pathway): Average groundwater flow rates (average travel time) and concentrations at the river's edge.
- Case 2 (west pathway): Average groundwater flow rates (average travel time) and examples of anticipated concentrations in the river.
- Case 3 (west pathway): Maximum groundwater flow rates (minimum travel time) and concentrations at the river's edge.
- Case 4 (west pathway): Maximum groundwater flow rates (minimum travel time) and examples of anticipated concentrations in the river.
- Case 5 (northeast pathway): Maximum groundwater flow rates (minimum travel time) and concentrations at Fishing Creek.
- Case 6 (northeast pathway): Maximum groundwater flow rates (minimum travel time) and calculated minimum surface water flow to achieve the unity rule at Fishing Creek.

The cases with the maximum groundwater velocities offer the more conservative approach as there is less time for radioactive decay to occur. Note that the analyses do not include retardation effects, which are significant for most radionuclides. Retardation slows migration down providing additional time for radioactive decay, which allows the unity rule to be met for those radionuclides that are retarded. Tritium is not retarded, and is the notable exception. Minimum mixing volumes estimated to meet the unity rule are discussed in Subsection 2.4.13.1.8.

For the west pathway, the estimates of average and maximum groundwater velocities in the Alluvium are based on the evaluation and calculation of hydraulic gradients for each of the twelve monthly measurement events. These events covered a variety of seasonal and tidal conditions, yielding an average and maximum hydraulic gradient. These estimates were coupled with the assumption of an effective porosity of 0.2 (Reference 2.4.13-4) along with estimates of average and maximum hydraulic conductivity. The conductivities were obtained from the results of slug tests performed in Alluvium aquifer monitoring wells in the proposed

**PSEG Site
ESP Application
Part 2, Site Safety Analysis Report**

power block area. Available historic groundwater level data on the Alluvium throughout the site, (References 2.4.12-1 and 2.4.12-2), when compared with the twelve months of water levels collected in 2009, and the more geographically extensive groundwater level measurements in September 2009, suggest that the water levels within the Alluvium are relatively stable across the site and over time. The minimum travel time for a hypothetical release of radionuclides to groundwater to arrive at a discharge location is based on the shortest pathway distance, the maximum hydraulic gradient, and the maximum hydraulic conductivity. The groundwater flow velocity developed from these site-specific hydrogeologic parameters results in a minimum travel time calculated at greater than 3000 days (>8 years).

For the migration pathway to the northeast only the maximum hydraulic parameters (hydraulic conductivity and estimated maximum gradient) are assumed. As described in Subsection 2.4.13.1.3, to calculate the maximum horizontal hydraulic gradient for the northeast migration pathway to Fishing Creek, the maximum water level along the east side of the power block and a groundwater elevation equivalent to mean sea level at the point of discharge are considered. The groundwater flow velocity developed from the site-specific hydrogeologic parameters and the estimated gradient for this pathway results in a minimum travel time calculated at greater than 270,000 days (>740 years).

Some of the radionuclides may decay to other radionuclides of concern. Other radionuclides are parents (have no other contributing species, so initial concentrations simply decay), and their decay products are termed progeny or daughter products. Decay of parent compounds follows simple first-order decay kinetics, while the equations governing the time-dependent concentrations of progeny are more complex and require solution of sequential differential equations. Further, a parent element may branch off into more than one progeny.

Input parameters necessary for modeling the radioactive decay of radionuclides include first-order decay rates (or half-lives), initial concentrations, and duration of decay. First-order decay rates are obtained from Table E.1 of NUREG/CR-5512, *Residual Radioactive Contamination from Decommissioning* or the chart of Nuclides (Reference 2.4.13-5). Equations (Eq.) governing the decay of radionuclides are developed and presented in Appendix B of NUREG/CR-5512. Results are presented in Tables 2.4.13-2 through 2.4.13-5.

The advective mean groundwater velocity is assumed to follow Darcy's Law (Reference 2.4.13-3).

$$V = Ki/n_e \quad \text{(Equation 2.4.13-1)}$$

where: V = mean groundwater velocity
 K = aquifer hydraulic conductivity
 i = aquifer hydraulic gradient
 n_e = effective porosity

with consistent units.

The duration of travel, t , for a particular radionuclide is given by:

$$t = (L/V) \quad \text{(Equation 2.4.13-2)}$$

**PSEG Site
ESP Application
Part 2, Site Safety Analysis Report**

where: L = the distance from the release to the receptor
 V = the mean groundwater velocity

with consistent units.

First-order radioactive decay of a parent is governed by the equation:

$$C_{P1} = C_{P0} \exp(-\lambda_1 t) \quad (\text{Equation 2.4.13-3})$$

where: C_{P1} = parent radionuclide concentration at time t
 C_{P0} = parent radionuclide concentration at time zero
 \exp = exponential function base e (2.718281828...)
 λ_1 = first-order decay rate of parent

with consistent units.

If decay rates are expressed in terms of half-lives ($t_{1/2}$), λ is obtained from Equation 2.4.13-4 by substituting $C_{P1} = 0.5C_{P0}$ and $t = t_{1/2}$ and solving for λ as:

$$\lambda = \ln 2 / t_{1/2} \quad (\text{Equation 2.4.13-4})$$

with consistent units.

For the first progeny in the decay chain (subscript 2), concentrations vary due to its formation from the parent (subscript 1 or P) and its loss due to its own decay. The equation expressing the concentration of the first progeny in the decay chain is:

$$C_2 = K_1 \exp(-\lambda_1 t) + K_2 \exp(-\lambda_2 t) \quad (\text{Equation 2.4.13-5})$$

λ_2 = first-order decay rate of progeny

where: C_2 = progeny radionuclide concentration at time t , and

$$K_1 = (d_{12}\lambda_2 C_{P0}) / (\lambda_2 - \lambda_1) \quad (\text{Equation 2.4.13-6})$$

$$K_2 = C_{20} - (d_{12}\lambda_2 C_{P0}) / (\lambda_2 - \lambda_1) \quad (\text{Equation 2.4.13-7})$$

with consistent units.

where: d_{12} = fraction of parent that goes to the first progeny, and
 C_{20} = initial concentration of the first progeny

with consistent units.

Equations Equation 2.4.13-2, 3, 5, 6, and 7 are analogous to those published in Appendix B of NUREG-CR-5512.

Fractions of some parent radionuclides may branch off to different progeny; however, for the radionuclides under consideration here, that is not the case and the more complex equations need not be considered.

**PSEG Site
ESP Application
Part 2, Site Safety Analysis Report**

2.4.13.1.5 Radionuclides Determined to be a Potential Migration Threat

Based on the high decay rate of many of the radionuclides potentially present in the radioactive waste tank (with half-lives less than a year), and considering that several bounding concentrations are already less than the ECLs, the list of potential migration threats are considered to be limited to 12 radionuclides, two of which are potential progeny. This process results in the elimination of radionuclides from further consideration. The list of radionuclides retained for further analysis and the assumed bounding (initial) concentrations are shown in Table 2.4.13-1.

2.4.13.1.6 Transport with Advection and Radioactive Decay Only (Cases 1, 3 and 5)

In this second screening analysis, no retardation or dispersion effects are considered. The radionuclide is assumed to be transported at the mean groundwater velocity, thus conservatively limiting the duration of the time of travel and minimizing the period for radioactive decay. For the west flow path, the average mean groundwater velocity through the Alluvium aquifer, considered to be the most rapid horizontal pathway, is 0.007875 ft/day, and estimated maximum velocity is 0.094 ft/day (Subsection 2.4.13.1.3). While some tidal effects have been noted in shallow aquifers at the site, the net migration rate of groundwater is represented by the average and maximum velocities estimated from site-specific data. Assuming a migration pathway of 285 ft., based on the assumption of the western edge of the proposed power block as the tank release location (Figure 2.4.13-1), the advective transport time from point of release to the Delaware River is 36,190 days (99.1 years) for the average velocity (Case 1) and 3,032 days (8.3 years) for the maximum velocity (Case 3).

For Case 5, northeast pathway to Fishing Creek, only the maximum velocity is estimated. Considering a migration pathway of 4200 ft. based on the hypothetical release at the northeast edge of the proposed power block as the tank release location (Figure 2.4.13-2), the advective transport time from point of release to Fishing Creek is 272,222 days (745.4 years) assuming the maximum groundwater flow velocity. Retardation of metal radionuclide migration, as likely occurs, is not considered.

Construction and installation of structures and fill will result in modifications of the existing groundwater flow patterns and rates. These are expected to decrease current flow rates due to longer flow paths around structures, decrease infiltration rates, and decrease hydraulic gradients in the Alluvium. While structural fill will replace some of the hydraulic fill currently present, overall flow rates in this evaluation and selected migration pathway are determined by the lower hydraulic conductivity materials outside of the excavation and fill replacement area. Releases to shallow groundwater are expected to stay shallow (in the Alluvium) and not migrate into the lower Kirkwood and Vincentown Formations and aquifers. Potentials for migration to deeper aquifers are discussed in Subsection 2.4.13.1.3.

While a few radionuclides could be eliminated due to ratios less than one percent of the respective ECLs for both average and maximum estimated groundwater flow rates, these elements are still carried forward in the next phase of analysis. The results of this step of the analysis are shown on Tables 2.4.13-2 (Case 1), 2.4.13-4 (Case 3) and 2.4.13-6 (Case 5).

**PSEG Site
ESP Application
Part 2, Site Safety Analysis Report**

2.4.13.1.7 Transport with Advection, Radioactive Decay and Dilution (Cases 2, 4 and 6)

Radionuclides in groundwater discharging to surface-water potentially are subject to dilution effects in the surface-water due to typically larger flow rates in the surface-water. The Delaware River is adjacent to the facility, and is 2.5 miles wide at the new plant location. As stated in Subsection 2.4.1, the flow of tidally-influenced water through this section ranges from 400,000 to 472,000 cubic feet per second (cfs), while Harleman cited flow rates as high as 800,000 cfs (Reference 2.4.13-2). For the western pathway, mixing of a discharge plume would not extend to the whole river width at the point of discharge, the circulation of water in the river adjacent to the site is still substantial. The flow reverses with the tides two times a day, subjecting the relatively low flux associated with a hypothetical discharge plume to substantial dilution. The estimated maximum groundwater flux rate of the release to the river (8.59 cubic feet per day) is very small relative to the flow in the river. It is estimated that mixing within a river flow rate of only 112 cfs (less than 0.03 percent of the low end of the available tidal flow, as cited above) would be sufficient to achieve the sum of fractions unity rule.

For the northeast migration pathway (Case 6), the minimum amount of dilution needed at the discharge point in Fishing Creek is calculated to achieve a sum of ratios unity rule. From the groundwater discharge rate (1.41 cubic feet per day) and the ECL ratio without dilution (1.38), it is estimated that a creek flow rate of only 0.53 cubic feet per day (0.000022 cfs) is needed to achieve the sum of ratios unity rule. This flow rate is considered very small in comparison to the size of the tributary which is approximately 3000 ft. long by 200 to 300 ft. wide with approximately 5 to 6 ft. of tidal water fluctuation. The flow needed to meet the unity rule is so small that additional groundwater discharge occurring 9 ft. on either side of the calculated 35-foot width discharge is sufficient by itself to provide the added flow to meet the unity rule (sum of ratios less than or equal to 1).

With the tidal cycles, there are periods of low flow adjacent to the shoreline at the river and creek during slack tide. These are for brief periods of time and the overall effect across the tidal cycle provides substantial dilution. In the analysis, as an example of the potential effects of dilution for the western pathway, a flow in the river over complete tidal cycles is taken as approximately two-thirds of the maximum flow rate. Discharging groundwater would be diluted only slightly during the brief period when the tide changes, but would dilute by several orders of magnitude when complete mixing is achieved during the normal tidal exchanges. The results of this analysis are shown on Tables 2.4.13-3 (Case 2, average groundwater velocity west flow path) and 2.4.13-5 (Case 4, maximum groundwater velocity west flow path) and 2.4.13-7, (Case 6, maximum groundwater velocity northeast flow path).

This analysis does not directly consider retardation effects. With the exception of tritium, the radionuclides evaluated have relatively large soil-water partition coefficients that would lead to very slow migration rates and increased travel times to allow decay to occur. The effects of retardation would then lessen the calculated concentrations discharging to the Delaware River for these radionuclides. Therefore, by not considering effects of retardation, this evaluation presents a conservative determination of the effects of the accidental release scenario.

Also, not considered in this analysis is the probable existence of a tidally-influenced mixing zone. In this zone, at the groundwater/surface-water interface, surface-water penetrates into the aquifer a short distance during the time the tide elevation is greater than the groundwater piezometric head and dilutes the flow until the tide cycle ebbs to allow the groundwater (mixed

**PSEG Site
ESP Application
Part 2, Site Safety Analysis Report**

with river water) to again discharge to surface-water. This additional dilution effect can be significant in lowering concentrations at the point of discharge.

2.4.13.1.8 Potential Effects from Increased Hydraulic Gradients (Mounding)

As described in Subsection 2.4.12, groundwater mounding in the power block area following construction is possible due to changes in grade elevation and placement of fill to support construction. However, under a conservative scenario, the unity rule is still met with increases in hydraulic gradients that are depicted in modeling output both on the east and west side of the power block.

Potential effects on post-construction groundwater gradients in the alluvium are depicted on Figure 2.4.12-28 under a conservative modeling scenario to develop estimates for maximum hydrostatic pressures inside a soil retention barrier. To the east of the power block, the steep portion of a potential increase in gradient is limited to approximately the first 400 feet of the total length of the estimated 4,200-foot long release pathway to Fishing Creek. If the length of the pathway were assumed to be shortened to 3,800 feet, the additional width of discharging groundwater bracketing the hypothetical accidental release plume reaching Fishing Creek to attain the unity rule through dilution would increase to about 24 feet on either side of the plume (from an estimated 9 feet on either side as described in Subsection 2.4.13.1.7). The amount of groundwater discharge to Fishing Creek needed to attain the unity rule is equivalent to an additional 1.59 cubic feet per day (2.12 cubic feet per day for the 3,800-foot long pathway versus 0.53 cubic feet per day for the 4,200-foot long pathway).

If dilution from adjacent groundwater discharge at Fishing Creek is discounted entirely, an equivalent dilution of 2.12 cubic feet per day is available from Fishing Creek flow. This amount of flow is expected to be only a small fraction of the tidally-induced flow in Fishing Creek as described in Subsection 2.4.13.1.7.

For a westerly release, the groundwater model for the post-construction scenario shows a gradient for the west flow path of 0.007 ft/ft. For comparison, the accidental release calculations show a maximum hydraulic gradient of 0.00235 ft/ft as cited in Subsection 2.4.13.1.3. Thus, the potential increase in hydraulic gradient over the full distance from the accidental release site to the Delaware River is approximately three times the maximum considered in the accidental release calculations. The accidental release calculation shows that mixing with only 112 cubic feet per second of flow in the Delaware River (about 0.03 percent of the available flow rate) is sufficient to meet the unity rule. Even if the ground water flow rate from a potential accidental release is tripled (due to the tripled hydraulic gradient), the required increase in river flow rate required to reach unity would still be well below (<0.2 percent) the minimum anticipated river flow rate.

In summary, if an increase in hydraulic gradient were to materialize for each release pathway (east and west sides), as suggested in the conservative scenario conducted to estimate maximum changes in hydraulic pressure within the power block, an unmitigated release does not result in an exceedance of the unity rule in the receiving body upon mixing.

**PSEG Site
ESP Application
Part 2, Site Safety Analysis Report**

2.4.13.1.9 Comparison with 10 CFR Part 20

For the average and maximum estimated groundwater velocities in the Alluvium aquifer (Cases 1, 3 and 5), the conservative analysis conducted above indicates that most of the radionuclides released remain under consideration relative to the 10 CFR Part 20 criteria. The results indicate that the concentrations reaching the Delaware River or Fishing Creek could be at levels where the ratio of concentration to ECL is greater than one percent and a total of these ratios for all constituents in the mixture is greater than 1 (see Tables 2.4.13-2, 2.4.13-4 and 2.4.13-6). Concentrations could still remain above the ECL at the point of discharge, but the receiving water dilution factors (Cases 2 and 4) reduce the exposure concentration to several orders of magnitude below the ECL (Tables 2.4.13-3, 2.4.13-5 and 2.4.13-7). The Delaware River and Fishing Creek, in the vicinity of the PSEG Site, are not sources of drinking water due to salinity. In addition, the Alluvium and Vincentown aquifers are also not potable water supplies due to elevated salinity. The nearest off-site public water supply wells are within the Mount Laurel-Wenonah aquifer and are located approximately 3.5 miles across the river in Delaware. These wells would not be impacted by a release to the Alluvium or the Vincentown aquifers.

Based on the sum of the fractions and without dilution, the unity rule is exceeded. However, a more refined analysis taking credit for retardation would result in only tritium reaching the Delaware River at concentrations significantly above the ECL. With dilution alone, and without any contribution from retardation, the resulting sum of the fractions would also be significantly less than 1 for all radionuclides. The amount of dilution that would take place at the edge of each receiving water body cannot be easily quantified. However, the very low rates of discharge of the maximum estimated rate of the hypothetical release, not considering other attenuation factors such as dispersion and retardation, requires only mixing within a river flow of 112 cfs (less than 0.03 percent of the low end of the available tidal flow, as cited above) to meet a sum of ratios of less than 1 for a release along the west side of the power block. Under similar assumptions (no dispersion or retardation) a flow of only 0.53 cubic feet per day in Fishing Creek would be needed to achieve the unity rule for a release at the northeast edge of the power block.

2.4.13.1.10 Conclusions

The above discussion presents a conservative analysis of the potential effects of the accidental release of liquid radioactive waste to groundwater in two independent locations within the power block. For a release along the western edge of the power block, a westerly migration path to the Delaware River is considered. For a release along the northeast edge of the power block, a northeasterly migration pathway to Fishing Creek is assessed. Each release does not take into account dispersion and retardation of the radionuclides. The analysis for the west flow path, a shorter pathway, indicates that most of the radionuclide releases considered in this hypothetical scenario could reach the potential receptor (at the point of discharge to the Delaware River) at concentrations above 10 CFR Part 20 ECLs. If retardation effects are included, all radionuclides, except for tritium, would likely be present at the discharge location at activities less than one percent of their respective ECLs. The Delaware River is tidal in the vicinity of the site, and the ebb and flow of the tidally-influenced estuary offers several orders of magnitude of dilution to the effluent release. Considering this dilution effect, all radionuclides are within the limits of 10 CFR Part 20.

**PSEG Site
ESP Application
Part 2, Site Safety Analysis Report**

The analysis of the northeast flow path indicates that without any consideration for the effects of dispersion, retardation, or dilution, all but one radionuclide would be present at the discharge point (Fishing Creek) below their respective ECLs. The calculated ECL ratio (1.38) for all radionuclides is slightly over the target ECL ratio of 1.00. Considering the effect of a small amount of flow contribution for dilution from Fishing Creek (0.53 cubic feet per day or more) all radionuclides are within the limits of 10 CFR Part 20 for this flow path.

Increased hydraulic gradients or mounding in the alluvium unit, which may occur following construction, are expected to result in only a limited increase in radionuclide concentrations at the discharge point that meets the unity rule, when taking into account a relatively small amount of dilution for each transport pathway.

In addition to the conservative assumptions of maximum estimated groundwater velocity, minimum travel path length, and no attenuation due to dilution and dispersion, or retardation along the migration pathway, further conservatism is inherent in the analysis. Additional conservative factors not assumed in calculating estimated concentrations at the river point of discharge include:

- 1) That a construction soil retention barrier, which could act as a seepage cutoff, may remain in place, and a bulkhead, constructed along the river's edge, will decrease groundwater flux rates for the westerly migration pathway,
- 2) Improved site surface drainage may decrease infiltration and flow through the Alluvium in the vicinity of the expansion,
- 3) The shallow aquifers are not usable as potable water sources,
- 4) There are no public water supply wells within 3.5 miles of the facility (the nearest being across the river in Delaware), and
- 5) Spill containment will be provided for tanks where release of radionuclides to groundwater could potentially occur.

2.4.13.2 Surface-Water

There are no potable surface-water bodies downgradient of the PSEG Site. Although the final plant design and specific layout have not been determined, any outdoor tanks that contain radionuclides will have secondary containment to ensure that a catastrophic release does not result in the release of liquid effluent directly to the surface-water. There will also be controlled release points for systems that could be in contact with radioactive liquids to prevent any potential releases from being discharged directly to surface waters.

2.4.13.3 References

2.4.13-1 Not Used

- 2.4.13-2 Harleman, D.R.F., "One-Dimensional Models," in "Estuarine Modeling: An Assessment, Capabilities and Limitations for Resource Management and Pollution

**PSEG Site
ESP Application
Part 2, Site Safety Analysis Report**

- Control,” by Tracor, Inc., for the Water Quality Office, Environmental Protection Agency, February 1971.
- 2.4.13-3 Kresic, N., “Hydrogeology and Groundwater Modeling,” 2nd edition, CRC Press, Boca Raton, Florida, 2007.
- 2.4.13-4 North Carolina Department of Environment and Natural Resources. Basic Hydrology.
http://www.ncwater.org/Education_and_Technical_Assistance/Ground_Water/Hydrogeology/#porosity, accessed 12/31/2009.
- 2.4.13-5 Parnington, J.R., et.al., “Nuclides and Isotopes,” 15th edition, General Electric, 1996.
- 2.4.13-6 U.S. Department of Commerce, National Oceanic and Atmospheric Administration, National Ocean Service, Reedy Point, C & D Canal, Delaware benchmark, <http://tidesandcurrents.noaa.gov/benchmarks/8551910.html#DatumsPage>, website, accessed 04/23/2012.

**PSEG Site
ESP Application
Part 2, Site Safety Analysis Report**

**Table 2.4.13-1 (Sheet 1 of 3)
Initial Concentrations of Radionuclides**

Radio-nuclide	Progeny	Bounding (uCi/cc)	Half-life (d)^(a)	Analysis (uCi/cc)
Br-82		3.50E-03	1.47E+00	*
Br-83		3.20E-02	9.96E-02	*
Br-84		1.70E-02	2.21E-02	*
Br-85		2.00E-03	1.99E-03	*
Rb-86m		3.00E-07	6.94E-04	*
Rb-86		1.10E-02	1.87E+01	*
Rb-88		1.50E+00	1.24E-02	*
Rb-89		6.90E-02	1.06E-02	*
Sr-89		1.53E-03	5.05E+01	*
Sr-90	Y-90	1.26E-04	1.06E+04	1.26E-04
Sr-91		2.10E-03	3.96E-01	*
Sr-92		1.59E-03	1.13E-01	*
Y-90		1.80E-04	2.67E+00	*
Y-91m		5.20E-04	3.45E-02	*
Y-91		6.01E-04	5.85E+01	*
Y-92		1.23E-03	1.48E-01	*
Y-93		2.04E-03	4.21E-01	*
Zr-95		1.60E-04	6.40E+01	*
Zr-97		6.70E-05	7.04E-01	*
Nb-95		1.80E-04	3.52E+01	*
Mo-99		2.10E-01	2.75E+00	*
Mo-101		5.00E-03	1.01E-02	*
Tc-99m		1.10E-01	2.51E-01	*
Ru-103		2.91E-04	3.93E+01	*
Ru-105		9.50E-05	1.85E-01	*
Ru-106	Rh-106	5.41E-05	3.68E+02	5.41E-05
Rh-103m		2.91E-04	3.90E-02	*
Rh-105		4.40E-05	1.47E+00	*
Rh-106		5.41E-05	3.46E-04	*
Ag-110m		1.74E-05	2.50E+02	*
Ag-110		1.10E-08	2.85E-04	*
Sb-125		8.00E-07	1.01E+03	**
Sb-127		5.00E-06	3.85E+00	* **
Sb-129		6.80E-06	1.85E-01	*
Te-125m		1.90E-04	5.80E+01	*
Te-127m		7.50E-04	1.09E+02	*
Te-127		2.20E-03	3.90E-01	*
Te-129m		2.50E-03	3.36E+01	*
Te-129		2.40E-03	4.83E-02	*
Te-131m		6.30E-03	1.25E+00	*
Te-131		2.60E-03	1.74E-02	*
Te-132		7.00E-02	3.26E+00	*

**PSEG Site
ESP Application
Part 2, Site Safety Analysis Report**

**Table 2.4.13-1 (Sheet 2 of 3)
Initial Concentrations of Radionuclides**

Radio-nuclide	Progeny	Bounding (uCi/cc)	Half-life (d)^(a)	Analysis (uCi/cc)
Te-133m		4.30E-03	3.85E-02	*
Te-134		7.60E-03	2.90E-02	*
I-129		4.60E-08	5.73E+09	**
I-130		5.00E-02	5.15E-01	*
I-131		7.40E-01	8.04E+00	*
I-132		3.70E-01	9.58E-02	*
I-133		1.30E+00	8.67E-01	*
I-134		2.40E-01	3.65E-02	*
I-135		7.90E-01	2.75E-01	*
Cs-132		2.20E-03	6.48E+00	*
Cs-134		2.00E+00	7.53E+02	2.00E+00
Cs-135m		2.40E-03	3.68E-02	*
Cs-136		1.00E+00	1.31E+01	*
Cs-137	Ba-137m	1.20E+00	1.10E+04	1.20E+00
Cs-138		3.70E-01	2.24E-02	*
Ba-137m		8.00E+00	1.77E-03	*
Ba-139		2.20E-02	5.74E-02	*
Ba-140		3.90E-03	1.27E+01	*
La-140		3.90E-03	1.68E+00	*
La-141		5.30E-05	1.64E-01	*
La-142		3.10E-05	6.42E-02	*
Ce-141		4.20E-04	3.25E+01	*
Ce-143		1.20E-04	1.38E+00	*
Ce-144		1.20E-04	2.84E+02	*
Pr-143		8.80E-05	1.36E+01	*
Pr-144		2.90E-03	1.20E-02	*
Pm-147		1.30E-05	9.58E+02	**
Nd-147		3.40E-05	1.10E+01	*
Eu-154		1.20E-06	3.21E+03	**
Np-239		2.04E-02	2.36E+00	*
Pu-238	U-234	2.00E-07	3.20E+04	2.00E-07
Pu-239		2.00E-08	8.79E+06	*
Pu-240		2.80E-08	2.39E+06	2.80E-08
Pu-241	Am-241	6.90E-06	5.26E+03	6.90E-06
Am-241		7.80E-09	1.58E+05	**
Cm-242		1.90E-06	1.63E+02	1.90E-06
Cm-244		1.00E-07	6.61E+03	1.00E-07
Na-24		3.70E-02	6.25E-01	*
P-32		2.07E-03	1.43E+01	*
Cr-51		8.11E-02	2.77E+01	*
Mn-54		1.23E-03	3.13E+02	*
Mn-56		4.00E-02	1.07E-01	*
Fe-55		1.80E-02	9.86E+02	1.80E-02

**PSEG Site
ESP Application
Part 2, Site Safety Analysis Report**

**Table 2.4.13-1 (Sheet 3 of 3)
Initial Concentrations of Radionuclides**

Radio-nuclide	Progeny	Bounding (uCi/cc)	Half-life (d)^(a)	Analysis (uCi/cc)
Fe-59		4.50E-04	4.45E+01	*
Co-58		3.30E-03	7.08E+01	*
Co-60		7.21E-03	1.93E+03	7.21E-03
Ni-63		1.80E-05	3.51E+04	**
Cu-64		1.92E-02	5.29E-01	*
Zn-65		3.60E-03	2.44E+02	*
W-187		1.80E-03	9.96E-01	*
H-3		3.50E+00	4.51E+03	3.50E+00

a) Half-lives from Table E.1 NUREG/CR-5512 or Chart of Nuclides

* Eliminated because half life is less than one year

** Eliminated because activity is below ECL

**PSEG Site
ESP Application
Part 2, Site Safety Analysis Report**

**Table 2.4.13-2
Radionuclide Concentrations - Advection and Decay Only
Average Groundwater Flow Rate Conditions^(f)**

Radionuclide	Progeny	Bounding (uCi/cc)	Half-life (days)^(a)	Decay Rate (1/day)	d12^(b)	d23^(c)	At Receptor Location (uCi/cc)	ECL^(e) (uCi/cc)	Ratio^(d)
Sr-90	Y-90	1.26E-04	10,600	6.54E-05	1		1.18E-05	5.00E-07	2.37E+01
Ru-106	Rh-106	5.41E-05	368	1.88E-03	1		1.36E-34	3.00E-06	4.55E-29
Cs-134		2.00E+00	753	9.20E-04			6.86E-15	9.00E-07	7.62E-09
Cs-137	Ba-137m	1.20E+00	11,000	6.3E-05	0.946		1.23E-01	1.00E-06	1.23E+05
Pu-241	Am-241	6.90E-06	5260	1.32E-04			5.86E-08	1.00E-06	5.86E-02
Cm-242		1.90E-06	163	4.25E-03	1		2.86E-73	7.00E-07	4.08E-67
	Pu-238 > U-234	2.00E-07	32,000	2.17E-05		1	9.58E-08	2.00E-08	4.79E+00
Cm-244		1.00E-07	6610	1.05E-04	1		2.25E-09	3.00E-08	7.50E-02
	Pu-240	2.80E-08	2,390,000	2.90E-07		1	2.80E-08	2.00E-08	1.40E+00
Fe-55		1.80E-02	986	7.03E-04			1.62E-13	1.00E-04	1.62E-09
Co-60		7.21E-03	1930	3.59E-04			1.64E-08	3.00E-06	5.46E-03
H-3		3.50E+00	4510	1.54E-04			1.35E-02	1.00E-03	1.35E+01
								SUM =	1.23E+05

a) Half lives from Table E.1 in NUREG/CR5512

b) d12 = fraction of parent decay to first progeny

c) d23 = fraction of first progeny to second

d) Ratio = the fraction receptor concentration divided by the ECL

e) ECL = Effluent Concentration Limit

f) Other Input Parameters.

Hydraulic Conductivity (K) = 3.75 ft/day.

Hydraulic Gradient (i) = 0.00042.

effective porosity (neff) = 0.2 (dim).

Groundwater Velocity (V) 0.007875 ft/day.

Receptor Distance = 285 ft.

Advective Time = 36,190.48 days, 99.084 years.

**PSEG Site
ESP Application
Part 2, Site Safety Analysis Report**

**Table 2.4.13-3
Radionuclide Concentrations - Advection, Decay and Dilution
Average Groundwater Flow Rate Conditions^{(a)(b)(c)(d)(e)(g)(h)(i)}**

Radionuclide	Receptor Concentration ^(f)	Diluted	ECL	Ratio
Sr-90	1.18253E-05	1.84584E-16	5.00E-07	3.69E-10
Ru-106	1.36485E-34	2.13041E-45	3.00E-06	7.10E-40
Cs-134	6.85618E-15	1.07019E-25	9.00E-07	1.19E-19
Cs-137	1.22741048E-01	1.91589E-12	1.00E-06	1.92E-06
Pu-241	5.86282E-08	9.15138E-19	1.00E-06	9.15E-13
Cm-242	2.85772E-73	4.46067E-84	7.00E-07	6.37E-78
Pu-238	9.57806E-08	1.49506E-18	2.00E-08	7.48E-11
Cm-244	2.24997E-09	3.51202E-20	3.00E-08	1.17E-12
Pu-240	2.79759E-08	4.36681E-19	2.00E-08	2.18E-11
Fe-55	1.61626E-13	2.52285E-24	1.00E-04	2.52E-20
Co-60	1.63816E-08	2.55704E-19	3.00E-06	8.52E-14
H-3	1.34576E-02	2.10062E-13	1.00E-03	2.10E-10
SUM =				1.92E-06

- a) The release volume is 80 percent of the tank volume.
b) The release volume displaces aquifer space.
c) The shape of the displacement is assumed to be square.
d) The flux rate is the area of the displacement times the specific discharge.
e) Average flow in the river is assumed to be 2/3 of the estimated maximum tidal flow past the site, i.e., 0.6667*800,000 cfs.
f) The receptor concentration is taken from the results for advection and decay.
g) No dispersion of the initial displacement is assumed.
h) Retardation is not considered in this scenario.
i) Input Parameters
- | | |
|-------------------------------------------------------------------|------------------------------------------|
| Tank Volume = 30,000 gallons | GW flow rate = 0.72 ft ³ /day |
| Release volume = 24,000 gallons (3208.556 ft ³) | Aquifer K = 3.75 ft/day |
| Aquifer thickness = 13 feet | Dilution Factor = 64,064,898,234 |
| Effective porosity = 0.2 (dimensionless) | |
| Area displaced = 1234.06 ft ² | Square side = 35.13 ft |
| Flow in river = 533,333 cfs (46,079,971,200 ft ³ /day) | |
| Hydraulic gradient = 0.00042 ft/ft | |

**PSEG Site
ESP Application
Part 2, Site Safety Analysis Report**

**Table 2.4.13-4
Radionuclide Concentrations Advection and Decay Only
Maximum Groundwater Flow Rate Conditions – West Flow Path^(f)**

Radionuclide	Progeny	Bounding (uCi/cc)	Half-life (in days) ^(a)	decay rate, 1/d	d12 ^(b)	d23 ^(c)	Concentration at Receptor Location (uCi/cc)	ECL ^(e) (uCi/cc)	Ratio ^(d)
Sr-90	Y-90	1.26E-04	10600	6.54E-05	1		1.03E-04	5.00E-07	2.07E+02
Ru-106	Rh-106	5.41E-05	368	1.88E-03	1		1.79E-07	3.00E-06	5.98E-02
Cs-134		2.00E+00	753	9.20E-04			1.23E-01	9.00E-07	1.36E+05
Cs-137	Ba-137m	1.20E+00	11000	6.3E-05	0.946		9.91E-01	1.00E-06	9.91E+05
Pu-241	Am-241	6.90E-06	5260	1.32E-04			4.63E-06	1.00E-06	4.63E+00
Cm-242		1.90E-06	163	4.25E-03	1		4.79E-12	7.00E-07	6.85E-06
	Pu-238 > U-234	2.00E-07	32000	2.17E-05		1	1.96E-07	2.00E-08	9.82E+00
Cm-244		1.00E-07	6610	1.05E-04	1		7.28E-08	3.00E-08	2.43E+00
	Pu-240	2.80E-08	2390000	2.90E-07		1	2.81E-08	2.00E-08	1.40E+00
Fe-55		1.80E-02	986	7.03E-04			2.14E-03	1.00E-04	2.14E+01
Co-60		7.21E-03	1930	3.59E-04			2.43E-03	3.00E-06	8.09E+02
H-3		3.50E+00	4510	1.54E-04			2.20E+00	1.00E-03	2.20E+03

SUM = 1.13E+06

- a) Half-lives from Table E.1 in NUREG/CR-5512.
b) d12 = fraction of parent decay to first progeny.
c) d23 = fraction of first progeny to second.
d) Ratio = the fraction receptor concentration divided by the ECL.
e) ECL = Effluent Concentration Limit.
f) Other Input Parameters.
K = hydraulic conductivity = 8 feet per day.
i = hydraulic gradient = 0.00235 feet per foot.
neff = effective porosity - 0.2 (dimensionless).
GW vel = groundwater velocity = 0.094 feet per day.
Receptor distance = 285 feet.
Advective time = 3032 days = 8.3 years.

**PSEG Site
ESP Application
Part 2, Site Safety Analysis Report**

**Table 2.4.13-5 (Sheet 1 of 2)
Radionuclide Concentrations – Advection, Decay, and Dilution
Maximum Groundwater Flow Rate Conditions – West Flow Path ^{(a)(b)(c)(e)(g)(h)}**

Radionuclide	Receptor Concentration ^(d)	Diluted	ECL ^(f)	Ratio
Sr-90	1.03E-04	1.93E-14	5.00E-07	3.85E-08
Ru-106	1.79E-07	3.34E-17	3.00E-06	1.11E-11
Cs-134	1.23E-01	2.29E-11	9.00E-07	2.54E-05
Cs-137	9.91E-01	1.85E-10	1.00E-06	1.85E-04
Pu-241	4.63E-06	8.62E-16	1.00E-06	8.62E-10
Cm-242	4.79E-12	8.93E-22	7.00E-07	1.28E-15
Pu-238	1.96E-07	3.66E-17	2.00E-08	1.83E-09
Cm-244	7.28E-08	1.36E-17	3.00E-08	4.52E-10
Pu-240	2.81E-08	5.23E-18	2.00E-08	2.61E-10
Fe-55	2.14E-03	3.98E-13	1.00E-04	3.98E-09
Co-60	2.43E-03	4.52E-13	3.00E-06	1.51E-07
H-3	2.20E+00	4.09E-10	1.00E-03	4.09E-07
			SUM =	2.11E-04

- a) The shape of the displacement is assumed to be square.
- b) The flux rate is the area of the displacement times the specific discharge.
- c) Average flow in the river is assumed to be 2/3 of the estimated maximum tidal flow past the site (Subsection 2.4.13.1.7).
- d) The receptor concentration is taken from the results for advection and decay.
- e) No dispersion of the initial displacement is assumed.
- f) ECL = Effluent Concentration Limits.
- g) Concentrations in microcuries per liter.

**PSEG Site
ESP Application
Part 2, Site Safety Analysis Report**

**Table 2.4.13-5 (Sheet 2 of 2)
Radionuclide Concentrations – Advection, Decay, and Dilution
Maximum Groundwater Flow Rate Conditions – West Flow Path^{(a)(b)(c)(e)(g)(h)}**

h) Input Parameter Values:

Tank Volume = 30,000 gallons
Release volume = 24,000 gallons (3208.56 ft³)
Aquifer thickness = 13 feet
Effective porosity = 0.2 (dimensionless)
Area displaced = 1234.06 ft²
Square side = 35.13 ft
Aquifer K = 8 ft/day
Hydraulic gradient = 0.00235 ft/ft
GW flow rate = 8.59 ft³/day
Flow in river = 533,333 cfs (46,076,971,200 ft³/day)
Dilution factor = 5,367,139,081

**PSEG Site
ESP Application
Part 2, Site Safety Analysis Report**

**Table 2.4.13-6
Radionuclide Concentrations – Advection and Decay Only
Maximum Groundwater Flow Rate Conditions – Northeast Flow Path^(f)**

Radionuclide	Progeny	Bounding (uCi/cc)	Half-life (in days) ^(a)	decay rate, 1/d	d12 ^(b)	d23 ^(c)	Concentration at Receptor Location (uCi/cc)	ECL ^(e) (uCi/cc)	Ratio ^(d)
Sr-90	Y-90	1.26E-04	10600	6.54E-05	1		2.35E-12	5.00E-07	4.70E-06
Ru-106	Rh-106	5.41E-05	368	1.88E-03	1		1.30E-227	3.00E-06	4.20E-222
Cs-134		2.00E+00	753	9.20E-04			3.10E-109	9.00E-07	3.50E-103
Cs-137	Ba-137m	1.20E+00	11000	6.3E-05	0.946		4.28E-08	1.00E-06	4.28E-02
Pu-241	Am-241	6.90E-06	5260	1.32E-04			1.83E-21	1.00E-06	1.83E-15
Cm-242		1.90E-06	163	4.25E-03	1		0	7.00E-07	0
	Pu-238 > U-234	2.00E-07	32000	2.17E-05		1	5.77E-10	2.00E-08	2.89E-02
Cm-244		1.00E-07	6610	1.05E-04	1		4.03E-20	3.00E-08	1.34E-12
	Pu-240	2.80E-08	2390000	2.90E-07		1	2.61E-08	2.00E-08	1.31E+00
Fe-55		1.80E-02	986	7.03E-04			1.45E-85	1.00E-04	1.45E-81
Co-60		7.21E-03	1930	3.59E-04			2.55E-45	3.00E-06	8.52E-40
H-3		3.50E+00	4510	1.54E-04			2.39E-18	1.00E-03	2.39E-15

SUM = 1.38E+00

- a) Half-lives from Table E.1 in NUREG/CR-5512.
b) d12 = fraction of parent decay to first progeny.
c) d23 = fraction of first progeny to second.
d) Ratio = the fraction receptor concentration divided by the ECL.
e) ECL = Effluent Concentration Limit.
f) Other Input Parameters.
K = hydraulic conductivity = 8 feet per day.
i = hydraulic gradient = 0.00039 feet per foot.
neff = effective porosity - 0.2 (dimensionless).
GW vel = groundwater velocity = 0.015 feet per day.
Receptor distance = 4200 feet.
Advective time = 272222 days = 745.3 years.

**PSEG Site
ESP Application
Part 2, Site Safety Analysis Report**

**Table 2.4.13-7 (Sheet 1 of 2)
Radionuclide Concentrations – Advection, Decay, and Dilution
Maximum Groundwater Flow Rate Conditions – Northeast Flow Path^{(a)(b)(c)(e)(g)(h)}**

Radionuclide	Receptor Concentration ^(d)	Diluted	ECL ^(f)	Ratio
Sr-90	2.04E-12	1.71E-12	5.00E-07	3.41E-06
Ru-106	1.25E-227	9.11E-228	3.00E-06	3.04E-222
Cs-134	3.14E-109	2.28E-109	9.00E-07	2.53E-103
Cs-137	4.28E-08	3.11E-08	1.00E-06	3.11E-02
Pu-241	1.83E-21	1.33E-21	1.00E-06	1.33E-15
Cm-242	0	0	7.00E-07	0
Pu-238	5.77E-10	4.19E-10	2.00E-08	2.10E-02
Cm-244	4.03E-20	2.93E-20	3.00E-08	9.76E-13
Pu-240	2.61E-08	1.90E-08	2.00E-08	9.49E-01
Fe-55	1.45E-85	1.06E-85	1.00E-04	1.06E-81
Co-60	2.55E-45	1.86E-45	3.00E-06	6.19E-40
H-3	2.39E-18	1.73E-18	1.00E-03	1.73E-15
			SUM =	1.00E+00

- a) The shape of the displacement is assumed to be square.
- b) The flux rate is the area of the displacement times the specific discharge.
- c) The minimum dilution equivalent is to the addition of 0.53 ft³/day flow in Fishing Creek is applied to meet SUM = 1.00.
- d) The receptor concentration is taken from the results for advection and decay.
- e) No dispersion of the initial displacement is assumed.
- f) ECL = Effluent Concentration Limits.
- g) Concentrations in microcuries per liter.

**PSEG Site
ESP Application
Part 2, Site Safety Analysis Report**

**Table 2.4.13-7 (Sheet 2 of 2)
Radionuclide Concentrations – Advection, Decay, and Dilution
Maximum Groundwater Flow Rate Conditions – Northeast Flow Path^{(a)(b)(c)(e)(g)(h)}**

h) Input Parameter Values:

Tank Volume = 30,000 gallons

Release volume = 24,000 gallons (3208.56 ft³)

Aquifer thickness = 13 feet

Effective porosity = 0.2 (dimensionless)

Area displaced = 1234.06 ft²

Square side = 35.13 ft

Aquifer K = 8 ft/day

Hydraulic gradient = 0.00039 ft/ft

GW flow rate = 1.41 ft³/day

Added Flow in Fishing Creek = (0.53 ft³/day)

Dilution factor = 1.38

**PSEG Site
ESP Application
Part 2, Site Safety Analysis Report**

2.5 GEOLOGY, SEISMOLOGY, AND GEOTECHNICAL INFORMATION

This section provides information on the geology, seismology, and geotechnical characteristics of the PSEG Site. The section follows the standard format and content prescribed in Regulatory Guide (RG) 1.206, *Combined License Applications for Nuclear Power Plants (LWR Edition)*, Revision 0, 2007. Further, the technical content complies with RG 1.208, *A Performance-Based Approach to Define the Site-Specific Earthquake Ground Motion*, Revision 0, 2007, for guidance respective to the level of investigation recommended at different distances from a proposed site for a nuclear facility. A particular focus is on data developed since the publication of the Updated Final Safety Analysis Report (UFSAR) for licensing Salem Generating Station (SGS) and the Hope Creek Generating Station (HCGS) in the same site area.

The PSEG Site is located on the southern part of Artificial Island on the east bank of the Delaware River in Lower Alloways Creek Township, Salem County, New Jersey. The SGS and HCGS are adjacent to the planned new plant location. The site is relatively level with existing surface grades ranging nominally from elevation 5 to 15 feet (ft.), North American Vertical Datum 88 (NAVD).

Investigations to obtain the data discussed in Section 2.5 were performed by MACTEC Engineering and Consulting, Inc. (with William Lettis Associates, Inc.) working under the overall direction of Sargent and Lundy, LLC. Field investigation work includes geologic mapping, geotechnical borings, surveying and geophysical testing as briefly described below. Laboratory testing of selected samples was performed.

Subsection 2.5.1 describes basic geological and seismological data compiled through literature reviews as well as regional and site-specific studies. Much of the site-specific data was gathered as part of the geotechnical exploration program described in detail within Subsection 2.5.4, which also provides information for Subsection 2.5.2 as well as Subsection 2.5.3.

Subsection 2.5.2 describes the vibratory ground motion at the site, including an updated seismicity catalog, description of seismic sources, and development of the Ground Motion Response Spectra (GMRS) and site-specific Safe Shutdown Earthquake (SSE). The site parameters to develop the GMRS and SSE are compiled from data acquired as part of the investigations described in Subsections 2.5.1 and 2.5.4.

Subsection 2.5.3 describes the potential for surface faulting in the site area and presents the results of both regional and site-specific studies discussed in Subsections 2.5.1 and 2.5.4.

Subsections 2.5.4 and 2.5.5 describe the stability of surface materials and slopes at the site. Included in Subsection 2.5.4 is a detailed discussion of site-specific investigations that provide supporting data for Subsections 2.5.1, 2.5.2, and 2.5.3.

In summary, the geologic, seismologic, and geotechnical conditions for the PSEG Site are characterized from investigations conducted specifically for the early site permit application (ESPA) and are consistent with conditions noted for the existing SGS and HCGS. The geologic, seismic and geotechnical site characteristics meet the requirements for safe location and operation of a nuclear power plant as considered at the ESPA stage. Detailed discussions are provided in the following subsections.

**PSEG Site
ESP Application
Part 2, Site Safety Analysis Report**

2.5.1 BASIC GEOLOGIC AND SEISMOLOGIC INFORMATION

This subsection presents information on the geological, seismological, and geotechnical engineering properties of the PSEG Site.

RG 1.208 provides guidance for the recommended level of investigation at different distances from a proposed site for a nuclear facility:

- The site region is that area within 200 miles (mi.) of the new plant location.
- The site vicinity is that area within 25 mi. of the new plant location.
- The site area is that area within 5 mi. of the new plant location.
- The site is that area within 0.6 mi. of the new plant location.

These terms — site region, site vicinity, site area, and site — are used in Subsections 2.5.1 through Subsection 2.5.5 to describe these specific areas of investigation and are not applicable to other subsections of the Site Safety Analysis Report (SSAR).

The geological and seismological information presented in this subsection is developed from a review of previous reports prepared for SGS and HCGS, published geologic literature, interpretation of aerial photography, subsurface investigations, geological mapping, and aerial reconnaissance conducted to support this ESPA. Previous site-specific reports reviewed include the HCGS UFSAR (Reference 2.5.1-176) and supporting referenced engineering reports and studies. A review of published geologic literature is used to supplement and update the existing geological and seismological information.

This subsection of the SSAR is intended to demonstrate compliance with the requirements of 10 CFR 100, *Reactor Site Criteria*, Section 100.23, *Geologic and seismic siting criteria*, paragraph (c), *Geological, seismological and engineering characteristics*.

2.5.1.1 Regional Geology

This subsection discusses the physiography, geologic history, stratigraphy, and tectonic setting within a 200-mi radius of the PSEG Site. The site region physiographic map (Figure 2.5.1-1) and regional geologic maps (Figures 2.5.1-2a, 2.5.1-2b, 2.5.1-3a, and 2.5.1-3b) show the physiography, geology, stratigraphy, and tectonic setting for the PSEG Site region. Summaries of the aspects of the regional geology are presented to provide the framework for evaluation of the geologic and seismologic hazards presented in the succeeding subsections.

2.5.1.1.1 Regional Physiography and Geomorphology

The PSEG Site lies within the Coastal Plain physiographic province (Figure 2.5.1-1). The site region includes parts of several other physiographic provinces: the Continental Rise, Continental Slope, and Continental Shelf (from east to west), all located in the eastern portions of the site region, and (to the west) the Piedmont, New England, Blue Ridge, Valley and Ridge and Appalachian Plateau provinces. These physiographic provinces are discussed in the following subsections.

**PSEG Site
ESP Application
Part 2, Site Safety Analysis Report**

2.5.1.1.1.1 Coastal Plain Physiographic Province

The Coastal Plain physiographic province is the sub-aerial portion of the North American continental shelf. In the site region, the Coastal Plain province extends eastward from the fall line to the Atlantic Ocean along the length of the North American Atlantic margin (Figure 2.5.1-1). The Coastal Plain province is characterized by low-lying, gently rolling terrain developed on sequences of deltaic, shallow, marine and continental shelf clastics consisting primarily of unconsolidated to semi-consolidated gravels, sands, silts, and clays that dip gently oceanward. The surface has been modified by erosional and depositional landforms associated with several transgressive and regressive marine cycles. In general, the Coastal Plain province exhibits lower topographic relief than the Piedmont province to the west. However, the land surface varies from flat to deeply incised. The mid-Atlantic Coastal Plain in the site region is traversed by major rivers and their associated valleys that are flooded to form estuaries, including Chesapeake Bay and Delaware Bay (Figures 2.5.1-1 and 2.5.1-4).

The mid-Atlantic Coastal Plain has been subdivided into four major physiographic subprovinces (based on their characteristic geomorphology): Inner Coastal Plain, Middle Coastal Plain, Outer Coastal Plain, and Alluvial and Estuarine Valleys (Figure 2.5.1-5). The Inner Coastal Plain is further subdivided into two regions: the dissected outcrop belt, the area of the oldest and most incised coastal plain sediments, and the upland sands and gravels area (Figure 2.5.1-5). In the mid-Atlantic region, the upland sands and gravels occur largely as discontinuous bodies confined to hilltops. However, in and around the site vicinity in New Jersey (NJ) and the Delmarva Peninsula, this unit constitutes laterally continuous strata that dip to the southeast to form a rolling upland that is dissected by underfit streams. The land surface of the Inner Coastal Plain is at least 5 million years old (Reference 2.5.1-11 and Figure 2.5.1-5).

The Middle Coastal Plain is a series of marine terraces and associated scarps developed in response to Pliocene and Early to Middle Pleistocene cyclic marine transgressions and regressions. These terraces have been exposed long enough to have well-developed drainages. In the site vicinity (Figure 2.5.1-6) and surrounding area, the Middle Coastal Plain occurs as a dissected upland with better-developed stream incision and drainages that were extended and entrenched during lowstands of sea level due to cyclic glaciations. The land surface of the Middle Coastal Plain is 200,000 – 3 million years old (Reference 2.5.1-11). In the site region, north of the Potomac River and in the site vicinity, the Coastal Plain has been located at a higher elevation since the late Pliocene and exposed longer than regions to the south (References 2.5.1-11 and 2.5.1-144). Consequently, deposition of Pleistocene marginal marine sequences is limited except for the Chesapeake and Delaware River valleys (Figures 2.5.1-5 and 2.5.1-6). In this region, the Middle Coastal Plain consists primarily of dissected uplands along with the terraces associated with the river valleys (Reference 2.5.1-11).

The Outer Coastal Plain lowland area near the modern coastline is characterized by a land surface that is flat and poorly drained, with drainages predominately tidally influenced. In the Outer Coastal Plain, the water table is relatively close to the land surface. The drainage network in the Outer Coastal Plain is poorly developed since the land surface is younger than approximately 120,000 years (Reference 2.5.1-11). The Outer Coastal Plain includes at least three scarp-bounded terraces composed of Quaternary marine and estuarine deposits that preserve landforms, including barrier bars, inlets, tidal deltas, and sand dunes. The outer margins of the terraces are surrounded by Holocene tidal marshes, bays, and barrier islands (Reference 2.5.1-144).

**PSEG Site
ESP Application
Part 2, Site Safety Analysis Report**

The fluctuating sea levels related to cyclic glaciation in the Quaternary have resulted in incision and enhanced erosion during lowstands. During highstands, transgression drowned the major river valleys and developed estuaries connected by barrier lagoon systems (Reference 2.5.1-179). The entire surface of the Coastal Plain in and around the site vicinity has been modified by climatic events related to glacial and interglacial periods. This is recorded as low-gradient slopes underlain by colluvium, surficial strata deformed by cryoturbation, and underfit streams. In addition, poorly-drained, closed depressions and loess and dune fields occur (Reference 2.5.1-144).

North of the site vicinity, the Delaware River makes an approximately 90-degree bend at the fall line, turning from a southeasterly to a southwesterly flow direction (Figure 2.5.1-4). The river subsequently follows a course along the inner edge of the Coastal Plain along the strike of the southeast-dipping Coastal Plain strata. It then turns approximately 90 degrees to resume a southeasterly course as it enters the Delaware Bay. The result is that the southeastward-dipping Coastal Plain strata to the east of the Delaware River Valley, as they follow the inner margin of the Coastal Plain, form a cuesta. Consequently, the drainage divide resulting from the cuesta and the Delaware Bay cause drainages in NJ that either flow southward into Delaware Bay, southeastward down the dip of the Coastal Plain strata to the Atlantic Ocean, or down the northwestward-facing slope of the cuesta across the strike of the Coastal Plain strata into the Delaware River (Reference 2.5.1-144).

There appear to have been instances in the Pleistocene in which the Delaware River Valley was obstructed, resulting in the formation of temporary lakes due to ponding of glacial meltwater. The presence of these temporary lakes has resulted in a series of shorelines at elevations 140 feet (ft.) mean sea level (msl), 100 ft. msl, and 60 ft. msl in the Delaware River Valley (Reference 2.5.1-124). During the Wisconsin glacial event this lake formed spillways in low areas of the cuesta drainage divide described above and overflowed to the Mullica River and subsequently the Atlantic Ocean. This overflow has resulted in the deposition of alluvial fans and braided stream channel deposits downstream from the spillway locations (References 2.5.1-124 and 2.5.1-66).

2.5.1.1.1.2 Continental Shelf, Slope, and Rise Physiographic Provinces

The Continental Shelf physiographic province is the submerged continuation of the Coastal Plain province. It extends from the shoreline to the continental slope (Figure 2.5.1-1). The Continental Shelf province is characterized by a gently sloping surface to the southeast. In the site region, the surface of the continental shelf has a series of coast-parallel ridges and related depressions that record relict shorelines from past ocean lowstands. In northern portions of the site region, off the southern New England coast, the topography of the shelf surface related to the relict shorelines has been infilled and smoothed over by very fine Holocene deposits resulting from winnowing of glacial sediments (Reference 2.5.1-208).

Several of the outer shelf Wisconsin shorelines (Figure 2.5.1-1) have been studied in detail and dated. These include the Nicholls shoreline (about 15,000 years old), the Franklin shoreline (about 13,000 years old), and the Atlantis shoreline (about 9000 years old). These shorelines, in addition to the Fortune shoreline, are relatively flat south of an inflection point off the NJ shore (Figure 2.5.1-1). North of this location, they become progressively deeper going northward. This has been attributed to the effects of glacial loading during their formation (Reference 2.5.1-51).

**PSEG Site
ESP Application
Part 2, Site Safety Analysis Report**

The continental shelf is transected by shelf valleys incised during sea level lowstands, some of which now are partially to completely filled with sediment. These valleys are associated with major rivers and constitute past and present cross-shelf fluvial systems (Reference 2.5.1-208). In the site region, the shelf valleys are the Block Shelf Valley, Hudson Shelf Valley, Great Egg Shelf Valley, and Delaware Shelf Valley (Figure 2.5.1-1).

The continental shelf extends eastward for 80 mi. to 100 mi., off the coast of NJ (Figure 2.5.1-1). The eastward margin of the continental shelf is delineated by a distinct escarpment (the continental slope) that drops to the continental rise.

The escarpment that marks the continental slope is highly dissected by submarine canyons, the largest of which are associated with the shelf valleys. The depth to the edge of the continental shelf that marks the shelf/slope break decreases from north to south. The break is about 394 ft. in the vicinity of Hudson Canyon, progressively decreasing to 197 ft. south of the site region (Reference 2.5.1-208). The base of the slope occurs at approximate depths of 6560 ft. to 7220 ft. In intercanyon regions, the slope changes gradient, with 1° to 2° slopes on the upper rise above approximate El -1312 ft. to -3280 ft. msl, and 3° to 8° on the lower slope. However, within the canyons, the slope topography is much steeper, with gradients from 30° to vertical (Reference 2.5.1-208).

The continental rise occurs at the base of the continental slope and is composed primarily of fine-grained sediments deposited by slope parallel currents. The continental rise consists of an upper rise that onlaps the base of the continental slope and forms a gently convex surface to the -13,100 ft. isobath. The lower rise is a relatively flat region with a very gentle seaward slope to the abyssal plain, which occurs at depths greater than 17,100 ft. The site region only encompasses the part of the upper rise near the base of the continental slope (Figure 2.5.1-1). The surface of the continental rise is incised by rise valleys that connect with the major submarine slope canyons and shelf valleys. The most prominent of these rise valleys are the Hudson and Wilmington (Figure 2.5.1-1).

2.5.1.1.1.3 Piedmont Physiographic Province

The Piedmont physiographic province extends southwest from New York (NY) to Alabama and borders the Coastal Plain physiographic province on the west (Figure 2.5.1-1). The Piedmont has gently rolling to hilly topography. It extends from the fall line at the edge of the Coastal Plain to the Blue Ridge physiographic province to the west. The eastern and southeastern limit of the Piedmont province, the fall line, forms a southeasterly facing topographic scarp southeast of Wilmington, Delaware (DE) (References 2.5.1-77 and 2.5.1-241). This feature, which in most cases corresponds closely with the edge of the Coastal Plain sediments, progressively increases in elevation from sea level in NJ to about 787 ft., in Georgia and Alabama (Reference 2.5.1-78).

In the site region, the Piedmont physiographic province has been subdivided into subprovinces on the basis of distinct physiographic characteristics (Figure 2.5.1-1). Extreme southwestern portions of the site region, southwest of the Rappahannock River in central Virginia (VA), contain the Piedmont Lowlands subprovince and the Foothills Zone subprovince (Figure 2.5.1-1). These two subprovinces protrude into the southwestern quadrant of the site region and are separated by a boundary that is defined on the basis of a slight steepening in regional slope to the northwest. Southeast of this boundary, the Piedmont Lowlands subprovince is characterized

**PSEG Site
ESP Application
Part 2, Site Safety Analysis Report**

by subdued rounded hills and drainages underlain by saprolite and crystalline rocks. Relief is typically rock-controlled and considered by Hack (Reference 2.5.1-77) to be related to the erosional resistance of lithologies. This area was probably once covered by a veneer of younger sediments based on inherited stream patterns. To the northwest, the Foothills Zone is characterized by topography and relief that becomes slightly steeper up to the transition to the Blue Ridge physiographic province (Figure 2.5.1-1). The Foothills Zone contains chains of isolated hills and ridges underlain by erosionally resistant lithologies. Although Hack considered erosional resistance to be the main control on relief for the Piedmont Lowlands and Foothills Zone provinces, on the basis of curvilinear alignment of high gradient reaches in major drainages, Weems (Reference 2.5.1-245) delineated seven “fall lines” in this area of the Piedmont (Figure 2.5.1-7), which he interpreted to be of neotectonic origin.

Most of the Piedmont physiographic province in the site region occurs northeast of the Potomac River and consists of the Northeastern Highlands subprovince (Figure 2.5.1-1). The Northeastern Highlands subprovince exhibits more topographic relief than the subprovinces to the south and has elevations that reach 984 ft msl. The northwestern portions of the Northeastern Highlands are underlain by sediments and volcanic rocks associated with Mesozoic rift basins. The sediments comprise shales, mudstones, and siltstone and are easily erodible. Consequently, this part of the subprovince forms a lowland with ridges and hills underlain by the more resistant volcanic lithologies. In contrast, the southeastern portions of the Northeastern Highlands are underlain by relatively resistant crystalline rocks. South of the Delaware River, the Northeastern Highlands is also characterized by drainages that have incised narrow valleys in the southeast near the fall line, and broad upland surfaces (Reference 2.5.1-77). These drainages also have complex longitudinal profiles with increased gradients near the fall line, indicating uplift. Based on these relationships and the coincidence of warped gravel beds, (Reference 2.5.1-34) inferred that the uplift formed a broad dome that he called the Westminster anticline. However, based on the observation that the upper surfaces of resistant lithologies in the lowlands to the northwest were level with the crystalline highlands to the southeast, Hack (Reference 2.5.1-77) interpreted the uplift to form more of a southeasterly facing monocline that appears anticlinal due to the more deeply eroded lowland areas.

The major drainages along the southeastern margin of the Northeastern Highlands around the site vicinity, including the Potomac, Susquehanna, and Delaware Rivers, exhibit right-stepping bends in the vicinity of the fall line. A southeasterly flow direction in the Piedmont portions of these drainages turns abruptly 90 degrees to the southwest for some distance and then turns abruptly 90 degrees to return to a southeasterly flow across the strike of the Coastal Plain strata (Figure 2.5.1-4 and Reference 2.5.1-120).

The Wisconsin glacier extended to the extreme northern end of the Newark Basin in the Piedmont province (Figure 2.5.1-1) where its extent is marked by a terminal moraine, glacial lake deltas, and lake deposits. Evidence of pre-Wisconsin glacial events is present to the south consisting of patchy, deeply weathered till and gravel deposits (Reference 2.5.1-78).

2.5.1.1.1.4 Blue Ridge Physiographic Province

The Blue Ridge physiographic province is bounded to the southeast by the Piedmont province and, to the northeast, by the Valley and Ridge province (Figure 2.5.1-1). The Blue Ridge province is divided into northern and southern portions, (Reference 2.5.1-78) separated by the Roanoke River. In the site region, the Northern Blue Ridge physiographic province occurs as a

**PSEG Site
ESP Application
Part 2, Site Safety Analysis Report**

narrow ridge of mountains called the Northern Blue Ridge Mountains (Reference 2.5.1-77). It has an average width of 9.3 mi. and lies entirely within the Atlantic drainage (Reference 2.5.1-78). These mountains are held up by a restricted range of Precambrian to Cambrian plutonic, volcanic, and resistant sedimentary rocks along their entire length. These rocks include coarse-grained granitoids, volcanic rocks of the Catoctin formation, and clastic sediments of the Chilhowee Group.

2.5.1.1.1.5 New England Physiographic Province

The New England physiographic province occurs primarily in New England. However, a portion of this province extends to the southwest as a narrow belt into the northeastern quadrant of the site region (Figure 2.5.1-1). The portions of the New England physiographic province in the site region comprise a narrow belt of low-grade Paleozoic metamorphic rocks in the Hudson Valley of NY, referred to as the Hudson Highlands, and Precambrian metamorphic and igneous rocks that form highlands of NJ and Pennsylvania (PA), referred to as the Reading Prong (Reference 2.5.1-78). These areas are characterized by rough topography with elevations less than 984 ft. msl, strongly related to the erosional resistance of the underlying lithologies (Reference 2.5.1-78).

The New England physiographic province records the late Wisconsinan terminal moraine, which coincides with Long Island and extends offshore, in addition to several discontinuously developed recessional moraines to the north. The uplands areas are generally scraped down to bare rock but, in areas of moderate relief, glacial till forms drumlins (Reference 2.5.1-78). Deltaic sediments are also present that were deposited at the margins of glacial lakes.

2.5.1.1.1.6 Valley and Ridge Physiographic Province

The Valley and Ridge physiographic province occurs in the northwestern portion of the site region (Figure 2.5.1-1) and is bounded on the southeast, progressing from south to north, by the Blue Ridge, Piedmont, and New England provinces. The Valley and Ridge is bounded to the northwest by the Appalachian Plateau province. The Valley and Ridge is underlain by Laurentian shelf clastic and carbonate sedimentary sequences along with overlying synorogenic deposits. The strata that comprise these sequences have been imbricated by faulting and folding above thrust ramps. The eastern portions of the Valley and Ridge province form a broad valley underlain by thick sequences of carbonate and shale (Reference 2.5.1-78). To the northwest, variably erosionally resistant lithologies of strata upturned by the thin-skinned thrust faulting and folding has produced the characteristic northeast-southwest aligned valleys and long strike ridges from which the province gets its name. Sandstone forms most of the ridges, and less-resistant shales and carbonate form the valleys.

Glacial effects in the Valley and Ridge are recorded as far south as the Delaware River and include deltaic and bottom deposits associated with glacial lakes (Reference 2.5.1-78).

2.5.1.1.1.7 Appalachian Plateau Physiographic Province

The Appalachian Plateau physiographic province occurs in the northwestern portions of the site region (Figure 2.5.1-1). This province is underlain by relatively flat, erosionally resistant strata. These strata result from the syn- to postorogenic clastic input from the Appalachian Mountains to the east. In locations in which the larger drainages have cut through the resistant cap strata,

**PSEG Site
ESP Application
Part 2, Site Safety Analysis Report**

they form deep gorges. Eastern portions of the province have rugged topography that becomes more subdued to the west (Reference 2.5.1-78).

Terminal moraines recording glacial advance are found in PA and Ohio. Elsewhere in the Appalachian Plateau glacial effects are recorded mainly by glaciofluvial sediments (Reference 2.5.1-78).

2.5.1.1.2 Regional Geologic History

The PSEG Site region bears geologic elements that altogether reflect a complex geologic and tectonic history. Tectonic events beginning in the Proterozoic have been overprinted by Paleozoic contractional deformation, Mesozoic extension, and Cenozoic erosion and deposition in response to uplift and sea level changes. This tectonic history imparts a pre-existing structural grain in the crust that provides context for understanding the current seismotectonic regime. Modern day seismicity may occur along faults or in terranes exposed at the surface, but within the site region it more often occurs within basement rocks buried beneath Paleozoic accreted terranes or younger sediments. Hence, understanding the complex structural setting at depth, as well as at the surface, is important for evaluating the distribution of historical seismicity within the tectonic context of the site region.

The PSEG Site lies on the Coastal Plain, oceanward of a belt of deformed Precambrian and Paleozoic rocks that yield evidence of the earliest tectonic events in the region. The map pattern of the site region indicates that this sinuous belt of rocks, oriented northeast-southwest through the site region, is flanked to the northwest by less-deformed Upper Paleozoic sedimentary strata, and to the southeast by the southeastward-dipping Lower Cretaceous and younger Coastal Plain strata (Figure 2.5.1.-2a). The deformed Precambrian and Paleozoic rocks in linear exposures parallel to the structural grain of the Appalachian orogen are interrupted by a series of Mesozoic basins that expose the characteristic synrift strata produced during Triassic rifting, seen on the map as the belt of Triassic and Jurassic units. Currently, the site region is located on the passive margin of the North American plate, far from a plate boundary where the majority of tectonic activity (such as faulting, seismicity, and volcanism) takes place. In the past, however, this was not necessarily the case and the tectonic events that have shaped the site region are described below.

2.5.1.1.2.1 Grenville Orogeny and Subsequent Rifting

Some of the earliest tectonic events recorded within the site region involve ancestral North America, a craton composed of old continental crust known as Laurentia. The Middle Proterozoic Grenville orogeny, 1.3 to 1.0 billion years ago (Ga), occurred as ancestral Africa collided with Laurentia to form a new supercontinent known as Rodinia. Metamorphism and deformation accompanied this collision (Reference 2.5.1-231). During the several hundred million years of tectonic quiescence following this orogeny, the mountains eroded and exposed the metamorphic basement rocks. These rocks are currently exposed in Maryland (MD), DE, and southeastern PA (Reference 2.5.1-183).

Eventually, in the late Proterozoic, the tectonic plate configuration changed, separating ancestral Africa and Laurentia. As these two continents moved apart, an ocean developed between them. This ocean, known as the Iapetus, can be thought of as a precursor to the Atlantic. The separation of the two continents was accomplished via continental rifting in which a

**PSEG Site
ESP Application
Part 2, Site Safety Analysis Report**

series of normal faults developed subparallel to the continental margin and extended the continental crust. This rift system was irregular and left Laurentia with a jagged network of fault-bounded basins filled with synrift strata along its margin. These basins and the thinned crust began to subside and accumulate sediment. The initial clastic sediment eventually was overlain by a transgressive clastic sequence overlain by thick carbonates. This characteristic passive margin stratigraphy developed from the Middle to Late Cambrian into Ordovician time (Reference 2.5.1-64).

After the rift-to-drift transition was complete, the Laurentian margin experienced multiple phases of contractional deformation throughout the Paleozoic. During this time the Iapetus Ocean continually closed as island arcs, smaller fragments of continental crust, and eventually ancestral Africa (Gondwana), collided with one another and the eastern margin of Laurentia.

2.5.1.1.2.2 Penobscot/Potomac Orogeny

Following development of Laurentia's passive margin, subduction developed island arcs in the Iapetus Ocean. The earliest Paleozoic collisional events in eastern North America are the Penobscot and Taconic orogenies, which involved Iapetan island arcs colliding with continental blocks. The offshore island arcs created a source of clastic sediment that was shed westward onto the Cambro-Ordovician passive margin carbonate platform. This clastic sediment filled the Appalachian Basin, which stretched from Canada to Alabama, roughly parallel to the Atlantic coastline. Early Cambrian deformation in the Penobscot region of Maine is thought to represent the offshore collision between island arcs and a micro-continent off of the Laurentian margin (References 2.5.1-233 and 2.5.1-37). In the PSEG Site region, this Penobscot equivalent, or the Potomac orogeny, is considered a pre-Taconic collision between fragments of continental crust (e.g., the Brandywine or Baltimore microcontinent) and the island arc (the Chopawamsic or Wilmington complex). Only later, during the Taconic, did these combined fragments accrete to the Laurentian margin (Reference 2.5.1-64).

2.5.1.1.2.3 Taconic Orogeny

The Taconic orogeny occurred in the Middle to Late Ordovician 480 to 435 million years ago (Ma) as amalgamated microcontinent and volcanic island arcs collided with the eastern margin of Laurentia via subduction on an east-dipping subduction zone. In the central Appalachians, this is represented by the Martic thrust, which carried the Westminster and Potomac terranes westward. The Potomac terrane, correlated with the Chopawamsic and Tugaloo terranes to the southwest, represents an Ordovician island arc (Reference 2.5.1-85). Locally, the Wilmington complex is a metaigneous unit representing a metamorphosed island arc, while the Wissahickon Formation represents a forearc or accretionary wedge deposit of Laurentian sediment. Altogether, the island arc and surrounding Laurentia-derived sediments were metamorphosed and intruded by a suite of igneous rocks in the Silurian. This Silurian metamorphism is interpreted as resulting from the collision of the arc with the Laurentian margin (Reference 2.5.1-4).

As Laurentia, the island arc/microcontinent, and the intervening basin collided (in the region of the present-day PSEG Site) the Taconic orogeny gave rise to the original deformation on many low-angle thrust faults, such as the Martic line and thrusts of the Hamburg Complex (Figures 2.5.1-8a and 2.5.1-8b and Reference 2.5.1-64).

**PSEG Site
ESP Application
Part 2, Site Safety Analysis Report**

2.5.1.1.2.4 Acadian Orogeny

In the northern Appalachians, the Devonian Acadian orogeny is linked to the collision of a microcontinent, Avalon, with the Laurentian margin. This orogeny led to metamorphism and intrusion of a suite of plutons in New England, and possibly in parts of the southern Appalachians (Reference 2.5.1-81). The significance of the Acadian orogeny is less certain within the central Appalachians, or large parts of the PSEG Site region. The Taconic loading of the Laurentian margin with the obducted arc/microcontinent led to further development of the Appalachian Basin. Most of the evidence of the Acadian orogeny in the central Appalachians comes from the sedimentary record of this basin (Reference 2.5.1-65). The Acadian orogeny ended the quiescent carbonate-dominated deposition as large amounts of clastic materials were shed from the Acadian mountains, producing the Acadian clastic wedge exposed in northeastern PA and NY (Figures 2.5.1-8a and 2.5.1-8b; Reference 2.5.1-65).

2.5.1.1.2.5 Alleghany Orogeny

The late Paleozoic Alleghanian orogeny represents the final closure of the Iapetus Ocean. This collision between Laurentia and Gondwana to form the supercontinent Pangea, occurred in the Carboniferous and is responsible for many of the contractional structures seen in the site region today (Figures 2.5.1-8a and 2.5.1-8b). This includes the northwestward transport of previously accreted terranes (such as the Potomac terrane) toward the core of the Appalachians and the folding and deformation in the Appalachian foreland, seen in central PA (Figure 2.5.1-2). Within the site region, the suture between peri-Laurentian rocks and rocks from Gondwana is probably covered by Coastal Plain sediments (Reference 2.5.1-85). However, northwest of the PSEG Site, a variety of Alleghanian-age faults are exposed in the Piedmont, such as the Pleasant Grove shear zone and the Yellow Breeches thrust (Figure 2.5.2-8a and Reference 2.5.1-85).

2.5.1.1.2.6 Mesozoic Opening of the Atlantic Basin

The next tectonic event that affected the region was the rifting apart of the supercontinent Pangea and the opening of the Atlantic Ocean basin. The progression from active continental rifting to seafloor spreading and a passive continental margin included: (1) initial rifting and hotspot plume development; (2) thinning of warm, buoyant crust with northwest-southeast extension, via normal faulting accompanied by deposition of synrift sedimentary and volcanic rocks; and (3) cooling and subsidence of thinned crust and deposition of postrift sediments on the Coastal Plain and continental shelf, slope, and rise (References 2.5.1-103 and 2.5.1-104). The second phase (rifting), like the Iapetan rifting before it, was accomplished via a series of normal faults subparallel to the margin. The normal faults developed a series of half-graben basins that were filled with synrift strata known as the Newark Supergroup (Figure 2.5.1-9). These rocks are well-dated and indicate that rifting occurred in the Triassic and Early Jurassic (Reference 2.5.1-117) which was accompanied by voluminous Early Jurassic volcanism (Reference 2.5.1-201). Within the site region, the normal faults and synrift strata are best seen in a series of rift basins exposed northwest of the site—the Newark, Gettysburg and Culpeper basins (Figure 2.5.1-9). Oceanward of these exposed basins, Mesozoic normal faults and basins are covered by Coastal Plain sediments (Figure 2.5.1-9). The spatial distribution of the buried normal faults and basins is uncertain, but evidence indicates that pre-Mesozoic basement underlies the site (Figure 2.5.1-9). This topic, as it relates to the PSEG Site, is discussed in Subsection 2.5.1.2.4.

**PSEG Site
ESP Application
Part 2, Site Safety Analysis Report**

The transition between the second (rifting) and third (drifting) phases during the Early Jurassic marked the initiation of a passive margin setting in the site region, in which active spreading migrated east away from the margin. As the thinned crust of the continental margin cooled and migrated away from the warm, buoyant crust at the mid-Atlantic spreading center, horizontal northwest-southeast tension changed to horizontal compression as gravitational potential energy from the spreading ridge exerted a lateral ridge push force on the oceanic crust. Northwest-southeast-directed postrift shortening, manifested in Mesozoic basin inversion structures, provides the clearest indication of this change in stress regime (Reference 2.5.1-254).

A postrift unconformity separates synrift from postrift deposits and represents the change in tectonic regime in the Middle Jurassic from continental rifting to the establishment of the passive margin (drifting). Sedimentary rocks below the unconformity are cut by numerous faults. In contrast, the later Jurassic and Cretaceous strata above the unconformity accumulated within the environment of a broadly subsiding passive margin, and are sparsely faulted. Sediments shed from the faulted blocks of the rifting phase and from the core of the Alleghany orogen accumulated on the Coastal Plain, continental shelf, slope, and rise above the postrift unconformity and contributed to subsidence of the cooling postrift crust by tectonic loading.

2.5.1.1.2.7 Cenozoic Passive Margin Development

The east coast of North America is characterized by passive margin development throughout the Cenozoic, which involves cooling and subsidence of extended (thinned) Atlantic margin continental crust and a net eastward mass redistribution from the eroding Appalachian core to Coastal Plain and offshore depocenters. These erosional processes have resulted in isostatic flexure of the crust about a hinge line located roughly along the Fall Zone, or the western edge of the Coastal Plain. Within the Coastal Plain, variations in subsidence have formed local arches and basins (such as the South New Jersey Arch and Salisbury Embayment) (Fig. 2.5.1-10) and deposition has increased since a hiatus in the Oligocene. As a result of this erosional unroofing, the Piedmont is experiencing uplift relative to the Coastal Plain, which is being isostatically loaded by fluvial deposition. Thus, the Fall Zone stands out as a topographic escarpment that is dominantly controlled by lithologic contrasts. Slow erosional exhumation of this region is recorded by low-temperature thermochronologic and geomorphic data sets.

Apatite fission track data from southeastern PA indicate roughly 0.6 to 1.2 mi. of post-Cretaceous uplift of the Piedmont relative to the Coastal Plain (Reference 2.5.1-259). Similar rates of relative uplift have been calculated from disequilibrium river profiles in VA and MD (Reference 2.5.1-190). Moreover, Pazzaglia and Gardner (Reference 2.5.1-164) simulated the observed deformation with a one-dimensional flexural model of an elastic crust, confirming that relative base level fall in the Appalachians has been driven by slow, steady isostatic rise of the orogen in response to erosional unroofing and late Cenozoic eustatic lowering.

The geologic history for the site involves formation of a basement complex of metaigneous and metasedimentary rocks in the Paleozoic that were subsequently extended and rifted in the Mesozoic to form the Atlantic Ocean basin. The basement complex is overlain by sedimentary successions deposited on the North American Atlantic margin that now form the Coastal Plain. In the site area, these successions begin in the Early Cretaceous and continue to the present. The lower units of the Coastal Plain sequence represent passive, trailing margin conditions in response to thermal relaxation of the lithosphere over slightly to moderately extended crust.

**PSEG Site
ESP Application
Part 2, Site Safety Analysis Report**

Upper units of the sedimentary successions lie above a regional unconformity and represent late Miocene to present increased clastic input.

2.5.1.1.3 Regional Stratigraphy

The site region encompasses portions of the entire Appalachian orogenic sequence (Figures 2.5.1-3a, 2.5.1-3b, 2.5.1-8a, and 2.5.1-8b) which records sedimentation, igneous activity, and metamorphism resulting from the opening and closing of the Iapetus and Rheic oceans in the Late Proterozoic and Paleozoic, and the formation and opening of the Atlantic Ocean basin in the Mesozoic and Cenozoic (Reference 2.5.1-85). Each of these oceans and surrounding continental landmasses has sedimentary and igneous successions that formed in response to the formation and closure of each of the ocean basins (References 2.5.1-85 and 2.5.1-88). The regional stratigraphy as it relates to NJ is illustrated on Figure 2.5.1-11.

Rifting of the Rodinian continental mass to form the Iapetus ocean basin was followed by development of continental shelf, continental slope, and continental rise sedimentary sequences associated with a passive Laurentian oceanic margin. Subduction activity on the margins of the Iapetus and Rheic oceans has also resulted in synorogenic sedimentary and igneous sequences, both preserved on the Laurentian continental shelf and as volcanic arc sediments and igneous rocks preserved in several of the terranes accreted to the Laurentian margin. Final closure of the Iapetus and Rheic oceans, in the Neoproterozoic and Paleozoic, resulted in the formation of the Pangean landmass as final juxtaposition of Laurentia and Gondwana was completed in the Late Permian. Breakup of the Pangean continent, starting in the Triassic, subsequently initiated a new ocean-forming cycle with rift facies deposition and igneous activity followed by passive margin sedimentation resulting in formation of the Atlantic margin continental shelf, continental slope, and continental rise. Since each of these sedimentary successions consists of stratigraphic sequences formed in unique environments, they are discussed separately below.

2.5.1.1.3.1 Laurentian Continental Margin Stratigraphy

The base of Laurentian continental margin stratigraphic successions was formed in response to the rifting of the Rodinian continental mass in the Late Proterozoic to Early Cambrian, and subsequent establishment of a stable Laurentian continental margin and formation of the Iapetus ocean basin. Subsequent to deposition of volcanic and fluvial sediments in extensional environments, Laurentian margin deposition is characteristic of that associated with passive, trailing-margin sedimentation with transition from early clastic facies to the development of an extensive carbonate shelf and associated slope and rise deposits (Reference 2.5.1-183). This depositional situation was maintained, in the site region, to the Early to Middle Ordovician.

Following the Middle Ordovician in the site region, upper Laurentian-margin stratigraphic successions involve easterly derived clastic components that comprise clastic wedges forming temporally and spatially discrete strata that thicken toward the source regions (Figures 2.5.1-8a and 2.5.1-8b). These clastic wedges were deposited in foreland basins and typically grade into carbonates both laterally and upward (Reference 2.5.1-84). These strata are composed of an early fine-grained synorogenic facies, followed by coarser-grained late- to post-orogenic material, typically separated by an unconformity. The clastic wedge sediments record multiple, enhanced erosional and depositional events resulting from tectonic uplift of distal portions of the Laurentian margin. These tectonic events were associated with closure of the Iapetus Ocean

**PSEG Site
ESP Application
Part 2, Site Safety Analysis Report**

and, finally, accretion of Laurentia and Gondwana. The late- and post-orogenic sediments resulting from the accretion of Laurentia and Gondwana properly belong to the newly formed Pangean continent. However, they are discussed as part of the Laurentian stratigraphic units since they form a continuum with these lower units.

The Rodinian continental crust in the site region was formed as a result of igneous and metamorphic activity associated with the Mesoproterozoic and Neoproterozoic Grenville Orogeny, which represents primarily convergent style tectonics in the 1.3 to 1.0 Ga (Giga Annum) interval (Reference 2.5.1-231). Grenville-aged Rodinian crustal lithologies occur in the site region in several settings. In the subsurface in western portions of the site region, Grenville-aged crystalline rocks occur as crystalline basement to overlying Laurentian sedimentary strata (Reference 2.5.1-196). These lithologies are also exposed as the basement component to several allochthonous, metamorphosed basement-cover sequences referred to as highlands, massifs, or prongs. These include the Housatonic massif, Hudson Highlands, Manhattan Prong, New Jersey Highlands, Reading Prong, and Honey Brook Upland, and associated rocks in central portions of the site region, and as the Shenandoah massif in the northern Blue Ridge (References 2.5.1-183, 2.5.1-33, and 2.5.1-230, Figures 2.5.1-8a and 2.5.1-8b). Additionally, Grenville-aged crystalline basement is exposed, along with metamorphosed cover as antiformal structures such as the Baltimore terrane (Reference 2.5.1-3) in MD and, possibly, in the Goochland terrane in VA (References 2.5.1-183 and 2.5.1-154). However, the relationship of the Goochland terrane to the Laurentian margin is unclear. Lithologies in the Grenville crystalline basement complex are primarily metaigneous but also contain a significant component of high-grade supracrustal material (Reference 2.5.1-243). Proximal to the site vicinity, crystalline basement is exposed in the New Jersey Highlands of the Reading Prong. Here, representative lithologies include metaigneous and both quartzofeldspathic and carbonate metasediments (Reference 2.5.1-183 and Figure 2.5.1-11). Metasediments of the Glenarm Group also probably represent Laurentian margin protoliths. Exposures of these units in the northern part of the site vicinity include marbles that have developed dissolution features and sinkholes (Reference 2.5.1-220).

Initial rifting and breakup of the Rodinian continental crust was accompanied by bimodal volcanic activity and deposition of primarily clastic sediments in rift-related basins along several portions of the Laurentian margin (Reference 2.5.1-183). These lithologies are exposed in the site region in the South Mountain anticline (Figures 2.5.1-8a and 2.5.1-8b) where they compose igneous and sedimentary components of the Swift Run and Catoctin formations (Reference 2.5.1-57). In addition, some of the volcanic and sedimentary components of the allochthonous basement-cover sequences mentioned above, including metamorphosed diabase dikes that intrude the basement components, are probably Neoproterozoic to Early Cambrian rift-related facies (Reference 2.5.1-57). Near the site vicinity, this may include components of the Chestnut Hill Formation (Figure 2.5.1-11).

Following the extension breakup of the Rodinian continental crust, the thermal relaxation and subsidence of the rifted Laurentian margin was accompanied by the formation of new lapetean ocean crust and trailing edge passive margin conditions as the Laurentian continent drifted away from Gondwana. The transition from the high-energy fluvial sedimentation to trailing edge conditions is preserved in the Neoproterozoic to Early Cambrian Chilhowee Group that forms the base of the Laurentian trailing margin section. Chilhowee Group sediments are exposed in the South Mountain anticline (Figures 2.5.1-8a and 2.5.1-8b) where they nonconformably overlay the Catoctin Formation (Reference 2.5.1-57). Near the site vicinity, probable

**PSEG Site
ESP Application
Part 2, Site Safety Analysis Report**

stratigraphically equivalent units occur as metamorphosed cover to the allochthonous basement – cover units such as the Chickies Quartzite (Reference 2.5.1-183 and Figure 2.5.1-11).

The basal clastic sequence was overlain by Early Cambrian carbonates on the Laurentian shelf and by slope and rise deposits on more distal portions of the Laurentian margin (Reference 2.5.1-183). In the site region, these units are succeeded by predominately passive margin deposition of carbonates and muds of the Kittatinny Supergroup up to the culmination in the Beekmantown Group (Figure 2.5.1-11). These strata consist primarily of carbonates with a minor siliciclastic component represented by calcareous shales and sandstone (Figure 2.5.1-11). Slope and rise equivalents occur in units imbricated during the Taconic orogeny in the Jutland klippe (Figure 2.5.1-11) and other Taconic arcs and accretionary complexes such as the Wilmington complex and Wissahickon schist. In addition, correlative rocks are probably represented by the Glenarm Series, which forms the metamorphosed cover sequence to allochthonous basement-cover sequences (References 2.5.1-98 and 2.5.1-228).

The development of the Taconian clastic wedge (Figures 2.5.1-8a and 2.5.1-8b) begins with the development of a Middle Ordovician regional unconformity (Reference 2.5.1-183). Above this unconformity, the beginning of a foredeep is indicated by deposition of dark-colored limestone and argillaceous limestones containing a fine-grained siliciclastic component. This deposition records the first indication of westerly clastic input and these strata also contain altered beds of volcanic ash (Reference 2.5.1-58). Near the site vicinity, these rocks form the Middle Ordovician Jacksonburg Limestone (Figure 2.5.1-11). This unit marks the base of a primarily coarsening upward sequence of synorogenic clastic detritus composing shales and turbidite deposits that constitute the Martinsburg Formation. The top of the Martinsburg Formation near the site vicinity is marked by an unconformity above which are coarse-grained clastic strata of the Shawangunk Formation (Figure 2.5.1-11). The conglomerates mark the deposition of the late orogenic sequences of the Taconian clastic wedge as the highland to the east, which developed due to tectonic imbrication of the crust, was eroded.

In addition to the Taconian clastic wedge that was deposited on the Laurentian shelf during the subduction that resulted in Taconic orogenic activity, the Laurentian slope and rise deposits along with fragments of Iapetan ocean floor formed an accretionary wedge that, along with the accompanying plutonic, volcanic, and sedimentary components of volcanic arc(s), were accreted to the Laurentian margin. Deformed and metamorphosed correlatives of these units are now probably preserved in the Westminster, Chopawamsic, Philadelphia, and Potomac terranes (Reference 2.5.1-64), and in the Hamburg Complex (Reference 2.5.1-85, Figures 2.5.1-8a, and 2.5.1-8b). Upon accretion of these terranes, the Laurentian margin became composite, in the sense that it was now composed of an imbricated passive margin along with accreted metaplutonic, metavolcanic, and metasedimentary volcanic arc material with overlying or adjacent synorogenic and postorogenic sequences composing a clastic wedge.

Following deposition of the late- to post-orogenic coarse clastic facies of the Taconic clastic wedge, the foredeep was filled by erosion of the Taconic highlands. Deposition on the Laurentian shelf became progressively more characteristic of a shallow sea, with fining-upward sequences and reestablishment of carbonate deposition throughout the rest of the Silurian to the Middle Devonian, beginning with the Bloomsburg Formation (Figure 2.5.1-11). In western portions of the site region, coarse clastic material representing advance of the Acadian and Neoacadian clastic wedge began to appear interfingered with carbonate units in the Middle Devonian. This is followed by thick marine and nonmarine clastic strata during the Late

**PSEG Site
ESP Application
Part 2, Site Safety Analysis Report**

Devonian to Early Mississippian. These units compose the synorogenic and late- to post-orogenic components of the Catskill (Acadian and Neoacadian) (Figures 2.5.1-8a and 2.5.1-8b) clastic wedge and are not present near the site vicinity.

During the Mississippian, carbonate deposition was re-established, resulting in deposition of the Loyalhanna – Greenbrier limestone in western portions of the site region. The restricted clastic input allowing deposition of limestone was followed by synorogenic red beds of the Mauch Chunk Formation and late orogenic conglomerates, sandstone, shale, and coal of the Pottsville and Llewellyn formations. These sediments compose the synorogenic – late-orogenic sequence composing the Mauch Chunk – Pottsville (Alleghanian) (Figures 2.5.1-8a and 2.5.1-8b) clastic wedges (Reference 2.5.1-84) in the site region.

The appearance of the late-orogenic sediments of the Alleghanian clastic wedge marked the final assembly of the Pangean continent in the Permian. Permian sediments of the Dunkard Group appear to the west of the site region (Reference 2.5.1-61).

2.5.1.1.3.2 Gondwanan and Peri-Gondwanan Stratigraphy

At approximately the same time as subduction-related processes were affecting the Laurentian margin of Iapetus, several volcanic arcs were developed in association with the Gondwanan side of the ocean. These volcanic arcs now compose several terranes with Gondwanan associations and are considered to be of peri-Gondwanan affinity (Reference 2.5.1-85, Figures 2.5.1-8a and 2.5.1-8b). Some of these peri-Gondwanan terranes occur in the subsurface beneath the Atlantic margin and consequently are not well-studied and are poorly known. This includes the Brunswick terrane in the site region (Figures 2.5.1-8a and 2.5.1-8b). The best-known of the peri-Gondwanan terranes is the Carolina superterrane (Reference 2.5.1-85, Figure 2.5.1-8a, and Figure 2.5.1-8b) also known as “Carolinia” (Reference 2.5.1-88). The Carolina superterrane is projected beneath the subsurface of the Coastal Plain to underlie most of the site vicinity (Figures 2.5.1-8a and 2.5.1-8b). Although the timing of the accretion of the peri-Gondwanan terranes and Laurentia is debated, current models postulate either a Late Ordovician to Silurian (References 2.5.1-87 and 2.5.1-88) or Neoacadian (Reference 2.5.1-85) docking.

The Carolina superterrane is composed of subduction-related volcanogenic sediments and associated plutonic complexes (Reference 2.5.1-85). The magmatic activity that resulted in the igneous sequences began as early as 670 Ma with the main activity picking up at 633 Ma and terminating in the early Cambrian (Reference 2.5.1-88). These rocks were deformed and metamorphosed and subsequently overlain by 0.6 to 1.2 mi. of fossiliferous carbonate and Middle Cambrian mudstone and greywacke of the Asbill Pond Formation (Reference 2.5.1-88). To the extent that these general lithologic characteristics of the Carolina superterrane are present in the projection of the terrane beneath the site vicinity, they may be considered characteristic of the site vicinity basement.

Although the best-understood features of the Gondwanan crust are available from south Georgia and Florida, Gondwanan (African) crust may exist in the subsurface in eastern portions of the current Atlantic margin (Figures 2.5.1-8a and 2.5.1-8b).

**PSEG Site
ESP Application
Part 2, Site Safety Analysis Report**

2.5.1.1.3.3 Pangean Stratigraphy

Final assembly of the Pangean continent in the Late Pennsylvanian and Permian lead to deposition of the Dunkard Group in western PA, as discussed in the section on Laurentian stratigraphy above. In the Late Triassic, rifting and breakup of Pangea resulted in deposition of clastic and evaporite sediments, along with volcanic intrusive and extrusive rocks in several extensional basins that were developed as the Pangean crust thinned. Thinning of the Pangean crust led to the development of two main basin types (Reference 2.5.1-117) associated with different degrees of crustal thinning. Rift basins exposed mostly onshore formed Newark-type basins that were filled with thick sequences of terrigenous clastic-lacustrine and volcanic sediments. In the site region, Newark-type basins include the Taylorsville, Richmond, Culpeper, Gettysburg, and Newark basins (Figures 2.5.1-8a and 2.5.1-8b). Seaward of the string of Newark-type basins, on more highly extended crust that floors the Baltimore Canyon Trough, basin sediments are characterized by evaporite facies along with mudstones and carbonates. The rocks that compose the basin fill are classified as the Newark Supergroup (Figure 2.5.1-11). In the site region, the Newark Supergroup is composed of synrift facies consisting primarily of siltstones, shales, mudstones, conglomerates, sandstones, evaporites, limestone, coal, and windblown material (Reference 2.5.1-117). Volcanic lithologies occur in the upper part of the sequence and were intruded and erupted in a relatively short interval (References 2.5.1-117 and 2.5.1-150). Upper termination of Pangean stratigraphic successions is marked by the deposition of unconformable clastic drift facies sediments that indicate the transition from a rift to drift margin and formation of new North Atlantic ocean crust during final separation of the North American and African continents in the Middle Jurassic.

Deposition in the rift basins shows systematic patterns (Reference 2.5.1-117). Aerially, grain sizes show an asymmetrical elongated concentric pattern with coarse-grained facies consisting of conglomerates and sandstones around the exterior near the basin margins, progressively transitioning to fine-grained lacustrine sediments in the basin interior. A characteristic vertical pattern is characterized by a lower fluvial interval, a middle deep-water lacustrine interval that is typically grey or black, and an upper, usually red, lacustrine interval. In addition, it is proposed (Reference 2.5.1-150) that the sediments of the Newark Supergroup could be organized into four tectonostratigraphic sequences that could be recognized over most of the Central Atlantic margin extensional basins. These four sequences consist of early Middle Triassic initial synrift sedimentary deposits, late Middle and early Late Triassic early synrift sedimentary rocks, Late Triassic to earliest Jurassic middle synrift sedimentary rocks, and late synrift sedimentary rocks of Early Jurassic age. These sequences are typically, but not uniformly bound by unconformities.

The Newark-type basin occurs to the north of the site vicinity and is the closest exposed basin to the site. The basal member of the Newark Supergroup in the Newark-type basin is the Stockton Formation (Figure 2.5.1-11), which consists of clastic fluvial to deltaic sediments. The Stockton Formation is overlain by the Lockatong Formation, which is mostly lacustrine in origin, followed by the basal member of the Brunswick Group, the Passaic Formation, which is mostly lacustrine and fluvial in origin (Figure 2.5.1-11). The remainder of the Brunswick Group are late synrift deposits with clastic sediments and volcanic lithologies (References 2.5.1-151 and 2.5.1-150).

**PSEG Site
ESP Application
Part 2, Site Safety Analysis Report**

2.5.1.1.3.4 North American Stratigraphy

Following rifting of the Pangean crust and development of a passive margin, deposition of sediments related to the North American Atlantic margin began as North America separated and drifted away from Africa. These North American sediments now comprise the basin fill to several depocenters along the current North American Atlantic margin and include the sediments of the Coastal Plain, continental shelf, continental slope, and continental rise. In the site region, North American sediments occur primarily in the Baltimore Canyon Trough and associated Salisbury Embayment (Figure 2.5.1-4).

The Baltimore Canyon Trough forms one of the largest depocenters of the North American Atlantic margin. The distal portions of the trough are associated with a reef complex that defines a Mesozoic paleoshelf edge. This paleoshelf edge extends oceanward of the continental–oceanic crust transition (Reference 2.5.1-170). Therefore, in western, more proximal, portions of the Baltimore Canyon Trough, the North American stratigraphic section is deposited on moderately to highly extended Pangean continental crust and synrift deposits. The Pangean crustal basement component probably consists of Carolina superterrane and Brunswick terrane peri-Gondwanan arc assemblages and, perhaps, remnants of African crust (Figure 2.5.1-8a, Figure 2.5.1-8b, and Reference 2.5.1-85). Distal portions of the Baltimore Canyon Trough that occur oceanward of the continent–ocean crustal transition would have Atlantic Ocean crust as basement to the North American stratigraphic section. The on-land northwestern portion of the Baltimore Canyon Trough occurs as the Salisbury Embayment overlain by coastal plain deposits.

2.5.1.1.3.4.1 Mesozoic Strata

In the Baltimore Canyon Trough, the initial transition from synrift deposition to postrift drift facies occurs as early Jurassic evaporites that form subhorizontal strata above an angular unconformity above synrift deposits. Early to Middle Jurassic strata above the evaporitic interval consists of carbonate reef bank facies in middle and distal portions of the basin and siliclastic sediments proximal to the newly-formed North American continent. Seaward progradation of this sequence resulted in an Upper Jurassic paleoshelf edge defined by an extensive reef bank in the Late Jurassic (Reference 2.5.1-170).

The strata in the Salisbury Embayment and Baltimore Canyon Trough overlying the Upper Jurassic paleoshelf sequences become predominately clastic in nature starting in the Early Cretaceous as coarse sandstones and shales that compose the Lower Cretaceous section buried the Upper Jurassic reef shelf edge complex (Reference 2.5.1-170) and onlapped the continental margin to bury the Jurassic section. The Lower Cretaceous section in the Salisbury Embayment forms the Potomac Group (considered a formation by the Delaware Geologic Survey) (Reference 2.5.1-18 and Figure 2.5.1-11). Potomac Group sediments formed an aggrading alluvial plain that onlapped the Piedmont (Reference 2.5.1-17). Lithofacies present in strata of the Potomac Group are predominately nonmarine fluvial and deltaic sands and gravels, with upper and lower flood plain and fringing swamp deposits (Reference 2.5.1-152). These were formed from an anastomosing river system that deposited channel and overbank sands, flood plain silts, and clays that form bodies in a matrix of floodplain mud. The upper surface of the Potomac Formation is truncated by an unconformity (Reference 2.5.1-17). In and around the site vicinity, Potomac Group lithologies outcrop in limited exposures in the most up-dip portions

**PSEG Site
ESP Application
Part 2, Site Safety Analysis Report**

of the Coastal Plain, (Figures 2.5.1-12a and 2.5.1-12b) but mostly subcrop beneath Quaternary deposits.

The Upper Cretaceous section lies unconformably on the Lower Cretaceous and represents a change from the fluvial and deltaic sequences to transgressive-regressive marine cycles. These sediments contain abundant glauconite, indicating relatively low sedimentation rates. The Raritan Formation is a transgressive fluvial sequence at the base of the Lower Cretaceous section (Figure 2.5.1-11). The Raritan Formation is unconformably overlain by the Magothy Formation, which is entirely marine, and represents another transgressive sequence composed of sands with thin beds of clay silt and lignite (Reference 2.5.1-152). The Magothy Formation is a facies of the overlying transgressive Merchantville Formation. The Merchantville Formation ranges in composition from a glauconitic sand to silty clay, which ranges in thickness from 40 to 60 ft. (Reference 2.5.1-155). These Upper Cretaceous transgressive strata, the Raritan and Magothy–Merchantville formations, record development of an extensive shelf margin along the North Atlantic (Reference 2.5.1-152).

The overlying Woodbury and Englishtown formations represent regression following development of the extensive shelf conditions. The Woodbury is gradational into the underlying Merchantville Formation and consists of an inner-shelf facies, poorly sorted, massive clayey silt that attains thicknesses of 50 ft. The Woodbury is overlain by sand and silts of the Englishtown, which marks the maximum regressive phase of deposition. The Englishtown Formation is transitional with the underlying Woodbury (Reference 2.5.1-155). The overlying Marshalltown Formation represents another transgressive cycle and is composed of glauconitic silty to fine sands that are extensively burrowed. The overlying formations in the Upper Cretaceous section exhibit complex facies relationships related to shifting depositional environments (Reference 2.5.1-152). The Wenonah and Mount Laurel Sand represent regression following the Marshalltown transgression. Strata of the Wenonah and Mount Laurel resulted from deposition of clays, sands and glauconitic sands in inner-shelf and near-shore environments. The overlying Navesink, Red Bank and Tinton formations represent locally developed transgressive and regressive units composed of sands, clayey sands, silts and glauconitic sands.

The Hornerstown Formation contains basal beds that are Late Cretaceous in age, and upper beds of Paleocene age, and is transitional across the Cretaceous–Tertiary boundary (Reference 2.5.1-152). The Hornerstown is a distinctive unit composed of pure, well-sorted, glauconitic sand that gives it a characteristic green color.

2.5.1.1.3.4.2 Cenozoic Strata

Cenozoic stratigraphy in the site region records a widespread unconformity that results in the lack of upper Eocene and lower Oligocene strata. The overlying Neogene strata reflect a distinct increase in clastic input beginning in the Lower Miocene.

2.5.1.1.3.4.3 Tertiary Strata

Paleogene Tertiary strata are characterized by glauconite-rich clastic and carbonate sediments. In contrast, Neogene strata are non-glauconitic and have rare carbonates. These contrasting characteristics indicate that the Paleogene represents relatively low clastic input and erosion rates on the North Atlantic margin, as opposed to the Neogene which appears to be a time-enhanced erosion and clastic deposition (Reference 2.5.1-152). In addition, Tertiary

**PSEG Site
ESP Application
Part 2, Site Safety Analysis Report**

stratigraphic units show geographic differences north and south of the Delaware River as a result of spatially variable sediment input (Reference 2.5.1-152).

The lower two Tertiary formations, the Hornerstown and Vincentown, are the only formations that outcrop both north and south of the Delaware River (Reference 2.5.1-152). Characteristics of the Hornerstown are discussed in the Mesozoic section above in that its basal beds appear to be of Late Cretaceous age. The Vincentown contains both clastic and carbonate components, represented by glauconitic sands and silts and fossil-rich calcarinite. These sequences were deposited in an inner to middle shelf environment and are rich in bryozoans and foraminifera. The formation thins rapidly and is replaced by silt in the subsurface (Reference 2.5.1-152).

The Vincentown Formation is unconformably overlain by the Lower Eocene Manasquan Formation. The lower beds of the Manasquan are glauconite-rich and upper beds consist of sand and silt. The sandy and silty upper beds thicken to replace the overlying Shark River Formation oceanward. Near the site vicinity in the coastal plain, the Middle Eocene section comprises the Shark River Formation, composed of glauconitic sand and mudstone and which lies unconformably above the Manasquan (Reference 2.5.1-152).

The Oligocene marks the development of an extensive unconformity. This unconformity cuts oceanward and occurs as a beveled erosional surface above Lower and Middle Eocene strata in the Coastal Plain, and Upper Eocene strata offshore. In NJ, above this unconformity, a Late Oligocene transgression is represented by the Piney Point Formation, which consists of glauconitic sands and reworked lithic material from the underlying Eocene section. Upper Eocene and Lower Oligocene strata are missing in the Coastal Plain (Reference 2.5.1-152). Paleogene strata in VA and MD comprise the Pamunkey Group, which displays similar unconformable relationships above the Eocene.

The overlying Neogene strata are predominately clastic sediments that were deposited in response to changes in sea level. The Neogene strata occur as both fluvial and marine facies in diverse settings throughout the site region and have a varied nomenclature in the area. Figure 2.5.1-13 (References 2.5.1-163 and 2.5.1-164) shows the regional correlation between these various units in the site region.

The lower two formations in the region of the site vicinity in NJ represent transgressional cycles. The lower unit, the Kirkwood Formation, is polycyclic and represents two or three transgressive phases (References 2.5.1-152 and 2.5.1-216) deposited in the inner to middle shelf. Sections of Kirkwood, as seen in outcrops, consist of three members distinguished based upon clay, silt and sand composition. These units were deposited on the inner to middle shelf.

The Cohansey Sand, which overlies the Kirkwood Formation, is a shoreline facies with poorly defined age constraints in that it contains few fossils, although pollen indicates a late Miocene to early Pliocene age (Reference 2.5.1-152). The strata overlying the Cohansey Sand are fluvial in origin and were deposited during a period when the Coastal Plain was emergent and undergoing dissection (Reference 2.5.1-152). These are typically coarse clastic facies that represent deltaic environments that in cases are transitional into marine conditions representative of lower delta plain and delta front conditions. The Bridgeton Formation occurs primarily in NJ, where it is unconformably overlain by the Pensauken Formation (Reference 2.5.1-152). The Pensauken Formation extends into the western portions of the site vicinity southwest of the Delaware River. The Cohansey, Bridgeton, and Pensauken formations are

**PSEG Site
ESP Application
Part 2, Site Safety Analysis Report**

correlative with marine members of the Chesapeake Group Miocene members (Reference 2.5.1-144).

2.5.1.1.3.4.4 Quaternary Strata

Quaternary deposition in the site region is closely related to the effects of glaciation and results from fluvial and marine processes associated with changes in sea level or with terminal glacial processes and glacial outwash. Deposits from terminal glacial effects and outwash occur in northern portions of the site region and include till and gravel deposits, terminal moraines, and delta and outwash lake gravel deposits.

The oldest marine Pleistocene unit in the site region outcrops from the Delmarva Peninsula to the southeast, and is known as the Omar Formation in DE. This unit is 200,000 years old and was extensively eroded during emplacement of younger Quaternary units (Reference 2.5.1-152). Sea level fluctuations resulting from glacial episodes result in drainage incision during lowstands that results in erosion of large parts of previously deposited sediments. Subsequently, during the transgressive phase, the eroded surface forms an unconformity above which successions of estuarine, barrier island, and inner-shelf sediments are deposited. Several such transgressive and regressive cycles result in complex stratigraphic sequences of similar lithologies (Reference 2.5.1-193). In the vicinity of the site region, at least three transgressive sea level cycles have resulted in marine and estuarine terrace formations that comprise the Cape May Formation and as fluvial deposits of uncertain association in the Van Scliver Lake Beds and the Spring Lake Beds (Reference 2.5.1-144). These have correlative units in Chesapeake Bay and the Atlantic Coast. The transgressive-regressive cycles in the Cape May occur at pre-30 to -28 thousand years ago (ka), 71 ± 7 ka, and 184 ± 20 ka. Each sequence associated with these transgressive-regressive cycles occurs in a deep valley cut in Coastal Plain sediments filled with coarse clastic facies and freshwater peat. These deposits are overlain by finer sediment and fauna that gradually become more marine upward, with pollen indicating an increasingly warm climate. The relationships indicate that the top of the sequence marks climatic cooling and lowering of sea level during glacial events (References 2.5.1-193 and 2.5.1-144). Holocene transgression has resulted in removal or overlap of the youngest Pleistocene sediments and deposition of fill in the major estuaries in the site region (Reference 2.5.1-152).

2.5.1.1.4 Regional Tectonic Setting

The PSEG Site region is located in the central and eastern U.S. (CEUS) which is a stable continental region (SCR) characterized by low rates of crustal deformation and no active plate boundary conditions. The purpose of this subsection is to summarize the current state of knowledge on the tectonic setting and tectonic structures in the site region relevant to the assessment of seismic sources. Subsection 2.5.2 provides an expanded discussion of the seismic source model used for the PSEG Site.

A global review of earthquakes in SCR shows that areas of Mesozoic and Cenozoic extended crust are positively correlated with large SCR earthquakes. Nearly 70 percent of SCR earthquakes with Magnitude (M) 6 occurred in areas of Mesozoic and Cenozoic extended crust (Reference 2.5.1-94). Additional evidence shows an association between Late Proterozoic rifts and modern seismicity in eastern North America (References 2.5.1-94, 2.5.1-247, and 2.5.1-60). Materials from unextended Proterozoic and Paleozoic crust to highly extended Mesozoic

**PSEG Site
ESP Application
Part 2, Site Safety Analysis Report**

extended crust underlie the entire 200 mi. PSEG Site region. However, as discussed in this subsection, there is no evidence for late Cenozoic seismogenic activity of any tectonic feature or structure in the site region (References 2.5.1-40 and 2.5.1-248; NUREG-2115).

The following subsections describe the tectonic setting of the site region by discussing the: (1) origin and orientation of tectonic stress; (2) principle tectonic features; (3) seismic zones defined by regional seismicity; and (4) gravity and magnetic data and anomalies. Historical seismicity occurring in the site region is described in Subsection 2.5.2. The geologic history of the site region is discussed in Subsection 2.5.1.1.2.

2.5.1.1.4.1 Regional Stress

An international effort to collate and evaluate stress indicator data resulted in publication of a world stress map (Reference 2.5.1-263) in 1989. Data for this map are ranked in terms of quality, where plate-scale trends in the orientations of principal stresses are assessed qualitatively based on analysis of high-quality data (Reference 2.5.1-260). Subsequent statistical analyses of stress indicators confirm that the trajectory of the maximum compressive principal stress is uniform across broad continental regions at a high level of statistical confidence. In particular, the northeast-southwest orientation of principal stress in the CEUS is statistically robust and is consistent with the theoretical trend of compressive forces acting on the North American plate from the mid-Atlantic ridge (Reference 2.5.1-36). As part of the CEUS-SSC project (NUREG-2115), the world stress map was updated for the CEUS region. The update reached the same conclusion of a northeast-southwest orientation of principal stress as presented in Reference 2.5.1-236. However, local variations in the regional stress field are also present in more recent datasets (References 2.5.1-99 and 2.5.1-191).

In addition to better documenting the orientation of stress, research has addressed quantitatively the relative contributions of various forces which may be acting on the North American plate, to the total stress within the plate. Richardson and Reding (Reference 2.5.1-192) performed numerical modeling of stress in the continental U.S. interior and considered the contribution to total tectonic stress to be from three classes of forces:

- Horizontal stresses that arise from gravitational body forces acting on lateral variations in lithospheric density. These forces commonly are called buoyancy forces. Richardson and Reding emphasize that what is commonly called ridge-push force is an example of this class of force. Rather than a line-force that acts outwardly from the axis of a spreading ridge, ridge-push arises from the pressure exerted by positively buoyant, young oceanic lithosphere near the ridge against older, cooler, denser, less buoyant lithosphere in the deeper ocean basins (Reference 2.5.1-234). The force is an integrated effect over oceanic lithosphere ranging in age from 0 to 100 million years (Reference 2.5.1-43). The ridge-push force is transmitted as stress to the interior of continents by the elastic strength of the lithosphere.
- Shear and compressive stresses transmitted across major plate boundaries (strike-slip faults and subduction zones).
- Shear tractions acting on the base of the lithosphere from relative flow of the underlying asthenospheric mantle.

Richardson and Reding (Reference 2.5.1-192) concluded that the observed northeast-southwest trend of principle stress in the CEUS dominantly reflects ridge-push body forces.

Rev. 4

**PSEG Site
ESP Application
Part 2, Site Safety Analysis Report**

They estimated the magnitude of these forces to be 2 to 3×10^{12} newtons per meter (the total vertically integrated force acting on a column of lithosphere 1 meter wide), which corresponds to average equivalent stresses of 40 to 60 megapascals (MPa) distributed across a 30 mi. (50 km) thick elastic plate. The fit of the model stress trajectories to data was improved by the addition of compressive stress (5 to 10 MPa) acting on the San Andreas Fault and Caribbean plate boundary structures. The fit of the modeled stresses to the data further suggested that shear stresses acting on these plate boundary structures are in the range of 5 to 10 MPa.

Richardson and Reding noted that the general northeast-southwest orientation of principle stress in the CEUS also could be reproduced in numerical models which assume a shear stress, or traction, acting on the base of the North American plate. Richardson and Reding (Reference 2.5.1-192) and Zoback and Zoback (Reference 2.5.1-262) do not favor this as a significant contributor to total stress in the mid-continent region. A basal traction predicts or requires that the horizontal compressive stress in the lithosphere increases by an order of magnitude moving east to west, from the eastern seaboard to the Great Plains. Zoback and Zoback (Reference 2.5.1-262) noted that the state of stress in the southern Great Plains is characterized by north-northeast to south-southwest extension, which is contrary to this prediction. They further observed that the level of background seismic activity is generally higher in the eastern United States than in the Great Plains, which is not consistent with the prediction of the basal traction model that compressive stresses (and presumably rates of seismic activity) should be higher in the middle parts of the continent than along the eastern margin.

To summarize, analyses of regional tectonic stress in the CEUS is characterized as a northeast-southwest orientation of the maximum compressive principal stress, which would apply to the PSEG Site region in general. The orientation of a planar tectonic structure relative to the principle stress direction determines the magnitude of shear stress resolved onto the structure. Thus, there is no significant change in the understanding of the regional static stress in the CEUS since the publication of the world stress map (Reference 2.5.1-263) in 1989 or NUREG-2115, and there are no significant implications for existing characterizations of potential activity of tectonic structures.

2.5.1.1.4.2 Principal Tectonic Structures

The principal tectonic structures within the 200-mi. PSEG Site region are categorized and discussed on the basis of their age of formation or most recent reactivation. These categories include Late Proterozoic, Paleozoic, Mesozoic, and Cenozoic. Late Proterozoic, Paleozoic, and Mesozoic structures are related to major plate tectonic events. These generally are mapped regionally on the basis of geological and/or geophysical data. Late Proterozoic structures include normal faults active during post-Grenville orogeny rifting and formation of the Iapetan passive margin. Paleozoic structures include thrust and reverse faults active during Taconic, Acadian, Alleghanian, and other contractional orogenic events. Mesozoic structures include normal faults active during break-up of Pangea and formation of the Atlantic Ocean basin. Cenozoic structures within the PSEG Site region are related to the tectonic environment of the Atlantic passive margin. This passive margin environment is characterized by southwest- to northeast-oriented, horizontal principle compressive stress and vertical crustal motions. The vertical crustal motions are associated with loading of the Coastal Plain and offshore sedimentary basins and erosion and exhumation of the Piedmont and westward provinces of the Appalachians. Commonly, these structures are localized and represent reactivated portions

**PSEG Site
ESP Application
Part 2, Site Safety Analysis Report**

of older bedrock structures. Several studies have compiled a list of tectonic features with potential Quaternary activity (References 2.5.1-40, 2.5.1-248 and 2.5.1-249). These potential Quaternary features are listed in Subsection 2.5.1.1.4.2.5. Zones of seismicity not clearly associated with a tectonic feature are discussed separately in Subsection 2.5.1.1.5.

2.5.1.1.4.2.1 Late Proterozoic Tectonic Structures

Extensional structures related to the Late Proterozoic-Early Cambrian rifting of the former supercontinent Rodinia and the formation of the Iapetus Ocean basin are located along a northeast-trending belt between Alabama and Labrador, Canada, and along roughly-orthogonal branches (References 2.5.1-247 and 2.5.1-94). The northwestern or cratonward limit of Iapetus normal faults separates unfaulted Laurentian basement to the northwest from the rifted basement to the southeast. The rifted basement generally has higher seismicity rates than the un rifted craton interior (Reference 2.5.1-247). The Rome Trough is a Middle to Late Cambrian graben system that stretched from PA southwest into Kentucky and formed during rifting of Rhodinia. The trough dies out in central PA, near the edge of the PSEG Site region (Reference 2.5.1-194).

The Grenville internal massifs or gneiss domes are a series of exposures of Grenville basement that occur within the core of the Paleozoic orogen. These exposures are generally the result of younger tectonic events, basement rocks that have been folded and transported to higher structural levels on thrust faults. But the high-grade metamorphic gneisses exposed in these massifs represent evidence of older orogeny. These include the domes that expose the Baltimore gneiss in southeastern PA, DE, and MD, as well as the Chester-Athens dome to the northeast and the Sauratown Mountains anticlinorium to the southwest (Reference 2.5.1-182). These exposures are key in that they indicate that the Grenville basement was located at least as far southeast as these exposures, and can help define the potential boundaries of the accreted terranes. Other notable exposures of Grenville basement are found in the Hudson Highlands, Manhattan Prong, Reading Prong, Trenton Prong, Honey Brook upland, and the Blue Ridge and Salem anticlinoria (Reference 2.5.1-183). Detailed work in these areas has revealed a complex tectonic history. For example, in the Hudson Highlands of NY, gneisses reveal three episodes of plutonic emplacement along with folding and mylonitization during the Proterozoic (Reference 2.5.1-188).

2.5.1.1.4.2.2 Paleozoic Tectonic Structures

Outside of the Coastal Plain physiographic province in which the PSEG Site is located, numerous tectonic structures are exposed. These thrust sheets, shear zones, regional folds, and sutures formed during convergent and transpressional Appalachian orogenic events of the Paleozoic Era. It is understood that many structures of the same style and age also exist, unexposed and buried beneath the Coastal Plain sediments. Paleozoic structures shown on Figures 2.5.1-8a and 2.5.1-8b include 1) sutures interpreted to separate tectonic terranes that collided with ancestral North America; 2) regionally extensive Appalachian thrust fault and oblique-slip shear zones; and 3) smaller faults and folds that accommodated Paleozoic deformation during collisional events. Most of the thrust faults are northwest-vergent and dip southeastward to sole into a basal decollement (Figure 2.5.1-14). Below this basal decollement is North American basement, generally thought of as Grenville or Laurentian crust. Given the number of faults within the site region (Figure 2.5.1-10), discussion of Paleozoic structures is limited to those of particular regional interest and those within the site vicinity.

**PSEG Site
ESP Application
Part 2, Site Safety Analysis Report**

Within the site region, several faults may represent the western boundary of terranes accreted to Laurentia in the Paleozoic while the Iapetus closed (Reference 2.5.1-182). Nearest the site, this structure is the Pleasant Grove-Huntingdon Valley fault (PGHV). To the northeast, near New York City, it is known as Cameron's Line, and the equivalent to the southwest is hypothetically located beneath the Culpeper Basin (Reference 2.5.1-182). These are northeast-striking, southeast-dipping thrusts. The PGHV fault is a 0.6 to 1.2 mi. wide mylonitic thrust fault which separates the rocks of the Westminster terrane from the Potomac terrane to the southeast (Figures 2.5.1-12 and 2.5.1-8). It probably originally formed as a northwest-vergent thrust during the Taconic orogeny, but was reactivated dextrally during the Alleghanian greenschist-grade deformation (Reference 2.5.1-106).

The Martic line or thrust developed during the Taconic orogeny and thrust ocean basin deposits (the Westminster terrane) west over Laurentian slope deposits before regional metamorphism (Reference 2.5.1-64). Similar thrusts developed during the Taconic orogeny are generally gently-dipping faults with sinuous traces that deform Cambro-Ordovician rocks exposed in klippen like the Hamburg complex (such as the Sinking Springs, Portland, Kutztown-Leinbacks, and Black River faults) (Reference 2.5.1-57). The Yellow Breeches thrust fault (Ybt) (Figures 2.5.1-8a and 2.5.1-8b) is thought to be the northern extension of the Blue Ridge thrust (Reference 2.5.1-84). Younger thrusts developed during the Alleghanian orogeny often either form the characteristic folds in the Appalachian foreland exposed, or are responsible for exposures of Grenville basement throughout the Appalachians (Figures 2.5.1-8a and 2.5.1-8b). Late Paleozoic faults with strike-slip deformation are common, such as the Spotsylvania fault in VA (Reference 2.5.1-137).

The only Paleozoic structure within the site vicinity is the Rosemont shear zone, a northeast-striking shear zone located approximately 17 mi. north of the site in the PA piedmont; sometimes being mapped extending into northern DE (References 2.5.1-199 and 2.5.1-22, Figures 2.5.1-12a and 2.5.1-12b). The mylonitic shear zone separates the Brandywine gneiss and Arden plutonic suite to the east and the West Chester and Avondale basement massifs to the northwest, and deforms rocks of the Wissahickon Formation. Deformed rocks have shallowly plunging lineations subparallel to the foliation of the shear zone, interpreted to indicate dextral deformation. Descriptions of the southern extension of this structure in DE, however, indicate that it is a steep high-angle reverse fault (Reference 2.5.1-255). Cross-cutting relationships indicate that the Rosemont shear zone was active after peak regional metamorphism, probably in the Devonian to early Mississippian (Reference 2.5.1-240). The Rosemont shear zone is deformed and cross-cut by the Pleasant Grove-Huntingdon Valley shear zone to the north (Reference 2.5.1-240).

2.5.1.1.4.2.3 Mesozoic Tectonic Structures

The primary tectonic features from the Mesozoic Era within the PSEG Site region are rift basins that accomplished the extension associated with the opening of the Atlantic Ocean. A series of such basins is exposed within the core of the Appalachian orogen north and west of the site (e.g., the Newark, Gettysburg, and Culpeper basins). They are easily identified by their characteristic fill of synrift Newark Supergroup (Figure 2.5.1-9). East of the exposed basins, a series of basins beneath the Cretaceous to Holocene sediment of the Coastal Plain is more difficult to identify and map. The Mesozoic faults associated with these basins are shown as dashed to indicate that they are concealed (Figure 2.5.1-10).

**PSEG Site
ESP Application
Part 2, Site Safety Analysis Report**

Borings and seismic lines can be used to identify Mesozoic synrift sediments and map basin-bounding normal faults, but these have a limited spatial distribution and only provide information at a point or along a finite line. Aeromagnetic and gravity data have a broader spatial coverage and can also be used to estimate the boundaries or spatial extent of basins identified on seismic lines or with borings, but the potential causes for observed magnetic and gravity highs or lows are non-unique. Hence, there is much uncertainty regarding the location of the buried basins and a variety of basin location maps are available (Figure 2.5.1-15). On review of the available compilations and representations of the buried basins, it is concluded that the Benson map (Reference 2.5.1-15 and Figure 2.5.1-9) is the most detailed and defensible regional representation of the potential basins along the central Atlantic margin. The Benson map was compiled and published at a larger scale than other compilations. It is explicit about what data was used to draw each basin on the map, and it distinguishes between basin boundaries that are more or less certain, with query symbols. In fact, other representations (Reference 2.5.1-254 and Figure 2.5.1-15) are often based upon the Benson compilation (References 2.5.1-15 and 2.5.1-19). The Benson map indicates that the nearest Mesozoic basin is a postulated and heavily queried extension of the Queen Anne basin, located approximately 15 mi. south of the site. Evidence that indicates the presence of pre-Mesozoic basement beneath the site is discussed in detail in Subsection 2.5.1.2.4.

Most Mesozoic normal faults in the area of the PSEG Site are regional structures in close association with the Mesozoic rift basins. Such faults include the Ramapo, Furlong-Flemington, and Chalfont faults (Figures 2.5.1-9 and 2.5.1-10). These structures are usually east-dipping faults which form the western edge of the half-graben basins, though the west-dipping basin-bounding faults in Connecticut (CT) are exceptions to this (Reference 2.5.1-15). Smaller, subsidiary normal faults mapped near the basins also exist and, if undated, are generally considered Mesozoic in age because the last regional episode of extensional deformation was related to the Triassic-Jurassic rifting of the Atlantic.

The Ramapo fault is located on the west edge of the Newark basin in NY and NJ (Figure 2.5.1-9). The fault clearly cuts Upper Triassic members of the Newark Supergroup, the characteristic synrift sedimentary sequences deposited in the rift basins during the opening of the Atlantic Ocean basin, and its Mesozoic history is clearly recognized (Reference 2.5.1-195). Work along the northeastern extension of the fault reveals a complex history in the Hudson Highlands of NY. Here, intense cataclasis restricted to portions of the fault juxtaposing Paleozoic and Precambrian units indicates periods of earlier repeated movements (Reference 2.5.1-184). Seismic imaging of the border faults at depth to the southwest in eastern PA reveals that the fault dips more gently there (as low as 25 degrees), exhibits kinematic indicators consistent with an older contractional history, and parallels older mylonitic thrusts at depth (Reference 2.5.1-189). Though the faults most recent movement is Mesozoic in age, it clearly was reactivating along a gently dipping stack of imbricate thrust slices related to Paleozoic contractional tectonics.

2.5.1.1.4.2.4 Cenozoic Tectonic Structures

Several Cenozoic tectonic faults and folds have been identified within the PSEG Site region (Figure 2.5.1-10), although some have very scant evidence for existence of Cenozoic activity. Only structures with suggested or demonstrated Cenozoic activity, not discussed in the potential Quaternary feature compilation studies of Crone and Wheeler (Reference 2.5.1-40), are

**PSEG Site
ESP Application
Part 2, Site Safety Analysis Report**

discussed here. The potential Quaternary features compiled by Crone and Wheeler are discussed in Subsection, 2.5.1.1.4.2.5. A summary for both sets of features, including information regarding the best estimate for latest deformation on these Cenozoic structures and Crone and Wheeler features is presented in Table 2.5.1-1.

2.5.1.1.4.2.4.1 The Hypothesized Fault of Pazzaglia (1993)

In an investigation of Quaternary sedimentary sequences near or on Elk Neck in MD, Pazzaglia (Reference 2.5.1-162) noted variations of approximately 26 ft. in the elevation of Pleistocene Turkey Point beds. A fault was postulated to cause the abnormal height of the Turkey Point beds relative to their elevation farther north (Figure 2.5.1-16). Pazzaglia indicated during expert interviews that there was no physical geologic evidence for faulting in the area and that original depositional relief on the strata was an equally plausible cause for the observed elevation differences. Field and aerial reconnaissance, as well as inspections of aerial imagery, found no indicators of faulting and, given the hypothetical nature of this structure, it is concluded that it is not a capable tectonic source.

2.5.1.1.4.2.4.2 Faults of Hansen (1978)

Hansen used a series of vibroseis lines in MD on the east and west sides of the Chesapeake Bay to infer faulting of the basement surface at depth beneath the Coastal Plain sediments. In one case, although the resolution of the seismic data did not allow for offset in the overlying Potomac sediments, Hansen used correlated well-log data to infer faulting that was as young as early Paleocene (the Hillville fault, located on the west side of Chesapeake Bay). Structure contour maps indicate that the top of the Cretaceous surface above the structures identified in seismic lines is unfaulted, therefore a late Mesozoic age is most likely for these features. (Reference 2.5.1-79)

2.5.1.1.4.2.4.3 River Bend Trend/Stafford Fault of Marple (2004)

Marple (Reference 2.5.1-120) hypothesized that the southwestern bends in many rivers of the east coast are related to a northeast-southwest striking structure extending from the well-characterized Tertiary Stafford fault system in VA, to central NJ (Figure 2.5.1-16). Yet, Marple presents no geologic or geomorphic evidence of faulting along this trace. Instead, the bends in these rivers likely represent the migration from older, entrenched channels in resistant Piedmont rocks to lower gradient meandering river systems flowing across younger, less-competent Coastal Plain sediments. It is likely that a very gentle regional tilt towards a local depocenter (such as the Salisbury Embayment) may control the tendency of the rivers to flow to the southwest. Review of records shows no evidence for the progressive deflection of rivers across a tectonic structure, such as abandoned meanders or beheaded channels, along this river bend trend. It is also well-known that many regional rivers bent to the southwest as early as the Miocene. For example, clasts in the Miocene Bridgeton formation indicate a source in the Adirondacks of NY, and paleoflow indicators indicate a southwestern flow direction along the present-day Delaware Valley, to deposit the Bridgeton across southern NJ, by a paleo-Hudson River (Reference 2.5.1-153). Hence, the southwest bend of the rivers are an effect of the location of depocenters in the Tertiary, and not related to Quaternary faulting.

**PSEG Site
ESP Application
Part 2, Site Safety Analysis Report**

2.5.1.1.4.2.4.4 National Zoo Faults

The National Zoo faults in Washington D.C. are located roughly 100 mi. southwest of the site (Figures 2.5.1-10 and 2.5.1-16). The National Zoo faults are primarily northwest-striking, southwest-dipping thrust faults that occur within a dense, 1.5 mi. long, north-trending elongate cluster (Reference 2.5.1-69). The faults were first identified by Darton (Reference 2.5.1-49) in historic excavations between the National Zoo and Massachusetts Avenue in Washington D.C. The mapped surface traces of these faults range from 500 to 2000 ft. with up to 20 ft. of post-Cretaceous reverse displacement visible in outcrops at the National Zoo (Reference 2.5.1-69).

The National Zoo faults generally offset the unconformity between underlying Paleozoic rocks and the Cretaceous Potomac formation, indicating they were active during the Mesozoic (References 2.5.1-49, 2.5.1-126 and 2.5.1-69). However, the youngest two faults thrust basement rocks over Pliocene Upland gravels (References 2.5.1-69 and 2.5.1-126) and an exposure of these two faults is still preserved along Adams Mill Road as a special monument (Reference 2.5.1-173). This fault zone is coincident with the mapped trace of the Early Paleozoic Rock Creek shear zone, which may indicate that the National Zoo faults represent reactivations of Paleozoic deformational features (Reference 2.5.1-126 and 2.5.1-69). These faults are probably Tertiary in age, and though new information has been published about them since the EPRI (Reference 2.5.1-62) studies, their timing and extent have remained unchanged.

2.5.1.1.4.2.4.5 Chesapeake Bay Impact Structure

The Chesapeake Bay impact crater was discovered in 1993 at the southern end of the Chesapeake Bay, approximately 150 mi. south of the PSEG Site (Reference 2.5.1-62). The 35-million year old Chesapeake Bay impact crater is a 56 mi. wide, complex structure with an inner and outer ring (Reference 2.5.1-172). Immediately after the impact with the large comet or meteorite, the crater filled with a characteristic breccia called the Exmore beds. The large crater was apparently not alone, in that multiple secondary craters of Eocene age have also been discovered (Reference 2.5.1-171). Normal faulting is developed within and around these structures. These faults are typical of such geomorphic features and accommodate the oversteepened edges of the crater and/or differential compaction or subsidence of sediment across these features. The faulting is mostly confined to Tertiary units, but does extend into younger, unconsolidated deposits. This faulting, like growth faults in the unconsolidated Coastal Plain sediments, is not expected to cause seismicity. The most significant effect of the crater is its effect on the depositional history of the east coast. The continued subsidence due to compaction at the crater site meant that this area acted as a regional depocenter for much of the Cenozoic (Reference 2.5.1-172).

2.5.1.1.4.2.4.6 Brandywine Fault System

The Brandywine fault system is located approximately 100 mi. southwest of the site, on the north side of the Potomac River near the Stafford fault system (Figures 2.5.1-10 and 2.5.1-16). The 12 to 30 mi. long Brandywine fault system consists of a series of en echelon northeast-trending, southeast-dipping reverse faults with east-side-up vertical displacement. Jacobeen (Reference 2.5.1-92) first described the fault system from vibroseis profiles and a compilation of borehole data. The fault system is composed of the Cheltenham and Danville faults, which are 4 mi. and 8 mi. long, respectively. These two faults are separated by a 0.6 to 1 mi. wide left step-over (Reference 2.5.1-92). Later work by Wilson and Fleck (Reference 2.5.1-253) interpret one

**PSEG Site
ESP Application
Part 2, Site Safety Analysis Report**

continuous 20 to 30 mi. long fault that transitions into a west-dipping flexure to the south near the Potomac River. Mixon and Newell (Reference 2.5.1-133) pointed out similarities between the Brandywine system and the nearby Stafford fault system.

The Brandywine fault system was active in the Early Mesozoic and reactivated during late Eocene and possibly middle Miocene time (Reference 2.5.1-92 and 2.5.1-253). Basement rocks have a maximum vertical displacement of approximately 250 ft. across the fault (Reference 2.5.1-92), and the Cretaceous Potomac Formation is 150 ft. thinner on the east (up-thrown) side of the fault indicating syndepositional faulting. The faulting extends upward into the Eocene units and dies out as a subtle 8-ft. flexure developed within the Miocene Calvert Formation (References 2.5.1-92 and 2.5.1-253). Hence, geologic information indicates that deformation on the Brandywine fault system ended during the Miocene.

2.5.1.1.4.2.5 Potential Quaternary Tectonic Features within the Site Region

In an effort to provide a comprehensive database of Quaternary tectonic features, Crone and Wheeler (Reference 2.5.1-40), and Wheeler (References 2.5.1-248 and 2.5.1-249) compiled geological information on Quaternary faults, liquefaction features, and possible tectonic features in the CEUS. Crone and Wheeler and Wheeler (Reference 2.5.1-248) evaluated and classified these features into one of four categories based on strength of evidence for Quaternary activity (Classes A, B, C, and D); see Table 2.5.1-2 for definitions (References 2.5.1-40 and 2.5.1-248). Work performed as part of the PSEG Site investigation, including literature review, interviews with experts, and geologic reconnaissance, did not identify any additional potential Quaternary tectonic features within the site region. Crone and Wheeler report only one feature described in the literature that exhibited evidence for Quaternary activity (Class A) (Figure 2.5.1-17). The only Crone and Wheeler feature within the PSEG Site vicinity is the faulting in New Castle County, a Class C feature (Figure 2.5.1-17 and Reference 2.5.1-40).

2.5.1.1.4.2.5.1 Central Virginia Seismic Zone

The Central Virginia seismic zone is an area of persistent, low-level seismicity in the Piedmont Province (Figures 2.5.1-1 and 2.5.1-18). The zone extends approximately 75 mi. in a north-south direction, and approximately 90 mi. in an east-west direction, from Richmond to Lynchburg, VA, coincident with the James River (Reference 2.5.1-24). The PSEG Site is located 170 mi. northeast of the northern boundary of the Central Virginia seismic zone. The largest historical earthquake to occur in the Central Virginia seismic zone was the estimated moment magnitude $E[M]$ 5.8 Mineral earthquake on August 23, 2011 (Reference 2.5.1-288). The maximum intensity estimated for this event was Modified Mercalli Intensity (MMI) VII in the epicentral region (see Subsection 2.5.2.1.3 for additional discussion of the Mineral earthquake). Several years prior to the Mineral earthquake an mb 4.5 earthquake (two closely-spaced events that when combined equal a moment magnitude (M_w) of 4.1) occurred on December 9, 2003 within the Central Virginia seismic zone (CVSZ). The December 9, 2003 earthquake occurred close to the Spotsylvania fault, but due to the uncertainty in the location of the epicenter (3.7 to 5 mi.) no attempt could be made to locate the epicenter with a specific fault or geologic lineament in the CVSZ (Reference 2.5.1-99).

Seismicity in the CVSZ ranges in depth from 2 to 8 mi. (Reference 2.5.1-251). It is suggested (Reference 2.5.1-38) that seismicity in the central and western parts of the zone may be associated with west-dipping reflectors that form the roof of a detached antiform, while

**PSEG Site
ESP Application
Part 2, Site Safety Analysis Report**

seismicity in the eastern part of the zone near Richmond may be related to a near-vertical diabase dike swarm of Mesozoic age. However, given the depth distribution of 2 to 8 mi. (Reference 2.5.1-251) and broad spatial distribution, it is difficult to uniquely attribute the seismicity to any known geologic structure, and it appears that the seismicity extends both above and below the Appalachian detachment. No capable tectonic sources have been identified within the CVSZ, but two paleoliquefaction sites have been identified within the zone (References 2.5.1-40 and 2.5.1-146). The presence of these paleoliquefaction features on the James and Rivanna rivers shows that the CVSZ reflects both an area of paleo-seismicity as well as observed historical seismicity. Based on the absence of widespread paleoliquefaction, however, it was concluded (Reference 2.5.1-146) that an earthquake of magnitude 7 or larger has not occurred within the seismic zone in the last 2000 to 3000 years, nor in the eastern portion of the seismic zone for the last 5000 years. It was also concluded that the geologic record of one or more magnitude 6 to 7 earthquakes might be concealed between streams, but that such events could not have been abundant in the seismic zone. In addition, these isolated locations of paleoliquefaction may have been produced by local, shallow, moderate magnitude earthquakes of M 5 to 6.

The paleoliquefaction sites reflect prehistoric occurrences of seismicity within the CVSZ, and do not indicate the presence of a capable tectonic source. Recently, Wheeler (Reference 2.5.1-249) hypothesizes that there may be two causative faults for the small dikes of Obermier and McNulty (Reference 2.5.1-146), and that earthquakes larger than those represented by historic seismicity are possible; whereas Marple and Talwani (Reference 2.5.1-123) interpret seismicity data to infer the presence of a hypothesized northwest-trending basement fault (Shenandoah fault) that coincides with the Norfolk fracture zone (Reference 2.5.1-120). However, no definitive causative fault or faults have been identified within the CVSZ (Reference 2.5.1-249).

2.5.1.1.4.2.5.2 Lancaster Seismic Zone and the Cacoosing Valley Earthquake

The Lancaster seismic zone of southeast PA, as defined by Armbruster and Seeber (Reference 2.5.1-10), has been a persistent source of seismicity for at least two centuries. The Cacoosing Valley earthquake occurred within the 80 square mile (sq. mi.) zone that spans a belt of allochthonous Appalachian crystalline rocks between the Great Valley and Martic Line northwest of the PSEG Site (Figure 2.5.1-18). The Lancaster seismic zone straddles exposed Piedmont rocks which include thrust faults and folds associated with Paleozoic collisional orogenies as well as the Newark-Gettysburg Triassic rift basin, which consists of extensional faults associated with Mesozoic rifting. Most well-located epicenters in the Lancaster seismic zone lie directly outside the Mesozoic basin (Reference 2.5.1-198). The epicenters of events with magnitudes 2.93 to 4.1 E[M], from the western part of the Lancaster seismic zone, define a north-south trend that intersects the juncture between the Gettysburg and Newark subbasins. This juncture is a hinge around which the two subbasins subsided, resulting in east-west oriented tensile stress. Numerous north-south trending fractures and diabase dikes are consistent with this hypothesis. It is likely that seismicity in at least the western part of the Lancaster seismic zone is due to present-day northeast-southwest compressional stress which is activating the Mesozoic fractures, with dikes perhaps serving as stress concentrators (Reference 2.5.1-10).

It also is probable that some recent earthquakes in the Lancaster seismic zone have been triggered by surface mining. For instance, the January 16, 1994, Cacoosing earthquake (E[M] 4.166) is the largest instrumented earthquake occurring in the Lancaster seismic zone. This

**PSEG Site
ESP Application
Part 2, Site Safety Analysis Report**

event was part of a shallow (depths generally less than 1.5 mi.) earthquake sequence linked to quarry activity (Reference 2.5.1-204). The earthquake sequence that culminated in the January 16, 1994 event initiated after a quarry was shut down and the quarry began to fill with water. Seeber (Reference 2.5.1-204) interprets the reverse-left lateral oblique earthquake sequence to be due to a decrease in normal stress caused by quarrying followed by an increase in pore fluid pressure (and decrease in effective normal stress) when the pumps were turned off and the water level increased. Because this earthquake is anthropogenic, it is not officially part of the CEUS-SSC seismic catalog (NUREG-2115).

Prior to the Cacoosing earthquake sequence, the April 23, 1984, Martic earthquake (mb 4.1) was the largest instrumented earthquake in the seismic zone and resembles pre-instrumental historical events dating back to the middle 18th century. The 1984 earthquake sequence appears centered at about 2.8 mi. in depth and may have ruptured a steeply east-dipping, north-to northeast-striking fault aligned subparallel to Jurassic dikes with a reverse-right lateral oblique movement, consistent with east-northeast horizontal maximum compression. These dikes are associated with many brittle faults and large planes of weakness suggesting that they too have an effect on the amount of seismicity in the Lancaster seismic zone. Most of the seismicity in the Lancaster seismic zone is occurring on secondary faults at high angles to the main structures of the Appalachians.

2.5.1.1.4.2.5.3 Fall Lines of Weems (1998)

In 1998, Weems defined seven fall lines across the Piedmont and Blue Ridge provinces of North Carolina (NC) and VA (Figure 2.5.1-7). The eastern fall line terminated approximately 100 mi. southwest of the PSEG Site. The fall lines, not to be confused with the fall zone separating the Piedmont and Coastal Plain provinces, are based on the alignment of short stream segments with anomalously steep gradients (i.e., knickpoints). Weems (Reference 2.5.1-245) explores possible ages and origins (rock hardness, climatic, and tectonic) of the fall lines and “based on limited available evidence favors a neo-tectonic origin” for these geomorphic features during the Quaternary. However, numerous studies in the Appalachians recognize widespread, development of knickpoints unrelated to tectonic activity and note that differences in bedrock strength and joint orientation are dominant controls on waterfall formation and evolution. These knickpoints can also be formed in response to changes in sea level differential uplift or subsidence of the Piedmont relative to the Coastal Plain due to isostatic adjustments from erosional unroofing and deposition (References 2.5.1-77, 2.5.1-132, 2.5.1-71, and 2.5.1-164).

Later studies, part of the North Anna ESPA, demonstrated that there are inconsistencies and ambiguities in Weems’ (Reference 2.5.1-245) correlations and alignment of steep reaches of streams used to define continuous fall lines (Reference 2.5.1-55). The North Anna ESPA study concludes that the characteristics of the fall zones can be readily explained by differential erosion due to variable bedrock hardness rather than Quaternary tectonism and that there is no geomorphic expression of recent tectonic activity (Reference 2.5.1-55). Similarly, Wheeler (Reference 2.5.1-248) notes that the fall zones reported by Weems (Reference 2.5.1-245) are not reproducible and are, thus, subjective, thereby invalidating the tectonic faulting origin model and designating the knickpoints as a Class C feature. In the safety evaluation report for the North Anna ESPA site study, the NRC staff agrees with the assessment that the fall lines of Weems (Reference 2.5.1-245) are unrelated to tectonic activity. In summary, based on review of published literature, field reconnaissance, and geologic and geomorphic analysis performed previously for the North Anna ESPA, the fall lines of Weems (Reference 2.5.1-245) are

**PSEG Site
ESP Application
Part 2, Site Safety Analysis Report**

erosional features related to contrasting lithologies of different erosional resistance and are not tectonic in origin.

2.5.1.1.4.2.5.4 Everona-Mountain Run Fault Zone

The Mountain Run fault zone is located along the eastern margin of the Culpeper Basin and lies approximately 150 mi. southwest of the site (Figure 2.5.1-17). The 75-mi. long, northeast-striking fault zone is mapped from the eastern margin of the Triassic Culpeper Basin near the Rappahannock River southwestward to near Charlottesville, in the western piedmont of VA (Reference 2.5.1-159). The fault zone consists of a broad zone of sheared rocks, mylonites, breccias, and phyllites of variable width.

The Mountain Run fault zone is interpreted to have formed initially as a thrust fault upon which back-arc basin rocks or mélangé deposits were accreted onto ancestral North America at the end of the Ordovician (Reference 2.5.1-160). This major suture separates the Blue Ridge and Piedmont terranes (Reference 2.5.1-161 and Figure 2.5.1-8a). Subsequent reactivation of the fault during the Paleozoic and/or Mesozoic produced strike-slip and dip-slip movements. Horizontal slickensides found in borehole samples and at several places near the base of the Mountain Run scarp suggest strike-slip movement, whereas small-scale folds in the uplands near the scarp suggest an oblique dextral sense of slip. The timing of the reverse and strike-slip histories of the fault zone, and associated mylonitization and brecciation, is constrained to be pre-Early Jurassic, based on the presence of undeformed Early Jurassic diabase dikes that cut rocks of the Mountain Run fault zone. The northeast-striking Mountain Run fault zone is moderately to well-expressed geomorphically (Reference 2.5.1-161). Two northwest-facing scarps occur along the fault zone, including: (1) the 1 mi. long Kelly's Ford scarp located directly northeast of the Rappahannock River and; (2) the 7 mi. long Mountain Run scarp located along the southeast margin of the linear Mountain Run drainage. Conspicuous bedrock scarps in the Piedmont, an area characterized by deep weathering and subdued topography, have led some experts to suggest that the fault has experienced a Late Cenozoic phase of movement (References 2.5.1-160 and 2.5.1-161).

Near Everona, VA, a small reverse fault, found in an excavation, vertically displaces probable Late Tertiary gravels by 5 ft. (Reference 2.5.1-161). The fault strikes northeast, dips 20 degrees northwest and, based on kinematic indicators, is an oblique strike-slip fault. More recently, it is estimated that the offset colluvial gravels are Pleistocene age (Reference 2.5.1-117). The Everona fault is located about 0.5 mi. west of the Mountain Run fault zone. Due to the close proximity of these two faults and their shared similar orientation and sense of slip, the Everona and Mountain Run faults are considered to be part of the same fault zone, hence the Everona-Mountain Run fault zone (Reference 2.5.1-40). Crone and Wheeler (Reference 2.5.1-40) assessed that the faulting at Everona is likely to be of Quaternary age, but because the likelihood has not been tested by detailed paleo-seismological or other investigations, this feature was assigned to Class C.

Field and aerial reconnaissance, and geomorphic analysis of deposits and features associated with the fault zone, recently performed for the North Anna ESPA, provide new information on the absence of Quaternary faulting along the Everona-Mountain Run fault zone (Reference 2.5.1-54). In response to NRC comments on the North Anna ESPA, geologic cross-sections and topographic profiles were prepared along the Mountain Run fault zone to further evaluate the inferred tectonic geomorphology coincident with the fault zone. The results of the additional

**PSEG Site
ESP Application
Part 2, Site Safety Analysis Report**

analysis were presented in the response to an NRC request for additional information (RAI) (Reference 2.5.1-54) and are summarized below:

- There is no consistent expression of a scarp along the Mountain Run fault zone in the vicinity of the Rappahannock River. The northwest-facing Kelly's Ford scarp is similar to a northwest-facing scarp along the southeastern valley margin of Mountain Run. Both scarps were formed by streams that preferentially undercut the southeastern valley walls, creating asymmetric valley profiles.
- There is no northwest-facing scarp associated with the Mountain Run fault zone between the Rappahannock and Rapidan Rivers. Undeformed late Neogene colluvial deposits bury the Mountain Run fault zone in this region, demonstrating the absence of Quaternary fault activity.
- The northwest-facing Mountain Run scarp southwest of the Rappahannock River alternates with a southeast-facing scarp on the opposite side of Mountain Run valley. Both sets of scarps have formed by the stream impinging on the edge of the valley.

Significant new information includes the work performed for the North Anna ESPA that shows the Mountain Run fault zone has not been active during the Quaternary. In addition, the NRC staff agrees that the scarps along the Mountain Run Fault zone were not produced by Cenozoic fault activity (Reference 2.5.1-145). Similarly, Crone and Wheeler (Reference 2.5.1-40) do not show the Mountain Run fault zone as a known Quaternary structure in their compilation of active tectonic features in the CEUS, having assigned it to Class C. Based on the findings of the previous studies performed for the North Anna ESPA and NRC issuance of the North Anna ESP, it is concluded that the Everona-Mountain Run fault zone is not a capable tectonic source.

2.5.1.1.4.2.5.5 New Castle County Faults

The New Castle County faults were inferred as the result of hydrologic well investigations in northern DE, approximately 15 mi. north of the PSEG Site (Figure 2.5.1-19). Spoljaric (References 2.5.1-210 and 2.5.1-211) mapped a set of buried basement normal faults using well data and a vibroseis profile. The faults defined a basement graben trending approximately 30 degrees northeast. In both studies, there was no evidence that the faults, which cut Paleozoic basement, extend into the overlying Potomac strata. Hence, the best age estimate for these structures is post-Paleozoic and pre-Cretaceous. Later work included a north-south seismic line, three borings, and five trenches located north of New Castle, DE, and along strike of the basement graben identified in the earlier studies (References 2.5.1-210 and 2.5.1-211). Together, these data indicated that Cretaceous and younger strata were undeformed and no evidence for young faulting was found (Reference 2.5.1-128).

Motivated by a single earthquake event (E[M] 3.77 on February 28, 1973) (Reference 2.5.1-197) near Wilmington, DE, Spoljaric (Reference 2.5.1-212) inspected satellite imagery in an attempt to identify structures that could be responsible for the seismic event. Numerous lineaments were identified throughout northern DE and southeastern PA using satellite data. Seven were classified as faults, all located more than 20 mi. north of the PSEG Site. Despite the breadth of the field and geomorphic study, evidence for faulting along any of the hypothesized structures was negligible. Locations of surface deformations are randomly distributed with respect to the postulated faults. In the conclusions of the study, Spoljaric (Reference 2.5.1-212) described tectonic activity as "imperceptible" at the surface and indicated that there was a "lack of observable movements along the faults." Similarly, Spoljaric (Reference 2.5.1-213) mapped

Rev. 4

**PSEG Site
ESP Application
Part 2, Site Safety Analysis Report**

many regional lineaments, faults, and probable faults across DE using Landsat data. No age assignment is given for these features, which were identified with satellite data. The limited evidence to support faulting on these lineaments almost always came from the earlier well data studies (References 2.5.1-210 and 2.5.1-211), which indicated faulting in basement or Cretaceous strata, with undisturbed Cretaceous or Tertiary units above the hypothesized structures (Reference 2.5.1-213). It is concluded that the postulated faults and lineaments of Spoljaric (References 2.5.1-212 and 2.5.1-213), and the basement faults identified by Spoljaric (References 2.5.1-210 and 2.5.1-211), do not exist or do not represent capable tectonic sources based upon the following sources of information:

- Work conducted for the Summit Site nuclear power plant investigated the faults postulated in the Spoljaric (Reference 2.5.1-212) study. This study was unable to verify any faulting along lineaments identified by Spoljaric. Instead, any deformational features found were concluded to have occurred near high-temperature metamorphism.
- Geologic mapping in northern DE (Reference 2.5.1-181) has not identified or corroborated any of the surficial structures postulated by Spoljaric (References 2.5.1-212 and 2.5.1-213) nor any deformation above the basement faults studied in Spoljaric (References 2.5.1-210 and 2.5.1-211).
- A Cretaceous stratigraphic study using over 100 wells in northern DE indicated that Cretaceous and younger units were unfaulted north and west of the PSEG Site for approximately 20 mi. (Reference 2.5.1-18).
- The trenches, seismic lines, and borings conducted just north of New Castle, DE, straddled at least one postulated fault (Reference 2.5.1-128).
- Aerial and field reconnaissance conducted as part of the PSEG Site investigation found no evidence for disrupted topography or Quaternary deformation along any of the lineaments identified in satellite imagery or above any of the faults mapped in basement.

Conclusions in this report regarding the New Castle county faults are consistent with other studies which concluded that Quaternary faulting was not demonstrated (References 2.5.1-248 and 2.5.1-56).

2.5.1.1.4.2.5.6 The Stafford Fault System

The Stafford fault system is a set of en echelon northwest dipping thrust faults near the fall line in northeastern VA (References 2.5.1-133 and 2.5.1-134). These faults include the Stafford, Dumfries, Fall Hill, Hazel Run, Brooke, and Tank Creek faults, as well as an unnamed fault. Two additional northeast-striking southeast-side-down faults, the Ladysmith and the Acadia, are located to the southwest. The individual faults are 10 to 25 mi. long and separated by 1 to 3 mi. wide en echelon, left step-overs. The left-stepping pattern and slickensides found on the Dumfries fault suggest a component of dextral shear on the fault system (Reference 2.5.1-137). The structures are located approximately 130 mi. south of the PSEG Hope Creek site and locally portions of the fault system coincide with the fall line and a northeast-trending portion of the Potomac River (Figures 2.5.1-10 and 2.5.1-16).

Slip on the fault system during the Mesozoic and Tertiary is documented by displacement of Ordovician bedrock over Lower Cretaceous bedrock along the Dumfries fault zone and abrupt thinning of the Paleocene Aquia Formation across multiple strands of the fault system (References 2.5.1-133 and 2.5.1-137). Most evidence indicates that faulting ceased during the Miocene because the Miocene Calvert Formation and overlying units are undeformed

Rev. 4

**PSEG Site
ESP Application
Part 2, Site Safety Analysis Report**

(Reference 2.5.1-134). However, two exposures of small Pliocene offsets exist, indicating minor Pliocene faulting. An offset of 11 to 14 inches (in.) has been measured along the Fall Hill fault of the base of a Rappahannock River terrace deposit correlated with the Pliocene Yorktown Formation (References 2.5.1-134 and 2.5.1-137). In addition, an offset of 18 in. of the base of a Pliocene gravel was mapped about six-tenths of a mi. southeast of the Hazel Run fault (References 2.5.1-134 and 2.5.1-178). In both cases, only the base of the Pliocene unit was offset, and the faulting was not traceable into the overlying portions of the deposit. Recent geomorphic analyses conducted as part of the North Anna ESPA provides additional data regarding the age of deformation (Reference 2.5.1-54). Structural contour maps and topographic profiles of the top and base of Neogene marine deposits and Pliocene and Quaternary fluvial terraces of the Rappahannock River indicate that these surfaces are not deformed within the resolution of the data across the Stafford fault system in northeastern VA (Reference 2.5.1-54). Field and aerial reconnaissance conducted as part of the North Anna study indicates no distinct scarps or anomalous topography on terraces straddling the fault traces. The NRC (Reference 2.5.1-145) agreed with the results of the North Anna ESPA study, and stated: "Based on the evidence cited by the applicant, in particular the applicant's examination of the topography profiles that cross the fault system, the staff concludes that the applicant accurately characterized the Stafford fault system as being inactive during the Quaternary Period." These data indicate that the Stafford fault system is not a capable tectonic source as defined in Appendix A of RG 1.165, *Identification and Characterization of Seismic Sources and Determination of Safe Shutdown Earthquake Ground Motion*.

The Skinkers Neck anticline is a broad, low-amplitude structure that plunges northeast, east of the Stafford fault system in northeastern VA (Figure 2.5.1-16). This fold is defined by structure contour mapping of Cretaceous and Tertiary strata, which indicates that this structure folds and thins rocks as young as Middle Eocene (Reference 2.5.1-137). A hypothesized connection between the anticline and the Brandywine fault system to the northeast has been suggested, but no mapping or documentation supports this suggestion (Reference 2.5.1-135). To the southeast and down dip is the Port Royal fault zone, a 2-mi. wide zone of downwarping or folding in Mesozoic and Tertiary strata (Reference 2.5.1-135). This structure indicates down-to-the-southeast deformation as the Coastal Plain section is thickened southeast of the north-northeast striking structure. Eocene and Miocene strata are deformed, but the deformation is potentially related to flexuring rather than faulting (Reference 2.5.1-137).

2.5.1.1.4.2.5.7 Upper Marlboro Faults

The Upper Marlboro faults are located in MD, approximately 160 mi. southwest of the PSEG Site (Reference 2.5.1-59) as three small faults offsetting coastal plain sediments apparently exposed in a road cut on Crain Highway at 3.3 mi. south of the railroad crossing in Upper Marlboro, MD (Reference 2.5.1-173). Two faults displace Miocene and Eocene sediments, and a third fault is shown offsetting a Pleistocene unit. Dryden (Reference 2.5.1-59) described offsets that could be as small as 1 to 2 ft. and as large as 15 ft., and noted that they could be erosional features rather than faults. These structures are not observed or mapped beyond this exposure. Based on a critical review of available literature, Wheeler (Reference 2.5.1-249) reinterprets the Upper Marlboro faults as likely related to surficial landsliding because of the very low dips and concavity of the fault planes. The Marlboro faults are classified by Crone and Wheeler (Reference 2.5.1-40) and Wheeler (Reference 2.5.1-249), as a Class C feature based on a lack of evidence for Quaternary faulting.

**PSEG Site
ESP Application
Part 2, Site Safety Analysis Report**

2.5.1.1.4.2.5.8 Lebanon Church Fault

The Lebanon Church fault is a poorly known northeast-striking reverse fault located in the Appalachian Mountains of VA, approximately 190 mi. southwest of the PSEG Site (Figure 2.5.1-17). The fault is exposed in a single road cut along U.S. Route 250 as a small reverse fault that offsets Miocene-Pliocene terrace gravels up to about 5 ft. (Reference 2.5.1-173). The terrace gravels overlie Precambrian metamorphic rocks of the Blue Ridge Province. While an early author (Reference 2.5.1-139) originally considered the gravels to be Pleistocene, more recent work (Reference 2.5.1-173) has interpreted the gravel to be Miocene to Pliocene and, hence, interpreted the Lebanon Church fault to be a Tertiary structure. No new literature, seismicity, or mapping indicates otherwise. Wheeler (Reference 2.5.1-249) classifies the Lebanon Church fault as a Class C feature, having insufficient evidence to demonstrate that faulting is Quaternary.

2.5.1.1.4.2.5.9 New York Bight Fault

Seismic surveys offshore of Long Island, NY, discovered an approximately 30 mi. long fault in the Coastal Plain strata (Figure 2.5.1-17 and Reference 2.5.1-91). The fault offsets Cretaceous through Eocene strata, and middle and late Quaternary deposits are not offset within the resolution of available data (Reference 2.5.1-202). Evidence of Quaternary faulting has not been demonstrated for this structure (References 2.5.1-40 and 2.5.1-249) and it likely is Tertiary in age.

2.5.1.1.4.2.5.10 East Border Fault

The East Border fault is the easternmost of the basin-bounding faults along the Hartford Basin in NY, CT, and Massachusetts (Figures 2.5.1-9 and 2.5.1-10). This west-dipping fault clearly offsets Jurassic and Cretaceous strata, but detailed examinations of salt marsh peat deposits straddling the projection of the fault indicated the possibility of offsets in deposits approximately 1200 years old (Reference 2.5.1-229). However, as pointed out by Wheeler (Reference 2.5.1-248), these offsets did not necessarily occur discretely in space or time. No fault surface was identified and no evidence for seismic slip has been produced. The authors also state that major erosion events, such as storms or tsunamis, could have produced a similar record in the peat deposits. Finally, the uncertainty in the age/offset data and its reproducibility are unclear. More data are needed to evaluate the hypothesis put forth by Thompson (Reference 2.5.1-229). Altogether, definitive evidence for Quaternary slip on this structure has not been presented. Thus, the best timing evidence indicates the East Border fault is a Mesozoic structure.

2.5.1.1.4.2.5.11 Ramapo Fault

The Ramapo fault is located in northern New Jersey and southern New York State, approximately 100 mi (160 km) north-northeast of the PSEG Site (Figure 2.5.1-8a). The fault extends for 50 mi (80 km) from Peapack, NJ to the Hudson River (Reference 2.5.1-184). The Ramapo fault is one segment of a system of northeast-striking, southeast-dipping, normal faults that bound the northwest side of the Mesozoic Newark Basin (References 2.5.1-184, 2.5.1-267 and 2.5.1-281). To the south the Ramapo fault splays into several fault strands and merges with the Flemington Fault zone. On the north side of the Hudson River the fault splays into several northeast- to east-trending faults in Rockland and Westchester Counties, New York. Bedrock mapping has indicated that there are primarily northwest-dipping Lower Jurassic and Upper

**PSEG Site
ESP Application
Part 2, Site Safety Analysis Report**

Triassic Newark Supergroup rocks in the hanging wall and tightly folded and faulted Paleozoic basement rocks in the footwall of the Ramapo fault (Reference 2.5.1-267).

Numerous studies of the potential capability of the Ramapo fault have been conducted since the 1970s when a potential strand of the fault was proposed to extend within several miles of the Indian Point nuclear power plant (References 2.5.1-2, 2.5.1-219, 2.5.1-268, 2.5.1-269, 2.5.1-271 and 2.5.1-279). However, none of these studies provide conclusive evidence that the Ramapo and related faults are capable structures.

Identification of the Ramapo fault as a potentially seismogenic fault was initially proposed by seismologists at what is now the Lamont Doherty Earth Observatory in Palisades, NY. Largely based on earthquake locations generated from local network data, these researchers noted a spatial association between earthquakes and the Ramapo fault and cited this association as evidence that the Ramapo fault was a capable structure (References 2.5.1-2, 2.5.1-96 and 2.5.1-273). Page et al. (Reference 2.5.1-273) used the location of four small earthquakes ($E[M] < 2.7$) within approximately 6 mi (10 km) of the Ramapo fault to conclude that the earthquakes were occurring on the Ramapo fault, and, therefore, the Ramapo was experiencing small slip events.

In a later study, Aggarwal and Sykes (Reference 2.5.1-2) located 33 earthquakes occurring between 1962 and 1977 with magnitudes less than or equal to $E[M] 3.0$ within the region surrounding the Ramapo fault. Based on the spatial association between the earthquakes and the Ramapo and related fault systems, Aggarwal and Sykes (Reference 2.5.1-2) concluded that the association “leave[s] little doubt that earthquakes in this area occur along preexisting faults” (page 426) (Reference 2.5.1-2). Focusing on the Ramapo fault, Aggarwal and Sykes (Reference 2.5.1-2) concluded that: (1) over half of the identified events occur along the Ramapo fault, and (2) the Ramapo fault is an active fault with the capability of generating large earthquakes. Aggarwal and Sykes (Reference 2.5.1-2) based this conclusion on: (1) the spatial association of seismicity; (2) focal mechanisms for earthquakes near the Ramapo fault that show high-angle thrust faulting along roughly northeast trending faults, implying a northwest maximum compressive stress direction; and (3) earthquake hypocenters from within 10 km of the Ramapo fault surface trace that align with a dip of approximately 60°.

Despite the strong wording from previous studies that there was little doubt the Ramapo fault is active, numerous studies post-dating those of Aggarwal and Sykes (Reference 2.5.1-2) and Page et al. (Reference 2.5.1-273) presented revised analyses of the seismicity that contradict the earlier work and demonstrate that there is considerable uncertainty as to whether or not slip on the Ramapo and related fault systems is causing the recorded seismicity (References 2.5.1-96, 2.5.1-274, 2.5.1-282 and 2.5.1-284). For example, Seborowski et al (Reference 2.5.1-282) analyzed aftershocks that occurred in 1980 near the northern end of the Ramapo fault near Annsville, NY. They demonstrated that the alignment of these aftershocks and their composite focal mechanism suggest thrusting on a north-northwest trending fault plane. This observation led Seborowski et al (Reference 2.5.1-282) to conclude that their observations are not consistent with the conclusion of Aggarwal and Sykes (Reference 2.5.1-2) that the Ramapo fault is active because the slip direction derived by Seborowski et al (Reference 2.5.1-282), and the corresponding maximum compressive stress direction, is perpendicular to that hypothesized by Aggarwal and Sykes (Reference 2.5.1-2).

**PSEG Site
ESP Application
Part 2, Site Safety Analysis Report**

Quittmeyer et al. (Reference 2.5.1-274) undertook another study with the goal of addressing the discrepancy between the expected slip directions, and thus maximum compressive stress directions, of the Aggarwal and Sykes (Reference 2.5.1-2) and Seborowski et al. (Reference 2.5.1-282) studies. Quittmeyer et al. (Reference 2.5.1-274) analyzed an earthquake sequence from 1983 that occurred approximately 7 miles from the sequence analyzed by Seborowski et al. (Reference 2.5.1-282) and also reanalyzed one of the earthquakes used by Aggarwal and Sykes (Reference 2.5.1-2). Quittmeyer et al. (Reference 2.5.1-274) demonstrated two main points: (1) a composite fault plane solution for the 1983 earthquake sequence indicates thrust faulting along faults striking northwest with a maximum compressive stress direction oriented to the northeast; and (2) the earthquake analyzed by Aggarwal and Sykes (Reference 2.5.1-2) has a non-unique fault plane solution consistent with either the results of Aggarwal and Sykes (Reference 2.5.1-2) or the fault plane solution for the 1983 earthquake sequence. Based on these observations, Quittmeyer et al. (Reference 2.5.1-274) hypothesized that the maximum compressive stress direction is directed roughly northeasterly and implied that the Ramapo fault is not likely a source of earthquakes within the region.

Kafka et al. (Reference 2.5.1-96) presented a revised and extended seismicity catalog for the New York – New Jersey area surrounding the Ramapo fault region extending from 1974 to 1983. Kafka et al. (Reference 2.5.1-96) described this compilation as an improvement over previous efforts because the seismic network during this timeframe was more robust and provides more accurate earthquake locations and uniform magnitude estimates. Kafka et al. (Reference 2.5.1-96) recorded a total of 61 earthquakes from 1974 to 1983, all with magnitudes less than or equal to $E[M] 3.0$, and estimates that the catalog is complete down to at least $E[M] 1.8$. Kafka et al. (Reference 2.5.1-96) noted that of the 27 earthquakes they identified with $E[M] > 1.2$, approximately half of them occurred within 6 mi (10 km) of the Ramapo fault. Kafka et al. (Reference 2.5.1-96) describe the remaining earthquakes as occurring around the outside of the Newark basin. Importantly, Kafka et al. (Reference 2.5.1-96) concluded that while “much emphasis was placed on the significance of the Ramapo fault and its relationship to seismicity” (page 1297), the other seismicity occurring throughout the region suggests that “the geologic structures associated with most (if not all) earthquakes in this region are still unknown” (page 1285). In a later publication in which Kafka and Miller (Reference 2.5.1-268) analyze updated seismicity with respect to geologic structures, Kafka and Miller (Reference 2.5.1-268) further discredit the association between seismicity and the Ramapo fault by saying, “...the currently available evidence is sufficient to rule out ... a concentration of earthquake activity along the Ramapo fault” (page 83).

Thurber and Caruso (Reference 2.5.1-284) also investigated seismicity in the region surrounding the Ramapo fault by using new, one- and three-dimensional crustal velocity models of the upper crust in the region of the northern Ramapo fault to provide better earthquake locations in that area. These velocity models were considered improvements over those used in previous studies (Reference 2.5.1-2), and allowed Thurber and Caruso (Reference 2.5.1-284) to refine the depths for some of the 15 earthquakes they examined. Thurber and Caruso (Reference 2.5.1-284) concluded that: (1) there are significant lateral velocity variations within the region surrounding the Ramapo fault that can impact earthquake locations made using simple velocity models; and (2) “the Ramapo fault proper is not such a salient seismic feature in New York State, unlike the findings of Aggarwal and Sykes” (page 151). As with the Quittmeyer et al. (Reference 2.5.1-274), Seborowski et al. (Reference 2.5.1-282) and Kafka et al. (Reference 2.5.1-96) studies, the conclusions of Thurber and Caruso (Reference 2.5.1-284)

**PSEG Site
ESP Application
Part 2, Site Safety Analysis Report**

indicate that there is considerable uncertainty surrounding the potential activity of the Ramapo fault based on the analysis of seismicity.

Following the earlier seismological studies that suggested the Ramapo fault is a potentially capable fault, geological investigations were conducted to look for evidence of Quaternary slip on the Ramapo fault. The researcher consistently involved in most of these efforts was Nicholas Ratcliffe of the U.S. Geological Survey. Ratcliffe and his colleagues conducted detailed geologic mapping, seismic reflection profiling, petrographic analysis, borings and core analysis along much of the Ramapo fault and its corollary northern and southern extension (References 2.5.1-185, 2.5.1-188, 2.5.1-189 2.5.1-275, 2.5.1-276, 2.5.1-277, and 2.5.1-280). Much of Ratcliffe's work was explicitly focused on investigating the potential relationship between the Ramapo fault and the seismicity that had been noted in the surrounding region (Reference 2.5.1-2). The primary conclusions of the cumulative work of Ratcliffe and his colleagues with respect to the potential for Quaternary slip on the Ramapo fault are:

- The most recent slip episode on the Ramapo fault, as determined from rock core samples taken across the fault, was in a normal sense with some along-strike slip motion (i.e., oblique normal faulting). Ratcliffe and others concluded that the evidence for extensional faulting, and thus lack of compression (i.e., thrust faulting) as would be required in the modern day stress field (References 2.5.1-261 and 2.5.1-286), is evidence that the Ramapo fault has not been reactivated since the latest episode of extension in the Mesozoic.
- In general the Ramapo fault dips less than that inferred from the earthquake epicenters of Aggarwal and Sykes (Reference 2.5.1-2), with the exception of the northernmost end of the fault where the dip measured from borings is approximately 70°.

The implication of this last observation based on Ratcliffe's work is that earthquakes near the Ramapo fault hypothesized as being due to slip on the Ramapo fault are most likely occurring within the Proterozoic footwall rocks of the Ramapo fault.

Taken together, Ratcliffe's and his colleagues results are additional evidence of the uncertainty with respect to the potential activity of the Ramapo fault because they found positive evidence for a lack of slip along the fault since the Mesozoic.

There has been some more recent research on the Ramapo fault. However, this research has not provided any additional certainty with respect to the potential for activity of the Ramapo fault. For example, a fieldtrip guidebook of Kafka et al. (Reference 2.5.1-269) for the New York region briefly discusses proposed geomorphic expressions of the Ramapo fault including valley tilting, concentrations of terraces on only one valley side, and tributary offsets as evidence of Quaternary activity along the Ramapo fault. The use of these observations of Kafka et al. (Reference 2.5.1-269) as evidence supporting Quaternary activity of the Ramapo fault should be treated cautiously because:

- Kafka et al. (Reference 2.5.1-269) present no data or evidence supporting these observations;
- Some of the noted geomorphic features may be older than Quaternary in age; and
- The observations themselves are not necessarily positive evidence of seismogenic, Quaternary faulting.

**PSEG Site
ESP Application
Part 2, Site Safety Analysis Report**

Newman et al. (References 2.5.1-271 and 2.5.1-272) also present observations that they interpret as evidence of Quaternary activity along the Ramapo fault. Newman et al. (References 2.5.1-271 and 2.5.1-272) used radiocarbon dating of peat deposits from a series of tidal marsh sites along the Hudson River where it crosses the Ramapo fault to construct marine transgression curves. Newman et al. (Reference 2.5.1-271) investigated eleven sites, six of which were within the Ramapo fault zone as it crosses the Hudson River. Of the six sites within the Ramapo fault zone, Newman et al. (Reference 2.5.1-271) report that three of the sites show a discontinuity in the transgression curves, and they conclude that these discontinuities reflect Holocene normal faulting within the Ramapo fault zone. These observations and conclusions of Newman et al. (References 2.5.1-271 and 2.5.1-272) are questionable and inconclusive with respect to supporting Quaternary faulting along the Ramapo fault because:

- The radiocarbon and elevation data used to develop the transgression curves have considerable uncertainties that were not clearly taken into account in testing the faulting or no faulting hypotheses;
- The transgression curves suggest normal faulting, a motion contrary to the current state of stress (reverse faulting is expected);
- Trenching studies across the Ramapo fault have not revealed any evidence of Quaternary faulting [Ratcliffe et al., (Reference 2.5.1-279); Stone and Ratcliffe (Reference 2.5.1-283)]; and
- If the inferred offsets within the transgression curves are from fault movement, there is no evidence that the movement was accommodated seismically (e.g., the offsets could have been accumulated through aseismic slip).

Finally, in an abstract for a regional Geological Society of America meeting, Nelson (Reference 2.5.1-270) reported the results of pollen analysis taken from a core adjacent to the Ramapo fault near Ladentown, NY. In the brief abstract Nelson (Reference 2.5.1-270) reports that the pollen history can be interpreted as either a “continuous, complete Holocene pollen profile suggesting an absence of postglacial seismicity along the fault” or as a pollen profile with a reversal, potentially suggesting a disruption of the infilling process caused by faulting. In summarizing his work, Nelson (Reference 2.5.1-270) concludes that, “the pollen evidence is equivocal but certainly not strongly suggestive of seismicity.”

More recently, the seismicity within the region surrounding the Ramapo fault has been reanalyzed by Sykes et al. (Reference 2.5.1-219). Sykes et al. (Reference 2.5.1-219) compiled a seismicity catalog with 383 earthquakes extending from 1677 through 2006 for the greater New York City – Philadelphia area. Sykes et al. (Reference 2.5.1-219) note that one of the striking characteristics of their seismicity catalog is the concentration of seismicity within what they refer to as the Ramapo Seismic Zone (RSZ), a zone of seismicity approximately 7.5 mi (12 km) wide extending from the Ramapo fault to the west and from northern New Jersey north to approximately the Hudson River. Most of the instrumentally located earthquakes within the RSZ have magnitudes less than $E[M] 3.1$. The largest earthquake in this zone is the historical $E[M] 4.73$ earthquake of 30 November 1783 (Reference 2.5.1-219). However, uncertainty in the location of this earthquake is thought to be as much as 100 km (62 mi) (Reference 2.5.1-219) raising significant uncertainty as to whether the event occurred near the Ramapo fault.

From analyzing cross sections of the earthquakes, Sykes et al. (Reference 2.5.1-219) concluded that the earthquakes within the RSZ occur within the highly deformed middle

**PSEG Site
ESP Application
Part 2, Site Safety Analysis Report**

Proterozoic to early Paleozoic rocks to the west of the Mesozoic Newark basin and not on the Ramapo fault proper. Sykes et al. (Reference 2.5.1-219) specifically noted that, with the exception of three earthquakes with magnitudes less than or equal to mb 1.0 that are poorly located, earthquake hypocenters are almost vertically aligned beneath the surface trace of the Ramapo fault and not aligned with the Ramapo fault at depth. Instead of associating the earthquakes with the Ramapo fault, Sykes et al. (Reference 2.5.1-219) attributed the observed seismicity within the RSZ to minor slip events on numerous small faults within the RSZ. However, neither Sykes et al. (Reference 2.5.1-219), nor any other researchers (References 2.5.1-96, 2.5.1-248, 2.5.1-249, 2.5.1-250, and 2.5.1-285), have identified distinct faults on which they believe the earthquakes may be occurring thus preventing the characterization of any potentially active faults. Also, Sykes et al. (Reference 2.5.1-219) only vaguely described the geometry of the RSZ and did not provide robust constraints on the geometry of the zone, the orientation of the potentially active faults they interpret to exist within the zone, or the maximum expected magnitude of earthquakes within the zone.

The work of Wheeler (Reference 2.5.1-249) provides a good summary of the current state of knowledge concerning the capability of the Ramapo fault, despite the fact that it did not consider the results of the Sykes et al. (Reference 2.5.1-219) study. Wheeler (Reference 2.5.1-249) states that: "No available arguments or evidence can preclude the possibility of occasional small earthquakes on the Ramapo fault or other strands of the fault system, or of rarer large earthquakes whose geologic record has not been recognized. Nonetheless, there is no clear evidence of Quaternary tectonic faulting on the fault system aside from the small earthquakes scattered within and outside the Ramapo fault system" (page 178). The CEUS-SSC study (NUREG-2115) does not include a discussion of the Ramapo fault, or consider it a source of repeated large magnitude earthquakes. Subsection 2.5.2 provides a discussion on site specific implications for the PSHA.

2.5.1.1.4.2.5.12 Kingston Fault

In central NJ, the Kingston fault is mapped as a normal fault that offsets Triassic and Jurassic rocks within the Newark basin (Figure 2.5.1-17) and is overlain by the Cretaceous Magothy formation (Reference 2.5.1-158), providing a Mesozoic age for the structure. Stanford (Reference 2.5.1-214) conducted an augering study and found that a gravel of Pliocene age thickened across the fault, while a Late Pleistocene glaciofluvial gravel overlies the fault without offset, indicating that the fault was active in the Pliocene or up to Middle Pleistocene. The reported thickening of the Pliocene gravel could be fluvial in nature and there is no evidence that this occurred via seismic faulting. Hence, Quaternary faulting has not been demonstrated (Reference 2.5.1-40).

2.5.1.1.4.2.5.13 Dobb's Ferry Fault Zone

A 1.2-mi. long northwest-trending zone of concentrated fractures and slickensides was mapped north of New York City in the Manhattan Prong referred to as "Dobbs Ferry fracture zone" (Figure 2.5.1-17; unpublished mapping by Hall, cited in Reference 2.5.1-50). In 1985, the expected moment magnitude 3.7 Ardsley earthquake occurred 1.2 to 1.9 mi. southeast of the fracture zone. Fault plane solutions for the Ardsley earthquake and its aftershocks indicate a small rupture area at a depth of approximately 3.1 mi., with left-lateral kinematics striking west-northwest and dipping steeply (Reference 2.5.1-203). Later fieldwork and mapping extended the fracture zone to the southeast for a total of 5 to 6 mi. The new mapping connected the Ardsley

**PSEG Site
ESP Application
Part 2, Site Safety Analysis Report**

epicenters and two additional fractured outcrops and lineaments identified in aerial photography or topography to the zone previously mapped. The fractured outcrops contain fractures, joints, and slickensides with limited kinematic information, or evidence of offset indicating left-lateral, right-lateral and dip-slip deformation (Reference 2.5.1-50). The authors interpreted the left-lateral deformation as the most recent, correlated it with the Ardsley earthquakes, and suggest that it represents the reactivation of older extensional structures seen at the same outcrops. However, the Ardsley earthquakes are too deep to be responsible for the deformation seen at the surface along the expanded Dobbs Ferry fault zone. No information suggests that there is a history of prehistoric seismicity (e.g., liquefaction, faulting of Quaternary deposits) (Reference 2.5.1-40). The best estimate of the age of this deformation is Paleozoic or younger, based on the age of the oldest rocks it deforms.

2.5.1.1.4.2.5.14 Mosholu Fault

The Mosholu fault is an approximately 7.5-mi. long northwest-striking, subvertical right-lateral oblique fault mapped in New York City (Figure 2.5.1-17 and Reference 2.5.1-13). Throughout the area, drainages flow southwestward in lithologically controlled channels underlain by weaker units such as the Inwood marble. The Bronx River, however, has diverted from this channel approximately 0.4 mi. north of its intersection with the Mosholu fault, flowing south across an upland out of a V-shaped gorge cut into resistant Precambrian and Paleozoic rocks to the southeast for a more northerly trend than the original broader lowland. Merguerian and Sanders (References 2.5.1-129 and 2.5.1-130) interpret the V-shaped gorge without glacial striae to indicate that the diversion of the river occurred in post-glacial time, or since the Pleistocene. A fine clay deposit, interpreted as resulting from a dammed-lake at the diversion point, is found overlying glacial till in the Inwood Valley north of the diversion point, but not south of it. An elongate, buried bedrock ridge is located north of and parallel to the Mosholu fault. This antiformal structure, called the East 204th Street Bulge, is a shallowing in the depth to bedrock of 10 to 20 ft., and approximately 2 mi. long. Merguerian and Sanders infer that the bulge was moved eastward on the Mosholu, dammed the river, and caused the diversion of the river to the south in post-glacial time. The authors caution that the movement of the uplift may not have occurred via seismic faulting and could have been an aseismic process (Reference 2.5.1-130). The faulting is not demonstrably of Quaternary age, and the only clear evidence regarding the timing of faulting is that it is younger than the Paleozoic deformation in the rocks it offsets.

2.5.1.1.4.2.5.15 Offset Glacial Surfaces

Throughout NY, Vermont, New Hampshire, and Canada, offsets have been recognized in surfaces bearing glacial polish or striations, indicating offset is post-glacial in age (Reference 2.5.1-149). The offsets range from 0.04 in. to 39 in., but are typically up to 3.9 in. in extent. These features strike nearly every orientation and no consistent or more frequent orientation commensurate with the present-day stress field is observed. The features are often associated with wedge-shaped voids in the outcrops, (Reference 2.5.1-186). In short, it is most likely that these features formed from ice-wedging or frost-heaving, rather than from a tectonic event (References 2.5.1-186, 2.5.1-40 and 2.5.1-249). In the unlikely event that they are tectonic features, their small extent allows only for small earthquakes and negligible seismic hazard (Reference 2.5.1-40).

**PSEG Site
ESP Application
Part 2, Site Safety Analysis Report**

2.5.1.1.4.2.5.16 Hopewell Fault

The Hopewell fault is located in central VA, approximately 89 mi. southwest of the PSEG Site (Figure 2.5.1-17). The Hopewell fault is a 30 mi.-long, north-striking, steeply east-dipping reverse fault (Reference 2.5.1-136 and 2.5.1-53). The fault was originally named the Dutch Gap fault by Dischinger (Reference 2.5.1-53), and was renamed the Hopewell fault by Mixon (Reference 2.5.1-136). The fault displaces a Paleocene-Cretaceous contact and is inferred to offset the Pliocene Yorktown Formation (Reference 2.5.1-53). Mixon (Reference 2.5.1-136) extends the mapping of Dischinger (Reference 2.5.1-53), and maps the fault as buried beneath Quaternary units.

2.5.1.1.4.2.5.17 East Coast Fault System

The postulated East Coast fault system (ECFS) of Marple and Talwani (Reference 2.5.1-122) trends N34°E, and is located approximately 170 mi. southwest of the site (Figure 2.5.1-17). The 370 mi.-long fault system consists of three approximately 125 mi.-long segments extending from the Charleston area in South Carolina (SC) northeastward to VA. The southern segment is located in SC, and the central segment is located primarily in NC. The northern segment, buried beneath Coastal Plain deposits, extends from northeastern NC to southeastern VA. Identification of the ECFS is based on the alignment of geomorphic features along Coastal Plain rivers, areas suggestive of uplift, and regions of local faulting.

The southern segment of the fault system, first identified by Marple and Talwani (Reference 2.5.1-121) as an approximately 125 mi.-long and 6 to 9-mi. wide zone of river anomalies, has been attributed to the presence of a buried fault zone. The southern end of this segment is associated with the Woodstock fault, a structure defined by fault plane solutions of microearthquakes and thought to be the causative source of the 1886 Charleston earthquake (Reference 2.5.1-122). The southern segment is geomorphically the most well-defined segment of the fault system and is associated with microseismicity at its southern end.

However, there is seismicity spatially associated with the northern and central segments of the fault system. The northern segment is based only upon a variety of anomalous river characteristics, and no coincidence with faulting has been demonstrated (Reference 2.5.1-122). While the southern segment has been considered in seismic source characterization studies, the central and northern segments have not, (Reference 2.5.1-70) and little evidence supports the concept of the central or northern segments existing as structures, let alone Quaternary, seismically active ones (Reference 2.5.1-248). Given the hypothetical nature of the northern segment of the ECFS, it is not a candidate for Quaternary faulting in the PSEG Site region.

2.5.1.1.5 Seismic Zones Defined By Regional Seismicity

Areas of apparently higher rates of seismicity and/or anomalous patterns of seismicity were considered as potential seismic sources both within the PSEG Site region and outside of it. Regionally, the Charleston seismic zone in SC, the New Madrid seismic zone within and around southeastern MO, and the Charlevoix seismic zone in southeastern Quebec are addressed in the CEUS Model (NUREG-2115) and are discussed in Subsection 2.5.2. Of local interest, the Ramapo seismic zone in NY and NJ, and the proposed Peekskill-Stamford seismic boundary of Sykes et al. (Reference 2.5.1-219) in NY and CT are discussed below. Figure 2.5.1-18 depicts the CEUS-SSC seismicity catalog outside of the PSEG Site region, and both the CEUS-SSC

**PSEG Site
ESP Application
Part 2, Site Safety Analysis Report**

earthquakes and earthquakes added as part of the regional update to the seismicity catalog within the PSEG Site update region (Reference 2.5.1-287).

2.5.1.1.5.1 Ramapo Seismic Zone

The Ramapo seismic zone (RSZ), is a region with an apparent increased rate of seismicity west of the Ramapo fault in northern NJ and southern NY (References 2.5.1-2, 2.5.1-184 and 2.5.1-185). Originally, activity within the RSZ was hypothesized to be due to slip on the Ramapo fault (Figure 2.5.1-17), but subsequent studies conclusively demonstrated that the Ramapo fault has not been active since the Jurassic (Reference 2.5.1-189) (Subsection 2.5.1.1.4.2.5.11).

The characteristics of the RSZ have been recently refined with the publication of an updated seismicity catalog by Sykes et al. (Reference 2.5.1-219) for the region surrounding the RSZ. Sykes et al. describe the RSZ as a zone approximately 7.5 mi. wide, extending to depths of 9.3 mi., trending northeast for approximately 80 mi. from northern NJ to southern NY. The RSZ, as defined by Sykes et al., is approximately 100 mi. from the PSEG Site. All of the instrumentally located earthquakes within the RSZ have magnitudes less than E[M] 3.1 (the expected moment magnitude) (Reference 2.5.1-219). The only earthquake with E[M] greater than 3.1 is the historical E[M] 4.73 earthquake of November 30, 1783. However, uncertainty of the location of this earthquake is thought to be as much as 62 mi. (Reference 2.5.1-219), raising significant suspicion as to whether the event occurred within the RSZ.

Earthquakes within the RSZ occur within highly deformed Middle Proterozoic to Early Paleozoic rock to the west of the Mesozoic Newark basin (Reference 2.5.1-219). Sykes et al. attribute the observed earthquakes within the RSZ to minor slip events on numerous small faults within the RSZ. However, neither Sykes et al. (Reference 2.5.1-219), nor any other researchers (References 2.5.1-96, 2.5.1-248, 2.5.1-249, 2.5.1-250, and 2.5.1-40) have identified distinct faults on which they believe the earthquakes may be occurring, thus preventing the characterization of any potentially active faults. Also, Sykes et al. (Reference 2.5.1-219) only vaguely describe the geometry of the RSZ and do not provide robust constraints on the geometry of the zone, the orientation of potentially active faults within the zone, and the maximum expected magnitude of earthquakes within the zone. As such, the only new information on the RSZ is the updated earthquake catalog of Sykes et al. (Reference 2.5.1-219). This new information on the RSZ is incorporated in the seismic hazard analysis for the PSEG Site by using the CEUS-SSC seismic catalog (NUREG-2115), which incorporated the Sykes et al. (Reference 2.5.1-219) information (see Subsection 2.5.2).

2.5.1.1.5.2 Proposed Peekskill-Stamford Seismic Boundary of Sykes et al.

Sykes et al. (Reference 2.5.1-219) present a seismicity catalog for the greater New York-Philadelphia area that is slightly updated from previous studies and a discussion of the tectonic setting of notable earthquakes and seismicity trends. One trend noted by Sykes et al. (Reference 2.5.1-219) is what they describe as an aseismic region that begins along the southern New York and Connecticut border between approximately Peekskill, NY and Stamford, CT and extends to the north-northeast. Sykes et al. (Reference 2.5.1-219) refer to the southeast boundary of this aseismic region as the Peekskill-Stamford seismic boundary.

Sykes et al. (Reference 2.5.1-219) describe the proposed seismic boundary as being along strike and/or spatially associated with a disparate set of features including: a bend in the

**PSEG Site
ESP Application
Part 2, Site Safety Analysis Report**

Hudson river; a short fault segment of unidentified age to the northwest of the boundary; an Ordovician to early Silurian age igneous complex; a reach of the Croton reservoir; and the northwestern end of the Newark basin. The only relationship Sykes et al. (Reference 2.5.1-219) make between their proposed boundary and potentially active faults is presented in their abstract where they state:

“[The Peekskill-Stamford seismic] boundary, which is subparallel to brittle faults farther south, is inferred to be a similar fault or fault zone. Those brittle features may have formed between the Newark, Hartford, and New York bight basins to accommodate Mesozoic extension” (p. 1696 of Reference 2.5.1-219).

However, Sykes et al. (Reference 2.5.1-219) do not present data, discussion, or detailed hypotheses to support this inference. Weighing this weak inference against the considerable amount of research that has been conducted within the region without identifying any geologic structure that may be related to the potential boundary (e.g., see discussion in Subsections 2.5.1.1.2 and 2.5.1.1.6), it was concluded that there is no new data within Reference 2.5.1-219 with respect to the proposed Peekskill-Stamford boundary to suggest that the current seismic source model (NUREG-2115) does not adequately represent the potential seismic hazard at the PSEG Site.

2.5.1.1.6 Site Regional Gravity and Magnetic Fields

The following two subsections describe the major anomalous features of the site regional gravity and magnetic fields. A discussion and interpretation of features present in the gravity and magnetic fields for the basement rocks for the Atlantic Coastal Plain can be found in Daniels and Leo (Reference 2.5.1-47). Some general relationships between lithologies and associated gravity and magnetic signatures are that granitic lithologies are associated with low-amplitude gravity and magnetic anomalies due to their relatively low densities and magnetizations. In contrast, the relatively higher-density and magnetization characteristic of mafic lithologies result in coincident high-amplitude gravity and magnetic anomalous fields. An exception to these generalizations is metagabbro, which may exhibit a relatively weak magnetization and anomalous magnetic signature. However, if subjected to metamorphism and serpentinitization, olivine-bearing lithologies may exhibit an intense induced magnetization due to the hydration of olivine and the production of magnetite.

2.5.1.1.6.1 Site Regional Gravity Field

The anomalous gravity field data for the PSEG Site region (Figures 2.5.1-20a through 2.5.1-20c) is obtained from the National Geophysical Data Center and was originally produced for the Decade of North America Geology (DNAG) Project (Reference 2.5.1-225). The DNAG data were originally presented on a 6-km grid but were subsequently regridded by the National Geophysical Data Center to a 2.5-minute grid spacing. These data represent free-air gravity anomalies over the oceans and Bouguer anomalies over land. The spatial density of the gravity stations from which the data were obtained to produce the grids is highly variable and in cases is insufficient to support the resolution implied on the basis of grid spacing. Therefore, detailed interpretation of the anomalous field in terms of resolution and spatial aliasing requires consideration of the available data density in the specific location under examination. Terrane corrections were computed and applied only in high-relief areas of the continent. Issues related

**PSEG Site
ESP Application
Part 2, Site Safety Analysis Report**

to comparison of free-air and Bouguer anomalies on these types of maps in terms of density variations are discussed in Costain et al. (Reference 2.5.1-39).

First-order features of the site regional gravity field are defined by two curvilinear anomalous gravity highs that transect the site region in a northeasterly-southwesterly orientation. The southeasternmost of these curvilinear gravity high anomalies is closely associated with bathymetry that defines the continental shelf break (shelf edge anomaly; (Figure 2.5.1-20b) so that the central peak of the curvilinear anomaly closely follows the shelf break (References 2.5.1-177, 2.5.1-125, and Figure 2.5.1-20b). Regionally, the shelf edge anomaly exhibits 75 to 150 mGal amplitudes and is 47 to 78 mi. wide, but shows variable amplitudes and shapes (Reference 2.5.1-103). It also exhibits a segmented nature that can be correlated with the locations of oceanic fracture zones (Reference 2.5.1-206). Along the gravity profile in the site region, (Figure 2.5.1-21) the shelf edge anomaly exhibits amplitudes of 40 mGal.

The shelf edge anomaly arises from a variety of related crustal effects that make confident interpretation of the free-air anomalous field complicated. It occurs near a transition from continental to oceanic crust (Reference 2.5.1-97). In addition, a contributing source of this anomaly is the edge effect related to the degree of isostatic compensation resulting from the interaction between sediment loading and rigidity of the lithosphere (References 2.5.1-97 and 2.5.1-258). However, a large contributing factor is the bathymetric relief at the shelf edge (+50 mGal) and change in depth to the mantle (-30 mGal) (Reference 2.5.1-206). Smaller-scale effects of bathymetry can also be discerned, in that the more prominent submarine canyons incised into the shelf break affect the regional shelf edge anomaly signature at small scales (Figure 2.5.1-20b). However, local variations in the anomaly amplitude are also present due to density variations in the underlying shelf edge (Reference 2.5.1-177). The shelf edge anomaly is asymmetric in cross-section with a steep southeastern gradient corresponding to the steep bathymetric gradient associated with the continental slope (Figure 2.5.1-21 and Reference 2.5.1-97). Southeast of this steep gradient, the anomalous gravity field is characterized by a broad low (Figures 2.5.1-20a and 2.5.1-20b) that reaches -50 mGal in the site region along the gravity profile (Figure 2.5.1-21). This low is associated with the deeper water column and low-density sediments of the continental rise floored by oceanic crust.

To the northwest of the shelf-edge anomaly maximum, the gravity field gradient exhibits lower values than that to the southeast and is characterized in cross-section by a longer tail that extends out over the shallower waters of the continental shelf and Baltimore Canyon Trough (Figures 2.5.1-21 and 2.5.1-4). In this region, the gravity field exhibits a broad, relatively low free-air anomalous field that reaches minimal value of -25 mGal on the gravity profile for the site region (Figure 2.5.1-21). However, the field in this region is characterized by higher values than the low field characteristic of the continental rise. The anomalous free-air field over the continental shelf also exhibits many localized linear and circular free-air anomalies (Figure 2.5.1-20a), indicating localized density variations due to variable underlying continental shelf lithologies and structure. Potentially, these localized gravity anomalies arise from density contrasts associated with carbonate reef complexes, diapiric salt, and igneous intrusions such as the Great Stone Dome (Figure 2.5.1-20b), and consolidated synrift sediments and volcanics. Variable topography on top of crystalline basement due to segmentation into fault-bounded blocks is also a contributor. However, these density variations are poorly characterized (References 2.5.1-206, 2.5.1-103, and 2.5.1-232).

Northwest of the shelf edge anomaly, another curvilinear regional anomalous gravity high transects the site region almost diametrically with an east-west inflection to the north of the

**PSEG Site
ESP Application
Part 2, Site Safety Analysis Report**

PSEG Site (Figures 2.5.1-20a and 2.5.1-20b). This feature is a fundamental component of the gravity field of the Appalachian orogen known as the Piedmont Gravity High (Reference 2.5.1-39, Figure 2.5.1-20b, and Figure 2.5.1-20c). The transition from a low regional gravity field in northwestern portions of the site, characterized by values of -70 to -40 mGal on the site regional gravity profile (Figure 2.5.1-21), to the Piedmont gravity high, which exhibits maximal values of 25 mGal on the site regional gravity profile (Figure 2.5.1-21), is marked by a southeasterly increasing field and associated gravity gradient. This transitional gravity gradient is referred to as the Appalachian gravity gradient. Several explanations have been proposed for the Appalachian gravity gradient (Reference 2.5.1-39 for a review). One explanation for the gravity gradient is that it represents a transition from low-density crust to the northwest, to crustal components with higher density to the southeast (Reference 2.5.1-83).

The ubiquitous presence of relatively high-amplitude magnetic anomalies in the terranes to the southeast of the Appalachian gravity gradient (Figures 2.5.1-22a, 2.5.1-22b, and 2.5.1-22c), relative to those to the northwest, indicate the presence of abundant mafic material and higher-density crustal components in these areas. These observations would indicate that the Appalachian gravity gradient results, at least in part, from an associated crustal density gradient. However, Mesozoic rift basins are intimately associated, both spatially and kinematically, with the axis of the Piedmont gravity high (Figure 2.5.1-20c and Reference 2.5.1-116). In the site region, the Culpeper Basin occurs along the axis of the Piedmont gravity high and the Gettysburg and Newark basins are aligned along the trend of the Piedmont gravity high just to the northeast of the anomaly axial maximum (Figure 2.5.1-20c). These spatial associations with crustal-scale extensional structures, and the presence of thinner crust to the southeast of the Appalachian gravity gradient, strongly indicate that this feature has a first-order cause in crustal thinning associated with formation of the Atlantic Ocean basin and elevation of the mantle (References 2.5.1-116 and 2.5.1-39).

The response of the regional gravity field to the presence of Mesozoic rift basins, in particular the Culpeper, Gettysburg, and Newark basins, is discussed in Manspeizer et al (Reference 2.5.1-117) and Daniels and Leo (Reference 2.5.1-47). The syn-rift sediments that fill the basins are typically less dense than the surrounding basement lithologies so, in general, the low-density basin fill should provide a density contrast that would result in a low-gravity-field anomaly shape that is correlated with the basin geometry. However, this general response is complicated in detail by such factors as the density contrast between the basin fill and the surrounding basement and the presence of high-density mafic lithologies within the basin (Reference 2.5.1-117) as well as higher-density basement ridges (Reference 2.5.1-100), in addition to the isostatic control related to elastic thickness of the crust (Reference 2.5.1-14).

Fundamental controls on the gravity signature related to extensional basins also result from the extensional shear mode of their formation. Bell et al. (Reference 2.5.1-14) have shown that crustal thinning by simple shear results in paired gravity anomalous highs in the hanging wall of the basin. These paired anomalies consist of a relatively short wavelength (50 km; 30 mi) "inner gravity high" with an amplitude of about 25 mGal that occurs close to the basin and a broader (100 km; 60 mi) and an outer gravity high with slightly lower amplitude of about 20 mGal. These anomalies are evident in a number of extensional basins in North America after removal of the dominating signature of the regional field, in particular the Newark, Gettysburg and Culpeper basins in the site region. The outer gravity high can be explained by the interaction at the base of the crust with simple shear extensional strain and flexural compensation. However, the inner gravity high is postulated to result from high-density mafic intrusions that are localized along the

**PSEG Site
ESP Application
Part 2, Site Safety Analysis Report**

extensional detachment. Bell et al. (Reference 2.5.1-14) show that the gravity anomalies associated with these phenomena can have significant influence on the gravity low associated with the low-density basin fill.

In the site region, the signature of the Culpeper Basin exhibits very little influence on the regional gravity field (Figure 2.5.1-20c). This is attributed to a low-density contrast between the Culpeper Basin fill and surrounding basement phyllites and to shallow basement depths associated thin syn-rift sediments. A low-amplitude north–northeast-trending linear gravity high is spatially correlative with the basin border fault along the northwestern portions of the Culpeper Basin (Figure 2.5.1-20c). However, this anomaly is attributed to metabasalt that underlies the basin (Reference 2.5.1-117). The Gettysburg and Newark basins are associated with regional gravity lows. However, on a regional scale, (Figure 2.5.1-20c) the correlation of the basin geometry to the regional anomalous gravity field is not well-defined in that the anomalous low field extends well beyond the basin borders. Analysis of the residual gravity after removal of the regional field does show low-gravity anomalies associated with thick low-density basin fill and high anomalous gravity values associated with high-density mafic material (References 2.5.1-117, 2.5.1-218, and 2.5.1-14) and basement ridges (Reference 2.5.1-100). In contrast, the Taylorsville Basin (Figure 2.5.1-20c) exhibits very good spatial correlation with a regional gravity low, and with linear gravity highs along its northwestern and southeastern flanks (Reference 2.5.1-47). This is presumably due to less interference from the regional field produced by the Piedmont gravity high to the west of the basin location. Although most of this basin is buried beneath Coastal Plain strata, the correlation of the basin geometry and the anomalous gravity field has been demonstrated based on boring control and seismic reflection profiles (References 2.5.1-252 and 2.5.1-131).

In summary, the signature of Mesozoic extensional basins on the gravity field in the site region is obscured by the regional field and indistinct in most cases. Constraining the presence, location, or geometry of the Mesozoic basins based on the anomalous gravity signature is made more certain by processing the field to remove the longer-wavelength components of the regional field (References 2.5.1-14 and 2.5.1-117) and by the availability of high-resolution gravity data in and around the basin (References 2.5.1-46 and 2.5.1-42).

Northeast of the Appalachian gravity gradient the anomalous gravity field in the site region is characterized by relatively broad elongate to circular anomalies. The most prominent of these is an elongate elliptical gravity high that has been described as the Scranton gravity high (Reference 2.5.1-52, Reference 2.5.1-111, and Figure 2.5.1-20b). The Scranton gravity high is flanked to the northwest by the Williamsport gravity low (Figure 2.5.1-20b) and to the southeast by the Reading gravity low (Figure 2.5.1-20b). Southwest of, and on trend of, the Scranton gravity high, the Newport gravity high occurs as a smaller circular-shaped anomaly (Figure 2.5.1-20b). Along this same trend to the southwest occurs the Chambersburg gravity low (Figure 2.5.1-20b). The source of most of these anomalies has been interpreted to be variable depths to basement with overlying thickened, lower-density sedimentary sections (Reference 2.5.1-111). However, the Newport gravity high is coincident with a magnetic high anomaly (Bloomfield High, Figure 2.5.1-22b) indicating a mafic component in the crust at this location and an associated density contrast (References 2.5.1-111 and 2.5.1-100).

To the southeast of, and subparallel to, the Piedmont gravity high an arcuate, curvilinear anomalous gravity high is present which crudely mimics the shape of the Salisbury Embayment (Figures 2.5.1-20b and 2.5.1-4). This anomalous feature exhibits a possible left-lateral offset just east of Chesapeake Bay and exhibits higher anomalous gravity field values in the southern

**PSEG Site
ESP Application
Part 2, Site Safety Analysis Report**

segment. The anomaly extends to the northeast and turns eastward in MD to extend into southern portions of the site vicinity south of the PSEG Site. This feature has been referred to as the Sussex-Leonardtown anomaly (Reference 2.5.1-47), and as the Salisbury anomaly by Sheridan et al. (Reference 2.5.1-207).

A more detailed map of the gravity field for portions of the site vicinity is shown in Figure 2.5.1-23 (Reference 2.5.1-74). The east-west to northeasterly oriented trend in the Piedmont gravity high forms a linear anomaly in northern portions of the site vicinity. The axial maximum for the Piedmont gravity high attains positive values of 40 mGal. South of the central axial maximum, the gravity field exhibits a steep negative gradient into an elongate east-west oriented gravity low with two circular minima with field values of less than -12 mGal. The PSEG Site is located approximately on the -8 mGal contour on the western edge of the westernmost minima. The other minimum is located approximately 30 mi. east of the PSEG Site. Portions of the eastern gravity low anomaly have been shown by seismic reflection profiling to be associated with synrift sediments within a Mesozoic extensional basin (Figure 2.5.1-23 and Reference 2.5.1-207).

The elongate gravity anomalous low discussed above is bounded to the east and northeast by a circular gravity high that attains values of +35 mGal and connects at the +22 mGal level with the Piedmont gravity high to the northwest (Figure 2.5.1-23). This gravity high corresponds to the South New Jersey uplift (Reference 2.5.1-95) and basement topography. To the south, the elongate anomalous low is bounded by an east-west oriented linear gravity anomaly that is defined by elongate gravity anomalies that attain positive values of 25 mGal. This linear anomaly is the extension of the Sussex-Leonardtown linear anomaly into the site vicinity. To the south of the Sussex-Leonardtown anomaly, the gravity field again exhibits a steep negative gradient. The southward negative gravity gradient also has a component due to the fact that top of basement becomes progressively deeper in this direction (Reference 2.5.1-16). However, it is uncertain how much of the gravity signature is due to compositional and associated density variations in the basement or to basement topography.

2.5.1.1.6.2 Site Region Magnetic Field

The anomalous magnetic field for the site region (Figures 2.5.1-22a, 2.5.1-22b, and 2.5.1-22c) is obtained from data compiled for the 2002 Magnetic Map of North America by the North American Magnetic Anomaly Group (Reference 2.5.1-138). These data are presented on a 0.62-mile grid. However, the data sets compiled into the Magnetic Map of North America come from both aeromagnetic and surface sources with a wide range of sample intervals. The aeromagnetic data sets, in particular, span a range of flight-line spacings from less than 0.62 mi. to greater than 5 mi., in addition to having variable orientations. This large range in acquisition parameters for the input data sets results in a corresponding range in resolution and degree of spatial aliasing represented on different portions of the Magnetic Map of North America. Therefore, detailed evaluation of the data presented on the Magnetic Map of North America, in terms of both resolution limits and degree of spatial aliasing present in the magnetic anomalies depicted on the map, requires that the sample distribution and flight-line orientations and spacing for the area of interest be evaluated.

The site regional anomalous magnetic field exhibits a band of linear, short-wavelength, relatively high-amplitude, magnetic highs and lows through the approximate center of the site region northwest of the coastal plain (Figures 2.5.1-22a, 2.5.1-22b, and 2.5.1-22c). These high

**PSEG Site
ESP Application
Part 2, Site Safety Analysis Report**

frequency magnetic anomalies impart a well-defined fabric to the magnetic field that in general mimics the Appalachian tectonic fabric for the region (Figures 2.5.1-22a, 2.5.1-22b, and 2.5.1-22c). This fabric can be discerned to extend into the Coastal Plain (Figure 2.5.1-22b), although the higher-frequency components of the anomalies become progressively damped to the southeast as the thickness of the nonmagnetic Coastal Plain cover sediments become thicker. These observations testify to the extension of Piedmont lithologies as basement to Coastal Plain stratigraphic sequences (Reference 2.5.1-47). Similar damping effects are seen in northwestern portions of the site region. The magnetic anomalies to the northwest of the well-defined band of Appalachian magnetic fabric are broader and lower-amplitude exhibiting longer spatial wavelengths. The source of these anomalies arises from magnetic variations in the basement beneath a thick cover of nonmagnetic sediments of the Appalachian Valley and Ridge and Appalachian Plateau in northwestern portions of the PSEG Site region (Reference 2.5.1-100). A distinctive feature in this region is the northeasterly trending New York-Alabama lineament (Figure 2.5.1-22b, Reference 2.5.1-85, Reference 2.5.1-100, and Reference 2.5.1-101).

In the PSEG Site region, the New York-Alabama lineament forms an abrupt linear boundary in the fabric of the magnetic field (Reference 2.5.1-100). To the southeast of the New York-Alabama lineament, the magnetic field is characterized by broad, low-amplitude, low-gradient magnetic anomalies that arise from relatively magnetically homogenous, deeply buried basement. To the northeast of the New York-Alabama lineament, relatively short-wavelength, high-amplitude circular to elongate anomalies indicate basement sources arising from more magnetically variable basement components. The New York-Alabama lineament appears to be a major crustal boundary (Reference 2.5.1-100) that may separate exotic crustal blocks (Reference 2.5.1-85). Southeast of the New York-Alabama lineament, a distinctive, triangular-shaped magnetic anomalous high is present (Figure 2.5.1-22 b). The magnetic expression of this anomaly has been called the New Bloomfield high (Reference 2.5.1-100). This magnetic feature coincides with the Newport gravity high (Figure 2.5.1-20b), indicating a high-density and magnetic mafic source for this anomaly (Reference 2.5.1-100).

The interpretation of the magnetic field for exposed portions of the Appalachian orogen in the site region is discussed in detail by Fisher et al. (Reference 2.5.1-68) and King (Reference 2.5.1-100). General conclusions presented by Fisher et al. (Reference 2.5.1-68) are that the crystalline basement rocks that compose the Grenville component to the allochthonous basement-cover sequences and the antiformal domes are variably magnetic. The basement massifs such as the Reading Prong have a high susceptibility due to significant amounts of magnetite, so that they produce a relatively large-amplitude dipole anomaly. In contrast, the domes, such as the Baltimore gneiss, are not magnetic or contain a reversely magnetized remnant component so that they are associated with a relatively low magnetic field. The Paleozoic sediments surrounding these bodies are also relatively nonmagnetic so that they contribute no significant magnetization to the field. The metamorphosed sedimentary cover sequences to the Grenville basement elements (Glenarm Supergroup) are variably magnetic and contain both magnetic and nonmagnetic components. This same behavior characterizes metamorphosed mafic and ultramafic inclusions within the Wissahickon Formation. A prominent linear feature in the magnetic field is associated with the Martic line (Reference 2.5.1-100), which marks the boundary of Laurentian margin sequences to the west from oceanic-affiliated arcs and oceanic crust to the east. The short-wavelength magnetic anomalies associated with these lithologic and structural elements result in an extremely variable behavior in the magnetic

**PSEG Site
ESP Application
Part 2, Site Safety Analysis Report**

signature exhibited on the regional magnetic profile over this region (Figures 2.5.1-22a, 2.5.1-22b, and 2.5.1-22c).

One of the most prominent magnetic anomalies in the region of the PSEG Site is a northeasterly trending linear magnetic high near the shelf edge that makes a sharp bend to the east near the eastern boundary of the PSEG Site region. This magnetic anomaly extends along the Atlantic margin and comprises the East Coast magnetic anomaly (Figure 2.5.1-22b and References 2.5.1-227, 2.5.1-125, and 2.5.1-103). Regionally, the East Coast magnetic anomaly exhibits amplitudes from 300 to 500 nanotesla (nT), and widths from 47 to 80 mi., being narrowest off Cape May, NJ (Reference 2.5.1-227). The anomaly is segmented at various scales corresponding to basin and platform structures at longer scales (190 – 1300 mi.) and to fracture zone spacings at smaller scales (30 to 60 mi.) (Reference 2.5.1-103). Seaward of the East Coast magnetic anomaly, the magnetic field exhibits low amplitudes and gradients, resulting in a relatively featureless magnetic quiet zone (Reference 2.5.1-125). This magnetic quiet zone persists eastward to the Blake Spur magnetic anomaly, which is outside of the PSEG Site region. In the site region, the East Coast magnetic anomaly occurs under the continental shelf and most concepts for its existence associate it with the transition from continental to oceanic crust and involve some combination of extended continental crust and magnetized intrusions, with primarily remnant components and edge effects (Reference 2.5.1-103).

To the northwest of the East Coast magnetic anomaly, the magnetic fabric is characterized by broad, long-wavelength, amplitude circular to elliptical anomalies over the continental shelf (Figure 2.5.1-22a). These are interpreted to reflect variable depth to magnetic basement associated with block faulting associated with extended crust. This fabric is interrupted by localized circular, high-amplitude magnetic highs that result from Late Cretaceous diapheric intrusions such as the Great Stone Dome (Figure 2.5.1-22b and Reference 2.5.1-76).

The signature produced by Mesozoic extensional basins of eastern North America on the anomalous magnetic field is discussed by Costain et al. (Reference 2.5.1-39) and Bond and Phillips (Reference 2.5.1-26). Generally, the relatively nonmagnetic synrift basin fill sediments tend to produce a subdued magnetic field over the basins characterized by reduced amplitude and gradients. However, several issues serve to complicate this generalized model. The presence of magnetic Mesozoic volcanic intrusives and extrusives in the synrift sequences produce localized magnetic sources that are hard to distinguish from the surrounding basement. Likewise, basement ridges within the basin have the same result (Reference 2.5.1-100). Also, the degree that the anomalous magnetic field is suppressed depends on the magnetic contrast between the basin fill and surrounding basement. If the surrounding basement rocks are not significantly more magnetic than the basin fill, then the magnetic field will be suppressed in the area in and around the basin so that no significant anomalous behavior is produced by the basin. In settings where the basement is strongly magnetic, high-amplitude anomalies may be produced beneath or extend into the basin with little suppression, particularly where the basin fill is thin (Reference 2.5.1-39). This type of behavior has the potential to mask the basin fill signature by spatially extensive, intense induced dipole or remnant anomalies associated with nearby strongly magnetic mafic bodies, particularly bodies that are near the southeastern margins of the basin (Reference 2.5.1-42).

Gravity and magnetic modeling has shown that the major contributor to the magnetic low field associated with a basin resulted from the negative induced dipole component from a strongly magnetized mafic body southeast of the basin, and that the effect of the basin field was

**PSEG Site
ESP Application
Part 2, Site Safety Analysis Report**

secondary (Reference 2.5.1-42). The association of mafic material with the borders of extensional basins may be a generic effect (Reference 2.5.1-14) and a relatively common occurrence associated with extensional basins in eastern North America. This leads to the possibility that this relationship may be used as a diagnostic signature in the gravity and magnetic fields to infer the existence and extent of extensional basins in the subsurface.

Effects in the regional magnetic field due to the issues discussed above can be observed in association with the exposed Mesozoic extensional basins in the site region (Figure 2.5.1-22c). The Gettysburg and Newark basins contain many short wavelength elongate to linear magnetic anomalous highs that are sourced by highly magnetic diabase intrusions or basement highs (References 2.5.1-166, 2.5.1-26, and 2.5.1-100). Also, the relatively thinly developed basin fill along the southern margin of the Newark Basin ineffectively dampens the magnetic signature of the underlying basement so that linear magnetic trends continue uninterrupted across the basin boundary (Reference 2.5.1-100).

The factors listed above result in considerable uncertainty in discerning the presence or geometry of Mesozoic extensional basins based on analysis of the anomalous magnetic field alone. However, in spite of the associated uncertainties, a primary geophysical signature used to infer the existence and extent of Mesozoic extensional basins beneath the Coastal Plain cover is the presence of broad regions of magnetic low-amplitude and subdued gradients that result from damping of the anomalous field due to the increased thickness of nonmagnetic synrift sediments present in the basins (References 2.5.1-90, 2.5.1-119, 2.5.1-48, 2.5.1-102, 2.5.1-252, and 2.5.1-85).

A variably resolved, curvilinear magnetic-high linear anomaly occurs in a coincident location with the Sussex-Leonardtown gravity anomaly. The magnetic expression of this anomaly follows the general shape of the Salisbury Embayment and exhibits very high anomalous amplitudes and gradients along the axis of the southern segment southeast of Chesapeake Bay. Northeast of Chesapeake Bay, the anomaly exhibits more subdued amplitudes and gradients across MD and DE until it passes through southern portions of the site vicinity. As the anomaly crosses the Delaware Estuary, it again exhibits increased amplitudes and gradients. Southern segments of the anomaly were originally referred to as the Sussex-Currioman trend by Hansen (Reference 2.5.1-79).

The northwestern portions of the site vicinity cover exposures of crystalline rocks in northern DE, northeastern MD, and southeastern PA. The magnetic anomaly map presented in Figure 2.5.1-24a is composed from the original flight-line data. The flight-line directions and spacings, along with a color scale for each data region, are presented in Figure 2.5.1-24b so that resolution and aliasing for each area may be evaluated. A northeasterly trending anomalous low magnetic field characterizes northwestern portions of this area. This region is underlain by relatively nonmagnetic Baltimore gneiss lithologies and forms the Mill Creek anticline (Reference 2.5.1-68). To the southeast, between the Mill Creek anticline and the Coastal Plain, the magnetic field is composed of several elongate to circular magnetic highs that coalesce to form northeasterly trending linear magnetic highs. This area is underlain by the magnetic lithologies of Wissahickon schist along with interlayered mafic and ultramafic lithologies (Reference 2.5.1-68). These anomalous highs can be seen to extend beneath the Coastal Plain sediments several miles, although with damped amplitudes and gradients. The Sussex-Leonardtown anomaly is also present in southern portions of the site vicinity.

**PSEG Site
ESP Application
Part 2, Site Safety Analysis Report**

2.5.1.1.6.3 Discussion and Synthesis of Regional Gravity and Magnetic Fields

Various elements that compose first-order anomalous features of the gravity and magnetic fields for the PSEG Site region mark the transitional boundaries that separate crustal zones characterized by various degrees of extensional strain and related thickness changes in continental crust (Reference 2.5.1-103 and Figure 2.5.1-25). These crustal zones relate to Mesozoic extensional tectonics which resulted in the formation of the Atlantic Ocean. The site region encompasses the entire transitional range from relatively unextended continental crust, in northeastern portions of the site region, to oceanic crust that floors the continental rise in southeastern portions of the site region.

Westernmost portions of the site region are underlain by continental crust that essentially preserved the crustal state of the Pangean craton before it was rifted to form the North American continent. Continental crust is greater than 19 mi. thick and records little to no Mesozoic extensional strain. However, the structural and lithologic state of continental crust is complex due to the protracted pre-Mesozoic polyorogenic history (Reference 2.5.1-103).

West-central portions of the site region are underlain by rifted continental crust (Figure 2.5.1-25). The western boundary between continental crust and rifted continental crust coincides with the westernmost crustal-penetrating Mesozoic extensional detachments. The location of this boundary is also marked by the Appalachian gravity gradient. Rifted continental crust extends eastward to the basement hinge zone, which occurs offshore in the site region, and subparallel to the Atlantic margin. The rifted condition of this crustal zone is also evident in the fact that, except for a few cases, this is the locus of the on-land extent of Mesozoic diabase dikes (References 2.5.1-182 and 2.5.1-127).

The hinge zone marks the location where the surface of continental basement exhibits a steep gradient in depth from 1.2 to 2.5 mi. to over 5 mi. (Reference 2.5.1-103). Rifted continental crust records slight to moderate extension, but still retains recognizable features of continental crust (Reference 2.5.1-103). Rift-related features include the exposed and sub-Coastal Plain Mesozoic rift basins. Additional features include half-grabens with easterly dipping border faults and tilted blocks with landward-dipping faults containing thick synrift sequences that occur landward of the hinge line (Reference 2.5.1-103). These features are the likely source of the anomalous magnetic lows that parallel the hinge line just to the west of its location.

East of the basement hinge zone and extending to approximately the landward edge of the East Coast magnetic anomaly, the marginal basins and Baltimore Canyon Trough are underlain by rift-stage transitional crust (Reference 2.5.1-103). Rift stage crust is significantly thinner than rifted continental crust and composite in nature, consisting of highly extended continental crust that has been intruded by significant quantities of rifting-related igneous material. The composite nature of rift-stage crust makes it transitional from continental to oceanic crust (Reference 2.5.1-103).

Many models for the source of the East Coast magnetic anomaly have been presented (Reference 2.5.1-206), and the source of this anomaly is not well-constrained (Reference 2.5.1-103). However, most of the models for the source of the East Coast magnetic anomaly involve combinations of continental crust with major amounts of mafic material that has a significant remnant magnetization (Reference 2.5.1-222). Talwani and Abreu (Reference 2.5.1-222) were able to show by improved migration focusing of seismic reflection profiles that the strongly

**PSEG Site
ESP Application
Part 2, Site Safety Analysis Report**

reflecting continental crust ends abruptly at a steeply, landward dipping interface. The East Coast magnetic anomaly overlies intrusive material that they interpret as initial oceanic crust and upper mantle generated when the Atlantic Ocean first opened. Since typical, nominally thick oceanic crust lies to the east of the East Coast magnetic anomaly, the anomaly is associated with a marginal crustal zone that marks the transition from rift-stage crust to oceanic crust (Reference 2.5.1-103). A transition also occurs in the nature of the magnetization to the east as the predominately remnant magnetization of oceanic mafic material gives way to the predominately induced magnetization characteristic of continental crustal material (Reference 2.5.1-222).

In summary, the crustal extension and thinning that resulted in rifting of the North American margin and formation of Atlantic oceanic crust imparted a discrete zonal structure to the crust along the Atlantic margin. Each of these zones is characterized by crust modified by variable degrees of extensional strain and igneous activity. The transitions between the zones are marked by anomalous geophysical features, and the zones exhibit characteristic magnetic and gravity geophysical field fabrics. In addition to the zonal nature imparted to the crust described above, variations in the rifting process along the length of the Atlantic margin also appear to have resulted in variations of the elastic thickness and isostatic response of the crust as determined from analysis of the gravity field (Reference 2.5.1-258). These variations in elastic thickness correlate spatially with arches and depressions along the Atlantic margin (Reference 2.5.1-30) and are probable first-order explanations for their existence (Reference 2.5.1-258). The PSEG Site vicinity and location occur on rifted continental crust west of the continental hinge line. East of the hinge line, the crustal state becomes highly extended with the addition of significant amounts of igneous components.

Secondary crustal transitions are also present in the site region. The Sussex-Leonardtown geophysical anomaly is associated with both a magnetic-high and a gravitational-high anomalous field (Reference 2.5.1-47), indicating a source consisting of dense, highly magnetic mafic material. Borings into the anomaly produced foliated mafic volcanic rocks, ultramafic rocks, gabbro, metadiorite, and phyllite (Reference 2.5.1-47). Two offsets in this anomaly are possibly related to fault-related displacement (Reference 2.5.1-47). These results have been interpreted by various researchers as oceanic crust associated with an Alleghanian suture, as a mélange, and a Taconic suture (Reference 2.5.1-182). Northeastern extensions of the Sussex-Leonardtown anomaly can be traced into southern portions of the site vicinity and probably mark a significant crustal transition related to a terrane boundary at this location (Reference 2.5.1-182).

The possible existence and extent of Mesozoic rift basins present beneath the Coastal Plain sedimentary cover in the PSEG Site region have been proposed by several researchers (References 2.5.1-254, 2.5.1-16, and 2.5.1-85). In many of these studies, a Mesozoic basin has been postulated to extend through the site vicinity south of the PSEG Site (References 2.5.1-254, 2.5.1-16 and Figure 2.5.1-26). In addition, smaller basins occur to the east of the PSEG Site. Most of these projections and interpretations of the existence and extent of the basins are based on analysis of broad low features in the anomalous magnetic field and have relatively large associated uncertainties, as discussed in the subsection above. With the exception of the Buena Basin that occurs 30 mi. east of the PSEG Site, the existence of these basins has not been proven and their presence and extent have large uncertainties.

**PSEG Site
ESP Application
Part 2, Site Safety Analysis Report**

2.5.1.2 Site Geology

2.5.1.2.1 Physiography and Geomorphology

2.5.1.2.1.1 Site Area

The PSEG Site is located on the eastern bank of the Delaware River Estuary (Figure 2.5.1-27). The site occurs almost completely within the Outer Coastal Plain physiographic subprovince (Reference 2.5.1-11). The Middle Coastal Plain Terrace subprovince occurs outside the site boundary to the east. The Middle Coastal Plain Terrace (Figure 2.5.1-6) along with Upland Sands and Gravels subprovinces fall within the extreme western portions of the PSEG Site area. West-central and south-central portions of the site are occupied by the Delaware River channel.

The physiographic expression in the Outer Coastal Plain shows significant differences on either side of the Delaware River (Figure 2.5.1-27). Eastern portions of the PSEG Site, east of the Delaware River, are characterized almost completely by extremely flat, low-lying topography only a few feet above sea level, underlain by Holocene Delaware Bay estuarine deposits. The exceptions being the artificially elevated island on which the PSEG Site is located, and the limited areas of remnants of deeply-incised and eroded Quaternary terraces underlain by the Cape May Formation (Figure 2.5.1-28) that occur along and near the northeastern and eastern boundaries of the site (Figure 2.5.1-27). In contrast, western portions of the site area in Delaware, west of the Delaware River, are characterized by incised Quaternary terrace uplands underlain mainly by the Scotts Corners Formation (Figure 2.5.1-28). The lowlands consist of Holocene estuarine deposits again only a few feet above sea level.

The lowland surfaces that are underlain by Holocene estuarine deposits consist mainly of tidal marsh and are drained by many low-gradient, tidally influenced streams. Major drainages in the site area on the NJ side of the Delaware River include Hope Creek east and south of the PSEG Site, and Alloway Creek north and northeast of the site. In DE, major drainages in the area of the PSEG Site include Blackbird Creek and Appoquinimink River to the southwest, and Augustine Creek to the west.

2.5.1.2.1.2 New Plant Location

The center of the new plant location occurs on an artificial island on the eastern bank of the Delaware River. Western portions of the site (area within 0.6 mi.) fall within the Delaware River. Eastern portions are underlain by artificial fill and, in northeastern portions, marsh deposits overlying artificial fill (Figures 2.5.1-29 and 2.5.1-30). Historical aerial photography (Figure 2.5.1-31) reveals that the PSEG Site center occurs on what was originally a bar in the Delaware River channel formed from dredge spoil. Figure 2.5.1-32 shows general topography of the site area based on LIDAR data (Reference 2.5.1-140). Current elevations within the site area range from sea level to 16 ft NAVD. A recent topographic survey of the site (Reference 2.5.1-118) shows elevations within the site range from 5 to 15 ft. NAVD with developed areas of the site nominally 10 to 12 ft. NAVD.

**PSEG Site
ESP Application
Part 2, Site Safety Analysis Report**

2.5.1.2.2 Site Stratigraphy and Lithology

2.5.1.2.2.1 Site Area

The PSEG Site falls entirely within the Salisbury Embayment and is underlain by Coastal Plain sediments that range in age from Early Cretaceous to Holocene. These sediments are covered by sequences to a basement complex composed of rifted continental crust (Figure 2.5.1-33). The stratigraphic column for the PSEG Site (Figure 2.5.1-33) is discussed below.

2.5.1.2.2.1.1 Basement Complex

There are considerable uncertainties in the nature of the basement terranes and lithologies that occur beneath the pre-Cretaceous unconformity that forms the base of the Coastal Plain, particularly as the distance east of the fall line becomes greater and extrapolation from known control increases (References 2.5.1-182 and 2.5.1-85). Based on the extrapolations presented by Hatcher et al. (Reference 2.5.1-85, Figures 2.5.1-8a and 2.5.1-8b), Carolina superterrane occurs beneath the pre-Cretaceous unconformity in the site area. However, Hatcher et al. (Reference 2.5.1-85) express uncertainty in the location of the boundary with the Philadelphia terrane to the northwest, indicating that this boundary between the Carolina superterrane and the Philadelphia terrane is not well-constrained in their analysis. Therefore, the rocks beneath the pre-Cretaceous unconformity in the site area could be Carolina superterrane lithologies or Philadelphia terrane lithologies. If the boundary passes through the site area, both terranes could be present, with Philadelphia terrane lithologies to the north and Carolina superterrane to the south. The nearest well-documented control is from the Delmarva Power Summit site located outside and northeast of the PSEG Site boundary. Basement samples at this location are reported to be pyroxenite. However, since no detailed petrographic information was provided, this sample is not diagnostic and could be Carolina superterrane or Philadelphia terrane. The possibility exists that the basement complex in the site area may be composed entirely or in part by lithologies of either the Carolina superterrane or the Philadelphia terrane, therefore the general lithologic characteristics of both terranes are discussed below.

In addition to the Carolina superterrane and Philadelphia terrane lithologies that may be present in the subsurface of the site area, subsurface Triassic rift basins have also been interpreted to occur in and around the site vicinity (References 2.5.1-15, 2.5.1-254, and 2.5.1-207). In most cases, the presence and extent of these basins are based on aeromagnetic anomalies, the exception being the Buena Basin in which portions of the basin were imaged by seismic reflection profiling (Reference 2.5.1-207). Due to the uncertainty associated with the inference on the existence and extent of rift basins based on magnetic data, there is considerable uncertainty in the existence and locations of these basins. However, Mesozoic synrift sediments may exist in the subsurface in the site area. Their possible presence is indicated on Figure 2.5.1-33.

2.5.1.2.2.1.1.1 Carolina Superterrane

The general lithologic sequences that characterize the Carolina superterrane are dominated by metaigneous lithologies and associated metasediments that developed in association with Neoproterozoic to Cambrian subduction-related volcanic arcs and some continental basement (References 2.5.1-86 and 2.5.1-85). The volcanic arc components range from mafic to felsic in composition and contain both a plutonic infrastructure and suprastructural volcanoclastic

**PSEG Site
ESP Application
Part 2, Site Safety Analysis Report**

elements along with unconformable sedimentary cover (References 2.5.1-86, 2.5.1-88, and 2.5.1-85).

The nearest exposure of Carolina superterrane lithotectonic sequences occur along strike southwest of the site region (Figure 2.5.1-8a). The components of the Carolina superterrane that occur nearest the PSEG Site include the Charlotte terrane, the Carolina terrane (particularly the Virgilina sequence), and the Roanoke Rapids terrane. The Charlotte terrane is an infrastructural component of the Carolina superterrane (or Carolinia) (Reference 2.5.1-86) and is composed of intermediate composition metaplutonic lithologies along with metamorphosed mafic and ultramafic components (Reference 2.5.1-86). The metaplutonic protoliths range in age from Neoproterozoic to late Paleozoic.

The Carolina terrane is a suprastructural component of the Carolina superterrane (Reference 2.5.1-86) that consists of low-grade metaigneous and associated metasedimentary rocks. The Virgilina sequence of the Carolina terrane records a stratigraphic succession consisting of a felsic to intermediate volcanic base, an intermediate unit of metaturbidites, and an upper unit of metabasalt (Reference 2.5.1-86). These units were deposited in an interval from 633 to 612 Ma and subsequently intruded by granites at about 546 Ma (Reference 2.5.1-86).

The Roanoke Rapids terrane consists of igneous and sedimentary protoliths metamorphosed from greenschist to epidote amphibolite facies. This terrane is composed of three main units, although their stratigraphic relationships are uncertain (Reference 2.5.1-86). One of the component units consists of low-grade metamafic to metaultramafic rocks with protoliths that range in composition from peridotite to diorite and basalt. These rocks have been interpreted to be ophiolite components and to represent oceanic crust that was substrate to a volcanic arc (Reference 2.5.1-86). Another component of the Roanoke Rapids terrane is a volcanic-plutonic complex composed of a trondhjemite to quartz diorite plutonic core surrounded by felsic metavolcanic and metavolcaniclastic rocks. The remaining component is composed of metavolcanics and foliated volcaniclastic unit of felsic composition.

2.5.1.2.2.1.1.2 Philadelphia Terrane

The Philadelphia terrane (Figure 2.5.1-8a and 2.5.1-8b) consists mostly of the Wissahickon Formation along with granodiorite and granitic intrusions of the Wilmington Complex. The characteristics of the Wissahickon Formation are described in Plank et al. (Reference 2.5.1-168). The primary lithologies comprising the Wissahickon Formation are aluminous to quartz-rich gneisses interlayered with amphibolites. The transition between the gneiss compositional variations is gradational and the contacts with the amphibolites are sharp. Most of the amphibolite layers are less than 30 ft. thick. Geochemically they exhibit either mid-ocean ridge basalt (MORB) or intraplate basalt affinities. The gneisses contain granitic pegmatites and are metamorphosed to upper amphibolite facies. This felsic gneiss-amphibolite complex contains lenses of serpentinite, monomineralic amphibolite and hornblende-plagioclase amphibolite whose protoliths were peridotite, pyroxinite, and gabbro respectively (Reference 2.5.1-168).

The Wilmington Complex represents an early Paleozoic magmatic arc (Reference 2.5.1-168) consisting of metavolcanic and metaplutonic units. The metavolcanic units are represented by amphibolites and gneiss. The plutonic protoliths range from felsic to mafic in composition and are now represented by felsic to intermediate composition gneisses, metagabbros, and undeformed plutonic suites of granites, gabbro, tonalite, and gabbro-norites (Reference 2.5.1-

**PSEG Site
ESP Application
Part 2, Site Safety Analysis Report**

168). The members of the Wilmington Complex were intruded and crystallized in the Ordovician between 475 to 485 Ma, except for an assemblage of granites to gabbros that intruded the complex at 434 Ma (Reference 2.5.1-4).

2.5.1.2.2.1.2 Coastal Plain Stratigraphic Sequences

2.5.1.2.2.1.2.1 Lower Cretaceous Strata

The Lower Cretaceous section in the vicinity of the PSEG Site consists entirely of the Potomac Group (considered a formation by the Delaware Geological Survey).

Potomac Group (Formation)

The Potomac Group strata (Figure 2.5.1-33) occur only in the subsurface at the PSEG Site. The unit consists of white, grey, and red interbedded variegated silts, clays, and quartzose sands (References 2.5.1-17 and 2.5.1-217). In the site vicinity, Potomac Group lithologies have been reported as clays, silty clays, and clayey silts with some sand bodies (Reference 2.5.1-217). These lithologies show complex lateral variations, so subdivision of the unit based on laterally continuous properties is tenuous (Reference 2.5.1-17). From north to south, across the PSEG Site, the Potomac Formation ranges in thickness from 800 ft. to 1650 ft. (Reference 2.5.1-18). This large thickness change is due mainly to a steep gradient in the surface of the basement that deepens to the southeast (Reference 2.5.1-18).

2.5.1.2.2.1.2.2 Upper Cretaceous Strata

Magothy Formation

The Magothy (Figure 2.5.1-33) unconformably overlies the Potomac Group and marks the transition to marine conditions. This unit represents beach and estuarine environments and consists of crossbedded sands interbedded with clay, silt, and some lignite (References 2.5.1-152, 2.5.1-217, and 2.5.1-20). These general characteristics are representative of those expected from a beach and estuarine setting. Benson (Reference 2.5.1-18) shows the Magothy to be approximately 50 ft. thick in southern portions of the PSEG Site and to pinch out near the northern boundary.

Merchantville Formation

The Merchantville formation (Figure 2.5.1-33) represents a transgression and is a facies of the underlying Magothy (Reference 2.5.1-152). The contact is shown as conformable in Olsson et al. (Reference 2.5.1-152). However, Owens et al. (Reference 2.5.1-155) report that the contact is sharp and disconformable. The Merchantville Formation ranges from a glauconitic sand to micaceous silty clay (References 2.5.1-152 and 2.5.1-20). Benson (Reference 2.5.1-18) shows the Merchantville strata to exhibit a relatively consistent thickness of approximately 120 ft. at the PSEG Site.

Woodbury Formation

The Woodbury Formation (Figure 2.5.1-33) formed during a regressive pulse and has gradational contact relationships with both the underlying Merchantville Formation and the

**PSEG Site
ESP Application
Part 2, Site Safety Analysis Report**

overlying Englishtown Formation. The Woodbury Formation is a micaceous, chloritic, silty clay (Reference 2.5.1-152). Owens et al. (Reference 2.5.1-155) report it as a massive clayey silt with abundant carbonaceous material. Benson (Reference 2.5.1-18) does not distinguish the Woodbury Formation as a separate unit on his cross-sections through the site area.

Englishtown Formation

The Englishtown Formation (Figure 2.5.1-33) marks the end of the regressive pulse succession. In southern NJ, it is a micaceous silt to very fine sand (References 2.5.1-152 and 2.5.1-155). Benson (Reference 2.5.1-18) shows that the Englishtown Formation is about 25 ft. thick across the site, but shows small variations in thickness.

Marshalltown Formation

The Marshalltown Formation (Figure 2.5.1-33) represents a transgressive event. It is an extensively burrowed, very silty fine sand with significant amounts of glauconite (References 2.5.1-152 and 2.5.1-155). Small pebbles occur at the base and in the middle of the formation, and it is moderately to poorly sorted (Reference 2.5.1-155). Owens et al. (Reference 2.5.1-155) report that the contact with the underlying Englishtown Formation is sharp. The Marshalltown is a relatively thin unit and is approximately 20 ft. thick beneath most of the site, but thins to about half this thickness in northern portions of the site (Reference 2.5.1-18).

Wenonah Formation

The Wenonah Formation (Figure 2.5.1-33) consists of a clayey, silty, slightly glauconitic fine quartz sand deposited in a regressive phase (Reference 2.5.1-152). It is poorly to moderately sorted (Reference 2.5.1-155). It has gradational contacts with the underlying Marshalltown Formation (Reference 2.5.1-155) and the Overlying Mount Laurel Sand (Reference 2.5.1-152). Benson (Reference 2.5.1-18) does not break the Wenonah Formation out as a separate unit and combines it with the overlying Mount Laurel Formation. However, it is included in the stratigraphic column for Salem County, NJ, by Olsson et al. (Reference 2.5.1-152), where it is reported to be indistinguishable from the Mount Laurel Formation.

Mount Laurel Formation

The Mount Laurel Formation (Figure 2.5.1-33) consists of several lithofacies, including thinly bedded clays and sands that may be crossbedded, massive sand beds, and thin pebbly sands (Reference 2.5.1-152). Olsson et al. (Reference 2.5.1-152) indicate that the Mount Laurel ranges in thickness in southern NJ and DE from 20 to 85 ft. The contact with the underlying Wenonah Formation is characteristically gradational but may be sharp in localized areas (Reference 2.5.1-155). Benson (Reference 2.5.1-18) shows the Wenonah-Mount Laurel interval to be approximately 100 ft. thick across the site, but to thin slightly to the north where it subcrops beneath Quaternary cover north of the site.

Navesink Formation

The Navesink Formation (Figure 2.5.1-33) consists of fossiliferous clayey glauconitic sands (References 2.5.1-152 and 2.5.1-155) that accumulated on midshelf conditions resulting from a transgressive phase (Reference 2.5.1-152). Prominent fossil content includes oysters,

**PSEG Site
ESP Application
Part 2, Site Safety Analysis Report**

brachiopods, and belemnites. In the site area, Benson (Reference 2.5.1-18) shows the Navesink Formation to be consistently approximately 20 ft. thick and to subcrop beneath Quaternary deposits near the northern site area boundary.

2.5.1.2.2.1.2.3 Lower Tertiary Strata (Paleocene)

Hornerstown Formation

The Hornerstown (Figure 2.5.1-33) is considered to be the base of the Lower Tertiary section in NJ and DE. However, the basal beds of the unit have been shown to be Cretaceous in age while the upper strata are Paleocene (Reference 2.5.1-152). The Hornerstown Formation is a well-sorted almost purely glauconitic sand that imparts a distinctive green color to the unit (Reference 2.5.1-152). Benson (Reference 2.5.1-18) shows the Hornerstown Formation to attain thicknesses of approximately 30 ft. in the area of the PSEG Site and to be of relatively uniform thickness. The Hornerstown Formation subcrops beneath Quaternary deposits in northern portions of the site area and outcrops along the northwestern limits of the site (Figure 2.5.1-28).

Vincentown Formation

The Vincentown (Figure 2.5.1-33) consists of two lithofacies consisting of massive quartz sand and a quartz-rich calcareous facies containing bryozoans and foraminifera (Reference 2.5.1-152). Benson (Reference 2.5.1-18) shows the Vincentown Formation to be consistently approximately 90 ft. thick beneath the site. The formation subcrops in the site area beneath Quaternary sediments north of the PSEG Site and crops out in valleys in northwestern portions of the site (Figure 2.5.1-28).

Manasquan Formation

The Manasquan Formation (Figure 2.5.1-33) lies unconformably above the Vincentown formation. The Manasquan Formation consists of a lower glauconite-rich member and an upper member composed of clayey sand to silt (Reference 2.5.1-152). Benson (Reference 2.5.1-18) shows the Manasquan to be of relatively constant thickness of 40 ft. beneath the PSEG Site and to subcrop just north of the PSEG No.6 production well (Figure 2.5.1-30 for well location). Sugarman and Monteverde (Reference 2.5.1-215) interpreted this same interval from the PSEG No. 6 production well to be composed of surficial deposits. Geotechnical studies at the PSEG Site have not identified Manasquan sediments in the subsurface.

Shark River Formation

The Shark River Formation (Figure 2.5.1-33) lies unconformably above the Manasquan Formation. Shark River Formation is a glauconitic sand and mudstone (Reference 2.5.1-152). Benson shows the Shark River strata to be a consistent thickness of approximately 70 ft. beneath the southern portions of the PSEG Site and to subcrop beneath thin Quaternary deposits to the south of the site.

**PSEG Site
ESP Application
Part 2, Site Safety Analysis Report**

2.5.1.2.2.1.2.4 Upper Tertiary Strata (Neogene)

Kirkwood Formation

The Kirkwood Formation (Figure 2.5.1-33) is divided into three members on the basis of variable amounts of clay, silt, and sand that were deposited in two or three marine cycles (Reference 2.5.1-152). Benson shows the Kirkwood Formation (his Calvert Formation) to be approximately 90 ft. thick in southern portions of the PSEG Site and to pinch out northward to subcrop beneath Quaternary cover.

2.5.1.2.2.1.2.5 Quaternary Strata

Quaternary strata exposed in the area of the PSEG Site consist mostly of several formal and informal formations and consist primarily of estuarine terrace or marsh deposits with isolated exposures of fluvial units. In DE, estuarine terrace deposits form the Delaware Bay Group (Reference 2.5.1-75). In NJ, in the site area, similar, possibly correlative, terrace deposits constitute the Cape May Formation (Reference 2.5.1-144).

Delaware Bay Group

The deposits of the Delaware Bay Group (Figure 2.5.1-33) comprise two formations that have the appearances of terraces, in that they form inset wedge-shaped deposits that thicken toward Delaware Bay and are separated by a scarp. These units are the Lynch Heights Formation and the Scotts Corners Formation. They are Pleistocene in age and comprised of estuarine, tidal marsh, and a few freshwater marsh sediments (References 2.5.1-180 and 2.5.1-75). Both units show variability in composition both stratigraphically and laterally (Reference 2.5.1-75).

Lynch Heights Formation

The oldest formation of the Delaware Bay Group is the Lynch Heights (Figures 2.5.1-28 and 2.5.1-33), which is middle Middle Pleistocene in age (Reference 2.5.1-75). The Lynch Heights Formation is stratified and consists of a basal bed of medium to coarse quartz sand, a middle bed of clayey silt, and an upper bed of medium to fine sand that fines upward (References 2.5.1-180 and 2.5.1-75). The surface of the Lynch Heights Formation is at an elevation of 20 to 30 ft. but may attain elevations of approximately 40 ft. (Reference 2.5.1-75).

Scotts Corners Formation

The Scotts Corners Formation (Figure 2.5.1-33) is Late Pleistocene in age (Reference 2.5.1-75) and rests unconformably on the Lynch Heights Formation. The Scotts Corners ranges in composition from light gray to brown, fine to coarse, sands and gravel. This clastic sequence contains laterally discontinuous beds of organic-rich clayey silt (References 2.5.1-180 and 2.5.1-75). The clastic component is primarily quartz with some feldspar and muscovite. Segregations of heavy minerals are also present (Reference 2.5.1-180). The organic silts and clayey silts are typically associated with channel-fill features (Reference 2.5.1-180). The base of the Scotts Corners Formation usually is delineated by a coarse sand to pebble gravel that overlies oxidized sand of Lynch Heights Formation. However, in some places, the contact is marked by pebbles and heavy minerals in a clean sand. The oxidized zone in Lynch Heights Formation beneath the

**PSEG Site
ESP Application
Part 2, Site Safety Analysis Report**

contact is not always present (Reference 2.5.1-180). The Scotts Corners Formation surface occurs at elevations of 15 ft. or less (Reference 2.5.1-175).

Cape May Formation

The Cape May Formation (Figure 2.5.1-33) includes sequences from at least three transgressive-regressive cycles (Reference 2.5.1-144). Cape May Formation exposed in the site area is mapped as either undivided Cape May Formation (Qcm) or as Unit 1 of the Cape May Formation (Qcm₁) (Figure 2.5.1-28). Newell et al. (Reference 2.5.1-144) report the age range for the Cape May Formation to be from about 184 ka to no younger than 28 ka, with the Qcm₁ unit being the youngest. These formations form estuarine terraces in the eastern portions of the site area (Figure 2.5.1-28).

Each transgressive-regressive cycle has a similar stratigraphic sequence that consists of a basal coarse clastic phase that fines upwards and transitions from marine to terrestrial conditions. Estuarine Cape May deposits include quartz-rich sands with concentrations of heavy minerals, in addition to variably colored pebble gravels. Fine-grained components include clayey silt and peat in upper portions of the unit (Reference 2.5.1-144).

Undifferentiated Cape May units also contain locally developed fluvial deposits of uncertain association referred to as Van Scriber Lake, and Spring Lake deposits (Reference 2.5.1-144).

Quaternary Marsh Deposits

Most of the low-lying regions in the site area that are a few feet above sea level are underlain by marsh deposits (Figure 2.5.1-28). These deposits are related to aggradation of the Delaware River Estuary and consist primarily of muck and peat, silt, clay, and sand. Silt and sand deposits are mainly related to deposition along tidal creek margins (References 2.5.1-156 and 2.5.1-144). Aggradation of the Delaware River Estuary and deposition of the marsh deposits began in the Pleistocene and continued into the Holocene (Reference 2.5.1-156).

2.5.1.2.2.2 Site Stratigraphy

The site (new plant location) stratigraphy is summarized in Figure 2.5.1-34 and discussed below.

2.5.1.2.2.2.1 Basement Complex

Control of the nature of basement lithologies that underlie the PSEG Site is provided by PSEG No. 6 production well located approximately 0.6 mi. from the site center (Figures 2.5.1-30 and 2.5.1-35). The log for this well reports residual clay, which is interpreted to be Wissahickon schist from a sidewall core at depth 1800 ft. Based on this information, lithostratigraphic sequences of the Philadelphia terrane underlie the site beneath the pre-Cretaceous unconformity.

**PSEG Site
ESP Application
Part 2, Site Safety Analysis Report**

2.5.1.2.2.2.2 Coastal Plain Stratigraphic Sequences

Information on the lithological properties and stratigraphic relationships for strata that comprise the Coastal Plain section in and around the site is provided from several borings on and near the site (Reference 2.5.1-114).

2.5.1.2.2.2.2.1 Lower Cretaceous Strata

Potomac Group (Formation)

Potomac Group (Formation) strata were sampled in one deep boring within the PSEG Site (NB-1, Reference 2.5.1-114), and in another deep boring (PSEG Well No. 6) located near the new plant location. The lithologies in these samples consisted of hard plastic, red, gray, and white mottled clay. These characteristics are consistent with those reported for the Potomac Group (Formation) regionally (References 2.5.1-152 and 2.5.1-17). Boring NB-1 within the PSEG Site encountered Potomac Group (Formation) at elevation 454 ft. Based on the information provided by Benson (Reference 2.5.1-18) from the PSEG No. 6 production well, the Potomac Group (Formation) strata are approximately 1300 ft. thick beneath the site.

2.5.1.2.2.2.2.2 Upper Cretaceous Strata

Magothy Formation

The Magothy Formation unconformably overlies the Potomac Group (Formation). The Magothy Formation consists primarily of interbedded gray to dark gray, locally mottled, silts and clays containing trace amounts of lignite and carbonaceous material. The silts and clays were interbedded with sands that contain variable amounts of silt and clay. The Magothy Formation is 52 ft. thick beneath the site location. Benson (Reference 2.5.1-16) shows the Magothy Formation to be approximately 60 ft. thick near the PSEG Site, in the PSEG No. 6 production well, consistent with the information provided by the deep boring.

Merchantville Formation

The Merchantville Formation is composed primarily of dark greenish-black glauconitic silts and clays with variable amounts of sand and mica. These characteristics are representative of those described regionally for this formation (Reference 2.5.1-152). Based on the deep boring NB-1, the Merchantville Formation is 30 ft. thick beneath the site. This thickness is generally consistent with those reported for this formation by Owens et al. (Reference 2.5.1-155), who gives a range of 40 to 60 ft. for this unit as sampled about 10 mi. to the north.

Woodbury Formation

The Woodbury Formation consists of black, micaceous and highly plastic clay. This formation is distinguished from the overlying Englishtown by increased clay and mica content. Based on boring NB-1, the Woodbury Formation is 36 ft. thick at the site. Benson (Reference 2.5.1-18) does not delineate the Woodbury Formation. However, Owens et al. (Reference 2.5.1-155) indicate that the Woodbury is gradational into the underlying Merchantville indicating that Benson (Reference 2.5.1-18) did not break the Woodbury Formation out separately from the Merchantville Formation on his cross-sections. Benson gives the combined interval for these

**PSEG Site
ESP Application
Part 2, Site Safety Analysis Report**

two formations as approximately 90 ft., which is greater than the 66 ft. measured beneath the site.

Englishtown Formation

The Englishtown Formation consists of dark grey to black sandy clay, to clayey sand with shell fragments, grading to black silt and clay with trace amounts of glauconite and mica. These characteristics are representative for those reported regionally (Reference 2.5.1-152). The Englishtown is 44 ft. thick beneath the site. Benson shows the Englishtown Formation to be approximately 15 ft. thick near the PSEG Site. It should be noted that the combined thickness of 110 ft. for the Merchantville, Woodbury and Englishtown Formations at the site is comparable to this same interval reported by Benson (Reference 2.5.1-17) at 105 ft.

Marshalltown Formation

The Marshalltown Formation consists of glauconitic, silty, and clayey fine sand. The presence of significant amounts of glauconite and fine-grained nature of the clastic component are characteristic of this unit regionally (Reference 2.5.1-152). Based on borings NB-1 and NB-2, the Marshalltown Formation is 25 ft. thick beneath the site. Near the site location, the Marshalltown is reported to be approximately 20 ft. thick (Reference 2.5.1-18).

Wenonah Formation

The Wenonah Formation exhibits a gradational contact with the underlying Marshalltown Formation. The Wenonah Formation consists of sandy clay and clayey sand. Average thickness in borings from the site and nearby areas is 15 ft. Benson (Reference 2.5.1-18) does not break the Wenonah Formation out as a separated unit on this section through PSEG Number 6 production well near the site location.

Mount Laurel Formation

The Mount Laurel Formation consists of a dense to very dense brownish-gray to dark green, fine to coarse-grained sand with variable amounts of silt and clay. This unit appears to exhibit a coarsening upward sequence in that glauconite content, in addition to grain size and fine content decrease with depth. Based on borings NB-1, NB-2 and NB-8, at the site, the Mount Laurel Formation ranges from 102 to 105 ft. thick. When combined with the Wenonah interval thickness, this is consistent with the thickness for the Mount Laurel Formation shown by Benson (Reference 2.5.1-18) near the PSEG Site.

Navesink Formation

The Navesink Formation consists of fossiliferous, dark green to greenish-black, extremely glauconitic sand. Fossils consisted primarily of pelecypod fragments. Based on all eight of the borings in the site location, the Navesink Formation is ranges from 23 to 26 ft. thick. These characteristics in composition and thickness are consistent with regional descriptions (Reference 2.5.1-152). Reference 2.5.1-18 reports a thickness for the Navesink Formation of approximately 15 ft. near the site.

**PSEG Site
ESP Application
Part 2, Site Safety Analysis Report**

2.5.1.2.2.2.3 Lower Tertiary Strata (Paleocene)

Hornerstown Formation

The Hornerstown Formation primarily consists of greenish-gray, to dark green, to greenish-black glauconitic sand with some indurated intervals. Borings at the site location give thickness of 16 to 21 feet. This is consistent with a thickness of approximately 15 ft. reported by Benson (Reference 2.5.1-18) near the PSEG Site.

Vincentown Formation

The Vincentown Formation is a greenish-grey, fine-grained to medium-grained silty sand with some zones of clayey sand. Glauconite is commonly present. This unit contains cemented zones from 0.1 to 3.0 ft. thick. The Vincentown thickness is highly variable at the PSEG Site, with thickness of ranging from 35 to 79 ft. thick. This variability is due in part to the fact that the top of the Vincentown Formation is a scour surface.

2.5.1.2.2.2.4 Upper Tertiary Strata (Neogene)

Kirkwood Formation

The Kirkwood consists of two distinct stratigraphic units. The upper unit consists of greenish-gray, silty fine sand, fine sand, and greenish-gray to brown, organic clay with zones of peat and occasional shell fragments. The lower member consists of fine to coarse sand and subrounded to subangular gravel with variable silt and clay content. Total thickness of the Kirkwood is highly variable at ranging from 12 to 29 ft. thick.

2.5.1.2.2.2.5 Quaternary Strata

Alluvium

A bed of alluvial material deposited on the bed of the adjacent Delaware River represents the uppermost geologic strata at the site. Units above this were emplaced as fill material. Alluvial deposits consist of fine to coarse sand and gravels interbedded with layers of peat and other organic rich soils. A lower bed of slightly organic to non-organic micaceous silts and clay is present locally. The alluvial material was highly variable in thickness at ranging from 5 to 23 ft. thick.

Hydraulic Fill

Hydraulic fill consists of soft, discontinuous lenses of clayey silts, silty sands, and organic clays. This fill material resulted from dredging operations in the nearby Delaware River. These dredging operations have intermittently placed materials in the site location from the early 1900's and continue currently in the northern most area.

Artificial Fill

Artificial fill is present at the PSEG Site with variable thicknesses up to 10 feet. The material comprising the fill consisted of clays, silts, and sands with variable silt and clay contents. Clayey

**PSEG Site
ESP Application
Part 2, Site Safety Analysis Report**

and silty gravels were also present. The structural fill was used for backfilling around various structures and for other general site grading during the construction of the Hope Creek and Salem Generating Stations.

2.5.1.2.3 Geologic History

2.5.1.2.3.1 Formation of Pangean Crust

The nature of the crystalline lithologies that form the basement complex beneath the PSEG Site are uncertain in that the site vicinity and site area fall near the projected boundary between the Philadelphia terrane and the Carolina superterrane (Reference 2.5.1-85). These two terranes were formed in two realms of the Iapetus and Rheic oceans (References 2.5.1-87, 2.5.1-88, and 2.5.1-85) so that their early histories were different until they were juxtaposed either in the Late Ordovician-Silurian (Reference 2.5.1-88) or the Early Mississippian (Reference 2.5.1-85).

The Carolina superterrane is composed of arc-related metaigneous rocks that were deposited, intruded, and metamorphosed in the Neoproterozoic to Early Cambrian (References 2.5.1-87, 2.5.1-88 and 2.5.1-85). These metaigneous units were subsequently overlain in the Cambrian to Ordovician by clastic sedimentary cover (References 2.5.1-87, 2.5.1-89, and 2.5.1-85). In contrast, the Philadelphia terrane consists of a metamorphosed sedimentary sequence that was intruded in the 475 to 485 Ma interval by a diverse suite of igneous rocks and again at approximately 434 Ma by a felsic to mafic suite.

In summary, the Carolina superterrane consists of a metaigneous basal sequence with overlying clastic sediments that formed mostly in the Neoproterozoic. The Philadelphia terrane consists of sedimentary basal units that were intruded in the Ordovician and Silurian (Reference 2.5.1-4). Subsequent to their formation, these two terranes were juxtaposed either in the Late Ordovician-Silurian (References 2.5.1-87 and 2.5.1-88) or the Early Mississippian (Reference 2.5.1-85) to form the Pangean crust and the crystalline component of the basement complex.

The Pangean crust was subjected to extensional strain and rifting in the Early to Middle Triassic that resulted in the formation of localized basins and deposition of synrift sequences. Based on geophysical analysis, these basins have been projected to occur in the site vicinity (Reference 2.5.1-15). The site vicinity is located west of the hinge line on slightly to moderately extended crust. Therefore, it probably occupied an elevated position relative to the developing Atlantic Ocean basin that was forming to the east. This resulted in a period of erosion and formation of a pre-Cretaceous unconformity above which Coastal Plain sedimentary successions were deposited.

Therefore, the basement complex may contain crystalline components that may record Neoproterozoic to Cambrian igneous activity followed by deposition of sedimentary sequences that could be as late as Ordovician. Crystalline components may also be present and record Neoproterozoic deposition followed by Ordovician intrusion and metamorphism. The two components form the Pangean crust subsequently rifted to form extensional basins and synrift depositional sequences. Over the site vicinity, the rifting was followed by a long period of erosion to form a regional unconformity.

**PSEG Site
ESP Application
Part 2, Site Safety Analysis Report**

2.5.1.2.3.2 Deposition of North American Sedimentary Sequences

Following development of Atlantic Ocean crust in the Jurassic, thermal relaxation of the crust resulted in subsidence and aggradation on the pre-Cretaceous unconformity surface. In the PSEG Site vicinity, the aggradational sequence is represented by the Early Cretaceous Potomac Group (Formation). Following aggradation over the pre-Cretaceous erosional surface, the establishment of widespread continental shelf marine conditions resulted in deposition of the Upper Cretaceous section, first the Magothy Formation, which is characterized by beach and estuarine environments, and then several glauconite-rich transgressive-regressive cycles. The Upper Cretaceous section is indicative of low clastic input and bioturbation.

The end of the Cretaceous was marked by a massive bolide event near Chicxulub, Mexico (Reference 2.5.1-266). Boreholes in New Jersey conducted approximately 40 miles northeast and 59 miles east of the PSEG Site as part of the Ocean Drilling Program recovered a continuous depositional record across the Cretaceous/Tertiary boundary. A thin (<10 cm.) layer in this sequence contains materials that appear to be from a tsunami. The tsunami may have been caused by submarine slumping on the Atlantic slope associated with the Chicxulub bolide impact (Reference 2.5.1-265).

Widespread marine conditions persisted into the Eocene, at which time continental ice sheets in Antarctica by the earliest Oligocene marked the beginning of the onset of cyclic continental glaciation. Oscillation of the earth's water-ice budget resulted in associated glacio-eustatic sea level changes. In the PSEG Site vicinity, glacio-eustasy resulted in several transgressive-regressive cycles that are recorded in the Oligocene and early Miocene stratigraphic sequence stratigraphy (Reference 2.5.1-165). However, no Oligocene sediments are present in the site area or site location having been cut out by the sub-Miocene unconformity at the base of the Kirkwood Formation. The Middle Miocene also marked the beginning of increased clastic input that continues to the Quaternary (Reference 2.5.1-169). This has probably resulted in drainage divide migration (Reference 2.5.1-29) and has components of climate change and increased weathering (Reference 2.5.1-28).

During the Pliocene, the onset of continental glaciation in the northern hemisphere began with a major glacial event at 2.4 Ma and settled into an orbital cyclic pattern with a 41-ka period with relatively low amplitude events (Reference 2.5.1-105). This condition persisted until the Middle to Late Pleistocene with the onset of large amplitude glacial-interglacial cycles (Reference 2.5.1-28). In the vicinity of the PSEG Site these events have resulted in the deposition of fluvial sequences and the formation of estuarine terraces that were formed during the transition to interglacial periods and the resulting rise in sea level. Transition into glacial periods and the resulting fall in sea level and base level resulted in incision of the terraces and fluvial sequences that were deposited in the preceding transgressive event and the development of unconformities.

However, the relatively nearby location of the Laurentide ice sheet to the site vicinity makes correlation of relative sea levels to landforms complicated, due to near-field effects on relative sea level. These effects include, in addition to relative sea level changes associated with glacio-eustasy, the effects of glacio-isostasy and hydro-isostasy (Reference 2.5.1-41). Deconvolution of the contributions of these effects from the relative sea level signal depends on the horizontal distance to the ice load on the crust and poorly known parameters, such as mantle rheology and elastic strength of the crust (Reference 2.5.1-246).

**PSEG Site
ESP Application
Part 2, Site Safety Analysis Report**

A sea level high stand at 188,000 years ago recorded in Marine Isotope Stages 6 to 7 transition (Reference 2.5.1-41) may correlate with deposition of the Lynch Heights Formation (Reference 2.5.1-75) and mark the middle Middle Pleistocene interglacial maximum. Subsequent interglacial transgressions in the Late Pleistocene resulted in the formation of the Scotts Corners and Cape May Formations which comprise incised terraces in the eastern and western portions of the site area.

Beginning in the Late Pleistocene and through the Holocene to the present, the Delaware Bay has experienced deposition of estuarine material in tidal marsh settings (Reference 2.5.1-156). This consists mainly of silts and clays with considerable organic content resulting from tidal marsh grasses and other vegetation. Locally, some sand is present as deposits at the mouths and bars in tidal creeks where transport energies are sufficient.

2.5.1.2.4 Structural Geology

The structural geology of the PSEG Site described in this section is based primarily on a review of published geologic mapping (References 2.5.1-199, 2.5.1-167, 2.5.1-157, and 2.5.1-144), detailed boring and geophysical log correlations of southern NJ, northern DE, and eastern MD (References 2.5.1-18 and 2.5.1-215), results of earlier investigations performed at the PSEG Site and the nearby Summit site (References 2.5.1-176 and 2.5.1-56), as well as PSEG Site reconnaissance and subsurface exploration performed for this permit application.

The Delmarva Summit Site (Summit site) is located about 9 miles to the north and west of the PSEG Site. The Summit site was explored in the early 1970's by Delmarva Power as a possible location for a new nuclear power plant. The Preliminary Safety Analysis Report (PSAR) provided useful information respective to the stratigraphy, structure and velocity profile of Coastal Plain sediments. Geotechnical borings indicate that the top of the Merchantville Formation is a planar, southeast-dipping horizon undisturbed by obvious faulting in the Summit site vicinity. These data and supporting studies located in the Delaware Geological Survey archives were used to evaluate conditions in the PSEG Site vicinity including discussions in Subsections 2.5.1.1.4.2.5.5 and 2.5.1.2.2.1.1.

2.5.1.2.4.1 Site Vicinity

No Mesozoic rift basins have been identified beneath the PSEG ESP site, though such basins are known and inferred to be buried nearby beneath the Coastal Plain strata of Virginia, Maryland, Delaware and New Jersey. In particular, Benson (Reference 2.5.1-15) hypothesized that a northern extension of a covered basin crosses the Delaware River into NJ and comes within 15 miles of the PSEG Site (Figure 2.5.1-35). Furthermore, the site lies on the edge of a gravity low (Figure 2.5.1-20a). In an effort to explore the possibility of the presence of Mesozoic basins extending beneath the site, data relevant to the basement beneath the site was investigated. This investigation aimed to determine the elevation and attitude of the basement surface and the age and lithology of the basement rocks, and to evaluate the likelihood that Triassic rift sediments exist at depth in the area.

In the original FSAR for the Hope Creek site, a well log indicated that 'residual clay above basement' was penetrated at a depth of 1800 ft. (Reference 2.5.1-174). The residual clay was interpreted as saprolite in Wissahickon schist, but lithologic descriptions for this and any overlying units were vague. Wells located within 10 miles of the site encountered crystalline

**PSEG Site
ESP Application
Part 2, Site Safety Analysis Report**

basement at depths varying from 1364 ft to 2295 ft, consistent with the expected southeast-dipping basement surface. Well logs and data from a seismic refraction survey to the east (Reference 2.5.1-63) indicate that the basement surface dips to the southeast at approximately 100 ft./mi. Calculated projections from these data indicate that basement should be encountered at a depth of approximately 1750 ft. below sea level at the PSEG Site, within a likely 10% error of the value obtained from the site well of 1800 ft (Figure 2.5.1-35). A review of well logs, cores, and cuttings of basement rocks in southern NJ and eastern DE indicates that saprolite is common at the basement surface in the region (Reference 2.5.1-244). Approximately 6 other wells within 10 miles of the PSEG ESP site did not encounter potential Triassic rift sediments, and instead record a thick section of Cretaceous sedimentary rocks above metamorphosed, crystalline rocks of probable Paleozoic or Precambrian age (Reference 2.5.1-244). Palynology from a deep well updip at Ft. Mott, NJ, confirms Cretaceous ages for units at a depth of 820 ft. (Reference 2.5.1-217), and a well located downdip in Cumberland County, NJ, has fossils indicating Cretaceous strata at a depth of 2300 ft. before encountering basement at 3616 ft. (Reference 2.5.1-30).

At least two other wells located in the regional gravity low drilled through no Triassic rift-related rocks to encounter crystalline basement (Reference 2.5.1-244). In addition, a seismic refraction line crosses the gravity low east of the PSEG Site (Reference 2.5.1-63). Retrieved depth-to-basement values are consistent with those expected from boring data (Figure 2.5.1-35). Seismic velocities from the refraction transect indicate that the basement velocities are approximately 18,000 feet per second, consistent with crystalline rocks, rather than Triassic rift sediments (Reference 2.5.1-63). An intermediate layer encountered above basement (interpreted as the Cretaceous-Tertiary boundary) has seismic velocities of 4,500 to 8000 feet per second, too low to be correlated with Triassic rift sediments (Reference 2.5.1-42). Certainly, data coverage is not ideal, particularly east of the PSEG Site and west of the seismic refraction line. However, the available data, from the site itself and from wells located 8 to 30 mi. distant from the site, refute the presence of a basin within the site area.

Faults mapped within the site vicinity fall into two categories: Piedmont faults exposed in northernmost DE, and basement faults beneath the Coastal Plain strata. The Piedmont faults in northernmost DE, approximately 15 mi. north of the PSEG Site, cut only Paleozoic units and have a maximum age of latest Paleozoic (Subsection 2.5.1.1.4.2.2). The availability of a variety of subsurface data (borings, geophysical logs, vibroseis data, seismic data) has allowed for the identification of many small offsets in the basement surface at depth beneath the Coastal Plain sediments in DE (see discussion of basement faults of Spoljaric (References 2.5.1-210 and 2.5.1-211) in Subsection 2.5.1.1.4.2.5.5). Borings are the most frequent type of data used, but only provide elevation of a layer at one location, therefore the apparent offsets could actually be the result of smooth variations in the elevation of the basement surface, rather than discrete faults. Nevertheless, the faults identified with such data generally cut metamorphic basement (with presumed Paleozoic age) and, in some cases, Cretaceous sedimentary units. The Tertiary and younger strata within the vicinity of the PSEG Site are undeformed (References 2.5.1-56 and 2.5.1-176).

2.5.1.2.4.2 Site Area and Site

The 5-mi. radius of the PSEG Site contains no tectonic faults, folds, or structures (Figure 2.5.1-28). The structure within the PSEG Site is best characterized by planar Cretaceous and Tertiary strata that dip gently to the southeast (Figure 2.5.1-36). Most recent geologic mapping indicates

**PSEG Site
ESP Application
Part 2, Site Safety Analysis Report**

that no faults have been mapped within 5 mi. of the site (Reference 2.5.1-157). Figure 2.5.1-37 shows the locations of two cross-sections constructed from the ESPA and nearby Hope Creek and Salem borings. These cross-sections (Figures 2.5.1-38 and 2.5.1-39) indicate that Tertiary and older units are flat, planar and undisrupted (Figures 2.5.1-37, 2.5.1-38, and 2.5.1-39). The one exception to this is the top of the Vincentown formation/base of the Kirkwood, which has an erosional, channelized character with many feet of relief (approximately 35 ft.) across the new plant location area (Figure 2.5.1-40). The Hope Creek Final Safety Analysis Report (FSAR) indicates that approximately 25 ft. of relief is present across the smaller area investigated with borings for the Salem and Hope Creek plants, shown as two linear ridges in the top of the Vincentown oriented roughly north-south (References 2.5.1-175 and 2.5.1-176). It is important to recognize that contacts between units both above and below the Vincentown are planar and undeformed, ruling out faulting as a potential source for the variability seen in the elevation of the Vincentown/Kirkwood contact (Figures 2.5.1-39 and 2.5.1-40).

2.5.1.2.5 Site Engineering Geology Evaluation

The engineering geology evaluation considered both natural and manmade conditions within the site vicinity, area, and location that may pose a hazard and include evidence for past conditions. Detailed investigations for the new plant location during subsequent combined license application (COLA) activities requires an update respective to conditions for the actual foundation locations. It is noted that subsurface conditions determined from the ESPA investigation are consistent with conditions noted in the existing Hope Creek FSAR and referenced engineering reports.

2.5.1.2.5.1 Dynamic Behavior During Prior Earthquakes

Subsection 2.5.2.7 discusses the location and proximity of prior earthquakes to the PSEG Site. No earthquakes larger than $E[M] 3.77$ have been recorded within the site vicinity as discussed in Subsection 2.5.2.1.3. Paleoliquefaction studies in the region (Reference 2.5.1-6) have not noted any evidence for liquefaction features. Much of the area surrounding the site location provides little exposure for evaluating the presence of liquefaction features and consists primarily of fine-grained silts and silty sands. Review of aerial photography, both historic and recent, as well as inspection from low altitude over-flight, does not indicate the presence of sand blows or fissures from lateral spread. However, these may be considered ephemeral features due to the low topography and relative sea level. Excavation mapping within the existing Hope Creek unit did not note the presence of earthquake-induced features. The physical properties of the soils within the new plant location are discussed in Subsection 2.5.4.7 respective to dynamic response.

2.5.1.2.5.2 Zones of Mineralization, Alteration, Weathering, Structural Weakness

Subsection 2.5.4.2 discusses the engineering properties of the soils within the new plant location. The soils within the upper section (approximately 80 ft.) include hydraulic fill, alluvium from the adjacent Delaware River, and Tertiary silty clays and sands of the Kirkwood Formation. All soils in this upper portion of the section shall be removed to an elevation within the underlying Vincentown Formation which provides the foundation bearing layer for backfill beneath all Category 1 structures, as described in Subsection 2.5.4.5.

**PSEG Site
ESP Application
Part 2, Site Safety Analysis Report**

The conditions of the Vincentown Formation are consistent with the conditions noted in the existing Hope Creek unit FSAR. It is noted from the ESPA investigation that there are areas in the uppermost portion of the Vincentown that are described as oxidized silty sands and locally have low N-values. The foundation-bearing layer (competent unit) considers the presence and removal of softer soils and will be confirmed during more detailed COLA investigations for the Category 1 structures and construction excavation mapping. The Vincentown Formation also contains varying amounts of calcium carbonate with varying amounts and secondary cementation. There is no evidence of karst conditions noted from the extensive boring investigation and excavation mapping of the existing Hope Creek unit, nor from review of aerial photography of the new plant location. The nearest noted karst terrain is approximately 20 mi. northwest of the site in the piedmont of DE and is associated with dissolution of the marble within the Cockeysville Formation, which subcrops and outcrops in northern DE (Reference 2.5.1-220). Karst conditions are not considered a hazard within the site area or location.

2.5.1.2.5.3 Unrelieved Residual Stresses in Bedrock

The PSEG Site is within the upper Coastal Plain physiographic province and consists of approximately 1750 ft. of normally consolidated to overconsolidated sediments overlying crystalline basement rock. Isostatic adjustment in the region due to glacial rebound is characterized by subsidence as measured from recent global positioning system studies in North America (Reference 2.5.1-205). Studies of paleoshorelines on the continental shelf offshore of NJ also indicate relatively stable isostatic conditions in the site vicinity. These effects are discussed in Subsection 2.5.3.1.7. The state of stress in the bedrock is discussed in Subsection 2.5.1.1.4.5. There is no evidence for unrelieved stress within the bedrock or overlying sediments that pose a hazard to the site location.

2.5.1.2.5.4 Groundwater Conditions

The PSEG Site is adjacent to the Delaware River as described in Subsection 2.5.4.1 and consists mainly of an artificial island constructed from the placement of hydraulic fill from dredging of the channel. The groundwater level is generally a few feet below the surface and is discussed in Subsection 2.4.12. Groundwater conditions for construction excavation are discussed in Subsection 2.5.4.6. The area is surrounded by numerous natural estuaries and tidal marshes as well as manmade channels and drainage cuts. These features do not pose a hazard to the site location.

2.5.1.2.5.5 Effects of Human Activity

As described in Subsection 2.5.4 the site location is within a manmade island constructed of dredge material from the adjacent Delaware River. The physical properties of these materials are discussed in Subsection 2.5.4. Also, the evaluation of dredging operations respective to stability of slopes is discussed in Subsection 2.5.5. Other conditions resulting from human activity include surface and subsurface mining, as well as oil and gas extraction and injection; none of which pose a risk to the new plant location because no such activity has been reported within the site area.

2.5.1.3 References

2.5.1-1 Not Used.

**PSEG Site
ESP Application
Part 2, Site Safety Analysis Report**

- 2.5.1-2 Aggrawal, Y. P. and L.R. Sykes, "Earthquakes, Faults, and Nuclear Power Plants in Southern New York and Northern New Jersey," in *Science* 200(4340): p. 425 – 429, 1978.
- 2.5.1-3 Aleinikoff, J. N., J.W. Horton Jr., A. A. Drake Jr., R.P. Wintsch, C.M. Fanning and K. Yi, "Deciphering Multiple Mesoproterozoic and Paleozoic Events Recorded in Zircon and Titanite from the Baltimore Gneiss, Maryland: SEM Imaging, SHRIMP U-Pb Geochronology, and EMP analysis," in *Proterozoic Tectonic Evolution of the Grenville Orogen in North America*, Geological Society of America Memoir 197: p. 411 – 443, 2004.
- 2.5.1-4 Aleinikoff, J.N., W.S. Schenck, M.O. Plank, L. Srogi, C.M. Fanning, S.L. Kamo, and H. Bosbyshell, "Deciphering Igneous and Metamorphic Events in High-Grade Rocks of the Wilmington Complex, Delaware: Morphology, Cathodoluminescence and Backscattered Electron Zoning, and SHRIMP U-Pb Geochronology of Zircon and Monzanite," *Geological Society of America Bulletin* 118(1/2): p. 39 – 64, 2006.
- 2.5.1-5 Not Used.
- 2.5.1-6 Amick, D., R. Gelinas, G. Maurath, R. Cannon, D. Moore, E. Billington, and H. Kemppinen, "Paleoliquefaction Features Along the Atlantic Seaboard," Nuclear Regulatory Commission, NUREG/CR-5613, 1990a.
- 2.5.1-7 Not Used.
- 2.5.1-8 Not Used.
- 2.5.1-9 Not Used.
- 2.5.1-10 Armbruster, J.G. and L. Seeber, "The 23 April 1984 Martic Earthquake and the Lancaster Seismic Zone in Eastern Pennsylvania," *Bulletin of the Seismological Society of America* 77(3): p. 877 – 890, 1987.
- 2.5.1-11 Ator, S. W., J.M. Denver, D.E. Krantz and W.L. Newell, "Surficial Hydrogeologic Framework for the Mid-Atlantic Coastal Plain," U. S. Geological Survey Professional paper 1680: 44 pp., 2005.
- 2.5.1-12 Not Used.
- 2.5.1-13 Baskerville, C.A., "Bedrock and Engineering Geologic Maps of Bronx County and Parts of New York and Queens Counties, New York, Sheet 1-Geologic Map," U.S. Geological Survey, Open-File Report 87-360, 1992.
- 2.5.1-14 Bell, R.E., G.D. Karner and M.S. Steckler, "Early Mesozoic Rift Basins of Eastern North America and Their Gravity Anomalies: The Role of Detachments During Extension," *Tectonics* 7(3): p. 447 – 462, 1988.

**PSEG Site
ESP Application
Part 2, Site Safety Analysis Report**

- 2.5.1-15 Benson, R.N., "Map of Exposed and Buried Early Mesozoic Rift Basins/Synrift Rocks of the U.S. Middle Atlantic Continental Margin," Delaware Geologic Survey Miscellaneous Map Series No. 5, 1992.
- 2.5.1-16 Benson, R.N., "Mesozoic Rift Basins of the U.S. Middle Atlantic Continental Margin," in Proceedings of the Third Symposium on Studies Related to Continental Margins: Bureau of Economic Geology: p. 99 – 105, 1994.
- 2.5.1-17 Benson, R.N., "Characterization of the Potomac Aquifer, an Extremely Heterogeneous Fluvial System in the Atlantic Coastal Plain of Delaware," in the Atlantic Coastal Plain of Delaware: Delaware Geological Survey Open File Report 45, 2004.
- 2.5.1-18 Benson, R.N., "Internal Stratigraphic Correlation of the Subsurface Potomac Formation, New Castle County, Delaware, and Adjacent Areas in Maryland and New Jersey," Delaware Geologic Survey Report of Investigations No. 71, 15 pp., 2006.
- 2.5.1-19 Benson, R.H. and R.G. Doyle, "Early Mesozoic Rift Basins and the Development of the United States Middle Atlantic Continental Margin," in W. Manspeizer, ed., Triassic-Jurassic Rifting, Continental Breakup and the Origin of the Atlantic Ocean Passive Margins, Part A, New York, Elsevier, p. 99 – 127, 1988.
- 2.5.1-20 Benson, R.N. and N. Spoljaric, "Stratigraphy of the Post-Potomac Cretaceous-Tertiary Rocks of Central Delaware," Delaware Geological Society Bulletin No. 20, 28 pp., 1996.
- 2.5.1-21 Not Used.
- 2.5.1-22 Blackmer, G.C., "Preliminary Bedrock Geologic Map of a Portion of the Wilmington 30- by 60-Minute Quadrangle, Southeastern Pennsylvania," Pennsylvania Geological Survey Open File Report OFBM-01-01.0, scale 1:50,000, 2005.
- 2.5.1-23 Bollinger, G.A. "Specification of Source Zones, Recurrence Rates, Focal Depths, and Maximum Magnitudes for Earthquakes Affecting the Savannah River Site in South Carolina," U.S. Geological Survey Bulletin 2017: 57pp., 1992.
- 2.5.1-24 Bollinger, G.A. and M.S. Sibol, "Seismicity, Seismic Reflection Studies, Gravity and Geology of the Central Virginia Seismic Zone: Part I, Seismicity," Geological Society of America Bulletin 95: p. 49 – 57, 1985.
- 2.5.1-25 Not Used.
- 2.5.1-26 Bond, K.R. and J.D. Phillips, "Aeromagnetic Imagery with Geologic Correlations for some Early Mesozoic Basins of the Eastern United States," in Studies of the Early Mesozoic Basins of the Eastern United States, U.S. Geological Survey Bulletin 1776: p. 253 – 257, 1988.

**PSEG Site
ESP Application
Part 2, Site Safety Analysis Report**

- 2.5.1-27 Not Used.
- 2.5.1-28 Braun, D.D., "Glacial and Periglacial Erosion of the Appalachians," *Geomorphology*, 2: p. 233 – 256, 1989.
- 2.5.1-29 Braun, D.D., F.J. Pazzaglia and N.Potter Jr., "Margin of Laurentide Ice to the Atlantic Coastal Plain: Miocene-Pleistocene Landscape Evolution in the Central Appalachians," in *Quaternary Geology of the United States INQUA 2003 Field Guide Volume*, p. 219 – 244, 2003.
- 2.5.1-30 Brown, P.M., J.A. Miller and F.M. Swain, "Structural and Stratigraphic Framework, and Spatial Distribution of Permeability of the Atlantic Coastal Plain, North Carolina to New York," U.S. Geological Survey Professional Paper 796: p. 1 – 79, 1972.
- 2.5.1-31 Not Used.
- 2.5.1-32 Burton, W.C. and N.M. Ratcliffe, "Attitude, Movement History, and Structure of Cataclastic Rocks of the Flemington Fault-Results of Core Drilling Near Oldwick, New Jersey," U. S. Geological Survey, Map MF-1781, 1985.
- 2.5.1-33 Burton, W.C. and S. Southworth, "Tectonic Evolution of the Northern Blue Ridge Massif, Virginia and Maryland," in *Proterozoic Tectonic Evolution of the Grenville Orogen in North America*, Geological Society of America Memoir 197: p. 477–493, 2004.
- 2.5.1-34 Campbell, M.R., "Late Geologic Deformation of the Appalachian Piedmont as Determined by River Gravels," *Proceedings of the National Academy of Sciences* 15: p. 156 – 161, 1929.
- 2.5.1-35 Chapman, M.C. and F. Krimgold, "Seismic Hazard Assessment for Virginia," Virginia Polytechnic Institute Seismological Observatory, 1994.
- 2.5.1-36 Coblenz, D.C. and R.M. Richardson, "Statistical Trends in the Intraplate Field," *Journal of Geophysical Research* 100(B10): p. 20,245 – 20,255, 1995.
- 2.5.1-37 Colman-Sadd, S.P., G.R. Dunning and T. Dec, "Dunnage-Gander Relationships and Ordovician Orogeny in Central Newfoundland; a Sediment Provenance and U/Pb Age Study," *American Journal of Science* 292: p. 317 – 355, 1992.
- 2.5.1-38 Coruh, C., G.A. Bollinger and J.K. Costain, "Seismogenic Structures in the Central Virginia Seismic Zone," *Geology* 16: p. 748 – 751, 1988.
- 2.5.1-39 Costain, J.K., R.D. Hatcher Jr., C. Coruh, T.L. Pratt, S.R. Taylor, J.J. Litehiser and I. Zietz, "Geophysical Characteristics of the Appalachian Crust," in *The Geology of North America*, Geological Society of America, v. F-2: p. 385 –416, 1989.

**PSEG Site
ESP Application
Part 2, Site Safety Analysis Report**

- 2.5.1-40 Crone, A.J. and R.L. Wheeler, "Data for Quaternary Faults, Liquefaction Features, and Possible Tectonic Features in the Central and Eastern United States, East of the Rocky Mountain Front," U.S. Geological Survey Open File Report 00-0260: 341 pp., 2000.
- 2.5.1-41 Cronin, T.M., B.J. Szabo, T.A. Ager, J.E. Hazel and J.P. Owens, "Quaternary Climates and Sea Levels of the U.S. Atlantic Coastal Plain," Science 211: p. 233 – 211, 1981.
- 2.5.1-42 Cumbest, R.J., V. Prive and E.E. Anderson, "Gravity and Magnetic Modeling of the Dunbarton Triassic Basin, South Carolina," Southeastern Geology 33 (1): p. 37 – 51, 1992.
- 2.5.1-43 Dahlen, F.A., "Isostasy and the Ambient State of Stress in the Oceanic Lithosphere," Journal of Geophysical Research 86(B9): p. 7801 – 7807, 1981.
- 2.5.1-44 Dames & Moore, "Report of Foundation Studies, Proposed Salem Nuclear Generating Station, Salem, New Jersey," Public Service Electric & Gas Company, August 28, 1968.
- 2.5.1-45 Dames & Moore, "Report of Foundation Studies, Proposed Hope Creek Generating Station, Lower Alloways Creek Township, New Jersey," Public Service Electric and Gas Company, May 23, 1974.
- 2.5.1-46 Daniels, D.L., "Gravimetric Character and Anomalies in the Gettysburg Basin, Pennsylvania – A Preliminary Appraisal," in Proceedings of the Second U.S. Geological Survey Workshop on the Early Mesozoic Basins of the Eastern United States, U.S. Geological Survey Circular 946: p. 128 – 132, 1985.
- 2.5.1-47 Daniels, D.L. and G. W. Leo, "Geologic Interpretation of Basement Rocks of the Atlantic Coastal Plain," U.S. Geological Survey Open-File Report 85-655, 45 pp., 1985.
- 2.5.1-48 Daniels, D.L., I. Zietz and P. Popenoe, "Distribution of Subsurface Lower Mesozoic Rocks in the Southeastern United States, as Interpreted from Regional Aeromagnetic and Gravity Maps," in Studies Related to the Charleston, South Carolina, Earthquake of 1886 – Tectonics and Seismicity, U.S. Geological Survey Professional Paper 1313: p. 1 – 24, 1983.
- 2.5.1-49 Darton, N.H., "Configuration of the Bedrock Surface of the District of Columbia and Vicinity," U.S. Geological Survey Professional Paper 0217: 41, 1950.
- 2.5.1-50 Dawers, N.H. and L. Seeber, "Intraplate Faults Revealed in Crystalline Bedrock in the 1983 Goodnow and 1985 Ardsley Epicentral Areas, New York," Tectonophysics 186: p. 115 – 131, 1991.
- 2.5.1-51 Dillon, W.P. and R.N. Oldale, "Late Quaternary Sea-Level Curve: Reinterpretation Based on Glaciotectonic Influence," Geology 6: p. 56 – 60, 1978.

**PSEG Site
ESP Application
Part 2, Site Safety Analysis Report**

- 2.5.1-52 Diment, W.H., O.H. Muller and P.M. Lavin, "Basement Tectonics of New York and Pennsylvania as Revealed by Gravity and Magnetic Studies," in D. R. Wones, ed., The Caledonides in the USA, Proceedings I. G. C. P. Project 27: p. 221 – 227, Caledonide Orogen 1979 meeting, Blacksburg, Virginia, published 1980.
- 2.5.1-53 Dischinger, J.B. Jr., "Late Mesozoic and Cenozoic Strategic and Structural Framework Near Hopewell, Virginia," U.S. Geological Survey, Bulletin No. 1567, 56 pp., 1987.
- 2.5.1-54 Dominion, "Response to 6/1/04 RAI 2.5.1-6, Letter No. 5," U.S. Nuclear Regulatory Commission, Serial No. 04-347, and Docket No. 52-008, dated August 19, 2004 (ML 042440365).
- 2.5.1-55 Dominion, "Response to 4/15/04 RAI 2.5.1-1, 2.5.1-2, 2.5.1-3, 2.5.1-4, 2.5.2-2, 2.5.2-3, 2.5.2-4, and 2.5.3-1, Letter No. 3," U.S. Nuclear Regulatory Commission, Serial No. 04-270, and Docket No. 52-008, dated July 8, 2004 (ML042310575).
- 2.5.1-56 Delmarva Power & Light, Delmarva Power and Light Summit Power Station, PSAR Amendment 24, 1974.
- 2.5.1-57 Drake, A. A. Jr., "Precambrian and Lower Paleozoic Metamorphic and Igneous Rocks – South Mountain and Reading Prong," in C.H. Schultz, ed., The Geology of Pennsylvania, Pennsylvania Geological Survey and Pittsburgh Geological Society, p. 37 – 50, 1999.
- 2.5.1-58 Drake, A.A. Jr., A.K. Sinha, J. Laird and R.E. Guy, "The Taconic Orogen," in R.D. Hatcher Jr., W.A. Thomas and G.W. Viele, The Appalachian – Ouachita Orogen in the United States F-2: p. 101 – 177, Geological Society of North America, The Geology of North America, 1989.
- 2.5.1-59 Dryden, A.L. Jr., "Geology-Faults and Joints in the Coastal Plain of Maryland," Journal of the Washington Academy of Sciences, Journal 22: p. 469 – 472, 1932.
- 2.5.1-60 Ebel, J.E. and M. Tuttle, "Earthquakes in the Eastern Great Lakes Basin from a Regional Perspective," Tectonophysics 353: p. 17 – 30, 2002.
- 2.5.1-61 Edmunds, W.E., "Pennsylvanian – Permian Transition and Permian," in C.H. Shultz, ed., The Geology of Pennsylvania, Pennsylvania Geological Survey and Pittsburgh Geological Society, p.171 – 177, 1999.
- 2.5.1-62 EPRI, "Seismic Hazard Methodology for the Central and Eastern United States," EPRI NP-4726, 1986.
- 2.5.1-63 Ewing, M., G.P. Woollard and A.C. Vine, "Geophysical Investigations in the Immersed and Submerged Atlantic Coastal Plain," Geological Society of America Bulletin 51: p. 1821 – 1840, 1940.

**PSEG Site
ESP Application
Part 2, Site Safety Analysis Report**

- 2.5.1-64 Faill, R.T., "A Geologic History of the North-Central Appalachians: Part 1. Orogenesis from the Mesoproterozoic through the Taconic Orogeny," American Journal of Science 297: p. 551 – 619, 1997a.
- 2.5.1-65 Faill, R.T., "A Geologic History of the North-Central Appalachians: Part 2. The Appalachian Basin from the Silurian through the Carboniferous," American Journal of Science 297: p. 729 – 761, 1997b.
- 2.5.1-66 Farrell, S.C., "Pleistocene Braided Stream Deposits in the Atsion Quadrangle Area Northwestern Atlantic County, New Jersey," in R.W. Talkington, ed., Geological Investigations of the Coastal Plain of Southern New Jersey, Second Annual Meeting of the Geological Association of New Jersey, Pomona, New Jersey, p. A-1 – A-12, 1985.
- 2.5.1-67 Fenneman, N.M. and D.W. Johnson, "Physiographic Divisions of the Conterminous U.S.," U.S. Geological Survey Publications, 1946.
- 2.5.1-68 Fisher, G.W., M.W. Higgins and I. Zietz, "Geological Interpretations of Aeromagnetic Maps of the Crystalline Rocks in the Appalachians, Northern Virginia to New Jersey," Maryland Geological Survey Report of Investigations No. 32, 43 pp., 1979.
- 2.5.1-69 Fleming, A.H., A.A. Drake Jr. and L. McCartan, "Geologic Map of the Washington West Quadrangle, District of Columbia, Montgomery and Prince Georges Counties, Maryland, and Arlington and Fairfax Counties, Virginia," U.S. Geological Survey, Geologic Quadrangle Map GQ-1748, 1994.
- 2.5.1-70 Frankel, A.D., M.D. Petersen, C.S. Muller, K.M. Haller, R.L. Wheeler, E.V. Leyendecker, R.L. Wesson, S.C. Harmsen, C.H. Cramer, D.M. Perkins and K.S. Rukstales, "Documentation for the 2002 Update of the National Seismic Hazard Maps," U.S. Geological Survey, Open-file Report 02-420: 33 pp., 2002.
- 2.5.1-71 Frankel, K., F.J. Pazzaglia and J.D. Vaughn, "Knickpoint Evolution in a Vertically Bedded Substrate, Upstream-Dipping Terraces, and Atlantic Slope Bedrock Channels," Geological Society of America Bulletin 119(3-4): 476 – 486, 2007.
- 2.5.1-72 Not Used.
- 2.5.1-73 Garrity, C.P. and D.R. Soller, "Database of the Geologic Map of North America," adapted from the map by J.C. Reed Jr. and others (2005): U.S. Geological Survey Data Series 424, Website, <http://pubs.usgs.gov/ds/424/>, accessed September 24, 2009.
- 2.5.1-74 Ghatge, S.L., "Bouguer Gravity Anomaly Map of New Jersey and Vicinity," New Jersey Geological Survey Open-File Map OFM 55, 2004.
- 2.5.1-75 Groot, J.J. and R.R. Jordan, "The Pliocene and Quaternary Deposits of Delaware: Palynology, Ages, and Paleoenvironments," Delaware Geological Survey Report of Investigations No. 58, 36 pp., 1999.

**PSEG Site
ESP Application
Part 2, Site Safety Analysis Report**

- 2.5.1-76 Grow, J.A., K.D. Klitgord and J.S. Schlee, "Structure and Evolution of Baltimore Canyon Trough," in R.E. Sheridan and J.A. Grow, eds., Continental Margin US, Geological Society of America, The Geology of North America I-2: p. 269 – 290, 1988.
- 2.5.1-77 Hack, J.T., "Physiographic Divisions and Differential Uplift in the Piedmont and Blue Ridge," U.S. Geological Survey Professional Paper 1265, 49 pp., 1982.
- 2.5.1-78 Hack, J.T., "Geomorphology of the Appalachian Highlands," in The Appalachian – Ouachita Orogen in the United States, in R.D. Hatcher, W.A. Thomas and G.W. Viele, eds., The Geology of North America, The Geological Society of America, F-2: p. 459 – 470, 1989.
- 2.5.1-79 Hansen, H.J., "Upper Cretaceous (Senonian) and Paleocene (Danian) Pinchouts on the South Flank of the Salisbury Embayment, Maryland, and Their Relationship to Antecedent Basement Structures," Maryland Geological Survey, Report of Investigations No. 29, 1978.
- 2.5.1-80 Not Used.
- 2.5.1-81 Hatcher, R.D. Jr., "A Tectonic Synthesis of the U.S. Appalachians," in R.D. Hatcher Jr., W.A. Thomas and G.W. Viele, eds., in The Geology of North America, The Geological Society of America, F-2: p. 511 – 535, 1989a.
- 2.5.1-82 Hatcher, R.D. Jr., "Appalachian Introduction," in R.D. Hatcher Jr., W.A. Thomas and G.W. Viele, eds., The Appalachian – Ouachita Orogen, The Geology of North America, The Geological Society of America, F-2:p. 1 – 6, 1989b.
- 2.5.1-83 Hatcher, R.D. Jr. and I. Zietz, (1980) "Tectonic Implications for Regional Aeromagnetic and Gravity Data from the Southern Appalachians," in D.R. Wones, ed., Proceedings, The Caledonides in the U.S.A.; IGCP Project 27: p. 235 – 244, Blacksburg, Virginia Polytechnic Institute and State University Memoir 2, 1980.
- 2.5.1-84 Hatcher, R.D. Jr., W.A. Thomas, P.A. Geiser, A.W. Snoke, S. Mosher and D.V. Wiltschko, "Alleghanian Orogen," in R.D. Hatcher Jr., W.A. Thomas and G.W. Viele, eds., The Appalachian – Ouachita Orogen, The Geology of North America, The Geological Society of America, F-2: p. 233 – 318, 1989.
- 2.5.1-85 Hatcher, R.D. Jr., B.R. Bream and A.J. Merschat, "Tectonic Map of the Southern and Central Appalachians: A Tale of Three Orogens and a Complete Wilson Cycle," in R.D. Hatcher Jr., M.P. Carlson and J.H. McBride, eds., 4-D Framework of Continental Crust, Geological Society of America, Memoir 200: p. 595 – 632, 2007.
- 2.5.1-86 Hibbard, J.P., E.F. Stoddard, D.T. Secor and A.J. Dennis, "The Carolina Zone: Overview of Neoproterozoic to Early Paleozoic Peri-Gondwanan Terranes along

**PSEG Site
ESP Application
Part 2, Site Safety Analysis Report**

the Eastern Flank of the Southern Appalachians,” *Earth Science Reviews* 57: p. 299 – 339, 2002.

- 2.5.1-87 Hibbard, J., C. van Staal, D. Rankin and H. Williams, “Geology, Lithotectonic Map of the Appalachian Orogen (South), Canada-United States of America,” Geological Survey of Canada, Map 02096A, scale 1:1500000, 2006.
- 2.5.1-88 Hibbard, J.P., C.R. van Staal and D.W. Rankin, “A Comparative Analysis of Pre-Silurian Crustal Building Blocks of the Northern and Southern Appalachian Orogen”. *American Journal of Science* 307: p. 23 – 45, 2007a.
- 2.5.1-89 Hibbard, J.P., C.R. van Staal and B.V. Miller, “Links among Carolina, Avalonia and Ganderia in the Appalachian Peri-Gondwanan Realm,” in J.W. Sears, T.A. Harms and C.A. Evenchick, eds., *Whence the Mountains? Inquiries into the Evolution of Orogenic Systems: A Volume in Honor of Raymond A. Price*, Geological Society of America Special Paper 433: p. 291 – 311, 2007b.
- 2.5.1-90 Higgins, M.W., I. Zietz and G.W. Fisher, “Interpretation of Aeromagnetic Anomalies Bearing on the Origin of Upper Chesapeake Bay and River Course Changes in the Central Atlantic Seaboard Region: Speculations,” *Geology* 2(1): p. 73 – 76, 1974.
- 2.5.1-91 Hutchinson, D.R. and J.A. Grow, “New York Bight Fault,” *Geological Society of American Bulletin* 96: p. 975 – 989, 1985.
- 2.5.1-92 Jacobeen, F.K. Jr., “Seismic Evidence for High Angle Reverse Faulting in the Coastal Plain of Prince Georges and Charles County, Maryland,” *Maryland Geological Survey, Information Circular No. 13*, 1972.
- 2.5.1-93 Not Used.
- 2.5.1-94 Johnston, A.C., K.J. Coppersmith, L.R. Kanter and C.A. Cornell, “The Earthquakes of Stable Continental Regions-Volume 1: Assessment of Large Earthquake Potential,” EPRI Report TR-102261-VI, 1994.
- 2.5.1-95 Jordan, R.R., “Stratigraphic Nomenclature of Nonmarine Cretaceous Rocks of Inner Margin of Coastal Plain in Delaware and Adjacent States,” *Delaware Geological Survey, Report of Investigations No. 37*, 1983.
- 2.5.1-96 Kafka, A.L., E.A. Schlesinger-Miller and N.L. Barstow, “Earthquake Activity in the Greater New York City Area: Magnitudes, Seismicity, and Geologic Structures,” *Bulletin of the Seismological Society of America* 75(5): p. 1285 – 1300, 1985.
- 2.5.1-97 Karner, G.D. and A.B. Watts, “On Isostasy at Atlantic-Type Continental Margins,” *Journal of Geophysical Research* 87(B4): p. 2923 – 2948, 1982.
- 2.5.1-98 Kauffman, M.E., “Eocambrian, Cambrian, and Transition to Ordovician,” in *The Geology of Pennsylvania*, C.H. Shultz, ed., *Pennsylvania Geological Survey and Pittsburgh Geological Society*, p. 59 – 73, 1999.

Rev. 4

**PSEG Site
ESP Application
Part 2, Site Safety Analysis Report**

- 2.5.1-99 Kim, W.Y. and M. Chapman, "The 9 December 2003 Central Virginia Earthquake Sequence: A Compound Earthquake in the Central Virginia Seismic Zone," Bulletin of the Seismological Society of America 95(6): p. 2428 – 2445, 2005.
- 2.5.1-100 King, E.R., "Aeromagnetism," in The Geology of Pennsylvania, C.H. Shultz, ed., Pennsylvania Geological Survey and Pittsburgh Geological Society, p. 323 – 327, 1999.
- 2.5.1-101 King, E.R. and I. Zietz, "The New York-Alabama Lineament; Geophysical Evidence for a Major Crustal Break in the Basement Beneath the Appalachian Basin," Geology 6: p. 312 – 318, 1978.
- 2.5.1-102 Klitgord, K.D. and D.R. Hutchinson, "Distribution and Geophysical Signatures of Early Mesozoic Rift Basins Beneath the U.S. Atlantic Continental Margin," in Proceedings of the Second U.S. Geological Survey Workshop on the Early Mesozoic Basins of the Eastern United States, U.S. Geological Survey Circular 946: p. 45 – 61, 1985.
- 2.5.1-103 Klitgord, K.D., D.R. Hutchinson and H. Schouten, "U.S. Atlantic Continental Margin; Structural and Tectonic Framework," in R.E. Sheridan and J.A. Grow, eds., The Geology of North America, The Atlantic Continental Margin, U.S., Geological Society of America, I-2: p. 19 – 55, 1988.
- 2.5.1-104 Klitgord, K.D., C.W. Poag, C.W., L. Glover, III, R.E. Sheridan, D.R. Hutchinson, R.B. Mixon and R.N. Benson, "Mid-Atlantic Continental Margin: The Mesozoic-Cenozoic Continent-Ocean Boundary," in E-3 Southwestern Pennsylvania to Baltimore Canyon Trough: Geological Society of America, Geology of North America, North American Continent/Ocean Transect Program, Explanatory Pamphlet for Transect 19, p. 50 – 68, 1995.
- 2.5.1-105 Krantz, D.E., "A Chronology of Pliocene Sea-Level Fluctuations: The U.S. Middle Atlantic Coastal Plain Record," Quaternary Science Reviews 10: p. 163 – 174, 1991.
- 2.5.1-106 Krol, M.A., P.D. Muller and B.D. Idleman, "Late Paleozoic Deformation within the Pleasant Grove Shear Zone, Maryland: Results from ⁴⁰Ar/³⁹Ar Dating of White Mica," Geological Society of America Special Papers 330: p. 93 – 111, 1999.
- 2.5.1-107 Not Used.
- 2.5.1-108 Not Used.
- 2.5.1-109 Not Used.
- 2.5.1-110 Not Used.

**PSEG Site
ESP Application
Part 2, Site Safety Analysis Report**

- 2.5.1-111 Lavin, P.M., "Gravity," in C.H. Shultz ed., The Geology of Pennsylvania, Pennsylvania Geological Survey and Pittsburgh Geological Society, p. 317 – 321, 1999.
- 2.5.1-112 Leblanc, G. and G. Buchbinder, "Second Microearthquake Survey of the St. Lawrence Valley near LaMalbaie, Quebec," Canadian Journal of Earth Sciences 14: p. 2778 – 2889, 1977.
- 2.5.1-113 Not Used.
- 2.5.1-114 MACTEC, "Geotechnical Exploration and Testing, PSEG Site Application, Lower Alloways Creek Township, New Jersey," Data Report Rev. A, 2009.
- 2.5.1-115 Not Used.
- 2.5.1-116 Manspeizer, W. and H.L. Cousminer, "Late Triassic – Early Jurassic Synrift Basins of the U.S. Atlantic Margin," in R.E. Sheridan and J.A. Grow, eds., The Geology of North America, The Atlantic Continental Margin, U.S., Geological Society of America, I-2: p. 197 – 216, 1988.
- 2.5.1-117 Manspeizer, W., J. deBoer, J.K. Costain, A.J. Froelich, C. Coruh, P.E. Olsen, G.J. McHone, J.H. Puffer and D.C. Prowell, "Post-Paleozoic Activity," in R.D. Hatcher Jr., W.A. Thomas and G.W. Viele, eds., The Geology of North America, The Appalachian – Ouachita Orogen in the United States, Geological Society of North America, F-2: p. 319 – 374, 1989.
- 2.5.1-118 Maser Consulting, PA, "ALTA/ACSM Land Title Survey for PSEG Nuclear LLC of Block 26, Lots 4, 4.01, 5 and 5.01, Job Number 05001649D, Index Number HASU023453", June 13, 2008.
- 2.5.1-119 Marine, L.W. and G.E. Siple, "Buried Triassic Basin in the Central Savannah River Area, South Carolina and Georgia," Geological Society of America Bulletin 85: p. 311 – 320, 1974.
- 2.5.1-120 Marple, R., "Relationship of the Stafford Fault Zone to the Right-Stepping Bends of the Potomac, Susquehanna, and Delaware Rivers and Related Upstream Incision along the U.S. Mid-Atlantic Fall Line," Southeastern Geology 42(3): p. 123 – 144, 2004.
- 2.5.1-121 Marple, R.T. and P. Talwani, "Evidence of Possible Tectonic Upwarping along the South Carolina Coastal Plain from an Examination of River Morphology and Elevation Data," Geology 21: p. 651 – 654, 1993.
- 2.5.1-122 Marple, R.T. and P. Talwani, "Evidence for a Buried Fault System in the Coastal Plain of the Carolinas and Virginia-Implications for Neotectonics in the Southeastern United States," Geological Society of America Bulletin 12(2): p. 200 – 220, 2000.

**PSEG Site
ESP Application
Part 2, Site Safety Analysis Report**

- 2.5.1-123 Marple, R. and P. Talwani, "Proposed Shenandoah Fault and East Coast-Stafford Fault System and Their Implications for Eastern U.S. Tectonics," *Southeastern Geology* 43(2): p. 57 – 80, 2004.
- 2.5.1-124 Marsh, E.R., "A Pleistocene Lake in Central New Jersey," in *Geological Investigations of the Coastal Plain of Southern New Jersey*, R.W. Talkington, ed., Second Annual Meeting of the Geological Association of New Jersey, Pomona, New Jersey, p. A-13 – A-22, 1985.
- 2.5.1-125 Mayhew, M.A., "Geophysics of Atlantic North America," in C.A. Burk and C.L. Drake, eds., *The Geology of Continental Margins*: p. 409 – 427, 1974.
- 2.5.1-126 McCartan, L., "Geologic Map of the Coastal Plain and Upland Deposits, Washington West Quadrangle, Washington, D.C., Maryland, and Virginia," U.S. Geological Survey Open file Report 90-654, Plate 1, 1990.
- 2.5.1-127 McHone, J.G., "Broad-Terrane Jurassic Flood Basalts across Northeastern North America," *Geology* 24(4): p. 319 – 322, 1996.
- 2.5.1-128 McLaughlin, P.P., S.J. Baxter, K.W. Ramsey, T.E. McKenna and S.A. Strohmeier, "Results of Trenching Investigations along the New Castle Railroad Survey-1 Seismic Line, New Castle, Delaware," Delaware Geological Survey, Open File Report No. 43, 2002.
- 2.5.1-129 Merguerian, C. and J.E. Sanders, "Diversion of the Bronx River in New York City-Evidence for Postglacial Faulting?" in G.N. Hanson, chairman, *Geology of Long Island and Metropolitan New York*, 20 April 1996, State University of New York at Stony Brook, NY, Long Island Geologists Program with Abstracts, p. 131 – 145, 1996.
- 2.5.1-130 Merguerian, C. and J.E. Sanders, "Bronx River Diversion: Neotectonic Implications," *International Journal of Rock Mechanics and Mining Science* 34(3-4): p. 1 – 11, 1997.
- 2.5.1-131 Milici, R.C., J.K. Costain, C. Coruh and P.A. Pappano, "Structural Section across the Atlantic Coastal Plain, Virginia and Southeasternmost Maryland," Virginia Department of Mines, Minerals, and Energy, Division of Mineral Resources, Publication 140, 1995.
- 2.5.1-132 Mills, H.H., "Apparent Increasing Rates of Stream Incision in the Eastern United States During the Late Cenozoic," *Geology* 28(10): p. 955 – 957, 2000.
- 2.5.1-133 Mixon, R.B. and W.L. Newell, "Stafford Fault System: Structures Documenting Cretaceous and Tertiary Deformation along the Fall Line in Northeastern Virginia," *Geology*, 5: p. 437 – 440, 1977.
- 2.5.1-134 Mixon, R.B. and W.L. Newell, "The Faulted Coastal Plain Margin at Fredericksburg, Virginia," in *Tenth Annual Virginia Geology Field Conference*, 48 pp., October 13 –14, 1978.

**PSEG Site
ESP Application
Part 2, Site Safety Analysis Report**

- 2.5.1-135 Mixon, R.B. and D.S. Powars, "Folds and Faults in the Inner Coastal Plain of Virginia and Maryland: Their Effects on Distribution and Thickness of Tertiary Rocks and Local Geomorphic History," in N.O. Frederickson and K. Krafft, eds., Cretaceous and Tertiary Stratigraphy, Paleontology, and Structure, Southwestern Maryland and Northeastern Virginia, American Association of Stratigraphic Palynologists Field Trip Volume and Guidebook, p. 112 – 122, 1984.
- 2.5.1-136 Mixon, R.B., C.R. Berquist Jr., W.L. Newell, G.H. Johnson, D.S. Powars, J.S. Schindler and E.K. Rader, "Geologic Map and Generalized Cross-Sections of the Coastal Plain and Adjacent Parts of the Piedmont, Virginia," U.S. Geological Survey, Miscellaneous Investigations Series Map I-2033, scale 1:250000, 1989.
- 2.5.1-137 Mixon, R.B., L. Pavlides, D.S. Powars, A.J. Froelich, R.E. Weems, J.S. Schindler, W.L. Newell., L.E. Edwards and L.W. Ward, "Geologic Map of the Fredericksburg 30' x 60' Quadrangle, Virginia and Maryland," U.S. Geological Survey, Geologic Investigation Series Map I-2607, 2000.
- 2.5.1-138 North American Magnetic Anomaly Group, "Digital Data Grids for the Magnetic Anomaly Map of North America," U.S. Geological Survey, Open-File Report 02-414, 2002.
- 2.5.1-139 Nelson, W.A., "Geology and Mineral Resources of Albemarle County, Virginia," Division of Mineral Resources, Bulletin 77, 92 pp., 1 folded map, scale 1: 62,500, 1962.
- 2.5.1-140 New Jersey Department of Environmental Protection, "Lidar Data for Cape May and Cumberland Counties, and portions of Salem County within the CAFRA Zone," U.S. Geological Survey, 2 m resolution, 2008.
- 2.5.1-141 New Jersey Geological Survey, "General Stratigraphic Table for New Jersey," Website, <http://www.state.nj.us/dep/njgs/enviroed/infocirc/njstratcol.pdf>, accessed September 25, 2009.
- 2.5.1-142 New Jersey Office of Information Technology, "1930s Aerial Photography from New Jersey Web Map Service, Office of Geographic Information Systems," scale 1:24,000, 2007.
- 2.5.1-143 New Jersey Office of Information Technology, "2007-2008 High Resolution Orthophotography of New Jersey, Office of Geographic Information Systems," scale 1:24,000, data downloaded on January 27, 2009 from https://njgin.state.nj.us/NJ_NJGINExplorer/DataDownloads.jsp, 2008.
- 2.5.1-144 Newell, W.L., D.S. Powars, J.P. Owens, S.D. Stanford and B.D. Stone, "Surficial Geologic Map of Central and Southern New Jersey," U.S. Geological Survey Map I-2540, 1998.

**PSEG Site
ESP Application
Part 2, Site Safety Analysis Report**

- 2.5.1-145 Nuclear Regulatory Commission, "Safety Evaluation Report for an Early Site Permit (ESP) at the North Anna ESP Site," NUREG-1835, Nuclear Regulatory Commission, September 2005.
- 2.5.1-146 Obermeier, S.F. and W.E. McNulty, "Paleoliquefaction Evidence for Seismic Quiescence in Central Virginia during Late and Middle Holocene Time," U.S. Geological Survey, 1998.
- 2.5.1-147 Not Used.
- 2.5.1-148 Not Used.
- 2.5.1-149 Oliver, J., T. Johnson and J. Dorman, "Postglacial Faulting and Seismicity in New York and Quebec," Canadian Journal of Sciences 7: p. 579 – 590, 1970.
- 2.5.1-150 Olsen, P.E., "Stratigraphic Record of the Early Mesozoic Breakup of Pangea in the Laurasia-Gondwana Rift System," Annual Review of Earth and Planetary Sciences 25: p. 337 – 401, 1997.
- 2.5.1-151 Olsen, P. E., D.V. Kent, B. Cornet, W.K. Witte and R.W. Schlische, "High-Resolution Stratigraphy of the Newark Rift Basin (Early Mesozoic, Eastern North America)," Geological Society of America Bulletin 108(1): p. 40 – 77, 1996.
- 2.5.1-152 Olsson, R.K., T.G. Gibson, H.J. Hansen and J.P. Owens, "Geology of the Northern Atlantic Coastal Plain: Long Island to Virginia," in R.E. Sheridan and J.A. Grow, eds., The Geology of North America, The Atlantic Continental Margin, U.S., Geological Society of America, I-2: p. 87 – 105, 1988.
- 2.5.1-153 Owens, J.P. and J.P. Minard, "Upper Cenozoic Sediments of the Lower Delaware Valley and the Northern Delmarva Peninsula, New Jersey, Pennsylvania, Delaware, and Maryland," U.S. Geological Survey, Professional Paper 1067-D, 1979.
- 2.5.1-154 Owens, B.E. and S.D. Sampson, "Nd Isotopic Constraints on the Magmatic History of the Goochland Terrane, Easternmost Grenvillian Crust in the Southern Appalachians," in R.P. Tollo, L. Corriveau, J. McLelland and M.J. Bartholomew, eds., Proterozoic Tectonic Evolution of the Grenville Orogen in North America, Geological Society of America Memoir 197: p. 601 – 608, 2004.
- 2.5.1-155 Owens, J.P., J.P. Minard, N.F. Sohl and J.P. Mello, "Stratigraphy of the Outcropping Post-Magothy Upper Cretaceous Formations in Southern New Jersey and Northern Delmarva Peninsula, Delaware and Maryland," U.S. Geological Survey Professional Paper 674, 60 pp., 1970.
- 2.5.1-156 Owens, J.P., K. Stefansson and L.A. Sirkin, "Chemical, Mineralogic, and Palynologic Character of the Upper Wisconsinan-Lower Holocene Fill in Parts of Hudson, Delaware, and Chesapeake Estuaries," Journal of Sedimentary Petrology 44(2): p. 390 – 408, 1974.

**PSEG Site
ESP Application
Part 2, Site Safety Analysis Report**

- 2.5.1-157 Owens, J.P., B.J. Sugarman, N.F. Sohl, R.A. Parker, H.F. Houghton, R.A. Volkert, A.A. Drake and R.C. Orndorff, "Bedrock Geologic Map of Central and Southern New Jersey," U.S. Geological Survey, Miscellaneous Investigations Series, Map I-2540-B, 1999.
- 2.5.1-158 Parker, R.A. and H.F. Houghton, "Bedrock Geologic Map of the Monmouth Junction Quadrangle, New Jersey," U.S. Geological Survey Open File Report 90-219, 1990.
- 2.5.1-159 Pavlides, L., "Mountain Run Fault Zone of Virginia," U.S. Geological Survey, NEHRP, Summaries of Technical Reports XXII, OFR 87-63: p. 93 – 93, 1986.
- 2.5.1-160 Pavlides, L., "Early Paleozoic Composite Melange Terrane, Central Appalachian Piedmont, Virginia and Maryland: Its Origin and Tectonic History," Geological Society of America Special Paper 288: p. 135 – 193, 1989.
- 2.5.1-161 Pavlides, L., A.R. Bobyarchick, W.L. Newell and M.J. Pavich, "Late Cenozoic Faulting Along the Mountain Run Fault Zone, Central Virginia Piedmont," Geological Society of America Abstracts with Programs, Southeastern Sedimentology Meeting 15(2): p. 55, 1983.
- 2.5.1-162 Pazzaglia, F.J., "Stratigraphy, Petrography, and Correlation of Late Cenozoic Middle Atlantic Coastal Plain Deposits: Implications for Late-Stage Passive-Margin Geologic Evolution," Geological Society of America Bulletin 105: p. 617 – 1634, 1993.
- 2.5.1-163 Pazzaglia, F.L. and T.W. Gardner, "Fluvial Terraces of the Lower Susquehanna River," Geomorphology 8: p. 83 – 113, 1993.
- 2.5.1-164 Pazzaglia, F.L. and T.W. Gardner, "Late Cenozoic Flexural Deformation of the Middle U.S. Atlantic Passive Margin," Journal of Geophysical Research 99(B6): p. 12,143 – 12,157, 1994.
- 2.5.1-165 Pekar, S.F., K.G. Miller and J.V. Browning, "New Jersey Coastal Plain Oligocene Sequences," in Proceedings of the Ocean Drilling Program, Scientific Results, 150X: p. 187 – 206, 1997.
- 2.5.1-166 Phillips, J.D., "Aeromagnetic Character and Anomalies of the Gettysburg Basin and Vicinity, Pennsylvania – A Preliminary Appraisal," in Proceedings of the Second U.S. Geological Survey Workshop on the Early Mesozoic Basins of the Eastern United States, U.S. Geological Circular 946: p. 133 – 135, 1983.
- 2.5.1-167 Pickett, T.E., N. Spoljaric, "Geology of the Middletown-Odessa Area, Delaware," Delaware Geological Survey Geologic Map Series, Number 2, 1971.
- 2.5.1-168 Plank, M.O., W.S. Schenck and L. Srogi, "Bedrock Geology of the Piedmont of Delaware and Adjacent Pennsylvania," Delaware Geological Survey Report of Investigations No. 59, 52 pp., 2000.

**PSEG Site
ESP Application
Part 2, Site Safety Analysis Report**

- 2.5.1-169 Poag, C.W. and W.D. Sevon, "A Record of Appalachian Denudation in Postrift Mesozoic and Cenozoic Sedimentary Deposits of the U.S. Middle Atlantic Continental Margin," *Geomorphology* 2: p. 119 – 157, 1989.
- 2.5.1-170 Poag, C.W. and P.C. Valentine, "Mesozoic and Cenozoic Stratigraphy of the United States Atlantic Continental Shelf and Slope," in R.E. Sheridan and J.A. Grow, eds., *The Geology of North America, The Atlantic Continental Margin, U.S.*, Geological Society of America, I-2: p. 67 – 85, 1988.
- 2.5.1-171 Poag, C.W., C. Koeberl and W.U. Reimold, "The Chesapeake Bay Crater, Springer-Verlag, New York, 522 pp., 2004.
- 2.5.1-172 Powars, D.S. and T.S. Bruce, "The Effects of the Chesapeake Bay Impact Crater on the Geological Framework and Correlation of Hydrogeologic Units of the Lower York-James Peninsula, Virginia," U.S. Geological Survey Professional Paper 1612: 82 pp., 1999.
- 2.5.1-173 Prowell, D.C., "Index of Faults of Cretaceous and Cenozoic Age in the Eastern United States," U.S. Geological Survey, Miscellaneous Field Studies Map MF-1269, 1983.
- 2.5.1-174 PSEG, Page, L.M., Engineering Geologist's Report No. 6 and Production Well Salem Generating Station, 1982.
- 2.5.1-175 Public Service Enterprise Group (PSEG), "Salem Generating Station Updated Final Safety Analysis Report," Revision 23, October 17, 2007.
- 2.5.1-176 Public Service Enterprise Group (PSEG), "Hope Creek Generating Station Updated Final Safety Analysis Report," Revision 16, May 15, 2008.
- 2.5.1-177 Rabinowitz, P.D., "The Boundary Between Oceanic and Continental Crust in the Western North Atlantic," in C.A. Burk and C.L. Drake, eds., *The Geology of Continental Margins*, p. 67 – 84, 1974.
- 2.5.1-178 Rader, E.K., W.L. Newell and R.B. Mixon, "Mesozoic and Cenozoic Compressional Faulting along the Coastal Plain Margin, Fredericksburg, Virginia," in T.L. Neathery, ed., *Geological Society of America Centennial Field Guide* 6: p. 309 – 314, 1986.
- 2.5.1-179 Ramsey, K.W., "Coastal Response to Late Pliocene Climate Change: Middle Atlantic Coastal Plain, Virginia and Delaware," in *Quaternary Coasts of the United States: Marine and Lacustrine Systems*, SEPM Special Publication No. 48: p. 121 – 127, 1992.
- 2.5.1-180 Ramsey, K.W., "Geology of the Milford and Mispillion River Quadrangles," Delaware Geological Survey Report of Investigations No. 55, 40 pp., 1997.
- 2.5.1-181 Ramsey, K.W., "Geologic Map of New Castle County, Delaware," Delaware Geological Survey, Geologic Map Series No. 13, 2005.

**PSEG Site
ESP Application
Part 2, Site Safety Analysis Report**

- 2.5.1-182 Rankin, D.W., "Continental Margin of the Eastern United States: Past and Present," in R.C. Speed, ed., Phanerozoic Evolution of North American Continent-Ocean Transitions, Geological Society of America, DNAG Continent-Ocean Transect Volume, pp.129 – 218, 1994.
- 2.5.1-183 Rankin, D.W., A.A. Drake Jr., L. Glover III, R. Goldsmith, L.M. Hall, D.P. Murray, N.M. Ratcliffe, J.F. Read, D.T. Secor Jr. and R.S. Stanley, "Pre-Orogenic Terranes," in R.D. Hatcher Jr., W.A. Thomas, and G.W. Viele, eds., Geology of North America, The Appalachian – Ouachita Orogen in the United States, F-2: p. 7 – 42, 1989.
- 2.5.1-184 Ratcliffe, N.M., "The Ramapo Fault System in New York and Adjacent Northern New Jersey: A Case of Tectonic Heredity," Geological Society of America Bulletin 82: p. 125 – 142, 1971.
- 2.5.1-185 Ratcliffe, N.M., "Brittle Faults (Ramapo Fault) and Phyllonitic Ductile Shear Zones and the Basement Rock of the Ramapo Seismic Zones New York and New Jersey, and Their Relationship to Current Seismicity," in Field Studies of New Jersey Geology and Guide to Field Trips: 52nd Annual Meeting New York State Geological Association: p. 278 – 312, 1980.
- 2.5.1-186 Ratcliffe, N.M., "Result of Core Drilling of the Ramapo Fault at Sky Meadow Road, Rockland County, New York, and Assessment of Evidence for Reactivation to Produce Current Seismicity," U.S. Geological Survey Map 1-1401, 1982.
- 2.5.1-187 Ratcliffe, N.M., "Orientation, Movement History, and Cataclastic Rocks of Ramapo Fault Based on Core Drilling and Trenching Along The Western Margin of The Newark Basin near Bernardsville, New Jersey," U.S. Geological Survey Map 1-1982, 1990.
- 2.5.1-188 Ratcliffe, N.M., "Bedrock Geology and Seismotectonics of the Oscawana Lake Quadrangle, New York," U.S. Geological Survey Bulletin 1941, 1992.
- 2.5.1-189 Ratcliffe, N.M., W.C. Burton, R.M. D'Angelo, and J.K. Costain, "Seismic Reflection Geometry of the Newark Basin Margin in Eastern Pennsylvania," NUREG/CR-4676, 1986.
- 2.5.1-190 Reed, J.C. Jr., "Disequilibrium Profile of the Potomac River near Washington, D.C. – A result of Lowered Base Level or Quaternary Tectonics Along the Fall Line?," Geology 9: p. 445 – 450, 1981.
- 2.5.1-191 Reinecker, J., O. Heidbach, M. Tingay, B. Sperner, and B. Müller, "The Release 2008 of the World Stress Map," <http://www.world-stress-map.org>, Heidelberg Academy of Sciences and Humanities, 2008.
- 2.5.1-192 Richardson, R.M. and L.M. Reding, "North American Plate Dynamics," Journal of Geophysical Research 96(B7): p. 201 – 12, 23, 1991.

**PSEG Site
ESP Application
Part 2, Site Safety Analysis Report**

- 2.5.1-193 Riggs, S.R., and D.F. Belknap, "Upper Cenozoic Processes and Environments of Continental Margin Sedimentation: Eastern United States," in R.E. Sheridan and J.A. Grow, eds., *The Geology of North America, The Atlantic Continental Margin, U.S.*, Geological Society of America, I-2: p. 131 – 176, 1988.
- 2.5.1-194 Ryder, R.T., "Restored Stratigraphic Section C-C' from Medina County, Ohio, Through Southwestern and South-Central Pennsylvania to Hampshire County, West Virginia, Showing the Cambrian and Ordovician Sequence," U.S. Geological Survey Bulletin 1839-K, Plate 1, 1992.
- 2.5.1-195 Sanders, J.E., "Late Triassic Tectonic History of Northeastern United States," *American Journal of Science* 261: p. 501 – 524, 1963.
- 2.5.1-196 Saylor, T.E., "Precambrian and Lower Paleozoic Metamorphic and Igneous Rocks – in the Subsurface," in C.H. Shultz, ed., *The Geology of Pennsylvania*, Pennsylvania Geological Survey and Pittsburgh Geological Society, p. 51 – 57, 1999.
- 2.5.1-197 Sbar, M.L., R.R. Jordan, C.D. Stephens, T.E. Pickett, K.D. Woodruff and C.G. Sammis, "The Delaware-New Jersey Earthquake of February 28, 1973," *Bulletin of the Seismological Society of America*, 65: p. 85 – 92, 1975.
- 2.5.1-198 Scharnberger, C.K., "The Lancaster Seismic Zone of SE Pennsylvania in Relation to the Gettysburg-Newark Basin," *Geological Society of America Abstracts with Programs* 38(2): p. 83, 2006.
- 2.5.1-199 Schenck, W.S., M.O. Plank and L. Srogi, "Bedrock Geologic Map of the Piedmont of Delaware and Adjacent Pennsylvania," Delaware Geological Survey, Geologic Map Series 10, scale 1:36000, 2000.
- 2.5.1-200 Schlische, R.W. and P.E. Olsen, "Quantitative Filling Model for Continental Extensional Basins with Applications to Early Mesozoic Rifts of Eastern North America," *Journal of Geology* v. 98, p. 135 – 155, 1990.
- 2.5.1-201 Schlische, R.W. and M.O. Withjack, "The Early Mesozoic Birdsboro Central Atlantic Margin Basin in the Mid-Atlantic Region, Eastern United States: Discussion," *Geological Society of America Bulletin* 116: p. 823 – 832, 2005.
- 2.5.1-202 Schwab, W.C., M.A. Allison, W. Corso, L.L. Lotto, B. Butman, M. Bucholtz ten Brink, J.F. Denny, W.W. Danforth and D.S. Foster, "Initial Results of High Resolution Sea-Floor Mapping Offshore of the New York-New Jersey Metropolitan Area Using Sidescan Sonar," *Northeastern Geology and Environmental Sciences* 19(4): p. 243 – 262, 1997.
- 2.5.1-203 Seeber, L. and J. Armbruster, "Seismicity Along the Atlantic Seaboard of the U.S.: Intraplate Neotectonics and Earthquake Hazard," in *The Geology of North America, The Atlantic Continental Margin, I-2*, Geological Society of America: p. 565 – 582, 1988.

**PSEG Site
ESP Application
Part 2, Site Safety Analysis Report**

- 2.5.1-204 Seeber, L., J. G. Armbruster, W.-Y. Kim, and N. Barstow, "The 1994 Cacoosing Valley Earthquakes near Redding, Pennsylvania: A Shallow Rupture Triggered by Quarry Unloading," *Journal of Geophysical Research* 103(B10): 24,505–24,521, 1998.
- 2.5.1-205 Sella, G.F., S. Stein, T.H. Dixon, M. Craymer, T.S. James, S. Mazzotti and R.K. Dokka, "Observation of Glacial Isostatic Adjustment in 'Stable' North America with GPS," *Geophysical Research Letters* 34: L02306, 2007.
- 2.5.1-206 Sheridan, R.E., J.A. Grow, and K.D. Kiltgord, "Geophysical Data," in R.E. Sheridan and J.A. Grow, eds., *The Geology of North America, The Atlantic Continental Margin, U.S.*, Geological Society of America, I-2: p. 177 – 196, 1988.
- 2.5.1-207 Sheridan, R.E., R.K. Olsson and J.J. Miller, "Seismic Reflection and Gravity Study of Proposed Taconic Suture Under the New Jersey Coastal Plain: Implications for Continental Growth," *Geological Society of America Bulletin*, 103: p. 402 – 414, 1991.
- 2.5.1-208 Shor, A.N. and C.E. McClenner, "Marine Physiography of the U.S. Atlantic Margin," in R.E. Sheridan and J.A. Grow, eds., *The Geology of North America, The Atlantic Continental Margin, U.S.*, Geological Society of America, I-2: p. 9 – 18, 1988.
- 2.5.1-209 Not Used.
- 2.5.1-210 Spoljaric, N., "Geology of the Fall Zone in Delaware," *Delaware Geological Survey Report of Investigations No. 19*, 1972.
- 2.5.1-211 Spoljaric, N., "Normal Faults in Basement Rocks of the Northern Coastal Plain, Delaware," *Geological Society of America Bulletin* 84: p. 2781 – 2784, 1973.
- 2.5.1-212 Spoljaric, N., "Subsurface Geological Investigation of a Pleistocene Braided Stream in the Northern Coastal Plain, Delaware (U.S.A.)," *Sedimentology* 21: p. 451 – 461, 1974.
- 2.5.1-213 Spoljaric, N., "Landsat View of Delaware," *Delaware Geological Survey Open File Report 12*, 1979.
- 2.5.1-214 Stanford, S.D., D.L. Jagel, D.W. Hall, "Possible Pliocene–Pleistocene Movement on a Reactivated Mesozoic Fault in Central New Jersey," (Abstract), *GSA Abstracts with Program, Northeastern Section*, No. 37762, 1995.
- 2.5.1-215 Sugarman, P.J. and D.H. Monteverde, "Correlation of Deep Aquifers Using Coreholes and Geophysical Logs in Parts of Cumberland, Salem, Gloucester and Camden Counties, New Jersey," *New Jersey Geological Survey, Geologic Map Series 08-1*, 2008.

**PSEG Site
ESP Application
Part 2, Site Safety Analysis Report**

- 2.5.1-216 Sugarman, P.J., K.G. Miller, J.P. Owens and M.D. Feigenson, "Strontium-Isotope and Sequence Stratigraphy of the Miocene Kirkwood Formation, Southern New Jersey," Geological Society of American Bulletin 105: p. 423 – 436, 1993.
- 2.5.1-217 Sugarman, P.J., K.G. Miller, J.V. Browning, A.A. Kulpecz, P.P. McLaughlin and D.H. Monteverde, "Hydrostratigraphy of the New Jersey Coastal Plain: Sequences and Facies Predict Continuity of Aquifers and Confining Units," Stratigraphy 2(3): p. 259 – 275, 2005.
- 2.5.1-218 Sumner, J.R., "Geophysical Investigation of the Structural Framework of the Newark – Gettysburg Triassic Basin, Pennsylvania," Geological Society of America Bulletin, 88: p. 935 – 942, 1977.
- 2.5.1-219 Sykes, L.R., J.G. Armbruster, W.-Y. Kim, and L. Seeber, "Observations and Tectonic Setting of Historic and Instrumentally Located Earthquakes in the Greater New York City-Philadelphia Area," Bulletin of the Seismological Society of America 98(4): p. 1696 – 1719, 2008.
- 2.5.1-220 Talley, J.H., "Sinkholes, Hockessin Area, Delaware," Delaware Geological Survey Open File Report No. 14, 16 pp., 1981.
- 2.5.1-221 Not Used.
- 2.5.1-222 Talwani, M. and V. Abreu, "Inferences Regarding Initiation of Oceanic Crust Formation from the U.S. East Coast Margin and Conjugate South Atlantic Margins," in Atlantic Rifts and Continental Margins, American Geophysical Union Geophysical Monograph 115: p. 211 – 233, 2000.
- 2.5.1-223 Not Used.
- 2.5.1-224 Not Used.
- 2.5.1-225 Tanner, J., "Gravity Anomaly Map of North America," Decade of North American Geology (DNAG), Geological Society of America, scale 1:500,000,000, 5 plates, 1987.
- 2.5.1-226 Not Used.
- 2.5.1-227 Taylor, P.T., I. Zietz, and L.S. Dennis, "Geologic Implications of Aeromagnetic Data for the Eastern Continental Margin of the United States," Geophysics 33(5): p. 755 – 780, 1968.
- 2.5.1-228 Thompson, A.M., "Ordovician," in C.H. Shultz, ed., The Geology of Pennsylvania, Pennsylvania Geological Survey and Pittsburgh Geological Society, p.75 – 89, 1999.
- 2.5.1-229 Thompson, W.G., J.C. Varekamp and E. Thomas, "Fault Motions Along the Eastern Border Fault, Hartford Basin, CT, Over the Last 2800 Years," Transactions of the American Geophysical Union, abstract, 2000.

**PSEG Site
ESP Application
Part 2, Site Safety Analysis Report**

- 2.5.1-230 Tollo, R.P., J.N. Aleinikoff, E.A. Borduas, P.C. Hackley and C.M. Fanning, "Petrologic and Geochronologic Evolution of the Grenville Orogen, Northern Blue Ridge Province, Virginia," in Proterozoic Tectonic Evolution of the Grenville Orogen in North America, Geological Society of America Memoir 197: p. 647 – 677, 2004b.
- 2.5.1-231 Tollo, R.P., L. Corriveau, J. McLelland and M.J. Bartholomew, "Proterozoic Tectonic Evolution of the Grenville Orogen in North America: An Introduction," in Proterozoic Tectonic Evolution of the Grenville Orogen in North America, Geological Society of America Memoir 197: p. 1 – 19, 2004a.
- 2.5.1-232 Trehu, A.M., K.D. Klitgord, D.S. Sawyer and R.T. Buffler, "Atlantic and Gulf of Mexico Continental Margins," in Geophysical Framework of the Continental United States, Geological Society of America Memoir 172: p. 349 – 382, 1989.
- 2.5.1-233 Tucker, R.D., P. Osberg and H.N. Berry, "The Geology of a Part of Acadia and the Nature of the Acadian Orogeny Across Central and Eastern Maine," American Journal of Science 301: p. 205 – 260, 2001.
- 2.5.1-234 Turcotte, D.L. and G. Schubert, "Geodynamics", 2nd Edition. Cambridge University Press, 2002, U.S. Geological Survey, Open-file Report 02-361, Website, http://pubs.usgs.gov/of/2002/ofr-02-361/mag_home.htm, accessed September 24, 2009.
- 2.5.1-235 U.S. Geological Survey, Open-file Report 99-577 mc0639, Website, <http://pubs.usgs.gov/of/1999/ofr-99-0557/data/md/md0639.jpg>, accessed September 24, 2009.
- 2.5.1-236 U.S. Geological Survey, Open-file Report 99-557 md0705, Website, <http://pubs.usgs.gov/of/1999/ofr-99-0557/data/md/md0705.jpg>, accessed September 24, 2009.
- 2.5.1-237 U.S. Geological Survey, Open-file Report 99-577 pa0046, Website, <http://pubs.usgs.gov/of/1999/ofr-99-0557/data/pa/pa0046.jpg>, accessed September 24, 2009.
- 2.5.1-238 U.S. Geological Survey, "Professional Paper 1680, Plate 1," Website, <http://pubs.usgs.gov/pp/2005/pp1680/pdf/Plate1.pdf>, accessed September 25, 2009.
- 2.5.1-239 Not Used
- 2.5.1-240 Valentino, D.W., R.W. Valentino and M.L. Hill, "Paleozoic Transcurrent Conjugate Shear Zones in the Central Appalachian Piedmont of Southeastern Pennsylvania," Journal of Geodynamics, 19: p. 303 – 324, 1995.

**PSEG Site
ESP Application
Part 2, Site Safety Analysis Report**

- 2.5.1-241 Vigil, J.F., R.J. Pike and D.G. Howell, "A Tapestry of Time and Terrain," a Pamphlet to Accompany Geologic Investigations Series I-2720, U.S. Geological Survey, 11 pp., 2000.
- 2.5.1-242 Not Used.
- 2.5.1-243 Volkert, R.A., "Mesoproterozoic Rocks of the New Jersey Highlands, North-Central Appalachians: Petrogenesis and Tectonic History," in Proterozoic Tectonic Evolution of the Grenville Orogen in North America, Geological Society of America Memoir 197: p. 697 – 728, 2004.
- 2.5.1-244 Volkert, R.A., A.A. Drake Jr. and P.J. Sugarman, "Geology, Geochemistry, and Tectonostratigraphic Relations of the Crystalline Basement Beneath the Coastal Plain of New Jersey and Contiguous Areas," U.S. Geological Survey Professional Paper 1565-B: 48 pp., 1996.
- 2.5.1-245 Weems, R.E., "Newly Recognized En Echelon Fault Lines in the Piedmont and Blue Ridge Provinces of North Carolina and Virginia, with a Discussion of Their Possible Ages and Origins," U.S. Geological Survey, Open-File Report 98-374, 1998.
- 2.5.1-246 Westaway, R., "Late Cenozoic Uplift of the Eastern United States Revealed by Fluvial Sequences of the Susquehanna and Ohio Systems: Coupling Between Surface Processes and Lower Crustal Flow," Quaternary Science Reviews 26: p. 2823 – 2843, 2007.
- 2.5.1-247 Wheeler, R.L., "Earthquakes and the Cratonward Limit of Iapetus Faulting in Eastern North America," Geology 23: p. 105 – 108, 1995.
- 2.5.1-248 Wheeler, R.L., "Known or Suggested Quaternary Tectonic Faulting, Central and Eastern United States-New and Updated Assessments for 2005," U.S. Geological Survey, Open-File Report 2005-1336, 2005.
- 2.5.1-249 Wheeler, R.L., "Quaternary Tectonic Faulting in the Eastern United States," Engineering Geology 82: p. 165 – 186, 2006.
- 2.5.1-250 Wheeler, R.L., "Paleoseismic Targets, Seismic Hazard, and Urban Areas in the Central and Eastern United States," Bulletin of the Seismological Society of America 98(3): p. 1572 – 1580, 2008.
- 2.5.1-251 Wheeler, R.L. and A.C. Johnston, "Geologic Implications of Earthquake Source Parameters in Central and Eastern North America," Seismological Research Letters 63(4): p. 491 – 505, 1992.
- 2.5.1-252 Wilkes, G.P., S.S. Johnson, and R.C. Milici, "Exposed and Inferred Early Mesozoic Basins Onshore and Offshore, Virginia," Virginia Division of Mineral Resources Publication 94, 1989.

**PSEG Site
ESP Application
Part 2, Site Safety Analysis Report**

- 2.5.1-253 Wilson, J.M. and W.B. Fleck, "Geology and Hydrologic Assessment of Coastal Plain Aquifers in the Waldorf Area, Charles County, Maryland," Maryland Geological Survey, Report of Investigations No. 53, 1990.
- 2.5.1-254 Withjack, M.O., R.W. Schlische and P.E. Olsen, "Diachronous Rifting, Drifting, and Inversion on the Passive Margin of Central Eastern North America: An Analog for Other Passive Margins," AAPG Bulletin 82: p. 817 – 835, 1998.
- 2.5.1-255 Woodruff, K.D. and A.M. Thompson, "Geology of the Wilmington Area, Delaware," Delaware Geological Survey Geologic Map Series 4, scale 1:24,000, 1975.
- 2.5.1-256 Not Used.
- 2.5.1-257 Not Used.
- 2.5.1-258 Wyer, P. and A.B. Watts, "Gravity Anomalies and Segmentation at the East Coast, USA Continental Margin," Geophysics Journal International 166: p. 1015 – 1038, 2006.
- 2.5.1-259 Zimmerman, R.A., "Apatite Fission Track Age Evidence of Post-Triassic Uplift in the Central and Southern Appalachians," Geological Society of America, Abstracts with Programs 11: p. 219, 1979.
- 2.5.1-260 Zoback, M.L., "Stress Field Constraints on Intraplate Seismicity in Eastern North America," Journal of Geophysical Research, 97(B8): p. 11,761 – 11,782, 1992.
- 2.5.1-261 Zoback, M.D. and M.L. Zoback, "Tectonic Stress Field of North America and Relative Plate Motions," Geology of North America, Decade Map 1(19): p. 339 – 366, 1991.
- 2.5.1-262 Zoback, M.L. and M.D. Zoback, "Tectonic Stress Field of the Continental United States," in Geophysical Framework of the Continental United States, Geological Society of America Memoir, 172: p. 523 – 539, 1989.
- 2.5.1-263 Zoback, M.L., M.D. Zoback, J. Adams, M. Assumpcao, S. Bell, E.A. Bergman, P. Blumling, N.R. Brereton, D. Denham, J. Ding, K. Fuchs, N. Gay, S. Gregersen, H.K. Gupta, A. Gvishiani, K. Jacob, R. Klein, P. Knoll, M. Magee, J.L. Mercier, B.C. Muller, C. Paquin, K. Rajendran, O. Stephansson, G. Suarez, M. Suter, A. Udias, Z.H. Xu and M. Zhizhin, "Global Patterns of Tectonic Stress," Nature, v. 341, p. 291 – 299, 1989.
- 2.5.1-264 Not Used.
- 2.5.1-265 Miller, K.G., J. V. Browning, P. J. Sugarman, P. P. McLaughlin, M. A. Kominz, R. K. Olsson, J. D. Wright, B. S. Cramer, S. F. Pekar, and W. Van Sickel, 2003, 174AX leg summary: Sequences, sea level, tectonics, and aquifer resources: Coastal plain drilling, in Miller, K.G., P. J. Sugarman, J. V. Browning, et al., eds., Proceedings of the Ocean Drilling Program, Initial Reports, 174AX (Supplement):

**PSEG Site
ESP Application
Part 2, Site Safety Analysis Report**

College Station TX (Ocean Drilling Program), 1-38.

- 2.5.1-266 Hildebrand, Alan R., Glen T. Penfield, David A. Kring, Mark Pilkington, Antonio Camargo Z., Stein B. Jacobsen and William V. Boynton, "Chicxulub Crater: a possible Cretaceous/Tertiary boundary impact crater on the Yucatan Peninsula, Mexico", *Geology*, v. 19 p.867, 1991.
- 2.5.1-267 Drake, A., Volkert, R., Monteverde, D., Herman, G., Houghton, H., Parker, R., and Dalton, R., 1996, *Bedrock Geological Map of Northern New Jersey*, US Geological Survey, 2 sheets, scale 1:100,000.
- 2.5.1-268 Kafka, A.L., and Miller, P.E., 1996, Seismicity in the area surrounding two Mesozoic rift basins in the northeastern United States: *Seismological Research Letters*, v. 67, p. 69-86.
- 2.5.1-269 Kafka, A.L., Winslow, M.A., and Barstow, N.L., 1989, Earthquake activity in the greater New York city area - A faultfinder's guide, in Weiss, D., ed., *New York Geological Association 61st Annual Meeting Field Trip Guidebook*: Middletown, New York, p. 177-203.
- 2.5.1-270 Nelson, S., 1980, Determination of Holocene fault movement along the Ramapo fault in southeastern New York using pollen stratigraphy: *Geological Society of America Abstracts with Programs*, v. 12, p. 75.
- 2.5.1-271 Newman, W.S., Cinquemani, L.J., Sperling, J.A., Marcus, L.F., and Pradi, R.R., 1987, Holocene neotectonics and the Ramapo fault zone sea-level anomaly: A study of varying marine transgression rates in the lower Hudson estuary, New York and New Jersey, in Nummedal, D., Pilkey, O.H., and Howard, J.D., eds., *Sea-Level Fluctuation and Coastal Evolution*, Society of Economic Paleontologists and Mineralogists, Special Publication No. 41, p. 97-111.
- 2.5.1-272 Newman, W.S., Cinquemani, L.J., Sperling, J.A., and Pardi, R.R., 1983, Holocene neotectonics of the lower Hudson Valley: *Geological Society of America Abstracts with Programs*, abstract 16786, v. 15, p. 148.
- 2.5.1-273 Page, R.A., Molnar, P.H., and Oliver, J., 1968, Seismicity in the vicinity of the Ramapo fault, New Jersey-New York: *Bulletin of Seismological Society of America*, v. 58, p. 681-687.
- 2.5.1-274 Quittmeyer, R.C., Statton, C.T., Mrotek, K.A., and Houlday, M., 1985, Possible implications of recent microearthquakes in southern New York state: *Earthquake Notes*, v. 56, p. 35-42.
- 2.5.1-275 Ratcliffe, N.M., 1983, Fault reactivation models for the origin of eastern United States seismicity: Does the solution to Charleston reside at Charleston, in Hays, W.W., and Gori, P.L., eds., *Proceedings of Conference XX: A workshop on the 1886 Charleston, South Carolina, earthquake and its implications for today*, US Geological Survey Open-File Report 83-843.

**PSEG Site
ESP Application
Part 2, Site Safety Analysis Report**

- 2.5.1-276 Ratcliffe, N.M., and Burton, W., 1985, Fault reactivation models for origin of the Newark basin and studies related to eastern U.S. seismicity, in Robinson, G.R., and Froelich, A.J., eds., Proceedings of the Second U.S. Geological Survey Workshop on the Early Mesozoic Basins of the Eastern United States, US Geological Survey Circular 946, p. 36-45.
- 2.5.1-277 Ratcliffe, N.M., Burton, W., D'Angelo, R.M., and Costain, J.K., 1986, Low-angle extensional faulting, reactivated mylonites, and seismic reflection geometry of the Newark basin margin in eastern Pennsylvania: *Geology*, v. 1986, p. 766-770.
- 2.5.1-278 Ratcliffe, N.M., and Burton, W., 1988, Structural analysis of the Furlong fault and the relation of mineralization to faulting and diabase intrusion, Newark basin, Pennsylvania, in Froelich, A.J., and Robinson, G.R., eds., Studies of the early Mesozoic Basins of the Eastern United States, US Geological Survey Bulletin 1776, p. 176-193.
- 2.5.1-279 Ratcliffe, N.M., Burton, W.C., and Pavich, M.J., 1990, Orientation, movement history, and cataclastic rocks of Ramapo fault based on core drilling and trenching along the western margin of the Newark basin near Bernardsville, New Jersey, US Geological Survey, Miscellaneous Investigations Map I-1982.
- 2.5.1-280 Ratcliffe, N.M., and Costain, J., 1985, Northeast Seismicity and Tectonics, in Jacobson, M.L., and R., R.T., eds., National Earthquake Hazards Reduction Program summaries of technical reports, Volume XX, US Geological Survey Open File Report 85-464, p. 54-58.
- 2.5.1-281 Schlische, R.W., 1992, Structural and stratigraphic development of the Newark extensional basin, eastern North America: Evidence for the growth of the basin and its bounding structures: *Geol. Soc. Am. Bull.*, v. 104, p. 1246-1263.
- 2.5.1-282 Seborowski, D.K., Williams, G., Kelleher, J.A., and Statton, C.A., 1982, Tectonic implications of recent earthquakes near Annsville, New York: *Bulletin of Seismological Society of America*, v. 72, p. 1601-1609.
- 2.5.1-283 Stone, B.M., and Ratcliffe, N.M., 1984, Faults in Pleistocene sediments at trace of Ramapo fault, Geological Survey Research, U.S. Geological Survey Professional Paper 1375, p. 49.
- 2.5.1-284 Thurber, C.H., and Caruso, T.C., 1985, Crustal structure along the Ramapo fault zone, New York State: *Earthquake Notes*, v. 56, p. 145-152.
- 2.5.1-285 Wheeler, R.L., and Crone, A.J., 2001, Known and suggested Quaternary faulting in the midcontinent United States: *Engineering Geology*, v. 62, p. 51-78.
- 2.5.1-286 Zoback, M., and Zoback, M., 1980, State of stress in the conterminous United States: *Journal of Geophysical Research*, v. 85, p. 6113-6156.
- 2.5.1-287 PSEG Power, LLC, 2012, Letter ND-2012-0057, Response to Request for Additional Information, RAI No. 61, Vibratory Ground Motion, October 2, 2012.

**PSEG Site
ESP Application
Part 2, Site Safety Analysis Report**

2.5.1-288 NEIC, 2012, NEIC PDE-W earthquake summary for 23 August 2011 155104 earthquake, USGS, <http://neic.usgs.gov/cgi-bin/epic/epic.cgi?SEARCHMETHOD=3&FILEFORMAT=1&SEARCHRANGE=HH&CLAT=37.93&CLON=-77.93&CRAD=10&SYEAR=2011&SMONTH=8&SDAY=23&EYEAR=2011&EMONTH=8&EDAY=23&LMAG=5.5&UMAG=6.1&NDEP1=&NDEP2=&IO1=&IO2=&SLAT2=0.0&SLAT1=0.0&SLON2=0.0&SLON1=0.0&SUBMIT=Submit+Search>

**PSEG Site
ESP Application
Part 2, Site Safety Analysis Report**

**Table 2.5.1-1 (Sheet 1 of 2)
Potential Cenozoic Features in the PSEG Site Region**

Feature	Notes^(a, b)	Assigned Age	Basis for Assigned Age
Hypothesized fault of Pazzaglia (1993)	Likely non-existent	Pleistocene (?) ^(c)	Offset could be the result of stratigraphic variations (Reference 2.5.1-162)
Faults of Hansen (1978)	Extent hypothetical	Tertiary (?) ^(c)	One Paleocene offset inferred along a seismic line (Reference 2.5.1-79)
River Bend Trend/Stafford fault of Mixon (2000)	Likely non-existent	Tertiary (?) ^(c)	River bends developed in Miocene (Reference 2.5.1-153)
National Zoo faults		Tertiary	Offset Pliocene gravels (Reference 2.5.1-69)
Chesapeake Bay Impact Structure		Tertiary; younger growth faulting	Eocene impact; younger subsidence-driven growth faulting probably not capable of producing earthquakes (Reference 2.5.1-172)
Brandywine fault system		Miocene	Faulting dies out within Miocene Calvert formation (Reference 2.5.1-92)
Central Virginia Seismic Zone	C&W Class A	Quaternary	Historical and paleo-seismicity record (Reference 2.5.1-146)
Lancaster Seismic Zone	C&W Class C	Quaternary	Historic seismicity (Reference 2.5.1-10)
Cacoosing Earthquake	C&W Class C; Probably triggered by mining	Quaternary	Likely non-tectonic (Reference 2.5.1-204)
Fall Lines of Weems (1998)	C&W Class C; Erosional feature	Tertiary (?) ^(c)	No Quaternary units are offset (Reference 2.5.1-245)
Everona-Mountain Run fault zone	C&W Class C	Mesozoic	Fault cut by undeformed Jurassic dikes (Reference 2.5.1-137)
New Castle County faults	C&W Class C	Mesozoic	Faults cut Precambrian-Paleozoic basement, don't cut Cretaceous units (References 2.5.1-210 and 2.5.1-211)
Stafford fault system	C&W Class C	Tertiary	2 <18 inch offsets of Pliocene units (Reference 2.5.1-134); Quaternary terraces undeformed (Reference 2.5.1-54)
Upper Marlboro faults	C&W Class C; probably erosional features	Pleistocene (?) ^(c)	Slump due to surficial erosion most likely cause (Reference 2.5.1-249)

**PSEG Site
ESP Application
Part 2, Site Safety Analysis Report**

**Table 2.5.1-1 (Sheet 2 of 2)
Potential Cenozoic Features in the PSEG Site Region**

Feature	Notes^(a, b)	Assigned Age	Basis for Assigned Age
Lebanon Church fault	C&W Class C	Tertiary	Offset of Miocene to Pliocene gravel (Reference 2.5.1-173)
New York Bight fault	C&W Class C	Tertiary	Offsets Eocene strata, Quaternary strata undeformed (Reference 2.5.1-202)
East Border fault	C&W Class C	Quaternary (?) ^(c)	Offsets not demonstrated to have occurred via earthquakes (References 2.5.1-229 and 2.5.1-248)
Ramapo fault	C&W Class C	Jurassic	Offsets Jurassic rocks, Quaternary strata undeformed (Reference 2.5.1-187)
Kingston fault	C&W Class C; faulting not demonstrated	Tertiary or Quaternary	Pliocene gravels thicken; late Pleistocene gravels undeformed (Reference 2.5.1-214)
Dobb's Ferry fault zone	C&W Class C	Post-Paleozoic	Youngest rocks deformed are Paleozoic (Reference 2.5.1-50)
Mosholu fault	C&W Class C	Post-Paleozoic	
Offset glacial features	C&W Class C; likely not capable of producing earthquakes	Quaternary	Small offsets of surfaces with Pleistocene striations (Reference 2.5.1-149)
Hopewell fault	C&W Class C	Tertiary	Offsets Pliocene units, Quaternary units are undeformed (Reference 2.5.1-136)

a) C&W refers to studies of Crone and Wheeler (References 2.5.1-40 and 2.5.1-248).

b) See Table 2.5.1-2 for definitions of Crone and Wheeler (Reference 2.5.1-40) classes.

c) “?” indicates uncertainty on geologic age.

**PSEG Site
ESP Application
Part 2, Site Safety Analysis Report**

**Table 2.5.1-2
Definition of Classes Used to Compile Quaternary Faults, Liquefaction Features, and Deformations
in the Eastern United States**

Class Category	Definition
Class A	Geologic evidence demonstrates the existence of a Quaternary fault of tectonic origin, whether the fault is exposed for mapping or inferred from liquefaction or other deformational features.
Class B	Geologic evidence demonstrates the existence of a fault or suggests deformation, but either (1) the fault might not extend deep enough to be a potential source of significant earthquakes, or (2) the currently available geologic evidence is too strong to confidently assign the features to Class C, but not strong enough to assign it to Class A.
Class C	Geologic evidence is insufficient to demonstrate (1) the existence of tectonic fault, or (2) Quaternary slip or deformations associated with the feature.
Class D	Geologic evidence demonstrates that the feature is not a tectonic fault or feature; this category includes features such as demonstrated joints or joint zones, landslides, erosional or fluvial scarps, or landforms resembling fault scarps, but of demonstrable non-tectonic origin.

Reference 2.5.1-40

**PSEG Site
ESP Application
Part 2, Site Safety Analysis Report**

2.5.2 VIBRATORY GROUND MOTION

This subsection provides a detailed description of vibratory ground motion assessments, specifically the criteria and methodology for establishing the Ground Motion Response Spectra (GMRS) for the PSEG Site. The development of the GMRS follows a methodology consistent with the approach recommended in RG 1.208 and, therefore, satisfies the requirements set forth in 10 CFR 100.23. This subsection begins with a review of the approach outlined in RG 1.208 and is followed by these subsections:

- Seismicity (Subsection 2.5.2.1)
- Geologic and Tectonic Characteristics of the Site and Region (Subsection 2.5.2.2)
- Correlation of Earthquake Activity with Seismic Sources (Subsection 2.5.2.3)
- Probabilistic Seismic Hazard Analysis and Controlling Earthquake (Subsection 2.5.2.4)
- Seismic Wave Transmission Characteristics of the Site (Subsection 2.5.2.5)
- Ground Motion and Site Response Analysis (Subsection 2.5.2.6)

RG 1.208 provides guidance on methods acceptable to the NRC for satisfying the requirements of developing the site-specific GMRS, which in turn represents the first step in developing the Safe Shutdown Earthquake (SSE) ground motion levels as a characterization of the seismic hazard at the PSEG Site. The process outlined in RG 1.208 for determining the GMRS includes:

- Geological, geophysical, seismological, and geotechnical investigations of the site and site region, including the identification of seismic sources significant to seismic hazard at the site
- Procedures for performing a Probabilistic Seismic Hazard Analysis (PSHA) and deaggregating the mean hazard
- Characterization of the seismic wave transmission characteristics of the site
- Development of the performance-based site-specific earthquake ground motion

RG 1.208 states that an acceptable starting point for developing probabilistic seismic hazards calculations for an ESP is a PSHA model that has been reviewed and accepted by the NRC. The PSEG ESPA uses the Central and Eastern United States Seismic Source Characterization (CEUS-SSC) for Nuclear Facilities PSHA model (NUREG-2115) as the starting point for determining the GMRS for the site. The CEUS-SSC model replaces the PSHA model developed by the Electric Power Research Institute Seismicity Owners Group (EPRI-SOG) (Reference 2.5.2-35) and was developed using a Senior Seismic Hazard Analysis Committee (SSHAC) Level 3 assessment process. As described in NUREG-2115, the CEUS-SSC study is a comprehensive compilation of geological, geophysical, and seismological data for the CEUS by the SSHAC team members, consisting of experts in geology, seismology, and geophysics, to develop seismic source characterizations for the CEUS. These characterizations explicitly incorporated uncertainty in source geometry, earthquake recurrence, and earthquake magnitude, providing a full assessment and rigorous treatment of uncertainties, and embracing a suite of various technical interpretations. Further discussion of the suitability of the CEUS-SSC seismic sources is presented in Subsection 2.5.2.2.1.

Following the guidance of RG 1.208, a comprehensive review of new geological, geophysical, and seismological data developed since the completion of the CEUS-SSC study was conducted to determine the need for updating the CEUS-SSC PSHA model for the PSEG Site. Site and regional geologic and geophysical data are discussed in Subsection 2.5.1, and site and regional

Rev. 4

**PSEG Site
ESP Application
Part 2, Site Safety Analysis Report**

seismological data are presented in Subsection 2.5.2.1. Additionally, post-CEUS-SSC seismic source characterizations for sources relevant to the PSEG Site are reviewed in Subsection 2.5.2.2.2.

Subsection 2.5.2.4 describes the PSHA calculations including the choice of ground motion equations and how the Cumulative Absolute Velocity (CAV) filter is considered for PSHA calculations to determine the GMRS. Also following guidance provided in RG 1.208, the horizontal GMRS developed in Subsection 2.5.2.6 is calculated using a performance-based, risk-consistent method based on the ASCE/SEI Standard 43-05, Seismic Design Criteria for Structures, Systems, and Components in Nuclear Facilities (Reference 2.5.2-4) that takes into account soil amplification factors and soil properties presented in Subsection 2.5.2.5. The method specifies the level of conservatism and rigor in the seismic design process such that the performance of structures, systems, and components of the plant achieve a uniform seismic safety performance. Subsection 2.5.2.6 also describes the development of the vertical GMRS through scaling of the horizontal GMRS. The GMRS is developed for the uppermost competent layer beneath the site.

2.5.2.1 Seismicity

The CEUS-SSC PSHA methodology that is used as the basis for determining the GMRS at the PSEG Site primarily relies on historical seismicity within the CEUS to estimate seismicity rate and relative magnitude recurrence parameters (i.e., activity rates and Gutenberg-Richter b-values) for seismic sources defined in the CEUS-SSC model (NUREG-2115). The seismicity catalog for the CEUS Study Region spans the years 1568 through December 31, 2008. The resultant catalog is briefly reviewed in Subsection 2.5.2.1.1. As part of evaluating the impact of post-CEUS-SSC information on seismic source characterizations relevant to the PSEG Site, an updated CEUS-SSC seismicity catalog was developed for the whole CEUS-SSC Study Region for the period January 1, 2009 through December 31, 2011. From the updated CEUS-SSC seismicity catalog, a seismicity catalog is developed for the PSEG Site region, a 320 km (200 mi.) radius around the PSEG Site, for the years 2009 through the end of 2011. The final seismicity catalog used for the PSEG Site PSHA is the combination of the original CEUS-SSC seismicity catalog (1568-2008) and the updated PSEG Site Region catalog (2009-2011) for the PSEG Site region. Subsection 2.5.2.1.2 describes the development of the updated CEUS-SSC seismicity catalog and the PSEG Site Region seismicity catalog. Significant recent and historical earthquakes with respect to the PSEG Site are discussed in Subsection 2.5.2.1.3.

2.5.2.1.1 Seismicity Catalog Used in CEUS-SSC Seismic Hazard Analysis

The seismicity catalog used in the CEUS-SSC (NUREG-2115) extends from longitudes approximately coincident with the Rocky Mountain foothills (105 degrees W) on the west, to 322 km (200 mi.) offshore of the Atlantic coastline on the east. The northern boundary extends a minimum of 322 km (200 mi.) north of the US-Canadian border, and the southern boundary extends a minimum of 322 km (200 mi.) into the Gulf of Mexico (Figure 2.5.2-56). The CEUS-SSC catalog published in NUREG-2115 is assumed to be complete throughout the historical record to the time of the catalog compilation (December 31, 2008) in that all instrumental earthquakes and significant historical earthquakes are included. In addition, the catalog applies uniform size measure to each earthquake and only includes main events of earthquake clusters (i.e., the catalog is declustered).

**PSEG Site
ESP Application
Part 2, Site Safety Analysis Report**

Given the characteristics of the seismicity catalog developed for the CEUS-SSC study, the CEUS-SSC seismicity catalog (through 2008) meets the requirement of RG 1.206 that a COL applicant shall “provide a complete list of all historically reported earthquakes that could have reasonably affected the region surrounding the site, including all earthquakes of Modified Mercalli intensity greater than or equal to IV or of magnitude greater than or equal to 3.0 that have been reported within 200 miles (322 kilometers) of the site.”

2.5.2.1.2 Updated Seismicity Catalogs

To examine seismicity that has occurred since 2008 in the region surrounding the PSEG Site, the CEUS-SSC seismicity catalog in NUREG-2115 is updated (2009 through 2011). From the updated catalog, a seismicity catalog for the 322 km (200 mi.) region surrounding the PSEG Site (PSEG Site Region) is created and declustered. The CEUS-SSC seismicity catalog in NUREG-2115 is combined with the PSEG Site Region seismicity catalog. Maximum magnitude (Mmax) values of events in each of the CEUS-SSC background source zones are compared to those in the updated CEUS-SSC to determine if the Mmax values require updating. An additional seismic source is also created to capture a small area in the PSEG Site Region that is not included in the NUREG-2115 CEUS-SSC Study Region.

2.5.2.1.2.1 Updating the NUREG-2115 CEUS-SSC Seismicity Catalog

The seismicity catalog presented in NUREG-2115 contains events from 1568 through December 31, 2008. An updated CEUS-SSC seismicity catalog encompassing the whole CEUS-SSC Study Region and the PSEG Site Region (bounded by 36° to 43° N and 71° to 80° W) is compiled using web-based searches of regional and national seismicity catalogs from each database start date to December 31, 2011. As shown in Figure 2.5.2-57, the PSEG Site southeastern regional boundary extends slightly beyond the CEUS-SSC Study Region boundary. The area outside the CEUS-SSC Study Region boundary is considered as an extension of the Atlantic Highly Extended Crust CEUS-SSC seismotectonic zone. An additional seismic source zone, named Atlantic Highly Extended Crust East (AHEx-E), is created for use in the seismicity analysis. The start date for each database is used to be sure all events in the AHEx-E are included in the search.

The regional catalogs searched are:

- Center for Earthquake Research and Information (CERI) (Reference 2.5.2-99)
- Lamont-Doherty Cooperative Seismographic Network (LCSN) (Reference 2.5.2-100)
- New England Seismic Network (NESN) (Reference 2.5.2-101)
- Southeastern U.S. Seismic Network (SEUSSN) (Reference 2.5.2-102)
- Ohio Seismic Network (OSN) (Reference 2.5.2-103)

The national catalogs searched are:

- USGS National Earthquake Information Center (NEIC) (Reference 2.5.2-104)
- Advanced National Seismic System (ANSS) (Reference 2.5.2-105)

The CERI regional catalog corresponds to the New Madrid Seismic Network (NMSN) “Authoritative Region” reported by ANSS and is illustrated in Figure 2.5.2-58. In addition, the CERI regional network is considered a primary source for the SEUSSN “Authoritative Region”

**PSEG Site
ESP Application
Part 2, Site Safety Analysis Report**

for events after 2007, because it is one of the contributors to the ANSS for events in the SEUSSN region. The OSN, while not an ANSS “Authoritative Region,” is considered to be the authority for events recorded within the border of the state of Ohio.

2.5.2.1.2.2 Mmax Distributions

After assembling the updated CEUS-SSC seismicity catalog from the various sources, events outside the CEUS-SSC Study Region are removed from the seismicity catalog. Next, all events prior to January 1, 2009 are removed from the catalog because the NUREG-2115 CEUS-SSC seismicity catalog is current through December 31, 2008. The magnitudes of the remaining events are then converted to moment magnitudes (**M**) using the methodology described in NUREG-2115. Figure 2.5.2-59 depicts the resultant updated CEUS-SSC seismicity catalog developed for the CEUS-SSC Study Region.

Events occurring on the same date, within a time frame of ± 5 seconds, a latitude or longitude window of ± 0.0001 degrees, and having the same magnitude value are flagged as duplicates and removed from the catalog. When an event is identified as a duplicate and it is listed in both a regional and national catalog, the event is searched to see if that event fell within the “Authoritative Region” (Figure 2.5.2-58) of the regional network.

The event generating the Mmax value in each of the CEUS-SSC source zones presented in Figures 2.5.2-60 through 2.5.2-65 is identified and declustered by comparing the event to all the other events in the zone. Events that occurred within the same 24 hours and within ± 0.1 degree longitude or ± 0.1 degree latitude from this particular event are flagged as a dependent event. In declustering, regional networks are given priority over national networks within their “Authoritative Regions.” When an event is identified as dependent and is listed in a regional and national catalog, the event location is evaluated to see if that event falls within the “Authoritative Region” of the regional network. The particular event listed in the regional network is flagged to be selected for the updated PSEG Site Region seismicity catalog. National networks are given priority over regional networks when events are outside the regional network’s corresponding “Authoritative Region” as defined by ANSS, or if the magnitude reported by the national NEIC catalog is higher than the magnitude reported by the regional networks, even if the event is reported by the regional network within its “Authoritative Region.” For this evaluation, the NEIC catalog always takes precedence over the ANSS catalog, except for events within the SEUSSN regional network from January 1, 2007 through December 31, 2011.

The largest magnitude event in each CEUS-SSC background source zone (Figures 2.5.2-60 – 2.5.2-65) is then compared to the lower-bound Mmax for the source zones containing the earthquake. Table 2.5.2-25 presents these comparisons. The largest magnitude event in each CEUS-SSC background source zone listed in Table 2.5.2-25 corresponds to the lowest Mmax in the Mmax distribution of NUREG-2115 (with a weight of 0.101). Based on Table 2.5.2-25, no earthquake in the updated CEUS-SSC seismicity catalog within any of the source zones exceeds the lower-bound Mmax as presented in NUREG-2115.

2.5.2.1.2.3 PSEG Site Region Seismicity Catalog Update

**PSEG Site
ESP Application
Part 2, Site Safety Analysis Report**

The PSEG Site Region seismicity catalog is declustered as previously discussed to remove dependent and duplicate events. Dependent events are considered those that occurred within the same 24-hr period and within ± 0.1 degree longitude and ± 0.1 degree latitude.

The final PSEG Site Region seismicity catalog, for the period January 1, 2009 to December 31, 2011, contains eighteen events. One additional event is included, an event within AHEx-E, outside the CEUS-SSC Study Region (**M** 3.38; May 5, 1990), resulting in a total of 19 events. Table 2.5.2-26 lists the events and Figure 2.5.2-66 shows the event locations. The **M** 5.8 Mineral VA Earthquake (August 23, 2011) is included in the events. The PSEG Site Region seismicity catalog is then combined with the original CEUS-SSC seismicity catalog (only those events within the PSEG Site Region boundary) to develop a complete composite regional catalog for the PSEG Site. The composite regional catalog includes 259 events.

2.5.2.1.2.4 Evaluation of AHEx-E Seismic Source Zone

The AHEx-E seismic source zone is defined as the area within the PSEG Site regional update boundary and outside the CEUS-SSC Study Region (see Figure 2.5.2-57). Figure 2.5.2-57 depicts two earthquake events in the AHEx-E seismic source zone; however, one of these events was found to be a duplicate event. As shown on Figure 2.5.2-66 and in Table 2.5.2-26, there is only a single earthquake event (**M** 3.38; May 5, 1990) which lies within the AHEx-E seismic source zone, but outside the 322 km (200 mi.) radius around the PSEG Site. As a result, the contribution of the AHEx-E seismic source zone to the hazard at the PSEG Site is expected to be minimal, thereby justifying the use of a simplified and conservative approach in defining the logic tree and seismic source parameters for the AHEx-E seismic source zone as discussed in Subsection 2.5.2.4.2.2.1.

2.5.2.1.3 Recent and Historical Seismicity

The NUREG-2115 CEUS-SSC seismicity catalog described in Subsection 2.5.2.1.1 and the updated seismicity catalog described in Subsection 2.5.2.1.2 are shown in Figures 2.5.2-56 and 2.5.2-57, respectively. Figure 2.5.2-57 depicts the location of the August 23, 2011 earthquake that occurred near Mineral, VA (referred to as the Mineral earthquake) (Reference 2.5.2-107). For the PSEG Site ESPA, the Mineral earthquake is characterized as an Emb 5.9 based on the mb 5.9 magnitude reported by the NEIC (Reference 2.5.2-107). These figures demonstrate that there is no significant difference in the spatial pattern of seismicity within the updated region between the CEUS-SSC catalog and the updated catalog. Subsection 2.5.2.4.2.1 provides a quantitative comparison of seismicity rates and shows also that there is no significant difference in seismicity rates determined between the two catalogs. As also noted in NUREG-2115, the most seismically active region within the extent of Figure 2.5.2-57 is the New England region in the northeast section of the figure, well outside of the PSEG Site Region. Within the PSEG Site Region, the largest concentration of earthquakes occurs within the Central Virginia Seismic Zone (CVSZ). The CVSZ is discussed in more detail in Subsection 2.5.1.1.4.2.5.1.

The Mineral earthquake is the only significant earthquake to have occurred within the PSEG Site Region since the end date of the CEUS-SSC seismicity catalog (i.e., 2008). This earthquake is discussed in additional detail below along with the seven additional earthquakes within the PSEG Site Region with Emb greater than or equal to 4.5.

**PSEG Site
ESP Application
Part 2, Site Safety Analysis Report**

23 August 2011, Emb 5.9, Mineral, Virginia

The 23 August 2011 Emb 5.9 earthquake (Reference 2.5.2-107) that occurred near Mineral, VA is one of the largest earthquakes to have been widely felt along the east coast since the 1897 Giles County, Virginia earthquake. The earthquake occurred within the CVSZ (see Subsection 2.5.1.1.4.2.5.1 for further discussion of the CVSZ) (Reference 2.5.2-108). The earthquake has yet to be positively associated with a causative fault (References 2.5.2-108, 2.5.2-109 and 2.5.2-110). The earthquake was felt throughout much of eastern North America including Michigan, Georgia, and Quebec. The highest levels of damage associated with the earthquake were felt in Louisa County, surrounding the epicenter of the earthquake. Reported Modified Mercalli intensities (MMI) reached VII (moderate to moderate/heavy damage) (Reference 2.5.2-108). Light damage (MMI VI) occurred throughout central Virginia and southern Maryland. The epicenter of the earthquake was approximately 270 km (170 mi.) from the PSEG Site. Reported MMI values for the area immediately surrounding the PSEG Site were between III and IV, indicating weak to light ground shaking and no damage (Reference 2.5.2-108).

10 August 1884, Emb 5.08, New York City

The location and magnitude of the 10 August 1884 earthquake are based on patterns of felt intensity. The earthquake was felt along the Atlantic coast from southern Maine to central Virginia and to the west (W) as far as northeast Ohio (References 2.5.2-79, 2.5.2-94, and 2.5.2-95). The highest Modified Mercalli intensity (MMI) was VI to VII in southern Long Island, and estimated intensities within the PSEG Site vicinity were MMI IV or less (References 2.5.2-65, 2.5.2-75, and 2.5.2-79). Reported effects of the earthquake include fallen chimneys, cracked walls, and ground shaking induced waves in the Housatonic River in Connecticut (References 2.5.2-79, 2.5.2-94, and NUREG/CR-4750, *A study of earthquake hazards in New York State and adjacent areas: final report covering the period 1982-1985*). The location of the earthquake is constrained to the greater New York City area and southern Long Island based on: (1) the concentration of the highest intensity observations in that region, (2) reports of short-period gravity waves within water bodies, and (3) reports of ground cracking only within this region (Reference 2.5.2-80, NUREG/CR-4750). However, most researchers note that the high population density within the New York City region may introduce bias into intensity-based epicenters for this earthquake (Reference 2.5.2-97, NUREG/CR-4750). The reported location is approximately 182 km (113 mi.) from the PSEG Site. The earthquake has not been positively correlated to any geologic structures (Reference 2.5.2-51, NUREG/CR-4750, 80).

19 December 1737, Emb 4.9, New York City

The location and magnitude of the 19 December 1737 earthquake is based on patterns of felt intensity. Based on the sparse number of felt reports, the earthquake location may be incorrectly located by up to 100 km (62 mi.) (Reference 2.5.2-80). However, intensity estimates near the PSEG Site for this event (MMI III) are significantly lower than those near New York city (MMI VI to VIII) indicating that the event location uncertainty does not accommodate the possibility of the earthquake being located significantly closer to the PSEG Site (References 2.5.2-75, 2.5.2-96, and NUREG/CR-4750). The location of the earthquake within the CEUS-SSC NUREG-2115 earthquake catalog is approximately 198 km (123 mi.) from the PSEG Site. Felt effects associated with this earthquake include the ringing of bells and the knocking down of chimneys in New York City. The earthquake was also felt in Boston, Philadelphia, and northern Delaware

**PSEG Site
ESP Application
Part 2, Site Safety Analysis Report**

(References 2.5.2-2.5.2-79, 2.5.2-94, and NUREG/CR-4750, 95). The earthquake has not been positively correlated to any geologic structures, and there were no reported ground failures associated with the earthquake.

27 August 1833, Emb 4.9, Central Virginia

The location and magnitude of the 27 August 1833 earthquake is based on patterns of felt intensity. The earthquake was felt along the Atlantic coastline from Baltimore, Maryland to Raleigh, North Carolina (References 2.5.2-14, 2.5.2-15, 2.5.2-59, and 2.5.2-79). The maximum felt intensities, estimated to be MMI IV to VI, occurred in the region between Richmond and Charlottesville, Virginia (References 2.5.2-14, 2.5.2-59, and 2.5.2-96). Commonly reported effects of the earthquake include the rattling of windows and the shaking of walls and fences. There was no reported significant damage caused by the earthquake (References 2.5.2-59 and 2.5.2-79). The location of the earthquake within the CEUS-SSC (NUREG-2115) earthquake catalog is approximately 290 km (180 mi.) from the PSEG Site. No felt effects were reported in the region immediately surrounding the PSEG Site (References 2.5.2-14 and 2.5.2-59). The earthquake has not been positively correlated to any geologic structures, and there were no reported ground failures associated with the earthquake.

10 April 1918, Emb 4.79, Page County, Virginia

The location and magnitude of the 10 April 1918 earthquake is based on patterns of felt intensity, but early seismographs in Washington, D.C., Ithaca, New York, and Cambridge, Massachusetts detected the earthquake (Reference 2.5.2-89). The earthquake was felt throughout much of Virginia and parts of West Virginia, Maryland, Delaware, Pennsylvania, and the District of Columbia (References 2.5.2-15, 2.5.2-79, and 2.5.2-89). The PSEG Site area is on the edge of the felt area of the event (Reference 2.5.2-15). The maximum reported intensities, estimated to be between MMI V to VI, occurred within a narrow northeast trending band along the Shenandoah valley on the border of Virginia and West Virginia (References 2.5.2-15, 2.5.2-79, and 2.5.2-89). Near the reported epicenter in Luau, Virginia the maximum felt effects included broken windows as well as cracked ceilings and plaster walls, but anomalously broken windows were also reported at Georgetown University in Washington, D. C. (References 2.5.2-79 and 2.5.2-89). The location of the earthquake within the CEUS-SSC NUREG-2115 earthquake catalog is approximately 262 km (163 mi.) from the PSEG Site. The earthquake has not been positively correlated to any geologic structures, and there were no reported ground failures associated with the earthquake (Reference 2.5.2-89).

1 September 1895, Emb 4.63, Hunterdon County, New Jersey

The location and magnitude of the 1 September 1895 earthquake is based on patterns of felt intensity. The earthquake was felt in New Jersey, New York, Pennsylvania, Delaware, Virginia, and Connecticut (Reference 2.5.2-75, NUREG/CR-6750, 79). The maximum felt intensities for the earthquake (MMI V to VI) were reported in north-central New Jersey (Reference 2.5.2-75, NUREG/CR-4750). Reported felt effects include rocking buildings, broken windows, cracked plaster walls, and items falling over on shelves and counters (Reference 2.5.2-79). The location of the earthquake within the CEUS-SSC NUREG-2115 earthquake catalog is approximately 150 km (93 mi.) from the PSEG Site. The earthquake has not been positively correlated to any geologic structures, and there were no reported ground failures associated with the earthquake.

**PSEG Site
ESP Application
Part 2, Site Safety Analysis Report**

16 January 1994, Emb 4.6, Cacoosing Valley, Pennsylvania

The 16 January 1994 Cacoosing Valley earthquake, near Reading, PA, was the largest instrumentally recorded earthquake within the site region, until the 23 August 2011, EMb 5.9 Mineral, Virginia earthquake. Some minor damage to chimneys, plaster walls, and loose objects within houses was reported due to the earthquake within the Reading, Pennsylvania area (References 2.5.2-64 and 2.5.2-76). The earthquake was felt in southeast Pennsylvania and as far away as Baltimore, Maryland, New York City, and Toronto, Canada (Reference 2.5.2-64). The earthquake is located approximately 109 km (68 mi.) from the PSEG Site, and isoseismal maps for the earthquake suggest that intensities at the PSEG Site would have been MMI I. There were a few reports of damage to underground piping that were related to a sinkhole collapse (no location provided in the two cited references) (Reference 2.5.2-76). Otherwise there were no reports of ground failure associated with the earthquake. A detailed seismological investigation of the earthquake was conducted by Seeber et al. (Reference 2.5.2-76) that included installation of temporary seismographs to map aftershock patterns, a regional stress analysis, relocation of the earthquake hypocenter, determination of the source focal mechanism from broadband recordings, and determination of a composite focal mechanism from early aftershocks. The main results of the study were that:

- The mainshock and aftershocks were constrained to the upper 2.5 km (1.6 mi.) of the crust within a roughly elliptical zone approximately 2 km (1.2 mi.) wide and 3 km (1.9 mi.) long trending northwest
- The depth of the mainshock was estimated to be 2 ± 1 km (1.2 ± 0.6 mi.);
- The slip direction and rupture plane for the event was reverse slip along a plane striking 135° and dipping 54° to the southwest
- The rupture plane does not correlate with any known faults or fault trends within the area
- The earthquake occurred below a quarry and was likely caused by changes in the local state of stress due to the excavation of large quantities of rock from the 1950s to 1992 and the flooding of the quarry in 1992

9 December 2003, Emb 4.5, Central Virginia

The 9 December 2003 earthquake in central Virginia is the third largest instrumentally located earthquake within the PSEG Site region. The earthquake was felt in Virginia, Maryland, North Carolina, New Jersey, New York, Pennsylvania, and West Virginia (References 2.5.2-86 and 2.5.2-87). The highest reported felt intensity was MMI VI near Bremo Bluffs and Kent Store, Virginia where minor damage occurred. The earthquake is located approximately 291 km (181 mi.) from the PSEG Site, and the USGS Community Internet Intensity Map for the earthquake does not have any felt reports from the region immediately surrounding the PSEG Site area (Reference 2.5.2-88). A detailed seismological investigation of the earthquake was conducted by Kim and Chapman (Reference 2.5.2-53) that reported on the results of a temporary installation of seismographs to map aftershock patterns, conducted a regional stress analysis, relocated the earthquake hypocenter, determined the earthquake focal mechanism, and determined potential fault planes for the earthquake. The main results of the study were that:

- The earthquake was a compound earthquake consisting of two nearly identical events occurring 12 seconds (sec.) apart and approximately 300 m (984 ft.) from one another
- It is ambiguous as to whether or not the two earthquakes occurred on the same fault planes because the lack of aftershocks and high-quality waveform data from nearby

**PSEG Site
ESP Application
Part 2, Site Safety Analysis Report**

stations prevent conclusive identification of a fault plane

- Focal mechanisms for the earthquakes indicate thrust faulting with a P axis trending 301° and plunging subhorizontal (19°)
- The depth of the earthquake is constrained to be at 10 ± 2 km (6.2 ± 1.2 mi.) indicating that the event occurred above the southern Appalachian detachment separating Precambrian basement from overlying Paleozoic and Mesozoic rocks and fault systems, consistent with the pattern of seismicity within the Central Virginia Seismic Zone;
- The earthquake cannot be attributed to any identified fault
- There is no reported ground deformation associated with the earthquake
- Measured peak ground acceleration at the closest station 47 km (29 mi.) from the epicenter was 0.028g

9 October 1871, Emb 4.45, Wilmington, Delaware

The location and magnitude of the 9 October 1871 earthquake is based on patterns of felt intensity. The earthquake was felt in New Jersey and Delaware (Reference 2.5.2-79). The maximum felt intensity for the earthquake, MMI VII, was felt near Wilmington, DE where chimneys were toppled and windows were broken (Reference 2.5.2-79). The location of the earthquake within the CEUS-SSC NUREG-2115 earthquake catalog is approximately 26 km (16 mi.) from the PSEG Site, and there are no known records of felt effects at the PSEG Site. The earthquake has not been positively correlated to any geologic structures, and there were no reported ground failures associated with the earthquake. The Hope Creek Generating Station UFSAR for Units 1 and 2 (Reference 2.5.2-70) discusses the earthquake in detail:

“This shock is the largest earthquake in historic time, originating in or near the Piedmont, and because of its close proximity to the site area is considered to be the most significant to the HCGS seismic design analysis. Accurate location of its epicenter is difficult because of limited available information. Based on damage reports and intensities felt, the epicenter has been located near Wilmington, Delaware, whereas the shock was felt from near Chester, Pennsylvania on the north, to Middletown, Delaware on the south and from Salem, New Jersey on the east to Oxford, Pennsylvania on the west. The initial shock was followed by a much smaller shock just after midnight on October 10th. A contemporary newspaper account indicates that the initial shock was felt at Wilmington “with great distinctness.” Buildings were shaken severely and a number of chimneys were damaged in the surrounding towns of Oxford, Pennsylvania, and New Castle and Newport, Delaware. An interesting aspect of this earthquake is the fact that it was accompanied by a very loud sound, as of an explosion. This loud noise, in fact, led to the belief that the shock was caused by an explosion, probably at the powder mill of E.I. DuPont de Neumours Company, near Wilmington. This possibility was carefully investigated at the time and it was concluded that the shock was a legitimate earthquake” (Reference 2.5.2-70).

2.5.2.2 Geologic and Tectonic Characteristics of the Site and Region

Guidance from the NRC regarding seismic source characterizations is presented in RG 1.208. This guidance states that:

“...PSHA should be conducted with up-to-date interpretations of earthquake sources, earthquake recurrence, and strong ground motion estimation”.

**PSEG Site
ESP Application
Part 2, Site Safety Analysis Report**

The issued guidance also states that:

“... seismic sources and data accepted by the NRC in past licensing decisions may be used as a starting point (for the PSHA).”

As part of the acceptance of these studies, RG 1.208 states that site-specific geological, geophysical, and seismological studies should be conducted to determine if these accepted source models adequately describe the seismic hazard for the site of interest given any new data developed since acceptance of the original models. The regulatory guidance explicitly states that:

“The results of these investigations will also be used to assess whether new data and their interpretation are consistent with the information used in recent probabilistic seismic hazard studies accepted by NRC staff. If new data, such as new seismic sources and new ground motion attenuation relationships, are consistent with the existing earth science database, updating or modification of the information used in the site specific hazard analysis is not required. It will be necessary to update seismic sources and ground motion attenuation relationships for sites where there is significant new information provided by the site investigation”.

For the case of new information requiring updated source characterizations, RG 1.208 recommends that the development of updated source characterizations conform to the guidance presented in NUREG/CR-6372, Recommendations for Probabilistic Seismic Hazard Analysis: Guidance on Uncertainty and Use of Experts. NUREG/CR-6372, prepared by a Senior Seismic Hazard Analysis Committee (SSHAC), provides recommendations on the development of PSHA studies for nuclear facilities. A primary recommendation of the SSHAC is that for a given technical issue (i.e., source zone characterization):

“The following should be sought ... (1) a representation of the legitimate range of technically supportable interpretations among the entire informed technical community...”

The SSHAC outlines four levels of study for developing the range of interpretations with the choice of level depending on the complexity of the issue to be addressed. The four levels, Level 1 through 4, are distinguished by the increasing levels of sophistication, resources, and participation by technical experts.

For the PSEG Site, the CEUS-SSC source characterization (NUREG-2115) is used as the base source model for determining the GMRS. The CEUS-SSC model is chosen because the CEUS-SSC model replaces the EPRI-SOG source characterizations (Reference 2.5.2-35) as an acceptable base model and because of the availability of detailed documentation describing the CEUS-SSC model (NUREG-2115). Another supporting reason for using the CEUS-SSC model is that the CEUS-SSC methodology and resultant source characterizations are consistent with a high level SSHAC study (Level 3), and the final aggregate source characterizations were developed to:

“...provide high levels of confidence that the data, models, and methods of the larger technical community have been considered and the center, body, and range of

**PSEG Site
ESP Application
Part 2, Site Safety Analysis Report**

technically defensible interpretations have been included” (Executive Summary page 1xxxv, NUREG-2115).

As required by RG 1.208, site and regional data collected for the PSEG Site and presented in Subsection 2.5.1, Subsection 2.5.2.1 and Subsection 2.5.4 have been reviewed to:

“...determine whether there are any new data or interpretations that are not adequately incorporated into the existing PSHA databases”

As stated within the regulatory guidance, if significant new data or interpretations are found, they require updating of the CEUS-SSC source characterizations. No new data or interpretations have been found since the publication of NUREG-2115, therefore, it has been determined that no new data exists that requires alteration of the CEUS-SSC source characterizations for the PSEG Site except for the inclusion of the AHEx-E seismic source zone (see Subsection 2.5.2.1.2).

The following subsections present the seismic source characterizations from the CEUS-SSC model in NUREG-2115 considered for the PSEG Site. The AHEx-E seismic source zone is presented in Subsection 2.5.2.1.2.

2.5.2.2.1 Summary of CEUS-SSC Source Model

The CEUS-SSC model has two types of seismic sources. The first, termed distributed seismicity sources, uses the recorded history of seismicity to model the frequency and spatial distribution of moderate to large earthquakes ($M \geq 5$). The background distributed seismicity sources are made up of Mmax and seismotectonic zones. The second type of seismic source uses the paleo-earthquake record to model the frequency and spatial distribution of repeated large magnitude earthquakes (RLMEs) at specific locations. Figure 2.5.2-67 illustrates the master logic tree for the CEUS-SSC model, showing the division of the Mmax, seismotectonic, and RLME sources.

2.5.2.2.1.1 Mmax Sources

The Study Region, which includes the whole study region of the CEUS-SSC (Figure 2.5.2-56) can be treated as a single background source. However, it can also be divided into multiple sources when there are zones of different Mmax distributions. These additional background sources are called Mmax zones. These zones are further divided into Mesozoic Extended and Mesozoic Non-extended zones, and can also be divided based on whether the boundary between the Mesozoic Extended and Mesozoic Non-extended zones is narrow or wide (Figure 2.5.2-68). A list of the Mmax zones is provided in Table 2.5.2-27. Each Mmax source has a unique geometry, seismogenic crustal thickness distribution, characteristic magnitude distribution, and seismicity rates.

2.5.2.2.1.2 Seismotectonic Sources

Similar to Mmax zones, the Study Region can be divided into a number of sources based on seismotectonic features (Figures 2.5.2-69a and 2.5.2-69b). Also, similar to Mmax zones, seismotectonic sources are further divided based on wide and narrow interpretations of source boundaries and whether or not certain sources are included in parts of other sources. A list of

**PSEG Site
ESP Application
Part 2, Site Safety Analysis Report**

the seismotectonic zones is provided in Table 2.5.2-28. Each seismotectonic source has a unique geometry, seismogenic crustal thickness distribution, characteristic magnitude distribution, and seismicity rates.

2.5.2.2.1.3 RLME Sources

RLME sources are additional seismic sources that are superimposed on the Mmax and seismotectonic sources. Table 2.5.2-29 lists the 11 RLME source zones in the CEUS-SSC model. Each RLME source has a unique geometry and/or faulting style, seismogenic crustal thickness distribution, characteristic magnitude distribution, and seismicity rates.

2.5.2.3 Correlation of Earthquake Activity with Seismic Sources

As discussed in Subsection 2.5.2.2.1, the CEUS-SSC published in NUREG-2115 provides a regional seismic source model for use in probabilistic seismic hazard analysis that, in part, uses the spatial distribution of seismicity to subdivide the CEUS-SSC Study Region into seismic source zones. The seismicity catalog used for the CEUS-SSC is described in Subsection 2.5.2.1.1. An updated catalog is developed for use in the PSEG Site efforts (Subsection 2.5.2.1.2), and the two catalogs are compared to assess any changes in the patterns of seismicity or if there exists any correlation between geologic structures and seismicity not identified within the CEUS-SSC study that needs to be accounted for at the PSEG Site. Comparison of the catalogs yields the following conclusions:

- The updated seismicity catalog does not contain any earthquakes within the site region that can be positively associated with a known geologic structure.
- The updated seismicity catalog does not show a pattern of seismicity different from that of the CEUS-SSC catalog that would suggest a new seismic source in addition to those included in the CEUS-SSC characterizations. For the PSEG ESPA, a new seismic source zone (AHX-E) is created, as this small area in and adjacent to the PSEG Site Region is not included in the original CEUS-SSC catalog (see Subsection 2.5.2.1.2).
- The updated seismicity catalog does show a similar spatial distribution of earthquakes to that of the CEUS-SSC catalog, suggesting that no significant revisions to the geometry of seismic sources defined in the CEUS-SSC characterization is required.
- The updated seismicity catalog does not contain any earthquakes that suggest revisions to the Mmax distributions for CEUS-SSC zones is required (see Subsection 2.5.2.1.2).
- Seismicity rates determined from the updated catalog are not significantly different than those determined from the original CEUS-SSC catalog (see Subsection 2.5.2.4.2.1.1).

2.5.2.4 Probabilistic Seismic Hazard Analysis and Controlling Earthquake

The Probabilistic Seismic Hazard Analysis (PSHA) conducted for the PSEG Site is presented in this subsection. Following the procedures outlined in RG 1.165 and RG 1.208, Subsection 2.5.2.4.1 discusses the basis for the PSHA, which uses the CEUS-SSC model in NUREG-2115. Subsection 2.5.2.4.2 presents revisions to the CEUS-SSC model. The only revision is the addition of seismic source zone AHX-E. The description of the ground motion models used is presented in Subsection 2.5.2.4.3. Finally, Subsection 2.4.2.4.4 presents results incorporating these revisions in the form of uniform hazard response spectra (UHS) for rock conditions, including deaggregations of hazard.

**PSEG Site
ESP Application
Part 2, Site Safety Analysis Report**

2.5.2.4.1 CEUS-SSC Probabilistic Seismic Hazard Analysis

The CEUS-SSC (NUREG-2115) was the starting point for probabilistic seismic hazard calculations. This follows the recommendation of RG 1.165 and 1.208. An underlying principle of the CEUS-SSC was that expert opinion on alternative, competing models of earthquake occurrence (size, location, and rates of occurrence) and of ground motion amplitude and its variability should be used to weight alternative hypotheses. The result is a family of weighted seismic hazard curves from which mean and fractile seismic hazard can be derived.

2.5.2.4.2 Revisions to CEUS-SSC Model Used for Probabilistic Seismic Hazard Analysis

The only revision made to the CEUS-SSC model is the addition of seismic source zone AHX-E. A detailed discussion of this source, including the reason for its creation, and its source parameters, is provided in Subsections 2.5.2.1.2 and 2.5.2.4.2.2.1. Table 2.5.2-30 lists the seismic sources used in the PSEG Site PSHA calculations.

2.5.2.4.2.1 Updated Seismicity Catalog

Subsection 2.5.2.1.2 describes the development of an updated seismicity catalog for the PSEG Site Region. This updated catalog documents additional earthquakes through 2011 that have occurred after the earthquake compilation for the CEUS-SSC (which included events through December 31, 2008).

2.5.2.4.2.1.1 Effect on Earthquake Occurrence Rates

The effect of the updated seismicity catalog on earthquake occurrence rates in the study area around the PSEG Site is assessed by computing earthquake recurrence parameters for the study area boundary around the PSEG Site (bounded by 36° to 43° N and 71° to 80° W).

To estimate the observed recurrence within the limit of updated seismicity, it is necessary to use a combined catalog of the original CEUS-SSC seismicity catalog in NUREG-2115 and the PSEG Site Region seismicity catalog update from 2009 through 2011 developed in Subsection 2.5.2.1.2. The observed recurrence is estimated using the methodology described in NUREG-2115 that uses the summation of the equivalent earthquake counts for each of the specified magnitude bins, after applying corresponding weights related to magnitude weighting cases per the logic tree presented in NUREG-2115.

The CEUS-SSC seismicity catalog in NUREG-2115 provides information on the equivalent earthquake counts for each event. The equivalent earthquake counts for the updated seismicity catalog from 2009 through 2011 are estimated using Eq. 3.3.1-12 in NUREG-2115. The value of equivalent earthquake counts is calculated as a function of the standard deviation of the moment magnitude and the magnitude type using Table 3.3-1 in NUREG-2115. The resulting observed earthquake counts for the CEUS-SSC seismicity catalog update are presented in Figure 2.5.2-70. The observed earthquake counts in Figure 2.5.2-70 are compared to the predicted “modeled” earthquake counts. Error bars presented for the observed earthquake counts represent \pm one standard deviation based on Reference 2.5.2-106.

The predicted earthquake values are based on summing up the total events within the specified region after applying corresponding weights related to magnitude weighting cases, the

**PSEG Site
ESP Application
Part 2, Site Safety Analysis Report**

corresponding contributing background sources per the logic tree presented in Appendix H of NUREG-2115, and by accounting for the corresponding completeness times for the corresponding completeness regions for each magnitude bin/magnitude weighting case. The full catalog includes three years past the catalog end date in the CEUS-SSC study and is considered complete for those three years. Hence the completeness times have three years added to them. Figure 2.5.2-70 illustrates that the modeled earthquake recurrence parameters are sufficient and that there is no need to update the earthquake recurrence parameters.

The PSEG Site Region updated seismicity catalog extends at least 380 km (235 mi.) from the PSEG Site and includes the August 23, 2011 Mineral, VA earthquake discussed in Subsection 2.5.2.4.4. The Mineral, VA earthquake occurred approximately 270 km (170mi.) from the PSEG Site, and background sources at that distance are not significant contributors to the mean hazard at the PSEG Site as demonstrated by the deaggregations presented in Subsection 2.5.2.4.4. In addition, the magnitude of the Mineral, VA earthquake of August 23, 2011 did not exceed the minimum Mmax in the Mmax distribution for the underlying Mmax and Paleozoic Extended Crust – Narrow and Wide seismotectonic zones in NUREG-2115. Considering these conditions, evaluation of the need for refinement of earthquake recurrence parameters of those seismotectonic zones is not necessary.

2.5.2.4.2.2 New Seismic Source Characterizations

The only revision made to the CEUS-SSC model is the addition of seismic source zone AHEx-E.

2.5.2.4.2.2.1 Atlantic Highly Extended Crust – East (AHEx-E) Seismic Source Zone

The AHEx-E seismic source zone is modeled as an independent seismic source zone with a probability of activity of 1.0 to eliminate the need to unnecessarily modify the current CEUS-SSC logic tree in NUREG-2115 or perform any refinements to the earthquake recurrence parameters in the CEUS-SSC background source zones (AHEx, STUDY-R, MESE-W, and MESE-N) that share a common boundary with the AHEx-E seismic source zone. The AHEx-E seismic source zone is modeled using uniform seismicity because there is only a single earthquake event in the AHEx-E seismic source zone and because the event occurred outside the 322 km (200 mi.) radius around the PSEG Site. The AHEx-E seismic source zone is added to the CEUS-SSC logic tree in NUREG-2115 as a separate branch with a weight of 1.0.

The earthquake recurrence parameters for the AHEx-E seismic source zone are developed using a methodology consistent with the NUREG-2115 guidance. The three magnitude weighting cases (A, B, and E) with their corresponding regional betas are adopted. The equivalent count of earthquakes (N^*) is computed for the single AHEx-E seismic source zone event using equation 3.3.1-12 from NUREG-2115. The Equivalent Periods of Completeness (TE) from NUREG-2115 are adopted. Three years are added to each of the three Magnitude Weighting Cases to account for the additional three years in the seismicity catalog developed for the PSEG Site (January 1, 2009 to December 31, 2011). Added conservatism is adopted whereby the recurrence rates computed using magnitude weighting cases A and B are given equal weights of 0.5 each in deriving the rate for the AHEx-E seismic source zone, because magnitude case E has a magnitude weight of 0.0 for the magnitude bin 2.9 to 3.6. The rate per unit time and area for the AHEx-E seismic source zone are then compared to the largest rate per unit time and area for the CEUS-SSC source zone boundary points adjacent to the AHEx-E

**PSEG Site
ESP Application
Part 2, Site Safety Analysis Report**

seismic source zone. The rate per unit time and area derived for the AHEx-E seismic source zone using the simplified approach are higher by 35 than those for the boundary points.

Finally, because the AHEx-E seismic source zone is essentially an extension of the AHEx seismic source, the AHEx-E seismic source zone is modeled using the AHEx seismic source crustal thicknesses and Mmax distributions presented in NUREG-2115. Figure 2.5.2-71 provides the logic tree for the AHEx-E seismic source zone.

2.5.2.4.2.2 Ramapo Seismic Zone

As discussed in Subsection 2.5.1.1.5.1, the Ramapo Seismic Zone (RSZ) was identified before the CEUS-SSC study (NUREG-2115) as a region with an apparent increased rate of seismicity west of the Ramapo fault in northern New Jersey and southern New York (References 2.5.2-3, 2.5.2-71, and 2.5.2-72). Originally, activity within the RSZ was hypothesized to be due to slip on the Ramapo Fault, but subsequent studies demonstrated that the Ramapo fault has not been active since the Jurassic (Subsection 2.5.1.1.5.1). Areas like the RSZ may have been classified as special source zones in past PSHA seismic source characterization models (i.e., EPRI-SOG, Reference 2.5.2-35), but, the CEUS-SSC study (NUREG-2115) did not classify the RSZ as a special source zone (i.e., RLME source zone). The magnitudes of the largest observed events in the area (less than **M** 5.5) and lack of evidence of Quaternary slip on faults in the area did not support the RSZ being classified as a special seismic source zone in NUREG-2115.

2.5.2.4.3 EPRI Ground Motion Models

The ground-motion equations presented in the EPRI characterization (GMC) model for the CEUS (Reference 2.5.2-39) are recommended for use by NUREG-2115. These equations estimate median spectral acceleration and its uncertainty as a function of earthquake magnitude and distance. Epistemic uncertainty is modeled using multiple ground motion equations with weights, and multiple estimates of aleatory uncertainty, also with weights. Different sets of equations are recommended for seismic sources that contribute to seismic hazard with moderate vs. large magnitude earthquakes, for sources that represent rifted vs. non-rifted regions of the earth's crust, and for travel paths that are primarily through the stable continental interior vs. through a region that skirts the Gulf of Mexico. Equations are available for hard rock site conditions at spectral frequencies of 100 hertz (Hz) (which is equivalent to peak ground acceleration, PGA), 25 Hz, 10 Hz, 5 Hz, 2.5 Hz, 1 Hz, and 0.5 Hz. All ground motion estimates are for spectral response with 5 percent of critical damping.

Aleatory uncertainties published in the EPRI GMC model were re-examined by Abrahamson and Bommer (Reference 2.5.2-41), because it was thought that the EPRI GMC aleatory uncertainties were probably too large, resulting in over-estimates of seismic hazard. The Abrahamson and Bommer study (Reference 2.5.2-41) recommends a revised set of aleatory uncertainties and weights that can be used to replace the original EPRI GMC estimates of aleatory uncertainty, and is also recommended for use by NUREG-2115.

No CAV filter is used for the PSHA calculations. Instead, a minimum moment magnitude of 5.0 is adopted in the calculations as specified in Reference 2.5.2-111.

**PSEG Site
ESP Application
Part 2, Site Safety Analysis Report**

In summary, the ground motion model used in the seismic hazard calculations consisted of the median equations from EPRI GMC combined with the updated aleatory uncertainties of Abrahamson and Bommer (Reference 2.5.2-41).

2.5.2.4.4 Updated Probabilistic Seismic Hazard Analysis and Deaggregation

A rock PSHA for the PSEG Site was conducted using the CEUS-SSC model and using the EPRI GMC ground motion model, with updated aleatory uncertainties and weights for the CEUS. The single refinement to the CEUS-SSC model is the addition of the single seismic source zone AHX-E, which is given a branch weight of 1.0 and the same EPRI GMC ground motions and updated aleatory uncertainties and weights are used as those used for the CEUS-SSC seismic source zone AHX (see Subsection 2.5.2.1.2).

The rates of earthquakes for the New Madrid Fault System (NMFS) (in-cluster branch) and Charleston (narrow source geometry branch) Repeated Large Magnitude Earthquakes (RLMEs) in the CEUS-SSC (NUREG-2115) are characterized using a time-dependent renewal model, based on the Brownian Passage Time (BPT) renewal model, and a time-independent model (i.e. Poissonian). NUREG-2115 assumes a plant start date of January 1, 2011, and a plant exposure time of 60 years. This start date is not appropriate for use at the PSEG Site, which has an anticipated start time of June 1, 2021. The plant exposure time is the same (60 years) as that assumed in NUREG-2115. Parameters for the renewal appropriate for the PSEG Site are developed to reflect the different start time.

For Charleston, the appropriate renewal parameters are input directly into the rock hazard input source files. To accommodate the clustered earthquake occurrences for NMFS sources, the mean seismic hazard contribution is calculated using a two-step process. First, the seismic hazard is calculated at the PSEG Site using the parameters from NUREG-2115. Second, the mean seismic hazard from the NMFS sources is scaled by the percentage increase in mean occurrence rate (compared to the NUREG-2115 mean recurrence rate) determined using parameters for the renewal model that are appropriate for the PSEG Site.

The first calculation is made for hard rock conditions, which is consistent with the EPRI GMC (Reference 2.5.2-39) ground motion model, and is made without applying the CAV filter. Instead, a minimum moment magnitude of 5.0 is adopted in the calculations as specified in Reference 2.5.2-111. Hard rock hazards are generated for seven spectral frequencies of 0.5, 1, 2.5, 5, 10, 25, and 100 Hz (PGA). The corresponding unsmoothed mean rock Uniform Hazard Response Spectra (UHRS) are derived for mean annual frequencies of exceedance (AFEs) of 10^{-4} , 10^{-5} , and 10^{-6} at the seven spectral frequencies per the guidelines of RG 1.208. Finally, the contribution of AHX-E is evaluated to justify the simplified conservative methodology used in developing the corresponding seismic source parameters.

A PSHA consists of calculating annual frequencies of exceeding various ground motion amplitudes for all possible earthquakes that are hypothesized in a region. The seismic sources specify the rates of occurrence of earthquakes as a function of magnitude and location, and the ground motion model estimates the distribution of ground motions at the site for each event. Multiple weighted hypotheses on seismic sources characteristics, including rates of occurrence and magnitude distribution, and ground motions (characterized by the median ground motion amplitude and its uncertainty) result in multiple weighted seismic hazard curves. From this

**PSEG Site
ESP Application
Part 2, Site Safety Analysis Report**

family of weighted curves, the mean and fractile seismic hazard can be determined. The calculation is made separately for background sources and each RLME source, and the seismic hazard distribution for the sources are combined, weighting each source equally. This combination gives the overall mean and distribution of seismic hazard at the site.

Figures 2.5.2-18 through 2.5.2-24 present mean and fractile (5th, 16th, median, 84th, and 95th) rock seismic hazard curves from this calculation for the spectral frequencies of 100 Hz (PGA), 25 Hz, 10 Hz, 5 Hz, 2.5 Hz, 1 Hz, and 0.5 Hz, respectively. Table 2.5.2-31 provides the fractile and mean rock seismic hazard curves for the seven spectral frequencies in tabular form. Figure 2.5.2-72 illustrates the total mean and median rock UHRS at the PSEG Site for 10^{-4} , 10^{-5} , and 10^{-6} mean annual frequencies of exceedances (AFEs). Table 2.5.2-32 provides the mean and median rock UHRS values for this calculation. Figures 2.5.2-73 through 2.5.2-75 illustrate the contribution of source AHX-E to the total mean site hazard at the PSEG Site for spectral frequencies 1 Hz, 10 Hz, and 100 Hz (PGA), respectively. These figures confirm that AHX-E has an insignificant impact on the hazard at the PSEG Site. The calculation of rock hazard without CAV was used to deaggregate the hazard and identify the magnitudes and distances appropriate to represent rock spectral shapes for site response calculations.

The rock seismic hazard without CAV is deaggregated following the guidelines of RG 1.208. Specifically, the mean contributions to seismic hazard for 1 Hz and 2.5 Hz are deaggregated by magnitude and distance from the PSEG Site (R) for the mean 10^{-4} ground motion amplitude at 1 Hz and at 2.5 Hz, and these deaggregations are combined (contributions for each magnitude and distance bin are averaged). Figure 2.5.2-25 depicts this combined deaggregation. Similar deaggregations of the mean hazard are performed for 5 Hz and 10 Hz spectral accelerations (Figure 2.5.2-26). Deaggregations of the mean hazard for 10^{-5} and 10^{-6} ground motions are shown in Figures 2.5.2-27 through 2.5.2-30. For these figures, deaggregation is given in terms of moment magnitude.

The deaggregation plots in Figures 2.5.2-25 through 2.5.2-30 indicate that local earthquakes are the major contributor to seismic hazard at the PSEG Site for both high frequencies (5 Hz and 10 Hz) and low frequencies (1 Hz and 2.5 Hz). The peaks around 1300 km (808 mi.), (Figures 2.5.2-25, 2.5.2-27, and 2.5.2-29) correspond with the NMFS RLME source. The Charleston RLME source is approximately 660-980 km (approximately 410-609 mi.) from the PSEG Site and the Charlevoix RLME source is approximately 930-1050 km (approximately 578-652 mi.) from the PSEG Site. These sources do not appear on the deaggregation plots due to their low percent contribution, except for the 1 Hz and 2.5 Hz 10^{-4} plot (Figure 2.5.2-25).

Table 2.5.2-33 provides the percent contributions for various magnitude and distance bins for the six deaggregations, and Table 2.5.2-34 indicates mean magnitudes and distances from the PSEG Site (R) calculated from the deaggregations, for all contributions to hazard and for contributions with R less than 100 km (62 mi) and exceeding 100 km (62 mi.). For the 1 Hz and 2.5 Hz results, contributions from events with $R > 100$ km (62 mi.) exceed 36 percent of the total hazard for the 10^{-4} and 15 percent of the total hazard for the 10^{-5} deaggregations, and is approximately 3 percent for the 10^{-6} deaggregation. As a result, following the guidance of RG 1.208, the controlling earthquakes for low-frequency (LF) ground motions are selected from the $R > 100$ km (62 mi.) calculations, and the controlling earthquakes for high-frequency (HF) ground motions are selected from the overall calculations. The values of the moment magnitude (**M**) and R selected in this way are provided in shaded cells in Table 2.5.2-34.

**PSEG Site
ESP Application
Part 2, Site Safety Analysis Report**

Smooth UHRS are developed from the UHRS amplitudes in Table 2.5.2-32, using controlling earthquake **M** and **R** values shown in Table 2.5.2-34 and using the hard rock spectral shapes for CEUS earthquake ground motions recommended in NUREG/CR-6728. Separate spectral shapes are developed for high frequency (HF) and low frequency (LF). In order to reflect accurately the UHRS values calculated by the PSHA as shown in Table 2.5.2-32, the HF spectral shape is anchored to the UHRS values from Table 2.5.2-32. For the 10^{-4} AFE hazard level, the HF spectral shape, derived from NUREG/CR-6728, is scaled to the UHRS amplitudes at 5, 10, 25, and 100 Hz (PGA). The NUREG/CR-6728 spectral shape defines the HF spectrum between 0.5 and 5 Hz anchored (scaled) to the UHRS amplitude at 5 Hz. For the 10^{-5} and 10^{-6} HF response spectrum, the HF spectral shape scaled to 5 Hz exceeds the 2.5 Hz UHRS value, therefore, the HF spectral shape, derived from NUREG/CR-6728, is scaled to the UHRS amplitudes at 2.5, 5, 10, 25, and 100 Hz (PGA). The NUREG/CR-6728 spectral shape defines the HF spectrum between 0.5 and 2.5 Hz anchored (scaled) to the UHRS amplitude at 2.5 Hz.

For each AFE hazard level, the LF spectral shape, derived from the NUREG/CR-6728, is scaled to the UHRS amplitudes at 0.5, 1, and 2.5 Hz. The NUREG/CR-6728 spectral shape defines the LF spectrum above 2.5 Hz when anchored (scaled) to the UHRS amplitude at 2.5 Hz. To create these spectral shapes, the single-corner and double-corner models recommended in NUREG/CR-6728 are weighted equally for each AFE hazard level, and for both HF and LF. For frequencies below 0.5 Hz, the spectral shape is extrapolated from the value at 0.5 Hz assuming a constant spectral velocity (i.e., spectral accelerations are assumed to scale linearly with frequency) down to 0.167 Hz (6 sec period). From 0.167 Hz to 0.1 Hz, spectral accelerations are assumed to scale as the square of the frequency. This follows the recommendation of Federal Emergency Management Agency (FEMA) 450 (Reference 2.5.2-21) for long periods. Some smoothing of the 10^{-4} and 10^{-5} AFE LF spectrum is applied between 0.6 Hz and 2 Hz to avoid bumps in this frequency range that are apparent if no smoothing is applied.

Figures 2.5.2-31 through 2.5.2-33 present the horizontal HF and LF spectra calculated in this way for 10^{-4} , 10^{-5} , and 10^{-6} annual frequencies of exceedance, respectively. As mentioned previously, these spectra accurately reflect the rock UHRS amplitudes in Table 2.5.2-32 that are calculated for the seven spectral frequencies. For each AFE hazard level, the envelope spectrum (smooth mean rock UHRS) is also calculated. Figure 2.5.2-76 shows the smooth mean rock 10^{-4} , 10^{-5} , and 10^{-6} AFE UHRS for the PSEG Site.

2.5.2.5 Seismic Wave Transmission Characteristics of the Site

The subsurface conditions necessary to predict and model the seismic wave transmission characteristics for the PSEG Site are determined from both site-specific and regional data. This data included both stratigraphic and representative shear-wave measurements, degradation properties of the soils, and the uncertainties associated with these parameters. A detailed presentation of these parameters, as well as a discussion of the data and methodology for developing them, are provided in Subsections 2.5.4.2 through 2.5.4.7.

The profile is divided into the shallow profile (surface to about 400 ft.) and the deep profile (about 400 ft. to "basement"). The shallow profile represents depth to which extensive characterization has been performed. The lateral and vertical control on the subsurface strata (layering) is defined primarily on lithology and material properties. The GMRS is developed for the top of the Competent Layer (Layer 1) (Figure 2.5.4.7-8a), following the guidance of RG

**PSEG Site
ESP Application
Part 2, Site Safety Analysis Report**

1.208, which has a mean elevation of -67 feet. Soils above this elevation are considered only for the purposes of calculating confining stresses.

2.5.2.5.1 Aleatory and Epistemic Uncertainty

The uncertainties in most of the site-characterization parameters are developed in Subsection 2.5.4.7 and are summarized here. Other necessary parameters not described in Subsection 2.5.4.7 are developed in this subsection.

Uncertainty in shear-wave velocities is specified by means of its Coefficient of Variation (COV). This COV takes a value of 0.25 for the top 160 ft. of the shallow profile, 0.30 for the deeper portion of the shallow profile, and 0.35 for the deep profile.

Uncertainty in the stratigraphy is also described in Subsections 2.5.4.1, 2.5.4.7.2, and 2.5.4.7.4, including uncertainty in the depth to basement rock. These uncertainties are specified as standard deviations or ranges for the elevation of the top of each layer.

Uncertainties in the degradation properties for soils in the shallow profile are discussed in Subsection 2.5.4.7.5. These values are roughly comparable to those recommended by Costantino (Reference 2.5.2-28) and by EPRI (Reference 2.5.2-38). For the deep profile and bedrock, which have strain-independent properties, the uncertainty in damping is characterized by a COV of 0.35 based on the recommendations in EPRI (Reference 2.5.2-38).

2.5.2.5.2 Description of Site Response Analysis

The site response analysis is conducted in three steps that are common to analyses of this type. First, the site geology and geotechnical properties in Subsections 2.5.4.1, 2.5.4.2, and 2.5.4.7, and the assessments of uncertainty described in Subsection 2.5.2.5.1 are reviewed and used to generate multiple synthetic profiles of site characteristics. Second, sets of rock spectra are selected to represent rock ground motions corresponding to mean annual exceedance frequencies of 10^{-4} , 10^{-5} , and 10^{-6} . Finally, site response is calculated using an equivalent-linear technique, using the multiple synthetic profile and the sets of rock spectra representing input motions. These three steps are described in detail in the following subsections.

2.5.2.5.2.1 Generation of Synthetic Profiles

To account for the epistemic and aleatory uncertainties in the site's dynamic properties, 60 synthetic profiles are generated using the stochastic model developed by Toro (Reference 2.5.2-84), with some modifications to account for the conditions at the PSEG Site. These synthetic profiles represent the site column from the top of the bedrock to the top of the Competent Layer, where the GMRS is defined. Bedrock is defined as having a shear-wave velocity of 9,200 ft/sec, in order to achieve consistency with the EPRI attenuation equations used for the rock hazard calculations (Reference 2.5.2-39). This stochastic model uses as inputs the following quantities, provided from Subsections 2.5.2.5.1 or 2.5.4.2, 2.5.4.4, and 2.5.4.7: (1) the mean shear-wave velocity profile, provided in Table 2.5.2-17; (2) the standard deviation of $\ln(V_s)$ (the natural logarithm of the shear-wave velocity) as a function of depth below the top of the Competent Layer, provided in Table 2.5.2-17 and is taken as identical to the COV values given in Subsection 2.5.2.5.1; (3) the correlation coefficient between $\ln(V_s)$ in adjacent layers, from generic results in Toro (Reference 2.5.2-84); and (4) the uncertainties in

**PSEG Site
ESP Application
Part 2, Site Safety Analysis Report**

the depths to the top of the various layers, provided in Table 2.5.2-18 (note that the standard deviations for the shallow profile take into account that the elevation of the top of Competent Layer is itself uncertain).

The correlation coefficient between $\ln(V_s)$ in adjacent layers is estimated using the inter-layer correlation model from Toro (Reference 2.5.2-84) for USGS category A+B, which corresponds to V_{s30} values of 360 m/s ($\sim 1,180$ ft./s) or greater. This correlation model predicts fairly high correlation coefficients, except for the very top of the profile. For instance, the correlation coefficient is approximately 75 percent at a depth of 50 ft. and higher values at greater depths.

Figures 2.5.2-34 and 2.5.2-35 present the V_s values of the 60 synthetic profiles, for the entire profile and shallow profile, respectively. Figures 2.5.2-36 and 2.5.2-37 compare the logarithmic means of these 60 V_s profiles to the $V_s \pm$ Variability values provided in Table 2.5.2-17, indicating excellent agreement. The difference near the bottom of the profile occurs because the values in Table 2.5.2-17 do not take into account the depth to bedrock and its uncertainty.

For the randomization of the degradation properties, the standard deviations given in Subsection 2.5.4.7.5 are read at a strain of $3.16E-2$, converted to logarithmic standard deviations and used as input to the randomization calculations. To account for a possible range in the Overconsolidation Ratio (OCR) of Layers 1 through 9B in Table 2.5.2-17 (varying from 2 to 6), idealized G/G_{max} and damping curves are developed whose median and standard deviations bound the respective curves for the range of OCRs as shown in Figures 2.5.2-77 through 2.5.2-80. The randomization software extends these uncertainty values to other strains, tapering them near the ends to achieve physically reasonable curves for the synthetic G/G_{max} and damping curves. The correlation coefficient between $\ln(G/G_{max})$ and $\ln(\text{damping})$ in the fill is specified as -0.75. This implies that in synthetic profiles where the fill has higher than average G/G_{max} , the fill tends to have lower than average damping. The degradation and damping properties are treated as fully correlated among layers with the same soil type, but independent between different soil types. In this analysis, damping values are truncated at 15 percent as is standard practice.

Figures 2.5.2-77 through 2.5.2-80 illustrate the modulus-degradation and damping curves for layers 1, 2-5, 6-8, and 9A/9B, respectively used in the 60 synthetic profiles.

Each set of 60 synthetic profiles, consisting of V_s and unit weight vs. depth, depth to bedrock, stiffness, and damping curves, is used to calculate and quantify site response and its uncertainty, as described below.

2.5.2.5.2.2 Selection of Rock Input Motions

Rock input motions are selected for input to the site response calculations using the seismic hazard and deaggregation results. Six separate input motions are considered, corresponding to HF and LF motions at 10^{-4} , 10^{-5} , and 10^{-6} . The development of spectra for these motions is presented in Subsection 2.5.2.4.4 and illustrated in Figures 2.5.2-31 through 2.5.2-33.

2.5.2.5.2.2.1 Site Response Calculations

The site response calculations for the PSEG Site are performed using the Random Vibration Theory (RVT) approach. In many respects, the inputs and assumptions are the same for an

**PSEG Site
ESP Application
Part 2, Site Safety Analysis Report**

RVT analysis and for a time-history based analysis (e.g., an analysis with the program SHAKE (Reference 2.5.2-47). Both the RVT and SHAKE procedures use a horizontally layered half-space representation of the site and use an equivalent-linear representation of dynamic response to vertically propagating shear waves. Starting from the same inputs (in the form of response spectra), both procedures result in similar estimates of site response (Reference 2.5.2-73). The main advantage of the RVT approach is that it does not require the spectral matching of multiple time histories to a given rock response spectrum. Instead, the RVT approach uses a probabilistic representation of the ensemble of all input motions corresponding to that given response spectrum and then calculates the response spectrum of the ensemble of dynamic responses.

Site-response calculations are performed for the six bedrock motions as described in the previous subsection.

In addition to the rock response spectra, the RVT site-response calculations require the following inputs: (1) the strong-motion duration (T) associated with each rock spectrum; and (2) the equivalent-strain ratio to use in the equivalent-linear calculations (this input is required for both the time-history and RVT approaches and depends on magnitude). The duration is calculated from the deaggregation results in Subsection 2.5.2.4.4 (Table 2.5.2-34), using standard seismological relations between magnitude, seismic moment, corner frequency (f_c), and duration (Reference 2.5.2-73), and stress-drop and crustal V_s values typical of the eastern United States. The effective strain ratio is calculated using the expression $(M-1)/10$ (Reference 2.5.2-47), where M is moment magnitude. Values smaller than 0.5 or greater than 0.65 are brought into the 0.5-0.65 range, which is the range recommended by Kramer (Reference 2.5.2-54). The calculated values of duration and effective strain ratio are given in Table 2.5.2-19.

For each rock-motion input, separate site response calculations are performed for the corresponding 60 synthetic profiles, and these results are used to calculate the logarithmic mean and standard deviation of the amplification factor. Figures 2.5.2-40 and 2.5.2-41 present the amplification factors computed for the 60 synthetic profiles, for the 10^{-4} HF and LF motions, and the resulting logarithmic mean and standard deviation. Figures 2.5.2-42 and 2.5.2-43 present the logarithmic mean and standard deviation of the amplification factor for all three exceedance frequencies considered. Tables 2.5.2-20 and 2.5.2-21 present these results in Tabular form.

Figures 2.5.2-44 and 2.5.2-45 provide the peak strains as a function of depth for the 60 synthetic profiles, for the 10^{-4} HF and LF rock motions. Results are shown only for the shallow portion of the profile because the properties of the deep profile are independent of strain.

2.5.2.6 Ground Motion and Site Response Analysis

2.5.2.6.1 Ground Motion Response Spectrum (GMRS)

With the site-specific amplification described in Subsection 2.5.2.5, the seismic hazard model described in Subsection 2.5.2.4 is reanalyzed incorporating the site amplifications into the hazard calculations. For ground motions below the 10^{-4} amplitudes, site amplification is assumed to be the same as for the 10^{-4} amplitudes (Tables 2.5.2-20 and 2.5.2-21). For ground motions greater than the 10^{-6} amplitudes, site amplification is assumed to be the same as for the 10^{-6} amplitudes (Tables 2.5.2-20 and 2.5.2-21). The logarithmic standard deviations in Tables

**PSEG Site
ESP Application
Part 2, Site Safety Analysis Report**

2.5.2-20 and 2.5.2-21 are used to represent uncertainties in site response. A minimum moment magnitude (**M**) of 5.0 is used in the calculations (no CAV filter was applied), using Vs30m for surface conditions for the PSEG Site - 730 m/s (2395 ft/sec) and using amplitudes at the surface after site effects have been taken into account.

The amplification factors for the HF input spectra are used for hazard calculations at 5, 10, 25, and 100 Hz (peak ground acceleration; PGA), and the amplification factors for the LF input spectra are used for hazard calculations at 0.5, 1, and 2.5 Hz. Figures 2.5.2-31 through 2.5.2-33 illustrate that the HF rock spectra dominate the high frequencies and the LF rock spectra dominate the low frequencies.

Figures 2.5.2-46 through 2.5.2-52 present seismic hazard curves for the seven spectral frequencies at which ground motion equations are available for the GMRS elevation. These figures cover a frequency range from PGA (100 hz) in Figure 2.5.2-46 to 0.5 hz (Figure 2.5.2-52). Seismic hazard data for the GMRS elevation are provided in Table 2.5.2-22. Table 2.5.2-23 provides mean and median amplitudes for annual frequencies of 10^{-4} , 10^{-5} , and 10^{-6} . The mean and median soil UHRS for 10^{-4} , 10^{-5} , and 10^{-6} are presented in Figure 2.5.2-53.

2.5.2.6.1.1 Horizontal GMRS Spectrum

The horizontal Ground Motion Response Spectra (GMRS) is developed from the horizontal soil UHRS using the approach described in ASCE/SEI Standard 43-05 (Reference 2.5.2-4) and RG 1.208.

The ASCE/SEI Standard 43-05 (Reference 2.5.2-4) approach defines the GMRS using the site-specific UHRS, which is defined for Seismic Design Category SDC-5 at a mean 10^{-4} annual frequency of exceedance. The procedure for computing the GMRS is as follows:

For each spectral frequency at which the UHRS is defined, a slope factor A_R is determined from:

$$A_R = SA(10^{-5}) / SA(10^{-4}) \quad (\text{Equation 2.5.2-2})$$

where $SA(10^{-4})$ is the spectral acceleration SA at a mean UHRS exceedance frequency of 10^{-4} /yr (and similarly for $SA(10^{-5})$). A Design Factor "DF" is defined based on A_R , which reflects the slope of the mean hazard curve between 10^{-4} and 10^{-5} mean annual frequencies of exceedance. The DF at each spectral frequency is given by:

$$DF = 0.6(A_R)^{0.80} \quad (\text{Equation 2.5.2-3})$$

and

$$GMRS = \max[SA(10^{-4}) \times \max(1, DF), 0.45 \times SA(10^{-5})] \quad (\text{Equation 2.5.2-4})$$

The derivation of DF is described in detail in Reference 2.5.2-4 and in RG 1.208. Table 2.5.2-24 tabulates the horizontal GMRS. The horizontal GMRS is plotted in Figure 2.5.2-54.

**PSEG Site
ESP Application
Part 2, Site Safety Analysis Report**

2.5.2.6.1.2 Vertical GMRS Spectrum

The vertical GMRS is developed using vertical-to-horizontal (V/H) ratios. NRC RG 1.60 and NUREG/CR-6728 provide proposed V/H ratios for design spectra for nuclear facilities, and these V/H ratios are plotted in Figure 2.5.2-55. The V/H ratios in the portion of Figure 2.5.2-55 labeled “NUREG/CR-6728 CEUS rock” are from Table 4-5 in NUREG/CR-6728. The values are those recommended for rock sites in the CEUS when the horizontal PGA ranges from 0.2g to 0.5g, which is the case for the horizontal GMRS at the PSEG Site. These V/H ratios are shown for background information only. For soil conditions, two ground motion prediction equations are used based on empirical data from the Western United States (WUS), Campbell and Bozorgnia (Reference 2.5.2-112) and Gülerce and Abrahamson (Reference 2.5.2-113) because these studies enable prediction of V/H ratios as a function of **M** and **R**. Two earthquakes are used for this calculation, corresponding to the **M** and **R** values presented in Table 2.5.2-34 for HF 10^{-4} and 10^{-5} spectra: **M**=5.9 and **R**=27 km (16.7 mi.), and **M**=6.0 and **R**=12 km (7.5 mi.). The GMRS is between the 10^{-4} and 10^{-5} UHRS as shown in Figure 2.5.2-81 but these **M** and **R** values are indicative of the magnitudes and distances that cause the GMRS ground motion.

Two sets of V/H ratios are presented on Figure 2.5.2-55 for each of the two WUS ground motion prediction equations. The first set is labeled “unshifted” and is taken directly from each respective ground motion prediction equation for the corresponding HF controlling earthquake. The second set of V/H ratios, labeled “shifted” recognizes that CEUS earthquake ground motions tend to have more high-frequency content than their WUS counterparts. To approximate what might be a V/H ratio for soil conditions in the CEUS, the WUS soil V/H ratios are shifted by scaling the frequency by a factor of 3, which shifts the peak V/H ratio to higher frequencies. The locations of the peak for the “shifted” V/H ratios are consistent with the peak in the “NUREG/CR-6728 CEUS rock” V/H ratio.

Based on these comparisons, the recommended V/H ratios for the PSEG Site are 1.15 at spectral frequencies between 40 Hz and 100 Hz, 0.75 for frequencies from 0.1 Hz to 5 Hz. Between the frequencies of 5 and 40 Hz the V/H ratio is assumed to vary linearly from 0.75 at 5 Hz up to 1.15 at 40 Hz. The recommended V/H ratios are depicted on Figure 2.5.2-55 as a solid black line. These recommended V/H ratios bound the V/H ratios described above, except the RG 1.60 ratio, which is considered obsolete because it is based on a small number of ground motions recorded prior to 1973.

Vertical spectra are scaled from the horizontal spectra using the V/H ratios. The vertical GMRS is calculated by multiplying the horizontal GMRS at each frequency by the V/H ratio depicted by the solid black line in Figure 2.5.2-55. Figure 2.5.2-54 illustrates the horizontal GMRS and the vertical GMRS calculated using this method. The V/H ratios and vertical GMRS values are provided in Table 2.5.2-24.

**PSEG Site
ESP Application
Part 2, Site Safety Analysis Report**

2.5.2.7	References
2.5.2-1	Not Used
2.5.2-2	Not Used
2.5.2-3	P. Aggarwal, Y., and L. Sykes. "Earthquakes, Faults, and Nuclear Power Plants in Southern New York and Northern New Jersey." <i>Science</i> 200, no. 28 (1978): 425-29.
2.5.2-4	American Society of Civil Engineers (ASCE). "Seismic Design Criteria for Structures, Systems, and Components in Nuclear Facilities." 81. Reston, VA: ASCE/SEI 43-05, 2005.
2.5.2-5	Not Used
2.5.2-6	Not Used
2.5.2-7	Not Used
2.5.2-8	Not Used
2.5.2-9	Not Used
2.5.2-10	Not Used
2.5.2-11	Not Used
2.5.2-12	Not Used
2.5.2-13	Not Used
2.5.2-14	Bollinger, G. A. "Seismicity of the Central Appalachian States of Virginia, West Virginia, and Maryland—1758 through 1968 " <i>Bulletin of Seismological Society of America</i> 59 (1969): 2103-11.
2.5.2-15	Bollinger, G. A. "Seismicity of the Southeastern United States." <i>Bulletin of Seismological Society of America</i> 63 (1973): 1785-808.
2.5.2-16	Not Used
2.5.2-17	Not Used
2.5.2-18	Not Used
2.5.2-19	Not Used
2.5.2-20	Not Used

**PSEG Site
ESP Application
Part 2, Site Safety Analysis Report**

2.5.2-21	Building Seismic Safety Council. "NEHRP Recommended Provisions for Seismic Regulations for New buildings and Other Structures (FEMA 450) 2003 Edition." FEMA Report 450, 2004.
2.5.2-22	Not Used
2.5.2-23	Not Used
2.5.2-24	Not Used
2.5.2-25	Not Used
2.5.2-26	Not Used
2.5.2-27	Not Used
2.5.2-28	Costantino, C. J. "Recommendations for Uncertainty Estimates in Shear Modulus Reduction and Hysteretic Damping Relationships." In Description and Validation of the Stochastic Ground Motion Model, edited by W. Silva, N. Abrahamson, G. Toro and C. J. Costantino: Dept. Nuclear Energy, Brookhaven National Laboratory, contract number 770573, 1996.
2.5.2-29	Not Used
2.5.2-30	Not Used
2.5.2-31	Not Used
2.5.2-32	Not Used
2.5.2-33	Not Used
2.5.2-34	Not Used
2.5.2-35	Electric Power Research Institute (EPRI). Seismic Hazard Methodology for the Central and Eastern United States (NP-4726), Vol. 1-3 & 5-10. 10 vols. Vol. Volumes 1-10: EPRI, 1986-1989.
2.5.2-36	Not Used
2.5.2-37	Not Used
2.5.2-38	Electric Power Research Institute (EPRI). Guidelines for Determining Design Basis Ground Motions (TR-102293). Palo Alto, CA: EPRI, 1993.
2.5.2-39	Electric Power Research Institute (EPRI). "CEUS Ground Motion Project Final Report." Palo Alto, CA: EPRI, report 1009684, 2004.

**PSEG Site
ESP Application
Part 2, Site Safety Analysis Report**

2.5.2-40	Not Used
2.5.2-41	Electric Power Research Institute (EPRI). "Truncation of the Lognormal Distribution and Value of the Standard Deviation for Ground Motion Models in the Central and Eastern United States." Palo Alto, CA: EPRI, report 1014381, 2006.
2.5.2-42	Not Used
2.5.2-43	Not Used
2.5.2-44	Not Used
2.5.2-45	Not Used
2.5.2-46	Not Used
2.5.2-47	Idriss, I., and J. I. Sun. "Users Manual for SHAKE91." 1992.
2.5.2-48	Not Used
2.5.2-49	Not Used
2.5.2-50	Not Used
2.5.2-51	Kafka, A. L., E. A. Schlesinger-Miller, and N. L. Barstow. "Earthquake Activity in the Greater New York City Area: Magnitudes, Seismicity, and Geologic Structures " Bulletin of Seismological Society of America 75 (1985): 1285-300.
2.5.2-52	Not Used
2.5.2-53	Kim, Won-Young, and Martin C. Chapman. "The 9 December 2003 Central Virginia Earthquake Sequence: A Compound Earthquake in the Central Virginia Seismic Zone." Bulletin of the Seismological Society of America 95 (2005): 2428-45.
2.5.2-54	Kramer, S. L. Geotechnical Earthquake Engineering: Prentice Hall, 1996.
2.5.2-55	Not Used
2.5.2-56	Not Used
2.5.2-57	Not Used
2.5.2-58	Not Used
2.5.2-59	MacCarthy, G. R. "A Note on the Virginia Earthquake of 1833." Bulletin of Seismological Society of America 48 (1958): 177-80.
2.5.2-60	Not Used

**PSEG Site
ESP Application
Part 2, Site Safety Analysis Report**

2.5.2-61	Not Used
2.5.2-62	Not Used
2.5.2-63	Not Used
2.5.2-64	National Earthquake Information Center (NEIC). "NEIC Monthly Earthquake Data Report File for Event 19940116014916.21." US Geological Survey, 2009.
2.5.2-65	Nottis, G. N., and W. Mitronovas. "Documentation of Felt Earthquakes in the Coastal Plain of Southeastern New York and East Central New Jersey: 1847-1954." 74. Albany, NY: New York State Geol. Surv. Open-File Report #4i020 (2003.00), 1983.
2.5.2-66	Not Used
2.5.2-67	Not Used
2.5.2-68	Not Used
2.5.2-69	Not Used
2.5.2-70	Public Service Enterprise Group (PSEG), "Hope Creek Generating Station Updated Safety Analysis Report, Rev. 16" Section 2.5, May 15, 2006.
2.5.2-71	Ratcliffe, N. M. "The Ramapo Fault System in New York and Adjacent Northern New Jersey: A Case of Tectonic Heredity." Geol. Soc. Am. Bull. 82 (1971): 125-42.
2.5.2-72	Not Used
2.5.2-73	Rathje, E. M., and M. C. Ozbey. "Site-Specific Validation of Random Vibration Theory-Based Seismic Site Response Analysis." J. Geotechnical and Geoenvironmental Engineering 132 (2006): 911-22.
2.5.2-74	Not Used
2.5.2-75	Seeber, L., and J. G. Armbruster. "Seismicity along the Atlantic Seaboard of the U.S.: Intraplate Neotectonic and Earthquake Hazard." In The Atlantic Continental Margin, edited by R. E. Sheridan and J. A. Grow: Geological Society of America, The Geology of North America, 1988.
2.5.2-76	Seeber, L., J. Armbruster, W.-Y. Kim, N. Barstow, and C. Scharnberger. "The 1994 Cacoosing Valley Earthquakes near Reading, Pennsylvania: A Shallow Rupture Triggered by Quarry Unloading." J. Geophys. Res. 103 (1998): 24,505-24,21.
2.5.2-77	Not Used

**PSEG Site
ESP Application
Part 2, Site Safety Analysis Report**

2.5.2-78	Not Used
2.5.2-79	Stover, C. W., and J. L. Coffman. "Seismicity of the United States, 1568-1989 (Revised)." U.S. Geological Survey, Professional Paper 1527, 1993.
2.5.2-80	Sykes, Lynn R., John G. Armbruster, Won-Young Kim, and Leonardo Seeber. "Observations and Tectonic Setting of Historic and Instrumentally Located Earthquakes in the Greater New York City–Philadelphia Area." Bulletin of the Seismological Society of America 98 (2008): 1696-719.
2.5.2-81	Not Used
2.5.2-82	Not Used
2.5.2-83	Not Used
2.5.2-84	Toro, G. "Probabilistic Models of Site Velocity Profiles for Generic and Site-Specific Ground-Motion Amplification Studies." In Description and Validation of the Stochastic Ground Motion Model, edited by W. Silva, N. Abrahamson, G. Toro and C. J. Costantino: Dept. Nuclear Energy, Brookhaven National Laboratory, contract number 770573, 1996.
2.5.2-85	Not Used
2.5.2-86	United States Geological Survey (USGS). "M4.5 Powhatan County, Virginia Earthquake of 9 December 2003." USGS, Earthquake Summary Map, 2003.
2.5.2-87	United States Geological Survey (USGS). "Preliminary Earthquake Report for Magnitude 4.5 - Virginia 2003 December 9 20:59:14 UTC." USGS, 2009.
2.5.2-88	United States Geological Survey (USGS). "USGS Community Intensity Map for 9 December 2003 Virginia Earthquake." USGS, 2009.
2.5.2-89	Watson, T. L. "The Virginia Earthquake of April 9, 1918." Bulletin of Seismological Society of America 8 (1918): 105-16.
2.5.2-90	Not Used
2.5.2-91	Not Used
2.5.2-92	Not Used
2.5.2-93	Not Used
2.5.2-94	Wheeler, Russell L., Nathan K. Trevor, Arthur C. Tarr, and Anthony J. Crone. "Earthquakes in and Near the Northeastern United States, 1638-1998." U.S. Geological Survey Fact Sheet FS-0006-01, 2001.

**PSEG Site
ESP Application
Part 2, Site Safety Analysis Report**

- 2.5.2-95 Wheeler, Russell L., Nathan K. Trevor, Arthur C. Tarr, and Anthony J. Crone. "Earthquakes in and Near the Northeastern United States, 1638-1998." U.S. Geological Survey Geologic Investigations Series, I-2737 2005.
- 2.5.2-96 Winkler, L. "Catalog of U.S. Earthquakes Before the Year 1850." Bulletin of Seismological Society of America 69 (1979): 569-602.
- 2.5.2-97 Yang, J.-P., and Y. P. Aggarwall. "Seismotectonics of Northeastern United States and Adjacent Canada." J. Geophys. Res. 86 (1981): 4981-98.
- 2.5.2-98 Not Used
- 2.5.2-99 Center for Earthquake Research and Information (CERI), New Madrid Earthquake Catalog Search, Accessed on 8-3-2012, http://folkworm.ceri.memphis.edu/catalogs/html/cat_nm.html.
- 2.5.2-100 Lamont-Doherty Cooperative Seismographic Network (LCSN), LCSN Earthquake Catalog Search, Accessed on 8-6-2012, <http://almaty.ldeo.columbia.edu:8080/data.search.html>.
- 2.5.2-101 New England Seismic Network (NESN), Earthquake Catalog Search, Accessed on 8-6-2012, http://aki.bc.edu/catalog_search.htm.
- 2.5.2-102 Southeastern U.S. Seismic Network (SEUSSN), Catalog Download, Accessed on 8-3-2012, <http://www.geol.vt.edu/outreach/vtso/anonftp/catalog/>.
- 2.5.2-103 Ohio Seismic Network (OSN), Catalogs and Maps of Ohio Earthquakes, Accessed on 8-3-2012, <http://www.dnr.state.oh.us/tabid/8302/Default.aspx>.
- 2.5.2-104 USGS National Earthquake Information Center (NEIC). Rectangular Area Earthquake Search, Accessed on 8-6-2012, http://earthquake.usgs.gov/earthquakes/eqarchives/epic/epic_rect.php.
- 2.5.2-105 Advanced National Seismic System (ANSS), ANSS Catalog Search, Accessed on 8-6-2012, <http://www.ncedc.org/anss/catalog-search.html>.
- 2.5.2-106 Weichert, D.H., 1980, Estimation of the Earthquake Recurrence Parameters for Unequal Observation Periods for Different Magnitudes, Bulletin of the Seismological Society of America, v. 70, no. 4, pp. 1337-1346.
- 2.5.2-107 NEIC, 2012, NEIC PDE-W earthquake summary for 23 August 2011 155104 earthquake, USGS, <http://neic.usgs.gov/cgi-bin/epic/epic.cgi?SEARCHMETHOD=3&FILEFORMAT=1&SEARCHRANGE=HH&CLAT=37.93&CLON=-77.93&CRAD=10&SYEAR=2011&SMONTH=8&SDAY=23&EYEAR=2011&EMONTH=8&EDAY=23&LMAG=5.5&UMAG=6.1&NDEP1=&NDEP2=&IO1=&IO2=&SLAT2=0.0&SLAT1=0.0&SLON2=0.0&SLON1=0.0&SUBMIT=Submit+Search>.

**PSEG Site
ESP Application
Part 2, Site Safety Analysis Report**

- 2.5.2-108 USGS, 2012, M5.8 Virginia Region Earthquake of 23 August 2011 (poster), US Geological Survey, <http://earthquake.usgs.gov/earthquakes/eqarchives/poster/2011/20110823b.php>.
- 2.5.2-109 Chapman, M., 2011, The M 5.7 Central Virginia Earthquake of August 23, 2011: A Complex Rupture, Meeting of the Eastern Section of the Seismological Society of America, October 16-18 2011: Little Rock, AR.
- 2.5.2-110 DGMR, 2012, August 23, 2011 1:51pm; 5.8 Magnitude Earthquake Virginia Department of Mines Minerals and Energy, Division of Geology and Mineral Resources, http://www.dmme.virginia.gov/DMR3/va_5.8_earthquake.shtml.
- 2.5.2-111 USNRC (2012). Request for Information Pursuant to Title 10 of the Code of Federal Regulations 50.54(f) Regarding Recommendations 2.1, 2.3, and 9.3, of the Near-Term Task Force Review of Insights from the Fukushima Dai-ichi Accident, ADAMS Accession No. ML12053A340.
- 2.5.2-112 Campbell, Kenneth W. and Yousef M. Bozorgnia. "Updated Near-Source Ground Motion (Attenuation) Relations for the Horizontal and Vertical Components of Peak Ground Acceleration and Acceleration Response Spectra." Bulletin of Seismological Society of America 93 (2003): 314-331.
- 2.5.2-113 Gülerce, Zeynep and Norman A. Abrahamson. "Site-Specific Design Spectra for Vertical Ground Motion," Earthquake Spectra 27, no. 4 (2011): 1023-1047.

**PSEG Site
ESP Application
Part 2, Site Safety Analysis Report**

Tables 2.5.2-1 through 2.5.2-16 Not Used

**PSEG Site
ESP Application
Part 2, Site Safety Analysis Report**

**Table 2.5.2-17
Base-Case Soil Profile
Mean Shear Wave Velocity**

Formation	Soil Curve Number	Soil Curve Description	Thickness (ft.)	Vs (ft/sec)	Unit Weight (pcf)^(a)	Sigma (ln Vs)	Depth to Top of layer – best estimate (ft.)^(c)
Layer 1 (Tvt, Tht and Knv) - Competent Layer for GMRS ^(b)	1	Layer 1	84.5	2250	121	0.25	0
Layer 2 (Kml)	2	Layers 2-5	18.5	3920	131	0.25	84.5
Layer 3 (Kml)	2	Layers 2-5	21.5	2490	131	0.25	103
Layer 4 (Kml)	2	Layers 2-5	34.5	3020	131	0.25	124.5
Layer 5 (Kml, Kwn, Kmt)	2	Layers 2-5	62.0	2490	128	0.25	159
Layer 6 (Ket, Kwb)	3	Layers 6-8	84.0	1710	125	0.30	221
Layer 7 (Kmv)	3	Layers 6-8	26.0	2290	130	0.30	305
Layer 8 (Kmg)	3	Layers 6-8	25.0	1780	130	0.30	331
Layer 9A (Kmg)	4	Layers 9a-9b	31.0	2490	130	0.30	356
Layer 9B (Kp)	4	Layers 9a-9b	51.0	2490	130	0.30	387
Upper Potomac	5	Deep Profile	365.0	2200	135	0.35	438
Middle Potomac	5	Deep Profile	430.0	2630	135.0	0.35	803
Lower Potomac	5	Deep Profile	450.0	3060	135.0	0.35	1233

a) pcf=pounds per cubic foot

b) Layer definitions are shown on Figure 2.5.4.7-8a

c) Depths are referenced to top of Competent Layer

**PSEG Site
ESP Application
Part 2, Site Safety Analysis Report**

**Table 2.5.2-18
Parameters for Layer-Depth Randomization**

Formation (top of)	Distribution Type	Depth 1 (ft.)^(a)	Depth 2 (ft.)^(a)
Layer 2 (Kml)	Normal	84.5	4.27
Layer 3 (Kml)	Normal	103	4.27
Layer 4 (Kml)	Normal	124.5	4.27
Layer 5 (Kml, Kwn, Kmt)	Normal	159	4.27
Layer 6 (Ket, Kwb)	Normal	221	4.27
Layer 7 (Kmv)	Normal	305	6.40
Layer 8 (Kmg)	Normal	331	6.40
Layer 9A (Kmg)	Normal	356	6.40
Layer 9B (Kp)	Normal	387	20.40
Upper Potomac	Uniform	433	443
Middle Potomac	Uniform	603	1003
Lower Potomac	Uniform	1033	1433
Bedrock	Uniform	1483	1883

- a) For normal distributions, Depth 1 is the mean depth below competent layer and Depth 2 is the standard deviation of depth; for uniform distributions, Depth 1 is the minimum depth to the top of the layer below top of competent layer and Depth 2 is the maximum depth to the top of the layer below top of competent layer.

**PSEG Site
ESP Application
Part 2, Site Safety Analysis Report**

**Table 2.5.2-19
Calculation of Durations and Effective Strain Ratios for Input Rock Motions**

Event	M	Distance (R) km (mi)	Mo (dyn-cm)^(a)	fc (Hz)	T (seconds)	Effective Strain Ratio
1E-4 HF	5.9	27 (16.7)	7.94E+24	0.42	3.71	0.5
1E-4 LF	7.3	540 (335.5)	1.00E+27	0.08	38.82	0.63
1E-5 HF	6.0	12 (7.5)	1.21E+25	0.38	3.25	0.5
1E-5 LF	7.6	570 (354)	2.82E+27	0.06	45.20	0.65
1E-6 HF	6.3	9 (5.6)	3.16E+25	0.27	4.19	0.53
1E-6 LF	7.7	420 (261)	3.98E+27	0.05	39.74	0.65

a) Mo=seismic moment; dyn-cm=Dyne-centimeters

**PSEG Site
ESP Application
Part 2, Site Safety Analysis Report**

**Table 2.5.2-20
Amplification Factors for High-Frequency (HF) Motions**

Frequency (Hz)	Logarithmic Mean Amplification Factors			Logarithmic Standard Deviations		
	1E-4	1E-5	1E-6	1E-4	1E-5	1E-6
100	1.07	0.77	0.48	0.21	0.23	0.30
90	0.97	0.70	0.43	0.21	0.23	0.30
80	0.85	0.60	0.37	0.22	0.24	0.30
70	0.72	0.51	0.30	0.23	0.24	0.31
60	0.62	0.42	0.25	0.25	0.26	0.31
50	0.57	0.38	0.21	0.28	0.28	0.32
45	0.57	0.37	0.20	0.29	0.30	0.33
40	0.59	0.37	0.19	0.30	0.32	0.34
35	0.63	0.38	0.19	0.31	0.34	0.36
30	0.67	0.41	0.19	0.31	0.36	0.39
25	0.76	0.46	0.21	0.30	0.36	0.43
20	0.89	0.57	0.25	0.30	0.36	0.46
15	1.06	0.73	0.33	0.27	0.33	0.48
12.5	1.14	0.84	0.42	0.23	0.29	0.47
10	1.27	0.97	0.52	0.22	0.27	0.43
9	1.38	1.07	0.59	0.22	0.27	0.43
8	1.51	1.19	0.69	0.21	0.26	0.43
7	1.63	1.31	0.80	0.22	0.26	0.40
6	1.74	1.43	0.92	0.19	0.22	0.37
5	1.80	1.53	1.03	0.28	0.25	0.32
4	1.64	1.50	1.10	0.32	0.31	0.33
3	1.42	1.37	1.17	0.22	0.25	0.34
2.5	1.47	1.39	1.22	0.26	0.27	0.35
2	1.69	1.57	1.35	0.23	0.26	0.33
1.5	1.93	1.83	1.57	0.23	0.25	0.31
1.25	2.05	1.96	1.70	0.24	0.25	0.34
1	2.18	2.17	1.98	0.26	0.23	0.24
0.9	2.06	2.10	2.03	0.26	0.25	0.23
0.8	1.97	2.02	2.02	0.23	0.23	0.23
0.7	2.00	2.05	2.08	0.24	0.23	0.21
0.6	2.16	2.22	2.29	0.23	0.23	0.21
0.5	2.44	2.49	2.57	0.23	0.23	0.22
0.4	2.75	2.82	2.89	0.30	0.30	0.30
0.3	2.34	2.41	2.48	0.38	0.39	0.39
0.2	1.60	1.64	1.69	0.32	0.33	0.35
0.15	1.36	1.39	1.41	0.18	0.19	0.21
0.125	1.31	1.33	1.34	0.14	0.15	0.16
0.1	1.29	1.31	1.30	0.11	0.12	0.13

**PSEG Site
ESP Application
Part 2, Site Safety Analysis Report**

**Table 2.5.2-21
Amplification Factors for Low-Frequency (LF) Motions**

Frequency (Hz)	Logarithmic Mean Amplification Factors			Logarithmic Standard Deviations		
	1E-4	1E-5	1E-6	1E-4	1E-5	1E-6
100	1.13	0.93	0.63	0.18	0.21	0.28
90	1.05	0.86	0.58	0.18	0.21	0.28
80	0.93	0.76	0.51	0.19	0.21	0.28
70	0.80	0.64	0.43	0.20	0.21	0.28
60	0.69	0.54	0.36	0.21	0.22	0.28
50	0.64	0.48	0.31	0.23	0.23	0.29
45	0.63	0.47	0.30	0.25	0.25	0.29
40	0.64	0.46	0.29	0.26	0.26	0.30
35	0.67	0.47	0.29	0.27	0.27	0.30
30	0.71	0.49	0.29	0.28	0.29	0.32
25	0.77	0.53	0.30	0.28	0.31	0.34
20	0.89	0.60	0.33	0.28	0.33	0.37
15	1.04	0.72	0.37	0.27	0.33	0.42
12.5	1.12	0.82	0.43	0.24	0.32	0.44
10	1.26	0.94	0.51	0.23	0.30	0.45
9	1.36	1.03	0.56	0.22	0.30	0.46
8	1.47	1.14	0.63	0.22	0.29	0.47
7	1.59	1.25	0.73	0.22	0.28	0.45
6	1.69	1.36	0.83	0.20	0.25	0.43
5	1.74	1.43	0.91	0.28	0.27	0.39
4	1.62	1.43	0.99	0.32	0.31	0.38
3	1.42	1.34	1.07	0.21	0.26	0.36
2.5	1.47	1.38	1.16	0.25	0.28	0.38
2	1.66	1.51	1.26	0.22	0.26	0.37
1.5	1.93	1.79	1.48	0.22	0.26	0.35
1.25	2.03	1.91	1.60	0.23	0.25	0.39
1	2.10	2.02	1.77	0.23	0.18	0.26
0.9	2.06	2.08	1.94	0.24	0.22	0.25
0.8	2.00	2.04	2.00	0.22	0.21	0.26
0.7	2.03	2.07	2.07	0.23	0.21	0.24
0.6	2.20	2.26	2.28	0.24	0.23	0.23
0.5	2.51	2.54	2.63	0.27	0.26	0.24
0.4	2.73	2.77	2.85	0.30	0.30	0.29
0.3	2.30	2.33	2.42	0.37	0.38	0.37
0.2	1.55	1.57	1.62	0.31	0.31	0.34
0.15	1.30	1.31	1.34	0.17	0.18	0.19
0.125	1.23	1.23	1.25	0.13	0.13	0.14
0.1	1.17	1.18	1.19	0.09	0.09	0.10

**PSEG Site
ESP Application
Part 2, Site Safety Analysis Report**

**Table 2.5.2-22 (Sheet 1 of 7)
Mean and Fractile Soil Seismic Hazard Curves at GMRS Elevation**

100 Hz (PGA) Hazard Curves						
Amplitude^(a)	MEAN	0.05^(b)	0.16	0.5^(c)	0.84	0.95
0.0005	6.08E-02	2.10E-02	2.83E-02	4.76E-02	1.04E-01	1.41E-01
0.0007	4.73E-02	1.70E-02	2.14E-02	3.41E-02	8.22E-02	1.16E-01
0.001	3.56E-02	1.29E-02	1.62E-02	2.44E-02	6.12E-02	8.97E-02
0.0015	2.54E-02	9.12E-03	1.13E-02	1.71E-02	4.45E-02	6.52E-02
0.002	1.98E-02	6.92E-03	8.56E-03	1.28E-02	3.43E-02	5.09E-02
0.003	1.36E-02	4.90E-03	6.04E-03	8.85E-03	2.29E-02	3.59E-02
0.005	8.29E-03	2.82E-03	3.72E-03	5.33E-03	1.37E-02	2.16E-02
0.007	5.86E-03	1.86E-03	2.63E-03	4.00E-03	8.85E-03	1.49E-02
0.01	3.98E-03	1.23E-03	1.74E-03	2.82E-03	5.97E-03	1.00E-02
0.015	2.50E-03	7.08E-04	1.07E-03	1.86E-03	3.80E-03	5.78E-03
0.02	1.76E-03	4.68E-04	7.08E-04	1.32E-03	2.65E-03	4.04E-03
0.03	1.04E-03	2.69E-04	4.07E-04	7.59E-04	1.52E-03	2.33E-03
0.05	5.06E-04	1.35E-04	1.91E-04	3.80E-04	7.59E-04	1.23E-03
0.07	3.09E-04	7.76E-05	1.10E-04	2.34E-04	4.68E-04	7.59E-04
0.1	1.82E-04	4.17E-05	6.31E-05	1.35E-04	2.88E-04	4.68E-04
0.15	9.89E-05	2.16E-05	3.16E-05	7.76E-05	1.66E-04	2.51E-04
0.2	6.35E-05	1.29E-05	1.95E-05	5.13E-05	1.02E-04	1.55E-04
0.3	3.33E-05	6.46E-06	1.08E-05	2.75E-05	5.89E-05	8.32E-05
0.5	1.38E-05	2.14E-06	3.98E-06	1.05E-05	2.57E-05	3.89E-05
0.7	7.23E-06	9.33E-07	1.86E-06	5.25E-06	1.38E-05	2.24E-05
1	3.41E-06	3.20E-07	7.08E-07	2.29E-06	6.46E-06	1.05E-05
1.5	1.29E-06	7.24E-08	2.04E-07	7.08E-07	2.29E-06	4.27E-06
2	5.93E-07	2.09E-08	6.53E-08	3.09E-07	1.00E-06	2.29E-06
3	1.71E-07	2.37E-09	1.05E-08	7.24E-08	2.88E-07	7.33E-07
5	2.69E-08	3.59E-15	4.68E-10	8.51E-09	4.79E-08	1.30E-07
7	6.55E-09	5.19E-29	4.73E-15	1.68E-09	1.12E-08	3.27E-08
10	1.24E-09	4.20E-29	6.31E-17	2.34E-10	2.00E-09	6.03E-09

- a) Spectral acceleration in g
b) Percentile
c) 0.5 fractile = median

**PSEG Site
ESP Application
Part 2, Site Safety Analysis Report**

**Table 2.5.2-22 (Sheet 2 of 7)
Mean and Fractile Soil Seismic Hazard Curves at GMRS Elevation**

25 Hz Hazard Curves						
Amplitude ^(a)	MEAN	0.05 ^(b)	0.16	0.5 ^(c)	0.84	0.95
0.0005	7.69E-02	1.82E-02	3.02E-02	7.55E-02	1.11E-01	1.71E-01
0.0007	6.18E-02	1.48E-02	2.44E-02	5.75E-02	9.10E-02	1.32E-01
0.001	4.84E-02	1.29E-02	1.84E-02	4.38E-02	7.00E-02	1.02E-01
0.0015	3.62E-02	1.05E-02	1.49E-02	2.91E-02	5.38E-02	7.49E-02
0.002	2.92E-02	9.12E-03	1.20E-02	2.21E-02	4.19E-02	5.86E-02
0.003	2.14E-02	7.41E-03	9.13E-03	1.45E-02	3.01E-02	4.57E-02
0.005	1.43E-02	4.90E-03	6.46E-03	9.39E-03	1.98E-02	3.01E-02
0.007	1.08E-02	3.98E-03	4.90E-03	7.05E-03	1.46E-02	2.29E-02
0.01	7.99E-03	2.82E-03	3.47E-03	5.30E-03	1.06E-02	1.72E-02
0.015	5.62E-03	1.86E-03	2.46E-03	3.73E-03	7.24E-03	1.16E-02
0.02	4.34E-03	1.32E-03	1.86E-03	3.02E-03	5.76E-03	8.97E-03
0.03	2.96E-03	8.13E-04	1.23E-03	2.14E-03	4.02E-03	6.00E-03
0.05	1.74E-03	4.22E-04	6.61E-04	1.23E-03	2.46E-03	3.55E-03
0.07	1.18E-03	2.69E-04	4.37E-04	8.13E-04	1.68E-03	2.48E-03
0.1	7.54E-04	1.66E-04	2.51E-04	5.37E-04	1.07E-03	1.74E-03
0.15	4.39E-04	8.91E-05	1.40E-04	3.09E-04	6.17E-04	1.07E-03
0.2	2.93E-04	5.89E-05	8.91E-05	2.04E-04	4.07E-04	7.08E-04
0.3	1.62E-04	3.16E-05	4.79E-05	1.18E-04	2.34E-04	4.07E-04
0.5	7.40E-05	1.29E-05	2.24E-05	5.50E-05	1.18E-04	1.97E-04
0.7	4.31E-05	6.92E-06	1.29E-05	3.16E-05	7.24E-05	1.22E-04
1	2.37E-05	3.47E-06	6.03E-06	1.70E-05	4.47E-05	6.31E-05
1.5	1.15E-05	1.41E-06	2.82E-06	8.22E-06	2.24E-05	3.39E-05
2	6.61E-06	6.38E-07	1.41E-06	4.42E-06	1.20E-05	2.09E-05
3	2.85E-06	1.91E-07	4.37E-07	1.62E-06	4.90E-06	9.77E-06
5	8.61E-07	3.06E-08	8.32E-08	3.80E-07	1.41E-06	3.02E-06
7	3.53E-07	6.24E-09	2.24E-08	1.26E-07	5.75E-07	1.32E-06
10	1.23E-07	5.56E-10	4.57E-09	3.63E-08	1.91E-07	5.01E-07

a) Spectral acceleration in g

b) Percentile

c) 0.5 fractile = median

**PSEG Site
ESP Application
Part 2, Site Safety Analysis Report**

**Table 2.5.2-22 (Sheet 3 of 7)
Mean and Fractile Soil Seismic Hazard Curves at GMRS Elevation**

10 Hz Hazard Curves						
Amplitude ^(a)	MEAN	0.05^(b)	0.16	0.5^(c)	0.84	0.95
0.0005	9.89E-02	3.91E-02	5.62E-02	9.32E-02	1.45E-01	1.84E-01
0.0007	7.94E-02	3.18E-02	4.27E-02	7.12E-02	1.19E-01	1.52E-01
0.001	6.15E-02	2.41E-02	3.24E-02	5.08E-02	9.14E-02	1.17E-01
0.0015	4.50E-02	1.82E-02	2.29E-02	3.63E-02	6.58E-02	9.03E-02
0.002	3.56E-02	1.48E-02	1.85E-02	2.76E-02	5.09E-02	7.07E-02
0.003	2.52E-02	9.78E-03	1.30E-02	1.82E-02	3.70E-02	5.21E-02
0.005	1.60E-02	6.46E-03	7.98E-03	1.10E-02	2.34E-02	3.45E-02
0.007	1.17E-02	4.57E-03	5.63E-03	8.21E-03	1.65E-02	2.54E-02
0.01	8.20E-03	3.02E-03	3.98E-03	5.73E-03	1.14E-02	1.76E-02
0.015	5.39E-03	2.00E-03	2.63E-03	4.01E-03	7.20E-03	1.16E-02
0.02	3.95E-03	1.41E-03	2.00E-03	3.03E-03	5.25E-03	7.90E-03
0.03	2.48E-03	8.13E-04	1.23E-03	2.00E-03	3.33E-03	4.86E-03
0.05	1.31E-03	4.07E-04	6.17E-04	1.07E-03	1.75E-03	2.59E-03
0.07	8.27E-04	2.51E-04	3.80E-04	6.61E-04	1.08E-03	1.66E-03
0.1	4.94E-04	1.45E-04	2.19E-04	4.07E-04	7.08E-04	1.01E-03
0.15	2.69E-04	7.76E-05	1.10E-04	2.19E-04	4.07E-04	5.77E-04
0.2	1.74E-04	4.79E-05	6.76E-05	1.45E-04	2.88E-04	3.81E-04
0.3	9.23E-05	2.32E-05	3.39E-05	7.76E-05	1.55E-04	2.04E-04
0.5	4.02E-05	8.51E-06	1.38E-05	3.39E-05	7.24E-05	9.55E-05
0.7	2.24E-05	4.57E-06	7.41E-06	1.82E-05	3.89E-05	5.50E-05
1	1.15E-05	2.21E-06	3.47E-06	9.12E-06	2.09E-05	3.16E-05
1.5	5.02E-06	8.71E-07	1.32E-06	3.47E-06	9.12E-06	1.38E-05
2	2.62E-06	3.80E-07	6.38E-07	1.86E-06	4.90E-06	7.41E-06
3	9.49E-07	1.02E-07	2.04E-07	6.17E-07	1.74E-06	2.82E-06
5	2.18E-07	1.20E-08	3.16E-08	1.35E-07	3.80E-07	6.61E-07
7	7.28E-08	1.57E-09	6.92E-09	3.89E-08	1.26E-07	2.34E-07
10	2.02E-08	7.50E-11	9.33E-10	9.12E-09	3.89E-08	7.24E-08

a) Spectral acceleration in g

b) Percentile

c) 0.5 fractile = median

**PSEG Site
ESP Application
Part 2, Site Safety Analysis Report**

**Table 2.5.2-22 (Sheet 4 of 7)
Mean and Fractile Soil Seismic Hazard Curves at GMRS Elevation**

5 Hz Hazard Curves						
Amplitude ^(a)	MEAN	0.05^(b)	0.16	0.5^(c)	0.84	0.95
0.0005	1.12E-01	5.91E-02	7.38E-02	9.97E-02	1.66E-01	2.04E-01
0.0007	8.95E-02	4.19E-02	5.62E-02	7.63E-02	1.36E-01	1.75E-01
0.001	6.88E-02	2.96E-02	4.27E-02	5.50E-02	1.05E-01	1.44E-01
0.0015	4.96E-02	2.09E-02	2.82E-02	3.94E-02	7.62E-02	1.11E-01
0.002	3.87E-02	1.48E-02	2.00E-02	3.03E-02	6.25E-02	8.58E-02
0.003	2.67E-02	9.78E-03	1.31E-02	2.02E-02	4.22E-02	6.24E-02
0.005	1.61E-02	5.62E-03	7.48E-03	1.23E-02	2.55E-02	3.84E-02
0.007	1.13E-02	3.72E-03	4.92E-03	8.01E-03	1.80E-02	2.77E-02
0.01	7.55E-03	2.46E-03	3.24E-03	5.50E-03	1.20E-02	1.87E-02
0.015	4.64E-03	1.46E-03	2.00E-03	3.32E-03	7.06E-03	1.12E-02
0.02	3.21E-03	1.00E-03	1.41E-03	2.32E-03	4.79E-03	7.60E-03
0.03	1.85E-03	5.37E-04	8.13E-04	1.42E-03	2.62E-03	4.28E-03
0.05	8.87E-04	2.51E-04	3.80E-04	6.84E-04	1.21E-03	1.91E-03
0.07	5.31E-04	1.55E-04	2.19E-04	4.07E-04	7.14E-04	1.13E-03
0.1	3.01E-04	8.32E-05	1.26E-04	2.34E-04	4.37E-04	6.29E-04
0.15	1.56E-04	4.17E-05	6.31E-05	1.18E-04	2.51E-04	3.56E-04
0.2	9.65E-05	2.40E-05	3.63E-05	7.24E-05	1.55E-04	2.19E-04
0.3	4.83E-05	1.12E-05	1.70E-05	3.63E-05	7.76E-05	1.10E-04
0.5	1.92E-05	3.98E-06	6.03E-06	1.48E-05	3.16E-05	4.79E-05
0.7	1.00E-05	1.86E-06	2.82E-06	7.94E-06	1.70E-05	2.57E-05
1	4.74E-06	7.59E-07	1.23E-06	3.72E-06	8.51E-06	1.29E-05
1.5	1.86E-06	2.51E-07	4.37E-07	1.41E-06	3.47E-06	5.25E-06
2	9.05E-07	1.02E-07	1.78E-07	6.61E-07	1.74E-06	2.63E-06
3	2.95E-07	1.82E-08	4.17E-08	2.04E-07	5.75E-07	9.33E-07
5	5.97E-08	5.07E-12	4.27E-09	3.16E-08	1.18E-07	2.19E-07
7	1.84E-08	7.50E-14	4.52E-10	7.67E-09	3.63E-08	7.24E-08
10	4.70E-09	9.66E-19	2.75E-14	1.51E-09	9.12E-09	2.09E-08

- A. Spectral acceleration in g
B. Percentile
C. 0.5 fractile = median

**PSEG Site
ESP Application
Part 2, Site Safety Analysis Report**

**Table 2.5.2-22 (Sheet 5 of 7)
Mean and Fractile Soil Seismic Hazard Curves at GMRS Elevation**

2.5 Hz Hazard Curves						
Amplitude ^(a)	MEAN	0.05 ^(b)	0.16	0.5 ^(c)	0.84	0.95
0.0005	1.03E-01	1.59E-02	6.44E-02	4.19E-02	1.56E-01	1.98E-01
0.0007	8.06E-02	1.13E-02	4.58E-02	3.07E-02	1.28E-01	1.70E-01
0.001	6.06E-02	7.17E-03	3.24E-02	2.10E-02	9.86E-02	1.36E-01
0.0015	4.26E-02	4.27E-03	2.01E-02	1.38E-02	7.20E-02	9.89E-02
0.002	3.26E-02	2.92E-03	1.42E-02	9.78E-03	5.60E-02	8.01E-02
0.003	2.18E-02	1.62E-03	8.68E-03	6.46E-03	3.81E-02	5.50E-02
0.005	1.25E-02	7.85E-04	4.61E-03	3.47E-03	2.18E-02	3.30E-02
0.007	8.34E-03	4.68E-04	3.03E-03	2.14E-03	1.40E-02	2.28E-02
0.01	5.25E-03	2.51E-04	1.87E-03	1.32E-03	8.61E-03	1.49E-02
0.015	2.97E-03	1.18E-04	1.07E-03	7.59E-04	4.76E-03	8.52E-03
0.02	1.93E-03	7.24E-05	6.61E-04	5.01E-04	2.82E-03	5.72E-03
0.03	1.02E-03	3.16E-05	3.55E-04	2.69E-04	1.39E-03	2.76E-03
0.05	4.35E-04	1.05E-05	1.45E-04	1.10E-04	5.59E-04	1.05E-03
0.07	2.42E-04	4.57E-06	7.76E-05	5.89E-05	3.36E-04	5.59E-04
0.1	1.27E-04	1.86E-06	4.17E-05	2.75E-05	1.79E-04	2.90E-04
0.15	5.98E-05	5.75E-07	1.95E-05	1.29E-05	9.56E-05	1.38E-04
0.2	3.45E-05	2.19E-07	1.12E-05	6.92E-06	5.89E-05	8.10E-05
0.3	1.56E-05	4.79E-08	4.90E-06	2.82E-06	2.75E-05	3.64E-05
0.5	5.47E-06	2.27E-10	1.41E-06	8.71E-07	9.77E-06	1.38E-05
0.7	2.61E-06	1.80E-12	5.75E-07	3.31E-07	4.90E-06	6.92E-06
1	1.13E-06	7.00E-14	2.04E-07	8.91E-08	2.14E-06	3.24E-06
1.5	3.99E-07	1.15E-15	4.79E-08	1.59E-08	8.13E-07	1.15E-06
2	1.78E-07	1.46E-18	1.25E-08	7.24E-11	3.80E-07	5.37E-07
3	5.15E-08	4.04E-29	8.91E-11	1.88E-14	1.10E-07	1.66E-07
5	8.85E-09	4.20E-29	2.07E-15	5.07E-29	1.82E-08	3.16E-08
7	2.44E-09	4.20E-29	4.32E-17	4.28E-29	4.90E-09	9.77E-09
10	5.53E-10	4.20E-29	3.55E-19	4.20E-29	1.07E-09	2.46E-09

- a) Spectral acceleration in g
b) Percentile
c) 0.5 fractile = median

**PSEG Site
ESP Application
Part 2, Site Safety Analysis Report**

**Table 2.5.2-22 (Sheet 6 of 7)
Mean and Fractile Soil Seismic Hazard Curves at GMRS Elevation**

1 Hz Hazard Curves						
Amplitude^(a)	MEAN	0.05^(b)	0.16	0.5^(c)	0.84	0.95
0.0005	5.94E-02	1.59E-02	3.04E-02	4.27E-02	1.05E-01	1.29E-01
0.0007	4.44E-02	1.13E-02	2.01E-02	3.12E-02	8.21E-02	1.07E-01
0.001	3.19E-02	7.17E-03	1.32E-02	2.16E-02	5.70E-02	7.91E-02
0.0015	2.14E-02	4.27E-03	8.10E-03	1.41E-02	3.94E-02	5.71E-02
0.002	1.59E-02	2.92E-03	5.32E-03	1.03E-02	2.93E-02	4.43E-02
0.003	1.02E-02	1.62E-03	2.84E-03	6.22E-03	1.87E-02	2.93E-02
0.005	5.47E-03	7.85E-04	1.32E-03	3.09E-03	1.02E-02	1.78E-02
0.007	3.49E-03	4.68E-04	7.09E-04	1.80E-03	6.12E-03	1.19E-02
0.01	2.08E-03	2.51E-04	4.08E-04	9.62E-04	3.57E-03	7.64E-03
0.015	1.10E-03	1.18E-04	2.04E-04	4.76E-04	1.66E-03	4.33E-03
0.02	6.84E-04	7.24E-05	1.18E-04	2.82E-04	9.18E-04	2.69E-03
0.03	3.35E-04	3.16E-05	5.31E-05	1.37E-04	3.79E-04	1.22E-03
0.05	1.27E-04	1.05E-05	1.82E-05	5.14E-05	1.44E-04	3.88E-04
0.07	6.41E-05	4.57E-06	9.12E-06	2.76E-05	7.94E-05	1.70E-04
0.1	2.96E-05	1.86E-06	4.27E-06	1.38E-05	4.20E-05	7.31E-05
0.15	1.18E-05	5.75E-07	1.51E-06	6.03E-06	1.95E-05	2.93E-05
0.2	6.09E-06	2.19E-07	6.61E-07	3.24E-06	1.12E-05	1.63E-05
0.3	2.40E-06	4.79E-08	1.91E-07	1.32E-06	4.90E-06	7.45E-06
0.5	7.30E-07	2.27E-10	2.02E-08	3.55E-07	1.62E-06	2.46E-06
0.7	3.21E-07	1.80E-12	1.78E-10	1.26E-07	7.59E-07	1.15E-06
1	1.27E-07	7.00E-14	1.48E-11	3.89E-08	2.88E-07	5.01E-07
1.5	4.01E-08	1.15E-15	1.97E-13	1.05E-08	8.61E-08	1.78E-07
2	1.65E-08	1.46E-18	9.44E-15	3.24E-09	3.39E-08	7.76E-08
3	4.26E-09	4.04E-29	1.45E-16	4.07E-10	8.51E-09	2.16E-08
5	6.28E-10	4.20E-29	2.88E-19	2.85E-11	1.15E-09	3.47E-09
7	1.55E-10	4.20E-29	5.28E-29	4.27E-12	2.51E-10	8.71E-10
10	3.12E-11	4.20E-29	5.28E-29	5.75E-13	4.47E-11	1.66E-10

a) Spectral acceleration in g

b) Percentile

c) 0.5 fractile = median

**PSEG Site
ESP Application
Part 2, Site Safety Analysis Report**

**Table 2.5.2-22 (Sheet 7 of 7)
Mean and Fractile Soil Seismic Hazard Curves at GMRS Elevation**

0.5 Hz Hazard Curves						
Amplitude ^(a)	MEAN	0.05 ^(b)	0.16	0.5 ^(c)	0.84	0.95
0.0005	3.34E-02	6.96E-03	1.28E-02	2.31E-02	6.08E-02	8.54E-02
0.0007	2.43E-02	4.59E-03	7.86E-03	1.72E-02	4.53E-02	6.67E-02
0.001	1.71E-02	2.82E-03	4.79E-03	1.23E-02	3.16E-02	4.92E-02
0.0015	1.12E-02	1.57E-03	2.54E-03	7.75E-03	2.11E-02	3.41E-02
0.002	8.24E-03	1.00E-03	1.55E-03	5.26E-03	1.57E-02	2.59E-02
0.003	5.17E-03	4.68E-04	7.68E-04	2.71E-03	9.97E-03	1.76E-02
0.005	2.73E-03	1.66E-04	2.89E-04	1.12E-03	5.27E-03	1.04E-02
0.007	1.74E-03	8.32E-05	1.55E-04	5.86E-04	3.17E-03	6.89E-03
0.01	1.04E-03	3.89E-05	7.25E-05	2.87E-04	1.71E-03	4.39E-03
0.015	5.56E-04	1.59E-05	2.95E-05	1.33E-04	7.20E-04	2.44E-03
0.02	3.47E-04	8.51E-06	1.59E-05	7.44E-05	3.64E-04	1.51E-03
0.03	1.74E-04	3.02E-06	6.03E-06	3.41E-05	1.48E-04	6.21E-04
0.05	7.08E-05	7.08E-07	1.74E-06	1.20E-05	5.47E-05	1.68E-04
0.07	3.70E-05	2.19E-07	6.61E-07	5.62E-06	2.82E-05	7.02E-05
0.1	1.70E-05	5.69E-08	2.19E-07	2.46E-06	1.39E-05	2.86E-05
0.15	6.24E-06	5.43E-09	4.79E-08	7.59E-07	6.03E-06	1.05E-05
0.2	2.86E-06	9.55E-11	1.05E-08	3.55E-07	3.47E-06	5.77E-06
0.3	9.03E-07	1.27E-12	1.10E-10	1.18E-07	1.32E-06	2.83E-06
0.5	2.11E-07	8.22E-15	3.98E-12	1.95E-08	4.07E-07	9.34E-07
0.7	8.32E-08	5.56E-16	1.84E-13	3.47E-09	1.91E-07	4.22E-07
1	3.09E-08	4.04E-29	4.42E-15	3.67E-10	7.76E-08	1.78E-07
1.5	9.53E-09	4.04E-29	8.61E-17	4.17E-11	2.40E-08	5.50E-08
2	3.88E-09	4.04E-29	4.73E-18	8.51E-12	9.77E-09	2.40E-08
3	9.81E-10	4.20E-29	5.28E-29	1.00E-12	2.29E-09	6.03E-09
5	1.41E-10	4.20E-29	5.28E-29	4.17E-14	2.51E-10	9.33E-10
7	3.43E-11	4.20E-29	4.47E-29	4.12E-15	4.79E-11	2.19E-10
10	6.76E-12	4.20E-29	4.47E-29	2.19E-16	7.41E-12	4.17E-11

- a) Spectral acceleration in g
b) Percentile
c) 0.5 fractile = median

**PSEG Site
ESP Application
Part 2, Site Safety Analysis Report**

**Table 2.5.2-23
Mean and Median UHRS Values for Soil Seismic Hazard (SA in g)**

Frequency, Hz	Mean 10⁻⁴	Mean 10⁻⁵	Mean 10⁻⁶
100 (PGA)	0.158	0.465	0.958
25	0.313	0.836	1.59
10	0.360	1.07	2.17
5.0	0.366	1.12	2.48
2.5	0.174	0.543	1.42
1.0	0.122	0.341	0.853
0.5	0.110	0.341	0.823
Frequency, Hz	Median 10⁻⁴	Median 10⁻⁵	Median 10⁻⁶
100 (PGA)	0.133	0.415	0.837
25	0.254	0.756	1.42
10	0.317	0.991	1.96
5.0	0.316	1.02	2.29
2.5	0.146	0.479	1.21
1.0	0.0767	0.251	0.665
0.5	0.0465	0.144	0.378

**PSEG Site
ESP Application
Part 2, Site Safety Analysis Report**

**Table 2.5.2-24
Calculation of Horizontal and Vertical GMRS**

Frequency (Hz)	Horizontal GMRS (g)	V/H Ratio	Vertical GMRS (g)
0.1	9.14E-03	0.75	6.86E-03
0.125	1.49E-02	0.75	1.12E-02
0.15	2.28E-02	0.75	1.71E-02
0.2	4.04E-02	0.75	3.03E-02
0.3	8.98E-02	0.75	6.74E-02
0.4	1.42E-01	0.75	1.07E-01
0.5	1.60E-01	0.75	1.20E-01
0.6	1.54E-01	0.75	1.16E-01
0.7	1.50E-01	0.75	1.12E-01
0.8	1.53E-01	0.75	1.15E-01
0.9	1.60E-01	0.75	1.20E-01
1	1.72E-01	0.75	1.29E-01
1.25	1.97E-01	0.75	1.48E-01
1.5	2.20E-01	0.75	1.65E-01
2	2.45E-01	0.75	1.84E-01
2.5	2.59E-01	0.75	1.94E-01
3	2.84E-01	0.75	2.13E-01
4	4.17E-01	0.75	3.13E-01
5	5.26E-01	0.75	3.95E-01
6	5.67E-01	0.79	4.45E-01
7	5.72E-01	0.81	4.66E-01
8	5.59E-01	0.84	4.70E-01
9	5.39E-01	0.86	4.65E-01
10	5.23E-01	0.88	4.62E-01
12.5	5.17E-01	0.93	4.79E-01
15	5.11E-01	0.96	4.91E-01
20	4.63E-01	1.02	4.71E-01
25	4.13E-01	1.06	4.37E-01
30	3.66E-01	1.09	4.01E-01
35	3.32E-01	1.12	3.73E-01
40	3.02E-01	1.15	3.47E-01
45	2.81E-01	1.15	3.23E-01
50	2.67E-01	1.15	3.07E-01
60	2.45E-01	1.15	2.81E-01
70	2.33E-01	1.15	2.68E-01
80	2.28E-01	1.15	2.62E-01
90	2.26E-01	1.15	2.60E-01
100	2.25E-01	1.15	2.59E-01

**PSEG Site
ESP Application
Part 2, Site Safety Analysis Report**

**Table 2.5.2-25
Mmax Comparisons Based on the CEUS-SSC Seismicity Catalog Update**

Mmax and Seismotectonic Zones	Lowest Mmax in CEUS-SSC Mmax Distribution	Mmax for CEUS-SSC Catalog Update
Study Region	6.5	5.80
MESE_N	6.4	5.80
NMESE_N	6.4	5.60
MESE_W	6.5	5.80
NMESE_W	5.7	5.60
AHEX	6.0	< 2.9 ^(a)
ECC_AM	6.0	5.80
ECC_GC	6.0	4.80
GHEX	6.0	3.58
GMH	6.0	5.20
IBEB	6.5	2.93
MID_A	5.6	5.60
MID_B	5.6	5.60
MID_C	5.6	5.60
MID_D	5.6	5.60
NAP	6.1	3.29
OKA	5.8	3.23
PEZ_N	5.9	3.46
PEZ_W	5.9	3.46
RR	6.2	3.69
RR_RCG	6.1	3.69
SLR	6.2	3.67

a) No events greater than **M** 2.9 are located in the AHEX zone in the final catalog

**PSEG Site
ESP Application
Part 2, Site Safety Analysis Report**

**Table 2.5.2-26
Regional Updated Seismicity Catalog for the PSEG Site ($M \geq 2.9$)**

Year	Month	Day	Hour	Min	Sec	Lat_N	Long_W	Depth	Mw^(a)	Catalog^(b)
1990	05	05	20	48	00.00	36.03	-71.67	10	3.38	NEIC
2009	02	03	03	34	00.00	40.87	-74.52	5	3.05	NEIC
2009	04	24	05	36	00.00	40.06	-77.03	1	2.97	NEIC
2009	05	18	00	53	00.00	42.57	-74.11	9	3.05	NEIC
2009	06	05	15	07	00.00	42.83	-78.25	5	2.97	NEIC
2009	10	21	01	32	00.00	42.57	-74.1	7	2.97	NEIC
2009	11	25	22	24	46.13	37.5602	-78.8702	0	2.93	ANSS
2009	12	13	22	00	00.00	42.57	-74.11	10	3.13	NEIC
2010	02	21	13	00	26.02	40.71	-74.64	9.73	2.97	NESN
2010	06	03	12	25	00.00	40.09	-76.97	1	2.97	NEIC
2010	07	16	09	04	00.00	39.18	-77.29	5	3.40	NEIC
2010	10	02	20	17	00.05	37.8532	-77.5187	19.2	3.16	ANSS
2010	11	30	15	45	59.08	39.798	-71.9273	6.63	3.78	ANSS
2011	08	23	17	51	00.00	37.94	-77.93	6	5.80	NEIC
2011	08	25	05	07	52.29	37.9468	-77.9672	6.81	4.30	ANSS
2011	08	27	14	38	00.00	42.69	-74.09	22	2.97	NEIC
2011	08	29	03	16	51.57	37.9347	-77.9877	3.72	2.93	ANSS
2011	09	01	09	09	37.96	37.9502	-77.932	3.42	3.46	ANSS
2011	10	12	16	40	00.37	37.9402	-77.983	4.01	3.16	ANSS

a) Mw = **M** in CEUS-SSC terminology

b) ANSS – Advanced National Seismic System
NEIC – National Earthquake Information Center
NESN – New England Seismic Network

**PSEG Site
ESP Application
Part 2, Site Safety Analysis Report**

**Table 2.5.2-27
CEUS-SSC Mmax Zones (Modified from Table H-3-1 of NUREG-2115)**

Zone Acronym	Mmax Source Zones
MESE-N	Mesozoic-and-Younger Extension – Narrow Interpretation
MESE-W	Mesozoic-and-Younger Extension – Wide Interpretation
NMESE-N	Non-Mesozoic-and-Younger Extension – Narrow Interpretation
NMESE-W	Non-Mesozoic-and-Younger Extension – Wide Interpretation
STUDY-R	CEUS-SSC Study Region

**PSEG Site
ESP Application
Part 2, Site Safety Analysis Report**

**Table 2.5.2-28
CEUS-SSC Seismotectonic Zones (Modified from Table H-4-1 of NUREG-2115)**

Zone Acronym	Seismotectonic Source Zones
AHEX	Atlantic Highly Extended Crust
ECC-AM	Extended Continental Crust – Atlantic Margin
ECC-GC	Extended Continental Crust – Gulf Coast
GHEX	Gulf Coast Highly Extended Crust
GMH	Great Meteor Hotspot
IBEB	Illinois Basin Extended Basement
MIDC-A	Midcontinent – Craton - Alternative interpretation A
MIDC-B	Midcontinent – Craton - Alternative interpretation B
MIDC-C	Midcontinent – Craton - Alternative interpretation C
MIDC-D	Midcontinent – Craton - Alternative interpretation D
NAP	Northern Appalachian
OKA	Oklahoma Aulacogen
PEZ-N	Paleozoic Extended Crust – Narrow Interpretation
PEZ-W	Paleozoic Extended Crust – Wide interpretation
RR	Reelfoot Rift
RR-RCG	Reelfoot Rift including Rough Creek Graben
SLR	St. Lawrence Rift including Ottawa and Saguenay grabens

**PSEG Site
ESP Application
Part 2, Site Safety Analysis Report**

**Table 2.5.2-29
CEUS-SSC RLME Sources (Modified from Table 4.2.2-1 of NUREG-2115)**

RLME	RLME Components
Charlevoix	Charlevoix Area Source
Charleston	Charleston Area Sources
Cheraw	Cheraw Fault
Meers	Meers Fault and Oklahoma Aulacogen Area Source
Reelfoot Rift Central Fault System – New Madrid North	New Madrid North Fault
Reelfoot Rift Central Fault System – New Madrid South	New Madrid South Fault
Reelfoot Rift Central Fault System – Reelfoot Thrust	Reelfoot Rift Fault
Reelfoot Rift Central Fault System – Eastern Rift Margin	Eastern Rift Margin – North Area Source Eastern Rift Margin – South Area Source
Reelfoot Rift - Marianna	Marianna Area Source
Reelfoot Rift – Commerce Fault Zone	Commerce Area Source
Wabash Valley	Wabash Valley Area Source

**PSEG Site
ESP Application
Part 2, Site Safety Analysis Report**

**Table 2.5.2-30
CEUS-SSC Seismic Sources Used in the PSEG Site PSHA Calculations**

Background Sources	Mmax	CEUS-SSC Study Region (STUDY-R)
		Mesozoic-and-Younger Extension - Wide (MESE-W)
		Mesozoic-and-Younger Extension - Narrow (MESE-N)
		Non-Mesozoic-and-Younger Extension - Wide (NMESE-W)
		Non-Mesozoic-and-Younger Extension - Narrow (NMESE-N)
	Seismotectonic	Atlantic Highly Extended Crust (AHEX)
		Atlantic Highly Extended Crust – East (AHEX-E) ^(a)
		Extended Continental Crust - Atlantic Margin (ECC-AM)
		Extended Continental Crust - Gulf Coast (ECC-GC)
		Gulf Coast Highly Extended Crust (GHEX)
		Great Meteor Hotspot (GMH)
		Illinois Basin Extended Basement (IBEB)
		Midcontinent-Craton (MIDC-A, MIDC-B, MIDC-C, and MIDC-D)
		Northern Appalachian (NAP)
		Oklahoma Aulacogen (OKA)
		Paleozoic Extended Crust - Wide (PEZ-W)
		Paleozoic Extended Crust - Narrow (PEZ-N)
		Reelfoot Rift (RR)
		Reelfoot Rift with Rough Creek Graben (RR-RCG)
		St. Lawrence Rift (SLR)
RLME Sources	Charleston (CHARLESTON)	
	Charlevoix (CHARLEVOIX)	
	Cheraw (CHERAW)	
	Meers (MEERS)	
	Reelfoot Rift - Central Fault System (NMFS) ^(b)	
	Reelfoot Rift - Eastern Rift Margin (ERM-N and ERM-S)	
	Reelfoot Rift - Marianna (MARIANNA)	
	Reelfoot Rift - Commerce (COMMERCE)	
	Wabash Valley (WABASH VALLEY)	

- a) AHEX-E is an additional seismic source zone created for the small area where the PSEG regional study area extends outside the CEUS-SSC study boundary (STUDY-R). Source parameters are taken from the AHEX source (NUREG-2115) as well as additional information from the updated CEUS-SSC catalog.
- b) The Reelfoot Rift – Central Fault System is made up of the New Madrid North fault (NMN), the New Madrid South fault (NMS) and the Reelfoot Thrust (RFT). These sources are combined into one RLME source that is called the New Madrid Fault System (NMFS).

**PSEG Site
ESP Application
Part 2, Site Safety Analysis Report**

**Table 2.5.2-31 (Sheet 1 of 7)
Mean and Fractile Rock Seismic Hazard Curves**

100 Hz (PGA) Hazard Curves						
Amplitude^(a)	MEAN	0.05^(b)	0.16	0.5^(c)	0.84	0.95
0.0005	6.08E-02	2.10E-02	2.83E-02	4.76E-02	1.04E-01	1.41E-01
0.0007	4.73E-02	1.70E-02	2.14E-02	3.41E-02	8.22E-02	1.16E-01
0.001	3.56E-02	1.29E-02	1.62E-02	2.44E-02	6.12E-02	8.97E-02
0.0015	2.54E-02	9.12E-03	1.13E-02	1.71E-02	4.45E-02	6.52E-02
0.002	1.98E-02	6.92E-03	8.56E-03	1.28E-02	3.43E-02	5.09E-02
0.003	1.36E-02	4.90E-03	6.04E-03	8.85E-03	2.29E-02	3.59E-02
0.005	8.29E-03	2.82E-03	3.72E-03	5.33E-03	1.37E-02	2.16E-02
0.007	5.86E-03	1.86E-03	2.63E-03	4.00E-03	8.85E-03	1.49E-02
0.01	3.98E-03	1.23E-03	1.74E-03	2.82E-03	5.97E-03	1.00E-02
0.015	2.50E-03	7.08E-04	1.07E-03	1.86E-03	3.80E-03	5.78E-03
0.02	1.76E-03	4.68E-04	7.08E-04	1.32E-03	2.65E-03	4.04E-03
0.03	1.04E-03	2.69E-04	4.07E-04	7.59E-04	1.52E-03	2.33E-03
0.05	5.06E-04	1.35E-04	1.91E-04	3.80E-04	7.59E-04	1.23E-03
0.07	3.09E-04	7.76E-05	1.10E-04	2.34E-04	4.68E-04	7.59E-04
0.1	1.82E-04	4.17E-05	6.31E-05	1.35E-04	2.88E-04	4.68E-04
0.15	9.89E-05	2.16E-05	3.16E-05	7.76E-05	1.66E-04	2.51E-04
0.2	6.35E-05	1.29E-05	1.95E-05	5.13E-05	1.02E-04	1.55E-04
0.3	3.33E-05	6.46E-06	1.08E-05	2.75E-05	5.89E-05	8.32E-05
0.5	1.38E-05	2.14E-06	3.98E-06	1.05E-05	2.57E-05	3.89E-05
0.7	7.23E-06	9.33E-07	1.86E-06	5.25E-06	1.38E-05	2.24E-05
1	3.41E-06	3.20E-07	7.08E-07	2.29E-06	6.46E-06	1.05E-05
1.5	1.29E-06	7.24E-08	2.04E-07	7.08E-07	2.29E-06	4.27E-06
2	5.93E-07	2.09E-08	6.53E-08	3.09E-07	1.00E-06	2.29E-06
3	1.71E-07	2.37E-09	1.05E-08	7.24E-08	2.88E-07	7.33E-07
5	2.69E-08	3.59E-15	4.68E-10	8.51E-09	4.79E-08	1.30E-07
7	6.55E-09	5.19E-29	4.73E-15	1.68E-09	1.12E-08	3.27E-08
10	1.24E-09	4.20E-29	6.31E-17	2.34E-10	2.00E-09	6.03E-09

- a) Spectral acceleration in g
b) Percentile
c) 0.5 fractile = median

**PSEG Site
ESP Application
Part 2, Site Safety Analysis Report**

**Table 2.5.2-31 (Sheet 2 of 7)
Mean and Fractile Rock Seismic Hazard Curves**

25 Hz Hazard Curves						
Amplitude^(a)	MEAN	0.05^(b)	0.16	0.5^(c)	0.84	0.95
0.0005	7.69E-02	1.82E-02	3.02E-02	7.55E-02	1.11E-01	1.71E-01
0.0007	6.18E-02	1.48E-02	2.44E-02	5.75E-02	9.10E-02	1.32E-01
0.001	4.84E-02	1.29E-02	1.84E-02	4.38E-02	7.00E-02	1.02E-01
0.0015	3.62E-02	1.05E-02	1.49E-02	2.91E-02	5.38E-02	7.49E-02
0.002	2.92E-02	9.12E-03	1.20E-02	2.21E-02	4.19E-02	5.86E-02
0.003	2.14E-02	7.41E-03	9.13E-03	1.45E-02	3.01E-02	4.57E-02
0.005	1.43E-02	4.90E-03	6.46E-03	9.39E-03	1.98E-02	3.01E-02
0.007	1.08E-02	3.98E-03	4.90E-03	7.05E-03	1.46E-02	2.29E-02
0.01	7.99E-03	2.82E-03	3.47E-03	5.30E-03	1.06E-02	1.72E-02
0.015	5.62E-03	1.86E-03	2.46E-03	3.73E-03	7.24E-03	1.16E-02
0.02	4.34E-03	1.32E-03	1.86E-03	3.02E-03	5.76E-03	8.97E-03
0.03	2.96E-03	8.13E-04	1.23E-03	2.14E-03	4.02E-03	6.00E-03
0.05	1.74E-03	4.22E-04	6.61E-04	1.23E-03	2.46E-03	3.55E-03
0.07	1.18E-03	2.69E-04	4.37E-04	8.13E-04	1.68E-03	2.48E-03
0.1	7.54E-04	1.66E-04	2.51E-04	5.37E-04	1.07E-03	1.74E-03
0.15	4.39E-04	8.91E-05	1.40E-04	3.09E-04	6.17E-04	1.07E-03
0.2	2.93E-04	5.89E-05	8.91E-05	2.04E-04	4.07E-04	7.08E-04
0.3	1.62E-04	3.16E-05	4.79E-05	1.18E-04	2.34E-04	4.07E-04
0.5	7.40E-05	1.29E-05	2.24E-05	5.50E-05	1.18E-04	1.97E-04
0.7	4.31E-05	6.92E-06	1.29E-05	3.16E-05	7.24E-05	1.22E-04
1	2.37E-05	3.47E-06	6.03E-06	1.70E-05	4.47E-05	6.31E-05
1.5	1.15E-05	1.41E-06	2.82E-06	8.22E-06	2.24E-05	3.39E-05
2	6.61E-06	6.38E-07	1.41E-06	4.42E-06	1.20E-05	2.09E-05
3	2.85E-06	1.91E-07	4.37E-07	1.62E-06	4.90E-06	9.77E-06
5	8.61E-07	3.06E-08	8.32E-08	3.80E-07	1.41E-06	3.02E-06
7	3.53E-07	6.24E-09	2.24E-08	1.26E-07	5.75E-07	1.32E-06
10	1.23E-07	5.56E-10	4.57E-09	3.63E-08	1.91E-07	5.01E-07

- a) Spectral acceleration in g
b) Percentile
c) 0.5 fractile = median

**PSEG Site
ESP Application
Part 2, Site Safety Analysis Report**

**Table 2.5.2-31 (Sheet 3 of 7)
Mean and Fractile Rock Seismic Hazard Curves**

10 Hz Hazard Curves						
Amplitude^(a)	MEAN	0.05^(b)	0.16	0.5^(c)	0.84	0.95
0.0005	9.89E-02	3.91E-02	5.62E-02	9.32E-02	1.45E-01	1.84E-01
0.0007	7.94E-02	3.18E-02	4.27E-02	7.12E-02	1.19E-01	1.52E-01
0.001	6.15E-02	2.41E-02	3.24E-02	5.08E-02	9.14E-02	1.17E-01
0.0015	4.50E-02	1.82E-02	2.29E-02	3.63E-02	6.58E-02	9.03E-02
0.002	3.56E-02	1.48E-02	1.85E-02	2.76E-02	5.09E-02	7.07E-02
0.003	2.52E-02	9.78E-03	1.30E-02	1.82E-02	3.70E-02	5.21E-02
0.005	1.60E-02	6.46E-03	7.98E-03	1.10E-02	2.34E-02	3.45E-02
0.007	1.17E-02	4.57E-03	5.63E-03	8.21E-03	1.65E-02	2.54E-02
0.01	8.20E-03	3.02E-03	3.98E-03	5.73E-03	1.14E-02	1.76E-02
0.015	5.39E-03	2.00E-03	2.63E-03	4.01E-03	7.20E-03	1.16E-02
0.02	3.95E-03	1.41E-03	2.00E-03	3.03E-03	5.25E-03	7.90E-03
0.03	2.48E-03	8.13E-04	1.23E-03	2.00E-03	3.33E-03	4.86E-03
0.05	1.31E-03	4.07E-04	6.17E-04	1.07E-03	1.75E-03	2.59E-03
0.07	8.27E-04	2.51E-04	3.80E-04	6.61E-04	1.08E-03	1.66E-03
0.1	4.94E-04	1.45E-04	2.19E-04	4.07E-04	7.08E-04	1.01E-03
0.15	2.69E-04	7.76E-05	1.10E-04	2.19E-04	4.07E-04	5.77E-04
0.2	1.74E-04	4.79E-05	6.76E-05	1.45E-04	2.88E-04	3.81E-04
0.3	9.23E-05	2.32E-05	3.39E-05	7.76E-05	1.55E-04	2.04E-04
0.5	4.02E-05	8.51E-06	1.38E-05	3.39E-05	7.24E-05	9.55E-05
0.7	2.24E-05	4.57E-06	7.41E-06	1.82E-05	3.89E-05	5.50E-05
1	1.15E-05	2.21E-06	3.47E-06	9.12E-06	2.09E-05	3.16E-05
1.5	5.02E-06	8.71E-07	1.32E-06	3.47E-06	9.12E-06	1.38E-05
2	2.62E-06	3.80E-07	6.38E-07	1.86E-06	4.90E-06	7.41E-06
3	9.49E-07	1.02E-07	2.04E-07	6.17E-07	1.74E-06	2.82E-06
5	2.18E-07	1.20E-08	3.16E-08	1.35E-07	3.80E-07	6.61E-07
7	7.28E-08	1.57E-09	6.92E-09	3.89E-08	1.26E-07	2.34E-07
10	2.02E-08	7.50E-11	9.33E-10	9.12E-09	3.89E-08	7.24E-08

- a) Spectral acceleration in g
b) Percentile
c) 0.5 fractile = median

**PSEG Site
ESP Application
Part 2, Site Safety Analysis Report**

**Table 2.5.2-31 (Sheet 4 of 7)
Mean and Fractile Rock Seismic Hazard Curves**

5 Hz Hazard Curves						
Amplitude^(a)	MEAN	0.05^(b)	0.16	0.5^(c)	0.84	0.95
0.0005	1.12E-01	5.91E-02	7.38E-02	9.97E-02	1.66E-01	2.04E-01
0.0007	8.95E-02	4.19E-02	5.62E-02	7.63E-02	1.36E-01	1.75E-01
0.001	6.88E-02	2.96E-02	4.27E-02	5.50E-02	1.05E-01	1.44E-01
0.0015	4.96E-02	2.09E-02	2.82E-02	3.94E-02	7.62E-02	1.11E-01
0.002	3.87E-02	1.48E-02	2.00E-02	3.03E-02	6.25E-02	8.58E-02
0.003	2.67E-02	9.78E-03	1.31E-02	2.02E-02	4.22E-02	6.24E-02
0.005	1.61E-02	5.62E-03	7.48E-03	1.23E-02	2.55E-02	3.84E-02
0.007	1.13E-02	3.72E-03	4.92E-03	8.01E-03	1.80E-02	2.77E-02
0.01	7.55E-03	2.46E-03	3.24E-03	5.50E-03	1.20E-02	1.87E-02
0.015	4.64E-03	1.46E-03	2.00E-03	3.32E-03	7.06E-03	1.12E-02
0.02	3.21E-03	1.00E-03	1.41E-03	2.32E-03	4.79E-03	7.60E-03
0.03	1.85E-03	5.37E-04	8.13E-04	1.42E-03	2.62E-03	4.28E-03
0.05	8.87E-04	2.51E-04	3.80E-04	6.84E-04	1.21E-03	1.91E-03
0.07	5.31E-04	1.55E-04	2.19E-04	4.07E-04	7.14E-04	1.13E-03
0.1	3.01E-04	8.32E-05	1.26E-04	2.34E-04	4.37E-04	6.29E-04
0.15	1.56E-04	4.17E-05	6.31E-05	1.18E-04	2.51E-04	3.56E-04
0.2	9.65E-05	2.40E-05	3.63E-05	7.24E-05	1.55E-04	2.19E-04
0.3	4.83E-05	1.12E-05	1.70E-05	3.63E-05	7.76E-05	1.10E-04
0.5	1.92E-05	3.98E-06	6.03E-06	1.48E-05	3.16E-05	4.79E-05
0.7	1.00E-05	1.86E-06	2.82E-06	7.94E-06	1.70E-05	2.57E-05
1	4.74E-06	7.59E-07	1.23E-06	3.72E-06	8.51E-06	1.29E-05
1.5	1.86E-06	2.51E-07	4.37E-07	1.41E-06	3.47E-06	5.25E-06
2	9.05E-07	1.02E-07	1.78E-07	6.61E-07	1.74E-06	2.63E-06
3	2.95E-07	1.82E-08	4.17E-08	2.04E-07	5.75E-07	9.33E-07
5	5.97E-08	5.07E-12	4.27E-09	3.16E-08	1.18E-07	2.19E-07
7	1.84E-08	7.50E-14	4.52E-10	7.67E-09	3.63E-08	7.24E-08
10	4.70E-09	9.66E-19	2.75E-14	1.51E-09	9.12E-09	2.09E-08

- a) Spectral acceleration in g
b) Percentile
c) 0.5 fractile = median

**PSEG Site
ESP Application
Part 2, Site Safety Analysis Report**

**Table 2.5.2-31 (Sheet 5 of 7)
Mean and Fractile Rock Seismic Hazard Curves**

2.5 Hz Hazard Curves						
Amplitude^(a)	MEAN	0.05^(b)	0.16	0.5^(c)	0.84	0.95
0.0005	1.03E-01	1.59E-02	6.44E-02	4.19E-02	1.56E-01	1.98E-01
0.0007	8.06E-02	1.13E-02	4.58E-02	3.07E-02	1.28E-01	1.70E-01
0.001	6.06E-02	7.17E-03	3.24E-02	2.10E-02	9.86E-02	1.36E-01
0.0015	4.26E-02	4.27E-03	2.01E-02	1.38E-02	7.20E-02	9.89E-02
0.002	3.26E-02	2.92E-03	1.42E-02	9.78E-03	5.60E-02	8.01E-02
0.003	2.18E-02	1.62E-03	8.68E-03	6.46E-03	3.81E-02	5.50E-02
0.005	1.25E-02	7.85E-04	4.61E-03	3.47E-03	2.18E-02	3.30E-02
0.007	8.34E-03	4.68E-04	3.03E-03	2.14E-03	1.40E-02	2.28E-02
0.01	5.25E-03	2.51E-04	1.87E-03	1.32E-03	8.61E-03	1.49E-02
0.015	2.97E-03	1.18E-04	1.07E-03	7.59E-04	4.76E-03	8.52E-03
0.02	1.93E-03	7.24E-05	6.61E-04	5.01E-04	2.82E-03	5.72E-03
0.03	1.02E-03	3.16E-05	3.55E-04	2.69E-04	1.39E-03	2.76E-03
0.05	4.35E-04	1.05E-05	1.45E-04	1.10E-04	5.59E-04	1.05E-03
0.07	2.42E-04	4.57E-06	7.76E-05	5.89E-05	3.36E-04	5.59E-04
0.1	1.27E-04	1.86E-06	4.17E-05	2.75E-05	1.79E-04	2.90E-04
0.15	5.98E-05	5.75E-07	1.95E-05	1.29E-05	9.56E-05	1.38E-04
0.2	3.45E-05	2.19E-07	1.12E-05	6.92E-06	5.89E-05	8.10E-05
0.3	1.56E-05	4.79E-08	4.90E-06	2.82E-06	2.75E-05	3.64E-05
0.5	5.47E-06	2.27E-10	1.41E-06	8.71E-07	9.77E-06	1.38E-05
0.7	2.61E-06	1.80E-12	5.75E-07	3.31E-07	4.90E-06	6.92E-06
1	1.13E-06	7.00E-14	2.04E-07	8.91E-08	2.14E-06	3.24E-06
1.5	3.99E-07	1.15E-15	4.79E-08	1.59E-08	8.13E-07	1.15E-06
2	1.78E-07	1.46E-18	1.25E-08	7.24E-11	3.80E-07	5.37E-07
3	5.15E-08	4.04E-29	8.91E-11	1.88E-14	1.10E-07	1.66E-07
5	8.85E-09	4.20E-29	2.07E-15	5.07E-29	1.82E-08	3.16E-08
7	2.44E-09	4.20E-29	4.32E-17	4.28E-29	4.90E-09	9.77E-09
10	5.53E-10	4.20E-29	3.55E-19	4.20E-29	1.07E-09	2.46E-09

- a) Spectral acceleration in g
b) Percentile
c) 0.5 fractile = median

**PSEG Site
ESP Application
Part 2, Site Safety Analysis Report**

**Table 2.5.2-31 (Sheet 6 of 7)
Mean and Fractile Rock Seismic Hazard Curves**

1 Hz Hazard Curves						
Amplitude^(a)	MEAN	0.05^(b)	0.16	0.5^(c)	0.84	0.95
0.0005	5.94E-02	1.59E-02	3.04E-02	4.27E-02	1.05E-01	1.29E-01
0.0007	4.44E-02	1.13E-02	2.01E-02	3.12E-02	8.21E-02	1.07E-01
0.001	3.19E-02	7.17E-03	1.32E-02	2.16E-02	5.70E-02	7.91E-02
0.0015	2.14E-02	4.27E-03	8.10E-03	1.41E-02	3.94E-02	5.71E-02
0.002	1.59E-02	2.92E-03	5.32E-03	1.03E-02	2.93E-02	4.43E-02
0.003	1.02E-02	1.62E-03	2.84E-03	6.22E-03	1.87E-02	2.93E-02
0.005	5.47E-03	7.85E-04	1.32E-03	3.09E-03	1.02E-02	1.78E-02
0.007	3.49E-03	4.68E-04	7.09E-04	1.80E-03	6.12E-03	1.19E-02
0.01	2.08E-03	2.51E-04	4.08E-04	9.62E-04	3.57E-03	7.64E-03
0.015	1.10E-03	1.18E-04	2.04E-04	4.76E-04	1.66E-03	4.33E-03
0.02	6.84E-04	7.24E-05	1.18E-04	2.82E-04	9.18E-04	2.69E-03
0.03	3.35E-04	3.16E-05	5.31E-05	1.37E-04	3.79E-04	1.22E-03
0.05	1.27E-04	1.05E-05	1.82E-05	5.14E-05	1.44E-04	3.88E-04
0.07	6.41E-05	4.57E-06	9.12E-06	2.76E-05	7.94E-05	1.70E-04
0.1	2.96E-05	1.86E-06	4.27E-06	1.38E-05	4.20E-05	7.31E-05
0.15	1.18E-05	5.75E-07	1.51E-06	6.03E-06	1.95E-05	2.93E-05
0.2	6.09E-06	2.19E-07	6.61E-07	3.24E-06	1.12E-05	1.63E-05
0.3	2.40E-06	4.79E-08	1.91E-07	1.32E-06	4.90E-06	7.45E-06
0.5	7.30E-07	2.27E-10	2.02E-08	3.55E-07	1.62E-06	2.46E-06
0.7	3.21E-07	1.80E-12	1.78E-10	1.26E-07	7.59E-07	1.15E-06
1	1.27E-07	7.00E-14	1.48E-11	3.89E-08	2.88E-07	5.01E-07
1.5	4.01E-08	1.15E-15	1.97E-13	1.05E-08	8.61E-08	1.78E-07
2	1.65E-08	1.46E-18	9.44E-15	3.24E-09	3.39E-08	7.76E-08
3	4.26E-09	4.04E-29	1.45E-16	4.07E-10	8.51E-09	2.16E-08
5	6.28E-10	4.20E-29	2.88E-19	2.85E-11	1.15E-09	3.47E-09
7	1.55E-10	4.20E-29	5.28E-29	4.27E-12	2.51E-10	8.71E-10
10	3.12E-11	4.20E-29	5.28E-29	5.75E-13	4.47E-11	1.66E-10

- a) Spectral acceleration in g
b) Percentile
c) 0.5 fractile = median

**PSEG Site
ESP Application
Part 2, Site Safety Analysis Report**

**Table 2.5.2-31 (Sheet 7 of 7)
Mean and Fractile Rock Seismic Hazard Curves**

0.5 Hz Hazard Curves						
Amplitude^(a)	MEAN	0.05^(b)	0.16	0.5^(c)	0.84	0.95
0.0005	3.34E-02	6.96E-03	1.28E-02	2.31E-02	6.08E-02	8.54E-02
0.0007	2.43E-02	4.59E-03	7.86E-03	1.72E-02	4.53E-02	6.67E-02
0.001	1.71E-02	2.82E-03	4.79E-03	1.23E-02	3.16E-02	4.92E-02
0.0015	1.12E-02	1.57E-03	2.54E-03	7.75E-03	2.11E-02	3.41E-02
0.002	8.24E-03	1.00E-03	1.55E-03	5.26E-03	1.57E-02	2.59E-02
0.003	5.17E-03	4.68E-04	7.68E-04	2.71E-03	9.97E-03	1.76E-02
0.005	2.73E-03	1.66E-04	2.89E-04	1.12E-03	5.27E-03	1.04E-02
0.007	1.74E-03	8.32E-05	1.55E-04	5.86E-04	3.17E-03	6.89E-03
0.01	1.04E-03	3.89E-05	7.25E-05	2.87E-04	1.71E-03	4.39E-03
0.015	5.56E-04	1.59E-05	2.95E-05	1.33E-04	7.20E-04	2.44E-03
0.02	3.47E-04	8.51E-06	1.59E-05	7.44E-05	3.64E-04	1.51E-03
0.03	1.74E-04	3.02E-06	6.03E-06	3.41E-05	1.48E-04	6.21E-04
0.05	7.08E-05	7.08E-07	1.74E-06	1.20E-05	5.47E-05	1.68E-04
0.07	3.70E-05	2.19E-07	6.61E-07	5.62E-06	2.82E-05	7.02E-05
0.1	1.70E-05	5.69E-08	2.19E-07	2.46E-06	1.39E-05	2.86E-05
0.15	6.24E-06	5.43E-09	4.79E-08	7.59E-07	6.03E-06	1.05E-05
0.2	2.86E-06	9.55E-11	1.05E-08	3.55E-07	3.47E-06	5.77E-06
0.3	9.03E-07	1.27E-12	1.10E-10	1.18E-07	1.32E-06	2.83E-06
0.5	2.11E-07	8.22E-15	3.98E-12	1.95E-08	4.07E-07	9.34E-07
0.7	8.32E-08	5.56E-16	1.84E-13	3.47E-09	1.91E-07	4.22E-07
1	3.09E-08	4.04E-29	4.42E-15	3.67E-10	7.76E-08	1.78E-07
1.5	9.53E-09	4.04E-29	8.61E-17	4.17E-11	2.40E-08	5.50E-08
2	3.88E-09	4.04E-29	4.73E-18	8.51E-12	9.77E-09	2.40E-08
3	9.81E-10	4.20E-29	5.28E-29	1.00E-12	2.29E-09	6.03E-09
5	1.41E-10	4.20E-29	5.28E-29	4.17E-14	2.51E-10	9.33E-10
7	3.43E-11	4.20E-29	4.47E-29	4.12E-15	4.79E-11	2.19E-10
10	6.76E-12	4.20E-29	4.47E-29	2.19E-16	7.41E-12	4.17E-11

- a) Spectral acceleration in g
b) Percentile
c) 0.5 fractile = median

**PSEG Site
ESP Application
Part 2, Site Safety Analysis Report**

**Table 2.5.2-32
Mean and Median UHRS Values for Rock Seismic Hazard at the PSEG Site
(Spectral Acceleration in g)**

Frequency, Hz	Mean 10⁻⁴	Mean 10⁻⁵	Mean 10⁻⁶
100 (PGA)	0.149	0.591	1.65
25	0.411	1.61	4.69
10	0.285	1.07	2.94
5.0	0.196	0.700	1.92
2.5	0.114	0.373	1.05
1.0	0.0563	0.161	0.437
0.5	0.0411	0.124	0.289
Frequency, Hz	Median 10⁻⁴	Median 10⁻⁵	Median 10⁻⁶
100 (PGA)	0.125	0.511	1.33
25	0.334	1.34	3.56
10	0.254	0.954	2.51
5.0	0.165	0.618	1.71
2.5	0.0971	0.325	0.888
1.0	0.0354	0.117	0.334
0.5	0.0173	0.0543	0.136

**PSEG Site
ESP Application
Part 2, Site Safety Analysis Report**

**Table 2.5.2-33 (Sheet 1 of 3)
Percent Contribution to Hazard by Magnitude and Distance^(a)**

Percent contribution by M-R Bin for 1 & 2.5 Hz, 10 ⁻⁴								
Distance (km)	Magnitude							
	5.25	5.75	6.25	6.75	7.25	7.75	8.25	8.75
0-20	8.6%	7.2%	3.9%	1.8%	3.8%	2.6%	<< 0.1%	<< 0.1%
20-40	3.7%	5.9%	4.7%	2.4%	0.7%	0.2%	<< 0.1%	<< 0.1%
40-60	0.8%	1.9%	2.8%	2.1%	0.7%	0.2%	< 0.1%	<< 0.1%
60-80	0.2%	1.0%	2.2%	1.5%	0.8%	0.1%	<< 0.1%	<< 0.1%
80-100	< 0.1%	0.4%	1.1%	1.4%	0.7%	0.2%	<< 0.1%	<< 0.1%
100-200	< 0.1%	0.8%	2.5%	3.4%	1.9%	0.5%	< 0.1%	<< 0.1%
200-300	<< 0.1%	0.1%	0.6%	1.3%	0.9%	0.4%	< 0.1%	<< 0.1%
> 300	<< 0.1%	< 0.1%	0.3%	1.5%	3.9%	13.8%	4.1%	<< 0.1%
Percent contribution by M-R bin for 5 & 10 Hz, 10 ⁻⁴								
Distance (km)	Magnitude							
	5.25	5.75	6.25	6.75	7.25	7.75	8.25	8.75
0-20	19.9%	10.7%	4.5%	1.7%	0.6%	0.2%	<< 0.1%	<< 0.1%
20-40	11.7%	10.1%	5.7%	2.5%	0.7%	0.2%	<< 0.1%	<< 0.1%
40-60	2.6%	3.1%	3.1%	2.0%	0.7%	0.2%	< 0.1%	<< 0.1%
60-80	0.5%	1.4%	2.0%	1.2%	0.6%	0.1%	<< 0.1%	<< 0.1%
80-100	0.3%	0.7%	1.0%	1.0%	0.5%	0.1%	<< 0.1%	<< 0.1%
100-200	0.3%	1.1%	2.2%	2.4%	1.2%	0.4%	< 0.1%	<< 0.1%
200-300	< 0.1%	< 0.1%	0.3%	0.5%	0.3%	0.2%	< 0.1%	<< 0.1%
> 300	<< 0.1%	<< 0.1%	< 0.1%	0.2%	0.3%	0.6%	0.3%	<< 0.1%

a) Magnitude is moment magnitude (**M**). The symbol "<<0.1%" indicates the percent contribution is <0.01%

**PSEG Site
ESP Application
Part 2, Site Safety Analysis Report**

**Table 2.5.2-33 (Sheet 2 of 3)
Percent Contribution to Hazard by Magnitude and Distance^(a)**

Percent contribution by M-R Bin for 1 & 2.5 Hz, 10⁻⁵								
Distance (km)	Magnitude							
	5.25	5.75	6.25	6.75	7.25	7.75	8.25	8.75
0-20	7.9%	14.0%	14.2%	9.0%	3.9%	1.6%	< 0.1%	<< 0.1%
20-40	0.7%	3.1%	6.4%	6.5%	3.3%	1.0%	< 0.1%	<< 0.1%
40-60	< 0.1%	0.4%	1.7%	2.9%	1.9%	0.7%	< 0.1%	<< 0.1%
60-80	<< 0.1%	< 0.1%	0.7%	1.2%	1.3%	0.4%	< 0.1%	<< 0.1%
80-100	<< 0.1%	< 0.1%	0.2%	0.8%	0.8%	0.4%	< 0.1%	<< 0.1%
100-200	<< 0.1%	< 0.1%	0.4%	1.3%	1.4%	0.8%	< 0.1%	<< 0.1%
200-300	<< 0.1%	<< 0.1%	< 0.1%	0.3%	0.4%	0.3%	< 0.1%	<< 0.1%
> 300	<< 0.1%	<< 0.1%	< 0.1%	0.2%	0.9%	5.9%	2.8%	<< 0.1%
Percent contribution by M-R bin for 5 & 10 Hz, 10⁻⁵								
Distance (km)	Magnitude							
	5.25	5.75	6.25	6.75	7.25	7.75	8.25	8.75
0-20	24.0%	22.5%	15.8%	8.4%	2.9%	0.6%	< 0.1%	<< 0.1%
20-40	2.0%	3.9%	5.2%	4.7%	2.3%	0.7%	< 0.1%	<< 0.1%
40-60	< 0.1%	0.3%	0.8%	1.3%	0.9%	0.4%	< 0.1%	<< 0.1%
60-80	<< 0.1%	< 0.1%	0.2%	0.3%	0.4%	0.2%	< 0.1%	<< 0.1%
80-100	<< 0.1%	< 0.1%	< 0.1%	0.2%	0.2%	0.1%	< 0.1%	<< 0.1%
100-200	<< 0.1%	< 0.1%	0.1%	0.3%	0.3%	0.2%	< 0.1%	<< 0.1%
200-300	<< 0.1%	<< 0.1%	<< 0.1%	< 0.1%	< 0.1%	< 0.1%	<< 0.1%	<< 0.1%
> 300	<< 0.1%	<< 0.1%	<< 0.1%	<< 0.1%	< 0.1%	< 0.1%	< 0.1%	<< 0.1%

a) Magnitude is moment magnitude (**M**). The symbol "<<0.1%" indicates the percent contribution is <0.01%

**PSEG Site
ESP Application
Part 2, Site Safety Analysis Report**

**Table 2.5.2-33 (Sheet 3 of 3)
Percent Contribution to Hazard by Magnitude and Distance^(a)**

Percent contribution by M-R Bin for 1 & 2.5 Hz, 10 ⁻⁶								
Distance (km)	Magnitude							
	5.25	5.75	6.25	6.75	7.25	7.75	8.25	8.75
0-20	2.7%	10.0%	20.0%	22.2%	12.1%	3.6%	0.2%	<< 0.1%
20-40	< 0.1%	0.5%	2.8%	6.5%	6.2%	2.8%	0.2%	<< 0.1%
40-60	<< 0.1%	< 0.1%	0.3%	1.3%	1.8%	1.3%	0.1%	<< 0.1%
60-80	<< 0.1%	<< 0.1%	< 0.1%	0.3%	0.8%	0.5%	< 0.1%	<< 0.1%
80-100	<< 0.1%	<< 0.1%	< 0.1%	0.2%	0.3%	0.3%	< 0.1%	<< 0.1%
100-200	<< 0.1%	<< 0.1%	< 0.1%	0.2%	0.4%	0.4%	< 0.1%	<< 0.1%
200-300	<< 0.1%	<< 0.1%	<< 0.1%	< 0.1%	< 0.1%	< 0.1%	< 0.1%	<< 0.1%
> 300	<< 0.1%	<< 0.1%	<< 0.1%	<< 0.1%	< 0.1%	0.7%	0.6%	<< 0.1%
Percent contribution by M-R bin for 5 & 10 Hz, 10 ⁻⁶								
Distance (km)	Magnitude							
	5.25	5.75	6.25	6.75	7.25	7.75	8.25	8.75
0-20	13.7%	20.5%	22.9%	18.6%	9.0%	2.5%	0.2%	<< 0.1%
20-40	0.1%	0.6%	1.8%	3.3%	3.1%	1.6%	0.1%	<< 0.1%
40-60	<< 0.1%	< 0.1%	< 0.1%	0.3%	0.5%	0.5%	< 0.1%	<< 0.1%
60-80	<< 0.1%	<< 0.1%	< 0.1%	< 0.1%	0.1%	0.1%	< 0.1%	<< 0.1%
80-100	<< 0.1%	<< 0.1%	<< 0.1%	< 0.1%	< 0.1%	< 0.1%	< 0.1%	<< 0.1%
100-200	<< 0.1%	<< 0.1%	<< 0.1%	< 0.1%	< 0.1%	< 0.1%	< 0.1%	<< 0.1%
200-300	<< 0.1%	<< 0.1%	<< 0.1%	<< 0.1%	<< 0.1%	<< 0.1%	<< 0.1%	<< 0.1%
> 300	<< 0.1%	<< 0.1%	<< 0.1%	<< 0.1%	<< 0.1%	<< 0.1%	<< 0.1%	<< 0.1%

a) Magnitude is moment magnitude (**M**). The symbol "<<0.1%" indicates the percent contribution is <0.01%

**PSEG Site
ESP Application
Part 2, Site Safety Analysis Report**

**Table 2.5.2-34
Mean Magnitudes (M) and Distances (R) from the 10^{-4} , 10^{-5} , and 10^{-6} Deaggregations at
Low and High Frequencies^(a)**

Structural Frequency	Annual Frequency of Exceedence	All R		R < 100 km		R > 100 km	
		M	R, km	M	R, km	M	R, km
5 & 10 Hz	1E-04	5.9	27	5.8	22	6.7	180
1 & 2.5 Hz	1E-04	6.6	68	6.2	21	7.3	540
5 & 10 Hz	1E-05	6.0	12	6.0	12	7.1	140
1 & 2.5 Hz	1E-05	6.6	27	6.4	16	7.6	570
5 & 10 Hz	1E-06	6.3	9	6.3	9	7.5	130
1 & 2.5 Hz	1E-06	6.7	13	6.7	12	7.7	420

a) Light-gray cells indicate high frequency controlling earthquakes and dark-gray cells indicate low frequency controlling earthquakes.

**PSEG Site
ESP Application
Part 2, Site Safety Analysis Report**

2.5.3 SURFACE FAULTING

The potential for tectonic and non-tectonic surface deformation at the PSEG Site is evaluated in this subsection. Information contained in Subsection 2.5.3 was developed in accordance with RG 1.208 which provides guidance for the recommended level of investigation at different distances from a proposed site for a nuclear facility:

- The site region is that area within 200 miles (mi.) of the new plant location.
- The site vicinity is that area within 25 mi. of the new plant location.
- The site area is that area within 5 mi. of the new plant location.
- The site is that area within 0.6 mi. of the new plant location.

This subsection is intended to demonstrate compliance with 10 CFR 100.23. RG 1.208 contains guidance on characterizing seismic sources, and defines a “capable tectonic source” as a tectonic structure that can generate both vibratory ground motion and tectonic surface deformation, such as faulting or folding at or near the earth’s surface, in the present seismotectonic regime.

In this subsection, the potential for surface faulting due to tectonic and non-tectonic sources is considered. This includes information on:

- Potential surface deformation associated with capable tectonic sources such as faults and folds
- Potential surface deformation associated with non-tectonic processes, such as collapse structures due to carbonate dissolution (karst), subsurface salt migration (salt domes), volcanism, and man-induced deformation (e.g., mining collapse and subsidence due to fluid withdrawal)

There are no capable faults and there is no potential for non-tectonic surface deformation within the site vicinity. Similarly, there is no potential for tectonic or non-tectonic deformation in the site area or the site. The following subsections contain the data, observations, and references to support these conclusions.

2.5.3.1 Geological, Seismological, and Geophysical Investigations

Geologic, seismological, and geophysical investigations performed at and around the PSEG Site characterize Quaternary tectonics, structural geology, stratigraphy, paleoseismology, and geological history for the site. Subsections 2.5.1 and 2.5.4 present the results of these investigations, including site and regional geologic maps and profiles illustrating lithology, stratigraphy, and structure. This subsection also presents investigations specifically relevant to the evaluation of surface faulting. The data presented regarding the potential for surface faulting at the PSEG Site is drawn from an extensive body of information documented in several primary sources:

- Geologic mapping of onshore and offshore areas published by the USGS, multiple state geological surveys, and other researchers – No faults or folds capable of surficial deformation are mapped within 25 mi. of the site. Compilation of existing data and literature, articles published by various researchers in referenced journals and field trip guidebooks were reviewed with emphasis on reports published since the HCGS UFSAR

**PSEG Site
ESP Application
Part 2, Site Safety Analysis Report**

(Reference 2.5.3-19) and the EPRI studies (Reference 2.5.3-6), including the Central and Eastern United States Seismic Source Characterization for Nuclear Facilities (CEUS-SSC, NUREG-2115).

- Review of seismicity data – A comprehensive review was completed of instrumental and historical seismicity data from published journal articles, EPRI Seismic Hazard Methodology for the Central and Eastern United States (Reference 2.5.3-6), and the updated seismicity catalog (Subsection 2.5.2).
- Previous site investigations performed for the Hope Creek (Reference 2.5.3-19) and Salem plants (Reference 2.5.3-18).

In addition to reviewing this existing information, the following investigations were performed to assess the potential for tectonic and non-tectonic deformation within the site area:

- Interpretation of aerial photography and remote sensing imagery
- Field and aerial reconnaissance
- Subsurface boring investigations

The following subsections discuss the results of these investigations.

2.5.3.1.1 Published Geologic Mapping

Review of geologic mapping in the area indicates no Quaternary faults within the site vicinity (Figures 2.5.1-12a and 2.5.1-28). All of Delaware within the site vicinity has been mapped at a scale of 1:24,000 (Reference 2.5.3-17); Maryland has been mapped at scales of 1:62,500 (Reference 2.5.3-10). Northern portions of the site vicinity within New Jersey (including the portion for the site vicinity) have been mapped at a scale of 1:24,000. The remainder of New Jersey portion of the site vicinity is available at 1:100,000 (References 2.5.3-14 and 2.5.3-15). None of these maps indicates the presence of Quaternary faults within the site vicinity.

2.5.3.1.2 Regional Geological Studies

A number of regional studies provide useful data for evaluating the possibility of near-surface faults or deformation. Extensive groundwater investigations have provided subsurface stratigraphic data in the region (References 2.5.3-2 and 2.5.3-30). These studies include boreholes surrounding the PSEG Site and report no faulting, except one buried potential offset in the Cretaceous Potomac strata northwest of the site (Reference 2.5.3-2 and Figure 2.5.3-1). This offset is located approximately 20 mi. north of the PSEG Site and does not deform the overlying Quaternary units (Reference 2.5.3-2).

The USGS has compiled information related to all known and postulated Quaternary faults, liquefaction features, and other tectonic features in the Central and Eastern United States (CEUS) (References 2.5.3-4 and 2.5.3-34). These compilations identify the New Castle County faults in Delaware (References 2.5.3-24, 2.5.3-26, 2.5.3-27, and 2.5.3-25) as potential Quaternary tectonic features within the site vicinity (Subsection 2.5.1.1.4.2.5) (Figure 2.5.1-17). These are concluded to be Class C features without proven evidence of Quaternary faulting (Reference 2.5.3-34) (Table 2.5.1-2). Review of published geological studies indicates that no Quaternary structures capable of producing surficial deformation exist within the site vicinity.

**PSEG Site
ESP Application
Part 2, Site Safety Analysis Report**

2.5.3.1.3 Seismicity Data

The CEUS-SSC study (NUREG-2115) compiled the latest information on seismicity, seismic source zones and sources of repeated large magnitude earthquakes. The CEUS-SSC seismicity catalog was updated to include post-2009 earthquakes (Subsection 2.5.2), and the resultant catalog indicates no earthquakes with expected moment magnitude estimates ($E[M]$) ≥ 3.0 within the site area (Figure 2.5.3-1). Within the site vicinity, less than 10 earthquakes have occurred with $E[M] \geq 3.0$. Most of these have magnitudes and locations based on non-instrumental intensity estimates. The largest event within the site vicinity was the instrumentally located $E[M]$ 3.77 event of February 28, 1973, which occurred roughly 19 miles north of the site. None of these events have been attributed to faults within the site vicinity (References 2.5.3-21 and 2.5.3-19).

2.5.3.1.4 Previous Site Investigations

The results of previous geological, geotechnical, and seismological studies were reviewed before planning the field and geotechnical investigations for the PSEG Site. The Hope Creek UFSAR (Reference 2.5.3-19) and the Salem UFSAR (Reference 2.5.3-18) summarize these previous studies. These studies included an extensive boring program, seismic refraction surveys, field reconnaissance and examination of the excavations during construction. These studies concluded that:

- No surficial folding or faulting exists within the site area.
- No evidence of prior earthquakes was found in the surficial materials in the site area.
- The near-surface geologic units are planar and undisrupted by folding or faulting beneath the site.

2.5.3.1.5 Aerial Imagery Analysis

The entire site area and up to 5 mi. beyond were inspected for linear features (lineaments). Aerial photography, satellite imagery, and topographic maps of varying scales and vintages reveal no evidence of geomorphic features indicative of potential tectonic surface deformation (e.g., faulting, warping, folding) within the site area. Imagery reviewed for the site area was obtained from the New Jersey Geographic Information Network and the Delaware Data Mapping and Integration Laboratory (Delaware DataMIL) and includes:

- Historical (1930's vintage) black and white aerial photographs
- Modern (2007) color aerial photographs
- Modern (2007 and 2008) imagery produced with high-resolution light detection and ranging (lidar) elevation data

The objective of reviewing the aerial photography and lidar imagery is to identify surficial features that may indicate the presence of near-surface structures (e.g., faults) within the site area (Figure 2.5.3-2). Features of interest are identified and classified, if possible, as the following types of lineaments:

- Vegetation lineament (VL): Interpreted linear features associated with noted changes in vegetation types, density, or distribution
- Stream lineament (SL): Reaches of streams, creeks, or rivers, which appear linear

**PSEG Site
ESP Application
Part 2, Site Safety Analysis Report**

- Topographic lineament (TL): Interpreted geomorphic feature associated with topographic relief
- Tonal contrast lineament (TC): Uninterrupted linear feature where distinguishable variation in tone is observed and appears aligned straight, which differs from adjacent features
- Paleoshoreline (PS): Curvilinear features bounding differences in topography

Linear features readily identified as anthropogenic or cultural artifacts are seen in imagery. These features included agricultural boundaries, fence lines, roads, railroads, pipelines and construction. The features are not classified because of the number and density of features present in each aerial photo and their obvious non-tectonic origin.

Fifty-eight lineaments are identified within the site area. Twenty-seven lineaments are identified in New Jersey, and 31 lineaments are identified in Delaware. Three vegetation (VL), 18 stream (SL), 21 tonal (TL), 10 (TC) and 6 PS lineaments are identified. Lidar imagery more readily identified topographic lineaments. Aerial photographs more readily identified stream lineaments and tonal contrast lineaments. Curvilinear topographic features are also noted and interpreted as remnant paleoshorelines. Although these features are not structurally controlled lineaments, the interpreted remnant shorelines are prominent along the western margin of Delaware Bay. These are easily identifiable as curvilinear topographic features within the lidar imagery, aligned subparallel to the modern shoreline of Delaware Bay. There was little to no topographic relief and heavy anthropomorphic modification on the eastern shores of Delaware Bay. Therefore, remnant shorelines east of Delaware Bay could not be identified.

While many features are not directly accessible, efforts were made to view the features on the ground from a nearby vantage point or during the aerial reconnaissance. The majority of these lineaments are not identifiable in the modern landscape, except for several shorelines identified parallel to the Delaware River in Delaware. In addition to field checking the topographic lineaments and stream lineaments, field reconnaissance was performed to verify any potential vegetation or tonal lineaments. None of the identified and accessible lineaments within the site area are determined to be structurally controlled features. These are often identified in the field as anthropogenic features associated with deforestation and land clearing for agricultural purposes. The majority of lineaments identified within the site area are identified as the edges of clumps of vegetation within the inaccessible tidal marshes southeast of the site. In summary, none of the lineaments investigated indicated any tectonic or geologic features indicative of surface faulting.

2.5.3.1.6 Current Aerial and Field Reconnaissance

Field reconnaissance included observing the landscape and available outcrops, visiting accessible locations of lineaments identified on aerial imagery, and evaluating the continuity of shorelines west of the PSEG Site. The low topographic relief of the site area results in minimal outcrop and exposure. Several linear features identified in the topography parallel the Delaware River and are interpreted as paleoshorelines. These paleoshorelines are dissected by drainages and are undeformed. Field reconnaissance identified no surficial deformation features. Aerial reconnaissance conducted to evaluate the region surrounding the site respective to faulting and deformation in the site area included:

- Viewing any potential lineaments identified in the historic or modern aerial imagery

**PSEG Site
ESP Application
Part 2, Site Safety Analysis Report**

- Inspecting the areas around the hypothetical features of Pazzaglia (Reference 2.5.3-16) and Marple (Reference 2.5.3-12) shown on Figure 2.5.3-1
- Looking for other faulting or paleoliquefaction evidence in the site vicinity (Figure 2.5.3-2)

Aerial reconnaissance observations indicate that much of the site vicinity has been modified by agriculture and development, but significant portions of the site area are less modified. No anomalous features clearly associated with faulting or deformations are identified within the site area. However, the presence of elliptical to round, lighter-colored patches in a field northeast of the site was noted. Examination of aerial photography shows that these features are numerous, and widely distributed around the Delaware Bay area. These features have been interpreted as resulting from periglacial processes (Reference 2.5.3-41) and formed either as eolian blowouts or thermokarstic depressions (References 2.5.3-37, 2.5.3-38, 2.5.3-39 and 2.5.3-40). Land adjacent to portions of the Chesapeake Bay, Susquehanna River and Delaware River near the Pazzaglia (Reference 2.5.3-16) and Marple (Reference 2.5.3-12) features show no evidence of faulting or deformation.

2.5.3.1.7 Current Site Subsurface Investigations

A geotechnical boring program evaluated the subsurface stratigraphy and structural geology at the PSEG Site. Sixteen new borings supplement the more than 130 borings completed as part of the earlier Hope Creek and Salem site investigations. The new borings extend the area of investigation to roughly one-half square mile. Altogether, the borings indicate that bedding is planar and undisrupted beneath the PSEG Site. Although the top of the Vincentown Formation, as discussed in Subsection 2.5.1.2.4.2, is an established erosional unconformity surface with tens of feet of relief in the site area, planar, unfaulted bedding is demonstrated both above and below that horizon and rules out faulting as the source (Figures 2.5.1-38 and 2.5.1-39). In summary, these investigations found no evidence for near-surface faulting at the site.

2.5.3.2 Geological Evidence, or Absence of Evidence, for Tectonic Surface Deformation

There are no faults identified within the PSEG Site area and very few faults or hypothesized faults are mapped within the site vicinity (Figure 2.5.3-1). In general, three categories summarize the features identified within the site vicinity:

- Paleozoic structures exposed in the Piedmont to the northwest
- Mesozoic faults truncated by undeformed Coastal Plain Cretaceous or Tertiary strata
- Hypothesized features with no recognized geologic or surficial deformation

As discussed in the following subsections, none of these represent a surficial faulting hazard at the PSEG Site.

2.5.3.2.1 Paleozoic Structures Exposed in the Piedmont

The Piedmont of New Jersey, Pennsylvania, Delaware, and Maryland exposes many structures that record the Paleozoic amalgamation of North America. These are primarily northwest-vergent thrust faults with varying degrees of obliquity that were most recently active during the late Paleozoic Alleghanian orogeny. Two primary structures are mapped within the PSEG Site vicinity, but do not extend within the site area. The faults are not active, do not disrupt the surface, and do not represent a surficial hazard for the PSEG Site.

**PSEG Site
ESP Application
Part 2, Site Safety Analysis Report**

The Rosemont shear zone is mapped as a northeast striking fault, interpreted variably as a dextral shear zone or high-angle thrust fault (References 2.5.3-32 and 2.5.3-36). This fault is often interpreted in the literature as separating the arc rocks of the Wilmington complex to the southeast from the Wissahickon Formation; representing a Cambro-Ordovician basin, to the northwest. In Pennsylvania, the shear zone cross-cuts foliations in adjacent units that developed during peak metamorphism. This zone is cross-cut by the Pleasant Grove-Huntingdon Valley (PG-HV) fault (Reference 2.5.3-32). In Maryland, argon (Ar) $^{40}\text{Ar}/^{39}\text{Ar}$ mica ages of approximately 311 million years ago on the PG-HV indicate it was active in the late Carboniferous period (Reference 2.5.3-11). Hence, the Rosemont shear zone was active in the Devonian to Carboniferous periods.

The thrust faults mapped bordering the exposures of Baltimore gneiss and its cover (Setters formation and Cockeysville marble) in the Pennsylvanian and Delaware Piedmont were responsible for uplifting the Greenville-aged basement massifs relative to the younger surrounding units (e.g., the Wissahickon) (Reference 2.5.3-35). These northeast-striking thrusts have led to the interpretation of the West Chester, Avondale, and Mill Creek massifs as nappes (Reference 2.5.3-33). Some of this deformation began in the early Paleozoic along with peak metamorphism, but the later phases of faulting or folding may be as young as late Paleozoic (References 2.5.3-1 and 2.5.3-7).

2.5.3.2.2 Faults Buried by Coastal Plain Sediments

Several faults have been mapped within the site vicinity that offset basement or overlying units, but are buried by younger Coastal Plain strata. These faults must be older than the oldest unfaulted unit that overlies them. These faults are Mesozoic in age, overlapped by Cretaceous to Quaternary units, and do not represent a surface faulting hazard at the PSEG Site.

Benson (Reference 2.5.3-3) interpreted gravity and magnetic anomaly maps, as well as available boreholes and seismic lines, to map Mesozoic basins buried beneath the Coastal Plain. As discussed in Subsection 2.5.1.1.4.2.3, three basins may extend into the southern portion of the PSEG Site vicinity (Figure 2.5.1-35). The Queen Anne basin has a single instance of potential synrift rocks identified in a boring from southern Maryland (Reference 2.5.3-3) and seismic lines that image pre-Cretaceous normal faults in Maryland (Reference 2.5.3-8). A vibroseis seismic reflection line crosses the southeastern boundary of the Buena basin. This was interpreted to cross “minor” normal faults that terminate upward within the Cretaceous Coastal Plain section and larger normal faults that offset basement units (Reference 2.5.3-23). Regardless of whether these three faults do or do not extend to within the site vicinity, as depicted in Figure 2.5.3-1, they do not cut rocks younger than Cretaceous. Therefore, they do not pose a surface faulting hazard for the PSEG Site.

A stratigraphic correlation study of the Cretaceous Potomac Formation used geophysical well log data from throughout eastern Maryland, northern Delaware, and westernmost New Jersey (Reference 2.5.3-2 and Figure 2.5.1-19). The vast majority of the data indicate that the Cretaceous units are planar and correlate without obvious disruptions between borings. However, one apparent offset of Cretaceous units was found in northern Delaware, approximately 15 mi. from the PSEG Site (Figure 2.5.3-1). The base of the overlying Quaternary units was not offset. Therefore, if this offset is due to faulting, it is pre-Quaternary in age and does not represent a surface faulting hazard for the PSEG Site.

**PSEG Site
ESP Application
Part 2, Site Safety Analysis Report**

As discussed in Subsection 2.5.1.1.4.2.5.5, a geologist working with the Delaware Geological Survey, Nenad Spoljaric, identified numerous lineaments, faults, and probable faults throughout Delaware, known broadly as the New Castle County faults. These features vary from offsets of the crystalline basement surface identified in boreholes to postulated lineaments and faults identified with satellite data or imagery (References 2.5.3-24, 2.5.3-26, 2.5.3-27, and 2.5.3-25). While many of these various features exist within the site vicinity, only two extend within the site area in Delaware. These two features, a “fault” and “possible fault” were drawn from lineaments interpreted in Landsat data (Reference 2.5.3-25).

The basement faulting of the earlier studies (References 2.5.3-24 and 2.5.3-26) is distinct from the lineaments mapped on the surface with satellite data (References 2.5.3-27 and 2.5.3-25). There is little doubt that offsets of the Precambrian to Paleozoic basement rocks exist (References 2.5.3-24 and 2.5.3-26). Evidence indicates that unfaulted Cretaceous and younger units overlie these faults (References 2.5.3-24 and 2.5.3-26). These faults are post-Paleozoic and pre-Cretaceous, therefore it is a reasonable interpretation that these offsets are probably due to faulting during Mesozoic rifting. More importantly, these offsets have been demonstrated to be pre-Cretaceous in age, and thus pose no surface faulting hazard. The existence and geologic relevance of the lineaments mapped by Spoljaric (References 2.5.3-27 and 2.5.3-25), however, are questionable and the interpretation that these lineaments are related to young faulting is not supported. The assessment that these lineaments may be faults primarily stems from the coincidence that part of the lineaments are located near areas where pre-Cretaceous basement faulting has been identified at depth in earlier studies (References 2.5.3-9, 2.5.3-24, and 2.5.3-26). The ‘fault’ or ‘possible fault’ assessments for the lineaments (References 2.5.3-27 and 2.5.3-25) are unsupported because:

- Boring investigations have failed to find offsets in near-surface units that cross the projection of these lineaments (References 2.5.3-5 and 2.5.3-2).
- The earlier studies of the basement offsets clearly indicate that the basement faults do not extend upward into the Cretaceous or Tertiary units (References 2.5.3-9, 2.5.3-24, and 2.5.3-25).
- Trenching, borings, and a seismic line near one of the lineaments north of the PSEG Site found unfaulted Cretaceous and Quaternary units at the surface (Reference 2.5.3-13).
- Spoljaric (Reference 2.5.3-27) noted that faulting at the surface was not evident.

In summary, neither lineaments nor the basement faults have been demonstrated to be associated with surficial faulting (Reference 2.5.3-34). In particular, the postulated “fault” and “possible fault” lineaments of Spoljaric (References 2.5.3-27 and 2.5.3-25) in the site area have not been corroborated by other workers (References 2.5.3-20 and 2.5.3-19). Additionally, no evidence from the current aerial imagery investigation or field and aerial reconnaissance supports their existence. These features do not pose a surface faulting hazard for the PSEG Site.

2.5.3.2.3 Hypothesized Features

Two additional faults have been hypothesized to exist within the PSEG Site vicinity. Portions of the River Bend Trend/Stafford fault of Marple (Reference 2.5.3-12) and the fault from Pazzaglia (Reference 2.5.3-16) are located within the northeastern portion of the site vicinity (Figure 2.5.3-

**PSEG Site
ESP Application
Part 2, Site Safety Analysis Report**

1). These features do not offset or disturb rocks within the site vicinity and do not pose a surface faulting hazard at the PSEG Site.

Marple drew the hypothesized extension of the Stafford fault to connect the southwest-trending portions of the Delaware and Susquehanna rivers. As discussed in Subsection 2.5.1.1.4.2.4.3, no faulting or fault-related deformation has been identified along this trace and rock units of varying ages are undeformed across its projection (References 2.5.3-22, 2.5.3-12, 2.5.3-20, 2.5.3-29, and 2.5.3-28). Field and aerial reconnaissance confirm the undeformed nature of rocks along this trace.

As discussed in Subsection 2.5.1.1.4.2.4.1, Pazzaglia (Reference 2.5.3-16) hypothesizes that a fault could be responsible for the apparent relief seen in the contact at the base of Pleistocene Turkey Point beds in eastern Maryland. He also noted in an interview that other causes (sedimentary relief, etc.) could be responsible and that no geologic offset, deformation, or other evidence for faulting exists in the area). Aerial reconnaissance indicates that no evidence for faulting exists where the hypothesized feature may extend onshore.

2.5.3.3 Correlation of Earthquakes with Capable Tectonic Sources

No capable tectonic sources exist within the PSEG Site vicinity. None of the 15 historical earthquakes occurring in the PSEG Site vicinity have been linked to any faults near or within the site vicinity (References 2.5.3-19, 2.5.3-21 and Figure 2.5.3-1). The only instrumentally located event, the E[M] 3.77 event in New Jersey, is not spatially associated with any faults, folds, or capable tectonic sources (Reference 2.5.3-21).

2.5.3.4 Ages of Most Recent Deformations

No faults, folds, or tectonic deformation have been identified at the surface within the PSEG Site area (Figure 2.5.1-28). Subsurface investigations readily demonstrate planar, unfaulted bedding throughout the Cretaceous and younger sections beneath the site (Figures 2.5.1-38 and 2.5.1-39) (References 2.5.3-18 and 2.5.3-19).

2.5.3.5 Relationship of Tectonic Structures in the Site Area to Regional Tectonic Structures

There are no tectonic bedrock faults within the PSEG Site area (Subsection 2.5.3.2). Consequently, there is no correlation of geologic structures in the site area to regional, capable tectonic structures.

2.5.3.6 Characterization of Capable Tectonic Sources

Data presented in Subsections 2.5.1, 2.5.2, and 2.5.3 indicates no capable tectonic sources within 5 mi. of the PSEG Site.

2.5.3.7 Designation of Zones of Quaternary Deformation in the Site Region

There are no zones of Quaternary deformation associated with tectonic faults requiring detailed investigation within the site region (Subsection 2.5.1). A review and interpretation of aerial photography and available geotechnical boring logs, coupled with aerial and field reconnaissance, identified no possible Quaternary deformation in the site area.

**PSEG Site
ESP Application
Part 2, Site Safety Analysis Report**

2.5.3.8 Potential for Surface Tectonic Deformation or Non-Tectonic Deformation at the Site

There is no potential for fault-related surface deformation at the PSEG Site. Current and previous subsurface investigations within the site area indicate that Miocene and younger strata are planar and nearly flat-lying. In addition, the investigation of aerial imagery and lidar data reveal no evidence of faulting, as discussed in Subsection 2.5.3.1.6.

Investigation of the potential for surface deformation aside from faulting was also conducted. This investigation included tectonic non-fault deformation, such as folding, and non-tectonic deformation such as glacial rebound, ground collapse, volcanic intrusions, salt movement, and human-related activities. None of these potential hazards pose a threat to deforming the surface near the PSEG Site. The site is far from any geologic, non-tectonic sources of deformation such as salt domes or volcanic intrusions. Some sinkholes and karst dissolution do exist within the site vicinity, but these are associated with surface exposures of the Cockeysville marble, a unit not present in the site area (Reference 2.5.3-31 and Figure 2.5.3-1). The Cockeysville marble occurrence is shown on Figure 2.5.3-1; the karst features described in Reference 2.5.3-31 are too small to show on Figure 2.5.3-1. There is no hazard due to human activity at the site. These non-tectonic and non-fault deformation activities and their associated hazards within the site vicinity are discussed in detail in Subsection 2.5.1.2.5.5.

2.5.3.9 References

- 2.5.3-1 Alcock, J., "The Discordant Doe Run Thrust: Implications for Stratigraphy and Structure in the Glenarm Supergroup, Southeastern Pennsylvania Piedmont," Geological Society of America Bulletin 106(7): p. 932 – 941, 1994.
- 2.5.3-2 Benson, R.N., "Internal Stratigraphic Correlation of the Subsurface Potomac Formation, New Castle County, Delaware, and Adjacent Areas in Maryland and New Jersey," Delaware Geologic Survey, University of Delaware, Report of Investigations No. 71, 15 pp., Newark, Delaware, 2006.
- 2.5.3-3 Benson, R.N., "Map of Exposed and Buried Early Mesozoic Rift Basins/Synrift Rocks of the U.S. Middle Atlantic Continental Margin," Delaware Geologic Survey, University of Delaware, Miscellaneous Map Series No. 5, Newark, Delaware, 1992.
- 2.5.3-4 Crone, A.J. and R.L. Wheeler, "Data for Quaternary Faults, Liquefaction Features, and Possible Tectonic Features in the Central and Eastern United States, East of the Rocky Mountain Front," U.S. Geological Survey Open File Report 00-0260: 341 pp., 2000.
- 2.5.3-5 Delmarva Power and Light, Preliminary Safety Analysis Report, Summit Power Station, Delmarva Power and Light, 1974.
- 2.5.3-6 Electric Power Research Institute, "Seismic Hazard Methodology for the Central and Eastern United States," EPRI NP-4726, 1986.

**PSEG Site
ESP Application
Part 2, Site Safety Analysis Report**

- 2.5.3-7 Faill, R.T., "A Geologic History of the North-Central Appalachians: Part 3. The Alleghany Orogeny," American Journal of Science 298: 131 – 179, 1998.
- 2.5.3-8 Hansen, H.J., "Buried Rift Basin Underlying Coastal Plain Sediments, Central Delmarva Peninsula," Maryland Geological Survey, Geology, v. 16, p. 779 – 782, 1988.
- 2.5.3-9 Hansen, H.J., "Upper Cretaceous (Senonian) and Paleocene (Danian) Pinchouts on the South Flank of the Salisbury Embayment, Maryland, and Their Relationship to Antecedent Basement Structures," Maryland Geological Survey, Report of Investigations No. 29, 1978.
- 2.5.3-10 Higgins, M.W. and L.B. Conant, "The Geology of Cecil County, Maryland," Maryland Geological Survey Bulletin 37, 183 p., 1990.
- 2.5.3-11 Krol, M.A., P.D. Muller and P.D. and B.D. Idleman, "Late Paleozoic Deformation Within the Pleasant Grove Shear Zone, Maryland: Results from 40Ar/39Ar Dating of White Mica," in D.W. Valentino, and A.E. Gates, eds., "The Mid-Atlantic Piedmont: Tectonic Missing Link of the Appalachians," Geological Society of America, Special Paper 330, Boulder, Colorado, 1999.
- 2.5.3-12 Marple, R., "Relationship of the Stafford Fault Zone to the Right-Stepping Bends of the Potomac, Susquehanna, and Delaware Rivers and Related Upstream Incision along the U.S. Mid-Atlantic Fall Line," Southeastern Geology 42(3): p. 123 – 144, 2004.
- 2.5.3-13 McLaughlin, P.P., S.J. Baxter, K.W. Ramsey, T.E. McKenna and S.A. Strohmeier, "Results of Trenching Investigations Along the New Castle Railroad Survey-1 Seismic Line, New Castle, Delaware," Delaware Geological Survey, Open File Report No. 43, 17 pp., 2002.
- 2.5.3-14 Newell, W.L., D.S. Powars, J.P. Owens, S.D. Stanford and B.D. Stone, "Surficial Geologic Map of Central and Southern New Jersey," U.S. Geological Survey Miscellaneous Investigations Series, Map I-2540-D, 2000.
- 2.5.3-15 Owens, J.P., P.J. Sugarman, N.F. Sohl, R.A. Parker, H.F. Houghton, R.A. Volkert, A.A. Drake and R.C. Orndorff, "Bedrock Geologic Map of Central and Southern New Jersey," U.S. Geological Survey, Miscellaneous Investigations Series, Map I-2540-B, 1999.
- 2.5.3-16 Pazzaglia, F.J., "Stratigraphy, Petrography, and Correlation of Late Cenozoic Middle Atlantic Coastal Plain Deposits: Implications for Late-Stage Passive-Margin Geologic Evolution," Geological Society of America Bulletin 105: p. 1617 – 1634, 1993.
- 2.5.3-17 Pickett, T.E. and N. Spoljaric, "Geology of the Middletown-Odessa Area, Delaware," Delaware Geological Survey, Geologic Map Series, Number 2, 1971.

**PSEG Site
ESP Application
Part 2, Site Safety Analysis Report**

- 2.5.3-18 Public Service Enterprise Group (PSEG), "Salem Generating Station Updated Final Safety Analysis Report," Revision 23, October 17, 2007.
- 2.5.3-19 Public Service Enterprise Group (PSEG), "Hope Creek Generating Station Updated Final Safety Analysis Report," Revision 16, May 15, 2008.
- 2.5.3-20 Ramsey, K.W., "Geologic Map of New Castle County, Delaware," Delaware Geological Survey, Geologic Map Series, Number 13, 2005.
- 2.5.3-21 Sbar, M.L., R.R. Jordan, C.D. Stephens, T.E. Pickett, K.D. Woodruff and C.G. Sammis, "The Delaware-New Jersey Earthquake of February 28, 1973," Bulletin of the Seismological Society of America, 65, p. 85 – 92, 1975.
- 2.5.3-22 Schenck, W.S., M.O. Plank and L. Srogi, "Bedrock Geologic Map of the Piedmont of Delaware and Adjacent Pennsylvania," Delaware Geological Survey, Geologic Map Series, Number 10, 2000.
- 2.5.3-23 Sheridan, R.E., R.K. Olsson and J.J. Miller, "Seismic Reflection and Gravity Study of Proposed Taconic Suture under the New Jersey Coastal Plain: Implications for Continental Growth," Geological Society of America Bulletin, 103: p. 402 – 414, 1991.
- 2.5.3-24 Spoljaric, N., "Geology of the Fall Zone in Delaware," Delaware Geological Survey Report of Investigations No. 19, 1972.
- 2.5.3-25 Spoljaric, N., "Landsat View of Delaware," Delaware Geological Survey, Open File Report 12, 1979.
- 2.5.3-26 Spoljaric, N., "Normal Faults in Basement Rocks of the Northern Coastal Plain, Delaware," Geological Society of America Bulletin 84: p. 2781 – 2784, 1973.
- 2.5.3-27 Spoljaric, N., "Subsurface Geological Investigation of a Pleistocene Braided Stream in the Northern Coastal Plain, Delaware (U.S.A.)," Sedimentology 21: p. 451 – 461, 1974.
- 2.5.3-28 Stanford, S.D. and P.J. Sugarman, "Bedrock Geology of the Bridgeport and Marcus Hook Quadrangles, Gloucester and Salem Counties, New Jersey," New Jersey Geological Survey, Geological Map Series 06-1, 2006.
- 2.5.3-29 Stanford, S.D., "Surficial Geology of the Bridgeport and Marcus Hook Quadrangles, Gloucester and Salem Counties, New Jersey," New Jersey Geological Survey, Geological Map Series 06-2, 2006.
- 2.5.3-30 Sugarman, P.J. and D.H. Monteverde, "Correlation of Deep Aquifers Using Coreholes and Geophysical Logs in Parts of Cumberland, Salem, Gloucester, and Camden Counties, New Jersey," New Jersey Geological Survey Geologic Map Series GMS 08-1, 2008.

**PSEG Site
ESP Application
Part 2, Site Safety Analysis Report**

- 2.5.3-31 Talley, J.H., "Sinkholes, Hockessin Area, Delaware," Delaware Geological Survey Open File Report No. 14, 16 pp., 1981.
- 2.5.3-32 Valentino, D.W., R.W. Valentino and M.L. Hill, "Paleozoic Transcurrent Conjugate Shear Zones in the Central Appalachian Piedmont of Southeastern Pennsylvania," Journal of Geodynamics, 19: p. 303 – 324, 1995.
- 2.5.3-33 Wagner, M.E. and L. Srogi, "Early Paleozoic Metamorphism at Two Crustal Levels and a Tectonic Model for the Pennsylvania-Delaware Piedmont," Geological Society of America Bulletin, v. 99, p. 113 – 126, 1987.
- 2.5.3-34 Wheeler, R.L., "Known or Suggested Quaternary Tectonic Faulting, Central and Eastern United States-New and Updated Assessments for 2005," U.S. Geological Survey, Open-File Report 2005-1336, 2005.
- 2.5.3-35 Woodruff, K.D. and M.O. Plank, "Geology of the Cockeysville Formation," Delaware Geological Survey Bulletin 19, 1995.
- 2.5.3-36 Woodruff, K.D. and A.M. Thompson, "Geology of the Wilmington Area, Delaware," Delaware Geological Survey Geologic Map Series 4, scale 1:24,000, 1975.
- 2.5.3-37 French, H. M., Demitroff, M. (2001) "Cold-climate origin of the enclosed depressions and wetlands ('Sprungs') of the Pine Barrens, southern New Jersey, USA". Permafrost and Periglacial Processes, v.12, p.337-350.
- 2.5.3-38 French, H. M., Demitroff, M., Forman, S. L. (2003) "Evidence for late-Pleistocene permafrost in the New Jersey Pine Barrens (Latitude 39 degrees N), eastern USA". Permafrost and Periglacial Processes, v.14, p.259-274.
- 2.5.3-39 French, H. M., Demitroff, M., Forman, S. L. (2005) "Evidence for late-Pleistocene thermokarst in the New Jersey Pine Barrens (Latitude 39 degrees N), eastern USA". Permafrost and Periglacial Processes, v. 16, p.173-186.
- 2.5.3-40 French, H. M., Demitroff, M., Forman, S. L., Newell, W. L. (2007) "A chronology of late-Pleistocene permafrost events in southern New Jersey, eastern USA.
- 2.5.3-41 Stanford, S. (2010) personal communication.

**PSEG Site
ESP Application
Part 2, Site Safety Analysis Report**

2.5.4 STABILITY OF SUBSURFACE MATERIALS AND FOUNDATIONS

This subsection presents information on the stability of subsurface materials and foundations at the PSEG new plant location. The information has been developed in accordance with the Standard Review Plan, NUREG-0800 following the guidance presented in RG 1.206, Section C.1.2.5.4.

2.5.4.1 Geologic Features

This subsection presents a summary of geologic features at the PSEG Site, located on the southern part of Artificial Island on the east bank of the Delaware River in Lower Alloways Creek Township, Salem County, New Jersey (NJ). Figure 2.5.4.1-1 shows the location of the PSEG Site. The regional geology, physiography and geomorphology, geologic history, stratigraphy, tectonic setting, and seismicity are discussed in Subsection 2.5.1.1. The site geology, physiography and geomorphology, geologic history, stratigraphy, structural geology, and a site engineering geology evaluation are discussed in Subsection 2.5.1.2. These subsections are incorporated by reference and not repeated in this subsection. . As described in Subsection 2.5.1.1.1.1, the site is within the Coastal Plain physiographic province which has laterally continuous strata that dip southeastward.

Subsection 2.5.4.1.1 describes the PSEG Site stratigraphy, Subsection 2.5.4.1.2 describes the PSEG Site stratigraphic units and geologic formations, and Subsection 2.5.4.1.3 describes the PSEG Site geologic stability.

2.5.4.1.1 PSEG Site Stratigraphy

The subsurface exploration for the ESPA includes 16 geotechnical borings, divided into two general groups (NB series and EB series). Figure 2.5.4.1-2 shows the locations of these borings. The NB series borings provide coverage of the northern portion of the PSEG Site. The EB series borings provide coverage of the eastern portion of the site. Boring logs from the ESPA exploration are contained in Appendix 2AA (Reference 2.5.4.1-8). Subsection 2.5.4.3 describes the field geotechnical exploration program of the ESPA investigation in detail.

A suite of borehole geophysical surveys was performed for the ESPA geotechnical investigation in two borings drilled in the northern portion and in two borings drilled in the eastern portion of the PSEG Site. Potential new plant locations were considered in selecting the boreholes for geophysical logging. The depth of geophysical logging was predetermined for geophysical purposes. Borehole geophysical testing completed included suspension compressional wave (P) and shear wave (S) velocity logging (commonly referred to as suspension P-S logging), natural gamma radiation, resistivity, spontaneous potential, caliper, and borehole deviation. The geophysical testing is discussed in Subsection 2.5.4.4.

Soil descriptions provided in the boring logs were assigned in the field by a geologist using the Unified Soil Classification System, in accordance with ASTM D 2488 (Reference 2.5.4.1-1). Field classifications were adjusted based on laboratory testing where appropriate, in accordance with ASTM D 2487 (Reference 2.5.4.1-2). The geophysical logs were used to supplement the stratigraphic interpretations from the field samples. Stratigraphic breaks, unless observed within the individual split-spoon samples, were placed at approximate depths between the samples where the change is interpreted to occur and adjusted based on the results of the

**PSEG Site
ESP Application
Part 2, Site Safety Analysis Report**

geophysical logging or field observations of drilling behavior where available. Stratigraphic breaks determined in this manner have an uncertainty of approximately +/- 2 feet (ft.) based on a 5-foot sample interval, and +/- 5 ft. based on a 10-foot sample interval. Final boring logs reflect geologic stratification based on sample review, geophysical log review, and the results of laboratory testing. Results of the laboratory testing are discussed in detail in Subsection 2.5.4.2.

Integration and comparison of the regional geologic stratigraphy, geophysical data, and geotechnical boring logs provide the basis for developing the site-specific stratigraphic model at the PSEG Site, shown in Figure 2.5.4.1-3. Fourteen stratigraphic layers, most of which can be correlated to the regional geologic strata described in Subsection 2.5.1.1, are identified in the borings. Table 2.5.4.1-1 contains a summary of the PSEG Site stratigraphic information. Interpretation of the geophysical data, specifically the natural gamma and resistivity measurements, aids in identifying stratigraphic formations, in correlating them across the site, and to regional geologic stratigraphy.

The results from the interpretations made using ESPA data (Reference 2.5.4.1-8) are compared to the stratigraphic information presented in previous geotechnical studies at the PSEG Site, specifically the Hope Creek Generating Station Updated Final Safety Analysis Report. Table 2.5.4.1-2 shows a comparison of the geologic stratigraphy and conditions within the area covered by the investigation to descriptions from the previous work. As shown in the table, there is general agreement with the previous work at the PSEG Site. Figure 2.5.4.1-2 shows the ESPA geotechnical boring locations, the locations of cross-sections, and the locations of some of the previous geotechnical borings completed at the site.

The fourteen stratigraphic layers encountered during the ESPA exploration at the PSEG Site (Figure 2.5.4.1-3) are grouped into the following five categories according to geologic age as discussed in Subsection 2.5.1.1 (from oldest to youngest):

- Lower Cretaceous
- Upper Cretaceous
- Paleogene (Lower Tertiary)
- Neogene (Upper Tertiary)
- Quaternary

Stratigraphic cross-sections oriented along the regional southeastward dip (Figure 2.5.4.1-4) and oriented perpendicular to the regional southeastward dip (Figure 2.5.4.1-5), a structure contour map of the top of the Vincentown Formation (Figure 2.5.4.1-6), and histograms of the field Standard Penetration Test (SPT) N-values for selected stratigraphic units (Figures 2.5.4.1-7 through 2.5.4.1-10), illustrate the stratigraphy and subsurface conditions at the PSEG Site. Subsection 2.5.4.1.1 provides a description of stratigraphic units present within each of the five above strata.

2.5.4.1.1.1 PSEG Site Stratigraphic Units and Geologic Formations

Several stratigraphic units are recognized within each of the five subsurface material categories. Region-related discussion of these units is provided in Subsection 2.5.1.1. Following is a description of these units as they relate to the PSEG Site.

**PSEG Site
ESP Application
Part 2, Site Safety Analysis Report**

The Lower Cretaceous strata encountered during the investigation at the PSEG Site is composed of a single unit, the Potomac Formation, which is recognized in only the deepest borings performed during the investigation. The top of this unit forms the base of the shallow subsurface profile at the site.

The Upper Cretaceous strata encountered during the investigation at the PSEG Site is composed of eight stratigraphic units listed from oldest to youngest:

- Magothy Formation
- Merchantville Formation
- Woodbury Formation
- Englishtown Formation
- Marshalltown Formation
- Wenonah Formation
- Mount Laurel Formation
- Navesink Formation

The Paleogene strata (Lower Tertiary) encountered during the ESPA investigation at the PSEG Site is composed of two Paleocene-age stratigraphic units, listed from oldest to youngest:

- Hornerstown Formation
- Vincentown Formation

The Neogene strata (Upper Tertiary) encountered during the investigation at the PSEG Site is composed of the Kirkwood Formation. The Kirkwood Formation is subdivided at the site into upper and lower units based on variations in lithology recognized in the subsurface in most, but not all, borings, though not formally divided into separate stratigraphic layers.

Note that one regional geologic cross section (Reference 2.5.4.1-4), shows the presence of the Manasquan Formation above the Vincentown Formation at the PSEG Site. The detailed site exploration did not encounter materials fitting the published description of Manasquan Formation. Materials encountered immediately above the Vincentown Formation in the borings were identified as the Kirkwood Formation. This identification is consistent with the geologic information from SGS and HCGS (References 2.5.4.1-10 and 2.5.4.1-11). The regional geologic cross section from Benson, 2006 also shows the Shark River Formation near the site, but not indicated as present at the site. Materials meeting the description of the Shark River Formation also were not identified in any of the ESPA or previous site explorations.

The boring shown on the regional geologic cross section of Benson, 2006 is the on-site PSEG No. 6 Production well, located approximately 1000 feet south of the northern portion of the PSEG Site and the area explored in the ESPA investigation. The regional cross section indicates the Manasquan Formation is present from elevation 0 NAVD to approximately elevation -40 ft. NAVD. At the PSEG Site, materials above elevation -40 ft. NAVD consist of the hydraulic fill or alluvium as discussed below.

The Quaternary Strata encountered during the ESPA investigation at the PSEG Site is composed of two stratigraphic units, listed from oldest to youngest:

- Alluvium
- Artificial and Hydraulic Fill

**PSEG Site
ESP Application
Part 2, Site Safety Analysis Report**

Detailed geologic material descriptions are provided in Subsection 2.5.4.1.2. Engineering material properties are described in Subsection 2.5.4.2.

2.5.4.1.2 Description of PSEG Site Stratigraphic Units and Geologic Formations

The 14 major stratigraphic layers defining the subsurface profile at the PSEG Site occur between the ground surface and 631.5 ft. below ground surface (elevation -615.0 ft. [NAVD]), which was the maximum depth drilled during the ESPA investigation. Table 2.5.4.1-1 provides a summary of the elevations of the tops of the stratigraphic layers for the ESPA investigation borings. The site stratigraphic layers and geologic formations are described and characterized in the following subsections, from the Potomac Formation (oldest formation encountered) to the ground surface. Table 2.5.4.1-3 provides a key to the terminology used in the following subsections and the geotechnical boring logs contained in Appendix 2AA. The presence of calcium carbonate can be inferred on the basis of the described reaction (none, weak, strong) of the sediments when tested with 10 percent hydrochloric acid solution, as calcium carbonate reacts strongly with dilute hydrochloric acid. The elevations given in this subsection and the following subsections are referenced to NAVD. Figures 2.5.4.1-11 through 2.5.4.1-14 show summary boring logs of encountered conditions for the four borings that included geophysical logging.

2.5.4.1.2.1 Lower Cretaceous Strata

2.5.4.1.2.1.1 Potomac Formation

The Potomac Formation is the deepest stratigraphic unit encountered by the ESPA borings at the PSEG Site. The Potomac Formation consists of Lower Cretaceous age non-marine, continentally-derived sediments deposited in anastomosing fluvial to deltaic environments (Reference 2.5.4.1-13). Two borings performed during the investigation penetrated the top of the Potomac Formation. The top of the formation is at approximate elevation -454 ft. NAVD in the northern portion of the site, and at approximate elevation -484 ft. NAVD in the eastern portion of the site. These two borings are along a southeasterly line, approximately in the regional dip direction. The vertical elevation difference corresponds to an apparent southeasterly dip of approximately 34 feet per mile (ft/mi.) (less than 1 percent)), consistent with the gentle dip reported for the NJ Coastal Plain in Subsection 2.5.1.1.

The top of the Potomac Formation is interpreted from the geophysical testing conducted in the two deepest borings completed as part of the ESPA investigation. The borings are compared to and correlated with published geophysical logs from the region (References 2.5.4.1-12 and 2.5.4.1-4) to aid in identification of the top of the stratigraphic unit. The results of the natural gamma and resistivity logging indicate the formation consists of interbedded layers of sand and clay in the upper portion of the formation, and mostly clay at the termination depths of the two deep borings. This interpretation is supported by the six soil samples collected in this unit. Sediments in the upper portion of the Potomac Formation are typically dark gray to gray, clay and sand with variable silt content. In the deeper portion of the formation, the sediments are typically mottled, gray and red clay. The sediments showed no reaction with 10 percent hydrochloric acid. Field values for the SPT resistance (N-Values) are high, ranging from 71 to greater than 100 blows per foot (bpf).

**PSEG Site
ESP Application
Part 2, Site Safety Analysis Report**

The bottom of the Potomac Formation was not encountered by any borings completed during the ESPA investigation. For the purposes of this study, the Raritan Formation, recognized by some geologic researchers as a distinct formation, is considered to be part of the Potomac Formation at the PSEG Site.

2.5.4.1.2.2 Upper Cretaceous Strata

2.5.4.1.2.2.1 Magothy Formation

The Magothy Formation unconformably overlies the Potomac Formation and consists of Upper Cretaceous age non-marine and marine sediments deposited in fluvial to marginal marine environments (Reference 2.5.4.1-13). The two deep borings performed during the ESPA investigation penetrated the top of the Magothy Formation at approximate elevation -402 ft. NAVD, in the northern portion of the PSEG Site; and at approximate elevation -429 ft. NAVD in the eastern portion of the site, which correspond to an apparent southeasterly dip of approximately 30 ft/mi. Borings showed the unit to range from 52 to 55 ft. thick. Sediments of the Magothy Formation typically consist of gray to very dark gray, carbonaceous/lignitic clay and silt at the top of the unit, interbedded with sands with variable silt and clay content at the bottom of the unit. The sediments showed no reaction with 10 percent hydrochloric acid. The results of the geophysical logging, specifically natural gamma and resistivity, aided in identifying the clay and sand layers where no SPT samples were collected. In general, the natural gamma response is higher and the resistivity is lower in the clay intervals, whereas the natural gamma response is lower and the resistivity is higher in the sand intervals. The field SPT N-values, where collected, were high and ranged from 53 to greater than 100 bpf.

The Magothy Formation is distinguished from the underlying Potomac Formation by comparing and correlating the geophysical logs for the two deep borings with published geophysical logs from the region (References 2.5.4.1-12 and 2.5.4.1-4). The contact between the two formations is placed to be where the basal sands interpreted to be part of the Magothy Formation transition to clays interpreted to be part of the Potomac Formation.

2.5.4.1.2.2.2 Merchantville Formation

The Merchantville Formation unconformably overlies the Magothy Formation. This formation consists of Upper Cretaceous age marine sediments deposited in a neritic environment during a marine transgression as described in Subsection 2.5.1.1.3.4.1. The two deep borings performed during the ESPA investigation penetrated the top of the Merchantville Formation at approximate elevation -372 ft. NAVD in the northern portion of the PSEG Site, and at approximate elevation -398 ft. NAVD in the eastern portion of the site, corresponding to an apparent southeasterly dip of approximately 29 ft/mi. The unit was found to be approximately 30 ft. thick. Sediments of the Merchantville Formation consist of greenish-black to black, glauconitic silt and clay with trace to some fine sand, trace mica; and locally with trace friable to moderately indurated layers. Glauconite content ranged from trace to little. The sediments showed no to weak reaction with 10 percent hydrochloric acid. Field SPT N-values within this unit ranged from 31 to 82 bpf, indicating the sediments are hard in consistency. The Merchantville Formation is distinguished from the overlying Woodbury Formation by the increase in glauconite content, general decrease in plasticity and mica content, and the change in color observed in the Merchantville Formation.

**PSEG Site
ESP Application
Part 2, Site Safety Analysis Report**

2.5.4.1.2.2.3 Woodbury Formation

The Woodbury Formation conformably overlies the Merchantville Formation. This formation consists of Upper Cretaceous age marine sediments deposited in an inner shelf environment associated with a marine regression (Reference 2.5.4.1-9). The top of the unit was penetrated by the two deep borings completed during the ESPA investigation at approximate elevation -336 ft. NAVD in the northern portion of the site, and at approximate elevation -368 ft. NAVD in the eastern portion of the site, corresponding to an apparent southeasterly dip of approximately 36 ft/mi. The thickness of the Woodbury Formation ranges from approximately 30 to 36 ft. across the PSEG Site. Sediments of the Woodbury Formation consist of very dark gray and black to greenish-black, highly plastic clay with trace glauconite, fine sand, mica, and shell fragments; and locally with trace indurated layers. The sediments showed no to weak reaction with 10 percent hydrochloric acid. Field SPT N-values within the Woodbury Formation indicate the sediments are typically very stiff in consistency with values ranging from 19 to 27 bpf, with isolated values as high as 49 bpf.

Sediments of the Woodbury Formation are very similar to those of the overlying Englishtown Formation, and the two formations appear to have a gradational contact. These units were distinguished in the field by the relative increase in clay and mica content observed in the Woodbury Formation sediments relative to the Englishtown Formation sediments. The results of the geophysical logging reveal little difference in natural gamma response or resistivity between these two units, or with the underlying Merchantville Formation.

2.5.4.1.2.2.4 Englishtown Formation

The Englishtown Formation conformably overlies the Woodbury Formation and consists of Upper Cretaceous age marine sediments deposited in a near-shore environment associated with a marine regression, as described in Subsection 2.5.1.1.3.4.1. The top of the unit was penetrated by four of the borings performed during the ESPA investigation at approximate elevation -291 ft. NAVD in the northern portion of the site, and at approximate elevation -319 ft. NAVD in the eastern portion of the site, corresponding to an apparent southeasterly dip of approximately 32 ft/mi. The thickness of the Englishtown Formation ranges from approximate 44 to 49 ft. across the PSEG Site. Sediments in the upper portion of the Englishtown Formation consist of micaceous, very dark greenish-gray to very dark gray and black sandy silt and clay to clayey sand, with trace shell fragments and trace to little glauconite; and grade downward into micaceous, black, highly plastic silt and clay with trace to few fine sand and trace shell fragments. The sediments of this unit showed no to weak reaction with 10 percent hydrochloric acid. Field SPT N-values in the Englishtown Formation indicate the sediments are typically very stiff to hard in consistency, with values ranging from 18 to 50 bpf, and isolated values as low as 10 bpf and as high as greater than 100 bpf.

2.5.4.1.2.2.5 Marshalltown Formation

The Marshalltown Formation conformably overlies the Englishtown Formation and consists of Upper Cretaceous age marine sediments deposited in a neritic environment during a marine transgression as described in Subsection 2.5.1.1.3.4.1. The top of the Marshalltown Formation was penetrated by five of the borings completed during the ESPA investigation at elevations ranging from approximately -265 to -277 ft. NAVD in the northern portion of the PSEG Site, and at approximate elevation -293 ft. NAVD in the eastern portion of the site, corresponding to an

**PSEG Site
ESP Application
Part 2, Site Safety Analysis Report**

apparent southeasterly dip of approximately 29 ft/mi. The Marshalltown Formation is approximately 25 ft. thick across the PSEG Site. Sediments of this unit typically consist of greenish-gray to very dark gray and black, clayey and silty, fine to medium sand, and fine sandy clay of variable plasticity, all with trace to little glauconite content. Trace amounts of shell fragments, pyrite nodules, friable layers, and subrounded fine gravel were locally encountered within the Marshalltown Formation. These sediments showed a weak to strong reaction with 10 percent hydrochloric acid. Field SPT N-values within this unit vary over a wide range (from as low as 22 to greater than 100 bpf), indicating the sediments are medium dense to very dense, and very stiff to hard in consistency.

Sediments of the Marshalltown Formation are very similar to those of the overlying Wenonah Formation, making the units difficult to distinguish in the field. A natural gamma peak occurring over a vertical distance of about 2 ft. is observed in the geophysical logs at the top of the Marshalltown Formation/base of the overlying Wenonah Formation. This peak in the gamma response is interpreted to represent a thin (less than 3 ft. thick) phosphatic hardground or lag deposit that formed during the transition from deposition of the Marshalltown Formation to deposition of the Wenonah Formation. This is used to differentiate the two formations at the PSEG Site. A small peak in the P-S velocity logging is also present at similar elevations to the peak observed in the natural gamma logging. The Marshalltown Formation, in general, shows an elevated natural gamma response in comparison to the overlying Wenonah Formation, but is similar in comparison to the underlying Englishtown Formation. The resistivity logging shows little difference between these formations.

2.5.4.1.2.2.6 Wenonah Formation

The Wenonah Formation conformably overlies the Marshalltown Formation. This formation consists of Upper Cretaceous age marine sediments deposited in a neritic environment during a marine regression (Reference 2.5.4.1-9). The top of the formation was penetrated by six of the borings completed during the ESPA investigation. The top of the Wenonah Formation was encountered at elevations ranging from -250 to -259 ft. NAVD in the northern portion of the PSEG Site, and at elevations ranging from -279 to -289 ft. NAVD in the eastern portion of the PSEG Site, corresponding to an apparent southeasterly dip of approximately 33 ft/mi. The Wenonah Formation has an average thickness of approximately 15 ft. across the PSEG Site. The formation typically consists of very dark gray to greenish-black, sandy clay with trace shell fragments and trace to few glauconite. Locally, the formation consists of clayey and silty, fine to medium sand with trace to few glauconite. Reaction with 10 percent hydrochloric acid is found to range from weak to strong. Field SPT N-values within the formation indicate the sediments are typically very stiff to hard in consistency, ranging from 17 to 40 bpf, with isolated values as low as 7 bpf and as high as 43 bpf.

2.5.4.1.2.2.7 Mount Laurel Formation

The Mount Laurel Formation conformably overlies the Wenonah Formation and consists of Upper Cretaceous age marine sediments deposited in a near-shore environment during a marine regression (Reference 2.5.4.1-9). The top of the formation was penetrated by all geotechnical borings performed during the ESPA investigation. The top of the Mount Laurel Formation was encountered at elevations ranging from -145 to -157 ft. NAVD in the northern portion of the PSEG Site, and at approximate elevations ranging from -168 to -177 ft. NAVD in the eastern portion of the PSEG Site; corresponding to an apparent southeasterly dip of

**PSEG Site
ESP Application
Part 2, Site Safety Analysis Report**

approximately 26 ft/mi. The unit has an average thickness of approximately 103 ft. in the northern portion of the site, thickening slightly to the southeast, with an average thickness of approximately 111 ft. in the eastern portion of the site.

Sediments of the Mount Laurel Formation typically consist of dark olive-gray, dark grayish-brown, and greenish-gray, clayey and silty, fine to medium sand, grading with depth into fine to medium sand with variable silt and clay content, all with trace to little glauconite and shell fragments. The amount of glauconite and shell fragments was found to decrease to trace amounts with increasing depth. The upper 15 to 20 ft. of the formation typically contains trace to little subrounded, coarse sand and fine gravel, and is locally composed of sandy clay. The sediments show a weak to strong reaction to 10 percent hydrochloric acid near the top of the formation. The reaction generally decreases to weak to none near the bottom of formation. Field SPT N-values within the Mount Laurel Formation indicate the sediments are typically very dense, with most being greater than 100 bpf, with isolated values as low as 23 bpf. Figure 2.5.4.1-7 illustrates the range and frequency of field SPT N-values from the Mount Laurel Formation in the northern portion of the PSEG Site.

A natural gamma peak occurring over a vertical distance of approximately 4 ft. is observed in the geophysical logging at the top of the Mount Laurel Formation/base of the overlying Navesink Formation. This peak in the gamma response is interpreted to represent a thin (less than 5 ft. thick) phosphatic hardground or lag deposit that formed during the transition from deposition of the Mount Laurel Formation to deposition of the Navesink Formation. An increase in the P-S velocity is also present at similar elevations to the peak observed in the natural gamma logging. The Mount Laurel Formation, in general, shows an elevated natural gamma response in the upper 25 ft. of the unit, similar to that in the overlying Navesink Formation, and a higher resistivity response throughout the formation relative to the overlying and underlying formations.

2.5.4.1.2.2.8 Navesink Formation

The Navesink Formation conformably overlies the Mount Laurel Formation. This formation consists of Upper Cretaceous age marine sediments deposited in a neritic environment during a marine transgression (Reference 2.5.4.1-9). The top of the Navesink Formation is encountered at elevations ranging from -121 to -133 ft. NAVD in the northern portion of the PSEG Site and at elevations ranging from -147 to -157 ft. NAVD in the eastern portion of the PSEG Site, corresponding to an apparent southeasterly dip of approximately 31 ft/mi. The thickness of the unit averages approximately 24 ft. in the northern portion of the site, thinning slightly to the southeast, with an average thickness of approximately 20 ft. in the eastern portion of the site.

Sediments of the Navesink Formation are typically composed of very dark greenish-gray to very dark grayish-green and greenish-black, silty and clayey, fine to medium grained glauconite, and quartz sand with trace to little shell fragments. The Navesink Formation is a distinctive marker unit across the PSEG Site due to its composition being almost entirely the mineral glauconite. The reaction of the sediments to 10 percent hydrochloric acid is found to range from none to strong, but typically shows a weak reaction. Field SPT N-values within the Navesink Formation indicate the sediments are typically dense to very dense, ranging from a low of 38 bpf to a high of greater than 100 bpf. Figure 2.5.4.1-8 illustrates the range and frequency of field SPT N-values from the Navesink Formation in the northern portion of the PSEG Site. Results of the geophysical logging show an elevated natural gamma response in comparison to the overlying formations, culminating in the gamma peak observed at the top of the underlying Mount Laurel

**PSEG Site
ESP Application
Part 2, Site Safety Analysis Report**

Formation. There is little difference in resistivity compared to the units above the Navesink Formation.

2.5.4.1.2.3 Paleogene Strata (Lower Tertiary)

2.5.4.1.2.3.1 Hornerstown Formation

The Hornerstown Formation conformably overlies the Navesink Formation. This formation consists of Upper Cretaceous to Paleocene age marine sediments deposited in a neritic environment during a marine transgression (Reference 2.5.4.1-9). The top of the Hornerstown Formation is encountered at elevations ranging from -105 to -114 ft. NAVD in the northern portion of the PSEG Site, and at elevations ranging from -127 to -137 ft. NAVD in the eastern portion of the PSEG Site, corresponding to an apparent southeasterly dip of approximately 26 ft/mi. The formation averages approximately 20 ft. in thickness across the PSEG Site.

Sediments of the Hornerstown Formation are typically composed of greenish- gray to very dark greenish-gray, silty and clayey, fine to medium sand, with trace to few shell fragments, and trace to some glauconite. Glauconite content typically increases with depth and is estimated from field sample observations to comprise greater than 30 percent of the sand fraction near the base of the formation. The unit exhibits a strong reaction to 10 percent hydrochloric acid. Field SPT N-values within the Hornerstown Formation indicate the sediments typically range from medium dense to very dense, with values ranging as low as 18 bpf and as high as greater than 100 bpf. Figure 2.5.4.1-9 illustrates the range and frequency of field SPT N-values from the Hornerstown Formation in the northern portion of the PSEG Site.

The formation contains numerous, discontinuous, friable to indurated calcium carbonate cemented sandstone layers. These cemented zones are typically 0.1 to 1 ft. thick, as observed from split spoon sampling and drilling operations. The results of the geophysical logging show a slight increase in the natural gamma response with depth to the top of the Navesink Formation. Results also show small spikes in the single point resistance logs which may represent the thin indurated layers discussed above. The sediments of the Hornerstown Formation are very similar to, and grade into, those of the overlying Vincentown Formation, making the units difficult to distinguish in the field. In general, the Hornerstown Formation is differentiated from the overlying Vincentown Formation on the basis of increasing silt/clay content and increasing glauconite content relative to the Vincentown Formation.

2.5.4.1.2.3.2 Vincentown Formation

The Vincentown Formation serves as the bearing layer for the foundations of the existing nuclear units (Hope Creek Unit 1 and Salem Units 1 and 2) (References 2.5.4.1-10 and 2.5.4.1-11). The formation conformably overlies the Hornerstown Formation and consists of Paleocene age marine sediments deposited in a neritic environment during a marine regression (Reference 2.5.4.1-9). The Vincentown Formation shows significant erosional relief on its upper surface, making both the elevation of its upper contact and its thickness somewhat variable. In the northern portion of the PSEG Site, the elevation of the top of the formation ranges from -33 to -70 ft. NAVD. In the eastern portion of the PSEG Site, the elevation ranges from -45 to -91 ft. NAVD. Figure 2.5.4.1-6 illustrates the variability of the top of the Vincentown Formation in the northern portion of the site. The thickness of the Vincentown Formation ranges from 35 to 79 ft.,

**PSEG Site
ESP Application
Part 2, Site Safety Analysis Report**

averaging approximately 52 ft. in the northern portion of the site. Thickness ranges from approximate 37 to 93 ft. and averages approximately 55 ft. in the eastern portion of the site.

Due to the erosional nature of the upper surface of the Vincenttown Formation, the sediments of the uppermost portion of the unit typically show signs of weathering characterized by oxidation of iron-bearing minerals such as glauconite. The weathering and oxidation of the formation is subject to the vagaries of post-depositional processes, such as subaerial exposure and fluvial erosion prior to deposition of the overlying sediments, as well as groundwater movement through the formation. This results in distinct but irregular contacts with the underlying unoxidized sediments that are not the result of depositional or stratigraphic control. Oxidized sediments are typically yellowish-brown to reddish-brown, and unoxidized sediments are typically light greenish-gray to dark greenish-gray. The oxidized and unoxidized Vincenttown Formation sediments are typically composed of glauconitic, calcareous, silty and clayey, fine to medium sand, and fine to medium sand with variable silt content. Glauconite and shell fragments are typically present in trace amounts with locally higher concentrations observed during field sampling.

The formation contains many discontinuous, friable to indurated, calcium carbonate cemented sandstone layers. These indurated layers are typically 0.1 to 1 ft. thick, as observed from split spoon sampling and drilling operations. The oxidized and unoxidized sediments display a weak to strong reaction with 10 percent hydrochloric acid. Field SPT N-values within the Vincenttown Formation indicate the sediments typically range from medium dense to very dense, with isolated values ranging from a low of 5 bpf near the top of the formation, to as high as greater than 100 bpf scattered throughout the unit. Figure 2.5.4.1-10 illustrates the range and frequency of field SPT N-values from the Vincenttown Formation in the northern portion of the PSEG Site. Results of the geophysical logging show a subdued natural gamma response for this formation and small spikes in the single point resistance logs which may be due to the thin, indurated layers, as discussed above.

2.5.4.1.2.4 Neogene Strata (Upper Tertiary)

2.5.4.1.2.4.1 Kirkwood Formation

The Kirkwood Formation unconformably overlies the Vincenttown Formation. This formation consists of Miocene age marine sediments deposited in a near-shore environment associated with a marine regression (Reference 2.5.4.1-13). The Kirkwood Formation rests on the erosional unconformity formed on top of the Vincenttown Formation, and the upper surface of the Kirkwood Formation forms an erosional unconformity with the overlying Alluvium, making the elevation of the unit's upper surface, as well as the thickness of the unit, somewhat variable. In the northern portion of the PSEG Site, the top of the Kirkwood Formation ranges from elevations of -34 to -43 ft. NAVD. In the eastern portion of the PSEG Site, the top of the formation ranges from elevations of -31 to -49 ft. NAVD. The thickness of the formation ranges from 12 to 29 ft., averaging approximately 17 ft. in the northern portion of the site. Thickness of the Kirkwood Formation ranges from 14 to 54 ft., and averages approximately 37 ft. in the eastern portion of the site. The large variation in thickness observed in the Kirkwood Formation is directly related to the erosional contact with the underlying Vincenttown Formation, which displays up to 37 ft. of relief in the northern portion of the site, and up to 51 ft. of relief in the eastern portion of the site. Where the top of the Vincenttown Formation is topographically low, the Kirkwood Formation is

**PSEG Site
ESP Application
Part 2, Site Safety Analysis Report**

generally thick. Where the top of the Vincentown Formation is topographically high, the Kirkwood Formation is generally thin.

The sediments of the Kirkwood Formation consist of two distinct units. The upper unit of the formation typically consists of dark gray, green, and brown to olive gray, highly plastic clay and silt, with trace fine sand and rounded gravel, trace shell fragments, and trace to little organic content. Locally, interbeds of silty and clayey, fine to medium sand occur within this upper unit. In the eastern portion of the PSEG Site, a thick section of light greenish-gray, silty, fine to medium sand is locally encountered above the finer grained sediments. Typical field SPT N-values within the upper unit of the Kirkwood Formation indicate the soils are very soft to stiff in the fine-grained sediments, with values ranging from weight-of-hammer (0) to 13 bpf, and medium dense to dense in the interbedded sand layers, with values ranging from 14 bpf to 33 bpf. An elevated gamma signature indicating the presence of clayey sediments was seen on the geophysics logs for borings NB-1 and EB-3, but not in borings NB-8 or EB-8G.

The lower, basal, unit of the Kirkwood Formation typically consists of a 2- to 14-ft. thick layer composed of dark greenish-gray, olive gray, and dark gray to brown, silty and clayey, fine to medium sand and fine to coarse gravel. The sand and gravel in this lower unit is typically rounded to subangular. Typical field SPT N-values within the lower Kirkwood Formation unit range from 11 bpf to greater than 100 bpf, indicating these soils are medium dense to very dense. The sediments of the upper and lower Kirkwood Formation typically show no reaction to 10 percent hydrochloric acid. Geophysical log results in the borings where lower Kirkwood was identified were similar to those for the Vincentown, indicating a similar composition.

Six of the 16 borings completed during the ESPA investigation did not encounter the lower unit sediments of the Kirkwood Formation, which may indicate the lower unit has some discontinuity across the site, or that the layer is thinner than the distance between the 5-ft. SPT sample interval at these locations. At boring NB-2, completed in the northern portion of the site, the upper unit of the Kirkwood Formation was not encountered. This is most likely due to fluvial scour during deposition of the overlying Alluvium at this location. At boring NB-7, completed in the northern portion of the site, sediments of the Kirkwood Formation are completely absent, with alluvial sand and gravel unconformably overlying strongly oxidized Vincentown Formation sediments. This condition is most likely due to fluvial scour during deposition of the Alluvium at this location.

2.5.4.1.2.5 Quaternary Strata

2.5.4.1.2.5.1 Alluvium

Alluvium unconformably overlies the Kirkwood Formation and consists of Quaternary age sediments representing the bed of a former location of the Delaware River (Reference 2.5.4.1-10). The Alluvium stratigraphic unit is typically encountered at elevations ranging from -22 to -35 ft. NAVD in the northern portion of the PSEG Site, and at elevations ranging from -16 to -25 ft. NAVD in the eastern portion of the site. As illustrated by Figure 2.5.4.1-5, the unit shows a slightly undulating upper surface, and the unit generally slopes gently westward towards the Delaware River. The thickness of the Alluvium ranges from 5 to 23 ft., averaging approximately 13 ft. in the northern portion of the site. Average thickness in the eastern portion of the site is approximately 18 ft., and ranges from 14 to 24 ft. thick. Alluvial soils consist typically of gray to

**PSEG Site
ESP Application
Part 2, Site Safety Analysis Report**

grayish-brown, fine to coarse sand with trace to little, rounded to angular, fine to coarse gravel, and trace to little silt and clay content.

In borings completed in the northern and eastern portions of the PSEG Site, 2- to 5-foot thick discontinuous layers of fine grained soils, consisting of sandy silts and clays and highly organic soils consisting of peat, were locally encountered intercalated with the alluvial sand and gravel layers. In the eastern portion of the site a 4-foot to 15-foot thick discontinuous layer of non-organic silt and clay was locally encountered below the alluvial sand and gravel. Field SPT N-values within the alluvium indicate the soils are typically loose to dense in the sand and gravel layers, with values ranging from 9 bpf to 38 bpf and isolated values as high as 65 bpf. Typical field SPT N-values in the silt and clay layers indicate the soils are soft to medium stiff, with values ranging from 2 bpf to 8 bpf. Geophysical logging did not encompass sufficient portions of the alluvium to allow an interpretation.

2.5.4.1.2.5.2 Artificial and Hydraulic Fill

Hydraulic fill is of manmade origin, deposited at the site as the result of channel dredging of the Delaware River (Reference 2.5.4.1-10). The combined Artificial and Hydraulic Fill stratigraphic unit overlies Alluvium at an average elevation of -29 ft. NAVD in the northern portion of the site, and at an average elevation of -21 ft. NAVD in the eastern portion of the site. Hydraulic fill consists typically of dark gray to dark greenish-gray, highly plastic clay and silt with trace to some organic material, and locally interbedded discontinuous layers of clayey and silty, fine to medium grained sand up to 5 ft. thick. Field SPT N-values within the hydraulic fill are typically very low, between weight-of-hammer (0) and 10 bpf, with isolated values as high as 36 bpf (due to gravel and wood debris), observed from SPT tests performed within 15 ft. of the ground surface. Thickness of the hydraulic fill ranges from 24 to 44 ft., with an average thickness of approximately 33 ft. across the northern and eastern portions of the site.

Artificial fill comprises the surface material at the PSEG Site, overlying hydraulic fill. Artificial fill consists of typically grayish-brown to brown, silt, clay, and sand with variable silt and clay contents, and clayey and silty gravels. Thickness of the artificial fill ranges from 2 to 10 ft., and averages approximately 4 ft. across the northern and eastern portions of the site. Field SPT N-values in the artificial fill vary over a wide range, from 2 bpf to 99 bpf, but typically indicate medium dense or stiff consistency and decrease with depth. These materials were placed at the site during previous construction activities and grade downward into the hydraulic fill.

2.5.4.1.3 Geologic Stability

As discussed in Subsection 2.5.1.2.3, the geologic formations underlying the PSEG Site record a long history of tectonic stability and sedimentary deposition. Formations also record transition from non-marine environments during the Lower Cretaceous, to marine environments during the Upper Cretaceous through the Paleogene, and increasing clastic sedimentation during the Neogene through to the present. Cross-sections drawn from the ESPA data (Figures 2.5.4.1-4 and 2.5.4.1-5) illustrate a lateral continuity of each stratigraphic layer, indicating that there are no significant faults, folds, areas of uplift or subsidence, or other subsurface structural weaknesses present at the site. The geotechnical data from previous investigations for the existing nuclear units at the PSEG Site was reviewed and compared to the data collected in this ESPA investigation. The stratigraphic layers, relationships, and conditions identified for the

**PSEG Site
ESP Application
Part 2, Site Safety Analysis Report**

Hope Creek and Salem generating stations are similar to the stratigraphic layers, relationships, and conditions identified for the ESPA investigation.

The dominant depositional processes for the strata were marine and fluvial over a series of regressive and transgressive events. Review of samples from the 16 soil borings performed in the area of the PSEG Site, all of which penetrated through the Cretaceous/Tertiary boundary, indicated strata or features that are consistent with the depositional environments described in the literature, and the samples are not interpreted to represent a paleotsunami occurrence at the PSEG Site.

The stratigraphic units overlying the Vincentown Formation are of low strength and are deemed unsuitable to serve as competent layers based on their physical properties. The Vincentown Formation will serve as the competent layer for any future nuclear units at the PSEG Site (as it is for the existing units at the site). The sediments immediately underlying the Vincentown Formation, and extending to the depths investigated, are composed of very dense, silty or clayey sands and hard silts and clays.

Observations during the drilling and sampling and review of the geophysical electrical logging, as discussed in Subsection 2.5.4.1.2.3.2, indicate the cementation of Vincentown Formation sediments is variable and ranges from non-cemented sands to discontinuous layers of indurated, calcareous sandstone. Calcium carbonate is present throughout the unit based on the weak to strong reaction of the samples to 10 percent hydrochloric acid observed during the ESPA investigation. Previous petrographic studies of the Vincentown Formation (Reference 2.5.4.1-7) indicate that the entire formation has been subjected to some degree of cementation and that, in some instances, samples visually classified as being uncemented in the field have been found to be partially cemented in the laboratory. Presence of these calcareous cemented sands would not have an impact on the concrete foundations because the Vincentown Formation is not in contact with the concrete.

The upper surface of the Vincentown Formation is somewhat variable due to subaerial exposure, weathering, and fluvial erosion of this unit prior to deposition of the overlying units, as illustrated on the structure contour map (Figure 2.5.4.1-6). The relief displayed by the upper surface of the Vincentown Formation is interpreted and concluded to be consistent with an erosional mechanism and not as the result of active dissolution of the unit. Post-depositional subaerial exposure and weathering of the upper portions of the Vincentown Formation, prior to deposition of the overlying units, resulted in zones of oxidation generally observed in the previous and present borings across the PSEG Site.

Previous studies conclude that some dissolution of the uppermost, oxidized portions of the Vincentown Formation is likely to have occurred during this period of subaerial exposure and weathering. Also, previous studies report that conditions favorable to dissolution of the Vincentown Formation are considered to have ended with the deposition of the overlying Kirkwood Formation, approximately 25 million years ago (Reference 2.5.4.1-7). The information obtained during this ESPA investigation is consistent with these previously reported conclusions and observations. No evidence of karst conditions or zones of dissolution has been found from the large number of geotechnical borings performed at the PSEG Site, or from the mapping of the foundation excavation conducted during construction of Hope Creek Unit 1. It is concluded there is no potential for karst conditions or presence of zones of dissolution at the PSEG Site.

**PSEG Site
ESP Application
Part 2, Site Safety Analysis Report**

Based on the results of the ESPA investigation geotechnical borings and geophysical logs, specifically the P-S velocities, the oxidized portion of the Vincentown Formation shows no significant divergence in density, composition, or cementation, to that observed in the unoxidized portions of the Vincentown Formation. Additional data to be collected during the combined license phase of field investigations will be used to further evaluate the nature of the oxidized Vincentown Formation.

2.5.4.1.4 References

- 2.5.4.1-1 ASTM, 2006a, "Standard Practice for Description and Classification of Soils," ASTM D 2488-06, 2006.
- 2.5.4.1-2 ASTM, 2006b, "Standard Practice for Classification of Soils for Engineering Purposes," ASTM D 2487-06, 2006.
- 2.5.4.1-3 ASTM, 2006c, "Standard Test Method for Standard Penetration Test (SPT) and Split Barrel Sampling of Soils," ASTM D 1586-08, 2008.
- 2.5.4.1-4 Benson, R. N., "Internal Stratigraphic Correlation of the Subsurface Potomac Formation, New Castle County, Delaware, and Adjacent Areas in Maryland and New Jersey," Delaware Geologic Survey Report of Investigations No. 71, 15 pp., 2006.
- 2.5.4.1-5 Dames & Moore, "Report of Foundation Studies, Proposed Hope Creek Generating Station, Lower Alloways Creek Township, New Jersey Public Service Electric and Gas Company," May 23, 1974.
- 2.5.4.1-6 Dames & Moore, "Report of Foundation Studies, Proposed Salem Nuclear Generating Station, Salem, New Jersey, Public Service Electric & Gas Company," August 28, 1968.
- 2.5.4.1-7 Dames & Moore, "Supplementary Foundation Studies Proposed Hope Creek Generating Station, Lower Alloways Creek Township, N.J., Public Service Electric and Gas Company," July, 1975.
- 2.5.4.1-8 MACTEC Engineering and Consulting, Inc., "Geotechnical Exploration and Testing, PSEG Site Application, Lower Alloways Creek Township, New Jersey," Rev. 0, Jul 10, 2009.
- 2.5.4.1-9 Olsson, R. K., T. G. Gibson, H. J. Hansen, and J. P. Owens, (1988) "Geology of the Northern Atlantic Coastal Plain: Long Island to Virginia," in R. E. Sheridan and J. A. Grow, Eds., The Geology of North America, The Atlantic Continental Margin, U. S., Geological Society of America, I-2: 87–105, 1988.

**PSEG Site
ESP Application
Part 2, Site Safety Analysis Report**

- 2.5.4.1-10 Public Service Enterprise Group (PSEG), “Hope Creek Generating Station Updated Final Safety Analysis Report,” Revision 16, Subsection 2.5.4, May 15, 2008.
- 2.5.4.1-11 Public Service Enterprise Group (PSEG), “Salem Generating Station Updated Final Safety Analysis Report,” Revision 23, Subsection 2.5.4, October 17, 2007.
- 2.5.4.1-12 Sugarman, P. J., and D.H. Monteverde , Correlation of Deep Aquifers Using Coreholes and Geophysical Logs in Parts of Cumberland, Salem, Gloucester, and Camden Counties, New Jersey Geological Survey, Geologic Map Series, GMS 08-1, 2008.
- 2.5.4.1-13 Sugarman, P. J., K. G. Miller, J. V. Browning, A. A. Kulpecz, P. P. McLaughlin, and D. H. Monteverde, “Hydrostratigraphy of the New Jersey Coastal Plain: Sequences and Facies Predict Continuity of Aquifers and Confining Units,” *Stratigraphy* 2(3): 259–275, 2005.

**PSEG Site
ESP Application
Part 2, Site Safety Analysis Report**

**Table 2.5.4.1-1
Summary of ESPA Investigation Stratigraphic Data
Elevation at the Top of Formations**

Collar Elev. (NAVD) U.S. ft.	15.9	14.1	16.5	20.3	13.8	13.7	17.0	15.3
GEOLOGIC UNIT	EB-1	EB-2	EB-3	EB-4	EB-5	EB-6	EB-7	EB-8
Hydraulic Fill ^(a)	11	7	12	16	9	10	14	13
Alluvium	-22	-25	-22	-23	-19	-19	-21	-16
Kirkwood Formation-Upper	-36	-49	-37	-44	-38	-39	-37	-31
Kirkwood Formation-Lower	NE ^(c)	-84	-77	-87	-73	NE ^(c)	-64	NE ^(c)
Vincentown Formation	-87	-90	-91	-89	-82	-54	-67	-45
Hornerstown Formation	-127	-129	-128	-127	-133	-129	-131	-137
Navesink Formation	-147	-149	-148	-149	-149	-149	-151	-157
Mount Laurel Formation	-170	-169	-168	-169	-168	-168	-171	-177
Wenonah Formation	-280	--	-279	--	--	--	--	-289 ^(b)
Marshalltown Formation	-293	--	-293	--	--	--	--	--
Englishtown Formation	-319	--	-319	--	--	--	--	--
Woodbury Formation	--	--	-368	--	--	--	--	--
Merchantville Formation	--	--	-398	--	--	--	--	--
Magothy Formation	--	--	-429	--	--	--	--	--
Potomac Formation	--	--	-484	--	--	--	--	--
Boring Termination	-335.6	-186.6	-615.0	-179.9	-185.5	-186.2	-183.3	-286.4
Collar Elev. (NAVD) U.S. ft.	12.8	8.2	7.4	11.5	7.8	9.3	6.2	8.9
GEOLOGIC UNIT	NB-1	NB-2	NB-3	NB-4	NB-5	NB-6	NB-7	NB-8
Hydraulic Fill ^(a)	11	4	2	10	3	0	2	7
Alluvium	-33	-35	-31	-26	-29	-29	-22	-24
Kirkwood Formation-Upper	-42	NE ^(c)	-43	-43	-37	-34	NE ^(c)	-39
Kirkwood Formation-Lower	-50	-58	NE ^(c)	-56	-54	-53	NE ^(c)	NE ^(c)
Vincentown Formation	-56	-70	-57	-58	-60	-63	-33	-55
Hornerstown Formation	-105	-105	-106	-113	-105	-108	-112	-114
Navesink Formation	-126	-121	-125	-131	-124	-125	-132	-133
Mount Laurel Formation	-150	-145	-151	-153	-149	-149	-157	-157
Wenonah Formation	-252	-250	--	--	--	--	--	-259
Marshalltown Formation	-267	-265	--	--	--	--	--	-277
Englishtown Formation	-292	-290	--	--	--	--	--	--
Woodbury Formation	-336	--	--	--	--	--	--	--
Merchantville Formation	-372	--	--	--	--	--	--	--
Magothy Formation	-402	--	--	--	--	--	--	--
Potomac Formation	-454	--	--	--	--	--	--	--
Boring Termination	-588.1	-293.3	-192.9	-189.8	-192.2	-190.7	-195.0	-292.1

Elevations shown for the geologic units are rounded to the nearest foot and obtained from the ESPA Geotechnical Boring Logs contained in Appendix 2AA

- a) Materials from ground surface to top of hydraulic fill are not included in this table. These materials are mixed debris and old fill (artificial fill).
- b) Interpreted strata break elevation from geophysical log for EB-8G.
- c) Not encountered

**PSEG Site
ESP Application
Part 2, Site Safety Analysis Report**

**Table 2.5.4.1-2
Comparison of PSEG ESPA and HCGS Stratigraphic Data**

FORMATION	PSEG ESPA Investigation Borings (Appendix 2AA)								Hope Creek Borings (Reference 2.5.4.1-5)			
	PSEG ESPA - NB Series Strata Summary (8 borings)				PSEG ESPA - EB Series Strata Summary (8 borings)				HOPE CREEK BORINGS ^(b) Strata Summary			
	Avg. Thickness (ft.)	Top of Formation			Avg. Thickness (ft.)	Top of Formation			Avg. Thickness (ft.)	Top of Formation		
		Avg. Elev. ^(a) (ft.)	Range (ft.)			Avg. Elev. ^(a) (ft.)	Range (ft.)			Avg. Elev. ^(a) (ft.)	Range (ft.)	
Highest Elev. ^(a) (ft.)	Lowest Elev. ^(a) (ft.)		Highest Elev. ^(a) (ft.)	Lowest Elev. ^(a) (ft.)	Highest Elev. ^(a) (ft.)		Lowest Elev. ^(a) (ft.)					
Vincentown	52.1	-56.4	-32.8	-69.8	54.6	-75.6	-44.7	-90.5	65.1	-52.0	-32.8	-64.8
Hornerstown	18.5	-108.4	-104.8	-114.1	19.7	-130.1	-126.7	-137.2	19.2	-117.1	-106.9	-124.6
Navesink	24.4	-126.9	-120.8	-132.6	20.1	-149.8	-147.1	-156.7	20.0	-136.3	-128.1	-147.9
Mount Laurel	103.0	-151.3	-144.8	-157.1	111.2	-169.9	-167.5	-176.7	109.3	-156.4	-150.3	-166.8
Wenonah	16.0	-253.7	-249.8	-259.1	13.5	-282.4	-278.5	-288.7	44.5 ^(c)	-265.7 ^(c)	-264.0 ^(c)	-267.3 ^(c)
Marshalltown	25.0	-269.7	-264.8	-277.1	26.0	-292.8	-292.5	-293.1				
Englishtown	44.0	-291.0	-289.8	-292.2	49.0	-318.8	-318.5	-319.1	75.5 ^(c)	-310.2 ^(c)	-310.0 ^(c)	-310.3 ^(c)
Woodbury	36.0	-336.2	--	--	30.0	-367.5	--	--				
Merchantville	30.0	-372.2	--	--	31.0	-397.5	--	--	25.0	-385.7	-385.0	-386.3
Magothy	52.0	-402.2	--	--	55.0	-428.5	--	--	--	-410.0	--	--
Potomac	--	-454.2	--	--	--	-483.5	--	--	--	--	--	--

a) All elevations shown in this table are referenced to North American Vertical Datum 88.

b) Borings B-201 through B-274 from Reference 2.5.4.1-5. Data from borings B-218 and B-233 was not used for all formations due to uncertainty of boring data.

c) The Hope Creek borings do not differentiate the Wenonah - Marshalltown Formations or the Englishtown - Woodbury Formations.

**PSEG Site
ESP Application
Part 2, Site Safety Analysis Report**

**Table 2.5.4.1-3
Key to Soil Descriptions at the PSEG Site**

Soils classified under the Unified Soil Classification System (USCS) and in accordance with ASTM D 2488-06 (Reference 2.5.4.1-3)					
CORRELATION OF SPT RESISTANCE WITH RELATIVE DENSITY-CONSISTENCY				MOISTURE CONTENT	
GRANULAR MATERIAL		SILTS AND CLAYS		DRY-Absence of moisture MOIST-Damp/no visible H2O WET-Visible free water	
RELATIVE DENSITY	SPT N-value (bpf)	CONSISTENCY	SPT N-value (bpf)		
VERY LOOSE	0 to 4	VERY SOFT	0 to 2	HCl Reaction NO/NONE - No visible reaction WEAK - Some reaction/slow STRONG - Violent reaction	
LOOSE	5 to 10	SOFT	3 to 4		
MEDIUM DENSE	11 to 30	MEDIUM STIFF	5 to 8		
DENSE	31 to 50	STIFF	9 to 15		
VERY DENSE	> 50	VERY STIFF	16 to 30		
		HARD	> 30		
MODIFIERS			INDURATION		
Modifiers provide an estimate of the percentages of gravel, sand, and fines (silt or clay size particles) or other material such as organics, shells, glauconite, indurated material, etc.			For sedimentary rocks, induration is the hardening of the material by cementing, heat, pressure, etc.		
TRACE			<5%	FRIABLE	Rubbing with finger frees numerous grains; gentle blow by hammer disintegrates sample.
FEW			5 to 10%	MODERATELY INDURATED	Grains can be separated from sample with steel probe/knife; breaks easily when hit with hammer.
LITTLE			15 to 25%	INDURATED	Grains are difficult to separate with steel probe/knife; difficult to break with hammer.
SOME			30 to 45%	EXTREMELY INDURATED	Sharp hammer blows required to break sample; sample breaks across grains.
MOSTLY			50 to 100%	SPT Sample Numbering: SS-1, SS-2, SS-3, etc. Undisturbed Sample Numbering: UD-1, UD-2, UD-3, etc. MEASUREMENTS: Horizontal measurements and vertical measurements, such as SPT sample recovery or penetration, sample depths, etc., are rounded to nearest tenth of a foot (0.1 ft). HORIZONTAL COORDINATES (Northing and Easting) = NAD83 (2007), New Jersey State Plane Coordinate System Zone (2900), U.S. Survey Feet. ELEVATIONS = North American Vertical Datum of 1988 (NAVD), U.S. Survey Feet. ABBREVIATIONS USED: Run = Soil cored length during rotosonic drilling TV = Torvane Test (tsf) PP = Pocket Penetrometer Test (tsf) tsf = tons per square foot ND = Not Determined	
COLOR of Soil: see Munsell Soil Color Charts Particle Size Range for Sand: Fine, Medium, Coarse Particle Size Range for Gravel: Fine or Coarse GROUND WATER: Fluid level observations were recorded at the boring locations at the start of each work day, when possible. Due to the use of drilling fluid additives, these values may not represent the ground water conditions at the site. See observation wells for measured ground water levels. FLUID LEVELS (ft.) : 0 HR = Measured fluid level in boring immediately after drilling completed 24 HR = Measured fluid level in boring prior to grouting					

**PSEG Site
ESP Application
Part 2, Site Safety Analysis Report**

2.5.4.2 Properties of Subsurface Materials

Subsection 2.5.4.2 presents a summary of subsurface material properties at the PSEG Site. Subsection 2.5.4.2.1 provides a description of laboratory testing and sample control procedures. Subsection 2.5.4.2.2 provides a summary of static and dynamic engineering properties of site materials. See Subsection 2.5.4.3 for a discussion of the PSEG ESPA exploration activities and sampling techniques.

Laboratory and field investigations were specifically developed to comply with guidance in:

- RG 1.132, *Site Investigations for Foundations of Nuclear Power Plants*
- RG 1.138, *Laboratory Investigations of Soils and Rocks for Engineering Analysis and Design of Nuclear Power Plants*

Subsection 2.5.4.2.2 summarizes the subsurface engineering profile and properties of materials by layer, based on the field and laboratory testing conducted. The descriptions of subsurface materials for this site are based on the recent field exploration for the ESPA (Reference 2.5.4.2-15) and a review of historical data. Historical information regarding subsurface conditions includes the Dames & Moore report, *Foundation Studies, Proposed Hope Creek Generation Station, Lower Alloways Creek Township, New Jersey*, dated May 23, 1974 (DMR) (Reference 2.5.4.2-13) and the HCGS UFSAR, (Reference 2.5.4.1-10). The field investigation conducted for the ESPA is described in Subsection 2.5.4.3.

Soils encountered during this exploration include artificial fill and hydraulic fill underlain by alluvium and coastal plain deposits. Coastal plain deposits consist of the Kirkwood, Vincentown, Hornerstown, Navesink, Mount Laurel, Wenonah, Marshalltown, Englishtown, Woodbury, Merchantville, Magothy and Potomac formations. Site geology and stratigraphy are discussed in detail in Subsections 2.5.1 and 2.5.4.1.

Geologic formations with similar engineering properties are grouped into geotechnical engineering strata for engineering purposes. The foundation-bearing stratum has been determined to be the Vincentown Formation as discussed in Subsection 2.5.4.5. The geotechnical engineering strata are divided into a group of strata above the foundation excavation level and a group of strata at the bearing or below the foundation-bearing level. The geotechnical engineering strata are listed below starting from the ground surface.

Material Above Anticipated Foundation Excavation Level

- Artificial Fill (mechanically placed)
- Hydraulic Fill
- Alluvium
- Kirkwood Formation

Material at or Below Foundation Excavation Level

- Vincentown and Hornerstown Formations
- Navesink Formation
- Mount Laurel Formation
- Wenonah and Marshalltown Formations

**PSEG Site
ESP Application
Part 2, Site Safety Analysis Report**

- Englishtown and Woodbury Formations
- Merchantville Formation
- Magothy Formation
- Potomac Formation

The static and dynamic properties of the engineering strata are determined by in-situ testing and laboratory testing. The engineering properties of the subsurface materials are presented in Subsection 2.5.4.2.2.

2.5.4.2.1 Laboratory Testing

2.5.4.2.1.1 Purpose and Scope

Split-spoon samples and intact samples recovered during the ESPA site investigation activities were submitted for static and dynamic laboratory analysis (see Table 2.5.4.2-1). Samples were selected for laboratory testing based on the following criteria.

- Representative samples for each stratigraphic unit of engineering interest.
- Coarse-grained samples with relatively low blow counts for liquefaction analysis.
- Samples used to evaluate excavation stability and foundation support.
- Spatial distribution of samples across the investigation area.

The safety analysis uses the test data to address geologic hazards and engineering design characteristics.

The scope of the static laboratory program included soil classification, index, shear strength, and consolidation testing. Table 2.5.4.2-1 summarizes the number and types of tests performed and applicable ASTM standards. Although the site exploration encountered some highly plastic clays they were not tested for expansion/shrinkage since they are expected to be saturated. As described in Section 2.5.4.5, the construction of safety-related facilities will require over excavation and backfill, concrete structure foundations will not be in contact with the in-situ materials. Therefore, testing of the in-situ soils for sulfate and chloride to determine the soils' effect on concrete was not performed for the ESPA. If in-situ soils are reused as backfill, they will be tested for sulfate and chloride at that time.

The static laboratory indices completed for the PSEG ESPA are shown in Table 2.5.4.2-2. Static laboratory strength data completed for the PSEG ESPA is shown in Table 2.5.4.2-3a and Table 2.5.4.2-4. Static laboratory consolidation data is shown in Table 2.5.4.2-5a.

Dynamic laboratory testing was performed on six intact samples using the resonant column and torsional shear (RCTS) method. The testing was conducted in accordance with the University of Texas procedure (Reference 2.5.4.2-17). The dynamic laboratory test results are shown in Table 2.5.4.2-9. Results from one test are not considered suitable for further analysis due to a high void ratio that is inconsistent with the character of the formation sampled. Results of that test are not included in Table 2.5.4.2-9.

**PSEG Site
ESP Application
Part 2, Site Safety Analysis Report**

2.5.4.2.1.2 Sample Control

Soil samples were obtained from split-spoon and intact tube samples taken under the observation of rig geologists as part of the geotechnical exploration program. Split-spoon samples were placed in glass jars and sealed using moisture-tight lids. Intact tube samples were sealed in the field using a microcrystalline wax. All samples were labeled with identifying information, transferred to secure site storage, and recorded into the sample inventory records. Samples not used for testing were transferred to a long-term sample storage area with access control.

Soil boring field records were reviewed by the project principal engineer and samples were identified for laboratory testing. Work instructions were issued listing samples to be removed from site storage and shipped to the laboratories. Samples were removed from the site storage area, prepared, and transported in accordance with the work instructions.

Samples were handled and transported to the appropriate laboratory location following handling methods in ASTM D 4220 (Reference 2.5.4.2-9). Samples for index testing were handled as Group B samples. Intact tube samples were handled as Group C samples. The intact samples were transported to the laboratory under the control of MACTEC project personnel. All samples were shipped under MACTEC chain-of-custody (COC) procedures. Samples were stored in controlled, limited access, laboratory environments. Laboratory assignment sheets and work instructions were prepared by the project principal engineer and provided to the testing laboratories.

COC forms were filled out by project personnel at the PSEG Site, and accompanied samples to the appropriate laboratories. COC forms were subsequently completed by the receiving laboratory. COC forms were then returned to the MACTEC Document Control Center (DCC) for inclusion in project records. All parties involved in sample transportation completed and signed COC forms to document the handling and transportation process.

2.5.4.2.1.3 Testing Procedures

All static testing was performed in accordance with ASTM standards listed in Table 2.5.4.2-1. RCTS tests were performed by a procedure developed at the University of Texas Geotechnical Research Laboratory (Reference 2.5.4.2-17) since ASTM has not published an applicable test standard. Methodology descriptions of testing for intact samples are provided below.

2.5.4.2.1.3.1 Consolidated-Undrained Triaxial Compression

Consolidated-undrained (CU) testing was performed in accordance with ASTM D 4767 (Reference 2.5.4.2-2) on intact test specimens extruded from sampling tubes and trimmed to appropriate dimensions. The specimens were encased in rubber membranes and saturated by back pressure prior to shearing. Specimen saturation was determined as prescribed in Subsection 8.2.3.1 of ASTM Standard D 4767. (Reference 2.5.4.2-2) The test specimen was permitted to drain during the consolidation phase, allowing equilibrium under the confining stress, but no drainage was allowed during the loading phase. Failure was determined to have occurred when the specimens had reached the maximum deviator stress or a deviator stress at a selected strain less than 15 percent.

**PSEG Site
ESP Application
Part 2, Site Safety Analysis Report**

Vertical load, vertical displacement, chamber pressure, and pore pressures generated during the loading phase were measured and recorded. The test is termed CU, and total stresses result if no pore pressure corrections are included. When the pore pressures generated during the loading phase are subtracted from the total stresses, effective stresses are calculated.

2.5.4.2.1.3.2 Unconsolidated-Undrained Triaxial Compression

Unconsolidated-undrained (UU) testing was performed in a manner similar to the CU testing described above, except that no drainage is allowed under the application of the confining pressure or the loading. Testing was performed in accordance with ASTM D 2850 (Reference 2.5.4.2-12).

2.5.4.2.1.3.3 One-Dimensional Consolidation

One-dimensional consolidation testing was performed in accordance with ASTM D 2435 (Reference 2.5.4.2-3) on an undisturbed test specimen of cohesive soil extruded from sampling tubes. The specimen was trimmed to form a disc approximately 2.5 inches (in.) in diameter and 1 in. thick. The soil sample was confined in a stainless steel ring, sandwiched between porous plates, and subjected to incrementally increasing vertical loads. The vertical load on the sample and number of loading increments varied slightly among the samples. Resulting changes in specimen height with respect to time were measured with a linear variable differential transducer and recorded on a data collector. Each load interval was considered complete when the specimen reached 100 percent consolidation. The time required for the specimen to reach 100 percent consolidation (T_{100}) was determined by the square root of time method. Load increments were doubled with each loading phase.

The consolidation test result for the sample from the Kirkwood Formation was used to estimate the coefficient of compression (C_c), the coefficient of recompression (C_r) and pre-consolidation stress (p_c) (Table 2.5.4.2-5a).

2.5.4.2.1.3.4 Resonant Column and Torsional Shear

Samples obtained from the Vincentown, Hornerstown and Navesink Formations were tested on resonant column and torsional shear (RCTS) using a University of Texas procedure (Reference 2.5.4.2-17). Each test specimen was subjected to a suite of tests at varying confining pressures and cyclic strain levels. In-situ confining pressures were estimated using layer unit weights and sample depths to obtain an estimated vertical effective stress. Then, an assumed coefficient of earth pressure at rest (K_0) was used to calculate the associated horizontal effective stresses (assumed isotropic). The value of K_0 chosen was 0.5, a value typical for generally normally consolidated soils. The mean confining pressure was then calculated by summing the vertical and two horizontal stresses and dividing by 3. To provide for variation in K_0 , RCTS tests were performed at confining pressures of 0.25, 0.5, 1, 2 and 4 times the estimated mean confining pressure.

In the resonant column portion of the RCTS test, a value for shear wave velocity was measured in the laboratory at small strains. In the torsion shear mode, samples were driven at increasing cyclic strain levels up to the limit of the equipment and were then excited in the resonant column mode to obtain results at higher strain levels. The test results are presented in Subsection 2.5.4.2.2.2.

**PSEG Site
ESP Application
Part 2, Site Safety Analysis Report**

2.5.4.2.2 Material Engineering Properties

2.5.4.2.2.1 Static Material Properties

Soil parameters obtained during the ESPA exploration (as discussed in Subsection 2.5.4.3.1.2) and laboratory analysis are presented in the following paragraphs for each geotechnical engineering strata. Additionally, pertinent data from the Hope Creek UFSAR (Reference 2.5.4.1-10) are summarized in the following paragraphs. Tables 2.5.4.2-2 through 2.5.4.2-6 present summaries of available data for both data sets.

This presentation of static material properties determined from the exploration of the PSEG Site indicates the uniformity of the various geotechnical engineering strata relative to material properties. The design values presented in Table 2.5.4.2-8 are primarily based on the values determined from the ESPA exploration.

2.5.4.2.2.1.1 Artificial Fill (Mechanically Placed)

Artificial Fill was encountered in all of the borings at the surface and extended to depths up to approximately 10 ft. Laboratory testing was not performed for these materials since they will be removed during construction. Based on visual manual examination, the lithologies were observed to be variable, and generally included clays, silts, sands with varying silt/clay contents, clayey/silty gravels and construction debris. Field Standard Penetration Test (SPT) N-Values range from 2 to 99 blows per foot (bpf). The higher N-values may be inflated due to the presence of rock fragments and other debris within the Artificial Fill.

2.5.4.2.2.1.2 Hydraulic Fill

Hydraulic Fill was encountered underlying the artificial fill in all of the borings performed for the ESPA subsurface investigation. Based on borings performed for the ESPA, hydraulic fill ranges in thickness from 24 to 44 ft. The Hydraulic Fill generally consists of soft, discontinuous lenses of clayey silts, silty sands, and organic clays. This unit represents dredge spoils deposited on the site from dredging conducted in the Delaware River since the early 1900's.

Static laboratory indices were determined for ten SPT samples and one intact sample of Hydraulic Fill collected during the ESPA subsurface investigation (Table 2.5.4.2-2, Sheet 1 of 18). Laboratory testing, including sieve analysis with hydrometer (ASTM D 422) (Reference 2.5.4.2-10), sieve analysis (No. 200 wash) (ASTM D 6913) (Reference 2.5.4.2-1), Atterberg limits (ASTM D 4318) (Reference 2.5.4.2-5), specific gravity (ASTM D 854) (Reference 2.5.4.2-6), moisture content (ASTM D 2216) (Reference 2.5.4.2-4) and organic content (ASTM D 2974) (Reference 2.5.4.2-11) were performed to classify and determine engineering properties of the Hydraulic Fill.

Samples of the Hydraulic Fill are generally classified as silt (ML, MH) and clay (CL, CH) and, less commonly, sand (SM, SC-SM), in accordance with the Unified Soil Classification System described in ASTM Standard D 2487 (Reference 2.5.4.2-7). The moisture content of tested samples ranges from 61 to 98 percent with an average of 79 percent and a median value of 77 percent. The percent fines (silt and clay; minus No. 200 sieve) of the Hydraulic Fill ranges from 15 to 99 percent, with an average of 73 percent, and a median value of 76 percent. The liquid limit of tested soils ranges from 18 to 97, with an average of 60, and a median value of 58. The

**PSEG Site
ESP Application
Part 2, Site Safety Analysis Report**

plastic limit ranges from 12 to 44, with an average of 28, and a median value of 29. The plasticity indices range from 6 to 53, with an average of 32, and a median value of 34. A specific gravity test was performed on one soil sample and indicated a value of 2.68. Soil index properties for the individual tests are shown in Table 2.5.4.2-2 (Sheet 1 of 18).

Soil index properties of the Hydraulic Fill reported in the HCGS UFSAR (Reference 2.5.4.1-10) were reviewed to determine if index properties determined for the ESPA are similar to the reported values in the HCGS UFSAR. Based on a review of the HCGS UFSAR, the liquid limit ranges from 29 to 94, with an average of 69, and a median value of 73. The plasticity indices of the tested samples range from 10 to 58 with an average of 34, and a median value of 37. The natural moisture of the tested samples ranges from 20 to 80 percent, with an average of 56 percent, and a median value of 61 percent. The specific gravity of the tested samples ranges from 2.50 to 2.69, with an average value of 2.58, and a median value of 2.58. Based on review, soil index properties reported in the HCGS UFSAR for the Hydraulic Fill are comparable to soil index properties determined for the ESPA. Soil index values reported in the HCGS UFSAR are shown in Table 2.5.4.2-2 (Sheet 2 of 18) for comparison purposes. Design values for the soil index properties are presented in Table 2.5.4.2-8.

Field SPT N-values ranged from weight-of-hammer (WOH) to 36 bpf. The average field SPT N-value for this layer is 3 bpf. The median SPT N-value is 0 bpf. SPT N-values corrected for field procedures, including hammer energy, (N_{60}) for this stratum range from 0 to 43 bpf, with an average value of 3 bpf, and a median value of 0 bpf. The design values for corrected and field N-values are shown on Table 2.5.4.2-8.

An intact sample of the Hydraulic Fill collected during the ESPA subsurface investigation was submitted for strength testing. Strength testing of the Hydraulic Fill included one UU triaxial compression ((ASTM D 2850-03a [2007]) (Reference 2.5.4.2-12) test at confining pressures of 0.756, 1.26 and 2.02 tons per square foot (tsf). Test results indicate undrained shear strength values ranging from 0.365 tsf to 0.507 tsf, with an average of 0.436 tsf. UU test results performed for the ESPA are shown in Table 2.5.4.2-3a.

Results of 22 UU triaxial compression tests are presented in the HCGS UFSAR and shown in Table 2.5.4.2-3b. The undrained shear strength of the Hydraulic Fill reported in the HCGS UFSAR range from 0.075 tsf to 0.560 tsf with an average value of 0.316 tsf and a median value of 0.306 tsf. Undrained shear strengths determined from tests of the Hydraulic Fill for the ESPA are consistent with UU compression tests reported in the HCGS UFSAR. Design values for the undrained shear strength of the Hydraulic Fill are included in Table 2.5.4.2-8.

No consolidation tests (ASTM D 2435-04) (Reference 2.5.4.2-3) were performed on samples from the Hydraulic Fill for the ESPA. Four consolidation tests on samples of Hydraulic Fill were performed for the HCGS UFSAR and the results are included on Table 2.5.4.2-5b. The consolidation test results reported in the HCGS UFSAR indicate a compression index, C_c , ranging from 0.42 to 0.70, with an average of 0.54, and a median of 0.52. Based on the tests, the pre-consolidation pressure, P_c , of the Hydraulic Fill ranges from 0.26 tsf to 1.30 tsf, with an average of 0.69 tsf. The design values for the consolidation properties are shown in Table 2.5.4.2-8.

The total unit weight determined from three portions of the intact sample collected from boring NB-1UD for shear testing was calculated to range from 90.9 to 94.9 pounds per cubic foot (pcf).

**PSEG Site
ESP Application
Part 2, Site Safety Analysis Report**

Results of individual tests are shown in Table 2.5.4.2-6. A summary of unit weights for the Hydraulic Fill reported in the DMR is presented in Table 2.5.4.2-7. The total unit weight of the 16 samples reported in the DMR for the Hydraulic Fill ranged from 78.2 to 132.3 pcf, with an average of 106.6 pcf and a median value of 100.5 pcf. The two unit weights reported in the DMR that were above 130 pcf were for samples collected within about 5 feet (ft.) of the ground surface and are not considered representative values. If these two unusually high values are ignored, the average and median of the DMR reported total unit weights for the Hydraulic Fill are 103 and 99 pcf, respectively. The design unit weight for the Hydraulic Fill, based on test results of the ESPA and the DMR, is presented in Table 2.5.4.2-8.

2.5.4.2.2.1.3 Alluvium

Alluvium was encountered in all of the borings performed for the ESPA investigation at elevations ranging from -16 to -35 ft. NAVD. Based on borings performed for the ESPA, Alluvium ranges in thickness from 5 to 24 ft. The Alluvium consists of fine to coarse sand and gravel deposits which formerly comprised the bed of the adjacent Delaware River. Layers of peat and other organic rich soils were also observed within this unit. A lower layer of slightly organic to non-organic micaceous silt and clay was locally encountered near the base of this formation in some borings. The Alluvium was overlain by Hydraulic Fill during the initial construction of Artificial Island.

Static laboratory indices were determined for seven SPT samples of the Alluvium collected during the ESPA subsurface investigation (Table 2.5.4.2-2, Sheet 4 of 18). Laboratory testing, including sieve analysis (No. 200 wash), Atterberg limits, and moisture content, were performed to determine the soil index properties of the Alluvium.

Samples of the Alluvium are generally classified as silty sands (SM, SP, SP-SM), and occasionally silt (ML) and clay (CL). The moisture content of tested samples ranges from 14 to 41 percent. The fine-grained component of Alluvium samples (silt and clay size fraction) range from 4 to 80 percent. An Atterberg limits test was performed on one sample of alluvial clay. The liquid limit of this clay sample was 40. The plastic limit was 24 and the plasticity index was 16. Soil index properties for the individual tests are shown in Table 2.5.4.2-2 (Sheet 4 of 18). Design values for the index properties are included in Table 2.5.4.2-8.

Field SPT N-values range from WOH to 65 bpf. The average SPT N-value for this layer is 14 bpf. The median SPT N-value is 13 bpf. SPT N-values corrected for field procedures, including hammer energy, (N_{60}) for this stratum range from 0 to 99 bpf, with an average value of 22 bpf, and a median value of 19 bpf. The design values for the corrected and field N-values are shown on Table 2.5.4.2-8.

The unit weight of Alluvium was not determined for the ESPA. Based on review of the DMR, the unit weight of one Alluvium sample, classified as SP, was determined to be 136.6 pcf, and is shown in Tables 2.5.4.2-7 and 2.5.4.2-8.

2.5.4.2.2.1.4 Kirkwood Formation

The Kirkwood Formation was encountered in all of the borings performed for the ESPA investigation, except boring NB-7, at elevations ranging from -31 to -49 ft. NAVD. The Kirkwood Formation encountered at the PSEG Site typically consists of two distinct stratigraphic units.

**PSEG Site
ESP Application
Part 2, Site Safety Analysis Report**

The upper unit is comprised of greenish-gray, silty, fine sand and greenish-gray to brown, organic clay with zones of peat and occasional shell fragments and was encountered at 14 of the 16 exploratory boring locations. The lower unit is comprised of fine to coarse sand and subrounded to subangular gravel, with variable silt and clay content and was encountered at 10 of the 16 exploratory boring locations. Based on borings performed for the ESPA, the upper, fine-grained portion of the Kirkwood Formation ranges in thickness from 8 to 51 ft., and the lower, coarse-grained portion ranges in thickness from 2 to 16 ft.

Static laboratory indices were determined for four SPT samples and one intact sample of the upper, fine-grained portion of the Kirkwood Formation and seven SPT samples of the lower, coarse-grained portion of the Kirkwood Formation collected during the ESPA subsurface investigation (Table 2.5.4.2-2, Sheets 6 and 8 of 18). Laboratory testing, including sieve analysis with hydrometer, sieve analysis (No. 200 wash), Atterberg limits, and moisture content, were performed to determine the soil index properties of the Kirkwood Formation.

Samples of the Kirkwood Formation are generally classified as silt (ML, MH), clay (CL, CH) in the upper portion, and sands (SP, SM, SP-SM, SC-SM) in the lower portion of the unit. The moisture content of samples tested for the ESPA range from 29 to 77 percent for six samples from the upper, fine-grained portion and from 16 to 21 for two samples from the lower, coarse-grained portion. The silt and clay size fraction (percent fines) ranges from 51 to 94 percent for four samples of the upper, fine-grained portion of the Kirkwood Formation and from 4 to 34 percent for seven samples of the lower, coarse-grained portion. The liquid limits for six ESPA samples from the upper fine grained portion of the Kirkwood Formation range from 27 to 63 with an average of 50 and a median of 53. The plasticity indices for six ESPA samples from the upper fine grained portion of the Kirkwood Formation range from 11 to 37 with an average of 25 and a median of 26. Soil index properties for the individual tests are shown in Table 2.5.4.2-2 (Sheet 6 and Sheet 8).

Soil index properties of the Kirkwood Formation reported in the HCGS UFSAR were reviewed and compared to results from the ESPA investigation. The liquid limit ranged from 37 to 81, with an average and median value of 58 for 16 samples of the upper, fine-grained portion of the Kirkwood Formation (identified as "Kirkwood Clays" in the HCGS UFSAR). The plasticity indices of the tested samples ranged from 16 to 50, with an average of 29, and a median value of 30. The natural moisture content of the tested samples ranged from 22 to 60 percent, with an average of 47 percent, and a median value of 50 percent. The specific gravity of the tested fine-grained samples ranges from 2.61 to 2.73, with an average value of 2.65, and a median value of 2.63. Void ratios calculated for 100 percent saturation ranged from 0.91 to 1.52. Based on this review, soil index properties reported in the HCGS UFSAR are comparable to soil index properties determined for the ESPA. Soil index values reported in the HCGS UFSAR are shown with the values determined from the ESPA Investigation in Table 2.5.4.2-2 (Sheet 5 and Sheet 7). Design values for the soil index properties are presented in Table 2.5.4.2-8.

An intact sample of the fine-grained portion of the Kirkwood Formation collected during the ESPA subsurface investigation (sample from UD-8 collected at boring NB-1UD) was submitted for strength and consolidation testing. UU triaxial compression testing was performed on a portion of the intact sample having a Unified Soil Classification System (USCS) classification of CL at a confining pressure of 2.52 tsf. The test result indicates an undrained shear strength value of 0.506 tsf (Table 2.5.4.2-3a).

**PSEG Site
ESP Application
Part 2, Site Safety Analysis Report**

Six UU triaxial compression tests were performed on the fine-grained portion of the Kirkwood Formation ("Kirkwood Clay") for the HCGS UFSAR and the test results are included in Table 2.5.4.2-3b. The undrained shear strength of the Kirkwood Formation clay reported in the HCGS UFSAR ranges from 0.510 tsf to 1.335 tsf with an average value of 0.735 tsf and a median value of 0.582 tsf. The undrained shear strength value determined in the Kirkwood Formation clay for the ESPA is consistent with the results of UU triaxial compression tests performed for the HCGS UFSAR. Design values for the undrained shear strength are included in Table 2.5.4.2-8.

The consolidation test was performed on a portion of the intact sample from UD-8 collected at boring NB-1UD having a USCS classification of MH. The consolidation test results indicated a pre-consolidation pressure, P_c , of 1.40 tsf, a coefficient of compression, C_c , of 0.535 and a coefficient of recompression, C_r , of 0.070 (Table 2.5.4.2-5a).

Five consolidation tests were performed on the fine-grained portion of the Kirkwood Formation for the HCGS UFSAR and the results are included in Table 2.5.4.2-5b. These consolidation test results indicate a compression index, C_c , ranging from 0.17 to 0.79, with an average of 0.44, and a median value of 0.42. Based on the tests, the pre-consolidation pressure, P_c , of the Kirkwood Formation ranges from 1.55 tsf to 8.00 tsf, with an average of 3.19 tsf and a median value of 2.10 tsf. Consolidation properties determined in the ESPA are consistent with the five consolidation tests performed for the HCGS UFSAR. The design values for the consolidation properties, based on tests performed from the ESPA and the HCGS UFSAR, are shown in Table 2.5.4.2-8.

The total unit weight determined for the portions of the intact sample of the fine-grained Kirkwood Formation collected at boring NB-1UD for strength and consolidation testing were 103.9 pcf for the MH portion of the sample, and 122.8 pcf for the CL portion of the sample, as shown in Table 2.5.4.2-6. Unit weights were determined on 11 samples of the upper, fine-grained portion of the Kirkwood Formation and reported in the DMR. The results of the unit weight determinations reported in the DMR are included in Table 2.5.4.2-7. The unit weights of the 11 samples of the fine-grained portion of the Kirkwood Formation ranged from 98.4 to 133.2 pcf, with an average of 111.0 pcf and a median value of 109.5 pcf. Total unit weights calculated for the ESPA are within the range of total unit weights reported in the DMR for the fine-grained portion of the Kirkwood Formation. The design unit weight for the fine-grained portion of the Kirkwood Formation, based on test results of the ESPA and the DMR, is presented in Table 2.5.4.2-8.

Field SPT N-values range from WOH to greater than 100 bpf. The average SPT N-value for this layer is 12 bpf. N-values greater than 100 bpf were treated as equal to 100 bpf for purposes of averaging. The median SPT N-value is 7 bpf. SPT N-values corrected for field procedures, including hammer energy, (N_{60}) for this stratum range from 0 to 140 bpf, with an average value of 18 bpf, and a median value of 10 bpf. The design corrected and field N-values are shown on Table 2.5.4.2-8.

2.5.4.2.2.1.5 Vincentown and Hornerstown Formations

For engineering purposes, the Vincentown and Hornerstown formations are combined into one engineering layer due to their similar engineering properties. The field and laboratory test results summarized here are for the Vincentown and Hornerstown formations.

**PSEG Site
ESP Application
Part 2, Site Safety Analysis Report**

The Vincentown Formation was encountered in all of the borings performed for this ESPA investigation. The Vincentown Formation serves as the bearing stratum for the adjacent Salem and Hope Creek generating stations and will serve as the bearing stratum for the new plant. Based on borings performed for the ESPA, thickness of the Vincentown Formation ranges from 35 to 93 ft. The elevation of the top of the Vincentown Formation ranges from elevation -33 to -91 ft. NAVD in the borings performed for this ESPA. The Vincentown Formation consists primarily of a greenish-gray, fine to medium grained silty sand with some zones of clayey sand. The mineral glauconite, which imparts the greenish color, was observed in most samples. Previous studies indicate that glauconite typically comprises less than 10 percent of the sand fraction of the Vincentown Formation, but can vary up to 20 percent. Based on drilling characteristics and recovered samples, friable to indurated (cemented) zones of 0.1 to 3.0 ft. in thickness are present throughout this formation. Previous studies, including geologic mapping of the HCGS excavation, have described the indurated zones as calcareous sandstone and limestone. An upper weathered or possibly reworked zone was observed in some of the borings. Where encountered, this upper weathered zone generally exhibited a lower degree of induration and was reddish-brown in color (likely due to oxidation).

The Hornerstown Formation was encountered in all of the borings performed for this exploration. Based on the borings, the Hornerstown Formation ranges in thickness from 16 to 22 ft. The Hornerstown Formation conformably underlies the Vincentown Formation and primarily consists of a greenish-gray to dark green silty and clayey, quartz and glauconitic sand with indurated zones, similar to the overlying Vincentown Formation. The contact between the Vincentown and Hornerstown formations was observed to be gradational. This contact was identified due to an increase in fines (silt and clay), and glauconite content.

Static laboratory indices were determined for 40 SPT samples and seven intact samples of the Vincentown and Hornerstown formations collected during the ESPA subsurface investigation (Table 2.5.4.2-2, Sheet 9 and 10 of 18). Laboratory testing, including sieve analysis with hydrometer, sieve analysis (No. 200 wash), Atterberg limits, specific gravity and moisture content, were performed to determine the soil index properties of the Vincentown and Hornerstown formations.

Samples of the Vincentown and Hornerstown formations are generally classified as silty sands (SM, SP-SM) and, less commonly, clayey sand (SC, SC-SM), silt (ML, MH) and clay (CL). The moisture content of tested samples ranges from 9 to 40 percent, with an average of 30 percent, and a median value of 30 percent. The fine-grained component of the Vincentown and Hornerstown formations (silt and clay; minus 200 sieve) ranges from 9 to 96 percent, with an average of 27 percent, and a median value of 23 percent. A grain size distribution envelope developed from 40 grain size distribution curves performed for the ESP investigation is presented as Figure 2.5.4.2-1.

Nine of the 22 samples submitted for Atterberg limits tests indicate no value for the liquid limit, and non-plastic for the plastic limit. For the remaining samples, the liquid limit ranges from no value to 36. The average value of the liquid limit is 26, and the median value is 25. The plastic limit ranges from non-plastic to 27. The average and median value of the plastic limit are 20 and 19, respectively. The plasticity indices range from non-plastic to 12. The average and median plasticity indices are 6. The average and median value of the liquid limit test, plastic limit test, and the calculated plasticity indices are based on tests having values for the liquid limit and plastic limit. The specific gravity ranges from 2.61 to 2.75, with an average of 2.70, and a

**PSEG Site
ESP Application
Part 2, Site Safety Analysis Report**

median value of 2.70. Soil index properties for the individual tests are shown in Table 2.5.4.2-2 (Sheet 9 and 10 of 18).

Soil index properties of the Vincentown Formation reported in the HCGS UFSAR were reviewed to determine if index properties determined in the ESPA are similar. Based on review of the HCGS UFSAR, the liquid limit ranges from 27 to 47, with an average of 36, and a median value of 35. The plasticity indices of the tested samples range from 6 to 20, with an average and median value of 11. The natural moisture of the tested samples ranges from 21 to 42 percent, with an average and median value of 30 percent. The specific gravity of the tested samples ranges from 2.60 to 2.73, with an average and median value of 2.68. Void ratios calculated for 100 percent saturation ranged from 0.55 to 1.06. Figure 2.5.4.2-1 shows the grain size envelope for the Vincentown and Hornerstown formations determined in the ESPA is consistent with the grain size envelope for the Vincentown Formation reported in the HCGS UFSAR. Based on review, soil index properties reported in the HCGS UFSAR are found to be comparable to soil index properties determined for the ESPA. Soil index values reported in the HCGS UFSAR are shown in Table 2.5.4.2-2 (Sheet 11 of 18). Design values for the soil index properties are presented in Table 2.5.4.2-8.

Representative intact samples of the Vincentown and Hornerstown strata collected during the ESPA subsurface investigation were submitted for strength and consolidation testing.

Three CU triaxial compression tests were performed on intact samples of the Vincentown and Hornerstown formations for the ESPA. Tests were performed on soils having an USCS classification of SM. Results of CU tests indicate average shear strength values of $c = 1.28$ tsf, and $\Phi = 20^\circ$ for total stress, and $c' = 0.40$ tsf, and $\Phi' = 37^\circ$ for effective stress. Shear strength properties for the individual tests performed for the ESPA are presented on Table 2.5.4.2-4.

Shear strength properties determined for the ESPA were compared with CU tests performed for the HCGS UFSAR. CU test results from the HCGS UFSAR indicate shear strength values ranging from $\Phi = 23^\circ$ to 37° for total stress, and $\Phi' = 31^\circ$ to 43° for effective stress. The CU tests performed for the HCGS UFSAR were one-point tests with the cohesion intercepts, c and c' assumed to be 0. Comparison of the strength test results between the ESPA samples and the HCGS UFSAR is not made due to the difference in test methods. Design shear strength values for the Vincentown and Hornerstown formations determined from CU tests performed for the ESPA are presented in Table 2.5.4.2-8.

The total unit weight determined from 13 intact samples of the Vincentown and Hornerstown formations was calculated to range from 110.9 to 130.2 pcf. The unit weight was calculated from the dry density and moisture content determined from intact samples selected for strength and consolidation testing. Results of individual tests performed for the ESPA investigation are shown in Table 2.5.4.2-6. A summary of unit weights for the Vincentown and Hornerstown formations reported in the DMR is shown in Table 2.5.4.2-7. Based on review of the DMR, unit weights calculated for the ESPA are consistent with unit weights of the Vincentown and Hornerstown formations reported in the DMR. The design unit weight for the Vincentown and Hornerstown formations, based on test results from the ESPA exploration and the DMR, is presented in Table 2.5.4.2-8.

Field SPT N-values range from 5 to greater than 100 bpf. The average SPT N-value for this layer is 47 bpf. The median SPT N-value is 33. N-values greater than 100 bpf were treated as

**PSEG Site
ESP Application
Part 2, Site Safety Analysis Report**

equal to 100 bpf for purposes of averaging. As noted in the ESPA boring logs (Appendix 2AA), cemented layers were encountered in the Vincentown Formation. The higher blow counts may be attributed to the presence of these cemented layers as evidenced by the angular, gravel-sized, cemented pieces recovered in the split-spoon barrel sampler. SPT N-values corrected for field procedures, including hammer energy, (N_{60}) for this stratum range from 7 to 160 bpf, with an average value of 70 bpf, and a median value of 50 bpf. The design corrected and field N-values are shown on Table 2.5.4.2-8. A histogram of the field N-values for the Vincentown Formation is shown in Figure 2.5.4.1-10, and one for the Hornerstown Formation is shown in Figure 2.5.4.1-9.

2.5.4.2.2.1.6 Navesink Formation

The Navesink Formation was encountered in all of the borings performed for the ESPA subsurface investigation at elevations ranging from -121 to -157 ft. NAVD. Based on the borings, the Navesink ranges in thickness from 19 to 26 ft. The Navesink Formation consists of dark green to greenish-black glauconitic sand, with varying silt and clay content. Fossils, consisting primarily of pelecypod fragments, were observed in many of the recovered samples. Examination of the samples obtained and data from previous studies indicates that glauconite comprises up to 95 percent of the sand fraction of this formation. Due to its unique characteristics, this unit was easily identified in the borings.

Static laboratory indices were determined for eight SPT samples and two intact samples of the Navesink Formation collected during the ESPA subsurface investigation (Table 2.5.4.2-2, Sheet 12 of 18). Laboratory testing, including sieve analysis with hydrometer, Atterberg limits, specific gravity, and moisture content, were performed to determine the soil index properties of the Navesink Formation.

Samples of the Navesink Formation are generally classified as silty and clayey sands (SM, SC-SM, SC). The moisture content for tested samples ranges from 15 to 36 percent, with an average of 22 percent, and a median value of 21 percent. The fine-grained component of Navesink Formation (silt and clay; minus 200 sieve) range from 13 to 40 percent, with an average of 22 percent, and a median value of 19 percent. A grain size distribution envelope developed from nine grain size distribution curves performed for the ESPA investigation is presented as Figure 2.5.4.2-2.

Four of the 10 samples submitted for Atterberg limits tests indicate no value for the liquid limit and non-plastic for the plastic limit. For the remaining samples, the liquid limit ranges from 21 to 37, with an average of 27, and a median value of 24. The plastic limit ranges from 13 to 18, with an average of 16, and a median value of 17. The plasticity indices range from 4 to 23, with an average of 11, and a median value of 8. The average and median value of the liquid limit test, plastic limit test and the calculation of the plasticity indices, are calculated from six tests that have a value for the liquid limit and plastic limit tests. The specific gravity ranges from 2.67 to 2.73, with an average of 2.70, and a median value of 2.71. Void ratios calculated for 100 percent saturation ranged from 0.52 to 0.61. Soil index properties for the individual tests are shown in Table 2.5.4.2-2, Sheet 12 of 18. Design values for index properties are included in Table 2.5.4.2-8.

Field SPT N-values range from 38 to greater than 100 bpf. N-values greater than 100 bpf were treated as equal to 100 bpf for purposes of averaging. The average SPT N-value for this layer is

**PSEG Site
ESP Application
Part 2, Site Safety Analysis Report**

72 bpf. The median SPT N-value is 74 bpf. SPT N-values corrected for field procedures, including hammer energy, (N_{60}) for this stratum range from 53 to 160 bpf with an average and median value of 108 bpf. The design corrected and field N-values are shown on Table 2.5.4.2-8. A histogram of the field N-values for the Navesink Formation is shown in Figure 2.5.4.1-8.

The total unit weight determined from two intact samples of the Navesink strata were calculated to be 115.5 and 131.8 pcf. The average unit weight for this stratum is 123.6 pcf. Results of individual tests are shown in Table 2.5.4.2-6. Based on review of the DMR, unit weights calculated for the ESPA are consistent with reported unit weights of the Navesink Formation in the DMR. The unit weight was calculated from the dry density and moisture content determined from intact samples selected for strength and consolidation testing. A summary of unit weights for the Navesink Formation reported in the DMR is shown in Table 2.5.4.2-7. The design unit weight for the Navesink Formation, based on test results of the ESPA and the DMR, is presented in Table 2.5.4.2-8.

2.5.4.2.2.1.7 Mount Laurel Formation

The Mount Laurel Formation was encountered in all of the borings performed for the ESP subsurface investigation at elevations ranging from -145 to -177 ft. NAVD, and ranged in thickness from 102 to 112 ft. The Mount Laurel Formation consists of a dense to very dense brownish-gray to dark green fine to coarse-grained sand with varying silt and clay content. The glauconite content in the Mount Laurel was observed to generally decrease with depth. Additionally, the grain size and fines content was also observed to decrease with depth such that the basal portion of the unit is composed of cleaner, finer-grained sand.

Static laboratory indices were determined for 17 SPT samples and three intact samples of the Mount Laurel Formation collected during the ESPA subsurface investigation (Table 2.5.4.2-2, Sheet 13 of 18). Laboratory testing, including sieve analysis with hydrometer, sieve analysis (No. 200 wash), Atterberg limits, specific gravity and moisture content, were performed to determine the soil index properties of the Mount Laurel Formation.

Samples of the Mount Laurel Formation are generally classified as silty and clayey sands (SM, SC-SM, SC). The moisture content for soils tested ranges from 13 to 29 percent, with an average of 20 percent, and a median value of 21 percent. The fine-grained component of the Mount Laurel Formation (silt and clay; minus 200 sieve) ranges from 15 to 38 percent, with an average of 24 percent, and a median value of 21 percent. A grain size distribution envelope developed from 18 grain size distribution curves performed for the ESPA investigation is presented as Figure 2.5.4.2-3.

Four of the 18 samples submitted for Atterberg limits tests indicate no value for the liquid limit, and non-plastic for the plastic limit. For the remaining samples, the liquid limit ranges from 19 to 42, with an average of 27, and a median value of 25. The plastic limit ranges from 13 to 26, with an average of 18, and a median value of 17. The plasticity index ranges from 3 to 19, with an average of 9, and a median value of 8. The average and median values of the liquid limit test, plastic limit test, and the calculation of the plasticity indices, are calculated from the 14 tests having a value for the liquid limit and plastic limit tests. The specific gravity ranges from 2.69 to 2.71, with an average and median value of 2.70. Void ratios calculated for 100 percent saturation ranged from 0.46 to 0.65. Soil index properties for the individual tests are shown in Table 2.5.4.2-2 (Sheet 13 of 18). Design soil index values are included in Table 2.5.4.2-8.

**PSEG Site
ESP Application
Part 2, Site Safety Analysis Report**

Representative intact samples of the Mount Laurel Formation collected during the ESPA subsurface investigation were submitted for strength and consolidation testing. One CU triaxial compression test was performed on a representative intact sample of the Mount Laurel Formation. The representative sample was a silty sand having a USCS classification of SM. Results of the CU tests indicate average shear strength values of $c = 7.63$ tsf, and $\Phi = 13^\circ$ for total stress, and $c' = 4.81$ tsf and $\Phi' = 20^\circ$ for effective stress (Table 2.5.4.2-4). Shear strength design values determined from the CU tests in the Mount Laurel Formation are included in Table 2.5.4.2-8.

The total unit weight determined from five intact samples of the Mount Laurel Formation were calculated to range from 129 to 132.5 pcf. Results of individual tests are shown in Table 2.5.4.2-6. The unit weight was calculated from the dry density and the moisture content determined in the consolidation test and the RCTS test. Design unit weight values are shown on Table 2.5.4.2-8.

Field SPT N-values range from 23 to greater than 100 bpf. N-values greater than 100 bpf were treated as equal to 100 bpf for purposes of averaging. The average SPT N-value for this layer is 91 bpf. The median SPT N-value is 100 bpf. SPT N-values corrected for field procedures, including hammer energy, (N_{60}) for this stratum range from 32 to 160 bpf with an average value of 137 bpf, and a median value of 146 bpf. The design corrected and field N-values are shown on Table 2.5.4.2-8. A histogram of the field N-values for the Mount Laurel Formation is shown in Figure 2.5.4.1-7.

2.5.4.2.2.1.8 Wenonah and Marshalltown Formations

The Wenonah and Marshalltown formations were encountered in five of the borings drilled at the site (EB-1, EB-3, NB-1, NB-2, and NB-8). The top of the Wenonah was encountered in boring EB-8. Due to their similarities, the Wenonah and Marshalltown formations can be considered as one unit for engineering purposes. The top of the Wenonah Formation was encountered at elevations ranging from -250 to -289 ft. NAVD. Based on the borings performed for the ESPA, the Wenonah and Marshalltown formations range in thickness from 39 to 40 ft. The Wenonah and Marshalltown formations were observed to be lithologically similar in the borings. These units lie in conformable relationship to each other and the underlying Englishtown Formation. The Wenonah generally consisted of sandy clay and clayey sand. The Wenonah was distinguished from the overlying Mount Laurel based on changes in color, glauconite content, and lithology, as well as SPT blow counts and reaction to hydrochloric acid. The Marshalltown generally consisted of glauconitic, silty and clayey fine sand. The Marshalltown was distinguished from the overlying Wenonah based on changes in lithology, and by a pronounced natural gamma spike observed in geophysical logs performed in the deep borings NB-1 and EB-3.

Static laboratory indices were determined for six disturbed SPT samples of the Wenonah and Marshalltown formations collected during the ESPA subsurface investigation (Table 2.5.4.2-2, Sheet 14 of 18). Laboratory testing, including sieve analysis with hydrometer, sieve analysis (No. 200 wash), Atterberg limits, specific gravity, and moisture content, were performed to determine the soil index properties of the Wenonah and Marshalltown formations.

Samples of the Wenonah and Marshalltown Formations were generally classified as clayey sands (SC) and, less commonly, silty sand (SM) and clay (CL). The moisture content for tested

**PSEG Site
ESP Application
Part 2, Site Safety Analysis Report**

samples ranges from 21 to 28 percent, with an average of 23 percent, and a median value of 22 percent. The fine-grained component of the Wenonah and Marshalltown formations (silt and clay; minus 200 sieve) ranges from 15 to 51 percent, with an average of 35 percent, and a median value of 39 percent. One of the six samples submitted for Atterberg limits tests indicated no value for the liquid limit and non-plastic for the plastic limit. For the remaining samples, the liquid limit ranges from no value to 42, with an average of 29, and a median value of 30. The plastic limit ranges from non-plastic to 23, with an average of 15, and a median value of 13. The plasticity indices range from non-plastic to 29, with an average of 14, and a median value of 9. The average and median value of the liquid limit test, plastic limit test, and the calculation of the plasticity indices, are calculated from the five tests having a value for the liquid limit and plastic limit tests. A specific gravity test was performed on one sample classified as SC and the specific gravity was determined to be 2.71. The void ratio for this sample was calculated to be 0.73 for 100 percent saturation. Soil index properties for the individual tests are shown in Table 2.5.4.2-2 (Sheet 14 of 18). Design values for index properties are included in Table 2.5.4.2-8.

Field SPT N-values range from 7 to greater than 100 bpf. N-values greater than 100 bpf were treated as equal to 100 bpf for purposes of averaging. The average SPT N-value for this layer is 41 bpf. The median SPT N-value is 37 bpf. SPT N-values corrected for field procedures, including hammer energy, (N_{60}) for this stratum range from 11 to 140 bpf, with an average value of 61 bpf, and a median value of 55 bpf. The design corrected and field N-values are shown on Table 2.5.4.2-8.

The unit weight was not determined for the Wenonah and Marshalltown formations for the ESPA or the HCGS UFSAR. The unit weights of soils for formations below the Mount Laurel were not determined for the ESPA.

2.5.4.2.2.1.9 Englishtown and Woodbury Formations

The Englishtown and Woodbury formations were penetrated in two borings performed for the ESPA investigation (NB-1 and EB-3). The top of the Englishtown was encountered in borings EB-1 and NB-2. Due to their similarities, the Englishtown and Woodbury formations can be considered one unit for engineering purposes. The top of the Englishtown Formation was encountered at elevations ranging from approximately -290 to -319 ft. NAVD. Based on the borings performed for the ESPA, the Englishtown and Woodbury formations were approximately 79 ft. thick at EB-3, and approximately 80 ft. thick at NB-1. The Englishtown and Woodbury formations were also observed to be lithologically similar in the borings. These units lie in conformable relationship to each other and the underlying Merchantville Formation. The Englishtown generally consisted of dark gray to black sandy clay, to clayey sand with shell fragments, grading to black silt and clay, with trace amounts of glauconite and mica. The Englishtown was distinguished from the overlying Marshalltown based on changes in color, occurrence of shell fragments, and increased silt and clay content. The Woodbury generally consisted of black, micaceous, highly plastic clay. The Woodbury was distinguished from the overlying Englishtown based on the increase in clay and mica content. Geophysical logging performed in borings NB-1 and EB-3 indicated a slight decrease in the natural gamma log and a more pronounced increase in the resistivity log at the Englishtown/Woodbury contact.

Static laboratory indices were determined for five SPT samples of the Englishtown and Woodbury formations collected during the ESPA subsurface investigation (Table 2.5.4.2-2, Sheet 15 of 18). Laboratory testing, including sieve analysis (No. 200 wash), Atterberg limits,

**PSEG Site
ESP Application
Part 2, Site Safety Analysis Report**

and moisture content, were performed to determine the soil index properties of the Englishtown and Woodbury formations.

Samples were generally classified as clay (CL, CH), except for one sample which was a clayey sand (SC). The moisture content of tested samples ranges from 25 to 31 percent, with an average and median value of 28 percent. The fine-grained component of the Englishtown and Woodbury formations (silt and clay; minus 200 sieve) ranges from 39 to 94 percent, with an average of 73 percent, and a median value of 79 percent. The liquid limit ranges from 32 to 75, with an average of 53, and a median value of 51. The plastic limit ranges from 16 to 21, with an average of 19, and a median value of 20. The plasticity indices range from 12 to 54, with an average of 34, and a median value of 31. Soil index properties for the individual tests are shown in Table 2.5.4.2-2 (Sheet 15 of 18). Design values for the index properties are included in Table 2.5.4.2-8.

Field SPT N-values range from 10 to greater than 100 bpf. N-values greater than 100 bpf were treated as equal to 100 bpf for purposes of averaging. The average SPT N-value for this layer is 32 bpf. The median SPT N-value is 25. SPT N-values corrected for field procedures, including hammer energy, (N_{60}) for this stratum range from 16 to 140 bpf with an average value of 47 bpf and a median value of 37 bpf. The design corrected and field N-values are shown on Table 2.5.4.2-8.

2.5.4.2.2.1.10 Merchantville Formation

The Merchantville Formation was encountered in two of the borings performed for the ESP investigation (NB-1 and EB-3) and consisted primarily of dark greenish-black glauconitic silts and clays with varying sand content. It was distinguished from the overlying Woodbury Formation by the increase in glauconite content, decrease in plasticity and mica content, and change in color. The top of the Merchantville was encountered at an elevation of approximately -372 ft. NAVD in boring NB-1, and at an elevation of approximately -398 ft. NAVD in boring EB-3. Based on borings performed for the ESPA, the Merchantville was approximately 31 ft. thick at EB-3 and approximately 30 ft. thick at NB-1.

Static laboratory indices were determined for two SPT samples of the Merchantville Formation collected during the ESPA subsurface investigation (Table 2.5.4.2-2, Sheet 16 of 18). Laboratory testing, including sieve analysis (No. 200 wash), Atterberg limits and moisture content, were performed to determine the soil index properties of the Merchantville Formation.

Samples of the Merchantville Formation were generally classified as clay (CL). The moisture content of tested samples ranges from 25 to 31 percent with an average and median value of 28 percent. The percent fines (silt and clay; minus 200 sieve) for one tested sample is 63 percent. The liquid limit ranges from 36 to 43, with an average and median value of 40. The plastic limit ranges from 18 to 21, with an average and median value of 20. The plasticity indices range from 18 to 22, with an average and median value of 20. Soil index properties for the individual tests are shown in Table 2.5.4.2-2, (Sheet 16 of 18). Design values for the index properties are included in Table 2.5.4.2-8.

Field SPT N-values range from 31 to 82 bpf. The average SPT N-value for this layer is 50 bpf. The median SPT N-value is 47. SPT N-values corrected for field procedures, including hammer

**PSEG Site
ESP Application
Part 2, Site Safety Analysis Report**

energy, (N_{60}) for this stratum range from 43 to 131 bpf, with an average value of 76 bpf, and a median value of 71 bpf. The design corrected and field N-values are shown on Table 2.5.4.2-8.

2.5.4.2.2.1.11 Magothy Formation

The Magothy Formation was encountered in two of the borings performed for the ESPA investigation (NB-1 and EB-3) and consists primarily of interbedded gray to dark gray, locally mottled, silts and clays, containing trace amounts of lignite and carbonaceous material. The top of the Magothy Formation was encountered at an elevation of approximately -402 ft. NAVD in boring NB-1, and at an elevation of approximately -429 ft. NAVD in boring EB-3. Based on the borings performed for the ESPA, the Magothy was approximately 55 ft. thick at EB-3, and approximately 52 ft. thick at NB-1. The silts and clays were interbedded with sands containing varying amounts of silt and clay. The interbedding was also indicated by the natural gamma and resistivity signatures on the geophysical logs performed in deep borings NB-1 and EB-3. This formation unconformably overlies the Potomac Formation.

Static laboratory indices were determined for two SPT samples of the Magothy Formation collected during the ESPA subsurface investigation (Table 2.5.4.2-2, Sheet 17 of 18). Laboratory testing, including sieve analysis (No. 200 wash), Atterberg limits, and moisture content, were performed to determine the soil index properties of the Magothy Formation.

Samples of the Magothy Formation were generally classified as clay (CH) and clayey sand (SC). The moisture content of tested samples ranges from 18 to 25 percent, with an average and median value of 21 percent. The percent fines (silt and clay; minus 200 sieve) ranges from 39 to 97 percent. The liquid limit ranges from 30 to 62, with an average and median value of 46. The plastic limit ranges from 14 to 27, with an average and median value of 21. The plasticity indices range from 16 to 35, with an average and median value of 26. Soil index properties for the individual tests are shown in Table 2.5.4.2-2 (Sheet 17 of 18). Design values for the index properties are included in Table 2.5.4.2-8.

Field SPT N-values range from 53 to greater than 100 bpf. N-values greater than 100 bpf were treated as equal to 100 bpf for purposes of averaging. The average SPT N-value for this layer is 85 bpf. The median SPT N-value is 100 bpf. SPT N-values corrected for field procedures, including hammer energy, (N_{60}) for this stratum range from 85 to 140 bpf, with an average value of 121 bpf, and a median value of 140 bpf. The design corrected and field N-values are shown on Table 2.5.4.2-8.

2.5.4.2.2.1.12 Potomac Formation

Soils of the Potomac Formation were encountered in borings NB-1 and EB-3, performed for the ESPA subsurface investigation. The top of the formation was encountered at an elevation of approximately -454 ft. NAVD in boring NB-1, and at an elevation of approximately -484 ft. NAVD in boring EB-3. The Potomac Formation was encountered to the depth of boring termination. The contact between the Potomac Formation and the overlying Magothy was identified from changes in drilling resistance and fluid color, and from the geophysical logs. These showed an increase in the natural gamma log, and a noticeable decrease in the resistivity log. Samples were obtained of the Potomac Formation soils at depths of approximately 600 ft. in boring NB-1, and approximately 630 ft. in boring EB-3. The samples consisted of hard plastic, red, gray, and white mottled clay.

**PSEG Site
ESP Application
Part 2, Site Safety Analysis Report**

Static laboratory indices were determined for three disturbed SPT samples of the Potomac Formation collected during the ESPA subsurface investigation (Table 2.5.4.2-2, Sheet 18 of 18). Laboratory testing, including sieve analysis (No. 200 wash), Atterberg limits, and moisture content, were performed to determine the soil index properties of the Potomac Formation.

Samples of the Potomac Formation were generally classified as clay (CL). The moisture content of tested samples ranges from 15 to 20 percent, with an average and median value of 18 percent. The percent fines (silt and clay; minus 200 sieve) for one sample tested is 96 percent. The liquid limit ranges from 33 to 38, with an average value of 36, and a median value of 37. The plastic limit ranges from 14 to 16, with an average and median value of 15. The plasticity indices range from 18 to 24, with an average and median value of 21. Soil index properties for the individual tests are shown in Table 2.5.4.2-2 (Sheet 18 of 18). Design values for the index properties are included in Table 2.5.4.2-8.

Field SPT N-values range from 79 to greater than 100 bpf. N-values greater than 100 bpf were treated as equal to 100 bpf for purposes of averaging. The average SPT N-value for this layer is 92 bpf. The median SPT N-value is 100. SPT N-values corrected for field procedures, including hammer energy, (N_{60}) for this stratum range from 112 to 140 bpf, with an average value of 131 bpf, and a median value of 140 bpf. The design corrected and field N-values are shown on Table 2.5.4.2-8.

2.5.4.2.2.2 Dynamic Material Properties

Table 2.5.4.2-9 presents the results of the laboratory RCTS tests. While values for shear wave velocity are presented in the table, these values represent small increments within the soil mass. As described in Subsection 2.5.4.1.1.2, the geologic strata are typically dense and contain cemented layers. Samples for RCTS testing from such materials are susceptible to disturbance. Samples used in the RCTS testing device can not include cemented zones or layers in the tested sample effectively, therefore use of in-situ shear wave velocity measurements as described in Subsection 2.5.4.4 is a more appropriate method to obtain the in-situ shear wave velocity for the overall strata. Subsection 2.5.4.7 discusses the selection of shear wave velocity for the site dynamic profile.

The RCTS testing also provides strain dependent variation of shear modulus and damping. These results from the RCTS testing conducted on samples from the Vincentown, Hornerstown and Navesink formations are shown in Figures 2.5.4.2-4 through 2.5.4.2-7. Results are presented as a function of the cyclic shear strain described by the damping ratio and the modulus reduction ratio (G/G_{\max}) (the shear modulus divided by the low strain shear modulus). The data are plotted on depth-dependent modulus reduction and damping ratio curves developed by the Electric Power Research Institute (EPRI) (Reference 2.5.4.2-14). The RCTS data range of shear strains is generally limited to strains less than about 10^{-2} percent and, thus, does not cover the full range of shear strain represented by the EPRI curves. The plotted data are similar to the shape of the EPRI curves within the range of the test strains, but more linear. This is because the presence of the cemented layers within the formations and the dense consistency (Subsections 2.5.4.1.2.2.8, 2.5.4.1.2.3.1, and 2.5.4.1.2.3.2) required use of rotating tube samplers (Pitcher barrel) with potential for causing sample disturbance.

**PSEG Site
ESP Application
Part 2, Site Safety Analysis Report**

RCTS testing was not performed on samples from formations below the Navesink for the ESPA. Computational methods, discussed in Subsection 2.5.4.7, were used to develop design shear modulus reduction and damping characteristics for the dynamic profile. Shear wave velocity measurements were made using in-situ geophysical testing as the primary data collection method. The in-situ testing methods and results are discussed in Subsection 2.5.4.4. Development of the dynamic properties is discussed in detail in Subsection 2.5.4.7.4.

2.5.4.2.3 References

- 2.5.4.2-1 ASTM, 2004a, "Standard Test Methods for Particle-Size Distribution (Gradation) of Soils Using Sieve Analysis," ASTM D 6913 - 04e1, 2004.
- 2.5.4.2-2 ASTM, 2004 b, "Standard Test Method for Consolidated Undrained Triaxial Compression Test for Cohesive Soils," ASTM D 4767-04, 2004.
- 2.5.4.2-3 ASTM, 2004c, "Standard Test Methods for One-Dimensional Consolidation Properties of Soils Using Incremental Loading," ASTM D 2435-04, 2004.
- 2.5.4.2-4 ASTM, 2005a, "Standard Test Methods for Laboratory Determination of Water (Moisture) Content of Soil and Rock by Mass," ASTM D 2216-05, 2005/
- 2.5.4.2-5 ASTM, 2005b, "Standard Test Methods for Liquid Limit, Plastic Limit, and Plasticity Index of Soils," ASTM D 4318-05, 2005.
- 2.5.4.2-6 ASTM, 2006a, "Standard Test Methods for Specific Gravity of Soil Solids by Water Pycnometer," ASTM D 854-06, 2006.
- 2.5.4.2-7 ASTM, 2006b, "Standard Practice for Classification of Soils for Engineering Purposes (Unified Soil Classification System)," ASTM D 2487-06e1, 2006.
- 2.5.4.2-8 ASTM, 2006c, "Standard Practice for Description and Identification of Soils (Visual-Manual Method)," ASTM D 2488-06, 2006.
- 2.5.4.2-9 ASTM, 2007a, "Standard Practices for Preserving and Transporting Soil Samples," ASTM D 4220 - 95(2007), 2007.
- 2.5.4.2-10 ASTM, 2007b, "Standard Test Method for Particle-Size Analysis of Soils," ASTM D 422 - 63(2007), 2007.
- 2.5.4.2-11 ASTM, 2007c – "Standard Test Methods for Moisture, Ash, and Organic Matter of Peat and Other Organic Soils," ASTM D 2974 - 07a, 2007.
- 2.5.4.2-12 ASTM, 2007d, "Standard Test Method for Unconsolidated-Undrained Triaxial Compression Test on Cohesive Soils," ASTM D 2850 - 03a (2007), 2007.
- 2.5.4.2-13 Dames & Moore, Report, Foundation Studies, Proposed Hope Creek Generation Station, Lower Alloways Creek Township, New Jersey, May 23, 1974
- 2.5.4.2-14 Electric Power Research Institute, "Guidelines for Determining Design Basis Ground Motions," Vol. 1, TR-102293, November, 1993.

**PSEG Site
ESP Application
Part 2, Site Safety Analysis Report**

- 2.5.4.2-15 MACTEC Engineering and Consulting, Inc., "Geotechnical Exploration and Testing, PSEG Site Application, Lower Alloways Creek Township, New Jersey," Rev. 0, Jul 10, 2009.
- 2.5.4.2-16 Public Service Enterprise Group (PSEG), "Hope Creek Generating Station Updated Final Safety Analysis Report," Revision 16, Subsection 2.5.4, May 15, 2008.
- 2.5.4.2-17 University of Texas at Austin, "Test Procedures and Calibration Documentation Associated with the RCTS and URC Tests at the University of Texas at Austin," August 4, 2006.
- 2.5.4.2-18 Coduto, Donald P., "Foundation Design Principles and Practices", Second Edition, Prentice Hall, p. 50.
- 2.5.4.2-19 Bowles, Joseph E., "Foundation Analysis and Design", Third Edition, McGraw-Hill Book Company, p.100-101.
- 2.5.4.2-20 US Department of Transportation, Federal Highway Administration, "Soil and Foundations Reference Manual - Volume 1", Publication No. FHWA NHI-06-088, December 2006, p. 5-13.

**PSEG Site
ESP Application
Part 2, Site Safety Analysis Report**

**Table 2.5.4.2-1
Summary of the Type and Number of Laboratory Tests Performed for the PSEG ESP Application**

Type of Test	Standard Test Method	Number of Tests Performed
Natural Moisture Content	ASTM D 2216-05	99
Specific Gravity of Soil Solids by Water Pycnometer	ASTM D 854-06	23
Particle-Size Distribution (Gradation) of Soils Using Sieve Analysis (for analysis not including hydrometer)	ASTM D 6913-04e1	46
Particle-Size Analysis of Soils	ASTM D 422-63-07	66
Liquid Limit, Plastic Limit, and Plasticity Index of Soils	ASTM D 4318-05	88
Unconsolidated-Undrained Triaxial Compression Test on Cohesive Soils	ASTM D 2850-03a (2007)	2
Consolidated-Undrained Triaxial Compression Test on Cohesive Soils	ASTM D 4767-04	4
One-Dimensional Consolidation Properties of Soils using Incremental Loading	ASTM D 2435-04	6
Resonant Column Torsional Shear	Test Procedures and Calibration Documentation Associated with the RCTS and URC Tests at the University of Texas at Austin, 2006	6
References: 2.5.4.2-1, 2.5.4.2-2, 2.5.4.2-3, 2.5.4.2-4, 2.5.4.2-5, 2.5.4.2-6, 2.5.4.2-10, 2.5.4.2-12, and 2.5.4.2-17		

**PSEG Site
ESP Application
Part 2, Site Safety Analysis Report**

**Table 2.5.4.2-2 (Sheet 1 of 18)
Summary of Static Indices Laboratory Analysis
for Hydraulic Fill Data from ESPA Investigation^(d)**

Boring Number	Sample Number	Sample Depth (ft.)	USCS Classification	Gravel^{(b)(f)} (%)	Sand^{(b)(f)} (%)	Fines^(b) (%)	Silt^(b) (%)	Clay^{(b)(f)} (%)	Natural Moisture^(b) (%)	LL^{(b)(e)}	PL^{(b)(e)}	PI^{(b)(e)}	G_s^(e)	Void Ratio^(c)	Stratum
NB-2	SS-5	19.9 – 21.4	CH	0	5	95	--	--	61	58	28	30	--	--	Hydraulic Fill
NB-3	SS-6	11.8 – 13.3	CH	0	24	76	--	--	98	69	31	38	--	--	Hydraulic Fill
NB-5	SS-7	15.0 – 16.5	MH	0	1	99	--	--	94	72	35	37	--	--	Hydraulic Fill
NB-8	SS-6	12.2 – 13.7	SC-SM	0	50	50	37	13	--	18	12	6	2.68	--	Hydraulic Fill
EB-1	SS-9	25.0 – 26.5	CH ^(a)	--	--	--	--	--	83	57	14	43	--	--	Hydraulic Fill
EB-2	SS-8	20.0 – 21.5	MH	0	2	98	--	--	72	85	41	44	--	--	Hydraulic Fill
EB-7	SS-6	12.5 – 14.0	CL	0	29	72	30	42	--	43	24	19	--	--	Hydraulic Fill
EB-8	SS-7A	14.8 – 15.4	CH	0	37	63	--	--	71	51	25	26	--	--	Hydraulic Fill
EB-8	SS-9	25.2 – 26.7	ML	0	12	88	--	--	71	49	30	19	--	--	Hydraulic Fill
NB-1UD	UD-3	19.6 – 21.6	MH ^(a)	--	--	--	--	--	81	97	44	53	--	--	Hydraulic Fill
NB-3	SS-9B	25.6-26.6	SM ^(a)	0	85	15	--	--	--	--	--	--	--	--	Hydraulic Fill

- a) Classification is based on quantitative and qualitative (visual inspection) information.
b) Test Results are rounded to the nearest percent.
c) Calculated value not reported in Reference (calculation assumes 100% saturation).
d) "--" Information not available
e) LL= Liquid Limit; PL= Plastic Limit; PI = Plasticity Index; G_s = Specific Gravity
f) Size Ranges: Gravel >2mm; 2mm>Sand>.074mm; .074mm>Silt>.005mm; >.005mm-Clay

Reference: 2.5.4.2-15

**PSEG Site
ESP Application
Part 2, Site Safety Analysis Report**

**Table 2.5.4.2-2 (Sheet 2 of 18)
Summary of Static Indices Laboratory Analysis
for Hydraulic Fill Data from the Hope Creek Generating Station UFSAR^(d)**

Boring Number	Sample Number	Sample Depth (ft.)	USCS Classification ^(a)	Gravel ^{(b)(f)} (%)	Sand ^{(b)(f)} (%)	Fines ^(b) (%)	Silt ^{(b)(f)} (%)	Clay ^{(b)(f)} (%)	Natural Moisture (%)	LL ^{(b)(e)}	PL ^{(b)(e)}	PI ^{(b)(e)}	G _s ^(e)	Void Ratio ^(c)	Stratum
211	1	5	--	--	--	--	--	--	54	73	--	26	--	--	Hydraulic Fill
211	4	20	--	--	--	--	--	--	58	61	--	23	--	--	Hydraulic Fill
216	1A	5	--	--	--	--	--	--	45	30	--	11	--	--	Hydraulic Fill
216	4	25	--	--	--	--	--	--	68	75	--	36	--	--	Hydraulic Fill
217	2	11	--	--	--	--	--	--	32	--	--	--	--	--	Hydraulic Fill
217	5	25	--	--	--	--	--	--	65	91	--	48	--	--	Hydraulic Fill
222	2	10	--	--	--	--	--	--	80	94	--	48	--	--	Hydraulic Fill
229	2	10	--	--	--	--	--	--	20	29	--	10	--	--	Hydraulic Fill
229	7	30	--	--	--	--	--	--	66	80	--	40	--	--	Hydraulic Fill
232	6A	25	--	--	--	--	--	--	52	69	--	38	--	--	Hydraulic Fill
232	6	28	--	--	--	--	--	--	--	--	--	--	2.58	--	Hydraulic Fill
238	1	5	--	--	--	--	--	--	63	90	--	37	--	--	Hydraulic Fill
238	5	20	--	--	--	--	--	--	64	73	--	30	--	--	Hydraulic Fill
239	1	6	--	--	--	--	--	--	20	--	--	--	--	--	Hydraulic Fill
239	7	35	--	--	--	--	--	--	54	52	--	13	--	--	Hydraulic Fill
253	6	25	--	--	--	--	--	--	76	89	--	43	--	--	Hydraulic Fill
253	2	20	--	--	--	--	--	--	--	--	--	--	2.6	--	Hydraulic Fill
AB-1	10	30	--	--	--	--	--	--	64	93	--	58	2.5	1.6	Hydraulic Fill
AB-1A	7	19	--	--	--	--	--	--	52	51	--	29	--	--	Hydraulic Fill
AB-2	8	19	--	--	--	--	--	--	64	74	--	45	2.58	1.65	Hydraulic Fill
AB-3	6	15	--	--	--	--	--	--	40	43	--	17	2.65	1.06	Hydraulic Fill
AB-4	2	5	--	--	--	--	--	--	54	70	--	41	2.69	--	Hydraulic Fill
AB-4	5	13	--	--	--	--	--	--	68	72	--	40	2.54	1.73	Hydraulic Fill
AB-5	3	6	--	--	--	--	--	--	64	66	--	37	2.54	--	Hydraulic Fill
AB-5	7	16	--	--	--	--	--	--	43	63	--	34	--	--	Hydraulic Fill
AB-5	14	33	--	--	--	--	--	--	69	79	--	47	2.58	1.78	Hydraulic Fill

a) Classification is based on quantitative and qualitative (visual inspection) information.

b) (Test Results are rounded to the nearest percent.

c) Calculated value not reported in Reference (calculation assumes 100% saturation).

d) "--" Information not available

e) LL= Liquid Limit; PL= Plastic Limit; PI = Plasticity Index; G_s = Specific Gravity

f) Size Ranges: Gravel >2mm; 2mm>Sand>.074mm; .074mm>Silt>.005mm; >.005mm-Clay

Reference: 2.5.4.1-10

**PSEG Site
ESP Application
Part 2, Site Safety Analysis Report**

**Table 2.5.4.2-2 (Sheet 3 of 18)
Summary of Static Indices Laboratory Analysis
for Alluvium Data from the Hope Creek Generating Station UFSAR^(d)**

Boring Number	Sample Number	Sample Depth (ft.)	USCS Classification ^(a)	Gravel ^{(b)(f)} (%)	Sand ^{(b)(f)} (%)	Fines ^(b) (%)	Silt ^{(b)(f)} (%)	Clay ^{(b)(f)} (%)	Natural Moisture ^(b) (%)	LL ^{(b)(e)}	PL ^{(b)(e)}	PI ^{(b)(e)}	G _s ^(e)	Void Ratio ^(c)	Stratum
217	7	35.5	--	--	--	--	--	--	12.3	--	--	--	--	--	Alluvium
228	11A	50	--	--	--	--	--	--	19.8	--	--	--	--	--	Alluvium
AB-1	12	35	--	--	--	--	--	--	18	--	--	--	--	--	Alluvium
	13	35	--	--	--	--	--	--	23	--	--	--	2.64	0.61	Alluvium
AB-1A	11	34	--	--	--	--	--	--	19	--	--	--	--	--	Alluvium
	12	38	--	--	--	--	--	--	20	--	--	--	--	--	Alluvium
AB-2	14	34	--	--	--	--	--	--	18	--	--	--	2.67	0.48	Alluvium
AB-3A	7	36	--	--	--	--	--	--	20	--	--	--	--	--	Alluvium

- a) Classification is based on quantitative and qualitative (visual inspection) information.
b) Test Results are rounded to the nearest percent.
c) Calculated value not reported in Reference (calculation assumes 100% saturation).
d) "--" Information not available
e) LL= Liquid Limit; PL= Plastic Limit; PI = Plasticity Index; G_s = Specific Gravity
f) Size Ranges: Gravel >2mm; 2mm>Sand>.074mm; .074mm>Silt>.005mm; >.005mm-Clay

References: 2.5.4.1-10 and 2.5.4.2-15

**PSEG Site
ESP Application
Part 2, Site Safety Analysis Report**

**Table 2.5.4.2-2 (Sheet 4 of 18)
Summary of Static Indices Laboratory Analysis
for Alluvium Data from the ESPA Investigation^(d)**

Boring Number	Sample Number	Sample Depth (ft.)	USCS Classification	Gravel^{(b)(f)} (%)	Sand^{(b)(f)} (%)	Fines^(b) (%)	Silt^{(b)(f)} (%)	Clay^{(b)(f)} (%)	Natural Moisture^(b) (%)	LL^{(b)(e)}	PL^{(b)(e)}	PI^{(b)(e)}	G_s^(e)	Void Ratio^(c)	Stratum
NB-3	SS-13	44.7 – 46.2	ML ^(a)	0	50	50	--	--	--	--	--	--	--	--	Alluvium
NB-5	SS-12	39.5 – 41.0	SP-SM ^(a)	37	52	11	--	--	--	--	--	--	--	--	Alluvium
EB-1	SS-13	45.0 – 46.5	SP ^(a)	1	95	4	--	--	--	--	--	--	--	--	Alluvium
EB-3	SS-12	40.0 – 41.5	SP-SM ^(a)	29	65	6	--	--	--	--	--	--	--	--	Alluvium
EB-3	SS-14	50.0 – 51.5	CL	0	20	80	--	--	41	40	24	16	--	--	Alluvium
EB-7	SS-13	45.0 – 46.5	SP-SM ^(a)	4	90	6	--	--	14	--	--	--	--	--	Alluvium
EB-7	SS-14	50.0 – 51.5	SP-SM ^(a)	25	65	10	--	--	--	--	--	--	--	--	Alluvium

- a) Classification is based on quantitative and qualitative (visual inspection) information.
b) Test Results are rounded to the nearest percent.
c) Calculated value not reported in Reference (calculation assumes 100% saturation).
d) "--" Information not available
e) LL= Liquid Limit; PL= Plastic Limit; PI = Plasticity Index; G_s = Specific Gravity
f) Size Ranges: Gravel >2mm; 2mm>Sand>.074mm; .074mm>Silt>.005mm; >.005mm-Clay

References: 2.5.4.1-10 and 2.5.4.2-15

**PSEG Site
ESP Application
Part 2, Site Safety Analysis Report**

**Table 2.5.4.2-2 (Sheet 5 of 18)
Summary of Static Indices Laboratory Analysis
for Upper (fine-grained) Kirkwood Formation Data from the Hope Creek Generating Station UFSAR^(d)**

Boring Number	Sample Number	Sample Depth (ft.)	USCS Classification ^(a)	Gravel ^{(b)(f)} (%)	Sand ^{(b)(f)} (%)	Fines ^(b) (%)	Silt ^{(b)(f)} (%)	Clay ^{(b)(f)} (%)	Natural Moisture ^(b) (%)	LL ^{(b)(e)}	PL ^{(b)(e)}	PI ^{(b)(e)}	G _s ^(e)	Void Ratio ^(c)	Formation
AB-1	14	40	CH	--	--	--	--	--	36	57	--	36	2.66	0.95	Kirkwood
AB-1	15	42	CH	--	--	--	--	--	46	60	--	35	2.73	1.26	Kirkwood
AB-1	21	57	CH-MH	--	--	--	--	--	51	66	--	34	2.63	1.34	Kirkwood
AB-1	24	65	CH	--	--	--	--	--	42	58	--	29	--	--	Kirkwood
AB-1A	18	68	MH or OH	--	--	--	--	--	60	71	--	35	--	--	Kirkwood
AB-2	15	37	CH	--	--	--	--	--	35	53	--	32	2.61	0.91	Kirkwood
AB-2	16	39	CH	--	--	--	--	--	52	55	--	30	2.63	1.37	Kirkwood
AB-2	24	59	MH	--	--	--	--	--	58	66	--	31	--	--	Kirkwood
AB-2	27	67	ML or OL	--	--	--	--	--	--	45	--	16	--	--	Kirkwood
AB-2A	8	35	CL	--	--	--	--	--	22	37	--	20	--	--	Kirkwood
AB-2A	9	41	CL	--	--	--	--	--	42	42	--	20	--	--	Kirkwood
AB-2A	13	61	MH or OH	--	--	--	--	--	50	53	--	19	--	--	Kirkwood
AB-3	17	43	CH	--	--	--	--	--	58	81	--	50	2.62	1.52	Kirkwood
AB-3	22	55	MH or OH	--	--	--	--	--	52	58	--	26	2.67	1.39	Kirkwood
AB-3	25	63	MH or OH	--	--	--	--	--	51	63	--	28	--	--	Kirkwood
AB-3A	13	65	MH or OH	--	--	--	--	--	42	55	--	18	--	--	Kirkwood

- a) Classification is based on quantitative and qualitative (visual inspection) information.
b) Test Results are rounded to the nearest percent.
c) Calculated value not reported in Reference (calculation assumes 100% saturation).
d) "--" Information not available
e) LL= Liquid Limit; PL= Plastic Limit; PI = Plasticity Index; G_s = Specific Gravity
f) Size Ranges: Gravel >2mm; 2mm>Sand>.074mm; .074mm>Silt>.005mm; >.005mm-Clay

References: 2.5.4.1-10 and 2.5.4.2-15

**PSEG Site
ESP Application
Part 2, Site Safety Analysis Report**

**Table 2.5.4.2-2 (Sheet 6 of 18)
Summary of Static Indices Laboratory Analysis
for Upper (fine-grained) Kirkwood Formation Data from the ESPA Investigation^(d)**

Boring Number	Sample Number	Sample Depth (ft.)	USCS Classification	Gravel^{(b)(f)} (%)	Sand^{(b)(f)} (%)	Fines^(b) (%)	Silt^{(b)(f)} (%)	Clay^{(b)(f)} (%)	Natural Moisture^(b) (%)	LL^{(b)(e)}	PL^{(b)(e)}	PI^{(b)(e)}	G_s^(e)	Void Ratio^(c)	Formation
EB-1	SS-23	90.0 – 91.0	CH ^(a)	--	--	--	--	--	31	63	31	32	--	--	Kirkwood
EB-2	SS-18	70.0 – 71.5	CL	0	39	61	--	--	40	48	25	23	--	--	Kirkwood
EB-3	SS-20	80.0 – 81.5	CH	0	20	80	--	--	77.	53	16	37	--	--	Kirkwood
NB-1UD	UD-8 UU	55.8 – 57.8	CL	1	48	51	--	--	29	27	16	11	--	--	Kirkwood
NB-1UD	UD-8	55.8 – 57.8	MH ^(a)	--	--	--	--	--	50	52	34	18	--	--	Kirkwood
NB-3	SS-15	54.6-56.1	CH	0	6	94	--	--	55	54	25	29	--	--	Kirkwood

- a) Classification is based on quantitative and qualitative (visual inspection) information.
b) Test Results are rounded to the nearest percent.
c) Calculated value not reported in Reference (calculation assumes 100% saturation).
d) "--" Information not available
e) LL= Liquid Limit; PL= Plastic Limit; PI = Plasticity Index; G_s = Specific Gravity
f) Size Ranges: Gravel >2mm; 2mm>Sand>.074mm; .074mm>Silt>.005mm; >.005mm-Clay

References: 2.5.4.1-10 and 2.5.4.2-15

**PSEG Site
ESP Application
Part 2, Site Safety Analysis Report**

**Table 2.5.4.2-2 (Sheet 7 of 18)
Summary of Static Indices Laboratory Analysis
for Lower (coarse-grained) Kirkwood Formation Data from the Hope Creek Generating Station UFSAR^(d)**

Boring Number	Sample Number	Sample Depth (ft.)	USCS Classification ^(a)	Gravel ^{(b)(f)} (%)	Sand ^{(b)(f)} (%)	Fines ^(b) (%)	Silt ^{(b)(f)} (%)	Clay ^{(b)(f)} (%)	Natural Moisture ^(b) (%)	LL ^{(b)(e)}	PL ^{(b)(e)}	PI ^{(b)(e)}	G _s ^(e)	Void Ratio ^(c)	Formation
206	10A	60.4	--	--	--	15	--	--	26	--	--	--	--	--	Kirkwood
211	8A	65.5	--	--	--	52	--	--	26	--	--	--	--	--	Kirkwood
214	8A	57.0	--	--	--	30	--	--	37	--	--	--	--	--	Kirkwood
217	10	50.5	--	--	--	57	--	--	24	--	--	--	--	--	Kirkwood
228	14	65.0	--	--	--	24	--	--	30	--	--	--	--	--	Kirkwood
231	10	50	--	--	--	5	--	--	26	--	--	--	--	--	Kirkwood
238	11	50	--	--	--	----	--	--	18	24.1	21.3	2.8	--	--	Kirkwood
242	12	60	--	--	--	83	--	--	27	--	--	--	--	--	Kirkwood
249	10C	46	--	--	--	19	--	--	15	--	--	--	--	--	Kirkwood
AB-1	26	70	--	--	--	----	--	--	18	--	--	--	--	--	Kirkwood
AB-2	28	69	--	--	--	----	--	--	20	--	--	--	2.63	0.53	Kirkwood
AB-3	26	65	--	--	--	----	--	--	38	--	--	--	2.57	0.98	Kirkwood
AB-4	23	57	--	--	--	----	--	--	26	--	--	--	--	--	Kirkwood
AB-5	20	48	--	--	--	----	--	--	27	--	--	--	2.70	0.73	Kirkwood

- a) Classification is based on quantitative and qualitative (visual inspection) information.
b) Test Results are rounded to the nearest percent.
c) Calculated value not reported in Reference (calculation assumes 100% saturation).
d) "--" Information not available
e) LL= Liquid Limit; PL= Plastic Limit; PI = Plasticity Index; G_s = Specific Gravity
f) Size Ranges: Gravel >2mm; 2mm>Sand>.074mm; .074mm>Silt>.005mm; >.005mm-Clay

References: 2.5.4.1-10 and 2.5.4.2-15

**PSEG Site
ESP Application
Part 2, Site Safety Analysis Report**

**Table 2.5.4.2-2 (Sheet 8 of 18)
Summary of Static Indices Laboratory Analysis
for Lower (coarse-grained) Kirkwood Formation Data from the ESPA Investigation^(d)**

Boring Number	Sample Number	Sample Depth(ft.)	USCS Classification	Gravel^{(b)(f)} (%)	Sand^{(b)(f)} (%)	Fines^(b) (%)	Silt^{(b)(f)} (%)	Clay^{(b)(f)} (%)	Natural Moisture^(b) (%)	LL^{(b)(e)}	PL^{(b)(e)}	PI^{(b)(e)}	G_s^(e)	Void Ratio^(c)	Formation
NB-2	SS-15	70.0 – 71.5	SM ^(a)	0	86	14	--	--	21	--	--	--	--	--	Kirkwood
EB-2	SS-24	100.0 – 101.5	SP-SM ^(a)	24	70	6	--	--	--	--	--	--	--	--	Kirkwood
EB-3	SS-23	95.0 – 96.5	SP-SM ^(a)	1	92	7	--	--	--	--	--	--	--	--	Kirkwood
EB-3	SS-24	100.0 – 101.5	SP-SM ^(a)	0	91	9	--	--	--	--	--	--	--	--	Kirkwood
EB-7	SS-19	75.0 – 76.5	SC-SM	0	66	34	27	7	--	23	19	4	--	--	Kirkwood
EB-8	SS-14	50.8 – 52.3	SC	0	70	30	--	--	16	66	30	36	--	--	Kirkwood
EB-1	SS-17	65.0-66.5	SP ^(a)	0	96	4	--	--	--	--	--	--	--	--	Kirkwood

- a) Classification is based on quantitative and qualitative (visual inspection) information.
b) Test Results are rounded to the nearest percent.
c) Calculated value not reported in Reference (calculation assumes 100% saturation).
d) "--" Information not available
e) LL= Liquid Limit; PL= Plastic Limit; PI = Plasticity Index; G_s = Specific Gravity
f) Size Ranges: Gravel >2mm; 2mm>Sand>.074mm; .074mm>Silt>.005mm; >.005mm-Clay

References: 2.5.4.1-10 and 2.5.4.2-15

**PSEG Site
ESP Application
Part 2, Site Safety Analysis Report**

**Table 2.5.4.2-2 (Sheet 9 of 18)
Summary of Static Indices Laboratory Analysis
for the Vincentown Formation and Hornerstown Formation Data from ESPA Investigation (MACTEC, 2009)^(d)**

Boring Number	Sample Number	Sample Depth (ft.)	USCS Classification	Gravel ^{(b)(f)} (%)	Sand ^{(b)(f)} (%)	Fines ^(b) (%)	Silt ^{(b)(f)} (%)	Clay ^{(b)(f)} (%)	Natural Moisture ^(b) (%)	LL ^{(b)(e)}	PL ^{(b)(e)}	PI ^{(b)(e)}	G _s ^(e)	Void Ratio ^(c)	Formation
NB-1	SS-21	85.0 – 86.5	SM	0	85	15	7	9		NV	NP	NP	2.71	--	Vincentown
NB-1	SS-23	95.0 – 96.5	SC-SM	0	76	24	17	7	35	25	20	5		--	Vincentown
NB-1	SS-26	110.0 – 111.5	SC-SM	0	77	23	13	10	--	24	17	7	2.70	--	Vincentown
NB-2	SS-19	90.1 – 91.6	SM ^(a)	0	73	27	12	15	--	--	--	--	--	--	Vincentown
NB-3	SS-18	69.6 – 71.1	SM ^(a)	0	79	21	15	6	40	--	--	--	--	--	Vincentown
NB-3	SS-24	99.6 – 101.1	SM ^(a)	0	70	31	7	24	35	--	--	--	--	--	Vincentown
NB-4	SS-27	70.0 – 71.5	SM ^(a)	0	65	35	28	7	38	--	--	--	--	--	Vincentown
NB-4	SS-38	100.0 – 101.5	SP-SM ^(a)	0	88	12	--	--	30	--	--	--	--	--	Vincentown
NB-4	SS-45	120.0 – 121.5	SM ^(a)	0	81	19	--	--	32	--	--	--	--	--	Vincentown
NB-5	SS-20	79.5 – 81.0	SM ^(a)	0	76	24	6	18	28	--	--	--	--	--	Vincentown
NB-7	SS-21	85.2 – 86.7	SM ^(a)	0	84	17	5	12	9	--	--	--	--	--	Vincentown
NB-8	SS-17	64.5 – 66.0	SM ^(a)	0	80	20	--	--	--				2.61	--	Vincentown
NB-8	SS-21	84.5 – 86.0	SC	0	67	33	10	23	--	24	16	8	--	--	Vincentown
NB-8	SS-23	94.5 – 96.0	SM ^(a)	0	74	26	--	--	28	--	--	--	2.72	0.76	Vincentown
NB-8	SS-27	114.5 – 116.0	SC-SM	0	75	25	12	13	32	25	19	6	--	--	Vincentown
EB-1	SS-27	109.8 – 111.3	MH ^(a)	0	4	97	53	44	21	--	--	--	--	--	Vincentown
EB-2	SS-25	105.0 – 106.1	SM ^(a)	23	58	19	--	--	--	--	--	--	--	--	Vincentown
EB-2	SS-30	129.8 – 131.3	SC ^(a)	0	80	20	6	13	--	--	--	--	--	--	Vincentown
EB-3	SS-27	115.0 – 116.5	SM ^(a)	0	66	34	18	16	28	--	--	--	--	--	Vincentown
EB-3	SS-32	139.6 – 140.8	SM ^(a)	0	71	29	12	17	30	--	--	--	--	--	Vincentown
EB-7	SS-23	95.0 – 96.5	SM ^(a)	0	81	19	--	--	31	--	--	--	2.70	0.84	Vincentown
EB-7	SS-24	100.0 – 100.7	CL	0	17	83	58	25	--	30	18	12	--	--	Vincentown

- a) Classification is based on quantitative and qualitative (visual inspection) information.
b) Test Results are rounded to the nearest percent.
c) Calculated value not reported in Reference (calculation assumes 100% saturation).
d) "--" Information not available
e) LL= Liquid Limit; PL= Plastic Limit; PI = Plasticity Index; G_s = Specific Gravity
f) Size Ranges: Gravel >2mm; 2mm>Sand>.074mm; .074mm>Silt>.005mm; >.005mm-Clay

Reference: 2.5.4.2-15

**PSEG Site
ESP Application
Part 2, Site Safety Analysis Report**

**Table 2.5.4.2-2 (Sheet 10 of 18)
Summary of Static Indices Laboratory Analysis
for the Vincentown Formation and Hornerstown Formation Data from ESPA Investigation^(d)**

Boring Number	Sample Number	Sample Depth (ft.)	USCS Classification	Gravel ^{(b)(f)} (%)	Sand ^{(b)(f)} (%)	Fines ^(b) (%)	Silt ^{(b)(f)} (%)	Clay ^{(b)(f)} (%)	Natural Moisture ^(b) (%)	LL ^{(b)(e)}	PL ^{(b)(e)}	PI ^{(b)(e)}	G _s ^(e)	Void Ratio ^(c)	Formation
EB-7	SS-25	105.0 – 106.5	SM	1	77	23	6	16	--	23	21	2		--	Vincentown
EB-7	SS-32	140.0 – 141.1	SC	0	64	36	17	19	--	22	14	8	2.75	--	Vincentown
EB-8	SS-16	60.0 – 61.5	ML	0	50	50	--	--	--	NV	NP	NP	--	--	Vincentown
EB-8	SS-18	69.5 – 71.0	SM ^(a)	0	78	22	--	--	--	--	--	--	--	--	Vincentown
EB-8	SS-22	90.0 – 91.5	SM ^(a)	0	79	21	--	--	--	--	--	--	--	--	Vincentown
EB-8	SS-29	125.1 – 126.6	SM ^(a)	0	70	30	--	--	36	--	--	--	--	--	Vincentown
NB-1UD	UD-13	75.0 – 77.5	SM ^(a)	--	--	--	--	--	23	NV	NP	NP	--	--	Vincentown
NB-1UD	UD-17	88.6 – 91.1	SM	0	82	18	11	7	32	NV	NP	NP	2.69	0.86	Vincentown
NB-1UD	UD-21	104.3 – 106.5	SM	0	80	21	13	8	26	NV	NP	NP	2.67	0.69	Vincentown
EB-3UD	UD-15	113.8 – 116.3	SM	0	78	22	14	8	32	NV	NP	NP	2.68	0.86	Vincentown
EB-3UD	UD-18	127.1 – 129.6	SM ^(a)	--	--	--	--	--	38	NV	NP	NP		--	Vincentown
NB-1	SS-28	120.0 – 120.8	SM	0	78	22	15	7	20	19	16	3	2.74	0.55	Hornerstown
NB-2	SS-25	120.0 – 121.5	SM ^(a)	0	83	17	3	14	27	--	--	--	--	--	Hornerstown
NB-3	SS-28	114.6 – 116.1	SM	0	86	13	2	12	28	20	NP	NP	--	--	Hornerstown
NB-3	SS-30	124.6 – 126.1	SM	0	80	20	7	13	33	25	24	1	--	--	Hornerstown
NB-5	SS-27	114.5 – 116.0	SM ^(a)	0	74	26	12	15	35	--	--	--	--	--	Hornerstown
NB-5	SS-30	129.5 – 131.0	SM	0	87	13	2	11	29	NV	NP	NP	--	--	Hornerstown
NB-8	SS-31	134.5 – 136.0	SM	0	76	24	8	17	30	22	19	3	2.71	0.81	Hornerstown
EB-1	SS-36	155.1 – 156.6	SM ^(a)	0	65	36	17	19	25	--	--	--	--	--	Hornerstown
EB-2	SS-35	155.0 – 156.5	SM ^(a)	0	75	25	10	15	--	--	--	--	--	--	Hornerstown
EB-3	SS-34	149.6 – 151.1	SC	0	66	34	20	15	34	33	22	11	--	--	Hornerstown
EB-7	SS-35	155.0 – 156.5	SM	0	68	33	15	18	39	32	27	5	2.73	1.06	Hornerstown
EB-8	SS-36	160.0 – 161.5	SC ^(a)	1	65	34	15	18	34	--	--	--	--	--	Hornerstown
NB-1UD	UD-24	121.5 – 124.0	SP-SM	1	91	9	3	6	28	NV	NP	NP	2.65	0.74	Hornerstown
NB-1UD	UD-25	125.6 – 128.1	SM ^(a)	--	--	--	--	--	29	36	26	10	--	--	Hornerstown

- a) Classification is based on quantitative and qualitative (visual inspection) information.
b) Test Results are rounded to the nearest percent.
c) Calculated value not reported in Reference (calculation assumes 100% saturation).
d) "--" Information not available
e) LL= Liquid Limit; PL= Plastic Limit; PI = Plasticity Index; G_s = Specific Gravity
f) Size Ranges: Gravel >2mm; 2mm>Sand>.074mm; .074mm>Silt>.005mm; >.005mm-Clay

**PSEG Site
ESP Application
Part 2, Site Safety Analysis Report**

**Table 2.5.4.2-2 (Sheet 11 of 18)
Summary of Static Indices Laboratory Analysis
for Vincentown Sands Data from the Hope Creek Generating Station UFSAR^(d)**

Boring Number	Sample Number	Sample Depth (ft.)	USCS Classification ^(a)	Gravel ^{(b)(f)} (%)	Sand ^{(b)(f)} (%)	Fines ^(b) (%)	Silt ^{(b)(f)} (%)	Clay ^{(b)(f)} (%)	Natural Moisture ^(b) (%)	LL ^{(b)(e)}	PL ^{(b)(e)}	PI ^{(b)(e)}	G _s ^(e)	Void Ratio ^(c)	Formation
201	18	100.0	--	--	--	--	--	--	30	--	--	--	--	--	Vincentown
201	19A	110.0	--	--	--	--	--	--	42	--	--	--	--	--	Vincentown
211	11A	80.5	--	--	--	--	--	--	30	--	--	--	--	--	Vincentown
214	10A	65.6	--	--	--	--	--	--	26	--	--	--	--	--	Vincentown
216	14A	75.5	--	--	--	--	--	--	35	--	--	--	--	--	Vincentown
216	14B	76.1	--	--	--	--	--	--	30	--	--	--	--	--	Vincentown
225	10D	57.5	--	--	--	--	--	--	21	--	--	--	--	--	Vincentown
225	11A-B	59.4	--	--	--	--	--	--	35	--	--	--	--	--	Vincentown
225	11A-C	59.9	--	--	--	--	--	--	22	--	--	--	--	--	Vincentown
231	12	60.0	--	--	--	--	--	--	32	--	--	--	--	--	Vincentown
238	17	75.5	--	--	--	--	--	--	--	--	--	--	2.64	--	Vincentown
239	14	70.5	--	--	--	--	--	--	35	--	--	--	--	--	Vincentown
239	15	75.5	--	--	--	--	--	--	--	--	--	--	2.68	--	Vincentown
239	16	80.5	--	--	--	--	--	--	31	--	--	--	--	--	Vincentown
220	14	70.5	--	--	--	--	--	--	--	--	--	--	2.66	--	Vincentown
220	16	80.0	--	--	--	--	--	--	--	--	--	--	2.67	--	Vincentown
220	20	120.0	--	--	--	--	--	--	--	--	--	--	2.60	--	Vincentown
257	13	65.5	--	--	--	--	--	--	--	--	--	--	2.69	--	Vincentown
257	17	85.0	--	--	--	--	--	--	--	--	--	--	2.68	--	Vincentown
257	20	100.0	--	--	--	--	--	--	--	--	--	--	2.70	--	Vincentown
259	14	65.0	--	--	--	--	--	--	--	--	--	--	2.67	--	Vincentown
275	33	91.0	--	--	--	--	--	--	25	44	--	15	2.68	0.67	Vincentown
275	44	113.4	--	--	--	--	--	--	27	47	--	20	2.72	0.73	Vincentown
277	16C	98.0	--	--	--	--	--	--	31	27	--	6	--	--	Vincentown
277	16E	98.5	--	--	--	--	--	--	32	33	--	6	2.73	0.88	Vincentown
277	25C	116.0	--	--	--	--	--	--	27	37	--	10	2.70	0.72	Vincentown
277	26C	118.5	--	--	--	--	--	--	28	27	--	11	2.721	0.76	Vincentown

- a) Classification is based on quantitative and qualitative (visual inspection) information.
b) Test Results are rounded to the nearest percent.
c) Calculated value not reported in Reference (calculation assumes 100% saturation).
d) "--" Information not available
e) LL= Liquid Limit; PL= Plastic Limit; PI = Plasticity Index; G_s = Specific Gravity
f) Size Ranges: Gravel >2mm; 2mm>Sand>.074mm; .074mm>Silt>.005mm; >.005mm-Clay
Reference: 2.5.4.1-10

**PSEG Site
ESP Application
Part 2, Site Safety Analysis Report**

**Table 2.5.4.2-2 (Sheet 12 of 18)
Summary of Static Indices Laboratory Analysis
for the Navesink Formation Data from ESPA Investigation^(d)**

Boring Number	Sample Number	Sample Depth (ft.)	USCS Classification	Gravel^{(b)(f)} (%)	Sand^{(b)(f)} (%)	Fines^(b) (%)	Silt^{(b)(f)} (%)	Clay^{(b)(f)} (%)	Natural Moisture^(b) (%)	LL^{(b)(e)}	PL^{(b)(e)}	PI^{(b)(e)}	G_s^(e)	Void Ratio^(c)	Formation
NB-1	SS-33	145.0 – 146.5	SM	4	81	16	8	8	21	NV	NP	NP	2.70	0.57	Navesink
NB-3	SS-34	144.6 – 146.1	SC	0	61	40	16	24	23	37	14	23	--	--	Navesink
NB-5	SS-33	144.5 – 146.0	SC	0	69	31	10	21	15	31	13	18	--	--	Navesink
NB-8	SS-35	154.5 – 156.0	SC-SM	4	77	19	8	10	19	22	16	6	2.73	0.52	Navesink
NB-8	SS-37	164.5 – 166.0	SC	1	74	25	11	14	21	26	17	9	2.71	0.57	Navesink
EB-1	SS-40	175.0 – 176.5	SC-SM	1	86	13	2	12	36	22	18	4	--	--	Navesink
EB-3	SS-40	179.6 – 181.1	SM	0	77	23	13	10	19	NV	NP	NP	--	--	Navesink
EB-7	SS-39	175.0 – 176.5	SC-SM	0	85	15	6	9	24	21	17	4	--	--	Navesink
NB-1UD	UD-27	140.0 – 142.5	SM	3	79	19	6	12	23	NV	NP	NP	2.67	0.61	Navesink
EB-3UD	UD-27	180.0 – 182.5	SM ^(a)	--	--	--	--	--	18	NV	NP	NP	--	--	Navesink

- a) Classification is based on quantitative and qualitative (visual inspection) information.
b) Test Results are rounded to the nearest percent.
c) Calculated value not reported in Reference (calculation assumes 100% saturation).
d) "--" Information not available
e) LL= Liquid Limit; PL= Plastic Limit; PI = Plasticity Index; G_s = Specific Gravity
f) Size Ranges: Gravel >2mm; 2mm>Sand>.074mm; .074mm>Silt>.005mm; >.005mm-Clay

Reference: 2.5.4.2-15

**PSEG Site
ESP Application
Part 2, Site Safety Analysis Report**

**Table 2.5.4.2-2 (Sheet 13 of 18)
Summary of Static Indices Laboratory Analysis
for the Mount Laurel Formation Data from ESPA Investigation^(d)**

Boring Number	Sample Number	Sample Depth (ft.)	USCS Classification	Gravel ^{(b)(f)} (%)	Sand ^{(b)(f)} (%)	Fines ^(b) (%)	Silt ^{(b)(f)} (%)	Clay ^{(b)(f)} (%)	Natural Moisture ^(b) (%)	LL ^{(b)(e)}	PL ^{(b)(e)}	PI ^{(b)(e)}	G _s ^(e)	Void Ratio ^(c)	Formation
NB-1	SS-37	165.0 – 166.5	SC	0	65	35	13	22	22	33	20	13	2.71	0.60	Mount Laurel
NB-1	SS-41	185.0 – 186.5	SC	0	78	22	11	11	23	33	22	11	--	--	Mount Laurel
NB-1	SS-49	250.0 – 251.5	SC	0	73	27	7	20	29	29	13	16	--	--	Mount Laurel
NB-2	SS-36	175.0 – 176.5	SC-SM	1	79	20	9	12	22	30	23	7	--	--	Mount Laurel
NB-3	SS-37	159.6 – 160.9	SC	0	62	38	20	18	21	42	26	16	--	--	Mount Laurel
NB-3	SS-44	194.6 – 195.4	SM	1	79	20	6	15	20	NV	NP	NP	--	--	Mount Laurel
NB-5	SS-41	184.5 – 186.0	SC	0	74	25	5	20	14	22	14	8	--	--	Mount Laurel
NB-7	SS-42	190.0 – 191.5	SC	3	77	20	4	16	13	26	16	10	--	--	Mount Laurel
NB-8	SS-44	199.5 – 201.0	SC ^(a)	0	78	22	--	--	24	--	--	--	2.71	0.65	Mount Laurel
NB-8	SS-49	249.5 – 251.0	SC-SM	0	82	19	7	12	21	23	19	4	--	--	Mount Laurel
EB-1	SS-46	210.0 – 211.5	SC-SM	1	79	20	8	12	20	22	16	6	--	--	Mount Laurel
EB-3	SS-41	184.6 – 186.1	SC	0	69	31	14	17	22	36	17	19	--	--	Mount Laurel
EB-3	SS-45	209.6 – 211.3	SM ^(a)	1	79	21	8	13	13	--	--	--	--	--	Mount Laurel
EB-3	SS-50	259.6 – 260.9	SM	0	84	16	10	6	23	21	18	3	--	--	Mount Laurel
EB-7	SS-43	195.0 – 195.4	SM	2	74	24	12	12	22	20	17	3	2.70	0.59	Mount Laurel
EB-8	SS-48	239.9 – 241.3	SM	0	85	15	9	6	21	NV	NP	NP	--	--	Mount Laurel
EB-8	SS-54	300.4 – 301.7	SC-SM	0	81	19	7	12	22	24	17	7	--	--	Mount Laurel
EB-3UD	UD-30	202.0 – 204.5	SM ^(a)	--	--	--	--	--	18	NV	NP	NP	--	--	Mount Laurel
EB-3UD	UD-31	208.0 – 210.5	SC-SM	0	63	37	25	12	17	19	14	5	2.69	0.46	Mount Laurel
EB-3UD	UD-32	220.1 – 222.6	SM ^(a)	--	--	--	--	--	18	NV	NP	NP	--	--	Mount Laurel

- a) Classification is based on quantitative and qualitative (visual inspection) information.
b) Test Results are rounded to the nearest percent.
c) Calculated value not reported in Reference (calculation assumes 100% saturation).
d) "--" Information not available
e) LL= Liquid Limit; PL= Plastic Limit; PI = Plasticity Index; G_s = Specific Gravity
f) Size Ranges: Gravel >2mm; 2mm>Sand>.074mm; .074mm>Silt>.005mm; >.005mm-Clay

Reference: 2.5.4.2-15

**PSEG Site
ESP Application
Part 2, Site Safety Analysis Report**

**Table 2.5.4.2-2 (Sheet 14 of 18)
Summary of Static Indices Laboratory Analysis
for the Wenonah Formation and Marshalltown Formation Data from ESPA Investigation^(d)**

Boring Number	Sample Number	Sample Depth (ft.)	USCS Classification^(a)	Gravel^{(b)(f)} (%)	Sand^{(b)(f)} (%)	Fines^(b) (%)	Silt^{(b)(f)} (%)	Clay^{(b)(f)} (%)	Natural Moisture^(b) (%)	LL^{(b)(e)}	PL^{(b)(e)}	PI^{(b)(e)}	G_s^(e)	Void Ratio^(c)	Formation
NB-1	SS-51	270.0 – 271.5	CL	0	49	51	--	--	28	42	13	29	--	--	Wenonah
NB-8	SS-52	279.5 – 281.0	SC	0	63	37	20	18	27	32	23	9	2.71	0.73	Wenonah
NB-1	SS-53	290.0 – 291.5	SM	0	85	15	--	--	22	NV	NP	NP	--	--	Marshalltown
EB-1	SS-57	315.0 – 316.5	SC	0	59	41	11	29	21	22	13	9	--	--	Marshalltown
EB-1	SS-59	329.0 – 330.5	SC	0	73	27	11	16	21	21	13	8	--	--	Marshalltown
EB-3	SS-56	319.6 – 321.1	SC	0	58	42	--	--	22	30	15	15	--	--	Marshalltown

- a) Classification is based on quantitative and qualitative (visual inspection) information.
b) Test Results are rounded to the nearest percent.
c) Calculated value not reported in Reference (calculation assumes 100% saturation).
d) "--" Information not available
e) LL= Liquid Limit; PL= Plastic Limit; PI = Plasticity Index; G_s = Specific Gravity
f) Size Ranges: Gravel >2mm; 2mm>Sand>.074mm; .074mm>Silt>.005mm; >.005mm-Clay

Reference: 2.5.4.2-15

**PSEG Site
ESP Application
Part 2, Site Safety Analysis Report**

**Table 2.5.4.2-2 (Sheet 15 of 18)
Summary of Static Indices Laboratory Analysis
for the Englishtown Formation and Woodbury Formation Data from ESPA Investigation^(d)**

Boring Number	Sample Number	Sample Depth (ft.)	USCS Classification	Gravel^{(b)(f)} (%)	Sand^{(b)(f)} (%)	Fines^(b) (%)	Silt^{(b)(f)} (%)	Clay^{(b)(f)} (%)	Natural Moisture^(b) (%)	LL^{(b)(e)}	PL^{(b)(e)}	PI^{(b)(e)}	G_s^(e)	Void Ratio^(c)	Formation
NB-1	SS-55	310.0 – 311.5	SC	0	61	39	--	--	25	36	16	20	--	--	Englishtown
NB-1	SS-57	330.0 – 331.5	CH	0	8	92	--	--	28	51	20	31	--	--	Englishtown
EB-3	SS-59	349.6 – 351.1	CL	0	34	66	--	--	28	32	20	12	--	--	Englishtown
NB-1	SS-62	380.0 – 381.5	CH	0	6	94	--	--	31	73	20	53	--	--	Woodbury
EB-3	SS-64	399.6 – 401.1	CH ^(a)	--	--	--	--	--	30	75	21	54	--	--	Woodbury

- a) Classification is based on quantitative and qualitative (visual inspection) information.
b) Test Results are rounded to the nearest percent.
c) Calculated value not reported in Reference (calculation assumes 100% saturation).
d) "--" Information not available
e) LL= Liquid Limit; PL= Plastic Limit; PI = Plasticity Index; G_s = Specific Gravity
f) Size Ranges: Gravel >2mm; 2mm>Sand>.074mm; .074mm>Silt>.005mm; >.005mm-Clay

Reference: 2.5.4.2-15

**PSEG Site
ESP Application
Part 2, Site Safety Analysis Report**

**Table 2.5.4.2-2 (Sheet 16 of 18)
Summary of Static Indices Laboratory Analysis
for the Merchantville Formation Data from ESPA Investigation^(d)**

Boring Number	Sample Number	Sample Depth (ft.)	USCS Classification	Gravel^{(b)(f)} (%)	Sand^{(b)(f)} (%)	Fines^(b) (%)	Silt^{(b)(f)} (%)	Clay^{(b)(f)} (%)	Natural Moisture^(b) (%)	LL^{(b)(e)}	PL^{(b)(e)}	PI^{(b)(e)}	G_s^(e)	Void Ratio^(c)	Formation
NB-1	SS-65	410.0 – 411.5	CL	0	37	63	--	--	31	43	21	22	--	--	Merchantville
EB-3	SS-68	439.6 – 441.1	CL ^(a)	--	--	--	--	--	25	36	18	18	--	--	Merchantville

- a) Classification is based on quantitative and qualitative (visual inspection) information.
b) Test Results are rounded to the nearest percent.
c) Calculated value not reported in Reference (calculation assumes 100% saturation).
d) "--" Information not available
e) LL= Liquid Limit; PL= Plastic Limit; PI = Plasticity Index; G_s = Specific Gravity
f) Size Ranges: Gravel >2mm; 2mm>Sand>.074mm; .074mm>Silt>.005mm; >.005mm-Clay

Reference: 2.5.4.2-15

**PSEG Site
ESP Application
Part 2, Site Safety Analysis Report**

**Table 2.5.4.2-2 (Sheet 17 of 18)
Summary of Static Indices Laboratory Analysis
for the Magothy Formation Data from ESPA Investigation^(d)**

Boring Number	Sample Number	Sample Dept (ft.)	USCS Classification^(a)	Gravel^{(b)(f)} (%)	Sand^{(b)(f)} (%)	Fines^(b) (%)	Silt^{(b)(f)} (%)	Clay^{(b)(f)} (%)	Natural Moisture^(b) (%)	LL^{(b)(e)}	PL^{(b)(e)}	PI^{(b)(e)}	G_s^(e)	Void Ratio^(c)	Formation
NB-1	SS-67	430.0 – 431.5	SC	0	61	39	--	--	18	30	14	16	--	--	Magothy
EB-3	SS-69	449.6 – 451.1	CH	0	3	97	--	--	25	62	27	35	--	--	Magothy

a) Classification is based on quantitative and qualitative (visual inspection) information.

b) Test Results are rounded to the nearest percent.

c) Calculated value not reported in Reference (calculation assumes 100% saturation).

d) "--" Information not available

e) LL= Liquid Limit; PL= Plastic Limit; PI = Plasticity Index; G_s = Specific Gravity

f) Size Ranges: Gravel >2mm; 2mm>Sand>.074mm; .074mm>Silt>.005mm; >.005mm-Clay

Reference: 2.5.4.2-15

**PSEG Site
ESP Application
Part 2, Site Safety Analysis Report**

**Table 2.5.4.2-2 (Sheet 18 of 18)
Summary of Static Indices Laboratory Analysis
for the Potomac Formation Data from ESPA Investigation**

Boring Number	Sample Number	Sample Depth (ft.)	USCS Classification	Gravel^{(b)(f)} (%)	Sand^{(b)(f)} (%)	Fines^(b) (%)	Silt^{(b)(f)} (%)	Clay^{(b)(f)} (%)	Natural Moisture^(b) (%)	LL^{(b)(e)}	PL^{(b)(e)}	PI^{(b)(e)}	G_s^(e)	Void Ratio^(c)	Formation
NB-1	SS-70	469.3 – 470.8	CL	0	4	96	--	--	21	33	15	18	--	--	Potomac
NB-1	SS-74	600.0 – 600.9	CL ^(a)	--	--	--	--	--	18	37	16	21	--	--	Potomac
EB-3	SS-70	630.0 – 631.5	CL ^(a)	--	--	--	--	--	15	38	14	24	--	--	Potomac

- a) Classification is based on quantitative and qualitative (visual inspection) information.
b) Test Results are rounded to the nearest percent.
c) Calculated value not reported in Reference (calculation assumes 100% saturation).
d) "--" Information not available
e) LL= Liquid Limit; PL= Plastic Limit; PI = Plasticity Index; G_s = Specific Gravity
f) Size Ranges: Gravel >2mm; 2mm>Sand>.074mm; .074mm>Silt>.005mm; >.005mm-Clay

Reference: 2.5.4.2-15

**PSEG Site
ESP Application
Part 2, Site Safety Analysis Report**

**Table 2.5.4.2-3a
Summary of Unconsolidated-Undrained (UU) Triaxial Test Results
Data from ESPA Investigation**

Boring No.	Sample No.	Sample Depth (ft.)	USCS Symbol^(a)	Initial Dry Unit Weight (pcf)	Initial Moisture Content (%)	Confining Pressure (tsf)	Undrained Shear Strength (tsf)	Formation
				49.9	82	0.756	0.435	Hydraulic Fill
NB-1UD	UD-3	19.6 to 21.6	MH	54.0	76	1.26	0.507	Hydraulic Fill
				50.0	87	2.02	0.365	Hydraulic Fill
NB-1UD	UD-8	55.8 to 57.8	CL	95.3	29	2.52	0.506	Kirkwood

a) Unified Soil Classification Symbol, ASTM D 2488 (Reference 2.5.4.2-8)

Reference: 2.5.4.2-15

**PSEG Site
ESP Application
Part 2, Site Safety Analysis Report**

**Table 2.5.4.2-3b (Sheet 1 of 2)
Summary of Unconfined Compression (UC) and Unconsolidated-Undrained (UU) Test Results
Data from the Hope Creek Generating Station UFSAR^(a)**

Type of Test	Boring No.	Sample No.	Sample Depth (ft.)	USCS Symbol	Initial Dry Unit Weight (pcf)	Moisture Content (%)	Confining Pressure (tsf)	Shear Strength (tsf)	Formation
UU	SS3	1	2	--	--	36.3	0.50	0.56	Hydraulic Fill
UU	SS2	2	4	--	--	41	0.50	0.265	Hydraulic Fill
UU	SS3	3	6	--	--	75.2	0.50	0.245	Hydraulic Fill
UU	AB5	3	6	--	--	47	0.252	0.195	Hydraulic Fill
UU	AB3	3	8	--	--	71	0.303	0.292	Hydraulic Fill
UU	AB5	7	16	--	--	43	0.598	0.271	Hydraulic Fill
UU	SS3	9	18	--	--	82.4	0.50	0.24	Hydraulic Fill
UU	AB1A	7	19	--	--	52	0.72	0.312	Hydraulic Fill
UC	216	3	20	--	--	52.4	--	0.263	Hydraulic Fill
UU	253	4	20	--	--	64.1	1.01	0.075	Hydraulic Fill
UU	AB2	9	22	--	--	61	0.792	0.322	Hydraulic Fill
UU	SS4	13	24	--	--	69.7	0.625	0.335	Hydraulic Fill
UU	SS1	13	25	--	--	52.1	0.625	0.385	Hydraulic Fill
UU	211	5	26	--	--	62.3	0.504	0.341	Hydraulic Fill
UU	SS3	13	26	--	--	64.4	0.625	0.263	Hydraulic Fill
UU	SS2	13	26	--	--	66.9	0.625	0.35	Hydraulic Fill
UU	AB2	11	27	--	--	60	1.0	0.275	Hydraulic Fill
UU	SS4	15	28	--	--	58.4	0.75	0.313	Hydraulic Fill
UU	SS3	15	30	--	--	66	0.75	0.3	Hydraulic Fill
UU	AB1	10	30	--	--	65	1.01	0.299	Hydraulic Fill
UU	211	1A	30 to 31.5	--	--	59.9	0.756	0.441	Hydraulic Fill
UU	SS4	17	32	--	--	72.2	0.875	0.425	Hydraulic Fill
UU	SS2	16	32	--	--	58.7	0.875	0.45	Hydraulic Fill
UU	AB2	15	37	--	--	35	1.51	0.604	Kirkwood Clay
UC	B1	8	43 to 45	--	--	35.5	--	1.08	Kirkwood Clay

**PSEG Site
ESP Application
Part 2, Site Safety Analysis Report**

**Table 2.5.4.2-3b (Sheet 2 of 2)
Summary of Unconfined Compression (UC) and Unconsolidated-Undrained (UU) Test Results
Data from the Hope Creek Generating Station UFSAR^(a)**

Type of Test	Boring No.	Sample No.	Sample Depth (ft.)	USCS Symbol	Initial Dry Unit Weight (pcf)	Moisture Content (%)	Confining Pressure (tsf)	Shear Strength (tsf)	Formation
UC	216	8	45	--	--	59.8	--	0.613	Kirkwood Clay
UU	AB5	19	46	--	--	40	2.016	0.51	Kirkwood Clay
UU	201	S-10C	46.2	--	--	37.1	2.43	0.56	Kirkwood Clay
UC	B2	8	46 to 48	--	--	50.5	--	0.67	Kirkwood Clay
UU	211	6A	55 to 56.5	--	--	51.8	1.15	0.854	Kirkwood Clay
UU	201	S-12C	57.5	--	--	19	3.1	0.55	Kirkwood Clay
UU	AB1	24	65	--	--	42	2.52	1.34	Kirkwood Clay

a) “—” Information not reported

Reference: 2.5.4.1-10

**PSEG Site
ESP Application
Part 2, Site Safety Analysis Report**

**Table 2.5.4.2-4
Summary of Consolidated Undrained Triaxial Test Results
Data from ESPA Investigation**

Boring No.	Sample No.	Sample Depth (ft.)	USCS ^(b)	Initial Dry Unit Weight (pcf) ^(d)	Initial Moisture Content (%)	Triaxial Test Data ^(a)				Formation
						c (tsf) ^(e)	ϕ (°)	c' (tsf) ^(e)	ϕ' (°)	
NB-1UD	UD-13	75.0 to 77.5	SM	94.4	29	ND ^(c)	ND	0.0	37.8	Oxidized Vincentown
				109.6	19	ND	ND	0.0	44.4	Oxidized Vincentown
NB-1UD	UD-25	125.6 to 128.1	SM	93.5	30					
				93.7	30	1.64	18.0	0.40	34.1	Hornerstown
				94.0	28					
EB-3UD	UD-18	127.1 to 129.6	SM	79.9	40					
				93.2	30	0.91	22.1	1.20	30.1	Vincentown
EB-3UD	UD-32	220.1 to 222.6	SM	110.5	20					
				109.1	20	7.63	12.8	4.81	20.4	Mount Laurel

a) ϕ = Total stress internal friction angle

c = Total stress cohesion intercept

ϕ' = Effective stress internal friction angle

c' = Effective stress cohesion intercept

b) Unified Soil Classification Symbol, ASTM D 2488 (Reference 2.5.4.2-8)

c) ND = Not Determined

d) pcf = pounds per cubic foot

e) tsf = tons per square foot

Reference: 2.5.4.2-15

**PSEG Site
ESP Application
Part 2, Site Safety Analysis Report**

**Table 2.5.4.2-5a
Summary of One-Dimensional Consolidation Test Results
Data from the ESPA Investigation^(c)**

Boring Number	Sample No.	Sample Depth (ft.)	USCS Symbol	Specific Gravity	Void Ratio	σ_v'^(a) (tsf)	Dry Unit Weight^(b)(pcf)	Initial Moisture Content^(b) (%)	p_c^(a) (tsf)	C_c^(a)	C_r^(a)	Formation
NB-1UD	UD-8	55.8 to 57.8	MH	--	--	1.50	68.7	51	1.40	0.535	0.070	Kirkwood

a) σ_v' = Overburden Pressure; p_c = Pre-consolidation Pressure; C_c = Coefficient of Compression; C_r = Coefficient of Recompression

b) Dry unit weight and moisture content values WERE determined prior to beginning test procedure.

c) "--" Information not available

Reference: 2.5.4.2-15

**PSEG Site
ESP Application
Part 2, Site Safety Analysis Report**

**Table 2.5.4.2-5b
Summary of One-Dimensional Consolidation Test Results
Data from the Hope Creek Generating Station UFSAR**

Boring Number	Sample No.	Sample Depth (ft.)	USCS Symbol	Specific Gravity	Void Ratio	σ_v' ^(a) (tsf)	Dry Unit Weight (pcf)	Initial Moisture Content (%)	p_c ^(a) (tsf)	C_c ^(a)	C_r ^(a)	Formation
232	2D	6.25	CH	2.66	1.33	--	--	50.0	1.55	.42	--	Kirkwood
216	9A	50.25	CH	2.62	1.53	--	--	58.4	1.80	.50	--	Kirkwood
232	6A	25.3	CH	2.65	1.42	--	--	52.3	1.30	.42	--	Fill
201	10D	46.5	CH	2.71	1.80	--	--	66.5	2.10	.79	--	Kirkwood
201	12D	57.75	CL-ML	2.78	0.59	--	--	20.4	8.0	.17	--	Kirkwood
AB1	10	30.0	CH	2.50	1.60	--	--	64.0	0.75	.62	--	Fill
AB4	5	13.0	CH	2.54	2.18	--	--	86.0	0.26	.70	--	Fill
AB5	3	6.0	CH	2.54	1.45	--	--	57.0	0.43	.42	--	Fill
AB1	14	40.0	CH	2.66	0.85	--	--	32.0	2.50	.33	--	Kirkwood

a) σ_v' = Overburden pressure, p_c = Pre-Consolidation pressure, C_c = Coefficient of Compression, C_r = Coefficient of Recompression

b) "--" Information not reported

Reference: 2.5.4.1-10

**PSEG Site
ESP Application
Part 2, Site Safety Analysis Report**

**Table 2.5.4.2-6
Summary of Unit Weight for Intact Samples
Data from ESPA Investigation^(e)**

Boring	UD #	Depth^(a)	Soil Classification^(b)	Formation	Natural Moisture (%)	Dry Unit Weight (pcf)	Total Unit Wt.^(c) (pcf)
NB-1UD	UD-3	19.6 to 21.6	MH	H. Fill	82	49.9	90.9
NB-1UD	UD-3	19.6 to 21.6	MH	H. Fill	76	54	94.9
NB-1UD	UD-3	19.6 to 21.6	MH	H. Fill	87	50	93.7
NB-1UD	UD-8	55.8 to 57.8	MH	Kirkwood	51	68.7	103.9
NB-1UD	UD-8	55.8 to 57.8	CL	Kirkwood	29	95.3	122.8
NB-1UD	UD-13	75.0 to 77.5	SM	OX. Vincentown ^(d)	29	94.4	121.8
NB-1UD	UD-13	75.0 to 77.5	SM	OX. Vincentown	19	109.6	130.2
NB-1UD	UD-17	90.65	SM	Vincentown	ND	ND	115.5
NB-1UD	UD-21	105.3	SM	Vincentown	ND	ND	113.5
EB-3UD	UD-15	115.5	SM	Vincentown	ND	ND	113.2
EB-3UD	UD-18	127.1 to 129.6	SM	Vincentown	40	79.9	111.9
EB-3UD	UD-18	127.1 to 129.6	SM	Vincentown	30	93.2	121.1
EB-3UD	UD-18	127.1 to 129.6	SM	Vincentown	41	78.7	110.9
NB-1UD	UD-25	125.6 to 128.1	SM	Hornerstown	29	93.5	120.8
NB-1UD	UD-25	125.6 to 128.1	SM	Hornerstown	30	93.7	121.4
NB-1UD	UD-25	125.6 to 128.1	SM	Hornerstown	28	94	120.7
NB-1UD	UD-25	125.6 to 128.1	SM	Hornerstown	29	92.2	118.8
NB-1UD	UD-24	122.9	SM	Hornerstown	ND	ND	120.3
EB-3UD	UD-27	180.0 to 182.5	SM	Navesink	20	109.8	131.8
NB-1UD	UD-27	142.5	SM	Navesink	ND	ND	115.5
EB-3UD	UD-31	210.5	SC-SM	Mount Laurel	ND	ND	130.3
EB-3UD	UD-30	202.0 to 204.5	SM	Mount Laurel	18	111.8	132
EB-3UD	UD-32	220.1 to 222.6	SM	Mount Laurel	20	110.5	132.5
EB-3UD	UD-32	220.1 to 222.6	SM	Mount Laurel	20	109.1	131.1
EB-3UD	UD-32	220.1 to 222.6	SM	Mount Laurel	17	109.9	129

a) Depth Indicates sample interval or tested sample depth

b) Soil classification by Unified Soil Classification System ASTM D 2488 (Reference 2.5.4.2-8)

c) Total Unit Weight Calculated from Dry Unit Weight and Moisture Content.

d) Oxidized portion of Vincentown Formation.

e) ND=Not Determined

Reference: 2.5.4.2-15

**PSEG Site
ESP Application
Part 2, Site Safety Analysis Report**

**Table 2.5.4.2-7 (Sheet 1 of 2)
Summary of Unit Weight of Soil
Data from Hope Creek Foundation Investigation**

Boring	Sample No.	Depth (ft)	Soil Classification^(a)	Formation^(b)	Natural Moisture (%)	Dry Unit Weight (pcf)	Total Unit Weight (pcf)
B-231	1	5	SM	FILL	25	105	130.7
B-238	1	5	ML	FILL	63	60.6	98.8
B-211	1	5.5	MH	FILL	54	64.3	99
B-239	1	5.5	SM	FILL	20	109.9	132.3
B-222	2	10	MH	FILL	80	53.1	95.8
B-229	2	10	ML	FILL	20	100.2	120.3
B-239	2	10.5	ML	FILL	32	83.2	109.4
B-217	2	11	ML	FILL	32	88.3	116.2
B-217	3	15	MH	FILL	66	61.3	101.9
B-216	3	20	MH	FILL	58	69.2	109.5
B-238	5	20	CL	FILL	64	60.8	99.7
B-211	4	21	MH	FILL	58	65.5	103.4
B-216	4	25.5	CL	FILL	68	46.5	78.2
B-217	5	25.5	MH	FILL	65	59.9	98.8
B-239	5	27.5	CL	FILL	53	68.6	105
B-229	7	30	CL	FILL	66	60.6	100.8
B-217	7	35.5	SP	ALLUVIUM	12	121.6	136.6
B-239	7	35.5	ML	FILL	54	66.3	102
B-249	8C	36	CH	KW	30	95.3	124
B-229	10	45	CH	KW	25	103.5	129.2
B-217	9	45.5	CH	KW	45	75.7	109.5
B-254	8A	46	MH	KW	61	62.3	100.3
B-254	8B	46	CH	KW	53	68.8	105.2
B-254	8C	46	CH	KW	54	67.8	104.7
B-231	10	50	SM	KW Basal	26	100	126.2
B-238	11	50	CH	KW	18	112.6	133.2
B-239	10	50.5	CH	KW	58	66.9	105.6
B-244	10A	51	MH	KW	57	66.5	104.1
B-244	10B	51	CH	KW	56	68.4	107
B-244	10C	51	MH	KW	68	58.6	98.4
B-225	10D	57.5	SM	OX VT	21	101.8	123.5
B-225	11A-B	59.4	SM	OX VT	35	84.2	113.8
B-225	11A-C	59.9	SM	OX VT	22	102.3	125
B-231	12	60	SM	OX VT	32	95	125.5
B-232	13	60	SM	OX VT	24	97.9	121.1
B-242	12	60	ML	KW Basal	27	99	125.9
B-206	10A	60.4	SP-SM	KW Basal	26	108.33	136.5

**PSEG Site
ESP Application
Part 2, Site Safety Analysis Report**

**Table 2.5.4.2-7 (Sheet 2 of 2)
Summary of Unit Weight of Soil
Data from Hope Creek Foundation Investigation**

Boring	Sample No.	Depth (ft)	Soil Classification ^(a)	Formation ^(b)	Natural Moisture (%)	Dry Unit Weight (pcf)	Total Unit Weight (pcf)
B-206	10A	60.4	SP-SM	KW Basal	26	108.33	136.5
B-211	7A	60.5	PT	KW Basal	156	29.1	74.6
B-214	10A	65.6	SM	VT	26	97.9	123.5
B-214	10B	66.2	SM	VT	32	89.7	118.1
B-214	10C	66.8	SM	VT	29	91.2	117.7
B-239	14	70.5	SM	OX VT	35	84.9	115
B-232	15	75	SM	OX VT	26	94.6	118.8
B-216	14A	75.5	SM	VT	35	86.4	116.5
B-216	14B	76.1	SM	VT	30	92.9	120.7
B-213	15	80	SM	VT	33	86.2	114.6
B-211	11A	80.5	SM	VT	30	92	119.1
B-239	16	80.5	SM	VT	31	88.7	115.8
B-206	13A	80.6	SP-SM	VT	22	77.6	95.2
B-206	13B	81.2	SP-SM	VT	25	81.6	101.7
B-206	13C	81.8	SP-SM	VT	32	82.8	109.1
B-206	14	85	SM	VT	22	84.5	103.3
B-201	18	100	SM	VT	30	93.2	121
B-201	19A	110	SM	VT	42	79.2	112.2
B-201	19C	111.6	SM	VT	39	81.9	113.5
B-201	19D	112.2	SM	VT	34	87.3	116.8
B-206	20B	115.9	SM	VT	31	90.1	118
B-206	20C	116.4	SM	VT	32	90.1	118.5
B-206	21A	120.6	SM	VT	36	85.7	116.3
B-206	21B	121.2	SM	VT	33	88.4	117.6
B-206	21C	121.7	SM	VT	34	87.4	116.9
B-232	25A	130	SM	HT	28	94.4	120.5
B-232	25B	130	SM	HT	25	99.4	124.3
B-206	22A	130.3	SM	HT	26	97.9	123.6
B-206	22B	131	SM	HT	26	98.9	124.9
B-206	22C	131.6	SM	HT	26	98.7	124.4
B-201	22A	140.4	SM	HT	26	99.6	125.7
B-201	22C	141.1	SM	HT	25	103.3	129.3
B-231	22	150	SM	NK	23	110	134.8
B-206	29	160	SC-SM	NK	21	104.8	126.6

(a) Unified Soil Classification System (USCS).

(b) Fill = Hydraulic Fill; KW = Kirkwood Formation; KW Basal = Lower portion of the Kirkwood Formation; OX VT = Oxidized Portion of the Vincentown Formation; VT = Vincentown Formation; HT = Hornerstown Formation; NK = Navesink Formation

Reference: 2.5.4.2-13

**PSEG Site
ESP Application
Part 2, Site Safety Analysis Report**

**Table 2.5.4.2-8 (Sheet 1 of 4)
Design Values for Static Engineering Properties of Subsurface Materials^(f)**

Parameter	Formation			
	Artificial Fill	Hydraulic Fill	Alluvium	Kirkwood ^(a)
Range of Thickness, feet	2 to 9.5	24 to 44	5 to 24	12 to 54
Average Thickness, feet	4.2	32.9	15.3	30.4
Range of Top Elevation, feet NAVD ^(c)	6.2 to 12.8	0 to 11	-35 to -22	-37 to -58
Average Top Elevation, feet NAVD	9	5	-29	-43
USCS Symbol	ND	SM, SC-SM, ML, MH, CL, CH	SP-SM, SP, SM, ML, CL, CH	SP-SM, SP, SM, MH, CL, CH
Natural Moisture, %	ND	79	28	47
Unit Weight, (pcf)	ND	100 ^(b)	136.6 ^(b)	(MH) 103.9 (CL) 122.8
Liquid Limit, (LL)	ND	60	40	50
Plastic Limit, (PL)	ND	28	24	25
Plasticity Index (PI)	ND	32	16	25
Field SPT N-value, bpf ^(d)	22	3	14	12
N ₆₀ , bpf ^{(d)(e)}	25	3	22	18
(N ₁) ₆₀ , bpf ^{(d)(g)}	56	13	26	20
Undrained Shear Strength (c _u), tsf	ND	0.436	ND	0.506
Total stress internal friction angle, Φ	ND	NA	ND	ND
Total stress cohesion intercept, c, tsf	ND	ND	ND	ND
Effective stress internal friction angle, Φ'	ND	ND	ND	ND
Effective stress cohesion intercept, c', tsf	ND	ND	ND	ND
Compression Index, C _c	ND	0.54	ND	0.535
Recompression Index, C _r	ND	ND	ND	0.070
Pre-consolidation Pressure, P _c (psf)	ND	1365	ND	2800

**PSEG Site
ESP Application
Part 2, Site Safety Analysis Report**

**Table 2.5.4.2-8 (Sheet 2 of 4)
Design Values for Static Engineering Properties of Subsurface Materials^(f)**

Parameter	Formation			
	Vincentown and Hornerstown	Navesink	Mount Laurel	Wenonah and Marshalltown
Range of Thickness, feet	51 to 112	19 to 26	102 to 112	18 to 40
Average Thickness, feet	72.4	22.3	107.1	35.4
Range of Top Elevation, feet NAVD ^(c)	-70 to -33	-133 to -121	-157 to -145	-259 to -250
Average Top Elevation, feet NAVD	-57	-127	-151.5	-256
USCS Symbol	SP-SM,SC-SM,SM,SC,MH,ML	SC-SM/SM/SC	SC-SM/SM/SC	SM/SC/CL
Natural Moisture, %	30	22	20	23
Unit Weight, (pcf)	118.5	123.6	131.0	125
Liquid Limit, (LL)	26	27	27	29
Plastic Limit, (PL)	20	16	18	15
Plasticity Index (PI)	6	11	9	14
Field SPT N-value, bpf ^(d)	37	72	91	41
N ₆₀ , bpf ^{(d)(e)}	56	108	137	61
(N ₁) ₆₀ , bpf ^{(d)(g)}	32	45	54	28
Undrained Shear Strength (c _u), tsf	ND	ND	ND	ND
Total stress internal friction angle, Φ	20	ND	13	ND
Total stress cohesion intercept, c , tsf	1.275	ND	7.640	ND
Effective stress internal friction angle, Φ'	37	ND	20	ND
Effective stress cohesion intercept, c', tsf	0.400	ND	4.810	ND
Compression Index, C _c	ND	ND	ND	ND
Recompression Index, C _r	ND	ND	ND	ND
Pre-consolidation Pressure, P _c (psf)	ND	ND	ND	ND

**PSEG Site
ESP Application
Part 2, Site Safety Analysis Report**

**Table 2.5.4.2-8 (Sheet 3 of 4)
Design Values for Static Engineering Properties of Subsurface Materials^(f)**

Parameter	Formation			
	Englishtown and Woodbury	Merchantville	Magothy	Potomac
Range of Thickness, feet	79 to 80	30 to 31	52 to 55	>133.9
Average Thickness, feet	79.5	30.5	53.5	NA
Range of Top Elevation, feet NAVD ^(c)	-292 to -290	-372	-402	-454
Average Top Elevation, feet NAVD	-292	-372	-402	-454
USCS Symbol	SC,CL,CH	CL	SC,CH	CL
Natural Moisture, %	28	28	21	18
Unit Weight, (pcf)	125 ^(h)	125 ^(h)	125 ^(h)	125 ^(h)
Liquid Limit, (LL)	53	40	46	36
Plastic Limit, (PL)	19	20	21	15
Plasticity Index (PI)	34	20	26	21
Field SPT N-value, bpf ^(d)	32	50	85	92
N ₆₀ , bpf ^{(d)(e)}	47	76	121	131
(N ₁) ₆₀ , bpf ^{(d)(g)}	19	NA	51	56
Undrained Shear Strength (c _u), tsf	ND	ND	ND	ND
Total stress internal friction angle, Φ	ND	ND	ND	ND
Total stress cohesion intercept, c, tsf	ND	ND	ND	ND
Effective stress internal friction angle, Φ'	ND	ND	ND	ND
Effective stress cohesion intercept, c', tsf	ND	ND	ND	ND
Compression Index, C _c	ND	ND	ND	ND
Recompression Index, C _r	ND	ND	ND	ND
Pre-consolidation Pressure, P _c , (psf)	ND	ND	ND	ND

**PSEG Site
ESP Application
Part 2, Site Safety Analysis Report**

**Table 2.5.4.2-8 (Sheet 4 of 4)
Design Values for Static Engineering Properties of Subsurface Materials(f)**

-
- a) Upper, fine-grained portion of Kirkwood Formation
 - b) Hope Creek data included in the value. (Reference 2.5.4.2-13)
 - c) Based on borings in new plat location (NB series). Artificial fill elevation from surveyed top of ground; all other elevations from boring log strata breaks rounded to nearest foot. No ranges where only one boring.
 - d) bpf = blows per foot
 - e) N_{60} = SPT N-values (field) corrected for field conditions, including hammer energy.
 - f) ND=Not Determined
 - g) $(N_1)_{60}$ = SPT N-values (field) corrected for field conditions, hammer energy and effective overburden pressure. Not applicable for cohesive soils.
 - h) Values based on information in References 2.5.4.2-19, 2.5.2.4-19 and 2.5.4.2-20.
 - i) NA = Not Applicable

**PSEG Site
ESP Application
Part 2, Site Safety Analysis Report**

**Table 2.5.4.2-9 (Sheet 1 of 2)
Summary of RCTS Test Results
Data from ESPA Investigation^{(b)(c)}**

Boring Number	Sample Number	Sample Depth (ft.)	USCS Symbol	Fines (%)	Total Unit Weight (pcf)	Initial Moisture (%)	PI (%)	Isotropic Confining Pressure, σ_o (psf)	Low-Amplitude Shear Modulus, G_{max} (ksf)	Low-Amplitude Shear Wave Velocity, $V_s^{(a)}$ (ft./sec.)	Low-Amplitude Material Damping Ratio, D_{min} (%)	Formation
NB-1UD	UD-17	90.65	SM	17.9	115.5	32	NP	850	1777	703	1.32	Vincentown
								1699	2582	847	1.24	Vincentown
								3398	3716	1015	1.05	Vincentown
								6797	5175	1196	0.82	Vincentown
								13,594	6965	1385	0.77	Vincentown
NB-1UD	UD-21	105.3	SM	20.9	113.5	26	NP	994	1243	593	1.49	Vincentown
								2002	1785	709	1.24	Vincentown
								4003	2587	852	0.99	Vincentown
								8006	3753	1024	0.91	Vincentown
								15,998	5732	1263	0.85	Vincentown
NB-1UD	UD-24	122.9	SP-SM	8.5	120.3	28	NP	1181	1679	670	1.98	Hornerstown
								2347	2387	798	1.57	Hornerstown
								4694	3375	947	1.32	Hornerstown
								9389	4726	1119	1.12	Hornerstown
								18,806	6513	1311	1.01	Hornerstown
NB-1UD	UD-27	142.5	SM	18.6	115.5	23	NP	1354	1862	685	4.55	Navesink
								2707	2720	827	4.45	Navesink
								5400	3936	993	4.19	Navesink
								10,800	5566	1178	4.03	Navesink
								21,600	7617	1373	3.84	Navesink

**PSEG Site
ESP Application
Part 2, Site Safety Analysis Report**

**Table 2.5.4.2-9 (Sheet 2 of 2)
Summary of RCTS Test Results
Data from ESPA Investigation^{(b)(c)}**

Boring Number	Sample Number	Sample Depth (ft.)	USCS Symbol	Fines (%)	Total Unit Weight (pcf)	Initial Moisture (%)	PI (%)	Isotropic Confining Pressure, σ_o (psf)	Low-Amplitude Shear Modulus, G_{max} (ksf)	Low-Amplitude Shear Wave Velocity, $V_s^{(a)}$ (ft./sec.)	Low-Amplitude Material Damping Ratio, D_{min} (%)	Formation
EB-3UD	UD-15	115.5	SM	22.3	113.2	32	NP	1181	1499	652	1.08	Vincentown
								2347	2184	786	0.74	Vincentown
								4694	3259	958	0.55	Vincentown
								9403	4838	1161	0.50	Vincentown
								18,806	7318	1413	0.49	Vincentown

a) Laboratory V_s results not representative of in-situ strata, and not used for dynamic profile (Subsections 2.5.4.2.2.2 and 2.5.4.7.1)

b) PI = Plasticity Index; psf = pounds per square foot; ksf = kips per square foot; ft./sec. = feet per second

c) All tests performed at ratios of 0.25, 0.5, 1, 2 and 4 times estimated in-situ confining pressure computed using $K_o = 0.5$

Reference: 2.5.4.2-15

**PSEG Site
ESP Application
Part 2, Site Safety Analysis Report**

2.5.4.3 Foundation Interfaces

This subsection presents a summary of foundation interface conditions at the PSEG Site based on findings of a site exploration conducted by MACTEC Engineering and Consulting, Inc. (Reference 2.5.4.3-11). Subsection 2.5.4.3.1 provides a description of the PSEG Site geotechnical exploration and testing activities. Subsection 2.5.4.3.2 summarizes the relationship of the planned foundations for safety-related structures and the engineering properties of underlying materials.

2.5.4.3.1 Site Exploration

2.5.4.3.1.1 Purpose and Scope

The purposes of the PSEG Site geotechnical exploration and testing were to:

- Obtain new data to meet current NRC and vendor design control document Tier 1 site characteristics requirements as appropriate for an ESPA
- Confirm and demonstrate the applicability of the existing field data from the previous site exploration work for the existing nuclear plants

Exploration activities were specifically developed to comply with requirements of 10 CFR 52, 10 CFR 50 Appendix B, and 10 CFR 100.23, using guidance provided in:

- NUREG-0800
- RG 1.132
- RG 1.138
- RG 1.206
- RG 1.208

The exploration program was designed to characterize, at a level appropriate for an ESPA, the geologic and geotechnical conditions at the new plant location, considering the lateral and vertical variability inherent in Coastal Plain sediments. Additionally, the depth of exploration considered factors such as depth to key geologic formations, anticipated foundation bearing pressures and geometry, and reasonable depths to obtain site-specific dynamic properties to evaluate the site response to vibratory ground motion and develop the GMRS.

Exploration activities involved the following modes of data collection:

- Exploratory borehole drilling and sampling
- In-situ geophysical testing
- Observation well installation and testing

The methodology and extent of each of the exploration activities is discussed below.

2.5.4.3.1.2 Exploratory Borehole Drilling and Sampling

Geotechnical borings were advanced to depths ranging from 151 to 631 feet (ft.) at 16 locations at the PSEG Site to characterize subsurface geologic conditions, to perform in-situ testing, and to obtain samples for geotechnical laboratory testing. Eight geotechnical borings, distinguished

Rev. 4

**PSEG Site
ESP Application
Part 2, Site Safety Analysis Report**

by the 'NB' boring identification prefix, were advanced within the northern portion of the PSEG Site. Nine geotechnical borings were advanced within the eastern portion of the PSEG Site, distinguished by the 'EB' boring identification prefix (two geotechnical borings were advanced at the EB-6 location to obtain a complete SPT profile at this location). Two boreholes were advanced adjacent to completed geotechnical borings (one designated NB-1UD adjacent to NB-1, and one designated NB-3UD adjacent to EB-3) for collection of intact soil samples. Three boreholes were advanced adjacent to NB-1 (designated CH NB-1A, CH NB-1B, CH NB-1C), and three boreholes were advanced adjacent to NB-8 (designated CH NB-8A, CH NB-8B, CH NB-8C) for crosshole seismic measurements. In-situ geophysical testing was conducted in boreholes NB-1, NB-8 and EB-3 and in a borehole advanced adjacent to completed geotechnical boring EB-8 (designated EB-8G). Thirty-two boreholes were advanced for installation of groundwater level observation wells. The record locations and ground surface elevations were determined for all of the completed boreholes by a New Jersey (NJ) professional land surveyor. The locations of the geotechnical, intact sample collection, in-situ geophysical testing, and observation well boreholes are shown on Figure 2.5.4.3-1. The location coordinates are shown on Tables 2.5.4.3-1 and 2.5.4.3-2.

Geotechnical drilling and observation well installation activities were performed by drillers licensed in NJ as soil borers or journeyman well drillers. Soil boring and well permits were obtained from the New Jersey Department of Environmental Protection by Craig Test Boring, Inc., of Mays Landing, NJ. All boreholes were advanced and sampled using either mud rotary wash drilling with unlined split-barrel drive sampling, or sonic drilling with continuous core sampling. Intact soil samples were collected from the boreholes in thin-wall, 3-inch (in.) diameter tubes, commonly called Shelby tubes, as described in ASTM D 1587 (Reference 2.5.4.3-8).

Mud rotary wash boring equipment was used to advance boreholes pursuant to ASTM D 5783 (Reference 2.5.4.3-3), and to collect disturbed samples pursuant to ASTM D 1586 (Reference 2.5.4.3-7). Powdered bentonite was the drilling fluid additive used during advancement of the geotechnical borings. A biodegradable drilling fluid additive was used during advancement of the boreholes drilled with mud rotary equipment for installation of observation wells. Borehole diameters ranged from 4 in. to 8 in., depending on the conditions encountered (e.g., 4-in. or 6-in. outside diameter casing was often necessary to facilitate recirculation of drilling fluid and stabilize the upper portion of boreholes advanced through the hydraulic fill or river gravels).

Drive sampling by the Standard Penetration Test (SPT) method was conducted with automatic trip hammers, generally at 2.5-ft., 5.0-ft., and 10-ft. intervals. Samples were collected using 18 in. long SPT unlined split-barrel drive samplers attached to drill rods (NWJ designation). All samplers were of standard manufacture, and were in good condition. The SPT sampling interval was typically 2.5-ft. from the ground surface to a depth of 15 ft., 5-ft. from a depth of 15 ft. to a depth of 200 ft., and 10-ft. from a depth of 200 ft. to a depth of 450 ft. Two borings (EB-4 and NB-4) were sampled at 2.5-ft. intervals to 200-ft. depth. SPT samples were obtained at larger than 10-ft. intervals below 450-ft. depth in borings NB-1 and EB-3, which were extended to respective depths of 600 ft. and 631 feet. The sampling interval below 450 ft. was extended because the purpose of boring below that depth was to obtain geologic information rather than engineering properties.

The automatic SPT hammers were calibrated by weighing the hammer and measuring the drop height. Calibrations were performed prior to start of work and prior to demobilization from the site. SPT energy measurements were conducted for each of the automatic hammers/drill rigs

**PSEG Site
ESP Application
Part 2, Site Safety Analysis Report**

performing SPT soil sampling, in accordance with ASTM D 4633 (Reference 2.5.4.3-2). The average energy transfer rates (ETR) measured for each rig are within the range of typical values for automatic hammers (66.0 to 82.6 percent of the theoretical potential energy) for the four rigs performing SPT sampling at the PSEG Site. A summary of the SPT energy measurements is presented in Table 2.5.4.3-3.

After recovery, representative portions of each SPT sample up to 4 in. long were selected by rig geologists/engineers and placed in one or more labeled glass jars with sealed, lined caps, in accordance with ASTM D 4220 (Reference 2.5.4.3-5). All samples were immediately assigned alphanumeric sample identifications, photographed, described in accordance with ASTM D 2488 (Reference 2.5.4.3-4), and recorded on field logs. The SPT samples were placed in compartmentalized cardboard boxes labeled to show contents. The boxes were transported daily from the field to a lockable area in the site trailer by the rig geologists/engineers, in accordance with ASTM D 4220 (Reference 2.5.4.3-5) for Group B samples as defined in ASTM D 4220 (disturbed samples collected for laboratory testing). A sample inventory log was kept at the sample storage facility. All samples entering the storage facility were logged in by the rig geologist/engineer or site manager/lead geologist. Selected samples were removed for laboratory testing. MACTEC chain-of-custody forms were completed for the samples removed.

Ranges and average of SPT results for each geologic layer are summarized in Subsection 2.5.4.2.2.1.

Intact soil samples were collected using standard Shelby tubes (Reference 2.5.4.3-8), Osterberg hydraulic samplers, or Pitcher barrel samplers (Reference 2.5.4.3-12). Shelby tubes were attached to the NWJ drill rod string with a fixed head sample holder with a check valve and advanced with a steady hydraulic push of the drill head. The Osterberg sampler is a type of hydraulically-pushed piston sampler that was used for collection of samples in the hydraulic fill and Kirkwood clay at boring EB-3UD. A Pitcher barrel sampler, which is a rotary sampler that drills ahead of the 3-in. thin-walled Shelby tube as it is advanced into the subsurface material, was used for collection of intact soil samples when the subsurface material was anticipated as being too dense or hard to allow hydraulic pushing of the Shelby tube. The Pitcher barrel sampler was generally used in sampling the Vincentown and deeper formations.

After recovery, Shelby tubes were purged of excess drilling fluid and drill cuttings while remaining upright. One to 2 in. of melted microcrystalline wax was poured into the top of each sample tube to preserve moisture and stabilize the sample. Plastic caps were then placed over each end and sealed with melted microcrystalline wax. Adhesive-backed tape was used to further secure the plastic end caps. All samples were immediately assigned alphanumeric sample identifications, photographed, described in accordance with ASTM D 2488 (Reference 2.5.4.3-4), and recorded on the field logs. The intact Shelby tube samples were transported from the field to the lockable area of the site trailer and handled as Group C samples (intact samples collected for laboratory testing) under ASTM D 4220 (Reference 2.5.4.3-5). A sample inventory log was maintained at the sample storage facility and the tube samples were stored upright in specially fabricated racks in the climate-controlled environment. Selected tube samples were removed from the storage trailers for off-site laboratory testing. Those tube samples transported for off-site laboratory analysis were secured upright in padded wooden crates, loaded in passenger vehicles, and then hand-delivered by project personnel under chain-of-custody protocol, in accordance with ASTM D 4220 (Reference 2.5.4.3-5).

**PSEG Site
ESP Application
Part 2, Site Safety Analysis Report**

Continuous soil core samples were obtained at 20 of the 32 observation well locations using roto sonic drilling methods to expedite the drilling process. The recovered core samples were obtained to establish the appropriate well screen intervals for the well cluster at those locations. Core run lengths were typically 5 to 10 ft. The cores were extruded from the core barrel into plastic sleeves. The plastic sleeves were opened at the drill site and the recovered materials were visually described, classified, and photographed by the rig geologist/engineer. Representative portions of the cores were placed in glass jars with sealed, lined caps and the remaining samples discarded. Sample jars were labeled, placed in cardboard boxes, and transported to the on-site secure sample storage trailer at the end of each work day.

2.5.4.3.1.3 In-Situ Geophysical Testing

Downhole geophysical testing was performed in four borings (NB-1, NB-8, EB-3, EB-8G). Borehole deviation, natural gamma, resistivity, and caliper logging was performed in each of the four boreholes. A suspension P-S velocity logging system was used to obtain in-situ compressional (P) wave and horizontal shear (S) wave velocity measurements in all four boreholes at 1.65 ft. to 3.3 ft. intervals.

Seismic velocity measurements were completed using crosshole techniques at two locations: in the vicinity of boring NB-1 (boreholes CH NB-1A, -B and -C), and in the vicinity of boring NB-8 (boreholes CH NB-8A, -B and -C). Downhole seismic velocity measurements were performed in borehole CH NB-1C. The crosshole testing was performed in 4-in. diameter PVC-cased boreholes, in general compliance with ASTM D 4428/4428M (Reference 2.5.4.3-6) to obtain compressional (P) wave and horizontal shear (S) wave velocities for use in validation of the data obtained at these two locations using the suspension P-S velocity logging system. Downhole testing was performed in accordance with an approved subcontractor procedure.

Subsection 2.5.4.4 presents a more detailed discussion of the in-situ geophysical data collection methods and presents the results.

2.5.4.3.1.4 Observation Well Installation and Testing

Thirty-two observation wells were installed in 16 locations during exploration at the PSEG Site (Figure 2.5.4.3-1 and Table 2.5.4.3-2). Eight well pairs were installed in the northern portion of the site, and 8 well pairs were installed in the eastern portion. Each well pair contained two 2-in. diameter PVC wells with a 10-ft. long machine slotted screen (0.010-in. wide slots) installed in a nominal 6-in. diameter borehole. One well at each pair was installed in the hydraulic fill or Alluvium (designated as the upper well with a "U" following the well number). The other well in the pair was installed in the Vincentown Formation (designated as the lower well with an "L" following the well number). The soil lithology identified in adjacent geotechnical borings was used to determine the screen interval and well completion depths. Where companion geotechnical borings had not been advanced adjacent to the well location prior to well installation, soil sampling and logging was conducted during the well installation to confirm that the lithology at the well sites was consistent with the overall site lithology. This condition occurred at only two well pair locations (EOW-9 and EOW-10).

Rotosonic drilling methods were used to advance the boreholes for installation of 20 of the 32 observation wells. The roto sonic cores were visually reviewed by the rig geologist/engineer and samples were collected from the cores and placed in sample jars.

**PSEG Site
ESP Application
Part 2, Site Safety Analysis Report**

Following installation, the wells were developed using a submersible pump to remove fines from the well and filter pack, under the supervision of a NJ licensed well driller. During the development process, the pump was cycled on and off and/or lifted up and down to create a surge effect in the well. The wells were considered developed when the pumped water was relatively clear and visually free of suspended sediment, or after a maximum of two hours.

Following well development, field hydraulic conductivity tests (also referred to as "slug tests") were performed at each well using procedures described in Section 8 of ASTM D 4044 (Reference 2.5.4.3-1). A minimum of two rising head tests and two falling head tests were completed at each location. The results of the hydraulic conductivity tests are presented in Subsection 2.5.4.6.

2.5.4.3.2 Foundation Interfaces

Figures 2.5.4.3-3 and 2.5.4.3-4 show cross-sections along, and perpendicular to, the dip of the Coastal Plain deposits underlying the northern area at the PSEG Site. These cross-sections are constructed from the geotechnical boring logs and demonstrate the position of subsurface stratigraphy relative to the upper and lower bounds of embedment depths for safety-related structures within the plant parameter envelope (PPE) described in Subsection 1.3.3. Figure 2.5.4.3-2 shows the location of the cross-sections relative to the geotechnical borings performed during the course of the PSEG Site exploration.

As discussed in Subsection 2.4.10, the site grade of the new plant will be at elevation 36.9 ft. NAVD. Between 25 and 30 ft. of fill will be required to achieve this site grade. The top of competent foundation materials, as evaluated in Subsection 2.5.4.5, occurs at approximate elevation -67 ft. NAVD at the new plant location. Table 1.3-1 lists the range of embedment depths for the four reactor technologies as 39 ft. to 84.3 ft. below the plant grade. Subtracting these depths from the site grade of elevation 36.9 ft, shows that the bottom of the foundations for the deepest base of the safety-related structures will lie at elevations -2.1 ft to -47.4 ft NAVD which corresponds to 20 to 65 ft. above the top of the competent foundation bearing material. Over-excavation of this unsuitable foundation support material and replacement with backfill material will be performed, as described in Subsections 2.5.4.5 and 2.5.4.10.

2.5.4.3.3 References

- 2.5.4.3-1 ASTM, 2008, "Standard Test Method (Field Procedure) for Instantaneous Change in Head (Slug) Tests for Determining Hydraulic Properties of Aquifers," ASTM D 4044-08, 2008.
- 2.5.4.3-2 ASTM, 2005, "Standard Test Method for Energy Measurement for Dynamic Penetrometers," ASTM D 4633-05, 2005.
- 2.5.4.3-3 ASTM, 2006a, "Standard Guide for Use of Direct Rotary Drilling with Water-Based Drilling Fluid for Geoenvironmental Exploration and the Installation of Subsurface Water-Quality Monitoring Devices," ASTM D 5783-06, 2006.
- 2.5.4.3-4 ASTM, 2006b, "Standard Practice for Description and Identification of Soils (Visual-Manual Procedure)," ASTM D 2488-06, 2006.

**PSEG Site
ESP Application
Part 2, Site Safety Analysis Report**

- 2.5.4.3-5 ASTM, 2007a, "Standard Practices for Preserving and Transporting Soil Samples," ASTM D 4220-07, 2007.
- 2.5.4.3-6 ASTM, 2007b, "Standard Test Methods for Seismic Crosshole Testing," ASTM D 4428/4428M-07, 2007.
- 2.5.4.3-7 ASTM, 2008a, "Standard Test Method for Standard Penetration Test (SPT) and Split-Barrel Sampling of Soils," ASTM D 1586-08, 2008.
- 2.5.4.3-8 ASTM, 2008b, "Standard Practice for Thin-Walled Tube Sampling of Soils for Geotechnical Purposes," ASTM D 1587-08, 2008.
- 2.5.4.3-9 Dames & Moore, "Report of Foundation Studies, Proposed Hope Creek Generating Station, Lower Alloways Creek Township, New Jersey Public Service Electric and Gas Company," May 23, 1974.
- 2.5.4.3-10 Dames & Moore, "Report of Foundation Studies, Proposed Salem Nuclear Generating Station, Salem, New Jersey, Public Service Electric & Gas Company," August 28, 1968.
- 2.5.4.3-11 MACTEC Engineering and Consulting, Inc., "Geotechnical Exploration and Testing, PSEG Site Application, Lower Alloways Creek Township, New Jersey", Rev. 0, Jul 10, 2009.
- 2.5.4.3-12 U.S. Army Corps of Engineers (USACE), "Geotechnical Investigations, U.S. Army Corps of Engineers, Engineering and Design," 2001.

**PSEG Site
ESP Application
Part 2, Site Safety Analysis Report**

**Table 2.5.4.3-1 (Sheet 1 of 2)
Summary of Exploratory Borehole Drilling, Sampling and Testing Locations^{(a)(d)}**

Boring Number	Boring Type		Depth (ft. bgs) ^(d)		Coordinates and Elevation (US Survey Feet)			In-Situ Testing							
	SPT	UD Tubes	Proposed	Actual	Northing	Easting	Ground Surface Elevation	P-S Suspension	Deviation	Natural Gamma	Resistivity	Caliper	Spontaneous Potential	Crosshole Seismic	Downhole Seismic
NB-1	--	NA	450.0	600.9	234567.6	198469.1	12.82	--	--	--	--	--	--	NA	NA
NB-1UD	NA	--	232.0	232.3	234556.0	198459.0	12.65	NA	NA	NA	NA	NA	NA	NA	NA
CH NB-1A	NA	NA	200.0	201.0	234544.4	198483.1	12.80	NA	--	NA	NA	NA	NA	--	NA
CH NB-1B	NA	NA	200.0	201.0	234537.1	198476.0	13.00	NA	--	NA	NA	NA	NA	--	NA
CH NB-1C	NA	NA	200.0	201.0	234529.8	198469.5	13.31	NA	--	NA	NA	NA	NA	--	--
NB-2	--	--	300.0	301.5	235205.0	197764.7	8.19	NA	NA	NA	NA	NA	NA	NA	NA
NB-3	--	NA	200.0	200.3	234554.7	197895.8	7.37	NA	NA	NA	NA	NA	NA	NA	NA
NB-4	--	--	200.0	201.3	233960.4	198139.0	11.52	NA	NA	NA	NA	NA	NA	NA	NA
NB-5	--	NA	200.0	200.0	234891.0	198445.7	7.81	NA	NA	NA	NA	NA	NA	NA	NA
NB-6	--	--	200.0	200.0	235251.5	198315.4	9.26	NA	NA	NA	NA	NA	NA	NA	NA
NB-7	--	NA	200.0	201.2	234965.7	199685.6	6.21	NA	NA	NA	NA	NA	NA	NA	NA
NB-8	--	NA	300.0	315.3	234140.4	199745.9	8.94	--	--	--	--	--	--	NA	NA
CH NB-8A	NA	NA	200.0	201.0	234137.6	199720.2	8.82	NA	--	NA	NA	NA	NA	--	NA
CH-NB-8B	NA	NA	200.0	201.5	234130.2	199713.0	8.85	NA	--	NA	NA	NA	NA	--	NA
CH-NB-8C	NA	NA	200.0	201.0	234122.3	199705.9	8.99	NA	--	NA	NA	NA	NA	--	NA
EB-1	--	NA	450.0	351.5	232316.7	202774.1	15.91	NA	NA	NA	NA	NA	NA	NA	NA
EB-2	--	NA	200.0	200.7	233264.7	202166.5	14.07	NA	NA	NA	NA	NA	NA	NA	NA
EB-3	--	NA	300.0	631.5	232349.0	202473.9	16.46	--	--	--	--	--	--	NA	NA
EB-3UD	NA	--	226.0	226.2	232350.2	202492.3	16.42	NA	NA	NA	NA	NA	NA	NA	NA
EB-4	--	NA	200.0	200.2	231783.2	202017.5	20.32	NA	NA	NA	NA	NA	NA	NA	NA
EB-5	--	NA	200.0	199.3	233048.3	203016.4	13.80	NA	NA	NA	NA	NA	NA	NA	NA
EB-6	--	NA	200.0	199.9	232587.2	203262.4	13.69	NA	NA	NA	NA	NA	NA	NA	NA

**PSEG Site
ESP Application
Part 2, Site Safety Analysis Report**

**Table 2.5.4.3-1 (Sheet 2 of 2)
Summary of Exploratory Borehole Drilling, Sampling and Testing Locations^{(a)(d)}**

Boring Number	Boring Type		Depth (ft. bgs) ^(d)		Coordinates and Elevation (US Survey Feet)			In-Situ Testing							
	SPT	UD Tubes	Proposed	Actual	Northing	Easting	Ground Surface Elevation	P-S Suspension	Deviation	Natural Gamma	Resistivity	Caliper	Spontaneous Potential	Crosshole Seismic	Downhole Seismic
EB-6A ^(c)	--	NA	151.0	151.1	232587.0	203251.3	14.10	NA	NA	NA	NA	NA	NA	NA	NA
EB-7	--	NA	200.0	200.3	232084.2	203023.1	16.97	NA	NA	NA	NA	NA	NA	NA	NA
EB-8	--	--	300.0	301.7	231160.7	203499.7	15.30	NA	NA	NA	NA	NA	NA	NA	NA
EB-8G	NA	NA	315.0	315.0	231153.3	203528.3	15.73	--	--	--	--	--	--	NA	NA

a) NA = Not Applicable

b) ft. bgs=feet below ground surface

c) EB-6A Drilled to Check SPT Values from 90 to 150 ft. in EB-6 due to hammer problems in EB-6

d) Horizontal Coordinates (Northing and Easting) = NAD83 (2007), New Jersey State Plane Coordinate System Zone (2900), U.S. Survey Feet; Elevations = North American Vertical Datum of 1988 (NAVD), U.S. Survey Feet

**PSEG Site
ESP Application
Part 2, Site Safety Analysis Report**

**Table 2.5.4.3-2 (Sheet 1 of 2)
Observation Well Location and Construction Summary**

Well Number	Type	Drilling Method	Depth (ft bgs)	Screen Interval (ft. bgs)		Coordinates and Elevations (US Survey Feet)						Well Diameter (I.D. in.)	Formation Screened
				Top	Bottom	Northing	Easting	TOC Elevation	Pad Elevation	Ground Elevation	Static Water Elevation 3/27/09		
EOW-1L	Observation Well	Mud Rotary	107.0	95.0	105.0	232297.6	202758.1	17.91	16.67	16.21	0.92	2	Kw/Vt
EOW-1U	Observation Well	Mud Rotary	50.0	38.0	48.0	232321.6	202758.0	18.01	16.46	16.02	1.20	2	ALLUVIUM
EOW-2L	Observation Well	Sonic	111.0	99.0	109.0	233271.5	202177.7	16.73	14.39	13.94	1.25	2	ALLUVIUM
EOW-2U	Observation Well	Sonic	51.0	39.0	49.0	233274.6	202157.9	16.51	14.32	13.98	2.83	2	Kw/Vt
EOW-4L	Observation Well	Mud Rotary	121.2	110.2	120.2	231772.9	202021.2	22.31	20.30	19.85	1.09	2	Vt
EOW-4U	Observation Well	Mud Rotary	33.0	22.0	32.0	231791.9	202012.1	22.73	20.37	19.98	12.90	2	FILL
EOW-5L	Observation Well	Mud Rotary	121.0	110.0	120.0	233039.7	203021.5	16.17	14.12	13.74	1.30	2	Vt
EOW-5U	Observation Well	Mud Rotary	46.0	35.0	45.0	233056.8	203007.3	15.85	13.85	13.45	1.16	2	ALLUVIUM
EOW-6L	Observation Well	Mud Rotary	102.0	90.0	100.0	232588.1	203300.7	15.23	13.70	13.25	1.30	2	Vt
EOW-6U	Observation Well	Mud Rotary	59.0	47.0	57.0	232587.1	203281.4	15.99	13.81	13.43	1.20	2	ALLUVIUM
EOW-8L	Observation Well	Sonic	79.0	67.0	77.0	231163.5	203516.0	17.89	15.82	15.44	0.60	2	Vt
EOW-8U	Observation Well	Sonic	42.0	30.0	40.0	231144.2	203520.4	18.38	16.04	15.53	1.47	2	FILL/ ALLUVIUM
EOW-9L	Observation Well	Sonic	128.7	117.5	127.5	230925.6	202844.6	18.21	18.40	17.91	0.68	2	Vt
EOW-9U	Observation Well	Sonic	62.2	50.0	60.0	230917.2	202826.0	20.67	18.26	17.85	0.50	2	ALLUVIUM
EOW-10L	Observation Well	Sonic	97.0	85.0	95.0	231706.7	203521.9	14.27	11.99	11.73	1.12	2	Vt
EOW-10U	Observation Well	Sonic	29.0	17.0	27.0	231687.2	203521.3	14.79	12.57	12.16	1.37	2	FILL
NOW-1L	Observation Well	Mud Rotary	92.3	80.0	90.0	234564.0	198449.8	15.19	13.01	12.52	0.56	2	Vt

**PSEG Site
ESP Application
Part 2, Site Safety Analysis Report**

**Table 2.5.4.3-2 (Sheet 2 of 2)
Observation Well Location and Construction Summary^{(a)(b)}**

Well Number	Type	Drilling Method	Depth (ft bgs)	Screen Interval (ft. bgs)		Coordinates and Elevation (US Survey Feet) ^(c)						Well Diameter (I.D. in.)	Formation Screened
				Top	Bottom	Northing	Easting	TOC Elevation	Pad Elevation	Ground Elevation	Static Water Elevation 3/27/09		
NOW-1U	Observation Well	Mud Rotary	58.3	46.1	56.1	234542.7	198443.4	15.20	13.03	12.56	0.61	2	ALLUVIUM
NOW-2L	Observation Well	Sonic	115.3	103.0	113.0	235227.7	197752.8	11.18	8.51	8.26	-0.32	2	Vt
NOW-2U	Observation Well	Sonic	64.3	52.0	62.0	235207.4	197754.9	10.80	8.31	8.05	-0.48	2	ALLUVIUM
NOW-3L	Observation Well	Sonic	102.3	90.0	100.0	234565.5	197897.9	7.66	7.91	7.42	-0.40	2	Vt
NOW-3U	Observation Well	Sonic	52.3	40.0	50.0	234552.8	197885.2	7.71	7.97	7.41	0.15	2	ALLUVIUM
NOW-4L	Observation Well	Mud Rotary	85.0	73.0	83.0	233972.7	198147.9	14.08	11.03	10.64	-0.01	2	Vt
NOW-4UB	Observation Well	Mud Rotary	54.5	42.2	52.2	233963.0	198147.1	13.56	11.45	10.92	0.46	2	KW
NOW-5L	Observation Well	Sonic	102.5	90.2	100.2	234927.5	198438.4	10.54	8.15	7.55	0.31	2	Vt
NOW-5U	Observation Well	Sonic	32.0	19.7	29.7	234907.5	198444.5	10.23	8.18	7.68	2.12	2	FILL
NOW-6L	Observation Well	Sonic	92.3	80.0	90.0	235287.9	198312.8	7.95	7.89	7.80	0.26	2	Vt
NOW-6U	Observation Well	Sonic	47.3	35.0	45.0	235269.4	198313.5	8.59	8.76	8.65	0.76	2	FILL/ ALLUVIUM
NOW-7L	Observation Well	Sonic	97.0	84.7	94.7	234973.4	199675.9	8.70	6.58	6.12	0.59	2	Vt
NOW-7U	Observation Well	Sonic	60.3	48.0	58.0	234975.8	199694.3	8.25	6.65	6.17	0.74	2	Vt
NOW-8L	Observation Well	Sonic	112.0	100.0	110.0	234139.1	199736.2	11.61	9.39	8.93	0.70	2	ALLUVIUM /Vt
NOW-8U	Observation Well	Sonic	49.0	37.0	47.0	234141.6	199755.9	11.68	9.58	9.11	0.84	2	Vt

a) NA = Not Applicable

b) ft bgs = feet below ground surface; I.D. in. = Inside Diameter of PVC Well Casing in Inches; TOC Elevation = Top of PVC Casing (Reference Mark) Elevation; Pad Elevation = Top of Concrete Pad Elevation; Ground Elevation = Ground Surface Elevation next to Concrete Pad; Static Water Elevation = Static Water Level Measurement collected on March 27, 2009

c) Horizontal Coordinates (Northing and Easting) = NAD83 (2007), New Jersey State Plane Coordinate System Zone (2900), U.S. Survey Feet; Elevations = North American Vertical Datum of 1988 (NAVD), U.S. Survey Feet; FILL=Hydraulic Fill; Vt=Vincentown Formation; Kw=Kirkwood Formation

**PSEG Site
ESP Application
Part 2, Site Safety Analysis Report**

**Table 2.5.4.3-3
Summary of SPT Energy Measurements**

Rig Serial No.	Boring No. Tested	Average Measured Energy (Average EFV) (ft.-lbs)^(a)	Energy Transfer Ratio (%)^(b) (Average ETR)
CTB-1 (CME 75 Truck)	EB-2	258.8	73.9%
CTB-2 (CME 75 Truck)	NB-1	245.1	70.0%
CTB-3 (CME 75 Truck)	EB-3	280.3	80.1%
CTB-4 (CME 850 Track)	EB-6	267.5	76.4%

- a) Measured energy is energy based on the EFV method, as outlined in ASTM D4633; two blows produced poor quality data, and were not used to calculate the Average Measured Energy. This may result in more or less blows evaluated for ETR than what is shown on the boring logs. EFV - $EMX * 1000 \text{ lbs/kip}$, where EMX equals the maximum transferred energy measured by the PDA.
- b) Energy Transfer Ratio is the measured energy divided by the theoretical SPT energy of 350 foot-pounds (140 pound hammer falling 2.5 feet). The average EFV and ETR values may differ slightly and insignificantly from those in the PDILOT tables due to roundoff.

**PSEG Site
ESP Application
Part 2, Site Safety Analysis Report**

2.5.4.4 Geophysical Surveys

This subsection presents a summary of geophysical data collected at the PSEG Site. The geophysical data was collected by GEOVision Geophysical Services, Inc. (GEOVision) under the observation of MACTEC Engineering and Consulting personnel. Reports describing the data collection procedures and presenting the results prepared by GEOVision are included in the MACTEC Data Report (Reference 2.5.4.4-2). Subsection 2.5.4.4.1 provides a description of the downhole geophysical testing and borehole suspension velocity logging procedures. Subsection 2.5.4.4.2 provides a description of crosshole seismic velocity measurement procedures. Subsection 2.5.4.4.3 provides a description of downhole seismic velocity measurement procedures. Subsection 2.5.4.7 provides a description of data set analysis and discussion of the response of site materials to dynamic loading.

2.5.4.4.1 Downhole Geophysical Testing and Suspension Velocity Logging

Downhole geophysical testing and suspension velocity logging were performed in three geotechnical boreholes (NB-1, NB-8, EB-3) and in one borehole (EB-8G) advanced adjacent to the geotechnical boring EB-8. Figure 2.5.4.4-1 provides a plan view of exploration locations. Table 2.5.4.4-1 provides details of the testing completed at each location.

The downhole geophysical testing was performed to aid in identification of stratigraphic transitions. Long and short normal resistivity, single point resistance, spontaneous potential, natural gamma, and 3-arm mechanical caliper measurements were completed at a nominal 0.05-foot (ft.) interval for the depth of the boring. The downhole geophysical testing results are presented on Figures 2.5.4.4-2 through 2.5.4.4-5.

There is currently no ASTM standard for the suspension P-S velocity testing procedure. The technical procedure used for the suspension velocity logging was developed by GEOVision and approved by the site exploration team. The approved technical procedure is described as follows.

The OYO/Robertson suspension P-S velocity logging system used at the PSEG Site uses a 19-ft. (5.8-meter [m]) probe. This probe contains a source near the bottom and two biaxial geophone receivers spaced 3.3 ft. (1 m) apart, suspended by a cable. The probe is lowered by winch to a specified depth into the uncased borehole within a flexible sleeve. The source in the probe generates a pressure wave in the borehole fluid (drilling fluid) that is converted to seismic waves (P- and S-waves) at the borehole wall. Along the borehole wall, at each receiver location, the P- and S-waves are converted back to pressure waves in the fluid and received by the geophones. The geophones send the data to the recorder on the surface. The receiver separation permits determination of the average wave velocity of a 3.3-ft. (1-m) high column of soil around the borehole by inversion of the wave travel time between receivers. This procedure is typically repeated every 1.65 ft. (0.5 m) or 3.3 ft (1 m) along the borehole as the probe is moved up the borehole. Comparisons of source-to-receiver and receiver-to-receiver travel time data sets are performed for quality assurance (Reference 2.5.4.4-2).

At the beginning of each survey, the instrument string is lowered to the bottom of the hole and then raised incrementally; recording data points every 1.65 ft. (0.5 m). A column of bentonite-weighted drilling fluid was kept within 2 ft. of the top of the borehole to maintain borehole wall

**PSEG Site
ESP Application
Part 2, Site Safety Analysis Report**

stability during suspension velocity logging. Drilling fluid was circulated in the borehole prior to the logging activities.

Recorded velocity data was processed upon completion of the surveys to develop the velocity-depth plots for the four logged boreholes presented in Figures 2.5.4.4-2 through 2.5.4.4-5 (Reference 2.5.4.4-2). The test shows similar results between P-wave and S-wave velocities along the four profiles logged, as well as the general velocity trends. A discussion of the uniformity of the dynamic profile revealed by the suspension velocity logging is presented in Subsection 2.5.4.7.

2.5.4.4.2 Crosshole Seismic Velocity Testing

Seismic velocity testing was also completed using crosshole techniques at two locations: in the vicinity of boring NB-1 (test holes CH NB-1A, B and C) and in the vicinity of boring NB-8 (test holes CH NB-8A, B and C) (Figure 2.5.4.4-1). Crosshole testing was completed in general compliance with ASTM D 4428 (Reference 2.5.4.4-1).

Crosshole seismic velocity testing was completed in a 3-hole array with hole separation of approximately 10 ft. center to center. Crosshole was completed to assist in validating the horizontal compressional (P) and shear (S) wave velocity measurements obtained with the suspension technique. Test holes for the crosshole testing consisted of 4-inch diameter flush joint PVC casing grouted into an 8-inch diameter (nominal) drilled hole. Casings extended approximately 200 ft. below grade. Borehole deviation logging was conducted in each of the six borings to determine the deviation of the boring from the vertical axis needed to calculate distances between the crosshole measurement points.

A comparison of the S-wave velocity measurements at the NB-1 boring location obtained using suspension and crosshole velocity testing procedures is presented on Figure 2.5.4.4-6. Crosshole P-wave data was not processed at the NB-1 location due to additional noise at that location. A comparison of P- and S-wave velocity measurements at the NB-8 boring location obtained using suspension and crosshole velocity testing procedures is presented on Figure 2.5.4.4-7. Both of these comparisons show agreement in test results for these two in-situ velocity measurement techniques.

2.5.4.4.3 Downhole Seismic Velocity Testing

In addition to the P-S and crosshole testing, seismic velocity testing was completed using downhole techniques in test hole number CH NB-1C, following the approved GEOVision procedure (Reference 2.5.4.4-2). Downhole seismic testing was completed to a depth of approximately 195 ft. at the single test location to further assist in validating the horizontal compressional (P) and shear (S) wave velocity measurements obtained with the crosshole and suspension techniques. A comparison of the P- and S-wave velocity model determined from downhole measurements, and suspension P-S velocity measurements in boring NB-1 is presented on Figure 2.5.4.4-8. As shown in Figure 2.5.4.4-8, there is good agreement between the downhole and suspension velocity measurements, except in the upper 50 ft. of the subsurface profile (within the hydraulic fill, Alluvium and Kirkwood Formation) where large variations in measured velocities occurred with both measurement techniques. The downhole measurements produced higher velocities than the suspension measurements in a thin layer between the 170 and 180 ft. depth. This is likely due to the limited number of downhole data

**PSEG Site
ESP Application
Part 2, Site Safety Analysis Report**

points in this thin layer and the potential error inherent in picking first arrival times with the downhole measurement technique.

2.5.4.4.4 References

- 2.5.4.4-1 ASTM, 2007, "Standard Test Methods for Seismic Crosshole Testing," ASTM D 4428/4428M-07, 2007.
- 2.5.4.4-2 MACTEC Engineering and Consulting, Inc., "Geotechnical Exploration and Testing, PSEG Site Application, Lower Alloways Creek Township, New Jersey," Rev. 0, July 10, 2009.

**PSEG Site
ESP Application
Part 2, Site Safety Analysis Report**

**Table 2.5.4.4-1
Summary of Exploratory Borehole Drilling, Sampling and Testing Locations^{(a)(b)(c)(d)}**

Boring Number	Boring Type		Boring Depth (ft., bgs)	Coordinates and Elevations (U.S. Survey Feet)			In-Situ Testing							
	SPT	UD Tubes	Actual	Northing	Easting	Ground Surface Elevation	P-S Suspension	Deviation	Natural Gamma	Resistivity	Caliper	Spontaneous Potential	Crosshole Seismic	Downhole Seismic
NB-1	x	NA	600.9	234567.6	198469.	12.82	x	x	x	x	x	x	NA	NA
NB-1UD	NA	x	232.3	234556.0	198459.	12.65	NA	NA	NA	NA	NA	NA	NA	NA
CH NB-1A	NA	NA	201.0	234544.4	198483.	12.80	NA	x	NA	NA	NA	NA	x	NA
CH NB-1B	NA	NA	201.0	234537.1	198476.	13.00	NA	x	NA	NA	NA	NA	x	NA
CH NB-1C	NA	NA	201.0	234529.8	198469.	13.31	NA	x	NA	NA	NA	NA	x	x
NB-2	x	x	301.5	235205.0	197764.	8.19	NA	NA	NA	NA	NA	NA	NA	NA
NB-3	x	NA	200.3	234554.7	197895.	7.37	NA	NA	NA	NA	NA	NA	NA	NA
NB-4	x	x	201.3	233960.4	198139.	11.52	NA	NA	NA	NA	NA	NA	NA	NA
NB-5	x	NA	200.0	234891.0	198445.	7.81	NA	NA	NA	NA	NA	NA	NA	NA
NB-6	x	x	200.0	235251.5	198315.	9.26	NA	NA	NA	NA	NA	NA	NA	NA
NB-7	x	NA	201.2	234965.7	199685.	6.21	NA	NA	NA	NA	NA	NA	NA	NA
NB-8	x	NA	315.3	234140.4	199745.	8.94	x	x	x	x	x	x	NA	NA
CH NB-8A	NA	NA	201.0	234137.6	199720.	8.82	NA	x	NA	NA	NA	NA	x	NA
CH-NB-8B	NA	NA	201.5	234130.2	199713.	8.85	NA	x	NA	NA	NA	NA	x	NA
CH-NB-8C	NA	NA	201.0	234122.3	199705.	8.99	NA	x	NA	NA	NA	NA	x	NA
EB-1	x	NA	351.5	232316.7	202774.	15.91	NA	NA	NA	NA	NA	NA	NA	NA
EB-2	x	NA	200.7	233264.7	202166.	14.07	NA	NA	NA	NA	NA	NA	NA	NA
EB-3	x	NA	631.5	232349.0	202473.	16.46	x	x	x	x	x	x	NA	NA
EB-3UD	NA	x	226.2	232350.2	202492.	16.42	NA	NA	NA	NA	NA	NA	NA	NA
EB-4	x	NA	200.2	231783.2	202017.	20.32	NA	NA	NA	NA	NA	NA	NA	NA
EB-5	x	NA	199.3	233048.3	203016.	13.80	NA	NA	NA	NA	NA	NA	NA	NA
EB-6	x	NA	199.9	232587.2	203262.	13.69	NA	NA	NA	NA	NA	NA	NA	NA
EB-6A	x	NA	151.1	232587.0	203251.	14.10	NA	NA	NA	NA	NA	NA	NA	NA
EB-7	x	NA	200.3	232084.2	203023.	16.97	NA	NA	NA	NA	NA	NA	NA	NA
EB-8	x	x	301.7	231160.7	203499.	15.30	NA	NA	NA	NA	NA	NA	NA	NA
EB-8G	NA	NA	315.0	231153.3	203528.	15.73	x	x	x	x	x	x	NA	NA

a) NA = Not Applicable

b) ft. bgs=feet below ground surface

c) EB-6A Drilled to Check SPT Values from 90 to 150 ft. in EB-6 due to hammer problems in EB-6

d) Horizontal Coordinates (Northing and Easting) = NAD83 (2007), New Jersey State Plane Coordinate System Zone (2900), U.S. Survey Feet; Elevations = North American Vertical Datum of 1988 (NAVD), U.S. Survey Feet

**PSEG Site
ESP Application
Part 2, Site Safety Analysis Report**

2.5.4.5 Excavation and Backfill

This subsection discusses the excavation, backfill, and earthwork requirements for the Seismic Category I structures. The following items are addressed in this subsection:

- The lateral and vertical limits of excavation
- Construction excavation and dewatering
- Backfill types, sources, properties, specifications, and quality control testing
- Foundation excavation monitoring

Earthwork for the proposed construction involves the removal of unsuitable materials, both in the overall power block area and below the Seismic Category I structures, and replacement with suitable backfill materials. Two categories of backfill are described later in this subsection – Category 1 and Category 2. Category 1 backfill materials will be placed below the base mat bearing grades of the Category I structures and adjacent to the below-grade walls of the Category I structures. Category 2 backfill will extend laterally beyond the Category 1 backfill areas out to the lateral limits of the power block area. The lateral and vertical extent of the excavation for the Category I structures within the approximately 70-acre power block area will depend on the plant technology chosen. Specific details regarding these items will be addressed in the COLA for the plant design technology selected.

2.5.4.5.1 Plans and Sections

The PPE defines bounding parameters for the four reactor technologies under consideration for the PSEG Site (Section 1.3, Table 1.3-1). A general layout for the limits of the excavation for the new plant location is developed (Figure 2.5.4.5-1). The general layout identifies a power block area within which all Seismic Category I structures for any of the four technologies are located, excluding the outlying river intake structure if required by the specific technology. No specific facility locations within the power block are identified.

With respect to vertical grading, flood studies (see Subsection 2.4.5) result in an external plant grade elevation of 36.9 ft. NAVD. The existing ground surface elevation within the new plant location is within a nominal range of 5 ft. to 15 ft. NAVD. The current grade will be raised to reach the proposed external plant grade. As discussed in Subsection 2.5.5, the proposed overall grading for the site will not result in cut or fill slopes that are close enough to the Seismic Category I structures to affect their performance or safety.

Discussion in the following subsections is based on the general plan shown on Figure 2.5.4.5-1, the plant grade requirements for flood protection, and the dimensional information for the four reactor technologies given in their respective design control documents or Final Safety Analysis Reports.

2.5.4.5.1.1 Lateral Limits of Excavation

The overall lateral limits of excavation extend to the boundaries of the power block area shown on Figure 2.5.4.5-1. The lateral excavation limits for the Seismic Category I structures depend on the plant technology chosen. The PPE does not include lateral dimensions as a parameter. For purposes of the ESPA, bounding plant dimensions encompassing the Seismic Category I structures (excluding the outlying river intake structure, if required by the specific technology),

**PSEG Site
ESP Application
Part 2, Site Safety Analysis Report**

are taken from technology-specific design documents (References 2.5.4.5-2, 2.5.4.5-6, 2.5.4.5-1, and 2.5.4.5-3). The four technologies, along with the dimensions of the nuclear island base mats, the overall lateral limits of the Category I structures and the depths for the foundations, are given in Table 2.5.4.5-1.

A conceptual, non-spatial, depiction of the lateral limits of excavation for the Category I structures is shown on Figure 2.5.4.5-1. The limits of excavation shown encompass the largest length and width of the four technologies. The limits are based on extending a 1(H):1(V) line downward and outward from the shallowest Category 1 structure foundation depth to the top of the competent layer (Subsection 2.5.4.5.1.2) to determine the length and width of the excavation area at the competent layer. The nuclear island excavation is inside the larger overall excavation.

2.5.4.5.1.2 Vertical Limits of Excavation

The PPE shows the bounding condition for reactor building embedment depths as 39 ft. (shallowest) to 84.3 ft. (deepest). These depths are for the reactor building/nuclear island base mat and are referenced to the external plant grade. For an external plant grade of elevation 36.9 ft. NAVD, the range of vertical limits by elevation is -2.1 ft. NAVD to -47.4 ft. NAVD. However, the materials at these elevations have a shear wave velocity less than 1000 ft/sec and are not considered to be a competent foundation layer, therefore additional excavation is needed to reach the competent foundation layer, which has been identified as the Vincentown layer. From the geotechnical evaluation, the elevation of the competent Vincentown layer is -67 ft. NAVD, with an estimated plus or minus variation of 4 ft. (Subsection 2.5.4.7). Therefore, regardless of the technology selected, the vertical excavation for Category 1 structures will extend to approximately elevation -67 ft. NAVD.

Outside of the Category 1 structure area, the hydraulic fill, as well as the soft/loose alluvium, require removal for stability and settlement considerations related to the fill placed to raise the existing ground up to the external plant grade. The excavation depth to accomplish this removal is estimated to be to the top of the Kirkwood Formation.

Figure 2.5.4.5-2 shows a conceptual illustration for the excavation within the power block. An initial excavation to the edges of the power block is made from ground surface down to the approximate top of the Kirkwood Formation. A second vertical excavation is then made in the area of the Category 1 structures to extend from the approximate top of the Kirkwood Formation down to the competent layer within the Vincentown Formation, which is at approximate elevation -67 ft. NAVD.

2.5.4.5.2 Construction Excavation and Dewatering

As discussed in Subsection 2.5.4.5.1.2, the excavation may be performed in two stages, with both stages requiring structural support. As discussed in Subsection 2.5.4.6, the average groundwater level is at approximate elevation 0.8 ft. NAVD. Dewatering is required during construction.

**PSEG Site
ESP Application
Part 2, Site Safety Analysis Report**

2.5.4.5.2.1 Excavation Support

The method of excavation support and the stability of temporary excavation slopes or support are evaluated in the combined license application (COLA). In concept, a combination of structural support, such as cellular cofferdams (used during construction of the Salem facility (Reference 2.5.4.5-5), sheet pile walls (part of the excavation method for the Hope Creek facility) (Reference 2.5.4.5-4) or other wall support systems, can be used for excavation support. Depending on excavation methods, a portion of one side of the excavation near the Delaware River may be partly sloped for dredge access. After dewatering, the initial mass excavation will be extended to the top of the Kirkwood Formation. After the excavation is completed to the Kirkwood, the excavation for the Category 1 structure area, will be to the top of the competent layer within the Vincentown Formation. This second, deeper, excavation is also supported by a structural system. The shoring methods will most likely be left in place as the backfill is placed.

2.5.4.5.2.2 Dewatering

Conceptually, dewatering is accomplished by installing wells around the outer and inner perimeters of the structural support system. The tops of the dewatering wells and the associated piping would be lowered progressively as the depth of the excavation increases. Water is pumped from the wells to one or more collection stations and discharged to the river, after passing through sediment traps or ponds.

Maintaining the water level below the excavation bottom by pumping creates a stable work area for placing fill outside of the plant area, and for preparing the foundations and placing fill to reach the bottom of the nuclear island base mat. The pumping creates a gradient toward the wells that precludes upward gradients into the base of the excavation. Thus, excavation degradation or instability due to upward water seepage or piping should not occur. Additional wells may be added in the bottom of the excavation to control localized seepage into the bottom of the excavation.

The construction dewatering system remains in operation until fill placement and building construction are completed. The influence of dewatering activities on existing structures is discussed in Subsection 2.5.4.6.

2.5.4.5.2.3 Excavation Mapping and Photography

Excavation mapping and photography are typically performed as needed to document the stratigraphy of the materials removed, check for indications of faulting, document the condition of the subgrade at the bearing levels, and check the condition of the structural support system. Mapping and photography also provide a means of verifying the data collected from the borings and providing an as-built record of the conditions present at the time of excavation.

2.5.4.5.3 Backfill

Backfill is required from the base of the excavation to the bearing grade of the Seismic Category I structures. Backfill is also required between the walls of the nuclear island structures and the adjacent excavation support system, and may also be used to raise the overall plant grade. The backfill below the Seismic Category I structures is designated Category I fill, while the fill placed

**PSEG Site
ESP Application
Part 2, Site Safety Analysis Report**

in other areas is designated Category 2 fill. Quantities, types, and sources of backfill are discussed conceptually below. Details for the backfill quantities, types and sources will be discussed in the COLA. Lateral loading conditions are not included as part of the ESPA because information on the type and characteristics of these backfill materials is not available. Additionally, the reactor technology, and its corresponding foundation depth, has not been selected. Lateral pressure evaluation from backfill materials will be evaluated during the COLA phase.

2.5.4.5.3.1 Materials

Possible backfill materials are lean concrete, roller-compacted concrete (RCC), or structural granular material. The sources would be local concrete batch plants or an on-site batch plant for lean concrete and RCC, and a local permitted borrow source for granular fill material. Materials removed from the excavation that meet engineering specification requirements may be considered for use as Category 2 fill.

2.5.4.5.3.2 Backfill Properties

Lean concrete or RCC for backfill purposes beneath and around mat foundations will meet the necessary structural requirements typical to nuclear construction to support Seismic Category I structures. An on-site concrete batch plant will likely be constructed to supply either the fill concrete or the RCC.

According to the previous study for the Hope Creek facility (Reference 2.5.4.5-4), granular fill material was obtained from off-site sources. For this ESPA, use of similar granular material from off-site sources is expected, and the properties are expected to be similar to those of the previously used material. In addition to the material properties requirements, the fill material below the nuclear island or other safety-related structures base grades must exhibit a shear wave velocity greater than 1000 ft/sec. Final granular backfill material properties determination, including shear wave velocity, will be performed as part of the COLA.

The material to be used to raise the overall plant grade above existing grade is designated Category 1 fill if it will support safety-related structures; otherwise it is designated Category 2 fill. Some of the excavated materials may be suitable for use as Category 2 fill.

Subsection 2.5.5 discusses the slopes of the fill above existing grades in the Power Block. Design of the fill slopes is performed for the COLA. As also discussed in Subsection 2.5.5, the outer slopes are protected from scour and erosion by using materials such as riprap, concrete blocks, or mats designed to resist the design basis flood and wave forces.

2.5.4.5.3.3 Compaction Specifications

2.5.4.5.3.3.1 Lean Concrete and Roller-Compacted Concrete

Specifications for placement and compaction of lean concrete and RCC will be developed for the COLA. Requirements of the American Concrete Institute (ACI) and test methods prescribed by ASTM are applied to the property testing during fill placement.

**PSEG Site
ESP Application
Part 2, Site Safety Analysis Report**

Compaction of lean concrete is typically not necessary. If needed, vibration of the concrete fill may be performed in confined areas to prevent the formation of voids or honeycombing of the concrete during placement. Concrete fill placement will be in horizontal layers in accordance with typical concrete placement specifications normally used for nuclear construction. Additional layers of lean concrete are not placed until the underlying lift has reached its initial set. The RCC is typically placed at a low slump and compacted using vibratory equipment. As with lean concrete, additional layers of RCC are not placed until the underlying lift has achieved its initial set.

2.5.4.5.3.3.2 Soil Backfill

Specifications for placing and compacting soil backfill will be developed for the COLA to be specific to the type of backfill identified. Procedures will be developed to control backfill placement including lift thickness, moisture conditioning, compacted density, and testing. Testing will also be performed to verify that the backfill material will exhibit a shear wave velocity greater than 1000 ft/sec below the nuclear island foundation depth. Inspections, Test, Analyses, and Acceptance Criteria (ITAAC) for the backfill and for shear wave velocity will be presented in the COLA as well.

Compacted fill outside of the wall backfill zone at the nuclear island areas is typically placed in near horizontal loose lifts. Backfill will be compacted in accordance with project specifications to be developed at the COL stage of the project. Prior to the commencement of filling operations, samples of potential fill material will be obtained and tested to determine that the index properties, sulfate and chloride content, particle size distribution, maximum dry density, and optimum moisture content values meet the established criteria. Laboratory testing will also be performed on a regular basis during placement to verify that the material being used is consistent and continues to meet design properties. This testing will also include dynamic laboratory testing, including cyclic resonant column/torsional shear testing.

Compaction equipment capable of providing the energy required to obtain the specified compaction will be used in open areas. Near the nuclear island foundation walls, smaller pieces of compaction equipment will be used to reduce the impact of compaction-induced lateral stresses on the adjacent wall. In confined areas, maximum lift thicknesses will be limited in order to achieve proper compaction using the smaller equipment.

A test fill pad may be constructed prior to beginning the backfilling operations to confirm the lift thicknesses, compaction equipment, and number of passes appropriate to achieve the required density.

2.5.4.5.3.4 Quality Control Testing

2.5.4.5.3.4.1 Lean Concrete or Roller-Compacted Concrete

A review of the concrete fill mix design or the RCC mix design will be performed to confirm that either material is acceptable for backfilling purposes. Unconfined compression tests with strain measurements will be performed on representative concrete cylinders made from trial batches of the concrete fill or RCC mix designs to determine the modulus of elasticity and shear wave velocity at design strength.

**PSEG Site
ESP Application
Part 2, Site Safety Analysis Report**

During concrete fill placement beneath the nuclear island base mat foundations, sampling and testing will be performed in accordance with normal nuclear construction practice to verify that the concrete meets the specified strength requirements. Field and laboratory testing of concrete will be performed in accordance with applicable ASTM and ACI standards.

2.5.4.5.3.4.2 Soil Backfill

Following is a description of general quality control procedures typical for controlling placement and compaction of backfill. Specific procedures will be presented during the COLA for the type of backfill identified.

After reaching the base of the excavation, the subgrade is inspected, mapped, and checked for suitability to receive fill. Checking may include probing, cone penetrometer soundings, borings or use of heavy equipment driven across the area (proofrolling) to look for conditions needing repair. Repairs are typically made by removal and replacement, or by aerating and compacting.

Field density testing is performed during fill placement to measure the degree of compaction being obtained. This is generally performed by qualified personnel. Test methods described in ASTM are typically used for field density control.

Shear wave velocity testing will be performed on the compacted backfill to verify that the shear wave velocity at the base elevation of the nuclear island foundation is greater than 1,000 ft./sec. An ITAAC will be prepared for the COLA addressing the testing and acceptance criteria for shear wave velocity.

2.5.4.5.4 Foundation Excavation Monitoring

Observations and monitoring of foundation excavations during construction will be performed by qualified personnel. These observations will be performed during general excavation (first stage of excavation) and during excavation to reach the competent layer for the nuclear island (second stage of excavation). Observation and monitoring will also be performed during placement of Category 1 fill. Fill placement will be documented on daily records.

Geotechnical instrumentation will be installed prior to excavation for the nuclear island structures in order to measure heave of the excavation bottom due to unloading from excavation. General discussion of the geotechnical instrumentation is provided in Subsection 2.5.4.5.4.2.

2.5.4.5.4.1 Mat Foundation Evaluation

Geotechnical personnel will observe and document the initial mat foundation excavation to the top of the competent bearing strata to confirm that the soil conditions conform to those used in design, and as depicted on the boring logs. Documentation will include:

- Types of soil penetrated
- Thicknesses of layers
- Presence and depths to perched groundwater tables
- Equipment used for excavation
- Relative difficulty of excavation

**PSEG Site
ESP Application
Part 2, Site Safety Analysis Report**

- Dewatering system water levels
- Geologic mapping of the exposed soils, including documentation of weathered zones, shear zones or fault traces, if observed

2.5.4.5.4.2 Geotechnical Instrumentation

Instrumentation around excavation support systems is typically installed to monitor deflections during the excavation. Instrumentation installed to measure heave or rebound of the excavation bottom typically consists of extensometers that include an anchor rod placed in a borehole extended some distance below the top of the competent Vincentown Formation. The number of extensometers will depend on the plant technology chosen. The extensometers can also be used to monitor settlement during concrete backfill placement. Long-term settlement of the nuclear island base mat or other safety-related structures is typically performed using survey reference points established at sensitive locations.

An instrumentation plan and monitoring schedule will be presented in the COLA.

2.5.4.5.5 References

- 2.5.4.5-1 AREVA, U.S. EPR Final Safety Analysis Report, Rev. 1, May, 2009.
- 2.5.4.5-2 General Electric-Hitachi, Design Control Document for the ABWR, Rev. 4, 1997.
- 2.5.4.5-3 Mitsubishi Heavy Industries, Ltd., Design Control Document for the US-APWR, Rev. 1, August, 2008.
- 2.5.4.5-4 Public Service Enterprise Group (PSEG), "Hope Creek Generating Station Updated Final Safety Analysis Report," Revision 16, Subsection 2.4.5, May 15, 2008.
- 2.5.4.5-5 Public Service Enterprise Group (PSEG), "Salem Generating Station Updated Final Safety Analysis Report," Revision 23, Subsection 2.4.5, October 17, 2007.
- 2.5.4.5-6 Westinghouse Electric Company, Design Control Document for the AP1000, Rev. 17, September, 2008.

**PSEG Site
ESP Application
Part 2, Site Safety Analysis Report**

**Table 2.5.4.5-1
Summary of Nuclear Plant Technologies**

Plant Technology and Associated Structures	Base Mat Dimensions (ft.) ^(a)	Nuclear Island Plan Dimensions (ft.) ^(a)	Category I Structures Plan Dimensions (ft.) ^(b)	Embedment Depths Below New Plant Grade (ft.) ^(a)
ABWR			890 x 775	
Nuclear Island	186 x 195	185 x 190		84.3
Control Building	79 x 184			76.1
US-APWR			700 x 750	
Nuclear Island	210 x 309	210 x 310		39
Power Source	69 x 115			34.7
UHS Buildings (4)	129 x 131(each)			47 (at sump)
AP1000			960 x 255	
Nuclear Island	165 x 260	160 x 255		39.5
U.S. EPR			960 x 745	
Nuclear Island	360 x 360	360 x 360		41
EPGB	95 x 178			5
ESWS	128 x 164			22

a) Plan dimensions (rounded to nearest foot) and embedment depths from new plant grade are taken from the following sources:

Reference 2.5.4.5-1

Reference 2.5.4.5-2

Reference 2.5.4.5-3

Reference 2.5.4.5-6

b) Dimensions are at the plant grade and encompass the Category 1 structures as shown in the cited DCD documents. Dimensions are rounded to nearest 5 feet.

**PSEG Site
ESP Application
Part 2, Site Safety Analysis Report**

2.5.4.6 Groundwater Conditions

This subsection includes information on the groundwater conditions at the PSEG Site relative to foundation stability for the safety-related structures. Subsection 2.5.4.6.1 discusses the occurrence of groundwater and the groundwater fluctuations. Subsection 2.5.4.6.2 discusses the results of field hydraulic conductivity tests. Subsection 2.5.4.6.3 discusses dewatering during construction, and provides an interpretation and analysis of seepage and potential piping conditions during construction.

2.5.4.6.1 Groundwater Occurrence

Geological and hydrogeological data are determined from the groundwater investigation conducted for the ESPA at the PSEG Site (Reference 2.5.4.6-3) and are discussed in Subsections 2.5.4.1 and 1.4.12.

For the ESPA site investigation, 16 geotechnical borings were drilled to characterize the geologic conditions at the PSEG Site. Subsection 2.5.4.3 provides details of the ESPA subsurface investigation. Subsection 2.5.4.1 provides a description of geologic conditions. Sixteen well pairs (32 groundwater observation wells) were installed as part of the ESPA investigation, generally at the locations of the geotechnical borings. Figure 2.5.4.6-1 shows the locations of the observation wells. Two well pairs (EOW-9U/9L and EOW-10U/L) were installed where no geotechnical boring was drilled.

Eight well pairs were installed in the north area of the site, and eight well pairs were installed at the east area of the site. The eight well pairs located in the north area of the site lie within the approximate limits of the new plant location and are used to characterize groundwater conditions in the area of the safety-related structures. Well NOW-4U was closed shortly after installation (due to a deficiency in the grout seal observed during well development) and replaced with NOW-4UB.

As described in Subsection 2.5.4.3, the lower or deeper well in each well pair was installed within the Vincentown or lower Kirkwood aquifer. With the exception of NOW-5U and NOW-7U, the upper or shallow well in each well pair was installed within the Alluvium. Observation well NOW-5U was installed in the hydraulic fill to assess the properties of the shallow hydraulic fill aquitard. NOW-7U was installed in the Vincentown Formation just below the Alluvium, as it was identified as the first adequate water-bearing zone encountered. Data from these observation wells is used to determine static groundwater levels and hydraulic conductivity for the respective water bearing zones. Data from the monitoring wells is presented and discussed in Subsection 2.4.12. A summary of observation well construction is presented in Table 2.5.4.3-2.

Subsection 2.5.4.1 describes the geologic units present at the site within the depth of interest. . The Vincentown Formation has been determined to be the competent layer for foundation-bearing. Excavation will be made to remove unsuitable materials down to the competent layer. Backfill will be placed from the competent layer up to the foundations of the safety-related structures. Subsection 2.5.4.5.3 describes the backfill.

The artificial fill materials were placed on the site during previous construction activities. Based on visual examination, the lithologies were observed to be variable, and generally included clays, silts, sands with varying silt and clay contents, and clayey and silty gravels. The artificial

**PSEG Site
ESP Application
Part 2, Site Safety Analysis Report**

fill is underlain by hydraulic fill. The hydraulic fill generally consists of soft, discontinuous lenses of clayey silts, silty sands, and organic clays. This unit represents dredge spoils previously deposited on the site from dredging conducted in the Delaware River. The hydraulic fill is underlain by alluvium associated with the Delaware River. The alluvium consists of fine to coarse sand and gravel deposits which formerly comprised the bed of the adjacent Delaware River. Layers of peat and other organic rich soils were also observed within this unit. A lower layer of slightly organic to non-organic micaceous silt and clay was locally encountered near the base of this formation in some borings.

The Alluvium is underlain by the Kirkwood Formation. The Kirkwood Formation consists of two distinct stratigraphic units. The upper unit consists of greenish-gray, silty, fine sand and greenish-gray to brown, organic clay with zones of peat and occasional shell fragments. The lower unit consists of fine to coarse sand and subrounded to subangular gravel with variable silt and clay content. The Vincentown consists primarily of a greenish-gray, fine-grained to medium-grained silty sand with some zones of clayey sand.

The upper water-bearing zone consists of hydraulic fill and Alluvium (riverbed sands and gravels), and is located above the upper unit of the Kirkwood Formation. The hydraulic fill and the Alluvium constitute the shallow groundwater flow system. The base of this flow system is the top of the alluvial clay, if present, or the top of the upper unit of the Kirkwood Formation (a clay-rich, semi-confining unit). The primary recharge to the upper water bearing zone is from direct infiltration of precipitation where not impeded by buildings, pavement, or other storm water diversion structures from the existing plants.

The hydraulic fill acts as an aquitard, therefore, the local estuary and shallow ponds are perched, creating moist to saturated soils, generally from the ground surface through the hydraulic fill.

The less permeable upper unit of the Kirkwood Formation is also considered an aquitard separating the Alluvium from the lower unit of the Kirkwood Formation and Vincentown Formation water-bearing zones. Locally, as indicated in borings NB-2 and NB-7, the upper unit of the Kirkwood Formation was not identified by the geotechnical boring or the adjacent observation wells (NOW-2 and NOW-7). In these areas the aquitard may be very thin or absent. Work performed for the SGS site reports the Kirkwood Formation aquitard (described as the Kirkwood confining unit) as laterally extensive (Reference 2.5.4.6-1) with respect to the SGS site footprint. Therefore, the absence of the upper unit of the Kirkwood Formation in two of the new plant area borings is interpreted as a localized condition.

The lower water-bearing zone consists of sands and gravel of the lower unit of the Kirkwood Formation and the Vincentown Formation. The lower unit of the Kirkwood Formation unconformably overlies the Vincentown Formation and is in hydraulic communication with the Vincentown Formation; where sands and gravels are present. The Vincentown Formation is in hydraulic communication with the Delaware River and, therefore, experiences greater tidal influences than the shallow water-bearing zone.

Historical groundwater elevations for all observed wells are presented in Subsection 2.4.12. A summary of groundwater elevations, measured from January to December, 2009, in observation wells located in the new plant area, is presented in Table 2.5.4.6-1. As shown on Table 2.5.4.6-1, groundwater elevations in the upper water-bearing zone range from -0.5 ft. to 2.2 ft. NAVD.

**PSEG Site
ESP Application
Part 2, Site Safety Analysis Report**

Groundwater elevations in the lower water-bearing zone range from -1.0 ft. to 2.8 ft. NAVD. The average groundwater elevations in the new plant location for observation wells screened in the upper and lower water-bearing zones are 0.82 ft. and 0.80 ft. NAVD, respectively. As shown on Table 2.5.4.6-1, groundwater levels in the upper water-bearing zone fluctuated an average of 1.58 ft., and groundwater levels in the lower water-bearing zone fluctuated an average of 2.18 ft. between January 2009 and December, 2009. The fluctuation is attributable to seasonal variations and, possibly, tidal influences.

The site grade for the new plant, as identified in Subsection 2.5.4.5, is 36.9 ft. NAVD, approximately 25 feet above the existing site grade. As discussed in Subsection 2.5.4.5, excavation of approximately 75 feet will be required to reach a competent layer in the area of the safety related structures. An excavation retention system will be constructed around the perimeter of the excavation as shown in Figure 2.5.4.5-2. A construction dewatering program, conceptually described in Subsection 2.5.4.5.2.2, will be operated until the construction excavation is backfilled.

Groundwater flow modeling results, discussed in Subsection 2.4.12.4, provide an estimate of post-construction groundwater elevation ranging from 6 to 10 ft. NAVD. Based on the planned site grade and the highest post-construction groundwater elevation estimate from the groundwater flow model in the area of the safety-related structures (10 ft. NAVD), the depth to groundwater at the new plant location after construction is more than 25 ft. below the plant grade. Thus, post-construction dewatering is not required.

2.5.4.6.2 Field Hydraulic Conductivity Testing

Field testing for hydraulic conductivity using the procedures described in Section 8 of ASTM D 4044 (Reference 2.5.4.6-2) was conducted in the sixteen observation wells installed in the new plant location as discussed in Subsection 2.5.4.3. The testing was conducted in wells screened in both the upper and lower water-bearing zones. Table 2.5.4.6-2 summarizes the results of the field hydraulic conductivity testing performed for the ESPA. Subsection 2.4.12.1.3.4 discusses the results of the field hydraulic conductivity testing and concludes the values from the ESPA testing are within the range of published values for the regional aquifers.

A tidal study was conducted as described in Subsection 2.4.12.1.3 to determine if the hydraulic conductivity tests were influenced by tidal shifts. The tidal study included the installation of four In-Situ Level TROLL 700 data loggers in two well pairs (NOW 1L and 1U, and NOW-3L and 3U) and the installation of one In-Situ Level TROLL 700 instrument at a Delaware River measuring point. Details and results of the tidal study are presented in Subsection 2.4.12.1.3.6

Based on the data collected during the tidal study, and the time duration of each slug test, water levels in the upper and lower water-bearing zones could have been tidally affected by up to 0.057 ft. and 0.39 ft., respectively, during the slug tests. These potential tidal effects are considered to be negligible.

2.5.4.6.3 Construction Dewatering

Construction dewatering is necessary to allow proper fill placement following the excavation to reach the competent layer. The conceptual dewatering scenario includes initial dewatering of the power block area down to the Kirkwood Formation using perimeter wells spaced

**PSEG Site
ESP Application
Part 2, Site Safety Analysis Report**

approximately 200 feet apart and installed into the Vincentown Formation. A second, smaller, excavation is then made in the area beneath the safety-related structures down to the competent layer with dewatering performed by a second set of wells spaced approximately 200 feet apart installed around that perimeter combined with continued pumping from the first set of wells. Both the power block area and the safety-related area have perimeter retention systems that will act as a barrier to groundwater flow laterally into the excavation. Figure 2.5.4.5-2 illustrates the cross section of the excavation. Figure 2.5.4.6-2 shows the conceptual position of the dewatering wells and the excavation retention used in the model.

As described in Subsection 2.4.12.4, a numerical groundwater flow model is used to aid in evaluating construction and post-construction effects of pumping from the dewatering system. The model covers approximately 1200 acres to simulate the effect on the groundwater elevation by dewatering within the power block area of the new plant location.

Maintaining the water level below the excavation bottom by pumping will create a stable work area for placing fill within the excavation limits of the plant area, and for preparing the bearing material surface and placing fill to reach the bottom of the nuclear island base mat. The pumping creates a gradient toward the wells that precludes upward gradients into the base of the excavation. Thus, degradation or instability of the bearing material due to upward water seepage or piping is not anticipated. Additional wells may be used in the bottom of the excavation to control localized seepage into the bottom of the excavation.

The retention system will provide a barrier to lateral seepage of groundwater into the excavation during construction.

2.5.4.6.3.1 Dewatering Effects on Adjacent Structures

The dewatering creates a decrease of the existing groundwater level in the fill materials and reduction in the existing piezometric surface head in the Alluvium and the Vincentown Formation that extends outward from the excavation in plan view. For purposes of considering dewatering effects, the groundwater surface within the hydraulic fill is used to estimate the effects of groundwater table lowering for the layers above the Vincentown Formation. The piezometric drop within the Vincentown Formation is used for the Vincentown Formation and layers below. Figures 2.5.4.6-3 and 2.5.4.6-4 show the piezometric heads within the hydraulic fill and within the Vincentown Formation after one year of dewatering as contours of depths below the static water levels used for the calibrated baseline model. Figures 2.5.4.6-5 and 2.5.4.6-6 show these contours overlaid onto a general layout plan of the existing HCGS and SGS plants.

From review of Figures 2.5.4.6-5 and 2.5.4.6-6, the existing structures listed below, in order of increasing distance from the new plant excavation, are within the projected zone of dewatering influence.

- Independent Spent Fuel Storage Installation (not safety-related; supported on soil-mix columns bearing in Kirkwood Formation)
- Fuel Oil Tank (not safety-related; supported on piles bearing in Vincentown Formation)
- HCGS Cooling Tower (not safety-related; supported on piles bearing in Vincentown Formation)
- Waste Treatment Plant (not safety-related; supported on shallow foundations)

**PSEG Site
ESP Application
Part 2, Site Safety Analysis Report**

- Auxiliary Boiler Building (not safety-related; supported on piles bearing in Vincentown Formation)
- Material Center (not safety-related; supported on piles bearing in Vincentown Formation)
- HCGS Switchyard (not safety-related; supported on piles bearing in Vincentown Formation)
- HCGS Intake Structure (safety-related; supported on Vincentown Formation)
- Learning and Development Center (not safety-related; supported on piles bearing in Vincentown Formation)
- HCGS Nuclear Island (safety-related; supported on Vincentown Formation)
- Low Level Radioactive Waste Building (not safety-related; supported on piles bearing in Vincentown Formation)
- SGS Nuclear Island (safety-related; supported on Vincentown Formation)
- SGS Intake Structure (safety-related; supported on Vincentown Formation).

Table 2.5.4.6-3 summarizes the drawdowns at the centers of the above structures, in feet below the base groundwater elevations used in the groundwater flow model. When the piezometric head is decreased, the effective vertical pressure exerted by the soil column is increased by the amount of that decrease times the unit weight of water. The increase in vertical effective pressure can cause settlement of soils. The settlement, in turn, can affect the performance of structures supported on the soil, or can add downward loads to pile foundations supporting the structures. The potential effects of the changes in vertical effective pressure on the above-listed structures are discussed in the following subsections. The groundwater flow model and the excavation system and sequence are preliminary at the ESPA stage; further evaluation of dewatering and potential impacts discussed in the subsections below will be performed during the COLA.

2.5.4.6.3.1.1 HCGS and SGS Nuclear Islands

Both the HCGS and SGS nuclear island structures are supported on concrete base mats that are underlain by granular fill and concrete fill that extends to the Vincentown Formation. The Vincentown Formation and underlying strata are generally dense granular materials. Applying the methods used for estimating settlement of the new plant mats that are discussed in Subsection 2.5.4.10.3, and using the same soil properties, potential settlement of the soils supporting the HCGS and SGS nuclear island base mats from the dewatering drawdown is estimated at less than 0.3 inch (in.) and less than 0.1 in., respectively.

2.5.4.6.3.1.2 HCGS Plant Area Buildings

Most permanent site structures in the HCGS Plant area outside of the nuclear island are supported on piles, and the pile design included provisions for additional loads resulting from settlement of surrounding soils (Reference 2.5.4.6-4). Thus, settlement of the hydraulic fill or Kirkwood Formation soils would not cause unanticipated loads on the piles. These structures are the Cooling Tower, the Fuel Oil Tank, the Auxiliary Boiler Building, the Switchyard Structures, the Learning and Development Center, the Material Center or the Low Level Radioactive Waste Building. The materials below the pile bottoms are estimated to have settlement due to drawdown-induced stress increases ranging from approximately 0.3 in. at the Learning and Development Center (most distant from the excavation) to approximately 0.6 in. at the Fuel Oil Tank and Cooling Tower (closest to the excavation). Such settlements move the entire structure and overlying soils down as a unit, resulting in minimal impacts.

Rev. 4

**PSEG Site
ESP Application
Part 2, Site Safety Analysis Report**

2.5.4.6.3.1.3 Independent Spent Fuel Storage Installation

The Independent Spent Fuel Storage Installation (ISFSI) foundation is a structural mat that is supported on soil-mixed columns that extend into the Kirkwood Formation. The soil-mixed columns create a block of improved soil with a bearing pressure suitable for the mat. The loads applied to the mat are analyzed as directly transferred to the material below the improved block.

For the drawdown range in Table 2.5.4.6-3, the estimated settlement of the soils below the improved block ranges from 1 to 1-1/2 in. The improved block of soil and the ISFSI mat on it could thus settle a similar amount. Because the improved soil block and the unimproved soils adjacent to it would each undergo settlement, development of downdrag forces within the improved soil block is not likely.

2.5.4.6.3.1.4 Buildings on Shallow Foundations

Various lightly-loaded buildings, including the Waste Treatment Plant (identified on earlier plant layouts as the sewage treatment plant) are supported on foundations bearing at shallow depths below the existing plant grade. These foundations are underlain by all the geologic strata described in Subsection 2.5.4.6.1. The primary source of settlement under increased stresses from drawdown is consolidation of the soft, clayey hydraulic fill and the clay portion of the Kirkwood Formation. Additional settlement arises from elastic compression of the Alluvium, Lower Kirkwood Formation, Vincentown Formation and deeper layers. The estimated consolidation settlement of hydraulic fill and Kirkwood Formation at the Waste Treatment Plant is estimated at approximately 1.3 in. The estimated settlement from the elastic compression is estimated at 0.6 in. for a total settlement estimate of 1.9 in. Buildings supported on shallow foundations where less drawdown is indicated will experience less settlement. The settlement will be an area settlement and will include pipes and other surrounding items such as roads and parking areas. Differential settlement between a building and adjacent areas is not expected.

2.5.4.6.4 References

- 2.5.4.6-1 ARCADIS G&M, Inc., "Remedial Investigation Report, PSEG Nuclear LLC, Salem Generating Station, Hancock's Bridge, New Jersey," March 2004.
- 2.5.4.6-2 ASTM, 2008, "Standard Test Method (Field Procedure) for Instantaneous Change in Head (Slug) Tests for Determining Hydraulic Properties of Aquifers," ASTM D 4044-08, 2008.
- 2.5.4.6-3 MACTEC Engineering and Consulting, Inc., "Geotechnical Exploration and Testing, PSEG Site Application, Lower Alloways Creek Township, New Jersey," Rev. 0, July 10, 2009
- 2.5.4.6-4 Public Service Enterprise Group (PSEG), "Hope Creek Nuclear Generating Station Updated Final Safety Analysis Report," Revision 16, Subsection 2.5.4, May 15, 2006.

**PSEG Site
ESP Application
Part 2, Site Safety Analysis Report**

**Table 2.5.4.6-1
Summary of Groundwater Elevations, January 2009 to December 2009 – New Plant Area**

Observation Well No.	Jan	Feb	Mar	Apr	May	Jun	Jul	Aug	Sept	Oct	Nov	Dec	Minimum Groundwater Elevation, ft.	Maximum Groundwater Elevation, ft.	Average Groundwater Elevation, ft.	Groundwater Elevation fluctuation, ft.
Shallow Hydraulic Fill Aquitard Observation Well Groundwater Elevation (ft. NAVD)																
NOW-5U ⁽¹⁾	2.54	2.04	2.12	2.07	1.20	2.74	2.59	2.12	2.55	2.87	2.53	3.20				
Upper Water Bearing Zone Observation Wells Groundwater Elevations (ft. NAVD)																
NOW-1U		0.36	0.61	0.59	0.66	1.32	1.14	0.94	1.13	1.22	1.18	-0.48	-0.48	1.32	0.79	1.80
NOW-2U	-0.10	-0.42	-0.48	-0.17	-0.08	2.04	-0.41	1.72	2.08	2.19	-0.20	0.88	-0.48	2.19	0.59	2.67
NOW-3U	-0.21	-0.36	0.15	-0.19	0.18	1.20	0.56	0.66	1.13	1.18	0.60	1.23	-0.36	1.23	0.51	1.59
NOW-4UB		0.03	0.46	0.36	0.40	1.18	1.00	0.75	0.95	1.09	0.95	1.34	0.03	1.34	0.77	1.31
NOW-6U	0.50	0.35	0.76	0.62	0.65	1.35	1.12	0.98	1.31	1.31	1.15	1.44	0.35	1.44	0.96	1.09
NOW-7U ⁽²⁾	0.40	0.18	0.74	0.77	0.79	1.40	1.14	1.07	1.41	1.46	1.01	1.64	0.18	1.64	1.00	1.46
NOW-8U	0.72	0.41	0.84	0.74	0.86	1.57	1.24	1.21	1.38	1.39	1.15	1.57	0.41	1.57	1.09	1.16
														Average	0.82	1.58
Lower Water Bearing Zone Observation Wells Groundwater Elevations (ft. NAVD)																
Observation Well No.	Jan	Feb	Mar	Apr	May	Jun	Jul	Aug	Sept	Oct	Nov	Dec	Minimum Groundwater Elevation, ft.	Maximum Groundwater Elevation, ft.	Average Groundwater Elevation, ft.	Groundwater Elevation fluctuation, ft.
NOW-1L		0.25	0.56	0.50	0.65	1.58	1.07	1.14	1.54	1.66	1.02	1.67	0.25	1.67	1.06	1.42
NOW-2L	-0.05	-0.31	-0.32	-0.20	0.74	2.16	-0.17	1.86	2.82	2.15	-0.01	1.10	-0.32	2.82	0.81	3.14
NOW-3L	-0.14	-0.25	-0.40	0.10	-0.99	1.63	0.10	1.69	1.90	1.38	0.61	1.25	-0.99	1.90	0.57	2.89
NOW-4L	-0.71	-0.30	-0.01	-0.16	0.37	1.70	0.43	1.20	1.80	1.56	0.43	1.45	-0.71	1.80	0.65	2.51
NOW-5L	0.54	-0.19	0.31	0.35	0.52	1.54	0.93	0.73	1.54	1.59	0.65	1.57	-0.19	1.59	0.84	1.78
NOW-6L	-0.11	-0.08	0.26	0.17	-0.58	1.56	0.88	0.80	1.54	1.63	1.04	0.21	-0.58	1.63	0.61	2.21
NOW-7L	0.39	-0.81	0.59	0.70	0.71	1.11	0.87	0.94	1.34	1.39	0.75	1.51	-0.81	1.51	0.79	2.32
NOW-8L	0.50	0.36	0.70	0.79	0.90	1.54	1.15	1.14	1.44	1.43	1.08	1.51	0.36	1.54	1.05	1.18
														Average	0.80	2.18

NOTES:

Elevations = North American Vertical Datum of 1988 (NAVD), U.S. Survey Feet

U = Wells screened in the upper water bearing zone; L = Wells screened in the lower water bearing zone.

NOW-4U replaced by NOW-4UB February 10, 2009. Blank Space = Well not installed at time of sampling event.

(1) Well screened in Hydraulic Fill. Water levels are perched and do not appear to be hydraulically connected to the upper water bearing zone.

(2) Well screened in Vincentown but appears to be hydraulically connected to the upper water bearing zone.

**PSEG Site
ESP Application
Part 2, Site Safety Analysis Report**

**Table 2.5.4.6-2
Summary of In-Situ Hydraulic Conductivity (Slug Test) Results^{(e)(i)}**

Upper Water Bearing Zone Observation Well ID^(a)	TOC Elevation (ft. NAVD)^{(f)(h)}	Screen Interval (ft. bgs)^(c)	Average coefficient of hydraulic conductivity, k (ft/day)^{(d)(g)}
NOW-1U	15.2	46 to 56	8.0
NOW-2U	10.8	52 to 62	8.0
NOW-3U	7.71	40 to 50	0.3
NOW-4UB	13.56	42.to 52	0.9
NOW-5U	10.23	19 to 29	0.2
NOW-6U	8.59	35 to 45	3.5
NOW-7U	8.25	48 to 58	1.4
NOW-8U	11.68	37 to 47	0.4

Lower Water Bearing Zone Observation Well ID^(b)	TOC Elevation (ft. NAVD)^{(f)(h)}	Screen Interval (ft. bgs)^(c)	Average k (ft/day)^{(d)(g)}
NOW-1L	15.19	80 to 90	4.5
NOW-2L	11.18	103 to 113	3.6
NOW-3L	7.66	90 to 100	1.4
NOW-4L	14.08	73 to 83	10.7
NOW-5L	10.54	90 to 100	1.7
NOW-6L	7.95	80 to 90	6.2
NOW-7L	8.7	84 to 94	2.4
NOW-8L	11.61	100 to 110	0.3

a) U = Observation wells screen in the upper water-bearing zone.

b) L = Observation wells screen in the lower water-bearing zone.

c) ft. bgs = feet below ground surface.

d) ft/day = feet per day.

e) Slug tests conducted in accordance with ASTM D 4044-96 (02).

f) TOC Elevation = Top of PVC Casing (Reference Mark) Elevation.

g) Average hydraulic conductivity determined by the average of the rising and falling head tests performed at each location.

h) Elevations = North American Vertical Datum of 1988 (NAVD), U.S. Survey Feet

i) No slug testing conducted on wells in the eastern portion of the site.

**PSEG Site
ESP Application
Part 2, Site Safety Analysis Report**

**Table 2.5.4.6-3
Summary of Drawdowns at Existing Structures**

Structure	Distance from Structure Center to Edge of Excavation, (ft.) ^(a)	Groundwater Drawdown in Hydraulic Fill after 1 year (ft.) ^(b)	Groundwater Drawdown in Vincentown Formation after 1 year (ft.) ^(d)
Independent Spent Fuel Storage Installation	330	9.5 - 14.5 ^(c)	36 - 51 ^(c)
Fuel Oil Tank	330	12.5	33.5
HCGS Cooling Tower	530	9.5	36
Waste Treatment Plant	550	11	33.5
Auxiliary Boiler Building	850	6	30
Material Center	1250	4.5	18.5
HCGS Switchyard	1600	5.5	18.5
HCGS Intake Structure	1625	1.5	10
Learning and Development Center (Nuclear Administration Building)	1700	4	17.5
HCGS Nuclear Island	1700	3.5	18.5
Low Level Radioactive Waste Building	1800	3	13.5
SGS Nuclear Island	3050	1	7.5
SGS Intake Structure	3500	1	4.5

a) Taken from Figure 1.2-3

b) Taken from Figure 2.5.4.6-3

c) Range is from end of structure nearest excavation to the ISFSI area most distant from the excavation.

d) Taken from Figure 2.5.4.6-4

**PSEG Site
ESP Application
Part 2, Site Safety Analysis Report**

2.5.4.7 Response of Soil and Rock to Dynamic Loading

This subsection discusses the subsurface properties at the PSEG Site (seismic wave velocity, shear modulus, damping, Poisson's ratio) applicable for evaluation of earthquake ground motion site response. Subsection 2.5.4.7.1 discusses the results of the field and laboratory data obtained as described in Subsections 2.5.4.2 and 2.5.4.4. Subsection 2.5.4.7.2 describes the general geology of the site, Subsection 2.5.4.7.3 discusses effects of past earthquakes, Subsection 2.5.4.7.4 discusses the development of the site dynamic profile. Subsection 2.5.4.7.5 discusses modulus reduction and damping values. Subsection 2.5.4.7.6 briefly discusses the development of the site GMRS that is more fully described in Subsection 2.5.2.6. For an ESPA, development of the GMRS at the top of a competent layer is the end result of the dynamic analyses; development of foundation input response spectra (FIRS) is performed during the COLA studies. Information in this subsection is referenced in Subsections 3.7.1 and 3.7.2 of the COLA for the Soil Structure Interaction (SSI) analysis.

2.5.4.7.1 Soil Dynamic Property Data

The following techniques were used to measure dynamic properties for the PSEG Site:

- Field measurements
 - Suspension P-S seismic velocity logging surveys ranging to a depth from approximately 300 ft. to 630 ft. in 4 boreholes
 - Crosshole seismic velocity measurements to depths of about 200 feet in 2 boreholes in the new plant location
 - Down-hole seismic velocity measurements to a depth of about 200 feet in 1 of the crosshole boreholes in the new plant location
- Laboratory measurements
 - Resonant column and torsional shear (RCTS) tests on 5 undisturbed soil samples

The field measurements and laboratory test methods and results are discussed in Subsections 2.5.4.4 and 2.5.4.2, respectively. As discussed in Subsection 2.5.4.2.2, shear wave velocities from the RCTS tests represent only small increments within the strata and, due to the presence of dense soils with cemented layers, the samples are susceptible to disturbance. As discussed in Subsection 2.5.4.4, the results from the crosshole and down-hole velocity methods show agreement with the results from the P-S suspension logging results in the adjacent boreholes. Therefore, for development of the site velocity profile, the P-S suspension logging results were used. The crosshole and P-S results were in good agreement and the P-S method provides closer spaced data for analysis.

2.5.4.7.2 Geologic Overview

Geologic units beneath the PSEG Site and above the crystalline basement rock include the following (described in detail in Subsection 2.5.4.1.2):

- Artificial Fill and Hydraulic Fill
- Alluvium (Quaternary)
- Kirkwood Formation (Neogene/Upper Tertiary)
- Vincentown Formation (Paleogene/Lower Tertiary)
- Hornerstown Formation (Paleogene/Lower Tertiary)

**PSEG Site
ESP Application
Part 2, Site Safety Analysis Report**

- Navesink Formation (Upper Cretaceous)
- Mount Laurel Formation (Upper Cretaceous)
- Wenonah Formation (Upper Cretaceous)
- Marshalltown Formation (Upper Cretaceous)
- Englishtown Formation (Upper Cretaceous)
- Woodbury Formation (Upper Cretaceous)
- Merchantville Formation (Upper Cretaceous)
- Magothy Formation (Upper Cretaceous)
- Potomac Formation (Lower Cretaceous)

Note that some geologic sections show the presence of the Manasquan Formation above the Vincentown Formation at the PSEG Site. The detailed site exploration did not encounter materials fitting the published description of Manasquan Formation. Materials encountered immediately above the Vincentown Formation in the borings were identified as the Kirkwood Formation, consistent with the geologic information from the Hope Creek and Salem plants (References 2.5.4.7-8 and 2.5.4.7-9).

The crystalline basement rock is a complex of metagranites and metavolcanic rocks. The depth to the crystalline basement rock is discussed in Subsection 2.5.4.7.4.2.

Table 2.5.4.7-1 presents average, maximum and minimum elevations for the Vincentown Formation and formations below the Vincentown Formation. As indicated on the table, stratigraphy in the PSEG Site is generally sub-horizontal and of consistent thickness, with the exception of an erosional surface at the top of the Vincentown Formation. Borings across the new plant location (NB series) show a relief of about 37 feet for this erosional surface. Subsection 2.5.4.1.3 contains a discussion of the lateral consistency of the formations. Borehole summary sheets show simplified borehole logs with corresponding suspension velocity survey data (Figures 2.5.4.7-1A, B, and C; 2.5.4.7-2A and B; 2.5.4.7-3A, B, and C; and 2.5.4.7-4A and B).

2.5.4.7.3 Effects of Prior Earthquakes on Site

As discussed in Subsection 2.5.3.1, no earthquakes larger than estimated body wave magnitude (E_{mb}) 4.45 have been recorded within the site vicinity. As discussed in Subsection 2.5.3.1.6, results of literature review, aerial photograph reviews and inspections of the area from low altitude over-flights has not noted evidence for liquefaction features. Much of the area surrounding the site location has ground cover from agriculture or development, therefore there is little exposure for evaluating the presence of liquefaction features such as sand blows, or fissures from lateral spreading. Excavation mapping within the existing Hope Creek unit did not note the presence of earthquake-induced features.

2.5.4.7.4 Calculation of Dynamic Soil Property Profiles

2.5.4.7.4.1 Shallow Soil Dynamic Profile.

Review of the boring and seismic velocity logging data shows the materials in the Hydraulic Fill, Alluvium and Kirkwood Formation are soft clays or silts and loose sands with shear wave velocities less than 1000 feet per second (ft/sec). These materials are considered unsuitable for the loadings that would be imposed by any of the reactor technologies under consideration.

Rev. 4

**PSEG Site
ESP Application
Part 2, Site Safety Analysis Report**

These materials will be removed below the Category I structures to reach a competent layer and replaced with a suitable backfill as discussed in Subsection 2.5.4.5. As allowed in Section 5.3 of RG 1.208, the GMRS is calculated at the outcrop of the competent layer that will exist after the excavation (to the top of the uppermost competent layer).

The boring information available and experience reported from the nearby Hope Creek excavation (Reference 2.5.4.7-8) indicates the upper 5 to 10 feet of the Vincentown Formation has variable weathering conditions that may require removal after foundation inspection. From review of the boring and geophysical logging data, the top of the competent layer for analysis has been taken at approximately elevation -67 ft. NAVD with an expected variation of plus or minus 4 feet. Elevation -67 ft. also is near the lower point of the relief in the surface of the Vincentown Formation.

Table 2.5.4.7-2 contains the thicknesses, from the top of the competent layer downward, of the strata in the new plant area (NB borings). The table values show consistent thicknesses of the underlying formations. Table 2.5.4.7-3 shows the lateral variation in shear wave velocity within the same geologic formation, as measured by the ratio of the highest to lowest velocity, is less than 1.4. Thus, one vertical dynamic profile is appropriate to characterize the velocity data for use as a base for the GMRS. The vertical dynamic profile is taken from the top of the competent layer in the Vincentown Formation with velocity data above that level not used.

Velocity layer models are developed for each of the P-S suspension velocity logs by plotting travel time measurements against depth and noting changes in the slope of the resulting lines (representing shear and compressional wave velocities). This analysis is demonstrated in Figures 2.5.4.7-5A, B, C and D, where data points are plotted as triangles, and best fit intervals for the regression line (e.g., mean velocity) are called out graphically. In these figures, the data points are frequently so well aligned that the regression line obscures them on the figure. Note that the layers above the Vincentown Formation are included for completeness of the data.

Each velocity layer model is checked and found to be satisfactory and mean shear wave (V_s) and compressional wave (V_p) velocities are determined using the equation (Reference 2.5.4.7-7):

$$b = \frac{\sum(x - \bar{x})(y - \bar{y})}{\sum(x - \bar{x})^2} \quad (\text{Equation 2.5.4-1})$$

to calculate the slope (b) of the least-squares regression line through depth and travel time data for each layer. In the equation, x is travel time (sec.), y is depth (ft.), \bar{x} is mean travel time (sec.), and \bar{y} is mean depth (ft.).

The resulting mean velocities determined from the slope analysis are overlaid on plots of the depth against shear and compressional wave velocity measurements as shown on Figures 2.5.4.7-6A, B, C, and D and observed to be reasonable.

Figures 2.5.4.7-6A, B, C, and D show that vertical variations in shear and compression wave velocities are associated closely with changes in the geologic strata. Within the geologic strata, though, similar shear wave velocity values exist in the four P-S suspension logged boreholes. Due to the dip of the geologic strata, depth-based plots of shear wave velocity cannot be directly compared. For purposes of analysis, the individual layer plots shown on Figures 2.5.4.7-6A, B,

**PSEG Site
ESP Application
Part 2, Site Safety Analysis Report**

C, and D were aligned by matching the elevations of the Navesink Formation, a layer that was easily distinguished in the field sampling by its distinctive color and composition, using boring NB-1, which is near the middle of the new plant location, as a base. Figure 2.5.6.7-7 shows the shear wave mean velocities from Figures 2.5.4.7-6A, B, C, and D aligned to the Navesink Formation. The site soil dynamic profile was developed using the information on Figure 2.5.4.7-7 and the geologic stratification from boring NB-1.

After developing the P-S suspension velocity layer model shown on Figure 2.5.4.7-7, V_s and V_p values of the layer velocity model were averaged horizontally by elevation using an arithmetic averaging approach. Some thinner layers that were identified within the same geologic formation with small changes in shear wave velocity were combined to form the final profile layering. The resulting means of suspension velocity data for the profile were used to calculate Poisson's ratio (σ) values (dimensionless) by layer elevation using the equation (Reference 2.5.4.7-6):

$$\sigma = \frac{0.5(V_p/V_s)^2 - 1}{(V_p/V_s)^2 - 1} \quad (\text{Equation 2.5.4-2})$$

Table 2.5.4.7-4 summarizes the layer-by-layer information on V_s , V_p and σ . Figures 2.5.4.7-8a (for shear wave velocity) and 2.5.4.7-8b (for compressive wave velocity) show the resulting layered vertical profile with variability assigned to each layer velocity. For variability, a Coefficient of Variation of 0.25 was applied to the layers where four sets of P-S suspension logging data were available (above a depth of about 300 feet). This variability encompasses the differences between the P-S logging results and the crosshole and downhole measurements. Below about 300 feet, where only two boreholes were logged using the P-S logging, a Coefficient of Variation of 0.3 was applied. The portions of Figures 2.5.4.7-8a and 2.5.4.7-8b extending to a depth of about 600 feet represents the soil dynamic profile where site-specific data are available. Below about 600 feet, no site-specific shear wave or compressive wave velocity data were obtained. The development of a deep profile extending to the crystalline basement rock is discussed in the following subsection.

2.5.4.7.4.2 Deep Soil Dynamic Profile.

The deep portion of the dynamic profile was taken to begin at the top of the Potomac Formation (about elevation -454 ft. NAVD) and extend into the crystalline basement rock (seismic basement). The seismic basement is defined as material with a shear wave velocity greater than 9200 ft./sec. and is the basis for existing attenuation relationships defined for generic rock conditions for the Central and Eastern United States (Reference 2.5.4.7-2). The crystalline basement rock is estimated to have a shear wave velocity greater than 9200 ft./sec. based on seismic refraction measurements reported for the Delmarva Power and Light Summit site (Reference 2.5.4.7-4) and discussed in a subsequent paragraph.

Figure 2.5.4.7-9 shows three basement surface contour maps that extend from Delaware across New Jersey. These maps indicate the top of the basement in the vicinity of the PSEG Site ranges between elevation -1500 ft. and -2000 ft NAVD. As discussed in Section 2.5.1.2.2.2., there is one deep well (PSEG-6) on the PSEG Site that indicated a top of basement rock at a depth of 1800 ft. (termination point of the well). The ground surface at the well location was not available, but a typical ground surface elevation of + 10 ft. is indicated on borings performed at the Hope Creek site (Reference 2.5.4.7-8), resulting in an approximate basement elevation of -1790 ft. NAVD for the PSEG-6 well. The top of basement rock directly below the PSEG Site was

Rev. 4

**PSEG Site
ESP Application
Part 2, Site Safety Analysis Report**

estimated as elevation -1750 ft. NAVD by interpolating among the nearest contour lines shown on Figure 2.5.4.7-9 and the PSEG-6 well information. A range in elevation of +/- 200 ft. was selected based on the regional contour maps in Figure 2.5.4.7-9.

The P-S suspension logging data from ESPA borings NB-1 and EB-3 and the resulting velocity layering discussed in Subsection 2.5.4.7.1 were used to the depth available. Below the depth of available site data, information from two seismic refraction survey lines reported in the Preliminary Safety Analysis Report (PSAR) for the Delmarva Power Summit Site (Reference 2.5.4.7-4) was correlated stratigraphically to the PSEG Site and the velocity layering used to develop a representative velocity profile. The stratigraphy from the PSEG Site to the Delmarva Summit Site was correlated using regional cross-sections A-A' and B-B' located as shown on Figure 2.5.4.7-10 (Reference 2.5.4.1-4) coupled with a review of the stratigraphy described in the Delmarva Summit Site PSAR (Reference 2.5.4.7-4) Figure 2.5.4.7-11 shows the correlation cross-section for the Summit Site and the PSEG Site. Figures 2.5.4.7-12 and 2.5.4.7-13 show the refraction survey lines for the Summit Site.

The regional stratigraphy correlated to the stratigraphy at the Summit Site and the Vp profile from the refraction surveys shown on Figures 2.5.4.7-12 and 2.5.4.7-13 is summarized on Figure 2.5.4.7-14.

Using estimates of Poisson's Ratio of 0.35 to 0.45 for the soil portion (Layers 2a and 2b on Figure 2.5.4.7-15) and 0.25 to 0.40 for the basement rock (Layer 3 on Figure 2.5.4.7-15), estimated Vs values were calculated by the equation in 2.5.4.7.4.1. Figure 2.5.4.7-15 shows the results. The resulting Vs estimate for Layer 2 was then used to compare with the P-S suspension velocity data for the upper portion of the Potomac Formation at the PSEG Site to determine the best estimate Vs profile for the remaining Potomac Formation. The resulting Vs for Layer 3 yielded a conservative estimate of Poisson's ratio with a more reasonable value being less than 0.37 resulting in a Vs higher than 9200 feet per second.

As discussed in Subsection 2.5.1.2.2.2.1, the Potomac Formation (deep profile) at the PSEG Site is about 1300 ft. thick. The top of the Potomac Formation as discussed in Subsection 2.5.4.1.2.1.1 is at about elevation -454 ft. NAVD. Thus the Potomac Formation extends from about elevation -454 ft NAVD to about elevation -1750 ft. NAVD. The deep profile was divided into layers of about 430 feet thick for the purpose of estimating an increasing Vs profile with depth to account for increasing overburden pressure. An evaluation of increasing Vs with increasing in-situ stress as well as variability of Vs measurements was made using P-S suspension log results from a Coastal Plain site in South Carolina (Washington Savannah River Company (Reference 2.5.4.7-12). Figure 2.5.4.7-16 shows a depth plot of Vs from the P-S logs as well as the calculated mean and +/- 1 sigma for the South Carolina site (Savannah River site). The effect of in-situ stress on Vs was estimated by scaling the increase in Vs over depth which indicated an increase of about 2 feet per second, per foot of depth. The +/- sigma was estimated to be the same as shown on Figure 2.5.4.7-16.

Figures 2.5.4.7-8a and 2.5.4.7-8b include the deep profile with the shallow profile. Where the site-specific P-S logging data extended below elevation -454 ft., the top of the deep profile, the shear wave velocity from the site data (2146 ft./sec.) was increased slightly to match the upper layer in the deep profile (Vs= 2200 ft/sec).

**PSEG Site
ESP Application
Part 2, Site Safety Analysis Report**

2.5.4.7.5 Evaluation of Modulus Reduction and Damping Values

Testing of five intact samples using the RCTS method samples was conducted as described in Subsection 2.5.4.2.1.3.4. These tests are on materials from the Vincentown, Hornerstown and Navesink Formations. A discussion of data analysis methods and conclusions is located in Subsection 2.5.4.2.2.2. Damping ratio and the modulus reduction ratio results plotted on the generic EPRI curves for Eastern North America (Reference 2.5.4.7-3) are shown in Figures 2.5.4.7-17 through 2.5.4.7-20.

The plotted data are similar to the shape of the EPRI curves within the range of the test strains, but more linear. This is because the presence of the cemented layers within the formations and the dense consistency as described in Subsections 2.5.4.1.2.2.8, 2.5.4.1.2.3.1 and 2.5.4.1.2.3.2 created difficulties in obtaining intact samples resulting in some sample disturbance. Also, because of the existence of cemented layers, the intact samples obtained would represent the sands between cemented layers. Thus, the RCTS test results are not representative of the behavior of the formation itself.

The plots of data from the tests conducted at four times the estimated in-situ confining pressure shown on Figures 2.5.4.7-19 and 2.5.4.7-20 show a closer match to EPRI curves from depths comparable to the sample depths, although the test data are still below the generic curves in most instances. Figure 2.5.4.7-20 also shows a wide scatter for the variation of damping with strain. The RCTS data were obtained on samples only from the Navesink Formation or higher. The RCTS test results were not used to predict modulus reduction and damping variation with shear strain because of the inconsistent RCTS test results compared to EPRI generic curves and because modulus reduction and damping curves are needed for materials deeper than the sampled depths. Computational techniques for modeling modulus reduction and damping variation related to shear strain, as described below, were used.

Work at the University of Texas (References 2.5.4.7-10 and 2.5.4.7-16) presents results of analysis of many RCTS tests on sandy and clayey soils to develop equations for modulus reduction and damping variation with shear strain as well as standard deviation. The equations, developed by Darendeli, use the confining pressure, plasticity index and overconsolidation ratio as inputs. For the PSEG Site, soils below the top of the competent layer and above the Potomac Formation were divided into four layers. Table 2.5.4.7-5 summarizes information about the layers.

For each layer, the effective confining pressure at the layer center was determined by using the depth of the layer below the top of the competent layer and soil unit weights. To account for the effects of materials above the competent layer, the confining pressure was increased to consider the weight of fill placed from the top of the competent layer to the new plant grade elevation. Stresses from removal of the existing materials were included. A range of overconsolidation ratios and associated K_0 values were applied as shown on Table 2.5.4.7-5. The curves computed using the data on Table 2.5.4.7-5 are shown in Figures 2.5.4.7-21 through 2.5.4.7-28. These curves provide input for the development of the GMRS as discussed in Subsection 2.5.2.5.

**PSEG Site
ESP Application
Part 2, Site Safety Analysis Report**

2.5.4.7.6 Development of Ground Motion Response Spectra

The GMRS for the ESPA is derived at the top of competent material. The average shear wave velocity seismic profile is shown on Figure 2.5.4.7-8a. Derivation of the GMRS based on this velocity profile is described in Subsection 2.5.2.5.

2.5.4.7.7 References

- 2.5.4.7-1 Benson, R. N., "Internal Stratigraphic Correlation of the Subsurface Potomac Formation, New Castle County, Delaware, and Adjacent Areas in Maryland and New Jersey", Delaware Geologic Survey Report of Investigations No. 71, 2006.
- 2.5.4.7-2 Electric Power Research Institute, "Seismic Hazard Methodology for the Central and Eastern United States," EPRI NP-4726, 1986.
- 2.5.4.7-3 Electric Power Research Institute, "Guidelines for Determining Design Basis Ground Motions," Vol. 1, TR-102293, November, 1993.
- 2.5.4.7-4 Delmarva Power and Light Company, "Preliminary Safety Analysis Report for Summit Power Station, Amendment 19," May 6, 1974.
- 2.5.4.7-5 Hansen, H. J., "Upper Cretaceous (Senonian) and Paleocene (Danian) Pinchouts on the South Flank of the Salisbury Embayment, Maryland, and their Relationship to Antecedent Basement Structures, Maryland Geological Survey," Report of Investigations No. 29, 1978.
- 2.5.4.7-6 Kramer, S. K., Geotechnical Earthquake Engineering, p. 155, Pearson Education, Inc., 1996.
- 2.5.4.7-7 Li, Jerome C. R., Statistical Inference, p. 287, Edwards Brothers, Inc, Ann Arbor, MI, 1965.
- 2.5.4.7-8 Public Service Enterprise Group (PSEG), "Hope Creek Generating Station Updated Final Safety Analysis Report," Revision 16, Subsection 2.5.4, May 15, 2008.
- 2.5.4.7-9 Public Service Enterprise Group (PSEG), "Salem Generating Station Updated Final Safety Analysis Report," Revision 23, Subsection 2.5.4, October 17, 2007.
- 2.5.4.7-10 Stokoe, H. H. II, Appendix B of Memorandum to Dr. Richard Lee dated 3 February, 2005, "Review of the Savannah River Site (SRS) Dynamic Soil Properties Recommended in the University of Texas (UT) Report of 1995", contained in Washington Savannah River Company, LLC, "Savannah River Site Probabilistic Seismic Hazard Assessment Update (U)," WSRC-TR-2006-00113, Rev. 0, December, 2007.

**PSEG Site
ESP Application
Part 2, Site Safety Analysis Report**

- 2.5.4.7-11 Volkert, R.A., Drake, Jr., A.A., and Sugarman, P.J., "Geology, Geochemistry, and Tectonostratigraphic Relations of the Crystalline Basement Beneath the Coastal Plain of New Jersey and Contiguous Areas," U.S. Geological Survey Professional Paper 1565-B, 1996.
- 2.5.4.7-12 Washington Savannah River Company, LLC, "Savannah River Site Probabilistic Seismic Hazard Assessment Update (U)," WSRC-TR-2006-00113, Rev. 0, p. 197, December, 2007.
- 2.5.4.7-13 Zapecza, O. S., "Hydrogeologic framework of the New Jersey coastal plain: USGS Professional Paper 1404-B," 1989.
- 2.5.4.7-14 Garrity, C.P. and D.R. Soller, "Database of the Geologic Map of North America," adapted from the map by J.C. Reed Jr. and others (2005): U.S. Geological Survey Data Series 424, Website, <http://pubs.usgs.gov/ds/424/>, accessed September 24, 2009.
- 2.5.4.7-15 MACTEC Engineering and Consulting Inc., "Geotechnical Exploration and Testing, PSEG Site ESPA Application, Lower Alloways Creek Township, New Jersey," Revision 0, July 10, 2009.
- 2.5.4.7-16 Darendeli, Mehmet B., "Development of a New Family of Normalized Modulus Reduction and Material Damping Curves," Dissertation, The University of Texas at Austin, August, 2001.

**PSEG Site
ESP Application
Part 2, Site Safety Analysis Report**

**Table 2.5.4.7-1
Summary of Geologic Strata Elevations**

FORMATION	PSEG ESPA Investigation Borings (Appendix 2AA)							
	PSEG ESPA - NB Series Strata Summary (8 borings)				PSEG ESPA - EB Series Strata Summary (8 borings)			
	Avg. Thickness (ft.)	Top of Formation			Avg. Thickness (ft.)	Top of Formation		
		Avg. Elev. ^(a) (ft.)	Range (ft.)			Avg. Elev. ^(a) (ft.)	Range (ft.)	
			Highest Elev. ^(a) (ft.)	Lowest Elev. ^(a) (ft.)			Highest Elev. ^(a) (ft.)	Lowest Elev. ^(a) (ft.)
Vincentown	52.1	-56.4	-32.8	-69.8	54.6	-75.6	-44.7	-90.5
Hornerstown	18.5	-108.4	-104.8	-114.1	19.7	-130.1	-126.7	-137.2
Navesink	24.4	-126.9	-120.8	-132.6	20.1	-149.8	-147.1	-156.7
Mount Laurel	103.0	-151.3	-144.8	-157.1	111.2	-169.9	-167.5	-176.7
Wenonah	16.0	-253.7	-249.8	-259.1	13.5	-282.4	-278.5	-288.7
Marshalltown	25.0	-269.7	-264.8	-277.1	26.0	-292.8	-292.5	-293.1
Englishtown	44.0	-291.0	-289.8	-292.2	49.0	-318.8	-318.5	-319.1
Woodbury	36.0	-336.2	--	--	30.0	-367.5	--	--
Merchantville	30.0	-372.2	--	--	31.0	-397.5	--	--
Magothy	52.0	-402.2	--	--	55.0	-428.5	--	--
Potomac	--	-454.2	--	--	--	-483.5	--	--

a) All elevations shown in this table are referenced to NAVD 88.

**PSEG Site
ESP Application
Part 2, Site Safety Analysis Report**

**Table 2.5.4.7-2
Summary of Stratigraphic Layer Thicknesses, New Plant Area^(b)**

GEOLOGIC UNIT/Boring No.	NB-1	NB-2	NB-3	NB-4	NB-5	NB-6	NB-7	NB-8
Vincentown Formation ^(a)	51	46	46	58	46	50	51	56
Hornerstown Formation	21	16	19	18	19	17	20	19
Navesink Formation	24	24	26	23	25	24	25	25
Mount Laurel Formation	102	105	--	--	--	--	--	102
Wenonah Formation	15	15	--	--	--	--	--	18
Marshalltown Formation	25	25	--	--	--	--	--	--
Englishtown Formation	44	-	--	--	--	--	--	--
Woodbury Formation	36	--	--	--	--	--	--	--
Merchantville Formation	30	--	--	--	--	--	--	--
Magothy Formation	52	--	--	--	--	--	--	--
Potomac Formation	--	--	--	--	--	--	--	--

- a) Materials from ground surface to top of competent layer within Vincentown Formation are not included in this table. The thickness shown for the Vincentown Formation begins at the top of the competent layer. (-67 NAVD)
- b) Thicknesses taken from strata breaks on ESPA Geotechnical Boring Logs contained in Appendix 2AA and rounded to the nearest foot.

**PSEG Site
ESP Application
Part 2, Site Safety Analysis Report**

**Table 2.5.4.7-3
Summary of Shear Wave Velocities and Layers^(a)**

Dynamic Profile Layer Number (See Figure 2.5.4.7-8a for Layer Numbers)	Highest Vs for all borings tested, ft./sec.	Lowest Vs for all borings tested, ft./sec.	Ratio of highest to lowest
1	2584	2036	1.3
2	4054	3763	1.1
3	2619	2336	1.1
4	3202	2928	1.1
5	2962	2087	1.4
6	1727	1698	1.0
7	2321	2260	1.0
8	1961	1613	1.2
9	2745	2189	1.3
10	2207	2085	1.1

a) Shear wave velocity data from P-S Logging analysis results shown on Figures 2.5.4.7-6A, 2.5.4.7-6B, 2.5.4.7-6C, and 2.5.4.7-6D

**PSEG Site
ESP Application
Part 2, Site Safety Analysis Report**

**Table 2.5.4.7-4
Shear Wave Velocity Parameters for Dynamic Profile Layers**

Layer No. (Figures 2.5.4.7-8a and 8b)	Coef of Variation Used	Mean Values, ft./sec.	Upper Bound, ft./sec.	Lower Bound, ft./sec.
1	0.25	2250	2813	1800
2	0.25	3920	4900	3136
3	0.25	2490	3113	1992
4	0.25	3020	3775	2416
5	0.25	2490	3113	1992
6	0.3	1710	2223	1315
7	0.3	2290	2977	1762
8	0.3	1780	2314	1369
9	0.3	2490	3237	1915
10	0.3	2200	2970	1430
Compressive Wave Velocity Parameters for Dynamic Profile Layers				
1	0.25	6200	7750	4960
2	0.25	7640	9550	6112
3	0.25	6350	7938	5080
4	0.25	6830	8538	5464
5	0.25	6450	8063	5160
6	0.3	5560	7228	4277
7	0.3	6190	8047	4762
8	0.3	5940	7722	4569
9	0.3	6600	8580	5077
10	0.3	6200	8370	4030
Poisson's Ratio Parameters for Dynamic Profile Layers				
1	(a)	0.43	0.43	0.43
2	(a)	0.32	0.32	0.32
3	(a)	0.41	0.41	0.41
4	(a)	0.38	0.38	0.38
5	(a)	0.41	0.41	0.41
6	(a)	0.45	0.45	0.45
7	(a)	0.42	0.42	0.42
8	(a)	0.45	0.45	0.45
9	(a)	0.42	0.42	0.42
10	(a)	0.44	0.44	0.44

a) Statistical variation too small to affect parameter

**PSEG Site
ESP Application
Part 2, Site Safety Analysis Report**

**Table 2.5.4.7-5
Summary of Modulus Reduction and Damping Layer Information**

Layer for Analysis	Related Dynamic Profile Layer(s) from Figure 2.5.4.7-8a^(b)	Soil Type	Plasticity Index (PI)	Over-consolidation Ratio (OCR)	Ko^(c)	Confining Pressure, (ksf)^(d)
A	1	Sand	NA	1	0.5	4.7
				2	0.6	5.1
				4	0.92	6.6
				6	1.17	7.8
B	2, 3, 4, and 5	Sand	NA	1	0.5	9.4
				2	0.83	12.5
				4	1.06	14.6
				6	1.21	16.0
C	6, 7, and 8	Clay with some sand	30	2	0.5	15.3
				2	0.71	18.5
				4	1.0	22.9
				6	1.22	26.2
D ^(a)	9a and 9b	Sand	NA	1	0.5	19.9
				2	0.6	21.9
				4	0.92	28.3
				6	1.17	33.2

a) Layers 9a and 9b are subdivision of Layer 9 with same properties - subdivided to accommodate geologic strata break.

b) Layer 10 shown on Figure 2.5.4.7-8a is combined with the Deep Profile

c) Coefficient of lateral earth pressure at rest

d) ksf = 1000 pounds per square foot

**PSEG Site
ESP Application
Part 2, Site Safety Analysis Report**

2.5.4.8 Liquefaction Potential

This subsection presents a discussion of liquefaction potential for the soils at the PSEG Site. RG 1.198, *Procedures and Criteria for Assessing Seismic Soil Liquefaction at Nuclear Power Plant Sites*, Revision 0, 2003, contains guidance on procedures for assessing soil liquefaction. The approach provides for screening using geologic criteria and soil characteristic criteria and calculation methods using field data and, if necessary, laboratory classification test data. If the screening methods conclude soils are not potentially liquefiable, the methods using laboratory cyclic strength test data are not necessary. Geologically based screening and Standard Penetration Test (SPT) based liquefaction analyses performed in accordance with RG 1.198 concluded the soils below elevation -67 ft. NAVD are not susceptible to liquefaction and more detailed analyses are not performed.

2.5.4.8.1 Site Conditions

Soil liquefaction is a process by which loose, saturated, granular deposits lose a significant portion of their shear strength due to pore pressure buildup resulting from cyclic loading, such as that caused by an earthquake. Soil liquefaction occurrence (or lack thereof) depends on geologic age, state of soil saturation, density, gradation, plasticity, and earthquake intensity and duration. Soil liquefaction can occur, leading to bearing failures and excessive settlements, when all of the following criteria are met:

- Design ground acceleration is high
- Soil is saturated (i.e., close to or below the water table)
- Site soils are sands or silty sands in a loose to medium dense condition

The PSEG Site geology, as described in Subsection 2.5.4.1, consists of layered sediments ranging in geologic age from Quaternary to Lower Cretaceous. These sediments overlie crystalline bedrock at an elevation of approximately -1750 ft. NAVD. The uppermost 50 (+/-) ft. of sediments are recent age and consist of soft fill placed by hydraulic disposal and some artificial fill placed during previous construction activity. Quaternary age (Pleistocene) deposits of loose to medium dense sandy alluvium underlie the recent deposits and are 10 to 15 ft. thick.

Below the alluvium, Tertiary age deposits of mostly sandy soils of the Kirkwood, Vincentown and Hornerstown formations are present to depths of approximately 160 ft. below the existing ground surface. Cretaceous age sediments begin at this approximately 160 ft. depth and extend to the crystalline bedrock.

As described in SSAR Subsection 2.5.4.3.1.2, boreholes were made using a clay mineral drilling fluid. Groundwater levels at the time of drilling can be affected by the presence of the drilling fluid. The depth to the groundwater table at each boring location used in the liquefaction evaluation was selected from water level measurements made in April 2009 (SSAR Table 2.5.4.6-1) in the shallow-depth observation wells installed adjacent to the geotechnical borings (U-series).

The Quaternary and Pleistocene deposits will be removed from the area of the safety-related structures because of their low shear wave velocity and unsuitable engineering characteristics. As discussed in Subsection 2.5.4.5, the removal is expected to extend to approximately elevation -67 ft. NAVD, or approximately 75 ft. below the present ground surface. Category 1

**PSEG Site
ESP Application
Part 2, Site Safety Analysis Report**

backfill materials will be placed between the top of the competent material and the foundation mats and adjacent to the walls for the safety-related structures. Category 1 backfill may consist of compacted granular fill, roller-compacted concrete or concrete fill. Compacted fill material (Category 2 backfill) will be placed from present ground up to the new plant grade. Category 2 backfill may consist of Category 1 materials, materials removed from the excavations or other materials meeting engineering requirements. Due to their strength and compacted condition, Category 1 backfill materials and compacted Category 2 backfill materials are not susceptible to liquefaction. Backfill characteristics and compaction requirements are described in Subsection 2.5.4.5.

RG 1.198 states that Cone Penetrometer Test (CPT) probes should be the tool of choice for initial site characterization in support of liquefaction potential assessment. CPT data is not obtainable because of the dense soils below the top of competent material at about elevation - 67 ft. NAVD. Results of STP tests, another acceptable method listed in RG 1.198, are used for the liquefaction potential assessment.

2.5.4.8.2 Geologically Based Liquefaction Assessment

The site investigation identifies 14 geologic formations above the crystalline bedrock at the site as follows, in order of increasing depth below the ground surface:

- a. Artificial and Hydraulic Fill
- b. Alluvium
- c. Kirkwood
- d. Vincentown
- e. Hornerstown
- f. Navesink
- g. Mount Laurel
- h. Wenonah
- i. Marshalltown
- j. Englishtown
- k. Woodbury
- l. Merchantville
- m. Magothy
- n. Potomac

As discussed in Subsection 2.5.4.5, the upper three formation soils, Artificial and Hydraulic Fill, Alluvium and Kirkwood, are to be removed from the area of the safety-related structures because of their unsuitable engineering characteristics. The Vincentown Formation at about elevation -67 ft. NAVD will form the competent layer for supporting the safety-related structures. The excavated area will be replaced with Category 1 backfill such as concrete, roller-compacted concrete, or compacted fill that will not liquefy. Because the upper three formations are to be removed, therefore they are not included in the liquefaction assessment.

Potential for liquefaction is evaluated using the screening methodology presented in RG 1.198 for each geologic formation below the top of the competent layer at the PSEG Site.

The liquefaction potential of each formation is first assessed based on the composition of each formation. The composition assessment is based on the general formation descriptions, Unified

**PSEG Site
ESP Application
Part 2, Site Safety Analysis Report**

Soil Classification System (USCS) designations shown on the test boring logs, and the results of Atterberg limit tests and grain size analysis tests performed on selected samples.

Based on their granular composition and position below the water table, the Vincentown, Hornerstown, Navesink, Mount Laurel, Wenonah, Marshalltown, Englishtown, Magothy and Potomac formations are potentially liquefiable. The Woodbury and Merchantville formations are clayey soils containing less than 50 percent sand and are not likely to liquefy.

The field SPT results (N-values) are corrected for field variables, sampling methods and effective overburden pressures. Based on the average corrected N-value of each formation, the Hornerstown, Wenonah and Englishtown formations are potentially liquefiable. The other formations have average corrected N-values equal to or greater than 30 blows per foot and are not likely to liquefy (Reference 2.5.4.8-2).

As discussed in Reference 2.5.4.8-2, resistance of soils to liquefaction increases with age – Pleistocene sediments are more resistant to liquefaction than younger sediments, and pre-Pleistocene sediments are generally not liquefiable. All formations below the top of the competent layer are pre-Pleistocene and are not likely to liquefy based on their age.

The results of the geologically based liquefaction screening evaluation are summarized on Table 2.5.4.8-1.

2.5.4.8.3 SPT-Based Liquefaction Assessment

A liquefaction assessment using a simplified SPT-based empirical procedure is performed for the geologic formations below the top of the competent layer using the methods described in Reference 2.5.4.8-2 and as described in RG 1.198. The liquefaction potential is presented as a factor of safety which is the ratio of the cyclic resistance ratio (CRR) to the cyclic stress ratio (CSR).

The CRR is based on the SPT N-values corrected for field variables, sampling methods, overburden pressure, and fines content of the soil. The CRR is initially computed for an earthquake magnitude of 7.5 and then modified by the Magnitude Scaling Factor which is based on the earthquake magnitude for the site being evaluated. Both lower bound and upper bound Magnitude Scaling Factors are used; the lower bound Magnitude Scaling Factor provides the lower factor of safety and thus is conservative.

Section 2.5.2 of NUREG-0800 states that if the controlling earthquakes for a site have magnitudes less than 6, the time history selected for the evaluation of liquefaction potential must have a duration and number of strong motion cycles corresponding to at least a magnitude 6 event. Table 2.5.2-34 presents controlling earthquakes for high and low frequency earthquakes and for annual frequencies of exceedance of 10^{-4} , 10^{-5} and 10^{-6} . Because liquefaction assessment is based on the GMRS, and because the GMRS is computed using only the high frequency controlling earthquakes for 10^{-4} and 10^{-5} annual frequencies of exceedance, only the values in Table 2.5.2-34 for those events are applicable for selecting the controlling earthquake. The applicable values in Table 2.5.2-34 are magnitude 6 or less, therefore magnitude 6 is used in the liquefaction analysis.

**PSEG Site
ESP Application
Part 2, Site Safety Analysis Report**

The CSR is a function of the maximum acceleration at the foundation level, the total and effective overburden pressures at the sample depth, and a stress reduction factor. A stress reduction factor is used because the soil column is not rigid but deformable, and shear stresses at depth are less than at the foundation level. The Ground Motion Response Spectrum (GMRS) is developed for the top of the competent layer (Vincentown Formation) and has a mean elevation of -67 ft. Therefore, the maximum acceleration is applied at the top of the competent layer and the stress reduction factor is referenced to the top of the competent layer in the evaluation. For conservatism, overburden stresses are referenced to existing ground surface at each boring location. The GMRS is shown on Figure 2.5.2-54. The maximum ground acceleration used in the analysis, 0.225 g, is the point at which the GMRS intersects the 100 Hz frequency. The use of 100 Hz to determine peak ground acceleration is standard practice and has been used on other soil sites.

Subsection 2.5.2.6 of the Hope Creek Generation Station (HCGS), UFSAR (Reference 2.5.4.8-1) presents the Safe Shutdown Earthquake (SSE) and peak acceleration for the HCGS site. Design acceleration of 20% g is recommended at the foundation level resulting from the occurrence of the SSE of Intensity VII (M ~ 5.7). These values are very comparable to the earthquake magnitude and peak acceleration used in this liquefaction evaluation.

The safety factor against liquefaction is computed for each SPT sample of granular soil obtained in borings NB-1 through NB-8 from the top of the competent layer at elevation -67 feet to the depth explored in the boring. Table 2.5.4.8-2 shows the minimum, maximum and average factors of safety against liquefaction and the distribution of safety factors for each geologic formation at the PSEG Site, based on the lower bound Magnitude Scaling Factor.

RG 1.198 states that in general factors of safety less than or equal to 1.1 against liquefaction are low, factors of safety between 1.1 and 1.4 are considered moderate, and factors of safety greater than or equal to 1.4 are considered high. A total of 257 SPT N-values are analyzed. There are 17 calculated liquefaction safety factors less than 1.1, 15 safety factors between 1.1 and less than 1.4, and 225 safety factors greater than 1.4. The SPT-based screening calculation results indicate that potentially liquefiable soils in the Vincentown Formation are isolated pockets surrounded by denser materials, not a continuous layer. Thus, liquefaction of granular soils below the top of the competent layer is not likely to occur.

The existing total and effective overburden pressures are used in computing the safety factor against liquefaction. The Artificial and Hydraulic Fill, Alluvium and Kirkwood Formation soils will be removed and replaced with controlled fill such as concrete or compacted fill having a unit weight greater than the existing soils. The higher unit weight materials will increase the total and effective overburden pressures and will result in higher safety factors against liquefaction. Therefore the computed liquefaction safety factors shown on Table 2.5.4.8-2 are conservative using existing total and effective overburden pressures.

2.5.4.8.4 Liquefaction Outside the Safety-Related Structure Area

The Artificial and Hydraulic Fill, Alluvium and Kirkwood Formation soils will be excavated to the top of the competent layer and replaced with Category 1 backfill material in the area of the nuclear island and other safety-related structures. Beyond this area of excavation and replacement, the Artificial and Hydraulic Fill, and Alluvium will be excavated to the Kirkwood Formation and replaced with Category 2 backfill material out to the limits of the power block

**PSEG Site
ESP Application
Part 2, Site Safety Analysis Report**

excavation. Subsection 2.5.4.2 and Figure 2.5.4.5-2 discuss and illustrate details of the excavation and replacement concept.

The excavation for the power block will be bounded by a structural support system located approximately 850 ft. from the centerline of the nuclear island structures depending on the technology selected. Outside of the structural support system, the Artificial and Hydraulic Fill, Alluvium, and Kirkwood Formation soils will remain in place. Liquefaction of these soils could result in settlement and lateral spread outside the excavation support structure. As a worst case, all soil outside the excavation support structure is considered as being removed during a possible liquefaction event. If this were to occur, the structural support system could fail, and soil inside the excavation support structure could fail back to the angle of repose for the compacted Category 2 soil fill. Figure 2.5.4.8-1 illustrates this condition. Based on this very conservative scenario, the top of failed slope would be approximately 180 ft. from the excavation support structure, leaving approximately 230 ft. of undisturbed soil in place between the top of slope and the nearest safety-related structure. The top of the slope would also be 670 ft. from the centerline of the nuclear island structures. The nuclear island structures and other safety-related structures would not be impacted by loss of soils outside the excavation support structure during a liquefaction event.

2.5.4.8.5 Non-Seismic Liquefaction Potential

NUREG-0800 states that non-seismic liquefaction potential from erosion, floods, wind loads on structures, and wave action should be considered. The soils impacted by such conditions will be fill placed either to replace excavated material or to reach the plant grade. The properties of these soils are not known at this time. Use of soils selected and compacted in accordance with the requirements given in Subsection 2.5.4.5.3 will provide a material resistant to liquefaction. Further evaluation of non-seismic liquefaction will be performed during the COLA.

2.5.4.8.6 References

- 2.5.4.8-1 Public Service Enterprise Group (PSEG), "Hope Creek Generating Station Safety Analysis Report," p. 2.5-104, Table 2.5-1, Footnote 2, 1988.
- 2.5.4.8-2 Youd, T.L., Idriss, I.M., Andrus, R.D., Arango, I., Castro, G., Christian, J.T., Dobry, R., Finn, W.D.L., Harder, Jr., L.F., Hynes, M.E., Ishihara, K., Koester, J.P., Liao, S.S.C., Marcuson, III, W.F., Martin, G.R. Mitchell, J.K. Moriwaki, Y., Power, M.S., Robertson, P.K., Seed, R.B., and Stokoe, II, K.H., 2001.
"Liquefaction resistance of soils: Summary report from the 1996 NCEER and 1998 NCEER/NSF Workshops on Evaluation of Liquefaction Resistance of Soils," J. Geotech. Geoenviron. Eng., ASCE, v 27 (10), 817-833, October 2001.

**PSEG Site
ESP Application
Part 2, Site Safety Analysis Report**

**Table 2.5.4.8-1
Screening for Potential Liquefaction**

Potential for Granular Soils to Liquefy				
Formation No.	Formation Name	Based on Composition ^(a)	Based on Average Corrected N-Value $(N_1)_{60}$ ^(b)	Based on Geologic Age ^(c)
4	Vincentown	Yes	No	No
5	Hornerstown	Yes	Yes	No
6	Navesink	Yes	No	No
7	Mount Laurel	Yes	No	No
8	Wenonah	Yes	Yes	No
9	Marshalltown	Yes	No	No
10	Englishtown	Yes	Yes	No
11	Woodbury	No	N/A	No
12	Merchantville	No	N/A	No
13	Magothy	Yes	No	No
14	Potomac	Yes	No	No

- a) "Yes" if sand content > 50%. "No" if sand content < 50%.
- b) Clean granular soils with $(N_1)_{60} \geq 30$ are too dense to liquefy (Reference 2.5.4.8-2).
- c) All Formations Pre-Pleistocene. "... Pre-Pleistocene sediments are generally not subject to liquefaction." (Reference 2.5.4.8-2)

**PSEG Site
ESP Application
Part 2, Site Safety Analysis Report**

**Table 2.5.4.8-2
Summary of Liquefaction Safety Factors (FS) for each Geologic Formation**

Formation No.	Formation Name	Safety Factor ^{(a), (b)}			Distribution of Safety Factors		
		Minimum	Maximum	Average	FS≤1.1	1.1<FS<1.4	1.4≤FS
4	Vincentown	0.8	10.0	3.6	15	13	48
5	Hornerstown	1.0	8.1	3.7	1	2	30
6	Navesink	2.8	21.4	8.1	0	0	44
7	Mount Laurel	1.4	10.6	8.9	0	0	90
8	Wenonah	0.9	2.4	1.7	1	0	1
9	Marshalltown	1.5	7.5	4.5	0	0	5
10	Englishtown	2.2	2.2	2.2	0	0	1
11	Woodbury	NL	NL	NL	0	0	0
12	Merchantville	NL	NL	NL	0	0	0
13	Magothy	6.1	6.7	6.5	0	0	3
14	Potomac	5.8	6.0	5.9	0	0	3
Total =					17	15	225

a) NL = Non-liquefiable silts and clays (USCS designations CL, CH, ML, MH, CL-ML, CH-MH)

b) Safety Factors based on lower bound Magnitude Scaling Factor

**PSEG Site
ESP Application
Part 2, Site Safety Analysis Report**

2.5.4.9 Earthquake Design Basis

This subsection briefly summarizes the derivation of the site-specific GMRS and SSE as detailed in Subsection 2.5.2.6.

The PSEG Site is in the Central and Eastern United States (CEUS). The CEUS, as discussed in Subsection 2.5.1.1.4, is a stable continental region characterized by low rates of crustal deformation and no active plate boundary conditions.

A performance-based, site-specific GMRS is developed in accordance with the methodology provided in RG 1.208. The PSEG Site is a deep soil site, therefore excavation is required to reach a competent layer. The GMRS is developed at the top of the competent layer as provided in Section 5.3 of RG 1.208. A site dynamic properties profile, developed as described in Subsection 2.5.4.7, and based on soil properties described in Subsections 2.5.4.2 and 2.5.4.4, forms the basic description of the site conditions used in developing the GMRS. The GMRS and the methodology for developing it are provided in Subsection 2.5.2.6. The GMRS satisfies the requirements of 10 CFR 100.23 for development of a site-specific SSE ground motion.

The approach to developing the GMRS follows the recommended steps in RG 1.208, as briefly described below:

- The seismic source characterization model used for the PSEG Site region (200-mile radius) is the Central and Eastern United States Seismic Source Characterization (CEUS-SSC) contained in NUREG-2115. As discussed in Subsection 2.5.2.2, no alterations to the CEUS-SSC were necessary, except to include the Atlantic Highly Extended Crust - East seismic source.
- Perform sensitivity studies and an updated probabilistic seismic hazard analysis (PSHA) to develop rock hazard spectra and define the controlling earthquakes (Subsection 2.5.2.4).
- Develop the site dynamic soil properties (Subsections 2.5.4.2, 2.5.4.4, and 2.5.4.7).
- Derive performance-based GMRS from the updated PSHA at a free field hypothetical outcrop at the top of the competent material beneath the site (defined as the upper portion of the Vincentown Formation) as described in Subsection 2.5.2.6.

The resulting GMRS is presented in Subsection 2.5.2.6.

2.5.4.9.1 References

2.5.4.9-1 Not Used

**PSEG Site
ESP Application
Part 2, Site Safety Analysis Report**

2.5.4.10 Static Stability

This subsection describes the analysis of the stability of safety-related facilities for static loading conditions. The safety-related structures evaluated in this subsection consist of the reactor building and associated buildings supported on a common base mat (nuclear island). Other safety-related structures are described in design control and final safety analysis documents for the four technologies under consideration. However, bearing pressures, bearing depths, and foundation embedment depths for these other safety-related structures are less than those for the nuclear island. Thus, by considering the largest and heaviest safety-related structures, the evaluation of bearing capacity and settlement is a conservative approach for the ESPA.

2.5.4.10.1 General Foundation Information

The reactor foundation design parameters are included in the reactor technology Design Control Documents (DCD), FSAR or the PPE (Table 1.3-1). The four reactor technologies are:

- ABWR
- AP1000
- U.S. EPR
- US-APWR

The following design parameters relative to the static stability of the foundations are given in the DCDs:

- Foundation embedment depth (39 ft. to 84.3 ft. below plant grade)
- Foundation plan dimensions
- Static bearing capacity (15,000 psf)

As described in Subsection 2.5.4.5, removal of soft/loose materials will be required to reach material suitable for supporting the loads imposed by the nuclear island structures. Material removal will extend to a competent layer located within the Vincentown Formation at approximately elevation -67 ft. NAVD. As discussed in Subsection 2.5.4.7, the competent layer and materials below this elevation have a shear wave velocity exceeding 1000 ft/sec.

The existing ground surface will be raised to elevation 36.9 ft. NAVD. For this plant grade, the highest present groundwater level as reported in Subsection 2.5.4.6 is elevation 2.8 ft. NAVD, or a distance of approximately 34.1 ft. below the plant grade.

The upper and lower bound embedment depths, to the bottoms of the nuclear island base mats, as listed in the PPE (Table 1.3-1), range between 39 ft. and 84.3 ft. below the plant grade. These depths correspond to bearing elevations between elevations -2.1 ft. and -47.4 ft. NAVD. A structural fill material will be placed in the space between the bottom of the nuclear island base mat and the top of the competent layer. The structural fill will consist of lean concrete, roller-compacted concrete or compacted granular backfill material. Outside of the building walls, a structural fill will be placed from the competent layer up to the plant grade to fill the excavation. Further discussion of excavation and backfill is provided in Subsection 2.5.4.5.

Plan dimensions of nuclear island base mats are described in the reactor technology DCDs or FSAR (References 2.5.4.10-1, 2.5.4.10-6, 2.5.4.10-7, and 2.5.4.10-9). These plan dimensions are used in the bearing capacity and settlement calculations with the exception of the U.S. EPR. The

**PSEG Site
ESP Application
Part 2, Site Safety Analysis Report**

U.S. EPR nuclear island foundation is a cruciform shape. For analysis, the contact area of the cruciform, converted to a rectangle of equivalent area, is used.

2.5.4.10.2 Soil Bearing Capacity

Bearing capacity under static and dynamic loading conditions is evaluated using three methodologies (Meyerhof, Terzaghi, and Vesic) described by Bowles (Reference 2.5.4.10-3). The bearing capacity for each of the four reactor technologies is evaluated because bearing capacity is related to the size of a mat foundation and the embedment.

The subsurface model used for bearing capacity evaluation included granular backfill placed from the bottom of the excavation up to the plant grade outside the mat and building limits. The source of backfill material is not known at the ESPA stage, thus properties of granular structural backfill are used, as reported in the Hope Creek UFSAR (Reference 2.5.4.10-8). The following properties (lower end of reported ranges) are used:

- Compacted maximum dry unit weight – 128 lbs/ft³
- Angle of internal friction – 35 degrees

Below the base mat, the analysis model assumed that the backfill is a compacted granular material with the same properties as above. This assumption is conservative, as the strength of the other two types of backfill (lean concrete or roller-compacted concrete) would be greater than that of the compacted granular backfill.

Unit weight is taken as a weighted average of those of the Vincentown, Hornerstown, Navesink and Mount Laurel formations, as these layers are the primary contributors to the bearing capacity. The angle of internal friction from tests on samples from the Vincentown Formation is used with calculation checks that are based on standard penetration resistance values corrected for field procedures, energy and overburden pressure $[(N_1)_{60}]$ for deeper formations. An average in-situ wet unit weight of 125 lbs/ft³ and an angle of internal friction of 37 degrees are used. Material properties used in this weighted averaging are presented in Table 2.5.4.2-9.

The position of the groundwater table is a parameter included in bearing capacity analysis. As discussed in Subsection 2.5.4.6, the average groundwater level measured between January, 2009 and December, 2009 was approximately elevation 0.8 ft. NAVD. The maximum groundwater level observed was elevation 2.8 ft. NAVD. For purposes of the bearing capacity analysis, a conservative groundwater level at the existing ground surface (elevation 10 ft. NAVD) is used. This is conservative because the potential to have a higher groundwater table within the fill placed to reach the plant grade is unlikely as the fill area is essentially a pedestal raised above the surrounding natural ground. In addition, normal site grading and stormwater management will prevent ponding water on the plant grade that would infiltrate over a period of time long enough to create a raised groundwater table.

For the model and the three analysis methods discussed above, the computed ultimate bearing capacity is 420,000 psf. The calculated ultimate bearing capacity does not include consideration of settlement. Settlement may be the governing performance criterion, and is discussed in Subsection 2.5.4.10.3.

**PSEG Site
ESP Application
Part 2, Site Safety Analysis Report**

2.5.4.10.3 Settlement

Criteria for total and differential settlement have not been established at this time. Settlement is greatly dependent on the position of the applied load relative to the subsurface layers, and on the size of the mat. An example of possible settlement at the new plant location is considered using the technology with the largest mat foundation (U.S. EPR) combined with a representative static bearing pressure of 15,000 psf. The approach to the calculation and the results are discussed below.

The soils below the top of the competent layer are primarily dense sands and very dense silty and clayey sands with some zones of hard clay. As discussed in Subsection 2.5.4.1.2.3.2, erosion has occurred in the geologic past, removing material above the Vincentown Formation. The soils in the Vincentown and below are thus over-consolidated. It is interpreted that these soils will deform elastically because of the sandy composition of the soil and the over-consolidation of the hard clay zones. Settlement calculations for the reactor building are performed using two methods that are based on theory of elasticity: the Timoshenko and Goodier method, and the Janbu method (Reference 2.5.4.10-3).

The Timoshenko and Goodier method uses a single layer of material subject to compression (taken for the ESPA analysis as twice the mat width) and a weighted average modulus of elasticity over this thickness. The Janbu method uses a layered subsurface model with the average vertical stress at the midpoint of each layer computed by stress distribution methods (Reference 2.5.4.10-4). The distributed stresses can be calculated for any point; stresses under the center point of the mat, a side point and a corner point are calculated for the evaluation discussed in this subsection. The elastic modulus for each layer is computed as described below, and the layer strain is determined by dividing the added stress by the modulus of elasticity. The individual layer strains are then summed to obtain a total settlement.

For the settlement calculation, the values for modulus of elasticity are calculated using the relationship between shear modulus and elastic modulus (Reference 2.5.4.10-5):

$$E_s = 2G(1 + \mu) \quad \text{(Equation 2.5.4.10-1)}$$

where:

E_s = Elastic Modulus (psf)

G = Shear Modulus (psf)

μ = Poisson's Ratio

The value of G decreases as the shear strain increases. For settlement analysis, the value of G in the above equation is selected for a shear strain level compatible with the soil deformation. The in-situ P-S suspension logging, described in Subsection 2.5.4.4, provides values of shear wave velocity at small shear strains. The small strain shear modulus, G_{\max} , is calculated from the shear wave velocity by the equation (Reference 2.5.4.10-5):

**PSEG Site
ESP Application
Part 2, Site Safety Analysis Report**

$$G_{\max} = V_s^2 \rho \quad (\text{Equation 2.5.4.10-2})$$

where:

G_{\max} = small-strain shear modulus (psf)

$\rho = \gamma_T / g$

g = gravitational constant = 32.2 ft/sec²

γ_T = total unit weight of soil (pcf), and

V_s = shear wave velocity of soil (ft/sec)

To account for the reduction of G with increasing shear strain, G_{\max} is reduced using plots of the ratio G/G_{\max} against shear strain, as described in Subsection 2.5.4.7.4. A typical shear strain for settlements is 10^{-3} (Reference 2.5.4.10-5). For purposes of the analysis, a reduction ratio of 0.4 is used above -300 ft. NAVD and 0.5 below that point. Poisson's ratio is taken as 0.3 above -300 ft. NAVD and 0.2 below. These values are less than values interpreted from the geophysical logging discussed in Subsection 2.5.4.7 and are based on general recommendations by the Federal Highway Administration (Reference 2.5.4-10-5). The layers, top elevations, unit weights, average shear wave velocities, shear modulus, Poisson's ratio, and elastic modulus used are shown in Table 2.5.4.10-1.

To consider differential settlement, settlement at the center of the base mat, a side point, and a corner are calculated. The differential settlement over the distance is calculated by dividing the distance into the settlement difference. Differential settlement occurs due to lateral changes in soil layer thicknesses or soil properties, and due to the difference in applied stresses below a corner and the center of the loaded area. As discussed in Subsections 2.5.4.1 and 2.5.4.7, the subsurface layers are subhorizontal and have similar thicknesses and properties across the site. Thus, the only contributor to differential settlement is the difference in applied stress conditions under the mat corner and the center.

As discussed in Subsection 2.5.4.5, the base mats for the technologies are constructed with their bottoms at an upper bound level of elevation -2.1 ft. NAVD, and a lower bound level of -47.4 ft. NAVD. However, excavation for all technologies extends to approximate elevation -67 ft. NAVD, to reach the competent layer. Rebound due to removal of soil in the excavation process occurs and recompression of the base of the excavation would occur upon application of the backfill loading. The weight of concrete fill placed below a base mat applies stresses of about the same as the weight of soil removed, or greater. Subsurface deformations related to the weight of the concrete fill are essentially completed before loads from the reactor building are added to the base mat because of the elastic character of the settlement. As a conservative approach for the calculations, the static bearing pressure is taken to be applied at the top of the competent layer (elevation -67 ft. NAVD).

The Janbu analysis method resulted in slightly greater estimated settlement than the Timoshenko and Goodier analysis method. The estimated settlement from the Janbu analysis described above is 1.6 in. for the center of the mat, and 1 in. for a side of the mat for the average modulus values. For the U.S. EPR mat dimension, the side to center differential settlement is 0.25 in. over 50 ft. Soils respond to load application in an elastic manner, therefore, much of the settlement occurs as the base mat and building wall loads are applied.

2.5.4.10.3.1 Deflection Monitoring

A settlement monitoring program will be conducted during construction of the facility to determine the magnitude of settlement that has occurred during construction to-date, and to better establish

**PSEG Site
ESP Application
Part 2, Site Safety Analysis Report**

post-construction settlement. Discussion of settlement monitoring is provided in Subsection 2.5.4.5.4.2.

2.5.4.10.4 References

2.5.4.10-1 AREVA, U.S. EPR Final Safety Analysis Report, Rev. 1, May, 2009.

2.5.4.10-2 Not used

2.5.4.10-3 Bowles, J.E., "Foundation Analysis and Design", Fourth Edition, Chapters 4, 5, pp 188-191, 232, 256-259., McGraw-Hill, 1988.

2.5.4.10-4 Bowles, J.E., "Foundation Analysis and Design", Third Edition, Chapter 5, pp 173-177, McGraw-Hill, 1982.

2.5.4.10-5 Federal Highway Administration (FHWA), Geotechnical Engineering Circular No. 5, Evaluation of Soil and Rock Properties, pp 150-151, April, 2002.

2.5.4.10-6 General Electric-Hitachi, Design Control Document for the ABWR, Rev. 0, 1997.

2.5.4.10-7 Mitsubishi Heavy Industries, Ltd., Design Control Document for the US-APWR, Rev. 1, August, 2008.

2.5.4.10-8 Public Service Enterprise Group (PSEG), "Hope Creek Generating Station Updated Final Safety Analysis Report," Revision 16, Subsection 2.5.4, May 15, 2008.

2.5.4.10-9 Westinghouse Electric Company, Design Control Document for the AP1000, Rev. 17, September, 2008.

**PSEG Site
ESP Application
Part 2, Site Safety Analysis Report**

**Table 2.5.4.10-1
Summary of Properties for Settlement Analysis
Properties for Average Shear Wave Velocity Values**

Analysis Layer		Total Unit Weight (pcf)	Average Shear Wave Velocity, V_s (ft/sec)	Small- strain Shear Modulus, $G_{max}^{(b)}$ (ksf)	Reduction Ratio, G/G_{max}	Reduced Shear Modulus, $G^{(b)}$ (ksf)	Poisson's Ratio	Average Static Modulus of Elasticity, $E_s^{(b)}$ (ksf)
From Elevation (ft. NAVD)	To Elevation (ft. NAVD)							
-67	-150	115	2250	18,100	0.4	7240	0.3	18,800
-150	-300	131	2500	25,200	0.4	10,080	0.3	26,200
-300	-370	128	1710	11,800	0.5	5900	0.2	14,100
-370	-505	125	2490	25,000	0.5	12,500	0.2	30,000
-505	(a)	130	2200	19,500	0.5	9750	0.2	23,400

a) Bottom elevation varies for each technology.

b) Numbers for G_{max} , G , and E_s are rounded

**PSEG Site
ESP Application
Part 2, Site Safety Analysis Report**

2.5.4.11 Design Criteria

The following geotechnical characteristics are evaluated in Subsection 2.5.4 and described in the cited subsections:

- Capable tectonic structures or sources – 2.5.4.9
- Groundwater level – 2.5.4.6
- Liquefaction potential – 2.5.4.8
- Static bearing capacity – 2.5.4.10
- Shear wave velocity – 2.5.4.7
- Soil angle of internal friction – 2.5.4.10

Consideration of settlement and construction groundwater control will be addressed in the COLA.

The design of the safety-related foundations for the nuclear island is based on the foundation mats being supported on backfill material. The backfill may consist of compacted granular fill, lean concrete fill, or roller-compacted concrete fill placed between the mat base and the competent sands of the Vincentown Formation. Removal of unsuitable soils below the nominal top elevation of the competent sands is expected locally, as required by the foundation inspection program described in Subsection 2.5.4.5.4. The backfill is placed between the suitable bearing soils and the foundation mat. The material requirements for backfill materials are discussed in Subsection 2.5.4.5. Quality control measures related to foundation material acceptance and to backfill material placement and compaction are described in Subsection 2.5.4.5. Inspections, Test, Analyses, and Acceptance Criteria (ITAAC) for the backfill will be presented in the COLA.

Discussion of assumptions and conservatism in static stability analyses is included in Subsection 2.5.4.10. Refer to Subsection 2.5.5 for slope stability design criteria. Computer analysis and methods of verification are discussed in the subsections in which they are used.

**PSEG Site
ESP Application
Part 2, Site Safety Analysis Report**

2.5.4.12 Techniques to Improve Subsurface Conditions

This subsection discusses techniques for soil improvement in the foundation areas of the safety-related structures. Depth below plant grade to the bottom of the common mats that support the safety-related structures within the nuclear island ranges from 39.0 ft. to 84.3 ft. (Table 1.3-1). As described in Subsection 2.5.4.5, the plant grade is elevation 36.9 ft. NAVD. Therefore, the base of the safety-related structures ranges from elevation -2.1 ft. to -47.4 ft. NAVD.

For the nuclear island, the materials within the range of the above stated base mat elevations are soft clays (hydraulic fill), loose sands (alluvium) and firm to soft clays (Kirkwood Formation). The geotechnical characteristics of these materials do not provide adequate bearing capacity for safety-related structures. Also, the shear wave velocities for these materials are less than 1000 feet per second. The improvement technique for these materials WILL be removal and replacement with backfill. The removal WILL extend down to competent sands present in the Vincentown Formation, as discussed in Subsection 2.5.4.5. Following the excavation and any localized soil improvements, the backfill WILL be placed in accordance with construction specifications for backfill, as discussed in Subsection 2.5.4.5.3.3. As discussed in Subsection 2.5.4.5.3, backfill may consist of granular material, fill concrete or roller-compacted concrete.

Based on the static stability analysis discussed in Subsection 2.5.4.10, deep soil improvement of foundation-bearing soils (such as vibro-compaction, vibro-replacement, vibro concrete columns, soil mix columns, or grouting) will not be necessary. Also, dental cleaning of rock defects and/or rock bolting will not be necessary because none of the foundations bear on or within rock.

Shallow-depth soil improvement techniques, including over-excavation and replacement, and bearing surface compaction, will apply to preparation of the foundation-bearing surfaces. These techniques are described briefly in this subsection, and in detail in Subsection 2.5.4.5.4.1.

2.5.4.12.1 Competent Layer Bearing Surface Preparation

Once a suitable bearing elevation is reached subgrade will be checked for general bearing surface conditions. Methods typically used for evaluating subgrade soils include probing, cone penetrometer testing, borings and use of heavy equipment driven across the area (proofrolling).

Areas identified by the subgrade check as potentially unsuitable may be further examined using additional probings, borings, and/or cone penetration test soundings to identify if unsuitable soils remain; and to determine their lateral extent and thickness. Areas identified as unsuitable may be compacted in place (using appropriate moisture content adjustments) to specified compaction requirements, or may be removed to expose competent materials in preparation for backfill placement. The final excavation surface will be observed, evaluated and approved by qualified personnel prior to placing any backfill or concrete. Materials compacted in place will be tested for compacted density using specified field density test methods.

Dewatering systems will be used to allow construction under dry conditions. Subsection 2.5.4.6.4 discusses the dewatering systems. The dewatering systems will remain active to keep water levels below the base of the excavation. Based on results of monitoring water levels within the excavation, additional dewatering wells may be added. Existing soils may be protected through use of a low-strength concrete mud mat until the backfill can be placed.

**PSEG Site
ESP Application
Part 2, Site Safety Analysis Report**

2.5.5 STABILITY OF SLOPES

This subsection discusses stability of earth slopes whose failure could affect safety-related structures, consistent with the information available for an ESPA. No rock exists at the PSEG Site within the area of the planned excavation; therefore, rock slopes are not discussed. The site characteristics related to stability of slopes are provided in Table 2.0-1. The pertinent site characteristics for stability of slopes are as follows:

- Capable tectonic structures
- Maximum flood
- Maximum groundwater level
- Liquefaction

Subsection 2.5.5.1 discusses characteristics of slopes as identifiable at the ESPA level. Subsection 2.5.5.2 reviews general design criteria and design analyses. However, specifics are deferred until the combined license application (COLA). Subsection 2.5.5.3 describes the results of investigations related to slopes. Subsection 2.5.5.4 discusses, in general terms, properties of borrow material, compaction and excavation specifications. However, specifics for design are deferred until the COLA.

2.5.5.1 Slope Characteristics

Temporary excavations are planned to remove unsuitable soils above a competent layer and replace them with compacted granular fill, lean concrete, or roller-compacted concrete. Subsection 2.5.4.5 discusses the excavation and backfill in more detail. Temporary excavations are planned with structural support designed to provide stability and safely retain the unexcavated soils.

As described in Subsection 2.5.4.5.1, the new plant grade will be raised to elevation 36.9 ft. NAVD. Fill material will need to be placed to reach the new plant grade, because the current ground elevations across the new plant location are 5 ft. to 15 ft. NAVD. The edges of the new fill will be sloped at 3 (horizontal): 1 (vertical) or flatter. The toe of the new slopes will be within the power block area, as illustrated on Figures 2.5.5-1 and 2.5.5-2. The fill below plant grade will be compacted as described in Subsection 2.5.4.3.3.2. The structural support system for the temporary excavation within the power block will be designed to provide appropriate support for the new fill should the sequence of construction require it.

An ultimate heat sink pond may be required for one of the four technologies included in the PPE. Slope stability analysis for an ultimate heat sink, if required, will be completed during the COLA phase of the project.

Slope stability analysis for the selected technology will include the evaluation of deep slope failure surfaces that may extend into the Delaware River and various water level considerations. This analysis will be completed during the COLA phase of the project. See Subsection 2.5.4.5 for discussion of excavation and backfill and Subsection 2.5.4.6 for discussion of groundwater conditions.

**PSEG Site
ESP Application
Part 2, Site Safety Analysis Report**

The portions of the site outside of the new plant power block area are relatively flat. There are no existing slopes on the site, either natural or manmade, that could affect the stability of the site.

2.5.5.2 Design Criteria and Analysis

This subsection will be completed for the COLA. Liquefaction potential is discussed in Subsection 2.5.4.8. Seismic forces for slope stability analysis will be based on controlling earthquakes, as discussed in Subsection 2.5.2.4.

The stability of slopes will be assessed during the COLA phase using limit equilibrium methods such as Bishop's simplified method (Reference 2.5.5-1); Janbu's simplified method (Reference 2.5.5-2) and the Spencer method (Reference 2.5.5-4). The stability analysis will evaluate the following loading conditions:

- End of construction
- Steady state
- Rapid drawdown
- Seismic events

2.5.5.3 Boring Logs

The locations of slopes are not known at the ESPA stage, therefore specific borings for slopes have not been performed. Figure 2.5.5-1 shows locations of the ESPA borings at the new plant location nearest to the approximate perimeter of the power block where the new fill slopes will be constructed. As discussed in Subsection 2.5.4.1, soils from the ground surface down to the Vincentown Formation are variable in thickness due to erosion and deposition in the geologic past. Soils below the Vincentown Formation show a consistent stratigraphy across the area of the new plant location. Boring logs for the borings shown on the plan and cross-sections are contained in Appendix 2AA. Based on the borings shown on Figure 2.5.5-1, soils in the area of fill placement for the new plant are expected to be similar throughout the area receiving fill. Further exploration for the design and analysis of slopes will be conducted for the COLA. This analysis will include evaluation of the required bearing elevation for fill material placement. Temporary excavations for removal of unsuitable soil will be conducted within the power block area. The new fill placed to reach the new plant grade is expected to be limited to the power block area. A general cross-section from the dredged channel in the Delaware River extended east into the power block area is shown on Figure 2.5.5-2. This cross-section indicates the approximate materials to be removed from within the power block and the general configuration of the new fill.

2.5.5.4 Compacted Fill

Material to form fills and associated slopes will be from on-site sources meeting required specifications or will be imported from off-site sources to the new plant location. Fill sources and characteristics are not identified for the ESPA. Subsection 2.5.4.5.3.2 describes characteristics of granular fill used for the Hope Creek backfill. Similar fill materials will be used at the new plant location. Subsection 2.5.4.5.3.3 describes general placement and compaction requirements. Subsection 2.5.4.5.3.4 describes quality control measures related to fill placement for slope construction.

**PSEG Site
ESP Application
Part 2, Site Safety Analysis Report**

Exterior slopes of the fill above the existing ground level will be protected from scour and erosion caused by river flooding by using armoring materials such as rock riprap, concrete blocks or mats designed to resist the design basis flood and wave forces. Details of the slope protection will be addressed in the COLA.

2.5.5.5 References

- 2.5.5-1 Bishop, A.W., "The Use of the Slip Circle in the Stability Analysis of Slopes", Geotechnique, Vol. 5 No. 1, 1955.

- 2.5.5-2 Janbu, N., "Slope Stability Computations", Soil Mechanics and Foundation Engineering, The Technical University of Norway, 1968.

- 2.5.5-3 National Oceanic and Atmospheric Administration (NOAA), "NOS Estuarine Bathymetry: Delaware Bay DE/NJ (M090)", Website <http://egisws01.nos.noaa.gov/servlet/BuildPage?template=bathy.txt&parm1=M090&B1=Submit>, accessed January 28, 2009.

- 2.5.5-4 Spencer, E., "A Method Analysis of the Stability of Embankments Assuming Parallel Inter-slice Forces", Geotechnique, Vol. 17 No. 1, 1967.